8

AFIP ATLAS OF TUMOR PATHOLOGY
Series 4

Tumors of the Adrenal Glands and Extraadrenal Paraganglia

Ernest E. Lack, MD

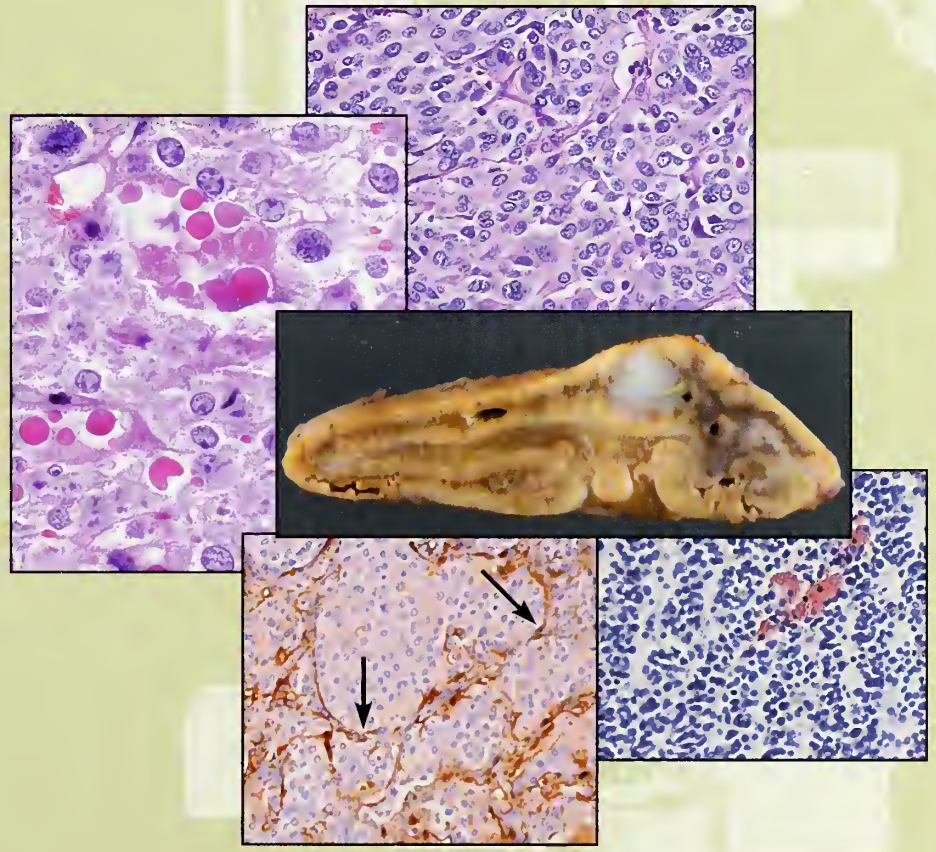

AFIP

ARP

Tumors of the Adrenal Glands and Extraadrenal Paraganglia

AFIP Atlas of Tumor Pathology

Silver Spring, Maryland

Editorial & Production Manager: Mirlinda Q. Caton
Production Editor: Dian S. Thomas
Editorial Assistant: Melanie J. De Boer
Copy Editor: Audrey Kahn

Available from the American Registry of Pathology
Armed Forces Institute of Pathology
Washington, DC 20306-6000
www.afip.org
ISBN 1-881041-01-8
978-1-881041-01-6

AFIP ATLAS OF TUMOR PATHOLOGY

Fourth Series
Fascicle 8

TUMORS OF THE ADRENAL GLANDS AND EXTRAADRENAL PARAGANGLIA

by

Ernest E. Lack, MD
Director of Anatomic Pathology
Washington Hospital Center
Washington, DC

Published by the
American Registry of Pathology
Washington, DC
in collaboration with the
Armed Forces Institute of Pathology
Washington, DC
2007

AFIP ATLAS OF TUMOR PATHOLOGY

EDITOR
Steven G. Silverberg, MD
Department of Pathology
University of Maryland School of Medicine
Baltimore, Maryland

ASSOCIATE EDITOR
Leslie H. Sobin, MD
Armed Forces Institute of Pathology
Washington, DC

EDITORIAL ADVISORY BOARD

EDITORS' NOTE

The Atlas of Tumor Pathology has a long and distinguished history. It was first conceived at a Cancer Research Meeting held in St. Louis in September 1947 as an attempt to standardize the nomenclature of neoplastic diseases. The first series was sponsored by the National Academy of Sciences-National Research Council. The organization of this Sisyphean effort was entrusted to the Subcommittee on Oncology of the Committee on Pathology, and Dr. Arthur Purdy Stout was the first editor-in-chief. Many of the illustrations were provided by the Medical Illustration Service of the Armed Forces Institute of Pathology (AFIP), the type was set by the Government Printing Office, and the final printing was done at the Armed Forces Institute of Pathology (hence the colloquial appellation "AFIP Fascicles"). The American Registry of Pathology (ARP) purchased the Fascicles from the Government Printing Office and sold them virtually at cost. Over a period of 20 years, approximately 15,000 copies each of nearly 40 Fascicles were produced. The worldwide impact of these publications over the years has largely surpassed the original goal. They quickly became among the most influential publications on tumor pathology, primarily because of their overall high quality but also because their low cost made them easily accessible the world over to pathologists and other students of oncology.

Upon completion of the first series, the National Academy of Sciences-National Research Council handed further pursuit of the project over to the newly created Universities Associated for Research and Education in Pathology (UAREP). A second series was started, generously supported by grants from the AFIP, the National Cancer Institute, and the American Cancer Society. Dr. Harlan I. Firminger became the editor-in-chief and was succeeded by Dr. William H. Hartmann. The second series' Fascicles were produced as bound volumes instead of loose leaflets. They featured a more comprehensive coverage of the subjects, to the extent that the Fascicles could no longer be regarded as "atlases" but rather as monographs describing and illustrating in detail the tumors and tumor-like conditions of the various organs and systems.

Once the second series was completed, with a success that matched that of the first, ARP, UAREP, and AFIP decided to embark on a third series. Dr. Juan Rosai was appointed as editor-in-chief, and Dr. Leslie H. Sobin became associate editor. A distinguished Editorial Advisory Board was also convened, and these outstanding pathologists and educators played a major role in the success of this series, the first publication of which appeared in 1991 and the last (number 32) in 2003.

The same organizational framework will apply to the current fourth series, but with UAREP no longer in existence, ARP will play the major role. New features will include a hardbound cover, illustrations almost exclusively in color, and an accompanying electronic version of each Fascicle. There will also be increased emphasis

Permission to use copyrighted illustrations has been granted with kind permission by:

American Journal of Pathology
American Journal of Pathology 1985;119:307. For figure 10.

American Medical Association
Archives of Pathology & Laboratory Medicine 1980;104:47. For figure 1.

American Society of Clinical Oncology
Journal of Clinical Oncology: official journal of the American Society of Clinical Oncology 1984;2:720-1. For figures 1 and 2.

Elsevier
Human Pathology 1977;8:39. For figure 4.
Major Problems in Pathology 1994;29:28-374. For figures 2-19, 3-9C, 5-11B, 9-3, 9-4, 9-5, 9-8, 9-9, 9-11, 10-22, 10-34, 10-37, 12-15A, 13-9, 14-4A, 14-4B, 14-6, 15-1, 15-5, and tables 1-1, 1-3, 14-1.
Pathology of the Adrenal Glands. New York: Churchill Livingston; 1990:1-378. For figures 1-3, 1-9, 1-11, 1-68B, 1-70B, 3-24, 4-57, 4-53B, 7-6B, 7-13, 7-19, 7-27, 7-30, 10-4A, and tables 5-1, 5-2B, 5-3A, 5-3B.

Humana Press
Journal of Urologic Pathology 1994;2:267. For figure 1A.
Endocrine Pathology 1992;3:116-128. For figure 1, table 4, and table 5.

Lippincott Williams & Wilkins
Diagnostic Surgical Pathology, 2nd ed. New York: Raven Press; 1994;600. For figure 2.
Journal of Computer Assisted Tomography 1991;15:773. For figure 2.
American Journal of Surgical Pathology 1979;3:86. For figures 1A and 1B.

Radiological Society of North America
Radiology 1979;132:102. For figure 5A.

McGraw-Hill Companies
Pathology of Infectious Diseases. Stamford, CN: Appleton & Lange; 1977;690-699. For figures 73-20, 73-24, and 73-25A.
Pathology Annual 1992:27:3-23. For figures 1, 2, 14, 14C, and 15.

Oxford University Press, Inc.
Pathology of the Pancreas, Gallbladder, Extrahepatic Biliary Tract, and Ampullary Region. New York: Oxford University Press; 2003:557. For figures 22-77A and 22-76B. (URL www.oup.com)

Springer Science and Business Media
Acta Physiologica Scandinavica 1951;22:14-43. For figure 10.
Anatomy and Embryology 1983;166:447. For figure 1.
Klinische Wochenschrift 1963;41:1025-6. For figure 1.
Zeitschrift für Zellforschung und Mikroskopische Anatomie 1968;87:562-70. For figures 1 and 2.

Wiley-Liss, Inc, a subsidiary of John Wiley & Sons, Inc.
Cancer 1979;43:270. For figure 2.

CONTENTS

1 DEVELOPMENTAL, PHYSIOLOGIC, AND ANATOMIC ASPECTS OF ADRENAL CORTEX AND MEDULLA

The adrenal cortex plays a vital role in the regulation of water and electrolyte balance, mainly by the secretion of mineralocorticoids. It also mediates important changes in the intermediary metabolism of proteins, carbohydrates, and fat. Glucocorticoids modulate a variety of processes including wound healing, growth, and inflammation, and affect the immune system. The adrenal glands are involved in reacting to stress and changes in the environment, which mandate rapid adaptations; this homeostatic role is mediated largely by the adrenal medulla, which secretes catecholamines, mainly epinephrine (1). The physiologic changes are rapid and the effects are short term. The adrenal cortex reacts to stress through the activation of the hypothalamic-pituitary axis, with trophic stimulation of the glands by adrenocorticotropic hormone (ACTH). The physiology and endocrinology of the adrenal cortex and medulla are far too complex to be adequately addressed in this text. It is essential, however, to have a fundamental knowledge of the physiology, structure, and function of the adrenal cortex and medulla in order to investigate endocrinologic and morphologic abnormalities of the adrenal glands.

EMBRYOLOGY AND BIOSYNTHETIC PATHWAYS

Embryologic Development of the Adrenal Cortex

Crowder (2) detailed the early events in the embryonic development of the adrenal cortex and medulla in staged human embryos; the important Carnegie stages of embryogenesis of the adrenal gland are shown in Table 1-1 (3). The Carnegie International Staging System is used worldwide; it correlates roughly with embryonic age, crown rump length, and main external characteristics, and allows for comparisons in growth and development to be made between different investigators.

The adrenal cortical primordia first appear at stage 14, just lateral to the dorsal mesentery near the cephalic end of the mesonephros; at this time there is a change in the characteristics of the cells of the coelomic epithelium, which are of mesodermal origin. The adrenal cortex, therefore, is of mesodermal origin. At stage 15, there is a cellular proliferation continuous with the overlying epithelium in an area designated the adrenal ridge (fig. 1-1). From stages 15 to 18, the adrenal primordia are cigar shaped and extend from vertebral segments T6 to L1, lateral to the aorta and mesogastrium (3). The first group of cells (C1) (fig. 1-2) migrate to the area of the adrenal ridge, enlarge, and become polyhedral cells with eosinophilic cytoplasm. According to Crowder, a new group of cells (C2) appears in the medial wall of the mesonephric glomeruli, and migrates into the adrenal primordium; these appear to give rise to the connective tissue framework and capsule of the developing adrenal gland. A second wave of cells (C3) from coelomic epithelium appears at Carnegie stage 16, and both C1 and C3 cells enter the adrenal primordia.

The developing adrenal gland grows as new cells accumulate in the subcapsular zone, also referred to as the zona glomerulosa. Mitotic

Table 1-1

IMPORTANT CARNEGIE DEVELOPMENTAL STAGES IN EARLY EMBRYOGENESIS OF HUMAN ADRENAL GLANDS[a,b]

Carnegie Stage	Size (mm)	Age (days)
15	7-9	33
16	8-11	37
17	11-14	41
19	16-18	47.5
23	27-31	56.5

[a]Table 1-1 from Fascicle 19, Third Series.
[b]Data from reference 3.

Figure 1-1

PRIMORDIA OF ADRENAL GLANDS

Schematic cross section of a human embryo shows primordia of adrenal glands, which are located lateral to the base of the dorsal mesentery. (Fig. 1-3 from Lack EE, Kozakewich HP. Embryology, developmental anatomy and selected aspects of nonneoplastic pathology. Pathology of the adrenal glands. New York: Churchill Livingstone; 1990:1-74.)

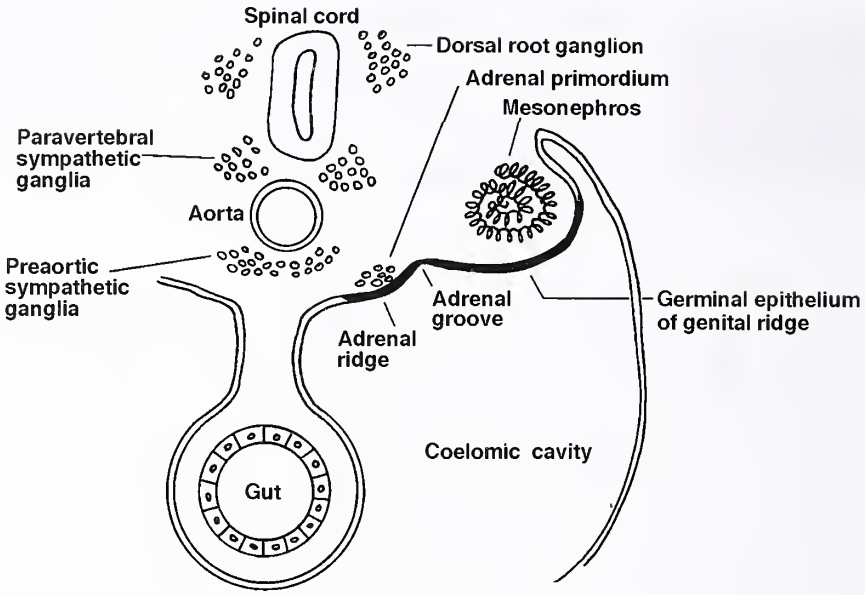

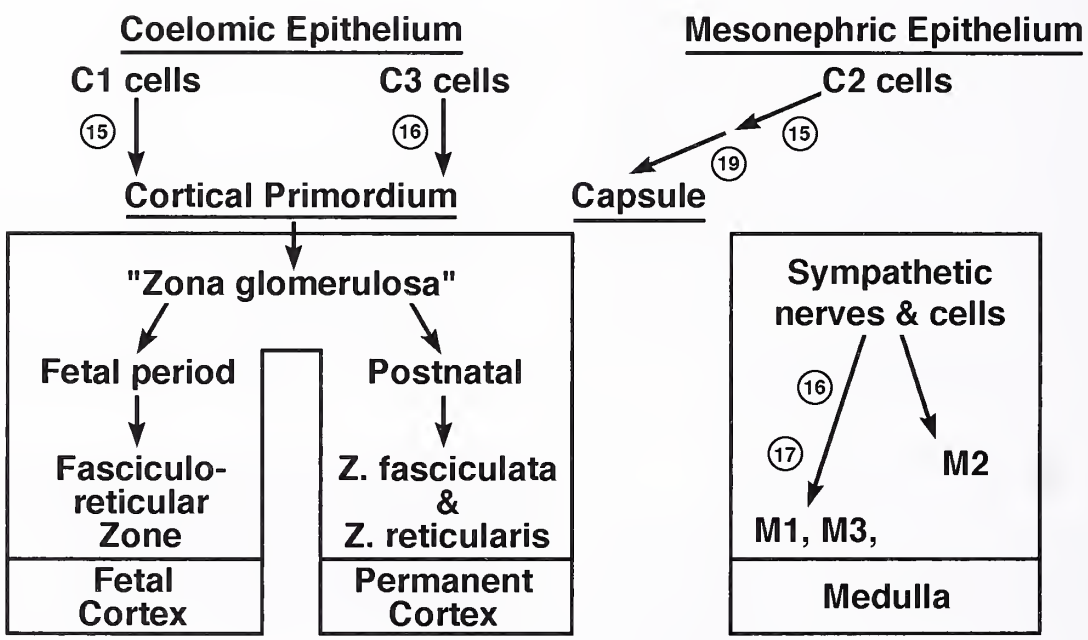

Figure 1-2

CROWDER'S INTERPRETATION OF DEVELOPMENTAL STAGES IN EMBRYOGENESIS OF THE ADRENAL GLANDS

Important stages appear as numerals within circles. C1, C2, C3: cell types in cortex; M1, M2, M3: cell types in medulla. (Modified from fig. 1 from O'Rahilly R. The timing and sequence of events in the development of the human endocrine system during the embryonic period proper. Anat Embryol 1983;166:439-451.)

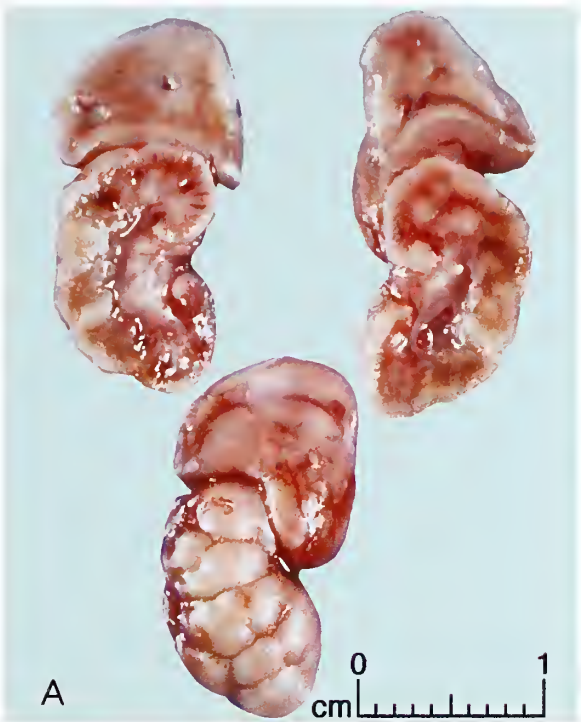

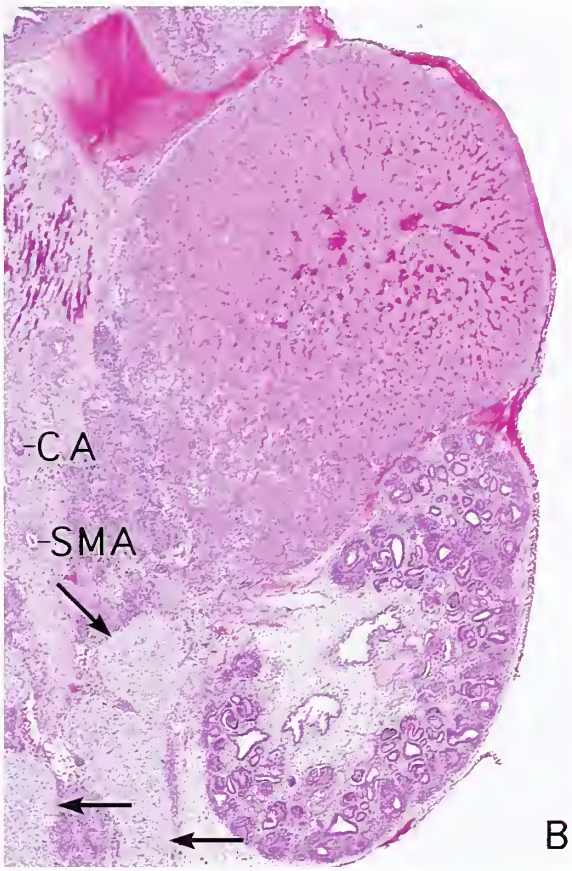

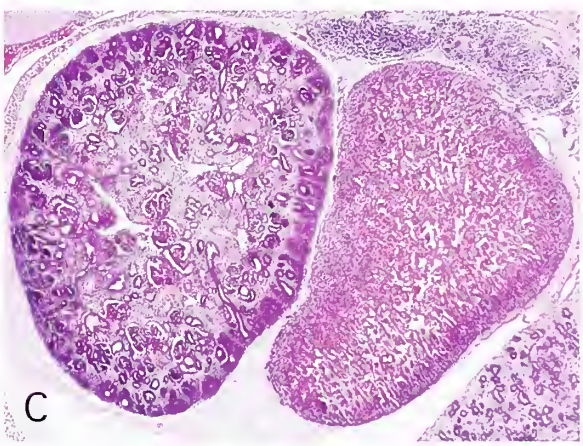

Figure 1-3

CORONAL SECTIONS OF FETAL ADRENAL GLAND AND KIDNEY

A: Coronal sections (left and right) of adrenal glands and kidneys are shown at top; external aspect of one specimen is at bottom. Chromaffin or medullary tissue is not evident macroscopically at this early stage of development. Organs were obtained from a fetus of about 18 weeks' gestational age.

B: Fetus at approximately 11 weeks' gestational age. The developing paraaortic sympathetic plexus has a close relationship with the medial and inferior aspects of the adrenal gland. Small pale-staining clusters of cells separate cords of fetal or provisional cortical cells in the inferomedial aspect of gland. The large collections of extramedullary chromaffin tissue (arrows) represent organs of Zuckerkandl. Celiac (CA) and superior mesenteric (SMA) arteries are also present. (Fig. 1-3 from Fascicle 19, Third Series.)

C: The left fetal adrenal gland lies medial to the upper pole of the kidney. Gestational age is about 10 weeks. Nearly all of the gland is composed of fetal or provisional cortical cells. A developing paravertebral sympathetic plexus is in the right upper corner and an oblique section of developing pancreas is at the bottom right.

figures can be identified in this area. New cells seem to migrate or are forced vis a tergo by replicating cells in a centripetal direction, thus forming the inner part of the gland, which consists of irregular cords of cortical cells and intervening sinusoids. The portion of the developing cortex that becomes most prominent is referred to as the fetal or provisional zone. At about 4 months' gestation, the adrenal gland is slightly larger than the kidney and is composed mostly of fetal cortical cells (fig. 1-3A,B). The orientation of the adrenal gland and kidney is seen in a transverse section of the upper abdomen of a fetus in figure 1-3C.

There are two polar theories explaining cell turnover and the replacement of adrenal cortical cells. The "cell migration" theory of Gottschau (4) proposes that cortical cells in the zona glomerulosa migrate centripetally, suggesting that a cell is sequentially capable of secreting all of the major classes of cortical steroids. The "zonation" theory of Chester Jones (5) suggests that each zone of the adrenal cortex replaces cells independently. A study using cellular kinetics in the experimental animal provided evidence supporting the "cell migration" theory with the displaced adrenocytes producing all three classes of steroids in sequence through their migration (6). In this experimental model, the "streaming" adrenal cortex is replenished by a subcapsular stem cell (capsular "blastema").

Biosynthetic Pathway of Adrenal Corticosteroids

There are three major classes of steroids that are synthesized in the adrenal cortex: mineralocorticoids, glucocorticoids, and sex steroids. Their respective biosynthetic pathways are illustrated in figure 1-4. Mineralocorticoids include several steroids (aldosterone being the most potent) whose major function is the maintenance of intravascular volume through conservation of sodium and the elimination of potassium. Glucocorticoids have wide-ranging effects on carbohydrate, lipid, and protein metabolism and also have regulatory effects on the immune system, growth, and development. The sex steroids include androgens and estrogens. The adrenal glands provide a small amount of biologically important androgens in men (most are of testicular origin); in women, roughly half of all androgen production is of adrenal origin. The precursor of the steroid hormones is cholesterol, which is stored as an esterified form in the lipid droplets of the cortical cells.

Aldosterone is produced by the cells of the zona glomerulosa, while cortisol is synthesized mainly in the zona fasciculata, with a smaller contribution from the zona reticularis. Sex steroids, mainly dehydroepiandrosterone sulfate, are synthesized in the zona reticularis, although the zona fasciculata is also capable of sex steroid production.

The secretion of cortisol is regulated by trophic stimulation by ACTH. Aldosterone secretion is stimulated by altered fluid and electrolyte status or a decrease in volume of extracellular fluid. The renin-angiotensin system is particularly important in physiologic stimulation of the zona glomerulosa, with angiotensin II acting on these cells to cause synthesis and secretion of aldosterone. Other stimulating factors that have a role in the regulation of aldosterone secretion are potassium, atrial natriuretic peptide, and ACTH. Adrenal androgen secretion rises throughout childhood, reaching a peak at puberty ("adrenarche"), and begins to decline at 40 to 50 years of age ("adrenopause"). The mechanism(s) regulating secretion of adrenal androgens is not entirely clear, but ACTH is a potent stimulant.

Embryologic Development of Adrenal Medulla

At Carnegie stages 16 and 17 (Table 1-1), a large paraaortic neural complex forms from paravertebral sympathetic ganglia T6 through T12, and usually including L1. Included in this complex are the primordia of the adrenal medullae, as well as celiac, superior mesenteric, and renal plexuses. The paravertebral sympathetic ganglia increase in size due to cell division and addition of nerve fibers from the rami communicantes. The ganglia contain three types of cells, designated M1, M2, and M3, which can be distinguished on the basis of size and shape (2).

Bundles of nerve fibers and small primitive cells (sympathicoblasts) pass laterally, and enter the dorsal and medial aspect of the adrenal glands. Small collections of cells separate cords of cortical cells (figs. 1-3B, 1-5). This process of separation and disruption of preexisting structures is referred to as "invasion" by Crowder (2), and involves mainly the medial and dorsal aspects of the glands; the ventrolateral part remains relatively intact. Nerve fibers from paravertebral ganglia accompany M1 and M3 cells. M2 cells remain within the ganglia to become sympathetic ganglion cells (fig. 1-2) (2,3). The M3 (or paraganglion) cells are scattered like seeds along the course of the nerve fibers; these immature cells have sometimes been referred to as pheochromoblasts. The nerve fibers entering the gland before the formation of the adrenal capsule maintain their place of entry indefinitely (2). The adrenal gland is richly innervated by the

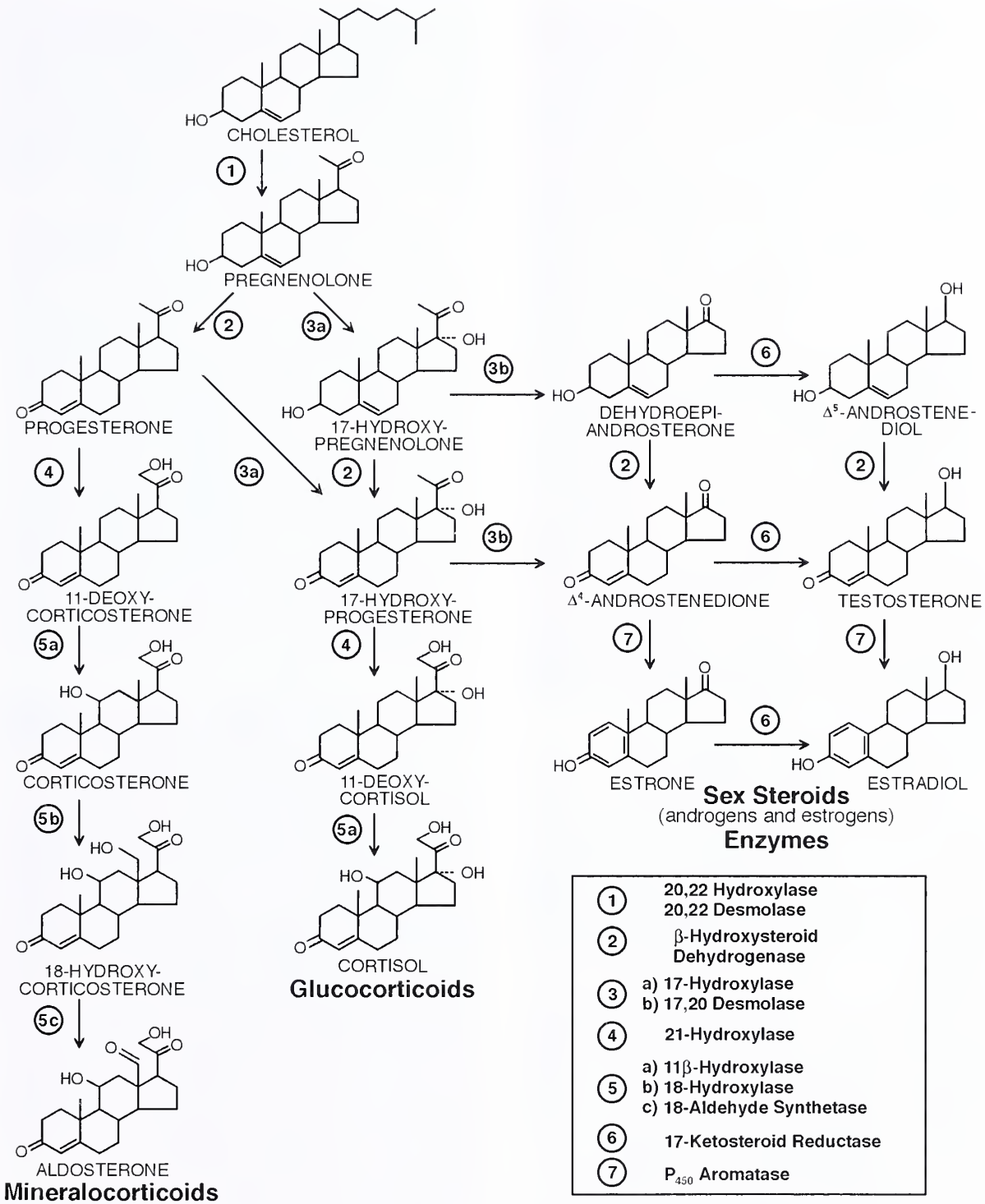

Figure 1-4

ADRENAL CORTICAL STEROIDS

Biosynthetic pathway of the three major classes of adrenal cortical steroids. (Fig. 1-4 from Fascicle 19, Third Series.)

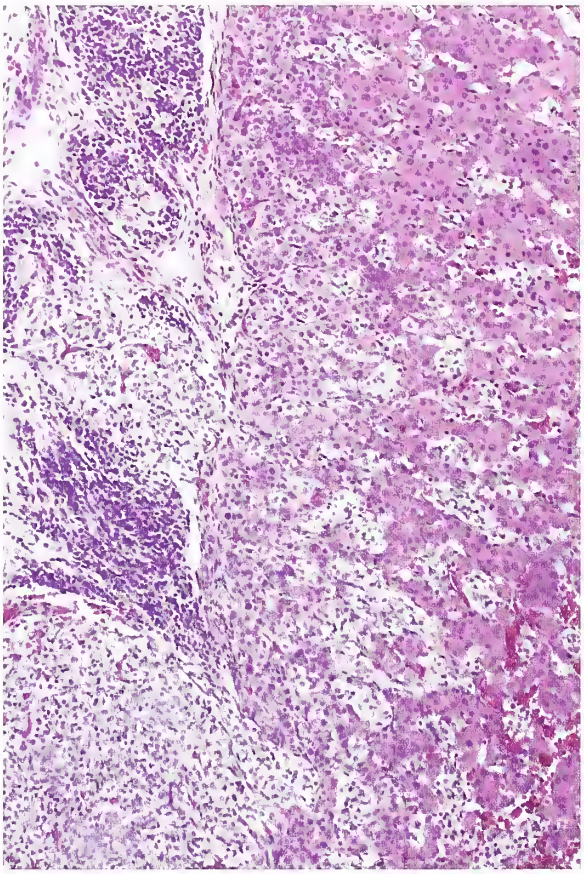

Figure 1-5

MEDIAL ASPECT OF DEVELOPING ADRENAL GLAND IN HUMAN FETUS

There is a close association between the developing sympathetic plexus and small nests of pale-staining cells (mostly future chromaffin cells) that are separating cords of fetal or provisional cortical cells. Primitive cells of the sympathetic plexus (left) contrast with pale-staining cells and those located between cords of cortical cells. Adult or definitive cortex is difficult to recognize in this area of the developing adrenal gland.

autonomic nervous system with largely preganglionic nerve fibers entering the adrenal medulla along the course of emerging or penetrating vessels or connective tissue trabeculae. The vast majority of nerve fibers terminate in the medulla or in the smooth muscle of the adrenal vessels.

At stage 19, there are small nests of immature cells scattered throughout most of the cortex, and at stage 23, paraganglion (M3) cells begin to multiple rapidly. There is some evidence of maturation into chromaffin cells. At embryonic size of 50 mm or more, a positive chromaffin reaction can be observed (2); these cells have also been referred to as medullary cells or pheochromocytes. Compared to the primitive sympathicoblasts, developing chromaffin cells have slightly enlarged nuclei with dispersed chromatin and pale-staining cytoplasm. With postnatal regression of the fetal cortex there is some loss of support for neural elements, which migrate to the area of the central vein.

Clusters of primitive sympathicoblasts (neuroblastic nodules) are an integral histologic component in the normal development of the adrenal glands (fig. 1-6), and may linger until birth or early infancy (7). Early neuroblastic nodules may be superficial and located near the adrenal capsule (fig. 1-6B), but in the older fetus are located more toward the central aspect of the gland due to inward migration, attrition, or relatively greater growth of the cortex. The presence of small neuroblastic nodules adjacent to or outside the capsule of the adrenal gland provides an explanation for the occurrence of chromaffin cells in the outer cortex or outside the adrenal gland.

There is an increase in the number and size of neuroblastic nodules with age, peaking at 17 to 20 weeks' gestational age, and there is a tendency to regress in older fetuses. Maturation into chromaffin cells may be seen in early neuroblastic nodules. This is apparent as cells with an increased amount of lightly amphophilic cytoplasm (fig. 1-6C). Some nodules may be cystic, but usually not until the 16th week of gestation (fig. 1-7). In all age groups combined, neuroblastic nodules range from 60 x 60 µm to a maximum size of 200 x 400 µm (7).

The neuroblastic nodules become significant in the differential diagnosis of in situ neuroblastoma. During embryogenesis, individual cells of neuroblastic nodules may: 1) mature into chromaffin or ganglion cells; 2) undergo spontaneous regression or programmed cell death (apoptosis); 3) become the nidus for in situ or clinically overt neuroblastoma (or a related tumor); and/or 4) contribute to the genesis of sustentacular cells (related to chromaffin cells) or satellite cells (related to ganglion cells).

Biosynthesis of Catecholamines

The biosynthetic pathway for catecholamines is shown in figure 1-8. The adrenal gland is the body's primary source of epinephrine production

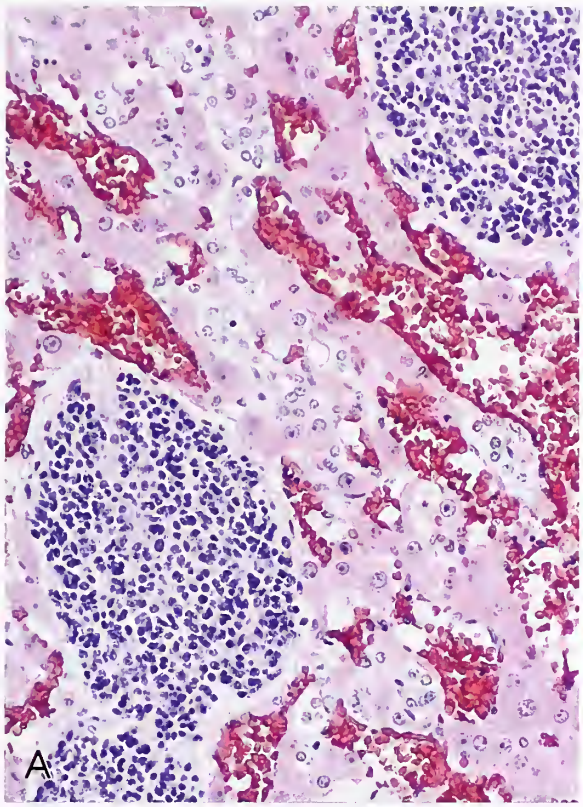

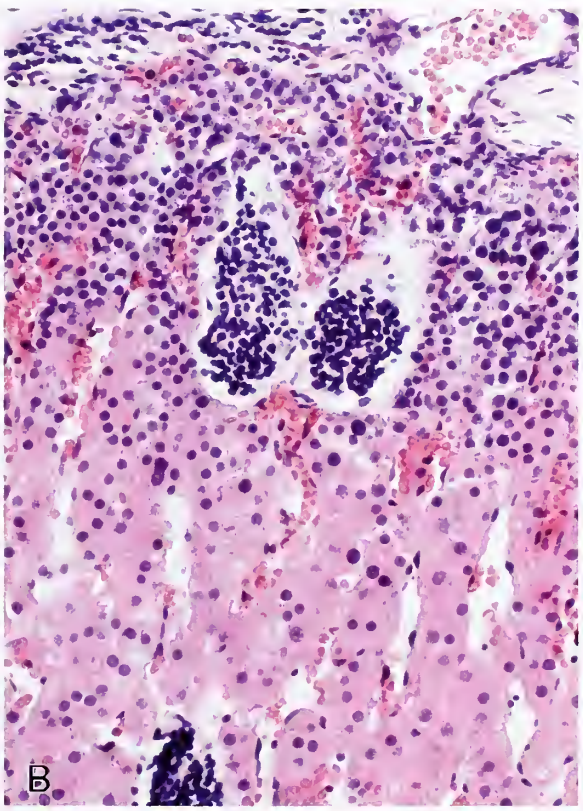

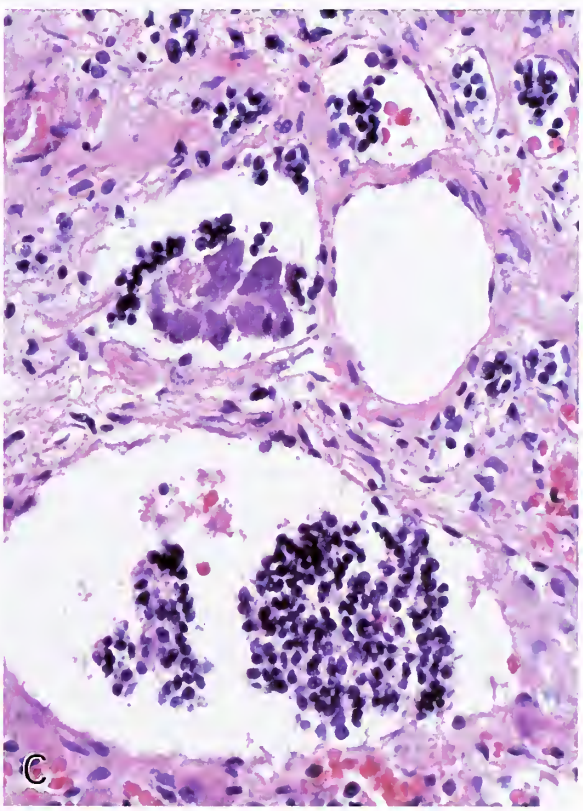

Figure 1-6

DEVELOPING FETAL ADRENAL GLAND

A: Small nodules of primitive neuroblastic cells are present within the inner aspect of the fetal or provisional cortex. A small amount of pale fibrillary matrix is evident in some neuroblastic nodules. Some cells with pale-staining cytoplasm and slightly larger nuclei show early chromaffin cell differentiation. (Fig. 1-6, left from Fascicle 19, Third Series.)

B: In a different fetus, nodules of primitive neuroblastic cells separate cords and columns of fetal or provisional cortical cells. Some are present near the adrenal capsule (top).

C: Neuroblastic nodules are set within cystic spaces. Early developed chromaffin cells are present near the center of the field.

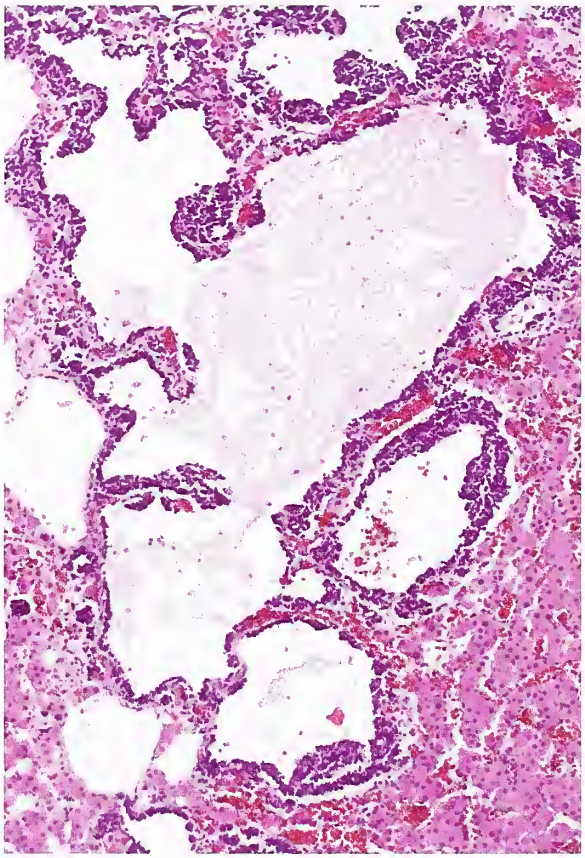

Figure 1-7

FETAL ADRENAL GLAND AT 16 WEEKS' GESTATION

Neuroblastic nodules show prominent cystic change, with pale, stringy, proteinaceous contents.

and release (8). Epinephrine production involves the conversion of the substrate for the cytosolic enzyme L-aromatic amino acid decarboxylase, 3,4 dihydroxyphenylalanine (DOPA), into dopamine. This substance is transported into the storage vesicle where the membrane-bound enzyme dopamine beta-hydroxylase forms norepinephrine. The terminal enzyme in catecholamine synthesis is phenylethanolamine N-methyltransferase (PNMT) (9), which is present in the cytosol. This enzyme methylates norepinephrine to form epinephrine, which is then taken up again into the vesicle for storage. Corticosteroids apparently work in conjunction with other transcriptional regulators to control the *PNMT* gene by increasing PNMT transcriptional activity and ensuring appropriate processing of PNMT messenger RNA (8). The chromaffin cell is, in essence, a postganglionic sympathetic neuron.

Following depolarization with the influx of calcium, the secretory vesicles move toward the plasma membrane, and through a process of exocytosis, the granule contents are expelled into the extracellular space (10). The clearance of catecholamines within the blood is rapid, and epinephrine and norepinephrine have a half life of only 1 to 2 minutes. The ratio of epinephrine to norepinephrine in the normal adrenal medulla in adults is about 4 to 1 (11).

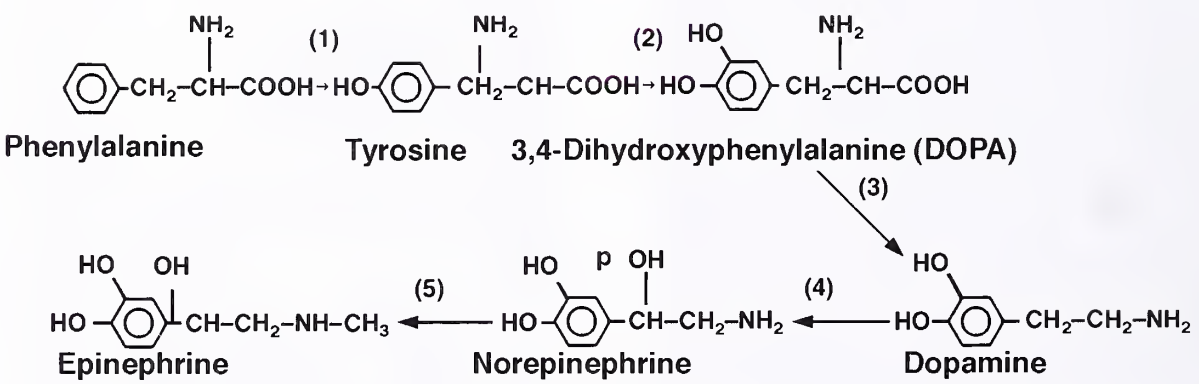

(1) phenylalanine hydroxylase, (2) tyrosine hydroxylase, (3) L-aromatic amino acid decarboxylase, (4) dopamine β-hydroxylase, (5) phenylethanolamine N-methyltransferase.

Figure 1-8

BIOSYNTHETIC PATHWAY OF CATECHOLAMINES AND VARIOUS INVOLVED ENZYMES

(Fig. 1-8 from Fascicle 19, Third Series.)

FUNCTION OF FETAL ADRENAL GLANDS

The adrenal glands are essentially two endocrine glands in one, with the medulla in humans completely enveloped by the cortex, thus ensuring a microenvironment rich in corticosteroids. The fetal adrenal gland exhibits functional zonation of fetal versus adult cortex. The corticosteroid produced in the largest quantity by the cells of the fetal zone is dehydroepiandrosterone sulfate (DHAS), while cells of the adult or definitive cortex produce mainly cortisol.

Glucocorticoids have an important role in the initiation of parturition in some animals, but such a function has not been established in humans. Cortisol may play an important role in the induction and maturation of different enzyme systems involved in lung maturation, deposition of glycogen in the liver, and induction of several enzymes in fetal brain, retina, pancreas, and gastrointestinal tract (12). Corticosteroids also facilitate the synthesis of epinephrine by the stimulation or induction of PNMT (8).

DHAS is metabolized in the fetal liver to 16-hydroxy DHAS, and both of these steroids can be hydrolyzed in the placenta, with subsequent aromatization to form estrone, estradiol, and estriol. Estriol is the major estrogen in the pregnant female. This underscores the interdependence of the fetus, placenta, and mother in the formation of estrogens. It has been shown that chronic stimulation of fetal cortical cells by ACTH in vitro can give rise to a functional phenotype similar to the cells of the adult cortex, with increased production of cortisol (13).

Most of the chromaffin tissue in fetal life resides in extraadrenal sites, particularly the organs of Zuckerkandl where norepinephrine is the predominant catecholamine. It is generally assumed that a high proportion of norepinephrine in the fetal adrenal medulla is indicative of functional immaturity. There is some suggestion that fetal chromaffin tissue may be involved in the homeostatic maintenance of vascular tone and blood pressure in utero. By 10 to 15 weeks' gestation, epinephrine (soon to be the major catecholamine in the medulla) and norepinephrine are detectable in medullary chromaffin cells.

ANATOMY OF ADRENAL GLANDS

Adrenal Weight

The individual or combined weight of the adrenal glands depends upon a number of factors including age, abnormalities in development, presence and chronicity of diseases of various types, and most important, the effort taken to carefully remove adherent connective tissue and fat for accurate specimen weight. Data regarding adrenal weights in infancy and childhood are based per force upon postmortem studies (1). Figure 1-9 shows the average combined weights of meticulously dissected adrenal glands from 226 individuals ranging from 30 weeks' gestational age to 35 years (1). The adrenal glands grow considerably toward the end of pregnancy but decrease postnatally. Tähkä (14) studied the average combined weight of adrenal glands from infants at various postnatal periods: 6.50 g at 0 to 7 days, 6.11 g at 8 to 14 days, and 4.52 g at 15 to 30 days. In another study involving adrenal glands from 84 children, the average combined weight at birth was 10 g (range, 2 to 17 g), by 7 days had decreased to 6 g (range, 3 to 12 g), and at 2 weeks was 5 g (range, 2 to 8 g) (15). The rather marked decrease in adrenal weight in the first few weeks of life (fig. 1-9) is attributed almost entirely to regression of the fetal cortex.

In a study of adrenal glands obtained surgically from adult females undergoing staged bilateral adrenalectomy for advanced breast cancer, the average weight of individual glands was 4.0 g (1 SD = 0.8 g); adrenal glands obtained at autopsy were heavier (average, 6.0 g), probably due to trophic stimulation by ACTH (16). Adrenal glands from patients given a crude extract of ACTH prior to surgery underwent a nearly two-fold enlargement (average weight, 8.1 g), and showed conversion of the pale, lipid-rich cells of the zona fasciculata to cells with compact, eosinophilic cytoplasm (16).

In children and adults there are no significant differences in adrenal weights with regard to sex or laterality. Since 98 percent of apparently normal glands removed surgically weigh less than 6 g, adrenal glands heavier than this may be abnormal (16), but this assessment must be based upon weights of meticulously dissected glands and correlation with clinical and

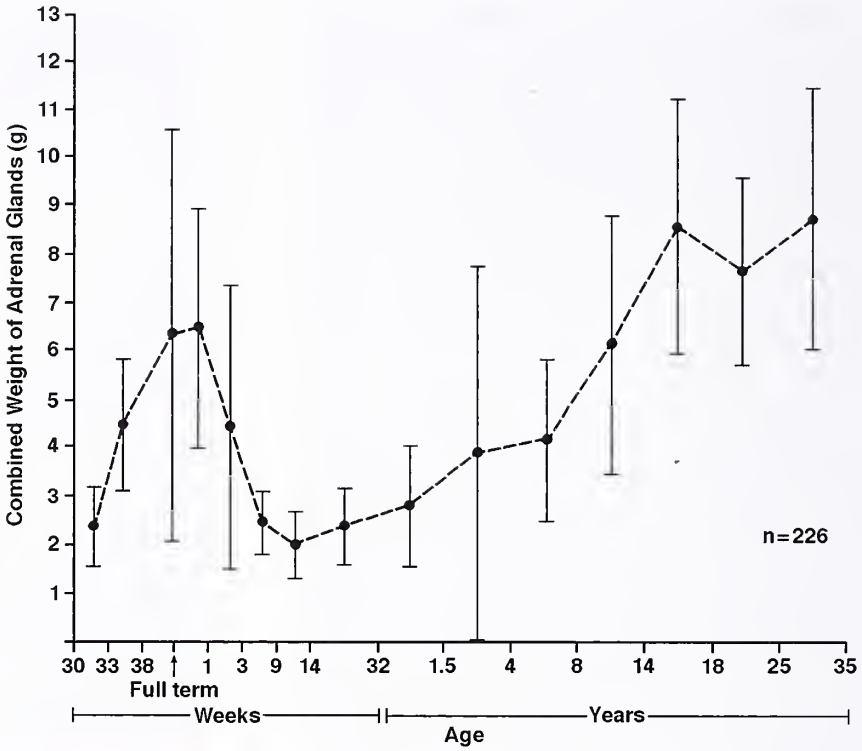

Figure 1-9

AVERAGE COMBINED WEIGHT OF ADRENAL GLANDS FROM 226 PATIENTS AT AUTOPSY

The patients ranged from 30 weeks' gestational age to 35 years in age. Vertical bars represent one standard deviation. There is a marked decrease in combined weight during the first few weeks of life. (Fig. 1-11 from Lack EE, Kozakewich HP. Embryology, developmental anatomy and selected aspects of non-neoplastic pathology. Pathology of the adrenal glands. New York: Churchill Livingstone; 1990:1-74.)

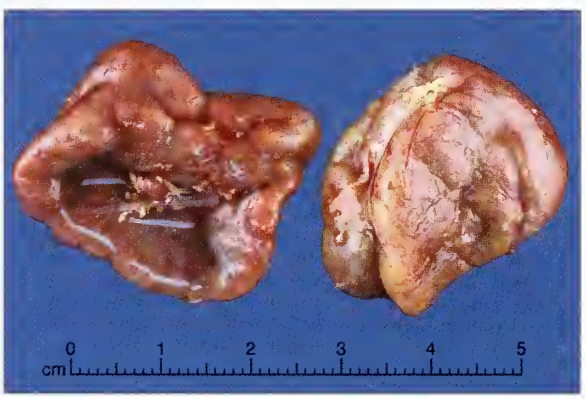

Figure 1-10

DORSAL ASPECT OF FETAL ADRENAL GLANDS

The dorsal surface of both adrenal glands from a 35-week premature infant shows a ridge (or crista) and a relatively smooth cortical surface. Each gland weighed 3 g.

endocrinologic data. Gross dissection and weighing of the adrenal medulla has shown that this component accounts for about 10 percent of the weight of the entire gland (0.431 g left, 0.448 g right) (17). In a recent study of a large Chinese population (n=333), patients with hypertension or lung cancer had significantly heavier adrenal glands; for those with lung cancer, ectopic ACTH production resulting in adrenal cortical hyperplasia was considered to be a possible factor in the increased weight of the glands (18).

Gross Anatomy

In newborns, the adrenal glands have a relatively smooth capsular surface (fig. 1-10). The gland may appear dark reddish brown on transverse section due to a combination of regression of fetal cortex, congestion, and increased density of vascular sinusoids (fig. 1-11). On gross inspection, this appearance may give the erroneous impression of adrenal hemorrhage or apoplexy; in addition, the glands may be quite soft. Medullary tissue is not grossly identifiable in the newborn gland under normal circumstances since it constitutes less than 1 percent of the total gland volume. Adrenal size and configuration can be altered with some congenital abnormalities such as a more rounded adrenal contour with ipsilateral renal agenesis and an extremely small gland in cases of congenital adrenal hypoplasia.

Figure 1-11

TRANSVERSE SECTIONS OF ADRENAL GLAND FROM A 35-WEEK PREMATURE INFANT

Much of the fetal or provisional cortex has a dark appearance. This may be a normal feature and should not be confused with adrenal hemorrhage.

In adults, the right adrenal gland is roughly pyramidal in shape while the left is elongated or crescentic (fig. 1-12, top). The anterior (or ventral) surface of the adrenal gland in situ is relatively smooth or flattened and there may be a shallow groove, usually on the left side, which contains a segment of the adrenal vein (fig. 1-12, bottom). The adrenal vein is much longer on the left side and normally drains into the renal vein; the right adrenal vein is short and empties directly into the inferior vena cava (fig. 1-13, top). The arterial supply to the adrenal gland is three-fold, with origin from the inferior phrenic artery, the aorta, and the renal artery (fig. 1-13, bottom). The posterior or dorsal surface of the gland is convex with a ridge (or crista) which is often more prominent in the tail of the gland on the superior and lateral aspect (fig. 1-14). The crista is flanked by flattened projections or alae (wings); these medial and lateral limbs are evident with computerized tomography (CT) or magnetic resonance imaging (MRI) (fig. 1-13, top).

Figure 1-12

DORSAL AND VENTRAL SURFACES OF ADULT ADRENAL GLAND

Top: In the adult, the dorsal surface of the right adrenal gland (right side) is pyramidal in shape, while the opposite gland is more elongated. A few cortical extrusions are present. (Fig. 1-12 from Fascicle 19, Third Series.)

Bottom: Central adrenal vein exits as a single vein from the relatively flat ventral surface of the adrenal gland near the junction of the head and body. The adrenal vein is most evident in the elongated left gland (right side of figure) and is associated with a well-developed groove. The pyramidal-shaped gland on right (left side of figure) has a shorter vein.

When sectioned in the transverse plane perpendicular to the long axis, the gland can arbitrarily be divided into three regions: the head (inferomedial one third), the body (middle one third), and the tail (superolateral one third). Chromaffin tissue is concentrated in the head and body of the gland, often with some extension into one or the other ala (figs. 1-14, 1-15).

The medulla has an ellipsoid shape near the extremity of the head and an omega or sickle shape near the body. It appears as a gray-white zone concentrated in the head and body of the gland (fig. 1-15). Using planimetry or other quantitative techniques, the ratio of the area

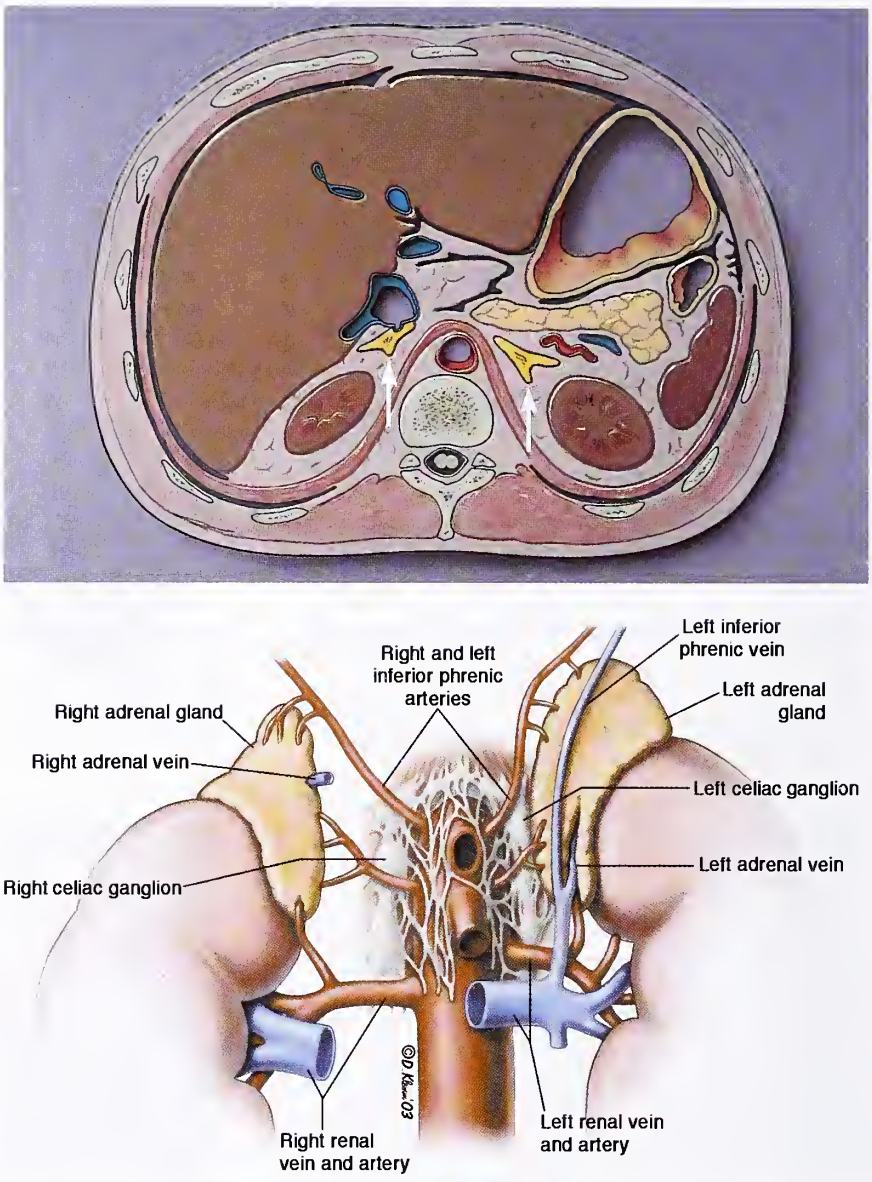

Figure 1-13

CONFIGURATION OF ADRENAL GLANDS IN SITU IN TRANSVERSE AND CORONAL PLANES THROUGH ABDOMEN

Top: The adrenal ridge (or crista) is located on the dorsal aspect (arrows) and is flanked by medial and lateral wings (or alae). The right adrenal gland has a relatively short adrenal vein which drains directly into the inferior vena cava. (Fig. 1-13 from Fascicle 19, Third Series.)

Bottom: In the coronal plane, the adrenal glands have a relatively flat ventral or anterior surface. Arterial supply is from the inferior phrenic artery, the aorta, and the renal artery. The left adrenal vein drains into the renal vein while the right adrenal vein is much shorter and drains into the inferior vena cava.

occupied by cortex to that of medulla is about 10 to 1, but in making this assessment it is necessary to exclude areas occupied by structures such as blood vessels and collections of cortical cells associated with vascular structures. Atrophy of the adrenal cortex makes the medulla appear relatively prominent (fig. 1-16), while the reverse occurs with cortical nodularity or hyperplasia. In some areas there may be no intervening medulla, and where cortex abuts upon cortex there is a raphé (cristal or interalar).

In children and adults the normal adrenal cortex has a radiant, yellow-gold hue due to the accumulation of lipid within the cortical cells (fig. 1-15), but this may not be uniform throughout. The thin zona reticularis is darker, and may contrast sharply with the gray-white medulla. Frequently, a partial or complete cuff of lipidized cortical cells is present about the intraglandular portion of the central vein or its tributaries. It is very common to see small (usually 1 to 2 mm), rounded extrusions of cortex (fig. 1-15, left) that may appear partially or entirely encapsulated, with or without connection to underlying cortex, or lying free in periadrenal connective tissue where they are regarded as accessory cortical tissue.

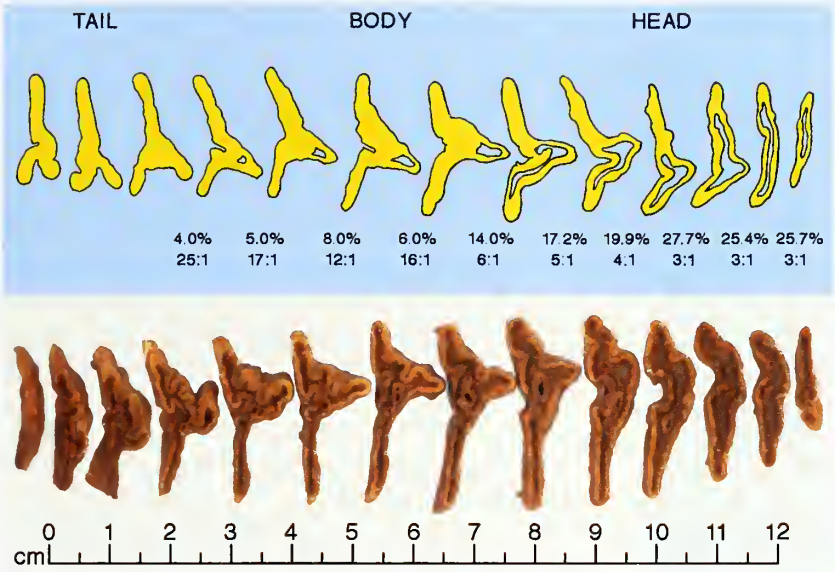

Figure 1-14

SERIAL TRANSVERSE SECTIONS OF ADULT ADRENAL GLAND

Top: Three regions of the gland are seen including the head (medial and inferior in situ), body, and tail (superior and lateral in situ). Most of the chromaffin tissue is concentrated in the body and head of the gland; none is present in the tail. The percentage of cross-sectional area occupied by medulla is indicated at the top along with the ratio of area occupied by cortex versus medulla (overall ratio about 10 to 1).

Bottom: In another adrenal gland, the medullary compartment is gray-white and is most prominent in body and head of the gland.

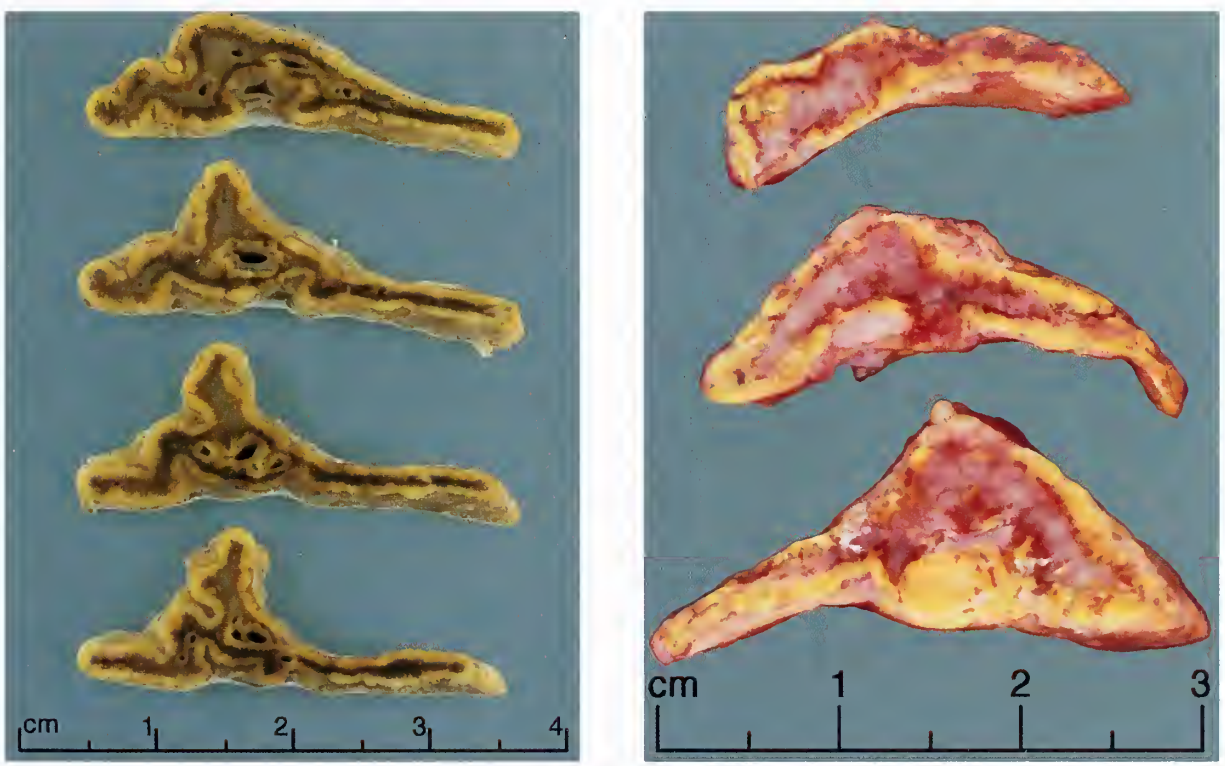

Figure 1-15

TRANSVERSE SECTIONS THROUGH BODY AND HEAD OF NORMAL ADRENAL GLAND

Left: The medullary compartment appears dull gray in contrast to the bright yellow cortex. Partial to complete cuffs of cortex are present around tributaries of the central adrenal vein. Note also the brown zona reticularis at the inner cortex. There is a small cortical extrusion on the left side of the top section. The adrenal gland was obtained at autopsy. (Fig. 1-15 from Fascicle 19, Third Series.)

Right: In this gland, the adrenal cortex is bright yellow with focal nodularity. Medullary tissue is gray-white and extends into both wings (alae) of the gland. The adrenal gland was obtained during radical nephrectomy.

Figure 1-16

ADULT ADRENAL GLAND AFTER CORTICOSTEROID TREATMENT

Transverse sections of adrenal glands at autopsy from an adult patient who had received suppressive doses of corticosteroids. The cortex is atrophic while the medullary compartment appears relatively prominent. Accurate morphometric evaluation for adrenal medullary hyperplasia (e.g., relative surface area of cortex versus medulla) may be affected by alterations in cortex such as atrophy or nodularity/hyperplasia. (Fig. 1-16 from Fascicle 19, Third Series.)

Microscopic Anatomy of Fetal and Newborn Adrenal Cortex

The adrenal cortex of the fetus and newborn has a biphasic structure that consists of a thin subcapsular adult or definitive zone and a wide inner zone composed of fetal, or provisional, cortical cells (fig. 1-17). At birth, the adult, or definitive, cortex is 0.1- to 0.2-mm thick, and by 9 days it is about 0.5-mm thick. The adult cortex is 0.8- to 1.0-mm thick by the end of the 12th year (15). It is only in the 2nd to 4th weeks of life that some differentiation of zona glomerulosa and zona fasciculata can be seen (15).

Cells of the adult cortex are relatively small, with dark-staining nuclei and scant cytoplasm, whereas the fetal cortical cells have larger, more vesicular nuclei, often with a small nucleolus and more voluminous, compact cytoplasm which is granular and eosinophilic. About 70 to 85 percent of the cortex in the normal newborn adrenal gland is composed of fetal, or provisional, cells; it is this prominent zone (much thicker than the adult cortex) that undergoes marked regression in the first few weeks of life. Various features of regression of the fetal cortex include foci of coagulative necrosis (occasionally with dystrophic calcification), cytolysis with nuclear pyknosis, evidence of recent and old hemorrhage and accentuation of vascular sinusoids. Prominent vascular sinusoids can simulate a hemangioma or lymphangioma. In anencephaly, the fetal cortex is markedly thin, although it is often normal in size and structure until approximately 20 weeks' gestation (1); by birth, the fetal cortex has undergone marked regression leaving the adult cortex relatively prominent. The adrenal glands in anencephalic newborns are quite small, with an average combined weight of 1.8 g, although a significant number weigh less than 1.0 g combined (1).

Microcysts have been reported in the adult, or definitive, cortex of premature stillborns and newborn infants (fig. 1-18), and have been attributed to a degenerative change associated with in utero stress (19), although some believe this may be a manifestation of the normal developmental process. Microcysts have been correlated with a shorter gestational period and shorter survival time following birth (20).

Vacuolar change of cells in the outer fetal cortex has been noted in infants with erythroblastosis fetalis, and nearly identical changes have been observed in those with thalassemia major (1). A connection with intrauterine stress and hypoxia has been proposed. Extramedullary hematopoiesis in the fetal adrenal gland has been observed by the author on rare occasion as an isolated finding.

Microscopic Anatomy of Adult Adrenal Cortex

Adrenal Cortex. The normal adrenal cortex in adults is almost 2-mm thick, but there may be variation from gland to gland, or thicker cortex in different areas of the same gland (fig. 1-19).

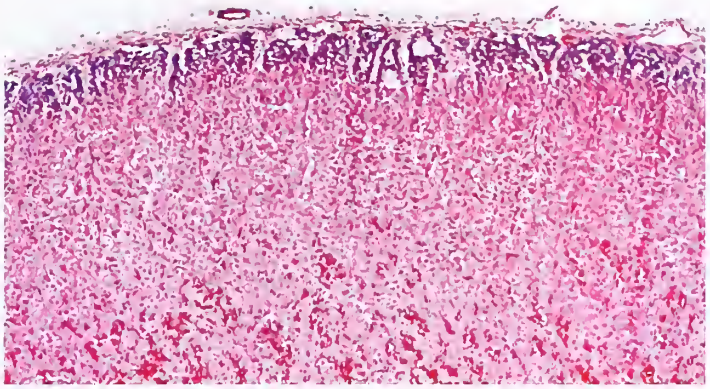

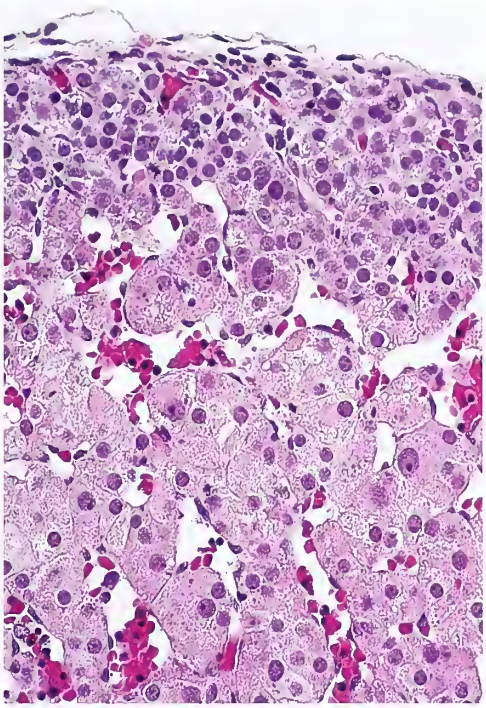

Figure 1-17

ADRENAL GLAND FROM A FETUS

Above: Most of this fetal adrenal gland is composed of fetal, or provisional, cortical cells having relatively abundant eosinophilic cytoplasm. A thin band of darker adult, or definitive, cortex is beneath the adrenal capsule (top).

Right: Adult, or definitive, cortex forms a thin rim of subcapsular cells, which have a high nuclear to cytoplasmic ratio. Most of the cortex is composed of fetal, or provisional, cortical cells. (Fig. 1-17 from Fascicle 19, Third Series.)

This variation is particularly evident in elderly individuals and those with hypertension or diabetes mellitus due to an increased incidence of cortical nodularity.

Distinct zonation can be found in the normal gland (fig. 1-20, left). The zona glomerulosa is a thin, usually discontinuous layer beneath the capsule with a ball-like arrangement of cells; it comprises about 5 to 10 percent of the cortex in some areas of the gland (fig. 1-20, right). Cells of the zona glomerulosa have less abundant cytoplasm compared with cells of the zona fasciculata. The zona fasciculata comprises about 70 percent of the thickness of the cortex and consists of radial columns or cords of cells which have ample, lipid-rich cytoplasm (fig. 1-20, left). Close scrutiny of these cells reveals a lattice-like partitioning or fine vacuolization of cell cytoplasm, which is pale-staining due to lipid accumulation (fig. 1-20). Where chromaffin cells are absent (e.g., tail of the gland), the opposing layers of adrenal cortex are demarcated by the interalar raphé; the raphé may appear as a wider pigmented zone because of the juxtaposition of zona reticularis on either side. There may be small clear spaces due to confluent lipid vacuoles, which in some instances are recognizable as lipomatous foci (fig. 1-21). On occasion,

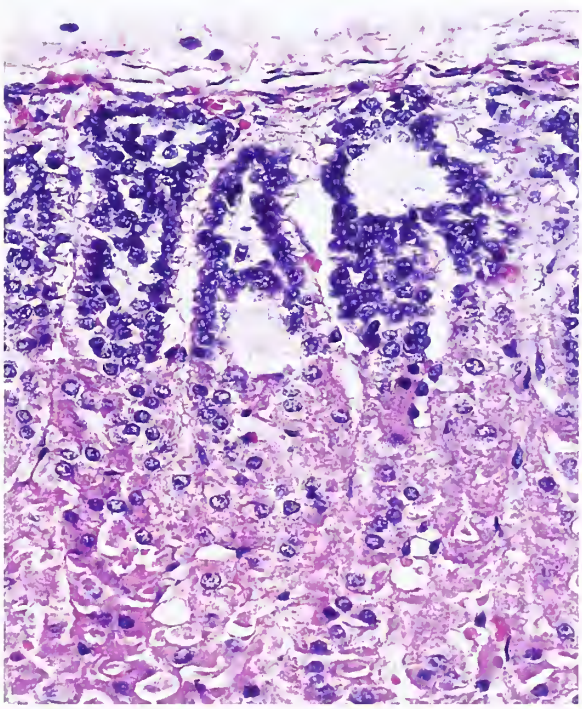

Figure 1-18

ADRENAL GLAND FROM A PREMATURE STILLBORN

Microcystic change is present in the adult, or definitive, cortex. (Fig. 1-18 from Fascicle 19, Third Series.)

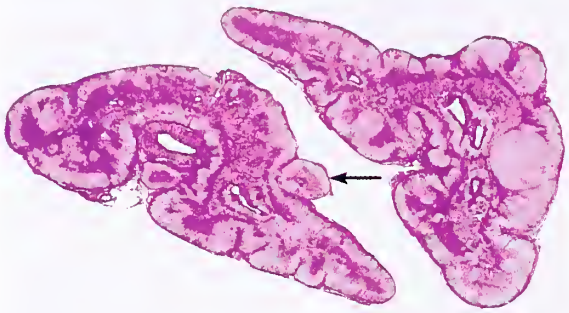

Figure 1-19

EUCORTICAL ADRENAL GLAND

Transverse sections through the body of an adrenal gland from an adult woman who underwent bilateral adrenalectomy for palliation of metastatic breast carcinoma. The patient was eucortical. There is irregular cortical nodularity. The darker zone next to the medulla is the zona reticularis. Tributaries of the central adrenal vein are surrounded by cuffs of cortical cells. Cortical extrusion is indicated by the arrow.

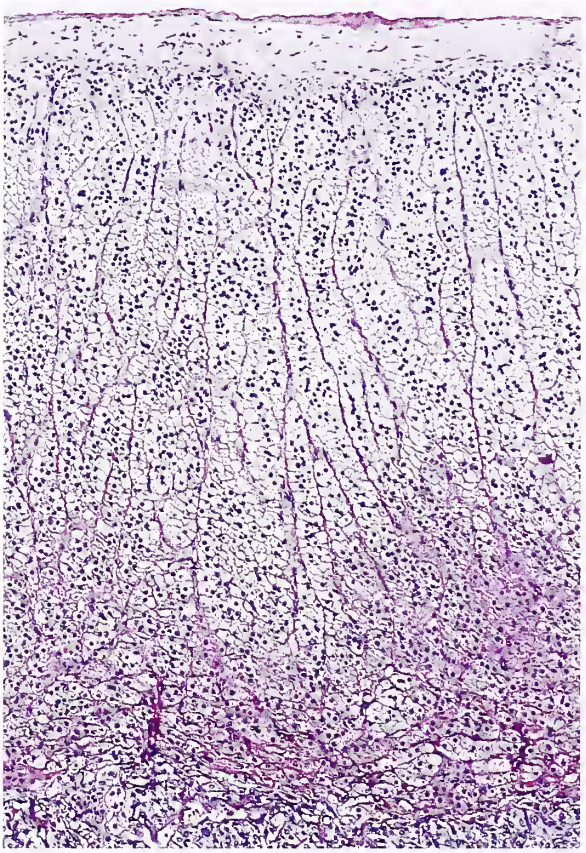

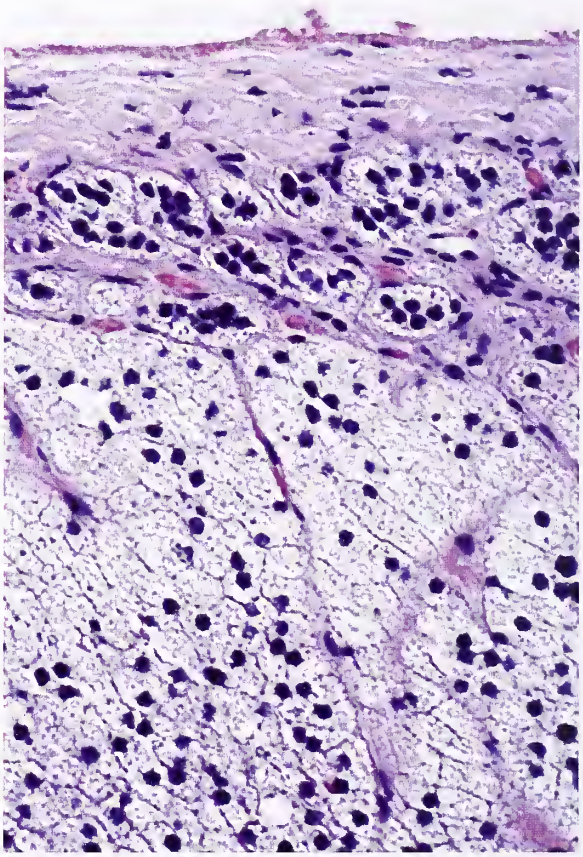

Figure 1-20

NORMAL ADRENAL GLAND

Left: Radial cords of lipid-rich cells of the zona fasciculata and an indistinct discontinuous zona glomerulosa are seen. (Fig. 1-20, left from Fascicle 19, Third Series.)

Right: The zona glomerulosa beneath the adrenal capsule has a ball-like arrangement of cells, with less abundant lipid-rich cytoplasm compared with cells of the zona fasciculata.

lipomatous foci may be accompanied by lymphocytes. This may represent a metaplastic process and does not appear to correlate with generalized adiposity. In a recent study, fat-cell metaplasia was observed in 5 percent of adrenal glands from adults, an incidence that increased with age with equal sex distribution (21). The incidence of fat-cell metaplasia or bone marrow

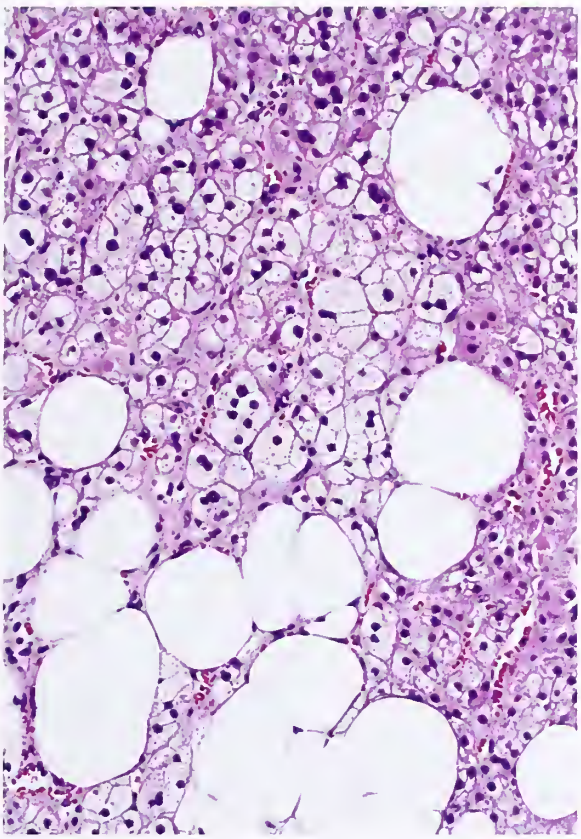

Figure 1-21

LIPOMATOUS CHANGE IN CORTEX

Normal adrenal gland from an adult shows a few areas of lipomatous change.

metaplasia correlated with arterial hypertension and severe coronary heart disease.

The inner zona fasciculata often merges imperceptibly with the zona reticularis; the latter is usually composed of cells with compact eosinophilic cytoplasm, and there may be prominent lipochrome pigment within the cytoplasm (fig. 1-22, top). The radial cord-like and reticular arrangement of cells can be accentuated by staining for reticulum (fig. 1-22, bottom). The corticomedullary interface is often smooth or delicately sinuous or undulating, but can be irregular, with the intermingling of cortical cells and chromaffin cells (fig. 1-23); this intermingling of cells can be vividly demonstrated by immunostains for neuroendocrine markers such as synaptophysin.

Adrenal Capsule. The adrenal capsule is composed of hypocellular fibrous tissue with coarse

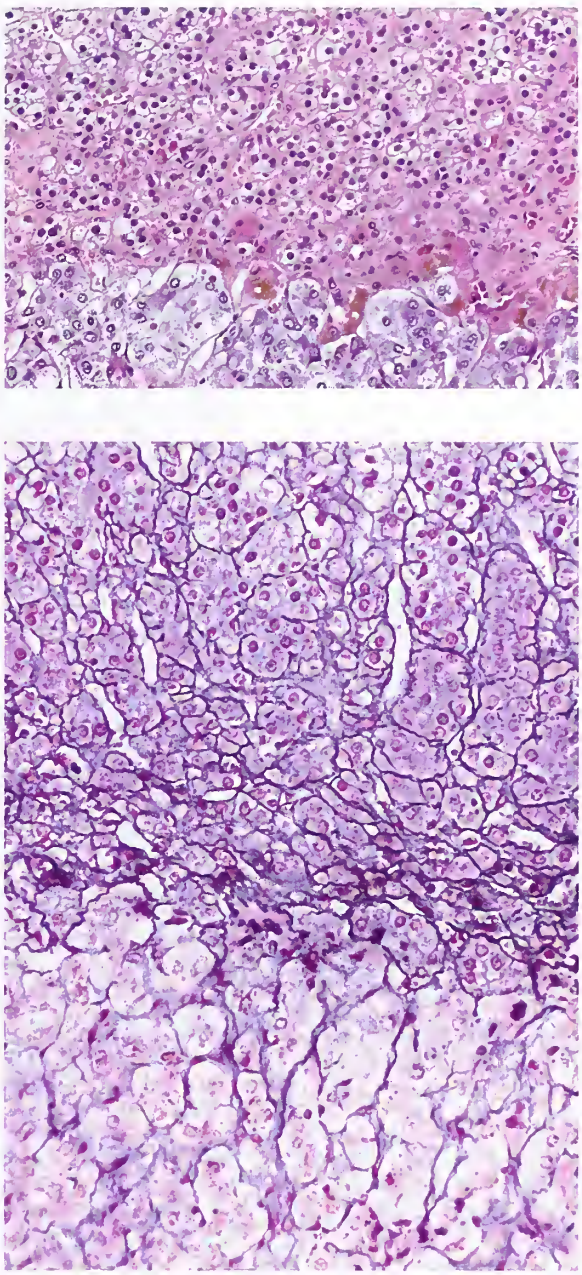

Figure 1-22

NORMAL ADRENAL GLAND

Top: Inner zona fasciculata merges with the zona reticularis. The cells of the latter have compact, eosinophilic cytoplasm and many contain brown granular pigment representing lipofuscin. The corticomedullary junction is sharply demarcated.

Bottom: Radial cords of the zona fasciculata contrast with a smaller nesting pattern of zona reticularis. The nesting pattern gives an apparent density to the reticulum. The lower portion of the field shows the organoid nesting pattern of the chromaffin cells of the adrenal medulla (reticulum stain).

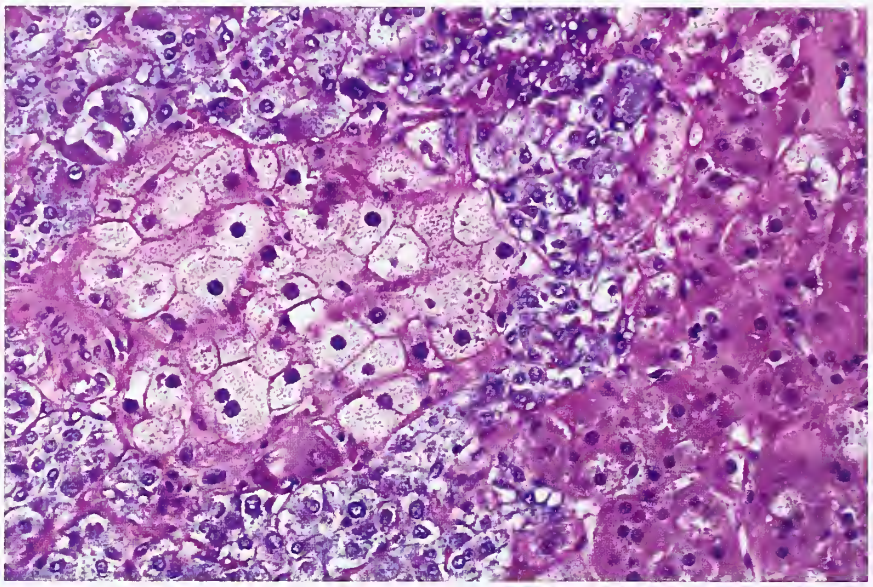

Figure 1-23

NORMAL ADRENAL GLAND

Partially lipid-depleted cortical cells intermingle with chromaffin cells. The zona reticularis is present on the right side of the field.

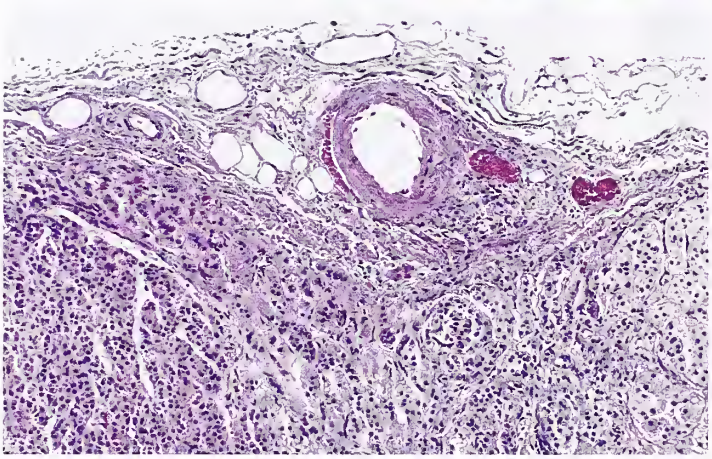

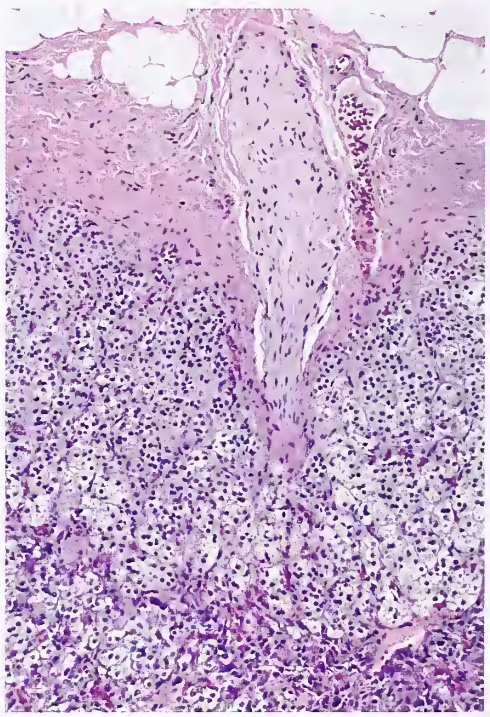

Figure 1-24

NORMAL ADRENAL GLAND

Above: The adrenal capsule may vary in thickness. Here the capsule appears very attenuated. A small capsular arteriole is on the surface of the gland.

Right: The adrenal capsule here is of normal thickness and is penetrated by a myelinated nerve bundle.

hyalinized collagen and elastic fibers. The capsule is usually thin, but may vary in thickness from gland to gland or even in different areas of the same gland (22). In some cases, the capsule is quite attenuated. Capsular arterioles are often present in random sections of the gland just outside the capsule (fig. 1-24, above). Immunostains for smooth muscle actin and muscle-specific actin may highlight even small vessels penetrating the capsule or in the subcapsular area. Small bundles of myelinated nerve also penetrate the adrenal capsule primarily on the posterior or dorsal surface of the gland (fig. 1-24, right) (22). A chance finding on ultrastructural study is a small neural bundle coursing through the adrenal cortex.

Cortical Extrusions and Accessory Cortical Nodules. Cortical extrusions are relatively

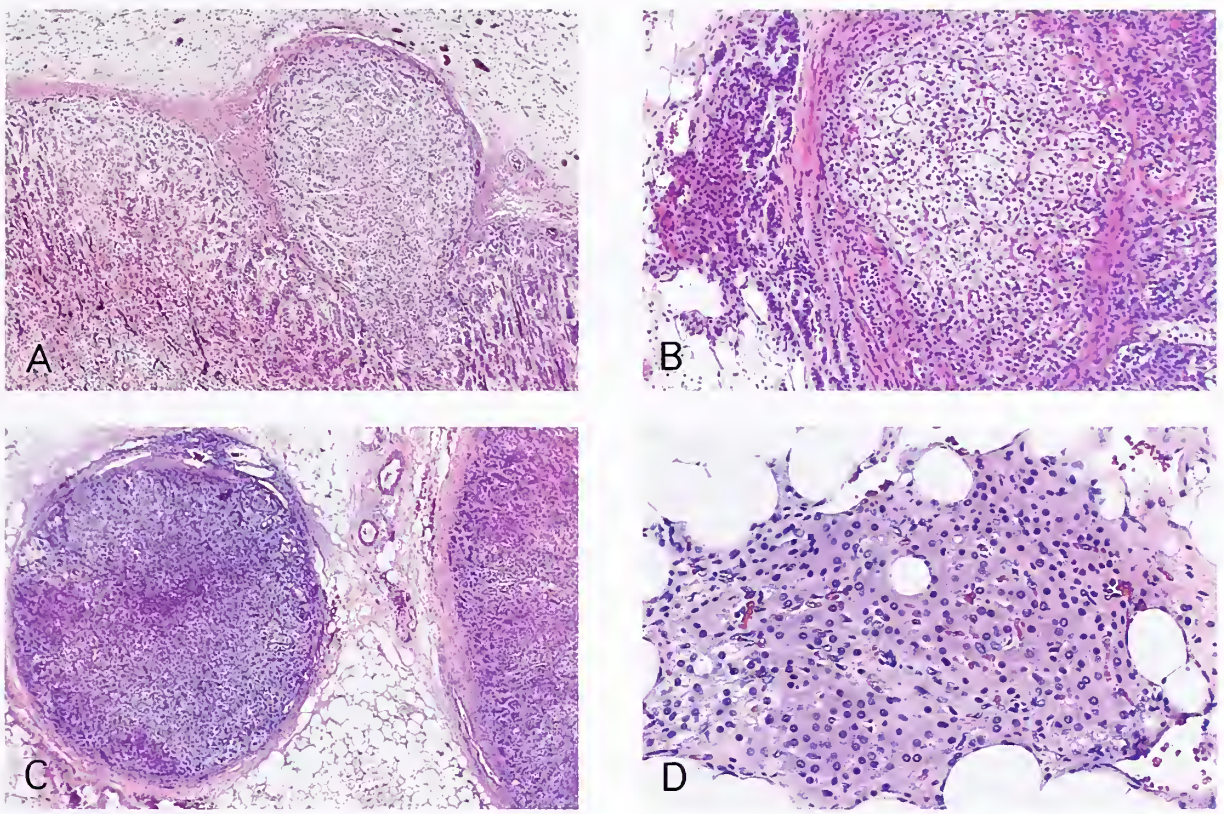

Figure 1-25

NORMAL ADRENAL GLAND

A: Partially encapsulated cortical extrusion in a normal adrenal gland has a "mushroom"-like configuration, with a narrow connection to the underlying cortex. (Fig. 1-23, left from Fascicle 19, Third Series.)

B: The cortical extrusion is attached to the adrenal capsule and extends freely into periadrenal fat. The capsule is very attenuated.

C: Accessory cortical nodule in periadrenal fat is completely encapsulated.

D: Accessory cortical nodule lies free in periadrenal fat without encapsulation.

common in adrenal glands from adults and elderly persons. Depending upon the plane of section, some of the cortical extrusions are connected to the underlying cortex (fig. 1-25A); other nodules lie on the surface of the gland and are encapsulated or extend from the adrenal capsule into periadrenal fat without encapsulation (fig. 1-25B). Nodules or clusters of cortical cells, which lie free in periadrenal fat, may be regarded as accessory cortical nodules (fig. 1-25C,D). The author has observed only rare examples of accessory cortical tissue admixed with chromaffin cells and a small ganglion.

"Fissure" Formation. Postmortem autolysis may result in "fissure" formation, with cavitation particularly after physical manipulation of the gland (fig. 1-26). In the extreme, there may be a cavity filled with detritus and blood and almost complete separation of medulla from cortex. The plane of separation seems, in some cases, to be at the corticomedullary junction or interalar raphé, but this is not a constant feature. The autolysis may be preceded by a toxic or infectious process. There is usually no significant inflammatory reaction. This postmortem change undoubtedly contributed to the misconception of the adrenal glands as hollow organs (hence the term "suprarenal capsules") and the early belief that they were involved in purifying or altering "black bile" (or "atrabilia").

Stress-Related Changes. An increase in tissue corticosteroid levels during illness is an

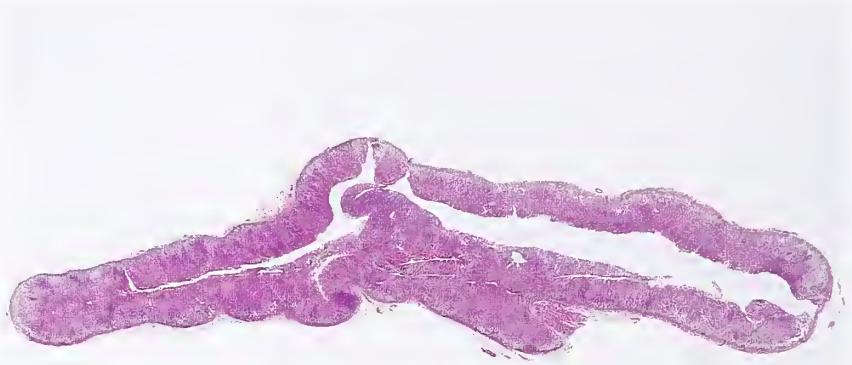

Figure 1-26

POSTMORTEM ARTIFACT WITH "FISSURE" FORMATION

Tissue separation, or "fissure" formation, is largely through the interalar raphé and corticomedullary junction, but may not indicate a clear demarcation between cortex and medulla. (Fig. 1-24 from Fascicle 19, Third Series.)

important protective response (23). The most common stress-related change in the adrenal glands is lipid depletion. In this situation, pale-staining, lipid-rich cells of the zona fasciculata convert to cells with compact, eosinophilic cytoplasm; the zona reticularis may appear widened and the entire thickness of the cortex may be involved. The macroscopic appearance may be striking, with uniform medium brown discoloration of the entire adrenal cortex (fig. 1-27, left); this discoloration is due to diffuse (or patchy) lipid depletion in cortical cells normally rich in cytoplasmic lipid (fig. 1-27, right). There is a pattern of patchy lipid depletion referred to as lipid reversion (fig. 1-28) in which lipid is absent in the outer cortex and usually scanty in the zona reticularis, but is prominent in the intervening zona fasciculata. This appearance suggests recovery from "stress" with replenishment of lipid in cells of the inner zona fasciculata (11). Tubular degeneration is evidenced by conversion of normally solid cords of cells in the outer cortex to tubular structures (fig. 1-29) lined by flattened cells, which may contain proteinaceous material or occasional degenerated cells. Rarely, intracytoplasmic globules are noted within the cells of the zona fasciculata in humans dying of such conditions as streptococcal meningitis, chronic renal failure, pneumonia, and overexposure to cold. Since these globules are induced in the experimental animal by ACTH administration, it is assumed that they are the result of overstimulation of the adrenal cortex (24).

Microscopic Anatomy of Adrenal Medulla

Adrenal Medulla. The chromaffin cells of the adrenal medulla are arranged in discrete nests or short anastomosing cords (fig. 1-30), a more diffuse or solid arrangement, or an admixture of different architectural patterns within the same gland. Staining for reticulum highlights the organoid arrangement of the cells.

Chromaffin cells have amphophilic to basophilic cytoplasm, indistinct borders, and usually a single nucleus that is often slightly eccentric in location. The nuclear contour and size may be quite regular, but in some glands there is considerable nuclear variation, with enlargement and hyperchromasia. Mitotic figures are virtually absent in the normal medulla, but can be found in diffuse or nodular adrenal medullary hyperplasia as seen in the multiple endocrine neoplasia (MEN) syndrome types 2a and 2b. Pinpoint basophilic granules, which are barely resolvable with the light microscope, are seen on close examination of cell cytoplasm (fig. 1-31); most of these correspond to dense-core neurosecretory granules.

Scattered ganglion cells can be found in the medulla either singly or in association with small myelinated nerve bundles. Occasionally, aggregates of ganglion cells are present. Depending upon the delay in or method of fixation,

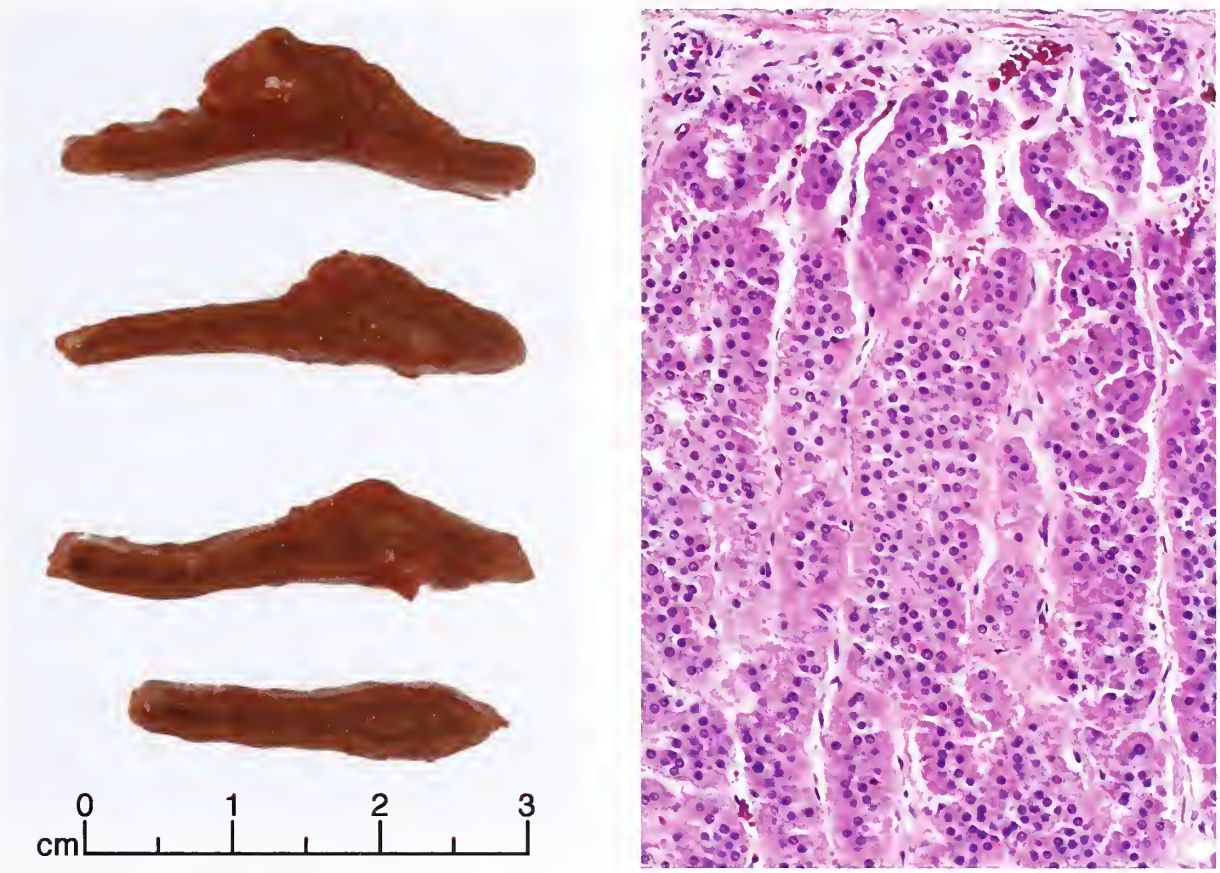

Figure 1-27

ADRENAL GLAND IN PATIENT WITH ACQUIRED IMMUNODEFICIENCY SYNDROME

Left: Adrenal gland from a patient who died of infectious complications of acquired immunodeficiency syndrome (AIDS). The adrenal cortex in the transverse sections is diffusely brown due to lipid depletion.

Right: The entire cortex shows marked lipid depletion and cells with compact, eosinophilic cytoplasm. This appearance was diffuse throughout both glands.

the cytologic detail of the chromaffin cells may be altered by cytoplasmic vacuolization or apparent disruption of cell membranes.

Intracytoplasmic hyaline globules have been reported in 79 percent of adrenal glands from adults, although they may be difficult to find on casual inspection (fig. 1-32). In 86 percent of cases in one study, the globules were scored as minimal in number, requiring an extensive search with the high dry microscope objective, while in only 3 percent were the globules numerous and present in nearly every high-power field (25). The globules are eosinophilic, range in size from 1 to 25 μm, and are periodic acid–Schiff (PAS) positive and resistant to diastase predigestion. There appears to be no correlation with sex, race, or age, but in the author's experience, they are uncommon in the pediatric age group. The globules have been described with increased frequency in patients with chronic neurologic disorders such as Parkinson's disease (26). In 1-μm thick sections stained with toluidine blue the globules are readily detected as blue-black structures which vary considerably in size (fig. 1-33); some may give the impression of having small budding projections, but this is probably due to superimposition of adjacent globules in most cases. Ultrastructurally, the globules may be partially or completely membrane bound, and have small curvilinear or circular profiles at the periphery with a size, shape, and electron density similar to adjacent dense-core neurosecretory

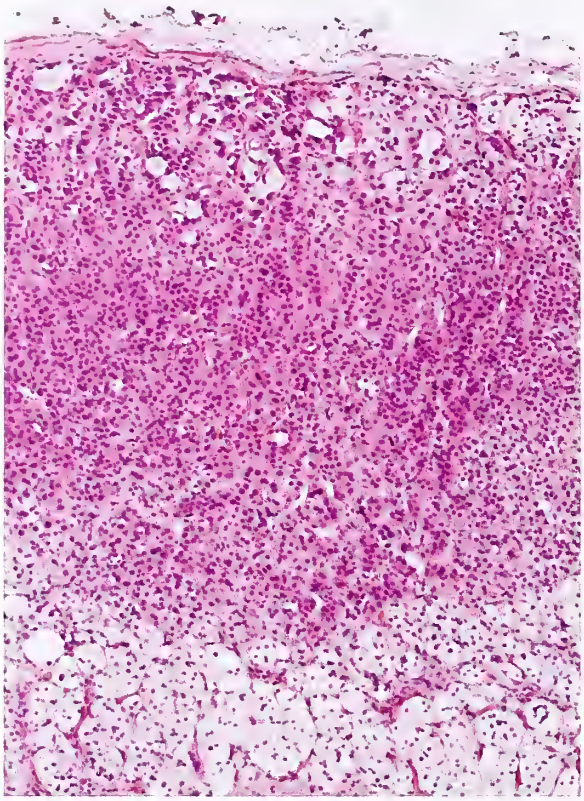

Figure 1-28

LIPID REVERSION

The outer aspect of the zona fasciculata is composed of cells with lipid-depleted, eosinophilic cytoplasm and the inner zone is composed of pale-staining, lipid-rich cells. This appearance suggests recovery from stress.

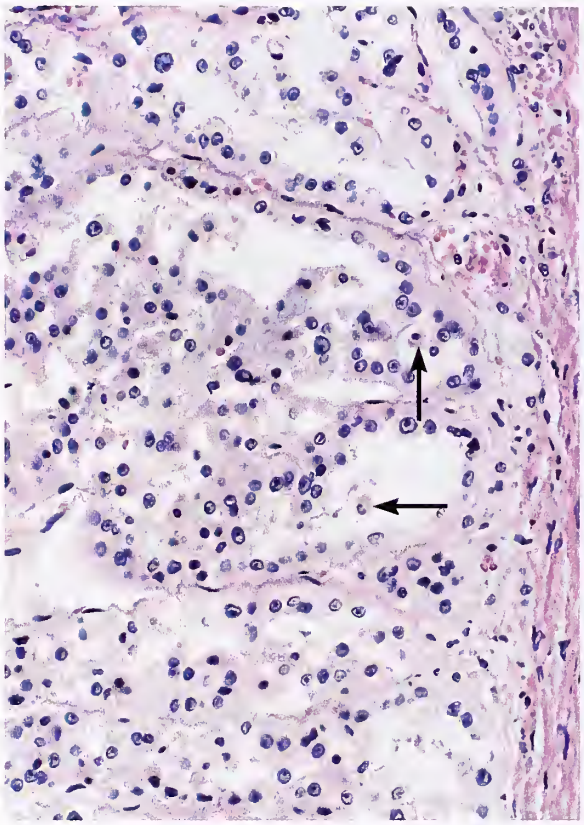

Figure 1-29

TUBULAR DEGENERATION OF OUTER ZONA FASCICULATA

Solid columns and cords of lipid-depleted cells are converted into hollow tubules, which contain rare necrobiotic cortical cells (arrows). (Fig. 1-27 from Fascicle 19, Third Series.)

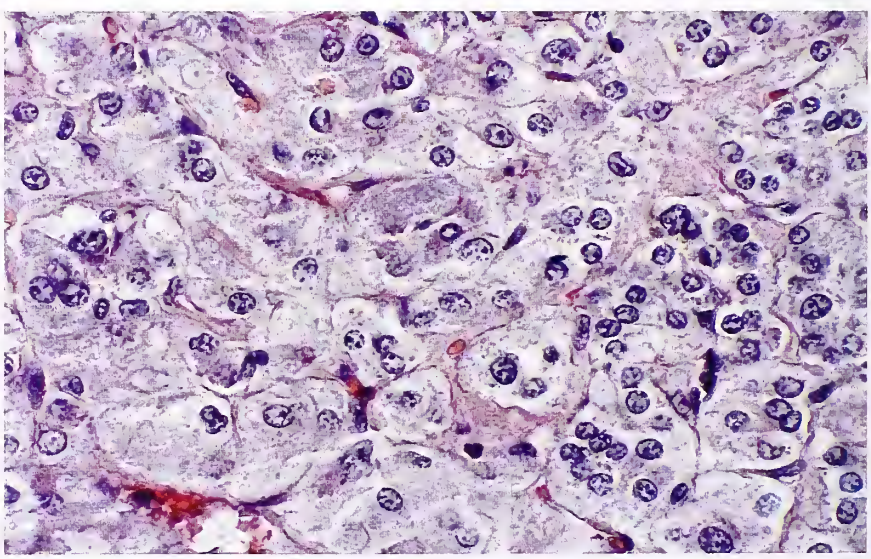

Figure 1-30

NORMAL ADRENAL MEDULLA IN AN ADULT

Chromaffin cells are arranged in nests and anastomosing short cords. (Fig. 1-28 from Fascicle 19, Third Series.)

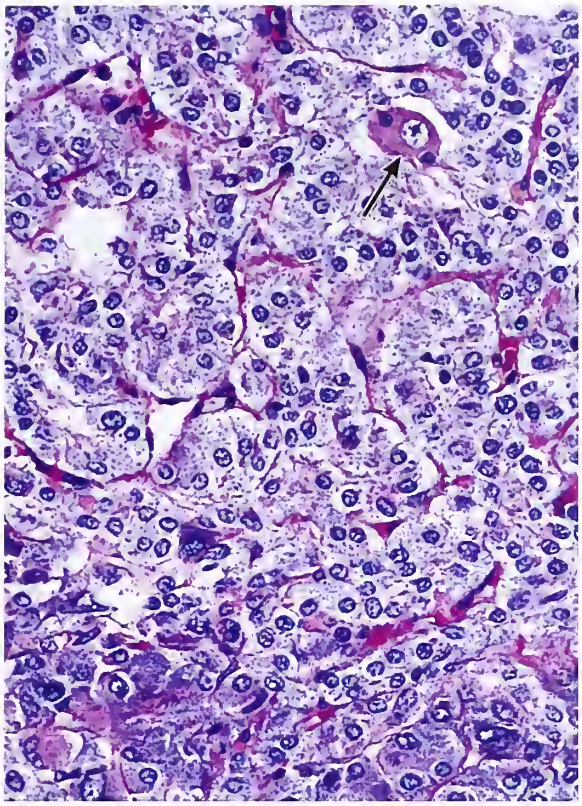

Figure 1-31

NORMAL ADRENAL MEDULLA IN AN ADULT

Chromaffin cells contain a myriad of pinpoint cytoplasmic granules. A mature ganglion cell is apparent (arrow). (Fig. 1-29, left from Fascicle 19, Third Series.)

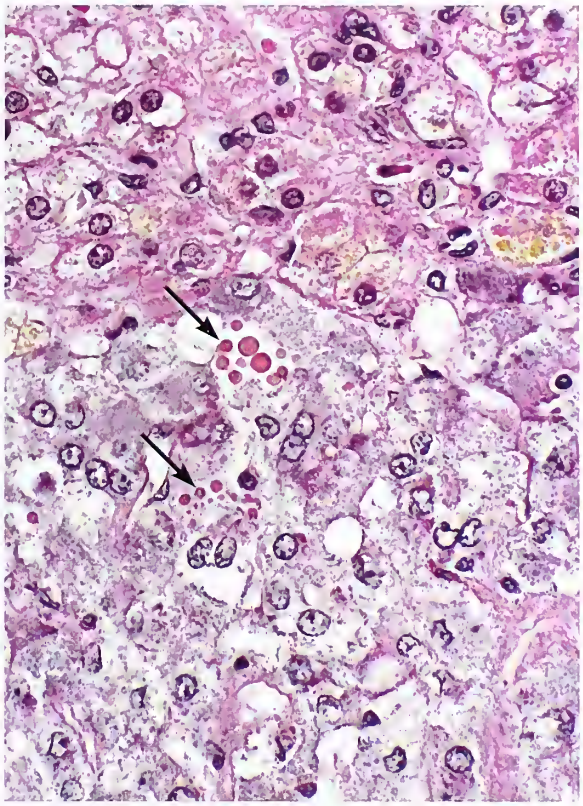

Figure 1-32

INTRACYTOPLASMIC HYALINE GLOBULES

Intracytoplasmic hyaline globules are present in several chromaffin cells near the corticomedullary junction (arrows). Cortical cells with finely vacuolated to eosinophilic cytoplasm are present in the upper portion of the field. The cells of the zona reticularis contain lipofuscin. (Fig. 1-30 from Fascicle 19, Third Series.)

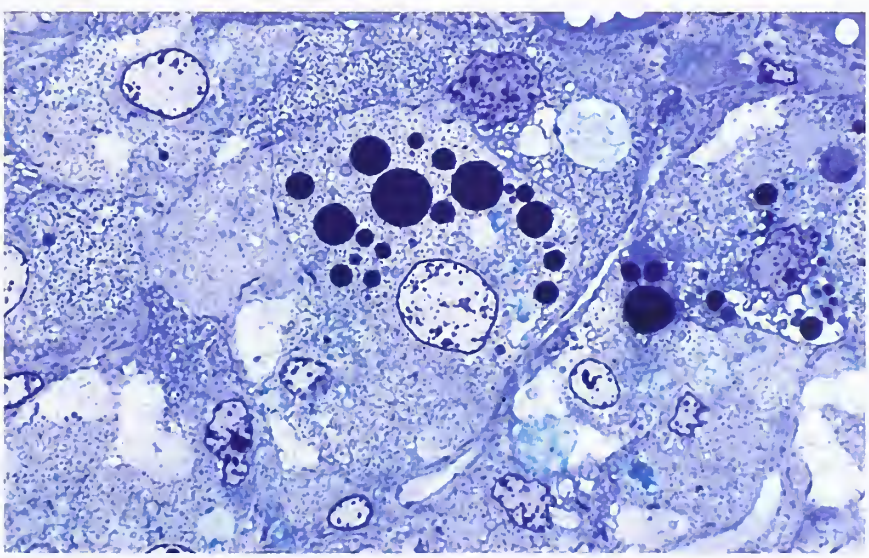

Figure 1-33

INTRACYTOPLASMIC HYALINE GLOBULES

Intracytoplasmic hyaline globules are numerous in this field; they are blue-black with the toluidine blue stain. The delicate microvasculature winds between nests and short cords of chromaffin cells. (Fig. 1-31 from Fascicle 19, Third Series.)

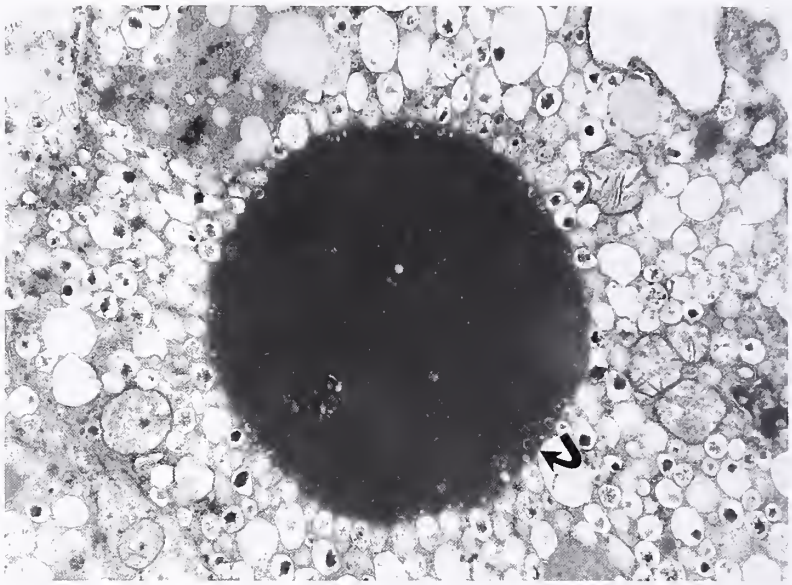

Figure 1-34

INTRACYTOPLASMIC HYALINE GLOBULES

The ultrastructure of normal chromaffin cells of the adult adrenal medulla is shown. The electron-dense structure represents an intracytoplasmic hyaline globule. Circular structures are at the periphery of the globule; some have the same electron density (curved arrow) as the cores of neurosecretory granules. Some partially empty secretory vesicles slightly indent the matrix of the globule. (Fig. 10-22 from Lack EE. Pathology of adrenal and extra-adrenal paraganglia. Major problems in pathology, Vol 29. Philadelphia: WB Saunders; 1994:202.)

granules (fig. 1-34). This feature suggests some association with the secretory activity of the chromaffin cells.

Medullary Extrusions and Accessory Chromaffin Cells. On rare occasion, extruded or "unmasked" medullary tissue is evident on gross examination of the intact gland (fig. 1-35A). Adrenal chromaffin cells are normally concentrated in the medulla, but occasionally are seen as small collections of cells near the capsule (fig. 1-35B), or as a circumscribed nest of cells in periadrenal connective tissue. Small collections of chromaffin cells outside the adrenal gland may be morphologically indistinguishable from extraadrenal paraganglia (see chapter 11). This localization may be explained by the pattern of migration of neuroblastic cells from the neural crest (see fig. 1-6B). Immunostaining for chromogranin may help to identify small nests of ectopic or accessory chromaffin cells, which might otherwise escape detection by routine light microscopy (fig. 1-35C).

Anatomy of Adrenal Vasculature

The three arteries supplying the adrenal glands divide repeatedly into as many as 50 branches, which partially invest the capsule as the capsular arterioles (see fig. 1-24, above) (27). There is a single central or main adrenal vein; typically an invaginated cuff of cortical tissue envelopes it throughout its length in much of the gland. It merges imperceptibly with the cortex in the tail of the gland; only in the head are there small venous radicles which lie free in the medulla (27). The microscopic anatomy of the central adrenal vein and its tributaries is remarkable for the very distinctive array of medial musculature organized into discontinuous pillars of longitudinal bundles (fig. 1-36). There is a selective gathering of muscle bundles in the medulla facing segments of veins in certain regions ("medullary tropism").

Once the arterioles penetrate the cortex they enter a thin subcapsular plexus that gives rise to capillary channels. The capillary channels course centrally through the zona fasciculata to reach the zona reticularis and then join a rich vascular plexus. Blood courses into venous sinuses in the medulla to enter tributaries of the central adrenal vein. In areas of the gland with no medulla, the blood from the reticular plexus courses directly into tributaries of the central adrenal vein. Contraction of the longitudinal muscle bundles is thought to aid in closure or damming up of blood in the venous sinuses and reticular plexus (fig. 1-37), and in this way the muscles act as "sluice gates" regulating the degree of congestion of the zona reticularis and inner zona fasciculata; with relaxation of muscle bundles and elastic recoil of venous sinuses there may be rapid, intermittent release of hormones into the central adrenal vein. One of

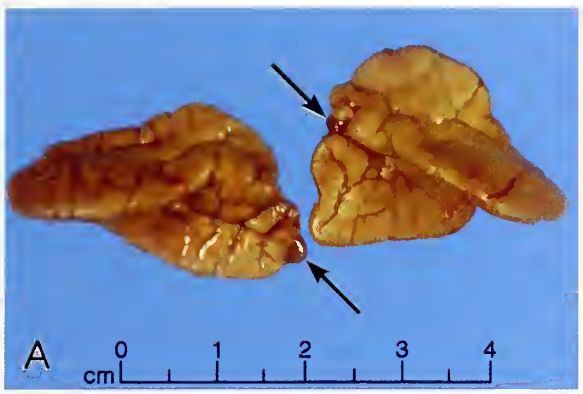

Figure 1-35

NORMAL ADRENAL GLAND

A: On the medial, inferior aspect of each adrenal gland from a young infant is a small nodule of extruded or "unmasked" medullary tissue (arrows) which was continuous with the adrenal medulla in the head of the gland. A longitudinal ridge or crista is on the dorsal surface of each gland and terminates in the outer (superolateral in situ) aspect of each gland.

B: Chromaffin cells lie within the outer aspect of the adrenal capsule.

C: Immunostain for chromogranin demonstrates small nests of chromaffin cells in the outer cortex just beneath the capsule of the adrenal gland (avidin-biotin peroxidase method).

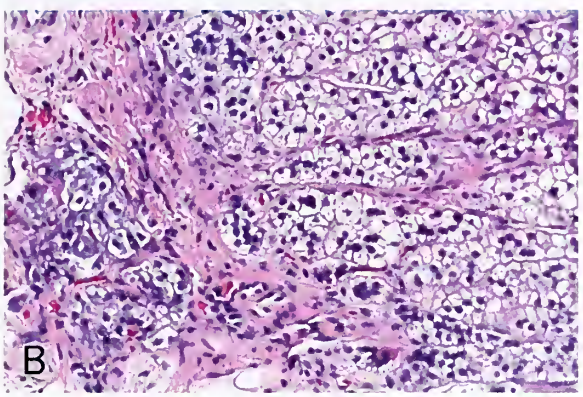

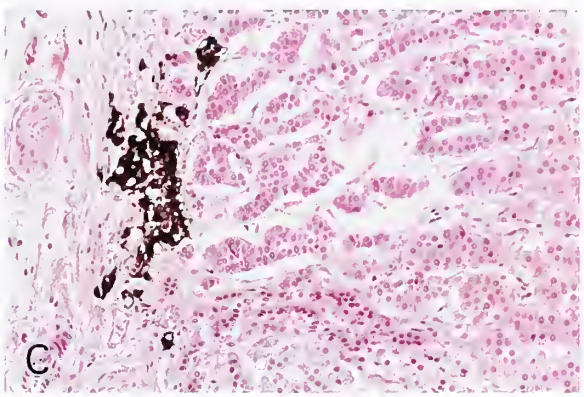

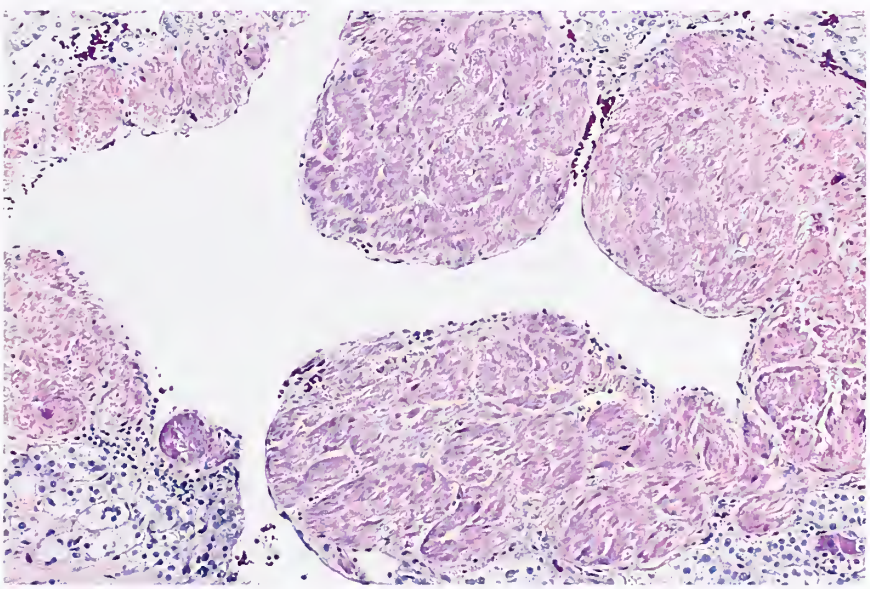

Figure 1-36

NORMAL ADRENAL GLAND

Distinctive arcades of smooth muscle surround a tributary of the central adrenal vein. Where smooth muscle is deficient, medullary (chromaffin) or cortical cells come into close proximity with the vascular space. (Fig. 1-33 from Fascicle 19, Third Series.)

the remarkable aspects of the venous structures is the close proximity which cortical and medullary cells have to the vascular lumen (fig. 1-38), a feature that is significant when interpreting vascular intrusions in hyperplastic and neoplastic conditions (28).

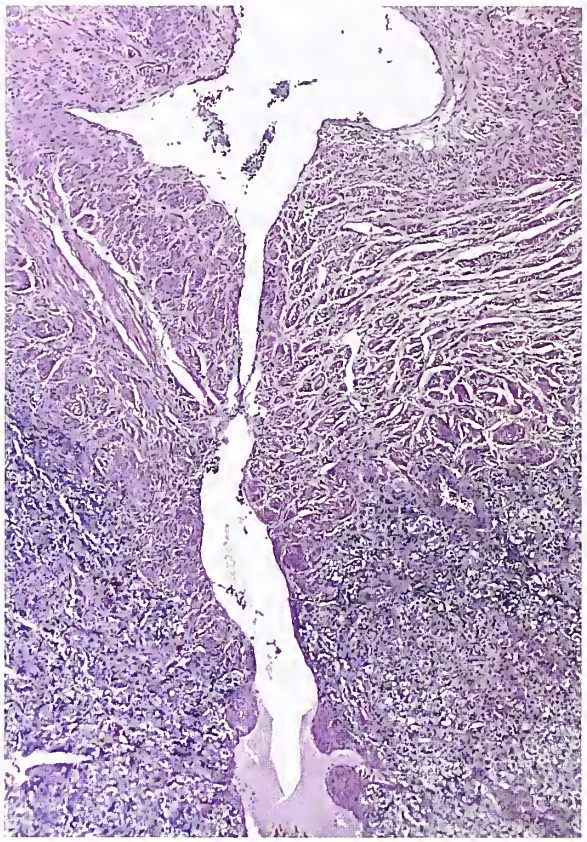

Figure 1-37

NORMAL ADRENAL GLAND

Venous sinusoids within the medullary compartment of the adrenal gland drain into a larger venous channel, which has stout bundles of smooth muscle. Contraction of smooth muscle may cause congestion of venous tributaries. (Fig. 1-34 from Fascicle 19, Third Series.)

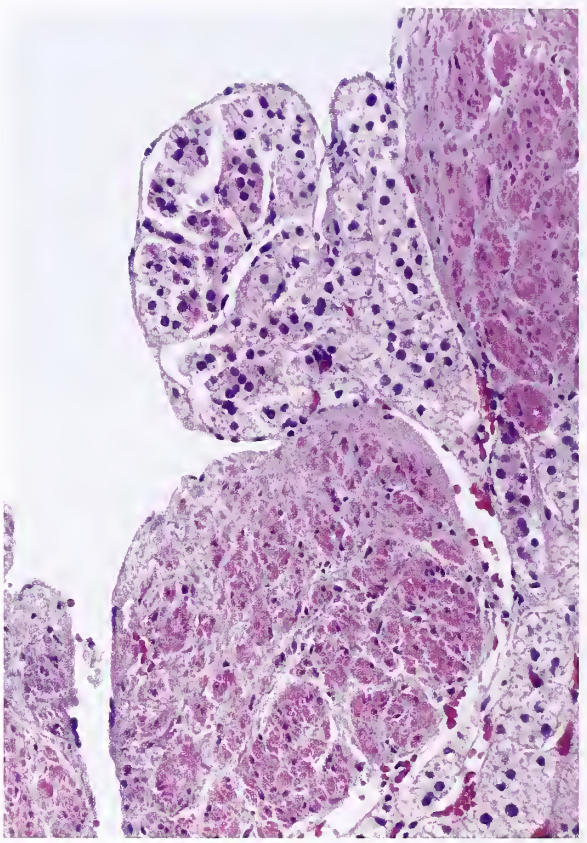

Figure 1-38

NORMAL ADRENAL GLAND

A cuff of cortical cells extends through the wall of the tributary of the central adrenal vein where there is discontinuity of smooth muscle bundles. The surface of a vascular "intrusion" is covered by endothelium.

IMMUNOHISTOCHEMISTRY OF ADRENAL CORTEX AND DISTRIBUTION OF STEROIDOGENIC ENZYMES

Immunohistochemistry

Immunofluorescent studies performed on frozen section specimens and immunoperoxidase staining of formalin-fixed paraffin-embedded tissue have shown cytokeratin expression localized within the cytoplasm of normal adrenal cortical cells (29). Immunostaining for vimentin is positive within stromal elements (e.g., endothelial cells), but also may stain cortical cells, particularly cells in the outer cortex (fig. 1-39A) (22). The neuroendocrine marker synaptophysin (fig. 1-39B) and neuron-specific enolase also stain some adrenal cortical cells to a variable degree, and this may be an important reason for the misdiagnosis of an adrenal cortical neoplasm as a pheochromocytoma. Other markers of cortical cells include inhibin (30), Melan-A (Mart-1) (fig. 1-39C) (31), and calretinin (fig. 1-39D). Some (or most) of these immunostains are nonspecific and correlation with anatomic features and pathology is indicated.

Other substances detected in the adrenal cortex are BCL2 (an antiapoptotic protein), transforming growth factor-alpha, epidermal growth factor, and insulin-like growth factor II (32). Cell proliferation studies of the human adrenal cortex using Ki-67 have shown some immunoreactivity, principally in the zona fasciculata (33),

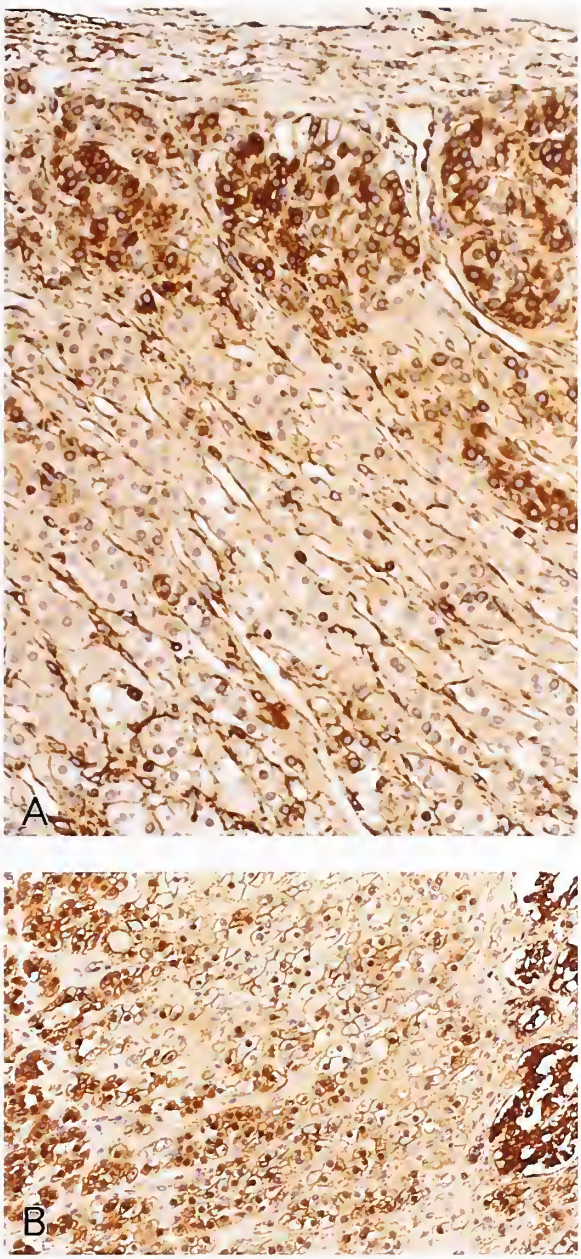

Figure 1-39

NORMAL ADRENAL GLAND

A: Immunostain for vimentin highlights delicate vascular spaces, but also stains the cytoplasm of some cortical cells, particularly in the zona glomerulosa.

B: Many of the cortical cells in this field are immunoreactive for synaptophysin, but more intense staining is present in the cytoplasm of chromaffin cells in the right part of the field.

C: Immunostain for Melan-A (Mart-1) is strongly positive in the cytoplasm of adrenal cortical cells. The adrenal capsule is on the left side.

D: Immunostain for calretinin shows diffuse positive staining of cortical cells. Adrenal capsule is on the right side (A–D: avidin-biotin peroxidase method).

but identifiable mitotic figures are extremely rare in the normal adrenal cortex. Nucleolar organizing regions have been studied to a limited degree in the normal adrenal cortex. Negative immunoreactivity has been reported for epithelial membrane antigen (29) and neurofilament protein. Lectin binding of wheat germ agglutinin and concanavalin has been reported in most adrenal cortical cells of all zones (34).

Distribution of Steroidogenic Enzymes

The intracortical distribution of P-450 cytochromes, which are important in corticosteroidogenesis, has been investigated using immunohistochemistry and results underscore the functional zonation of the adrenal cortex (34). P-450$_{17\alpha}$ was not present in the zona glomerulosa, thus confirming the exclusive localization of glucocorticoid and androgen biosynthesis in the zona fasciculata and zona

Figure 1-40

NORMAL ADRENAL GLAND

A: Immunostain for chromogranin at low magnification shows intense staining of virtually all the chromaffin cells of the adrenal medulla. In this section of the body of the gland, the adrenal medulla has roughly an omega shape and extends into both wings or alae. This configuration of adrenal medulla resembles "Napoleon's cap."

B: Sustentacular cells are vividly demonstrated with this immunostain for S-100 protein. There is intense staining of nuclei and dendritic cytoplasmic processes.

C: Immunostain for neurofilament protein highlights numerous thin neuritic processes between individual and small nests of chromaffin cells (A–C: avidin-biotin peroxidase method).

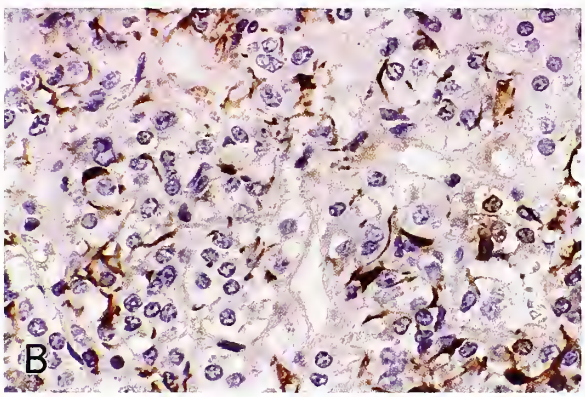

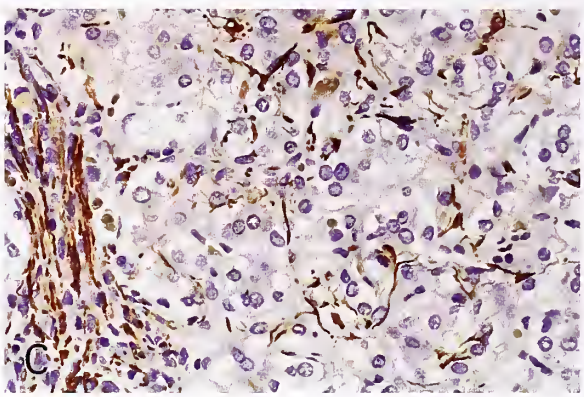

reticularis; immunoreactivity for P-450$_{C21}$ (C21 hydroxylation) was present in all three zones of the adrenal cortex, which reflects an important enzymatic step in biosynthesis of both mineralocorticoids and glucocorticoids. Some data suggest that the outer zona fasciculata is the most active area of corticosteroid biosynthesis (34).

CHROMAFFIN REACTION AND IMMUNOHISTOCHEMISTRY OF ADRENAL MEDULLA

The chromaffin reaction is rarely used today and is largely of historical interest. It depends on the oxidation of catecholamines in the presence of dichromate-containing fixatives with formation of adrenochrome pigments (28). The chromaffin reaction may be observed macroscopically as a darkening of medullary tissue, but it can also be detected on microscopic examination (26). Immunostaining for neuroendocrine markers such as chromogranin can highlight chromaffin cells to a remarkable degree (fig. 1-40A), demonstrate intermingling with cortical cells, and even highlight small nests of chromaffin cells out near the capsule of the gland (see fig. 1-35C). Cells that typically escape detection with routine light microscopy, and even electron microscopic study, are sustentacular cells, located at the periphery of small clusters, and cords of chromaffin cells. These cells are most vividly demonstrated by immunostaining for S-100 protein (fig. 1-40B). Immunostain for neurofilament protein demonstrates fine neuritic processes, which largely correspond to the rich splanchnic innervation by sympathetic fibers (fig. 1-40C).

MISCELLANEOUS MICROSCOPIC FEATURES

Adrenal Cytomegaly

Adrenal cytomegaly has been reported in about 3 percent of adrenal glands from newborns and 6.5 percent from premature stillborns (35); it is usually an incidental finding in glands which are otherwise grossly normal. It occurs in infants up to 2 months of age (35), and occasionally in older patients, even adults (36). Affected cells are limited to the fetal cortex and

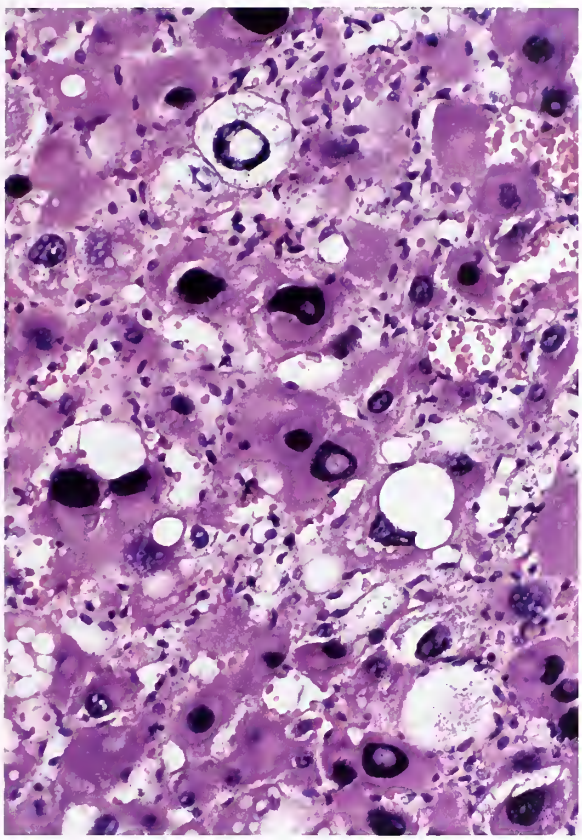

Figure 1-41

ADRENAL CYTOMEGALY IN A STILLBORN

Nuclear "pseudoinclusions" and a copious amount of eosinophilic, lipid-depleted cytoplasm are seen. Patchy areas of cytomegaly were present in cells of the fetal, or provisional, cortex.

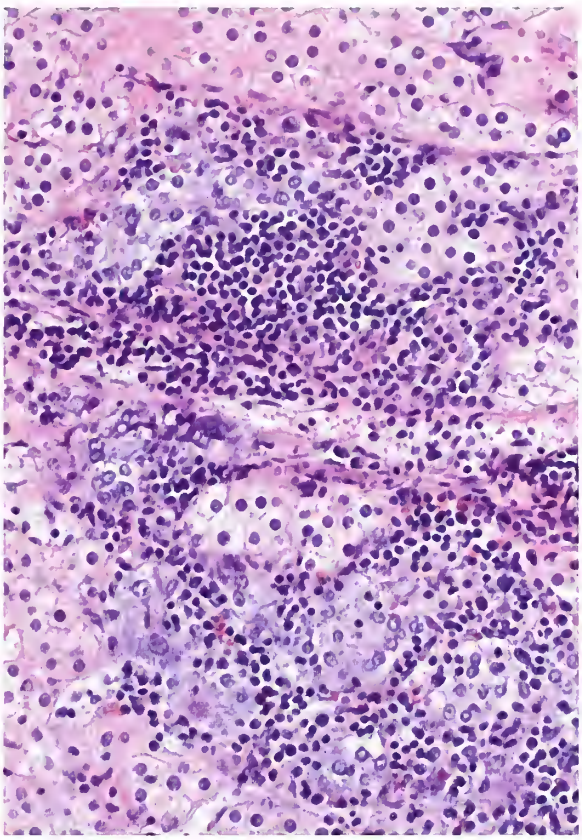

Figure 1-42

CHRONIC INFLAMMATION OF ADRENAL GLAND

A chronic inflammatory infiltrate, consisting mainly of lymphocytes, is present near the corticomedullary junction.

may be focal or diffuse (fig. 1-41). Cells may be as large as 120 µm in diameter (35), and show marked nucleomegaly with pleomorphism and hyperchromasia. These cells were once thought to be precursors of virilizing adrenal cortical tumors of childhood, but their presence is almost always an incidental finding. Cytomegalic cells may contain over 25 times the normal amount of nuclear DNA, underscoring the fact that polyploidy/aneuploidy is not an entirely specific marker of neoplasia or even malignancy (36). Characteristically, there are no identifiable mitotic figures. The occasional nuclear "pseudoinclusions," which in the past caused some concern for a viral etiology, have been shown ultrastructurally to have no viral inclusions; instead there is nuclear indentation or folding with intranuclear protrusion of cell cytoplasm.

Focal "Adrenalitis"

Rather than being an intrinsic adrenal disease, *focal "adrenalitis"* consists of small foci of lymphocytes and plasma cells, mainly interstitial (fig. 1-42) or in a perivenous location. These accompany retroperitoneal chronic inflammatory processes, such as chronic pyelonephritis. The significance of these cellular infiltrates is not known. Focal "adrenalitis" has been reported in 48 percent of patients at autopsy and is most frequent in elderly patients of both sexes (37).

Ovarian Thecal Metaplasia

Occasionally, small, partially hyalinized fibroblastic nodules are present which are often wedge-

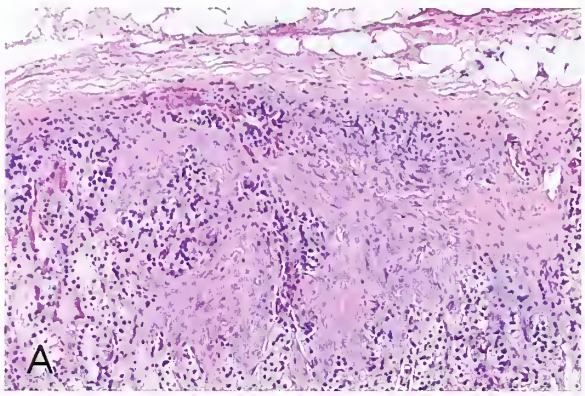

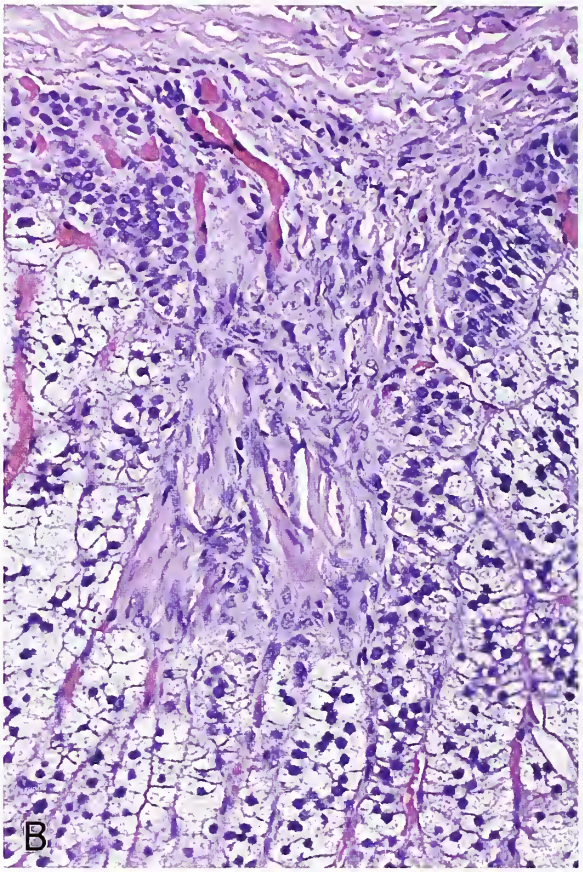

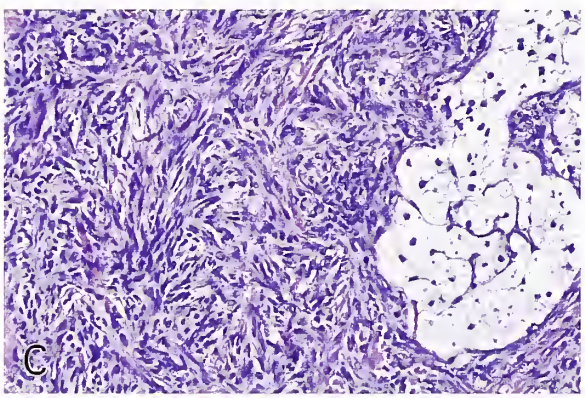

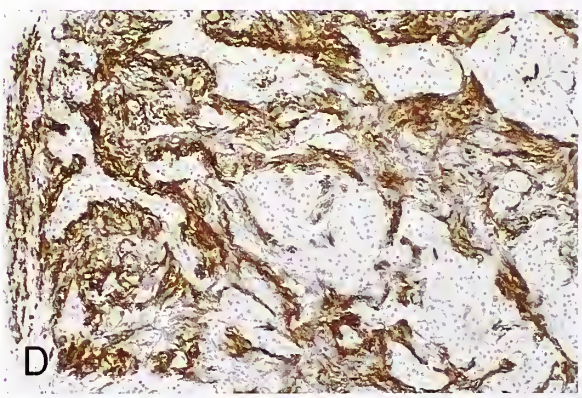

Figure 1-43

OVARIAN THECAL METAPLASIA

A: Ovarian thecal metaplasia appears as a broad, roughly wedge-shaped zone of bland spindle cells attached to the adrenal capsule.

B: At higher magnification, another case shows a slender tongue-like extension of compact spindle cells located between cords of cortical cells.

C: Ovarian thecal metaplasia is more cellular here, and extends around a collection of lipid-rich cortical cells (right side).

D: Interlacing bundles of spindle cells are immunoreactive for smooth muscle actin. Areas of negative staining represent nests of cortical cells. Cells were also immunoreactive for muscle-specific actin. The adrenal capsule at the far left also contains immunoreactive cells (avidin-biotin peroxidase method).

shaped and attached to the adrenal capsule (fig. 1-43A,B). Groups of spindle cells often extend between or surround small nests of cortical cells (fig. 1-43C). This mesenchymal proliferation, which is most common in postmenopausal females, was referred to as nodular hyperplasia of adrenal cortical blastema (38), but morphologically resembles mesenchymal cells of ovarian stroma, thus prompting the designation *ovarian thecal metaplasia* (39). This lesion is present in 4.3 percent of female patients (40), but has also been documented in men on rare occasion (38). The maximum size of the nodules is about 2 mm, and the lesions are multiple in about half of the cases and bilateral in roughly a third (40).

Ovarian thecal metaplasia varies in cellularity. Some foci are quite hyalinized while others are more cellular (fig. 1-43C). An occasional

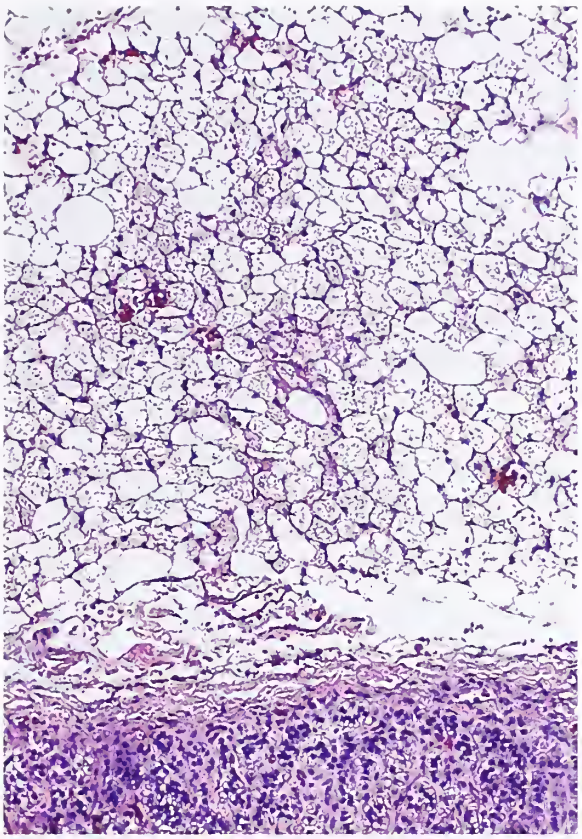

Figure 1-44

NORMAL ADRENAL GLAND

Periadrenal brown fat is occasionally seen in adults. It is well developed here.

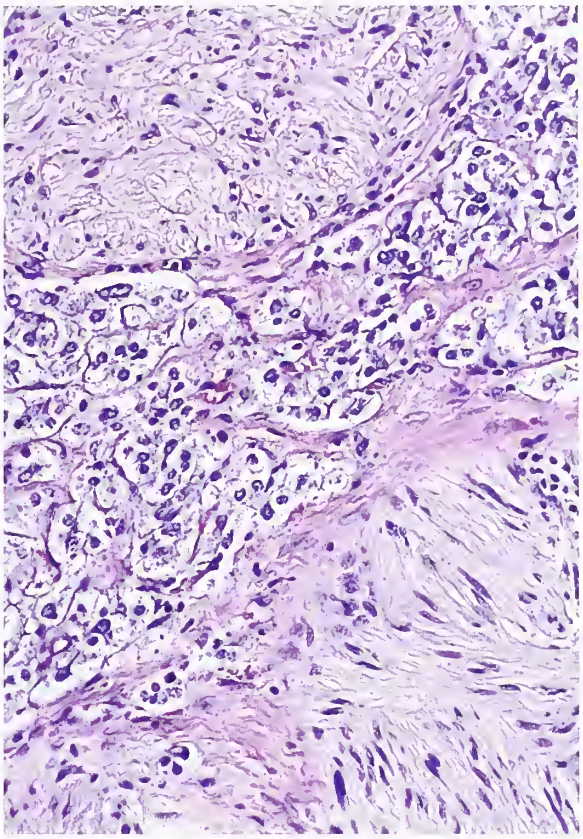

Figure 1-45

NEURAL HYPERTROPHY

On rare occasion, hypertrophic nerve bundles are seen in the medullary compartment of an otherwise normal adrenal gland.

focus may have dystrophic calcification. The histogenesis of ovarian thecal metaplasia is not entirely settled; in several cases studied by the author the cells were immunoreactive for smooth muscle actin (fig. 1-43D) and muscle-specific actin. The morphology and immunoprofile would suggest origin from myofibroblasts in some cases. Rarely, macroscopic spindle cell lesions occur which also resemble ovarian cortical stroma, but in one case there was a suggestion of origin from Schwann cells (41).

Other Features

Periadrenal brown fat is a normal constituent in early infancy and occasionally is well-developed in the adult (fig. 1-44). It has been more frequently associated with pheochromocytomas, but also occurs in those without pheochromocytoma (26). Bundles of myelinated nerve are found in the adrenal medulla, which may show some variation in size; on occasion, nerve bundles appear hypertrophied in a gland that is otherwise normal (fig. 1-45). The primordium of the adrenal cortex is in very close proximity to the adrenal ridge (see fig. 1-1), and accessory or heterotopic rests of adrenal cortical tissue can occur anywhere along the line of descent of the gonads in males and females; this includes adnexal structures and, rarely, within the substance of the gonad (see chapter 2). The presence of normal gonadal elements within the adrenal cortex is a rare occurrence. The author has seen one example of intracortical hilus (or Leydig) cells replete with crystalloids of Reinke (fig. 1-46) (42). Ectopic thyroid tissue has been reported in the adrenal gland, but a plausible

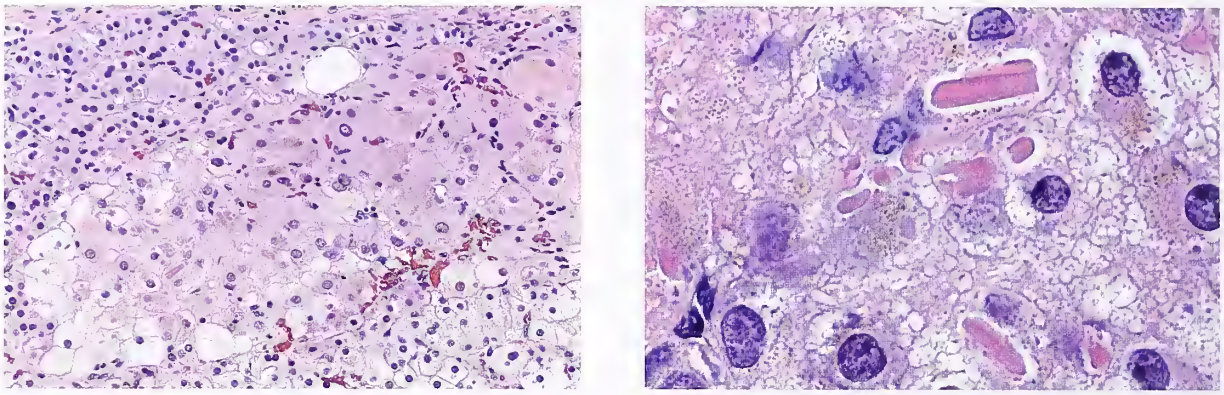

Figure 1-46

INTRACORTICAL HILUS (OR LEYDIG) CELLS

Left: A 49-year-old woman with an aldosterone-producing adrenal cortical adenoma underwent unilateral adrenalectomy. The normal adrenal cortex shows a solitary cluster of hilus (or Leydig) cells with numerous crystalloids of Reinke. Some cells of the adjacent zona glomerulosa contain "spironolactone bodies." The patient had been treated with the aldosterone antagonist spironolactone for primary hyperaldosteronism.

Right: Several intracortical hilus cells contain typical crystalloids of Reinke. Most cells also contain granular brown pigment representing lipofuscin.

embryologic explanation is difficult to envision (43). Intraadrenal hepatic heterotopia has also been reported (see chapter 2).

ELECTRON MICROSCOPY

Adrenal Cortex

The normal ultrastructure of the adrenal cortex in humans has been addressed in selected studies. Optimal results depend upon examination of glands obtained surgically without significant derangement in factors that would impact upon physiologic function by induction of stress. In a study of glands surgically resected from three women for palliative treatment of breast cancer, the three traditional zones of the cortex could be distinguished on the basis of size, shape, and internal architecture of mitochondria (44). All three zones of the adult cortex have a basement membrane surrounding clusters of several cells. The zona glomerulosa is distinguished by cells with relatively little lipid and lower cytoplasmic volume compared with cells of the zona fasciculata, and mitochondria that are elongated to round with lamellar or plate-like cristae (fig. 1-47) (11,44). Lipofuscin granules and lysosomes are sparse. The surface of cortical cells may have short microvillous projections that are most prominent in the inner zona fasciculata.

Intracellular lipid droplets are a prominent feature of the zona fasciculata (fig. 1-48, left) and may be quite large; some droplets appear as empty vacuoles, depending upon the method of fixation and processing for electron microscopic study. Cells of the zona fasciculata have mitochondria that are usually round to ovoid, and possess short and long tubular cristae (fig. 1-48, right). Cells often contain abundant smooth endoplasmic reticulum, which may form a complex network of anastomosing tubules. Profiles of rough endoplasmic reticulum may also be present, but in small amount. The cytoplasmic volume of the cells in the zona fasciculata tends to be large relative to the other zones. Microvillous cytoplasmic projections can be prominent. Junctional complexes are scanty, with close opposition of the plasmalemma of adjacent cortical cells resembling tight junctions (44). The zona reticularis is distinguished by cells with sparse lipid and often numerous lipofuscin granules and lysosomes (fig. 1-49). Mitochondria are usually spherical to ovoid, and have cristae with a mixture of short and long tubular invaginations of the inner membrane (44).

Ultrastructural study of early fetal cortical cells shows abundant smooth endoplasmic reticulum, which accounts in large part for the granular eosinophilic appearance by light microscopy. Mitochondria are spherical to ovoid, have

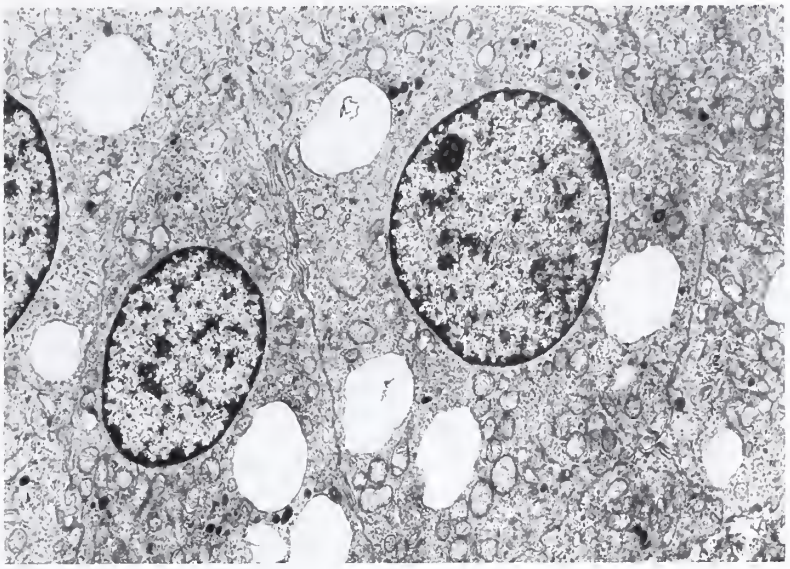

Figure 1-47

ZONA GLOMERULOSA OF NORMAL ADRENAL CORTEX

Cells of the zona glomerulosa contain relatively sparse lipid and have mitochondria that are round to oval. On closer view, the mitochondria had lamellar cristae. A few small clusters of cells in other areas were surrounded by a continuous basement membrane. Both smooth and rough endoplasmic reticulum are present.

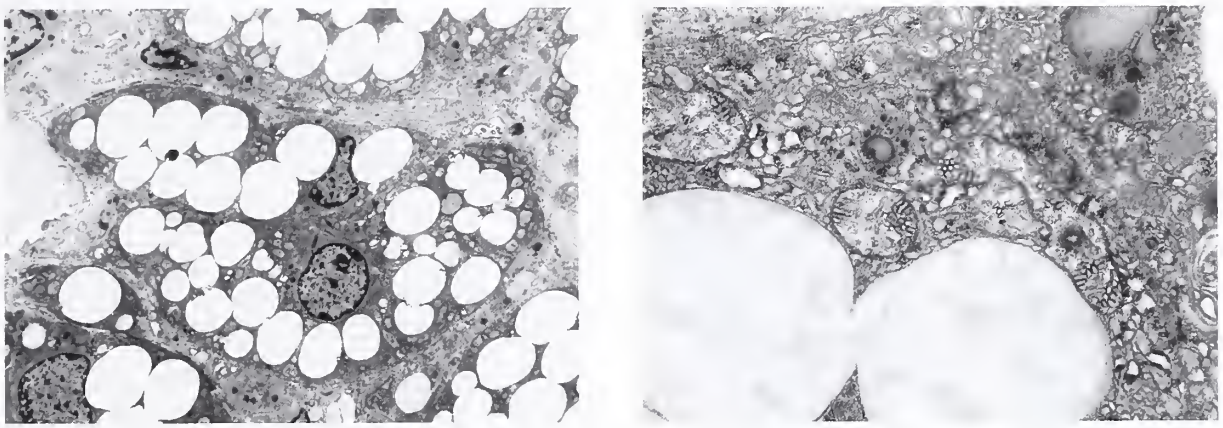

Figure 1-48

ZONA FASCICULATA OF NORMAL ADRENAL CORTEX

Left: Cells of the zona fasciculata contain abundant large lipid droplets. Focally, lipid droplets impinge upon and indent the nuclear contour.

Right: Cells of the zona fasciculata contain mitochondria, which are round to oval with short tubular or vesicular cristae. Smooth endoplasmic reticulum is also prominent.

tubular cristae, and contain very sparse lipid at about 8 weeks' gestation (45). The cell surface is covered with short microvilli, which project both into the intercellular space and toward the sinusoidal endothelium. Cells often contain a large Golgi complex with numerous associated dense bodies. The latter are described as lysosome-like and are perhaps involved in the fetal pattern of steroid metabolism (45).

Almost all of the cortical cells are in close proximity to capillary channels. Capillary spaces are lined by an attenuated endothelium with fenestrations, and in most areas there is a continuous, well-developed basal lamina with scattered pericytes (fig. 1-50). The perivascular spaces within the adrenal cortex are similar to the space of Dissé in the liver, and occasional macrophages have been noted in this area.

Adrenal Medulla

The chromaffin cells in the adult adrenal gland show some interdigitation of blunt to elongated

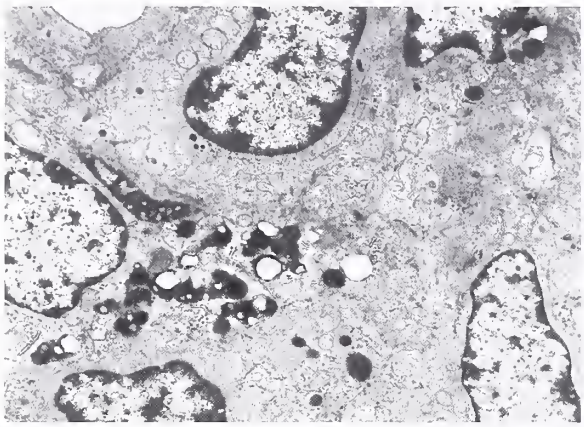

Figure 1-49

ZONA RETICULARIS OF NORMAL ADRENAL CORTEX

Cells of the zona reticularis are relatively depleted of lipid droplets. Lipofuscin granules are prominent and lysosomes are also present. Some mitochondria have cristae which appear as short and long tubular extensions of the inner membrane.

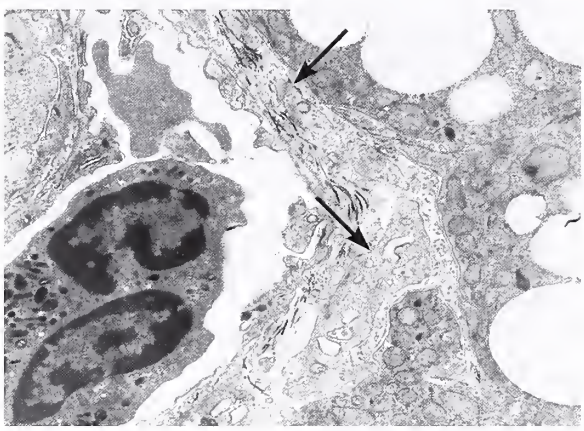

Figure 1-50

VASCULAR PATTERN OF NORMAL ADRENAL CORTEX

A vascular sinusoid is lined by endothelial cells with cytoplasmic fenestrations. Occasional Weibel-Palade bodies are present. Cytoplasmic processes of pericytes (arrows) partially encircle the vascular sinusoid. Basement membrane surrounds cortical cells in the right half of the field. A polymorphonuclear leukocyte is present in the vascular lumen.

cytoplasmic processes, with a few small, rudimentary intercellular attachments (not true desmosomes). The density of the cellular organelles may vary from cell to cell, contributing to the impression of a dichotomous or dual cell population of "dark" and "light" cells. The dominant ul-

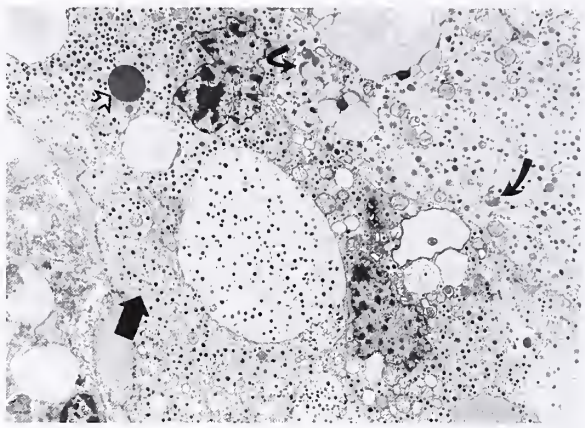

Figure 1-51

NORMAL ADRENAL CHROMAFFIN CELLS

The density of dense-core neurosecretory granules may vary from cell to cell. Some neurosecretory granules vary slightly in size and shape. The variation in the electron density of the cytoplasm gives the impression of a "light" (near center) and "dark" (thick arrow) population of endocrine cells. The open arrow indicates an electron-dense structure representing a small hyaline globule. Some cells contain lipofuscin (curved arrows). (Fig. 10-34 from Lack EE. Pathology of adrenal and extra-adrenal paraganglia. Major problems in pathology, Vol 29. Philadelphia: WB Saunders; 1994:213.)

trastructural feature is the presence of dense-core neurosecretory type granules, which also vary in density from one cell to another, and even in the same cell (fig. 1-51). The granules range in morphology from small, uniform dense cores having a tight limiting membrane and symmetric halo to granules with a wide asymmetric halo (fig. 1-52); the former granules have been associated with epinephrine storage, and the latter with norepinephrine (46). Granule morphology can vary considerably, consisting of pleomorphic, elongated, crescentic, or "dumbbell" shaped granules. Association of granule morphology by itself with storage of any particular regulatory peptide or hormone is not reliable. Neurosecretory granules usually range in size from 150 to 250 nm (46).

A small to moderate amount of rough endoplasmic reticulum is present in some chromaffin cells but smooth endoplasmic reticulum is sparse. Lipochrome pigment is present in some cells in association with sparse lipid, and is typically not as large or electron dense as the structures corresponding to the hyaline globules. Nuclei often show peripheral aggregation

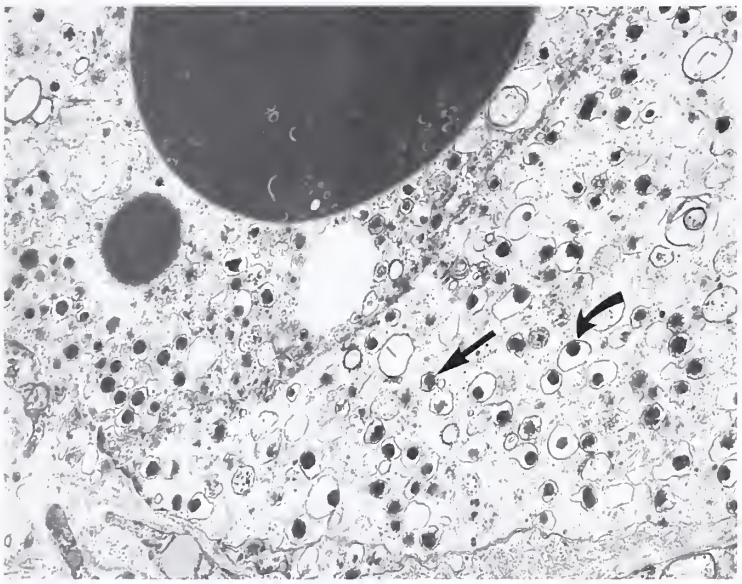

Figure 1-52

CHROMAFFIN CELLS IN NORMAL MEDULLA

Two adjacent chromaffin cells contain numerous neurosecretory granules. Some granules have a wide, asymmetric halo between the electron-dense core and limiting membrane (curved arrow), a morphologic feature associated with norepinephrine storage. Other granules have a more uniform morphology with a narrow, symmetric halo (straight arrow), which has been associated with the storage of epinephrine. The ultrastructural features by themselves may not be reliable in predicting the granule content of any particular hormone or neuropeptide. Note also the large intracytoplasmic hyaline globule with small round to oval structures at the periphery. (Fig. 10-37 from Lack EE. Pathology of adrenal and extra-adrenal paraganglia. Major problems in pathology, Vol 29. Philadelphia: WB Saunders; 1994:215.)

of chromatin, and the nuclear membrane is usually smooth and regular in contour, but may show some indentation or folding. Occasionally, there are simple intercellular attachments between chromaffin cells, and rarely, even with adjacent cortical cells (26). Sometimes the chromaffin cells and cortical cells intermingle, but this is much clearer in sections stained immunohistochemically for neuroendocrine makers. A feature noted in some pheochromocytomas is the presence of dilated spaces in the cytoplasm resembling "pseudoacini." The vascular network is delicate and lined by endothelial cells with some cytoplasmic fenestrations, similar to those in the cortex.

MOLECULAR MEDIATION OF ENDOCRINE DEVELOPMENT

The nuclear transcription factor, steroidogenic factor 1 (SF-1), has emerged as an essential regulator of endocrine development and function. It was initially identified as a tissue-specific transcriptional regulator of the cytochrome P-450 steroid hydroxylases but the role of SF-1 appears to be much broader (47). In studies of knockout or null mice lacking SF-1, the adrenal glands and gonads failed to develop, and the animals had adrenal cortical insufficiency and died within the first week after birth. Only rare examples of SF-1 mutations have been described in humans and have resulted in adrenocortical insufficiency. Another nuclear transcription factor, *DAX-1* (dosage-sensitive sex reversal adrenal hypoplasia congenital critical region on the X chromosome) was initially described as the gene responsible for human X-linked congenital adrenal hypoplasia (48). In mice, another gene product, acd (adrenal cortical dysplasia), has been shown to have a central role in development of the adrenal cortex (48).

DAX-1 mutations have been reported to be a relatively frequent cause of adrenal failure in male patients; *SF-1* mutations causing adrenal failure in humans are rare and are more likely to be associated with significant underandrogenization and gonadal dysfunction in 46, XX individuals (49). A complex genetic cascade of factors affecting the growth and development of the adrenal cortex is beginning to unfold.

REFERENCES

Embryology and Biosynthetic Pathways

1. Lack EE, Kozakewich HP. Embryology, developmental anatomy and selected aspects of nonneoplastic pathology. In: Lack EE, ed. Pathology of the adrenal glands. New York: Churchill Livingstone; 1990:1-74.
2. Crowder RE. The development of the adrenal gland in man, with special reference to origin and ultimate location of cell types and evidence in favor of the "cell migration" theory. Contributions to embryology, Vol 36. Nos 242-51, Carnegie Institute of Washington, publication #611, 1957:193-210.
3. O'Rahilly R. The timing and sequence of events in the development of the human endocrine system during the embryonic period proper. Anat Embryol (Berl) 1983;166:439-451.
4. Gottschau M. Struktur und embryonale entwickelung der nebennieren bei säugetieren. Arch fur Anat und Endwicklungsgeschichte. Anatomischer Abteilung 1883;9:412-458.
5. Chester Jones I. Variation in the mouse adrenal cortex with special reference to the zona reticularis and to brown degeneration, together with a discussion of the 'cell migration' theory. Q J Microsc Sci 1948;89:53-74.
6. Zajicek G, Ariel I, Arber N. The streaming adrenal cortex: direct evidence of centripetal migration of adrenocytes by estimation of cell turnover rate. J Endocr 1986;111:477-482.
7. Turkel SB, Itabashi HH. The natural history of neuroblastic cells in the fetal adrenal gland. Am J Pathol 1974;76:225-236.
8. Wong DL. Why is the adrenal adrenergic? Endocr Pathol 2003;14:25-36.
9. Wurtman RJ. Catecholamines. N Engl J Med 1965;273:637-646, 693-700, 746-753.
10. Coupland RE. The natural history of the chromaffin cell—twenty-five years on the beginning. Arch Histol Cytol 1989;52:331-341.
11. Symington T. Functional pathology of the human adrenal gland. Baltimore: Williams & Wilkins; 1969.

Function of Fetal Adrenal Glands

12. Pepe GJ, Albrecht ED. Regulation of the primate fetal adrenal cortex. Endocr Rev 1990;11:151-176.
13. Simonian MH, Capp MW. Characterization of steroidogenesis in cell clusters of the human fetal adrenal cortex: comparison of definitive zone and fetal zone cells. J Clin Endocrinol Metab 1984;59:643-651.

Anatomy of Adrenal Glands

14. Tähkä H. On the weight and structure of the adrenal glands and the factors affecting them in children of 0-2 years. Acta Pediatrica 1951;40 (Suppl 81):4-95.
15. Stoner HB, Whiteley HJ, Emery JL. The effect of systemic disease on the adrenal cortex of the child. J Pathol Bacteriol 1953;66:171-183.
16. Studzinski GP, Hay DC, Symington T. Observations on the weight of the human adrenal gland and the effect of preparations of corticotropin of different purity on the weight and morphology of the human adrenal gland. J Clin Endocrinol Metab 1963;23:248-254.
17. Quinan C, Berger AA. Observations on human adrenals with especial reference to the relative weight of the normal medulla. Ann Int Med 1933;6:1180-1192.
18. Lam KY, Chan AC, Lo CY. Morphological analysis of adrenal glands: a prospective analysis. Endocr Pathol 2001;12;33-38.
19. Oppenheimer EH. Cyst formation in the outer adrenal cortex. Studies in the human fetus and newborn. Arch Pathol 1969;87:653-659.
20. Rodin AE, Hsu FL, Whorton EB. Microcysts of the permanent adrenal cortex in perinates and infants. Arch Pathol Lab Med 1976;100:499-502.
21. Saeger W, Reinhard K. Fat-cell metaplasia in the adrenal cortex: incidence, structure and correlation to basic diseases in a postmortem series. Endocrine Pathol 1998;9:241-247.
22. Carney JA. Adrenal gland. In: Sternberg SS, ed. Histology for pathologists, 2nd ed. Philadelphia: Lippincott-Raven; 1997:1107-1131.
23. Cooper MS, Stewart PM. Corticosteroid insufficiency in acutely ill patients. N Engl J Med 2003;348:727-734.
24. Wilbur OM Jr, Rich AR. A study of the role of adrenocorticotropic hormone (ACTH) in the pathogenesis of tubular degeneration of the adrenals. Bull Johns Hopkins Hosp 1954;93:321-347.
25. Dekker A, Oehrle JS. Hyaline globules of the adrenal medulla of man. A product of lipid peroxidation? Arch Pathol 1971;91:353-364.
26. Lack EE. Pathology of adrenal and extra-adrenal paraganglia. Major problems in pathology, Vol 29. Philadelphia: WB Saunders; 1994.
27. Dobbie JW, Symington T. The human adrenal gland with special reference to the vasculature. J Endocrinol 1966;34:479-489.

28. Lack EE. Adrenal medullary hyperplasia and pheochromocytoma. In: Lack EE, ed. Pathology of the adrenal glands. New York: Churchill Livingstone; 1990:173-235.

Immunohistochemistry and Distribution of Steroidogenic Enzymes

29. Gaffey MJ, Traweek ST, Mills SE, et al. Cytokeratin expression in adrenocortical neoplasia: an immunohistochemical and biochemical study with implications for the differential diagnosis of adrenocortical, hepatocellular, and renal cell carcinoma. Hum Pathol 1992;23:144-153.
30. McCluggage WG, Burton J, Maxwell P, Sloan JM. Immunohistochemical staining of normal hyperplastic and neoplastic adrenal cortex with a monoclonal antibody against alpha inhibin. J Clin Pathol 1998;51:114-116.
31. Busam, KJ, Iversen K, Coplan, et al. Immunoreactivity for A103, an antibody to melan-A (Mart-1), in adrenocortical and other steroid tumors. Am J Surg Pathol 1998;22:57-63.
32. Lloyd RV, Douglas BR, Young WF Jr. Endocrine diseases. Atlas of Nontumor Pathology, 1st Series, Fascicle 1. Washington, DC: American Registry of Pathology; 2002.
33. Sasano H, Imatani A, Shizawa S, Suzuki T, Nagura H. Cell proliferation and apoptosis in normal and pathologic human adrenal. Mod Pathol 1995;8:11-17.
34. Sasano N, Sasano H. The adrenal cortex. In: Kovacs K, Asa SL, eds. Functional endocrine pathology. Boston: Blackwell Scientific Publications; 1991:546-584.

Miscellaneous Microscopic Features

35. Craig JM, Landing BH. Anaplastic cells of fetal adrenal cortex. Am J Clin Pathol 1951;21:940-949.
36. Favara BE, Steele A, Grant JH, Steele P. Adrenal cytomegaly: quantitative assessment by image analysis. Pediatr Pathol 1991;11:521-536.
37. Griffel B. Focal adrenalitis. Its frequency and correlation with similar lesions in the thyroid and kidney. Virchows Arch A Pathol Anat Histol 1974;364:191-198.
38. Reed RJ, Patrick JT. Nodular hyperplasia of the adrenal cortical blastema. Bull Tulane Univ Med Fac 1967;26:151-157.
39. Wong TW, Warner NE. Ovarian thecal metaplasia in the adrenal gland. Arch Pathol 1971;92: 319-328.
40. Fidler WJ. Ovarian thecal metaplasia in adrenal glands. Am J Clin Pathol 1977;67:318-323.
41. Carney JA. Unusual tumefactive spindle-cell lesions in the adrenal glands. Hum Pathol 1987;18: 980-985.
42. Lack EE, Nauta RJ. Case report. Intracortical Leydig cells in a patient with an aldosterone-secreting adrenal cortical adenoma. J Urol Pathol 1993;1:411-418.
43. Shiraishi T, Imai H, Fukutome K, Watanabe M, Yatani R. Ectopic thyroid in the adrenal gland. Hum Pathol 1999;30:105-108.

Electron Microscopy

44. Long JA, Jones AL. Observations on the fine structure of the adrenal cortex of man. Lab Invest 1967;17:355-370.
45. McNutt NS, Jones AL. Observations on the ultrastructure of cytodifferentiation in the human fetal adrenal cortex. Lab Invest 1970;22:513-527.
46. Tannenbaum M. Ultrastructural pathology of adrenal medullary tumors. Pathol Annu 1970;5:145-171.

Molecular Regulatory Factors

47. Parker KL, Rice DA, Lala DS, et al. Steroidogenic factor 1: an essential mediator of endocrine development. Recent Prog Horm Res 2002;57:19-36.
48. Beuschlein F, Keegan CE, Bavers DL, et al. SF-1, DAX-1, and ACD: molecular determinants of adrenocortical growth and steroidogenesis. Endocr Res 2002;28:597-607.
49. Lin L, Gu WX, Ozisik G, et al. Analysis of DAX1 (NR0B1) and steroidogenic factor-1 (NR5A1) in children and adults with primary adrenal failure: ten years experience. J Clin Endocrinol Metab 2006;91:3048-3054.

2 CONGENITAL ADRENAL HETEROTOPIA, HYPERPLASIA, AND BECKWITH-WIEDEMANN SYNDROME

ADRENAL ADHESION, UNION, AND FUSION

Adrenal adhesion and *adrenal union* are distinguished by the presence or absence, respectively, of a continuous connective tissue capsule (1). In adrenal adhesion to either kidney or liver, there is an intervening thick or thin capsule (fig. 2-1, left), while with adrenal union there is intermingling of respective parenchymal cells (fig. 2-1, right). The term fusion has been used synonymously with union (1). With adrenal union the intermingling may lead to separated, discontinuous nests of adrenal cortical cells which should not be misinterpreted as "invasion" (see fig. 2-7A). The morphologic features are probably identical to those of adrenal-renal heterotopia; both involve the liver and kidney. *Adrenal fusion* is a rare anomaly in which the adrenal glands are united in the midline (fig. 2-2),

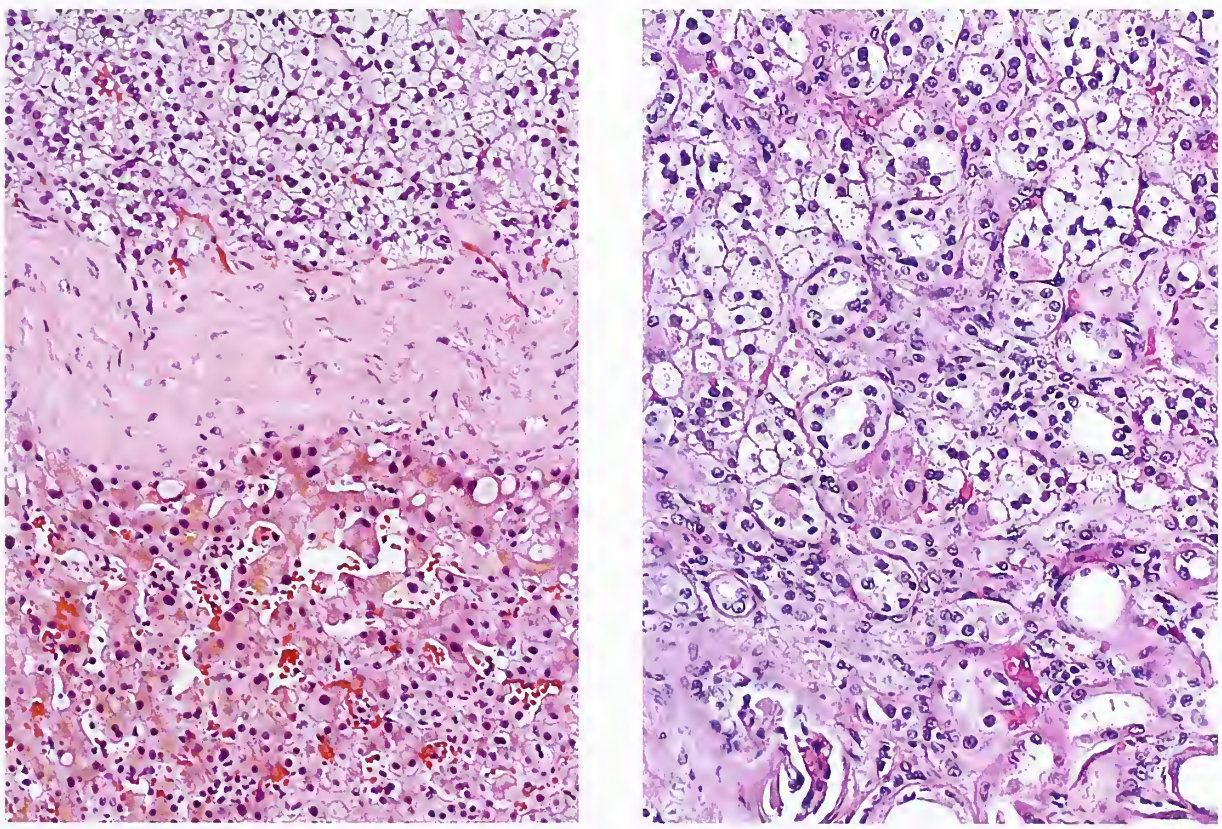

Figure 2-1

ADRENAL-HEPATIC ADHESION AND ADRENAL-RENAL UNION

Left: A thick capsule separates adrenal cortex (top) from hepatic parenchyma (bottom) in adrenal-hepatic adhesion.
Right: In adrenal-renal union (or fusion), there is no intervening capsule between adrenal cortex and renal parenchyma. (Fig. 2-1, right from Fascicle 19, Third Series.)

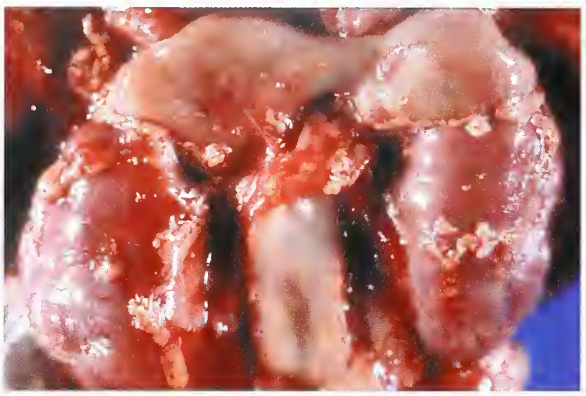

Figure 2-2

FUSION OF ADRENAL GLANDS

Newborn infant at autopsy with adrenal glands fused in the midline anterior to the aorta.

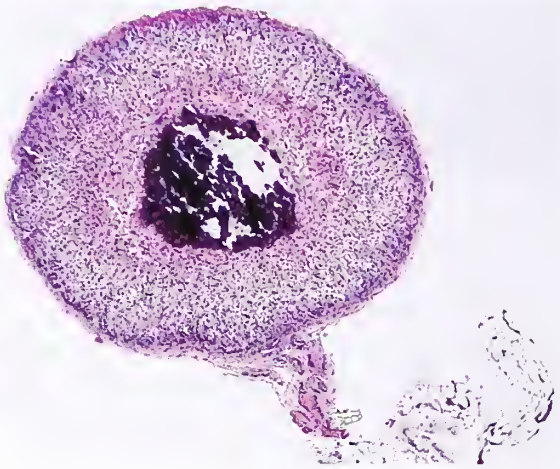

Figure 2-3

HETEROTOPIC ADRENAL CORTICAL TISSUE

A small nodule of heterotopic (or accessory) adrenal cortical tissue located along the spermatic cord was removed during inguinal hernia repair. Dystrophic calcification is present centrally. (Fig. 2-3 from Fascicle 19, Third Series.)

with some medial deviation of the kidneys in most cases. This abnormality is sometimes associated with midline congenital defects such as spinal dysraphism and indeterminate visceral situs, and occasionally, the Cornelia de Lange syndrome (mental and growth retardation, synophrys, anteverted nostrils, low-set ears, and spade-like hands with short tapering fingers) (1). *Renal agenesis* is sometimes associated with an adrenal gland of abnormal shape, which may be oval with a smooth contour. Complete absence or aplasia of adrenal glands has been rarely described, and may be familial (2).

HETEROTOPIC AND ACCESSORY ADRENAL TISSUES

Heterotopic and *accessory adrenal tissues* are found in the upper abdomen or anywhere along the path of descent of the gonads (fig. 2-3). This anatomic localization can be explained on an embryologic basis given the close spatial relationship between the gonadal ridge and adrenal glands. In rare cases, adrenal heterotopia occurs in bizarre anatomic sites which defy logical embryologic explanation, e.g., placenta (3), lung (4), and intracranial cavity (5). Rare examples of intraadrenal hepatic (6) and thyroid (7) heterotopia have also been reported. One of the most frequent sites for accessory adrenal tissue is the area of the celiac axis; in a study of 100 consecutive autopsies, accessory adrenal cortical tissue was identified in the area of the celiac plexus in 32 percent of cases, and in half of these (16 percent) the accessory tissue consisted of both cortex and medulla (8). Accessory or heterotopic adrenal cortical tissue has been noted in the kidney, usually in a subcapsular location in the upper pole, in 0.1 to 6.0 percent of individuals at autopsy (9). Complete removal of the renal capsule with exposure of the entire cortical surface may facilitate recognition of accessory adrenal tissue, which is usually less than 3 to 4 mm in size.

The resemblance of adrenal cortex to cells of renal cell carcinoma led Grawitz in 1883 to postulate that hypernephromas arise from misplaced adrenal tissue. Ectopic cortical tissue has also been noted within the wall of the gallbladder (10). Small adrenal cortical rests should be distinguished from adrenal-renal (or adrenal-hepatic) heterotopia, which can be complete or incomplete. In the complete form of adrenal-renal heterotopia, the entire adrenal gland is located beneath the renal capsule, over the superior pole or anterior surface of the kidney; in the incomplete form, the subcapsular portion of the gland is firmly attached to the surface of the kidney while a part of the gland may be contained in peculiar folds of the capsule, or a large part may be outside the capsule. The incomplete form of adrenal heterotopia is quite rare, and was seen in only 0.16 percent of autopsies in one study (11).

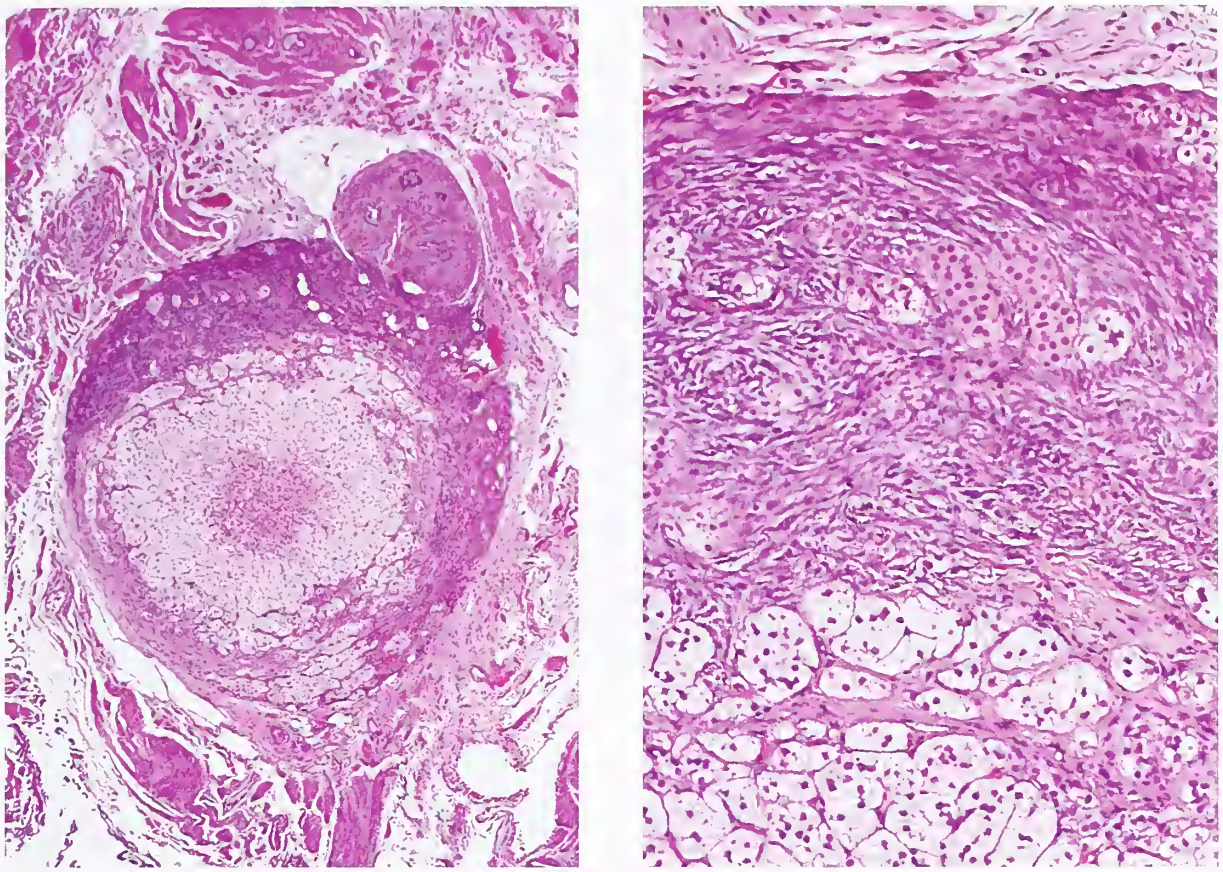

Figure 2-4

ACCESSORY ADRENAL CORTICAL TISSUE WITH OVARIAN THECAL METAPLASIA

Left: The heterotopic adrenal cortical rest was located near the broad ligament in an adult woman. Cortical cells are present in the center of the nodule and are surrounded by a mantle of ovarian thecal metaplasia.

Right: Adrenal cortical cells, some with lipid-depleted cytoplasm, are present within the spindle cell stroma of ovarian thecal metaplasia.

Accessory adrenal tissue in sites further removed from the upper abdomen consists almost solely of cortex, without a medullary component. Marchand (12) identified accessory adrenal tissue in the broad ligament near the ovary in human infants (fig. 2-4). In 23.3 percent of cases in one study (Table 2-1), accessory cortical tissue was identified in the broad ligament anywhere from the junction with the mesosalpinx to its lateral attachment; it was bilateral in 6.7 percent of cases (13). Accessory adrenal cortical tissue was found along the spermatic cord in 3.8 percent of children undergoing inguinoscrotal surgery, and in 9.3 percent who were operated on for an undescended testis where a longer segment of spermatic cord was dissected (14).

Table 2-1

LOCATION OF ACCESSORY AND HETEROTOPIC ADRENAL TISSUES[a]

Location	Incidence
Area of celiac axis	32%
Kidney, usually subcapsular upper pole	<0.1-6 %
Broad ligament	23%
Adnexa of testes	7.5%
Spermatic cord	3.8-9.3%
Rare sites: placenta, liver, lung, intracranial	

[a]Table 2-1 from Fascicle 19, Third Series.

Using a serial blocking technique, accessory adrenal cortical tissue was found in 15 of 200

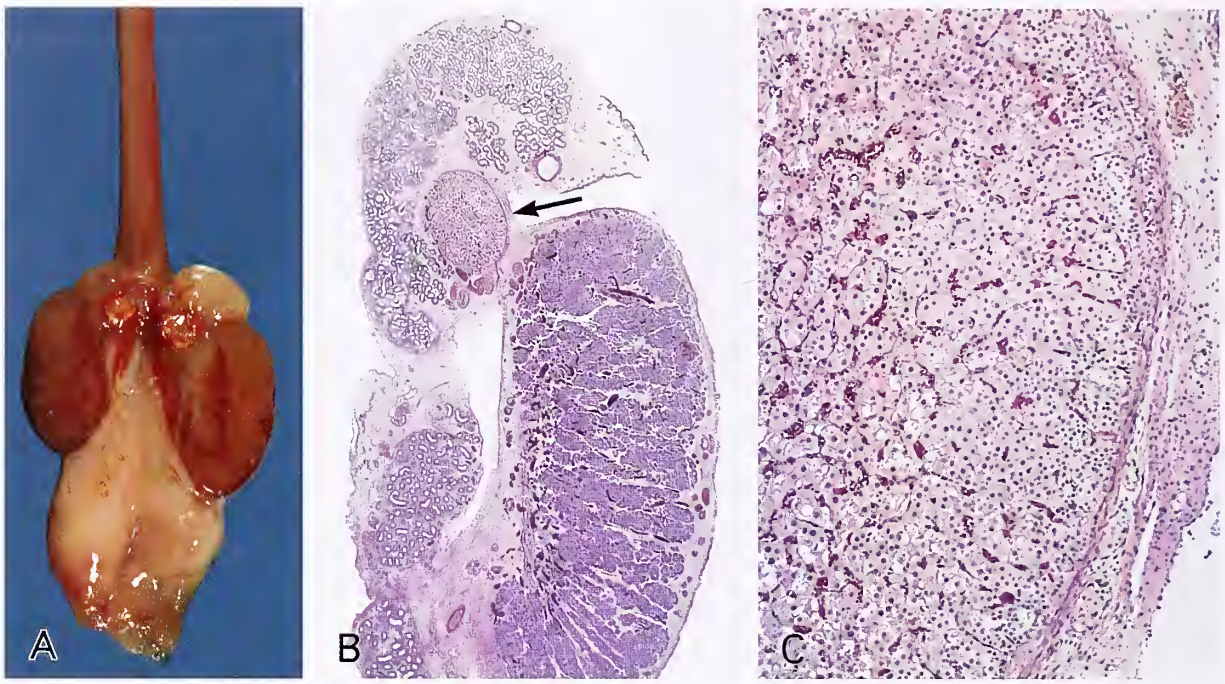

Figure 2-5

ACCESSORY ADRENAL CORTICAL TISSUE

A: Bisected testis from a newborn infant who died of disseminated herpes simplex infection. A small nodule of heterotopic or accessory adrenal cortical tissue is present in the hilum of the testis near the junction with the head of the epididymis. Microscopically, herpetic necrosis similar to the necrosis in orthotopic adrenal glands was seen. Intranuclear viral inclusions were readily identified. Attached pale connective tissue was markedly edematous. (A–C: Fig. 2-4 from Fascicle 19, Third Series.)

B: Longitudinal section of a newborn testis in a different case shows a nodule of heterotopic/accessory adrenal cortical tissue in the hilum of the testis (arrow) adjacent to the head of the epididymis.

C: The adrenal tissue from the case seen in B is composed of only cortical cells, without a medullary component.

testes from 100 male infants less than 1 year of age (7.5 percent); it was bilateral in 4 percent (15). The nodules were circumscribed, round to ovoid, measured 0.5 to 7.0 mm in diameter, and were located in connective tissue of the distal spermatic cord or the area of the hilum of the testis (fig. 2-5). It is rare to see an adrenal cortical rest located within testicular parenchyma (fig. 2-6) (16) or in the substance of the ovary (17). The occurrence of adrenal tissue in ectopic locations helps explain adrenal cortical neoplasms which arise in unusual sites, such as scrotum (18) and liver (fig. 2-7) (19), although some examples defy ready embryologic explanation.

CONGENITAL ADRENAL HYPERPLASIA

The first unmistakable and thorough account of *congenital adrenal hyperplasia* (CAH), also known as *adrenogenital syndrome*, was given by the Italian anatomist de Crecchio in 1865 (20). CAH results from a defect in any one of five enzymatic steps involved in steroid synthesis (fig. 2-8). This disorder is an inborn error of metabolism which has an autosomal recessive mode of inheritance and is the most common cause of ambiguous genitalia in infants (21). CAH is the most common cause of primary adrenal insufficiency in the pediatric age group. About 90 to 95 percent of all cases of CAH are due to 21-hydroxylase deficiency, a disorder of cortisol and aldosterone biosynthesis due to mutations in the *CYP21* gene that encodes adrenal 21-hydroxylase P-450_{c21} (21).

There are several forms of CAH: 1) a "classic" form that has an incidence between 1/5,000 and 1/15,000 live births in most white populations; 2) a "nonclassic" form, one of the most frequent autosomal recessive disorders in the general white population; and 3) a "cryptic" form in which biochemical abnormalities may exist, but the

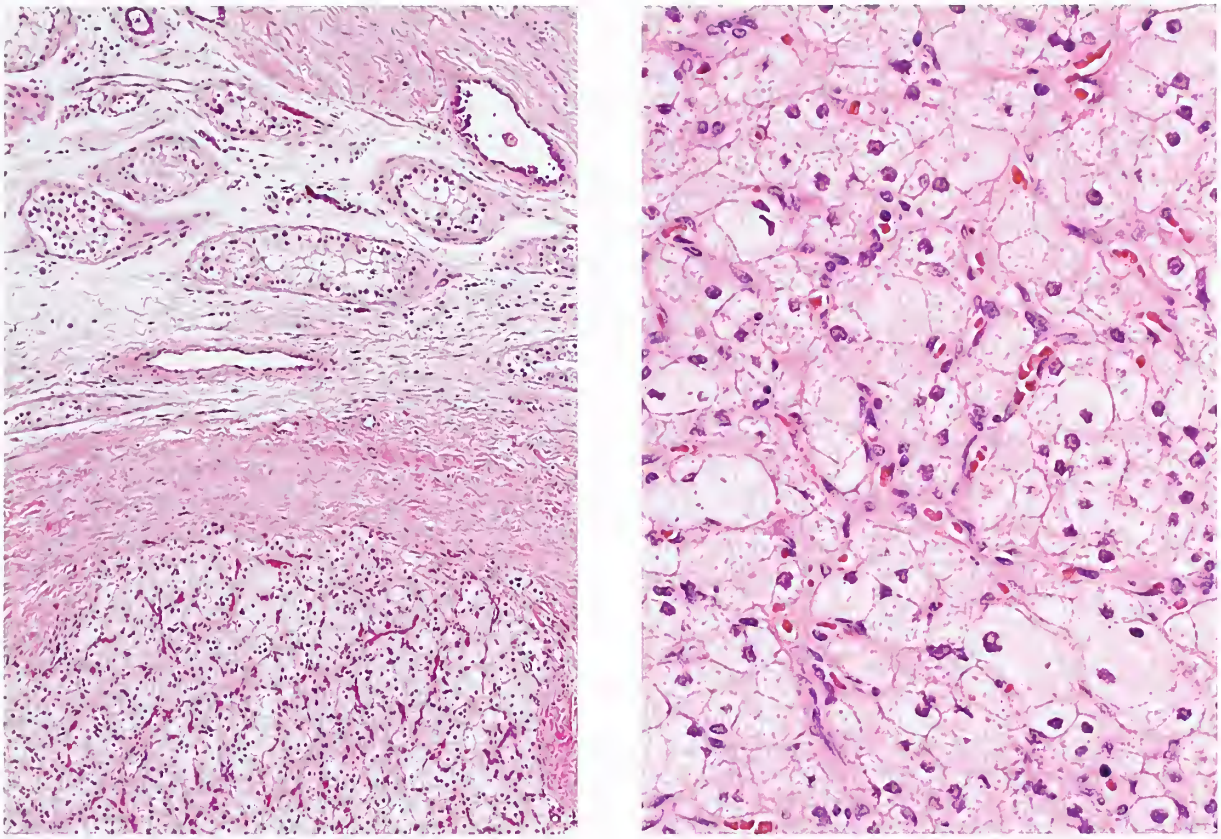

Figure 2-6

HETEROTOPIC/ACCESSORY ADRENAL CORTICAL TISSUE WITHIN THE TESTIS

Left: Heterotopic or accessory adrenal cortical tissue is encapsulated and presents as a small nodule within the testicular parenchyma. Seminiferous tubules are at the top of field. Inguinal orchiectomy was performed for possible malignancy.

Right: The nodule measured 1.4 cm in diameter. It is composed of cells with pale-staining, lipid-rich, finely vacuolated cytoplasm.

patients are asymptomatic. In two thirds of patients with the classic form of CAH, biosynthesis of aldosterone is blocked, resulting in "salt wasting"; the remaining one third have a simple virilizing form of the disease.

Other enzymatic deficiencies causing CAH include: 1) 11-beta-hydroxylase deficiency which causes virilization and often hypertension due to the accumulation of deoxycorticosterone; 2) 3-beta-hydroxysteroid dehydrogenase deficiency which results in intersexuality and salt-wasting in severe cases; 3) 17-alpha-hydroxylase deficiency which is associated with hypertension, hypokalemia, and incomplete masculinization; and 4) a mutation in the steroidogenic acute regulatory protein (StAR) which plays a critical role in regulating the rate-limiting stop in steroid hormone biosynthesis, cholesterol side-chain cleavage. The StAR protein facilitates the entry of cholesterol into mitochondria to initiate steroidogenesis. Mutations in this protein cause *congenital lipoid adrenal hyperplasia*, the most severe form of CAH (22). The disorder is usually fatal despite replacement therapy.

The clinical manifestations of CAH are the result of a deficiency of a particular steroid such as cortisol and/or the effects of steroids that accumulate proximal to the site of enzymatic deficiency and may be shunted into alternate biosynthetic pathways, particularly androgen synthesis. Males with the salt-losing form of 21-hydroxylase deficiency are at particular risk for salt-wasting and may have signs and symptoms (e.g., vomiting, dehydration, and hypotension) that resemble an Addisonian crisis within a few

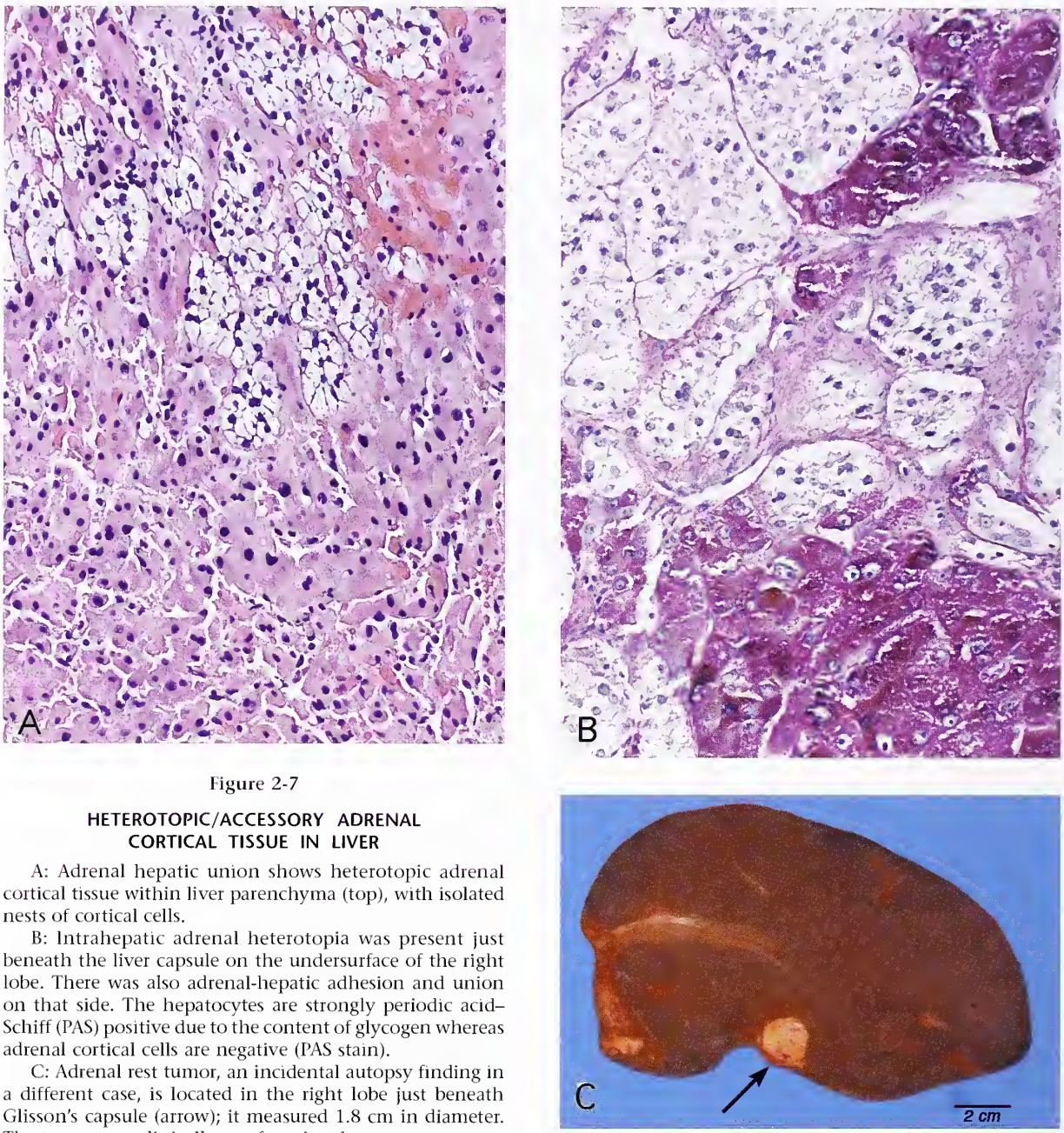

Figure 2-7

HETEROTOPIC/ACCESSORY ADRENAL CORTICAL TISSUE IN LIVER

A: Adrenal hepatic union shows heterotopic adrenal cortical tissue within liver parenchyma (top), with isolated nests of cortical cells.

B: Intrahepatic adrenal heterotopia was present just beneath the liver capsule on the undersurface of the right lobe. There was also adrenal-hepatic adhesion and union on that side. The hepatocytes are strongly periodic acid–Schiff (PAS) positive due to the content of glycogen whereas adrenal cortical cells are negative (PAS stain).

C: Adrenal rest tumor, an incidental autopsy finding in a different case, is located in the right lobe just beneath Glisson's capsule (arrow); it measured 1.8 cm in diameter. The tumor was clinically nonfunctional.

weeks of birth. If the female fetus is exposed to increased androgens in utero there is a variable degree of virilization of external genitalia, while the internal female organs are relatively normal. The typically ambiguous genitalia in these female infants include clitoromegaly and fusion of labioscrotal folds, which may be bulbous and rugated, thus simulating a scrotum (fig. 2-9). The clitoris may be bound somewhat by a "chordee." In a small number of infants, the degree of virilization is so marked that there is a fully masculinized penile urethra. The masculinized female may be incorrectly classified as a male (fig. 2-9), but the error is recognized when a salt-losing crisis develops at 1 to 4 weeks of age. Sociocultural problems may arise if gender reassignment becomes an issue in masculinized female patients with delayed presentation.

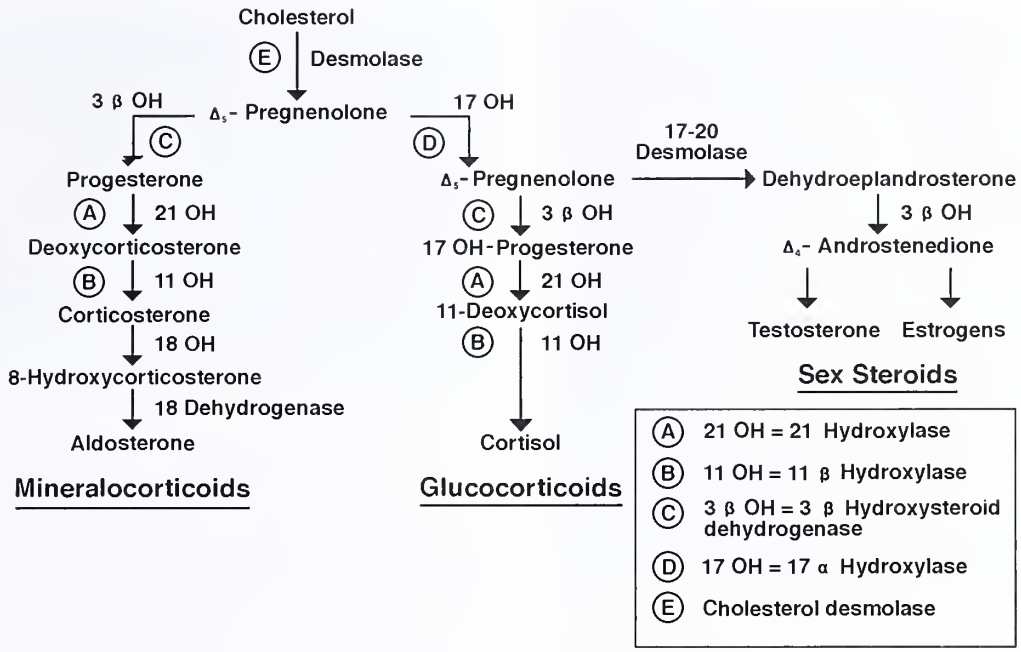

Figure 2-8

BIOSYNTHETIC PATHWAYS OF MINERALOCORTICOIDS, GLUCOCORTICOIDS, AND SEX STEROIDS

Sites of enzymatic block in congenital adrenal hyperplasia (CAH) are indicated by letters, with the corresponding enzymes. (Fig. 2-5 from Fascicle 19, Third Series.)

Figure 2-9

CONGENITAL ADRENAL HYPERPLASIA

This 18-month-old female was mistakenly assigned a male gender. The markedly enlarged clitoris resembles a penis. The hypertrophied clitoris had a urethral opening near the base. The rugosity of the partially fused labioscrotal folds simulates a scrotum. (Fig. 2-7 from Fascicle 19, Third Series.)

Masculinization of the external genitalia begins by 8 weeks of gestation (23). A prenatal diagnosis is possible, and maternal dexamethasone treatment may prevent virilization of the female fetus, thus obviating the need for corrective genital surgery after birth (21,23). Treatment failures may be due to early cessation of therapy, late start of treatment, noncompliance, suboptimal dosing, or differences in dexamethasone metabolism (23).

Figure 2-10

CONGENITAL ADRENAL HYPERPLASIA

Autopsy of an infant who died of the severe salt-losing form of 21-hydroxylase deficiency shows enlargement of both adrenal glands (arrows). The glands have a convoluted or cerebriform surface and are darker than normal due to intense persistent stimulation by adrenocorticotropic hormone (ACTH).

Figure 2-11

CONGENITAL ADRENAL HYPERPLASIA

The adrenal glands are enlarged and appear dark brown due to intense and persistent stimulation of the adrenal cortex by ACTH, which converts cortical cells into cells with compact, lipid-depleted cytoplasm. (Fig. 2-9 from Fascicle 19, Third Series.)

Pathology of Adrenal Glands in CAH

CAH may be fatal if unrecognized or untreated. At autopsy, the adrenal glands are enlarged, often tan or brown, and have a convoluted or cerebriform surface with redundant folds due to cortical hyperplasia (fig. 2-10). Individual adrenal glands in children weigh 10 to 15 g, while in older patients are 30 to 35 g (1). In most untreated cases of CAH the adrenal glands are darker than normal (fig. 2-11). In cholesterol desmolase deficiency (congenital lipoid adrenal hyperplasia), the accumulation of cholesterol and cholesterol esters may give rise to a nodular cortex which is bright yellow or whitish. Microscopically, there may be cholesterol clefts with a foreign body giant cell reaction and dystrophic calcification.

In CAH, persistent and intense trophic stimulation by adrenocorticotropic hormone (ACTH) results in marked hyperplasia of the zona fasciculata with conversion of pale-staining, lipid-rich cells into lipid-depleted cells with compact, eosinophilic cytoplasm similar to those of the zona reticularis (fig. 2-12); these morphologic findings, however, may vary if the patient is partially treated with exogenous corticosteroids. This contributes, in large measure, to the dark color of the glands. With partial or incomplete steroid replacement, the histologic picture may become altered, with columns and cords of lipid-rich cells admixed with some cells having lipid-depleted cytoplasm. Heterotopic or accessory adrenal cortical tissue can also become enlarged and hyperplastic (fig. 2-13).

Adrenal Cortical Neoplasms in the Setting of CAH

Persistent trophic stimulation of adrenal cortical tissue by ACTH gives rise to diffuse, and at times, slightly nodular hyperplasia, and there have been rare cases of adrenal cortical neoplasia occurring in the setting of CAH (1). The reported tumors have included both adrenal cortical adenomas (24) and carcinomas (25). In two cases, adrenal cortical carcinomas developed in patients with a longstanding (30 years and 36 years) history of virilization with onset in childhood, suggesting untreated CAH (1,26). Activation of virilizing adrenal rest tumors has been reported in a patient with Nelson's syndrome (27), in areas of accessory adrenal cortical tissue, originally described by Marchand (12). An increased incidence of incidental adrenal

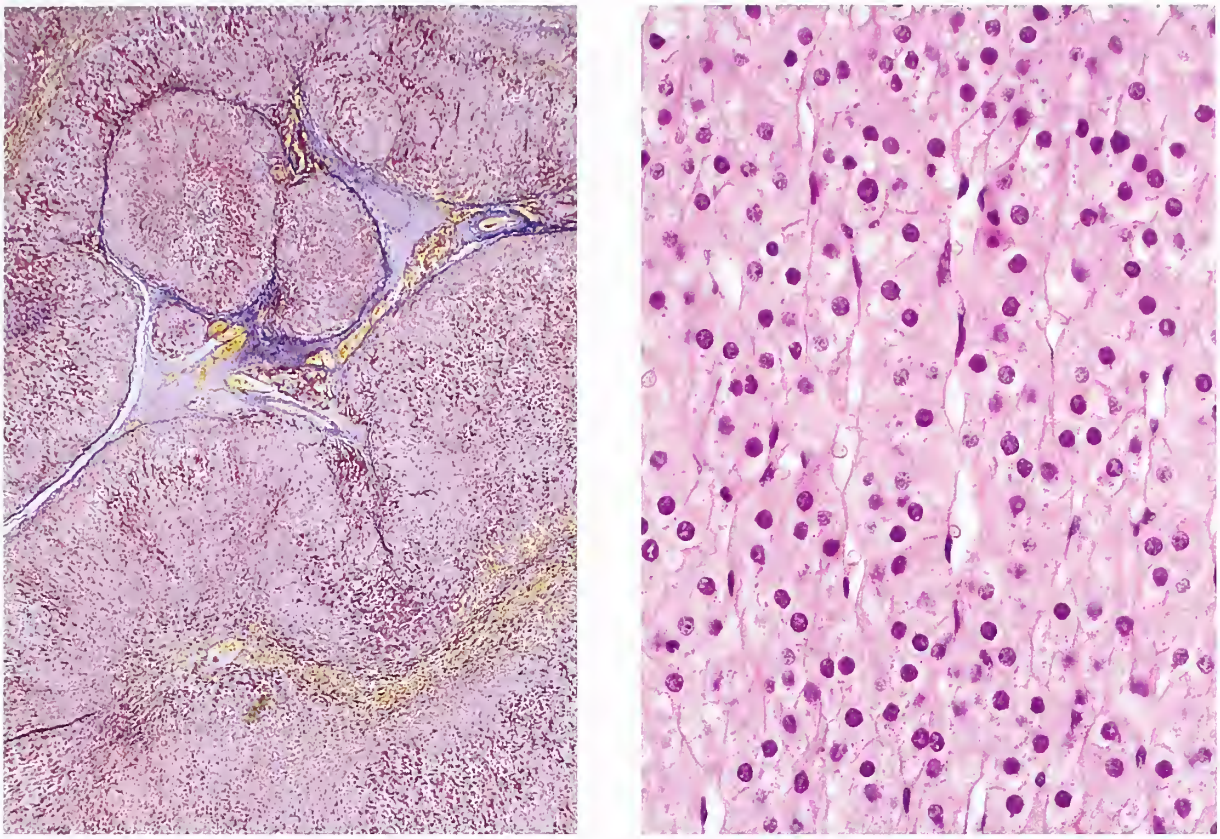

Figure 2-12

CONGENITAL ADRENAL HYPERPLASIA

Left: Marked expansion of the zona fasciculata in a child with CAH. Many cells have lipid-depleted cytoplasm due to sustained stimulation by ACTH. There are enlarged, hyperplastic accessory cortical nodules, or extrusions (toluidine blue eosin stain). (Fig. 2-10, top from Fascicle 19, Third Series.)

Right: Hyperplastic zona fasciculata in CAH is composed of cells with lipid-depleted, compact, eosinophilic cytoplasm.

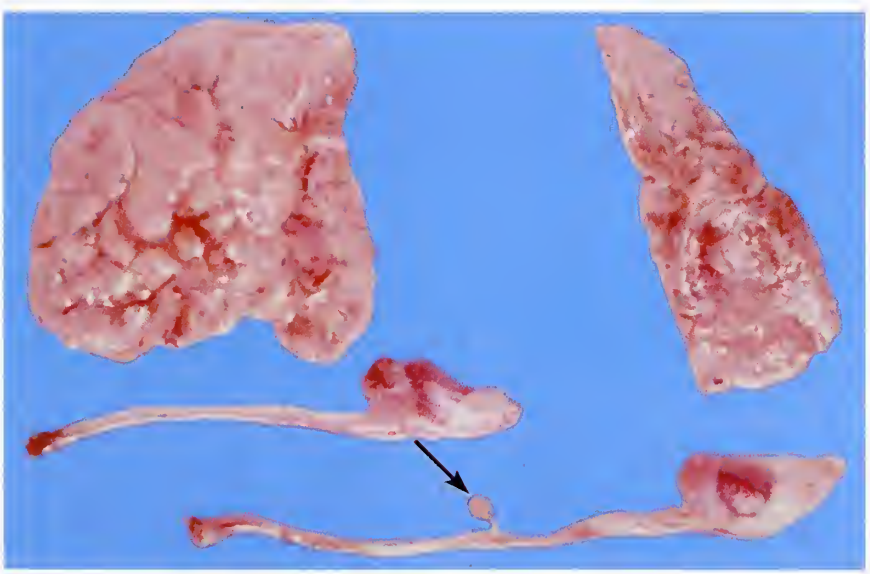

Figure 2-13

ENLARGED HYPERPLASTIC ADRENAL GLANDS IN A FATAL CASE OF CAH

An enlarged heterotopic/accessory nodule of adrenal cortex is present along the spermatic cord (arrow).

nodule(s) has been seen in patients with homozygous (82 percent of patients; 2 cases were bilateral) and heterozygous (45 percent of patients) traits for CAH; the lesions were assumed to be adrenal cortical adenomas without evidence of excess steroid secretion (28). In the group of patients with the homozygous trait, tumors were 5 to 9 mm (9 patients), 1 to 2 cm (7 patients), and over 5 cm (2 patients); the tumors in the heterozygous group showed a similar size distribution. It is uncertain whether these lesions represent a true cortical neoplasm which is nonhyperfunctional, or a dominant macronodule arising in a background of cortical hyperplasia.

Testicular Tumors in the Setting of CAH

Definition. *Testicular tumors* associated with CAH are tumefactive lesions of uncertain histogenesis which histologically resemble a Leydig or interstitial cell tumor, but may have features in common with hyperplastic adrenal cortical cells under the trophic influence of ACTH. Endocrinologic evaluation of the testicular lesions may reveal ACTH dependency and the ability to produce glucocorticoids.

General Considerations. Testicular hilar nodules have been identified in a large proportion of patients with CAH (29), and while most of these collections of cells morphologically resemble Leydig cells (1), some consider them to be a primordial rest (29). Extratesticular Leydig-like cells have been noted in tunica albuginea, rete testis, epididymis, and spermatic cord; in one prospective study, extratesticular Leydig cells were detected in 87 percent of surgical specimens that included paratesticular connective tissue as compared with a 30 percent detection rate in a retrospective analysis (30). Extratesticular Leydig cells are usually seen in association with nerves or, occasionally, small vascular channels. Curiously, they do not stain immunohistochemically for testosterone as do intratesticular Leydig cells (30).

Ultrasonography is more sensitive for detecting testicular nodules than manual palpation (31) and is the cheapest and quickest imaging technique; using this modality, testicular abnormalities are noted in 27 (32) to 94 percent (33) of postpubertal male patients with CAH. In a recent study, lesions were typically located adjacent to the hilum of the testis and the diameter of the lesions varied from 2 to 40 mm (33). Many of these testicular nodules are clinically undetectable. In another study, the nodules were hypoechoic, ranged in size from 0.2 to 2.8 cm (average, 1.6 cm), were bilateral in 6 of 8 patients (75 percent), and multifocal in each case (32). In another study, 3 of 36 males with CAH (8.2 percent) followed over a 30-year period developed a testicular mass 1 to 2 cm in size; the nodules were bilateral in 2 patients, and typically occupied the upper half of the testicle near the hilum (note the location of the adrenal cortical rest in figure 2-5) (34). In case of partial orchiectomy, magnetic resonance imaging (MRI) has been recommended because it shows lesion margins optimally (33).

Poor medical compliance with replacement steroid therapy in patients with CAH has in some cases led to excess ACTH stimulation. Bilateral adrenal rest tumors of the testicles were reported in a male cushinoid patient with von Hippel-Lindau disease after bilateral adenalectomy; bilateral testicular venous sampling revealed elevated glucocorticoids that were responsive to dexamethasone suppression. Conservative management with appropriate steroid therapy and radiographic evaluation was successful in this case (35). Adrenal rest tumors and hyperplasia have also been noted in patients with Nelson's syndrome (36) and primary Addison's disease (31). Bilateral ovarian tumors that are histologically identical to the testicular tumors have been reported in a patient with 21-hydroxylase deficiency (37), but in a recent study of 13 female patients with CAH, no ovarian adrenal rest tumors were detected by ovarian imaging, suggesting that these tumors are rare (38).

Pathologic Findings. A review of testicular tumors in CAH showed that two thirds were palpable (up to 10 cm), occurrence was usually in early adult life (average age, 22.5 years), smaller tumors (less than 2 cm) were usually seen in children, and 86 percent were located in the hilum of the testis (39). The tumors were bilateral in 83 percent of patients (39) compared to only 2.5 percent bilaterality for Leydig cell tumors (40).

On cross section, the larger tumors are unencapsulated, bulging, multinodular masses separated by prominent bands of fibrous connective tissue (fig. 2-14). They are often light tan-brown, due in part to lipochrome pigment and probably

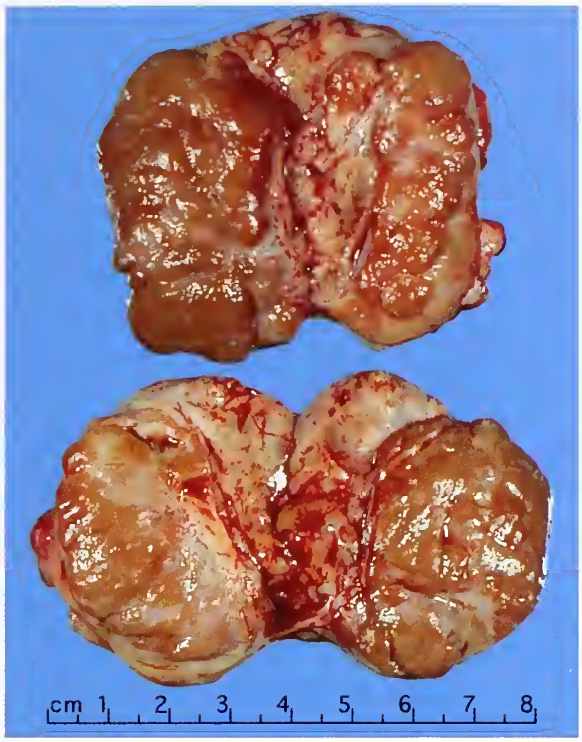

Figure 2-14

BILATERAL ORCHIECTOMY SPECIMENS FROM A 25-YEAR-OLD MALE WITH SALT-LOSING FORM OF 21-HYDROXYLASE DEFICIENCY

On cross section, both testes are almost completely replaced by bulging nodules of tan tumor. Surgery was done to alleviate severe pain and swelling which was not adequately controlled with suppressive doses of dexamethasone. The testicular tumor was shown to be ACTH dependent. (Fig. 2-13 from Fascicle 19, Third Series.)

diminished cytoplasmic lipid, particularly in cases with inadequate suppression of ACTH. In several cases there have been multiple extratesticular nodules as large as 1.5 cm along the spermatic cord or adjacent to the epididymis (39).

Microscopically, there are interconnecting sheets and nests of cells with granular pink cytoplasm and relatively distinct cell borders (fig. 2-15, top). The tumor also has an intimate pattern of reticulum, with isolation of individual or small nests of cells (fig. 2-15, bottom). This is in contrast to the broad radial cords of cells usually seen in hyperplasia of entopic or heterotopic adrenal cortex. Occasionally, there are interstitial adipocytes (fig. 2-16). Sections taken through the testicular hilum and rete testis may show involvement by tumor (fig. 2-17).

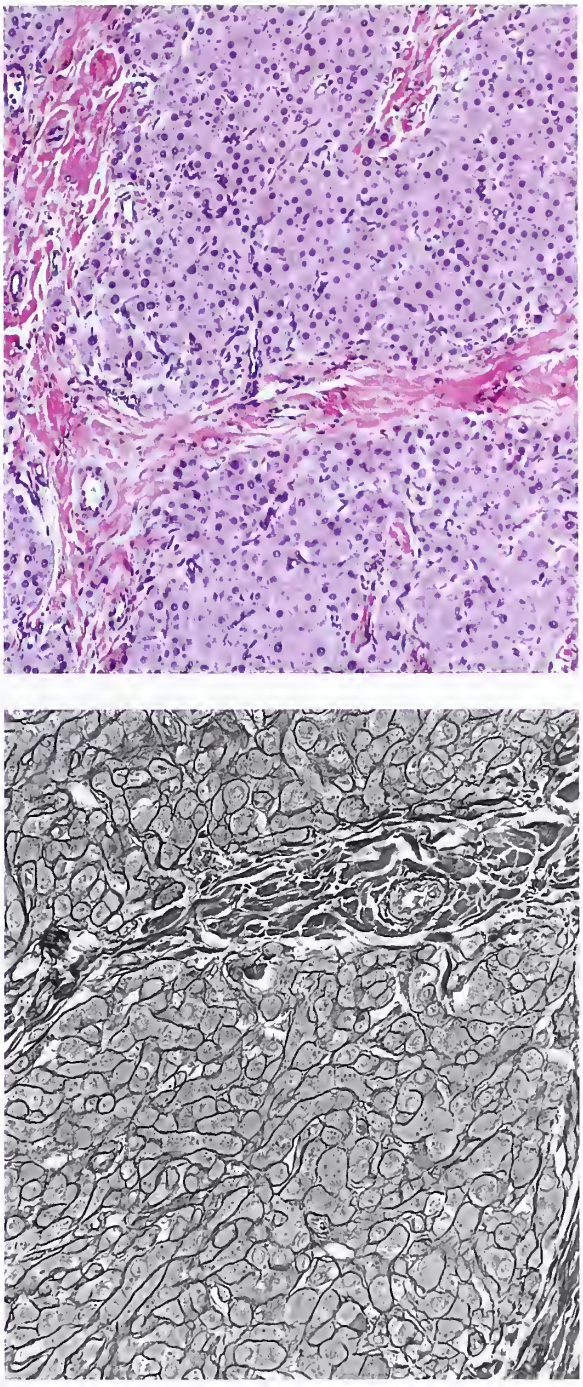

Figure 2-15

TESTICULAR TUMOR IN PATIENT WITH SALT-LOSING FORM OF 21-HYDROXYLASE DEFICIENCY

Top: Tumor cells are in lobules and solid sheets, with some intervening fibrous stroma.

Bottom: The reticulum staining pattern isolates individual and small groups of cells (reticulum stain). (T&B: Fig. 2-14 from Fascicle 19, Third Series.)

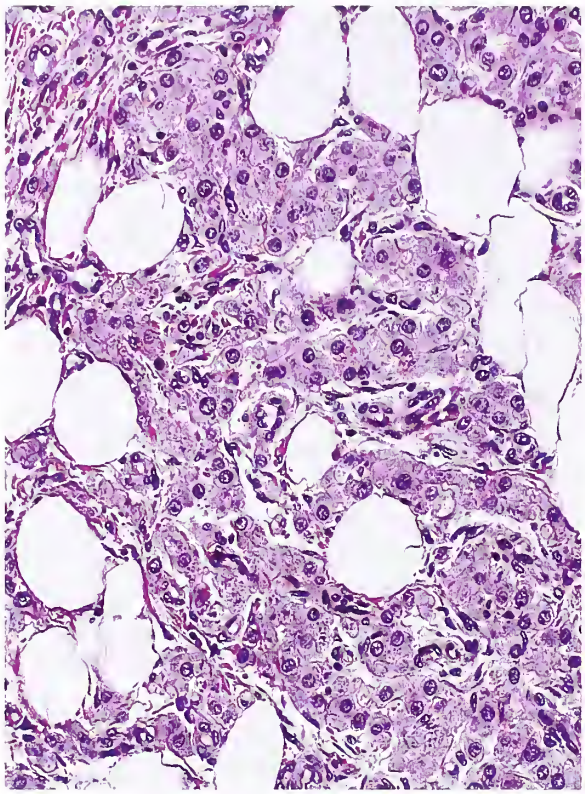

Figure 2-16

TESTICULAR TUMOR IN CAH

The small clusters of mature adipose tissue represent lipomatous metaplasia. (Fig. 2-15 from Fascicle 19, Third Series.)

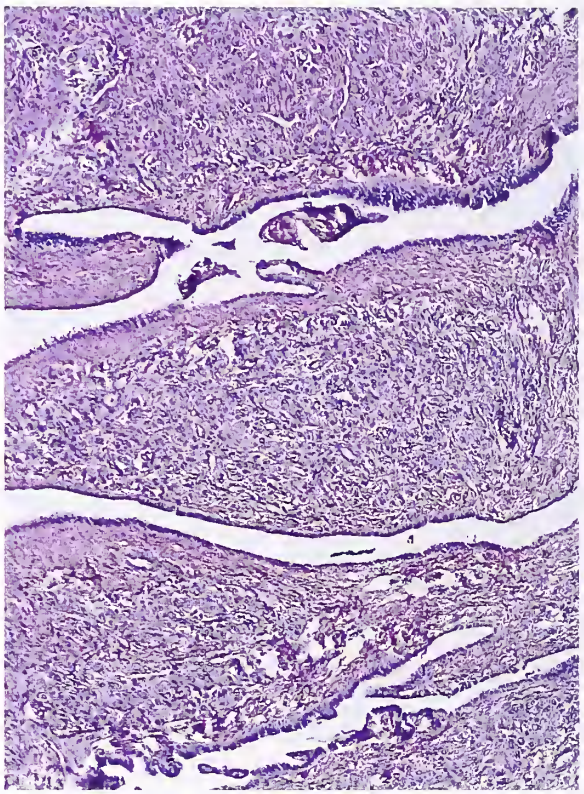

Figure 2-17

TESTICULAR TUMOR IN CAH

The rete testis is involved by the testicular tumor. Under normal conditions, heterotopic/accessory adrenal cortical tissue can be found in this area (see figure 2-5). (Fig. 2-16 from Fascicle 19, Third Series.)

Most tumor cells contain prominent lipochrome pigment (lipofuscin). Nuclei are fairly uniform and round to oval, with one or two small, central to eccentric nucleoli (fig. 2-18); occasionally there may be some nuclear enlargement. Mitotic figures are uncommon. There is a great resemblance to Leydig cells, and indeed the diagnosis usually made is Leydig or interstitial cell tumor. The cells also resemble the lipid-depleted cells of adrenal myelolipoma which arise in the setting of CAH. Reinke crystalloids, a pathognomonic marker for Leydig cells, and found in about 35 percent of Leydig cell tumors (40), are not a feature of testicular tumors of CAH. Adjacent testicular parenchyma may appear almost normal or atrophic with sclerosis and decreased spermatogenesis.

Ultrastructurally, the cells have features of steroid-producing cells: abundant smooth endoplasmic reticulum, numerous mitochondria, and accumulation of lipofuscin (fig. 2-19, left). The mitochondrial cristae may be lamellar or vesicular (fig. 2-19, above).

Histogenesis and Biologic Behavior. The cell of origin for these tumors is uncertain, but they can be distinguished from Leydig cell tumors by their distinctive clinical, biochemical, and pathologic features. Several studies have documented a dependence on ACTH, with increased levels of steroids (17-hydroxyprogesterone, cortisol, and 11-beta-hydroxylated steroids) in the testicular venous effluent (41). Suppression of ACTH with dexamethasone can greatly decrease testicular size to near normal, while trophic stimulation can cause testicular enlargement with recurrence of pain and tenderness (fig. 2-14). Orchiectomy may not be necessary since the tumor may not be truly

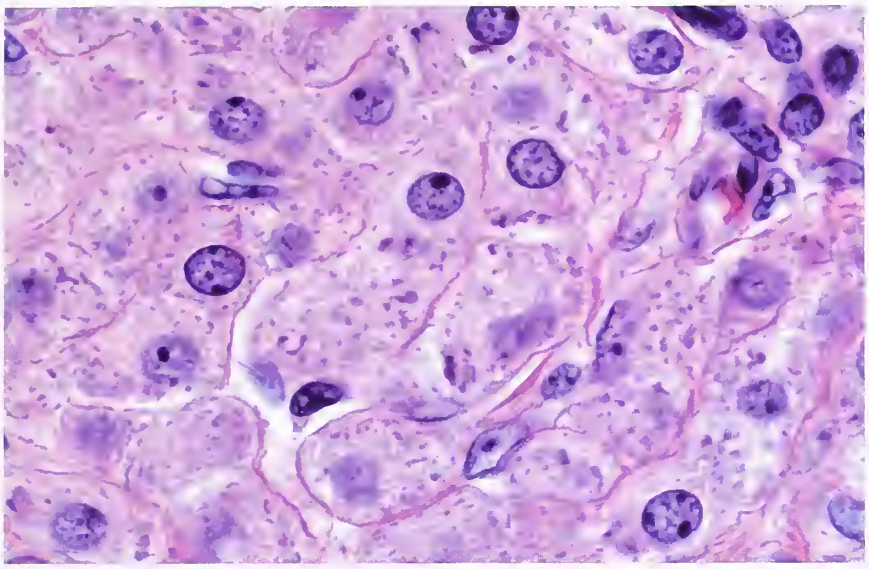

Figure 2-18

TESTICULAR TUMOR IN CAH

Individual cells have distinct cell borders and rounded nuclei, often with one or two eccentric nucleoli. Many cells contain coarse, granular pigment, which is lipofuscin.

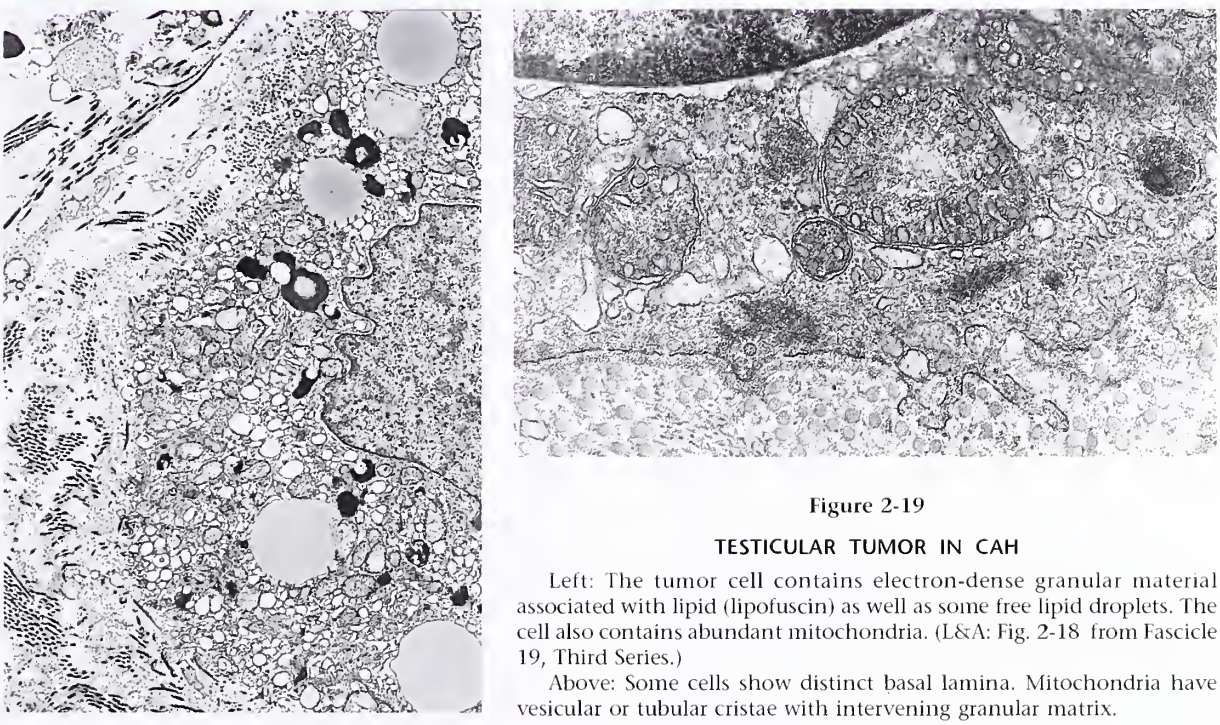

Figure 2-19

TESTICULAR TUMOR IN CAH

Left: The tumor cell contains electron-dense granular material associated with lipid (lipofuscin) as well as some free lipid droplets. The cell also contains abundant mitochondria. (L&A: Fig. 2-18 from Fascicle 19, Third Series.)

Above: Some cells show distinct basal lamina. Mitochondria have vesicular or tubular cristae with intervening granular matrix.

neoplastic in view of its dependence on ACTH and the lack of malignant behavior in cases reported to date (35,39). Conflicting opinions exist as to whether the tumor arises from Leydig cells, adrenal cortical rests, or multipotent testicular stromal cells that are capable of multidirectional differentiation depending upon the microenvironment and hormonal milieu.

Other Tumors in the Setting of CAH

Adrenal myelolipoma has been reported in the setting of CAH in a patient with 21-hydroxylase deficiency (42), and in another with deficiency of 17-hydroxylase (43); in these cases there was marked hyperplasia of adrenal cortical cells admixed with the myelolipoma (fig. 2-20). Several extraadrenal, seemingly unrelated

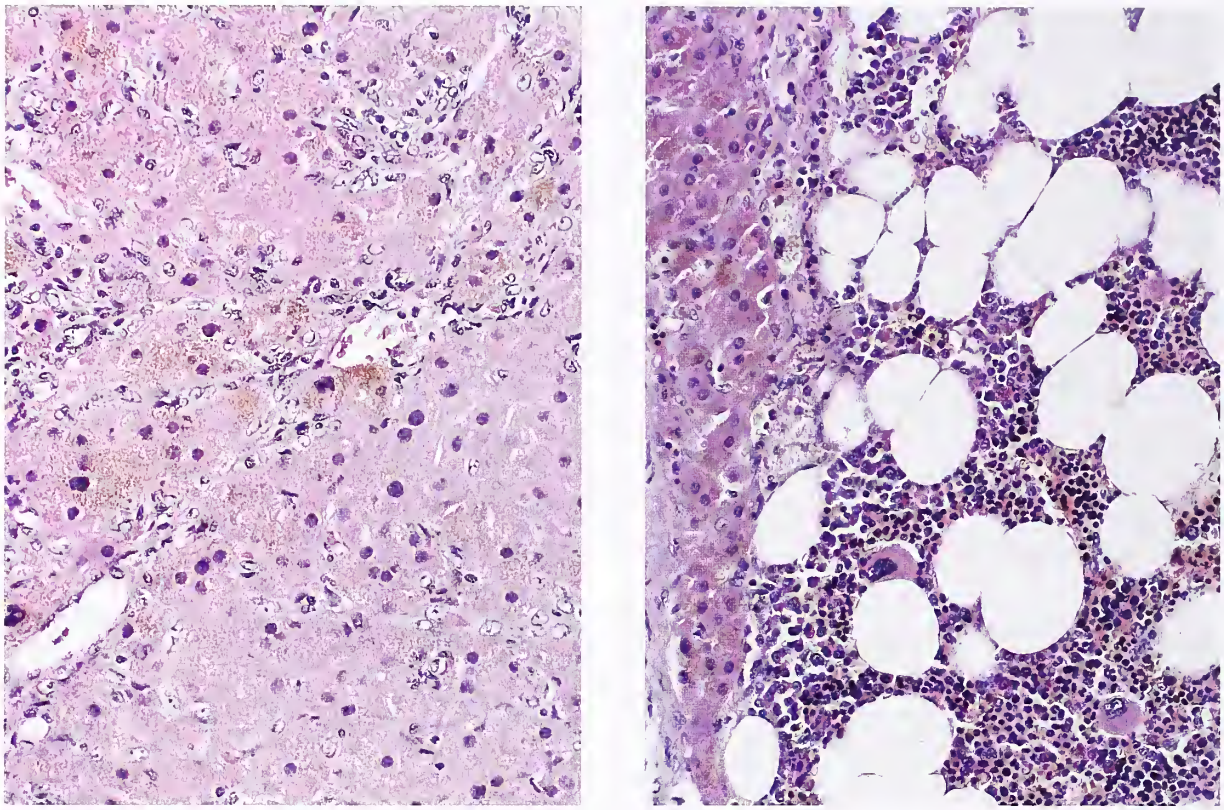

Figure 2-20

ADRENAL MYELOLIPOMA IN CAH

Left: Huge, bilateral adrenal myelolipomas in an adult male with CAH. The hyperplastic adrenal cortical tissue is remarkably similar to that of the testicular tumors of CAH illustrated previously. The granular pigment within some cells represents lipofuscin. Right: Most of the bilateral adrenal tumors was composed of myelolipoma. (L&R: Fig. 2-19 from Fascicle 19, Third Series.)

neoplasms have been reported such as *osteosarcoma, Ewing's sarcoma,* and *astrocytoma* (44).

BECKWITH-WIEDEMANN SYNDROME

Beckwith-Wiedemann syndrome (BWS) is a congenital human overgrowth disorder associated with dysregulation of the imprinting of genes in chromosome 11p15.5 (45). BWS is sometimes referred to by the acronym *EMG (exomphalos, macroglossia,* and *gigantism) syndrome.*

The estimated frequency of BWS is 1/13,000 births, of which 85 percent are sporadic. Some form of mendelian inheritance is responsible for familial cases; one study reported an autosomal dominant pattern with incomplete penetrance (46). The infant death rate is about 20 percent (46). The main clinical manifestation, hyperinsulinemic hypoglycemia, is related to defects in the function of pancreatic beta-cell adenosine triphosphate (ATP)-sensitive potassium channels (47). Failure to recognize the hypoglycemia may lead to permanent brain damage, mental deficiency, or death.

In a review by Wiedemann (48), 7.5 percent of children with BWS developed a malignant tumor, usually nephroblastoma (Wilms' tumor) or adrenal cortical carcinoma. Other associated neoplasms include neuroblastoma, pancreatoblastoma (49), pheochromocytoma (50), and rare cardiac tumors (51).

Cytogenetic abnormalities include loss of somatic heterozygosity for a locus on chromosome 11 in patients with adrenal cortical neoplasms associated with this disorder. The gene involved in the predisposition to adrenal cortical neoplasms has been mapped to region

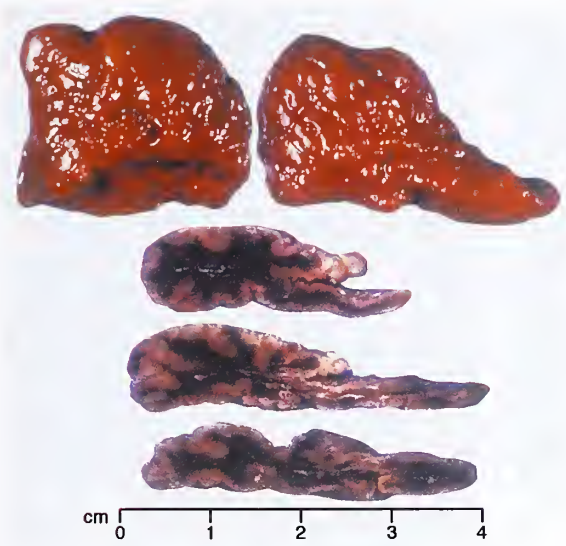

Figure 2-21

BECKWITH-WIEDEMANN SYNDROME

Adrenal glands from a 3-week-old infant with Beckwith-Wiedemann syndrome are enlarged and show excessive cortical nodularity and redundant folds on the external aspect (top). Cytomegaly affected much of the fetal, or provisional, zone.

11p15.5 (52). BWS overlaps with Sotos' syndrome, another overgrowth disorder (53).

BWS was described by Beckwith in 1963 (54) and by Wiedemann the following year (55), and includes a variety of abnormalities: craniofacial features such as ear creases and/or pits, nevus flammeus, midfacial hypoplasia, abdominal wall defects, visceromegaly, gigantism, and macroglossia. Giant omphalocele and "prune belly" have been reported as rare lethal complications (56). The adrenal glands are enlarged with a combined weight often up to 16 g, and due to cortical hyperplasia, may show redundant cortical folds and nodularity which may have a cerebriform configuration (fig. 2-21). Marked adrenal cytomegaly is a characteristic feature, and is bilateral, usually affecting most cells in the fetal cortex (fig. 2-22); in addition to enlarged pleomorphic nuclei, pseudoinclusions can be seen (fig. 2-22). Chromaffin cells have been reported to be strikingly hyperplastic within adrenal (fig. 2-23) and extraadrenal sites (49,54). Cortical microcysts may be present in the adult cortex on histologic examination. Rarely, hemorrhagic macrocysts of the adrenal cortex are the cause of an abdominal mass in the fetus and neonate with BWS (57). BWS has been associated with ectopic pancreatic tissue on rare occasion (58).

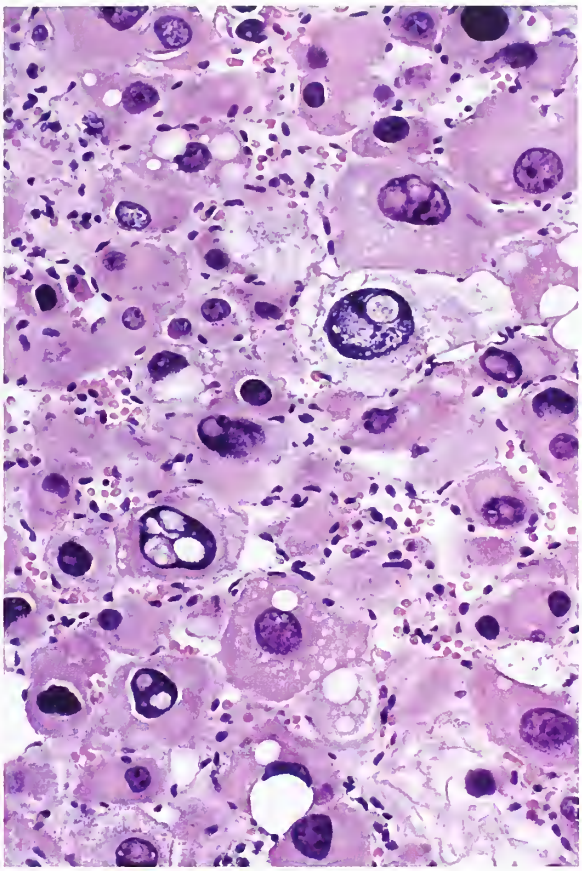

Figure 2-22

BECKWITH-WIEDEMANN SYNDROME

Marked adrenal cytomegaly involves cells of the fetal, or provisional, cortex. Note the nucleomegaly and hyperchromasia, and the presence of nuclear "pseudoinclusions." Mitotic figures were not identified.

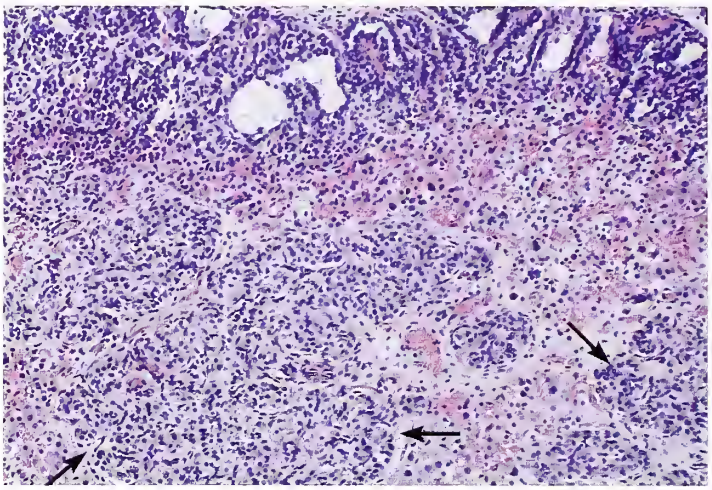

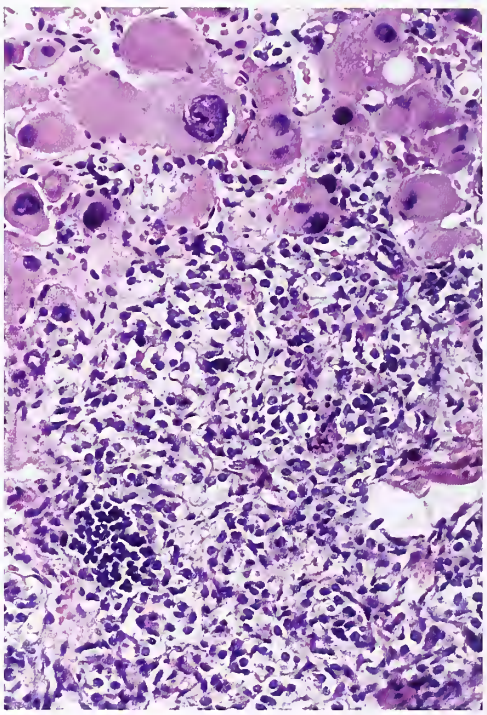

Figure 2-23

NEWBORN WITH BECKWITH-WIEDEMANN SYNDROME

Above: Nests of adrenal chromaffin cells are hyperplastic and inappropriately mature for this stage of development (arrows). Microcysts are present in the adult cortex. (Fig. 2-22 from Fascicle 19, Third Series.)

Right: Hyperplastic chromaffin cells contrast with the cytomegalic cells of the fetal cortex.

REFERENCES

Adrenal Adhesion, Union, and Fusion

1. Lack EE, Kozakewich HP. Embryology, developmental anatomy, and selected aspects of nonneoplastic pathology. In: Lack EE, ed. Pathology of the adrenal glands. New York: Churchill Livingstone; 1990:1-74.
2. Pakravan P, Kenny FM, Depp R, Allen AC. Familial congenital absence of adrenal glands; evaluaton of glucocorticoid, mineralocorticoid, and estrogen metabolism in the perinatal period. J Pediatr 1974;84:74-78.

Heterotopic and Accessory Adrenal Tissue

3. Labarrere CA, Caccamo D, Telenta M, Althabe O, Gutman R. A nodule of adrenocortical tissue within a human placenta: light microscopic and immunocytochemical findings. Placenta 1984;5:139-144.
4. Armin A, Castelli M. Congenital adrenal tissue in the lung with adrenal cytomegaly. Case report and review of the literature. Am J Clin Pathol 1984;82:225-228.
5. Wiener MF, Dallgaard SA. Intracranial adrenal gland; a case report. AMA Arch Pathol 1959;67: 120-125.
6. Honoré LH. Intra-adrenal hepatic heterotopia. J Urol 1985;133:652-654.
7. Shiraishi T, Imai H, Fukutome K, Watanabe M, Yatani R. Ectopic thyroid in the adrenal gland. Hum Pathol 1999;30:105-108.
8. Graham LS. Celiac accessory adrenal glands. Cancer 1953;6:149-152.
9. Apitz K. Die geschwülste und Gewebsmissbildungen der Nierenrinde. I. Mitteilng: Die intrarenalen Nebenniereninseln. Virchows Arch (Pathol Anat) 1943;311:285-305.
10. Busuttil A. Ectopic adrenal within the gall-bladder wall. J Path 1974;113:231-233.
11. O'Crowley CR, Martland HS. Adrenal heterotopia, rests and the so-called Grawitz tumor. J Urol 1943;50:756-768.
12. Marchand F. Ueber accessorische nebennieren im ligamentum latum. Virchows Arch 1883;92:11-19.
13. Falls JL. Accessory adrenal cortex in the broad ligament: incidence and functional significance. Cancer 1955;8:143-150.

14. Mares AJ, Shkolnik A, Sacks M, Feuchtwanger MM. Aberrant (ectopic) adrenocortical tissue along the spermatic cord. J Ped Surg 1980;15: 289-292.
15. Dahl EV, Bahn RC. Aberrant adrenal cortical tissue near the testis in human infants. Am J Pathol 1962;40:587-598.
16. Roosen-Runge EC, Lund J. Abnormal sex cord formation and an intratesticular adrenal cortical nodule in a human fetus. Anat Rec 1972;173: 57-67.
17. Symonds DA, Driscoll SG. An adrenal cortical rest within the fetal ovary: report of a case. Am J Clin Pathol 1973;60:562-564.
18. Morimoto Y, Hiwada K, Nanahoshi M, et al. Cushing's syndrome caused by malignant tumor in the scrotum: clinical, pathologic and biochemical studies. J Clin Endocrinol Metab 1971; 32:201-210.
19. Wallace EZ, Leonidas JR, Stanek AE, Avramides A. Endocrine studies in a patient with functioning adrenal rest tumor of the liver. Am J Med 1981;70:1122-1125.

Congenital Adrenal Hyperplasia

20. de Crecchio L. Sopra un caso di apparenze virili in una donna. Morgagni 1865;7:151-188.
21. New MI. An update of congenital adrenal hyperplasia. Ann N Y Acad Sci. 2004;1038:14-43.
22. Chen X, Baker BY, Abduljabbar MA, Miller WL. A genetic isolate of congenital lipoid adrenal hyperplasia with atypical clinical findings. J Clin Endocrinol Metab 2005;90:835-840.
23. Merke DP, Bornstein SR. Congenital adrenal hyperplasia. Lancet. 2005;365:2125-2136.
24. Pang S, Becker D, Cotelingam J, Foley TP Jr, Drash AL. Adrenocortical tumor in a patient with congenital adrenal hyperplasia due to 21-hydroxylase deficiency. Pediatrics 1981;68:242-246.
25. Bauman A, Bauman CG. Virilizing adrenocortical carcinoma. Development in a patient with salt-losing congenital adrenal hyperplasia. JAMA 1982;248:3140-3141.
26. Nogeire C, Fukushima DK, Hellman L, Boyar RM. Virilizing adrenal cortical carcinoma. Cancer 1977;40:307-313.
27. Verdonk C, Guerin C, Lufkin E, Hodgson SF. Activation of virilizing adrenal rest tissues by excessive ACTH production. An unusual presentation of Nelson's syndrome. Am J Med 1982;73:455-459.
28. Jaresch S, Kornely E, Kley HK, Schlaghecke R. Adrenal incidentaloma and patients with homzygous or heterozygous congenital adrenal hyperplasia. J Clin Endocrinol Metab 1992;74:685-689.
29. Shanklin DR, Richardson AP Jr, Rothstein G. Testicular hilar nodules in adrenogenital syndrome. The nature of the nodules. Am J Dis Child 1963;106:43-50.
30. Grignon DJ, Ro JY, Ordonez NG, Ayala AG. Extratesticular interstitial cells. Am J Surg Pathol 1988;12:735-736.
31. Seidenwurm D, Smathers RL, Kan P, Hoffman A. Intratesticular adrenal rests diagnosed by ultrasound. Radiology 1985;155:479-481.
32. Vanzulli A, DelMaschio A, Paesano P, et al. Testicular masses in association with adrenogenital syndrome: US findings. Radiology 1992;183:425-429.
33. Stikkelbroeck NM, Suliman HM, Otten BJ, Hermus AR, Blickman JG, Jager GJ. Testicular adrenal rest tumours in postpubertal males with congenital adrenal hyperplasia: sonographic and MR features. Eur Radiol 2003;13:1597-1603.
34. Srikanth MS, West BR, Ishitani M, Isaacs H Jr, Applebaum H, Costin G. Benign testicular tumors in children with congenital adrenal hyperplasia. J Ped Surg 1992;27:639-641.
35. Weeks DC, Walther MM, Stratakis CA, Hwang JJ, Linehan WM, Phillips JL. Bilateral testicular adrenal rests after bilateral adrenalectomies in a cushingoid patient with von Hippel-Lindau disease. Urology 2004;63:981-982.
36. Johnson RE, Scheithauer B. Massive hyperplasia of testicular adrenal rests in a patient with Nelson's syndrome. Am J Clin Pathol 1982;77: 501-507.
37. Al-Ahmadie HA, Stanek J, Liu J, Mangu PN, Niemann T, Young RH. Ovarian 'tumor' of the adrenogenital syndrome: the first reported case. Am J Surg Pathol 2001;25:1443-1450.
38. Stikkelbroeck NM, Hermus AR, Schouten D, et al. Prevalence of ovarian adrenal rest tumours and polycystic ovaries in females with congenital adrenal hyperplasia: results of ultrasonography and MR imaging. Eur Radiol 2004;14:1802-1806.
39. Rutgers JL, Young RH, Scully RE. The testicular "tumor" of the adrenogenital syndrome. A report of six cases and review of the literature on testicular masses in patients with adrenocortical disorders. Am J Surg Pathol 1988;12:503-513.
40. Kim I, Young RH, Scully RE. Leydig cell tumors of the testis. A clinicopathological analysis of 40 cases and review of the literature. Am J Surg Pathol 1985;9:177-192.
41. Radfar N, Bartter FC, Easley R, Kolins J, Javadpour N, Sherins RJ. Evidence for endogenous LH suppression in a man with bilateral testicular tumors and congenital adrenal hyperplasia. J Clin Endocrinol Metab 1977;45:1194-1204.

42. Boudreaux D, Waisman J, Skinner DG, Low R. Giant adrenal myelolipoma and testicular interstitial cell tumor in a man with congenital 21-hydroxylase deficiency. Am J Surg Pathol 1979;3:109-123.
43. Condom E, Villabona CM, Gómez JM, Carrera M. Adrenal myelolipoma in a woman with congenital 17-hydroxylase deficiency. Arch Pathol Lab Med 1985;109:1116-1118.
44. Duck SC. Malignancy associated with congenital adrenal hyperplasia. J Pediatr 1981;99:423-424.

Beckwith-Wiedemann Syndrome

45. Lew JM, Fei YL, Aleck K, Blencowe BJ, Weksberg R, Sadowski PD. CDKN1C mutation in Wiedemann-Beckwith syndrome patients reduces RNA splicing efficiency and identifies a splicing enhancer. Am J Med Genet A 2004:15; 127:268-276.
46. Pettenati MJ, Haines JL, Higgins RR, Wappner RS, Palmer CG, Weaver DD. Wiedemann-Beckwith syndrome: presentation of clinical and cytogenetic data on 22 new cases and review of the literature. Hum Genet 1986;74:143-154.
47. Hussain K, Cosgrove KE, Shepherd RM, et al. Hyperinsulinemic hypoglycemia in Beckwith-Wiedemann syndrome due to defects in the function of pancreatic beta-cell adenosine triphosphate-sensitive potassium channels. J Clin Endocrinol Metab 2005;90:4376-4382.
48. Wiedemann HR. Tumours and hemihypertrophy associated with Wiedemann-Beckwith syndrome. Eur J Pediatr 1983;141:129.
49. Lack EE. Pathology of adrenal and extra-adrenal paraganglia. Major problems in pathology, Vol 29. Philadelphia: WB Saunders; 1994.
50. Schnakenburg K, Müller M, Dörner K, Harms D, Schwarze EW. Congenital hemihypertrophy and malignant giant pheochromocytoma—a previously undescribed coincidence. Europ J Pediatr 1976;122:263-273.
51. Satge D, Vidalo E, Desfarges F, de Geeter B. A third case of cardiac neoplasm in a fetus with Beckwith-Wiedemann syndrome: epicardial angiofibroma. Fetal Diagn Ther 2005;20:44-47.
52. Porteus MH, Narkool P, Neuberg D, et al. Characteristics and outcome of children with Beckwith-Wiedemann syndrome and Wilms' tumor: a report from the National Wilms Tumor Study Group. J Clin Oncol. 2000;18:2026-2031.
53. Baujat G, Rio M, Rossignol S, et al. Paradoxical NSD1 mutations in Beckwith-Wiedemann syndrome and 11p15 anomalies in Sotos syndrome. Am J Hum Genet 2004;74:715-720.
54. Beckwith JB. Macroglossia, omphalocele, adrenal cytomegaly, gigantism, and hyperplastic visceromegaly. Birth Defects: Original Article Series 1969;5:188-196.
55. Wiedemann HR. Complexe malformatif familial avec hernie ombilicale et macroglossie—un "syndrome nouveau"? J Genet Hum 1964;13: 223-232.
56. Sinico M, Touboul C, Haddad B, et al. Giant omphalocele and "prune belly" sequence as components of the Beckwith-Wiedemann syndrome. Am J Med Genet A 2004;129:198-200.
57. Anoop P, Anjay MA. Bilateral benign haemorrhagic adrenal cysts in Beckwith-Wiedemann syndrome: case report. East Afr Med J 2004;81: 59-60.
58. Rahmah R, Yong JF, Sharifa NA, Kuhnle U. Bilateral adrenal cysts and ectopic pancreatic tissue in Beckwith-Wiedemann syndrome: is a conservative approach acceptable? J Pediatr Endocrinol Metab. 2004;17:909-912.

3 ADRENAL CORTICAL NODULES AND TUMOR-LIKE LESIONS

ADRENAL CORTICAL HYPERPLASIA

Adrenal cortical hyperplasia is a non-neoplastic condition characterized by an increase in the number of cortical cells. The hyperplasia can be diffuse, localized with the formation of one or more nodules, or a mixture of both patterns. There is usually an increase in size or weight of the adrenal glands, which may be symmetric or asymmetric. *Nodular hyperplasia,* in which one or more nodules are dominant, may simulate an adrenal cortical neoplasm.

Hyperplasia of the adrenal cortex is virtually always bilateral, although rare cases of putative unilateral hyperplasia have been reported (1). Diffuse hyperplasia appears as a generalized thickening of the adrenal cortex, usually without any well-defined nodularity, although an occasional small nodule may be detected with the use of a magnifying glass or a microscope. Nodular hyperplasia is divided into micronodular and macronodular types based upon the size of the nodules. Some classify micronodules as less than 0.5 cm in diameter, while others designate nodules 1.0 cm or more as macronodules (1). Diffuse, micronodular, and macronodular forms of adrenal cortical hyperplasia appear to be a continuum of morphologic alterations, making their distinction in some cases somewhat arbitrary. With the sensitive imaging of computerized tomography (CT) and magnetic resonance imaging (MRI), adrenal cortical nodules less than 1.0 cm in size can be detected.

The correct pathologic identification of adrenal cortical hyperplasia can be difficult, particularly if the gross and microscopic morphology shows only subtle changes. For this reason, careful gross dissection of the adrenal glands with removal of all periadrenal connective tissue and fat may be necessary for the accurate determination of the size and weight of the gland (1). Some of the smaller nodules may not be apparent on external examination of the intact gland, therefore, transverse sectioning at about 3-mm intervals is recommended.

The gross morphologic classification of adrenal cortical hyperplasia is shown in Table 3-1. A functional classification system based upon the presence or absence of a particular endocrine syndrome is shown in Table 3-2. The most common presentation of cortical hyperplasia, or neoplasia with adrenomegaly, is an asymptomatic patient who is eucortical. Adrenal cortical hyperplasia associated with noniatrogenic hypercortisolism can be pituitary dependent (Cushing's disease); associated with ectopic production of adrenocorticotropic hormone (ACTH) (or rarely corticotropin-releasing factor [CRF]); or due to primary pigmented nodular adrenocortical disease (PPNAD) or macronodular hyperplasia with marked adrenal enlargement. The functional approach to classification usually requires careful correlation of morphologic findings with clinical and endocrinologic data. Virilization is typically associated with congenital adrenal hyperplasia while feminization either is poorly characterized or exists only with cortical neoplasia (1).

Table 3-1

MORPHOLOGIC CLASSIFICATION OF ADRENAL CORTICAL HYPERPLASIA[a]

Bilateral Adrenal Cortical Hyperplasia
Diffuse hyperplasia
Nodular hyperplasia
Micronodular (less than 1 cm in diameter)
Macronodular (equal to or greater than 1 cm)
Combined micronodular and macronodular
Combined diffuse and nodular hyperplasia
Dominant cortical nodule with diffuse hyperplasia
Multiple nodules with diffuse hyperplasia
Macronodular hyperplasia with marked adrenal enlargement
Primary pigmented nodular adrenocortical disease
Incidental pigmented nodules
Unilateral Adrenal Cortical Hyperplasia
Diffuse and/or nodular hyperplasia
Incidental pigmented nodule(s)

[a]Table 3-1 from Fascicle 19, Third Series.

Table 3-2

CLINICAL ENDOCRINE SYNDROMES ASSOCIATED WITH DIFFUSE OR NODULAR HYPERPLASIA[a]

Endocrine Syndrome	Adrenal Cortical Hyperplasia
Hypercorticalism	
Cushing's syndrome	
Pituitary-dependent (Cushing's disease)	Diffuse and/or nodular
Ectopic ACTH[b] production	Predominantly diffuse
Primary pigmented nodular adrenocortical disease	Predominantly micronodular
Macronodular hyperplasia with marked adrenal enlargement	Macronodular
Ectopic secretion of CRF[b]	Predominantly diffuse
Hyperaldosteronism	Diffuse and/or micronodular
Virilization (congenital adrenal hyperplasia)	Predominantly diffuse
Eucorticalism	Diffuse and/or nodular

[a]Table 3-2 from Fascicle 19, Third Series.

[b]ACTH = adrenocorticotropic hormone; CRF = corticotropin-releasing factor.

Figure 3-1

NODULAR ADRENAL GLAND

Diagram of transverse section shows cortical extrusions with various configurations. Some lie free in periadrenal area. A larger, dominant intracortical nodule is present (left). There is intermingling of nests of cortical cells with chromaffin cells and both the cortex and medulla have a close anatomic relationship with the vascular space due to discontinuity of smooth muscle in the vessel walls. (Fig. 3-1 from Fascicle 19, Third Series.)

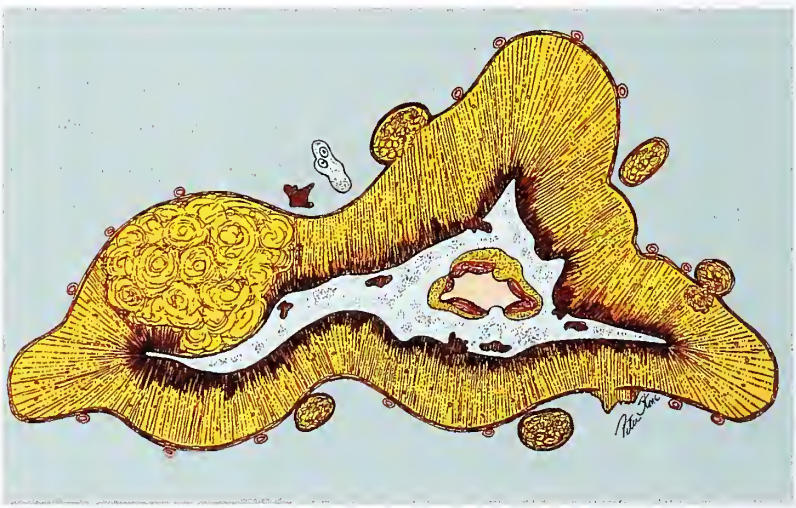

ADRENAL CORTICAL ADENOMA (NODULE) WITH EUCORTICALISM

Adrenal Cortical Nodule(s) at Autopsy

Incidence. The nodular adrenal gland from autopsy material and even in tissue obtained at surgery from individuals without evidence of hypercorticalism can be a diagnostic challenge for the pathologist (fig. 3-1). Much of the confusion about the nodular adrenal gland results from a combination of factors: vague terminology; continuing difficulty in distinguishing an adrenal cortical neoplasm from a dominant macronodule; overlap in morphology of adrenal cortical lesions in patients with different endocrine syndromes; absence of correlation between pathology and clinical/endocrinologic data; and incomplete understanding of the etiology and pathogenesis of the nodular gland in patients who have no evidence of cortical hyperfunction. Prior to the availability of CT scanning and other sensitive imaging techniques, the "nonfunctioning" nodular adrenal gland was usually an incidental finding at autopsy. Currently, it often presents as an incidental finding on high-resolution CT scan during examination for an unrelated problem or during the staging workup of a patient with a known malignancy elsewhere.

The incidence of cortical nodules at autopsy is difficult to estimate since there are no universally accepted morphologic criteria to define a cortical "nodule" in terms of size, number,

and other distinguishing characteristics. Early studies considered any solitary adrenal cortical nodule more than 3 to 5 mm in diameter to be a "nonfunctioning adenoma." In several large autopsy studies, cortical adenomas were detected in 1.4 to 2.9 percent of autopsies (1).

Several autopsy series report a higher incidence of cortical nodules or adenomas in elderly individuals (2,3) and in patients with hypertension (2,4). Spain and Weinsaft (3), for example, identified solitary "adenomas" in 29 percent of 100 consecutive autopsies on elderly females (average, 81 years). Other autopsy studies report adenomas of 1.5 cm or more in as many as 20 percent of patients with systemic hypertension (4). Adenomas 2 mm to 4 cm in size were identified in 8.7 percent of 739 consecutive autopsies, but roughly twice as many occurred in patients with diabetes mellitus (5).

Functional Considerations and Classification. A dominant macronodule might be regarded as an adenoma even though there is no evidence of autonomous hyperfunction or even if close inspection of multiple transverse sections of the ipsilateral or contralateral gland shows coexisting diffuse or micronodular hyperplasia. By routine morphology, it can be very difficult or impossible to prove that the macronodule is indeed a neoplasm (i.e., an adenoma), and the final classification can be quite arbitrary. In a study of clonality utilizing the methylation pattern of the androgen receptor alleles, polyclonal patterns were found in most cases of nodular adrenal cortical hyperplasia (78 percent) and a monoclonal pattern was present in most adrenal cortical adenomas (86 percent), but there was still some overlap in clonality (22 percent of nodular hyperplasias were monoclonal) (6). A solitary lesion with evidence of autonomous growth favors a diagnosis of neoplasia. Because some cortical nodules are related to vascular sclerosis and aging, it is not always appropriate to use the designation adenoma, which means a true neoplasm. Since these lesions are nonfunctional (or nonhyperfunctional), use of the term adrenal "nodule" or "nodular adrenal" seems preferable to hyperplasia in spite of the undoubted increase in mass of the cortical cells.

By definition, hyperplasia denotes an increase in the number of cells in a tissue or organ, and is usually associated with hypertrophy. When the adrenal cortex becomes hyperplastic (i.e., diffuse or nodular hyperplasia), it may cause adrenal hyperfunction or hypercorticalism; this is uncommon, however, based upon the prevalence of nodular adrenal glands in large autopsy studies or the frequency of serendipitous nodules or adenomas discovered in vivo. Scintigraphic studies utilizing radioiodinated cholesterol, a precursor in steroid biosynthesis, have provided some insight into the functional status of these silent adrenal nodules or adenomas detected in living patients (7,8). The adrenal nodule or adenoma is visualized using this technique, and quantification of cortisol levels in the adrenal vein shows the largest concentration on the side of the mass (unilateral cases), or on the side of the largest nodule in patients with bilateral adrenal masses (7). The nodule or adenoma, therefore, appears to be nonhyperfunctional. The findings suggest a condition analogous to nodular euthyroid (nontoxic) goiter, with partial suppression of normal tissue characterized scintigraphically by heterogeneous foci of increased tracer accumulation compared to overall normal hormone secretion (7). Prolonged follow-up of some of these incidentally discovered adrenal nodules or adenomas would be of interest to see if an endocrine syndrome does develop. A variety of enzymes involved in steroid biosynthesis have been detected immunohistochemically in small adrenal cortical adenomas found incidentally in asymptomatic patients, indicating a capacity to produce biologically active steroids, including cortisol (9).

Even in some cases with apparent atrophy of the attached cortex, the secretion of cortisol may be insufficient to cause detectable clinical or laboratory abnormalities. A recent study of 15 small adrenal cortical nodules or adenomas without apparent endocrinologic hyperfunction indicated a capability for producing biologically active steroids, including cortisol, although this was not associated with obvious hypercorticalism (9). Using immunohistochemical analysis of various steroidogenic enzymes (i.e., P-450 side-chain cleavage enzyme, 3-beta-hydroxysteroid dehydrogenase, P-450 C21-hydroxylase, P-450 17-alpha-hydroxylase, and P-450 11-beta-hydroxylase), results of this study indicated that autonomous neoplastic production and secretion of cortisol was present, but

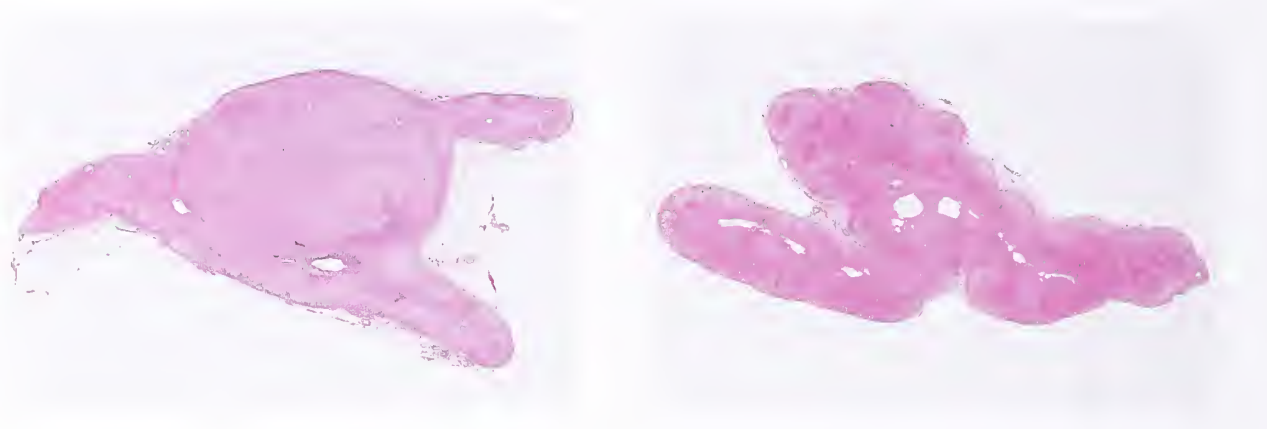

Figure 3-2

NODULAR ADRENAL GLAND

Left: Cross section of a nodular adrenal gland from an adult who had no evidence of hypercorticalism. The dominant macronodule simulates an adrenal cortical adenoma. Areas of diffuse and micronodular hyperplasia were also present.

Right: The opposite adrenal gland has discrete and confluent nodularity and several cortical extrusions.

insufficient to cause clinical or routine laboratory abnormalities. This nonhyperfunction may be sufficient to subtly alter the hypothalamic-pituitary-adrenal axis by suppressing ACTH or CRF secretion, or both, which can lead to atrophy of the attached ipsilateral adrenal cortex in some cases (9).

Pathologic Findings. A detailed study of the nodular adrenal gland was provided by Dobbie (2) who identified mild to distinct nodularity in 65 percent of glands obtained from 113 consecutive autopsies on adult patients. When large nodules or adenomas were encountered (fig. 3-2, left), careful examination of the glands revealed that they were not solitary; in each case, smaller nodules and capsular extrusions were identified in other parts of the ipsilateral or contralateral gland, suggesting that the larger nodules were an extension of the hyperplastic process (fig. 3-2, right). The range of cortical nodularity illustrated schematically in figure 3-1 underscores the fact that nodules are frequently multiple and bilateral.

Small intracortical nodules are best appreciated on microscopic study and can have a variety of appearances (fig. 3-3). The most common nodules are extrusions of cortex that project in a hemispheric or "hourglass" configuration (fig. 3-2, right), often with a continuous extension of the adrenal capsule. Sometimes, the nodule appears to reside on the surface of the gland, completely encapsulated or connected to the adrenal capsule. Depending upon the plane of section, however, there is usually a point of continuity with the underlying cortex (see fig. 3-1), a configuration likened to a "mushroom" or "door handle" (1,2). At times, the cortical cells are unencapsulated and stream into periadrenal fat (fig. 3-4), or form a discrete cortical nodule on the surface of the gland or in adjacent connective tissue without any attachment to the gland. With hyperplasia, these cortical extrusions and juxtaadrenal nodules may become accentuated (fig. 3-5), as can the cuff of cortical cells associated with the central adrenal vein or its tributaries.

Nodules can be seen in every region of the cortex, and the degree of nodularity can vary widely from gland to gland. The larger nodules may be greater than 2 cm in diameter, and may have areas of lipomatous, myelolipomatous, or even osseous metaplasia (2). An association between cortical nodularity and degenerative change in capsular arteries and arterioles (capsular arteriopathy) has been reported, suggesting that focal hyperplasia may be a response to localized ischemia (fig. 3-6) (2). It should be noted that nodular hyperplasia can be found without detectable capsular arteriopathy.

There are many architectural patterns associated with the nodular adrenal gland (fig. 3-7): alveolar, trabecular, gyriform or ribbon-like, and pseudoglandular. It may be difficult or impossible to distinguish an individual dominant macronodule from a cortical neoplasm on

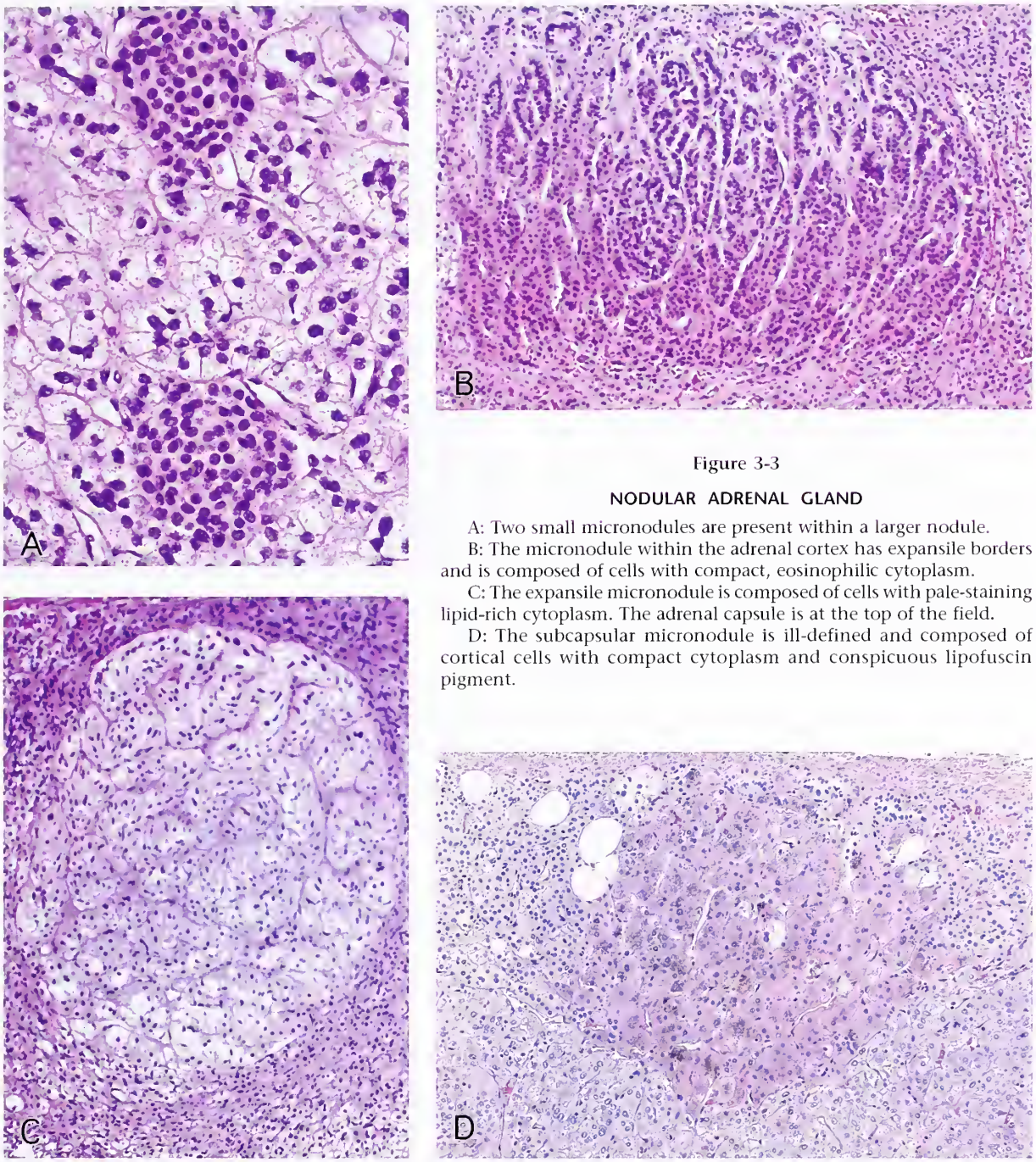

Figure 3-3

NODULAR ADRENAL GLAND

A: Two small micronodules are present within a larger nodule.

B: The micronodule within the adrenal cortex has expansile borders and is composed of cells with compact, eosinophilic cytoplasm.

C: The expansile micronodule is composed of cells with pale-staining lipid-rich cytoplasm. The adrenal capsule is at the top of the field.

D: The subcapsular micronodule is ill-defined and composed of cortical cells with compact cytoplasm and conspicuous lipofuscin pigment.

purely morphologic grounds since one or more of these varied patterns are also seen in the latter (see chapter 4). Pseudoglandular areas are rare but may have well-defined luminal borders and contents that consist of stringy amorphous eosinophilic or basophilic material (fig. 3-7D) or a few degenerated cortical cells. An occasional nodule may have a component of oncocytic cells having abundant compact eosinophilic cytoplasm (fig. 3-8). The adrenal medulla may be deformed due to compression by nodules or penetration of the medulla by cortical cells (2). The functional status of a dominant nodule or adenoma may sometimes be determined by

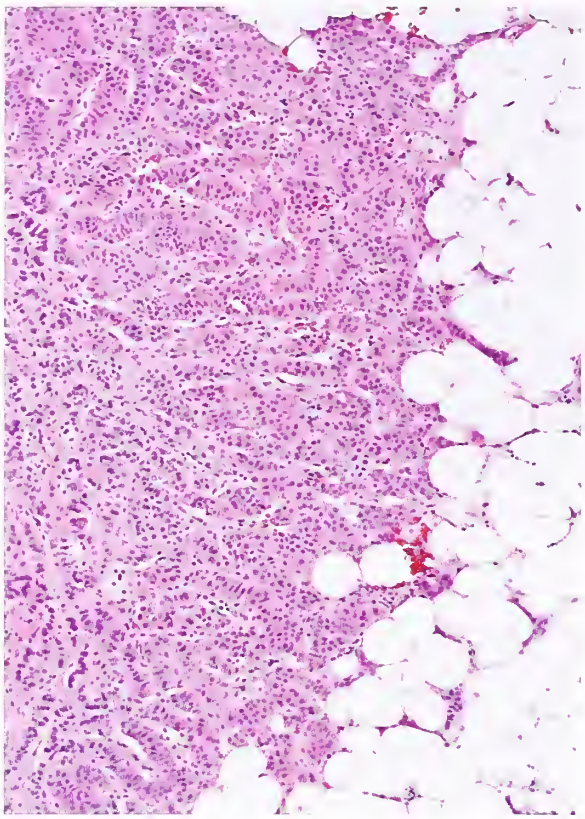

Figure 3-4

NODULAR ADRENAL GLAND

Irregular extrusion of cortical cells into the periadrenal fat without any encapsulation.

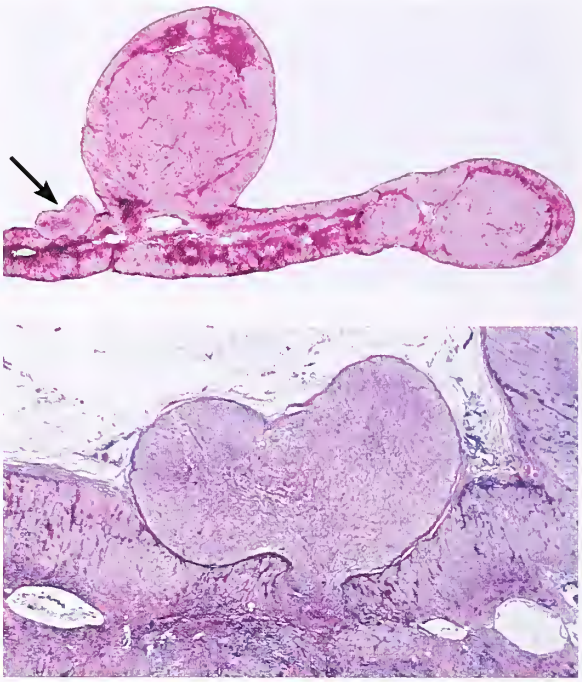

Figure 3-5

DIFFUSE AND NODULAR ADRENAL CORTICAL HYPERPLASIA

Top: Macronodular adrenal cortical hyperplasia in a patient with pituitary-dependent Cushing's disease. Several smaller nodules are present, including a cortical extrusion (arrow).

Bottom: Higher magnification shows the "door-handle" or "mushroom" configuration of the hyperplastic nodule.

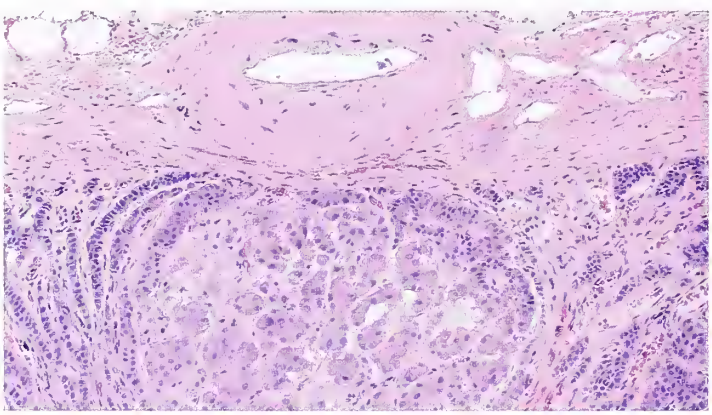

Figure 3-6

INCIDENTAL NODULAR ADRENAL GLAND

Above: Incidental nodular adrenal gland obtained surgically from a patient without any evidence of cortical hyperfunction. A micronodule is present in the outer cortex. Medial sclerosis of a capsular arteriole is seen.

Right: The adrenal cortical nodule beneath the capsule contains several sclerotic vessels.

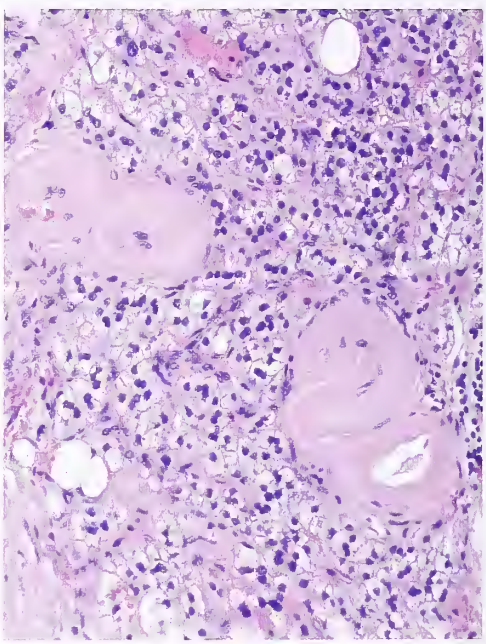

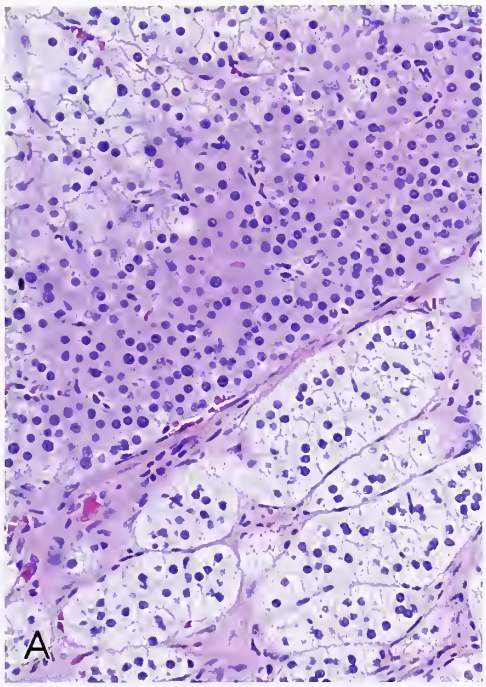

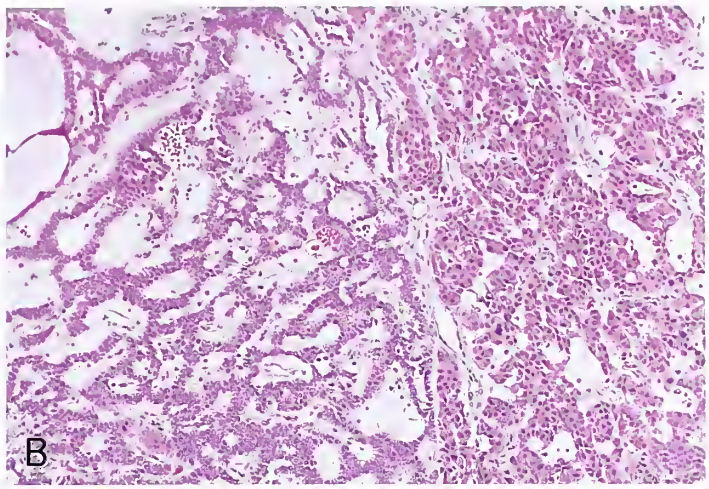

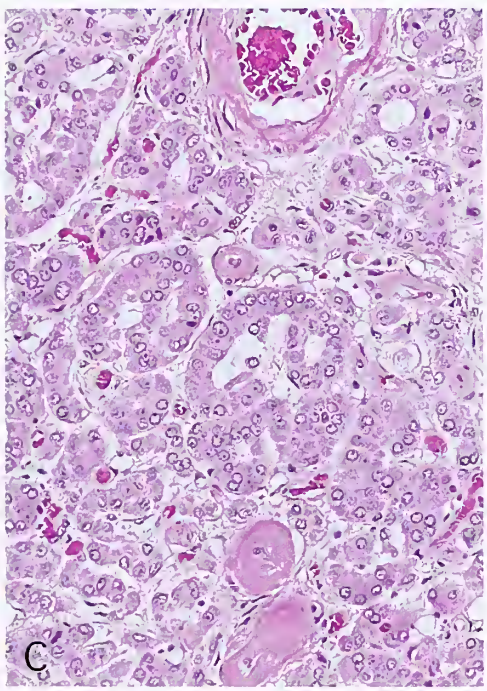

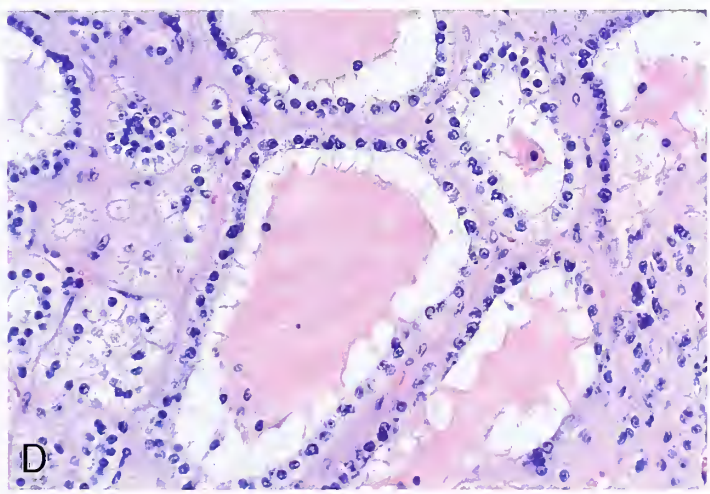

Figure 3-7

INCIDENTAL NODULAR ADRENAL GLAND FROM AN ADULT WHO HAD NO EVIDENCE OF HYPERCORTICALISM

A: Cords and sheets of cells vary in lipid content. Lipid-rich, pale-staining cells in the lower half of the field resemble cells of the zona fasciculata. Other cells have compact, eosinophilic cytoplasm.

B: Two poorly demarcated nodules are composed of blunt cords and trabeculae as well as thin serpentine columns of cells (left).

C: Irregular cords and clusters of cells have compact eosinophilic cytoplasm. A few hyalinized vessels are present. (B&C: Fig. 3-6B&C from Fascicle 19, Third Series.)

D: Alveolar (or nesting) arrangement of cells, some of which have gland-like spaces with eosinophilic proteinaceous contents.

examination of the remaining ipsilateral or contralateral cortex. The presence of cortical atrophy may indicate hypercortisolism while hyperplasia of the zona glomerulosa may indicate hyperaldosteronism. The large, nonhyperfunctional cortical nodule or adenoma may show some advanced degenerative features such as cystic change, sclerosis, or old hemorrhage. The sclerosis may be patchy or involve much of the nodule, and may be accompanied by dystrophic calcification. Rarely, areas resembling amyloid are present (figs. 3-9, 3-10).

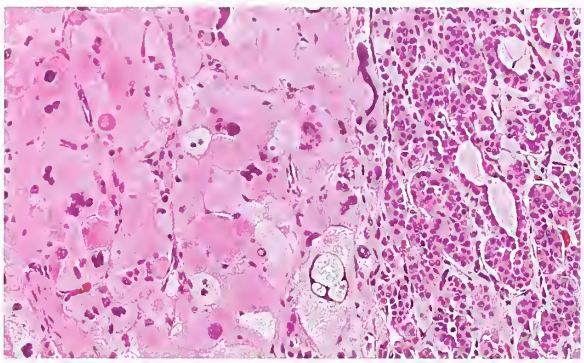

Figure 3-8

ONCOCYTIC CHANGE WITHIN NODULAR ADRENAL GLAND

There are a few areas in which cells have abundant eosinophilic cytoplasm. The nucleus in one cell (near bottom of field) has several nuclear pseudoinclusions.

Incidental Pigmented Cortical Nodule(s)

Small, brown or black pigmented nodules of the adrenal cortex are sometimes detected at autopsy or in surgical material. These nodules usually range in size from 1.0 mm to 1.5 cm or more in diameter. When the nodule is large, it can grossly distort the gland and be seen beneath the capsular surface (fig. 3-11, top); in transverse sections it may present as a tumefactive lesion (fig. 3-11, bottom). Retrospective autopsy studies have revealed pigmented nodules in 2.2 to 10.4 percent of cases (10,11); when these lesions were prospectively searched for in 3-mm sections from both adrenal glands, they were found in 37 percent of patients (10). As many as five separate pigmented nodules have been found in a single gland, and in 11 percent of

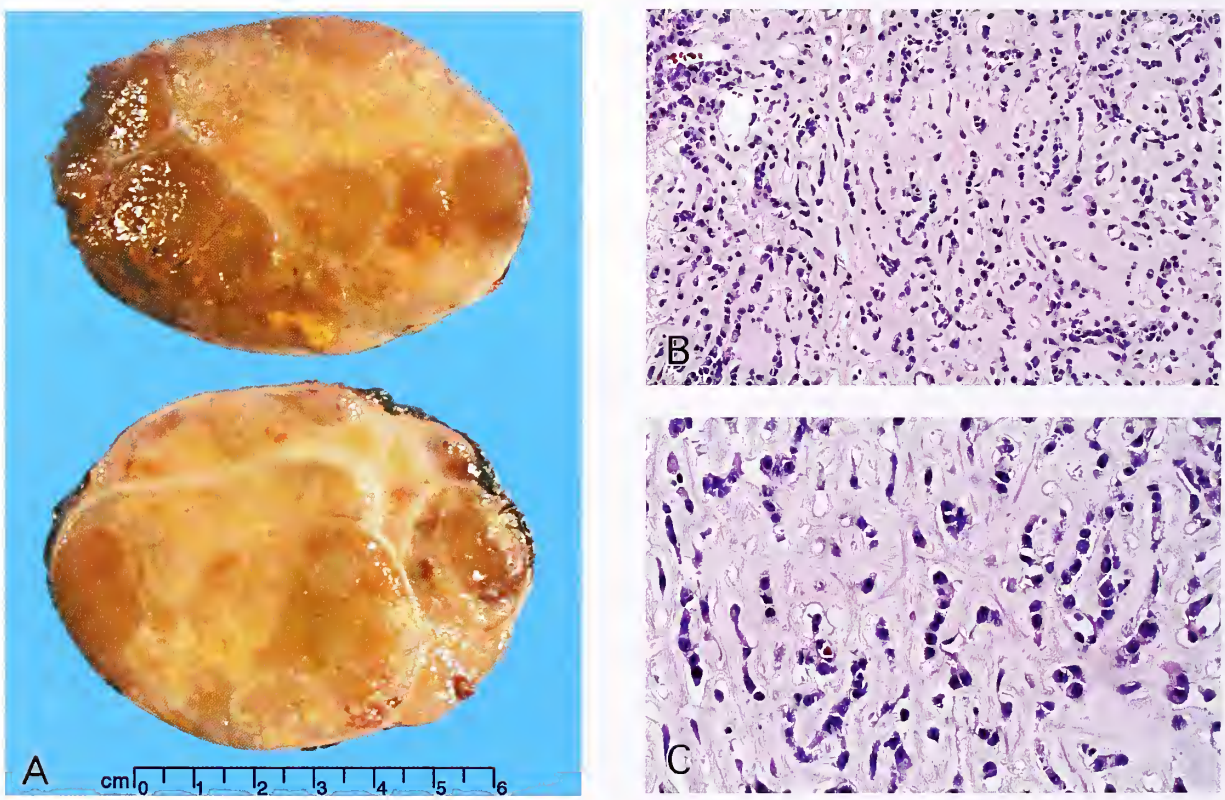

Figure 3-9

HYALINIZED (SCLEROSED) AND PARTIALLY CALCIFIED ADRENAL MASS

A: Cross section of an 8-cm adrenal cortical tumor from a 4-year-old girl. The tumor weighed 169 g and was classified as an atypical adenoma. On cut surface there are mottled to confluent areas of pallor representing intense sclerosis. (Courtesy of Dr. Michael Teitell, Los Angeles, CA.)

B: An adrenal cortical adenoma in a different case shows extensive stromal sclerosis isolating individual and small clusters of cortical cells. The tumor was nonfunctional. (B and C are from the same patient.)

C: Intense sclerosis in some areas resembles amyloid, but the Congo red stain was negative.

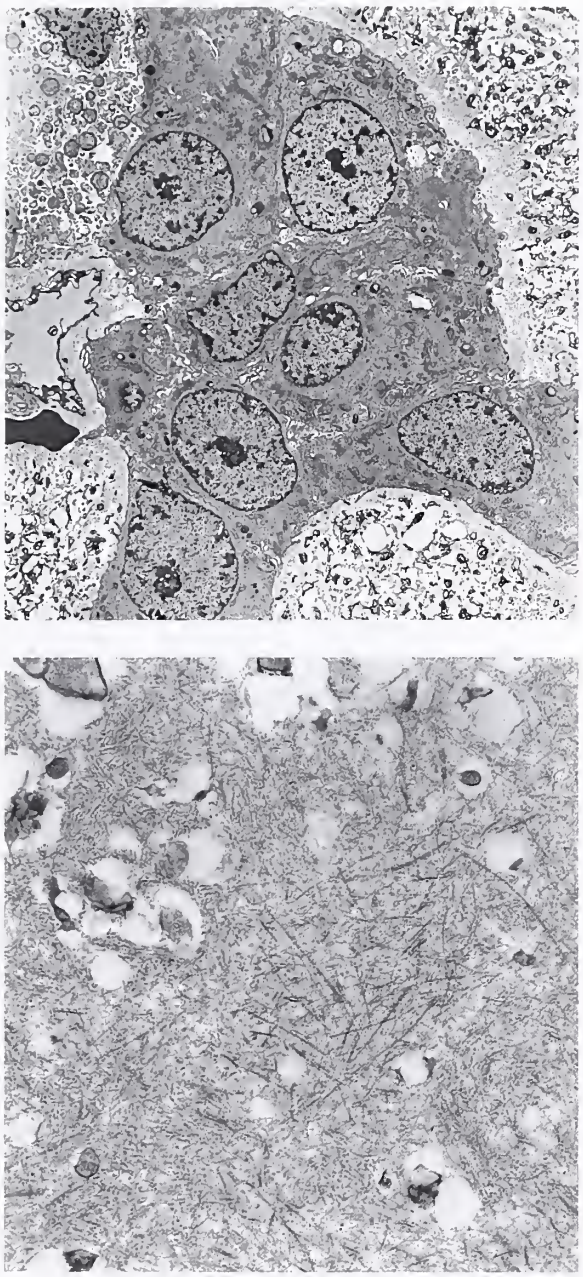

Figure 3-10

HYALINIZED AND PARTIALLY CALCIFIED ADRENAL MASS

This mass was discovered incidentally in an 11-year-old girl. (Same case as figure 3-9B,C.) (Fig. 3-8 from Fascicle 19, Third Series.)

Top: The cortical cells have lipid-depleted cytoplasm and a moderate number of mitochondria with slight pleomorphism. Amorphous matter and fibrillar material separate cells.

Bottom: Ultrastructure of intensely hyalinized stroma. Some of the rigid, nonbranching filaments resemble amyloid. (Courtesy of Ms. L. Farr, Providence, RI.)

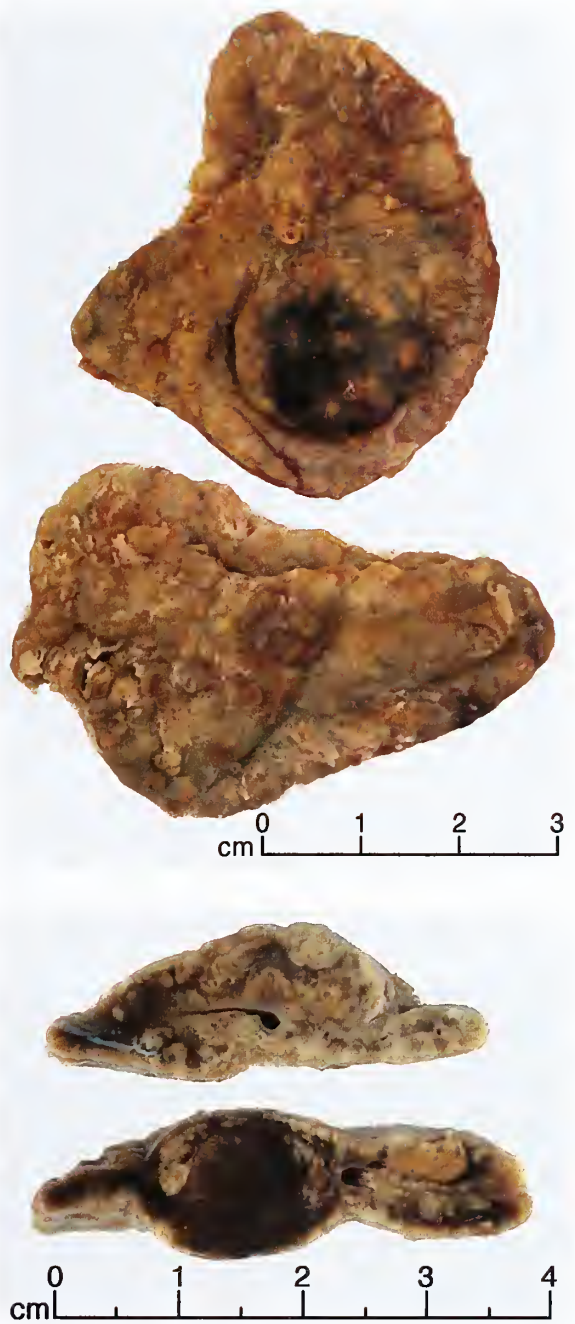

Figure 3-11

NODULAR ADRENAL GLAND WITH INCIDENTAL PIGMENTED MACRONODULE

Top: A darkly pigmented nodule projects beneath the capsule on the dorsal surface of a nodular adrenal gland.

Bottom: Transverse section shows numerous micronodules in the adjacent cortex. (T&B: Fig. 3-9 from Fascicle 19, Third Series.)

Figure 3-12

INCIDENTAL PIGMENTED ADRENAL NODULE

The nodule (white arrow) has expansile borders but lacks encapsulation. A small focus of lipomatous metaplasia (black arrow) as well as capsular extrusion (black arrowhead) are shown. (Fig. 3-10 from Fascicle 19, Third Series.)

cases the lesions were bilateral (10). In some reports, the small pigmented nodules were referred to as adenomas although there was no known functional significance attached to them. Distinction from a true neoplasm may be impossible, but when the lesions are multiple and bilateral, a hyperplastic process is favored.

The microscopic nature of the lesion at low magnification may not be as distinctive as that seen on gross examination (fig. 3-12). When the pigmented nodule is small it is characteristically centered on the zona reticularis, and there may be some indentation or distortion of the adrenal medulla or cortex (fig. 3-13, left). Occasional pigmented nodules may be present in the outer cortex (see fig. 3-3D). The pigmented lesions are unencapsulated, and are composed largely of cells with compact, eosinophilic cytoplasm, although there may be an admixture of cells with lipid-rich, vacuolated cytoplasm. The dark color of the lesion is imparted to a minor degree by the lipid-depleted cells, but a more conspicuous component is the intracytoplasmic, coarse granular pigment representing lipofuscin (fig. 3-13, right). Nuclei are usually uniform, round to oval, with a single, small, dot-like nucleolus, although occasionally there may be some nuclear irregularity. The cells strongly resemble cells of the zona reticularis although greatly expanded in cell density and volume. One study suggested the presence of a component of neuromelanin (11).

Serendipitous Cortical Adenoma Discovered in Vivo ("Incidentaloma")

An unsuspected, nonhyperfunctioning adrenal mass has been reported in 1 to 3 percent of patients examined by CT scan of the upper abdomen (1,12,13). This incidence could be even higher depending upon the patient population: patients with hypertension and diabetes mellitus, and elderly patients may theoretically have an increased frequency of such a mass. The prevalence may vary depending upon whether patients with known malignancy are excluded or whether other lesions with classic CT characteristics of cysts or myelolipoma are eliminated.

An *incidental nonhyperfunctional adrenal cortical adenoma (or nodule)* on CT scan is usually round to oval with a smooth contour, has a well-delineated margin clearly separate from adjacent structures (fig. 3-14), and typically shows little to no detectable growth on serial scanning of the abdomen. A smaller nodule may distort the medial or lateral limb of the gland. The average patient age in one series was 62 years and nearly 60 percent of patients were female (14). The average nodule size in several studies was 2.4 to 3.3 cm (12,14); the largest lesions are usually 5 to 6 cm in size. Subclinical or preclinical Cushing's syndrome (autonomous cortisol production without signs or symptoms of hypercortisolism) has been reported in 1 percent (14) up to 20 percent (15) of patients with incidentally discovered adrenal tumors who have been

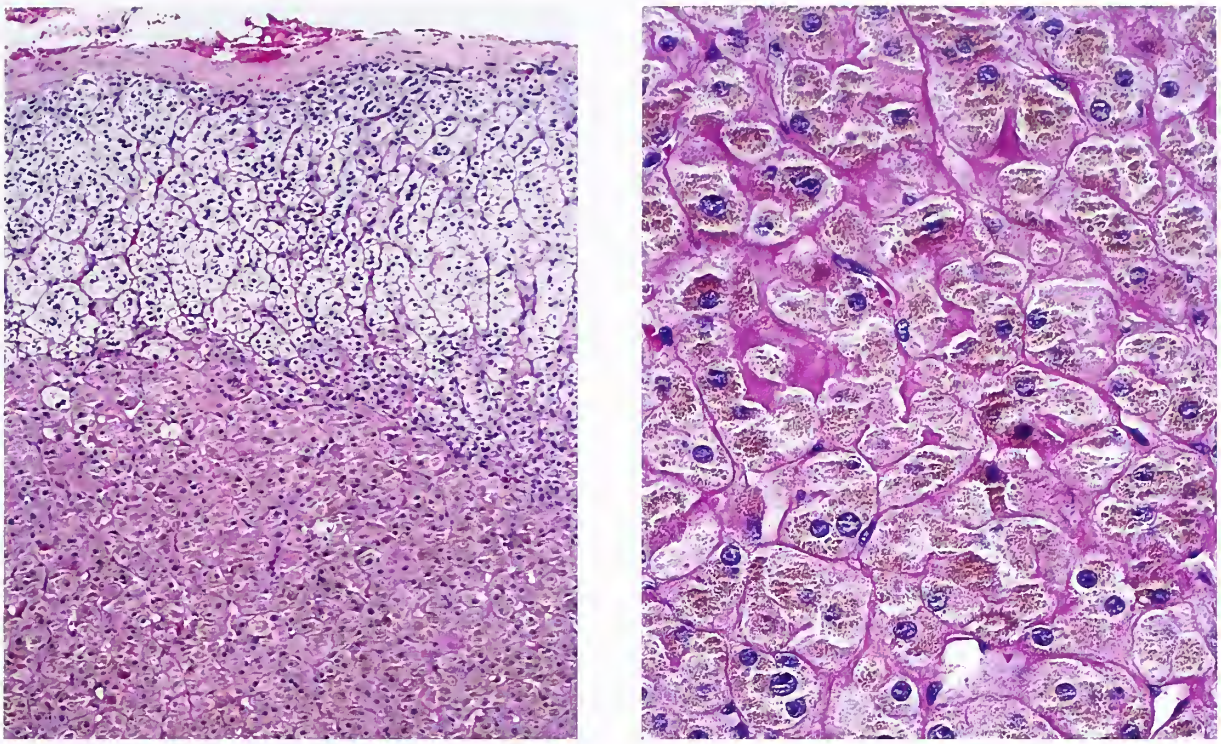

Figure 3-13

INCIDENTAL PIGMENTED ADRENAL NODULE

Left: Incidental pigmented nodule has its epicenter in the zona reticularis and expansile borders impinging slightly on the outer cortex.

Right: Cortical cells contain a variable amount of granular, dark brown pigment. Nuclei tend to be round to oval and vary only slightly in size. (L&R: Fig. 3-11 from Fascicle 19, Third Series.)

studied biochemically. A prevalence as high as 24 percent subclinical Cushing's syndrome has been reported (16). A major risk of adrenalectomy in patients with such tumors is adrenal cortical insufficiency (fig. 3-15).

With the availability of high resolution CT scan, an adrenal mass less than 1 cm may be visualized, and with wider application of this imaging modality, an increasing number of asymptomatic patients with an adrenal mass will likely be detected. The benign nonhyperfunctioning adrenal cortical adenoma (or macronodule) is the most common type of incidentally discovered adrenal mass, followed by a metastasis from a known primary tumor elsewhere, especially lung and breast (1). It may not be possible to reliably distinguish a metastasis from an adrenal cortical neoplasm on CT scan, and fine needle aspiration biopsy under CT or ultrasound guidance (fig. 3-16) can provide valuable

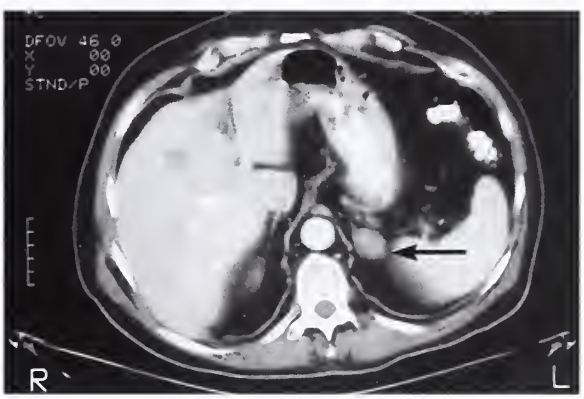

Figure 3-14

INCIDENTAL NONHYPERFUNCTIONAL ADRENAL CORTICAL ADENOMA

On computerized tomography (CT) scan, the incidental nonfunctional adrenal cortical adenoma of the left adrenal gland of a 63-year-old man (arrow) is round to oval and well circumscribed. There was low attenuation with intravenous contrast. CT-guided fine needle aspiration was performed. The patient had carcinoma of the urinary bladder.

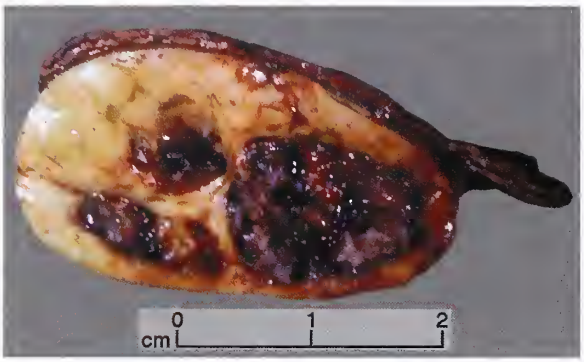

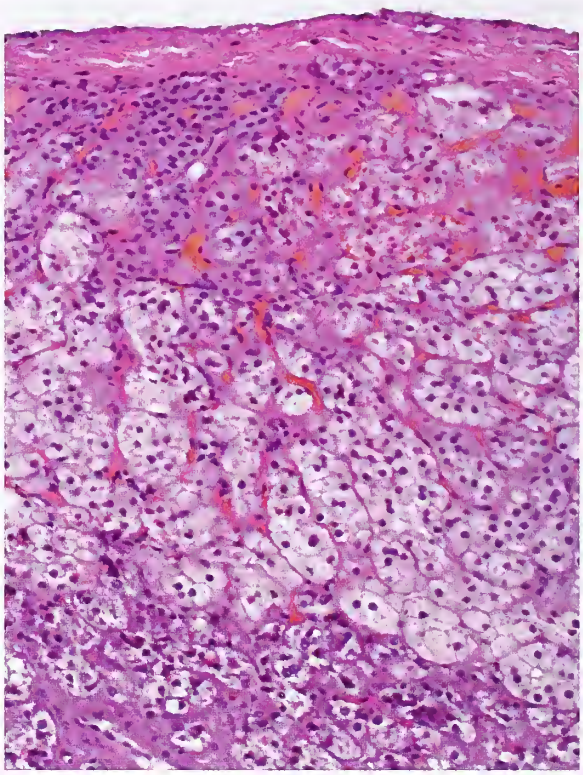

Figure 3-15

PRECLINICAL CUSHING'S SYNDROME

Above: An incidental, 4.2-cm adrenal cortical adenoma was detected in a 48-year-old woman with a history of carcinoma of the nose. On cross section, the tumor is pale yellow with central areas of degeneration and hemorrhage. Atrophy of the attached adrenal cortex is present, which in areas was well under 1 mm in thickness.

Right: Soon after resection of this incidental adenoma in another patient with preclinical Cushing's syndrome, signs and symptoms of adrenal cortical insufficiency developed. The patient was treated with intravenous hydrocortisone. Note the atrophy of the adrenal cortex. A portion of the adrenal medulla is at the bottom of the field.

information, which must be correlated with imaging characteristics of the lesion as well as any available clinical or endocrinologic data. Needle biopsy of an adrenal tumor may result in hemorrhage and hematoma formation (fig. 3-16E). Care must be taken to distinguish hepatic parenchyma, which may be mistaken for an adrenal cortical neoplasm (fig. 3-17). Occasionally in aspirates of benign cortical nodules, one may see "bare" or "stripped" nuclei having no apparent cytoplasm; this may superficially mimic a small, round cell malignancy (fig. 3-18). The nuclei, however, tend to be relatively uniform, without molding, and there is typically no evidence of necrosis. High diagnostic accuracy has also been reported with adrenal core biopsies (17). Cell block preparations also provide valuable information as well as the opportunity for additional stains if necessary (fig. 3-16A).

For the large group of adrenal lesions that appear unexpectedly on CT scans in the nononcologic patient, size and imaging characteristics become important criteria in determining the future course of action, i.e., observation with a repeat scan several months later or surgical resection. MRI can separate some nonhyperfunctional adenomas (low signal intensity) and pheochromocytomas (high signal intensity) (18), but some lesions have overlapping patterns. The size of the adrenal mass is important since adrenal cortical carcinoma (ACC) is usually over 6 cm in diameter, whereas adenomas are typically smaller in size. Assuming that the prevalence of biochemically silent ACC is about 1/250,000 population, it has been estimated that over 60 operations would have to be done on patients with an adrenal mass 6 cm or greater to remove one ACC (19). Based upon a large data base, it was estimated that the probability of malignancy at a size threshold of 4 cm or greater was 10 percent; 6 cm or greater, 19 percent; and 8 cm or greater, 47 percent (20). In a large series from the Mayo Clinic, 4 of 342 patients with an incidentally discovered adrenal tumor (55 underwent adrenalectomy) had an ACC (tumor diameters, 5.5 cm, 8.5 cm, 8.7 cm, and 17.0 cm); the three patients with the larger tumors died, while the patient with the smallest tumor had no evidence of tumor at 5 years follow-up (14). It

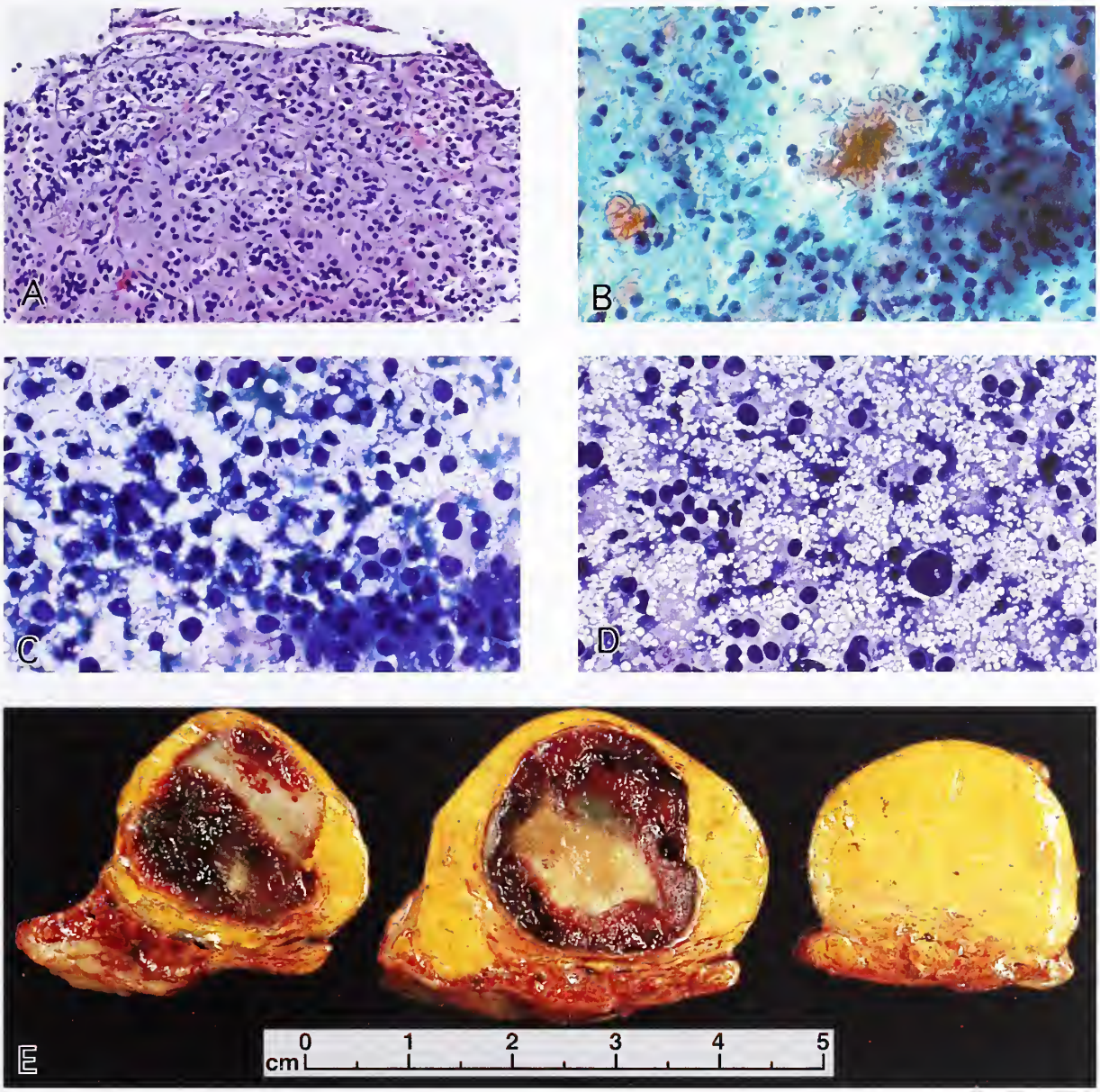

Figure 3-16

FINE NEEDLE ASPIRATION BIOPSY OF INCIDENTAL ADRENAL CORTICAL ADENOMA

A: Cell block preparation of fine needle aspiration of an incidental nonfunctional adrenal cortical adenoma. The cortical cells have an alveolar (or nesting) pattern, with pale-staining cytoplasm.

B: Fine needle aspiration specimen shows cells with uniform round to oval nuclei and ample, pale-staining cytoplasm. Some cells contained fine intracytoplasmic vacuoles (Papanicolaou stain).

C: Fine needle aspiration specimen has been air dried and stained with Diff Quik. Nuclei are relatively uniform and most cells have compact cytoplasm. Some cells contain small cytoplasmic vacuoles.

D: The cytoplasm of the cortical cells has been disrupted. The nuclei appear to float in an area of dispersed cytoplasmic vacuoles, which represent lipid droplets. Note the enlarged nucleus in bottom half of the field with a small nuclear "pseudoinclusion" (Diff Quik stain).

E: Incidental nonfunctional adrenal cortical adenoma in a 73-year-old man who had gallstones. Fine needle aspirate did not yield sufficient material for diagnosis. Right adrenalectomy was performed during elective cholecystectomy. The adrenal adenoma weighed 28 g and measured nearly 3.5 cm in diameter. Note the central organizing hematoma following the attempt at fine needle aspiration. (Fig. 3-13C from Fascicle 19, Third Series.)

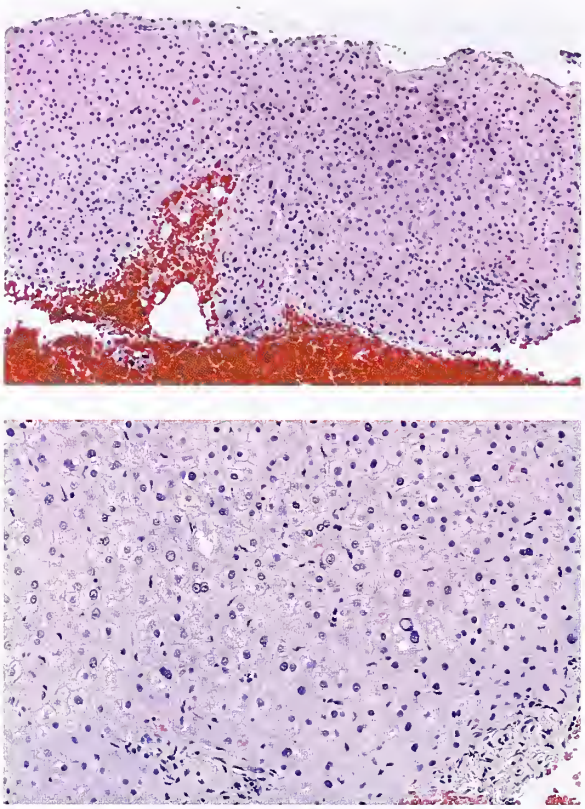

Figure 3-17

HEPATIC PARENCHYMA MIMICKING AN ADRENAL CORTICAL NEOPLASM

Top: Cell block preparation from a fine needle aspiration biopsy of a right adrenal mass shows a portion of liver parenchyma with fresh blood. Aspirate smears were insufficient for diagnosis.

Bottom: Hepatic tissue was initially regarded as a possible adrenal cortical neoplasm. Note the small portal tract in the right lower corner (compare with figure 3-16A).

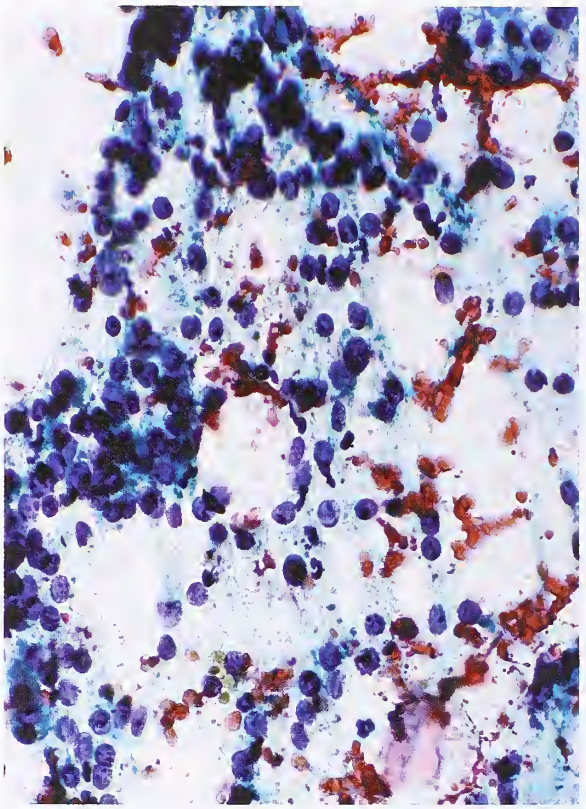

Figure 3-18

FINE NEEDLE ASPIRATION BIOPSY OF INCIDENTAL ADRENAL CORTICAL ADENOMA

CT-guided fine needle aspiration biopsy of a benign incidental nonhyperfunctional adrenal cortical adenoma. The cells are arranged in a loosely cohesive array with many having "bare" or "stripped" nuclei. At first glance, the pattern may suggest a metastatic small cell carcinoma but the lack of nuclear molding and the absence of necrotic background suggest the correct diagnosis (Papanicolaou stain).

should be remembered, however, that the threshold of size as a distinguishing feature varies from 3 to 5 cm, or slightly larger depending upon the source. The variegated gross appearance of a relatively large incidentally discovered adrenal cortical tumor is illustrated in figure 3-19A. A different case is illustrated in figure 3-19B–D, which was histologically very pleomorphic but proved to be clinically benign.

Many histopathologic features are seen in the incidentally discovered adrenal cortical adenoma. Some of the degenerative and stromal changes seen in these nonhyperfunctional tumors are of interest since they may cause diagnostic confusion. Marked degenerative change can simulate an adrenal hematoma or cyst and organization within the mass may simulate a hemangioma. The author has seen an incidental nonfunctional adrenal cortical adenoma with adrenal hepatic union and intermingling of cortical and hepatic cells; this should not be misinterpreted as "invasion."

ADRENAL CORTICAL HYPERPLASIA WITH HYPERCORTISOLISM

There are several major causes of *noniatrogenic Cushing's syndrome* (fig. 3-20) (21–24). In adults, noniatrogenic hypercortisolism due to pituitary-dependent ACTH overproduction (*Cushing's disease*) accounts for about 60 to 70 percent of cases

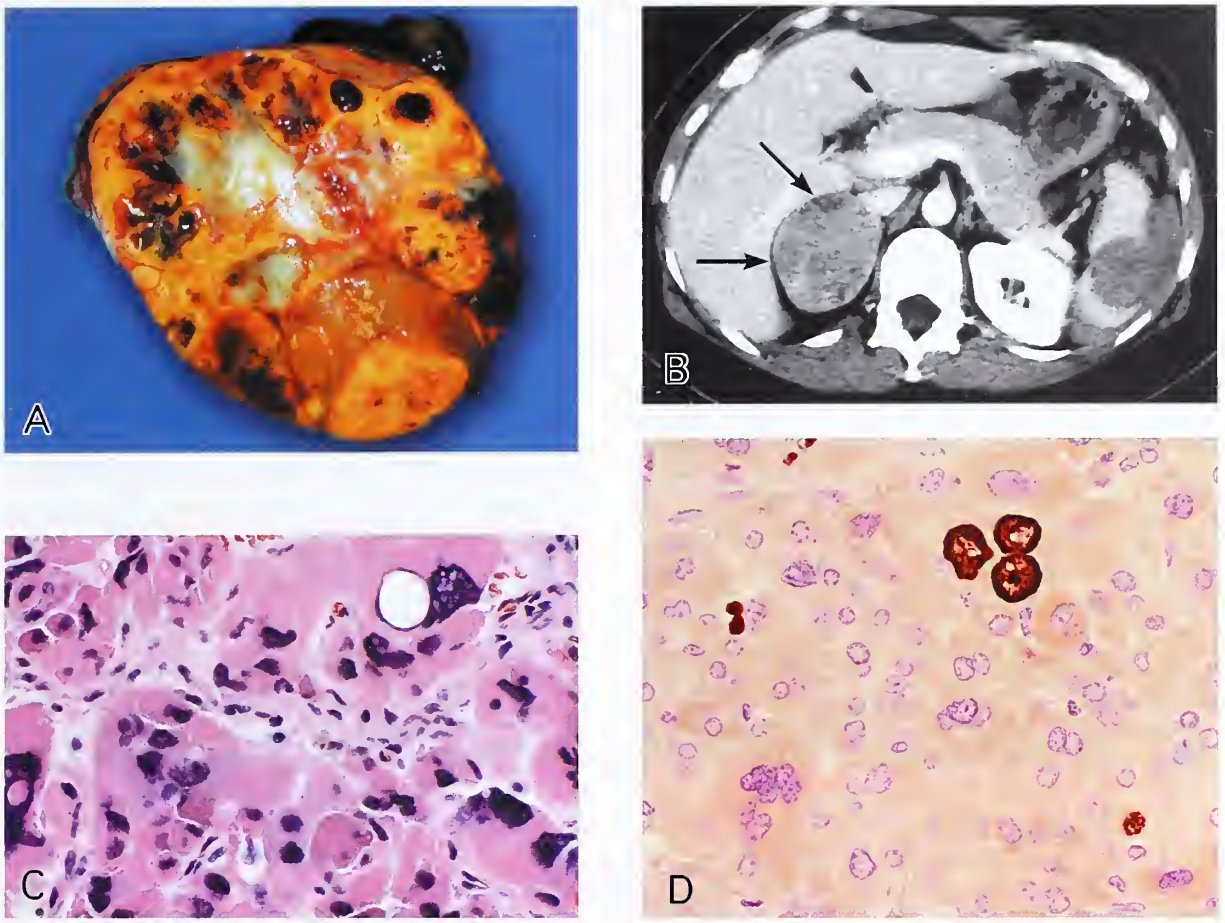

Figure 3-19

INCIDENTAL ADRENAL CORTICAL NEOPLASM

A: Cross section of an incidentally discovered adrenal cortical adenoma which was clinically nonfunctional. The tumor was 7 cm in diameter and weighed 128 g. The tumor had marked degenerative changes including hyalinization, recent and old hemorrhage, dystrophic mineralization, and areas of myxoid stroma. Areas of lipomatous metaplasia were also present. (Courtesy of Dr. Michael Barnan, New York, NY.)

B: Abdominal CT scan with contrast in a 45-year-old woman who, in an automobile accident, sustained blunt trauma to the spleen. There is a large splenic subcapsular hematoma on the left side and a well-circumscribed adrenal mass on the right (arrows) which was 6 cm in diameter. The patient had been essentially asymptomatic. Following splenectomy, an endocrinologic evaluation was essentially negative. The adrenal mass was surgically resected at a separate operation and was regarded as an atypical adrenal cortical adenoma. The tumor weighed 99.5 g. The patient was alive and well 11 years later.

C: Marked nuclear pleomorphism and hyperchromasia were present in this adrenal cortical adenoma. The tumor was well encapsulated without necrosis or vascular invasion and after prolonged search no mitotic figures were found. Cells throughout the tumor had abundant, compact eosinophilic cytoplasm.

D: Immunolabeling for Ki-67 (MIB-1) showed a very low labeling index for proliferative activity. Three nuclei near the top of the field show positive labeling but numerous other fields did not show any immunoreactivity.

(1,22–24); an autonomously secreting adrenal cortical neoplasm (or rare forms of pituitary- or ACTH-independent adrenal cortical hyperplasia) accounts for 18 (24) to 25 percent (22) of cases; ectopic production of ACTH is seen in 12 percent of cases (24); and rarely, hypercortisolism is due to ectopic production of CRF (25). Ectopic production of both ACTH and CRF has been reported, and the biochemical pattern may be that of pituitary ACTH-dependent hypercortisolism (26).

The age and sex of the patient may have some influence on the relative incidence of the

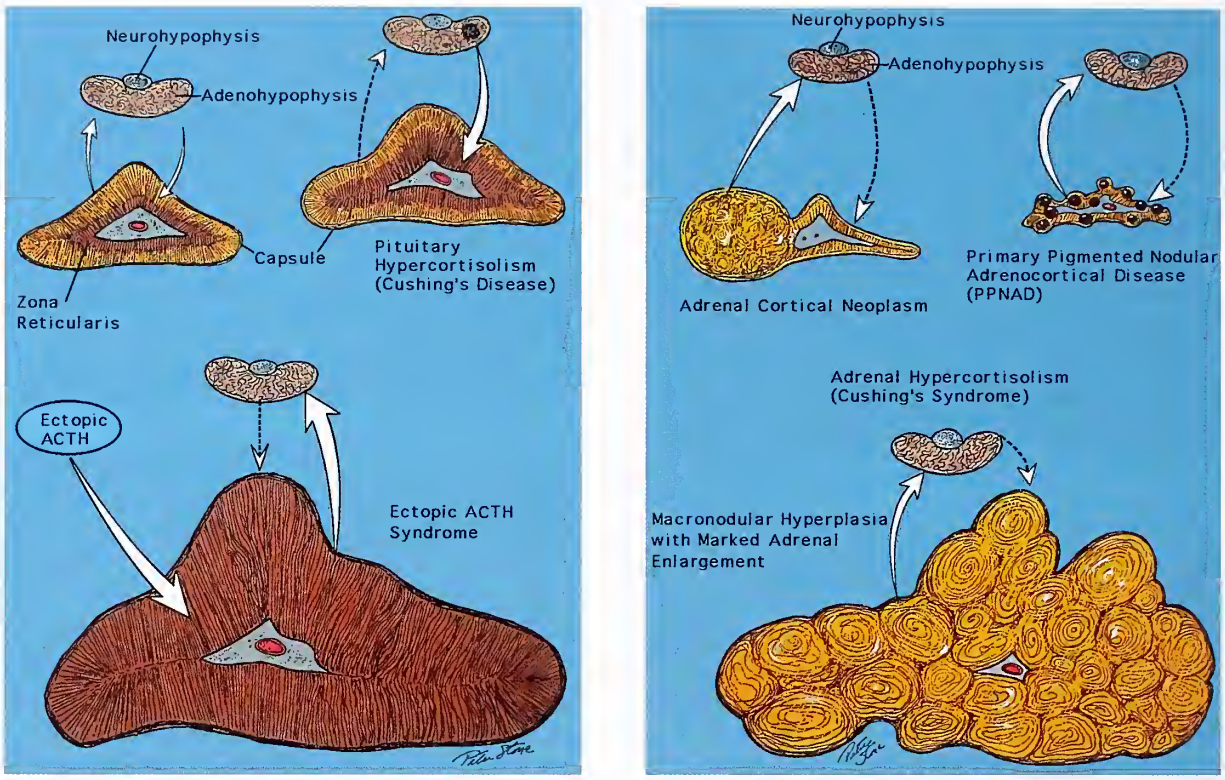

Figure 3-20

ETIOLOGY OF NONIATROGENIC CUSHING'S SYNDROME (SCHEMATIC DIAGRAM)

Left: The normal hypothalamic-pituitary-adrenal axis (upper left), pituitary-dependent Cushing's disease (upper right), and ectopic adrenocorticotropic hormone (ACTH) syndrome.

Right: Adrenal Cushing's syndrome due to either an adrenal cortical adenoma or carcinoma (upper left); primary pigmented nodular adrenocortical disease (PPNAD) (upper right), a rare form of pituitary (or ACTH)-independent Cushing's syndrome; and macronodular hyperplasia with marked adrenal enlargement (lower half), another rare form of pituitary (or ACTH)-independent Cushing's syndrome. (L&R: Fig. 3-15 from Fascicle 19, Third Series.)

different forms of hypercortisolism. The adrenal form of Cushing's syndrome, for example, predominates in children, particularly those in the first decade of life (1). Cushing's syndrome due to ectopic ACTH production is largely a disease of men, while most patients with Cushing's disease are women of reproductive age (1). In children under the age of 7 years, an adrenal cortical neoplasm appears to be a more common cause of Cushing's syndrome (either adrenal cortical adenoma or carcinoma) (1). When there is a pituitary source for ACTH overproduction (i.e., Cushing's disease) in childhood, Nelson's syndrome can develop following bilateral adrenalectomy, and some studies indicate a higher risk of this complication in children than in adults (27).

There are other causes of Cushing's syndrome that are rare, but provide insight into the regulatory mechanisms at the molecular level. The McCune-Albright syndrome consists of a triad of polyostotic fibrous dysplasia, skin pigmentation with café au lait spots, and sexual precocity, but there may be associated endocrine disorders including Cushing's syndrome. The McCune-Albright syndrome is due to a somatic mutation within exon 8 of the lambda subunit of stimulatory G protein, a protein that activates adenylate cyclase, which in turn causes authentic autonomous overproduction of cortisol in multiple adrenal cortical nodules in which this mutation is expressed (28). Food-dependent Cushing's syndrome has been reported secondary to inappropriate sensitivity of the adrenal glands to the normal postprandial increase in secretion of gastric inhibitory polypeptide (GIP) (29). The primary cause does

not appear to be GIP, but more likely "illicit" or "ectopic" expression of GIP receptors on the plasma membrane of adrenal cortical cells. There are also atypical forms of Cushing's syndrome which may be difficult to diagnosis, as for example the pseudo-Cushing's syndrome (23), a reversible form of hypercortisolism related to alcohol abuse, or cyclic Cushing's disease with intermittent hypersecretion of ACTH (30). Highly active antiretroviral therapy in patients infected with human immunodeficiency virus (HIV) is associated with a pseudo-Cushing's syndrome and may be related to a lipodystrophy with local regeneration of cortisol from inactive cortisone catalyzed by the enzyme 11-beta-hydroxysteroid dehydrogenase type 1 (31).

PITUITARY-DEPENDENT HYPERCORTISOLISM (CUSHING'S DISEASE)

Cushing provided a detailed description in 1932 of the disease which came to bear his name (32). An in depth biography of Cushing was written by Fulton in 1946 (33). Most cases of *Cushing's disease* are due to an ACTH-producing pituitary adenoma, usually a microadenoma (less than 10 mm in diameter), which may be difficult to identify with even the most contemporary imaging techniques. Advances in dynamic laboratory testing such as bilateral petrosal venous sinus sampling or, in some cases, internal jugular vein (34), and improvements in pituitary microsurgical techniques have increased the surgical remission rate for patients with microadenomas and macroadenomas confined to the sella turcica to 86 percent and 83 percent respectively (35). Plasma ACTH levels are usually within the normal range or only moderately elevated in ACTH (or pituitary)-dependent Cushing's disease (24). The microadenoma can be very small, and located deep in the central wedge of the pituitary gland near the neurohypophysis, making surgical (or pathologic) detection difficult; nonetheless, transsphenoidal adenomectomy remains the treatment of choice for most patients with Cushing's disease. When the tumor cannot be identified or removed, bilateral adrenalectomy may be indicated and laparoscopic resection has been successfully performed (36). A small proportion of patients with pituitary-dependent Cushing's disease appear to have underlying hyperplasia of ACTH-producing corticotroph cells, either as a primary abnormality or one due to entopic (hypothalamic) or ectopic excess production of CRF.

Figure 3-21

CUSHING'S DISEASE WITH DIFFUSE AND MICRONODULAR HYPERPLASIA

Transverse sections of adrenal gland in a patient with ACTH-dependent hypercortisolism (Cushing's disease). The adrenal gland was only mildly enlarged and shows both diffuse and micronodular hyperplasia. Much of the adrenal cortex is tan to brown although pale yellow areas can be seen.

Diffuse and Micronodular Hyperplasia

The pathologist seldom has the opportunity to examine adrenalectomy specimens from patients with Cushing's disease. Because excess corticosteroid secretion is detected at an earlier phase today, resected adrenal glands may be only mildly stimulated, with very subtle changes, and thus the gland may be regarded as "normal." Careful correlation of morphology with clinical and hormonal data may be necessary.

The adrenal glands usually show *diffuse* or *diffuse and micronodular hyperplasia* (fig. 3-21). Gland enlargement is usually mild with individual weights of 6 to 12 g (1). On transverse sections the gland may appear expanded with

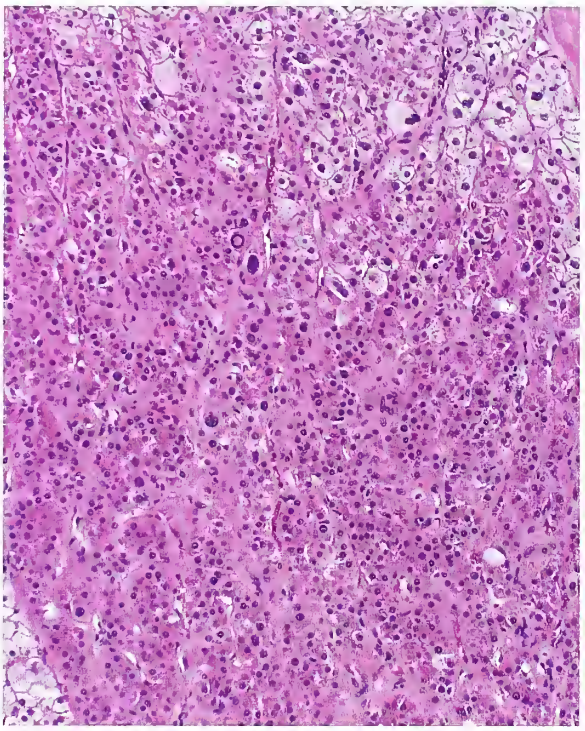

Figure 3-22

CUSHING'S DISEASE

Under the trophic influence of ACTH, much of the zona fasciculata is converted to cells with lipid-depleted, compact, eosinophilic cytoplasm. (Fig. 3-17 from Fascicle 19, Third Series.)

rounded edges, and careful inspection may reveal a faint, somewhat irregular junction between the pale yellow outer aspect of the cortex and the inner darker, often tan to light brown, one third to half due to conversion of vacuolated, lipid-rich cells to lipid-depleted cells with more compact, eosinophilic cytoplasm (fig. 3-22). The extent to which lipid-rich cells of the zona fasciculata are converted to compact lipid-poor cells is variable, and physiologic factors may have some bearing on the overall morphology (1). Micronodular hyperplasia may be evident as small irregular nests of cortical cells with expansile pushing borders, occasionally with compression of adjacent cortex.

There may be irregular extension of zona fasciculata cells into periadrenal fat, and a conspicuous mantle of cortical cells may be present around tributaries of the central adrenal vein. The adrenal medulla appears normal, although there may be accentuated intermingling of cortical and chromaffin cells. Ultrastructural changes have been reported in cortical cells, but dynamic endocrinologic and physiologic changes must be kept in mind.

Macronodular Hyperplasia

Macronodular hyperplasia (MNH), often used synonymously with *nodular hyperplasia*, has been reported in 10 (37) to 20 percent (38) of patients with pituitary-dependent Cushing's disease. A relatively high incidence of 40 percent was recorded by Smals et al. (39), but the definition of macronodular is entirely arbitrary. A macronodule is defined by Doppman et al. (37) as any nodule visible on CT scan; when they used 5-mm–thick sections, the smallest nodule was 6 mm in diameter.

MNH is considered to be a distinct form of ACTH-dependent hypercortisolism with rather confusing biochemical and radiologic findings (39). When it is characterized by a single dominant nodule, there is a risk of confusing this lesion with a unilateral autonomous adrenal cortical adenoma, and performing an inappropriate unilateral adrenalectomy (37). The term multinodular adrenal gland has been used to emphasize that the nodules are rarely, if ever, solitary. MNH is defined by others as the presence of one or more prominent yellow nodules visible to the naked eye in glands in which the remaining cortex is hyperplastic (38).

In MNH, the adrenal glands are enlarged and often show a multinodular configuration on transverse sections (fig. 3-23, top). One or more dominant nodules may distort the intact gland, and form a rounded projection from virtually any region. In one study, the average individual weight of the adrenal gland in MNH was about 16 g, and in one case, the weight of both adrenal glands was 87.5 g (39). In an earlier series of patients with Cushing's disease undergoing subtotal (about 90 percent) adrenalectomy, most glands had a combined weight of 14 to 26 g (40). Some patients undergoing subtotal bilateral adrenalectomy developed "adenoma-like" recurrences (41), thus underscoring the possibility of confusing MNH with an adrenal cortical neoplasm. Nodules vary in size from 0.5 to over 5 cm in size (37,39), but most are less than 2 cm. There may be a disparity between the size and weight of individual glands.

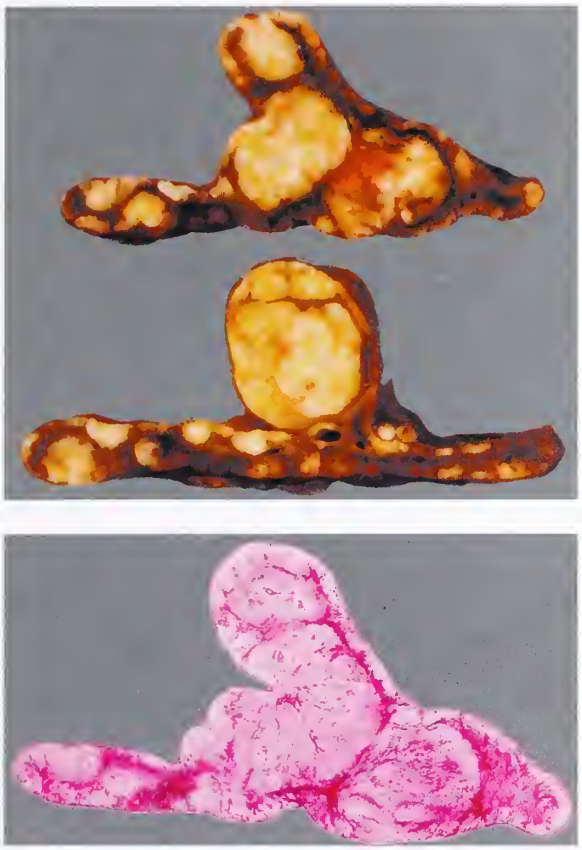

Figure 3-23

MACRONODULAR ADRENAL CORTICAL HYPERPLASIA IN CUSHING'S DISEASE

Top: The pale yellow cortical nodules range in size from 0.5 cm to over 1.0 cm. There are a few areas of capsular extrusion. The patient was a 36-year-old man with multiple endocrine neoplasia (MEN) syndrome type 1 who underwent right radical nephrectomy for an angiomyolipoma that simulated a renal cell carcinoma.

Bottom: Irregular expansile cortical nodules merge with adjacent hyperplastic cortex.

Grossly, the nodules appear discrete and sharply demarcated, and some dominant macronodules give the impression of encapsulation; on microscopic study, however, the nodules are less well defined, and blend almost imperceptibly with the adjacent hyperplastic cortex (fig. 3-23, bottom). There is a variable mixture of pale-staining, lipid-rich cells and lipid-depleted cells with compact, eosinophilic cytoplasm (fig. 3-24). Some nodules are composed almost exclusively of lipid-rich cells, which correspond to the yellow nodules seen on gross inspection. Prominent cortical nodules may compress and distort the

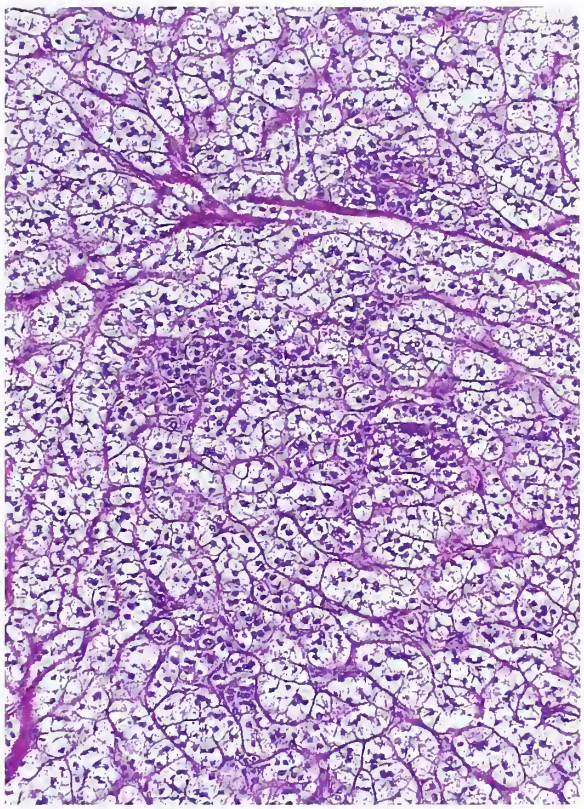

Figure 3-24

MACRONODULAR ADRENAL CORTICAL HYPERPLASIA IN CUSHING'S DISEASE

The nodules are composed of predominantly pale-staining, lipid-rich cells with scattered collections of lipid-depleted cells.

Table 3-3

COMPARISON OF DIFFUSE AND MICRONODULAR HYPERPLASIA WITH MACRONODULAR HYPERPLASIA IN CUSHING'S DISEASE[a,b]

	Diffuse and Micronodular Hyperplasia	Macronodular Hyperplasia
Female to male	5 to 1	5 to 1
Age (average)	31 yrs	44 yrs
Duration of disease (avg.)	2 yrs	8 yrs
Adrenal weight (avg.)	8 g each (less disparity in weight)	16 g each (may be some disparity in weight)
Nodule size	Less than 0.5 cm	0.5 to 5.3 cm

[a]Table 3-4 from Fascicle 19, Third Series.
[b]Data from reference 39.

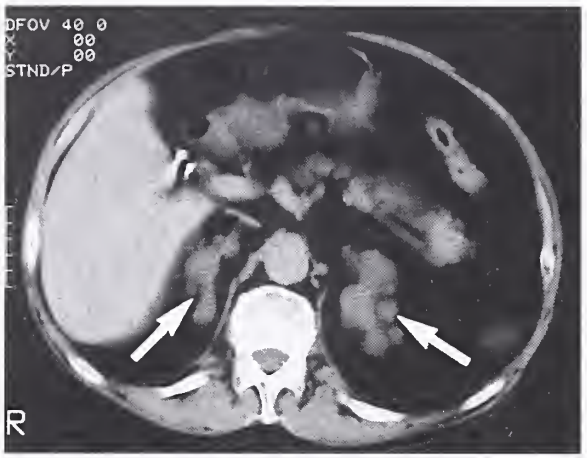

Figure 3-25

MACRONODULAR HYPERPLASIA WITH MARKED ADRENAL ENLARGEMENT

Extensive endocrine evaluation and imaging studies of the sella turcica and pituitary fossa indicated a primary adrenal form of Cushing's syndrome. The normal configuration of the adrenal glands (arrows) is obscured by multiple macronodules up to 3.8 cm in diameter. This marked enlargement can simulate a neoplasm. The combined weight of adrenal glands was 94 g. (Fig. 2 from Doppman JL, Nieman LK, Travis WD, et al. CT and MR imaging of massive macronodular adrenocortical hypercorticolism. J Computr Assist Tomogr 1991;15:773-779.)

adrenal medulla, and it may be difficult to recognize the medullary compartment in histologic sections (40). There may be foci of lipomatous or myelolipomatous metaplasia.

There are data suggesting that MNH may be the result of longstanding Cushing's disease with varying degrees of pituitary dependency and adrenal cortical autonomy (39). In one study there was a good correlation between the weight of the adrenal gland and the duration of the disease (Table 3-3) (39). Some data suggest that the cortical cells of MNH may require lower circulating levels of ACTH to sustain hypercortisolism compared with diffuse hyperplasia (42). The plasma levels of ACTH in some cases may be lower than in classic Cushing's disease, or even undetectable, and there may be absence of suppression with low-dose and high-dose dexamethasone. Some have advocated bilateral adrenalectomy as the treatment of choice for some cases of MNH in this setting (39). It is difficult to determine whether these dominant macronodules are truly neoplastic, or represent autonomous hyperplasia that requires no ACTH or only very low levels to maintain the hypercortisolism. In one study there was evidence of transition from pituitary-dependent to adrenal-dependent Cushing's syndrome (43); the situation may be similar to nodular goiter in which one or more thyroid nodules become "toxic" and acquire autonomous hyperfunction (1).

MACRONODULAR HYPERPLASIA WITH MARKED ADRENAL ENLARGEMENT

Definition. *Macronodular hyperplasia with marked adrenal enlargement* (MHMAE), as defined by sensitive imaging and endocrinologic study, is a primary (autonomous) adrenal cause of Cushing's syndrome. It may simulate an adrenal cortical neoplasm. The adjective "marked" in MHMAE is merely a descriptive term since some of the adrenal glands in this disorder are not greatly enlarged.

General Considerations. MHMAE is a very rare cause of primary autonomous adrenal hypercortisolism in which there is often tumefactive enlargement of both adrenal glands (fig. 3-25). MHMAE is a heterogeneous disorder in which cortisol secretion can be mediated by hormones other than ACTH following the aberrant or ectopic expression of various hormone receptors (44). Ectopic receptors for GIP, beta-adrenergic receptor agonists, vasopressin, 5-hydroxytryptamine, and probably angiotensin II have been identified (45,46).

The primary etiology of MHMAE remains unclear (45). Several candidate genes that may be responsible for MHMAE formation and/or progression have been identified, suggesting pathways that affect the cell cycle and transcription as possible mediators of adrenal cortical hyperplasia (44). Endocrine studies, including dynamic testing, indicate elevated plasma cortisol levels with loss of diurnal rhythmicity and very low or undetectable plasma ACTH levels; there is no suppression of adrenal cortisol secretion with dexamethasone, but some studies indicate a response to ACTH stimulation (47). There is no abnormality of the sella turcica or pituitary fossa on imaging studies, even in one patient who was reinvestigated almost 26 years later (47), the original case of MHMAE reported by Kirschner et al. in 1964 (48). Results of petrosal venous sinus sampling are also negative for a low-level pituitary source of ACTH.

Table 3-4

CUSHING'S SYNDROME DUE TO MACRONODULAR ADRENAL CORTICAL HYPERPLASIA WITH MARKED ADRENAL ENLARGEMENT[a]

Bilateral macronodular hyperplasia; combined adrenal weights often 60 to 180 g
Bilateral adrenalectomy considered treatment of choice in most cases
Elevated plasma cortisol with loss of diurnal variation
No suppression of adrenal cortisol secretion by dexamethasone
Variable response to ACTH[b] stimulation
No abnormality on petrosal venous sinus sampling
Lack of abnormality of sella or pituitary fossa

[a]Table 3-5 from Fascicle 19, Third Series.
[b]ACTH = adrenocorticotropic hormone.

MHMAE has also been reported to be a cause of subclinical Cushing's syndrome (49).

A few series reported to date suggest a slight predilection for female patients (47,50), although some data suggest a more equal sex distribution (50). The average age at diagnosis in one study was 56.2 years (50). Another study reported that the duration of the Cushing's syndrome ranged from 4 months to 10 years. Patients are usually older than those with diffuse and micronodular hyperplasia or MNH associated with Cushing's disease (39). Some of the features of MHMAE are summarized in Table 3-4.

Gross Findings. The adrenal glands in MHMAE can be markedly enlarged, with a combined weight of 28 to 297 g (fig. 3-26) (47). There is an extraordinary degree of nodular cortical hyperplasia, which is macronodular, with gross distortion of the glands on external examination. In one study, the nodules ranged in size from 0.1 to 5.5 cm (47). On gross examination, the external aspect of the intact adrenal gland is often coarsely bosselated, with discrete to closely aggregated nodules, which are rounded or have a distorted shape due to close apposition. On cross section, the nodules have a yellow to golden yellow hue, sometimes with small, irregular, light brown foci. The nodules are unencapsulated, and may give the impression of coalescence or fusion (fig. 3-27). The medullary compartment may be distorted and difficult to recognize, and random sections of the gland may fail to reveal it. A gland that is grossly distorted by macronodules may be difficult to orient in order to obtain good transverse sections. It is easy to see why MHMAE can simulate a tumor.

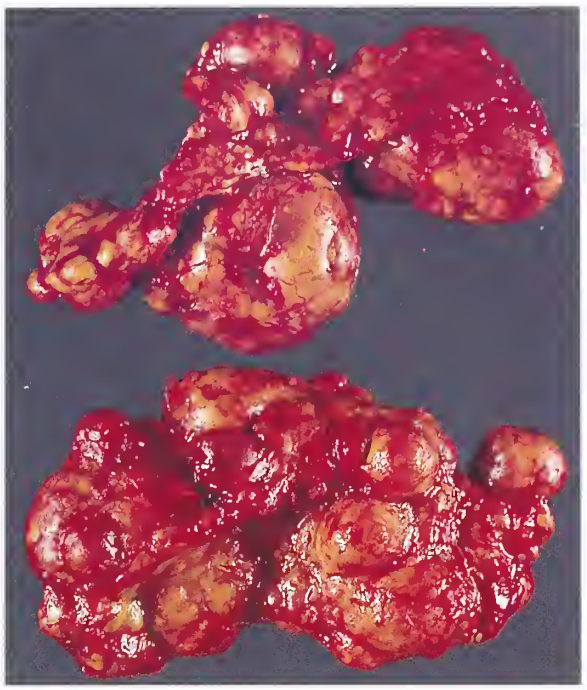

Figure 3-26

MACRONODULAR HYPERPLASIA WITH MARKED ADRENAL ENLARGEMENT

The combined weight of both adrenal glands was about 85 g. The external contour of both glands is greatly distorted by large cortical nodules. Endocrinologic workup and sensitive imaging studies indicated a primary adrenal form of Cushing's syndrome. (Fig. 3-23 from Fascicle 19, Third Series.)

Microscopic Findings. The cortical cells have a variable amount of lipid-rich, pale, vacuolated cytoplasm (fig. 3-28), and there may be some cells, random in distribution, with compact, eosinophilic cytoplasm. Rarely, cells with "ballooned" vacuolated cytoplasm are present (fig. 3-29, above). Nuclear pleomorphism is usually inconspicuous and mitotic figures are rare. An unusual feature is the presence of pseudoglandular foci with stringy, lightly basophilic material, but staining for mucin or glycogen is negative (fig. 3-29, right). It may be difficult or impossible to identify an intervening normal or diffusely hyperplastic cortex. In one study, the non-nodular cortex appeared atrophic in some areas, consistent with a disorder that is ACTH independent

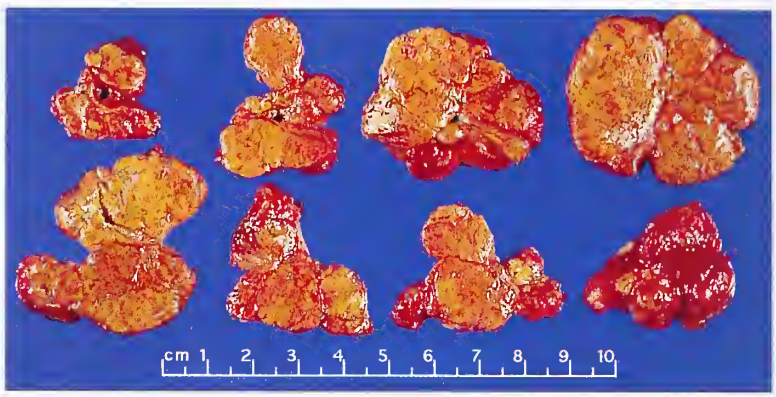

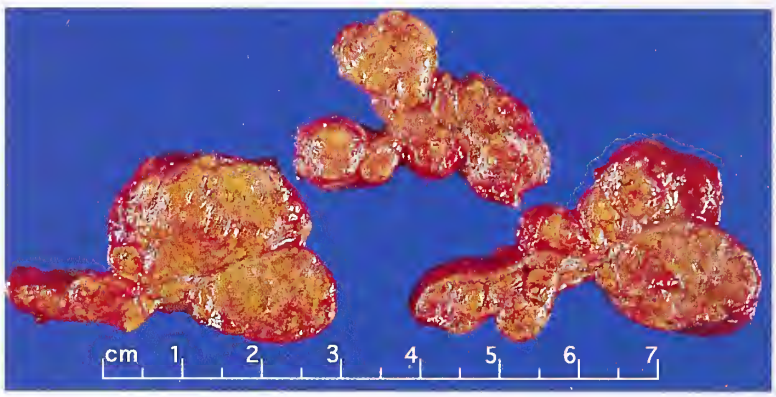

Figure 3-27

MACRONODULAR HYPERPLASIA WITH MARKED ADRENAL ENLARGEMENT

Transverse sections of both adrenal glands show marked thickening and nodularity of the golden yellow cortex. The nodules have ill-defined borders. The medulla is not evident. (Fig. 3-24 from Fascicle 19, Third Series.)

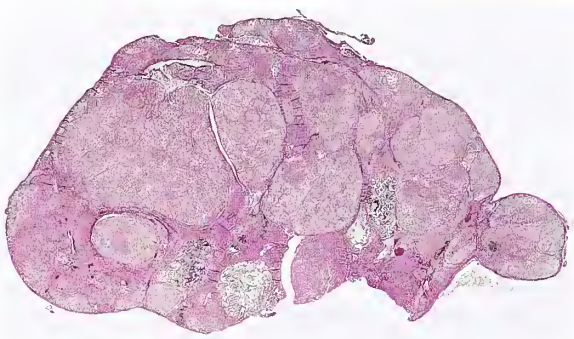

Figure 3-28

MACRONODULAR HYPERPLASIA WITH MARKED ADRENAL ENLARGEMENT

The gland is greatly distorted by large cortical nodules composed predominantly of pale-staining, lipid-rich cells. Some hyperplastic cortical cells extended into the periadrenal fat. (Fig. 3-25 from Fascicle 19, Third Series.)

(51). Irregular capsular extensions of cortical cells may be seen in sections from the periphery of the hyperplastic gland (fig. 3-30, left), and circumscribed capsular extrusions may appear more prominent than usual. Occasionally, there are lipomatous or myelolipomatous foci with rare bony metaplasia (fig. 3-30, right). The author has seen one case in which there was focal ischemic necrosis with dystrophic calcification (fig. 3-31). Weak reactivity for 3-beta-hydroxysteroid dehydrogenase and other enzymes involved in steroidogenesis has been reported in MHMAE in comparison with stronger staining in the usual adrenal cortical adenoma (51).

Ultrastructural study shows a poorly developed smooth endoplasmic reticulum (51). In situ hybridization of P-450$_{c17}$ can be used to localize the site of steroidogenesis (52). These studies suggest that effective corticosteroidogenesis by individual cortical cells is limited, and that a significant increase in cell number (i.e., hyperplasia) is necessary before excess cortisol production occurs, with resultant Cushing's syndrome. By contrast, cortical cells within nodules of primary pigmented nodular adrenocortical disease (PPNAD) have intense activity for steroidogenic enzymes (53,54); the nodules consist largely of cells with compact, eosinophilic cytoplasm and show a significantly developed smooth endoplasmic reticulum. A possible

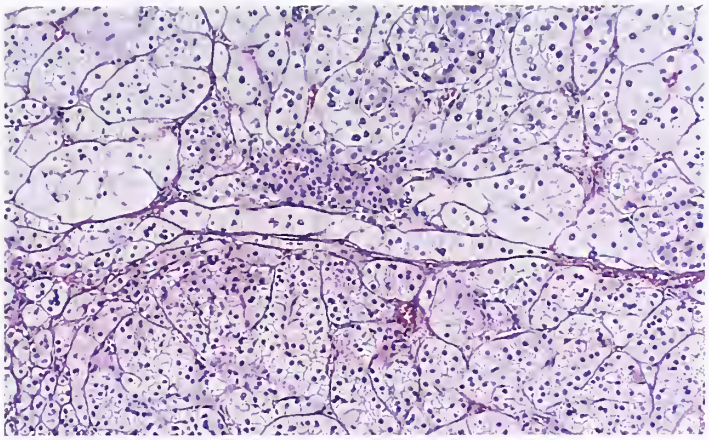

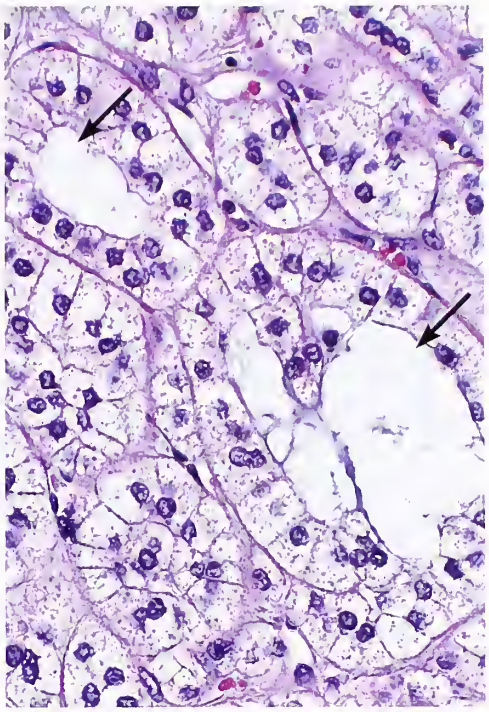

Figure 3-29

MACRONODULAR HYPERPLASIA
WITH MARKED ADRENAL ENLARGEMENT

Above: The cells have prominent pale-staining cytoplasm which is finely vacuolated due to abundant lipid. Some cells have a "ballooned" appearance. (A&R: Fig. 3-26 from Fascicle 19, Third Series.)

Right: Most hyperplastic cortical cells resemble those of the zona fasciculata. There are several pseudoglandular spaces (arrows).

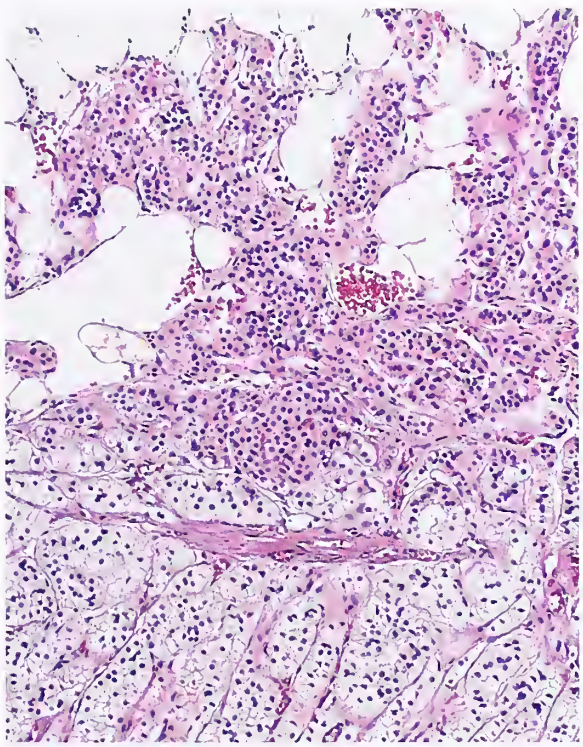

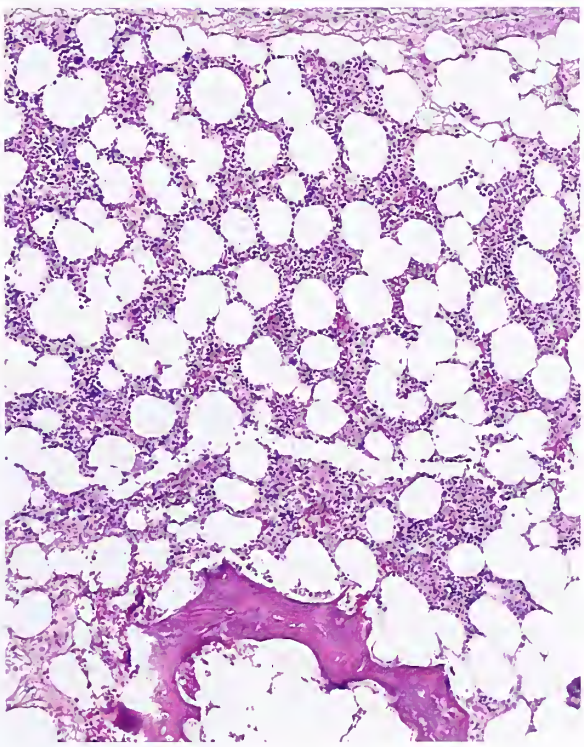

Figure 3-30

MACRONODULAR HYPERPLASIA WITH MARKED ADRENAL ENLARGEMENT

Left: Hyperplastic cortical cells stream out into periadrenal adipose tissue. Some cells have compact, lipid-depleted cytoplasm.
Right: Myelolipomatous metaplasia with bone formation. (L&R: Fig. 3-27 from Fascicle 19, Third Series.)

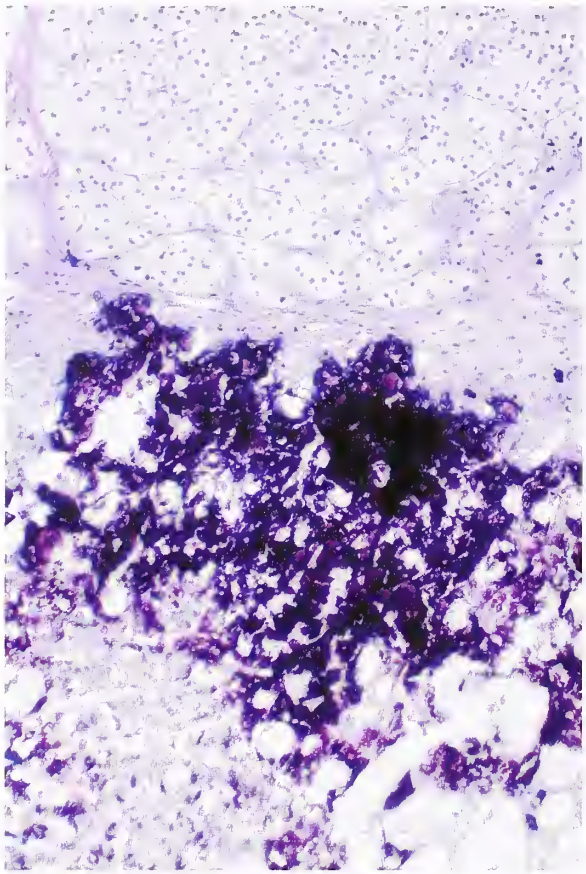

Figure 3-31

MACRONODULAR HYPERPLASIA WITH MARKED ADRENAL ENLARGEMENT

A small zone of ischemic necrosis is accompanied by dystrophic calcification.

relationship between MHMAE and MNH of Cushing's disease cannot be established with certainty in most cases reported to date (fig. 3-32). Immunostains contribute little to the diagnosis of MHMAE, but these hyperplastic lesions may be positive for endocrine markers such as synaptophysin.

Treatment. Bilateral adrenalectomy is currently the treatment of choice for this rare form of primary (autonomous) Cushing's syndrome. Nelson's syndrome has not been reported. The identification of aberrant or ectopic adrenal G-protein-coupled receptors offers the potential for novel pharmacologic therapies that either suppress the endogenous ligand or block the receptor with specific antagonists (46).

PRIMARY PIGMENTED NODULAR ADRENOCORTICAL DISEASE

Definition. *Primary pigmented nodular adrenocortical disease* (PPNAD) is a descriptive term for a distinctive but rare form of ACTH- or pituitary-independent Cushing's syndrome. PPNAD consists of bilateral nodular (usually micronodular) hyperplasia, with a variable degree of pigmentation within the nodules due to the accumulation of lipofuscin (see fig. 3-20, right). The adrenal glands may be small, normal in size, or mildly enlarged.

Clinical and Endocrinologic Features. This disorder has been referred to by a wide variety of terms which reflect an incomplete understanding of the etiology and pathogenesis.

Figure 3-32

MACRONODULAR ADRENAL CORTICAL HYPERPLASIA WITH MARKED ADRENAL ENLARGEMENT (SCHEMATIC DIAGRAM)

Sensitive endocrinologic testing and imaging studies indicate a rare primary form of ACTH-independent Cushing's syndrome. Some have wondered whether macronodular hyperplasia in Cushing's disease (left) can progress to bilateral autonomous Cushing's syndrome (right). (Fig. 3-28 from Fascicle 19, Third Series.)

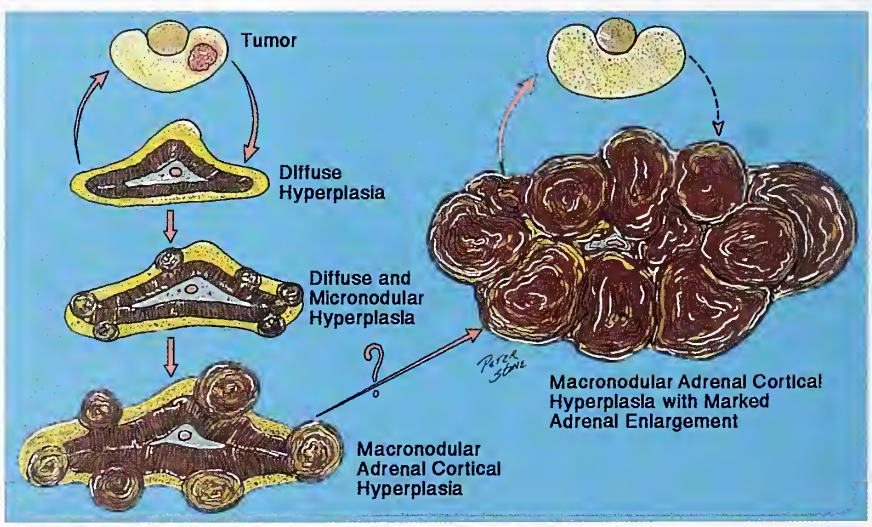

Table 3-5

CLINICAL FEATURES OF PRIMARY PIGMENTED NODULAR ADRENOCORTICAL DISEASE (PPNAD)[a,b]

Slight female predominance: 60%
Young age at diagnosis: average, 18 years; range, 4 to 32 years
Signs or symptoms of hypercortisolism: 82%; overt PPNAD
Associated conditions as main manifestation: 18%; subclinical or latent PPNAD
Average duration of hypercortisolism: 4.3 years (range, 0.3 to 18.0 years)
Osteoporosis, often severe: 39%
Cyclic hypersecretion of glucocorticoids: 4%
Treatment of choice: bilateral adrenalectomy; 35% of patients with unilateral or subtotal adrenalectomy required completion of total adrenalectomy
Spontaneous regression of Cushing's syndrome: rare
50% of cases familial and associated with unusual conditions

[a]Table 3-6 from Fascicle 19, Third Series.
[b]Data from reference 55.

Table 3-6

SIGNS AND SYMPTOMS OF CUSHING'S SYNDROME IN 72 PATIENTS WITH PRIMARY PIGMENTED NODULAR ADRENOCORTICAL DISEASE[a,b]

Sign or Symptom	Frequency (%)
Central obesity	62
Weight gain	61
Hirsutism	44
Hypertension	42
Osteoporosis	39
Abdominal striae	35
Menstrual cycle changes	33
Short stature	29
Muscular weakness	24
Acne	23
Easy bruising	20
Back pain	11
Depression	11
Precocious puberty	9
Renal lithiasis	9
Hypokalemia	8

[a]Table 3-7 from Fascicle 19, Third Series.
[b]Data from reference 55.

PPNAD typically affects relatively young individuals, often females, and the associated Cushing's syndrome may be severe (Tables 3-5, 3-6). PPNAD can be overt, subclinical, or latent with no clinical or laboratory evidence of Cushing's syndrome. The cyclic or intermittent hypersecretion of glucocorticoids (55) that occurs with PPNAD causes relapsing and remitting symptoms, which may arouse suspicion of a factitious etiology or Munchausen's syndrome, and some have questioned whether it was an early form of PPNAD or a new entity (56).

Endocrinologic studies, including dynamic testing, indicate a primary adrenal source for the hypercortisolism (Table 3-7). Sensitive imaging of the sella turcica and pituitary fossa shows no abnormalities, and selective venous sampling of the inferior petrosal sinus has not indicated a pituitary source of ACTH. Some patients have undergone unsuccessful pituitary ablation because the correct nature of the condition was not recognized. In several reports, the adrenal glands in PPNAD have been described as normal on CT scan, but unilateral or bilateral nodularity also has been reported using CT or MRI, and in older subjects macronodules (larger than 1 cm) have been detected (56). Patients with PPNAD have responded to dexamethasone with a paradoxical increase in glucocorticoids, a feature that distinguishes PPNAD from Cushing's syndrome caused by other primary adrenal disorders (57).

Gross Findings. The weights of adrenal glands vary from 0.9 to 13.4 g, with an average combined weight of 9.6 g (range, 4.3 to 17.0 g); about half of the individual weights are under 4 g and the rest are 4 g or more (55,58). The glands are usually normal in size. Gross examination of the external surface of the intact gland may reveal scattered pigmented nodules, usually 1 to 3 mm in size, beneath the capsule or bulging into periadrenal connective tissue (fig. 3-33). The "lumpy bumpy" contour of some glands may interfere with complete removal of adherent fat and connective tissue, which may make some recorded weights spuriously high. In transverse sections, there may be a spectacular array of small pigmented nodules studding the cortex, ranging in color from light gray, gray-brown, dark brown, to jet black (figs. 3-34, 3-35); a few nodules are yellow. Some glands contain pigmented or nonpigmented

Table 3-7

ENDOCRINOLOGIC FEATURES OF PRIMARY PIGMENTED NODULAR ADRENOCORTICAL DISEASE[a,b]

Autonomous Hypersecretion of Glucocorticoids	
Plasma ACTH[c]	Low or undetectable, 92% Normal, 8%
Plasma cortisol	High, 94% Normal, 6%
24-hour urine levels	
Cortisol	High, 95% Normal, 5%
17-OHCS/KGS[d]	High, 97% Normal, 3%
17-Ketosteroids	High, 49% Normal, 46% Low or undetectable, 5%
Results of Dynamic Testing	
Lack of dexamethasone suppression, low and high dose	
Occasional paradoxical increase in glucocorticoids with high-dose dexamethasone	
Failure of stimulation of glucocorticoid secretion with metyrapone	
Uptake of [6β[131]I] Iodomethyl-19-Norcholesterol on Adrenal Scintigraphy	

[a]Table 3-8 from Fascicle 19, Third Series.
[b]Data from reference 55.
[c]ACTH = adrenocorticotropic hormone.
[d]OHCS = hydroxycorticosteroids; KGS = ketogenic steroids.

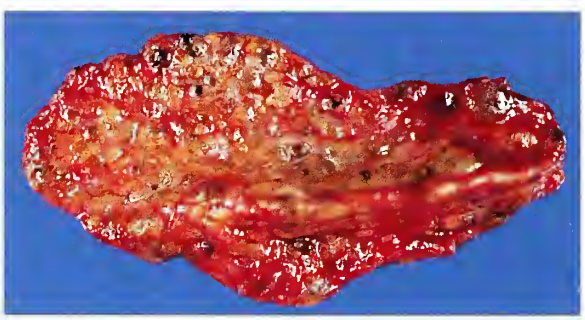

Figure 3-33

PRIMARY PIGMENTED NODULAR ADRENOCORTICAL DISEASE

Numerous jet black nodules are visible through the capsule on the dorsal surface of the intact gland. Both adrenal glands were small in size and low in weight, and the internodular cortex showed marked atrophy. (Fig. 3-29 from Fascicle 19, Third Series.)

macronodules measuring 1.8 to 3.0 cm in diameter; in some cases this appears to result from a confluence of smaller micronodules. The term

Figure 3-34

PRIMARY PIGMENTED NODULAR ADRENOCORTICAL DISEASE

Transverse sections of adrenal gland are studded by pigmented micronodules. Many are located along the inner aspect of the cortex. The cortex between the nodules is atrophic. (Fig. 3-30 from Fascicle 19, Third Series.)

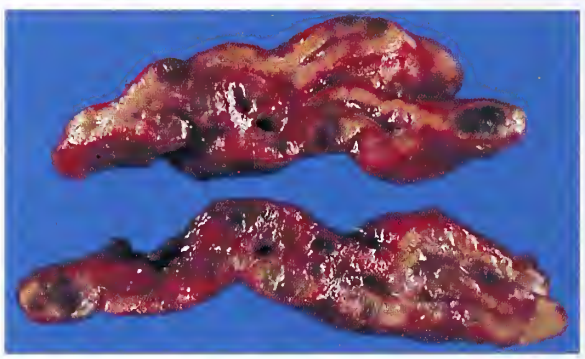

Figure 3-35

PRIMARY PIGMENTED NODULAR ADRENOCORTICAL DISEASE

There is no atrophy of the internodular cortex and pigmented nodules are not as deeply pigmented or jet black compared with figure 3-34. (Fig. 3-31 from Fascicle 19, Third Series.)

micronodular is entirely arbitrary since many of the intensely pigmented nodules are detected on gross examination even when they are smaller than 1 mm.

Microscopic Findings. The conspicuous nature of PPNAD on gross examination may become less obvious once the gland is evaluated histologically (fig. 3-36). The pigmented nodules are usually round to oval or have an

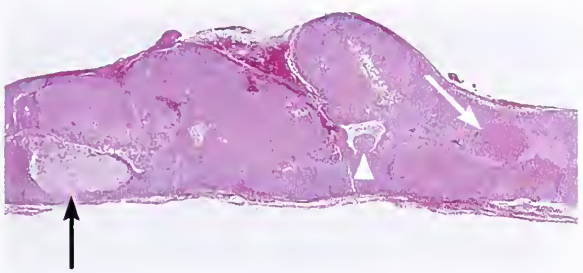

Figure 3-36

PRIMARY PIGMENTED NODULAR ADRENOCORTICAL DISEASE

Transverse section through the body of the gland shows micronodules that are less well-defined compared with the gross appearance. Some nodules straddle the corticomedullary junction and impinge on chromaffin cells (white arrow). Note the nodule composed of lipid-rich cells (black arrow) and the small hyperplastic nodule protruding into the vascular lumen between discontinuous bundles of smooth muscle (white arrowhead). (Fig. 3-32 from Fascicle 19, Third Series.)

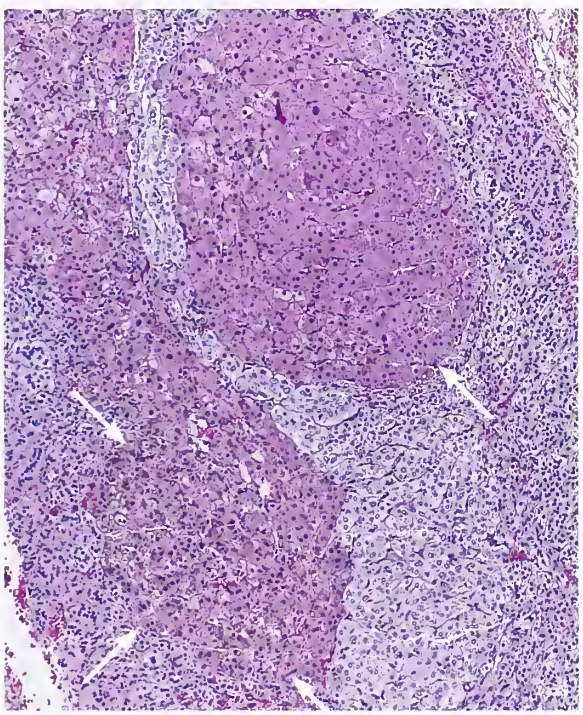

Figure 3-37

PRIMARY PIGMENTED NODULAR ADRENOCORTICAL DISEASE

Micronodules (arrows) are present at the corticomedullary junction on either side of the medulla. The nodules contain cells with compact, eosinophilic cytoplasm and focally prominent pigment. (Fig. 3-33 from Fascicle 19, Third Series.)

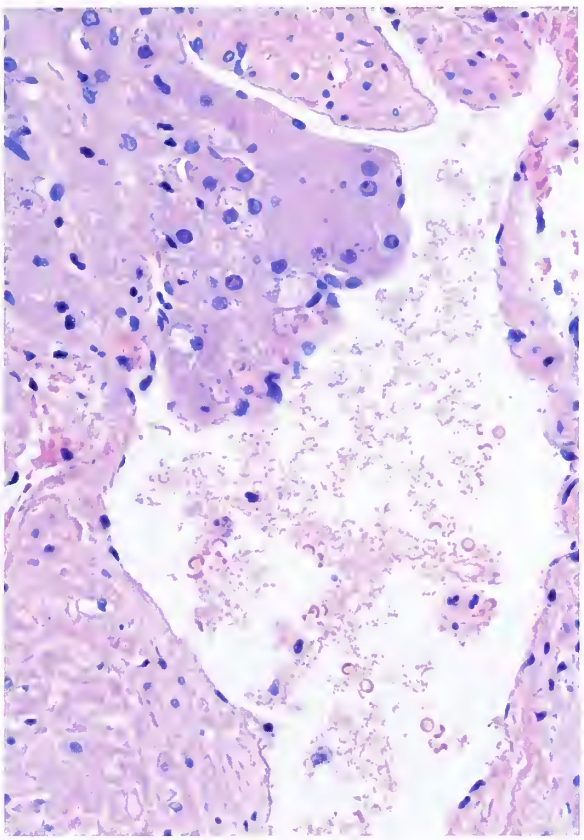

Figure 3-38

PRIMARY PIGMENTED NODULAR ADRENOCORTICAL DISEASE

The intravascular protrusion maintains continuity with the cortical cells in the gap of muscular arcades in the vessel wall.

irregular contour; some may have a silhouette that is reminiscent of an "hourglass," "string of beads," or "links of sausage." The nodules are unencapsulated, and are often deep within the cortex, centered on the zona reticularis, or straddle the corticomedullary junction with expansile borders (fig. 3-37). Some nodules may appear to occupy nearly the entire thickness of the cortex, and occasionally, they extend into periadrenal fat without any encapsulation. Occasionally, there is intraluminal projection of a nodule into tributaries of the central adrenal vein in association with discontinuities in bundles of smooth muscle (fig. 3-38). Depending upon the plane of section, the nodule may appear to lie free in the vascular lumen or have only a tenuous attachment (fig. 3-39).

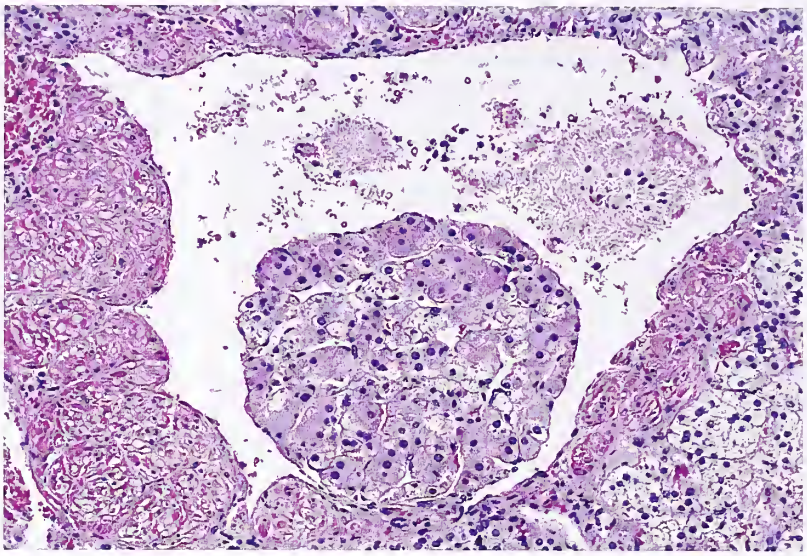

Figure 3-39

PRIMARY PIGMENTED NODULAR ADRENOCORTICAL DISEASE

A hyperplastic micronodule extends into the tributary of the central adrenal vein. There is a deficiency of smooth muscle in the vessel wall and intact endothelium over the surface of the micronodule projecting into the lumen. (Fig. 3-35 from Fascicle 19, Third Series.)

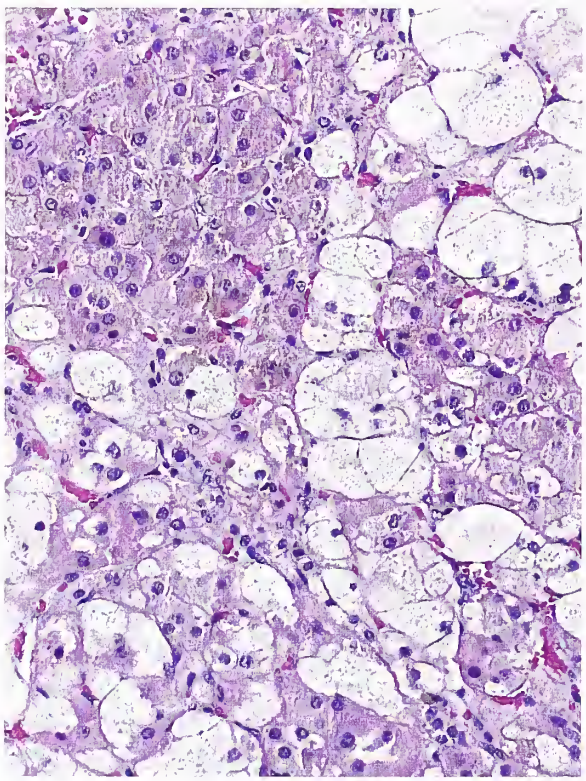

Figure 3-40

PRIMARY PIGMENTED NODULAR ADRENOCORTICAL DISEASE

This nodule is composed of cells with vacuolated, lipid-rich cytoplasm along with compact, lipid-depleted cells, both of which contain a variable amount of finely granular pigment representing lipofuscin. There is a mild degree of nuclear pleomorphism. (Fig. 3-36 from Fascicle 19, Third Series.)

Most cells within the nodules have lipid-depleted, compact, eosinophilic cytoplasm, although there may be an admixture of cells with more lipid-rich, vacuolated cytoplasm. Cellular enzymes, which are markers for steroidogenesis (53,54), are intensely active in almost all of the cells, especially those with abundant eosinophilic cytoplasm; this enzymatic profile may help to explain the paradox that adrenal glands that are normal in size or small can cause Cushing's syndrome (53). In one study, there was strong reactivity of enzymes in cells located in the zona reticularis, but not elsewhere in the adjacent internodular cortex, suggesting an abnormality of the zona reticularis in the pathogenesis of PPNAD (54). Some nodules contain abundant lipid-rich cells which may show some "ballooning" (fig. 3-40). Occasionally, a lipomatous (fig. 3-41) or even myelolipomatous component is present which represents a metaplastic phenomenon. This may also be apparent in other adrenal cortical lesions (hyperplastic and neoplastic) that are characterized by hyperfunction. Sparse lymphocytic infiltrates have been noted rarely, mainly around vessels, but also within the nodules (59,60). These cells are characterized as suppressor cytotoxic T cells or T-helper cells (59).

The cytologic features may be uniform, although occasionally cells are binucleated or multinucleated, or have enlarged hyperchromatic nuclei and prominent nucleoli (60). Mitotic figures are rare. The intracytoplasmic

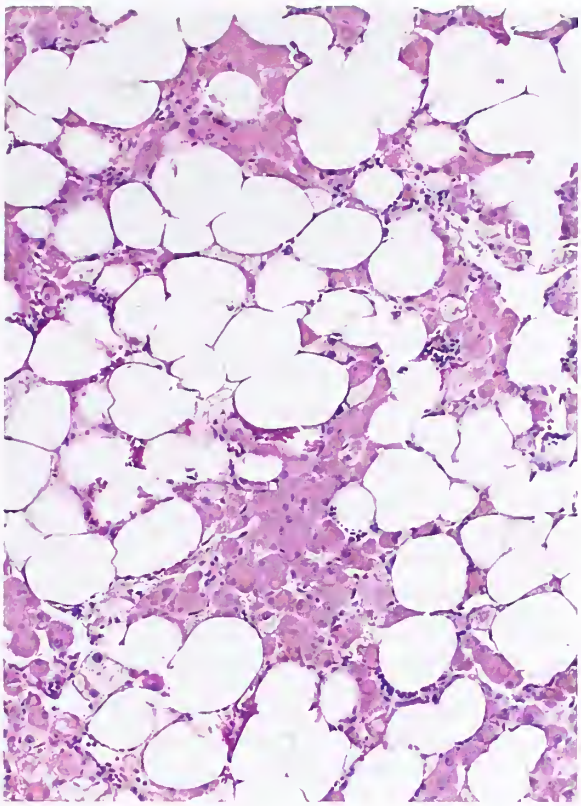

Figure 3-41

PRIMARY PIGMENTED NODULAR ADRENOCORTICAL DISEASE

This nodule has prominent lipomatous metaplasia with a small component of lymphocytes. Myeloid metaplasia is also found in some cases. (Fig. 3-37 from Fascicle 19, Third Series.)

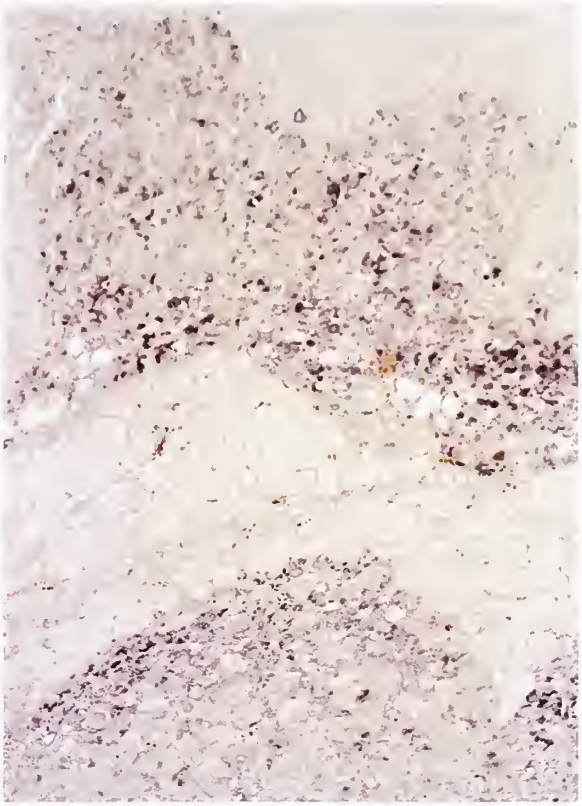

Figure 3-42

PRIMARY PIGMENTED NODULAR ADRENOCORTICAL DISEASE

Many of the cells of the micronodules are strongly argentaffin positive (Fontana-Masson stain).

pigment has the staining characteristics (fig. 3-42) and ultrastructural morphology of lipofuscin. Occasionally, treatment of sections with $KMNO_4$ abolishes this reaction, suggesting a component of neuromelanin (1).

Etiology and Pathogenesis. The etiology and pathogenesis of PPNAD are unknown, but the following have been proposed: 1) hamartomatous malformation or dysplasia of the adrenal cortex, a view supported in part by the varying amount of mature fat cells within the nodules; 2) a primary abnormality of the zona reticularis (53); 3) an occult ACTH-secreting pituitary tumor with cortical nodules becoming functionally autonomous; 4) an embryonic developmental error in adrenal cortex at the adrenarche (55); 5) a block in the evolution of

Table 3-8

VARIOUS THEORIES FOR THE ETIOLOGY AND PATHOGENESIS OF PRIMARY PIGMENTED NODULAR ADRENOCORTICAL DISEASE[a]

Hamartomatous malformation or dysplasia of adrenal cortex
Primary abnormality of zona reticularis
Occult ACTH[b]-producing pituitary adenoma with adrenal cortical nodules becoming functionally autonomous
Embryonic developmental error in adrenal cortex at the adrenarche
Block in evolution of zona fasciculata type cells into cells of zona reticularis with accumulation of autonomous cells at interface
Organ-specific form of autoimmune hypercortisolism (Cushing's syndrome)

[a]Table 3-9 from Fascicle 19, Third Series.

[b]ACTH = adrenocorticotropic hormone.

zona fasciculata–type cells to cells of the zona reticularis, with accumulation of cells at the interface, and formation of hyperfunctioning nodules that eventually become autonomous or ACTH independent (55); and 6) a form of autoimmune hypercortisolism (Table 3-8). The last theory is based upon reports of circulating adrenal-stimulating immunoglobulin (ASI) which has a stimulatory effect on segments of guinea pig adrenal gland in vitro as indicated by quantification of nuclear DNA (59,61,62). These observations support the hypothesis that PPNAD may represent an organ-specific autoimmune form of Cushing's syndrome with the ASI directed against the ACTH receptor or domains of this receptor (61). Atrophy of the internodular cortex may be due to heterogeneous responsiveness of cortical cells to autoimmune stimulation or some paracrine effect (62). The micronodules of PPNAD, but not the extranodular adrenal cortex, have shown intense immunostaining for synaptophysin (63). Further investigation is needed to determine whether PPNAD is truly an autoimmune disorder or one in which the circulating ASI is merely an epiphenomenon. Kindreds have been reported with circulating ASI, yet there is no clinical or biochemical evidence of hypercortisolism (62); an analogous situation may exist with patients who have circulating thyroid-stimulating antibodies, but are euthyroid on clinical evaluation and laboratory testing. Mutations in the gene coding for the protein kinase A type 1-alpha regulatory subunit (PRKAR1A) have been reported in patients with sporadic PPNAD and PPNAD associated with Carney's complex (64).

Treatment. Bilateral adrenalectomy is considered to be the treatment of choice for PPNAD (65), although some cases may permit less than total resection (55). The surgeon must be prepared to remove both adrenal glands, which may appear normal in size or even small. About one third of the patients initially treated by unilateral or subtotal adrenalectomy require subsequent total adrenalectomy due to persistence or recurrence of signs or symptoms of Cushing's syndrome (55). Nelson's syndrome has not been reported following bilateral adrenalectomy in patients with PPNAD. Rarely, Cushing's syndrome has been reported to regress spontaneously although dynamic endocrine testing showed persistent autonomous adrenal cortical function (62). It is of interest that one of the patients originally described by Cushing in 1932 (Minnie G) experienced gradual resolution of Cushing's syndrome (32).

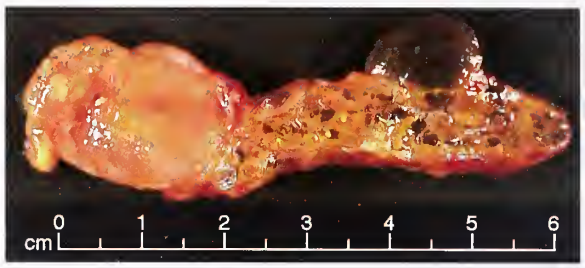

Figure 3-43

PRIMARY PIGMENTED NODULAR ADRENOCORTICAL DISEASE

A large pigmented macronodule and a larger pale yellow nodule with small areas of necrosis are seen. The patient was part of a family pedigree with the complex of myxomas, spotty pigmentation, and endo-crine overactivity (Carney's complex). There was a complex history of a retrogastric melanotic schwannoma, fibro-lamellar hepatoma, hyperpigmentation of the inner canthus of both eyes, and most recently, an ovarian serous cysta-denoma. The patient developed multiple pulmonary nodules which histologically were consistent with an adrenal cortical origin (possible metastases), but paradoxically was in good health for several years. The patient apparently died of metastatic melanotic schwannoma but autopsy was not performed. (Fig. 3-39 from Fascicle 19, Third Series.)

COMPLEX OF MYXOMAS, SPOTTY PIGMENTATION, AND ENDOCRINE OVERACTIVITY (CARNEY'S COMPLEX)

Originally proposed in 1985 (66), *Carney's complex* consists of an array of diverse abnormalities, which in many cases has an autosomal dominant mode of inheritance (67,68). In a review of PPNAD, about half of the cases occurred in a nonfamilial or sporadic setting, and the rest were familial (fig. 3-43). In a recent review of 338 patients with Carney's complex, 70 percent of cases were familial and often associated with the unusual conditions indicated in Table 3-9 (69). Some examples of this complex have been published with acronyms such as the *LAMB syndrome* (lentigines, atrial myxoma, mucocutaneous myxomas, blue nevi) (70) and the *NAME syndrome* (nevi, atrial myxoma, myxoid neurofibroma, ephelides) (71).

The molecular defects leading to Carney's complex have been mapped to chromosomes 2p16 and 17q22-24 (71a). There may be involvement in the regulation of genomic stability of dividing cells, in particular, the structure of telomeres in replicating chromosomes and/or the function of the mitotic apparatus (72). Recently, the tumor suppressor gene *PRKAR1A* at the 17q22-24 locus was found to be mutated in approximately half of the known kindreds with the complex (69).

The criteria for the diagnosis of Carney's complex are listed in Table 3-9 (69). If patients are identified with two or more elements of this complex, particularly PPNAD, bilateral large cell calcifying Sertoli cell tumors of testis, or mucocutaneous pigmentation (fig. 3-44), investigation for possible cardiac myxoma is recommended to permit early detection and treatment (69). Cardiac tumors present at a relatively early age (average, 24 years), and are frequently multiple (66).

Table 3-9

DIAGNOSTIC CRITERIA FOR CARNEY'S COMPLEX[a]

1. Spotty skin pigmentation with typical distribution (lips, conjunctiva and inner or outer canthi, vaginal and penile mucosa)
2. Myxoma (cutaneous and mucosal)[b]
3. Cardiac myxoma[b]
4. Breast myxomatosis[b] or fat-suppressed magnetic resonance imaging findings suggestive of this diagnosis[c]
5. Primary pigmented nodular adrenocortical disease or paradoxical positive response of urinary glucocorticoids to dexamethasone administration during Liddle's test[d]
6. Acromegaly due to growth hormone (GH)-producing adenoma[b]
7. Large cell calcifying Sertoli cell tumor[b] or characteristic calcification on testicular ultrasonography
8. Thyroid carcinoma[b] or multiple, hypoechoic nodules on thyroid ultrasonography, in a young patient
9. Psammomatous melanotic schwannoma[b]
10. Blue nevus, epithelioid blue nevus (multiple)[b]
11. Breast ductal adenoma (multiple)[b]
12. Osteochondromyxoma[b]

Supplemental Criteria

1. Affected first-degree relative
2. Inactivating mutation of the *PRKAR1A* gene

[a]To make a diagnosis of Carney's complex, a patient must either: 1) exhibit two of the manifestations of the disease listed or 2) exhibit one of these manifestations and meet one of the supplemental criteria.
[b]With histologic confirmation.
[c]Data from reference 68.
[d]Data from reference 57.

ECTOPIC ACTH SYNDROME WITH HYPERCORTISOLISM

About 12 percent of Cushing's syndrome in adults is due to ectopic production of ACTH (24). The source is usually a neoplasm, but there have been isolated reports of unusual non-neoplastic conditions associated with the syndrome (73,74). Almost all normal tissues produce small amounts of a biologically inactive precursor of the ACTH molecule, probably proopiomelanocortin (POMC). Cancers produce this same substance in increased quantities, although only a select number convert POMC into biologically active ACTH to produce the *"ectopic" ACTH syndrome*; in this context ectopic ACTH production is not necessarily ectopic (75). It may be possible to detect mRNA expression of POMC by the use of molecular probes such as in situ hybridization. Since pituitary microsurgery is the treatment of choice for Cushing's disease, correct identification of the source of ACTH secretion becomes essential, and unfortunately, failure to recognize it may occasionally result in unnecessary pituitary surgery. Cushing was correct in assuming that secretions from pituitary basophilic adenomas were responsible for the pluriglandular syndrome, but two of his original nine patients who were autopsied had no evidence of a pituitary lesion (32,76).

The neoplastic sources of ectopic ACTH production include bronchial carcinoid tumor (77), pulmonary and extrapulmonary small cell carcinoma (fig. 3-45), pancreatic islet cell carcinoma (fig. 3-46), medullary thyroid carcinoma, thymic carcinoid, pheochromocytoma (fig. 3-47), and a variety of other tumors. There are also cases of ectopic CRF production (78), which may also be accompanied by ectopic ACTH secretion (26). In some instances, the ectopic ACTH production is clinically and biochemically indistinguishable from pituitary-dependent Cushing's disease (79); in the ectopic ACTH syndrome, however, ACTH levels are usually

Figure 3-44

COMPLEX OF MYXOMA AND SPOTTY PIGMENTATION

Left: A young girl with multiple pigmented lesions about the mouth. The patient also had a darkly pigmented lesion on the vulva, probably a blue nevus.

Right: Cutaneous myxoma on the breast of the same patient, who also had a cardiac myxoma. There was no evidence of an adrenal abnormality or Cushing's syndrome. (L&R: Fig. 3-40 from Fascicle 19, Third Series.)

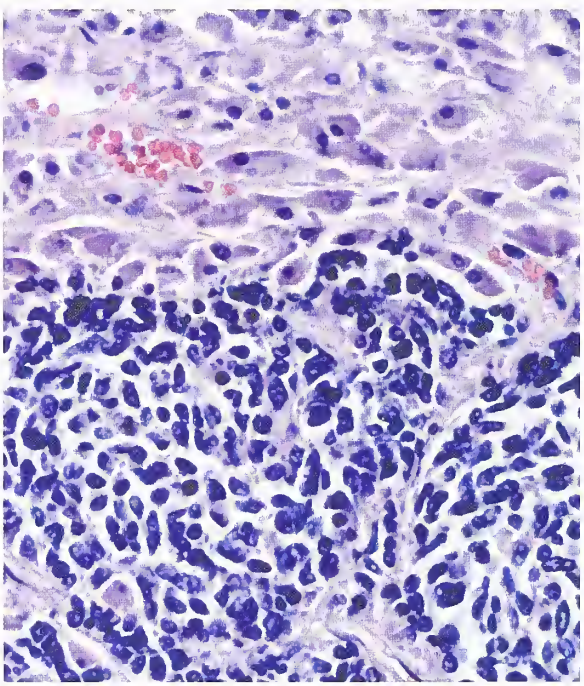

Figure 3-45

ECTOPIC ACTH SYNDROME

Adrenal gland at autopsy of an elderly man who had disseminated small cell (oat) carcinoma of lung. There was no clinical evidence of Cushing's syndrome, but both adrenal glands were markedly enlarged, weighing about 20 g each. The cortex was diffusely hyperplastic, and below in this field is metastatic small cell carcinoma.

quite elevated (24), sometimes over 250 pg/mL, whereas in Cushing's disease ACTH levels are often "normal" (upper range of normal) or only slightly elevated (75), and only rarely are levels of ACTH over 200 pg/mL. Rare ovarian neoplasms of various types are associated with Cushing's syndrome (80). A remarkable case of severe Cushing's syndrome has been reported due to a corticotroph cell pituitary adenoma arising in a benign cystic teratoma of the ovary (81).

The clinical features of Cushing's syndrome may be absent in patients with aggressive neoplasms such as bronchogenic small cell carcinoma, and instead the clinical picture may be dominated by cachexia or electrolyte disturbances with hypokalemia and metabolic acidosis (1). Other neoplasms, such as bronchial carcinoid tumors, may be associated with florid Cushing's syndrome, while the primary tumor remains indolent and occult, sometimes for several years. The *occult ectopic ACTH syndrome* has been defined as ACTH-dependent hypercortisolism of greater than 6 months' duration without emergence of an obvious cause or source (82).

The adrenal glands in patients with ectopic ACTH syndrome are symmetrically enlarged with rounded contours, and usually weigh 10 to 15 g each (fig. 3-48); sometimes the individual weight may exceed 20 g and rarely 30 g (1). Under

conditions of rather intense and constant stimulation by ACTH, there is diffuse hyperplasia, sometimes accompanied by vague nodularity. On transverse sections, the glands are usually tan to brown due to the conversion of pale-staining, lipid-rich cells into cortical cells with compact, eosinophilic cytoplasm (fig. 3-49, left). The cortex is often 0.3- to 0.4-cm thick, but may be even wider. The hyperplastic cortex may thus resemble a greatly expanded zona reticularis. Some cortical cells may be hypertrophied, with abundant eosinophilic cytoplasm and moderately enlarged nuclei (fig. 3-49, right), an appearance similar to the enlarged cortical cells in advanced idiopathic or autoimmune Addison's disease. There may also be small clusters of lipid-rich cortical cells randomly distributed in the zona fasciculata. Occasionally, there is lipomatous metaplasia.

MULTIPLE ENDOCRINE NEOPLASIA SYNDROME TYPE 1

Multiple endocrine neoplasia (MEN) *syndrome type 1*, also referred to as *Wermer's syndrome*, is inherited as an autosomal dominant trait; expression is variable and it may appear in sporadic form or affect family members in whom manifestations are detectable only after close scrutiny. MEN type 1 causes combinations of over 20 different endocrine and nonendocrine tumors (Table 3-10) (83). Factors other than heredity may be important in MEN type 1 as evidenced by nonidentical expression of the syndrome in identical twins (84). The MEN type 1 gene is located at chromosome 11(11q13) (83).

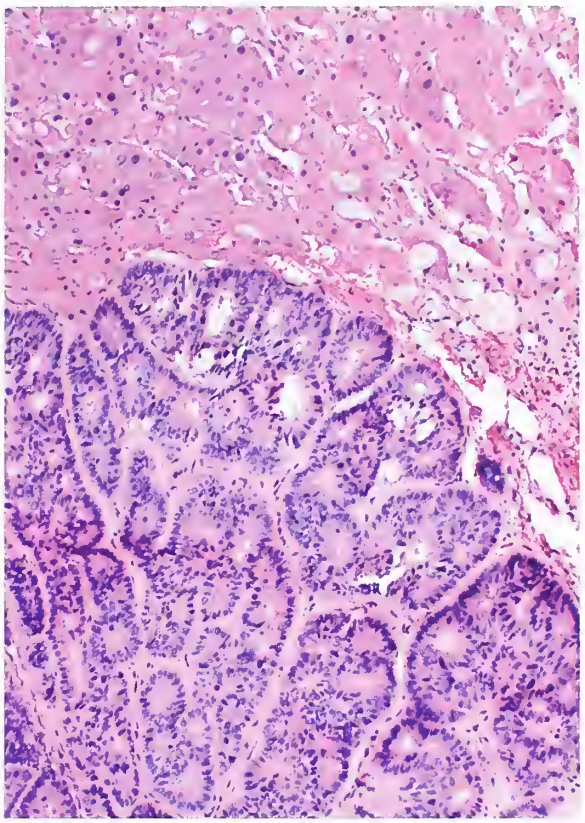

Figure 3-46

ECTOPIC ACTH SYNDROME

Ectopic ACTH syndrome in a patient with a malignant pancreatic endocrine neoplasm which here metastasized to the hyperplastic adrenal gland. Hyperplastic cortical cells are evident at top of field. The tumor has a well-developed acinar pattern.

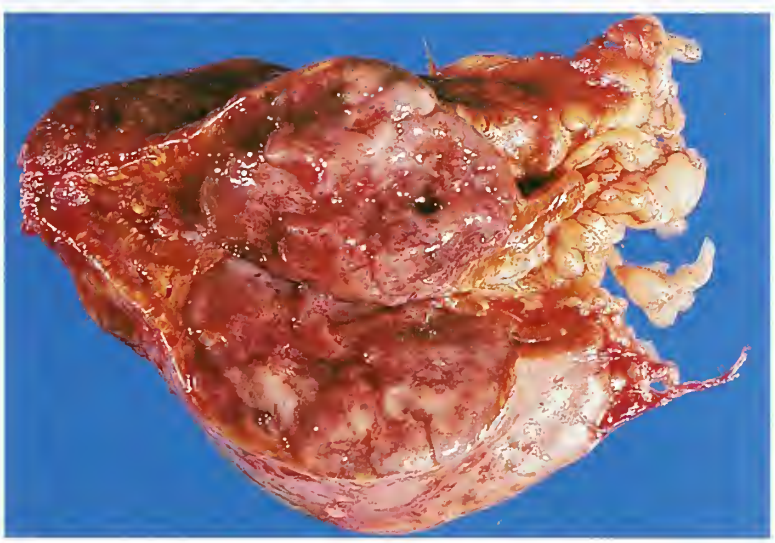

Figure 3-47

ECTOPIC ACTH SYNDROME DUE TO PHEOCHROMOCYTOMA

A 51-year-old white female presented with hypertension, facial swelling, and hirsutism. There were elevated steroid metabolites in the urine which could not be suppressed with high-dose dexamethasone. Skull X rays showed no abnormalities of the sella turcica. Following surgical removal of this 3-cm pheochromocytoma, hirsutism regressed and steroid levels normalized. Surgery was compli-cated by hypotensive episodes. The hyperplastic adrenal cortex was largely lipid depleted. Biopsy of the opposite hyperplastic adrenal gland was identical. (Fig. 3-43 from Fascicle 19, Third Series.)

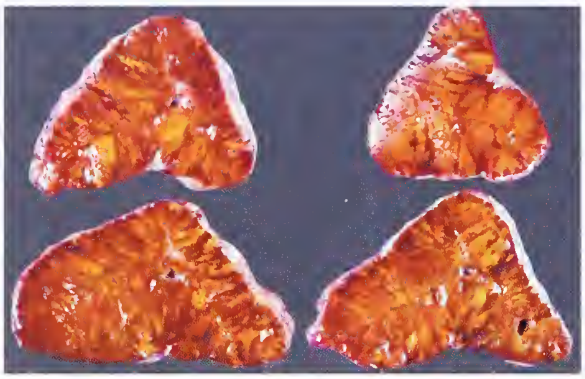

Figure 3-48

ECTOPIC ACTH SYNDROME

Left: Transverse sections of adrenal glands surgically resected from a patient with ectopic ACTH syndrome due to a bronchial carcinoid tumor. The tumor had remained occult for several years. The right adrenal gland weighed 12 g and the left 11 g. The dark appearance is due to intense stimulation by ACTH. Vague nodularity is seen in some areas. (Courtesy of Dr. W. D. Travis, Bethesda, MD).

Right: Ectopic ACTH syndrome due to a clinically malignant pancreatic endocrine neoplasm. Both adrenal glands were surgically resected because the patient had residual tumor that ectopically produced ACTH. The adrenal gland here was enlarged due to diffuse cortical hyperplasia. On transverse sections the gland appeared darker than normal due to persistent trophic stimulation by ACTH.

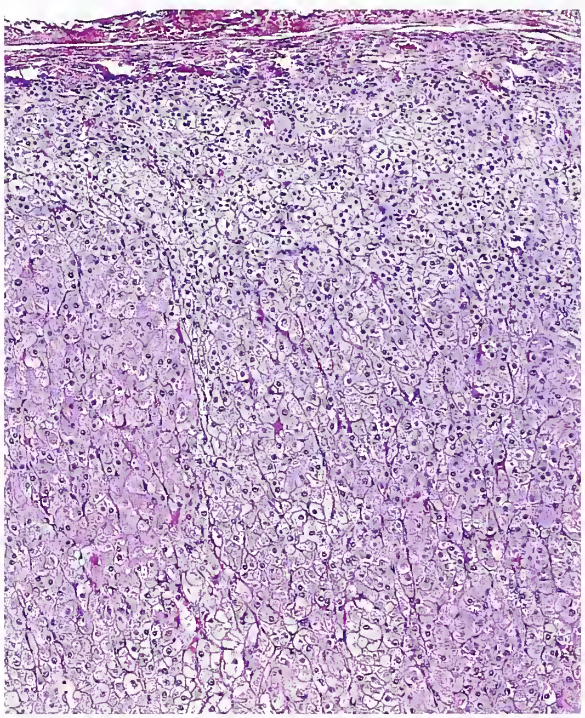

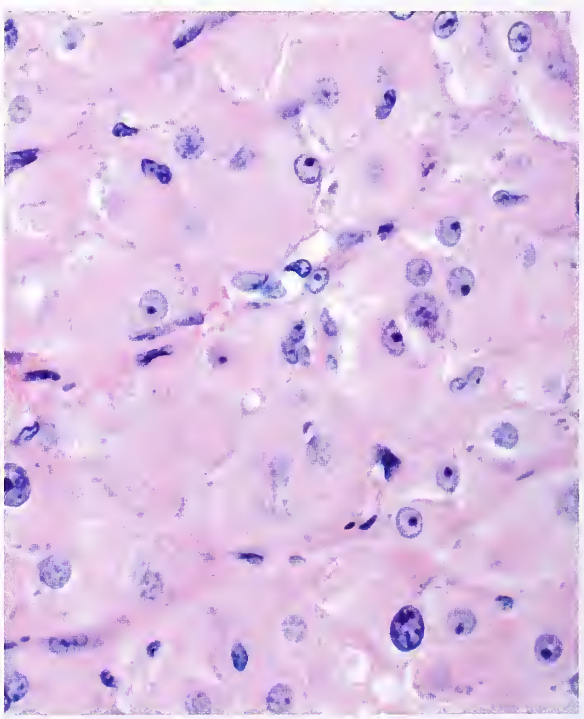

Figure 3-49

ECTOPIC ACTH SYNDROME DUE TO OCCULT BRONCHIAL CARCINOID TUMOR

Left: The cortex shows diffuse hyperplasia with lipid depletion in most cells of the zona fasciculata. (Fig. 3-45, left from Fascicle 19, Third Series.)

Right: Same case showing hypertrophy of the cortical cells, which have compact eosinophilic cytoplasm. Some cells contained sparse granular lipofuscin pigment.

In a review by Ballard et al. (85) of cases of MEN 1, the most common abnormalities were hyperparathyroidism (87 percent), pancreatic islet cell tumors (81 percent), and pituitary adenomas (65 percent). Autopsy protocols of 31 patients described adrenal pathology consisting of cortical adenomas, miliary adenomas, hyperplasia, multiple adenomas, and nodular hyperplasia, but only one patient had clinical hypercorticalism with increased aldosterone secretion. The pituitary-independent adrenal cortical proliferation does not appear to be the primary lesion in MEN type 1, and it has been postulated that it may be a secondary phenomenon, perhaps related to growth factors produced by the pancreatic endocrine neoplasm. Surprisingly, there is little clinical significance ascribed to these adrenal cortical alterations, even though they occur in about 25 percent of patients with MEN type 1 (83). Cushing's disease has been reported in patients with MEN type 1 (see fig. 3-23), but it is very uncommon (86).

In a series of 1,500 pituitary adenomas surgically resected at the Mayo Clinic, 41 (2.7 percent) arose in patients with MEN type 1; these included three corticotroph adenomas, two of which occurred in the setting of Nelson's syndrome and one classified as a "silent corticotrophic adenoma" (87). One of two monozygotic twins had Cushing's disease due to corticotroph cell hyperplasia, but abnormal CRF secretion either from the hypothalamus or an ectopic source is also a possibility.

Table 3-10

EXPRESSIONS OF MULTIPLE ENDOCRINE NEOPLASIA (MEN) TYPE 1 WITH ESTIMATED PENETRANCE (IN PARENTHESES) AT AGE 40 YEARS

Endocrine Features	Nonendocrine Features
Parathyroid adenoma (90%)	Lipomas (30%) Facial angiofibromas (85%) Collagenomas (70%)
Enteropancreatic tumor **Gastrinoma**[a] (40%) Insulinoma (10%) NF[b] including **pancreatic polypeptide** (20%[c]) Other: **glucagonoma, VIPoma, somatostatinoma** (2%)	Rare, maybe innate, endocrine or nonendocrine features
Foregut carcinoid **Thymic carcinoid** NF (2%) **Bronchial carcinoid** NF (2%) Gastric enterochromaffin-like tumor NF (10%)	Ependymoma (1%)
Anterior pituitary tumor Prolactinoma (20%) Other: GH + PRL, GH, NF (each 5%) ACTH (2%), TSH (rare)[d]	
Adrenal cortex tumor NF (25%)	
Pheochromocytoma (<1%)	

[a]Bold indicates tumor type with substantial malignant potential (above 25% of patients with that tumor).

[b]NF = nonfunctioning. May synthesize a peptide hormone or other factors (such as small amine), but does not usually oversecrete enough to produce a hormonal expression.

[c]Omits nearly 100% prevalence of NF and clinically silent tumors, some of which are detected incidental to pancreaticoduodenal surgery in patients with multiple endocrine neoplasia type I.

[d]GH = growth hormone; PRL = prolactin; ACTH = adrenocorticotropic hormone; TSH = thyroid-stimulating hormone.

ADRENAL HYPERFUNCTION WITH PRIMARY HYPERALDOSTERONISM

Primary hyperaldosteronism results from excessive secretion of aldosterone by the adrenal glands (88,89). Under normal conditions, the most important regulators of aldosterone secretion are the renin-angiotensin system and potassium, but ACTH can also stimulate secretion of this mineralocorticoid.

The clinical spectrum of primary hyperaldosteronism is complex and several unusual forms are recognized. The glucocorticoid-remediable (or dexamethasone-suppressible) form of primary hyperaldosteronism is a disorder with an autosomal dominant inheritance pattern (90). Glucocorticoid-remediable aldosteronism (GRA) appears to be the most common monogenic form of human hypertension (91). There are high levels of abnormal adrenal steroids (18-hydroxycortisol and 18-oxocortisol) which are under the control of ACTH and suppressible with glucocorticoids (90). A genetic abnormality has been discovered in which the coding sequence for aldosterone synthetase fuses with the 5'-regulatory region of the 11-beta-hydroxylase gene, thus permitting illicit or ectopic production of aldosterone by the zona fasciculata (91, 92). A syndrome of apparent mineralocorticoid excess has also been reported in children and young adults in which the levels of aldosterone

and all known mineralocorticoids are either very low or absent; it seems likely that the functioning "mineralocorticoid" in this disorder is cortisol, which circulates in normal amounts but exerts a mineralocorticoid effect because of incomplete metabolism at target tissues (90). This syndrome has an autosomal recessive pattern of inheritance. Rare cases of hyperaldosteronism have been ascribed to autonomous production of aldosterone by ovarian tumors (93).

It has been estimated that 15 to 35 percent of cases of primary hyperaldosteronism are idiopathic, with bilateral hyperplasia of the zona glomerulosa (38), although with increased awareness of milder forms of primary hyperaldosteronism, an incidence of 45 percent or even greater has been reported (94). In the idiopathic form, the clinical features such as hypertension, headache, easy fatigability, and weakness are often less pronounced than with cases of primary hyperaldosteronism due to an adrenal cortical neoplasm (95). Pathologists rarely have the opportunity to study the nontumorous adrenal glands in these patients since adrenalectomy is reserved almost exclusively for patients with an aldosterone-producing adenoma because of the much more predictable response in terms of amelioration or normalization of systemic hypertension (88,89, 94). Patients with idiopathic hyperaldosteronism due to hyperplasia are usually managed medically (88,89). Adrenal venous sampling is an essential diagnostic step in most patients with primary aldosteronism to distinguish between unilateral and bilateral adrenal aldosterone hypersecretion (95). Two unusual subsets of primary hyperaldosteronism have been described in which cure or amelioration of the effects of aldosterone excess can be achieved by subtotal or total adrenalectomy; one was designated primary adrenal hyperplasia and the other an aldosterone-producing renin-responsive adenoma (96).

On gross inspection, the adrenal glands in idiopathic primary hyperaldosteronism may not demonstrate distinguishing features, or they may be slightly enlarged with grossly visible micronodules (fig. 3-50, top) or macronodules. The hyperplastic zona glomerulosa may form a continuous band of cells, or the hyperplasia may be focal and vary from one part of the gland to another, thus necessitating multiple sections to detect the abnormality (1,38). In a study involving patients with primary hyperaldosteronism and no evidence of a neoplasm, 50 percent of cases showed hyperplasia of the zona glomerulosa with micronodules, and the remainder were divided into three groups: 1) hyperplasia of the zona glomerulosa with micronodules and macronodules; 2) hyperplasia of the zona glomerulosa without nodules (fig. 3-50, bottom); and 3) normal-appearing zona glomerulosa with micronodules (38). The etiology of this disorder is unclear, but some investigators have implicated an aldosterone-stimulating factor of anterior pituitary origin (94).

There are a variety of conditions that can cause activation of the renin-angiotensin system

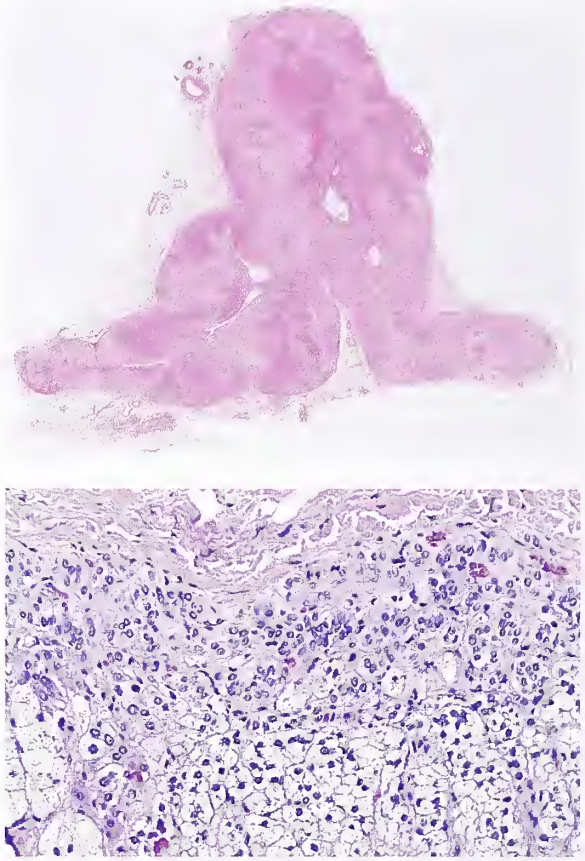

Figure 3-50

IDIOPATHIC PRIMARY HYPERALDOSTERONISM

Top: On gross examination, the adrenal gland was only slightly enlarged and on low magnification has only slight nodularity.

Bottom: Hyperplasia of the zona glomerulosa was present throughout with no evidence of micronodules, or macronodules.

resulting in secondary hyperaldosteronism. Hyperplasia of the zona glomerulosa has been reported in patients with cystic fibrosis and may be related to chronic loss of salt (97). An unusual cause of secondary hypermineralocorticoidism is excess ingestion of licorice which can cause sodium and water retention leading to systemic hypertension, but renin levels are low; a study suggests that licorice probably inhibits an enzyme system in the cortical cells resulting in a state analogous to children with 11-beta-hydroxysteroid dehydrogenase deficiency (98). Conn (99) emphasized that when concentrations of both renin and aldosterone are low it is likely that the cause of the hypertension is a potent sodium-retaining substance other than aldosterone; in the case of licorice it is ammonium glycorrhizate.

UNILATERAL ADRENAL CORTICAL HYPERPLASIA

A few cases of putative *unilateral adrenal cortical hyperplasia* have been reported in association with Cushing's syndrome (100), hyperaldosteronism (101), and ectopic ACTH syndrome (102). In the latter case it was speculated that local ACTH stimulation by metastatic tumor in one gland caused unilateral hyperplasia, and the resulting hypercortisolemia caused feedback inhibition of endogenous ACTH production, resulting in atrophy of the contralateral gland.

REFERENCES

Adrenal Cortical Hyperplasia

1. Lack EE, Travis WD, Oertel JE. Adrenal cortical nodules, hyperplasia and hyperfunction. In: Lack EE, ed. Pathology of the adrenal glands. New York: Churchill Livingstone; 1990:75-113.

Adrenal Cortical Nodules with Eucorticalism

2. Dobbie JW. Adrenocortical nodular hyperplasia: the ageing adrenal. J Pathol 1969;99:1-18.
3. Spain DM, Weinsaft P. Solitary adrenal cortical adenoma in elderly female; frequency. Arch Pathol 1964;78:231-233.
4. Shamma AH, Goddard JW, Sommers SC. A study of the adrenal status in hypertension. J Chronic Dis 1958;8:587-595.
5. Hedeland H, Östberg G, Hökfelt B. On the prevalence of adrenocortical adenomas in an autopsy material in relation to hypertension and diabetes. Acta Med Scand 1968;184:211-214.
6. Diaz-Cano SJ, de Miguel M, Blanes A, Tashjian R, Galera H, Wolfe HJ. Clonality as expression of distinctive cell kinetics patterns in nodular hyperplasias and adenomas of the adrenal cortex. Am J Pathol 2000;156:311-319.
7. Gross MD, Wilton GP, Shapiro B, et al. Functional and scintigraphic evaluation of the silent adrenal mass. J Nucl Med 1987;28:1401-1407.
8. Rizza RA, Wahner HW, Spelsberg TC, Northcutt RC, Moses HL. Visualization of nonfunctioning adrenal adenomas with iodocholesterol: possible relationship to subcellular distribution of tracer. J Nucl Med 1978;19:458-463.
9. Suzuki T, Sasano H, Sawai T, et al. Small adrenocortical tumors without apparent clinical endocrine abnormalities. Immunolocalization of steroidogenic enzymes. Path Res Pract 1992;188: 883-889.

Incidental Pigmented Cortical Nodules

10. Robinson MJ, Pardo V, Rywlin AM. Pigmented nodules (black adenomas) of the adrenal. An autopsy study of incidence, morphology, and function. Hum Pathol 1972;3:317-325.
11. Damron TA, Schelper RL, Sorensen L. Cytochemical demonstration of neuromelanin in black pigmented adrenal nodules. Am J Clin Pathol 1987;87:334-341.

Incidental Cortical Nodule In Vivo ("Incidentaloma")

12. Schteingart DE. Management approaches to adrenal incidentalomas. A view from Ann Arbor, Michigan. Endocrinol Metab Clin North Am 2000;29:127-139.
13. Grumbach MM, Biller BM, Braunstein GD, et al. Management of the clinically inapparent adrenal mass ("incidentaloma"). Ann Intern Med 2003;138:424-429.
14. Herrera MF, Grant CS, van Heerden JA, Sheedy PF, Ilstrup DM. Incidentally discovered adrenal tumors: an institutional perspective. Surgery 1991;110:1014-1021.
15. Sippel RS, Chen H. Subclinical Cushing's syndrome in adrenal incidentalomas. Surg Clin North Am 2004;84:875-885.

16. Rossi R, Tauchmanova L, Luciano A, et al. Subclinical Cushing's syndrome in patients with adrenal incidentaloma: clinical and biochemical features. J Clin Endocrinol Metab 2000;85: 1440-1448.
17. Saeger W, Fassnacht M, Chita R, et al. High diagnostic accuracy of adrenal core biopsy: results of the German and Austrian adrenal network multicenter trial in 220 consecutive patients. Hum Pathol 2003;34:180-186.
18. Doppman JL, Reinig JW, Dywer AJ, et al. Differentiation of adrenal masses by magnetic resonance imaging. Surgery 1987;102:1018-1026.
19. Copeland PM. The incidentally discovered adrenal mass. Ann Intern Med 1983;98:940-945.
20. Sturgeon C, Shen WT, Clark OH, Duh QY, Kebebew E. Risk assessment in 457 adrenal cortical carcinomas: how much does tumor size predict the likelihood of malignancy? J Am Coll Surg 2006;202:423-430.

Adrenal Cortical Hyperplasia with Hypercortisolism

21. Miller J, Crapo L. The biochemical diagnosis of hypercortisolism. The Endocrinol 1994;4:7-16.
22. Invitti C, Pecori Giraldi F, de Martin M, Cavagnini F. Diagnosis and management of Cushing's syndrome: results of an Italian multicentre study. Study Group of the Italian Society of Endocrinology on the Pathophysiology of the Hypothalamic-Pituitary-Adrenal Axis. J Clin Endocrinol Metab 1999;84:440-448.
23. Boscaro M, Barzon L, Sonino N. The diagnosis of Cushing's syndrome: atypical presentations and laboratory shortcomings. Arch Intern Med 2000;160:3045-3053.
24. Boscaro M, Barzon L, Fallo F, Sonino N. Cushing's syndrome. Lancet 2001;357:783-791.
25. Carey RM, Varma S, Drake, CR Jr, et al. Ectopic secretion of corticotropin-releasing factor as a cause of Cushing's syndrome. A clinical, morphologic, and biochemical study. N Engl J Med 1984;311:13-20.
26. Zárate A, Kovacs K, Flores M, Morán C, Félix I. ACTH and CRF-producing bronchial carcinoid associated with Cushing's syndrome. Clin Endocrinol (Oxf) 1986;24:523-529.
27. Thomas CG Jr, Smith AT, Benson M, Griffith J. Nelson's syndrome after Cushing's disease in childhood: a continuing problem. Surgery 1984;96:1067-1077.
28. Weinstein LS, Shenker A, Gejman PV, Merino MJ, Friedman E, Spiegel AM. Activating mutations of the stimulatory G protein in McCune-Albright syndrome. N Engl J Med 1991;325:1688-1695.
29. Antonini SR, N'Diaye N, Baldacchino V, Hamet P, Tremblay J, Lacroix A. Analysis of the putative regulatory region of the gastric inhibitory polypeptide receptor gene in food-dependent Cushing's syndrome. J Steroid Biochem Mol Biol 2004;91:171-177.
30. Grizzle WE, Dunlap N. Cushing's syndrome. Diagnosis of the atypical patient. Arch Pathol Lab Med 1989;113:727-728.
31. Sutinen J, Kannisto K, Korsheninnikova E, et al. In the lipodystrophy associated with highly active antiretroviral therapy, pseudo-Cushing's syndrome is associated with increased regeneration of cortisol by 11beta-hydroxysteroid dehydrogenase type 1 in adipose tissue. Diabetologia. 2004;47:1668-1671.

Pituitary-Dependent Hypercortisolism

32. Cushing H. The basophil adenomas of the pituitary body and their clinical manifestations (pituitary basophilism). Bull Johns H Hosp 1932;50: 137-195.
33. Fulton JF. Harvey Cushing: a biography. Springfield: Charles C. Thomas; 1946.
34. Erickson D, Huston J 3rd, Young WF Jr, et al. Internal jugular vein sampling in adrenocorticotropic hormone-dependent Cushing's syndrome: a comparison with inferior petrosal sinus sampling. Clin Endocrinol (Oxf) 2004;60: 413-419.
35. Hammer GD, Tyrrell JB, Lamborn KR, et al. Transsphenoidal microsurgery for Cushing's disease: initial outcome and long-term results. J Clin Endocrinol Metab 2004;89:6348-6357.
36. Vella A, Thompson GB, Grant CS, van Heerden JA, Farley DR, Young WF Jr. Laparoscopic adrenalectomy for adrenocorticotropin-dependent Cushing's syndrome. J Clin Endocrinol Metab 2001;86:1596-1599.
37. Doppman JL, Miller DL, Dwyer AJ, et al. Macronodular adrenal hyperplasia in Cushing's disease. Radiology 1988;166:347-352.
38. Neville AM, O'Hare MJ. Histopathology of the human adrenal cortex. Clin Endocrinol Metab 1985;14:791-820.
39. Smals AG, Pieters GF, van Haelst UJ, Kloppenborg PW. Macronodular adrenocortical hyperplasia in long-standing Cushing's disease. J Clin Endocrinol Metab 1984;58:25-31.
40. Cohen RB, Chapman WB, Castleman B. Hyperadrenocorticism (Cushing's disease): a study of surgically resected adrenal glands. Am J Pathol 1959;35:537-561.
41. Cohen, RB. Observations on cortical nodules in human adrenal glands. Their relationship to neoplasia. Cancer 1966;19:552-556.

42. Lamberts SW, Bons EG, Bruining HA. Different sensitivity to adrenocorticotropin of dispersed adrenocortical cells from patients with Cushing's disease with macronodular and diffuse adrenal hyperplasia. J Clin Endocrinol Metab 1984;58: 1106-1110.
43. Hermus AR, Pieters GF, Smals AG, et al. Transition from pituitary-dependent to adrenal-dependent Cushing's syndrome. N Engl J Med 1988; 318:966-970.

Macronodular Hyperplasia with Marked Adrenal Enlargement

44. Bourdeau I, Antonini SR, Lacroix A, et al. Gene array analysis of macronodular adrenal hyperplasia confirms clinical heterogeneity and identifies several candidate genes as molecular mediators. Oncogene 2004;23:1575-1585.
45. Bourdeau I. Clinical and molecular genetic studies of bilateral adrenal hyperplasias. Endocr Res 2004;30:575-583.
46. Lacroix A, Baldacchino V, Bourdeau I, Hamet P, Tremblay J. Cushing's syndrome variants secondary to aberrant hormone receptors. Trends Endocrinol Metab 2004;15:375-382.
47. Doppman JL, Chrousos GP, Papanicolaou DA, Stratakis CA, Alexander HR, Nieman LK. Adrenocorticotropin-independent macronodular adrenal hyperplasia: an uncommon cause of primary adrenal hypercortisolism. Radiology 2000;216: 797-802.
48. Kirschner MA, Powell RD Jr, Lipsett MB. Cushing's syndrome: nodular cortical hyperplasia of adrenal glands with clinical and pathological features suggesting adrenocortical tumor. J Clin Endocr 1964;24:947-955.
49. Tatsuno I, Uchida D, Tanaka T, et al. Vasopressin responsiveness of subclinical Cushing's syndrome due to ACTH-independent macronodular adrenocortical hyperplasia. Clin Endocrinol (Oxf) 2004;60:192-200.
50. Swain JM, Grant CS, Schlinkert RT, et al. Corticotropin-independent macronodular adrenal hyperplasia: a clinicopathologic correlation. Arch Surg 1998;133:541-546.
51. Aiba M, Hirayama A, Iri H, et al. Adrenocorticotropic hormone-independent bilateral adrenocortical macronodular hyperplasia as a distinct subtype of Cushing's syndrome. Enzyme histochemical and ultrastructural study of four cases with a review of the literature. Am J Clin Pathol 1991;96:334-340.
52. Sasano, H, Suzuki, T, Nagura H. ACTH-independent macronodular adrenocortical hyperplasia: immunohistochemical and in situ hybridization studies of steroidogenic enzymes. Mod Pathol 1994;7:215-219.
53. Aiba M, Hirayama A, Iri H, et al. Primary adrenocortical micronodular dysplasia: enzyme histochemical and ultrastructural studies of two cases with a review of the literature. Hum Pathol 1990;21:503-511.
54. Sasano H, Miyazaki S, Sawai T, et al. Primary pigmented nodular adrenocortical disease (PPNAD): immunohistochemical and in situ hybridization analysis of steroidogenic enzymes in eight cases. Mod Pathol 1992;5:23-29.

Primary Pigmented Nodular Adrenocortical Disease

55. Carney JA, Young WF Jr. The adrenal gland. Primary pigmented nodular adrenocortical disease and its associated conditions. Endocrinology 1992;2:6-21.
56. Doppman JL, Travis WD, Nieman L, et al. Cushing syndrome due to primary pigmented nodular adrenocortical disease: findings at CT and MR imaging. Radiology 1989;172:415-420.
57. Stratakis CA, Sarlis N, Kirschner LS, et al. Paradoxical response to dexamethasone in the diagnosis of primary pigmented nodular adrenocortical disease. Ann Intern Med. 1999;131:585-591.
58. Shenoy BV, Carpenter PC, Carney JA. Bilateral primary pigmented nodular adrenocortical disease. Rare cause of the Cushing syndrome. Am J Surg Pathol 1984;8:335-344.
59. Teding van Berkhout F, Croughs RJ, Kater L, et al. Familial Cushing's syndrome due to nodular adrenocortical dysplasia. A putative receptor-antibody disease? Clin Endocrinol 1986;24:299-310.
60. Travis WD, Tsokos M, Doppman JL, et al. Primary pigmented nodular adrenocortical disease. A light and electron microscopic study of eight cases. Am J Surg Pathol 1989;13:921-930.
61. Wulffraat NM, Drexhage HA, Wiersinga WM, van der Gaag RD, Jeucken P, Mol JA. Immunoglobulins of patients with Cushing's syndrome due to pigmented adrenocortical micronodular dysplasia stimulate in vitro steroidogenesis. J Clin Endocrinol Metab 1988;66:301-307.
62. Young WF Jr, Carney JA, Musa BU, Wulffraat NM, Lens JW, Drexhage HA. Familial Cushing's syndrome due to primary pigmented nodular adrenocortical disease. Reinvestigation 50 years later. N Engl J Med 1989;321:1659-1664.
63. Stratakis CA, Carney JA, Kirschner LS, et al. Synaptophysin immunoreactivity in primary pigmented nodular adrenocortical disease: neuroendocrine properties of tumors associated with Carney complex. J Clin Endocrinol Metab. 1999;84:1122-1128.
64. Groussin L, Horvath A, Jullian E, et al. A PRKAR1A mutation associated with primary pigmented nodular adrenocortical disease in 12 kindreds. J Clin Endocrinol Metab 2006;91: 1943-1949.

65. Grant CS, Carney JA, Carpenter PC, van Heerden JA. Primary pigmented nodular adrenocortical disease: diagnosis and management. Surgery 1986;100:1178-1184.

Complex of Myxomas, Spotty Pigmentation, and Endocrine Overactivity

66. Carney JA, Gordon H, Carpenter PC, Shenoy BV, Go VL. The complex of myxomas, spotty pigmentation, and endocrine overactivity. Medicine 1985;64:270-283.
67. Carney JA, Hruska LS, Beauchamp GD, Gordon H. Dominant inheritance of the complex of myxomas, spotty pigmentation and endocrine overactivity. Mayo Clin Proc 1986;61:165-172.
68. Courcoutsakis NA, Chow CK, Shawker TH, Carney JA, Stratakis CA. Syndrome of spotty skin pigmentation, myxomas, endocrine overactivity, and schwannomas (Carney complex): breast imaging findings. Radiology 1997;205: 221-227.
69. Stratakis CA, Kirschner LS, Carney JA. Clinical and molecular features of the Carney complex: diagnostic criteria and recommendations for patient evaluation. J Clin Endocrinol Metab. 2001;86:4041-4046.
70. Rhodes AR, Silverman RA, Harrist TJ, Perez-Atayde AR. Mucocutaneous lentigines, cardiomucocutaneous myxomas and multiple blue nevi: the "LAMB" syndrome. J Am Acad Dermatol 1984;10:72-82.
71. Atherton DJ, Pitcher DW, Wells RS, MacDonald DM. A syndrome of various cutaneous pigmented lesions, myxoid neurofibromata and atrial myxoma: the NAME syndrome. Br J Dermatol 1980;103:421-429.
71a. Sandrini F, Stratakis C. Clinical and molecular genetics of primary pigmented nodular adrenocortical disease. Arq Bras Endocrinol Metabol 2004;48:637-641.
72. Stratakis CA, Jenkins RB, Pras E, et al. Cytogenetic and microsatellite alterations in tumors from patients with the syndrome of myxomas, spotty skin pigmentation, and endocrine overactivity (Carney complex). J Clin Endocrinol Metab 1996; 81:3607-3614.

Ectopic ACTH Syndrome

73. Drasin GF, Lynch T, Temes GP. Ectopic ACTH production and mediastinal lipomatosis. Radiology 1978;127:610.
74. Dupont AG, Somers G, van Steirteghem AC, Warson F, Vanhaelst L. Ectopic adrenocorticotropin production: disappearance after removal of inflammatory tissue. J Clin Endocrinol Metab 1984;58:654-658.
75. Odell WD. Ectopic ACTH secretion. A misnomer. Endocrinol Metab Clin North Am 1991;20: 371-379.
76. Findling JW. Eutopic or ectopic adrenocorticotropic hormone-dependent Cushing's syndrome? A diagnostic dilemma. Mayo Clin Proc 1990;65:1377-1380.
77. Scanagatta P, Montresor E, Pergher S, et al. Cushing's syndrome induced by bronchopulmonary carcinoid tumours: a review of 98 cases and our experience of two cases. Chir Ital 2004; 56:63-70.
78. Schteingart DE, Lloyd RV, Akil H, et al. Cushing's syndrome secondary to ectopic corticotropin-releasing hormone-adrenocorticotropin secretion. J Clin Endocrinol Metab 1986;63:770-775.
79. Aniszewski JP, Young WF Jr, Thompson GB, Grant CS, van Heerden JA. Cushing syndrome due to ectopic adrenocorticotropic hormone secretion. World J Surg 2001;25:934-40.
80. Clement PB, Young RH, Scully RE. Clinical syndromes associated with tumors of the female genital tract. Semin Diagn Pathol 1991;8:204-233.
81. Axiotis CA, Lippes HA, Merino MJ, de Lanerolle NC, Stewart AF, Kinder B. Corticotroph cell pituitary adenoma within an ovarian teratoma. A new cause of Cushing's syndrome. Am J Surg Pathol 1987;11:218-224.
82. Doppman JL. Neuroendocrinology. The search for occult ectopic ACTH-producing tumors. Endocrinologist 1992;2:41-46.

Multiple Endocrine Neoplasia Syndrome Type 1

83. Brandi ML, Gagel RF, Angeli A, et al. Guidelines for diagnosis and therapy of MEN type 1 and type 2. J Clin Endocrinol Metab 2001 ;86:5658-5671.
84. Bahn RS, Scheithauer BW, van Heerden JA, Laws ER Jr, Horvath E, Gharib H. Nonidentical expressions of multiple endocrine neoplasia, type I, in identical twins. Mayo Clin Proc 1986; 61:689-696.
85. Ballard HS, Frame B, Hartsock RJ. Familial multiple endocrine adenoma-peptic ulcer complex. Medicine (Baltimore) 1964;43:481-516.
86. Miyagawa K, Ishibashi M, Kasuga M, Kanazawa Y, Yamaji T, Takaku F. Multiple endocrine neoplasia type I with Cushing's disease, primary hyperparathyroidism, and insulin-glucagonoma. Cancer 1988;61:1232-1236.
87. Scheithauer BW, Laws ER Jr, Kovacs K, Horvath E, Randall RV, Carney JA. Pituitary adenomas of the multiple endocrine neoplasia type I syndrome. Sem Diagn Pathol 1987;4:205-211.

Adrenal Hyperfunction with Hyperaldosteronism

88. Ganguly A. Primary aldosteronism. N Engl J Med 1998;339:1828-1834.
89. Young WF Jr. Primary aldosteronism: management issues. Ann N Y Acad Sci 2002;970:61-76.
90. Ulick S. Two uncommon causes of mineralocorticoid excess. Syndrome of apparent mineralocorticoid excess and glucocorticoid-remediable. Endocrinol Metab Clin North Am 1991;20: 269-276.
91. McMahon GT, Dluhy RG. Glucocorticoid-remediable aldosteronism. Cardiol Rev 2004;12:44-48.
92. Lifton RP, Dluhy RG, Powers M, et al. A chimaeric 11-beta-hydroxylase/aldosterone synthase gene causes glucocorticoid-remediable aldosteronism and human hypertension. Nature 1992;355:262-265.
93. Kulkarni JN, Mistry RC, Kamat MR, Chinoy R, Lotlikar RG. Autonomous aldosterone-secreting ovarian tumor. Gynecol Oncol 1990;37:284-289.
94. Gill JR Jr. Hyperaldosteronism. In: Becker KL, ed. Principles and practice of endocrinology and metabolism. Philadelphia: JB Lippincott; 1990: 631-643.
95. Young WF, Stanson AW, Thompson GB, Grant CS, Farley DR, van Heerden JA. Role for adrenal venous sampling in primary aldosteronism. Surgery 2004;136:1227-1235.
96. Irony I, Kater CE, Biglieri EG, Shackleton CH. Correctable subsets of primary aldosteronism. Primary adrenal hyperplasia and renin responsive adenoma. Am J Hypertens 1990;3:576-582.
97. Hawkins E, Singer DB. The adrenal cortex in cystic fibrosis of the pancreas. Am J Clin Pathol 1976;66:710-714.
98. Farese RV Jr, Biglieri EG, Shackleton CH, Irony I, Gomez-Foutes R. Licroice-induced hypermineralocorticoidism. N Engl J Med 1991;325;1223-1227.
99. Schteingart DE. The 50th anniversary of the identification of primary aldosteronism: a retrospective of the work of Jerome W. Conn. J Lab Clin Med 2005;145:12-16.

Unilateral Adrenal Cortical Hyperplasia

100. Jenkins PJ, Chew SL, Lowe DG, Reznek RH, Wass JA. Adrenocorticotrophin-independent unilateral macronodular adrenal hyperplasia occurring with myelolipoma: an unusual cause of Cushing's syndrome. Clin Endocrinol (Oxf) 1994;41:827-830.
101. Lam KY, Lo CY. The clinicopathologic significance of unilateral adrenal cortical hyperplasia: report of an unusual case and a review of the literature. Endocr Pathol 1999;10:243-249.
102. Sigman LM, Wallach L. Unilateral adrenal hypertrophy in ectopic ACTH syndrome. Arch Intern Med 1984;144:1869-1870.

4 ADRENAL CORTICAL ADENOMA

Adrenal cortical adenoma (ACA) is a benign neoplasm arising from adrenal cortical cells. The cells may or may not have functional activity, as evidenced by a recognizable endocrine syndrome or biochemical evidence of hypercorticalism.

INCIDENCE AND CLINICAL FEATURES

ACAs are typically unilateral, solitary, benign neoplasms. When they are associated with an endocrine syndrome, there is excess secretion of one or more of the three major classes of adrenal steroids. The incidence of ACA is low if the incidentally discovered adrenal adenoma, which is typically nonhyperfunctional, is excluded. The most frequent endocrine abnormality associated with ACA is primary hyperaldosteronism, followed by Cushing's syndrome, virilization, and occasionally, feminization (1). Many nonfunctional tumors are capable of taking up radiolabeled steroid precursor, but are unable to secrete sufficient steroids to cause the signs or symptoms of hypercorticalism (hence the term nonhyperfunctional).

Hypersecretion of adrenal steroids manifests as: 1) a fully developed endocrine syndrome that is often "pure," i.e., primary hyperaldosteronism or Cushing's syndrome; 2) abnormal laboratory data; or 3) cortical atrophy of the ipsilateral or contralateral adrenal cortex. The presence of virilization as either part of a pure or mixed endocrine syndrome (e.g., Cushing's syndrome and virilization), is associated with possible malignancy, particularly in large neoplasms weighing over 100 g. The presence of feminization can be a particularly ominous endocrine feature.

In general, ACAs have a predilection for female patients, and are equally distributed in both glands. Although there are some gross and microscopic features that are more likely to be associated with tumors producing a particular endocrine syndrome, it is sometimes difficult (or impossible) to predict the associated endocrine syndrome based upon morphologic features alone, without correlation with clinical or endocrinologic data. This chapter deals with ACAs associated with a particular endocrine syndrome. In some cases, there may be significant overlap in morphology; indeed, the range in morphology of even a dominant macronodule (nonhyperfunctional adenoma or nodule) can mimic almost any ACA associated with a known endocrine syndrome of various types. On rare occasion an ACA is associated with concurrent primary hyperaldosteronism and hypercortisolism; a recent case was reported in which the Cushing's syndrome was preclinical, or subclinical (2).

On computerized tomography (CT) scan, ACA (and nonhyperfunctional adenoma or nodule) is usually well defined, has a smooth contour, and is homogeneous, with attenuation values less than normal adrenal tissue, depending upon the amount of lipid present. The tumor may enhance mildly after contrast administration. On magnetic resonance imaging (MRI), ACAs tend to be homogeneous, with signal intensity less than fat but greater than muscle on all pulse sequences; the intensity is similar to liver on T1- and T2-weighted sequences. The tumor may enhance mildly; it may also appear darker than the remainder of the gland, when out-of-phase imaging, which is highly sensitive to the presence and amount of lipid, is used.

ADRENAL CORTICAL ADENOMA WITH CUSHING'S SYNDROME

Gross Findings. ACAs associated with Cushing's syndrome are usually solitary, unilateral, and unicentric neoplasms that often weigh less than 50 g. Only rarely have bilateral ACAs been reported in association with Cushing's syndrome (3). In those few instances of bilateral ACA, the contralateral adenoma is sometimes nonhyperfunctional (4). Occasionally, unusual cases of macronodular hyperplasia with marked adrenal enlargement (MHMAE) may appear to be a primary autonomous cause of Cushing's syndrome, and may stimulate a neoplasm (see chapter 3).

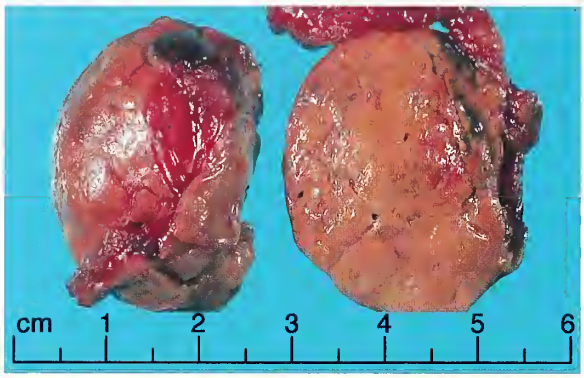

Figure 4-1

ADRENAL CORTICAL ADENOMA ASSOCIATED WITH CUSHING'S SYNDROME

This adrenal cortical adenoma is from a 33-year-old patient with Cushing's syndrome. The tumor is yellow-orange on cross section and has vague lobulations. It measured 3.5 x 3.0 x 2.5 cm. (Fig. 4-4 from Fascicle 19, Third Series.)

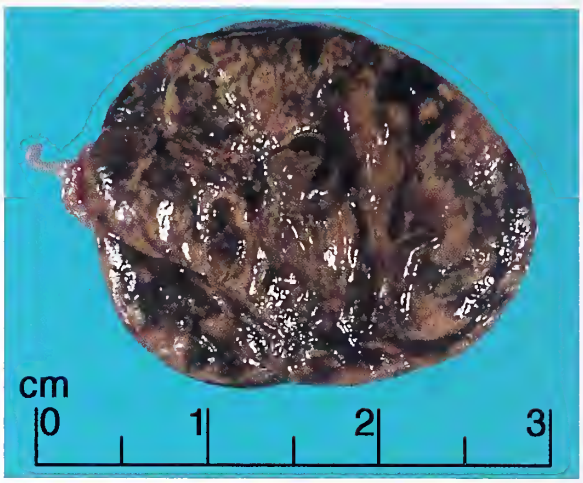

Figure 4-2

ADRENAL CORTICAL ADENOMA ASSOCIATED WITH CUSHING'S SYNDROME

This adrenal cortical adenoma from a 32-year-old woman with Cushing's syndrome measured 2.1 cm in diameter. The geographic to mottled zones of dark pigmentation are due to lipid depletion of neoplastic cortical cells as well as an accumulation of lipofuscin. (Fig. 4-2 from Fascicle 19, Third Series.)

ACAs are sharply circumscribed and appear encapsulated (fig. 4-1). In one study, the average diameter of the ACA causing Cushing's syndrome was 3.6 cm (range, 1.5 to 6.0 cm) (5). Many tumors weigh between 10 and 40 g (6). The largest ACA reported by Bertagna and Orth (7) weighed 126 g, and on occasion the tumor can weigh several hundred grams. There is some suggestion in the literature that an adrenal cortical neoplasm weighing over 100 g is probably a carcinoma until proven otherwise. Tumor weight alone, however, is insufficient to categorically type an adrenal cortical tumor as benign or malignant. While it is true that adrenal cortical carcinomas tend to be quite large, often 400 g or more, some very large tumors associated with Cushing's syndrome fail to metastasize, and rare tumors less than 50 g prove to be malignant (1). Clearly, criteria other than weight alone are necessary to predict biologic behavior.

On cross section, ACAs may appear yellow or golden yellow throughout, or there may be irregular foci of dark discoloration. The latter can be attributed to recent or old hemorrhage, areas of lipid-depletion within the tumor, or the presence of increased lipofuscin (fig. 4-2). Microscopic examination may reveal lipofuscin in most adrenal cortical lesions (including ACAs) associated with Cushing's syndrome. When the tumor is diffusely dark brown (fig. 4-3) or black, the term *black adenoma* has been used (1). Occasionally, areas of degeneration with fibrosis and cystic change are seen, but areas of confluent or geographic tumor necrosis are uncommon (1). Some tumors have vague nodularity on cross section, but typically without the coarse lobulations with broad fibrous bands associated with adrenal cortical carcinoma. If these features are present in larger tumors, malignancy should be suspected. Use of all available histologic and nonhistologic parameters may be necessary for a correct diagnosis (1).

Microscopic Findings. While ACA may appear encapsulated on gross examination, on histologic study the tumor may have a relatively smooth "pushing" border without a well-defined fibrous capsule. In some tumors, the compressed fibrous connective tissue at the periphery is, in essence, a fibrous pseudocapsule, whereas others acquire a fibrous capsule from the adrenal capsule itself. While a "classic" ACA is easy to recognize in many instances, particularly in adults, the tumor may reside in nodular cortex, making a straightforward diagnosis difficult (1).

Most tumors have broad fields of pale-staining, lipid-rich cells with relatively uniform nuclei; the cytoplasm appears optically "clear"

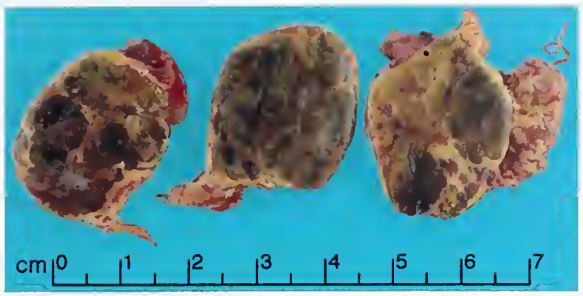

Figure 4-3

ADRENAL CORTICAL ADENOMA
ASSOCIATED WITH CUSHING'S SYNDROME

This adrenal cortical adenoma is from a 35-year-old female with Cushing's syndrome. The tumor has a confluent brown color due to cells with compact, lipid-depleted cytoplasm and intracellular lipochrome pigment. The attached adrenal cortex is markedly atrophic. The tumor weighed 16 g including the attached adrenal remnant. (Fig. 4-3 from Fascicle 19, Third Series.)

at low magnification (fig. 4-4). The most common architectural patterns are cells in a nesting or alveolar arrangement (fig. 4-5, left), short cords, narrow interconnecting trabeculae (fig. 4-5, right), or a mixture of these patterns in the same tumor. Occasionally, the tumor cells are focally aligned in slender cords reminiscent of normal zona fasciculata. A small area with a spindle cell pattern is only rarely encountered (fig. 4-6), but should not pose a problem in diagnosis since more typical histology is almost always evident elsewhere in the tumor.

Compared with normal cortical cells, ACA cells are usually larger, with a different quality of cytoplasm and variation in nuclear size and configuration. Most tumors have an abundance of cells with relatively distinct cell borders, similar to the cells of the zona fasciculata (fig. 4-5, right). A few tumors are composed purely of lipid-rich cells, which gives the tumor a vivid yellow or yellow-orange hue. Other tumors contain a variable component of compact lipid-poor cells with eosinophilic cytoplasm, sometimes with conspicuous lipochrome pigment. Some tumors have cells with varied cytologic features, recalling the diversity of cell types in the normal adrenal cortex, although the neoplastic cells are usually larger. There may be cells that have intermediate or transitional cytologic features, sometimes in the same histologic field. Clusters of tumor cells with greatly enlarged lipid-rich cytoplasm, "balloon

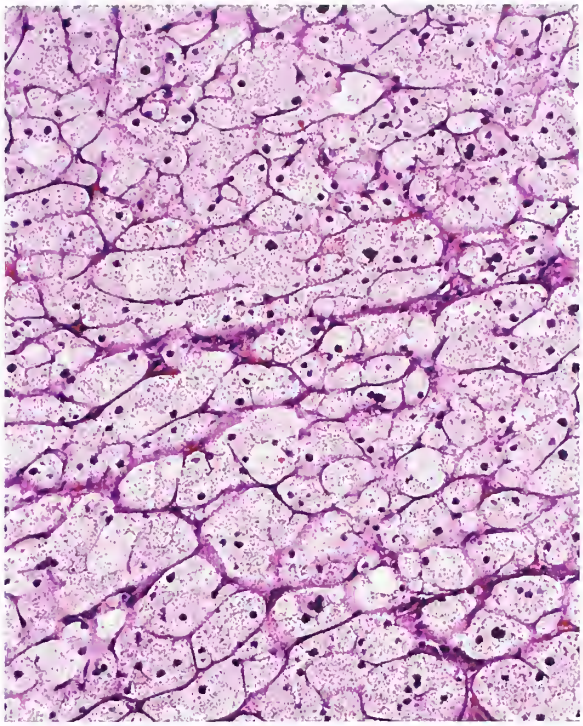

Figure 4-4

ADRENAL CORTICAL ADENOMA
ASSOCIATED WITH CUSHING'S SYNDROME

Tumor cells are arranged in small clusters and short cords with pale-staining, lipid-rich cytoplasm. Nuclear enlargement and pleomorphism are not present.

cells," stand out in stark contrast to cells with compact, eosinophilic cytoplasm (fig. 4-7).

The pale-staining quality of the cytoplasm has sometimes been referred to as "clear," but close examination of well-fixed specimens shows cytoplasm that is not optically clear or empty as in renal cell carcinoma, but finely vacuolated due to dispersed intracytoplasmic lipid droplets of various sizes. Staining of fresh frozen tumor with oil red-O demonstrates the abundant amount of intracytoplasmic lipid (fig. 4-8). In occasional tumors, there are cells with abundant, deeply eosinophilic cytoplasm that gives an oncocytic appearance (fig. 4-9); this is more likely to be focal, and lipid-rich cells are seen in other areas. In tumors that have a dark brown appearance (see fig. 4-3), cells contain conspicuous amounts of lipofuscin (fig. 4-10). Lipofuscin is often present in cells with compact eosinophilic cytoplasm which on ultrastructural study have a relatively sparse lipid content (fig. 4-11).

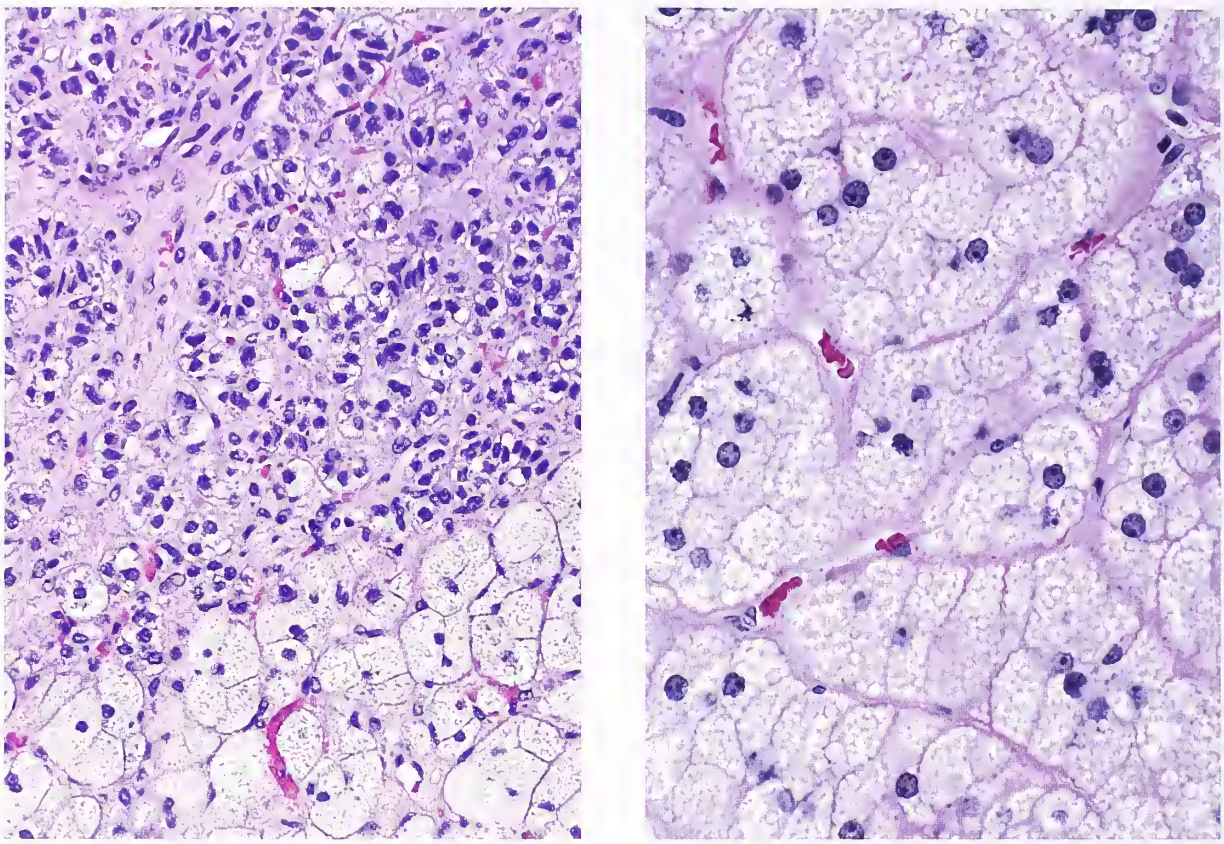

Figure 4-5

ADRENAL CORTICAL ADENOMA ASSOCIATED WITH CUSHING'S SYNDROME

Left: The tumor cells are arranged in rounded to ovoid clusters or alveoli, with a delicate intersecting vasculature. Cells at the bottom of the field have relatively abundant lipid-rich cytoplasm.

Right: A different area of the same tumor shows cells arranged in short cords. The finely vesicular quality of the pale staining cytoplasm is due to the lipid content. (Fig. 4-6, right from Fascicle 19, Third Series.)

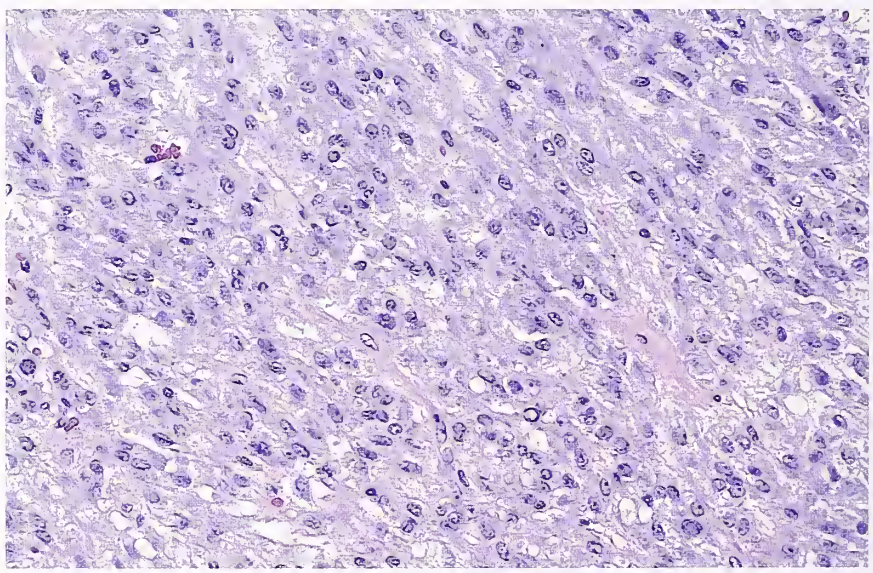

Figure 4-6

ADRENAL CORTICAL ADENOMA ASSOCIATED WITH CUSHING'S SYNDROME

Areas of this cortisol-producing adrenal adenoma show an ill-defined spindle cell pattern. More conventional histology was present in other fields. (Fig. 4-7 from Fascicle 19, Third Series.)

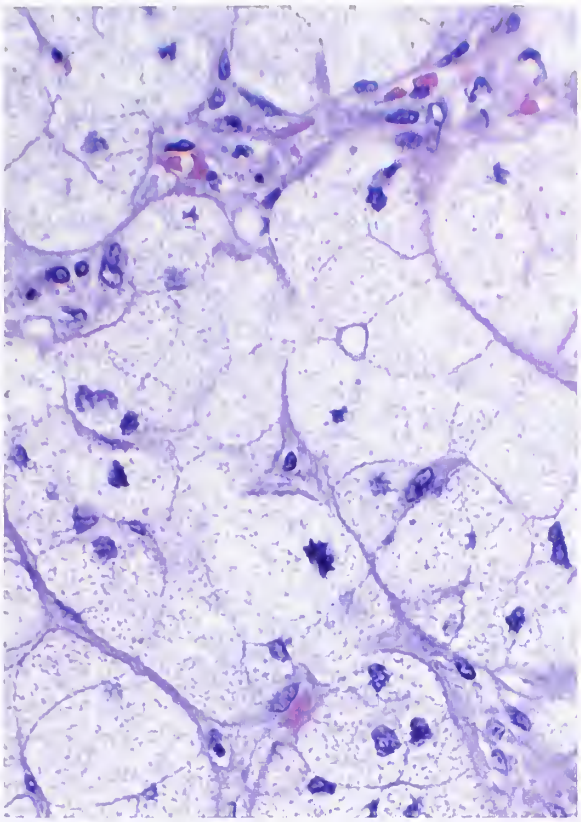

Figure 4-7

ADRENAL CORTICAL ADENOMA WITH "BALLOON CELLS"

The enlarged "balloon cells" in an adrenal cortical adenoma from a patient with Cushing's syndrome have greatly expanded, lipid-rich cytoplasm. Some cells were nearly 10-fold larger in diameter than other cells in the adenoma.

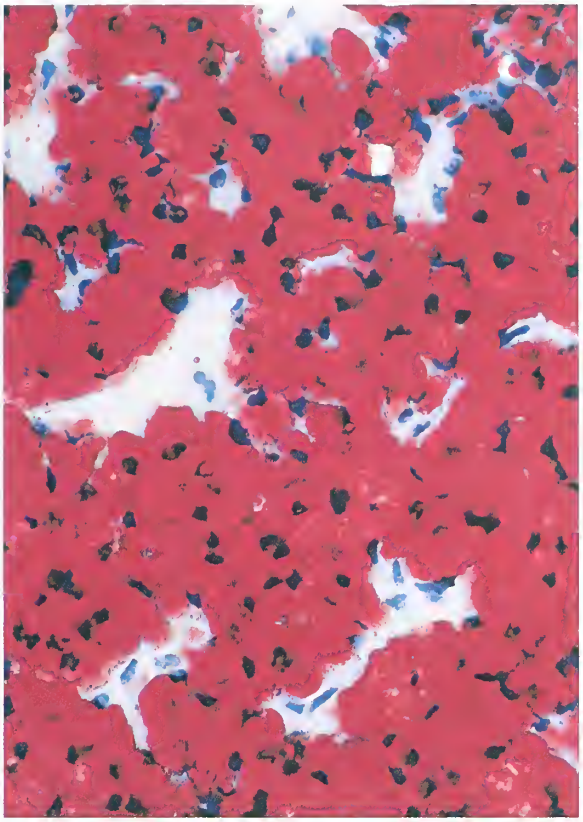

Figure 4-8

ADRENAL CORTICAL ADENOMA ASSOCIATED WITH CUSHING'S SYNDROME

The cells contain abundant neutral lipid (oil red-O stain). (Fig. 4-11 from Fascicle 19, Third Series.)

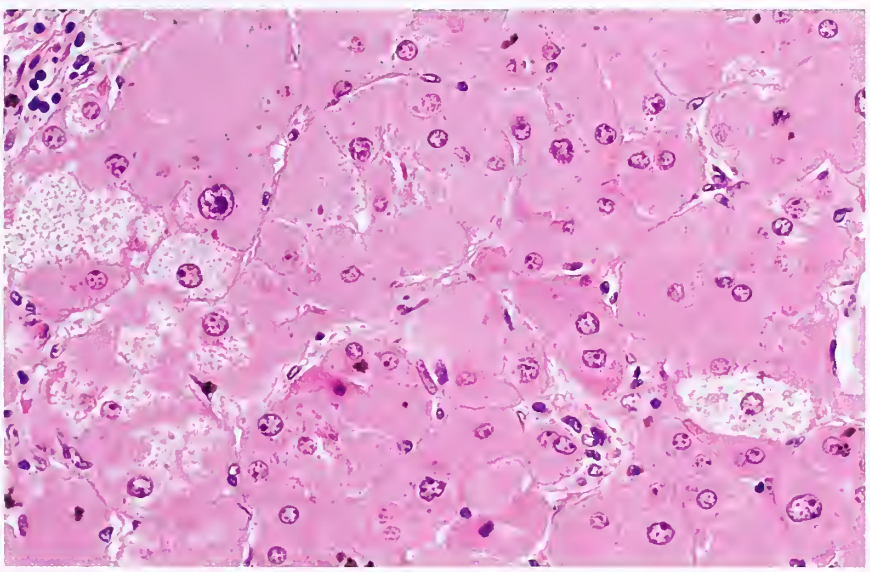

Figure 4-9

ADRENAL CORTICAL ADENOMA ASSOCIATED WITH CUSHING'S SYNDROME

Many cells in this adrenal cortical adenoma have abundant compact, eosinophilic cytoplasm that gives an oncocytic appearance. A few cells have finely vacuolated, pale-staining cytoplasm.

Figure 4-10

ADRENAL CORTICAL ADENOMA ASSOCIATED WITH CUSHING'S SYNDROME

On gross examination this tumor had diffuse areas of brown coloration. Microscopically, most of the tumor cells have compact, eosinophilic cytoplasm with pigmented granular material representing lipofuscin. Some nuclei are enlarged and hyperchromatic and a large nuclear pseudoinclusion is present in the left part of the field. (Fig. 4-12 from Fascicle 19, Third Series.)

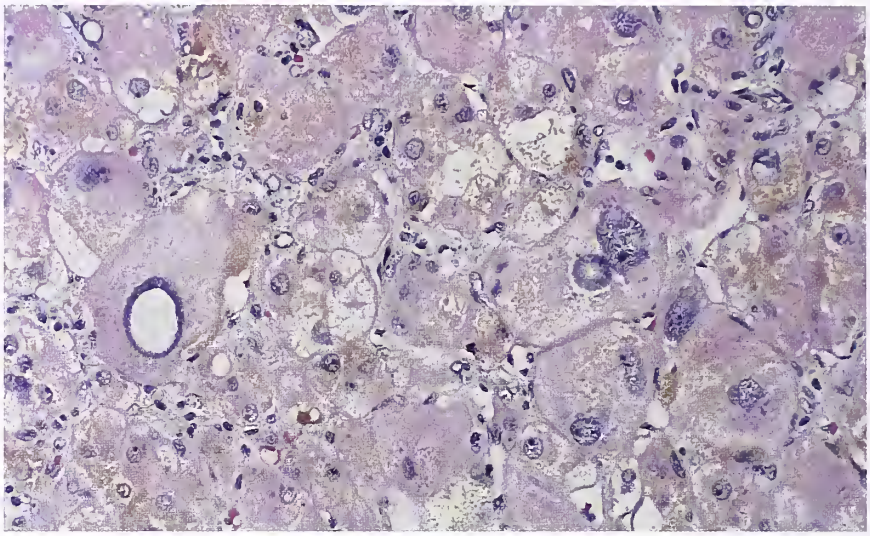

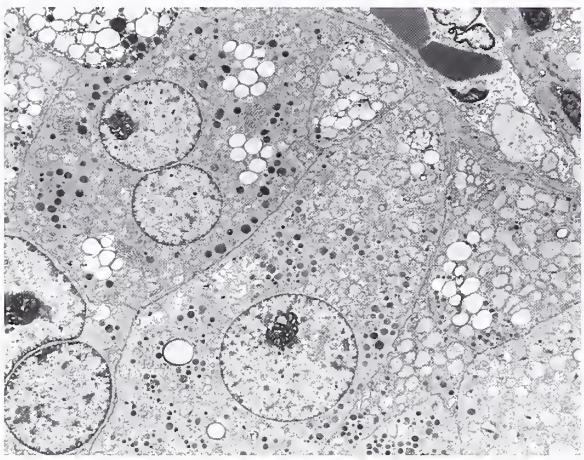

Figure 4-11

ADRENAL CORTICAL ADENOMA ASSOCIATED WITH CUSHING'S SYNDROME

The tumor cells contain small to medium-sized electron-dense granules, which represent lipofuscin. Some cells contain sparse lipid droplets.

Tumor cell nuclei are usually single and round to oval; margination of chromatin along the nuclear membrane produces a vesicular appearance. Most nuclei contain a single dot-like nucleolus, which is central or eccentric in location. There may be some nuclear enlargement and hyperchromasia (fig. 4-12), but these changes are usually focal in distribution and moderate in degree. There may be a few nuclear pseudoinclusions, which may have the same quality and intensity of cytoplasmic staining

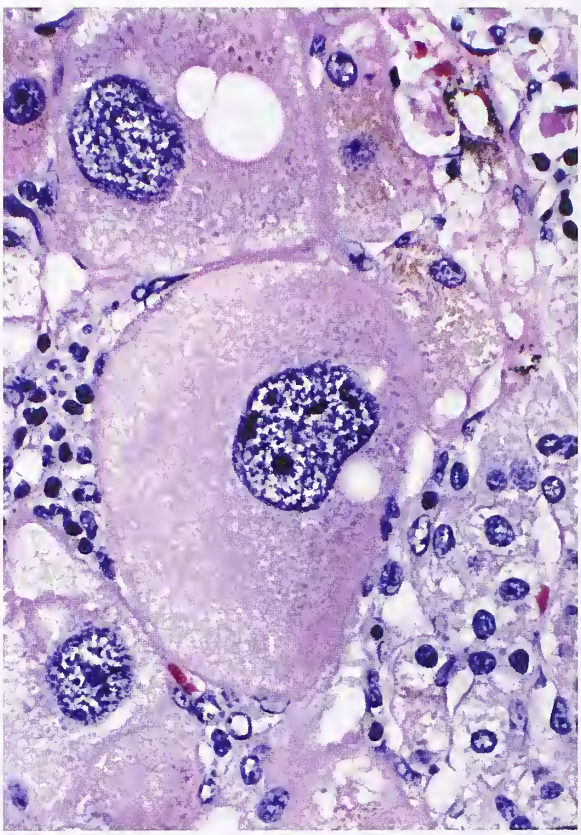

Figure 4-12

ADRENAL CORTICAL ADENOMA ASSOCIATED WITH CUSHING'S SYNDROME

Greatly enlarged pleomorphic nuclei are seen in some cells, which are markedly different than the nuclei of adjacent tumor cells. A few cells also contain finely granular brown lipofuscin pigment.

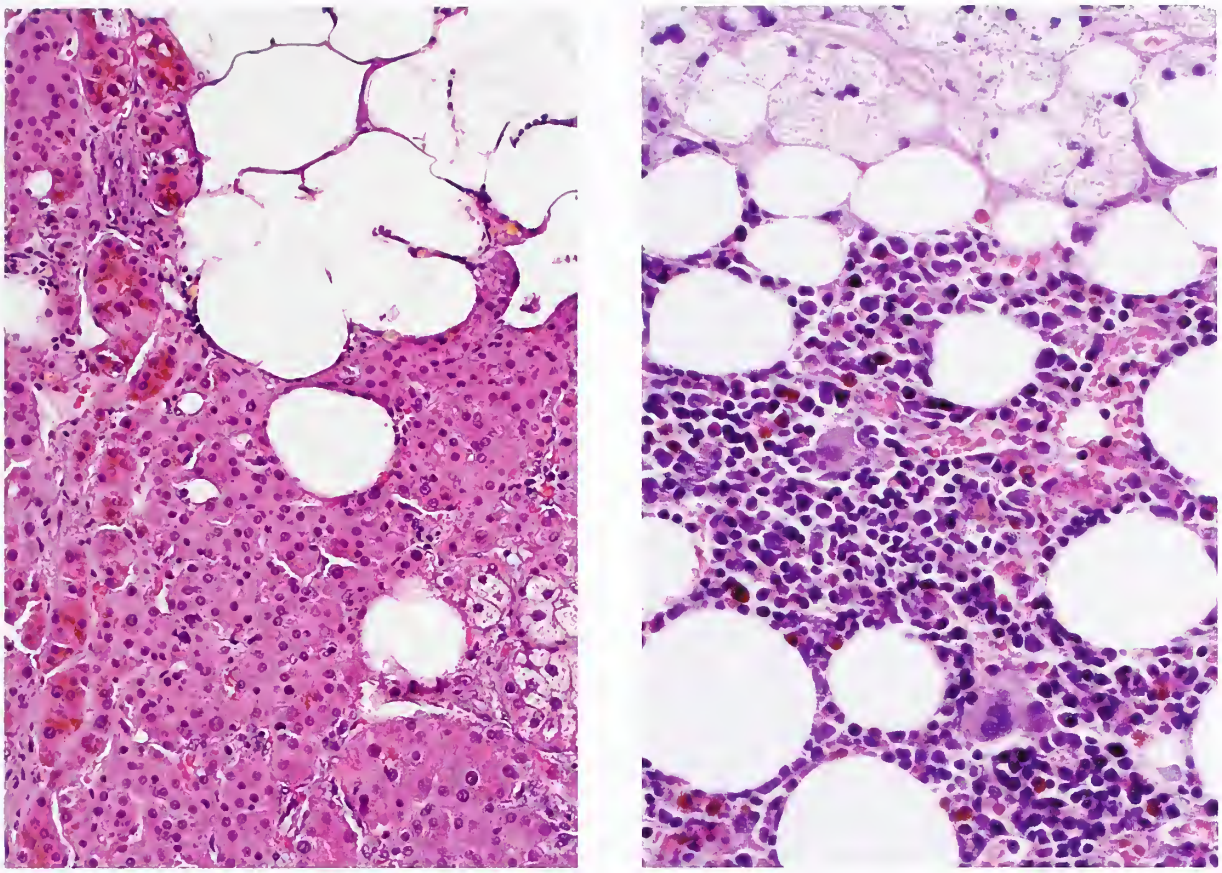

Figure 4-13

ADRENAL CORTICAL ADENOMA ASSOCIATED WITH CUSHING'S SYNDROME

Left: The tumor cells have predominantly compact, eosinophilic cytoplasm. There is a component of lipomatous metaplasia. Other areas of the tumor had numerous cells with pale-staining, lipid-rich cytoplasm. Some cells contain lipofuscin, imparting a brown appearance.

Right: A different adrenal cortical adenoma has areas of myelolipomatous metaplasia.

as the rest of the cell, or adjoining cells, or may be pale or vacuolated (fig. 4-10). There may be areas of lipomatous (fig. 4-13, left) or myelolipomatous metaplasia (fig. 4-13, right). On rare occasion, monomorphous aggregates of mature lymphocytes are observed, and it may be difficult to distinguish between a metaplastic process or an inflammatory reaction. Another unusual feature is the presence of dilated spaces, which if empty, appear pseudoglandular or angiomatous if congested. Mitotic figures are quite rare, at least in the ACAs occurring in adults, and atypical mitotic figures are exceptional. If several mitoses or atypical mitoses are present in consecutive high-power fields of a cortical neoplasm in an adult, these findings should be correlated with other clinical and pathologic features that might indicate malignancy.

An unusual finding in ACA is protrusion of tumor into venous tributaries of the central vein. The intact layer of endothelium over the tumor is usually due to intraluminal extension through discontinuities in the muscular wall of the vessel and not true vascular invasion (fig. 4-14, left). The discontinuity in the muscular wall and continuity of the cortical extension may not be apparent in every plane of section. The presence of loose plugs of histologically benign cortical tissue within vascular spaces is an artifact (fig. 4-14, right).

Similar to the incidentally discovered adrenal nodules outlined in chapter 3, some ACAs

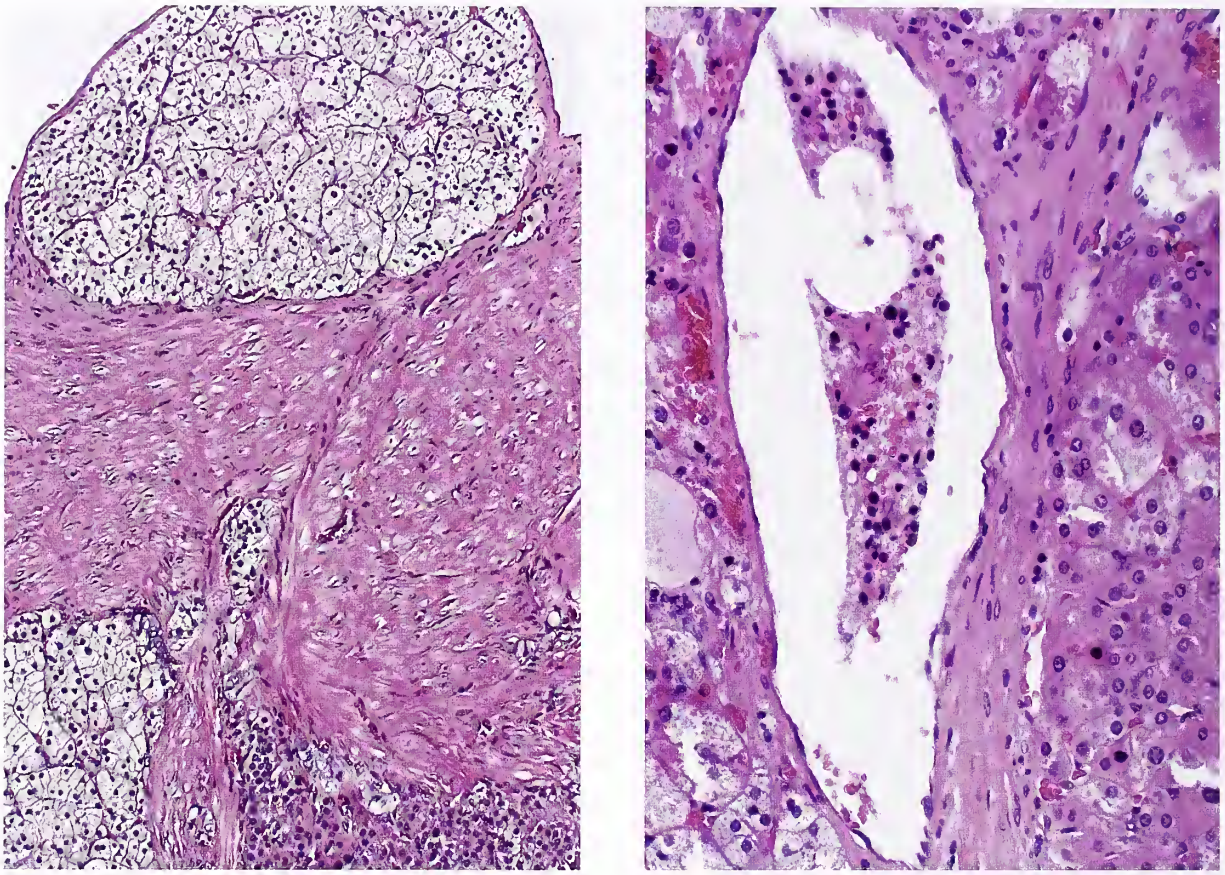

Figure 4-14

ADRENAL CORTICAL ADENOMA ASSOCIATED WITH CUSHING'S SYNDROME

Left: This adrenal adenoma weighed 17 g and measured 2.7 cm in diameter. Complete discontinuity in the smooth muscle bundles can account for the rare intraluminal vascular protrusion, but it is not always apparent in a particular plane of section. This fortuitous finding does not constitute true vascular invasion. (Fig. 4-15 from Fascicle 19, Third Series.)

Right: Benign cortical cells are lying loose in a vascular channel. This is most likely an artifact.

have degenerative features such as fibrosis, organizing fibrin-rich thrombi within sinusoids (fig. 4-15, left), dystrophic calcification, or even metaplastic bone formation (fig. 4-15, right). Myxoid change is rare but has been noted in adrenal cortical neoplasms, both adenomas and carcinomas (8).

While these architectural and cytologic features are characteristic for ACAs associated with Cushing's syndrome, they are not pathognomonic, and clinical and endocrinologic correlation is needed to ascertain the associated endocrine syndrome (1). Without proper correlation it may not be possible to distinguish the ACA from an incidental dominant macronodule or nonhyperfunctional adenoma. Important clues are provided by careful examination of the attached adrenal remnant (or the contralateral gland, as the case may be), since there is almost invariably some degree of adrenal cortical atrophy in association with Cushing's syndrome (fig. 4-16).

Pheochromocytomas with lipid degeneration are occasionally seen which can mimic an ACA grossly and microscopically (9). If the pheochromocytoma also happens to be ectopically producing adrenocorticotropic hormone (ACTH) with Cushing's syndrome, the distinction may become even more difficult. It may be very difficult to distinguish an ACA from a pheochromocytoma with an alveolar or nesting pattern, compact cytoplasm, and eosinophilic hyaline

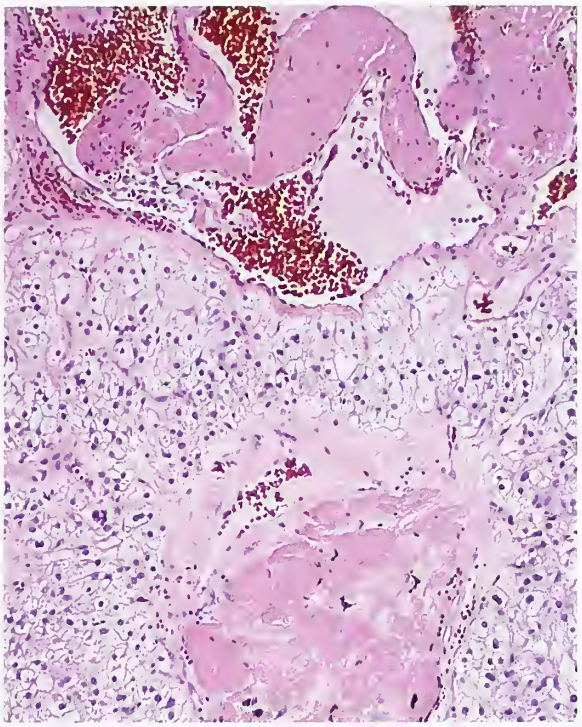

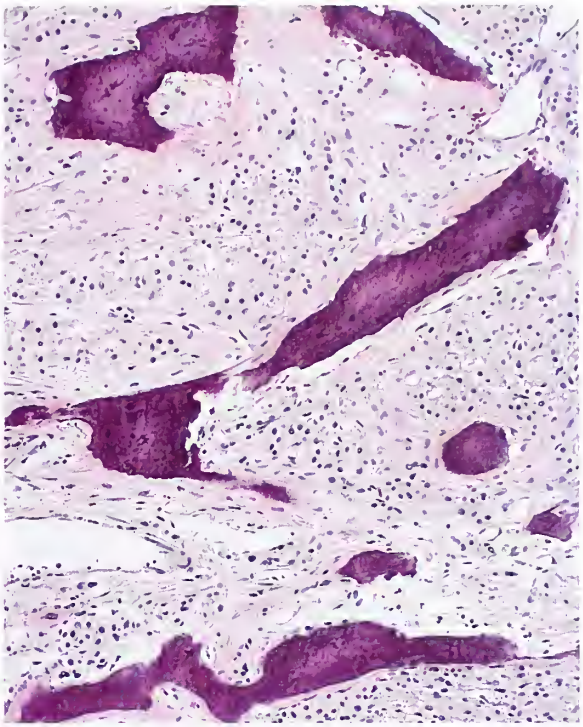

Figure 4-15

ADRENAL CORTICAL ADENOMA ASSOCIATED WITH CUSHING'S SYNDROME

Left: Central areas of this adrenal cortical adenoma have irregular vascular spaces partially occluded by organizing fibrin-rich thrombi. (L&R: Fig. 4-16 from Fascicle 19, Third Series.)

Right: Another area shows metaplastic bone formation in association with fibrotic stroma.

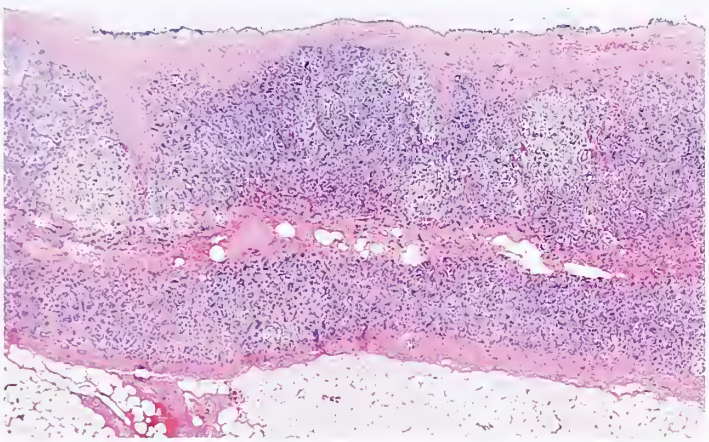

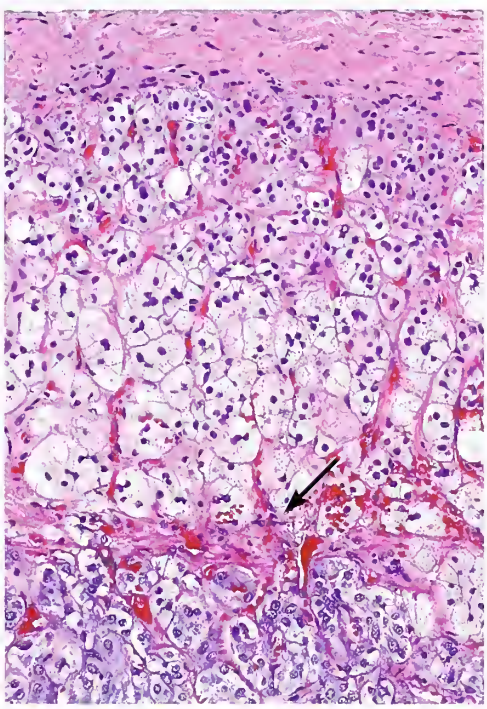

Figure 4-16

ATTACHED ADRENAL REMNANT IN CORTICAL ADENOMA ASSOCIATED WITH CUSHING'S SYNDROME

Above: The adrenal cortex on either side of the interalar raphé is markedly atrophic.

Right: A marked degree of cortical atrophy in Cushing's syndrome. The cortex measured well under 1 mm in thickness throughout. The cortical-medullary junction (arrow) is present in lower third of the field.

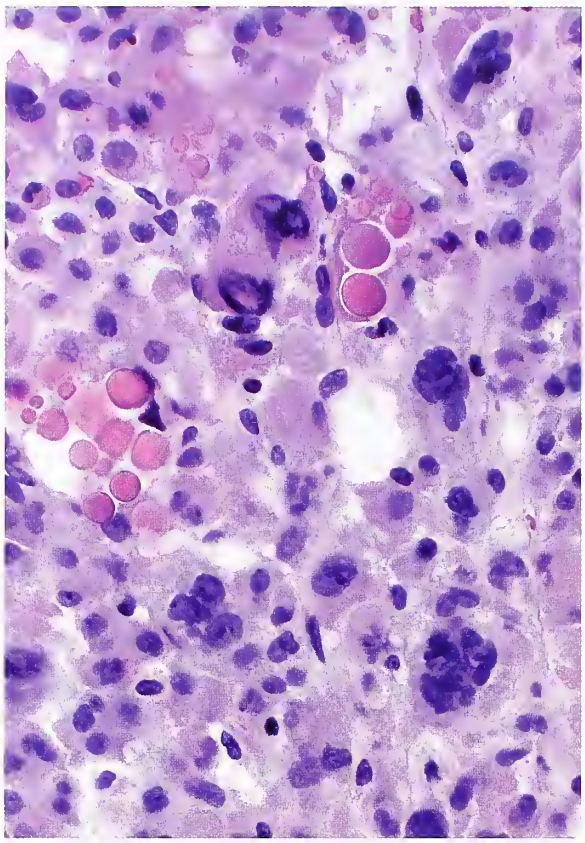

Figure 4-17

ADRENAL CORTICAL ADENOMA
ASSOCIATED WITH CUSHING'S SYNDROME

The tumor cells have compact eosinophilic cytoplasm and contain eosinophilic hyaline globules.

globules (fig. 4-17). A mixed ACA-pheochromocytoma (corticomedullary adenoma) has been reported in association with Cushing's syndrome (10), but one must be cautious in this diagnosis since normally there may be intermingling of cortical and medullary cells. Other unusual associations include a separate "nonfunctional" ACA in the same adrenal gland with a pheochromocytoma; adrenal medullary hyperplasia associated with ACA, with or without Cushing's syndrome; ACA and ganglioneuroblastoma in a child with both Cushing's syndrome and virilization; and a case of pseudohermaphroditism in a woman with an ACA associated with both Cushing's syndrome and virilization (1). Exacerbation of autoimmune thyroid dysfunction has been reported after removal of an ACA in a patient with Cushing's syndrome;

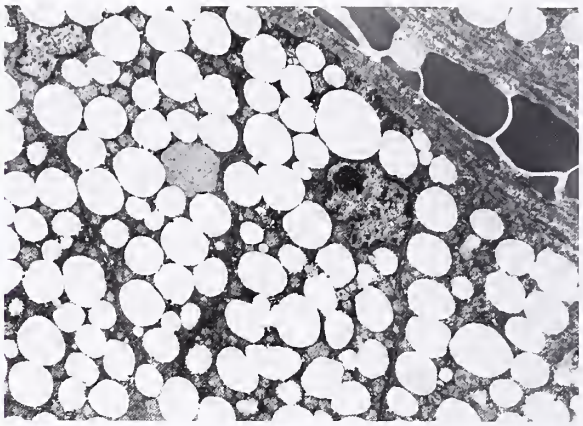

Figure 4-18

ADRENAL CORTICAL ADENOMA
ASSOCIATED WITH CUSHING'S SYNDROME

Prominent lipid droplets vary slightly in size and shape. The capillary channel is present in the right upper corner. The lipid droplets impart a finely vesicular quality by light microscopy (see figure 4-5, right).

it was postulated to be related to a decrease in glucocorticoid secretion by the tumor (11).

Ultrastructural and Immunohistochemical Findings. Most tumor cells are remarkable for the abundant amount of intracytoplasmic lipid droplets, which vary in size and density from cell to cell (fig. 4-18). As expected from the light microscopic heterogeneity of some of these tumors, some cells contain little or no lipid (fig. 4-19). As in the normal adrenal gland, there may be prominent microvillous projections along the cell borders and abundant smooth endoplasmic reticulum (fig. 4-20). Occasional rudimentary intercellular attachments may be present. The nuclear pseudoinclusion is due to an irregularity in the nuclear membrane, with indentation and infolding of cell cytoplasm, often with the same complement and density of cellular organelles (fig. 4-21). Mitochondria may be prominent, and are usually round to oval, although some may be elongated or distorted in shape. The mitochondrial cristae often have a tubular or vesicular profile (fig. 4-22) similar to the cells of the zona fasciculata, or there may be lamellar cristae resembling the morphology of zona reticularis cells (1,12).

Immunohistochemistry is seldom needed in the diagnosis of ACA. It may prove helpful when the tumor has unusual features that mimic a pheochromocytoma (see fig. 4-17) or

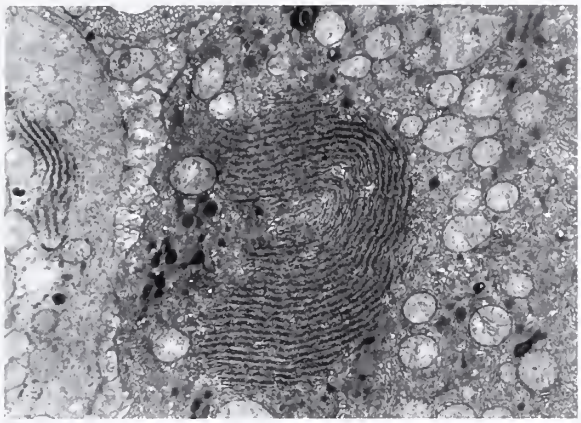

Figure 4-19

ADRENAL CORTICAL ADENOMA
ASSOCIATED WITH CUSHING'S SYNDROME

Tumor cells contain only scant to minimal lipid droplets. Stacks of rough endoplasmic reticulum and prominent smooth endoplasmic reticulum are seen. Clusters of dense granules probably represent primary lysosomes.

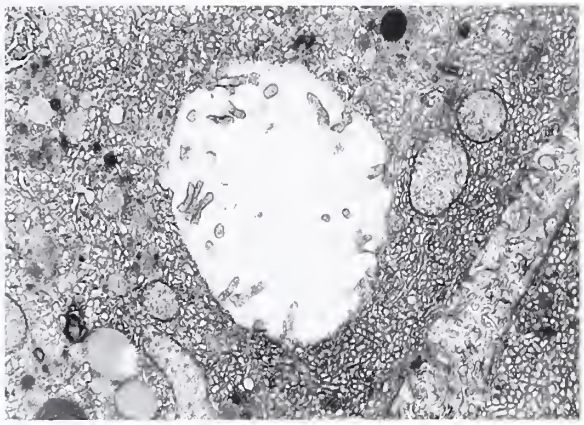

Figure 4-20

ADRENAL CORTICAL ADENOMA
ASSOCIATED WITH CUSHING'S SYNDROME

The abundant smooth endoplasmic reticulum appears as tubular or vesicular profiles, depending on the plane of section. Cells have prominent microvillous projections along cytoplasmic borders and in the center is a lumen with microvillous projections.

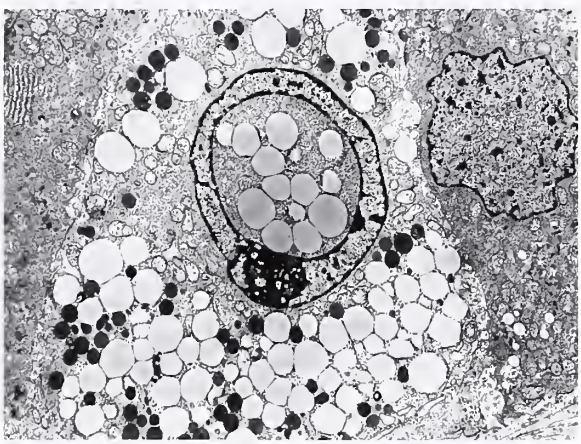

Figure 4-21

ADRENAL CORTICAL ADENOMA
ASSOCIATED WITH CUSHING'S SYNDROME

A nuclear pseudoinclusion viewed en face in an adrenal cortical adenoma from a patient with Cushing's syndrome. The structure is nonspecific and results from irregular deep infolding of the nuclear membrane. (Fig. 4-21 from Fascicle 19, Third Series.)

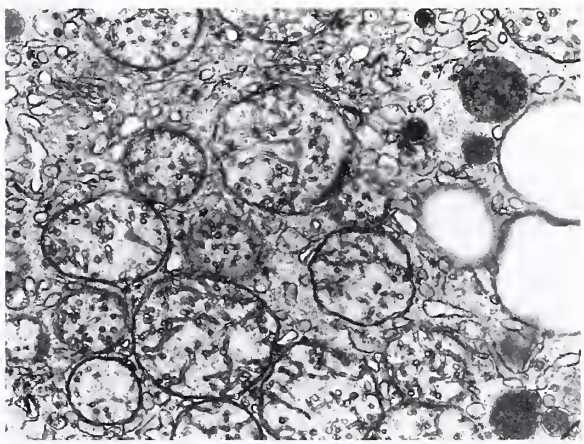

Figure 4-22

ADRENAL CORTICAL ADENOMA
ASSOCIATED WITH CUSHING'S SYNDROME

Cristae of mitochondria have a tubular or vesicular profile typical of steroid-producing cells. There is prominent smooth endoplasmic reticulum as well as a few free polyribosomes.

when the tumor occurs in an unusual or unexpected location within the abdomen or spinal canal (fig. 4-23) (13–15). Useful markers of adrenal cortical neoplasia include the alpha subunit of inhibin (16,17) and Melan-A (or Mart-1) (18). Vimentin may be positive in ACAs in keeping with the mesodermal derivation of adrenal cortical cells. ACAs can be positive for synaptophysin and neuron-specific enolase, and the tumor should not be mistaken for a pheochromocytoma. Immunoreactivity for chromogranin is negative.

Figure 4-23

ECTOPIC ONCOCYTIC ADRENAL CORTICAL ADENOMA

A: An intramedullary oncocytic adrenal cortical adenoma was present within the spinal cord at the level of the conus medullaris. The tumor was well circumscribed and light brown, and measured approximately 3 cm in diameter. Signs and symptoms of cord compression resulted. The tumor cells have abundant eosinophilic cytoplasm, but the tumor was nonfunctional.

B: Immunostain for inhibin is strongly positive in all cells (avidin-biotin peroxidase method).

C: The tumor cells are positive for Melan-A (Mart-1), but the immunoreaction is less intense compared with figure B (avidin-biotin peroxidase method).

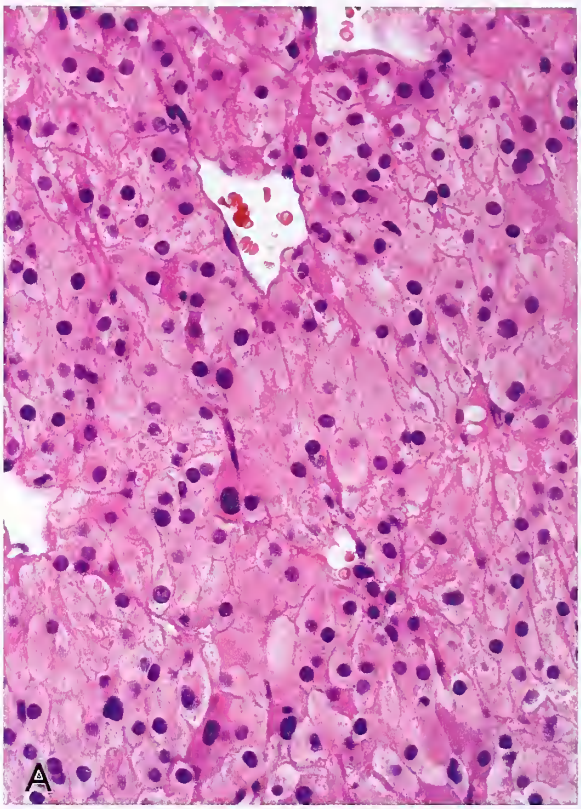

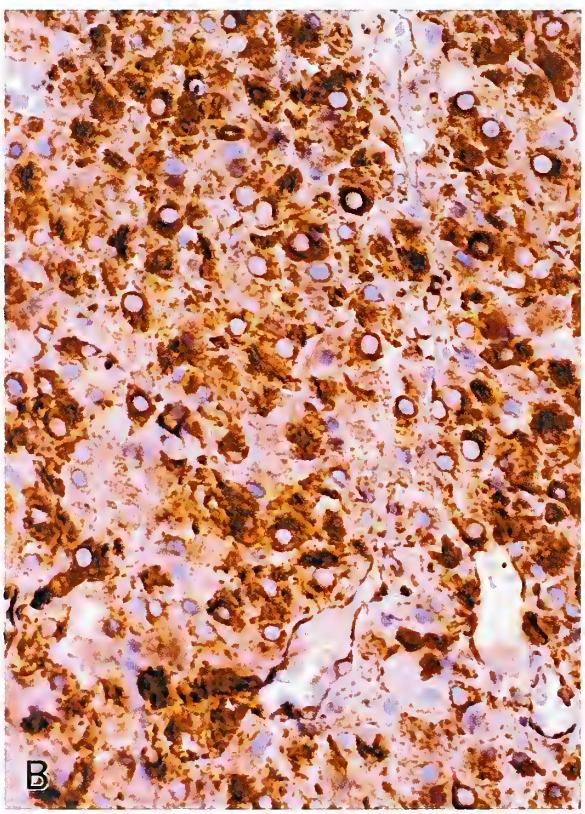

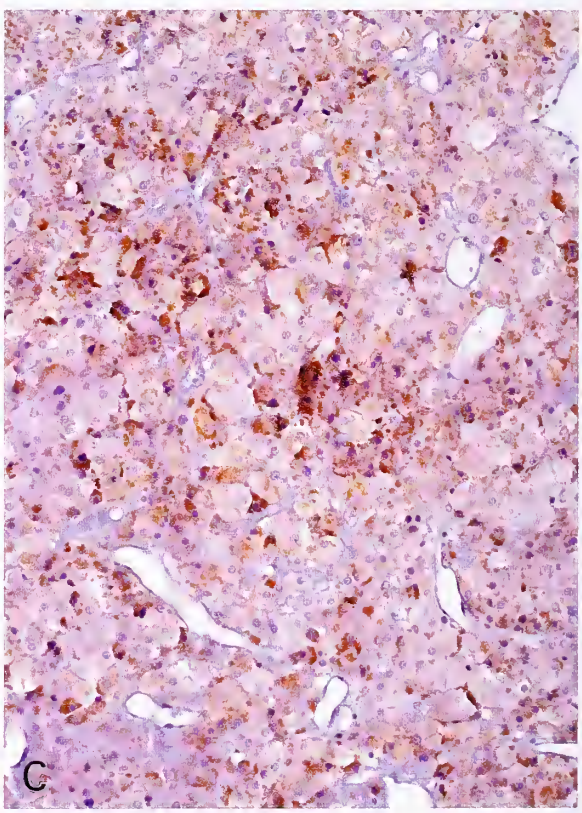

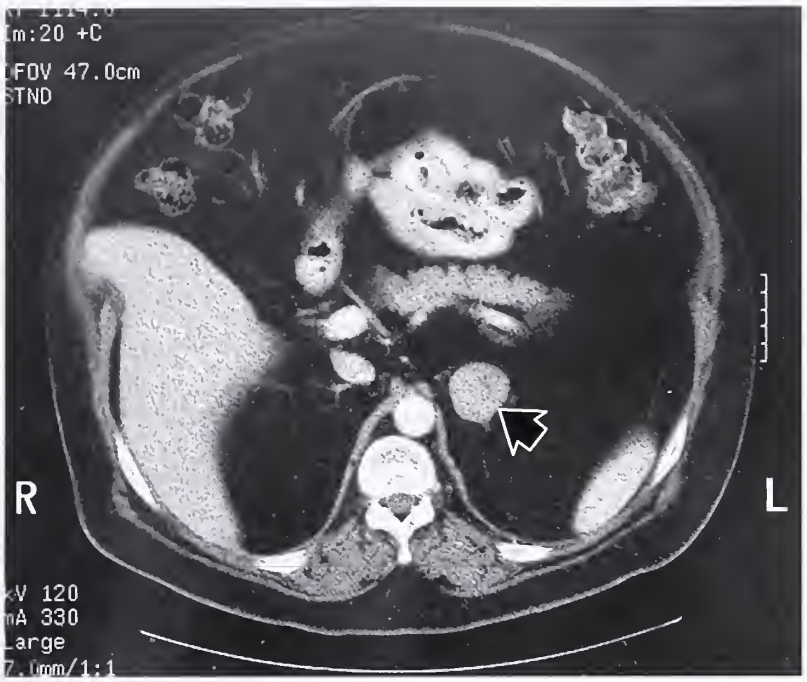

Figure 4-24

"BLACK" ADRENAL CORTICAL ADENOMA CAUSING CUSHING'S SYNDROME

The adrenal tumor on the left (arrow) was mildly heterogeneous both before and after contrast enhancement. There is slight contrast enhancement on computerized tomography (CT) scan, raising the possibility of either primary or secondary malignancy. (Figs. 4-24 and 4-25 are from the same case.) (Fig. 4-23 from Fascicle 19, Third Series.)

Cytogenetic Findings. Although the genetic background of ACA remains poorly understood, most, whether benign or malignant, appear to be monoclonal. A recent study reported a marked difference in the number of genetic events observed in adrenal cortical carcinomas (ACCs) versus ACAs (19). Comparative genomic hybridization (CGH) allows the entire genome of a tumor to be surveyed for gains and losses of DNA copy sequences. The mean number of CGH changes in ACCs was 7.6 (range, 1 to 15) with an equal number of gains and losses, while ACAs had a mean of 1.1 changes (range, 0 to 4), again with a roughly equal number of gains and losses. Several chromosomal loci were implicated in adrenal cortical tumorigenesis, including activation of oncogenes on chromosomes 5 and 12 and inactivation of tumor suppressor genes on chromosome arms 1p and 17p (19).

FUNCTIONAL PIGMENTED ("BLACK") ADENOMAS

Clinical Features. A *diffusely pigmented,* or *"black," adenoma* is quite rare, particularly when small incidental pigmented nodules, many of which are not truly neoplastic in the classic sense, are excluded (1). Over 20 black adenomas have been recorded in the literature, mostly as individual case reports, and most have been associated with Cushing's syndrome (1) or preclinical Cushing's syndrome (20). Occasionally, these adenomas have resulted in primary hyperaldosteronism (1).

There is a distinct predilection for female patients, and most tumors are diagnosed in the 3rd to 5th decades of life. The tumors usually weigh less than 35 g, and measure 2 to 3 cm in diameter (1). Black ACAs have been reported to have a higher radiologic density on CT scans (21); this is probably due to the predominance of cells with compact, lipid-depleted cytoplasm and abundant lipofuscin (fig. 4-24). The designation "adrenal cortical adenoma with excess pigment deposition," has been proposed for these tumors since there does not appear to be ample justification for their separation from the more prevalent "yellow" adenomas.

Pathologic Findings. Black ACAs can present a striking gross appearance, which in the extreme seems to warrant a separate designation even if it is merely a descriptive one (fig. 4-25). Some tumors are dark brown to yellowish (light) brown. When the pigmented adrenal mass is dark brown to black, other adrenal lesions enter the differential diagnosis, such as an adrenal hematoma and metastatic (or primary) malignant melanoma.

Figure 4-25

BLACK ADRENAL CORTICAL ADENOMA

Top: The adenoma was resected from a 58-year-old man with Cushing's syndrome. The dark exterior aspect of the tumor is evident through the intact adrenal capsule and thin investing fat.

Bottom: The tumor measured 2.9 x 2.8 x 2.5 cm and weighed 30 g. On cross section, the tumor became even darker after exposure of the cut surface to air. The adrenal cortex at the bottom of the field is markedly atrophic. Fat could not be removed entirely because the atrophic gland was so friable. (Fig. 4-24 from Fascicle 19, Third Series.)

Microscopically, the architectural patterns of black ACAs are comparable to other ACAs without excessive lipochrome pigment (fig. 4-26A), and most tumors are composed predominantly or entirely of cells with compact, eosinophilic cytoplasm similar to, but larger than, cells of the zona reticularis. There is a variable amount of brown or golden brown pigment within the cytoplasm, which may spare the immediate perinuclear zone. Clusters of pale-staining, lipid-rich cells are found, and occasionally, there are foci of lipomatous or myelolipomatous metaplasia within the tumor (fig. 4-26B); the case illustrated in figure 4-26C also had striking lipomatous metaplasia in the atrophic attached cortex. Recently, a case of functional black adenoma (with Cushing's syndrome) and a well-developed myelolipoma was reported (22).

Special stains document the presence of lipofuscin: a positive argentaffin reaction with the Fontana-Masson stain that is susceptible to bleaching procedures, a reddish orange tint with the periodic acid–Schiff (PAS) stain, and a negative reaction to iron stain (1). A study of black pigmented adrenal nodules (23) suggested that neuromelanin may be present.

On ultrastructural study, the tumor cells have a variable amount of cytoplasm. The cytoplasm is relatively poor in lipid droplets, and the lipid droplets that are present may be few in number and small in size (fig. 4-27). Other cells have such electron-dense cytoplasm that evaluation of cellular organelles such as mitochondria may be difficult in survey views. The tumor cells are polygonal or rounded, with occasional simple intercellular attachments; there may be microvillous projections along cell borders. Most cells contain a variable number of electron-dense granules (fig. 4-28, top), often with a small lipid component, which is typical for lipofuscin (fig. 4-28, bottom). Some granules appear membrane bound. There are typically no pigmented granules with the ultrastructural features of melanosomes or premelanosomes. There may be prominent mitochondria, which are rounded to elongated and have irregular tubular (or lamellar) cristae. Profiles of rough and smooth endoplasmic reticulum may be found along with free ribosomes.

ADRENAL CORTICAL ADENOMA WITH PRIMARY HYPERALDOSTERONISM (CONN'S SYNDROME)

Adrenal cortical adenoma with primary hyperaldosteronism (Conn's syndrome) is characterized by hypertension, suppressed plasma renin activity, increased plasma aldosterone levels, and an insuppressible aldosterone level in the blood or urine. Conn (24) described the clinical syndrome which came to bear his name in a publication in 1955, but his findings were presented in his presidential address on October 29th, 1954 before the Central Society for Clinical Research in Chicago, Illinois (25).

The etiology of Conn's syndrome has classically been attributed to an underlying aldosterone-secreting ACA ("aldosteronoma"), although

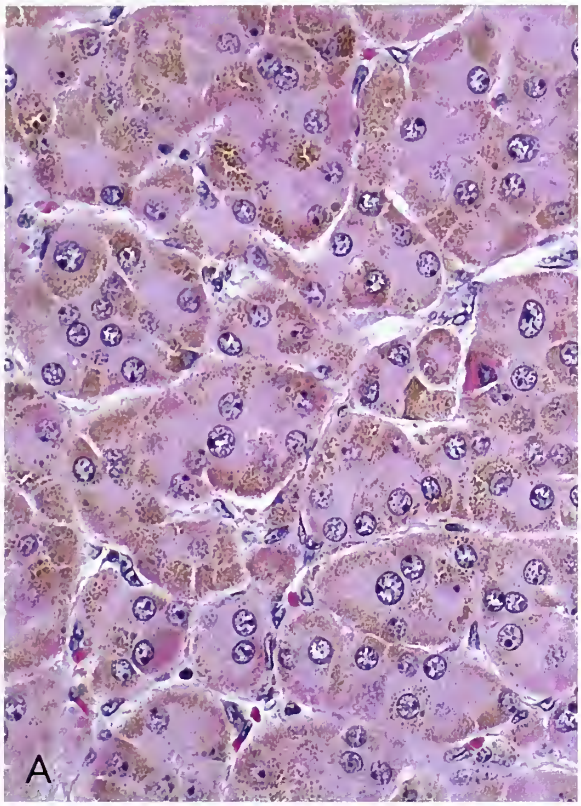

Figure 4-26

BLACK ADENOMA ASSOCIATED WITH CUSHING'S SYNDROME

A: Tumor cells have compact, eosinophilic cytoplasm and abundant lipofuscin. The nuclei have dispersed chromatin with small central to eccentric nucleoli. The cells are arranged in short cords and alveoli. (Fig. 4-25A from Fascicle 19, Third Series.)

B: Areas of prominent lipomatous metaplasia are present. A myelolipomatous component was present elsewhere.

C: The attached adrenal remnant shows marked cortical atrophy with prominent lipomatous metaplasia. (Fig. 4-25C from Fascicle 19, Third Series.)

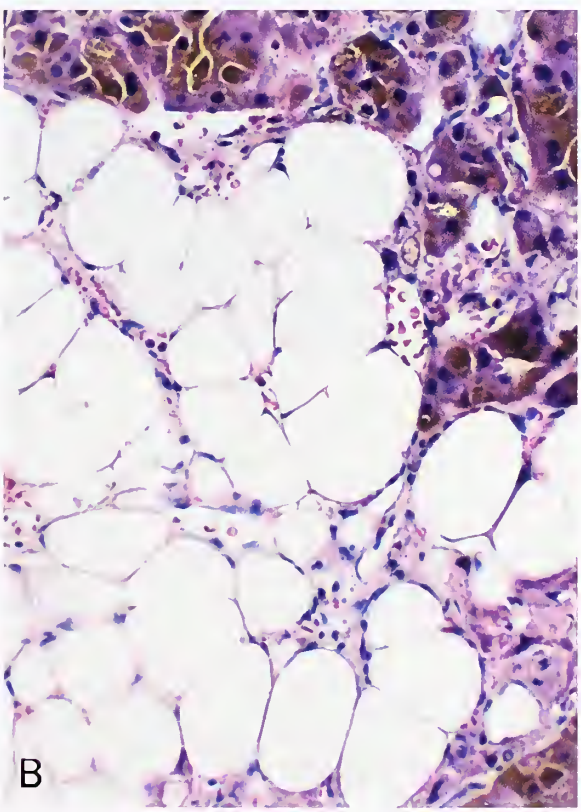

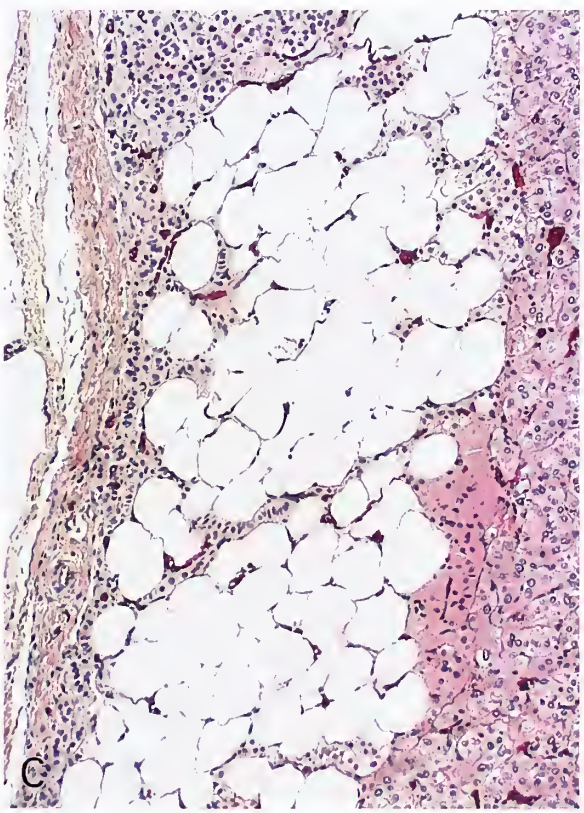

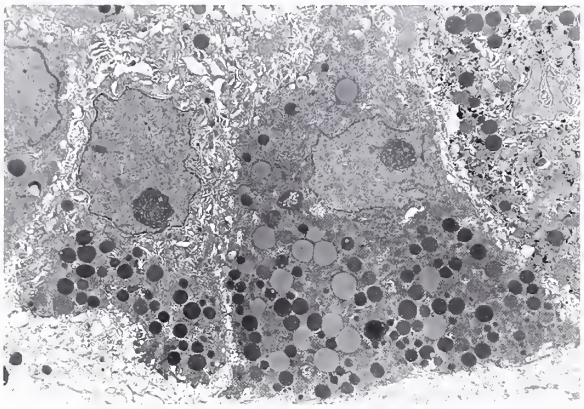

Figure 4-27

BLACK ADENOMA ASSOCIATED WITH CUSHING'S SYNDROME

The tumor cells contain abundant lipofuscin and have only sparse lipid droplets. Note the microvillous projections along the cytoplasmic borders. (Figs. 4-27 and 4-28 are from the same case.)

on occasion, the primary hyperaldosteronism is due to an adrenal cortical carcinoma (1). Primary hyperaldosteronism occurs in about 2 percent of patients with systemic hypertension, although some estimate that the prevalence among unselected hypertensive patients is less than 1 percent (26). With improved screening methods and the recognition that most patients with primary hyperaldosteronism are normokalemic, it appears that primary hyperaldosteronism is the most common form of secondary hypertension; current prevalence estimates range from 5 to 10 percent of the hypertensive population (27). Conn (28) suggested that primary hyperaldosteronism (due to an ACA) may be the cause of as many as 20 percent of all cases of essential hypertension. This was based, in part, on an autopsy study that reported ACAs or cortical "adenomas" of 1.5 cm or larger in as many as 20 percent of hypertensive patients (29). It is unclear whether the adrenal adenoma (or nodule) was the cause of the hypertension or perhaps a result of it (e.g., from localized ischemia due to capsular arteriopathy) (30). It has also been suggested that Conn's syndrome may exist for many years before symptoms or signs of potassium deficiency appear (28). Since studies have shown that patients may be normokalemic, or even hypokalemic, measurement of this electrolyte is not a reliable screening test.

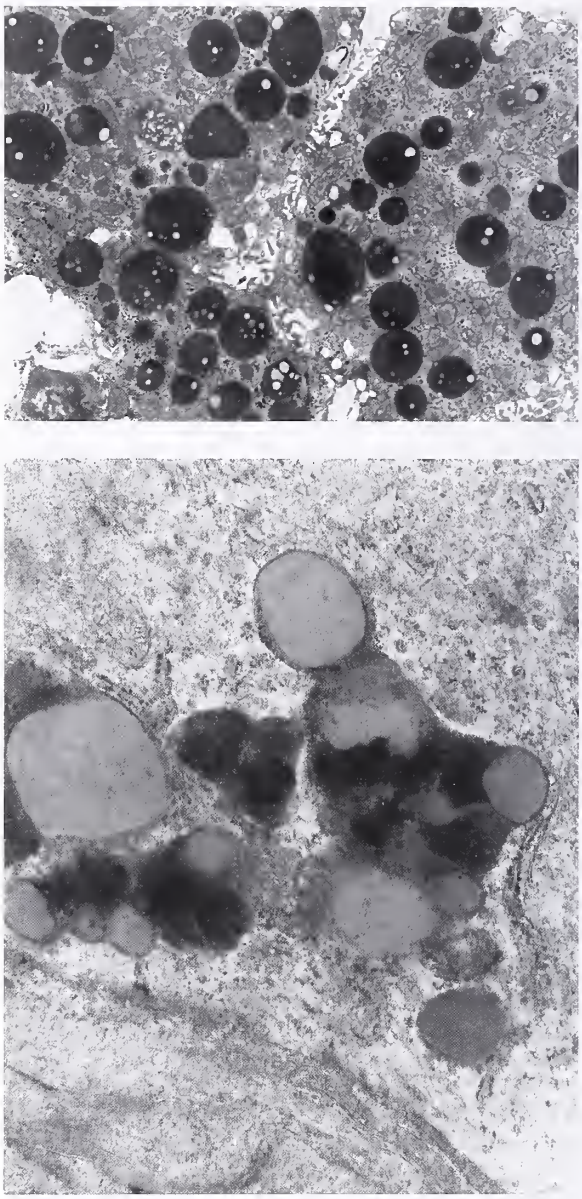

Figure 4-28

BLACK ADENOMA ASSOCIATED WITH CUSHING'S SYNDROME

Top: Granules of lipofuscin are electron dense and many are associated with small lipid droplets. The cells contained smooth endoplasmic reticulum along with short profiles of rough endoplasmic reticulum and free polyribosomes.

Bottom: Lipofuscin granules are heterogenous and associated with some lipid component.

There are few population-based studies on the incidence of Conn's syndrome. In one study, the average annual incidence in the Danish National Registry was 0.8/million population

(31). Most series report a predilection for female patients with ACA (1), but the preponderance of females overall with primary hyperaldosteronism appears to be declining with increasing recognition of the idiopathic form of the disorder. Most aldosterone-producing ACAs are diagnosed in patients in the 3rd to the 5th decades of life (1,32), whereas about 80 percent of incidental cortical nodules are seen in the 50- to 80-year-old age group (30).

Prevalence of Different Forms of Primary Hyperaldosteronism. Early data suggested that 60 to nearly 90 percent of cases of primary hyperaldosteronism were due to an aldosterone-producing ACA (5,26), but with increasing recognition of mild forms of hyperaldosteronism, different data have emerged. Prior to 1970, 70 percent of cases at the Mayo Clinic were due to an aldosterone-producing ACA and 26 percent due to bilateral adrenal hyperplasia, but from 1978 through 1987, ACAs accounted for 54 percent of cases and 45 percent were due to hyperplasia (33). A different source estimates that idiopathic bilateral hyperplasia of the zona glomerulosa may account for as many as 70 to 80 percent of cases of primary hyperaldosteronism (26).

Gross Findings. The aldosterone-producing ACA is usually a small, unicentric neoplasm measuring only a few centimeters in diameter (fig. 4-29) (1). In one study, 92 percent of tumors were less than 2 cm in diameter (6). In a review by Conn et al. (35), 72 percent of tumors were less than 3 cm, and 69 percent weighed less than 6 g, although it is not clear whether this represented the entire adrenal gland or just the neoplasm. One of the larger ACAs reported by Neville and Symington (34) weighed 75 g, but the recorded weights of most tumors were under 10 g; the largest tumor among the 18 patients with Conn's syndrome was an adrenal cortical carcinoma weighing over 2,000 g. In another study, the median size of ACAs was 1.7 cm and the smallest tumor detected on abdominal CT scan was 0.7 cm (36).

Most tumors are unilateral and solitary, but bilateral ACAs have been reported in 1 to 6 percent of cases (1). Bilateral ACAs were reported in a patient who had concurrent hypersecretion of aldosterone and cortisol (37). In a small percentage of cases, ACAs have been described as being multiple but still unilateral (6). Most tumors are large enough to be readily detected on abdominal CT scan or MRI (fig. 4-30); the sensitivity with CT scan is reported to be over 80 percent (36). The tumor may be obvious on gross examination of the intact gland, but occasionally, it is difficult to appreciate because of its small size, and it may become apparent

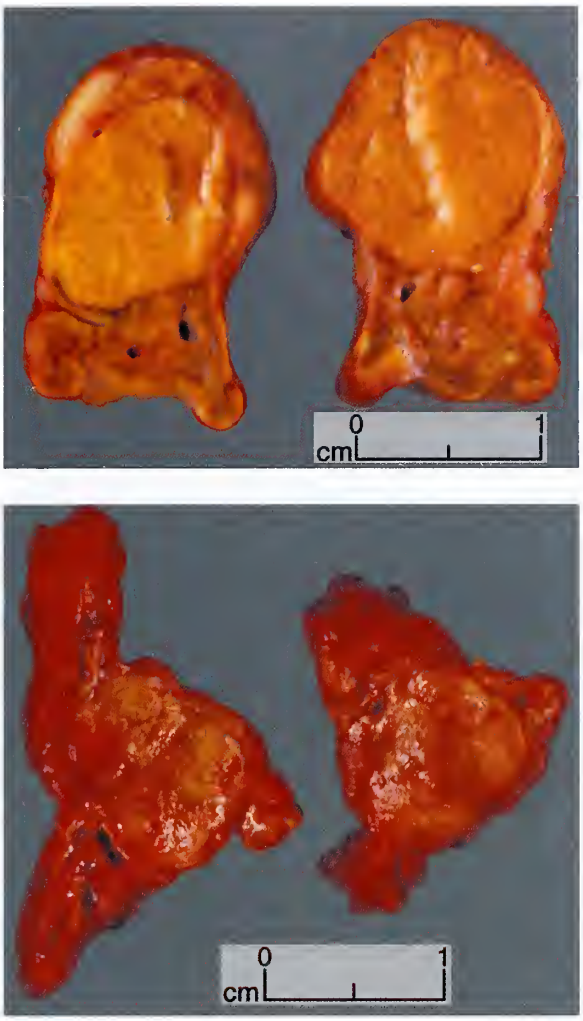

Figure 4-29

ALDOSTERONE-SECRETING ADRENAL CORTICAL ADENOMA

Top: On cross section the tumor is sharply demarcated and appears encapsulated, particularly where it expands the contours of the adrenal capsule. The tumor measured 1 cm in diameter and is a uniform yellow-orange.

Bottom: Resected aldosterone-producing adrenal cortical adenoma in a different case is less well-defined and has a mottled appearance on cross section. The tumor measured 1 cm in diameter.

only after transverse sectioning of the gland. ACAs are usually round to ovoid, and sharply demarcated, with what appears to be true encapsulation. The residual or attached adrenal cortex usually appears grossly normal without the atrophy expected with Cushing's syndrome. ACAs have been described as homogeneous, yellow-orange or "canary yellow" on cross section.

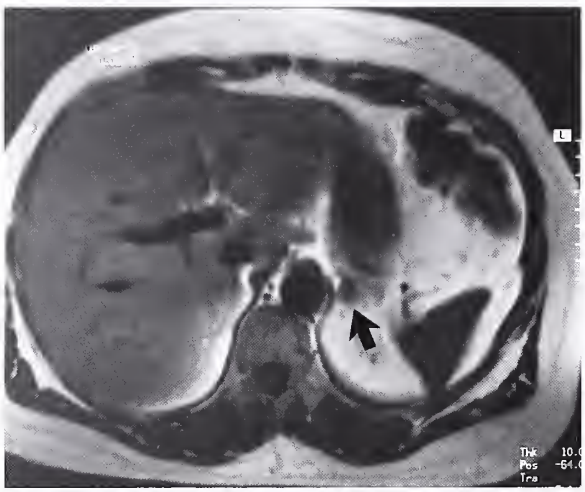

Figure 4-30

ALDOSTERONE-SECRETING ADRENAL CORTICAL ADENOMA

An aldosterone-secreting adrenal cortical adenoma was localized on abdominal magnetic resonance imaging (MRI) (left, arrow). The patient had systemic hypertension and hypokalemia. (Fig. 4-29 from Fascicle 19, Third Series.)

Larger tumors may have areas of hemorrhage or cystic change (1,34).

Microscopic Findings. In many instances, the gross impression of complete encapsulation is not borne out on low-power scanning of the pushing edges of the tumor (fig. 4-31). The ACA may appear partially or even completely encapsulated, but often there is a compressed fibrous rim or fibrous pseudocapsule at the expansile border of the tumor or the tumor acquires part of its "capsule" from expansion of the adrenal capsule itself. A high incidence of associated small cortical nodules have been noted (58 percent) which may be related to the effects of hypertension rather than an additional cause of it (6). Tumor cells are arranged in a nesting or alveolar pattern (fig. 4-32, left), short cords (fig. 4-32, right), blunt anastomosing trabeculae, or a mixture of these architectural patterns.

Theoretically, most or the entire tumor should be composed of cells that strongly resemble those of the zona glomerulosa, which is responsible for mineralocorticoid production, but such is far from the case. The morphology of individual cells may be quite heterogeneous (fig. 4-33) (1). Four different types of cells have been recognized: 1) pale-staining, lipid-rich cells that resemble zona fasciculata cells, although they tend to be larger; 2) cells resembling zona glomerulosa cells with a higher nuclear to cytoplasmic ratio and only a small amount of vacuolated, lightly eosinophilic

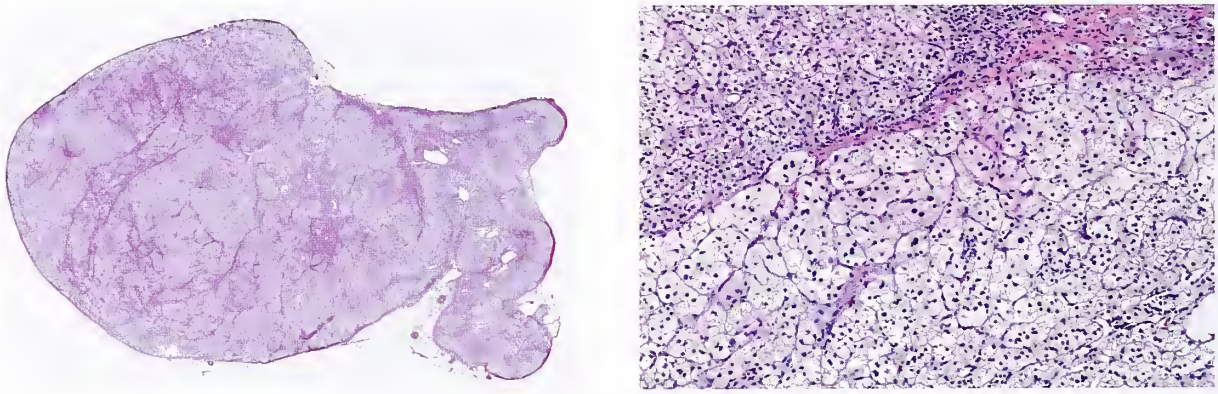

Figure 4-31

ALDOSTERONE-SECRETING ADRENAL CORTICAL ADENOMA

Left: The tumor has expansile smooth borders that compress adjacent adrenal parenchyma and expand the adrenal capsule.
Right: The borders of the adenoma are sharply demarcated from the adjacent cortex (left upper portion of field), but there is no well-developed fibrous capsule.

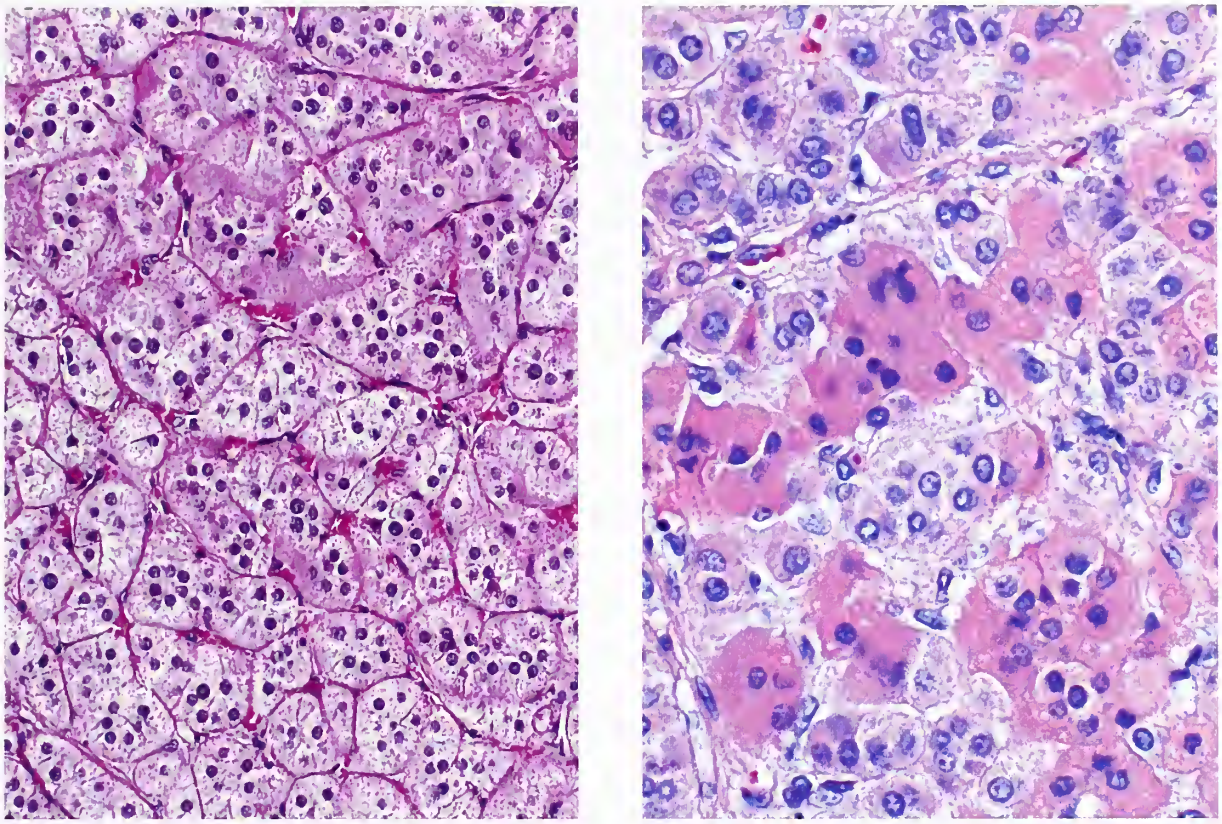

Figure 4-32

ALDOSTERONE-SECRETING ADRENAL CORTICAL ADENOMA

Left: Tumor cells have a predominantly nesting or alveolar pattern along with short cords. (Fig. 4-32, right from Fascicle 19, Third Series.)

Right: Cells are arranged in short cords. Focal areas within the tumor have oncocytic cells with dense, granular, eosinophilic cytoplasm.

cytoplasm; 3) compact cells indistinguishable from those of the zona reticularis (although usually larger) or occasionally cells with oncocytic features (fig. 4-32, right); and 4) a group of cells designated as "hybrid" cells with cytologic features of both the zona glomerulosa and zona fasciculata cells (34).

Origin of ACA from a transitional or hybrid cell is consistent with the functional behavior of these tumors, such as modulation of aldosterone secretion by ACTH, the lack of responsiveness to angiotensin II, the ability to produce cortisol, and the secretion of hybrid steroids. Some tumors probably arise from glomerulosa type cells (38). Studies have reported that the zona glomerulosa type cells and compact cells are more frequently present at the periphery of the tumor (34), whereas pale-staining cells are concentrated in more central areas (39). The large lipid-rich cells are most common; these cells, coupled with the other lipid-rich cells, give the tumor its characteristic golden yellow hue.

It may be very difficult on routine histologic study to distinguish one or more dominant macronodules in a surgically resected adrenal gland from an aldosterone-producing ACA without knowledge of the clinical and endocrinologic data. A recent study used mRNA expression of the gene *CYP11B2* (indicating aldosterone production) as an aid in the postoperative differentiation of unilateral ACA and bilateral adrenal hyperplasia (40); at present this in situ hybridization method for expression of genes coding for steroidogenic enzymes is of special value for analysis of cases not cured by adrenalectomy (40).

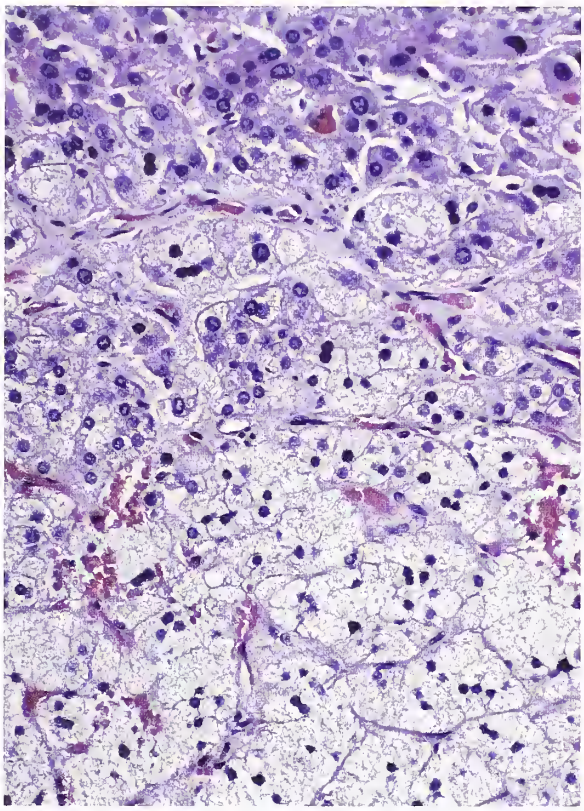

Figure 4-33

ALDOSTERONE-SECRETING ADRENAL CORTICAL ADENOMA

Morphologically, there is a heterogeneous cell population ranging from cells that are large and lipid-rich (analogous to zona fasciculata) to smaller cells with relatively sparse lipid (similar to zona glomerulosa) and cells with compact, eosinophilic cytoplasm resembling zona reticularis type cells.

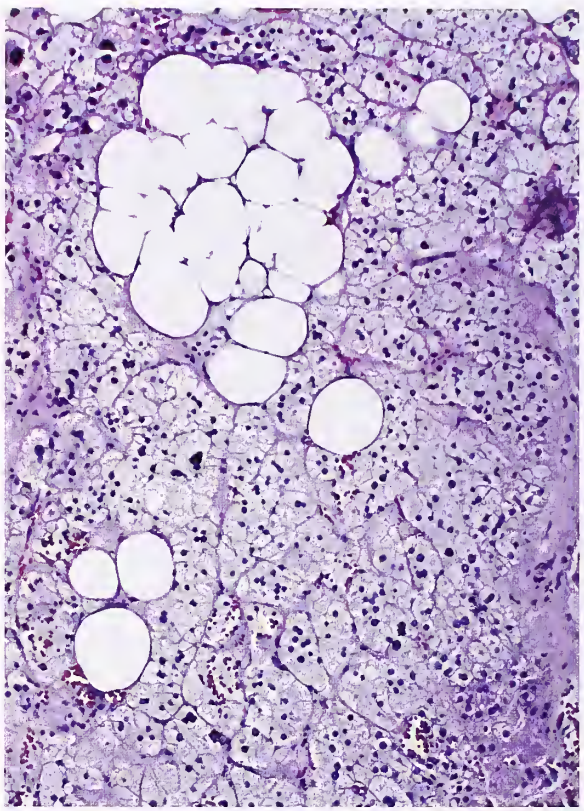

Figure 4-34

ALDOSTERONE-SECRETING ADRENAL CORTICAL ADENOMA

Small areas of lipomatous metaplasia are present.

Balloon cells, small clusters of cells with abundant lipid-rich cytoplasm, similar to those in ACAs associated with a different endocrine syndrome, may be present. The term hybrid cells, used in reference to the pale, lipid-rich cells of aldosterone-producing ACAs, emphasizes the capacity of these cells to elaborate hormones normally produced by either the zona glomerulosa (aldosterone) or the zona fasciculata (cortisol) (34). Production of either hormone is based upon the enzyme systems in the zona glomerulosa (18-oxidase system) and zona fasciculata (17-alpha-hydroxylase). In vitro studies of tumors from patients with Conn's syndrome show the production of aldosterone, cortisol, and a variety of other corticosteroids (1), which also can occur with ACTH stimulation.

Many cells have round to oval vesicular nuclei, often with a small, dot-like nucleolus. Some nuclei are darkly pyknotic. There may also be a mild degree of nuclear pleomorphism. Lipomatous or myelolipomatous metaplasia is an uncommon finding (fig. 4-34). Other unusual features include areas of interstitial fibrosis, which are typically small and localized (fig. 4-35); chronic inflammatory infiltrates (fig. 4-36); and pseudoglandular foci with stringy basophilic material (fig. 4-37). These features are nonspecific, however, and must be correlated with clinical and endocrinologic findings. A prominent infiltrate of mast cells was reported in a large adrenal cortical tumor producing 11-deoxycorticosterone, with associated signs and symptoms of primary hyperaldosteronism (41), but ordinarily mast cells are inconspicuous in ACAs associated with primary hyperaldosteronism or other endocrine syndromes.

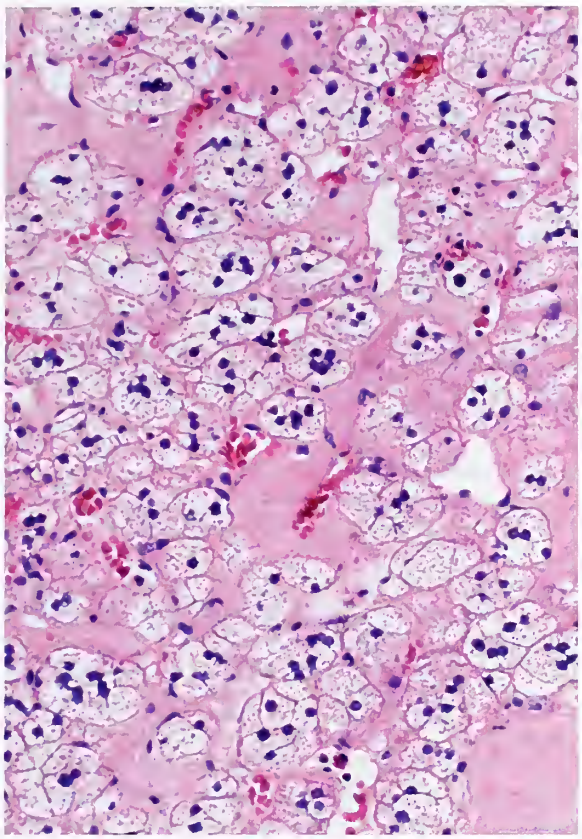

Figure 4-35

ALDOSTERONE-SECRETING ADRENAL CORTICAL ADENOMA

Areas of fibrosis in this adenoma separate alveolar clusters of pale-staining, lipid-rich tumor cells.

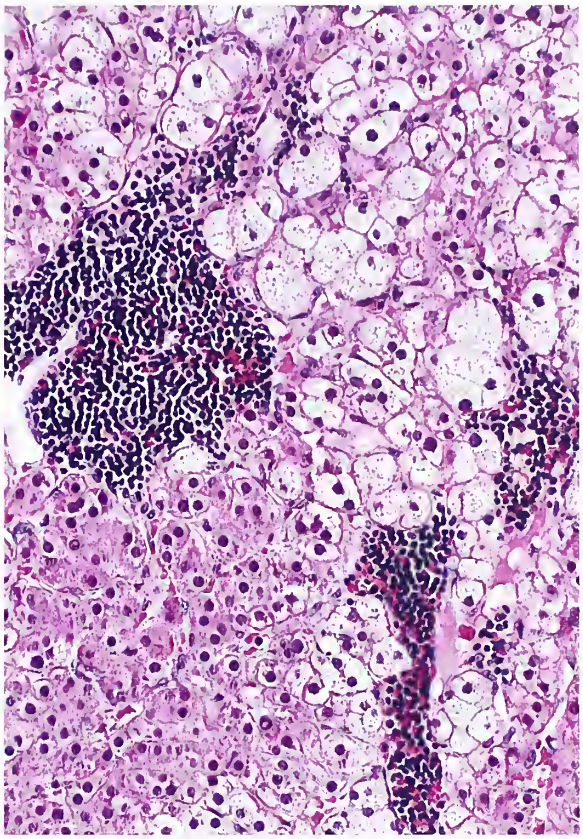

Figure 4-36

ALDOSTERONE-SECRETING ADRENAL CORTICAL ADENOMA

A few aggregates of lymphocytes are present. (Fig. 4-38 from Fascicle 19, Third Series.)

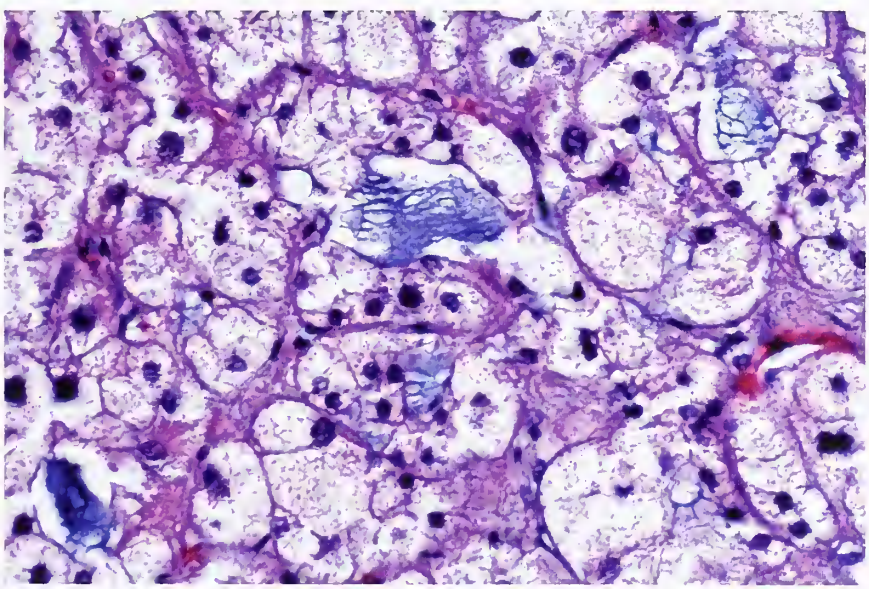

Figure 4-37

ALDOSTERONE-SECRETING ADRENAL CORTICAL ADENOMA

A few small pseudoglandular spaces have pale blue mucoid contents. No mucosubstances were identified with special stains.

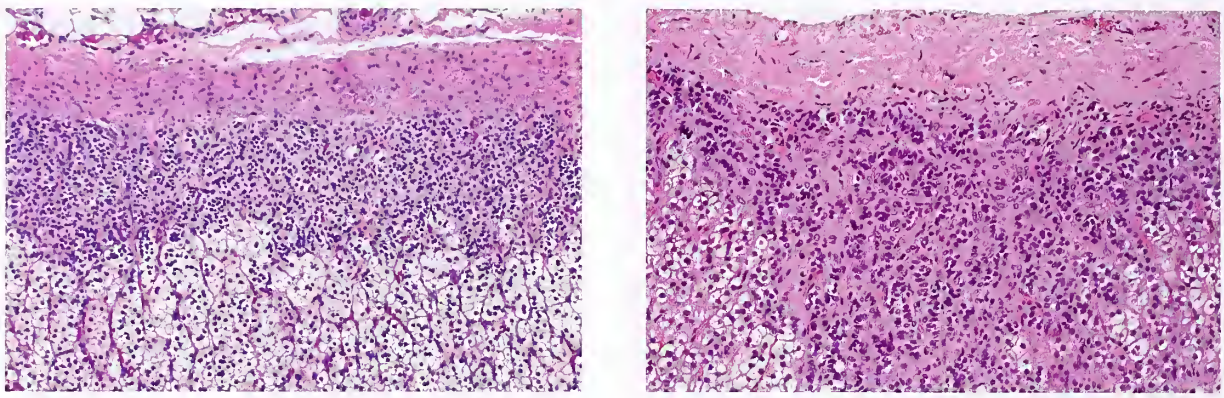

Figure 4-38

ALDOSTERONE-SECRETING ADRENAL CORTICAL ADENOMA

Left: A continuous zone of hyperplastic zona glomerulosa was present in the non-neoplastic adrenal remnant.
Right: In a different case, the hyperplastic zona glomerulosa is thickened with tongue-like extension in outer zona fasciculata.

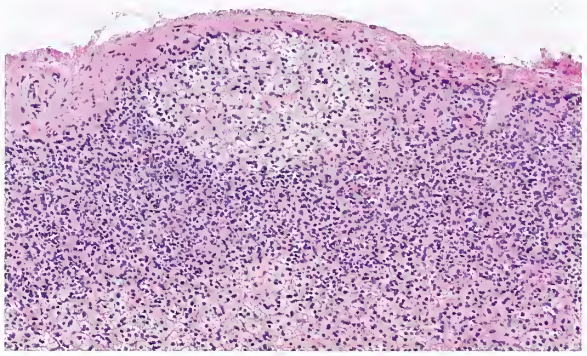

Figure 4-39

ALDOSTERONE-SECRETING ADRENAL CORTICAL ADENOMA

The hyperplastic zona glomerulosa merges with the outer zona fasciculata. The hyperplasia here is both diffuse and focally micronodular in the center beneath the adrenal capsule. This adrenal remnant was attached to an aldosterone-secreting adrenal cortical adenoma.

Hyperplasia of Zona Glomerulosa. Conn (24) first noted that the nontumorous zona glomerulosa was not atrophic in most cases, but often appeared wider than normal. The zona glomerulosa is thought to be hypoplastic in some cases (26), but confirmation is difficult with routine morphology since this zone is normally quite thin and discontinuous. The hyperplastic zona glomerulosa may form a broad zone focally or a continuous thickened zone at the periphery of the entire cortex (fig. 4-38, left), sometimes with extension of small tongues of glomerulosa type cells from the subcapsular region into the adjacent cortex (fig. 4-38, right). Occasionally, the hyperplastic zona glomerulosa has a small nodular component (fig. 4-39). This is very different from the cortical atrophy that regularly occurs with Cushing's syndrome. There may be micronodules or macronodules in the tumor-bearing or contralateral gland. Their presence might help explain some examples of multiple or bilateral tumors, but they may represent nonhyperfunctional cortical nodules possibly related to the underlying hypertension.

Ultrastructural Findings. Ultrastructural studies document the presence of cellular heterogeneity in aldosterone-producing ACAs (39). At the polar ends of the spectrum, there are cells with abundant or relatively sparse intracytoplasmic lipid (fig. 4-40) and cells that have essentially no lipid droplets, analogous to cells of the zona reticularis. The hybrid cell is as difficult to characterize at the ultrastructural level as by routine light microscopy. A smooth endoplasmic reticulum is prominent, often more so than the normal zona glomerulosa cell, and there may be short profiles of rough endoplasmic reticulum as well as free polyribosomes. Occasionally, concentric lamellar wraps of smooth endoplasmic reticulum associated with lipid material are seen. Mitochondria are round to oval, with short tubular or vesicular cristae (fig. 4-41), but abnormal shapes may be seen, depending in large part on the plane of section. Some mitochondria have lamellar or plate-like

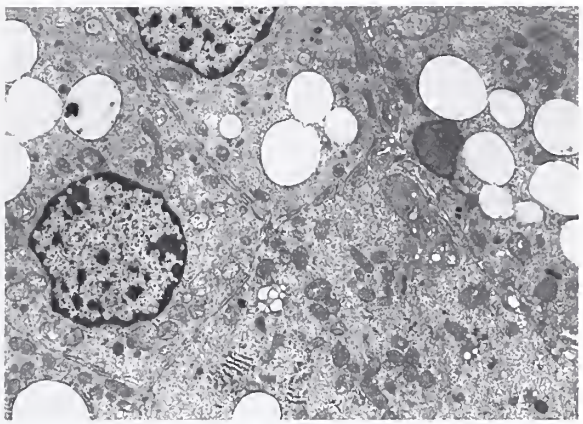

Figure 4-40

ALDOSTERONE-SECRETING ADRENAL CORTICAL ADENOMA

The tumor cells have much smooth endoplasmic reticulum and a few lipid droplets, which vary in size. Microvillous cytoplasmic extensions are evident along the cell borders. Mitochondria have tubulovesicular cristae. (Fig. 4-42 from Fascicle 19, Third Series.)

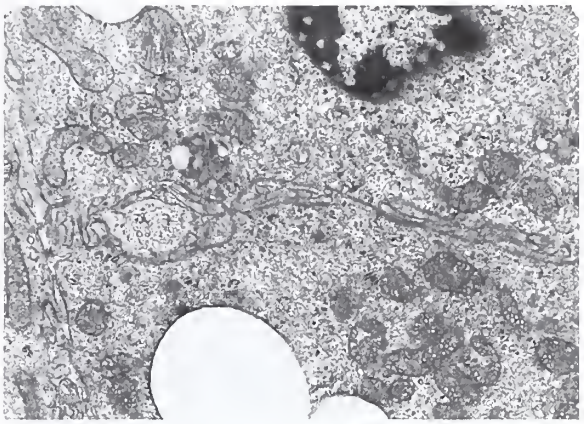

Figure 4-41

ALDOSTERONE-SECRETING ADRENAL CORTICAL ADENOMA

Most mitochondria have tubular cristae, some of which are slightly dilated. A few mitochondria with lamellar, plate-like cristae are also present.

cristae, a feature that is more characteristic of zona glomerulosa type cells.

Spironolactone Bodies. Spironolactone bodies are characteristically small intracytoplasmic inclusions that are lightly eosinophilic, with a laminated, scroll-like appearance (fig. 4-42). They develop in the cells of the zona glomerulosa (and sometimes cells deeper in the cortex) following treatment with the aldosterone antagonist spironolactone (42). These inclusions have been reported within the tumor cells of aldosterone-producing ACAs (43,44) and in the zona glomerulosa cells in the nontumorous cortex, and can often be readily identified in zona glomerulosa cells in adrenal glands from patients who have been treated for secondary hyperaldosteronism with spironolactone.

Spironolactone bodies are round to oval, measuring 2 to more than 12 μm in diameter, with 2 to 6 concentric laminations, and are often demarcated from the surrounding cytoplasm by a small clear halo. The spironolactone body is usually solitary within cells, and occurs mainly in cells with relatively compact eosinophilic cytoplasm (44). Due to their rich content of phospholipid, the inclusions may stain medium blue with the Luxol fast blue stain (fig. 4-43).

Ultrastructurally, the spherical laminated whorls consist of a central core with amorphous

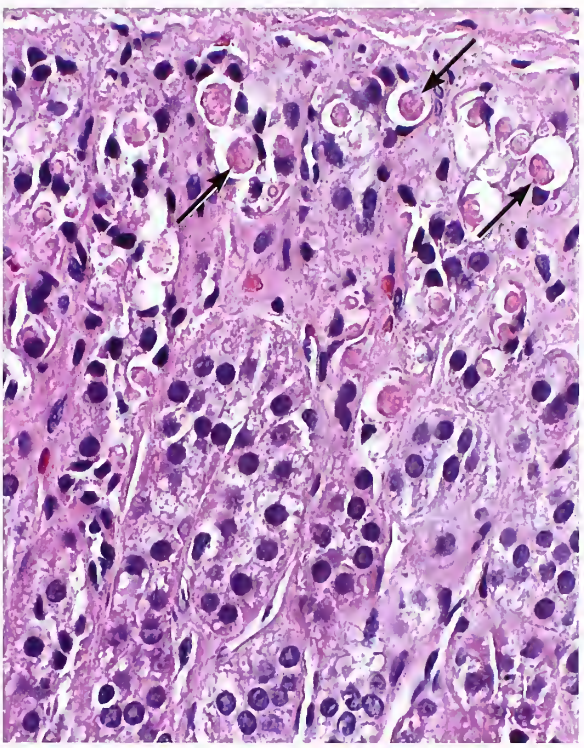

Figure 4-42

SPIRONOLACTONE BODIES

Spironolactone bodies appear as eosinophilic inclusions (arrows) within the cytoplasm of zona glomerulosa cells and are often surrounded by a clear halo. Occasional inclusions are seen in what appears to be cells of the outer zona fasciculata. (Fig. 4-44, right from Fascicle 19, Third Series.)

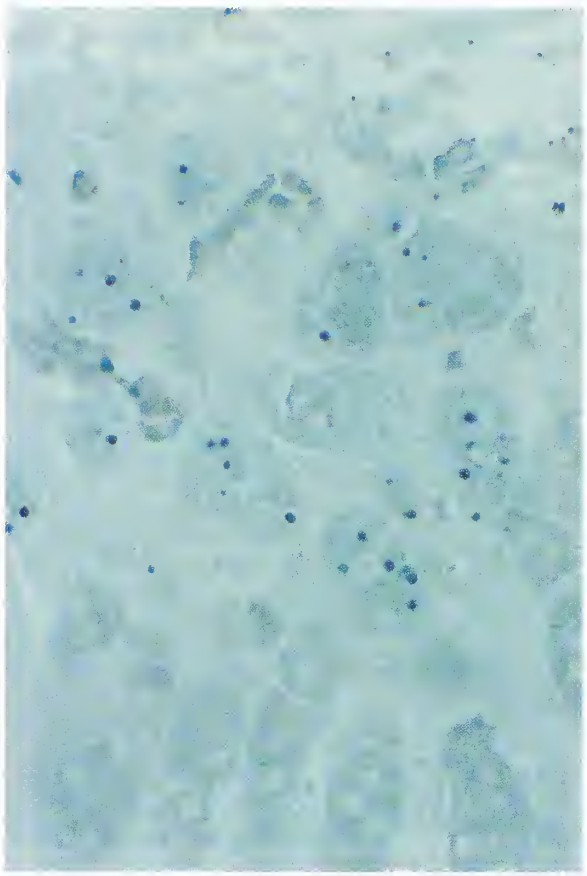

Figure 4-43

SPIRONOLACTONE BODIES

Spironolactone bodies appear as blue-black cytoplasmic inclusions in cells of the zona glomerulosa (luxol-fast blue stain).

electron-dense material surrounded by numerous, smooth-walled, concentric membranes continuous with the endoplasmic reticulum (45). Aldosterone has been demonstrated immunohistochemically in the concentric laminations (46). Carbonic anhydrase has been proposed as an immunochemical marker for zona glomerulosa cells of human adrenal glands and its localization suggests possible involvement in aldosterone biosynthesis or secretion (47).

Although there may be rare exceptions, intracytoplasmic inclusions are regarded as specific markers for spironolactone treatment (1). With time and continued administration of spironolactone, the inhibitory effect on aldosterone production by the ACA lessens or disappears, and spironolactone bodies may also diminish or disappear (43). The frequency of occurrence of spironolactone bodies in ACA correlates with the number or percentage of zona glomerulosa type cells in the ACA (48).

Localization and Treatment. Once the diagnosis of primary hyperaldosteronism is confirmed, the two major subtypes must be separated: unilateral aldosterone-producing ACA and bilateral idiopathic hyperplasia. When abdominal CT imaging shows normal-appearing adrenal glands or ambiguous findings, adrenal venous sampling may help to resolve the clinical dilemma (27,49,50). Adrenal venous sampling is the only dependable way to differentiate an aldosterone-producing ACA from bilateral idiopathic hyperplasia of the zona glomerulosa (51). The adrenal veins are catheterized via the percutaneous femoral vein approach and the position of the catheter tip is verified by gentle injection of a small amount of nonionic contrast medium and radiographic documentation (fig. 4-44A) (51). Rarely, adrenal venography is complicated by venous thrombosis and marked intraadrenal hemorrhage (fig. 4-44B,C) due to overzealous injection of contrast medium or wedging of the selective catheter; these complications are more likely in patients with Cushing's syndrome or Conn's syndrome because of excessive vascular fragility (52). On rare occasion, this vascular complication may result in prolonged remission from the manifestations of primary hyperaldosteronism (53).

The treatment options for patients with primary hyperaldosteronism largely depend on whether there is unilateral (e.g., ACA) or bilateral (e.g., hyperplasia) adrenal disease. The subtypes of primary hyperaldosteronism that may be treated surgically for cure are aldosterone-producing adenoma (or carcinoma) and primary unilateral adrenal hyperplasia. Unilateral laparoscopic adrenalectomy is a reasonable option in many cases. Cortical-sparing (subtotal) adrenalectomy has been used in a handful of cases but long-term results are still limited (54). Hypertension persists in most patients with bilateral adrenal hyperplasia who are treated surgically, therefore, the initial treatment is usually pharmacologic (27,33).

The mean cure rate after unilateral or bilateral adrenalectomy for about 100 cases of idiopathic hyperaldosteronism reported in the

Figure 4-44

VENOGRAM FOR SAMPLING OF ADRENAL VEIN CORTISOL AND ALDOSTERONE

A: Selective adrenal vein catheterization on the right side was done in a 47-year-old patient with uncontrolled hypertension. Venography was done for catheter placement. A sample for adrenal vein renin and cortisol was also obtained. The patient had an ipsilateral small aldosterone-secreting adrenal cortical adenoma.

B: Different case of aldosterone-secreting adrenal cortical adenoma in which venography was complicated by venous thrombosis and hemorrhagic infarction of the adrenal tumor.

C: The extensive hemorrhagic necrosis obliterated the architecture of the tumor.

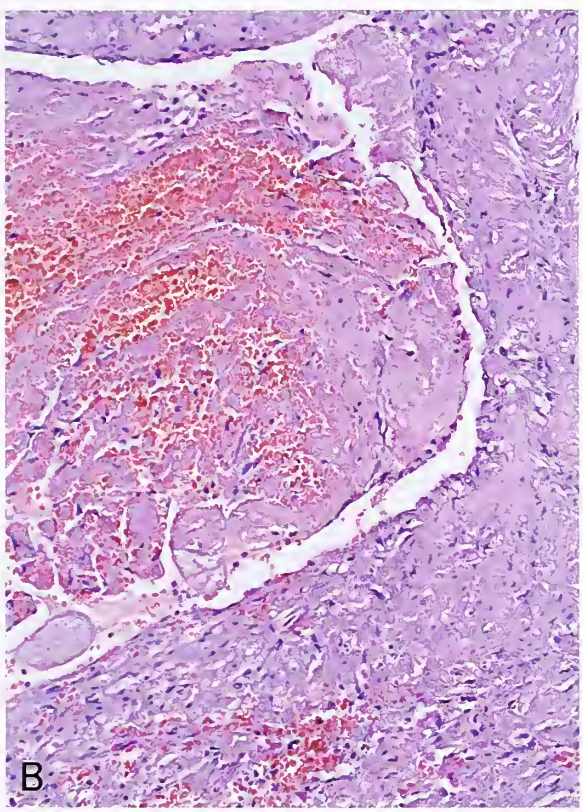

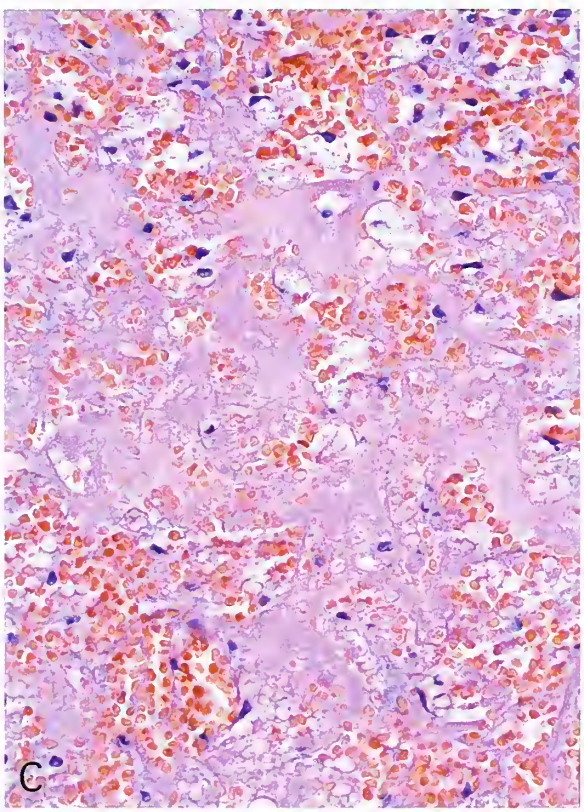

literature was only 19 percent (33), compared with 70 to 80 percent for patients with an aldosterone-producing ACA (26,33). An unusual subset of patients with primary aldosteronism, designated primary adrenal hyperplasia, also appears to be surgically correctable and resembles the rare ACTH-independent bilateral hyperplasia associated with autonomous cortisol production

and Cushing's syndrome (55). A case was recently reported using radiofrequency ablation of the aldosterone-producing ACA with subsequent normalization of blood pressure (56). Patients with bilateral idiopathic hyperplasia and glucocorticoid-remediable aldosteronism should be treated medically (27).

ADRENAL CORTICAL NEOPLASMS WITH VIRILIZATION OR FEMINIZATION

Adrenal cortical neoplasms causing virilization or feminization are uncommon, and are a cause for concern regarding the potential for malignancy. In a series of 190 adrenal tumors collected over three decades, there were only 10 virilizing cortical tumors (5.3 percent) of which 7 were malignant (57). Correlation with the pathologic features is essential to rule out malignancy. In a review of testosterone-producing adrenal cortical neoplasms in 47 adult females, the average tumor weight, when recorded, was 473 g (range, 13 to 1,500 g); at least 8 tumors (17 percent) were malignant, but follow-up in other cases was either limited or nonexistent (58). Most of the feminizing adrenal cortical neoplasms occurred in adults 25 to 45 years old, whereas virilizing tumors are more prevalent in the pediatric age group (59,60). In a review of 52 feminizing tumors, the average tumor weight, when recorded, was nearly 1,000 g (range, 175 to 2,650 g), and most tumors measured more than 12 cm in diameter (59). Feminizing adrenal cortical neoplasms are particularly ominous. In male patients, gynecomastia is the most frequent presenting sign, with or without breast tenderness, and may be accompanied by testicular atrophy, decreased libido or potency, and feminizing hair changes.

Grossly, the tumors may appear sharply circumscribed and even encapsulated, particularly smaller neoplasms, but some of the larger neoplasms may have ominous features such as hemorrhage and necrosis. There may be a predominance of cells with compact, eosinophilic cytoplasm faintly resembling cells of the zona reticularis (which elaborate sex steroids) (fig. 4-45). Correlation with biochemical and endocrinologic data is essential since there are no reliable morphologic features (either gross or microscopic) that permit an accurate and reproducible prediction of the accompanying endocrine syndrome, if one exists at all (1). Because these tumors do not secrete excess glucocorticoids (if endocrinologically "pure"), the attached adrenal remnant or contralateral adrenal cortex is not atrophic. Rare examples of virilizing adrenal neoplasms have been reported as Leydig cell adenomas of the adrenal gland, and although the cells specifically resemble lipid-depleted adrenal cortical cells, Reinke crystalloids have been identified (61).

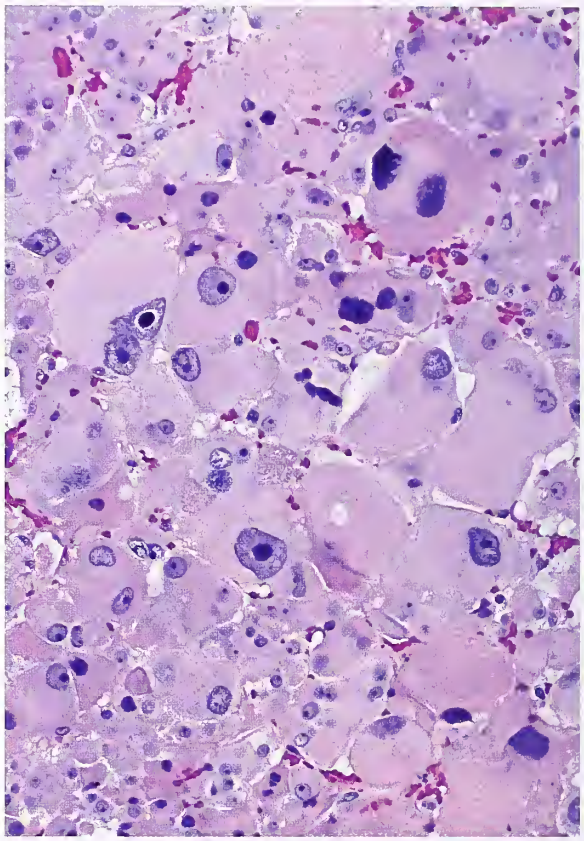

Figure 4-45

FEMINIZING ADRENAL CORTICAL ADENOMA

This feminizing adrenal cortical adenoma is composed of sheets of cells with abundant compact, eosinophilic cytoplasm. Moderate nuclear atypia is present. The tumor measured 3.5 cm in diameter and weighed 27 g.

ONCOCYTIC ADRENAL CORTICAL ADENOMA

Oncocytic adrenal cortical adenoma (or *adrenal cortical oncocytoma*) is composed of cells with abundant granular eosinophilic cytoplasm (62). The tumor may be dark tan or mahogany brown on gross examination (fig. 4-46), similar to

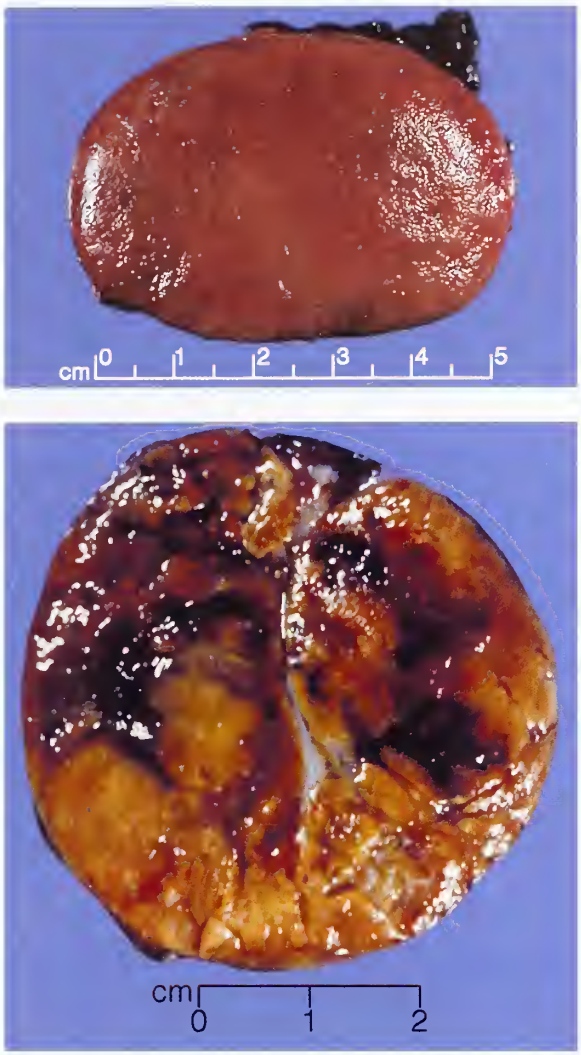

Figure 4-46

ONCOCYTIC ADRENAL CORTICAL ADENOMA

Top: This nonfunctional oncocytic adrenal cortical adenoma weighed 70 g and was 4 cm in diameter. On cross section the tumor is uniformly mahogany brown. (Fig. 4-48 from Fascicle 19, Third Series.)

Bottom: Cross section of another oncocytic cortical adenoma shows a tan yellow tumor with variegated areas of hemorrhage. The tumor was 4.2 cm in diameter.

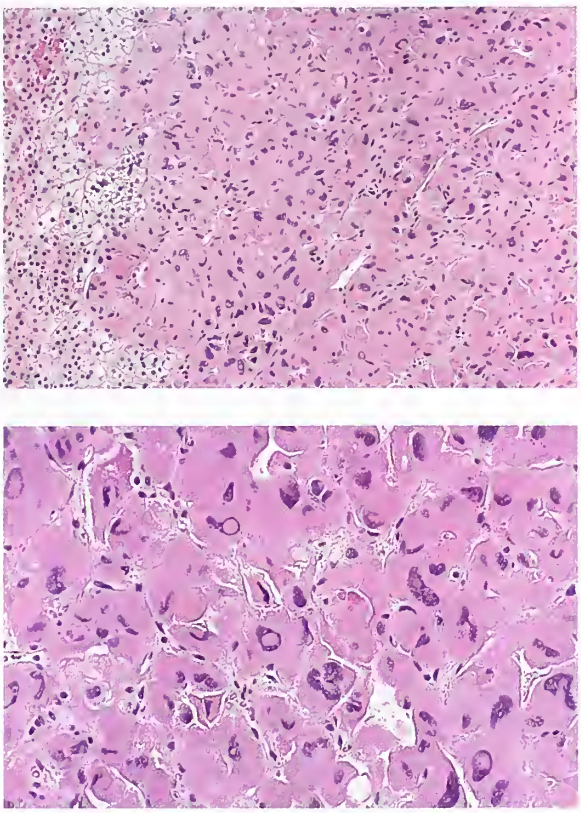

Figure 4-47

ONCOCYTIC ADRENAL CORTICAL ADENOMA

Top: The oncocytic adrenal cortical adenoma weighed 12 g and measured 3 cm in diameter. It was discovered incidentally on abdominal CT scan in a 67-year-old man who underwent surgical resection of a colonic adenocarcinoma. The tumor compresses the adjacent adrenal cortex.

Bottom: The tumor cells have an oncocytic appearance, with abundant eosinophilic, granular cytoplasm. There is a marked degree of nuclear pleomorphism and numerous nuclear pseudoinclusions. (Figs. 4-47 and 4-49 are from the same case.) (T&B: Fig. 4-49 from Fascicle 19, Third Series.)

oncocytomas in other anatomic sites. It is uncertain whether a tumor should be predominantly or entirely oncocytic to merit the designation oncocytoma. Occasionally, an adrenal cortical neoplasm designated as either adenoma (see fig. 4-9) or carcinoma has focal areas of oncocytic change. The architectural patterns are similar to other ACAs (fig. 4-47, top) and some tumors have prominent nuclear pleomorphism (fig. 4-47, bottom). An unusual pattern is a loose dyscohesive arrangement of cells (fig. 4-48). The lipid content within these cells tends to be sparse or almost nonexistent. The oncocytic appearance of the tumors is due to abundant mitochondria (fig. 4-49). A recent study noted peculiar cytoplasmic inclusions (63).

The term oncocytoma has been applied to a number of different neoplasms, but it is a relatively new concept for adrenal cortical tumors. Oncocytic adrenal cortical neoplasms have been reported both as adenoma and carcinoma

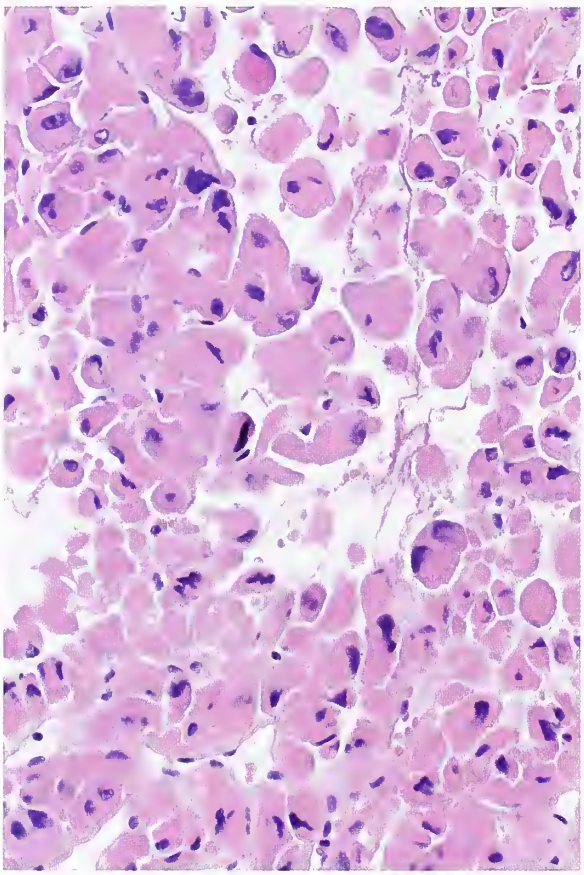

Figure 4-48

ONCOCYTIC ADRENAL CORTICAL ADENOMA

The oncocytic adrenal cortical adenoma was discovered incidentally on a CT scan of the abdomen. The tumor cells have abundant granular, eosinophilic cytoplasm and in many areas are loosely dispersed and appear almost acantholytic.

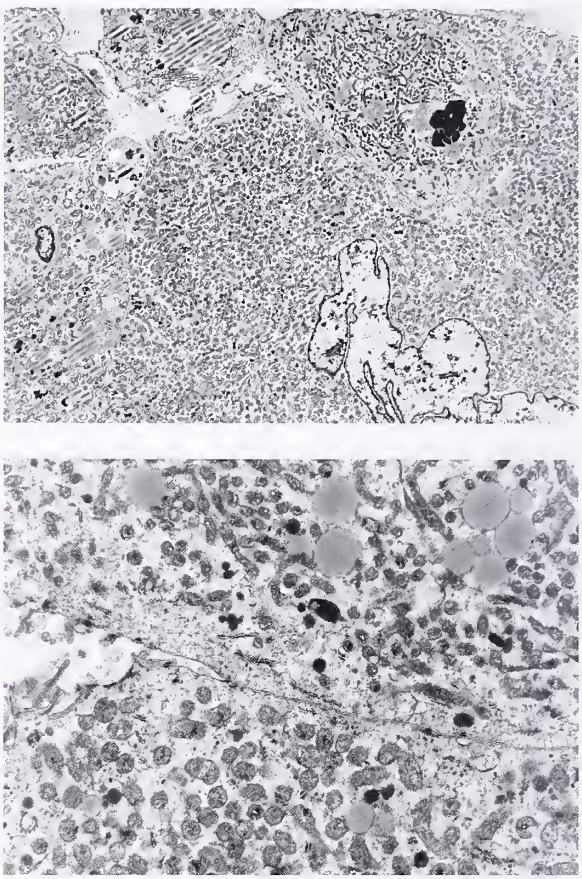

Figure 4-49

ONCOCYTIC ADRENAL CORTICAL ADENOMA

Top: Cells of this oncocytic adrenal cortical adenoma contain numerous round to elongated mitochondria. There are few small lipid droplets. The nuclear folds and clefts may form nuclear pseudoinclusions detectable on routine light microscopy.

Bottom: There are numerous mitochondria with predominantly tubular cristae. Relatively few lipid droplets are present, along with a few primary lysosomes. Microvillous projections are seen along the cell borders on the left side. (Courtesy of Dr. JMB Bloodworth, Madison, WI.)

(64,65). The small number of cases reported to date prevents any conclusive remarks regarding biologic behavior or even functional capacity. A recent report of 10 cases and review of the literature outlined criteria for diagnostic categorization of oncocytic adrenal cortical tumors (65). In a study of three cases, the tumors were considered to be truly nonfunctional since none expressed activity of enzymes involved in steroidogenesis (66).

REFERENCES

Adrenal Cortical Neoplasms and Adrenal Cortical Adenoma with Cushing's Syndrome

1. Lack EE, Travis WD, Oertel JE. Adrenal cortical neoplasms. In: Lack EE, ed. Pathology of the adrenal glands. New York: Churchill Livingston; 1990:115-171.
2. Sugawara A, Takeuchi K, Suzuki T, Itoi K, Sasano H, Ito S. A case of aldosterone-producing adrenocortical adenoma associated with a probable post-operative adrenal crisis: histopathological analyses of the adrenal gland. Hypertens Res 2003;26:663-668.
3. Tung SC, Wang PW, Huang TL, Lee WC, Chen WJ. Bilateral adrenocortical adenomas causing ACTH-independent Cushing's syndrome at different periods: a case report and discussion of corticosteroid replacement therapy following bilateral adrenalectomy. J Endocrinol Invest 2004;27:375-379.
4. Kato S, Masunaga R, Kawabe T, et al. Cushing's syndrome induced by hypersecretion of cortisol from only one of bilateral adrenocortical tumors. Metabolism 1992;41:260-263.
5. Harrison JH, Mahoney EM, Bennett AH. Proceedings: Tumors of the adrenal cortex. Cancer 1973;32:1227-1235.
6. Neville AM, O'Hare MJ. Histopathology of the human adrenal cortex. Clin Endocrinol Metab 1985;14:791-820.
7. Bertagna C, Orth DN. Clinical and laboratory findings and results of therapy in 58 patients with adrenocortical tumors admitted to a single medical center (1951 to 1978). Am J Med 1981; 71:855-875.
8. Brown FM, Gaffey TA, Wold LE, Lloyd RV. Myxoid neoplasms of the adrenal cortex: a rare histologic variant. Am J Surg Pathol 2000;24:396-401.
9. Unger PD, Cohen JM, Thung SN, Gordon R, Pertsemlidis D, Dikman SH. Lipid degeneration in a pheochromocytoma histologically mimicking an adrenal cortical tumor. Arch Pathol Lab Med 1990;114:892-894.
10. Wieneke JA, Thompson LD, Heffess CS. Corticomedullary mixed tumor of the adrenal gland. Ann Diagn Pathol 2001;5:304-308.
11. Takasu N, Komiya I, Nagasawa Y, Asawa T, Yamada T. Exacerbation of autoimmune thyroid dysfunction after unilateral adrenalectomy in patients with Cushing's syndrome due to an adrenocortical adenoma. N Engl J Med 1990;322:1708-1712.
12. Mackay A. Atlas of human adrenal cortex ultrastructure. In: Symington T, ed. Functional pathology of the human adrenal gland. Baltimore: Williams & Wilkins; 1969:346-484.
13. Kepes JJ, O'Boynick P, Jones S, Baum D, McMillan J, Adams ME. Adrenal cortical adenoma in the spinal canal of an 8-year-old girl. Am J Surg Pathol 1990;14:481-484.
14. Corsi A, Riminucci M, Petrozza V, et al. Incidentally detected giant oncocytoma arising in retroperitoneal heterotopic adrenal tissue. Arch Pathol Lab Med 2002;126:1118-1122.
15. Cassarino DS, Santi M, Arruda A, et al. Spinal adrenal cortical adenoma with oncocytic features: report of the first intramedullary case and review of the literature. Int J Surg Pathol 2004;12:259-264.
16. Munro LM, Kennedy A, McNicol AM. The expression of inhibin/activin subunits in the human adrenal cortex and its tumours. J Endocrinol 1999;161:341-347.
17. Zhang PJ, Genega EM, Tomaszewski JE, Pasha TL, LiVolsi VA. The role of calretinin, inhibin, melan-A, BC1-2, and C-kit in differentiating adrenal cortical and medullary tumors: an immunohistochemical study. Mod Pathol 2003;16:591-597.
18. Loy TS, Phillips RW, Linder CL. A103 immunostaining in the diagnosis of adrenal cortical tumors: an immunohistochemical study of 316 cases. Arch Pathol Lab Med 2002;126:170-172.
19. Sidhu S, Marsh DJ, Theodosopoulos G, et al. Comparative genomic hybridization analysis of adrenocortical tumors. J Clin Endocrinol Metab 2002;87:3467-3474.

Functional Pigmented ("Black") Adenomas

20. Tokunaga H, Miyamura N, Sasaki K, et al. Preclinical Cushing's syndrome resulting from black adrenal adenoma. A case report. Horm Res 2004;62:60-66.
21. Komiya I, Takasa N, Aizawa T, Yamada, T, et al.. Black (or brown) adrenal cortical adenoma: its characteristic features on computed tomography and endocrine data. J Clin Endocrinol Metab 1985;61:711-717.
22. Armand R, Cappola AR, Horenstein RB, Drachenberg CB, Sasano H, Papadimitriou JC. Adrenal cortical adenoma with excess black pigment deposition, combined with myelolipoma and clinical Cushing's syndrome. Int J Surg Pathol 2004;12:57-61.
23. Damron TA, Schelper RL, Sorensen L. Cytochemical demonstration of neuromelanin in black pigmented adrenal nodules. Am J Clin Pathol 1987;87:334-341.

Adrenal Cortical Adenomas with Primary Hyperaldosteronism (Conn's Syndrome)

24. Conn JW. Primary aldosteronism. J Lab and Clin Med 1955;45:661-664.
25. Schteingart DE. The 50th anniversary of the identification of primary aldosteronism: a retrospective of the work of Jerome W. Conn. J Lab Clin Med 2005;145:12-16
26. Gill JR Jr. Hyperaldosteronism. In: Becker KL, ed. Principles and practice of endocrinology and metabolism. Philadelphia: JB Lippincott Co; 1990:631-643.
27. Young WF Jr. Primary aldosteronism: management issues. Ann N Y Acad Sci 2002;970:61-76.
28. Conn JW. Plasma renin activity in primary aldosteronism. Importance in differential diagnosis and in research of essential hypertension. JAMA 1964;190:222-225.
29. Shamma AH, Goddard JW, Sommers SC. A study of the adrenal status in hypertension. J Chronic Dis 1958;8:587-595.
30. Dobbie JW. Adrenocortical nodular hyperplasia: the ageing adrenal. J Pathol 1969;99:1-18.
31. Anderson GS, Lund JO, Toftdahl D, Strandgaard S, Nielsen PE. Pheochromocytoma and Conn's syndrome in Denmark 1977-1981. Acta Medica Scand [Suppl] 1986-1987;714:11-14.
32. Melby JC. Diagnosis of hyperaldosteronism. Endocrinol Metab Clin North Am 1991;20:247-255.
33. Young WF Jr, Hogan MJ, Klee GG, Grant CS, van Heerden JA. Primary aldosteronism: diagnosis and treatment. Mayo Clin Proc 1990;65: 96-110.
34. Neville AM, Symington T. Pathology of primary aldosteronism. Cancer 1966;19:1854-1868.
35. Conn JW, Knopf RF, Nesbit RM. Clinical characteristics of primary aldosteronism from an analysis of 145 cases. Am J Surg 1964;107:159-172.
36. Dunnick NR, Leight GS Jr, Roubidoux MA, Leder RA, Paulson E, Kurylo L. CT in the diagnosis of primary aldosteronism: sensitivity in 29 patients. AJR Am J Roentgenol 1993;160:321-324.
37. Nagae A, Murakami E, Hiwada K, Kubota O, Takada Y, Ohmori T. Primary aldosteronism with cortisol overproduction from bilateral adrenal adenomas. Jpn J Med 1991;30:26-31.
38. Ganguly A. Cellular origin of aldosteronomas. Clin Investig 1992;70:392-395.
39. Eto T, Kumamoto K, Kawasaki T, Omae T, Masaki Z, Yamamoto T. Ultrastructural types of cells in adrenal cortical adenoma with primary aldosteronism. J Path 1979;128:1-6.
40. Enberg U, Volpe C, Hoog A, et al. Postoperative differentiation between unilateral adrenal adenoma and bilateral adrenal hyperplasia in primary aldosteronism by mRNA expression of the gene CYP11B2. Eur J Endocrinol 2004;151:73-85.
41. Aiba M, Iri H, Suzuki H, et al. Numerous mast cells in 11-deoxycorticosterone producing adrenocortical tumor. Histologic evaluation of benignancy and comparison with mast cell distribution in adrenal glands and neoplastic counterparts of 67 surgical specimens. Arch Pathol Lab Med 1985;109:357-360.
42. Janigan DT. Cytoplasmic bodies in the adrenal cortex of patients treated with spironolactone. Lancet 1963;1:850-852.
43. Conn JW, Hinerman DL. Spironolactone-induced inhibition of aldosterone biosynthesis in primary aldosteronism: morphological and functional studies. Metabolism 1977;26:1293-1307.
44. Aiba M, Suzuki H, Kageyama K, et al. Spironolactone bodies in aldosteronomas and in the attached adrenals. Enzyme histochemical study of 19 cases of primary aldosteronism and a case of aldosteronism due to bilateral diffuse hyperplasia of the zona glomerulosa. Am J Pathol 1981;103:404-410.
45. Kovacs K, Horvath E, Singer W. Fine structure and morphogenesis of spironolactone bodies in the zona glomerulosa of the human adrenal cortex. J Clin Path 1973;26:949-957.
46. Hsu SM, Raine L, Martin HF. Spironolactone bodies. An immunoperoxidase study with biochemical correlation. Am J Clin Pathol 1981;75:92-95.
47. Sasano H, Kato K, Nagura H, et al. Carbonic anhydrases in the human adrenal gland and its disorders: immunohistochemical and biochemical study of the enzymes. Endocr Pathol 1994:5:100-106.
48. Cohn, D, Jackson, RV, Gordon, RD. Factors affecting the frequency of occcurence of spironolactone bodies in aldosteronomas and non-tumorous cortex. Pathology 1983;15:273-277.
49. Gordon RD, Stowasser M, Rutherford JC. Primary aldosteronism: are we diagnosing and operating on too few patients? World J Surg 2001;25:941-947.
50. Young WF, Stanson AW, Thompson GB, Grant CS, Farley DR, van Heerden JA. Role for adrenal venous sampling in primary aldosteronism. Surgery 2004;136:1227-1235.
51. Stowasser M, Gordon RD. Primary aldosteronism—careful investigation is essential and rewarding. Mol Cell Endocrinol 2004;217:33-39.
52. Dedrick CG. Adrenal arteriography and venography. Urol Clin North Am 1989;16:515-526.
53. Melby JC. Identifying the adrenal lesion in primary aldosteronism. Ann Intern Med 1972; 76:1039-1041.

54. Walz MK. Extent of adrenalectomy for adrenal neoplasm: cortical sparing (subtotal) versus total adrenalectomy. Surg Clin North Am 2004;84: 743-753.
55. Irony I, Kater CE, Biglieri EG, Shackleton CH. Correctible subsets of primary aldosteronism. Primary adrenal hyperplasia and renin responsive adenoma. Am J Hypertens 1990;3:576-582.
56. Al-Shaikh AA, Al-Rawas MM, Al-Asnag MA. Primary hyperaldosteronism treated by radiofrequency ablation. Saudi Med J 2004;25:1711-1714.

Adrenal Cortical Neoplasms with Virilization and Feminization

57. Del Gaudio AD, Del Gaudio GA. Virilizing adrenocortical tumors in adult women. Report of 10 patients, 2 of whom each had a tumor secreting only testosterone. Cancer 1993;72: 1997-2003.
58. Mattox JH, Phelan S. The evaluation of adult females with testosterone producing neoplasms of the adrenal cortex. Surg Gynecol Obstet 1987;164:98-101.
59. Gabrilove JL, Sharma DC, Wotiz HH, Dorfman RI. Feminizing adrenocortical tumors in the male. A review of 52 cases including a case report. Medicine (Baltimore) 1965;44:37-79.
60. Zerbini C, Kozakewich HP, Weinberg DS, Mundt DJ, Edwards JA, Lack EE. Adrenocortical neoplasms in childhood and adolescence: analysis of prognostic factors including DNA content. Endocr Pathol 1992;3:116-128.
61. Pollock WJ, McConnell CF, Hilton C, Lavine RL. Virilizing Leydig cell adenoma of adrenal gland. Am J Surg Pathol 1986;10:816-822.

Oncocytic Adrenal Cortical Adenoma

62. Kitching PA, Patel V, Harach HR. Adrenocortical oncocytoma. J Clin Pathol 1999;52:151-153.
63. Seo IS, Henley JD, Min KW. Pecular cytoplasmic inclusions in oncocytic adrenal cortical tumors: an electron microscopic observation. Ultrastruct Pathol 2002;26:229-235.
64. el-Naggar AK, Evans DB, Mackay B. Oncocytic adrenal cortical carcinoma. Ultrastr Pathol 1991;15:549-556.
65. Bisceglia M, Ludovico O, Di Mattia A, et al. Adrenocortical oncocytic tumors: report of 10 cases and review of the literature. Int J Surg Pathol 2004;12:231-243.
66. Sasano H, Suzuki T, Sano T, Kameya T, Sasano N, Nagura H. Adrenocortical oncocytoma. A true nonfunctioning adrenocortical tumor. Am J Surg Pathol 1991;15:949-956.

5 ADRENAL CORTICAL CARCINOMA

Adrenal cortical carcinoma (ACC) is a malignant neoplasm arising from adrenal cortical cells, which may or may not have functional activity as evidenced by a clinically recognizable endocrine syndrome, biochemical abnormalities indicative of hypercorticalism, or both.

INCIDENCE AND CLINICAL FEATURES

The estimated frequency of ACC in the United States is about 1 to 2 cases/million population (1,2). This chapter deals almost solely with tumors in adult patients, although large clinical series often include a few patients in the pediatric age group. Adults in the 4th and 5th decades of life are most frequently affected, although ACC can occur at any age. A bimodal peak in age incidence has been reported in the 1st and 5th decades (3). There does not appear to be a significant racial predilection, although an epidemiologic study showed a trend of an increased rate among blacks (2). Most large clinical series indicate a slight predilection for female patients (4,5–8); in several studies, however, there was a predilection for male patients (9) including one which reviewed all "nonhormonal" tumors (10). In a review of ACCs reported in the English language literature from 1952 to 1992, 58.6 percent of patients were female and 41.4 percent were male (3). In some series, female patients with ACC were diagnosed at an earlier age than males (11).

The left adrenal gland is involved slightly more often than the right (52.8 percent versus 47.2 percent) (3,4). Bilateral ACC is extremely rare (4), although there may be metastases to the opposite adrenal gland up to 13 percent of cases (12). In several large studies, metastases were noted on initial presentation; in a study by King and Lack (9), pulmonary (fig. 5-1), skeletal, or mediastinal metastases were noted on initial chest X ray in 24 percent of patients. An extraordinarily high incidence of metastases (67 percent) at the time of diagnosis has been reported (13).

The frequency of ACCs that function endocrinologically varies depending upon whether "function" is defined as a clinically recognizable "pure" syndrome, such as Cushing's syndrome; a "mixed" endocrine syndrome (fig. 5-2); or any biochemical evidence of excess steroid production. In a large review of ACCs (1,881 patients), the tumors were reported to be "nonfunctional" in 40.7 percent (3). In a review of nonhormonal adrenal cortical neoplasms, the tumors were considered capable of forming precursor steroids without hormonal activity and, therefore, the tumors were not actually nonfunctional (10).

Data suggest that ACCs are less efficient in steroidogenesis due to the decreased activity of 3-beta-hydroxysteroid dehydrogenase, 17-hydroxylase, and 17,20-desmolase (14). An immunohistochemical study has shown that

Figure 5-1

ADRENAL CORTICAL CARCINOMA

A large adrenal cortical carcinoma (ACC) was found on the right side of an adult female who presented with abdominal and flank pain. Multiple hepatic and pulmonary metastases were present at the time of diagnosis. Chest X ray shows multiple nodular densities representing metastatic ACC. The patient died within 9 months of diagnosis with widespread metastases. (Fig. 5-1 from Fascicle 19, Third Series.)

Figure 5-2

ADRENAL CORTICAL CARCINOMA

A 37-year-old woman presented with mixed endocrinopathy of Cushing's syndrome and virilization. The patient died within a year of diagnosis of widespread ACC. At autopsy there was massive invasion of the inferior vena cava. The contralateral adrenal gland had marked cortical atrophy due to suppression of adrenocorticotropic hormone (ACTH). (Fig. 5-2 from Fascicle 19, Third Series.)

some tumor cells in ACC do not express all the enzymes involved in steroidogenesis, whereas other cells do, suggesting that there may be malregulation in individual cells (15). These findings may help to explain the large size of ACC when signs or symptoms of hypercorticalism first appear. Culture of tumor cells in vitro has demonstrated multiple pathways of steroidogenesis including formation of corticosteroids, mineralocorticoids, androgens, and estrogens, with all of the major enzyme systems required in their synthesis (16). A blunted or absent response to adrenocorticotropic hormone (ACTH) has also been reported in malignant cells maintained in vitro (17). Feminization is an uncommon endocrine syndrome, and it is usually only recognized in the male patient as gynecomastia and sometimes decreased potency.

Aldosterone-producing ACC is a rare cause of hypertension. A recent literature review identified 58 cases reported over the last 50 years: 10 percent of patients had metastases at initial diagnosis and an additional 48 percent had metastases at follow-up (18). A rare cause of mineralocorticoid-induced hypertension by an ACC is production of 11-deoxycorticosterone; a recent review described 10 cases reported in the literature (19).

The most common presenting complaints are abdominal or flank pain, discomfort, or fullness, and in a study involving 110 patients, 30 percent had a palpable abdominal mass (fig. 5-3) (20). Weight loss can also be a prominent feature. Intermittent, low-grade fever has been reported (4) and may be related to extensive tumor necrosis. Hypoglycemia and hypercalcemia have been reported in association with ACC, with the latter attributed to elaboration of a hypercalcemic hormone of malignancy (21). Other unusual presentations include overwhelming disseminated intravascular coagulation (22) and hemorrhagic shock due to spontaneous rupture of the ACC (23).

Figure 5-3

ADRENAL CORTICAL CARCINOMA
SIMULATING RENAL CELL CARCINOMA

A 57-year-old woman presented with abdominal pain, and had a large right upper quadrant mass on physical examination. The tumor could not be separated from the kidney on imaging studies and the patient underwent radical nephrectomy since the tumor simulated a renal cell carcinoma. There were no signs or symptoms of an endocrine syndrome due to hypercorticalism. Abnormal tortuous vessels are seen in an early phase of selective arteriogram along with stretching of the renal artery and its branches. (Fig. 3-24 from Lack EE, Travis WD, Oertel JE. Adrenal cortical neoplasms, In: Lack EE, ed. Pathology of the adrenal glands. New York: Churchill Livingstone; 1990:115-171.) (Figs. 5-3 and 5-7 are from the same case.)

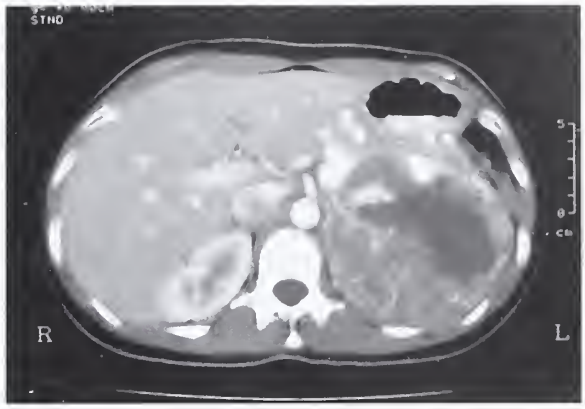

Figure 5-4

COMPUTERIZED TOMOGRAPHY
SCAN OF THE ABDOMEN

The 10-cm ACC present in the left upper quadrant has a hypodense center due to necrosis. The periphery of the mass has irregular enhancement following intravenous contrast injection.

IMAGING CHARACTERISTICS

On computerized tomography (CT) scan ACCs are usually large, with low intensity areas corresponding to necrosis; they have irregular contrast enhancement (fig. 5-4). Magnetic resonance imaging (MRI) usually appears heterogeneous on T1-weighted images while on T2-weighted images ACC usually has a signal intensity greater than fat. Enhancement may be very heterogeneous and there may be evidence of extension to retroperitoneal lymph nodes, renal vein, and/or inferior vena cava. Calcification may be present in the tumor (fig. 5-5) and is usually associated with necrosis.

GROSS FINDINGS

ACC is often a bulky neoplasm with the average weight in several series ranging from 510 g (24) to 1,210 g (25). Tumor weight has been reported to be an important prognostic factor (see also chapter 6): in the study by Tang and Gray (26), all tumors weighing 95 g or more were malignant, while tumors less than 50 g were benign. Clearly, there are exceptions since some tumors weighing less than 50 g can metastasize (27,28), and some in excess of 1,000 g may fail to do so on prolonged follow-up. Some of the heavier ACCs can be 4,500 g or more (8,10). The average size of tumors recorded in several series ranged from 12 (8) to 16 cm, but there is a wide range of 3 to 40 cm (1).

On external examination and in cross section, ACCs often have a coarsely lobulated appearance, with soft, bulging nodules ranging from yellow-orange to tan (fig. 5-6). Often, there are more variegated areas of necrosis and

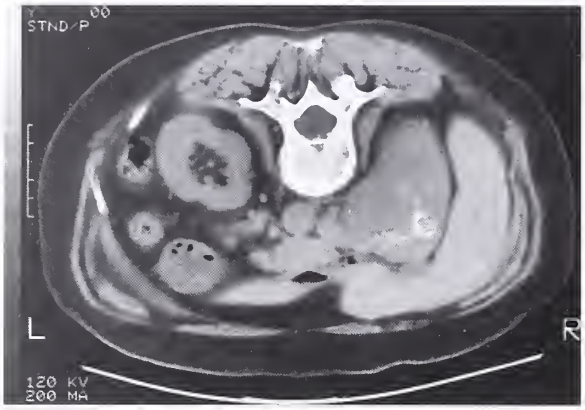

Figure 5-5

COMPUTERIZED TOMOGRAPHY SCAN OF THE ABDOMEN

A 52-year-old woman presented with abdominal pain and a palpable mass. CT scan showed a large suprarenal mass in the right upper quadrant. The mass has nonuniform density and areas of dystrophic calcification. The patient is in the prone position in preparation for fine needle aspiration biopsy. Pulmonary metastases were also present. A preliminary evaluation had suggested the possibility of primary hyperaldosteronism.

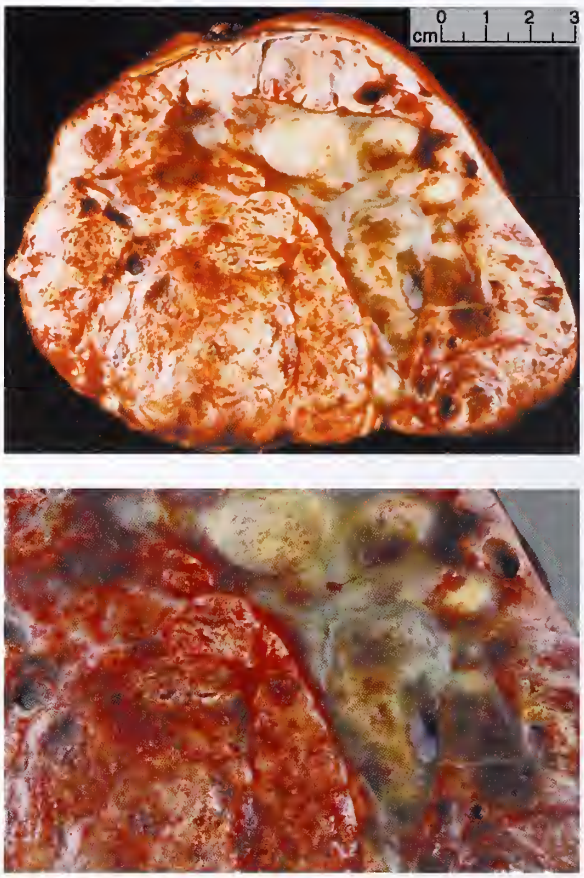

Figure 5-6

ADRENAL CORTICAL CARCINOMA

Top: A cross section of a 695-g ACC from a 41-year-old woman. The tumor has a variegated appearance, with bulging tan-yellow nodules as well as areas of necrosis.

Bottom: Higher magnification shows tan-yellow viable tumor and areas of necrosis.

hemorrhage (fig. 5-7). The nodularity may be related to intersecting broad fibrous bands. Necrotic areas appear pale tan or yellow-white, with a putty-like consistency (fig. 5-8). Areas of cystic degeneration may be seen. Rarely, adrenal neoplasms are macroscopically cystic and appear benign: six were identified at the Mayo Clinical over a 25-year period (two ACCs, two adrenal cortical adenomas, and two pheochromocytomas) (29). The overall appearance may be quite variegated, however, giving the unmistakable impression of malignancy on the basis of size, weight, and gross morphology. Some of the smaller ACCs are not as heterogeneous on sectioning, and therefore less suspicious of malignancy. ACC can invade adjacent organs or tissues and en bloc surgical removal of involved structures may be necessary for total gross resection (fig. 5-9).

MICROSCOPIC FINDINGS

Architectural Patterns

A variety of architectural patterns can be found in ACCs, sometimes admixed in the same neoplasm. One of the more characteristic is a broad trabecular growth pattern with anastomosing columns and cords of cells, often 10 to 20 or more cells wide, separated by delicate, gaping sinusoids lined by an attenuated endothelial layer (fig. 5-10). Occasionally, the trabeculae are oriented in a more parallel, elongated array, or have an irregular contour with a daisy-like or clover-leaf configuration, sometimes with areas of necrosis. Where anastomosing trabeculae are cut in various planes of section they may appear "free-floating" and unattached. This may give the impression of vascular or sinusoidal invasion (fig. 5-11). A perithelial arrangement of viable tumor cells may be present in association with tissue necrosis (fig. 5-12). The trabecular pattern can also be seen as an

Figure 5-7

ADRENAL CORTICAL CARCINOMA

A large adrenal cortical carcinoma from a 57-year-old woman simulated a renal cell carcinoma. The patient had no recognizable endocrine syndrome. Over half of the neoplasm was necrotic. (Fig. 5-4 from Fascicle 19, Third Series.)

Figure 5-8

ADRENAL CORTICAL CARCINOMA

An ACC from a 32-year-old female weighed 2,200 g and measured 21 cm in diameter. There were extensive areas of necrosis with foci of vascular invasion. The patient also had pulmonary metastases at the time of diagnosis. (Fig. 5-5 from Fascicle 19, Third Series.)

alignment of cells in slender elongated cords (fig. 5-13), sometimes with myxoid stromal change or fibrosis. In rare cases, there is a serpiginous arrangement of cells as might be seen in a carcinoid or pancreatic endocrine neoplasm (fig. 5-14). A trabecular pattern as seen in figure 5-10 is ominous even in the absence of other histologic features such as nuclear pleomorphism, and with tumors that are large (i.e., several hundred grams), the diagnosis is seldom benign.

Another architectural pattern is a nesting or alveolar arrangement of cells, which may be only focally distributed within a particular neoplasm (fig. 5-15); in areas, this pattern may blend with the trabecular arrangement noted above, which itself can be somewhat heterogeneous. There may be a diffuse or solid pattern, which may be focal, or less commonly, diffuse in distribution. With this pattern, the endocrine nature of the tumor, and specifically, an adrenal histogenesis, may not be obvious, particularly when coupled with significant cytologic pleomorphism (fig. 5-16). A spindle cell or frankly sarcomatous pattern in ACC is rare.

Occasional myxoid foci may cause diagnostic problems either in the primary tumor or even in distant metastases. Superficially, a myxoid pattern may resemble a chordoma or other myxoid neoplasms (fig. 5-17). This feature is usually focally distributed within a particular tumor. Myxoid changes in adrenal cortical neoplasms may be present in both adenomas and carcinomas but is more common in ACC (30). A myxoid ACC was recently reported with extensive lipomatous metaplasia (31).

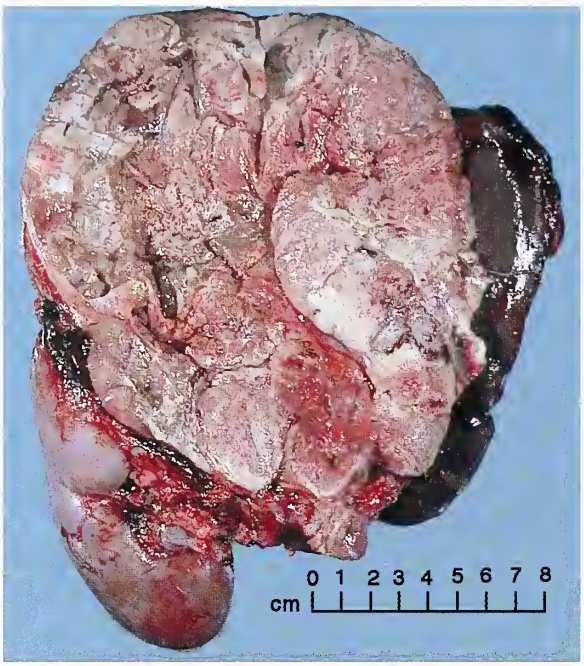

Figure 5-9

ADRENAL CORTICAL CARCINOMA

This large ACC was resected from a 27-year-old woman with virilization. The tumor measured 17 cm in diameter and invaded both kidney and spleen, which necessitated en bloc removal of these organs along with the tumor. (Fig. 5-6 from Fascicle 19, Third Series.)

A distinctive histologic pattern has been described in an ACC associated with hyperaldosteronism. The alveolar arrangement of cells was separated by prominent, thick-walled, dilated vascular spaces with zona glomerulosa type cells (32). This appearance, however, is nonspecific. A pseudopapillary arrangement of cells is another uncommon architectural pattern (fig. 5-18).

Cellular Morphology

Most ACCs contain a predominance of cells with lipid-depleted or acidophilic, compact cytoplasm; however, this feature alone does not have a statistically significant bearing on prognosis. Occasionally, coarse granular pigment representing lipofuscin is seen within the cytoplasm (fig. 5-19). Some tumors contain an abundance of lipid-rich, pale-staining cells. The presence (focal or diffuse) of cells with compact, eosinophilic cytoplasm does not correlate with any particular endocrine syndrome. On rare occasion, a tumor classified as ACC has such abundant eosinophilic cytoplasm that a designation of "oncocytic" may be appropriate (fig. 5-20), but as noted in chapter 4, this variant of adrenal cortical neoplasm needs further characterization since both clinically benign and malignant forms have been reported (33).

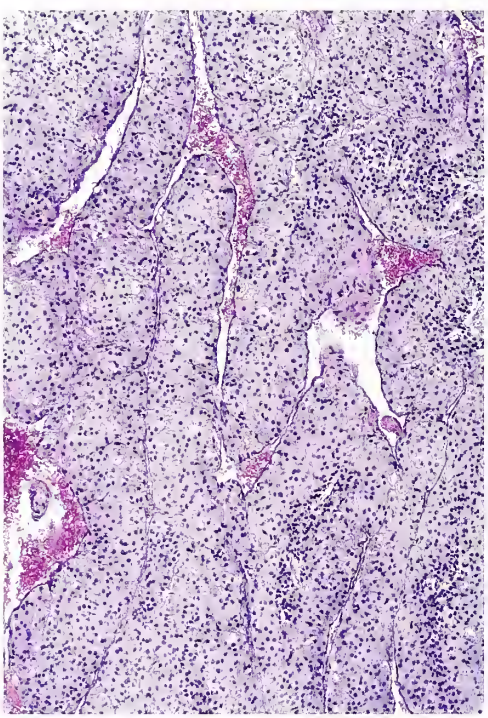

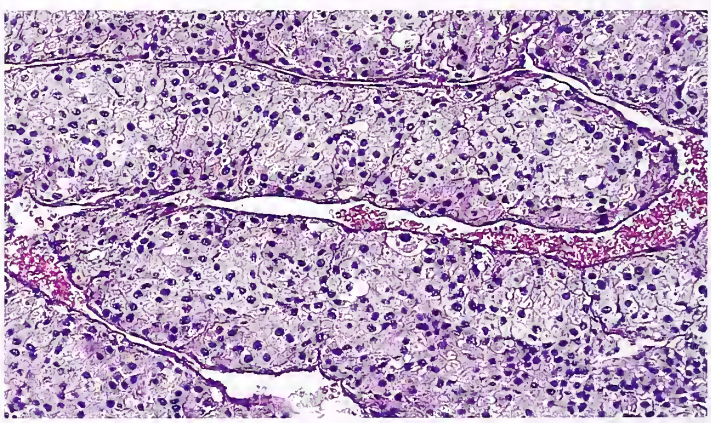

Figure 5-10

ADRENAL CORTICAL CARCINOMA

Left: The tumor has a broad anastomosing, trabecular pattern with slit-like delicate sinusoids. Some trabeculae appear as slender tongue-like extensions into sinusoids.

Above: Despite the absence of significant nuclear atypia, this histologic pattern was associated with aggressive biologic behavior and the patient died within 12 months of diagnosis with widespread metastases. (Left and above are from the same case as figure 5-2.)

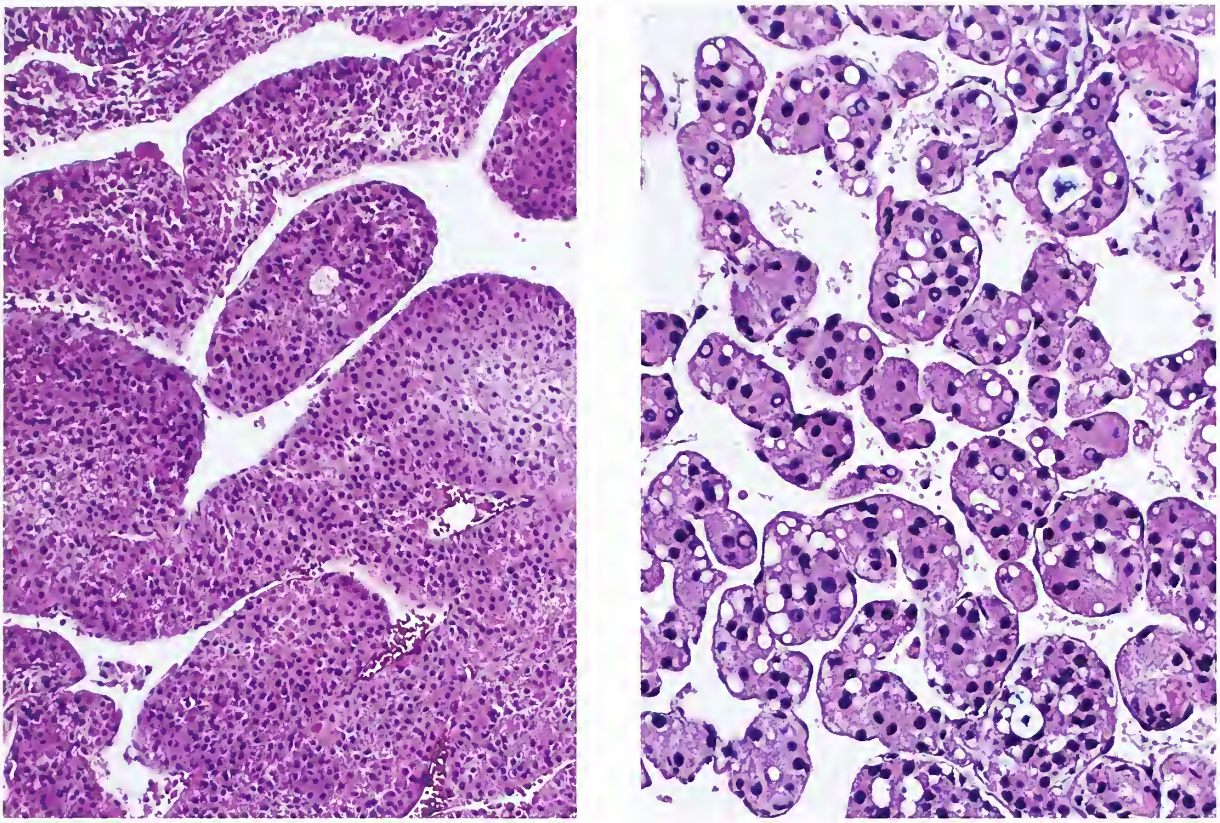

Figure 5-11

ADRENAL CORTICAL CARCINOMA

Left: ACC from an adult male who had primary hyperaldosteronism. Occasional nests of tumor appear to be "free floating" but additional sections may reveal sites of attachment.

Right: Fortuitous plane of section in a different case showing numerous "free floating" nests of tumor. Some cells have coarse cytoplasmic vacuoles representing lipid.

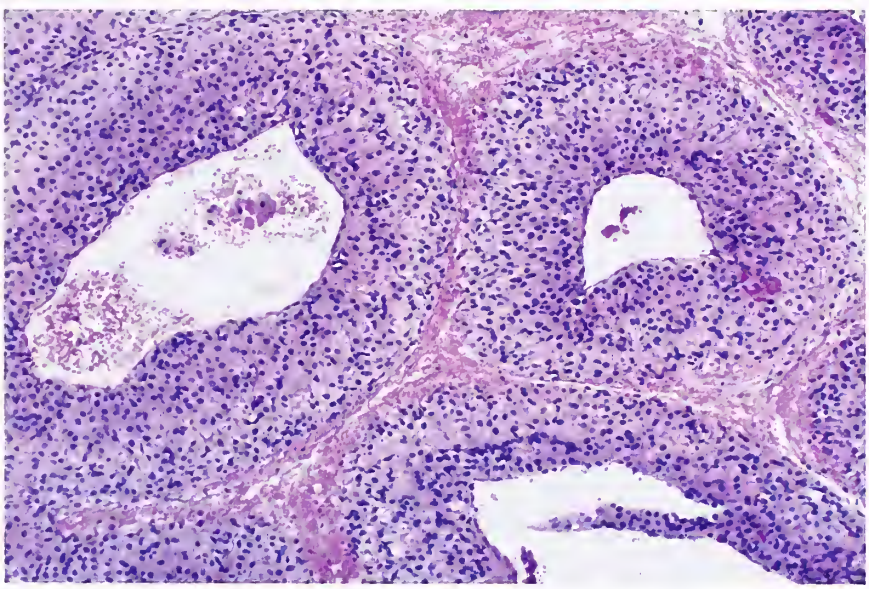

Figure 5-12

ADRENAL CORTICAL CARCINOMA

Perithelial distribution of tumor cells with intervening thin zones of necrosis.

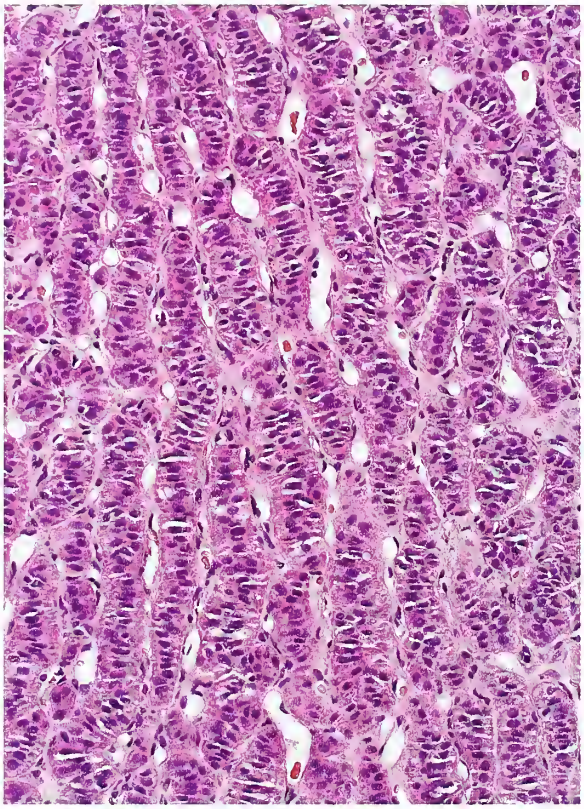

Figure 5-13

ADRENAL CORTICAL CARCINOMA

An unusual trabecular pattern was present in small areas of this tumor. Columns of cells are closely aligned in a narrow elongated profile.

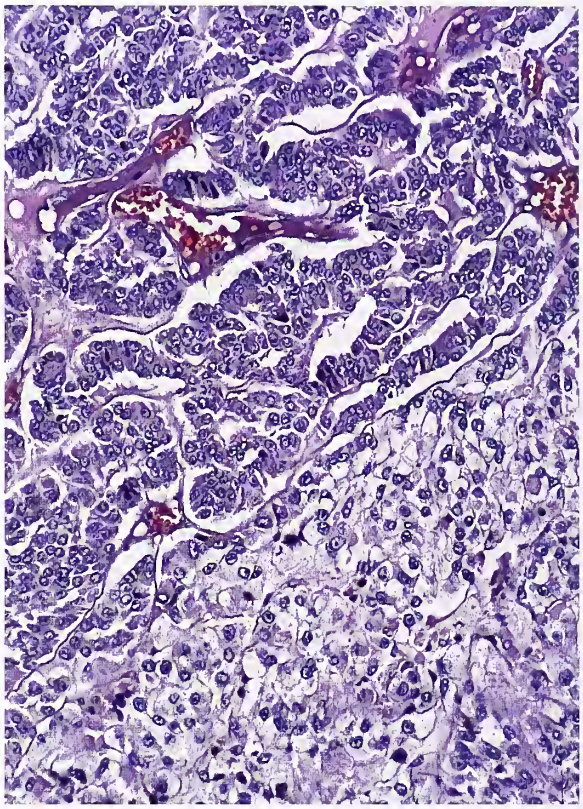

Figure 5-14

ADRENAL CORTICAL CARCINOMA

At the top are serpentine cords of cells while a more diffuse or solid pattern is present in other areas. Cells at the bottom have predominantly lipid-rich, pale-staining cytoplasm, but some cells had eosinophilic condensation of the cytoplasm. (Fig. 5-10 from Fascicle 19, Third Series.)

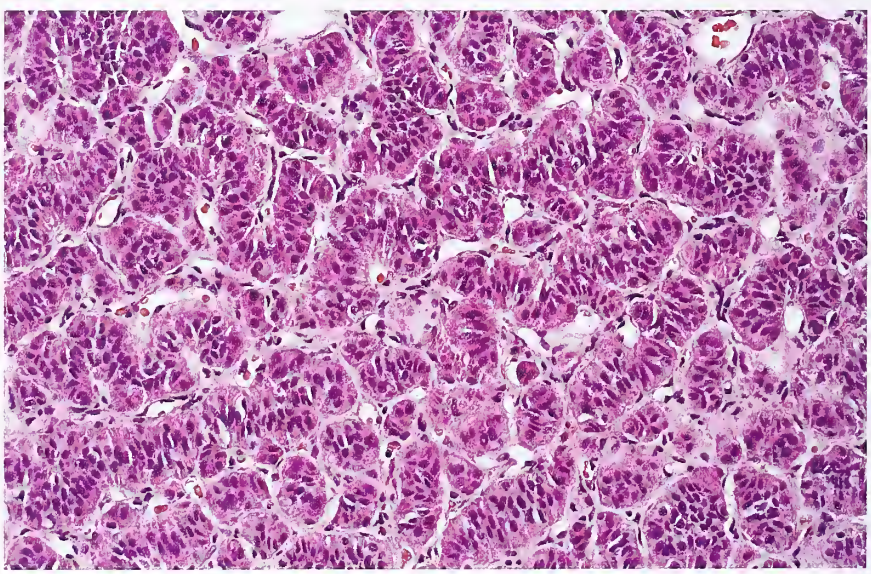

Figure 5-15

ADRENAL CORTICAL CARCINOMA

An alveolar or nesting pattern is admixed with blunt short cords of cells. The tumor cells have compact, eosinophilic cytoplasm.

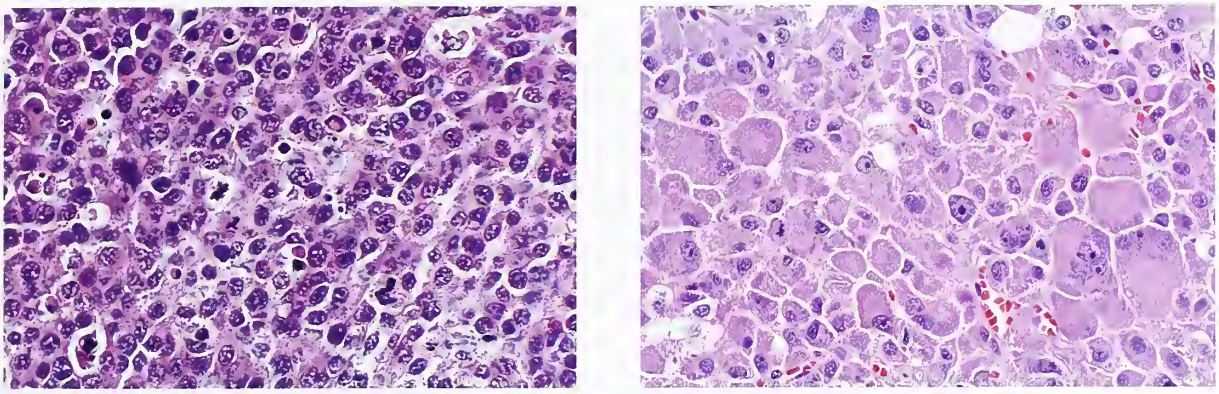

Figure 5-16

ADRENAL CORTICAL CARCINOMA WITH DIFFUSE OR SOLID ARCHITECTURE

Left: The ACC has a diffuse or solid pattern of irregular pleomorphic cells with a high nuclear to cytoplasmic ratio. Most cells have compact, eosinophilic cytoplasm. Mitotic figures were numerous, with many atypical forms. (Fig. 5-12 from Fascicle 19, Third Series.)

Right: A different ACC has loosely arranged cells with a diffuse or solid architecture. The tumor cells have abundant compact, eosinophilic cytoplasm.

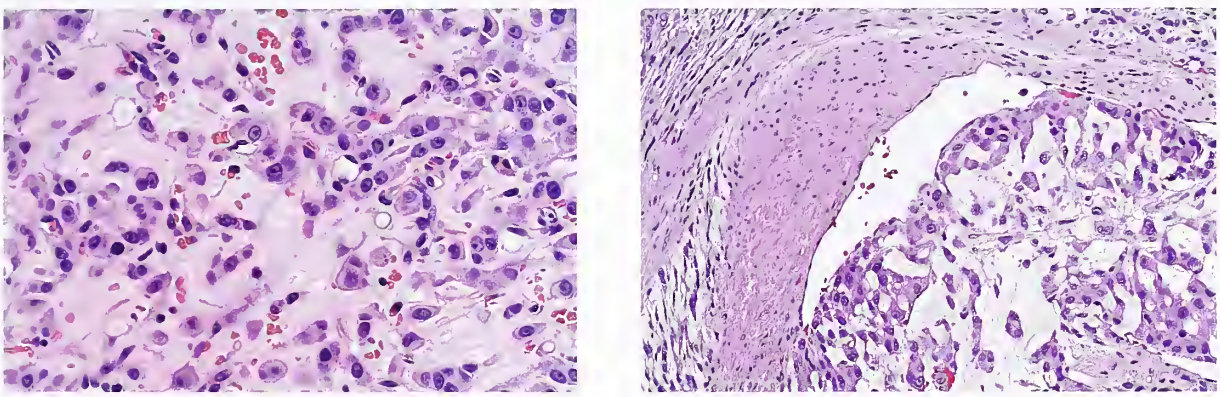

Figure 5-17

ADRENAL CORTICAL CARCINOMA

Left: Areas of marked myxoid stroma separate cords of tumor cells with predominantly compact, eosinophilic cytoplasm.
Right: A different ACC with myxoid stroma and areas of blood vessel invasion.

Cytologically, the borders of ACCs (and adenomas) are often fairly well defined. Some ACCs contain conspicuous intracellular lipid with finely dispersed vacuoles. Occasionally, the lipid is more sharply defined and the nucleus is peripherally displaced (fig. 5-21).

Nuclear pleomorphism and hyperchromasia can be a spectacular feature in ACCs (fig. 5-22), but such nuclear atypia is occasionally seen in clinically benign tumors. The presence of this feature alone is not sufficient to classify an adrenal cortical neoplasm as malignant, and this may have considerable importance in interpretation of cytologic material obtained by fine needle aspiration. On occasion, nuclei appear hyperlobated or multinucleated (fig. 5-23). Nuclei may contain one or more prominent nucleoli. Nuclear pseudoinclusions are found in some ACCs (fig. 5-19), as well as in some cortical adenomas and pheochromocytomas. These may be solitary or multiple, and appear as sharply outlined structures that stain as the remaining cell cytoplasm, or show pallor or vacuolar change. These pseudoinclusions result from irregularities or

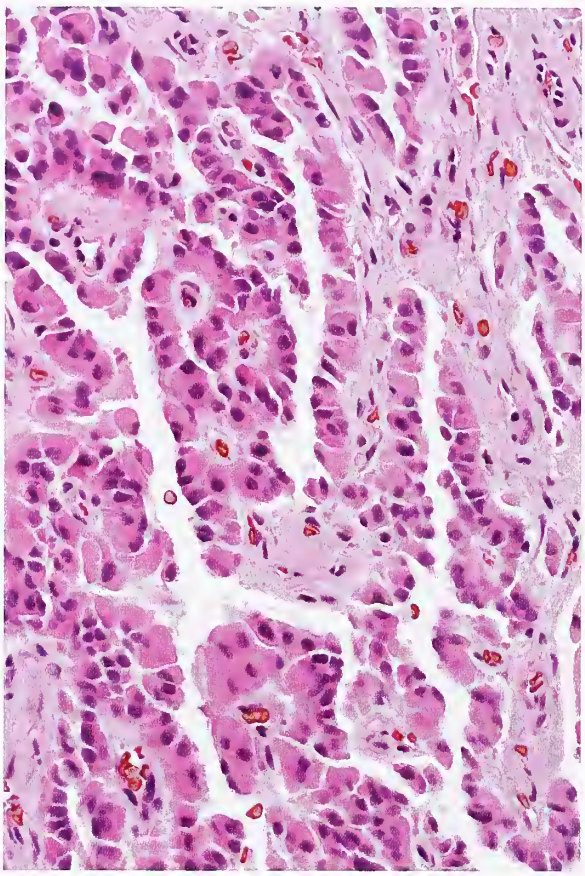

Figure 5-18

ADRENAL CORTICAL CARCINOMA

The pseudopapillary pattern focally present in this ACC is due to dyscohesion of cells.

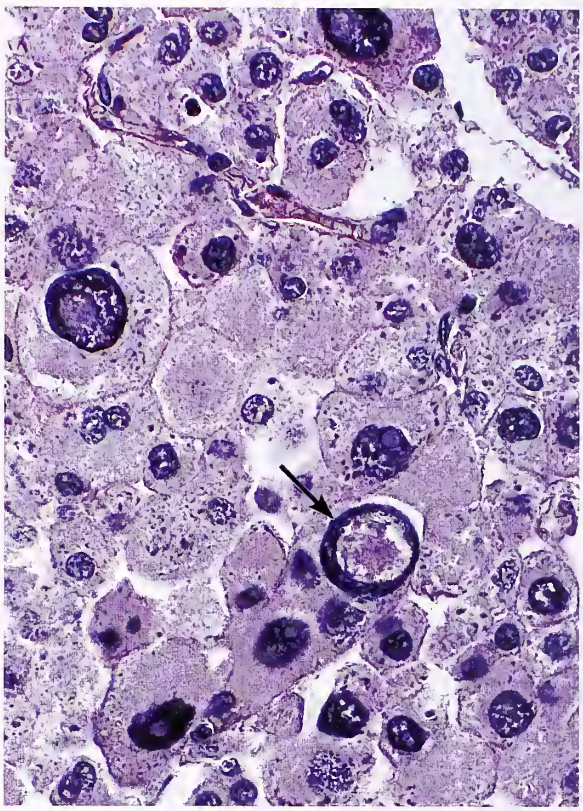

Figure 5-19

ADRENAL CORTICAL CARCINOMA

The compact, eosinophilic cytoplasm contains granular pigment, most likely lipofuscin. Note the large nuclear pseudoinclusion (arrow). (Fig. 5-14 from Fascicle 19, Third Series.)

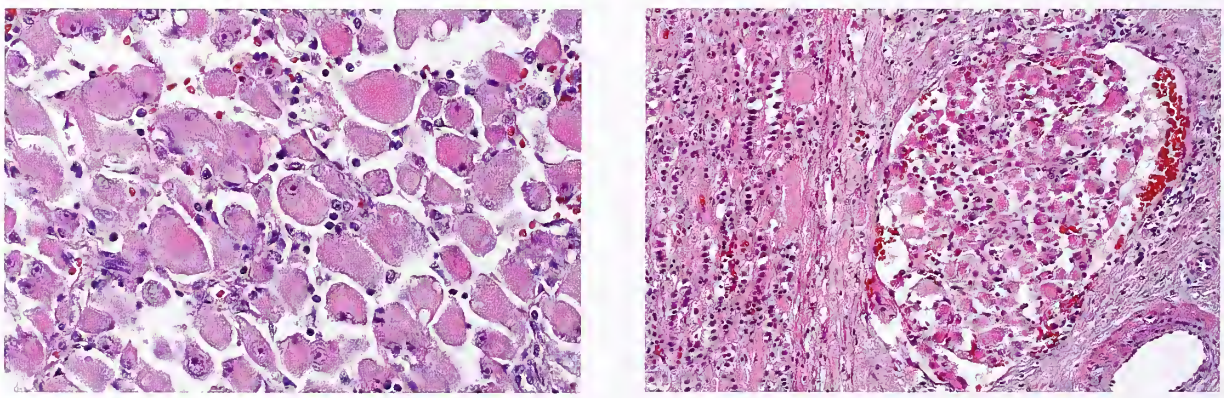

Figure 5-20

ADRENAL CORTICAL CARCINOMA WITH ONCOCYTIC FEATURES

Left: Tumor cells are dyscohesive and have abundant granular cytoplasm which is intensely eosinophilic.
Right: Other areas of same tumor show foci of blood vessel invasion.

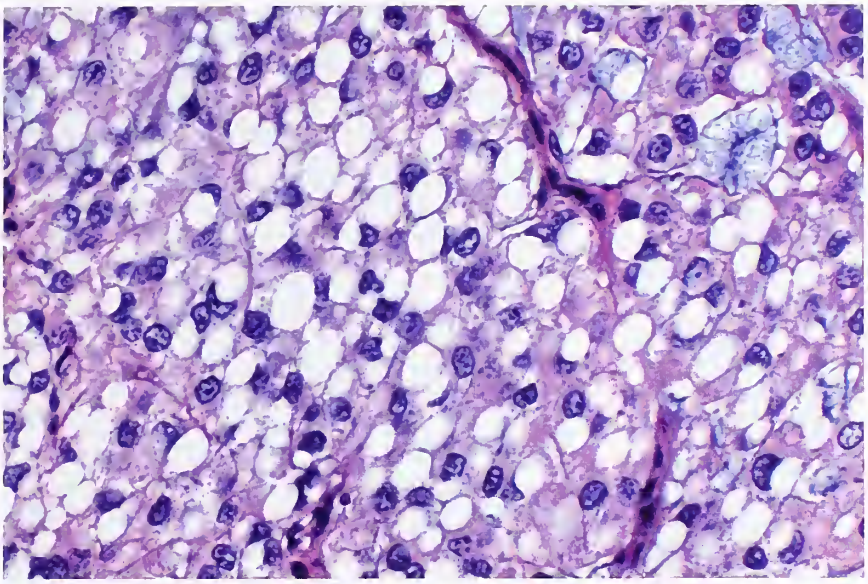

Figure 5-21

ADRENAL CORTICAL CARCINOMA

Most tumor cells have large, coarse cytoplasmic vacuoles which distend many cells and displace the nucleus to the periphery. Some cells have a "signet ring" appearance.

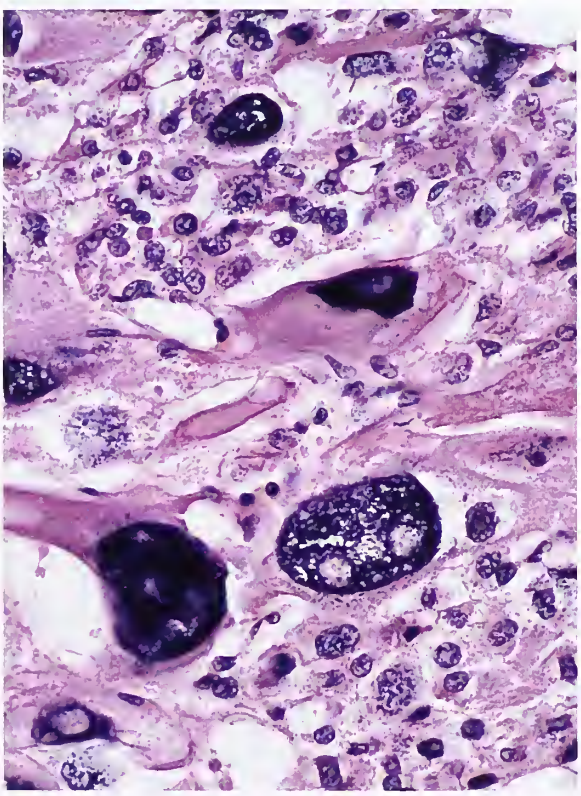

Figure 5-22

ADRENAL CORTICAL CARCINOMA

There is marked nuclear hyperchromasia, and great disparity in nuclear size and shape. Compare these remarkable features with the smaller tumor cells, which in turn are larger than normal adrenal cortical cells. (Fig. 5-15 from Fascicle 19, Third Series.)

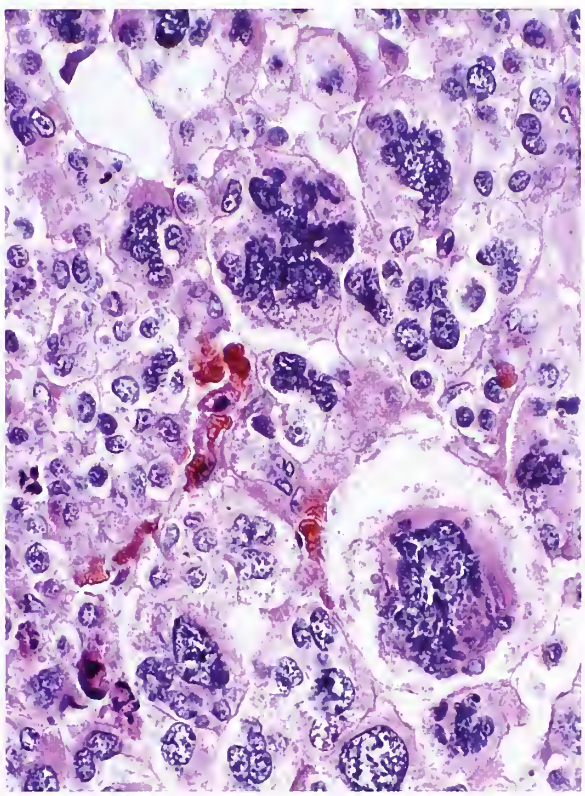

Figure 5-23

ADRENAL CORTICAL CARCINOMA

Foci of tumor cells have enlarged, hyperlobated nuclei. Some are multinucleated. (Fig. 5-16 from Fascicle 19, Third Series.)

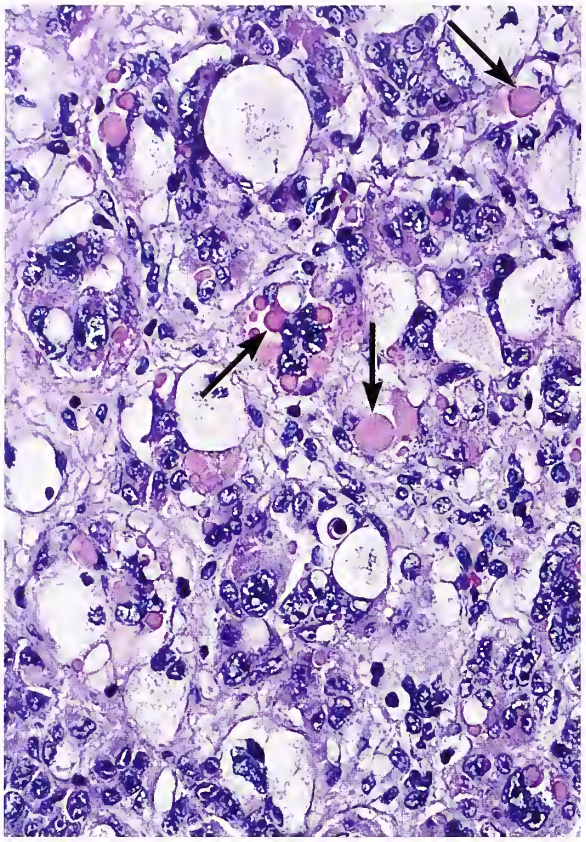

Figure 5-24

ADRENAL CORTICAL CARCINOMA

This ACC is composed of cells with predominantly eosinophilic granular cytoplasm although some cells are vacuolated with pale-staining cytoplasm. Numerous intracytoplasmic hyaline globules of various sizes are seen (arrows), with some as large or larger than the nucleus. (Fig. 5-17 from Fascicle 19, Third Series.)

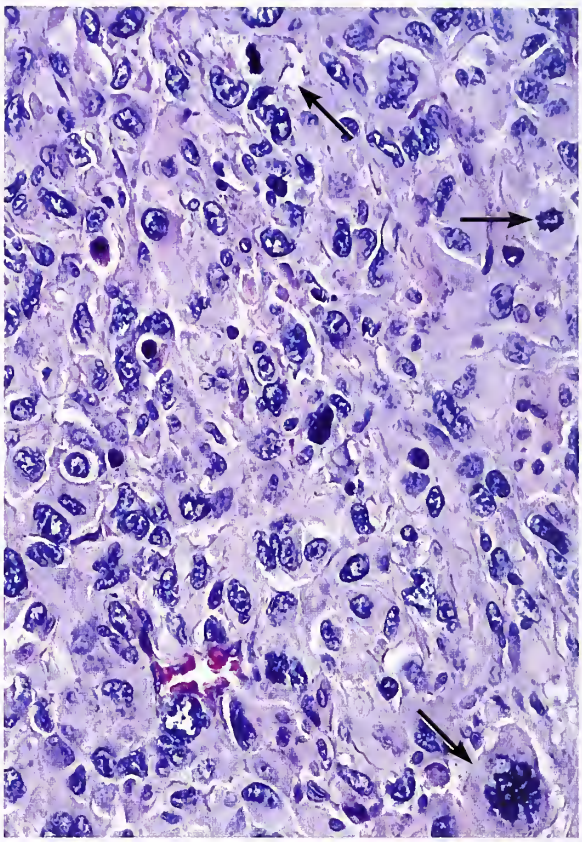

Figure 5-25

ADRENAL CORTICAL CARCINOMA

The tumor cells have compact, eosinophilic cytoplasm and hyperchromatic, pleomorphic nuclei. Numerous mitotic figures are present (arrows), some of which are atypical (right lower corner). (Fig. 5-19 from Fascicle 19, Third Series.)

infolding of the nuclear membrane and intranuclear extension of the cell cytoplasm.

An important feature of some adrenal cortical tumors, both benign and malignant, is the presence of intracytoplasmic hyaline globules (fig. 5-24). These globules are round to oval, slightly refractile, and deeply eosinophilic. They are identical by light microscopic morphology and special staining characteristics (i.e., periodic acid-Schiff [PAS] positive and variably resistant to diastase predigestion) to globules that are seen much more frequently in pheochromocytomas. In rare instances, it is difficult to distinguish an adrenal cortical neoplasm from a pheochromocytoma, and differentiation may necessitate immunohistochemical stains (e.g., pheochromocytomas are positive for chromogranin) or even ultrastructural study to identify dense-core neurosecretory granules. An adrenal cortical tumor with an alveolar or anastomosing trabecular pattern, compact eosinophilic cytoplasm, and these globules can be confused with a pheochromocytoma (see chapter 10).

Mitotic figures are relatively common in ACCs, and atypical forms may be present. The presence of mitotic figures in several consecutive high-power fields (fig. 5-25) is suspicious for malignancy, and other histologic and nonhistologic features that might be supportive should be sought. Weiss (24) found three histologic features specific to metastasizing or recurring adrenal cortical tumors: a mitotic rate of 6 or more per 50 high-power fields, atypical mitoses, and

invasion of venous structures. These findings do not necessarily apply to adrenal cortical tumors in the pediatric age group (see chapter 6). In adults, a mitotic rate greater than 20 per 50 high-power fields is associated with a shortened median survival period (14 months) compared with tumors having 20 or fewer mitoses (58 months median survival, p value < 0.02) (34).

Invasion

Vascular invasion is an ominous finding in an adrenal cortical neoplasm. It is very unusual to recognize angioinvasion on gross examination of the resected tumor or in preoperative imaging studies, although some tumors have been detected as invading large veins such as the inferior vena cava (35) and even extending on into the right atrium (1). Laparoscopic radical adrenalectomy for ACC has been reported with adrenal vein tumor thrombectomy (36). Vascular invasion is usually seen in histologic sections as loose plugs of tumor within the lumen of large veins (fig. 5-26), or sometimes in smaller vascular spaces, with some suggesting lymphatic channels. Invasion of the inferior vena cava can be associated with malignant ascites and lower extremity edema and, if unrecognized, may pose a danger in surgical resection if intraoperative mechanical manipulation results in a major tumor embolus. The tumor may extend in a sausage-like fashion into the vena cava without firm attachment to the vein wall (fig. 5-27).

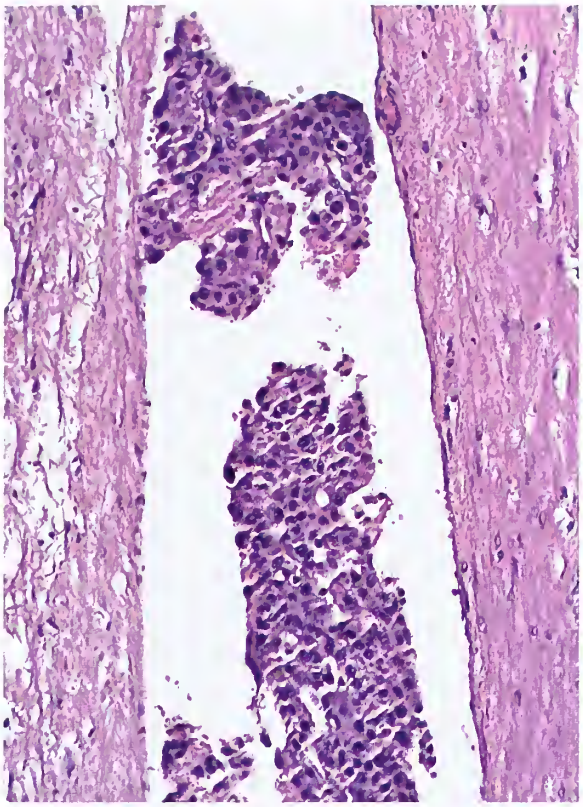

Figure 5-26

ADRENAL CORTICAL CARCINOMA

There are several large tumor plugs within the venous channels. (Fig. 5-20 from Fascicle 20, Third Series.)

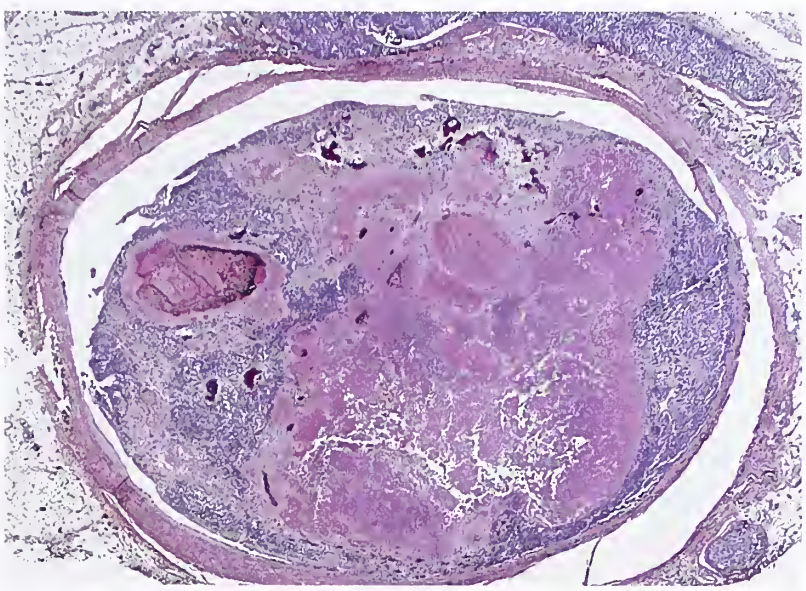

Figure 5-27

ADRENAL CORTICAL CARCINOMA

This ACC caused almost complete occlusion of the lumen of the inferior vena cava. The tumor shows extensive necrosis. One portion is attached to the wall of the vein. A few areas of dystrophic calcification are present. (Fig. 5-21 from Fascicle 19, Third Series.)

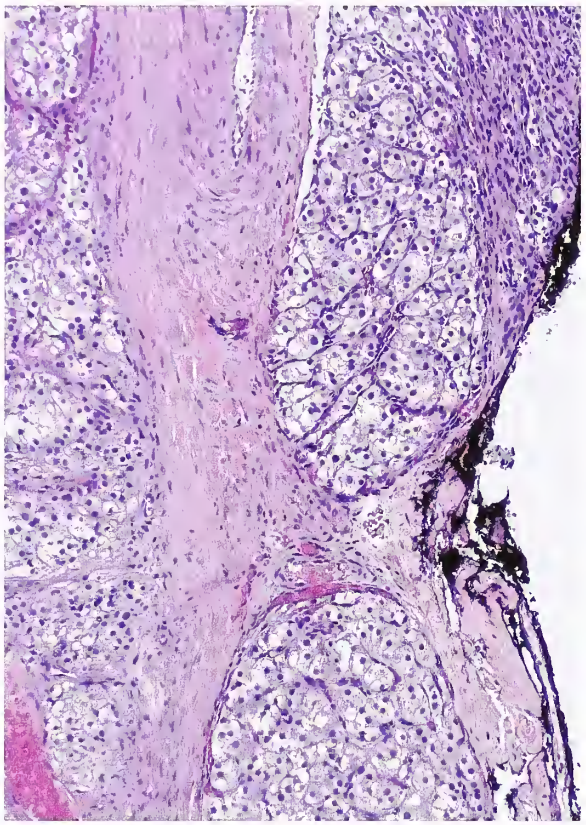

Figure 5-28

ADRENAL CORTICAL CARCINOMA

The tumor invades through the capsule and in this area approximates the inked surgical margin. The tumor was regarded as low grade based upon the low mitotic count.

Capsular invasion can be difficult to recognize in ACC since the expanded capsule (or fibrous pseudocapsule) may be, in part, preexisting adrenal capsule. This pattern of invasion is apparent as one or more blunt extensions of tumor through the fibrous pseudocapsule (fig. 5-28). Invasion of adjacent soft tissues or organs such as kidney or liver is a priori evidence of malignancy and extension beyond the adrenal capsule. Identification of capsular invasion is seldom essential in establishing the malignant nature of the tumor.

Stromal Alterations in Tumor

Broad fibrous bands may intersect the tumor, subdividing it into irregular macroscopic nodules. There may be broad confluent areas of necrosis, and occasionally, most of the tumor is necrotic (see fig. 5-7). Irregular foci of dense dystrophic calcifications may be present, usually following in the wake of tumor necrosis (fig. 5-29A); this may be detected by radiographic study or CT scan of the abdomen (see fig. 5-5). Hamper et al. (37) found that almost 20 percent of ACCs had calcification on sonographic evaluation as evidenced by a heterogeneous pattern of echopenic or echogenic zones. At times the calcification has a dust-like quality associated with individual necrotic cells (fig. 5-29B). Metaplastic bone formation is rarely seen (fig. 5-29C). Rarely, extensive tumor necrosis highlights the delicate vasculature with hematoxylinophilic material (fig. 5-29D).

Other features include myxoid alteration of the stroma and formation of lipomatous or myelolipomatous metaplasia. The presence of myxoid stroma may significantly alter the architecture of an ACC. Occasionally, one can get important clues as to an associated endocrine syndrome, even when the clinical features and endocrinologic data are not available for correlation. The presence of cortical atrophy usually indicates hypercortisolism with Cushing's syndrome or a mixed endocrine syndrome such as Cushing's syndrome and virilization. In the rare cases of ACC associated with primary hyperaldosteronism, there may be hyperplasia of the zona glomerulosa in the attached adrenal remnant.

ULTRASTRUCTURAL FINDINGS

There is a range of ultrastructural features of ACC (38). As might be expected from the light microscopic findings, the abundance of cells with compact, eosinophilic cytoplasm indicates a cell population with little to no intracytoplasmic lipid droplets (fig. 5-30); this is in sharp contrast to neoplastic lipid-rich cortical cells and normal cortical cells of the zona fasciculata. The cytoplasmic eosinophilia seen by light microscopy may be contributed to, in part, by a prominent smooth endoplasmic reticulum and abundant mitochondria (fig. 5-31); the latter may give the cytoplasm a finely granular appearance. An overabundance of mitochondria can give the tumor cells an oncocytic appearance. Most tumors contain cells with short, flattened profiles of rough endoplasmic reticulum; occasionally, it is seen as small stacks (38). The smooth endoplasmic

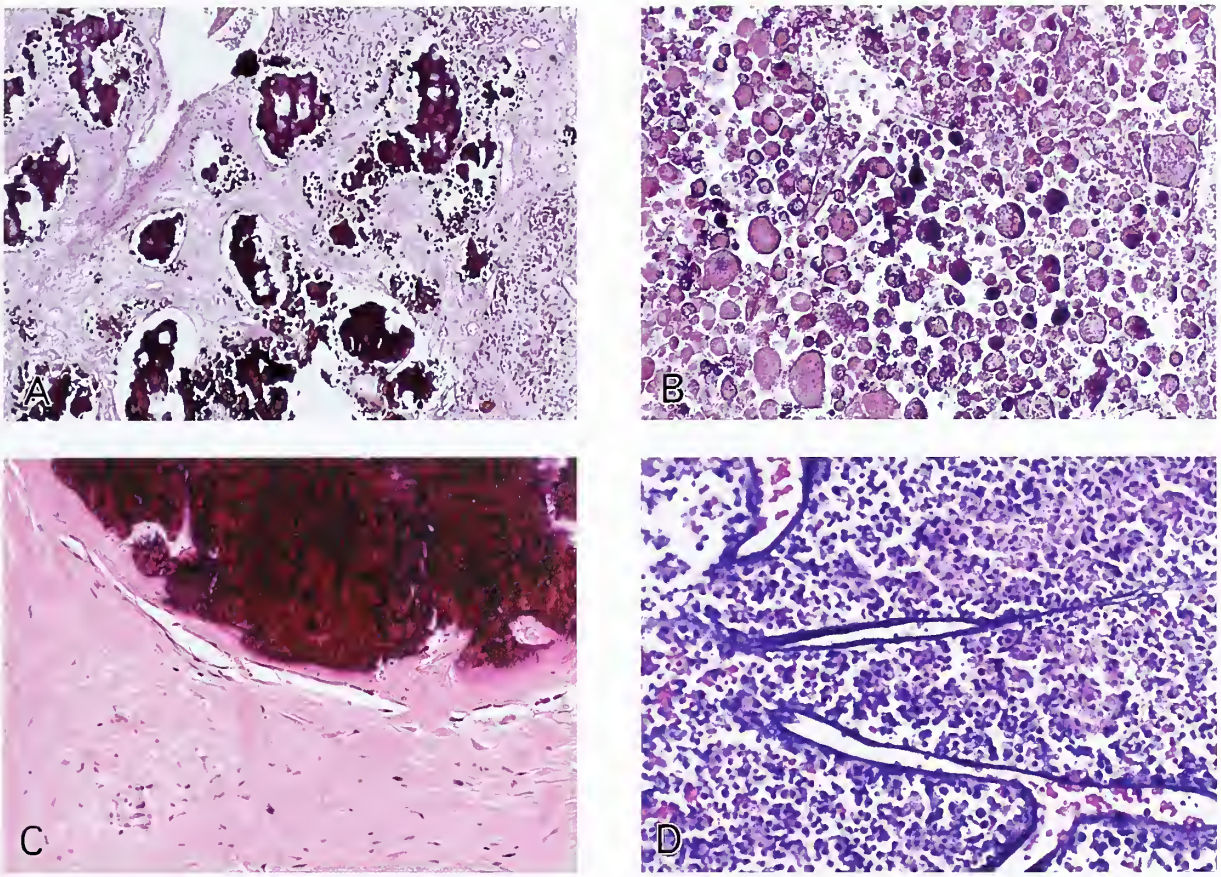

Figure 5-29

ADRENAL CORTICAL CARCINOMA

A: Areas of granular to coarse dystrophic calcification are in a background of extensive tumor necrosis.

B: Most necrotic tumor cells show granular, punctuate to dust-like dystrophic mineralization. (A&B: Fig. 5-23 from Fascicle 19, Third Series.)

C: Area of fibrosis and metaplastic bone formation in a tumor with extensive necrosis.

D: Extensive confluent tumor necrosis in an ACC is associated with mild hematoxylin staining of delicate vessel walls due to the application of DNA (Azzopardi effect).

reticulum may form concentric whorls or a tangled skein (fig. 5-32), or there may be sparse lamellated structures resembling myelin figures.

The nucleus becomes a dominant feature in some cells, and may have marginated chromatin dispersed on the nuclear membrane or densely clumped. Tumor cells may show stubby, microvillous projections, but these are usually not as well developed as those seen in adenomas (see chapter 4). Simple intercellular junctions are occasionally seen, but they tend to be sparse in number. In one study, about one third of ACCs failed to show convincing evidence of steroid cell differentiation (38).

Mitochondria may vary in size and shape, but are often small and round to oval. They may have a primitive cristal component which can be tubular, vesicular, or lamellar (shelf-like) (fig. 5-33). A granular matrix may be prominent within individual mitochondria. Cells of virilizing ACC can resemble the compact cells of the zona reticularis with lamellar and tubular cristae, lipofuscin pigment, and scant lipid, but it is virtually impossible to accurately predict the presence or absence of any particular endocrine syndrome solely from the ultrastructural appearance. Small intracytoplasmic lakes of glycogen have been reported in ACC, but are uncommon;

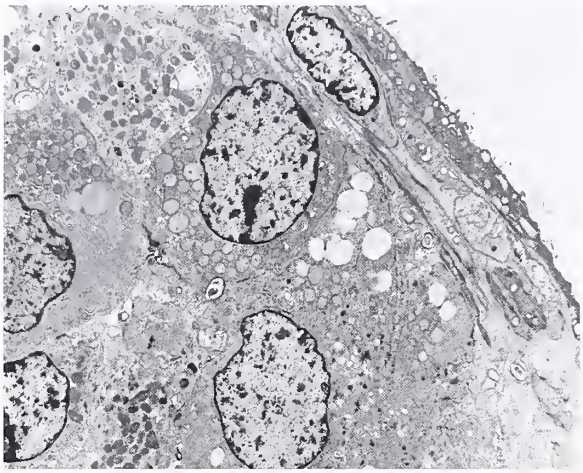

Figure 5-30

ADRENAL CORTICAL CARCINOMA

Tumor cells contain sparse lipid droplets; some have small, irregular microvillous extensions of cytoplasm along the cell border. The cells contain ample mitochondria and smooth endoplasmic reticulum. The delicate vasculature is illustrated by a vascular channel in the right upper corner that is lined by endothelial cells and partially surrounded by pericytes.

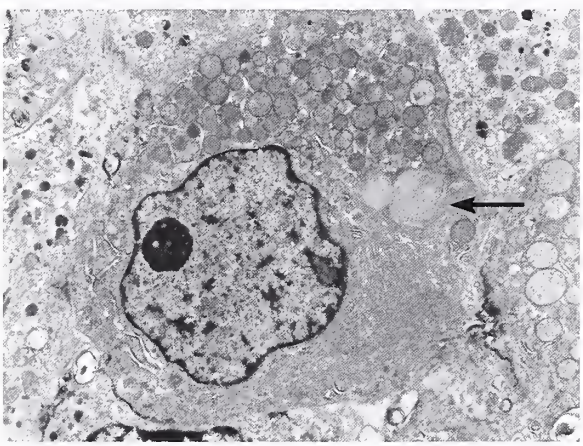

Figure 5-31

ADRENAL CORTICAL CARCINOMA

The tumor cell is essentially devoid of lipid droplets but contains abundant smooth endoplasmic reticulum and some profiles of rough endoplasmic reticulum. A few concentric whorls of smooth endoplasmic reticulum are also present (arrow).

in one study, glycogen was noted in a metastatic ACC while the primary tumor did not show the same extensive accumulation of glycogen (38). Sparse, membrane-bound, dense-core granules

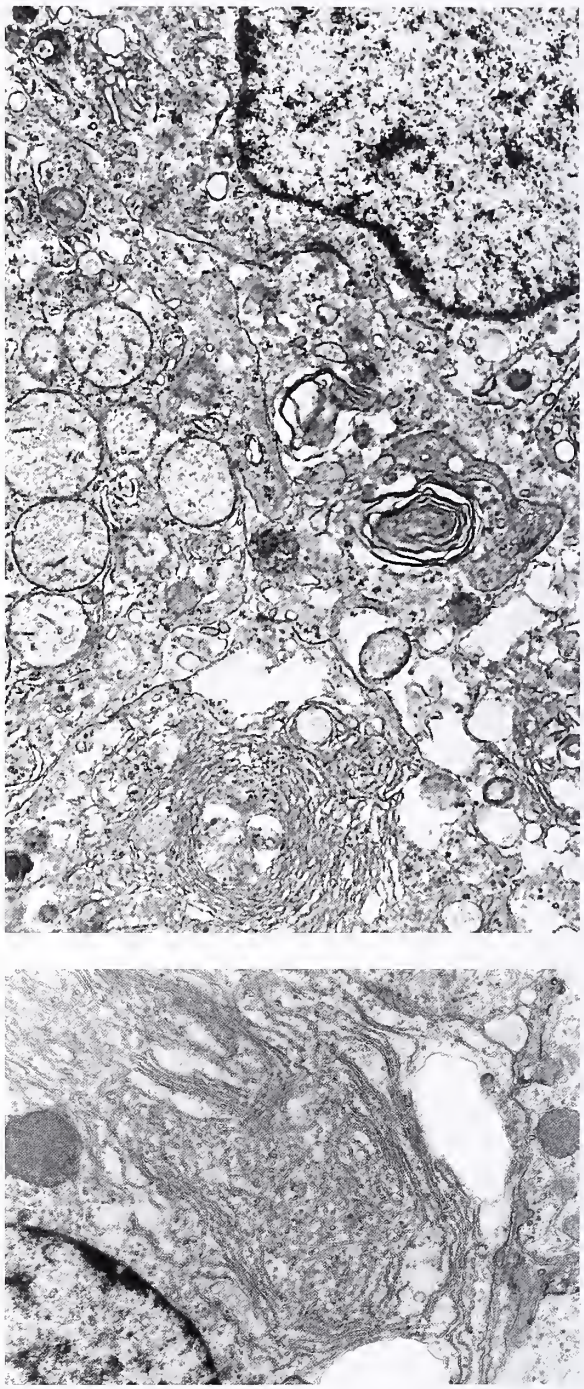

Figure 5-32

ADRENAL CORTICAL CARCINOMA

Top: There is a concentric whorl of smooth endoplasmic reticulum as well as a myelin figure. The mitochondria have sparse lamellar cristae (Fig. 5-27, left from Fascicle 19, Third Series.)

Bottom: ACC with a tangled skein of smooth endoplasmic reticulum.

have been reported, and in one study were considered consistent with neuroendocrine type granules even though the cells were not immunoreactive for chromogranin A (39).

IMMUNOHISTOCHEMICAL FINDINGS

At present, there is no immunohistochemical profile pathognomonic for ACC, but even negative results can sometimes aid in a difficult differential diagnosis. ACCs are typically negative for cytokeratin (40–42), although occasional positive results may be obtained using fresh frozen tissue or sections pretreated with a protease such as trypsin (40,43). In a study by Schröder et al. (41), only 2 of 72 adrenal cortical neoplasms (57 adrenal cortical adenomas [ACAs] and 15 ACCs) stained for cytokeratin (1 ACA and 1 ACC); Cote et al. (44) reported positive results in normal cortical cells and ACA, but none of the ACC cells expressed cytokeratin. Nakano (43) reported that 24 of 62 ACCs contained cytokeratin-positive cells, while all of the 42 ACAs were negative. Vimentin has been reported to be positive in tumor cells of ACC (fig. 5-34A), but the frequency reported in the literature varies considerably: 8 percent among 57 ACAs and 15 ACCs (41), 65 percent (all ACCs) (40), 73 percent ACCs (versus only 14 percent ACAs) (43), and 100 percent (44). Despite the variable results reported in the literature, as a general rule, a neoplasm that has the typical morphology, either in tissue sections or cytologic preparations, and has features of an ACC (large size, suprarenal location, adverse imaging characteristics), would statistically be expected to be vimentin positive and cytokeratin negative (at least most tumor cells). ACCs can also be immunoreactive for Melan-A, inhibin (fig. 5-34B), and calretinin (42), findings that may provide valuable information in the differential diagnosis.

MOLECULAR GENETICS, DIFFERENTIAL DIAGNOSIS, AND CELLULAR PROLIFERATION

Molecular genetic and chromosomal abnormalities have been identified in adrenal cortical neoplasms. Most adrenal cortical tumors, whether benign or malignant, have been characterized as monoclonal, indicating that genetic changes at specific loci in the genome are needed for tumor development (45). Loss of heterozygosity and other studies of these loci have identified genes with tumor suppression or other oncogenic functions, including genes coding for p53 (on chromosome 17p13.1), p57 on 11p15, and insulin-like growth factor-2 on 11p15.5 (46,47). Although some have found molecular genetics potentially useful in distinguishing benign from malignant adrenal cortical tumors (46), others have shown that multimolecular phenotyping is complex and heterogeneous in ACCs, thus making classification and targeted immunotherapy a significant challenge. Comparative genomic hybridization (CGH) analysis of ACCs has shown a complex array of genetic aberrations; the mean number of CGH changes was 7.6 (range, 1 to 15), with an equal distribution of gains and losses (48).

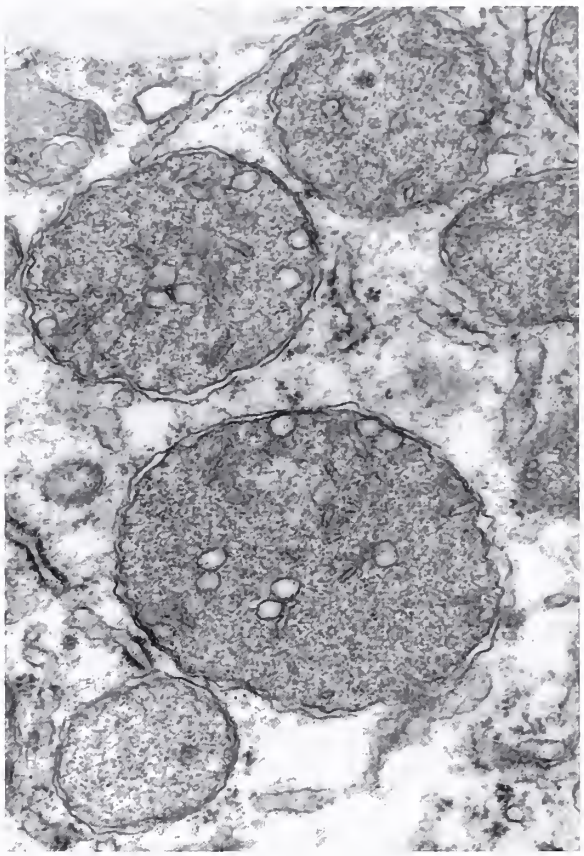

Figure 5-33

ADRENAL CORTICAL CARCINOMA

Mitochondrial cristae are relatively sparse. Both vesicular and tubular profiles are seen, along with an abundant granular matrix (Fig. 5-28 from Fascicle 19, Third Series.)

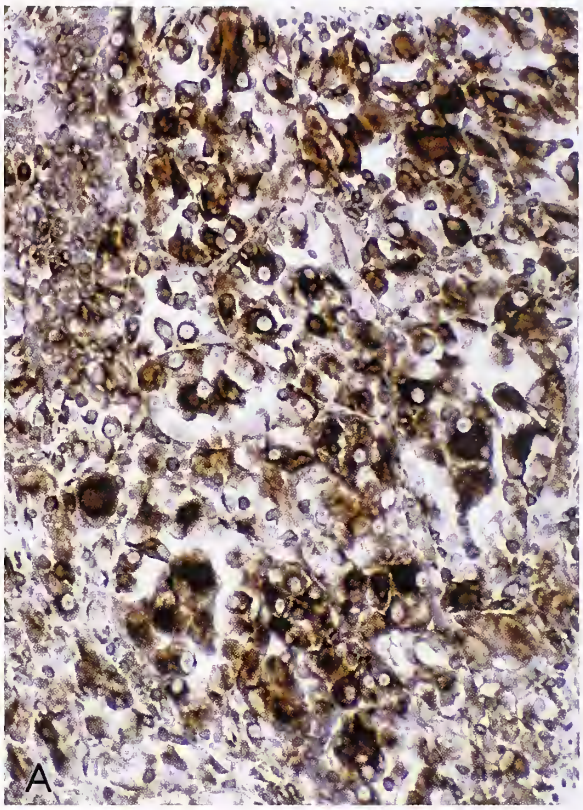

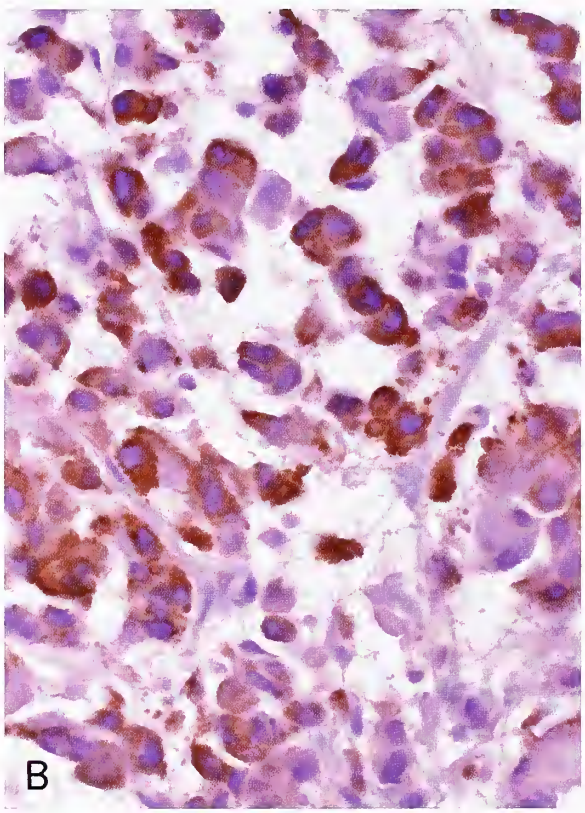

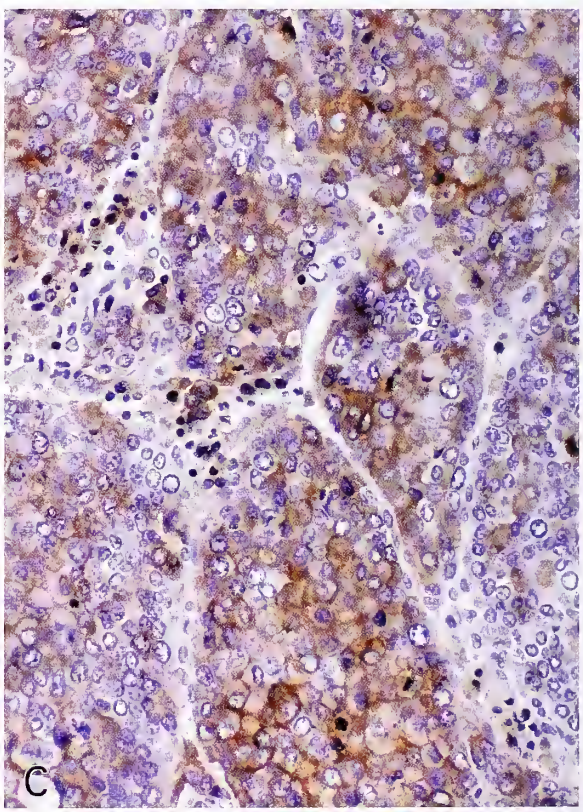

Figure 5-34

ADRENAL CORTICAL CARCINOMA

A: The tumor cells of an ACC are strongly immunoreactive for vimentin.

B: A myxoid variant shows positive immunostaining for inhibin.

C: ACC with strong immunoreactivity for synaptophysin, a staining reaction that may lead to a misdiagnosis of an endocrine tumor such as pheochromocytoma (A–C: avidin-biotin peroxidase method).

The differential diagnosis of ACC includes hepatocellular carcinoma (HCC), renal cell carcinoma (RCC), and various metastatic carcinomas. Careful morphologic evaluation and close correlation with other features such as clinical presentation, location, or results of special stains for intracellular glycogen or mucosubstances often provide definitive information as to the correct diagnosis. In a few cases, however, there may be lingering uncertainty. Most RCCs are positive for cytokeratin and other epithelial markers, such as epithelial membrane antigen. In one study, 33 of 33 HCCs (100 percent) were positive for cytokeratin and 6 (18 percent) were positive for vimentin, while 24 of 37 RCCs were positive for keratin (65 percent) and 22 of 37 were positive for vimentin (60 percent) (40). A recent large immunoprofile study of HCC, RCC, and ACC used the tissue array technique for comprehensive antibody testing (49). It appears that the immunophenotypic overlap of ACC, RCC, and HCC may hinder interpretation in some cases, but again, careful scrutiny of morphology, and use of basic special stains may resolve the dilemma.

Immunostaining for the alpha subunit of inhibin (fig. 5-34B) (50) and Melan-A (Mart-1) (51) have proven useful in the identification of adrenal cortical neoplasms, both benign and malignant, and may help resolve problems in the differential diagnosis. These and other immunostains, however, may be positive in different types of tumors and close correlation is recommended. A significant proportion of adrenal cortical tumors are immunoreactive for calretinin (over 90 percent) (52). Nuclear D11 immunoreactivity allows identification of well-differentiated ACC, and distinguishes carcinomas metastatic to the adrenal gland, including RCC, as well as other primary tumors such as pheochromocytoma (53). A potentially important immunocytochemical finding is staining for synaptophysin or neuron-specific enolase in a significant proportion of ACCs (39), which can lead to misdiagnosis unless close attention is paid to routine morphology (fig. 5-34C). In one study, 8 of 10 ACCs were positive, at least focally, and 3 showed extensive positivity of more than 30 percent of tumor cells (39). None of the ACCs were positive for chromogranin A or a variety of neuropeptides (39, 54), and all tumors were negative for cytoplasmic argyrophilia (41). Chromogranin immunoreactivity is not detected in either the normal adrenal cortex, ACA, or ACC (55). Clusters of dense-core granules have been identified ultrastructurally in some tumors (39), but they may be difficult to distinguish from primary lysosomes.

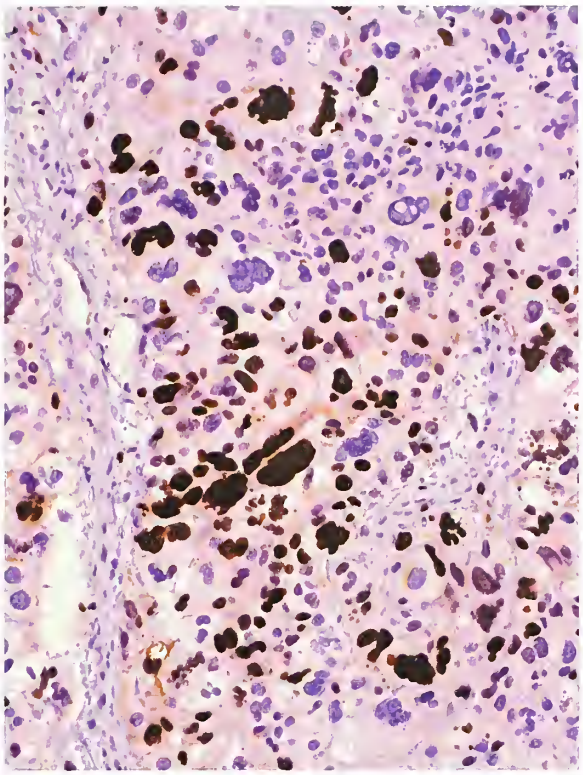

Figure 5-35

ADRENAL CORTICAL CARCINOMA

A high labeling index for proliferation marker Ki-67 (approximately 50 percent) is present (avidin-biotin peroxidase method).

An immunohistochemical study of markers of proliferative activity using a scoring system of proliferating cell nuclear antigen (PCNA) and Ki-67 has demonstrated a correlation with mitotic counts and clinical outcome (56,57). In a recent study, a high Ki-67 ACC labeling index was defined as more than 5 percent of tumor nuclei being stained (fig. 5-35) (57); other studies report an average labeling index of about 20 percent (56). Suzuki et al. (58) found immunoreactivity for PCNA and epidermal growth factor receptor in all ACAs (n = 6) and ACCs (n = 15) studied, and concluded that only DNA ploidy determination and immunolocalization

patterns of C-myc expression had any practical value in the pathologic evaluation of adrenal cortical tumors.

Determination of nucleolar organizer regions (AgNORs) appears to offer little value in distinguishing between ACA and ACC, but may correlate with increased steroid hormone production (59). Some of these molecular markers may be important for tumor progression through autocrine stimulation, oncogene overexpression, and other mechanisms, but the fundamental distinction between benign and malignant adrenal cortical neoplasms depends largely upon morphologic evaluation.

FINE NEEDLE ASPIRATION BIOPSY

Percutaneous fine needle aspiration biopsy is a diagnostic procedure that is very useful in the evaluation of an adrenal mass, particularly for staging an extraadrenal primary malignancy. There are very few reports in which ACC was diagnosed by fine needle aspiration biopsy (60), and caution should be used when distinguishing an ACC from a benign cortical neoplasm on the basis of cytologic findings alone. In several reported cases, the malignant nature of the tumor was clearly evident with fine needle aspiration biopsy, including sites of metastases such as liver, lung, lymph node, soft tissue, and bone, but correlation with clinical and radiologic information may be necessary (61) as well as comparison with the original primary tumor if material is available (61). Careful correlation with clinical and endocrinologic data is essential, as well as awareness of size, location, and imaging characteristics of the adrenal mass. As noted in chapter 3, the chances of diagnosing an ACC in an incidentally discovered adrenal nodule are remote, particularly when the adrenal mass is small (3 cm or less). A cell block preparation (fig. 5-36A) may contain fragments of tissue that can yield important diagnostic information and enable further investigation using immunohistochemistry.

The cytologic features of ACC can be very atypical, with loosely cohesive clusters or individual cells having vacuolated or compact cytoplasm (fig. 5-36B). The nucleus tends to dominate the cell, thus giving a high nuclear to cytoplasmic ratio, and sometimes the nuclear enlargement and irregularity can be an outstanding feature (fig. 5-36C,D). Additional information can be obtained by using special stains for intracytoplasmic glycogen or mucin (expect negative results in ACC), cytokeratin (typically negative), and vimentin (often positive). Positive immunostains for Melan-A and inhibin may provide confirmatory evidence of the diagnosis.

Occasionally, one may see bare or "stripped" nuclei having no apparent cytoplasm in aspirates of benign cortical nodules; this finding may superficially mimic a small, round cell malignancy (62). The nuclei, however, tend to be relatively uniform without molding and there is typically no evidence of necrosis. Conversely, pulmonary adenocarcinoma metastatic to the adrenal gland has been reported in which the aspirate of malignant cells closely resembled normal cortical cells (63).

A large, upper quadrant mass sometimes can be difficult to separate from the kidney or liver, and the fine needle aspiration specimen of a primary renal or hepatic neoplasm may be confused with an adrenal cortical tumor. An adrenal metastasis from RCC was diagnosed by fine needle aspiration, but required close correlation with the clinical history and radiographic findings to distinguish it from an ACC (64). RCC has been reported to have eosinophilic globules (65), and potentially an ACC could present with similar findings.

DNA QUANTIFICATION AND PLOIDY PATTERNS

There are conflicting interpretations of the quantitative DNA profiles in adrenal cortical neoplasms. Most studies have used flow cytometry analyses of material extracted from paraffin-embedded tissue or static image analysis of Feulgen-stained sections. In a large study of adenomas of various endocrine organs, unequivocal evidence of DNA aneuploidy was reported in 29 percent of 44 pituitary adenomas, 25 percent of 49 thyroid tumors, 35 percent of 54 parathyroid tumors, and 53 percent of 17 ACAs; none of the tumors were malignant (66). In one study, 9 of 31 (29 percent) ACAs had aneuploid DNA (67).

Quantification of the DNA content in the nonneoplastic adrenal gland with cytomegaly has revealed considerable heterogeneity in the DNA profile, indicating that polyploidy (aneuploidy) is not a specific marker of neoplasia (68). Some studies report that DNA ploidy (nondiploid/

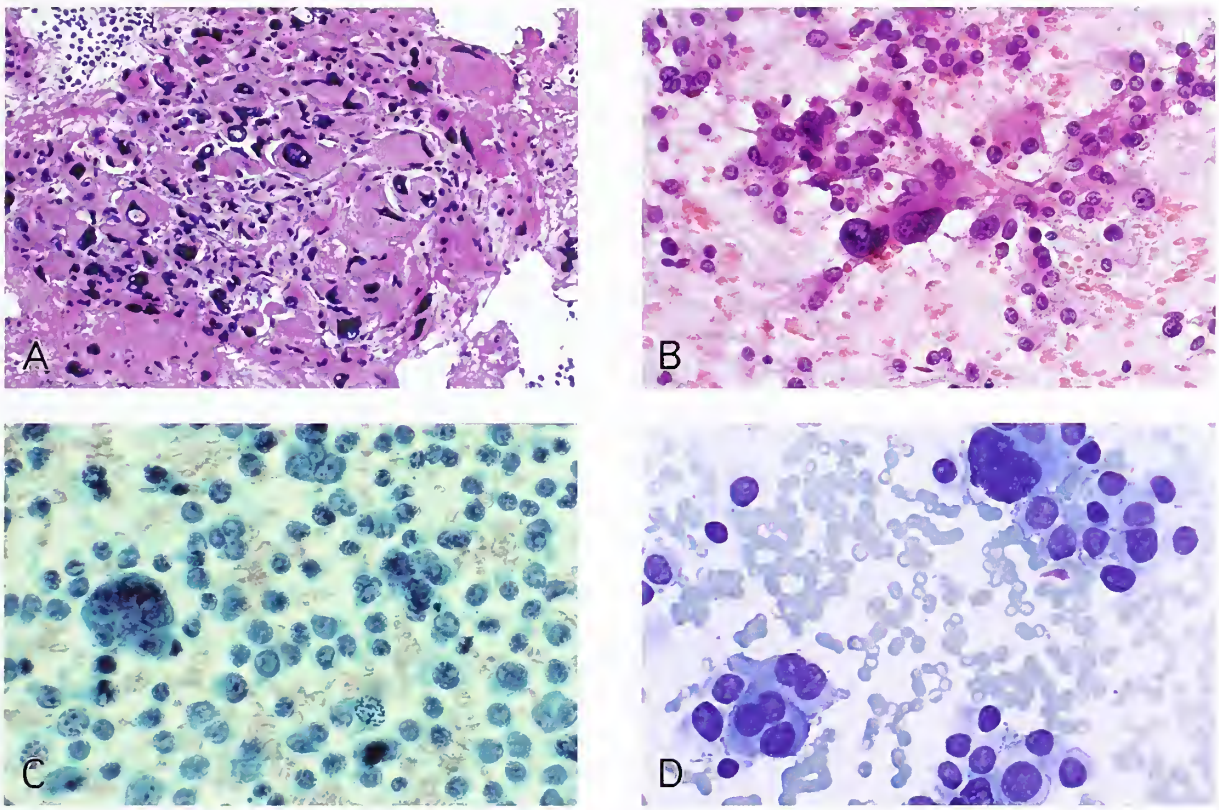

Figure 5-36

ADRENAL CORTICAL CARCINOMA

A: Cell block preparation from a fine needle aspiration biopsy of a large adrenal cortical neoplasm. There is marked nuclear pleomorphism and hyperchromasia, along with a few nuclear pseudoinclusions. Tumor size, location, and heterogeneous imaging features (necrosis, calcifications, and extraadrenal extension) correlated with a diagnosis of ACC.

B: Aspirate smear preparation of an ACC shows cells with compact, eosinophilic cytoplasm (hematoxylin and eosin [H&E] stain). (A and B are the same case).

C: Fine needle aspirate is quite cellular, with loosely dispersed malignant cells, some with gigantic hyperchromatic nuclei. Most cells have compact cytoplasm and a high nuclear to cytoplasmic ratio (Papanicolaou stain).

D: Another field in same case as C shows marked variation in nuclear size. Tumor cells are dispersed or loosely aggregated in small clusters (Diff Quik stain).

aneuploid peaks) helps distinguish benign from malignant adrenal cortical neoplasms in adults and children (69–73). Of 52 ACCs analyzed by Hosaka et al. (71) by flow cytometry, the value of the DNA ploidy determination was restricted to patients undergoing curative resections. In this subgroup, however, the number of patients with DNA diploid tumors was small, and the cases did not achieve statistical significance. A poor prognosis was associated with ACCs having two stemline DNA aneuploidy. Occasionally, different DNA profiles and aneuploid cell populations are identified by analyzing separate blocks of tumor (fig. 5-37).

Other studies, however, report no statistically significant correlation between aneuploidy or heterogeneous DNA content and biologic behavior (67,74–76), including two studies in the pediatric age group (77,78). In one study, DNA ploidy correlated with tumor size, mitotic rate, and nuclear grade, but did not correlate significantly with clinical outcome; aneuploid stemlines were identified in 9 of 13 ACCs (69 percent), but were also present in 6 of 30 ACAs (20 percent) (75). The literature regarding DNA ploidy in adrenal cortical neoplasms is briefly summarized by Zerbini et al. (77), who also noted that aneuploidy was relatively

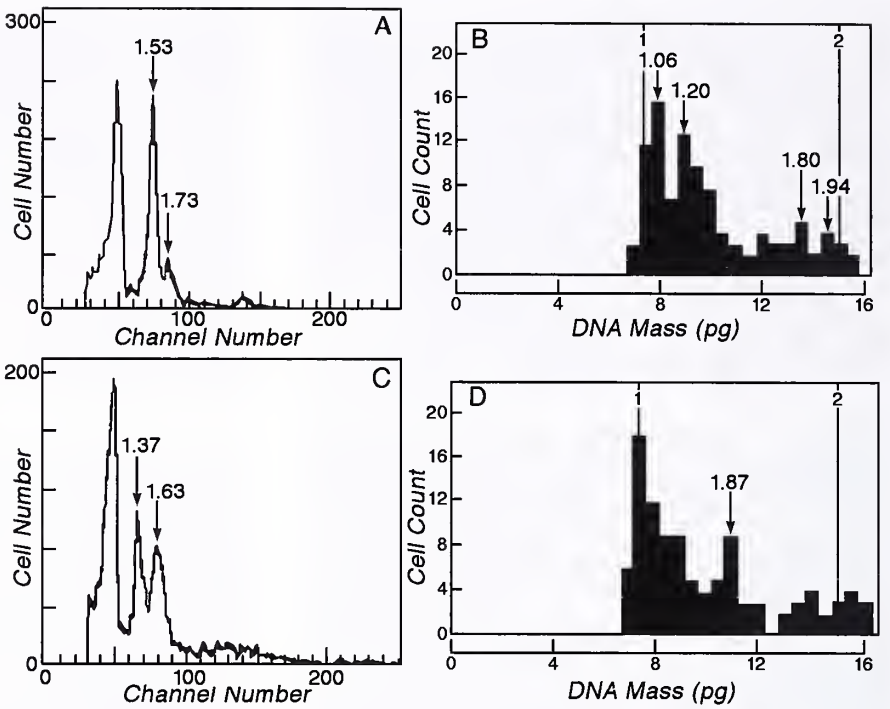

Figure 5-37

ADRENAL CORTICAL NEOPLASM

DNA histograms using flow cytometry and static image analysis on two separate tissue blocks from an adrenal cortical neoplasm (classified pathologically as an adenoma) from a 14-year-old female. The histograms are complex and multiple aneuploid peaks in both flow cytometric and static image analysis are present. A: flow cytometry; B: image analysis of first block; C: flow cytometry; and D: image analysis of second block. (Fig. 5-34 from Fascicle 19, Third Series.)

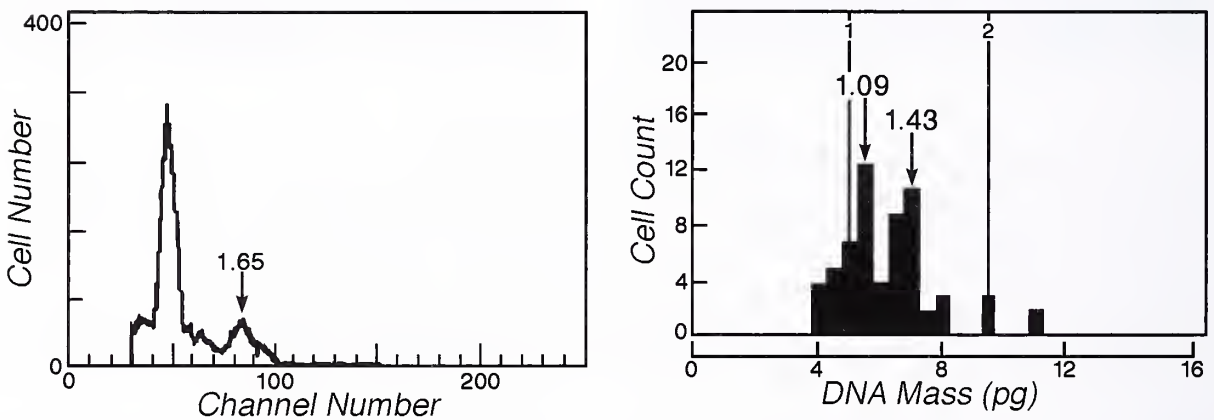

Figure 5-38

ANEUPLOID DNA HISTOGRAM FROM AN ADRENAL CORTICAL ADENOMA

The tumor (4 cm, 23 g) is from a 6-year-old girl with Cushing's syndrome. The patient was alive and well 17 years later. Flow cytometric (left) and image analysis (right) histograms are shown. Note the aneuploid and associated diploid peaks. (Fig. 5-35 from Fascicle 19, Third Series.)

frequent in benign pediatric adrenal cortical tumors (fig. 5-38).

CRITERIA FOR MALIGNANCY AND GRADING

Early studies of ACCs proposed various criteria of malignancy without rigorous testing using statistical methods. Features such as venous invasion, capsular invasion, documentation of distant metastases, extensive necrosis, and marked nuclear pleomorphism with one or more prominent nucleoli (79) were considered to be particularly useful in assessing malignant potential. Recent statistical analyses have identified histologic as well as nonhistologic parameters of

prognostic value. Significant criteria for predicting malignant behavior include clinical evidence of weight loss, broad fibrous bands, diffuse growth pattern, vascular invasion, tumor necrosis, and increased tumor mass, although no single criterion is reliable in separating benign from malignant tumors (80). Weiss (24) reported three histologic features present only in metastasizing/recurring tumors: mitotic rate of 6 or more per 50 high-power fields, atypical mitoses, and venous invasion; this series included cases of relatively small, innocuous ACAs associated with hyperaldosteronism which might skew the statistical analysis. A study using a histologic index identified tumor weight and mitotic activity as parameters with the highest discriminating value (25). ACC can be reliably diagnosed in most cases, but there remains a small group in which it is extremely difficult to reliably predict biologic behavior, and in some cases, use of the designation "adrenal cortical neoplasm of indeterminate malignant potential" may be appropriate (1). Long-term clinical follow-up may prove to be the final arbiter in the diagnosis of these troublesome cases. Although scintigraphic vizualization of a unilateral adrenal cortical neoplasm with ^{131}I-6-beta-iodomethylnorcholesterol (NP-59) has been considered diagnostic of ACA, particularly in a patient with Cushing's syndrome, recent evidence indicates that this finding does not represent uniformly benign disease (81).

The grading of ACC has not been uniform due to the variability in criteria used. Grading has been based upon the extent of cellular pleomorphism, anaplastic versus differentiated (82) or grades 1 through 3 (43), or overall level of differentiation (e.g., Broder grades 1 through 4) (6). More objective criteria have been proposed such as mitotic rate: ACCs having 20 or fewer mitoses per 50 high-power fields are low grade (median survival, 58 months) and tumors with more than 20 mitoses per 50 high power fields are high grade (median survival, 14 months) (34,83).

PROGNOSIS AND PATTERNS OF METASTASIS

The mortality rate for adult patients with ACC ranges from 50 percent mortality within 2 years (84), to 84 percent at 5 years (6), to 90 percent at 10 years (85); many large series report an overall mortality rate of 70 percent or more (1). Death due to metastatic ACC often occurs within the first 12 months after diagnosis, but in some cases there may be a lingering course of up to a decade or more (86). In the study by van Slooten et al. (25), 93 percent of patients developed metastases within 10 years of diagnosis.

Table 5-1

ANATOMIC SITES OF REGIONAL AND DISTANT METASTASES OF ADRENAL CORTICAL CARCINOMA[a,b]

Site	No. (%)
Liver	46 (92)
Lung	39 (78)
Retroperitoneum	24 (48)
Inferior vena cava	14 (28)
Serosa of intestine	11 (22)
Lymph nodes:	
Abdominal	16 (32)
Thoracic	13 (26)
Bone	9 (18)
Peritoneum	8 (16)
Kidney	6 (12)
Diaphragm	6 (12)
Heart	6 (12)
Spleen	4 (8)
Pancreas	4 (8)
Thyroid	3 (6)
Brain	2 (4)
Skin	1 (2)

[a]Table 5-1 from Fascicle 19, Third Series.
[b]Distribution of metastases in 50 autopsies at the National Institutes of Health.

The pattern of metastasis reflects both lymphatic and hematogenous avenues of spread, although there may be local intraabdominal recurrence or peritoneal spread by tumor. Retroperitoneal carcinomatosis is an unusual pattern of dissemination that was recently reported in a patient with primary hyperaldosteronism who had undergone laparoscopic resection of a relatively small adrenal tumor (87). Table 5-1 shows the distribution of metastases of ACCs among 50 patients autopsied at the National Institutes of Health (1). The most common sites of metastases are liver (fig. 5-39), lung (fig. 5-40A), retroperitoneum, and lymph nodes. The inferior vena cava may be invaded by tumor (see fig. 5-27), sometimes with signs of obstruction such as lower extremity edema and ascites.

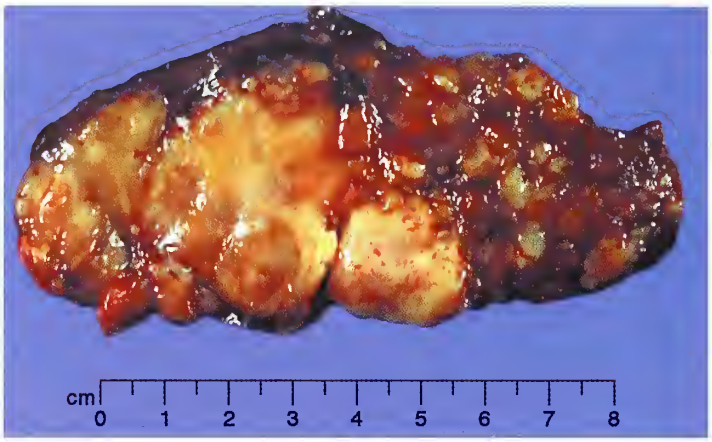

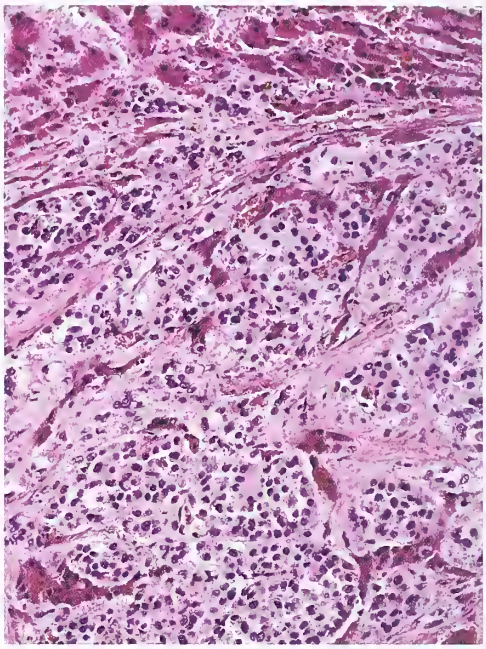

Figure 5-39

ADRENAL CORTICAL CARCINOMA METASTATIC TO LIVER

Above: Hepatic lobectomy specimen is largely replaced by metastatic ACC. The tumor is mottled tan-yellow.

Right: Metastatic ACC disrupts the liver parenchyma and has a large nesting pattern.

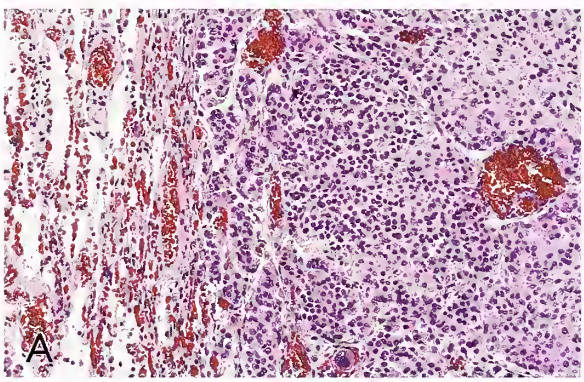

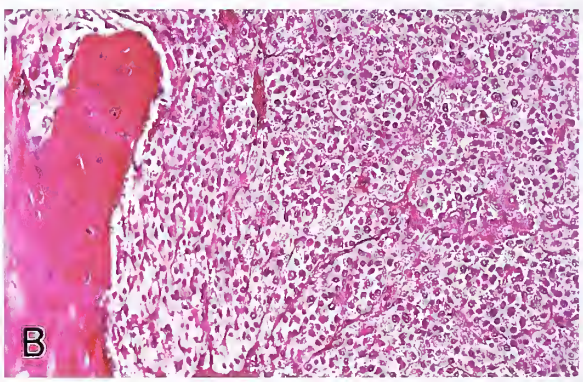

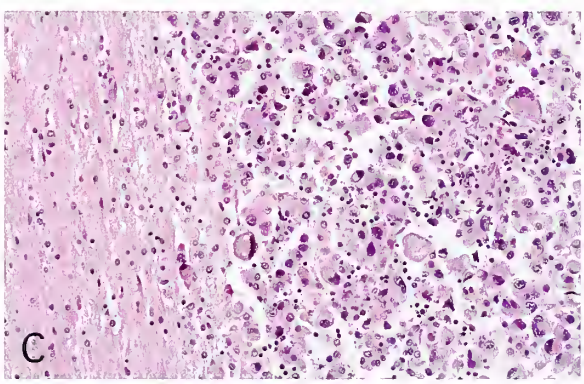

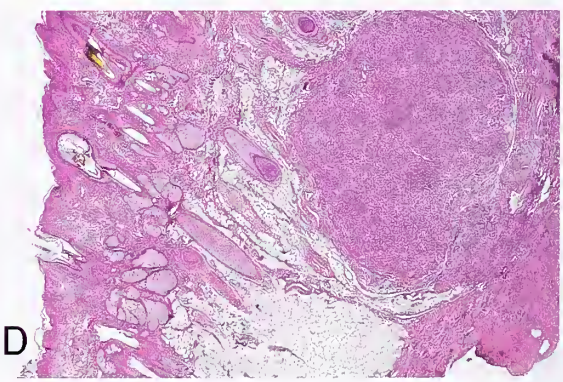

Figure 5-40

OTHER SITES OF METASTASIS BY ADRENAL CORTICAL CARCINOMA

Lung (A) is the second most common site of metastasis by ACC in a series of 50 autopsies performed at the National Institutes of Health. Bone (B) and brain (C) metastases are relatively uncommon (18 percent and 4 percent of cases, respectively) while cutaneous metastasis (D) (a surgically excised nodule on the scalp) is the least common site of involvement (2 percent).

Bony metastases are usually lytic in nature (fig. 5-40B). Metastases to brain (fig. 5-40C) and skin are uncommon. Cutaneous involvement of the scalp has been reported to simulate an angiosarcoma (88), but with clinical correlation there should be little problem in making the correct diagnosis (fig. 5-40D). ACC metastatic to the orbit (89) and breast (90) has also been reported.

STAGING

An extensive review by Wooten and King (3) using the staging criteria proposed by MacFarlane (5) and used by Sullivan et al. (91), showed that most patients with ACC have relatively advanced disease at the time of diagnosis (Table 5-2). Disease-free and overall survival rates strongly correlate with the stage of ACC (92). In the study by Schulick and Brennan (93), patients presenting with early stage I or II disease (n = 57) had a median survival period of 101 months (5-year survival rate, 60 percent), whereas those with late stage III and IV disease (n = 56) had a median survival period of 15 months (5-year survival rate, 10 percent).

Table 5-2

STAGING OF ADRENAL CORTICAL CARCINOMA[a,b,c]

Percent	Stage		Staging Criteria	
2.8	I	T1N0M0	T1	Tumor less than or equal to 5 cm, no invasion
			T2	Tumor greater than 5 cm, no invasion
29.0	II	T2N0M0	T3	Tumor any size, locally invasive but not involving adjacent organs
			T4	Tumor of any size with invasion of adjacent organs
19.3	III	T1N1M0	N0	Negative regional node(s)
		T2N1M0	N1	Positive regional node(s)
		T3N0M0	M0	No distant metastasis
			M1	Distant metastasis
48.9	IV	Any T, any N, T3, N1, T4	M1	

[a]Modified from Table 5-2 from Fascicle 19, Third Series.
[b]Data from references 3, 6, and 91.
[c]TX, primary tumor cannot be assessed; T0, no evidence of primary tumor; NX, regional lymph node(s) cannot be assessed; MX, distant metastasis cannot be assessed.

UNUSUAL VARIANTS OF ADRENAL CORTICAL CARCINOMA

Oncocytic Adrenal Cortical Carcinoma

Several examples of *oncocytic adrenal cortical neoplasms* have been reported; most are clinically benign and nonfunctional (oncocytoma, chapter 4), but on occasion the tumor may be malignant (see fig. 5-20) (94,95). These tumors contain cells rich in mitochondria. Oncocytic features are usually diffuse throughout. Occasionally, there are focal areas with sheets of oncocytic cells in an otherwise typical ACC.

Adrenal Carcinosarcoma

Adrenal carcinosarcoma is a rare adrenal malignancy that combines features of more conventional ACC with areas of sarcoma, including rhabdomyosarcoma (96,97), and areas showing osteogenic and chondroid differentiation (98). An example of adrenal carcinosarcoma is illustrated in figure 5-41. Embryologically, the adrenal cortex is of mesodermal origin, but growth of ACC in part as a sarcoma is exceptional.

Adrenal Cortical Blastoma

A unique *adrenal cortical blastoma* was reported in a young infant (see chapter 6) (99). It is not known whether tumors with this morphology are restricted to the pediatric age group.

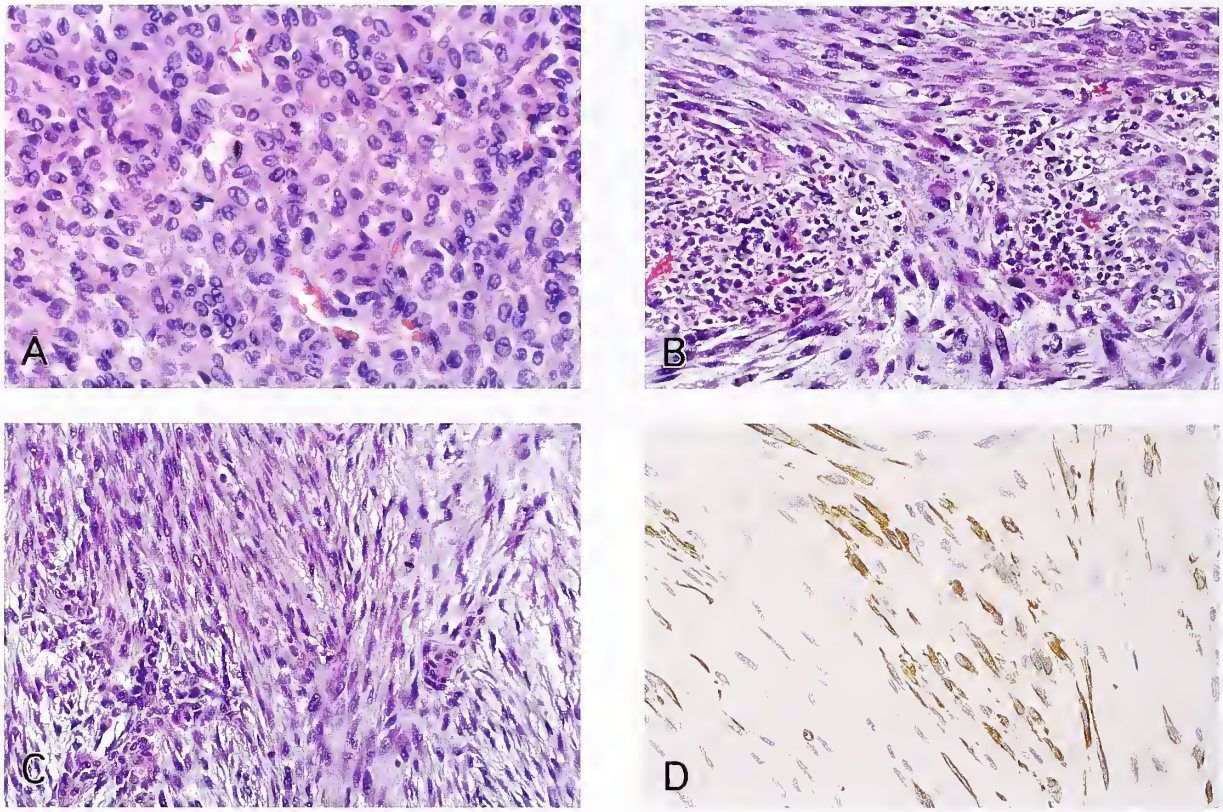

Figure 5-41

ADRENAL CARCINOSARCOMA

A: An ACC from an elderly woman has a diffuse or solid growth pattern. Tumor cells have compact, eosinophilic cytoplasm and a high nuclear to cytoplasmic ratio.

B: Portion of tumor growing as a spindle cell sarcoma. In this field, tumor surrounds smaller cells, probably residual adrenal cortex.

C: A component of tumor growing as sarcoma is composed of intersecting fascicles of spindle cells.

D: The sarcoma portion of the tumor shows cells that are strongly immunoreactive for smooth muscle actin, thus raising the possibility of leiomyosarcoma.

REFERENCES

Incidence, Clinical Aspects, and Pathology

1. Lack EE, Travis WD, Oertel JE. Adrenal cortical neoplasms. In. Lack EE, ed. Pathology of the adrenal glands. New York: Churchill Livingstone; 1990:115-171.
2. Correa P, Chen VW. Endocrine gland cancer. Cancer 1995;75(Suppl 1):338-352.
3. Wooten MD, King DK. Adrenal cortical carcinoma. Epidemiology and treatment with mitotane and a review of the literature. Cancer 1993;72:3145-3155.
4. Ng L, Libertino JM. Adrenocortical carcinoma: diagnosis, evaluation and treatment. J Urol 2003;169:5-11.
5. MacFarlane DA. Cancer of the adrenal cortex; the natural history, prognosis and treatment in a study of fifty-five cases. Ann R Coll Surg Engl 1958;23:155-186.
6. Henley DJ, van Heerden JA, Grant CS, Carney JA, Carpenter PC. Adrenal cortical carcinoma—a continuing challenge. Surgery 1983;94:926-931.

7. Luton JP, Cerdas S, Billaud L, et al. Clinical features of adrenocortical carcinoma, prognostic factors, and the effect of mitotane therapy. N Eng J Med 1990;322:1195-1201.
8. Icard P, Chapuis Y, Andreassian B, Bernard A, Proye C. Adrenocortical carcinoma in surgically treated patients: a retrospective study on 156 cases by the French Association of Endocrine Surgery. Surgery 1992;112:972-980.
9. King DR, Lack EE. Adrenal cortical carcinoma: a clinical and pathologic study of 49 cases. Cancer 1979;44:239-244.
10. Lewinsky BS, Grigor KM, Symington T, Neville AM. The clinical and pathologic features of "nonhormonal" adrenocortical tumors. Report of twenty new cases and review of the literature. Cancer 1974;33:778-790.
11. Huvos AG, Hajdu SI, Brasfield RD, Foote FW Jr. Adrenal cortical carcinoma. Clinicopathologic study of 34 cases. Cancer 1970;25:354-361.
12. Nader S, Hickey RC, Sellin RV, Samaan NA. Adrenal cortical carcinoma. A study of 77 cases. Cancer 1983;52:707-711.
13. Hogan TF, Gilchrist KW, Westring DW, Citrin DL. A clinical and pathological study of adrenocortical carcinoma: therapeutic implications. Cancer 1980;45:2880-2883.
14. D'Agata R, Malozowski S, Barkan A, Cassorla F, Loriaux D. Steroid biosynthesis in human adrenal tumors. Horm Metabol Res 1987;19:386-388.
15. Sasano H, Suzuki T, Nagura H, Nishikawa T. Steroidogenesis in human adrenocortical carcinoma: biochemical activities, immunohistochemistry, and in situ hybridization of steroidogenic enzymes and histopathologic study in nine cases. Hum Pathol 1993;24:397-404.
16. Gazdar AF, Oie HK, Shackleton CH, et al. Establishment and characterization of a human adrenocortical carcinoma cell line that expresses multiple pathways of steroid biosynthesis. Cancer Res 1990;50:5488-5496.
17. O'Hare MJ, Monaghan P, Neville AM. The pathology of adrenocortical neoplasia: a correlated structural and functional approach to the diagnosis of malignant disease. Hum Pathol 1979;10: 137-154.
18. Seccia TM, Fassina A, Nussdorfer GG, Pessina AC, Rossi GP. Aldosterone-producing adrenocortical carcinoma: an unusual cause of Conn's syndrome with an ominous clinical course. Endocr Relat Cancer 2005;12:149-159.
19. Mussig K, Wehrmann M, Horger M, Maser-Gluth C, Haring HU, Overkamp D. Adrenocortical carcinoma producing 11-deoxycorticosterone: a rare cause of mineralocorticoid hypertension. J Endocrinol Invest 2005;28:61-65.
20. Venkatesh S, Hickey RC, Sellin RV, Fernandez JF, Samaan NA. Adrenal cortical carcinoma. Cancer 1989;64:765-769.
21. Orland SM, Stewart AF, LiVolsi VA, Wein AJ. Detection of the hypercalcemic hormone of malignancy in adrenal cortical carcinoma. J Urol 1968;136:1000-1002.
22. Lee KW, Chon SB, Kim DY, et al. Adrenal cortical carcinoma initially presented with overwhelming disseminated intravascular coagulation. Ann Hematol 2003;82:596-598.
23. Stamoulis JS, Antonopoulou Z, Safioleas M. Haemorrhagic shock from the spontaneous rupture of an adrenal cortical carcinoma. A case report. Acta Chir Belg 2004;104:226-228.
24. Weiss LM. Comparative histologic study of 43 metastasizing and nonmetastasizing adrenocortical tumors. Am J Surg Pathol 1984;8:163-169.
25. van Slooten H, Schaberg A, Smeenk D, Moolenaar AJ. Morphologic characteristics of benign and malignant adrenocortical tumors. Cancer 1985;55:766-773.
26. Tang CK, Gray GF. Adrenocortical neoplasms. Prognosis and morphology. Urology 1975;5:691-695.
27. Gandour MJ, Grizzle WE. A small adrenocortical carcinoma with aggressive behavior. An evaluation of criteria for malignancy. Arch Pathol Lab Med 1986;110:1076-1079.
28. Saracco S, Abramowsky C, Taylor S, Silverman RA, Berman BW. Spontaneous regressing adrenocortical carcinoma in a newborn. A case report with DNA ploidy analysis. Cancer 1988; 62:507-511.
29. Erickson LA, Lloyd RV, Hartman R, Thompson G. Cystic adrenal neoplasms. Cancer 2004;101: 1537-1544.
30. Brown FM, Gaffey TA, Wold LE, Lloyd RV. Myxoid neoplasms of the adrenal cortex: a rare histologic variant. Am J Surg Pathol 2000;24:396-401.
31. Izumi M, Serizawa H, Iwaya K, Takeda K, Sasano H, Mukai K. A case of myxoid adrenocortical carcinoma with extensive lipomatous metaplasia. Arch Pathol Lab Med 2003;127:227-230.
32. Neville AM, Symington T. Pathology of primary aldosteronism. Cancer 1966;19:1854-1868.
33. Hoang MP, Ayala AG, Albores-Saavedra J. Oncocytic adrenocortical carcinoma: a morphologic, immunohistochemical and ultrastructural study of four cases. Mod Pathol 2002;15:973-978.
34. Weiss LM, Medeiros LJ, Vickery AL Jr. Pathologic features of prognostic significance in adrenocortical carcinoma. Am J Surg Pathol 1989;13:202-206.
35. Chesson JP, Theodorescu D. Adrenal tumor with caval extension—case report and review of the literature. Scand J Urol Nephrol 2002;36:71-73.

36. Kim JH, Ng CS, Ramani AP, et al. Laparoscopic radical adrenalectomy with adrenal vein tumor thrombectomy: technical considerations. J Urol 2004;171:1223-1226.
37. Hamper UM, Fishman EK, Hartman DS, Roberts JL, Sanders RC. Primary adrenocortical carcinoma: sonographic evaluation with clinical and pathologic correlation in 26 patients. AJR Am J Roentgenol 1987;148:915-919.

Ultrastructural Findings

38. Mackay B, El-Naggar A, Ordonez NG. Ultrastructure of adrenal cortical carcinoma. Ultrastr Pathol 1994;18:181-190
39. Miettinęn M. Neuroendocrine differentiation in adrenocortical carcinoma. New immunohistochemical findings supported by electron microscopy. Lab Invest 1992;66:169-174.

Immunohistochemistry, Molecular Genetics, and Cellular Proliferation

40. Gaffey MJ, Traweek ST, Mills SE, et al. Cytokeratin expression in adrenocortical neoplasia: an immunohistochemical and biochemical study with implications for the differential diagnosis of adrenocortical, hepatocellular and renal cell carcinoma. Hum Pathol 1992;23:144-153.
41. Schröder S, Padberg BC, Achilles E, Holl K, Dralle H, Klöppel G. Immunocytochemistry in adrenocortical tumors: a clinicopathological study of 72 neoplasms. Virchows Arch A Pathol Anat 1992;420:65-70.
42. DeLellis RA, Mangray S. The adrenal glands. In: Mills SE, Carter D, Greenson JK, Oberman HA, Reuter V, Stoler MH, eds. Sternberg's diagnostic surgical pathology. Philadelphia: Lippincott Williams & Wilkins; 2004:621-667.
43. Nakano M. Adrenal cortical carcinoma. A clinicopathological and immunohistochemical study of 91 autopsy cases. Acta Pathol Jpn 1988;38:163-180.
44. Cote RJ, Cordon-Cardo C, Reuter VE, Rosen PP. Immunopathology of adrenal and renal cortical tumors. Coordinated change in antigen expression is associated with neoplastic conversion in the adrenal cortex. Am J Pathol 1990;136:1077-1084.
45. Bornstein SR, Stratakis CA, Chrousos GP. Adrenocortical tumors: recent advances in basic concepts and clinical management. Ann Intern Med 1999;130:759-771.
46. Fogt F, Vargas MP, Zhuang Z, Merino MJ. Utilization of molecular genetics in the differentiation between adrenal cortical adenomas and carcinomas. Hum Pathol 1998;29:518-521.
47. Erickson LA, Jin L, Sebo TJ, et al. Pathologic features and expression of insulin-like growth factor-2 in adrenocortical neoplasms. Endocr Pathol 2001;12:429-435.
48. Sidhu S, Marsh DJ, Theodosopoulos G, et al. Comparative genomic hybridization analysis of adrenocortical tumors. J Clin Endocrinol Metab 2002;87:3467-3474.
49. Pan CC, Chen PC, Tsay SH, Ho DM. Differential immunoprofiles of hepatocellular carcinoma, renal cell carcinoma, and adrenocortical carcinoma: a systemic immunohistochemical survey using tissue array technique. Appl Immunohistochem Mol Morphol 2005;13:347-352.
50. Pelkey TJ, Frierson HF Jr, Mills SE, Stoler MH. The alpha subunit of inhibin in adrenal cortical neoplasia. Mod Pathol 1998;11:516-524.
51. Loy TS, Phillips RW, Linder CL. A103 immunostaining in the diagnosis of adrenal cortical tumors: an immunohistochemical study of 316 cases. Arch Pathol Lab Med 2002;126:170-172.
52. Zhang PJ, Genega EM, Tomaszewski JE, Pasha TL, LiVolsi VA. The role of calretinin, inhibin, melan-A, BCL-2, and C-kit in differentiating adrenal cortical and medullary tumors: an immunohistochemical study. Mod Pathol 2003;16: 591-597.
53. Tartour E, Caillou B, Tenenbaum F, et al. Immunohistochemical study of adrenocortical carcinoma. Predictive value of the D11 monoclonal antibody. Cancer 1993;72:3296-3303.
54. Komminoth P, Saremaslani P, Schröder S, Heitz PU, Roth J. Immunohistochemical marker profiles and polysialic acid expression in pheochromocytomas and adrenocortical carcinomas. Mod Pathol 1994;7:52A.
55. Lack EE. Tumors of the adrenal gland and extraadrenal paraganglia. AFIP Atlas of Tumor Pathology, 3rd Series, Fascice 19. Washington, DC: American Registry of Pathology; 1997.
56. Aubert S, Wacrenier A, Leroy X, et al. Weiss system revisited: a clinicopathologic and immunohistochemical study of 49 adrenocortical tumors. Am J Surg Pathol 2002;26:1612-1619.
57. Stojadinovic A, Brennan MF, Hoos A, et al. Adrenocortical adenoma and carcinoma: histopathological and molecular comparative analysis. Mod Pathol 2003;16:742-751.
58. Suzuki T, Sasano H, Nisikawa T, Rhame J, Wilkinson DS, Nagura H. Discerning malignancy in human adrenocortical neoplasms: utility of DNA flow cytometry and immunohistochemistry. Modern Pathol 1992;5:224-231.
59. Sasano H, Saito Y, Sato I, Sasano N, Nagura H. Nucleolar organizer regions in human adrenocortical disorders. Mod Pathol 1990;3:591-595.

Fine Needle Aspiration Biopsy

60. Wadih GE, Nance KV, Silverman JF. Fine needle aspiration cytology of the adrenal gland. Fifty biopsies in 48 patients. Arch Pathol Lab Med 1992;116:841-846.
61. Ren R, Guo M, Sneige N, Moran CA, Gong Y. Fine-needle aspiration of adrenal cortical carcinoma: cytologic spectrum and diagnostic challenges. Am J Clin Pathol 2006;126:389-398.
62. Suen KC, McNeely TB. Adrenal cortical cells mimicking small cell anaplastic carcinoma in a fine-needle aspirate. Mod Pathol 1991;4:594-595.
63. Mitchell ML, Ryan FP Jr, Shermer RW. Pulmonary adenocarcinoma metastatic to the adrenal gland mimicking normal adrenal cortical epithelium on fine needle aspiration. Acta Cytol 1985;29:994-998.
64. Duggan MA, Forestell CF, Hanley DA. Adrenal metastases of renal-cell carcinoma 19 years after nephrectomy. Fine needle aspiration cytology of a case. Acta Cytopathol 1987;31:512-516.
65. Unger P, Hague K, Klein G, Gordon RE, Thung SN, Szporn A. Fine needle aspiration of a renal cell carcinoma with eosinophilic globules. A case report. Acta Cytol 1993;37:201-204.

DNA Quantitation and Ploidy Patterns

66. Joensuu H, Klemi PJ. DNA aneuploidy in adenomas of endocrine organs. Am J Pathol 1988;132:145-151.
67. Haak HR, Cornelisse CJ, Hermans J, Cobben L, Fleuren GL. Nuclear DNA content and morphological characteristics in the prognosis of adrenocortical carcinoma. Br J Cancer 1993;68:151-155.
68. Favara BE, Steele A, Grant JH, Steele P. Adrenal cytomegaly: quantitative assessment by image analysis. Pediatr Pathol 1991;11:521-536.
69. Klein FA, Kay S, Ratliff JE, White FK, Newsome HH. Flow cytometric determination of ploidy and proliferation patterns of adrenal neoplasms: an adjunct to histological classification. J Urol 1985;134:862-866.
70. Bowlby LS, DeBault LE, Abraham SR. Flow cytometric analysis of adrenal cortical tumor DNA. Relationship between cellular DNA and histopathologic classification. Cancer 1986;58:1499-1505.
71. Hosaka Y, Rainwater LM, Grant CS, et al. Adrenocortical carcinoma: nuclear deoxyribonucleic acid ploidy studies by flow cytometry. Surgery 1987;102:1027-1034.
72. Taylor SR, Roederer M, Murphy RF. Flow cytometric DNA analysis of adrenocortical tumors in children. Cancer 1987;59:2059-2063.
73. Blanes A, Diaz-Cano SJ. DNA and kinetic heterogeneity during the clonal evolution of adrenocortical proliferative lesions. Hum Pathol 2006;37:1295-1303.
74. Amberson JB, Vaughan ED Jr, Gray GF, Naus GJ. Flow cytometry analysis of nuclear DNA from adrenocortical neoplasms. A retrospective study using paraffin-embedded tissue. Cancer 1987;59:2091-2095.
75. Cibas ES, Medeiros LJ, Weinberg DS, Gelb AB, Weiss LM. Cellular DNA profiles of benign and malignant adrenocortical tumors. Am J Surg Pathol 1990;14:948-955.
76. Camuto P, Schinella R, Gilchrist K, Citrin D, Fredrickson G. Adrenal cortical carcinoma: flow cytometric study of 22 cases. An ECOG study. Urology 1991;37:380-384.
77. Zerbini C, Kozakewich HP, Weinberg DS, Mundt DJ, Edwards JA III, Lack EE. Adrenocortical neoplasms in childhood and adolescence: analysis of prognostic factors including DNA content. Endocr Pathol 1992;3:116-128.
78. Bugg MF, Ribeiro RC, Roberson PK, et al. Correlation of pathologic features with clinical outcome in pediatric adrenocortical neoplasia. A study of a Brazilian population. Brazilian Group for Treatment of Childhood Adrenocortical Tumors. Am J Clin Pathol 1994;101:625-629.

Criteria for Malignancy and Grading

79. O'Hare MJ, Monaghan P, Neville AM. The pathology of adrenocortical neoplasia: a correlated structural and functional approach to the diagnosis of malignant disease. Hum Pathol 1979;10:137-154.
80. Hough AJ, Hollifield JW, Page DL, Hartmann WH. Prognostic factors in adrenal cortical tumors. A mathematical analysis of clinical and morphologic data. Am J Clin Pathol 1979;72:390-399.
81. Pasieka JL, McLeod MK, Thompson NW, Gross MD, Schteingart DE. Adrenal scintigraphy of well-differentiated (functioning) adrenocortical carcinomas: potential surgical pitfalls. Surgery 1992;112:884-890.
82. Karakousis CP, Rao U, Moore R. Adrenal adenocarcinomas: histologic grading and survival. J Surg Oncol 1985;29:105-111.
83. Medeiros LJ, Weiss LM. New developments in the pathologic diagnosis of adrenal cortical neoplasms. A review. Am J Clin Pathol 1992;97:73-83.

Prognosis and Patterns of Metastases

84. Lipsett MB, Hertz R, Ross GT. Clinical and pathophysiologic aspects of adrenocortical carcinoma. Am J Med 1963;35:374-383.

85. Venkatesh S, Hickey RC, Sellin RV, Fernandez JF, Samaan NA. Adrenal cortical carcinoma. Cancer 1989;64:765-769.
86. Meyer A, Behrend M. Long-term survival over 28 years of a patient with metastatic adrenal cortical carcinoma—case report. Anticancer Res 2004;24:1901-1904.
87. Deckers S, Derdelinckx L, Col V, Hamels J, Maiter D. Peritoneal carcinomatosis following laparoscopic resection of an adrenocortical tumor causing primary hyperaldosteronism. Horm Res 1999;52:97-100.
88. Milchgrub S, Wiley EL. Adrenal carcinoma presenting as a lesion resembling a cutaneous angiosarcoma. Cancer 1991;67:3087-3092.
89. Bartley GB, Campbell RJ, Salomao DR, Bradley EA, Marsh WR, Bite U. Adrenocortical carcinoma metastatic to the orbit. Ophthal Plast Reconstr Surg 2001;17:215-220.
90. Francois C, Rangachari B, Bova D. Mammography and sonography of pathologically proven adrenal cortical carcinoma metastatic to the breast. AJR Am J Roentgenol 2005;184:1279-1281.

Staging

91. Sullivan M, Boileau M, Hodges CV. Adrenal cortical carcinoma. J Urol 1978;120:660-665.
92. Icard P, Goudet P, Charpenay C, et al. Adrenocortical carcinomas: surgical trends and results of a 253-patient series from the French Association of Endocrine Surgeons study group. World J Surg 2001;25:891-897.
93. Schulick RD, Brennan MF. Long-term survival after complete resection and repeat resection in patients with adrenocortical carcinoma. Ann Surg Oncol 1999;6:719-726.

Unusual Variants

94. Hoang MP, Ayala AG, Albores-Saavedra J. Oncocytic adrenocortical carcinoma: a morphologic, immunohistochemical and ultrastructural study of four cases. Mod Pathol 2002;15:973-978.
95. Bisceglia M, Ludovico O, Di Mattia A, et al. Adrenocortical oncocytic tumors: report of 10 cases and review of the literature. Int J Surg Pathol 2004;12:231-243.
96. Decorato JW, Gruber H, Petti M, Levowitz BS. Adrenal carcinosarcoma. J Surg Oncol 1990;45: 134-136.
97. Fischler DF, Nunez C, Levin HS, McMahon JT, Sheeler LR, Adelstein DJ. Adrenal carcinosarcoma presenting in a woman with clinical signs of virilization. A case report with immunohistochemical and ultrastructural findings. Am J Surg Pathol 1992;16:626-631.
98. Barksdale SK, Marincola FM, Jaffe G. Carcinosarcoma of the adrenal cortex presenting with mineralocorticoid excess. Am J Surg Pathol 1993;17:941-945.
99. Molberg K, Vuitch F, Stewart D, Albores-Saavedra J. Adrenocortical blastoma. Hum Pathol 1992; 23:1187-1190.

6 ADRENAL CORTICAL NEOPLASMS IN CHILDHOOD

Adrenal cortical neoplasms are uncommon in childhood. They are described separately, however, since they can differ significantly from similar neoplasms in adults with regard to epidemiology, clinical manifestations, and biologic behavior, particularly those of early infancy. The biologic behavior of some of these adrenal cortical neoplasms can be difficult to predict, even when the tumor has clearly adverse prognostic findings similar to those outlined in chapter 5 for tumors in adults.

INCIDENCE AND EPIDEMIOLOGY

Of 141 cases of adrenal neoplasms in the Manchester Children's Tumor Registry prior to 1973, 92 percent were classified as neuroblastoma, 6 percent as adrenal cortical carcinoma (ACC), and 2 percent as pheochromocytoma (1). Based upon an update of the third National Cancer Survey, ACC now comprises an estimated 0.2 percent of childhood malignancies in white patients under 15 years of age; about 13 new cases are diagnosed yearly in the United States (2). The annual incidence of all malignant neoplasms in children under 15 years of age is 124.5/million in whites and 97.8/million in blacks (3).

Updates of this cancer survey continue in different regions of the United States as an ongoing monitoring of cancer incidence in the form of the SEER (Surveillance, Epidemiology, and End Results) Program of the National Cancer Institute (4). From 1973 through 1987, 28 ACCs were recorded in patients under age 20 years, indicating an estimated 19 new cases a year. The SEER Program does not track benign neoplasms such as adrenal cortical adenoma (ACA), and assuming that about 26 percent of all adrenal cortical neoplasms are ACA (or classified pathologically as such), an estimated 25 adrenal cortical tumors occur each year in the United States in patients under 20 years of age (5). The annual incidence rate is about 3/million children under 20 years; rates are slightly higher in females than males (fig. 6-1), but the sex difference appears to be limited to the first 5 years of life (5). Only 6 percent of ACCs occur in patients under age 20 years of age (5), the age at which a modal peak is formed, in addition to that seen in adults (5,6).

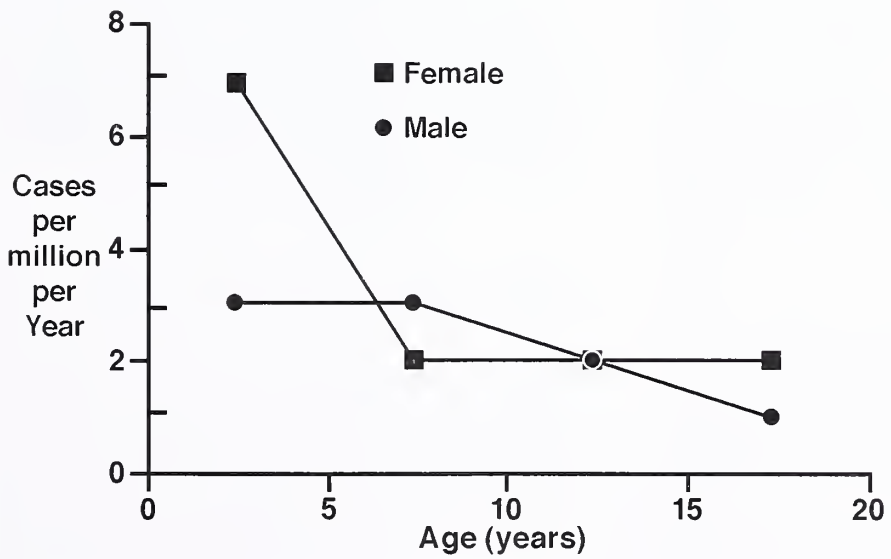

Figure 6-1

ADRENAL CORTICAL CARCINOMA

Sex- and age-specific incidence of adrenal cortical carcinoma in the United States, 1973-1987. (Fig. 1 from Lack EE, Mulvihill JJ, Travis WD, Kozakewich HP. Adrenal cortical neoplasms in the pediatric and adolescent age group. Clinicopathological study of 30 cases with emphasis on epidemiological and prognostic factors. Pathol Annu 1992;27:1-53.)

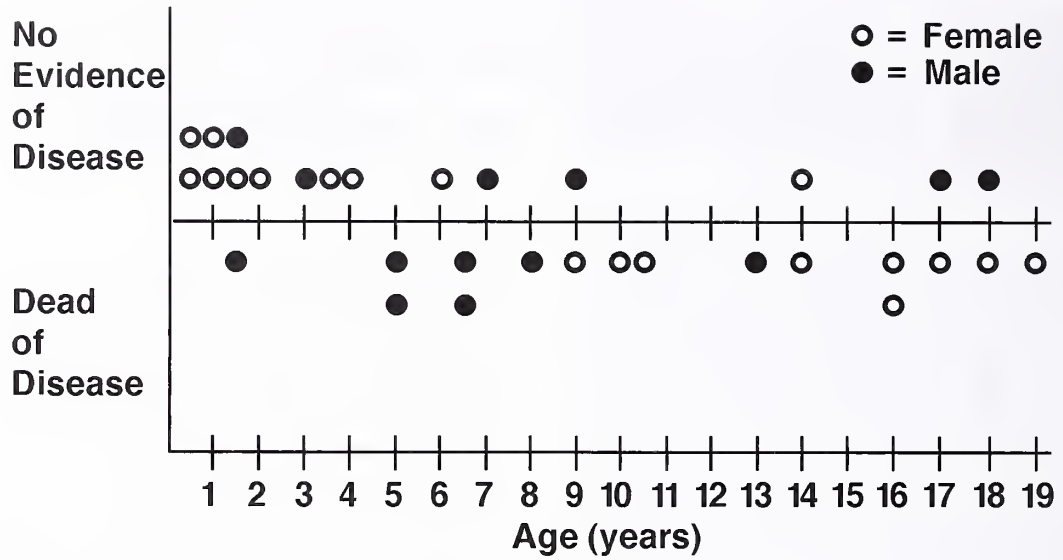

Figure 6-2

CLINICAL OUTCOME OF PATIENTS WITH ADRENAL CORTICAL TUMORS

Age and sex distribution of 32 children and adolescents with adrenal cortical tumors plotted according to clinical outcome, i.e., no evidence of disease or dead of disease. One patient in group A (no evidence of recurrent or metastatic adrenal tumor) and one in group B (recurrent or metastatic tumor) developed second primary tumors and died. Another child in group A died suddenly 1 year after diagnosis. (Fig. 1 from Zerbini C, Kozakewich HP, Weinberg DS, Mundt DJ, Edwards JA III, Lack EE. Adrenocortical neoplasms in childhood and adolescence: analysis of prognostic factors including DNA content. Endocr Pathol 1992;3:116-128.)

AGE, SEX DISTRIBUTION, AND LATERALITY

In a study of 32 patients (19 females, 13 males) with adrenal cortical neoplasms, the average age at diagnosis was 8 years (range, 6 months to 19 years), with a median age of 5 years. There was a clustering of cases in the age group of 5 years or less (fig. 6-2) (7). A similar clustering of cases in this younger age group was seen in a large series of cases (8) and in a comprehensive review of reported cases (9). Congenital adrenal cortical neoplasms are extremely rare and in a recent review, 23 cases were identified in the medical literature (10). A recent literature review of adrenal cortical neoplasms in childhood indicated a predominance in girls (female to male ratio, 2 to 1) (9). Adrenal cortical tumors constitute only about 0.2 percent of all pediatric malignancies; there is apparently a remarkably high incidence in southern Brazil (11). A registry has been established for pediatric adrenal cortical tumors and in a recent report of 254 patients, the female to male ratio was 1.6 to 1.0 (12). An uneven age distribution has been noted in the first two decades of life, with an "infantile group" having a peak incidence in the first year of life, and an "adolescent group" with the peak more evenly distributed between 9 and 16 years (13).

In a review by Lack et al. (5), 18 tumors arose in the right adrenal gland (60 percent) and 12 in the left (40 percent). Bilateral adrenal cortical tumors are extremely rare, as are ectopic tumors. A fascinating case of congenital ACC was reported in which the newborn had apparent spontaneous regression of cutaneous metastases and cerebral lesions (14).

CLINICAL FEATURES

Most children with an adrenal cortical neoplasm have signs or symptoms of an endocrine abnormality; fewer than 10 percent have no endocrine syndrome at presentation (11). In a large review of reported series, the rate of functionally active tumors was over 80 percent (9). Most children present with virilization, followed by Cushing's syndrome, which is often (60 percent) a mixed endocrine syndrome with virilization (5); pure Cushing's syndrome is

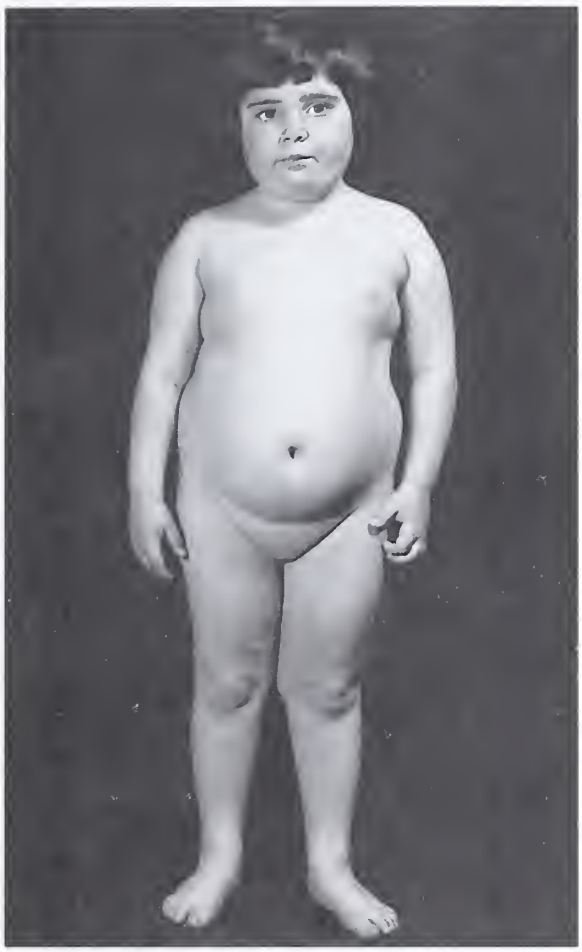

Figure 6-3

ADRENAL CORTICAL ADENOMA WITH CUSHING'S SYNDROME

A 6-year-old girl with "pure" Cushing's syndrome had an 11-month history of obesity, increasing abdominal girth, and hirsutism. The child had facial plethora. The generalized obesity was more pronounced centrally. Cutaneous striae were evident over the upper thighs and lower abdomen. The patient was alive and well 17 years following right adrenalectomy. The resected tumor weighed 23 g and measured 4 cm in diameter. (Fig. 6-3 from Fascicle 19, Third Series.)

Figure 6-4

ADRENAL CORTICAL CARCINOMA WITH VIRILIZATION

Virilization in a 3½-year-old female due to a right adrenal cortical tumor (classified pathologically as an adrenal cortical carcinoma). The tumor weighed 110 g and measured 7.5 cm in diameter. Clitoromegaly was noted shortly after birth. The child displayed remarkable development in terms of size and strength during the 2nd and 3rd years. She had a low-pitched voice, very well-developed musculature, and abundant pubic hair. The child died suddenly 1 year following surgical removal of the adrenal tumor, but there was no evidence of recurrent or metastatic tumor. (Fig. 14 from Lack EE, Mulvihill JJ, Travis WD, Kozakewich HP. Adrenal cortical neoplasms in the pediatric and adolescent age group. Clinicopathological study of 30 cases with emphasis on epidemiological and prognostic factors. Pathol Annu 1992;27:1-53.) (Figs. 6-4, 6-6, and 6-14 from the same case.)

uncommon. While obesity is reported by some to have a more truncal distribution in adults, in infants it tends to be generalized, with involvement of the extremities as well as the trunk (fig. 6-3). Feminization as a pure endocrine syndrome is unusual, particularly in childhood, as is primary hyperaldosteronism (15). Adrenal cortical tumors that secrete androgens exclusively are uncommon (16,17).

The features of virilization in females include increased muscle mass, sometimes resulting in a "herculean" habitus (fig. 6-4), as well as clitoromegaly (figs. 6-5, 6-6), facial hair, deepening of the voice, and the appearance of pubic hair (fig. 6-7). Excess androgen secretion in male patients usually causes isosexual precocity with penile enlargement and pubic hair (fig.

Figure 6-5

ADRENAL CORTICAL ADENOMA WITH VIRILIZATION

In a young girl, virilization is apparent as mild pubic hair and slight clitoral enlargement.

Figure 6-6

VIRILIZATION WITH MARKED CLITOROMEGALY

The clitoris in this 3½-year-old girl measured 3.5 cm in length and the glans measured 1.4 x 1.5 cm. (Fig. 14C from Lack EE, Mulvihill JJ, Travis WD, Kozakewich HP. Adrenal cortical neoplasms in the pediatric and adolescent age group. Clinicopathological study of 30 cases with emphasis on epidemiological and prognostic factors. Pathol Annu 1992;27:1-53.)

6-8) (5). Conversion of an endocrine syndrome of virilization to feminization has been reported (18). On rare occasion, the clinical presentation can mimic pheochromocytoma. Feminization in the male is usually associated with breast enlargement (gynecomastia), which may be symmetric or asymmetric (fig. 6-9). Rupture of an ACC is a rare cause of pediatric acute abdomen (19).

GROSS FINDINGS

Adrenal cortical tumors can range widely in size (2.4 to 19.0 cm) and weight (18 to 6,000 g) (5). In a study of 32 adrenal cortical neoplasms in children and adolescents, patients were segregated into two general groups: group A (15 patients) consisted of patients who were alive (or died of other causes) without evidence of recurrent or metastatic adrenal cortical neoplasm (i.e., clinically benign tumors) and group B (17 patients) had documented metastases or fatal outcome due to tumor (i.e., clinically malignant tumors) (7). Included in group A were tumors classified on initial pathology review as ACA (5 tumors), ACC (9 tumors), and indeterminate malignant potential (1 tumor). The average size of tumors in group A was 5.8 cm (median weight, 44 g) (fig. 6-10), while tumors in group B were significantly larger (11.9 cm) with a median weight of 560 g (7). In the review by Neblett et al. (20), 27.9 percent of childhood adrenal cortical neoplasms were classified pathologically as ACA (average weight of 43.3 g, average diameter of 4.6 cm), and 72.1 percent as ACC (average weight of 466.8 g, average diameter of 8.6 cm); this classification was based upon gross and microscopic features and not on biologic behavior. The average weight of ACAs in the study by Weatherby and Carney was 54 g (range, 30 to 122 g) (15). The gross appearance of some tumors can easily lead to a presumptive diagnosis of ACC (fig. 6-11). Even some of the smaller tumors, however, which prove to be clinically benign, have areas of tumor necrosis

Figure 6-7

MIXED ENDOCRINE SYNDROME

A 1-year-old female had a mixed endocrine syndrome consisting of virilization and Cushing's syndrome. Increased body hair is present in the pubic region, thighs, and lower abdomen. The child also had clitoromegaly. A right adrenal tumor (classified pathologically as adrenal cortical carcinoma) weighed 44 g and measured 5 cm in diameter. The patient was alive and well 9 years later. (Fig. 6-6 from Fascicle 19, Third Series.)

Figure 6-8

ADRENAL CORTICAL CARCINOMA WITH VIRILIZATION

A 6½-year-old boy came to medical attention because of penile enlargement, appearance of pubic hair, and recent onset of abdominal pain. Radiographs of hands and wrists showed advanced bone age. The child had pulmonary and hepatic metastases at presentation. The adrenal tumor weighed 475 g and measured 15 cm in diameter. The tumor invaded the inferior vena cava and the child died intraoperatively due to massive tumor embolization to the right ventricle and main pulmonary artery. (Fig. 15 from Lack EE, Mulvihill JJ, Travis WD, Kozakewich HP. Adrenal cortical neoplasms in the pediatric and adolescent age group. Clinicopathological study of 30 cases with emphasis on epidemiological and prognostic factors. Pathol Annu 1992;27:1-53.)

Figure 6-9

FEMINIZING ADRENAL CORTICAL CARCINOMA ASSOCIATED WITH GYNECOMASTIA

A young boy from South America has asymmetric gynecomastia due to a feminizing adrenal cortical carcinoma. The patient had recently undergone surgical resection of the right adrenal tumor.

Figure 6-10

ADRENAL CORTICAL CARCINOMA

Adrenal cortical carcinoma from a 7-month-old female with virilization. The tumor weighed 27 g and had confluent areas of necrosis (25 percent), dystrophic calcification, broad trabecular growth pattern, about 10 mitoses per 50 high-power fields, and atypical mitoses. The child was alive and well about 4 years later. India ink has been applied to the surgical margin of resection. (Fig. 6-11 from Fascicle 19, Third Series.)

(fig. 6-10), but such areas are seldom more than 25 percent in visual estimation of extent in histologic sections.

MICROSCOPIC FINDINGS

The histopathologic features of adrenal cortical tumors shown in Table 6-1 are from a review by Zerbini et al. (7), along with the tumors that were initially classified as ACCs in their study of groups A and B (7). From this table it is apparent that many of the pediatric tumors that prove to be clinically benign have the adverse morphologic findings commonly associated with malignancy in tumors from adult patients. Most tumors have architectural patterns that can be classified as alveolar (or nesting), diffuse (or solid), trabecular, or an admixture of these major patterns (fig. 6-12). An alveolar or blunt cord-like pattern is most common in tumors classified pathologically as ACA. Nuclear pleomorphism and hyperchromasia can be found in both ACA (fig. 6-13) and ACC, and this finding alone is usually not helpful in distinguishing between the two. Rarely, a tumor has oncocytic features as evidenced by greatly enlarged cells with abundant granular, eosinophilic cytoplasm (fig. 6-14) or a myxoid pattern (fig. 6-15). Occasionally, there appears to be capsular invasion in an otherwise clinically benign tumor (fig. 6-16); similar to cortical neoplasms in adults, capsular invasion may be difficult to recognize in histologic sections. At times, a priori evidence of capsular invasion or extraadrenal extension can be assumed by intraoperative assessment or gross examination. Other rare histologic features that are encountered include pseudoglandular areas (fig. 6-17, left) and extramedullary hematopoiesis (fig. 6-17, right).

Some tumors that prove to be clinically benign have areas of confluent necrosis (fig. 6-18), sometimes with small amounts of dystrophic calcification. Cagle et al. (21) found that clinically benign adrenal cortical tumors in children were significantly more likely to have mitoses, necrosis, broad fibrous bands, and moderate to marked pleomorphism than tumors in adults. Significant necrosis (25 percent

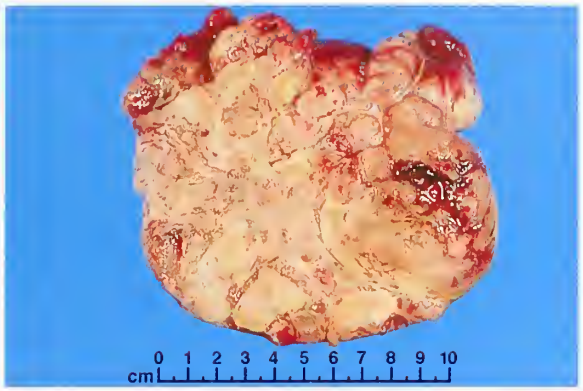

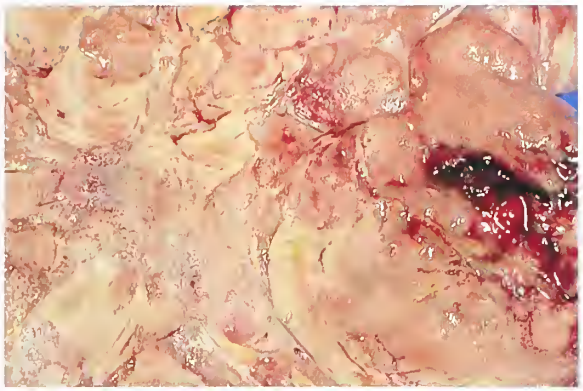

Figure 6-11

ADRENAL CORTICAL CARCINOMA

Left: Adrenal cortical carcinoma from a 16-year-old girl with virilization. The tumor weighed 1,250 g and measured 15.5 cm in diameter. The patient died 14 months following surgical resection due to massive intraabdominal recurrence and metastases to lung, liver, and peritoneum. Neoplasm in cross section is coarsely nodular and most of the tumor is necrotic. Geographic zones of pale-yellow tumor necrosis are confluent. (L&R: Fig. 6-10 from Fascicle 19, Third Series.)

Right: Viable areas of the same tumor appear as bulging tan nodules. The tumor had intersecting fibrous bands.

Table 6-1

HISTOPATHOLOGIC FEATURES OF ADRENAL CORTICAL TUMORS[a]

	Group A (n = 15)[b]	Group B (n = 17)
Number initially classified as ACC[c]	9/15 (60%)	17/17 (100%)
Number with mitotic figures	10/15 (67%)	16/17 (94%)
Average number mitoses (range)	11 per 50 high-power fields (1-61)	31 per 50 high-power fields (1-88)
Atypical mitoses	4/15 (27%)	5/17 (29%)
Tumor necrosis (greater than 25%)	3/15 (20%) (7 of 17 tumors had necrosis)	10/17 (59%) (15 of 17 tumors had necrosis)
Vascular invasion	1/15 (7%)	4/17 (24%)
Capsular invasion	6/15 (37%)	6/17 (35%)
Broad fibrous bands	4/15 (27%)	7/17 (41%)
Calcifications	5/15 (33%)	11/17 (65%)

[a]Table 5 from Zerbini C, Kozakewich HP, Weinberg DS, Mundt DJ, Edwards JA 3rd, Lack EE. Adrenocortical neoplasms in childhood and adolescence: analysis of prognostic factors including DNA content. Endocr Pathol 1992;3:116-28.

[b]Group A patients were alive (or dead of other causes) without evidence of recurrent or metastatic tumor; group B patients had documented metastasis, recurrence, or fatal outcome because of adrenal tumor. Note the number of cases initially classified as ACC in group A (60%) and group B (100%).

[c]ACC = adrenal cortical carcinoma.

or more by visual estimation in histologic sections), however, has been found to be an adverse prognostic finding (7). A broad anastomosing trabecular pattern can be found in both benign and malignant cortical neoplasms in childhood, although it is more prevalent in clinically malignant tumors.

Depending upon the plane of section, an attached (fig. 6-19) or what appears to be a free-floating portion of tumor within a vascular sinusoid is seen; careful inspection may reveal a continuous layer of endothelial cells indicating that this is probably not true vascular invasion. This may be similar to the sinusoidal invasion

Figure 6-12

ADRENAL CORTICAL ADENOMA

A: This tumor in a young child with virilization is composed of cells with predominantly compact, eosinophilic cytoplasm. The tumor had a predominantly trabecular pattern. There were about 10 mitotic figures per 50 high-power fields; one is present near the center of the field.

B: In a different case with virilization, the adenoma has an alveolar pattern with short cords and trabeculae.

C: Diffuse (or solid) growth in adrenal cortical adenoma from a 3-year-old female. Nuclei are moderately pleomorphic. Two nuclear pseudoinclusions are near the center of the field.

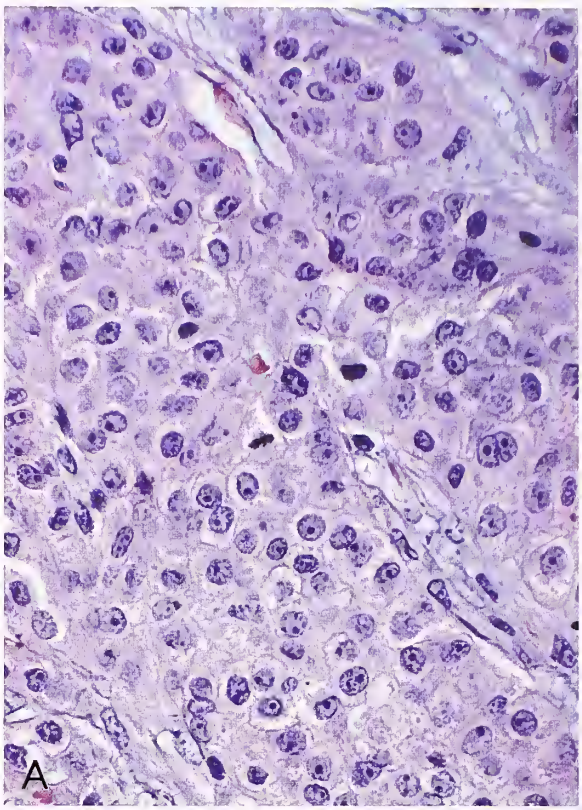

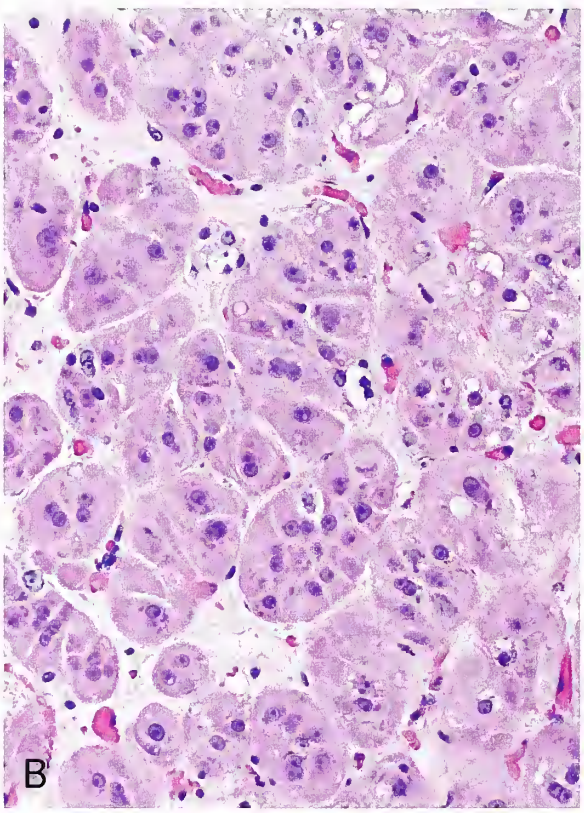

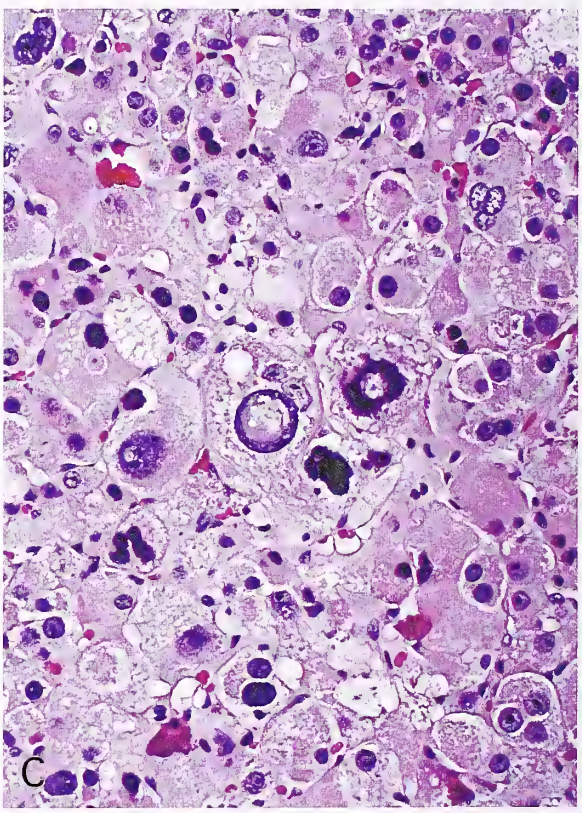

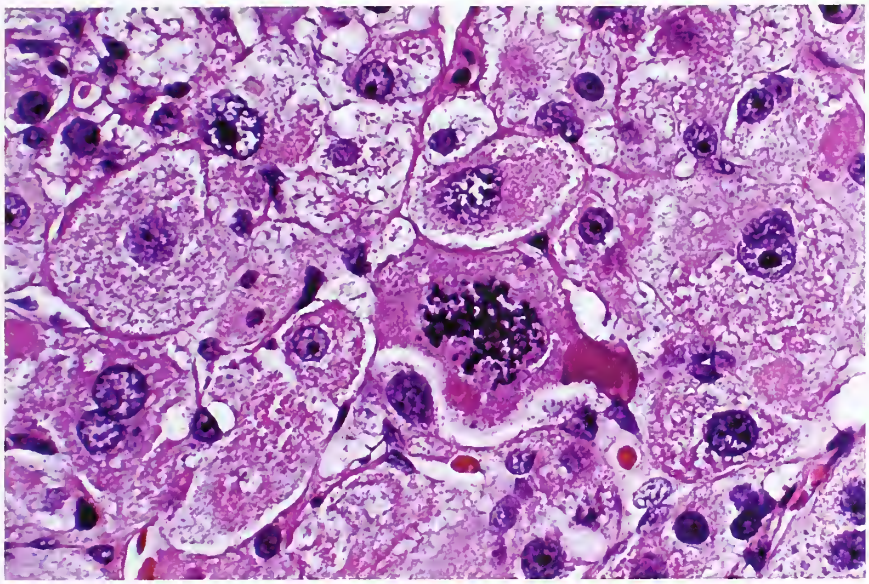

Figure 6-13

MASCULINIZING ADRENAL CORTICAL ADENOMA

This tumor in a 1½ -year-old male weighed 18 g and was 5 cm in diameter. There is nuclear pleomorphism and hyperchromasia, along with an atypical mitotic figure near the center of the field. The patient was alive and well 17 years later, but eventually died of massive liposarcoma of the retroperitoneum.

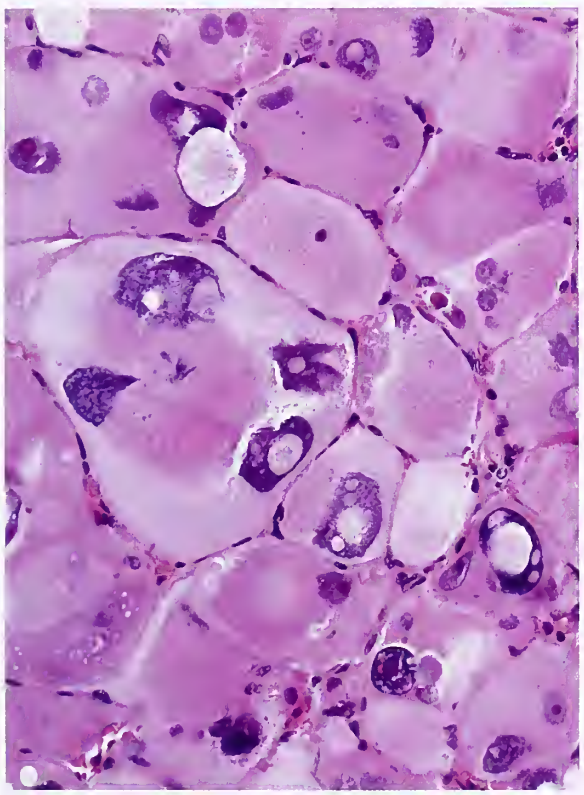

Figure 6-14

VIRILIZING ADRENAL CORTICAL NEOPLASM

This neoplasm from a 3½ -year-old female was classified initially as a carcinoma. The tumor cells have abundant cytoplasm, which is compact and eosinophilic. Numerous nuclear pseudoinclusions are evident. (Fig. 6-14 from Fascicle 19, Third Series.)

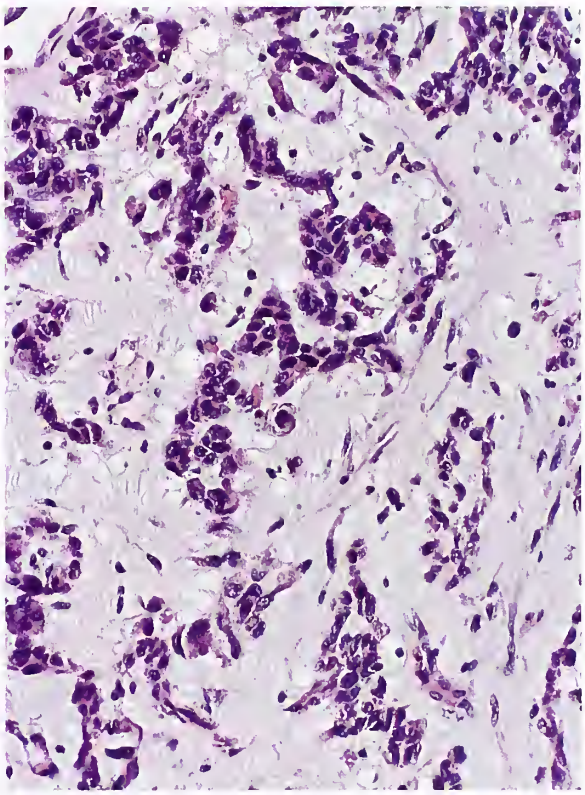

Figure 6-15

ADRENAL CORTICAL ADENOMA

Tumor from a young child with hypertension shows a marked myxoid stromal component. (Fig. 6-15 from Fascicle 19, Third Series.)

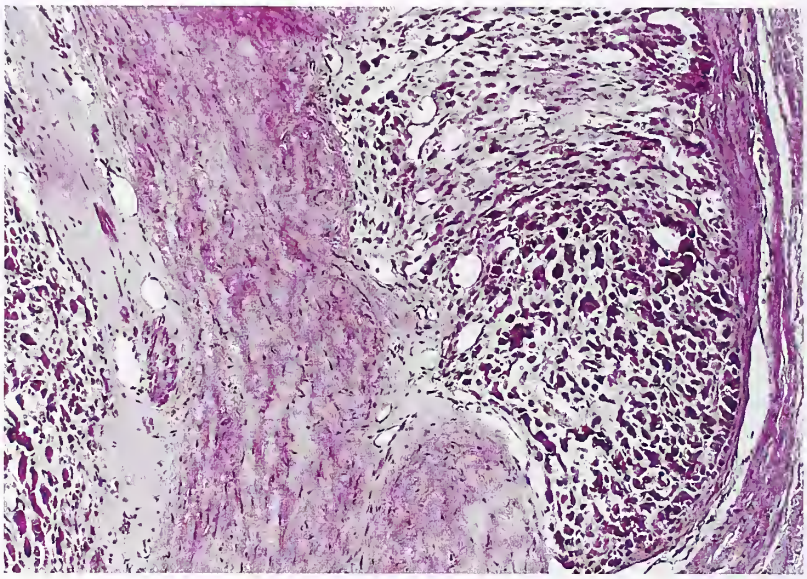

Figure 6-16

ADRENAL CORTICAL ADENOMA

This fibrous capsule (or pseudocapsule) was well-developed except for a few areas where tumor extended into and almost through as blunt, "mushroom-like" projections. A thin portion of connective tissue at the right represents the capsule of the adrenal gland. (Fig. 6-16 from Fascicle 19, Third Series.)

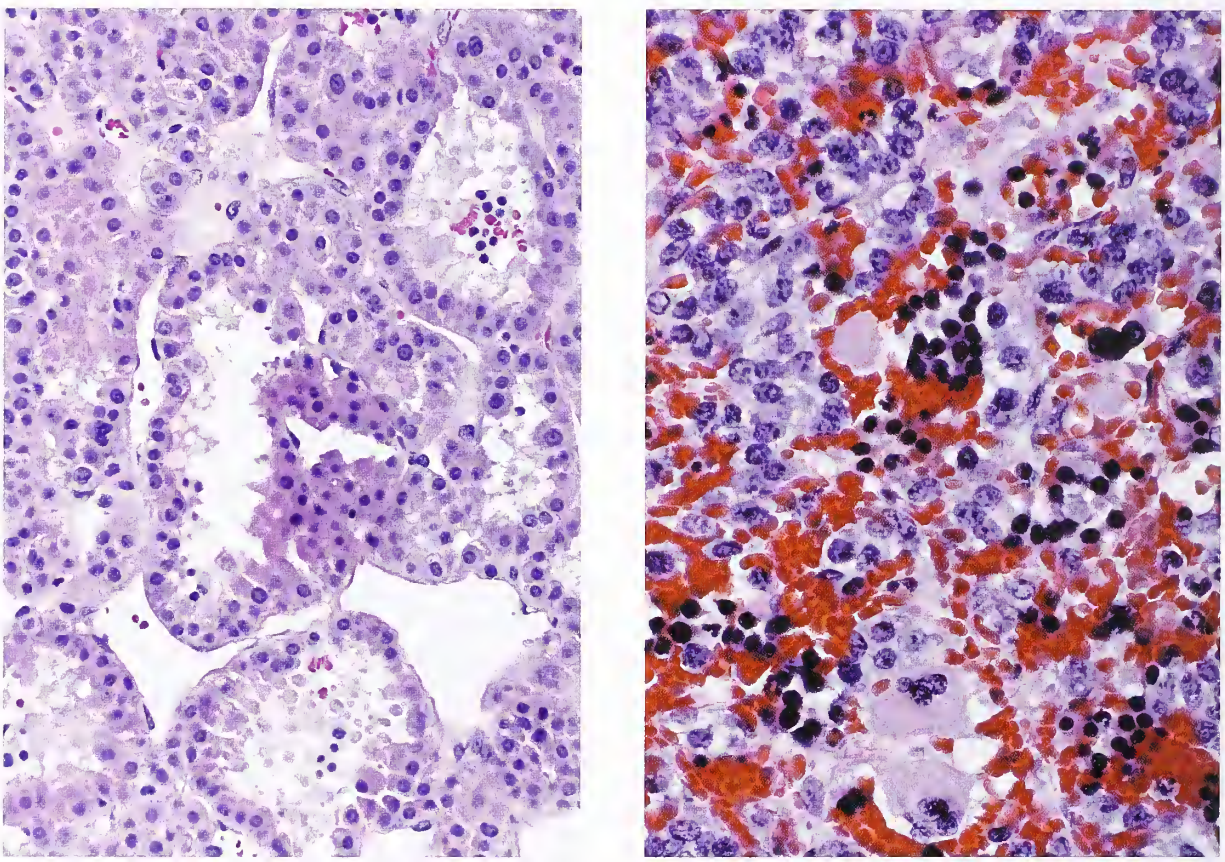

Figure 6-17

VIRILIZING ADRENAL CORTICAL ADENOMA

Left: Tumor from a 14-year-old girl has a trabecular pattern with dyscohesion of cells forming gland-like spaces.

Right: Tumor from a 7-day-old female had hemorrhagic foci with components of extramedullary hematopoiesis. Erythroid precursors and a few megakaryocytes are present at the bottom of the field.

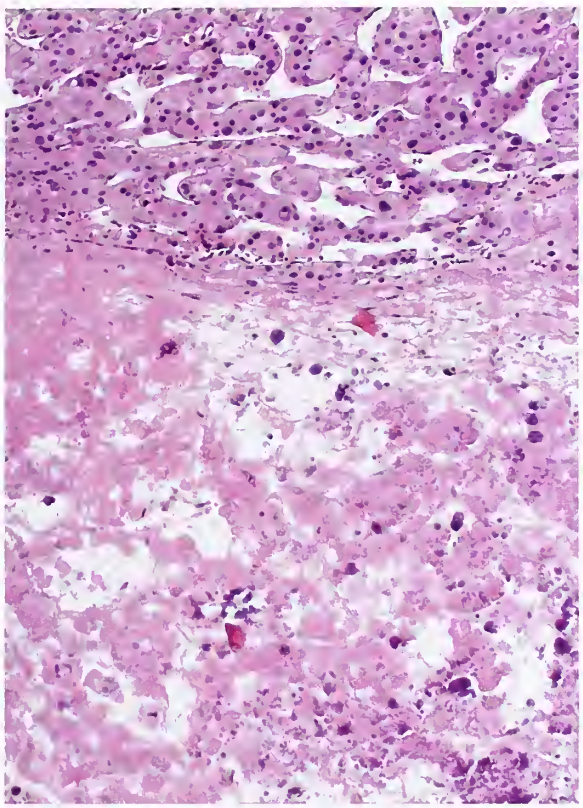

Figure 6-18

VIRILIZING ADRENAL CORTICAL NEOPLASM

This virilizing adrenal cortical neoplasm from a 7-month-old female was classified pathologically as carcinoma. The tumor had confluent areas of necrosis (25 percent total area in histologic sections) as well as spotty dystrophic calcification. The patient was alive and well 3½ years later. (Fig. 6-17 from Fascicle 19, Third Series.)

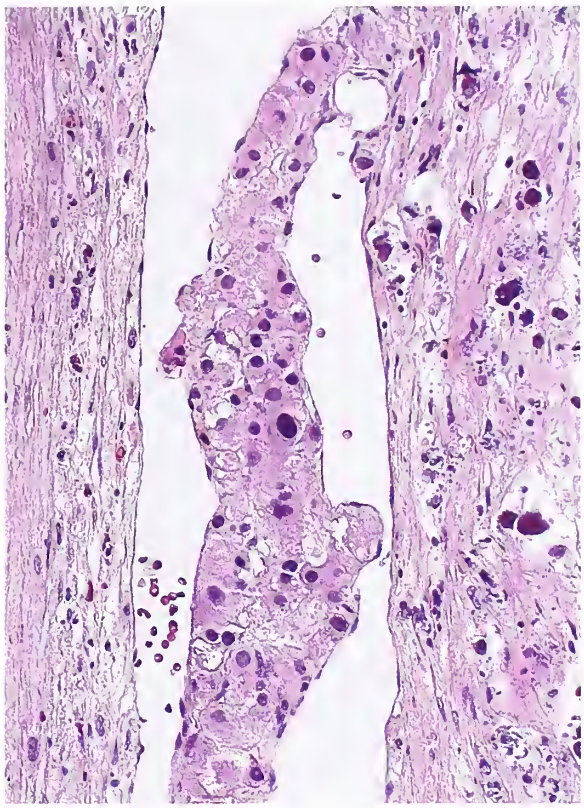

Figure 6-19

VIRILIZING ADRENAL CORTICAL NEOPLASM

Areas show occasional trabeculae of tumor with small tenuous attachments and an intact endothelial covering. Other areas of same tumor showed a "free-floating" island of tumor, which in that plane of section, gave the impression of angioinvasion. A different plane of section might reveal a site of attachment as shown here. (Fig. 6-18, left from Fascicle 19, Third Series.)

referred to by Weiss (22). True vascular invasion usually appears as loose plugs within vascular channels, which indicate malignancy (fig. 6-20). Rarely, the tumor can propagate through the remaining gland via tributaries of the venous network. Extension of tumor into the inferior vena cava may result in malignant ascites or pose potential problems during surgery due to mobilization of tumor thrombi (23).

Finding an occasional mitotic figure may not be an adverse feature (see fig. 6-13), but the finding of numerous mitoses (average of 31 or more per 50 high-power fields) is ominous, particularly if the tumor is large and the patient is in an older, or adolescent, age group (5,7). Intracytoplasmic hyaline globules are found in about 10 percent of adrenal cortical neoplasms, both ACAs and ACCs (fig. 6-21). The immunohistochemical profile of pediatric tumors is identical to that of tumors in adults, including the rare case that is unexpectedly immunoreactive for cytokeratin.

PROGNOSTIC FACTORS AND BIOLOGIC BEHAVIOR

Because of the rarity of adrenal cortical neoplasms in the pediatric age group it is difficult to draw definitive conclusions regarding the prognostic impact of morphologic features. The limited experience of most pathologists with these tumors may contribute to a tendency to overdiagnose these rare tumors as carcinoma (6,21). Based in large part on data in the older literature, a relatively poor prognosis had been

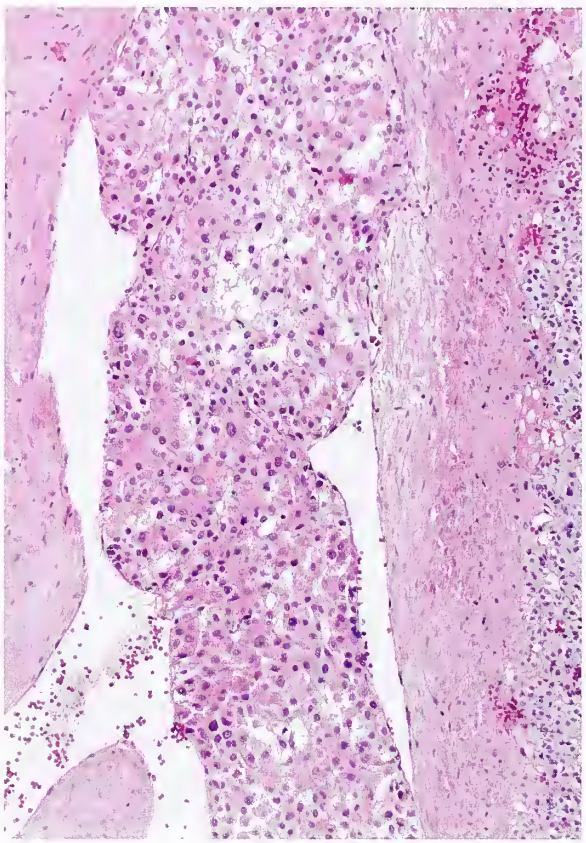

Figure 6-20

VIRILIZING ADRENAL CORTICAL CARCINOMA

Adrenal cortical carcinoma in a 6-month-old child had large embolic plugs of tumor in major tributaries of the central adrenal vein. Vascular invasion such as this can propagate into the inferior vena cava. Multiple pulmonary metastases became evident several months later.

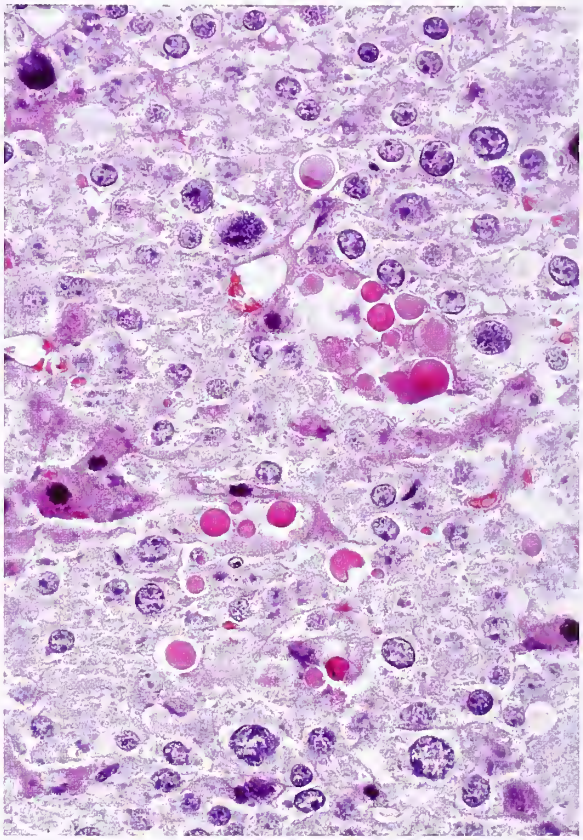

Figure 6-21

ADRENAL CORTICAL NEOPLASM

A 15-month-old female with an atypical adrenal cortical neoplasm, most likely adenoma. Some tumor cells contain cytoplasmic hyaline globules.

attached to adrenal cortical tumors in the pediatric age group (5). Of 222 cases of adrenal cortical tumors reported in children up to 1962, only 23 patients were recorded as surviving 2 or more years after treatment (24). There are a variety of factors contributing to this poor survival rate, such as far advanced disease, presentation in an era prior to the availability of cortisone, and the varied experience of surgical and life support teams in the management of the pediatric patient. A study by Cagle et al. (21), however, concluded that in the pediatric age group, adrenal cortical tumors are more likely to be benign than previously thought.

In some studies, adverse histologic findings are present more often in clinically benign tumors in the pediatric age group (21) compared with tumors seen in adults (25–27). In a univariate statistical analysis of various adverse prognostic factors, five factors were found to be statistically significant (Table 6-2) (7). 1) Age at diagnosis: in one study, the survival rate for patients older than 5 years with a pathologic diagnosis of ACC was only 13 percent, compared with 70 percent for children 5 years or younger (5); in the review by Humphrey et al. (13), the overall survival rate in the infantile group was 53 percent compared with 17 percent in the adolescent group. 2) Mitotic rate: this may be useful in distinguishing low-grade (20 mitoses or less per 50 high-power fields) from high-grade ACC (more than 20 mitoses per 50 high-power fields) in adults (27), however, a recent study of pediatric adrenal cortical neoplasms found mitoses not

Table 6-2

ADVERSE PROGNOSTIC FACTORS[a]

Variables[b]	Overall	Group A	Group B	P Values
Age (years)	8.3	5.9	10.3	0.04
Average tumor size (cm)	8.6	5.8	11.9	0.0003
Median tumor weight (g)	210	44	560	0.0001
Mitotic count (per 50 high-power fields)	20	11	31	0.04
Tumor necrosis greater than or equal to 25% (visually estimated)	41%	20%	59%	0.03

[a]Table 4 from Zerbini C, Kozakewich HP, Weinberg DS, Mundt DJ, Edwards JA 3rd, Lack EE. Adrenocortical neoplasms in childhood and adolescence: analysis of prognostic factors including DNA content. Endocr Pathol 1992;3:116-128.

[b]Parameters with statistically significant predictive value relating to prognosis.

to be a statistically significant prognostic indicator (7). A recent large study of expression of Ki-67 (fig. 6-22) and/or p53 did not appear to predict poor patient outcome (28). 3) Tumor size: clinically malignant adrenal cortical tumors are often much larger than benign tumors (11,28–30), although exceptions occur. 4) Tumor weight: Cagle et al. (21) found tumor weight to be the only reliable morphologic predictor of malignant behavior in the pediatric age group, with all tumors over 500 g being malignant. One study found that tumor weight of 100 g or more was an adverse prognostic finding, along with the histologic typing of tumors as low-grade and high-grade ACC; tumor diameter was not significantly predictive of biologic behavior, but this parameter was available in relatively few cases (31). Exceptions exist regarding weight criteria and prognosis: rarely tumors of more than 1,000 g prove to be clinically benign, and rare tumors under 40 g (22g [29] and 35 g [14]) are malignant with metastases. 5) Tumor necrosis.

Biochemical evidence of a deficiency of 11-beta-hydroxylation has been reported in childhood ACC (32), but its significance in terms of predicting biologic behavior is not known. Analysis of 83 cases identified the following features as predicting malignancy: tumor weight over 400 g, vena cava invasion, capsular and/or vascular invasion, extension into periadrenal soft tissue, confluent necrosis, severe nuclear atypia, more than 15 mitoses per 20 high-power fields, and the presence of atypical mitoses (28).

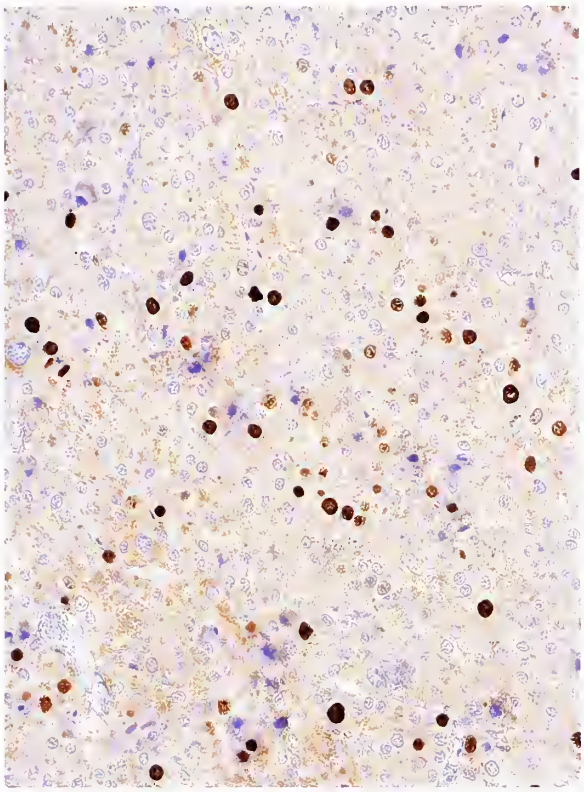

Figure 6-22

ADRENAL CORTICAL ADENOMA

Immunostain for Ki-67, a proliferation marker, shows a relatively low labeling index (avidin-biotin peroxidase method).

The review by Zerbini et al. (7) summarizes data from nine studies of DNA ploidy in adrenal cortical tumors; in their own study, 23 tumors (14 clinically benign and 9 clinically malignant) were analyzed by static image analysis (10 tumors) and by both static image analysis and flow cytometry (13 tumors). There was no discrepancy between the results of DNA ploidy analysis in tumors studied by both methods. Twelve of 14 clinically benign tumors were found to be aneuploid (4 with multiple aneuploid peaks) (fig. 6-23), compared with 5 of 9 clinically malignant tumors (1 with multiple aneuploid peaks); 4 of 9 clinically malignant tumors were found to have a diploid DNA value (fig. 6-24) (7). The results indicate no statistically significant

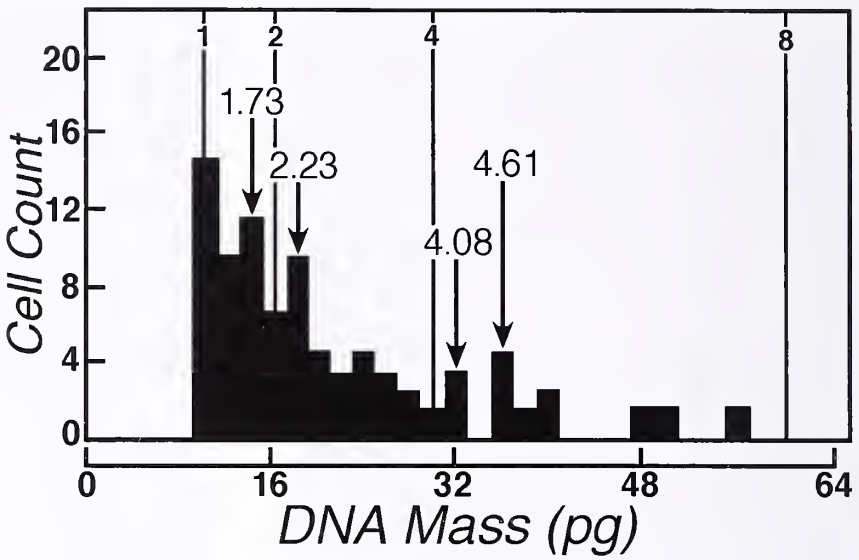

Figure 6-23

ADRENAL CORTICAL ADENOMA

DNA histogram by static image analysis shows multiple aneuploid peaks. The tumor weighed only 12 g. The child was alive and well 4½ years later. (Fig. 6-19 from Fascicle 19, Third Series.)

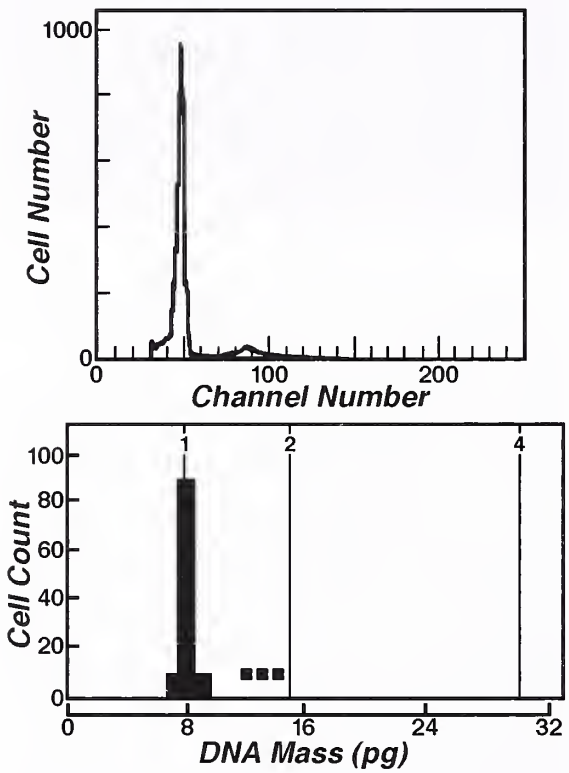

Figure 6-24

ADRENAL CORTICAL CARCINOMA WITH VIRILIZATION

Flow cytometric histogram (top) and image analysis histogram (bottom) of adrenal cortical carcinoma in a 16-year-old girl. The tumor had a diploid DNA content, but the patient died of massive intraabdominal recurrence and metastases a little over 1 year after diagnosis. (Fig. 6-20 from Fascicle 19, Third Series.)

association between clinical outcome and DNA ploidy pattern. A study of over 50 adrenal cortical tumors in the pediatric age group also concluded that ploidy does not reliably predict outcome: 21 of 29 patients with aneuploid tumors were disease-free following diagnosis (median, 1.75 years) (31). A relatively high incidence of aneuploidy was noted by Taylor et al. (4 of 4 cases) (33), but it was also apparent in one tumor which was clinically benign. Aspects of molecular genetics are briefly covered in a recent review (9).

Most deaths caused by ACC occur within 1 (5) to 2 years (13) following diagnosis, but some patients survive longer with recurrent or metastatic tumor. The most frequent sites of metastases are lung (fig. 6-25) followed by liver. Invasion of the inferior vena cava was reported in 6 of 17 patients with clinically malignant adrenal cortical neoplasms (35 percent), with obstruction in a number of instances resulting in lower extremity and truncal edema (5). Other sites of metastasis include peritoneum (29 percent), pleura and/or diaphragm (24 percent), abdominal lymph nodes (24 percent), and kidney (18 percent) (5). Cerebral metastasis also occurs (34).

HEMIHYPERTROPHY AND OTHER ABNORMALITIES

In 1967, Fraumeni and Miller (35) highlighted the association between adrenal cortical neoplasms and hemihypertrophy in the pediatric age group. In a clinical chart review of

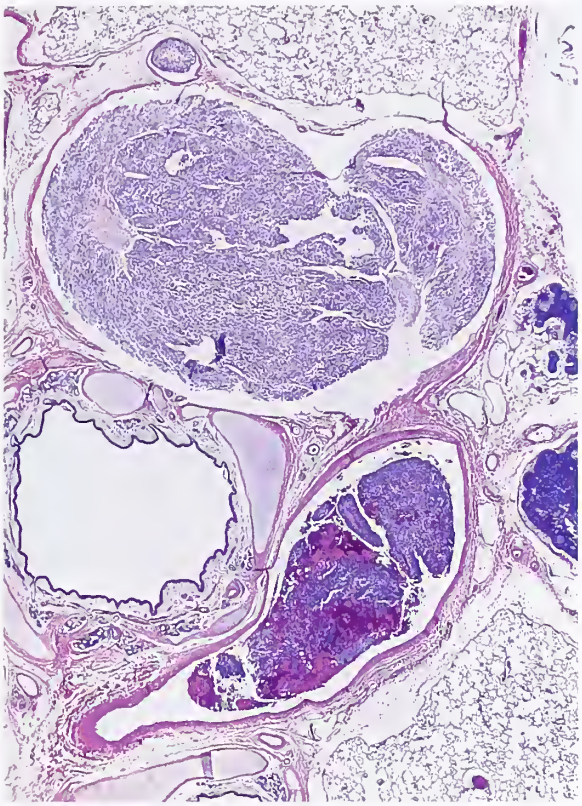

Figure 6-25

ADRENAL CORTICAL CARCINOMA

Large tumor emboli are evident in the venous channels of the lung. (Fig. 6-22 from Fascicle 19, Third Series.)

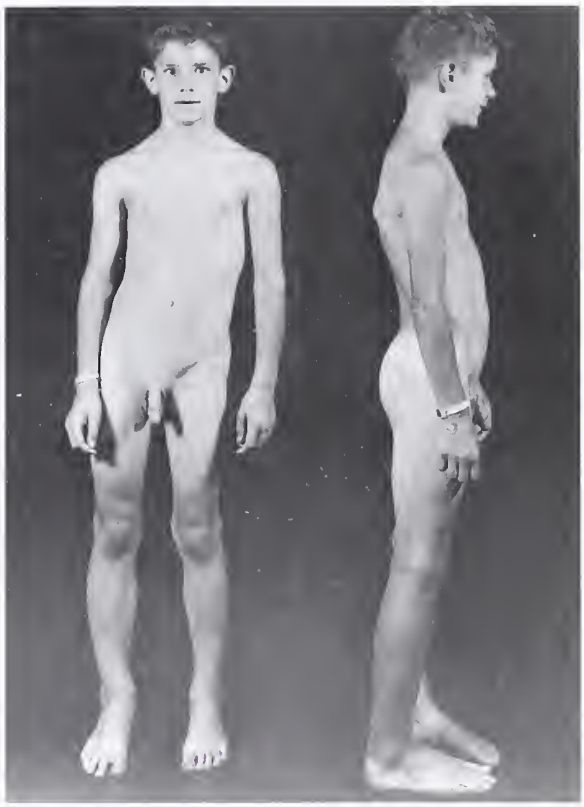

Figure 6-26

VIRILIZING ADRENAL CORTICAL ADENOMA

In infancy this 7-year-old boy had right-sided hemihypertrophy. Evaluation revealed advanced skeletal age, onset of acne, deepening of voice, enlarged genitalia, and appearance of pubic hair. The resected adrenal tumor weighed 40 g and measured 7 cm in diameter. The patient was alive and well 5 years later. (Fig. 2 from Lack EE, Mulvihil JJ, Travis WD, Kozakewich HP. Adrenal cortical neoplasms in the pediatric and adolescent age group. Clinicopathologic study of 30 cases with emphasis on epidemiological and prognostic factors. Pathol Annu 1992;27:1-53.)

62 children with adrenal cortical neoplasms from 12 hospitals, 46 tumors were designated pathologically as ACC (74.2 percent) and 16 were classified as ACA (25.8 percent); of all of these patients, 2 (3 percent) had congenital hemihypertrophy (fig. 6-26). The adrenal cortical tumors are not necessarily located on the same side as the hemihypertrophy. Other pediatric tumors reported in association with hemihypertrophy include nephroblastoma (Wilms' tumor) (36) and hepatoblastoma (35,37), but it has also been reported with malignant pheochromocytoma (38), as well as in a patient with ACA and medullary sponge kidney (39). Urinary tract abnormalities such as duplication of the collecting system and polycystic kidney have also been noted in children with adrenal cortical tumors. Rare cortical neoplasms have been reported in association with ganglioneuroma (40) and ganglioneuroblastoma (41).

BECKWITH-WIEDEMANN SYNDROME AND ADRENAL CYTOMEGALY

Adrenal cytomegaly is a very characteristic feature of *Beckwith-Wiedemann syndrome* (BWS), which has an association with adrenal cortical neoplasms (9,42) as well as other tumors, both benign and malignant (see chapter 2). Nephroblastoma is the main associated neoplasm followed by ACC and hepatoblastoma. A case of congenital metastasizing ACC was reported in which cytomegaly was present in the fetal adrenal cortex and elsewhere (43).

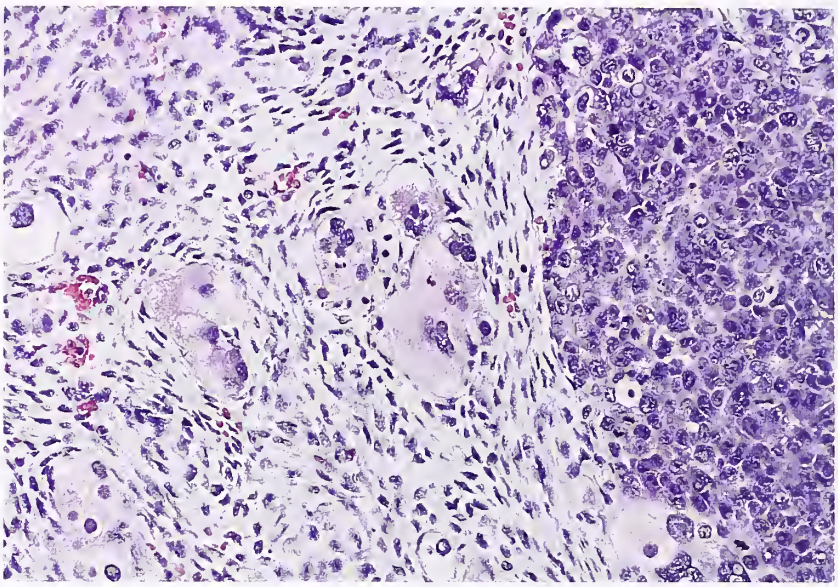

Figure 6-27

ADRENAL CORTICAL BLASTOMA

The tumor contains small nests of pleomorphic cells and more primitive spindle cells. (Fig. 6-24 from Fascicle 19, Third Series.)

CANCER FAMILY SYNDROME (LI-FRAUMENI OR SBLA SYNDROME)

In 1969, a remarkable familial aggregation of cancers was defined as a possible syndrome by Li and Fraumeni (44) based upon a review of hospital records of children with rhabdomyosarcoma. The acronym *SBLA cancer syndrome* (sarcoma; breast and brain tumors; leukemia, laryngeal carcinoma, and lung cancer; and adrenal cortical carcinoma) was later proposed based upon the complex of tumors (45). Based upon a large number of kindreds with the syndrome, an autosomal dominant mode of inheritance has been reported. The most common associated neoplasms are soft tissue sarcomas, bone sarcomas, and breast carcinoma, (44, 46,47). ACC comprises 10 percent of neoplasms other than sarcomas and breast cancer in the 0 to 44-year-old age group, whereas in the United States overall, ACC accounts for less than 1 percent of malignant neoplasms (48).

Alterations in the *p53* tumor suppressor gene have been detected in many patients with the Li-Fraumeni syndrome; the gene is located on chromosome 17p13 and encodes a 53-kDa nuclear phosphoprotein that appears to function as a negative regulator of cell growth and proliferation (49). The incidence of pediatric ACC in southern Brazil is 10 to 15 times higher than that of pediatric ACC worldwide, and recently a very high incidence of germline mutations of *p53* was reported there. This is similar to the Li-Fraumeni syndrome, but there is no history of increased cancer among family members (50).

CONGENITAL ADRENAL HYPERPLASIA

Rare adrenal cortical neoplasms, both ACA and ACC, have been reported in association with *congenital adrenal hyperplasia* (CAH), also known as the *adrenogenital syndrome* (see chapter 2) (6). One case of ACC raised the possibility of untreated CAH that later became neoplastic (51). Testicular "tumors" of adrenal cortical type are frequent in patients with CAH (see chapter 2), but large tumors (usually bilateral) necessitating orchiectomy are uncommon. It has been suggested that persistent trophic stimulation of adrenal cortical tissues by adrenocorticotropic hormone (ACTH) might induce neoplastic transformation, but this remains speculative (5).

ADRENAL CORTICAL BLASTOMA

A unique case of a virilizing malignant adrenal cortical tumor was reported by Molberg et al. (52) as an *adrenal cortical blastoma* in a 21-month-old infant who had increased serum alpha-fetoprotein. The tumor contained a mixture of immature epithelial and mesenchymal elements (fig. 6-27), as well as occasional foci of vascular invasion (fig. 6-28), but no metastases were evident at the time of autopsy. The tumor focally recapitulated the morphology of the developing fetal cortex.

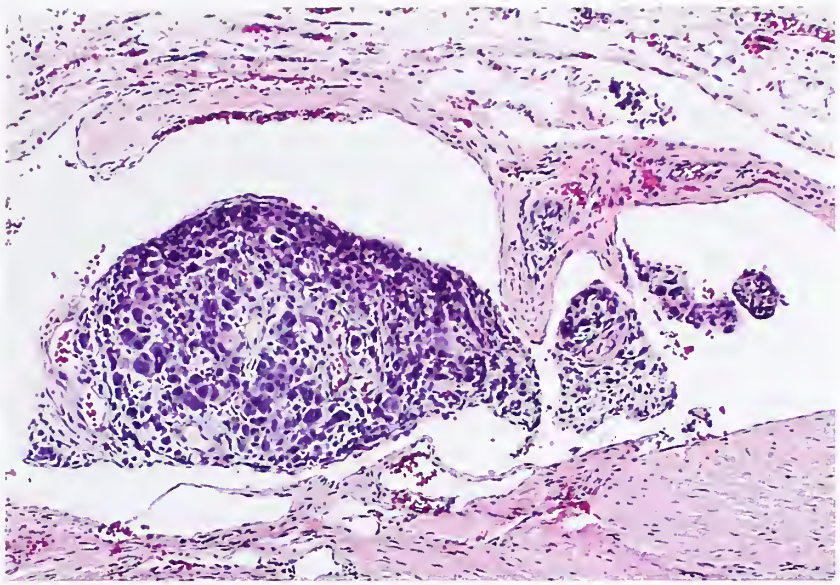

Figure 6-28

ADRENAL CORTICAL BLASTOMA

A large area of vascular (venous or lymphatic) invasion is present. (Fig. 6-25 from Fascicle 19, Third Series.)

REFERENCES

Clinical and Pathologic Features

1. Stewart DR, Jones PH, Jolleys A. Carcinoma of the adrenal gland in children. J Pediatr Surg 1974;9:59-67.
2. Miller RW, Young JL Jr, Novakovic B. Childhood Cancer. Cancer 1995;75(Suppl 1):395-405.
3. Young JL Jr, Miller RW. Incidence of malignant tumors in U.S. children. J Pediatr 1975;86:254-258.
4. Young JL Jr, Peroy CL, Asire AJ, et al. Cancer incidence and mortality in the United States, 1973-1977. Natl Cancer Inst Monogr 1981;57:1-187.
5. Lack EE, Mulvihill JJ, Travis WD, Kozakewich HP. Adrenal cortical neoplasms in the pediatric and adolescent age group. Clinicopathological study of 30 cases with emphasis on epidemiological and prognostic factors. Pathol Annu 1992;27:1-53.
6. Lack EE, Travis WD, Oertel JE. Adrenal cortical neoplasms. In: Lack EE, ed. Pathology of the adrenal glands. New York: Churchill Livingstone; 1990:115-171.
7. Zerbini C, Kozakewich HP, Weinberg DS, Mundt DJ, Edwards JA 3rd, Lack EE. Adrenocortical neoplasms in childhood and adolescence: analysis of prognostic factors including DNA content. Endocr Pathol 1992;3:116-128.
8. Teinturier C, Pauchard MS, Brugieres L, Landais P, Chaussain JL, Bougneres PF. Clinical and prognostic aspects of adrenocortical neoplasms in childhood. Med Pediatr Oncol. 1999;32:106-11.
9. Liou LS, Kay R. Adrenocortical carcinoma in children. Review and recent innovations. Urol Clin North Am 2000;27:403-421.
10. Sarwar ZU, Ward VL, Mooney DP, Testa S, Taylor GA. Congenital adrenocortical adenoma: case report and review of literature. Pediatr Radiol 2004;4:991-994.
11. Ribeiro RC, Figueiredo B. Childhood adrenocortical tumours. Eur J Cancer 2004;40:1117-1126.
12. Michalkiewicz E, Sandrini R, Figueiredo B, et al. Clinical and outcome characteristics of children with adrenocortical tumors: a report from the International Pediatric Adrenocortical Tumor Registry. J Clin Oncol 2004;22:838-845.
13. Humphrey GB, Pysher T, Holcombe J, et al. Overview on the management of adrenocortical carcinoma (ACC). In: Humphrey GB, Grindey GB, Dehner LP, Acton RT, Pysher TJ, eds. Adrenal and endocrine tumors in children. Boston: Martinus Nijhoff Publ; 1983:349-358.
14. Saracco S, Abramowsky C, Taylor S, Silverman RA, Berman BW. Spontaneously regressing adrenocortical carcinoma in a newborn. A case report with DNA ploidy analysis. Cancer 1988; 62:507-511.
15. Weatherby RP, Carney JA. Pathologic features of childhood adrenocortical tumors. In: Humphrey GB, Grindey GB, Dehner LP, Acton RT, Pysher TJ, eds. Adrenal and endocrine tumors in children. Boston: Martinus Nijhoff Publ; 1983:217-248.

16. Cordera F, Grant C, van Heerden J, Thompson G, Young W. Androgen-secreting adrenal tumors. Surgery 2003;134:874-880.
17. Bonfig W, Bittmann I, Bechtold S, et al. Virilising adrenocortical tumours in children. Eur J Pediatr 2003;162:623-628.
18. Halmi KA, Lascari AD. Conversion of virilization to feminization in a young girl with adrenal cortical carcinoma. Cancer 1971;27:931-935.
19. Leung LY, Leung WY, Chan KF, Fan TW, Chung KW, Chan CH. Ruptured adrenocortical carcinoma as a cause of paediatric acute abdomen. Pediatr Surg Int 2002;18:730-732.
20. Neblett, WW, Frexes-Steed M, Scott HW Jr. Experience with adrenocortical neoplasms in childhood. Am Surg 1987;53:117-125.
21. Cagle PT, Hough AJ, Pysher TJ, et al. Comparison of adrenal cortical tumors in children and adults. Cancer 1986;57:2235-2237.
22. Weiss LM. Comparative histologic study of 43 metastasizing and nonmetastasizing adrenal cortical tumors. Am J Surg Pathol 1984;8:163-169.
23. Godine LB, Berdon WE, Brasch RC, Leonidas JC. Adrenocortical carcinoma with extension into inferior vena cava and right atrium: report of 3 cases in children. Pediatr Radiol 1990;20:166-168.
24. Hayles AB, Hahn HB Jr, Sprague RG, Bahn RC, Priestly JT. Hormone-secreting tumors of the adrenal cortex in children. Pediatrics 1966;37:19-25.
25. Hough AJ, Hollifield JW, Page DL, Hartmann WH. Prognostic factors in adrenal cortical tumors. A mathematical analysis of clinical and morphological data. Am J Clin Pathol 1979;72: 390-399.
26. Weiss LM, Medeiros LJ, Vickery AL Jr. Pathologic features of prognostic significance in adrenal cortical carcinoma. Am J Surg Pathol 1989;13: 202-206.
27. Medeiros LJ, Weiss LM. New developments in the pathologic diagnosis of adrenal cortical neoplasms. A review. Am J Clin Pathol 1992;97:73-83.
28. Wieneke JA, Thompson LD, Heffess CS. Adrenal cortical neoplasms in the pediatric population: a clinicopathologic and immunophenotypic analysis of 83 patients. Am J Surg Pathol 2003;27: 867-881.
29. Lefevre M, Gerard-Marchant R, Gubler JP, Chaussain JL, Lemerle J. Adrenal cortical carcinoma in children: 42 patients treated from 1958 to 1980 at Villejuif. In: Humphrey GB, Grindey GB, Dehner LP, Acton RT, Pysher TJ, eds. Adrenal and endocrine tumors in children. Boston: Martinus Nijhoff Publ; 1983:265-276.
30. Michalkiewicz EL, Sandrini R, Bugg MF, et al. Clinical characteristics of small functioning adrenocortical tumors in children. Med Pediatr Oncol. 1997;28:175-178.
31. Bugg MF, Ribeiro RC, Roberson PK, et al. Correlation of pathologic features with clinical outcome in pediatric adrenocortical neoplasia. A study of a Brazilian population. Brazilian Group for Treatment of Childhood Adrenocortical Tumors. Am J Clin Pathol 1994;101:625-629.
32. Doerr HG, Sippell WG, Drop SL, Bidlingmaier F, Knorr D. Evidence of 11 beta-hydroxylase deficiency in childhood adrenocortical tumors. The plasma corticosterone/11-deoxycorticosterone ratio as a possible marker for malignancy. Cancer 1987;60:1625-1629.
33. Taylor SR, Roederer M, Murphy RF. Flow cytometric DNA analysis of adrenocortical tumors in children. Cancer 1987;59:2059-2063.
34. Romaguera RL, Minagar A, Bruce JH, et al. Adrenocortical carcinoma with cerebral metastasis in a child: case report and review of the literature. Clin Neurol Neurosurg 2001;103:46-50.

Hemihypertrophy and Other Abnormalities

35. Fraumeni JF Jr, Miller RW. Adrenocortical neoplasms with hemihypertrophy, brain tumors and other disorders. J Pediatr 1967;70:129-138.
36. Fraumeni JF Jr, Geiser CF, Manning MD. Wilms' tumor and congenital hemihypertrophy: report of five new cases and review of literature. Pediatrics 1967;40:886-899.
37. Fraumeni JF Jr, Miller RW, Hill JA. Primary carcinoma of the liver in childhood: an epidemiologic study. J Natl Cancer Inst 1968;40:1087-1099.
38. Schnakenburg KV, Muller M, Dorner K, Harms D, Schwarze EW. Congenital hemihypertrophy and malignant giant pheochromocytoma—a previously undescribed coincidence. Eur J Pediatr 1976;122:263-273.
39. Tomooka Y, Onitsuka H, Goya T, et al. Congenital hemihypertrophy with adrenal adenoma and medullary sponge kidney. Br J Radiol 1988;61: 851-853.
40. Gershanik JJ, Elmore M, Levkoff AH. Congenital concurrence of adrenal cortical tumor, ganglioneuroma, and toxoplasmosis. Pediatrics 1973;51: 705-709.
41. Dahms WT, Gray G, Vrana M, New MI. Adrenocortical adenoma and ganglioneuroblastoma in a child. A case presenting as Cushing's syndrome with virilization. Am J Dis Child 1973;125:608-611.

Beckwith-Wiedemann Syndrome

42. Hertel NT, Carlsen N, Kerndrup G, et al. Late relapse of adrenocortical carcinoma in Beckwith-Wiedemann syndrome. Clinical, endocrinological and genetic aspects. Acta Paediatr 2003;92:439-443.

43. Sherman FE, Bass LW, Fetterman GH. Congenital metastasizing adrenal cortical carcinoma associated with cytomegaly of the fetal adrenal cortex. Am J Clin Pathol 1958;30:439-446.

Cancer Family Syndrome

44. Li FP, Fraumeni JF Jr. Soft-tissue sarcomas, breast cancer and other neoplasms. A familial syndrome? Ann Intern Med 1969;71:747-752.
45. Lynch HT, Mulcahy GM, Harris RE, Guirgis HA, Lynch JF. Genetic and pathologic findings in a kindred with hereditary sarcoma, breast cancer, brain tumors, leukemia, lung, laryngeal, and adrenal cortical carcinoma. Cancer 1978;41: 2055-2064.
46. Kjellman M, Larsson C, Backdahl M. Genetic background of adrenocortical tumor development. World J Surg 2001;25:948-956.
47. Koch CA, Pacak K, Chrousos GP. The molecular pathogenesis of hereditary and sporadic adrenocortical and adrenomedullary tumors. J Clin Endocrinol Metab 2002;87:5367-5384.
48. Li FP, Fraumeni JF Jr, Mulvihill JJ, et al. A cancer family syndrome in twenty-four kindreds. Cancer Res 1988;48:5358-5367.
49. Malkin D. The Li-Fraumeni syndrome. Prin Pract Oncol Updates 1993;7:1-14.
50. Ribeiro RC, Sandrini F, Figueiredo B, et al. A inherited p53 mutation that contributes in a tissue-specific manner to pediatric adrenal cortical carcinoma. Proc Natl Acad Sci U S A 2001; 31;98:9330-9335.

Congenital Hyperplasia/Blastoma

51. Nogeire C, Fukushima DK, Hellman L, Boyar RM. Virilizing adrenal cortical carcinoma. Cancer 1977;40:307-313.
52. Molberg K, Vuitch F, Stewart D, Albores-Saavedra J. Adrenocortical blastoma. Hum Pathol 1992; 23:1187-1190.

7 OTHER NEOPLASMS AND TUMOR-LIKE LESIONS OF THE ADRENAL GLANDS

There are a variety of neoplastic and nonneoplastic lesions that can cause enlargement of the adrenal glands, and on occasion, clinical or radiologic confusion with an adrenal neoplasm, either primary or secondary (1). In some cases, the clinical features, and in particular the imaging characteristics on computerized tomography (CT) scan or magnetic resonance imaging (MRI), allow for a presumptive diagnosis, but in most instances diagnosis is by fine needle aspiration biopsy or examination of surgically resected specimens.

ADRENAL ENLARGEMENT DUE TO INFECTION OR ABSCESS FORMATION

Adrenal gland involvement by disseminated fungal infection has been recognized at autopsy in up to 80 percent of patients with histoplasmosis and paracoccidioidomycosis, and less commonly, disseminated blastomycosis, coccidioidomycosis, and cryptococcosis. There is often bilateral adrenal enlargement, but a unilateral adrenal mass may be evident. Disseminated fungal infection, particularly histoplasmosis, can cause extensive adrenal necrosis and result in subclinical or overt Addison's disease (fig. 7-1). Goodwin et al. (2) reported Addison's disease in 7 percent of patients with disseminated histoplasmosis. The extensive adrenal destruction caused by histoplasmosis appears to be associated with extracapsular adrenal vasculitis, which leads to adrenal infarction and caseation necrosis (fig. 7-2). Numerous organisms can be found within macrophages (fig. 7-3). Some of the parasitized cells are adrenal cortical cells. Involvement by tuberculosis can cause tumefactive enlargement of the adrenal glands. Less than 2 percent of patients with disseminated infection, however, present with signs or symptoms of adrenal cortical insufficiency (3).

Adrenal abscess formation due to bacterial infection is a rare cause of adrenal enlargement. It is usually unilateral, but on occasion, there is bilateral adrenal involvement. Radiographically,

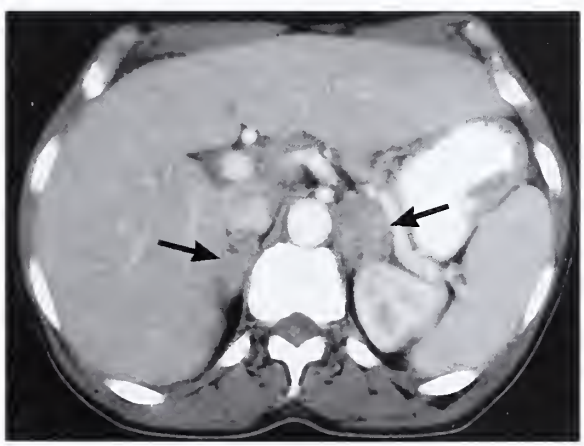

Figure 7-1

DISSEMINATED HISTOPLASMOSIS

An adult patient with disseminated histoplasmosis had chronic adrenal cortical insufficiency (Addison's disease). Both adrenal glands are enlarged (arrows) and nonhomogeneous on computerized tomography (CT) scan.

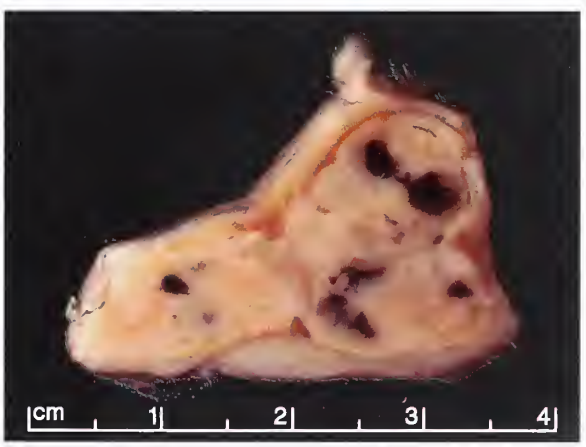

Figure 7-2

DISSEMINATED HISTOPLASMOSIS

Transverse section of an enlarged adrenal gland from a patient with disseminated histoplasmosis. There are broad zones of caseous necrosis and small areas of hemorrhage. (Fig. 7-2 from Fascicle 19, Third Series.)

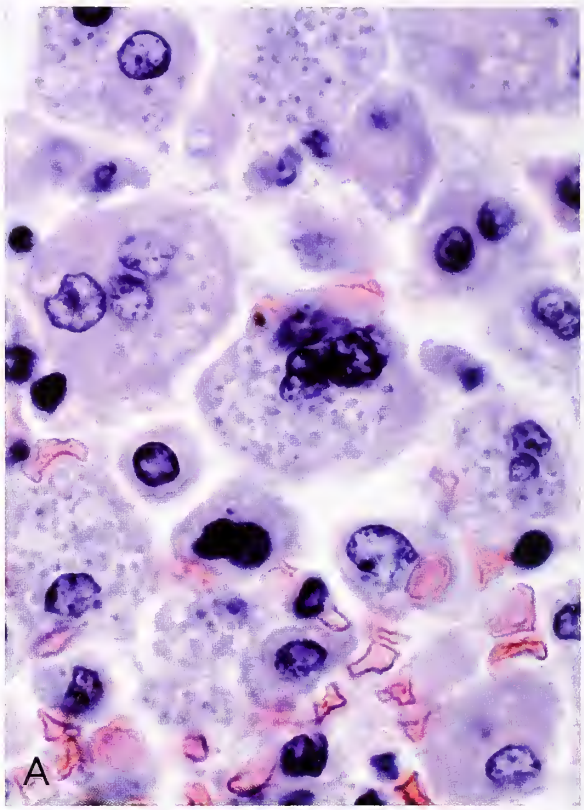

Figure 7-3

ADRENAL HISTOPLASMOSIS

A: Numerous intracellular organisms typical for *Histoplasma capsulatum* are present within sinusoids of the adrenal cortex.

B: Histiocytes contain numerous organisms typical for *H. capsulatum*, which are sharply delineated with periodic acid–Schiff (PAS) stain.

C: Cell block preparation of fine needle aspiration biopsy of enlarged adrenal gland (same case as figure 7-1) shows numerous yeast forms of *H. capsulatum*, which are round to ovoid. Some organisms are isolated and single while others have a budding configuration (Gomori methenamine silver stain).

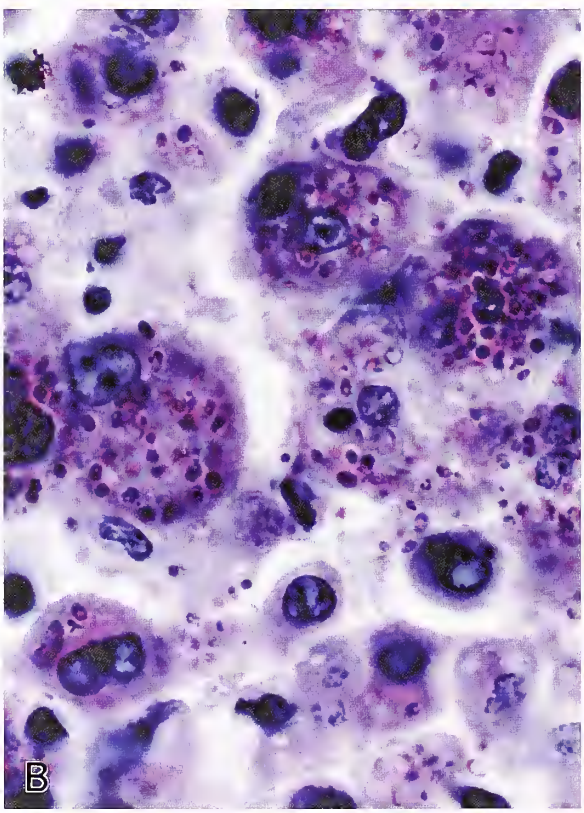

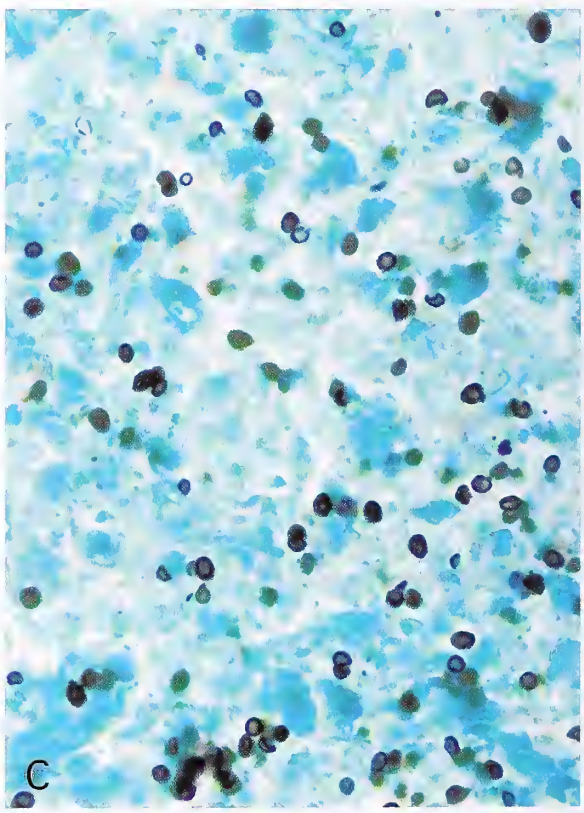

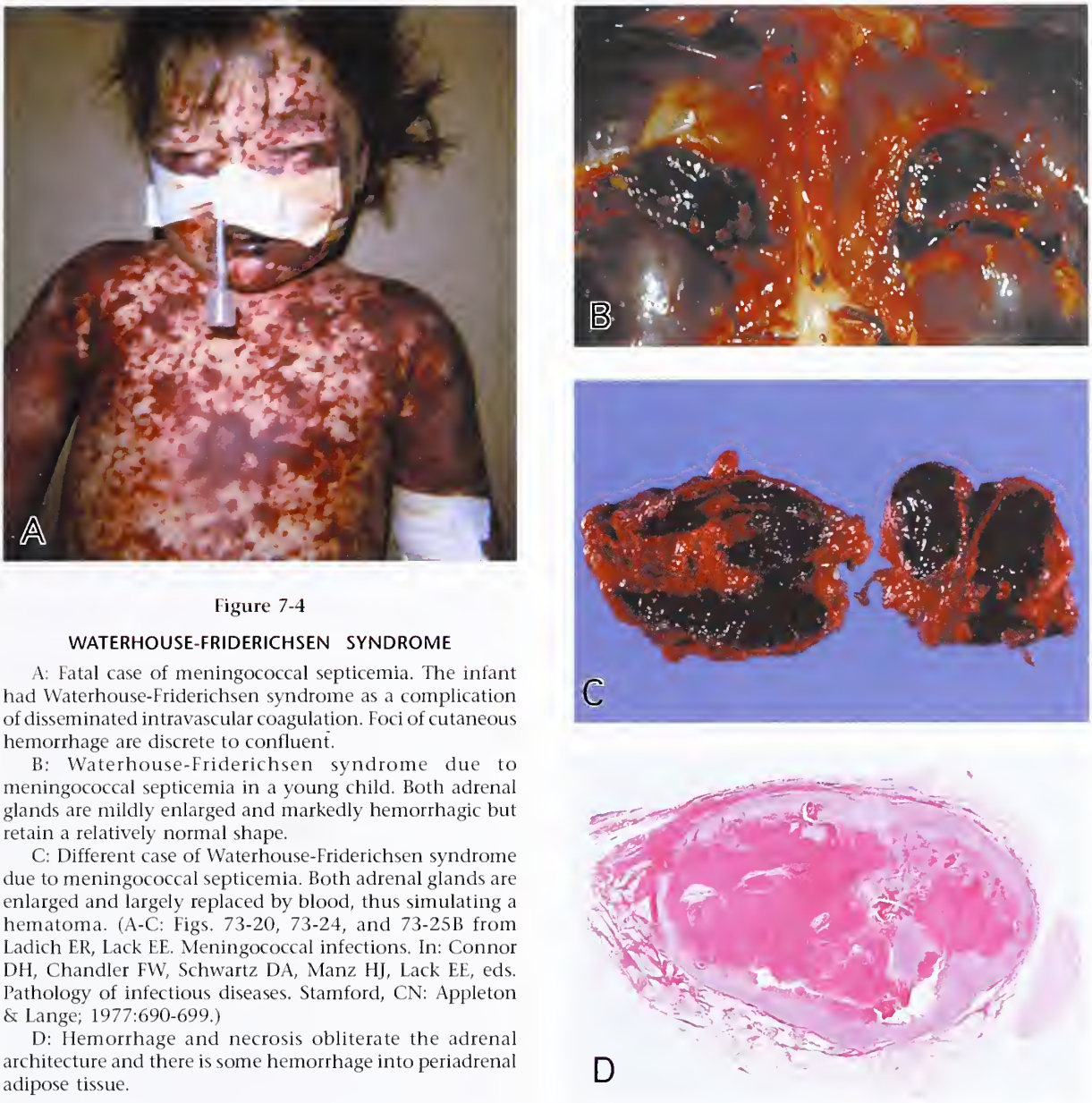

Figure 7-4

WATERHOUSE-FRIDERICHSEN SYNDROME

A: Fatal case of meningococcal septicemia. The infant had Waterhouse-Friderichsen syndrome as a complication of disseminated intravascular coagulation. Foci of cutaneous hemorrhage are discrete to confluent.

B: Waterhouse-Friderichsen syndrome due to meningococcal septicemia in a young child. Both adrenal glands are mildly enlarged and markedly hemorrhagic but retain a relatively normal shape.

C: Different case of Waterhouse-Friderichsen syndrome due to meningococcal septicemia. Both adrenal glands are enlarged and largely replaced by blood, thus simulating a hematoma. (A-C: Figs. 73-20, 73-24, and 73-25B from Ladich ER, Lack EE. Meningococcal infections. In: Connor DH, Chandler FW, Schwartz DA, Manz HJ, Lack EE, eds. Pathology of infectious diseases. Stamford, CN: Appleton & Lange; 1977:690-699.)

D: Hemorrhage and necrosis obliterate the adrenal architecture and there is some hemorrhage into periadrenal adipose tissue.

it may be difficult to differentiate an adrenal abscess from a primary or secondary adrenal neoplasm. Adrenal abscess formation has been reported more often in children where the suppurative process may complicate neonatal adrenal hemorrhage (1). In most cases, involvement by bacteria, usually *Escherichia coli*, followed by group B *Streptococcus* and *Bacteroides*, is attributable to hematogenous dissemination. Malakoplakia of the adrenal gland has also been reported in association with *E. coli* infection (4).

ADRENAL ENLARGEMENT WITH HEMORRHAGE, HEMATOMA FORMATION, AND CALCIFICATION

Adrenal hemorrhage can present antemortem as unilateral or bilateral adrenal enlargement (fig. 7-4). Hemorrhage is associated with a wide variety of factors including mechanical trauma, sepsis with or without Waterhouse-Friderichsen syndrome, coagulopathies, steroid or adrenocorticotropic hormone (ACTH) administration,

Figure 7-5

ADRENAL HEMORRHAGE

Right adrenal hemorrhage and large hematoma formation complicate extensive thromboemboli in the aorta of a 3-week-old infant. The child had a ductus arteriosus aneurysm and probably multiple emboli. (Fig. 7-5 from Fascicle 19, Third Series.)

primary or metastatic tumors, adrenal vein thrombosis, and as a complication of adrenal venography (1).

Adrenal enlargement due to hemorrhage appears on CT scan as a hyperintense mass with "streaky infiltration" of periadrenal tissues; older lesions may appear as a nonspecific mass. On MRI, subacute hemorrhage has a high signal intensity on both T1- and T2-weighted images in most cases. This imaging modality may be useful in estimating the age of the hematoma. Only rarely is an adrenal hematoma removed as a surgical specimen simulating a nonfunctional adrenal tumor. Over time, the adrenal hematoma may undergo resolution and shrinkage, with dystrophic calcification and possibly cyst formation (1).

Neonatal adrenal hemorrhage is associated with complicated delivery or asphyxia, and is most often confined to the right adrenal gland (fig. 7-5). Adrenal hematoma in the neonate may simulate the radiographic features of neuroblastoma complicated by hemorrhage (fig. 7-6) (5).

Adrenal hemorrhage can be focal or diffuse, ranging in size from only a few millimeters to 15 cm, and involve up to 2 L of blood. Adrenal hemorrhage or necrosis can be seen (fig. 7-7) in viral diseases such as varicella-zoster virus or cytomegalovirus, fungal infection due to disseminated mucormycosis, or opportunistic infection by *Pneumocystis carinii*; with these infections there may be a mild degree of adrenal enlargement. There is fresh or clotted blood in various stages of organization, and the adjacent adrenal cortex or medulla may have areas of necrosis.

Adrenal hemorrhage can be complicated by adrenal insufficiency, secondary infection with abscess formation, or retroperitoneal hemorrhage, and it may be life-threatening in some patients who have associated sepsis, malignancy, history of anticoagulant or steroid treatment, or major surgery (6). Aside from heparin-associated thrombocytopenia, adrenal hemorrhage is also associated with the phospholipid antibody syndrome and it may be associated with bilateral hemorrhagic infarction of the adrenal glands (7). The peculiar susceptibility of the adrenal gland to massive hemorrhage has been attributed to its vascular supply and pivotal role in physiologic response to stress; likened to a "vascular dam," any rise in adrenal venous pressure (e.g., vasoconstriction during shock) can lead to hemorrhage into the gland.

Calcification of the adrenal gland visible on radiographs, sonography, or CT scan is uncommon but has been associated with adrenal tumors such as neuroblastoma, adrenal cortical adenoma and carcinoma, pheochromocytoma, adrenal cysts, and some infectious diseases such as histoplasmosis (8). Marked bilateral adrenal calcifications were seen in a child with adenosine-deaminase-deficient severe combined immunodeficiency (fig. 7-8A-C). On rare occasion, the adrenal gland may contain metaplastic bone (fig. 7-8D), presumably as a remote consequence of necrosis or hemorrhage. Bilateral adrenal enlargement with stippled dystrophic calcification is a characteristic feature of Wolman's disease (fig. 7-9), a rare autosomal recessive disorder of lipid metabolism due to the deficiency of lysosomal

Figure 7-6

ADRENAL HEMORRHAGE

A: Right adrenal hemorrhage and necrosis in a newborn with nonspecific abdominal symptoms. Abdominal roentgenogram showed a mass effect and ultrasound revealed an adrenal mass that did not decrease in size on repeat study. There was also an elevated serum ferritin level which heightened suspicion for a neuroblastoma. Adrenalectomy was performed. (A–C: Fig. 7-6 from Fascicle 19, Third Series.)

B: Adrenal hemorrhage and necrosis affect mainly the fetal, or provisional, cortex. The fetal zone is largely necrotic and replaced by amorphous matter.

C: Dystrophic calcification is present in the outer aspect of the necrotic fetal cortex. Hemosiderin deposition was also present as an indication of old hemorrhage.

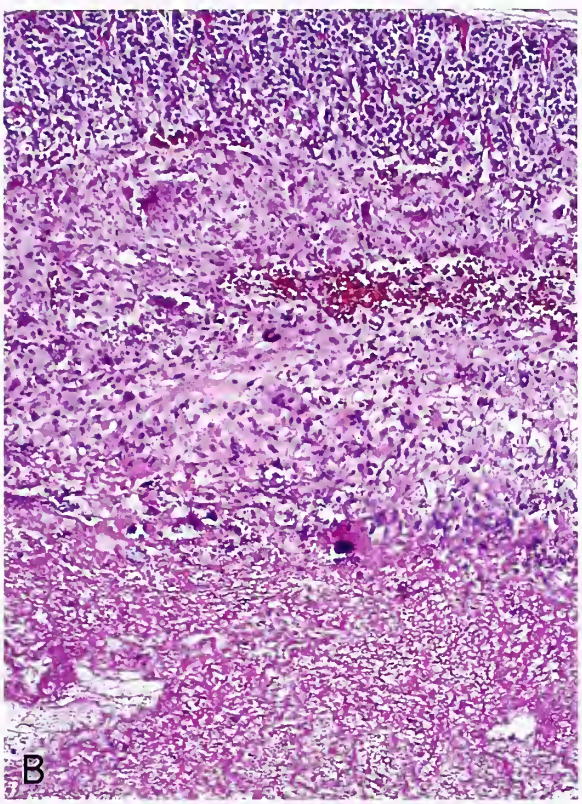

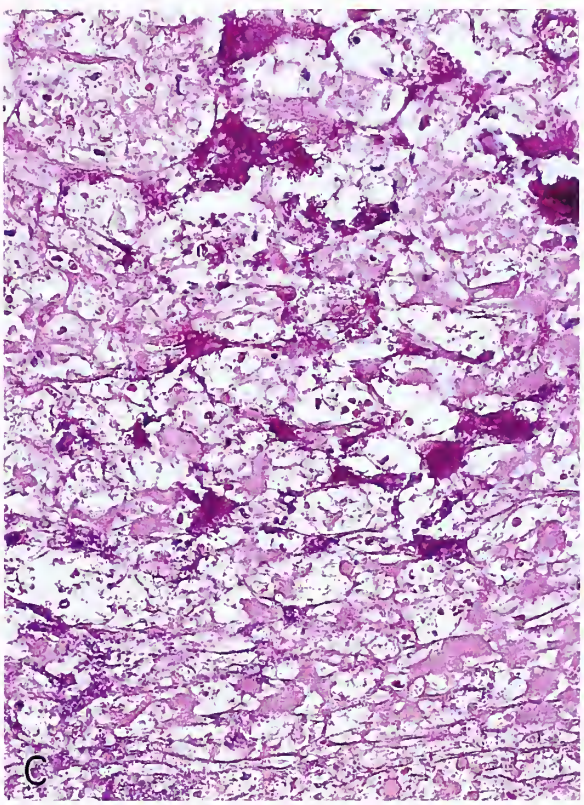

acid lipase. It is characterized by accumulation of cholesterol esters and triglycerides in a variety of tissues. The disease is invariably fatal, usually by 6 months of age.

ADRENAL CYSTS

Adrenal cysts are rare tumefactive lesions that occur at any age, but are more commonly seen in the 5th and 6th decades of life (1). Less than 5 percent of adrenal cysts occur in children, and these lesions are very rare in the neonatal period. In a review by Abeshouse (9), there was a three-fold greater incidence of adrenal cysts in female patients. The adrenal cyst is most often unilateral (only 5 to 8 percent are bilateral) (1). In one review, it was detected at autopsy in 45 percent of cases and during surgery in 55 percent (10). The frequency of adrenal cysts at autopsy is estimated to be 0.06 percent.

Signs and symptoms, when present, are usually vague and nonspecific, and include dull flank pain, various gastrointestinal complaints

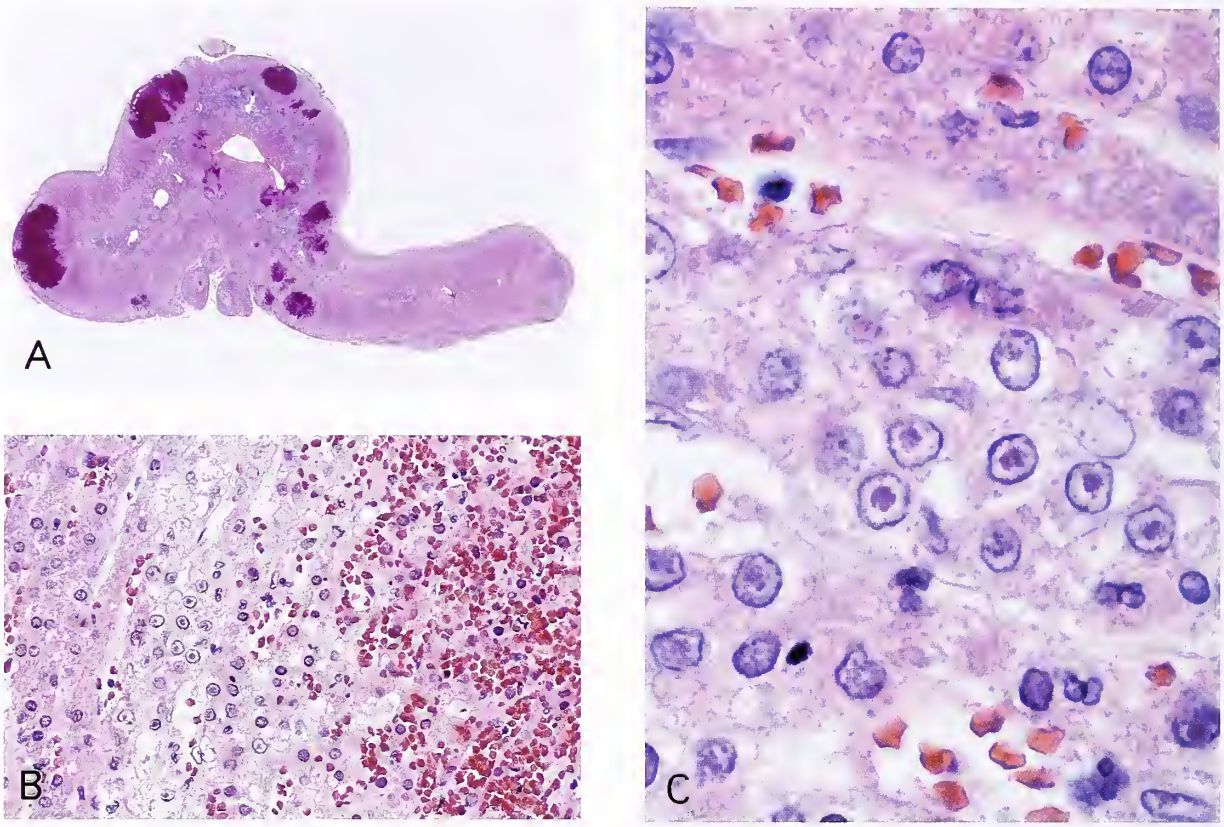

Figure 7-7

DISSEMINATED VARICELLA-ZOSTER INFECTION

A: Both adrenal glands in this fatal case had numerous sharply defined foci of hemorrhagic necrosis.
B: Many of the cortical cells bordering a zone of hemorrhagic necrosis have intranuclear viral inclusions.
C: The nuclei of infected cells contain a single eosinophilic inclusion with a surrounding halo, an appearance typical for Cowdry type A viral inclusions.

such as epigastric distress or indigestion, and a palpable abdominal mass (1). There may be constitutional symptoms such as malaise and weakness. Fever with leukocytosis is rare. Intracystic hemorrhage can result in anemia and a slowly growing abdominal mass (9). Rarely, an adrenal cyst can mimic metastatic disease.

Adrenal cysts have been classified into four major types (9,10): 1) parasitic cysts (7 percent), which are usually echinococcal and discovered incidentally at autopsy; 2) epithelial cysts (9 percent), which are divided into true glandular or retention cysts, embryonal cysts, and cystic adrenal tumors such as cystic pheochromocytoma; 3) endothelial cysts (45 percent), usually lymphangiomatous, but occasionally angiomatous; and 4) adrenal pseudocysts (39 percent), which are the most common clinically recognized type of adrenal cyst encountered during surgery. The adrenal pseudocyst may be a heterogenous subtype as well since some have an apparent vascular origin (11), which is supported immunohistochemically by positive staining for endothelial markers. A mesothelial origin has been reported for an adrenal cyst, with a pathogenesis analogous to the proposed origin of some splenic cysts (12). A cystic adrenal mass was due to isolated visceral leishmaniasis (13).

The adrenal pseudocyst is discovered with increased frequency due to improved imaging procedures. The characteristics of the cyst on CT scan provide valuable information. The cyst illustrated in figure 7-10 was thought to be a cystic renal cell carcinoma. On CT scan, adrenal cysts are usually well defined, with near water density. The cyst wall may have areas of

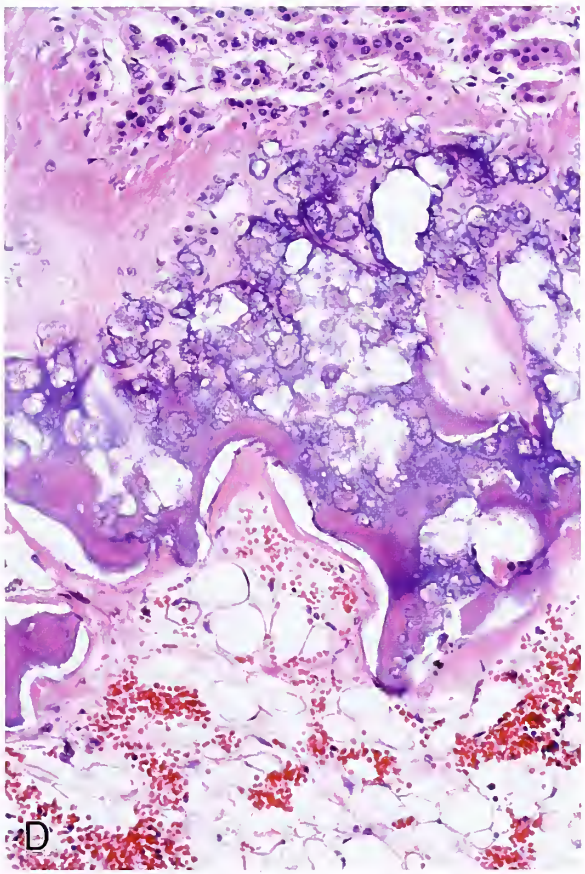

Figure 7-8

MARKED ADRENAL CALCIFICATION

A: At autopsy, plain roentgenogram shows bilaterally calcified adrenal glands (arrows, right side more than left) in a 16-month-old child with adenosine deaminase-deficient severe combined immunodeficiency.

B: The adrenal glands in the same case are slightly enlarged and markedly firm, with chalky white areas of calcification, best noted in the right adrenal gland.

C: Dense adrenal calcifications are most marked on the right side. (Fig. 1-68B from Lack EE, Kozakewich HP. Embryology, developmental anatomy, and selected aspects of non-neoplastic pathology. In: Lack EE, ed. Pathology of the adrenal glands. New York: Churchill Livingstone; 1990:1-74.)

D: Both adrenal glands have areas of dense calcification and in this field there is metaplastic bone formation.

calcification or enhance following contrast administration. There may be internal septations, and it may be difficult to distinguish a low-density adrenal cortical adenoma from a cyst. On MRI, adrenal cysts usually have a low signal intensity on T1-weighted images and a high signal intensity on T2-weighted images with enhancement, characteristics similar to those on CT scan. As with MRI scans in general, small areas of calcification are usually not detected. The average cyst size in one study was 9.2 cm (range, 6 to 16 cm) (11), but there are reports in which the cyst filled most of the abdomen (fig. 7-11), reaching a size of 33 cm, weighing 20.5 kg, and containing about 12 L of mahogany brown fluid (10). The major finding on roentgenogram of the abdomen is a peripheral curvilinear calcification.

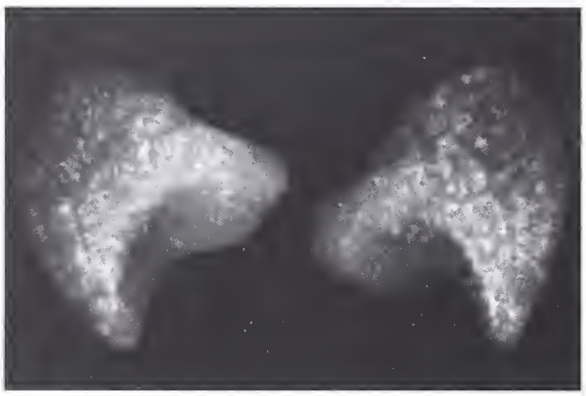

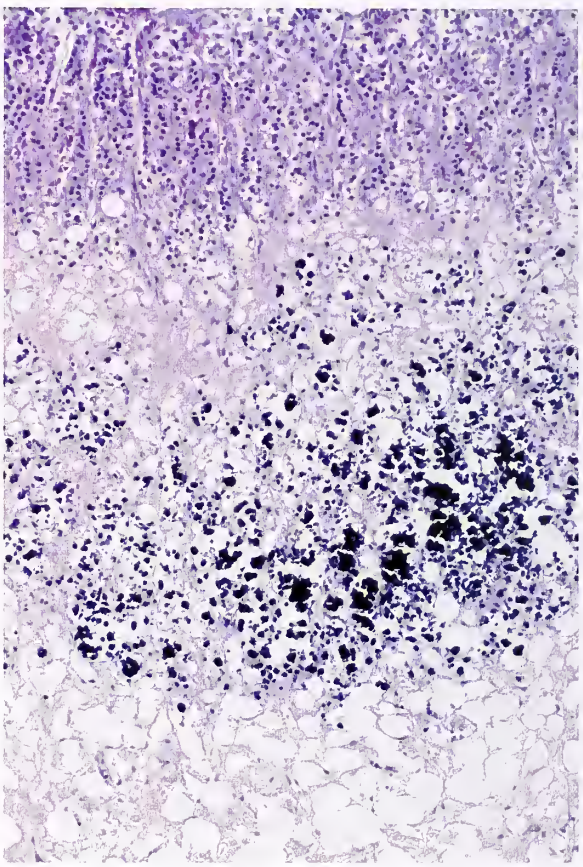

Figure 7-9

ADRENAL GLANDS IN INFANT WITH WOLMAN'S DISEASE

Above: Both adrenal glands in this 3-month-old infant were symmetrically enlarged. In this specimen radiograph at autopsy, numerous dystrophic calcifications are apparent. (Fig. 1-70B from Lack EE, Kozakewich HP. Embryology, developmental anatomy, and selected aspects of non-neoplastic pathology. In: Lack EE, ed. Pathology of the adrenal glands. New York: Churchill Livingstone; 1990:1-74.)

Right: The outer zona fasciculata is relatively well preserved whereas the inner fasciculata and entire zona reticularis are replaced by haphazardly arranged cells with vacuolated cytoplasm and needle-like clefts. Empty spaces represent lipid which has been extracted out in tissue processing. Dystrophic calcification is a prominent feature.

Grossly, the adrenal pseudocyst is unilocular, with a wall usually 1- to 5-mm thick, filled with yellow-brown or bloody amorphous material. The lining is smooth or shaggy (fig. 7-12), and may contain elevated nodules or plaques. The dense fibrous connective tissue capsule may be hyalinized, with spotty areas of calcification, and on close inspection, mottled yellow areas representing residual adrenal cortex may be seen. The cyst lining may have a partially organized, fibrinoid appearance without any apparent cellular lining when observed by routine light microscopy (fig. 7-13, above). The wall can be thick and hyalinized in areas (fig. 7-13, right) and may contain areas of calcification. Some cysts have smooth muscle in the wall that is continuous with the smooth muscle of the adrenal vein (14).

The pseudocyst contents may be fresh or altered blood (fig. 7-14A) or an amorphous fibrin-rich exudate (fig. 7-14B). There may be evidence of old hemorrhage with hemosiderin deposition and collections of foamy macrophages and cholesterol clefts. The macrophages can be distinguished from cortical cells by positive immunostaining for histiocyte markers (fig. 7-14C). Unusual variants of adrenal pseudocysts have been reported with intracystic fat, myelolipomatous metaplasia (15), and even a rare example of mammary carcinoma manifesting as an intracystic metastasis (15,16).

Endothelial or vascular adrenal cysts have flat to cuboidal endothelial cells in some areas; in a chance plane of section, these cells may communicate with the microvasculature of the adjacent adrenal cortex (fig. 7-15A). The endothelial component is very delicate and easily demonstrated by immunostains (fig. 7-15B). Areas of the cyst may be hemorrhagic and show evidence of organization of fibrin-rich exudates along with fibrosis, dystrophic calcification, and even metaplastic bone and fat (fig. 7-15C). Many of these features suggest that the initial event in some cases is adrenal hemorrhage with hematoma formation, followed by an attempt at organization with endothelialization from the adrenal microvasculature.

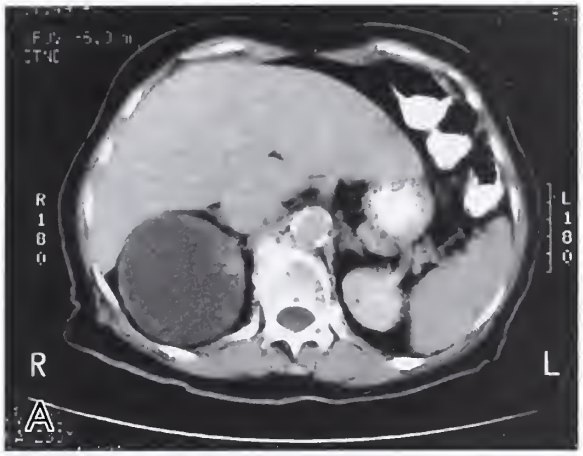

Figure 7-10

ADRENAL PSEUDOCYST MIMICKING CYSTIC RENAL CELL CARCINOMA

A: A large cystic mass is present at the superior pole of the right kidney. The mass could not be separated from the kidney on contrast studies, including selective angiography, and there was suspicion of a cystic renal cell carcinoma.

B: Percutaneous needle core biopsy was performed and yielded three cores of tissue, one of which is clearly kidney (bottom of field). The middle core was misinterpreted as a neoplasm consistent with renal cell carcinoma.

C: At higher magnification, adrenal cortex is seen. A radical nephrectomy was performed and the cyst turned out to be an adrenal pseudocyst. During surgery the cyst was found to be adherent to the undersurface of the liver and appeared to be "spreading" into it. A small portion of liver was removed with the cyst and it showed adrenal hepatic adhesion and union (or fusion), with free intermingling of cortical cells and hepatocytes (see figure 2-7).

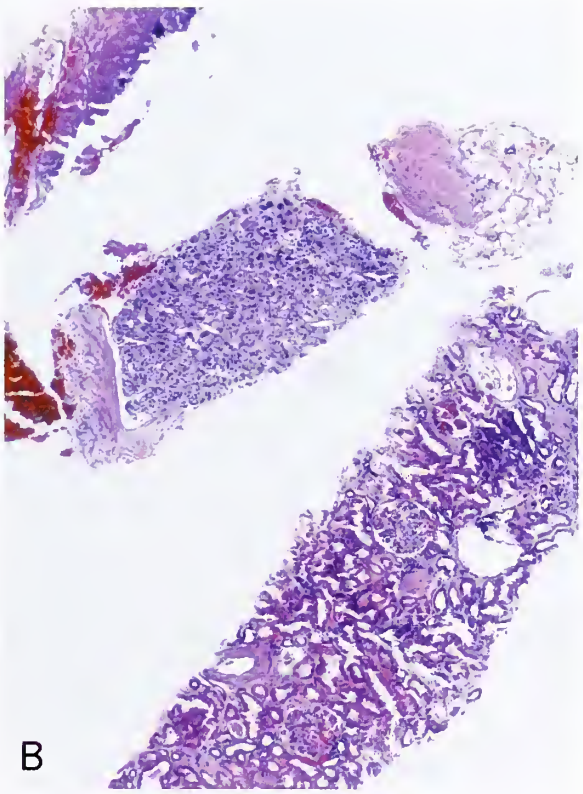

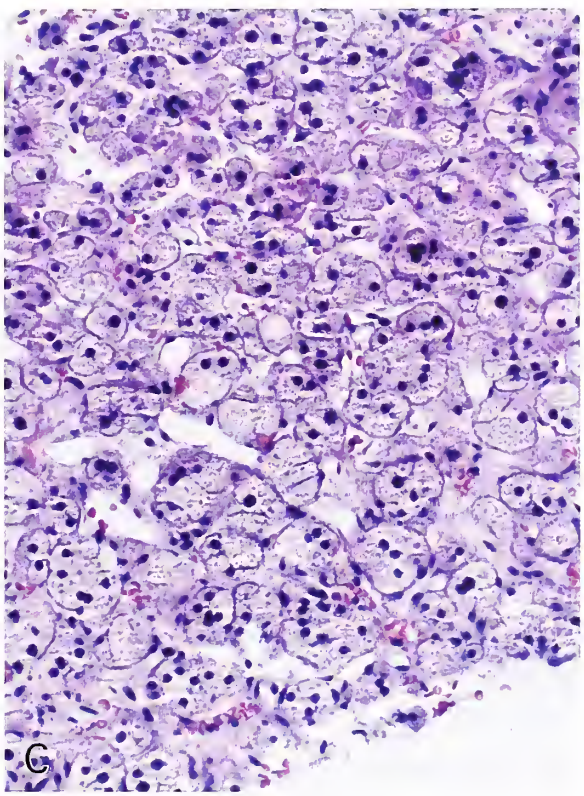

MYELOLIPOMA

Adrenal myelolipoma is a benign tumor-like lesion composed of mature adipose tissue admixed with hematopoietic elements in various proportions (1). While most of these lesions arise in the adrenal gland, extraadrenal myelolipomas have been reported, usually in the presacral area of the retroperitoneum (1), but also in unusual sites such as the renal sinus (17), thorax (18), liver (19), stomach, leptomeninges, and lung (20). Myelolipoma has also been reported in a heterotopic adrenal gland (21).

The age range of patients with adrenal myelolipoma in a study by Plaut (22) was 17 to 93 years; the average age at diagnosis is about 50 years (23). It is rare in individuals under 30 years

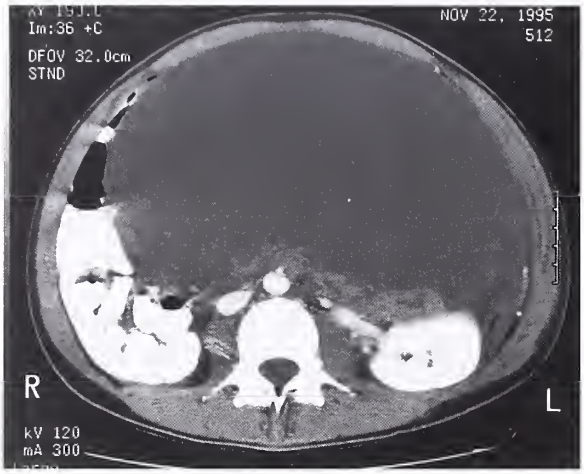

Figure 7-11

GIGANTIC ADRENAL PSEUDOCYST

This gigantic adrenal pseudocyst in a 29-year-old female was suspected preoperatively to be an ovarian cyst. The pseudocyst has relatively homogenous water density and in this CT scan occupies much of the abdomen. It extended into the true pelvis. In this plane of imaging, the pseudocyst is nearly 24 cm in diameter.

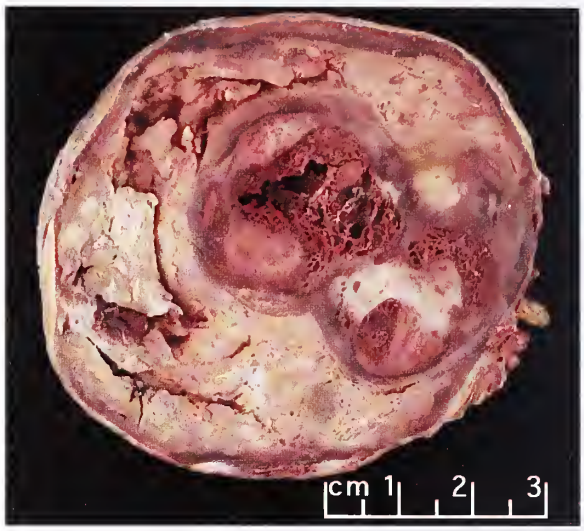

Figure 7-12

ADRENAL PSEUDOCYST

The contents of this adrenal pseudocyst, which measured nearly 7 cm in diameter, were creamy and curd-like. The cyst wall averaged about 0.2 cm in thickness and contained foci of calcification. (Fig. 7-8C from Fascicle 19, Third Series.)

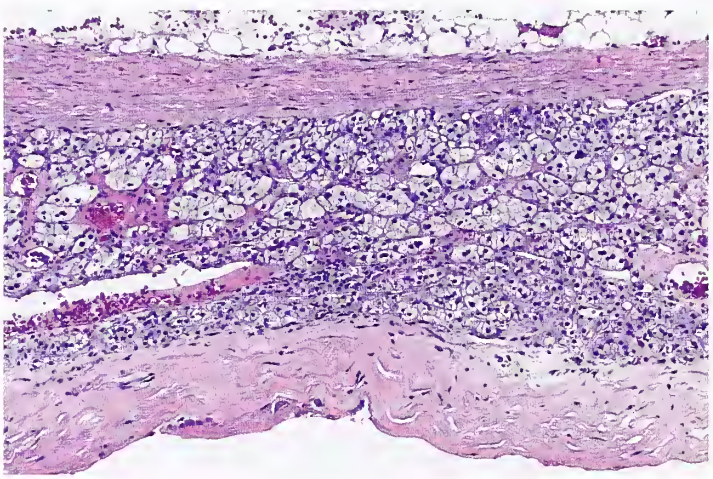

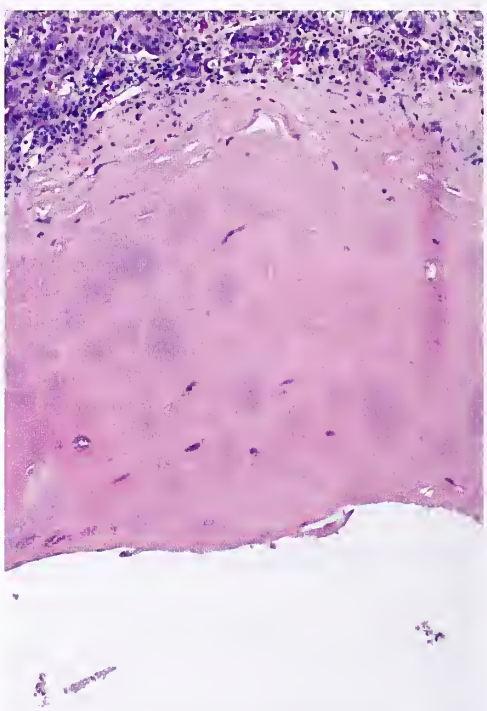

Figure 7-13

ADRENAL PSEUDOCYST

Above: The thin fibrous wall of an adrenal pseudocyst is at the bottom of field. There was no endothelial or other lining identified. The adrenal capsule with periadrenal fat is at the top.

Right: Adrenal pseudocyst in a different case has a thickened, hyalinized wall. Foci of calcification were present in other areas.

of age. Almost all adrenal myelolipomas are unilateral and solitary, and equally distributed on either side; only rarely is the lesion bilateral (23). There is a roughly equal sex distribution. The estimated incidence at autopsy varies from 0.08 to 0.2 percent; in one study it was 0.01 percent for the age group between 36 and 65 years (22). With the increasing use of sensitive

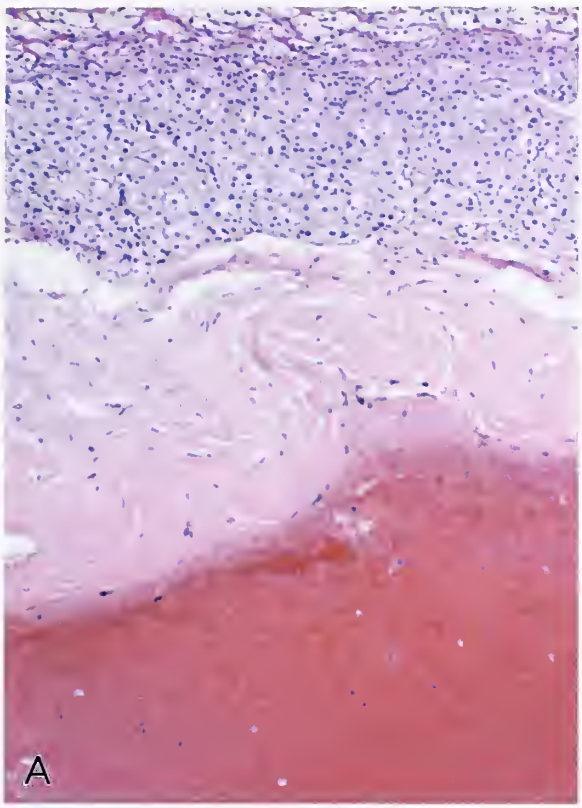

Figure 7-14

VARIED CONTENTS OF ADRENAL PSEUDOCYST

A: Adrenal pseudocyst contains fresh hemorrhage. The fibrous wall had no identifiable lining.

B: The cyst contains fibrin-rich matter.

C: Numerous foamy macrophages are present, with a few cholesterol clefts. Immunostain for histiocyte marker CD68 highlights macrophages (avidin-biotin peroxidase method).

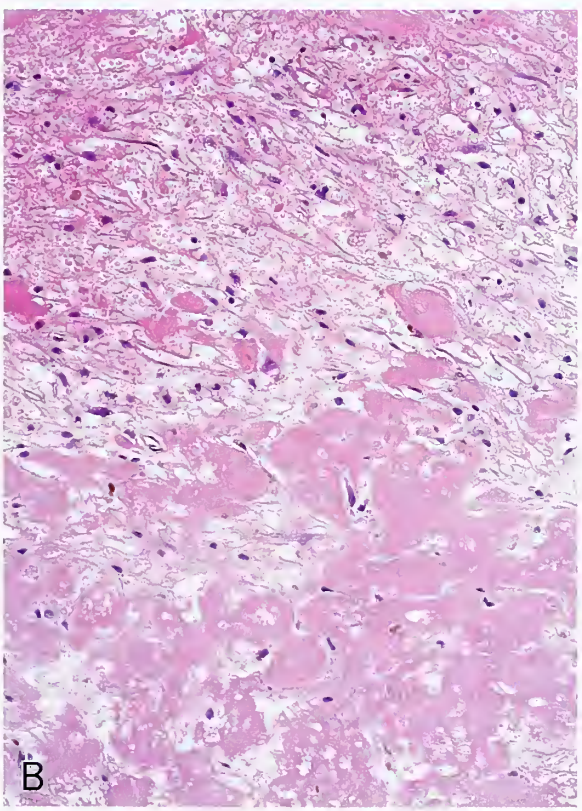

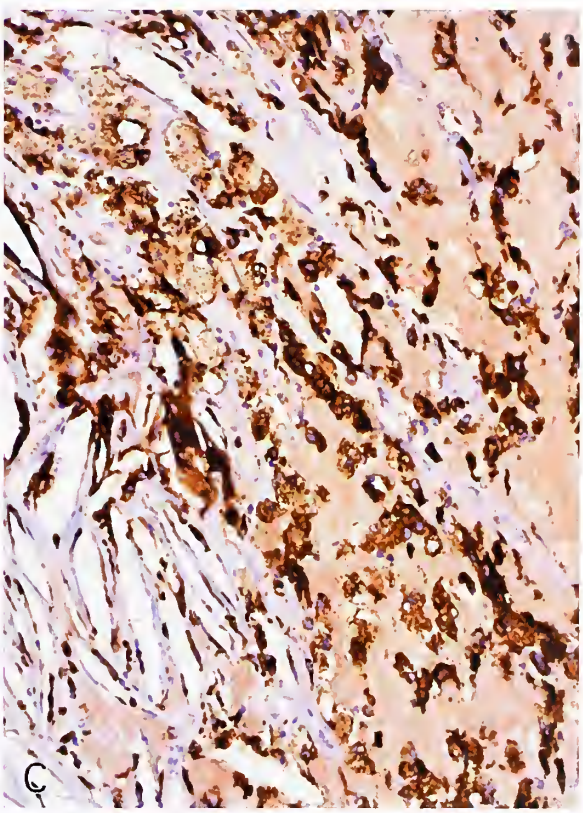

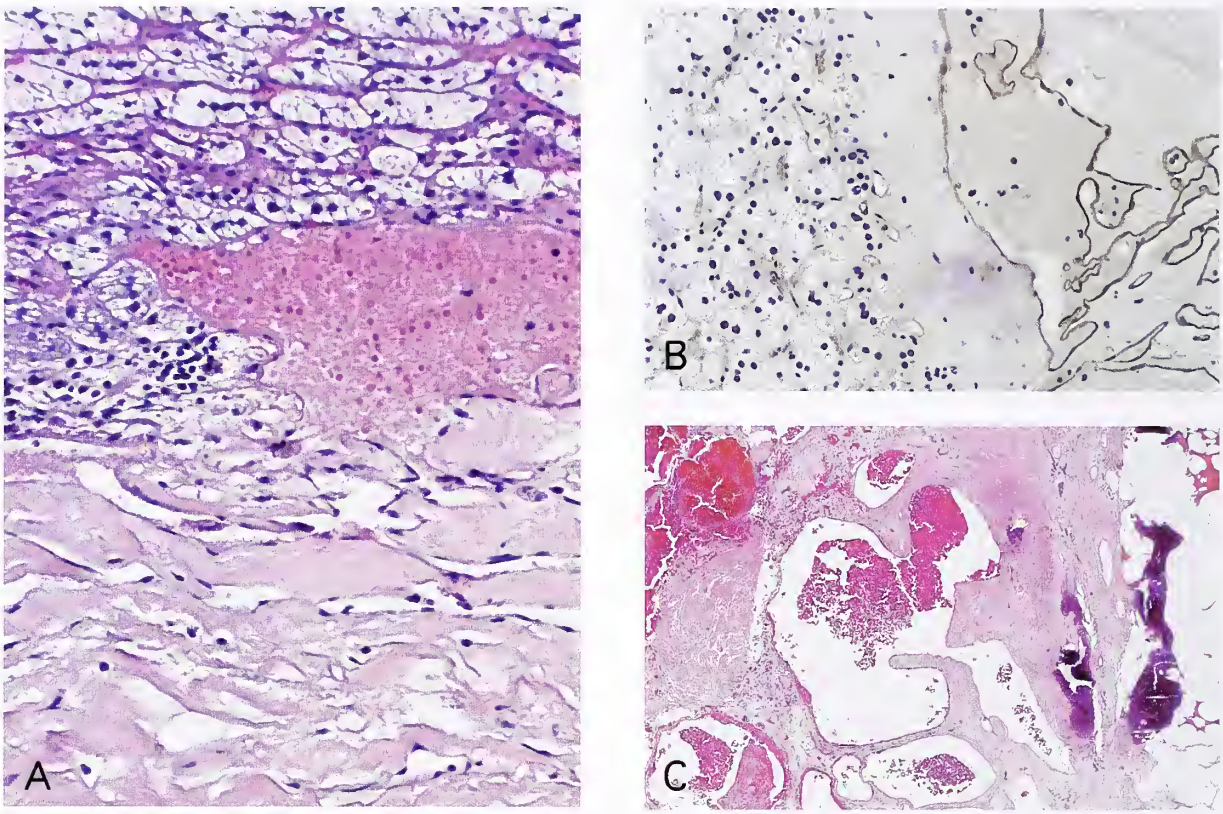

Figure 7-15

ENDOTHELIAL OR VASCULAR ADRENAL CYST

A: The contents of an adrenal cyst are beginning to endothelialize due to direct continuity with the adrenal microvasculature.

B: Immunostain for CD34 shows the microvasculature of the adrenal cortex on the left and endothelial-lined channels of the adrenal cyst on the right (avidin-biotin peroxidase method).

C: Adrenal cyst has irregular cavernous spaces containing fresh blood. There is also fibrosis with a fibrin-rich exudate. Fat and a few spicules of metaplastic bone are present on the right.

imaging techniques such as CT scan and MRI (fig. 7-16) (24), a larger number of asymptomatic patients with adrenal myelolipoma may be diagnosed during life.

On CT scan, myelolipomas are usually well-circumscribed, with a variable appearance depending upon the amount of fat present. The lesions may show internal enhancement or low attenuation due to the fat content. Lesions with little or no adipose tissue may be difficult to distinguish from other adrenal tumors (similar to MRI features). On MRI, myelolipomas tend to have an appearance based upon a high fat signal on T1-weighted images, with heterogeneous enhancement following contrast (fig. 7-16).

Roughly half of the patients undergoing surgical resection of an adrenal myelolipoma are asymptomatic while others have a variety of complaints or findings such as abdominal or flank pain, hematuria, a palpable mass, and hypertension; rarely, the patient presents with a near calamitous episode of retroperitoneal hemorrhage (1). Myelolipomas have been associated with a variety of endocrine disturbances including Cushing's syndrome (combined with an adrenal cortical adenoma), pituitary-dependent Cushing's disease, Addison's disease, virilism, and pseudohermaphroditism (1,22). Adrenal myelolipomas have also been reported in association with congenital adrenal hyperplasia due to deficiency of 21-hydroxylase and 17-hydroxylase

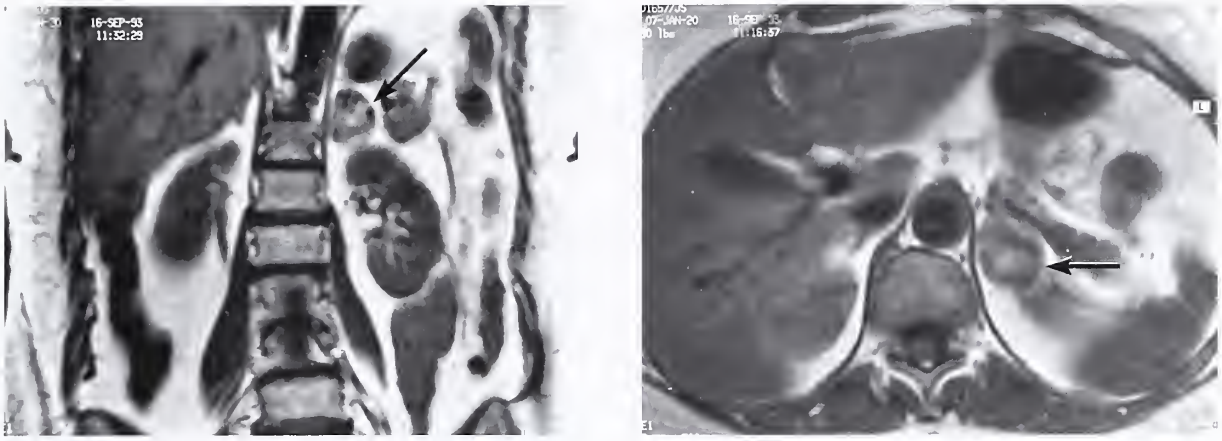

Figure 7-16

ADRENAL MYELOLIPOMA

Left: Left adrenal myelolipoma in a 73-year-old woman seen in the coronal plane (arrow). The T1-weighted image on magnetic resonance imaging (MRI) shows a high central signal from a fatty component.

Right: Adrenal myelolipoma in transverse plane (arrow). The high central signal is due to the fatty component. The T1-weighted "fat saturation" image showed selective nulling of the fat signal, proving the fatty content of the tumor. (L&R: Fig. 7-11 from Fascicle 19, Third Series.)

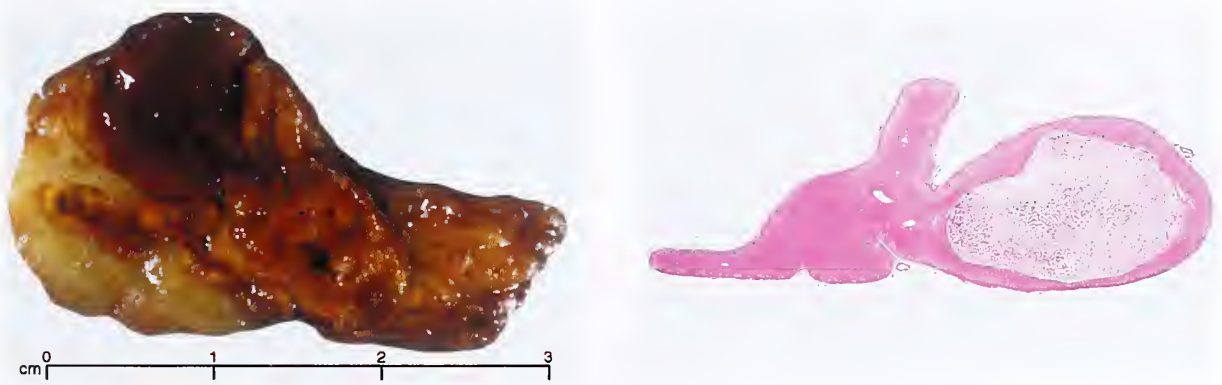

Figure 7-17

ADRENAL MYELOLIPOMA

Left: Adrenal myelolipoma was an incidental finding at autopsy. The tumor measures about 1 cm in diameter and is reddish brown on cross section due to the abundance of hematopoietic elements.

Right: Whole mount section shows one wing, or ala, of the gland expanded by a sharply demarcated myelolipoma.

(25). There is no relationship to anemia or other disturbance of the hematopoietic system (22). Some studies indicate a higher incidence in obese patients (1). Adrenal myelolipomas are occasionally associated with hypertension, and rarely may simulate a pheochromocytoma (1). A patient with alimentary tract ganglioneuromatosis-lipomatosis, adrenal myelolipomas, pancreatic telangiectasia, and multinodular goiter had been reported as having a possible neuroendocrine syndrome (26). An adrenal myelolipoma was reported in association with Castleman's disease (27) and adrenal ganglioneuroma (28).

Adrenal myelolipomas vary considerably in size, ranging from the small lesion discovered incidentally at autopsy (fig. 7-17) to an immense mass measuring up to 34 cm and weighing 5,900 g (1). The giant myelolipoma in figure 7-18 was discovered incidentally in a patient undergoing

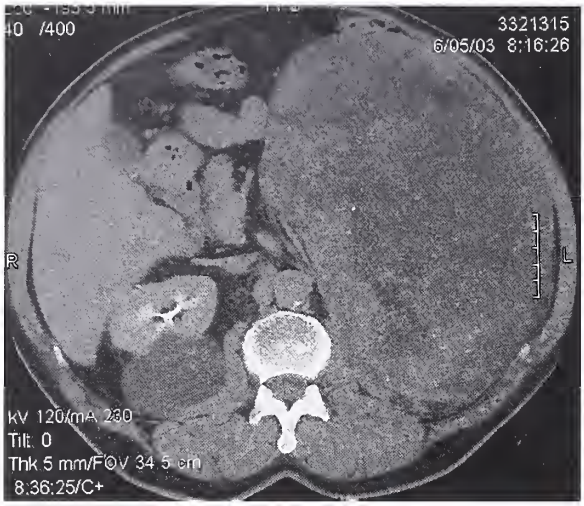

Figure 7-18

LARGE ADRENAL MYELOLIPOMA

Top: A 73-year-old asymptomatic man was found on screening colonoscopy to have a large left upper quadrant mass impinging on the left colon. The adrenal mass has a somewhat heterogenous imaging intensity on CT scan due to fibrosis and areas of recent and old hemorrhage. A benign renal cyst was present on the right side. The preoperative diagnosis was retroperitoneal sarcoma.

Bottom: At surgery, a large adrenal myelolipoma was seen, which measured nearly 30 cm in diameter and weighed 4,000 g. (Courtesy of Dr. Mark Steves, Washington, DC.)

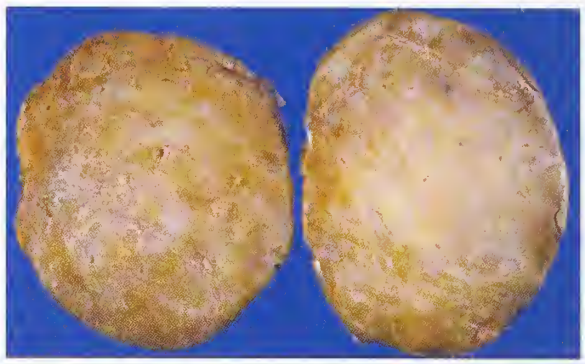

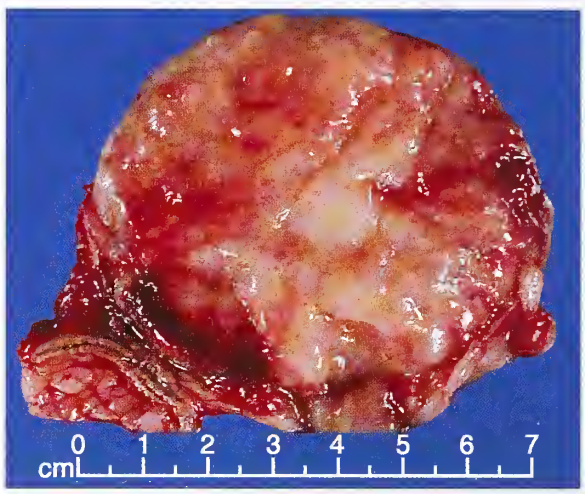

Figure 7-19

ADRENAL MYELOLIPOMA

Top: Adrenal myelolipoma is homogeneously bright yellow on cross section due to the predominance of mature adipose tissue. The tumor measures 8.5 cm in diameter and weighed 240 g. Patient was a 65-year-old female who presented with vague abdominal pain.

Bottom: Yellow areas rich in adipose tissue are admixed with darker red areas in a punctuate to confluent distribution, reflecting the content of hematopoietic elements. (Fig. 7-13, bottom from Fascicle 19, Third Series.)

screening colonoscopy. The lesion is well circumscribed on gross inspection, but is rarely encapsulated. The color varies from pale yellow (fig. 7-19, top) to deep red or red-brown depending upon the relative proportions of fat and hematopoietic elements (fig. 7-19, bottom).

The contour of the adrenal myelolipoma is smooth, wavy, or irregular, and may show intermingling of cortical cells with elements of the myelolipoma. The surrounding cortical cells can be relatively normal in appearance (fig. 7-20A) or compressed. There is a variable mixture of mature fat with hematopoietic elements, often with full representation of the major cell lines (fig. 7-20B). Occasionally, infarction or hemorrhage occurs along with secondary hematoma formation or fibrosis (1). The myelolipoma can grossly resemble a hematoma (fig.

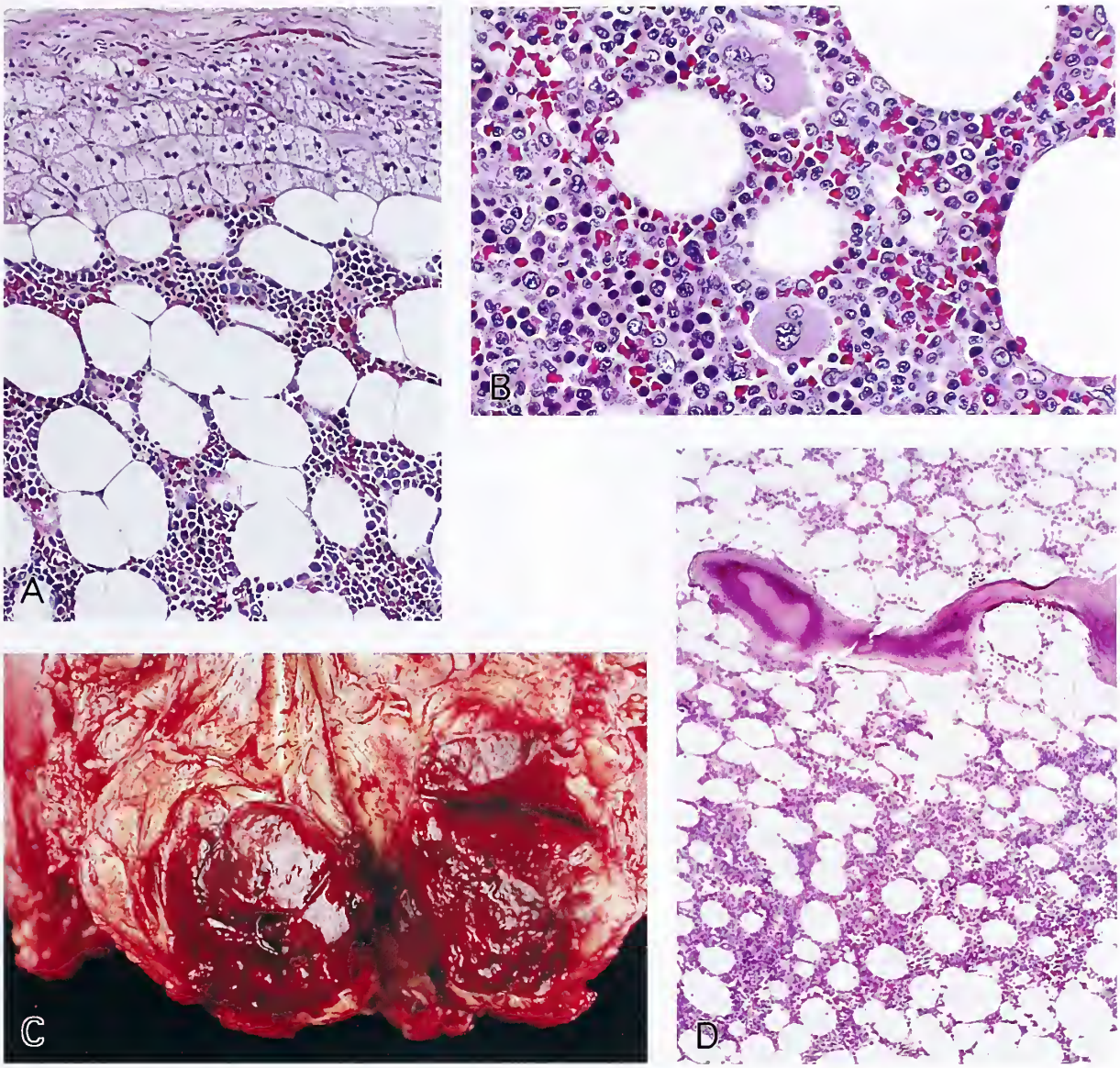

Figure 7-20

ADRENAL MYELOLIPOMA

A: Myelolipoma abuts directly against a rim of cortical cells with lipid-rich, pale-staining cytoplasm. The adrenal capsule is at the top of field. (A–C: Fig. 7-14 from Fascicle 19, Third Series.)

B: In this juxtaadrenal myelolipoma, trilinear hematopoietic cells are evident. Myeloid cells predominate, along with a few clusters of erythroid cells and occasional megakaryocytes.

C: This extraadrenal myelolipoma arose in the retroperitoneum adjacent to, but separate from, the adrenal gland. On cross section, it is deep red-brown and resembles a hematoma.

D: Histologic section of the myelolipoma seen in C shows a component of osseous metaplasia.

7-20C). Rarely, foci of ossification are present (fig. 7-20D). The diagnosis can sometimes be established by fine needle aspiration biopsy in conjunction with a typical appearance on imaging studies (fig. 7-21) (1).

The etiology of myelolipomas is obscure. Foci of lipomatous and myelolipomatous metaplasia can be found in a variety of adrenal cortical disorders, many characterized by cortical hyperfunction, such as adrenal cortical hyperplasia

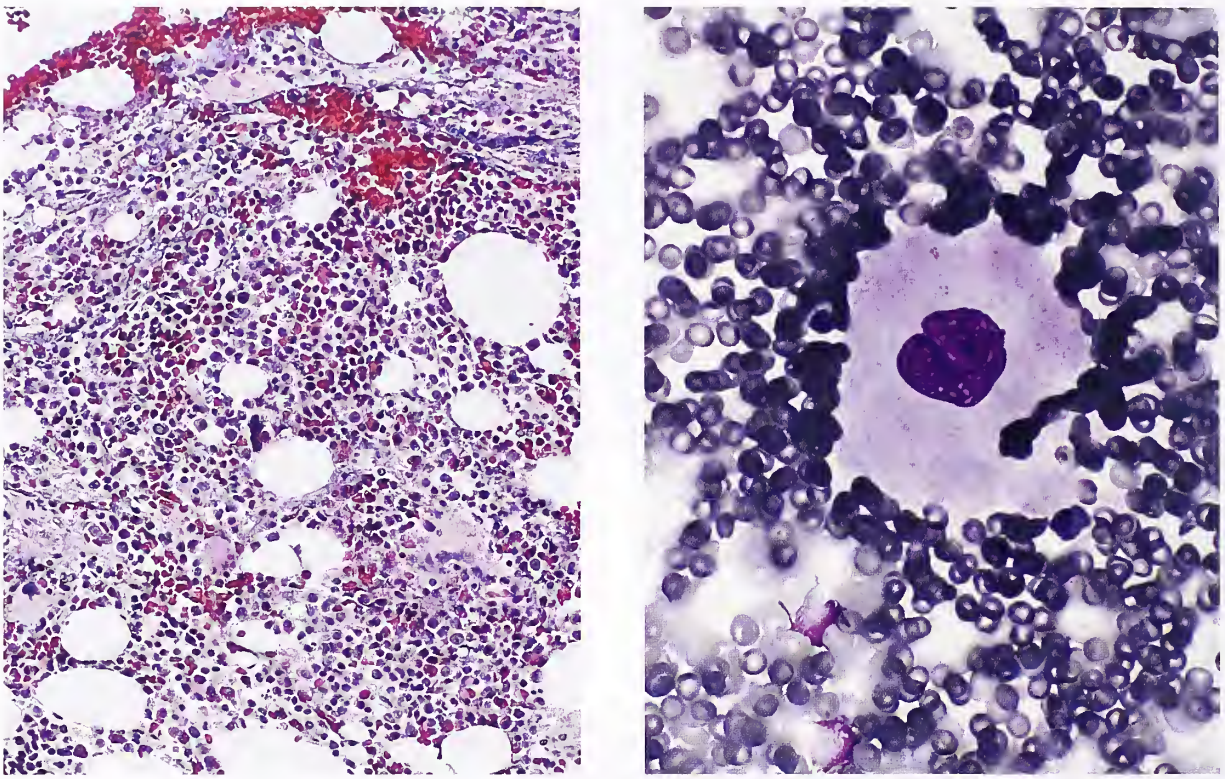

Figure 7-21

ADRENAL MYELOLIPOMA

Left: Cell block preparation of fine needle aspiration biopsy of myelolipoma. The aspirate consisted of blood and a few small tissue fragments composed of hematopoietic cells and mature fat.

Right: An occasional megakaryocyte was present. (L&R: Fig. 7-15 from Fascicle 19, Third Series.)

and neoplasia. A number of theories have been proposed for the origin of fat and hematopoietic cells in the adrenal gland: 1) bone marrow embolization by the hematogenous route; 2) intraadrenal embryonic rests of bone marrow; 3) metaplasia of adrenal cortical cells; and 4) metaplasia of uncommitted or pluripotential adrenal stromal cells (1). Lipomatous and myeloid transformation has been induced experimentally in the rat by administration of methyltestosterone and crude pituitary extracts rich in ACTH (29). Recently, nonrandom X-chromosome inactivation in hematopoietic elements and adipose tissue of myelolipomas has been reported, suggesting a clonal origin for these tumefactive lesions; results of this study, however, did not directly refute any of the previous theories for etiopathogenesis of myelolipomas (30).

PRIMARY MALIGNANT MELANOMA

Primary malignant melanoma of the adrenal gland is extremely uncommon. Proposed diagnostic criteria include: presence of malignant melanoma in only one adrenal gland; no prior or current pigmented lesions of the skin, mucosal surfaces, or eye; no history of removal of pigmented skin or eye lesions; and failure to detect an extraadrenal primary by a thorough autopsy (31). A review of primary malignant melanoma of the adrenal gland identified six cases since 1946, and proposed an origin from pheochromocytes, hence, these tumors were regarded as melanotic pheochromocytomas and not true melanocytic tumors (32). Melanin or melanin-like pigment has rarely been reported in pheochromocytomas (33), although it may be difficult to distinguish from neuromelanin, a pigment related to altered lipofuscin.

Figure 7-22

PRIMARY MALIGNANT MELANOMA OF ADRENAL GLAND

A 48-year-old female complained of abdominal pain and imaging studies of the upper abdomen revealed a right adrenal mass. Ultrasound showed an ovoid mass measuring about 5.5 cm in diameter. There was no history of a mucocutaneous pigmented lesion, and intensive investigation failed to reveal a primary source. (Figs. 7-22 through 7-25 are from the same case.) (Fig. 7-16 from Fascicle 19, Third Series.)

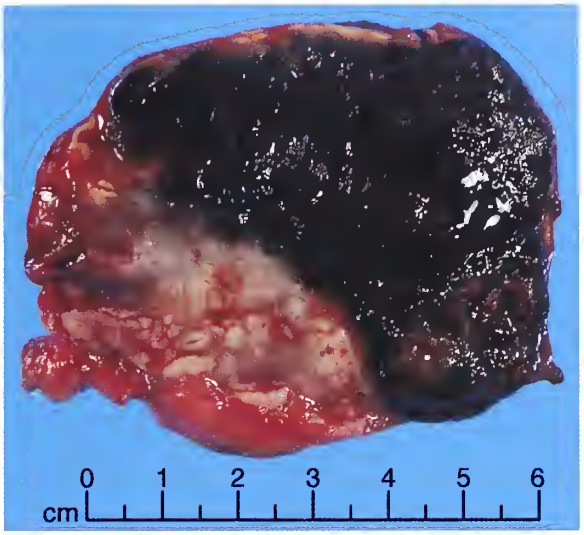

Figure 7-23

PRIMARY MALIGNANT MELANOMA OF ADRENAL GLAND

In cross section, much of the tumor is jet black and coarsely nodular. Periadrenal adipose tissue is attached to the tumor. The tumor measured about 6 cm in diameter. (Fig. 7-17 from Fascicle 19, Third Series.)

Neuromelanin has also been detected in ganglioneuroblastomas and in ganglioneuromas (34). A distinguishing feature of melanocytic melanin pigment is the presence of typical melanosomes or premelanosomes on ultrastructural study.

The author has encountered only one case of malignant melanoma primary in the adrenal gland, in a patient who had no evidence of malignant melanoma in any other site following a rigorous investigation utilizing a multidisciplinary approach (fig. 7-22). The tumor is brown to black (fig. 7-23), but the degree of pigmentation may vary and some tumors are amelanotic. There may be hemorrhage and focal necrosis. Grossly, the mass may look like another tumor, such as pheochromocytoma. The histology is typical for malignant melanoma arising in more conventional sites (fig. 7-24); confirmation includes immunohistochemical staining for S-100 protein, Melan-A, and HMB45, and the ultrastructural presence of premelanosomes or melanosomes. Primary malignant melanoma of the adrenal gland may have diagnostic features on fine needle aspiration (fig. 7-25). Other "pigmented" adrenal lesions such as adrenal hematoma with hemosiderin-laden macrophages, pigmented (black) adenomas, and even pigmented pheochromocytomas are part of the differential diagnosis. Primary malignant melanoma of the adrenal gland is highly malignant and usually fatal within 2 years of diagnosis (32).

PRIMARY MALIGNANT LYMPHOMA

Malignant lymphoma has been reported on rare occasion to be primary in the adrenal gland (35), but adrenal involvement almost always occurs with more widespread disease. This is covered further in chapter 8.

PRIMARY MESENCHYMAL TUMORS

Vascular Neoplasms

Hemangioma. Hemangiomas of the adrenal gland are extremely rare and most are discovered incidentally at autopsy. The files of the Armed Forces Institute of Pathology listed one adrenal angioma for every 10,000 autopsy protocols accessioned between 1943 and 1958 (frequency of 0.01 percent) (36). Very few adrenal hemangiomas have been detected during life as a surgical lesion (1), and only rarely

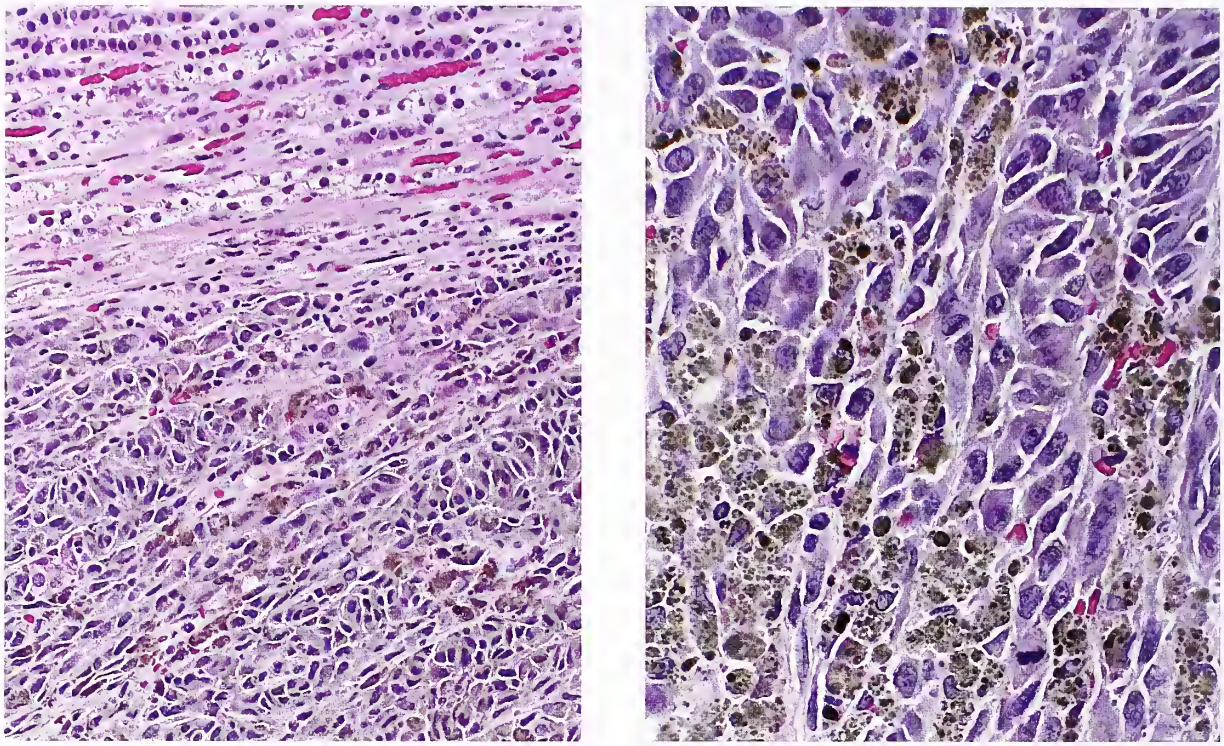

Figure 7-24

PRIMARY MALIGNANT MELANOMA OF ADRENAL GLAND

Left: The tumor compresses the residual cortex (top). (L&R: Fig. 7-18 from Fascicle 19, Third Series.)
Right: Melanin pigment is abundant. Nuclei are pleomorphic, with some having prominent nucleoli.

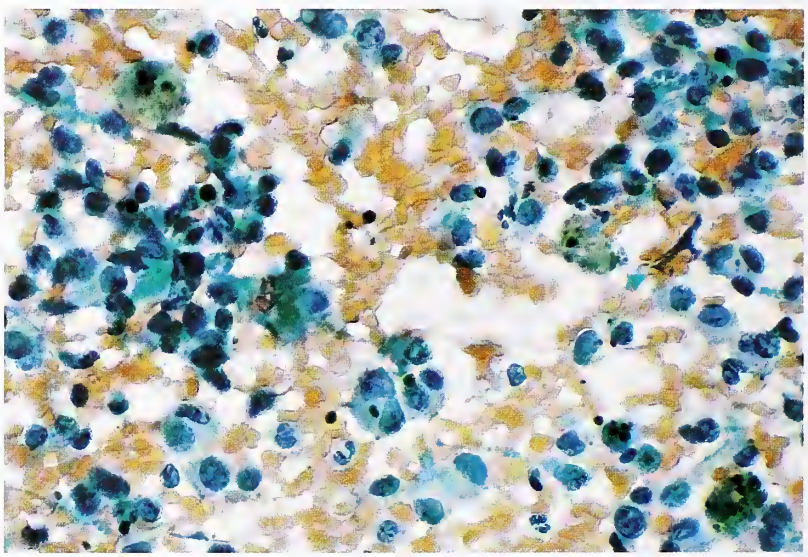

Figure 7-25

PRIMARY MALIGNANT MELANOMA OF ADRENAL GLAND

Fine needle aspiration specimen shows many tumor cells with partially disrupted cytoplasm. The abundant pigment is melanin. On ultrastructural study, typical melanosomes were present (Papanicolaou stain). (Fig. 7-19 from Fascicle 19, Third Series.)

do patients present with symptoms related to a mass effect by the adrenal tumor. The primary capillary hemangioma of the adrenal gland in figure 7-26 simulated a pheochromocytoma.

The age range of patients is usually the 3rd to the 8th decades of life, and most are female. The size of an adrenal hemangioma discovered at autopsy is usually less than 2 cm while those

Figure 7-26

PRIMARY ADRENAL HEMANGIOMA MIMICKING PHEOCHROMOCYTOMA

A: A 48-year-old woman with a history of hypertension was found to have a 0.9-cm nodule in the left adrenal gland by CT scan. A 24-hour urine collection showed elevated norepinephrine, metanephrine, and normetanephrine. On MRI the adrenal nodule showed intermediate to slightly high signal intensity on T2-weighted imaging. Adrenal venous sampling showed significant elevation in epinephrine and norepinephrine levels on the left side. The preoperative diagnosis was pheochromocytoma. The hemangioma here is present beneath the capsule and at the periphery, extending between nests of cortical cells. The vascular tumor has a capillary pattern.

B: Hemangioma in another area has a more cavernous pattern with dilated vascular spaces and delicate septa.

C: A portion of the adrenal hemangioma is located within the lumen of a large venous tributary of the central adrenal vein. Endothelial cells are immunostained with CD34 (avidin-biotin peroxidase method). (See chapter 10 for pseudopheochromocytoma.)

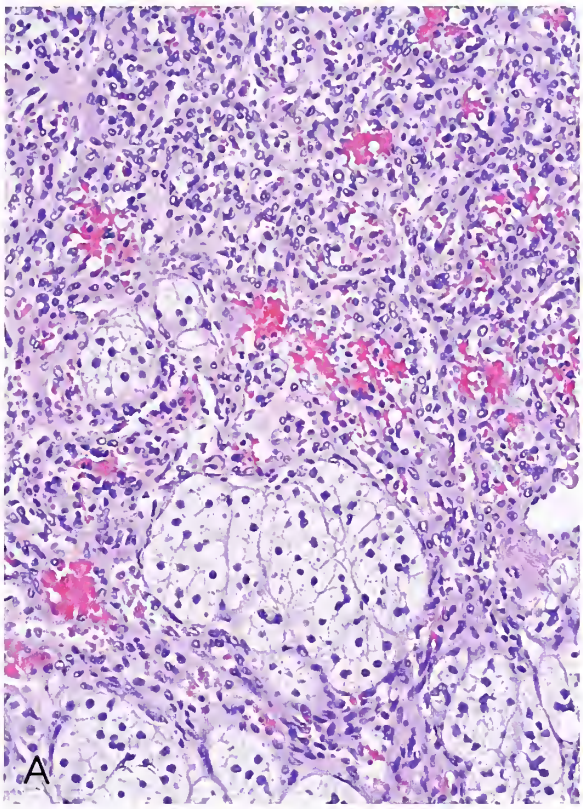

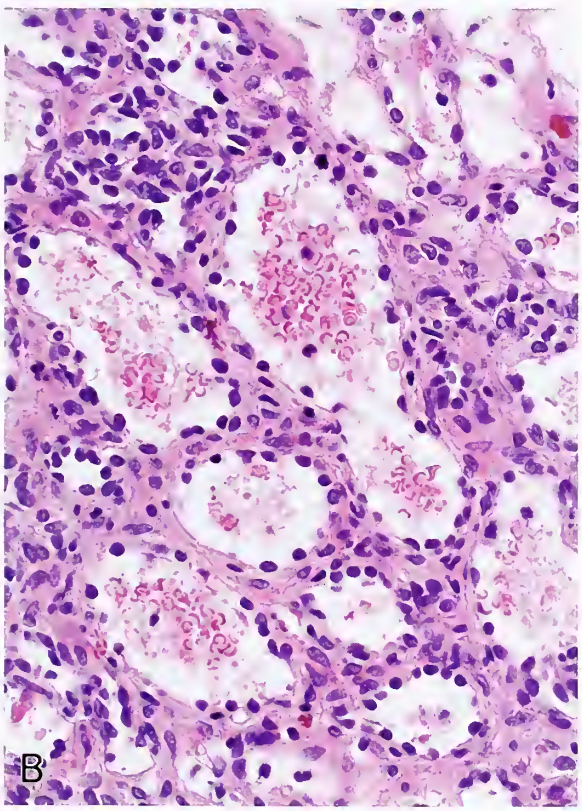

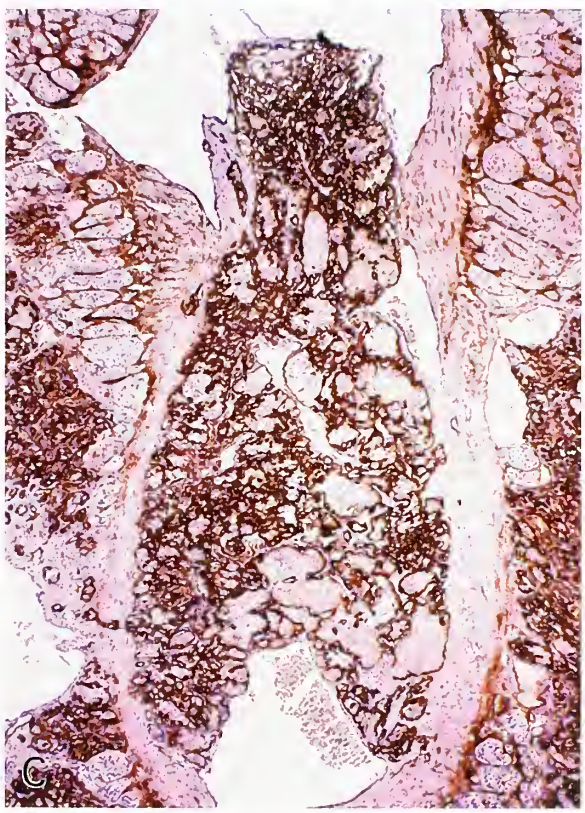

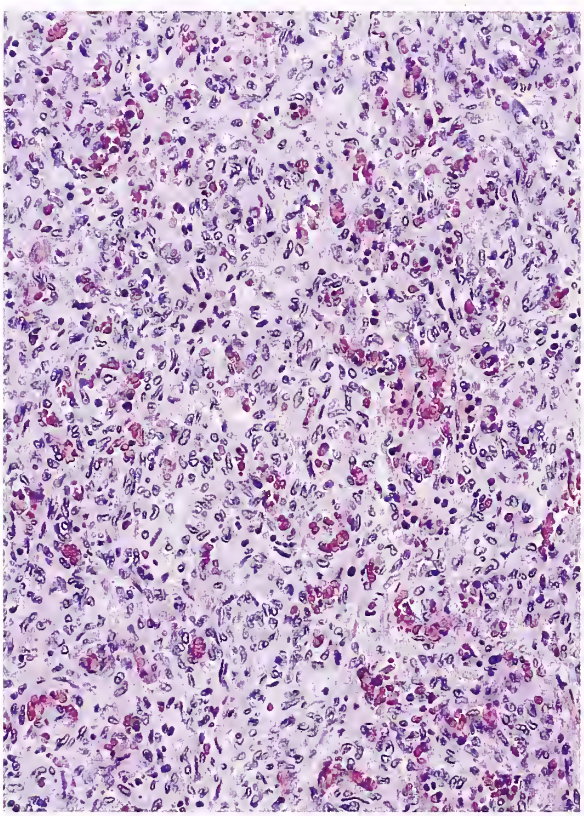

Figure 7-27

JUVENILE (OR CAPILLARY) HEMANGIOMA OF ADRENAL GLAND

Top: A small juvenile hemangioma of the adrenal gland in a newborn. There were numerous cutaneous hemangiomas and a large vascular tumor of the liver with identical histology. The adrenal tumor is uniformly tan, about 5 mm in diameter, and is located in the ridge or crista of the gland. The infant also had the Kasabach-Merritt syndrome with thrombocytopenia.

Bottom: The growth pattern in this juvenile hemangioma is more solid (similar to figure 7-26A), with plump endothelial cells and relatively inconspicuous vascular lumens. (T&B: Fig. 7-21 from Fascicle 19, Third Series.)

removed surgically are usually much larger, measuring up to 22 cm in diameter. Most are unilateral and solitary, but occasional bilateral hemangiomas have been reported (1). Although visceral hemangiomas and telangiectasias occur in the setting of hereditary hemorrhagic telangiectasia, involvement of the adrenal glands is rare (37). Most adrenal hemangiomas are of cavernous type. The author has seen one case of multifocal juvenile hemangioma (benign hemangioendothelioma of infancy) in which the newborn infant had a large hepatic hemangioma as well as a much smaller adrenal tumor (fig. 7-27, top) with identical histology (fig. 7-27, bottom). The child also had the Kasabach-Merritt syndrome and died of high output cardiac failure.

Lymphangioma. Lymphangioma of the adrenal gland has been reported, but it is exceedingly rare. Two of the three cases reported by Plaut (38) would be best classified as adenomatoid tumor. The author has seen only one case of well-developed cavernous lymphangioma of the adrenal gland (fig. 7-28).

Angiosarcoma. Angiosarcoma is another rare primary mesenchymal tumor of the adrenal gland (fig. 7-29). Over a dozen examples have been reported (39), one coexisting with an adrenal hemangioma (40). A case of an epithelioid angiosarcoma was reported in a 59-year-old male who worked as a vineyard cultivator; the tumor was presumed to be related to a long history of exposure to arsenicals (41). One case was also reported in association with mesenteric fibromatosis (42).

Adrenal angiosarcoma usually presents little difficulty in diagnosis when there is a clear vasoformative pattern (fig. 7-29B), but problems arise when the tumor has more of a solid epithelioid pattern, as seen focally in figure 7-29C. Nine epithelioid angiosarcomas of the adrenal gland were reported by Wenig et al. (39) and endothelial differentiation was confirmed by immunohistochemistry (including factor VIII–related antigen, CD34, and *Ulex europaeus* lectin binding) and by ultrastructural features; immunoreactivity for cytokeratin was reported in seven of the nine cases. A massive hemorrhagic adrenal cortical adenoma has been reported mimicking an angiosarcoma (43).

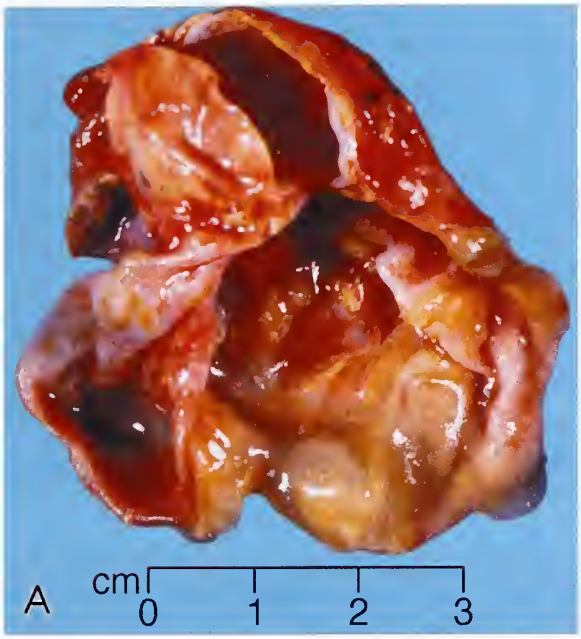

Figure 7-28

LYMPHANGIOMA OF ADRENAL GLAND

A: The tumor appears as a multilocular cyst that has a smooth glistening lining. The cyst had clear watery contents.

B: Lymphangioma has a cavernous (or cystic) architecture with proteinaceous fluid and some collections of lymphocytes. The lymphoid aggregates were also present in the interstitium elsewhere in this lymphangioma. Mildly compressed adrenal cortex is present (left upper corner).

C: Flattened endothelium of adrenal lymphangioma is markedly positive for factor VIII–related antigen (avidin-biotin peroxidase method).

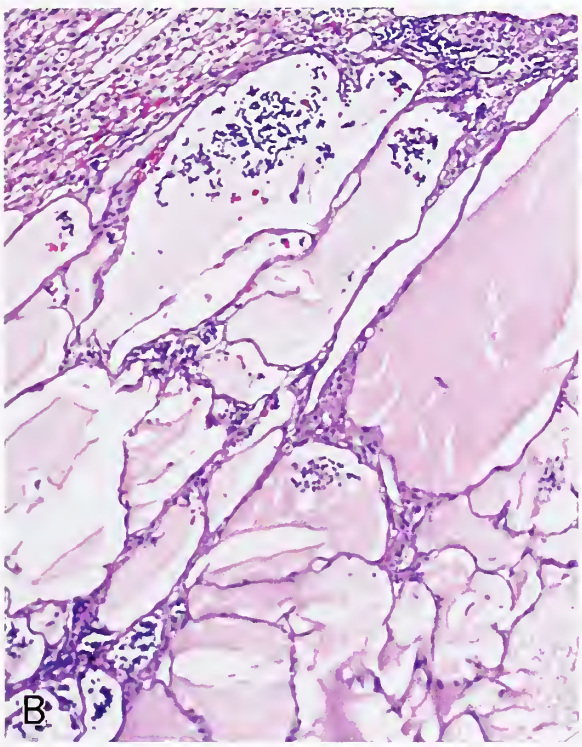

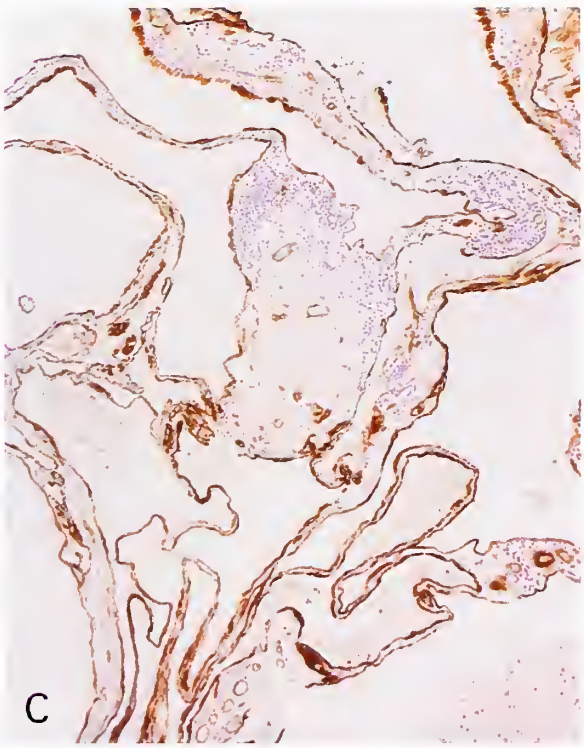

Smooth Muscle Neoplasms

Leiomyoma. Primary adrenal leiomyoma is a very rare tumor associated with the adrenal vein or its tributaries (44). Histologically, adrenal leiomyoma (fig. 7-30) has features identical to benign smooth muscle tumors occurring in other sites.

Leiomyosarcoma. Only a few cases of primary adrenal leiomyosarcoma have been reported (45), including a case in a man with acquired immunodeficiency syndrome (AIDS) (46). Smooth muscle tumors most likely arise from the smooth muscle associated with the central adrenal vein

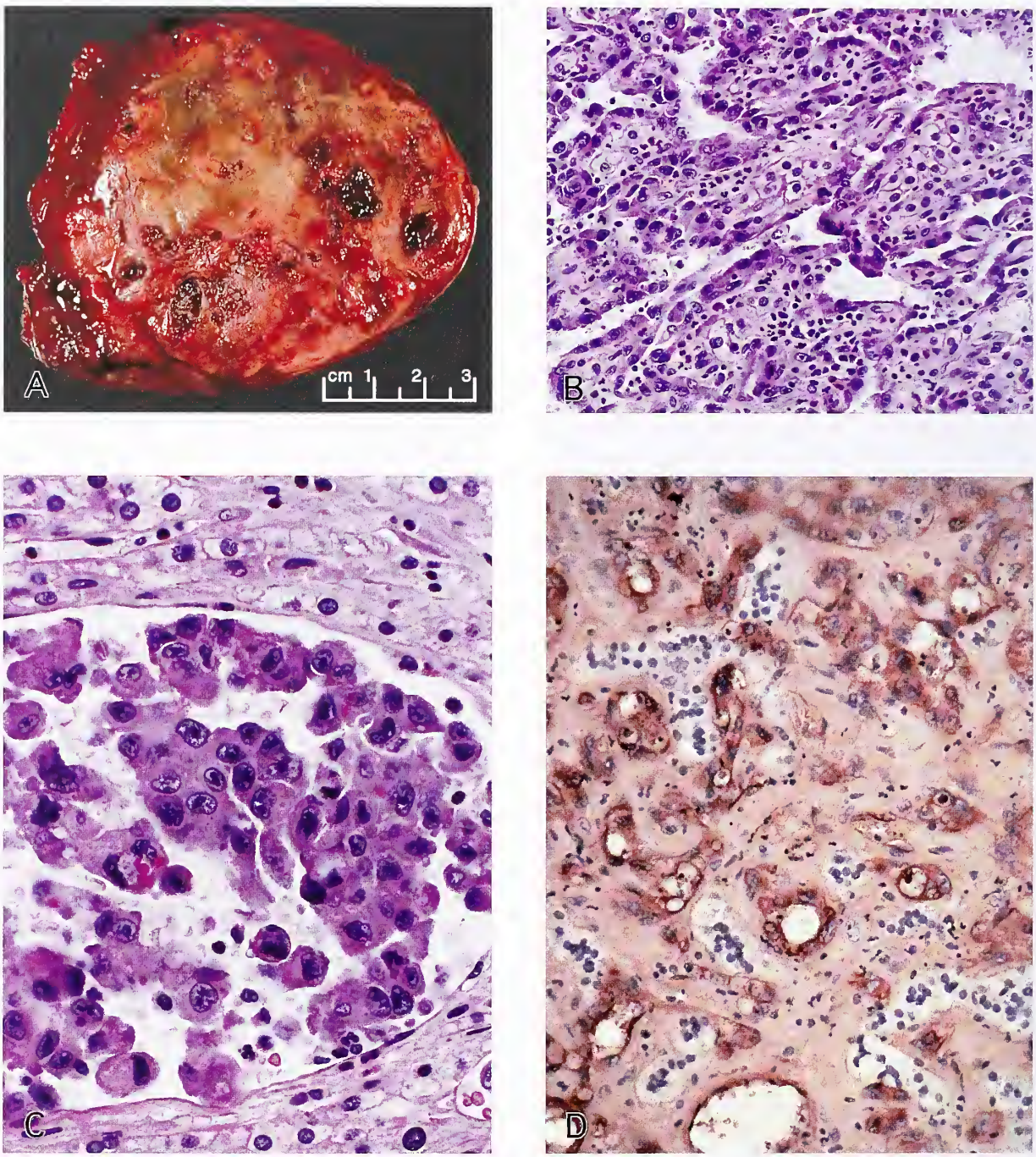

Figure 7-29

PRIMARY ANGIOSARCOMA OF ADRENAL GLAND

A: In cross section, the tumor is markedly variegated and has areas of hemorrhage and necrosis.

B: Primary adrenal angiosarcoma (different case than A). Note the well-developed vasoformative architecture with sinusoidal growth between cords of vacuolated cortical cells. Acute inflammatory cells are also present.

C: Primary adrenal angiosarcoma (same case as B) growing in part as a high-grade tumor with epithelioid features. Residual adrenal cortical cells are also present. (A–C: Fig. 7-22A-C from Fascicle 19, Third Series.)

D: Immunostain of primary adrenal angiosarcoma is markedly positive for factor VIII–related antigen (avidin-biotin peroxidase method). (Figures A and D courtesy of Dr. Sambasiva Rao, Chicago, IL.)

Figure 7-30

PRIMARY LEIOMYOMA OF ADRENAL GLAND

A: In cross section, the leiomyoma has an attached portion of residual adrenal gland (right upper corner). (Courtesy of Dr. Manuel Marcial, San Juan, Puerto Rico.)

B: Primary adrenal leiomyoma was surgically excised. Residual adrenal cortex is at top of field.

C: Primary adrenal leiomyoma is composed of interlacing fascicles of spindle cells in various planes of section. No mitotic figures were identified and there was no necrosis. (A–C: Fig. 7-23 from Fascicle 19, Third Series.)

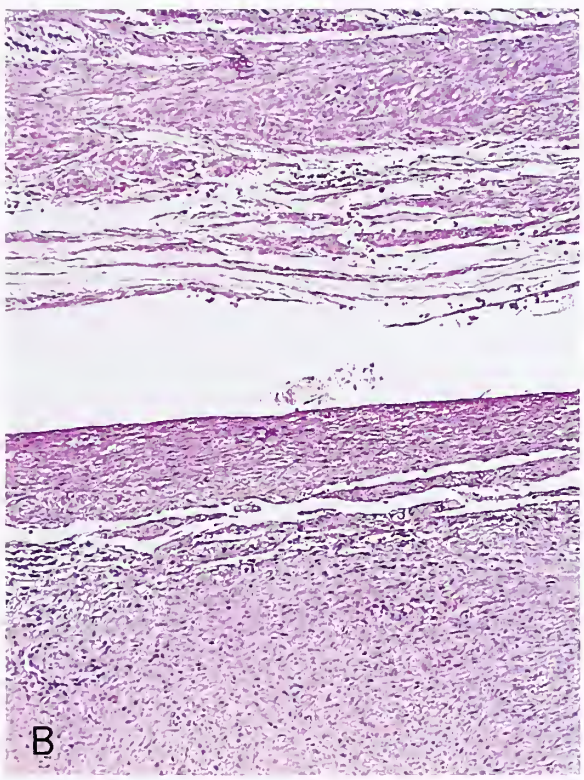

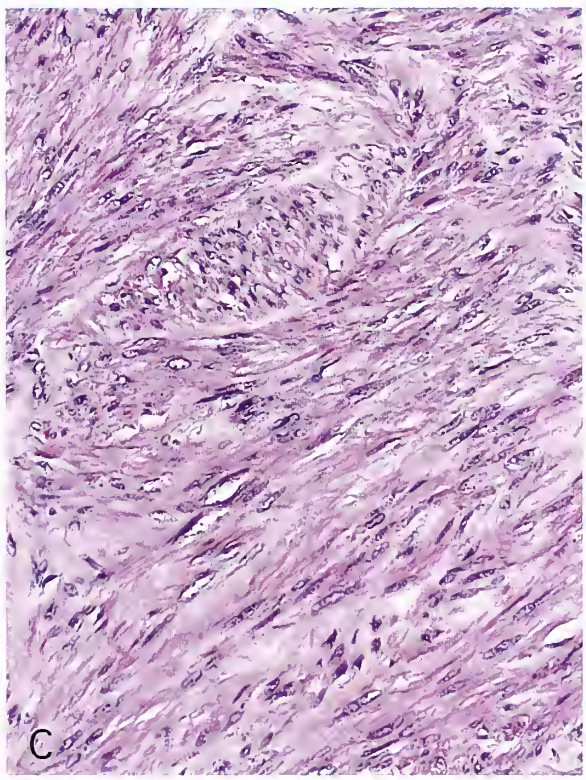

and its tributaries. Macroscopically, the tumor can have large areas of hemorrhage and necrosis (fig. 7-31). Microscopically, residual adrenal gland is seen, particularly in sections taken through the periphery of the tumor (fig. 7-32, left). The tumor may have a high mitotic rate (fig. 7-32, right), and be quite cellular, similar to leiomyosarcomas at other sites. Electron microscopy or immunohistochemistry (fig. 7-33) can confirm the smooth muscle nature of the sarcoma.

Figure 7-31

PRIMARY LEIOMYOSARCOMA OF ADRENAL GLAND

Right adrenal tumor and kidney have been bisected in the coronal plane. The tumor measured 11 x 8 x 7.5 cm. Areas of hemorrhage and necrosis are present. (Fig. 7-24 from Fascicle 19, Third Series.)

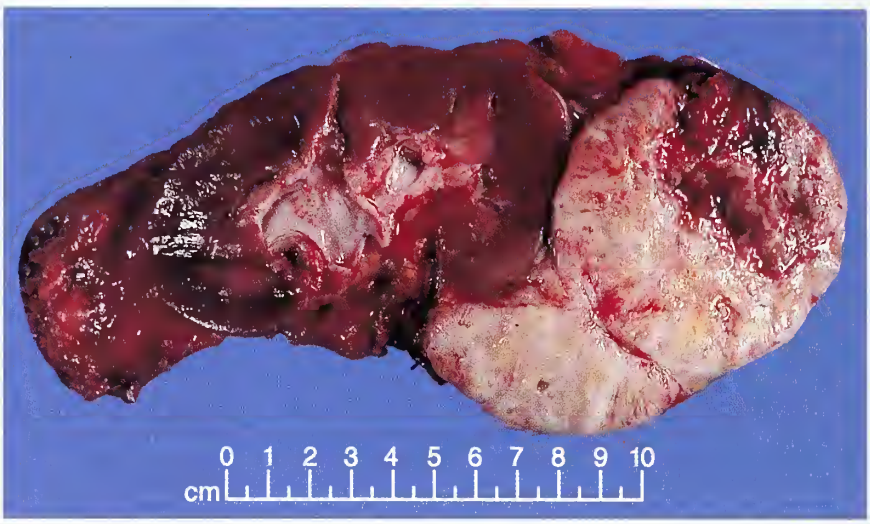

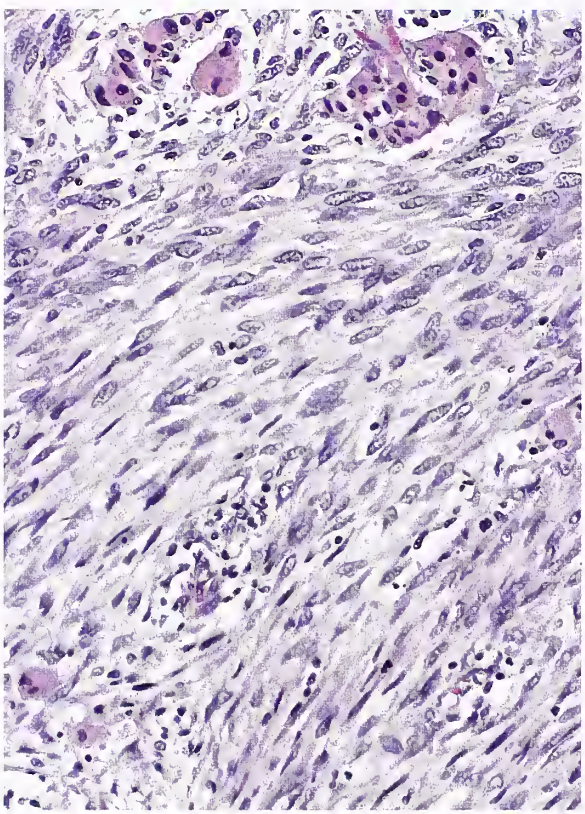

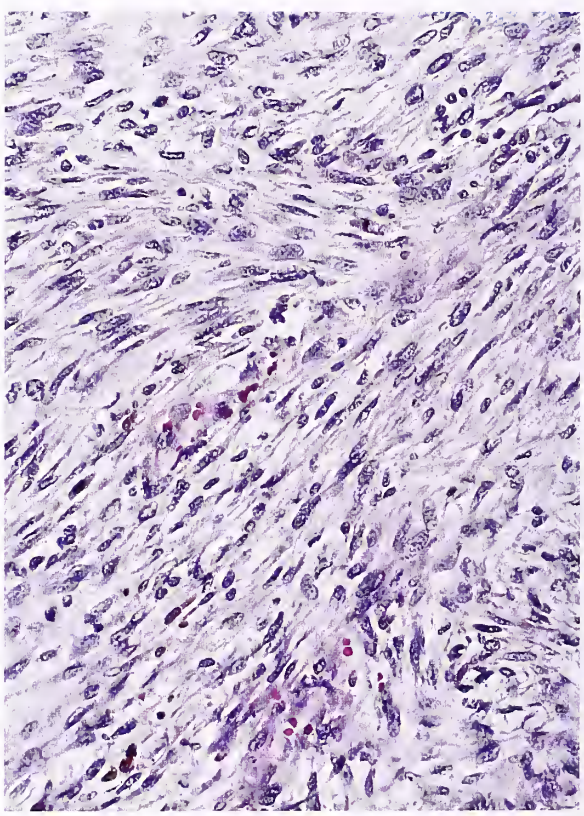

Figure 7-32

PRIMARY LEIOMYOSARCOMA OF ADRENAL GLAND

Left: Leiomyosarcoma infiltrates the adrenal gland. A few residual nests of cortical cells are present at the top and occasional individual cells at the bottom of the field. (L&R: Fig. 7-25 from Fascicle 19, Third Series.)

Right: This leiomyosarcoma had areas of confluent tumor necrosis. The mitotic rate averaged 15 per 10 high-power fields in some of the more active areas. Electron microscopy confirmed smooth muscle differentiation.

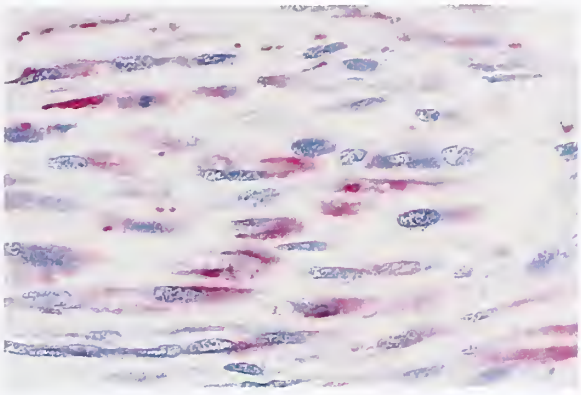

Figure 7-33

PRIMARY LEIOMYOSARCOMA OF ADRENAL GLAND

Tumor cells are positive for smooth muscle actin, which stains dark red (streptavidin-alkaline phosphatase method). (Fig. 7-26 from Fascicle 19, Third Series.)

Figure 7-34

LARGE PRIMARY CYSTIC ADRENAL SCHWANNOMA

This large primary cystic schwannoma of the adrenal gland in a 29-year-old female measured 14 cm in diameter. CT scan shows the marked cystic change (left). At surgery the cystic mass contained abundant clotted and altered blood.

OTHER UNUSUAL PRIMARY TUMORS

Neural Tumors

Primary adrenal or *jnxtaadrenal sclnvannomas* have been documented on rare occasion (1,47). The author has seen a large schwannoma that presented as a large, left upper quadrant cystic mass in a 29-year-old woman (fig. 7-34). The tumor was surgically resected, and while the adrenal gland was difficult to identify, random sections clearly revealed it as an attenuated structure over the surface of portions of the tumor. Although the adrenal gland is a very rare primary site for schwannoma (fig. 7-35), it should not be unexpected given the neural innervation of the gland (see chapter 1). *Adrenal neurofibroma* has also been reported (fig. 7-36) (1). Equally rare is the primary adrenal *malignant sclnvannoma*, or *malignant peripheral nerve sheath tumor* (fig. 7-37) (48). One example occurred in association with an ipsilateral pheochromocytoma, an example of a rare composite tumor (49), while another case arose in an adrenal ganglioneuroma in an adult male homosexual who was human immunodeficiency virus (HIV) positive (50). The histologic features of an adrenal malignant schwannoma are shown in figure 7-38 (48). The identification of tumor cells positive for S-100 protein by immunohistochemistry can help in the diagnosis (fig. 7-39).

Adenomatoid Tumor

Primary adenomatoid tumor of the adrenal gland is rare (51–53). Two of the three cases reported by Plaut (38) as "locally invasive lymphangioma" of adrenal gland appear to be adenomatoid tumors; both were discovered at autopsy. On gross examination, the tumor is smooth, white, and homogeneous. On microscopic examination the tumor is not truly encapsulated (fig. 7-40), hence Plaut's term "locally invasive" (38). This rare tumor is of mesothelial origin, and has the classic histomorphology of adenomatoid tumors including a sieve-like appearance due to cytoplasmic vacuoles and gland-like spaces (fig. 7-41, left). Nuclei have a vesicular quality, often with a single, small, dot-like nucleolus (fig. 7-41, right). There is usually a small amount of interlacing connective tissue. A mesothelial origin can be confirmed by positive immunohistochemical staining for cytokeratin (fig. 7-42), and ultrastructural demonstration of characteristic long, "bushy" cytoplasmic microvilli (51).

Other Rare Primary Tumors

Other rarely described adrenal tumors include lipoma (fig. 7-43), liposarcoma, angiomyolipoma (54), granulosa cell tumor (55), and several examples of adrenal Leydig cell tumor (56) and adrenal adenoma containing crystalloids of

Figure 7-35

PRIMARY SCHWANNOMA OF ADRENAL GLAND

A: This schwannoma has a more solid configuration, with uniform spindle cells. Some areas suggest vague palisading. The adrenal cortex is on the left.

B: Primary adrenal schwannoma (B and C same case as figure 7-34) shows a mild degree of nuclear hyperchromasia and pleomorphism. Other areas had an Antoni A pattern and poorly formed Verocay bodies. (Fig. 7-28B from Fascicle 19, Third Series.)

C: Virtually all nuclei and cytoplasmic extensions are strongly immunoreactive for S-100 protein (avidin-biotin peroxidase method).

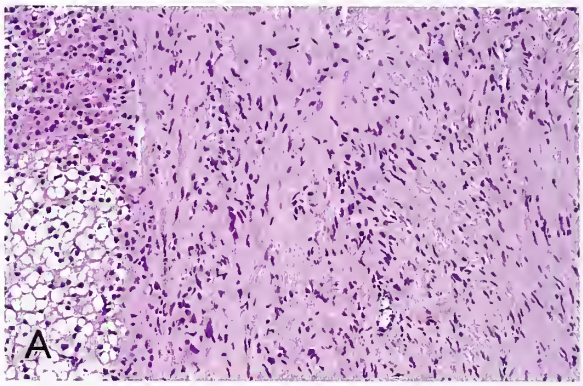

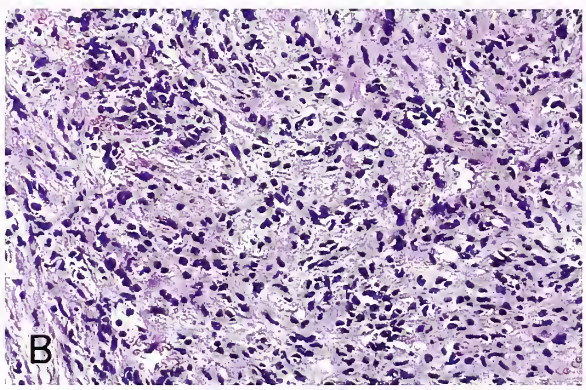

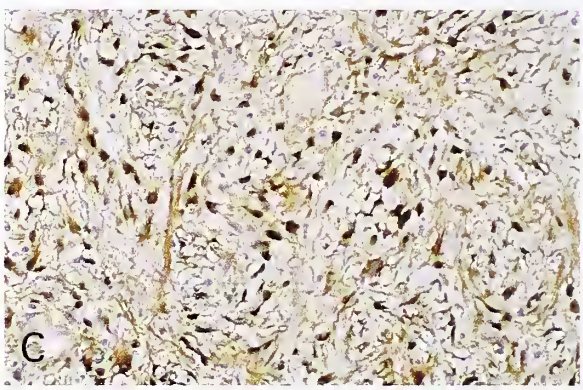

Figure 7-36

ADRENAL NEUROFIBROMA

A: A neurofibroma expands one ala, or wing, of the adrenal gland (arrows). The tumor is relatively well circumscribed but unencapsulated.

B: The adrenal neurofibroma (same case as A) was an incidental finding at autopsy of an adult who had no history of von Recklinghausen's disease (neurofibromatosis 1 [NF1]). The tumor is unencapsulated and interdigitates with adjacent cortical cells. No ganglion cells were identified.

C: Fascicles of spindle cells intermingle with clusters of normal chromaffin cells. (B,C: Fig. 7-29B,C from Fascicle 19, Third Series.)

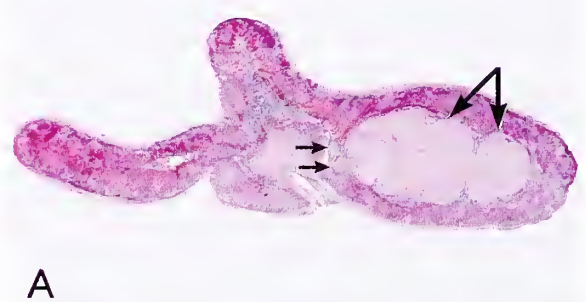

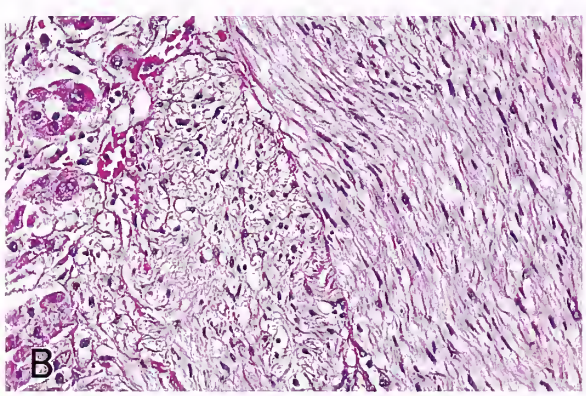

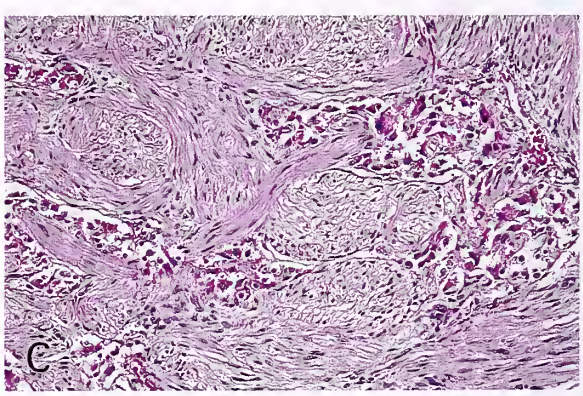

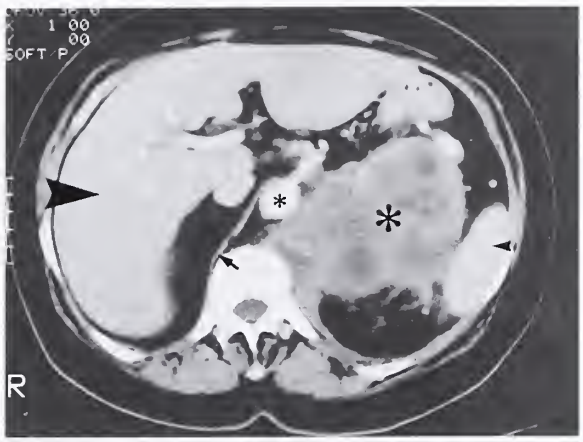

Figure 7-37

PRIMARY MALIGNANT PERIPHERAL NERVE SHEATH TUMOR OF ADRENAL GLAND

Primary malignant peripheral nerve sheath tumor of the left adrenal gland of a 60-year-old female. CT scan shows an 8 x 7 x 7 cm left suprarenal mass (large asterisk) which is nonhomogeneous. The tumor abuts upon the paravertebral (psoas) muscles medially and spleen (small arrowhead). It also invades and obliterates the right crus of the diaphragm (small arrow). Upper abdominal aorta is seen (small asterisk) as well as liver (large arrowhead). (Fig. 1A from Ayala GE, Ettinghausen SE, Epstein AH, Travis WD, Lack EE. Primary malignant schwannoma of the adrenal gland. Case report and literature review. J Urol Pathol 1994;2:265-272.)

Reinke with masculinization (57). Ovarian thecal metaplasia, which has been covered in chapter 1, may morphologically have a sex-cord stromal derivation. Leydig cells are rare within the adrenal gland, but the existence of these cells and tumors derived from them can be explained, in part, by the close embryologic relationship between the developing gonad and the adrenal primordium. The presence of crystalloids of Reinke provides definitive evidence of Leydig cells. Many (but not all) of the masculinizing adrenal cortical neoplasms contain abundant cells that superficially resemble Leydig cells due to their compact, finely granular, eosinophilic cytoplasm, but crystalloids of Reinke are typically not a feature. On only one occasion has the author observed hilus (or Leydig) cells within the adrenal cortex, in an adult female with an aldosterone-producing adrenal cortical adenoma (see fig. 1-46) (58). Intraadrenal Leydig-like cells have been reported in a patient with the ectopic ACTH syndrome (59). Spindle-shaped cells with crystalline inclusions that are ultrastructurally similar to Reinke crystalloids have been identified in the adrenal cortex of male patients (60).

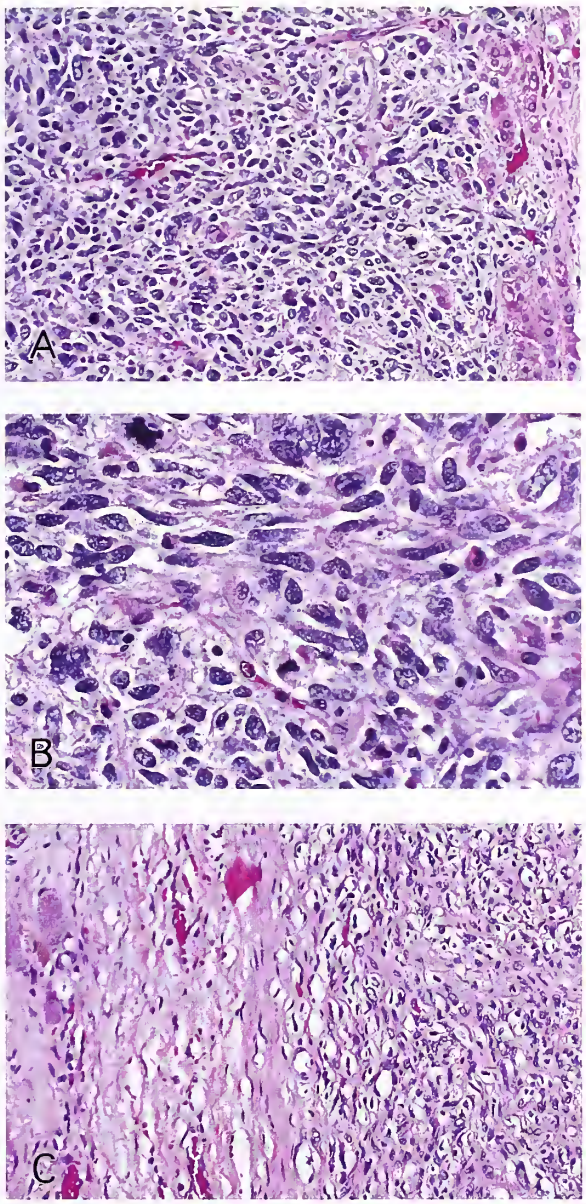

Figure 7-38

PRIMARY MALIGNANT PERIPHERAL NERVE SHEATH TUMOR OF ADRENAL GLAND

A: Residual cortex is seen on the right.

B: Areas were densely cellular, and in selected fields there were 1 to 2 mitoses per high-power field. Many tumor cells were positive for S-100 protein.

C: The tumor involved several adjacent nerve trunks. Residual compressed nerve and ganglion cells are present on the left. (A-C: Fig. 7-31 from Fascicle 19, Third Series.)

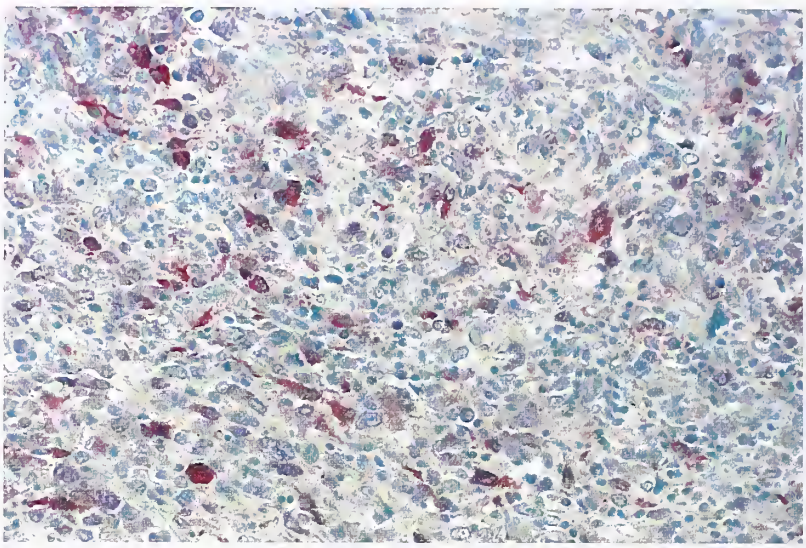

Figure 7-39

PRIMARY MALIGNANT PERIPHERAL NERVE SHEATH TUMOR OF ADRENAL GLAND

Numerous tumor cells are immunoreactive for S-100 protein (streptavidin-alkaline phosphatase method). (Fig. 7-32 from Fascicle 19, Third Series.)

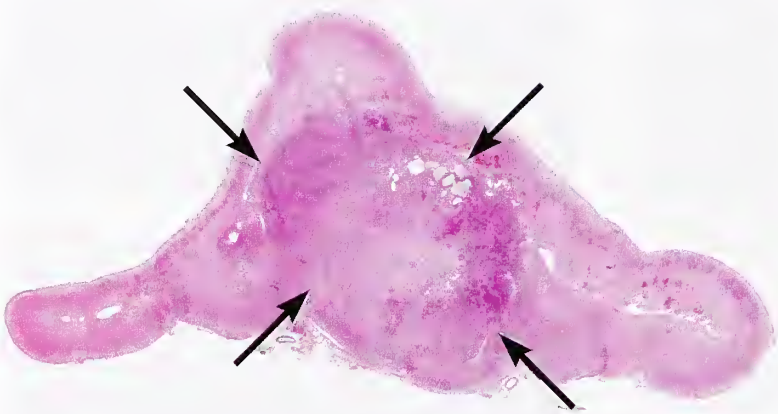

Figure 7-40

ADENOMATOID TUMOR OF THE ADRENAL GLAND

Unilateral, solitary adenomatoid tumor of adrenal gland in a patient with ectopic adrenocorticotropic hormone (ACTH) syndrome. The tumor expands the mid-portion of the gland (arrows) and is ill-demarcated on low-power examination. The edges of the tumor are expansile but unencapsulated, and the tumor measured about 1 cm in diameter. Adrenalectomy was done to rule out the possibility of ectopic ACTH production by a small pheochromocytoma.

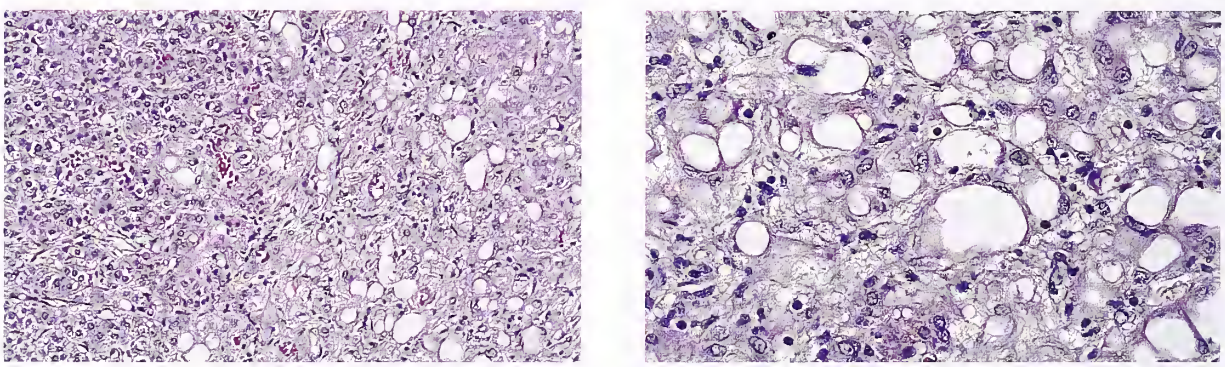

Figure 7-41

PRIMARY ADENOMATOID TUMOR OF ADRENAL GLAND

Left: Primary adrenal adenomatoid tumor has numerous small gland-like spaces. The tumor insinuates between cortical cells at the periphery and has enveloped small nests of adrenal cortical cells.

Right: The tumor cells have light, eosinophilic cytoplasm with vacuoles of various sizes. (L&R: Fig. 7-34 from Fascicle 19, Third Series.)

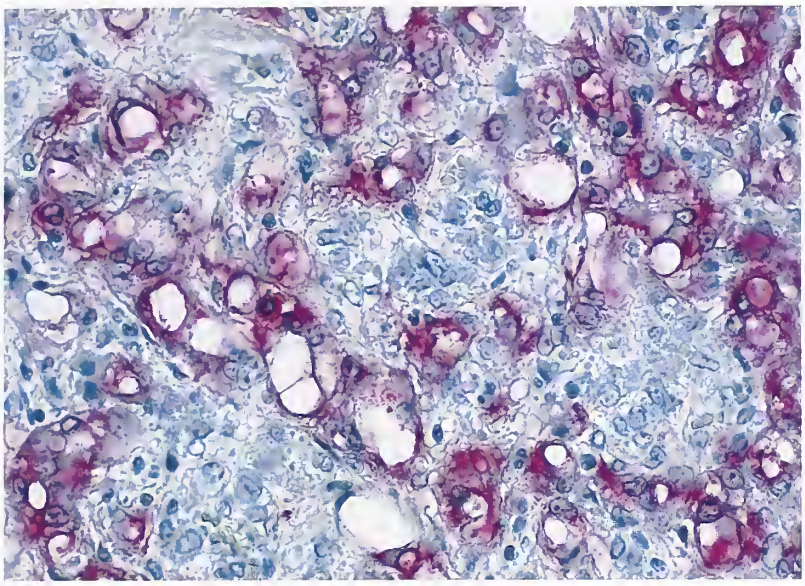

Figure 7-42

PRIMARY ADENOMATOID TUMOR OF ADRENAL GLAND

The tumor cells are positive for cytokeratin. The staining reaction highlights cells extending out into the adjacent cortex (streptavidin-alkaline phosphatase method). (Fig. 7-35 from Fascicle 19, Third Series.)

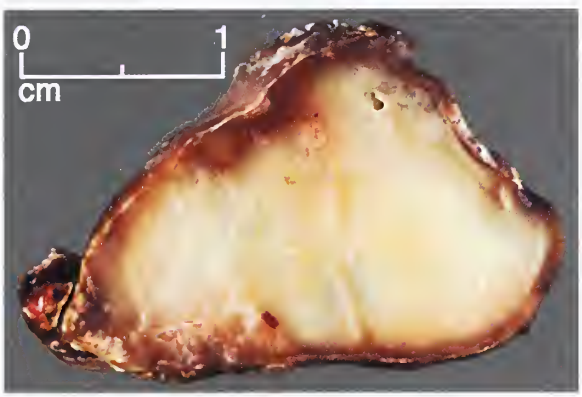

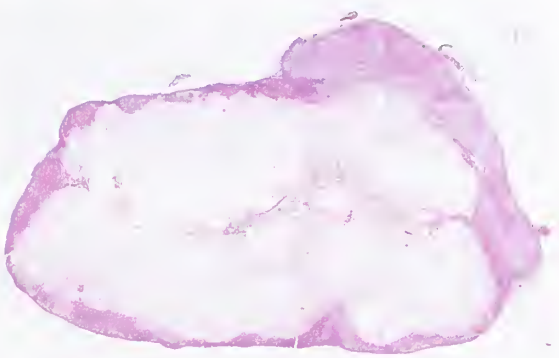

Figure 7-43

ADRENAL LIPOMA

Left: Incidental adrenal nodule was found on CT scan of the abdomen. Cross section shows a uniform, yellowish white mass approximately 2 cm in diameter.

Right: Low-power magnification shows expansion of the adrenal contour by adipose tissue. No hematopoietic cells were present.

A solitary fibrous tumor of the adrenal gland has been reported (61). Inflammatory myofibroblastic tumor of the adrenal gland is another rare tumor; the author has seen two examples, one a small incidental finding and the other presenting as a large adrenal mass (fig. 7-44). This is a neoplasm of intermediate biologic potential that may recur locally, but rarely metastasizes. A recent study indicated abdomen, retroperitoneum, or pelvis as the most common location (64 percent) and provided immunohistochemical data including expression of anaplastic lymphoma kinase (62). Castleman's disease of the adrenal gland has also been reported (63). There is an unusual example of retroperitoneal bronchogenic cyst presenting as an adrenal mass, but the lesion was found to be in an immediate juxtaadrenal location at surgery and the gland was left intact (64). A poorly differentiated neuroendocrine carcinoma (or primitive neuroectodermal tumor [PNET] different from neuroblastoma) presenting as a suprarenal mass without

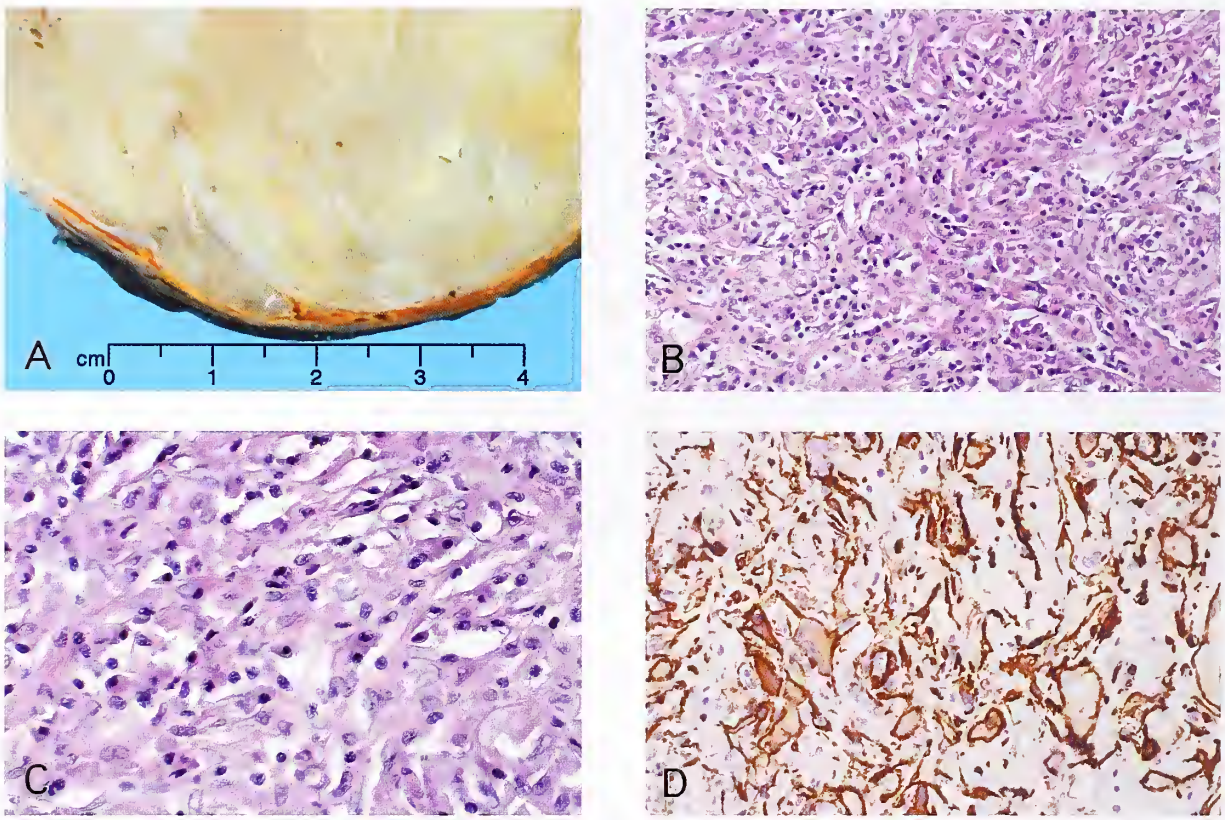

Figure 7-44

INFLAMMATORY MYOFIBROBLASTIC TUMOR OF ADRENAL GLAND

A: 49-year-old female complained of right flank pain for several weeks and was found to have a 14-cm tumor of the right adrenal gland. The mass, separate from the kidney, was resected along with the right kidney. On cross section, pale yellow-white areas show a compressed rim of residual adrenal gland. The adrenal tumor weighed 510 g. (Courtesy of Drs. B. M. Al-Khafaji and N. Bakshi, Detroit, MI.)

B: This cellular tumor had an irregular fascicular arrangement of fibroblastic/myofibroblastic cells. The inflammatory component is prominent, and mainly composed of plasma cells.

C: Higher magnification shows myofibroblastic cells admixed with plasma cells.

D: Spindle cells stain for vimentin, smooth muscle actin, and here, calponin, supporting a myofibroblastic lineage (avidin-biotin peroxidase method).

clear evidence of a primary tumor elsewhere may be an adrenal primary, remote as it may seem (65). A primary tumor with morphologic features of an extrarenal Wilms' tumor (nephroblastoma) has been reported in a 4-year-old boy (66). The author has also seen two examples of large, partially necrotic mesenchymal neoplasms of the adrenal gland with the morphologic features of malignant fibrous histiocytoma (fig. 7-45). A juxtaadrenal malignant fibrous histiocytoma was recently reported mimicking a pheochromocytoma (67), another example of the pseudopheochromocytoma. A myofibrosarcoma of the adrenal gland also has been reported (68), as well as a teratoma (69).

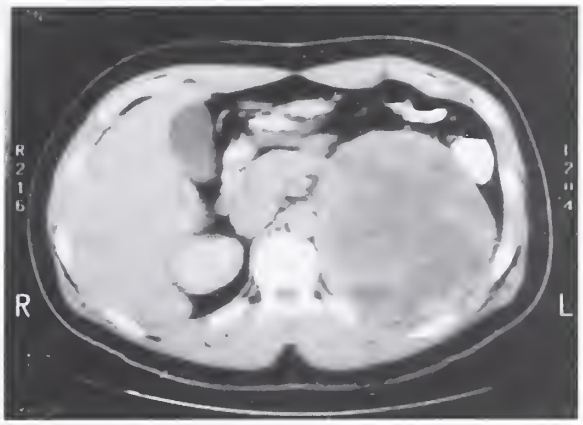

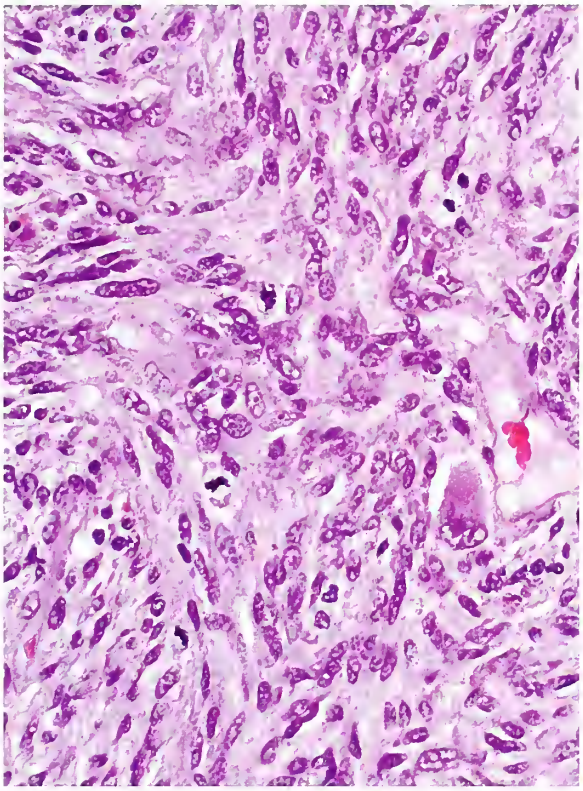

Figure 7-45

MALIGNANT FIBROUS HISTIOCYTOMA OF ADRENAL GLAND

Above: An adult male patient with abdominal pain/discomfort had a 17-cm left upper quadrant mass, which on CT scan was nonhomogeneous, suggesting tumor necrosis. The adrenal tumor weighed a little over 1,000 g.

Right: The tumor has a storiform pattern with nuclear pleomorphism and hyperchromasia as well as a few mitotic figures per high-power field. Immunostaining for vimentin was positive; other immunostains (cytokeratin, chromogranin, and S-100 protein) were negative.

REFERENCES

Adrenal Infection and Abscess Formation

1. Travis WD, Oertel JE, Lack EE. Miscellaneous tumors and tumefactive lesions of the adrenal gland. In: Lack EE, ed. Pathology of the adrenal glands. New York: Churchill Livingstone; 1990:351-378.
2. Goodwin RA Jr, Shapiro JL, Thurman GH, Thurman SS, Des Prez RM. Disseminated histoplasmosis: clinical and pathological correlations. Medicine (Baltimore) 1980;59:1-33.
3. Slavin RE, Walsh TJ, Pollack AD. Late generalized tuberculosis: a clinical pathological analysis and comparison of 100 cases in the preantibiotic and antibiotic eras. Medicine (Baltimore) 1980;59:352-366.
4. Benjamin E, Fox H. Malakoplakia of the adrenal gland. J Clin Pathol 1981;34:606-611.

Adrenal Hemorrhage, Hematoma Formation, and Calcification

5. Eklöf O, Mortensson W, Sandstedt B. Suprarenal hematoma versus neuroblastoma complicated by haemorrhage. A diagnostic dilemma in the newborn. Acta Radiol Diagn [Stockh] 1986;27:3-10.
6. Vella A, Nippoldt TB, Morris JC 3rd. Adrenal hemorrhage: a 25-year experience at the Mayo Clinic. Mayo Clin Proc. 2001;76:161-168.
7. Berneis K, Buitrago-Tellez C, Müller B, Keller U, Tsakiris DA. Antiphospholipid syndrome and endocrine damage: why bilateral adrenal thrombosis? Eur J Haematol. 2003;71:299-302.
8. Kenney PJ, Stanley RJ. Calcified adrenal masses. Urol Radiol 1987;9:9-15.

Adrenal Cysts

9. Abeshouse GA, Goldstein RB, Abeshouse BS. Adrenal cysts; review of the literature and report of three cases. J Urol 1959;81:711-719.
10. Foster DG. Adrenal cysts. Review of literature and report of case. Arch Surg 1966;92:131-143.
11. Torres C, Ro JY, Batt MA, Park YW, Ordonez NG, Ayala AG. Vascular adrenal cysts: a clinicopathologic and immunohistochemical study of six cases and a review of the literature. Mod Pathol 1997;10:530-536.

12. Medeiros LJ, Weiss LM, Vickery AL Jr. Epithelial-lined (true) cyst of the adrenal gland: a case report. Hum Pathol 1989;20:491-492.
13. Brenner DS, Jacobs SC, Drachenberg CB, Papadimitriou JC. Isolated visceral leishmaniasis presenting as an adrenal cystic mass. Arch Pathol Lab Med 2000;124:1553-1556.
14. Medeiros LJ. Lewandrowski KB, Vickery AL Jr. Adrenal pseudocyst: a clinical and pathologic study of eight cases. Hum Pathol 1989;20:660-665.
15. Gaffey MJ, Mills SE, Medeiros LJ, Weiss LM. Unusual variants of adrenal pseudocysts with intracystic fat, myelolipomatous metaplasia and metastatic carcinoma. Am J Clin Pathol 1990;94:706-713.
16. Gaffey MJ, Mills SE, Fechner RE, Bertholf MF, Allen MS Jr. Vascular adrenal cysts. A clinicopathologic and immunohistochemical study of endothelial and hemorrhagic (pseudocystic) variants. Am J Surg Pathol 1989;13:740-747.

Myelolipoma

17. Clark PE, Farver CF, Ulchaker JC, Angermeier K. A rare case of an extra-adrenal myelolipoma arising in the renal sinus: a case report and review of the literature. ScientificWorldJournal 2005;5:109-117.
18. Franiel T, Fleischer B, Raab BW, Fuzesi L. Bilateral thoracic extraadrenal myelolipoma. Eur J Cardiothorac Surg 2004;26:1220-1222.
19. Nishizaki T, Kanematsu T, Matsumata T, Yasunaga C, Kakizoe S, Sugimachi K. Myelolipoma of the liver. A case report. Cancer 1989; 63:930-934.
20. Hunter SB, Schemankewitz EH, Patterson C, Varma VA. Extraadrenal myelolipoma. A report of two cases. Am J Clin Pathol 1992;97:402-404.
21. Damjanov I, Katz SM, Catalano E, Mason D, Schwartz AB. Myelolipoma in a heterotopic adrenal gland: light and electron microscopic findings. Cancer 1979;44:1350-1356.
22. Plaut A. Myelolipoma in the adrenal cortex: myeloadipose structures. Am J Pathol 1958;34: 487-503.
23. Del Gaudio A, Solidaro G. Myelolipoma of the adrenal gland: report of two cases with a review of the literature. Surgery 1986;99:293-301.
24. Elsayes KM, Mukundan G, Narra VR, et al. Adrenal masses: mr imaging features with pathologic correlation. Radiographics 2004;24(Suppl 1):S73-86.
25. Allison KH, Mann GN, Norwood TH, Rubin BP. An unusual case of multiple giant myelolipomas: clinical and pathogenetic implications. Endocr Pathol 2003;14:93-100.
26. Hegstrom JL, Kircher T. Alimentary tract ganglioneuromatosis-lipomatosis, adrenal myelolipomas, pancreatic telangiectasias, and multinodular thyroid goiter. A possible neuroendocrine syndrome. Am J Clin Pathol 1985;83:744-747.
27. Seniuta P, Cazenave-Mahe JP, Le Treut A, Trojani M. [Adrenal myelolipoma and Castleman's pseudotumor. A case of association in a retroperitoneal tumor.] J Urol (Paris) 1989;95:511-514. [French.]
28. Merchant SH, Herman CM, Amin MB, Ro JY, Troncoso P. Myelolipoma associated with adrenal ganglioneuroma. Arch Pathol Lab Med 2002; 126:736-737.
29. Selye H, Stone H. Hormonally induced transformation of adrenal into myeloid tissue. Am J Pathol 1950;26:211-233.
30. Bishop E, Eble JN, Cheng L, et al. Adrenal myelolipomas show nonrandom X-chromosome inactivation in hematopoietic elements and fat: support for a clonal origin of myelolipomas. Am J Surg Pathol 2006;30:838-843.

Malignant Melanoma

31. Carstens PH, Kuhns JG, Ghazi C. Primary malignant melanomas of the lung and adrenal. Hum Pathol 1984;15:910-914.
32. Dao AH, Page DL, Reynolds VH, Adkins RB Jr. Primary malignant melanoma of the adrenal gland. A report of two cases and review of the literature. Am Surg 1990;56:199-203.
33. Chetty R, Clark SP, Taylor DA. Pigmented adrenal pheochromocytomas of the adrenal medulla. Hum Pathol 1993;24:420-423.
34. Lack EE. Pathology of adrenal and extra-adrenal paraganglia. Major problems in pathology, vol 29. Philadelphia: WB Saunders Co; 1994.

Malignant Lymphoma

35. Case records of the Massachusetts General Hospital: Case 35-2000. An 82-year-old woman with bilateral adrenal masses and low-grade fever. N Engl J Med 2000;343:1477-1483.

Primary Mesenchymal Tumors

36. Plaut A. Hemangiomas and related lesions of the adrenal gland. Virchows Arch Path Anat Physiol Klin Med 1962;335:345-355.
37. Mellor JA. Hereditary haemorrhagic telangiectasia. Br J Clin Pract 1983;37:234-236.
38. Plaut A. Locally invasive lymphangioma of adrenal glands. Cancer 1962;15:1165-1169.
39. Wenig BM, Abbondanzo SL, Heffess CS. Epithelioid angiosarcoma of the adrenal glands. A clinicopathologic study of nine cases with a discussion of the implications of finding "epithelial-specific" markers. Am J Surg Pathol 1994;18:62-73.
40. Nakagawa N, Takahashi M, Maeda K, Fujimura N, Yufu M. Case report: adrenal haemangioma coexisting with malignant haemangioendothelioma. Clin Radiol 1986;37:97-99.
41. Livaditou A, Alexiou G, Floros D, Filippidis T, Dosios T, Bays D. Epithelioid angiosarcoma of the adrenal gland associated with chronic arsenical intoxication? Path Res Pract 1991;187:284-289.

42. Ben-Izhak O, Auslander L, Rabinson S, Lichtig C, Sternberg A. Epithelioid angiosarcoma of the adrenal gland with cytokeratin expression. Report of a case with accompanying mesenteric fibromatosis. Cancer 1992;69:1808-1812.
43. Granger JK, Houn HY, Collins C. Massive hemorrhagic functional adrenal adenoma histologically mimicking angiosarcoma. Report of a case with immunohistochemical study. Am J Surg Pathol 1991;15:699-704.
44. Jacobs IA, Kagan SA. Adrenal leiomyoma: a case report and review of the literature. J Surg Oncol 1998;69:111-112.
45. Lack EE, Graham CW, Azumi N, et al. Primary leiomyosarcoma of the adrenal gland. Case report with immunohistochemical and ultrastructural study. Am J Surg Pathol 1991;15:899-905.
46. Zetler PJ, Filipenko JD, Bilbey JH, Schmidt N. Primary adrenal leiomyosarcoma in a man with acquired immunodeficiency syndrome (AIDS). Further evidence for an increase in smooth muscle tumors related to Epstein-Barr infection in AIDS. Arch Pathol Lab Med 1995;119:1164-1167.

Other Unusual Primary Adrenal Tumors

47. Lau SK, Spagnolo DV, Weiss LM. Schwannoma of the adrenal gland: report of two cases. Am J Surg Pathol 2006;30:630-634.
48. Ayala GE, Ettinghausen SE, Epstein AH, Travis WD, Lack EE. Primary malignant peripheral nerve sheath tumor of the adrenal gland. Case report and literature review. J Urol Pathol 1994;2:265-272.
49. Min KW, Clemens A, Bell J, Dick H. Malignant peripheral nerve sheath tumor and a pheochromocytoma. A composite tumor of the adrenal. Arch Pathol Lab Med 1988;112:266-270
50. Chandrasoma P, Shibata D, Radin R, Brown LP, Koss M. Malignant peripheral nerve sheath tumor arising in an adrenal ganglioneuroma in an adult male homosexual. Cancer 1986;57:2022-2025.
51. Travis WD, Lack EE, Azumi N, Tsokos M, Norton J. Adenomatoid tumor of the adrenal gland with ultrastructural and immunohistochemical demonstration of a mesothelial origin. Arch Pathol Lab Med 1990;114:722-724.
52. Isotalo PA, Keeney GL, Sebo TJ, Riehle DL, Cheville JC. Adenomatoid tumor of the adrenal gland: A clinicopathologic study of five cases and review of the literature. Am J Surg Pathol 2003;27:969-977.
53. Garg K, Lee P, Ro JY, Qu Z, Troncoso P, Ayala AG. Adenomatoid tumor of the adrenal gland: a clinicopathologic study of 3 cases. Ann Diagn Pathol 2005;9:11-15.
54. Lam, KY, Lo CY. Adrenal lipomatous tumours: a 30-year clinicopathologic experience at a single institution. J Clin Pathol 2001;54:707-712.
55. Orselli RC, Bassler TJ. Theca granulosa cell tumor arising in adrenal. Cancer 1973;31:474-477.
56. Pollock WJ, McConnell CF, Hilton C, Lavine RL. Virilizing Leydig cell adenoma of adrenal gland. Am J Surg Pathol 1986;10:816-822.
57. Vasiloff J, Chideckel EW, Boyd CB, Foshag LJ. Testosterone-secreting adrenal adenoma containing crystalloids characteristic of Leydig cells. Am J Med 1985;79:772-776.
58. Lack EE, Nauta RJ. Intracortical Leydig cells in a patient with an aldosterone-secreting adrenal cortical adenoma. J Urol Pathol 1993;1:411-418.
59. Horvath E, Chalvardjian A, Kovacs K, Singer W. Leydig-like cells in the adrenals of a woman with ectopic ACTH syndrome. Hum Pathol 1980;11: 284-287.
60. Magalhaes MC. A new crystal-containing cell in human adrenal cortex. J Cell Biol 1972;55:126-133.
61. Prévot S, Penna C, Imbert JC, Wendum D, de Saint-Maur PP. Solitary fibrous tumor of the adrenal gland. Mod Pathol 1996;9:1170-1174.
62. Coffin CM, Hornick JL, Fletcher CD. Inflammatory myofibroblastic tumor. Comparison of clinicopathologic, histologic, and immunohistochemical features including ALK expression in atypical and aggressive cases. Am J Surg Pathol 2007;31:509-520.
63. Debatin JF, Spritzer CE, Dunnick NR. Castleman's disease of the adrenal gland: MR imaging features. Am J Roentgenol 1991;157:781-783.
64. Foerster HM, Sengupta EE, Montag AG, Kaplan EL. Retroperitoneal bronchogenic cyst presenting as an adrenal mass. Arch Pathol Lab Med 1991;115:1057-1059.
65. Marina NM, Eteubarias E, Parham DM, Bowman LC, Green A. Peripheral primitive neuroectodermal tumor (peripheral neuroepithelioma) in children. A review of the St. Jude experience and controversies in diagnosis and management. Cancer 1989;64:1952-1960.
66. Santonja C, Diaz MA, Dehner LP. A unique dysembryonic neoplasm of the adrenal gland composed of nephrogenic rests in a child. Am J Surg Pathol 1996;20:118-124.
67. Pekic S, Damjanovic S, Djurovic M, et al. Retroperitoneal malignant fibrous histiocytoma mimicking pheochromocytoma. Endocrine. 2004;24: 99-103.
68. McLaughlin SA, Schmitt TM, Huguet KL, Menke DM, Nguyen JH. Myofibrosarcoma of the adrenal gland. Am Surg. 2005;71:191-193.
69. Malogolowkin MH, Monforte HL, Kovanlikaya A, Siegel SE. Pediatric germ cell tumors. In: American Cancer Society. Germ cell tumors. Atlas of Clinical Oncology. Hamilton, London: BC Decker, Inc; 2003:265-286.

8 TUMORS METASTATIC TO ADRENAL GLANDS

INCIDENCE AND PRIMARY SITES OF TUMORS METASTATIC TO ADRENAL GLANDS

While much discussion has been devoted to primary adrenal tumors of various types, including the uncommon and rare neoplasms in chapter 7, the adrenal glands are much more frequently involved by metastatic tumors from other primary sites. Per unit weight the adrenal glands are the organs most frequently involved by metastases, and as a specific anatomic site are reported to be the fourth most common site of spread, surpassed in frequency only by lung, liver, and bone (1). In an autopsy study by Abrams et al. (2) involving 1,000 carcinomas, the adrenal glands were secondarily involved in 27 percent of cases; the leading sources of adrenal metastases were breast (53.9 percent), lung (35.6 percent) (fig. 8-1), kidney (24 percent), stomach (21 percent), pancreas (19 percent), ovary (17 percent), and colon (14.4 percent).

The pattern of adrenal blood supply (threefold source of arterial supply), with high flow and sinusoidal vasculature, has been offered as an explanation for the high incidence of metastases despite the relatively small size of the adrenal gland. Spread of tumor within sinusoids of the involved adrenal gland may be evident adjacent to the main site of metastases (fig. 8-2, left), and may extend into small capsular extrusions of cortex (fig. 8-2, right). Bilateral adrenal metastases have been reported in 41 percent of patients with metastatic cancer involving the adrenal glands (3).

Autopsy studies have shown that the frequency of adrenal metastases decreases with age in patients with mammary carcinoma (4), and there appears to be a lower frequency in patients with small cell carcinoma of lung who have received chemotherapy and radiation (5). Metastases from extraadrenal primary malignancies have been reported rarely in primary adrenal neoplasms; neoplasm to neoplasm metastases have

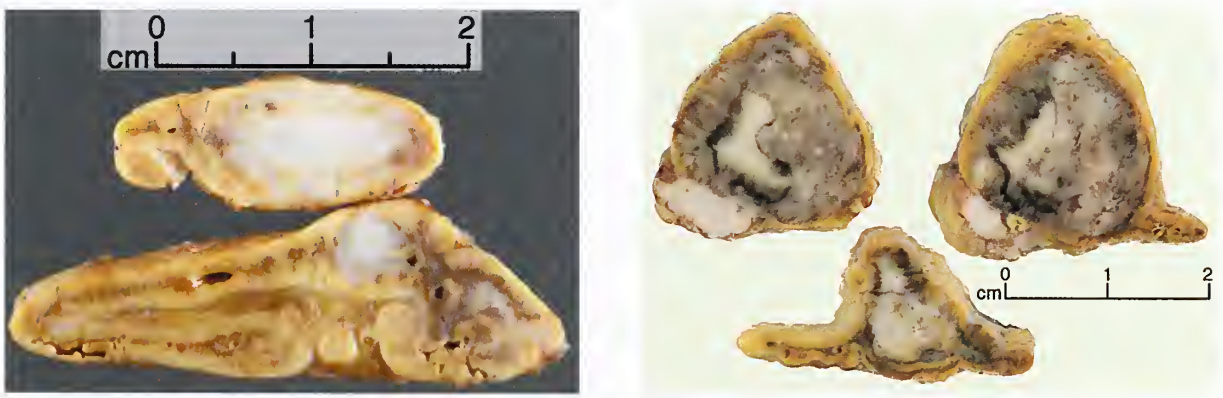

Figure 8-1

METASTATIC ADENOCARCINOMA OF LUNG TO ADRENAL GLAND

Left: Two metastases appear as pale white nodules within the medullary zone. They impinge on the corticomedullary junction.

Right: Poorly differentiated adenocarcinoma metastatic to adrenal gland in a 58-year-old man with bronchogenic carcinoma. The opposite gland was less extensively involved. The tumor is gray to cream colored, and greatly expands the contour of the adrenal gland. There were a few areas of confluent necrosis.

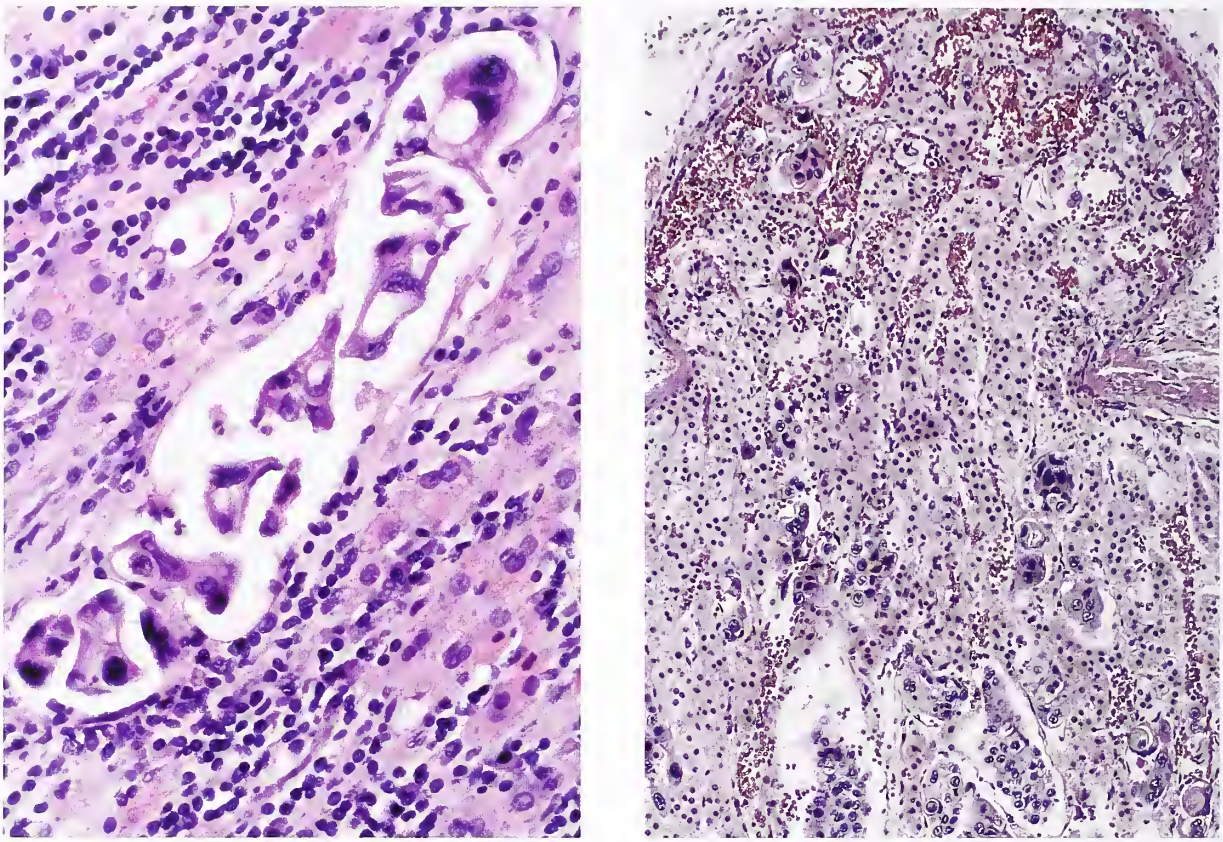

Figure 8-2

SINUSOIDAL INVASION BY ADENOCARCINOMA METASTATIC TO ADRENAL GLAND

Left: Tumor invades the sinusoids of the adrenal cortex and is accompanied by chronic inflammation.
Right: Different case shows sinusoidal invasion by metastatic bronchogenic adenocarcinoma with involvement of the capsular extrusion at top. (Fig. 8-2 from Fascicle 19, Third Series.)

been reported for pheochromocytoma (6) as well as adrenal cortical adenoma (7).

With the aid of high resolution imaging studies such as computerized tomography (CT) scan and magnetic resonance imaging (MRI) (8), adrenal metastases are more frequently recognized during life. The prevalence of adrenal metastases in 91 autopsied lung cancer patients was 35 percent, with adenocarcinoma and squamous cell carcinoma the most frequent; the metastases were bilateral in 23 percent (9). Although the sensitivity of CT scan varied from 20 to 41 percent in this study, the specificity was 85 percent or more.

During the staging workup for patients with a known malignancy elsewhere, the finding of an adrenal mass can be very significant in terms of prognosis. In this setting, CT or ultrasound-guided fine needle aspiration biopsy of the adrenal mass is a very useful method for distinguishing between a metastasis and a primary adrenal tumor (fig. 8-3). A metastatic carcinoma can clinically and pathologically simulate a primary adrenal cortical carcinoma. With lung carcinoma, for example, there may be marked unilateral adrenal enlargement (fig. 8-4) and multiple pulmonary nodules suggesting metastases from a primary adrenal cortical carcinoma. There may be involvement of tributaries of the central adrenal vein (fig. 8-5), which with overgrowth of the adrenal vascular system may result in retrograde extension into the inferior vena cava (fig. 8-6).

Occasionally, the adrenal mass is surgically resected (see fig. 8-4C). Adrenalectomy for a clinically isolated adrenal metastasis can prolong

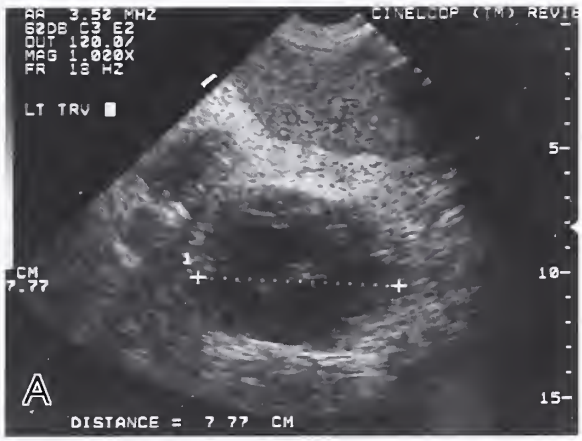

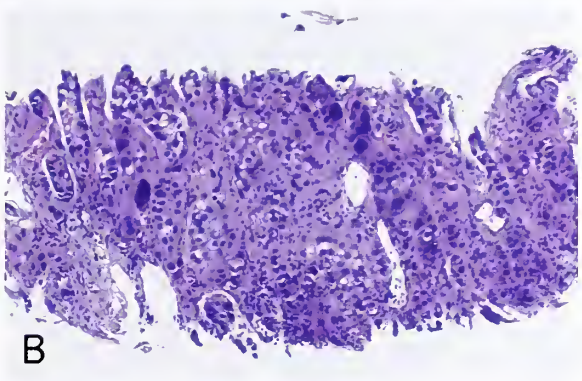

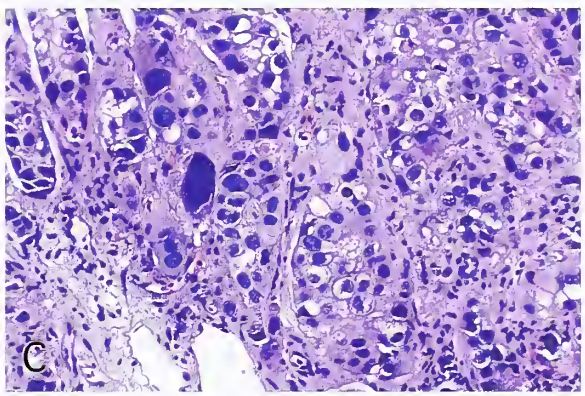

Figure 8-3

ADENOCARCINOMA METASTATIC TO ADRENAL GLAND

A: Abdominal ultrasound showed an adrenal mass in a 61-year-old patient who had a previous diagnosis of bronchogenic adenocarcinoma. Ultrasound-guided fine needle aspiration biopsy was diagnostic for metastatic adenocarcinoma.

B: Cell block preparation of fine needle aspiration may yield diagnostic tissue fragments, as seen here.

C: Metastatic poorly differentiated adenocarcinoma grows within the sinusoids of the adrenal cortex.

survival in selected patients (10). Laparoscopic adrenalectomy also plays an emerging role in adrenal surgery for removal of isolated metastases (11,12). CT-guided radiofrequency ablation of adrenal neoplasms (including metastases) is one of the newer modalities in achieving local control (13). Large cell carcinoma and poorly differentiated adenocarcinoma may cause difficulties in interpretation of biopsy or even adrenalectomy specimens obtained surgically (fig. 8-7), and may be misinterpreted as adrenal cortical carcinoma. A unilateral adrenal metastasis from a large cell carcinoma of lung is illustrated in figure 8-7 D-F; the patient presented suddenly with adrenal rupture and retroperitoneal hemorrhage.

SECONDARY ADRENAL CORTICAL INSUFFICIENCY (ADDISON'S DISEASE)

Bilateral metastases to the adrenal glands may lead to latent (borderline) or overt adrenal cortical insufficiency, or Addison's disease (14). It has been estimated that 80 to 90 percent of the adrenal gland must be replaced or destroyed before adrenal insufficiency is detected (15), which attests to the remarkable endocrine reserve of the adrenal gland with regard to cortical function. A variety of physiologic or "stress-related" factors, such as superimposed illness or surgery, play a pivotal role in borderline cases in this adrenoprival state.

Thomas Addison in his classic monograph in 1855 (16) first drew attention to a peculiar "bronzing" of the skin along with progressive weakness and other symptoms (such as "irritability of stomach") occurring in association with extensive destruction of the adrenal glands (or "suprarenal capsules"); most of the 11 cases in his 39-page monograph were due to tuberculosis that nearly completely destroyed the adrenal glands and caused "conversion into a mass of strumous disease"; several cases were due to carcinoma metastatic to the adrenal glands (case VII-breast carcinoma, case VIII-gastric carcinoma, case XI-carcinoma most likely pulmonary in origin). In two of these cases, extensive replacement of only one gland was noted at

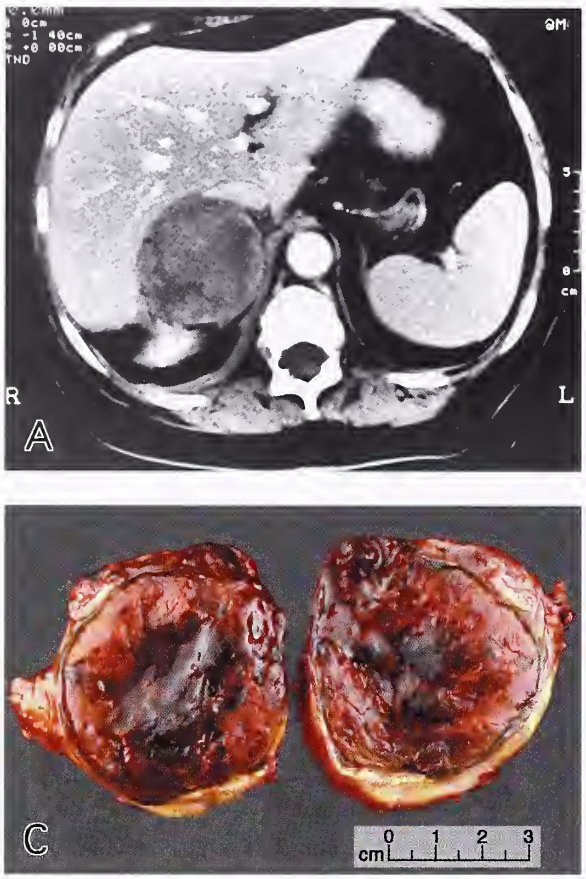

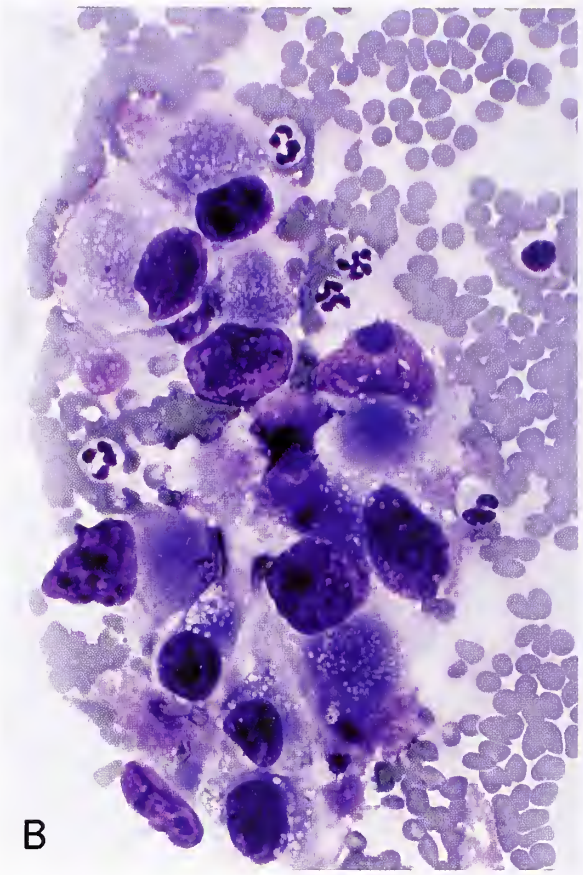

Figure 8-4

ADENOCARCINOMA METASTATIC TO ADRENAL GLAND

A: A 64-year-old woman had been treated previously for poorly differentiated bronchogenic adenocarcinoma. A right adrenal mass was picked up on CT scan of the abdomen. The tumor is round, has a smooth contour, and has soft tissue density with mild heterogeneity. Fine needle aspiration biopsy was diagnostic for metastatic adenocarcinoma (B) and the adrenal tumor was resected (C) since there was no other evidence of metastasis elsewhere.

B: Fine needle aspiration biopsy shows metastatic poorly differentiated adenocarcinoma. Some cells have a signet ring configuration (Diff Quik stain).

C: Cross section of the surgically resected adrenal tumor. Metastatic carcinoma expands the smooth contour of the adrenal gland. In the center is recent hemorrhage due to the fine needle aspiration biopsy procedure a few days before.

autopsy while the state of the opposite gland was not given in detail.

The true incidence of Addison's disease due to adrenal metastases is difficult to determine since the relatively nonspecific symptoms of adrenal insufficiency may be confused with cachexia or the fluid and electrolyte imbalance associated with cancer in some cases, and often there is no endocrinologic testing for adrenal reserve in patients with metastases and bilateral adrenal enlargement (14). Two studies reported adrenal insufficiency in 19 to 33 percent of patients with known metastatic tumor and CT evidence of bilateral adrenal enlargement (17,18). A wide variety of primary malignancies cause Addison's disease by massive adrenal replacement, most commonly metastatic lung and breast carcinomas; other primaries include renal cell carcinoma, gastric carcinoma, colonic adenocarcinoma, seminoma, pancreatic carcinoma, transitional cell carcinoma, and malignant melanoma (fig. 8-8) (14). Adrenal cortical carcinoma has also been reported to cause Addison's disease due to bilateral adrenal involvement (19).

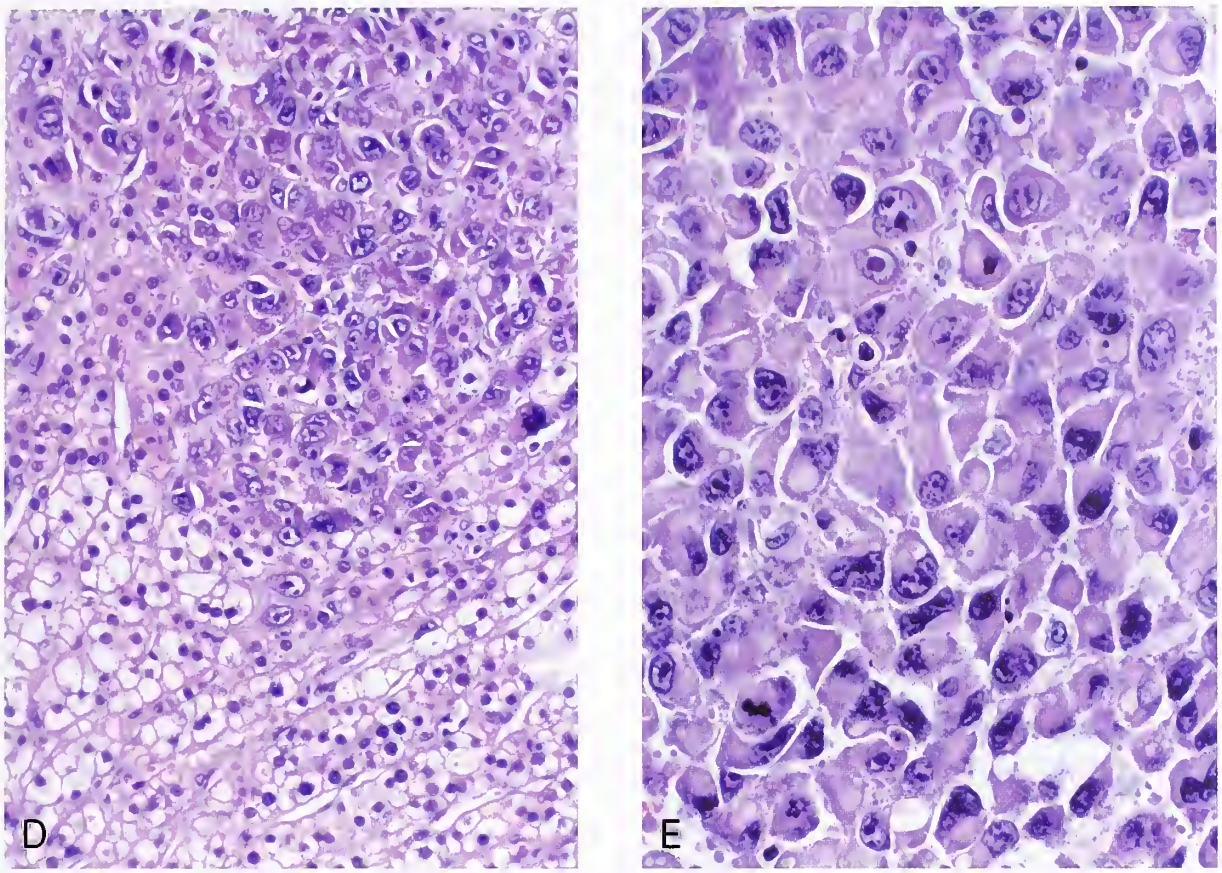

Figure 8-4 (Continued)

D: Tissue section shows confluent growth of metastatic adenocarcinoma (top) with compressed adrenal cortex (bottom). Frank gland formation was very difficult to identify.

E: Loosely cohesive growth by tumor cells. Many cells have a signet ring configuration.

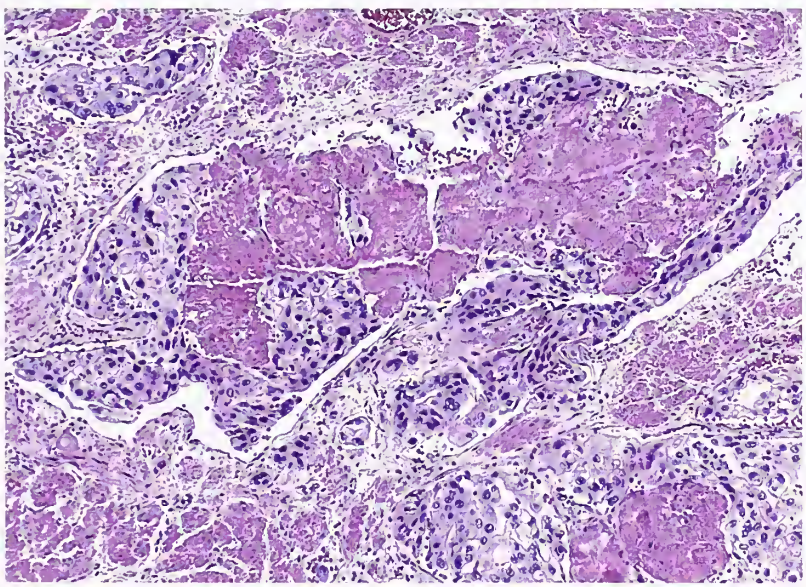

Figure 8-5

ADENOCARCINOMA METASTATIC TO ADRENAL GLAND

Poorly differentiated bronchogenic adenocarcinoma metastatic to the adrenal gland with involvement of a large tributary of the central adrenal vein. The tumor has a confluent zone of necrosis and molds to the contour of the venous channel. (Fig. 8-6 from Fascicle 19, Third Series.)

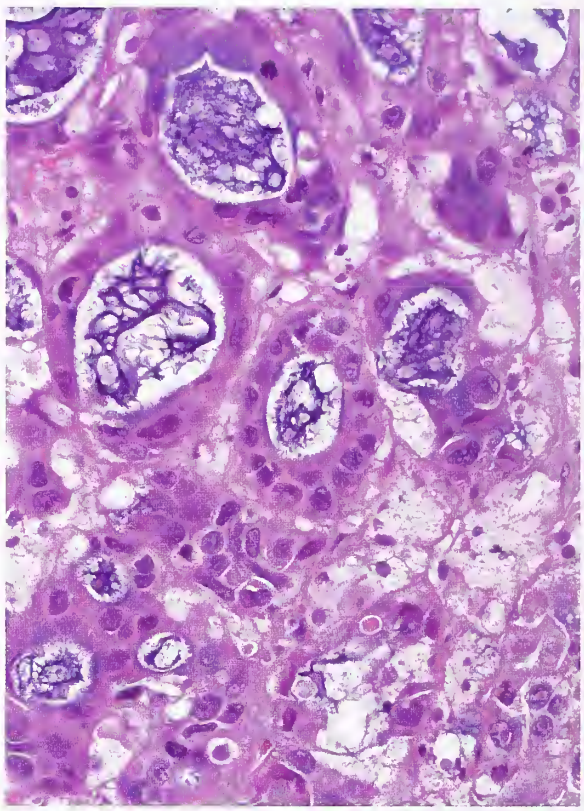

Figure 8-6

METASTATIC PULMONARY CARCINOMA MIMICKING A PRIMARY ADRENAL TUMOR

Left: The patient had a large suprarenal mass on the left side and multiple pulmonary nodules. At autopsy, the gross appearance of the tumor and its extension into the inferior vena cava suggested an adrenal cortical carcinoma, but proved to be a metastatic poorly differentiated adenocarcinoma of pulmonary origin. (Fig. 8-5 from Fascicle 19, Third Series.)

Right: Metastatic bronchogenic adenocarcinoma has a well-developed glandular pattern with mucin secretion.

IMAGING CHARACTERISTICS OF METASTATIC DISEASE

On CT scan, the involved adrenal gland is variable in size; sometimes the changes are bilateral. The involved gland is usually round or oval and may have a smooth or lobulated contour. Most glands involved by metastatic tumor are of soft tissue density unless large and necrotic. Variable enhancement is evident on CT scan. On MRI, the involved adrenal gland usually has a heterogeneous signal intensity on T2-weighted images and sometimes T1-weighted images as well, in which the gland may appear isointense or hypointense to liver. If there is hemorrhage internal to the metastatic tumor, there is usually a high signal on T1- and T2-weighted images. An adrenal metastasis may appear like an adrenal cortical adenoma on CT scan, so MRI should be performed on any solitary adrenal mass discovered in a patient with known malignancy and no other signs or symptoms of metastasis. A scoring system has been reported to help distinguish adrenal adenomas from metastases (20).

PATHOLOGY AND DIFFERENTIAL DIAGNOSIS

Grossly, a metastatic malignancy (rarely seen as a surgically resected specimen) may appear gray-white, with or without zones of tumor necrosis (see fig. 8-1, left); it usually lacks the yellow-orange hue of an adrenal cortical primary. Gross black to brown pigmentation may arouse suspicion for a metastatic malignant melanoma. There is usually no problem in making the histologic or cytologic diagnosis of metastatic carcinoma, although some tumors, such

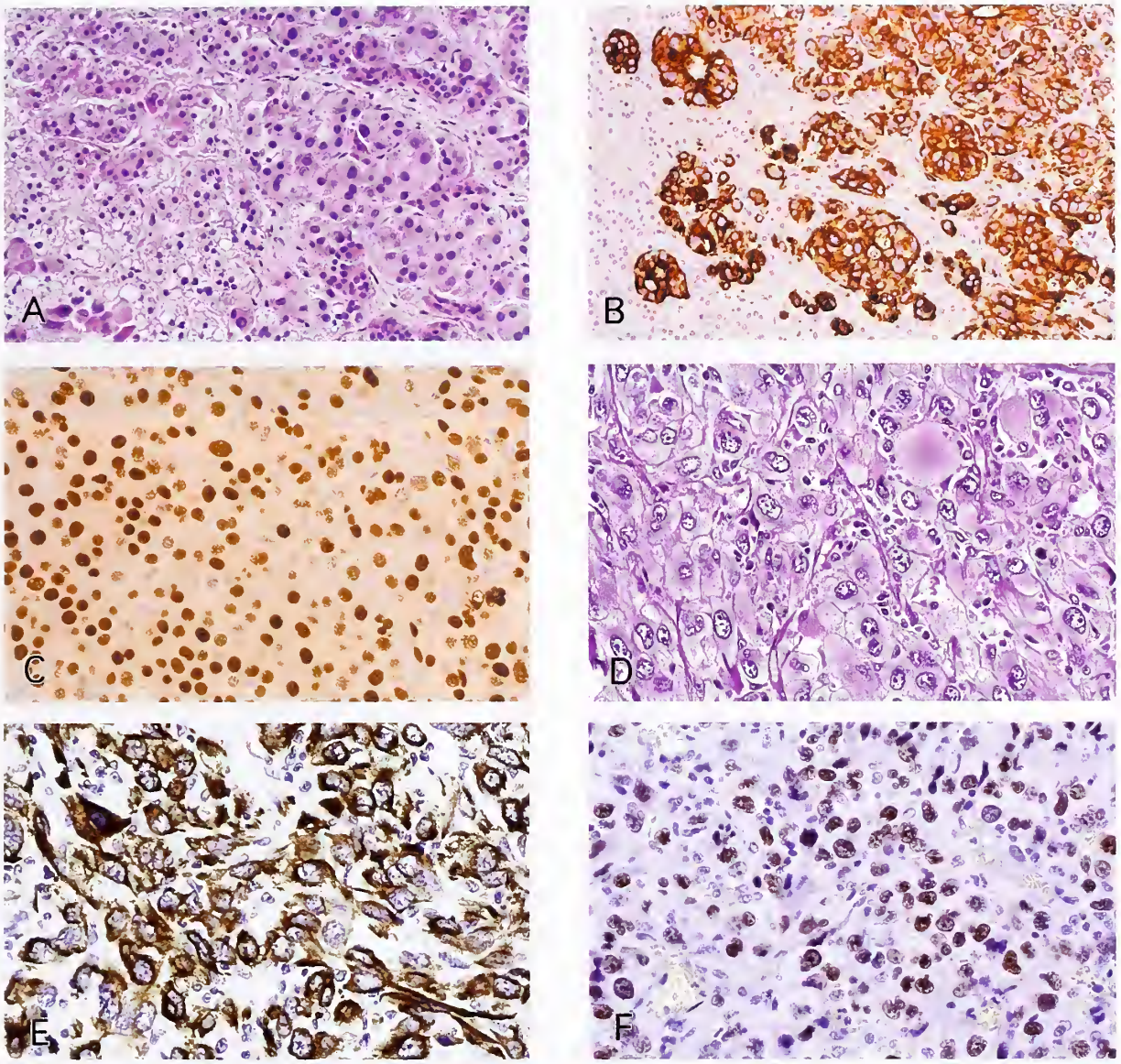

Figure 8-7

CARCINOMA METASTATIC TO ADRENAL GLAND

A: A 49-year-old woman with a history of breast cancer underwent surgical resection of a partially cystic adrenal neoplasm. This is regarded on both frozen section and permanent sections to be a malignant neoplasm, most likely an adrenal cortical carcinoma. The tumor had areas with a nesting and short trabecular pattern and which diffusely permeated the adrenal gland. Adrenal cortical cells are present in this field.

B: Immunostain for the pancytokeratin marker AE1/AE3 was strongly positive and accentuates the permeative pattern of the tumor (avidin-biotin peroxidase method).

C: Immunostain for estrogen receptor protein is also strongly positive, with dark staining of almost all tumor cell nuclei. The diagnosis is metastatic poorly differentiated mammary adenocarcinoma (avidin-biotin peroxidase method).

D: A 58-year-old woman had acute abdominal pain due to rupture and hemorrhage of a 95-g adrenal tumor. The adrenal mass was surgically resected and showed a poorly differentiated carcinoma which was felt to be an adrenal cortical carcinoma. The patient also had a solitary lung nodule measuring only a few centimeters in diameter.

E: Immunostain for cytokeratin (AE1/AE3) is strongly positive (avidin-biotin peroxidase method).

F: Immunostain for thyroid transcription factor-1 (TTF-1) is strongly positive within the nuclei of tumor cells. The diagnosis is metastatic large cell carcinoma of lung. The patient underwent lobectomy to remove the lung primary. No other sites of metastasis were evident (avidin-biotin peroxidase method).

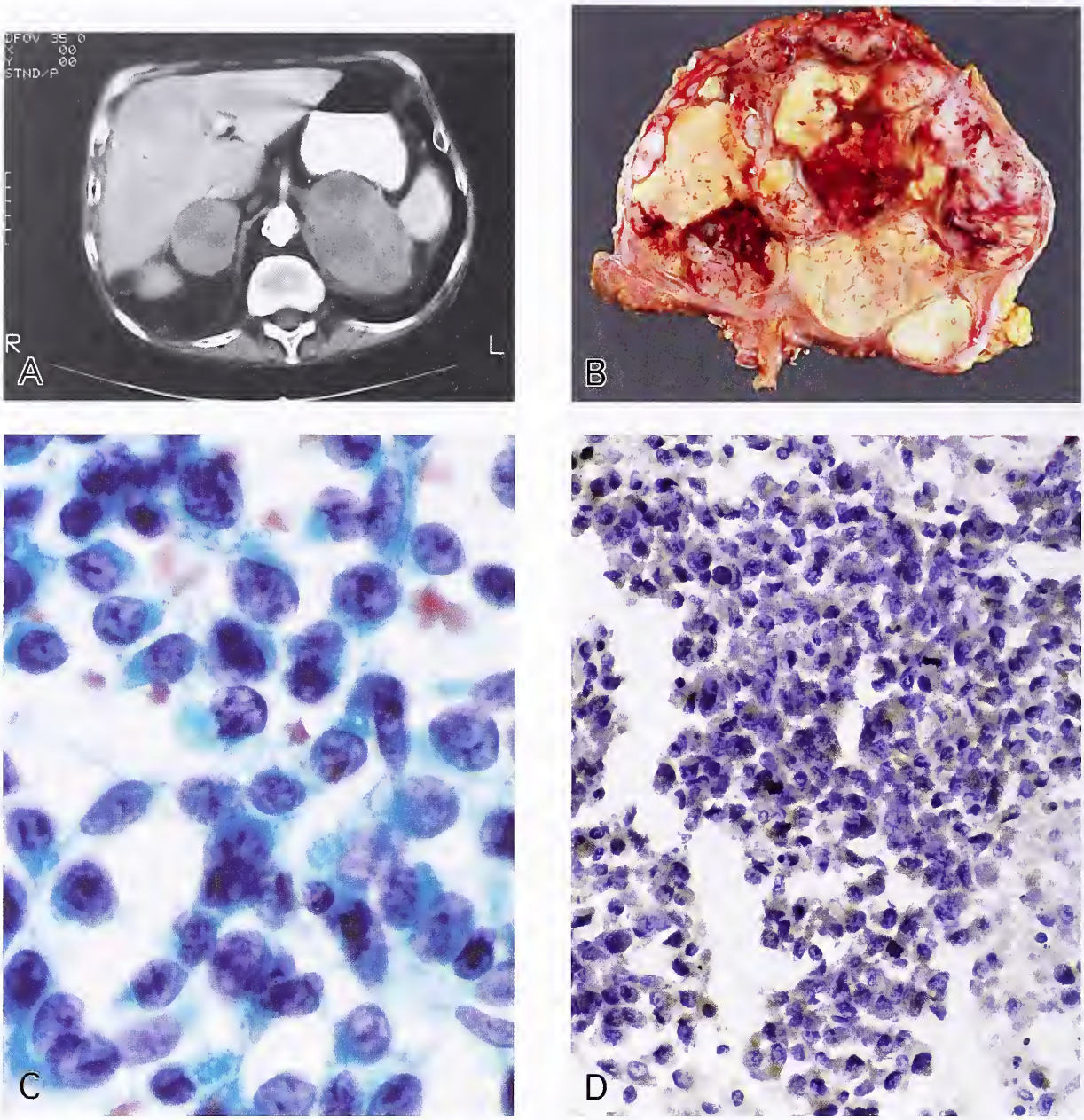

Figure 8-8

MALIGNANT MELANOMA METASTATIC TO ADRENAL GLANDS

A: A 73-year-old man had amelanotic malignant melanoma of the right nostril diagnosed 4 years previously. Huge bilateral adrenal masses were seen on CT scan. The patient had presented with weakness, dehydration, and hyponatremia probably due in part to acute Addisonian crisis. The patient also had septicemia. There was also a remote history of disseminated histoplasmosis (note calcified areas in spleen and one in liver).

B: Same case as A. Both adrenal glands were extensively replaced by metastatic malignant melanoma, which has coarsely nodular areas of necrosis. (A,B: Fig. 8-8 from Fascicle 19, Third Series.)

C: Different case of metastatic malignant melanoma to the adrenal gland. Fine needle aspiration biopsy smear shows cells that are loosely cohesive, with a high nuclear to cytoplasmic ratio and relatively prominent nucleoli. Occasional nuclear pseudoinclusions were present. No pigment was identified (Papanicolaou stain).

D: Cell block preparation in same case as C shows positive immunostaining for HMB45 (avidin-biotin peroxidase method).

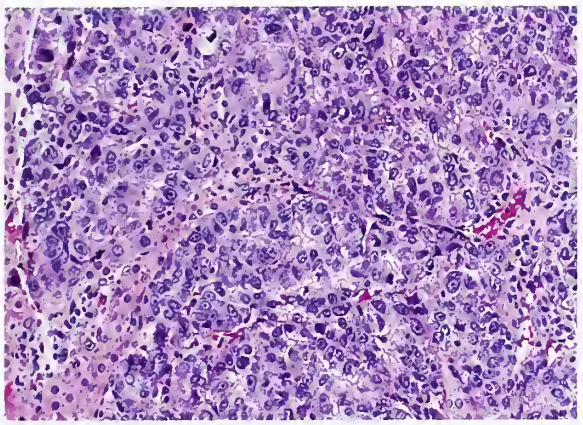

Figure 8-9

HEPATOCELLULAR CARCINOMA METASTATIC TO ADRENAL GLAND

The hepatocellular carcinoma metastatic to the adrenal gland simulated a primary adrenal tumor. The metastasis has a vague trabecular pattern and the tumor cells have prominent nucleoli. (Fig. 8-9 from Fascicle 19, Third Series.)

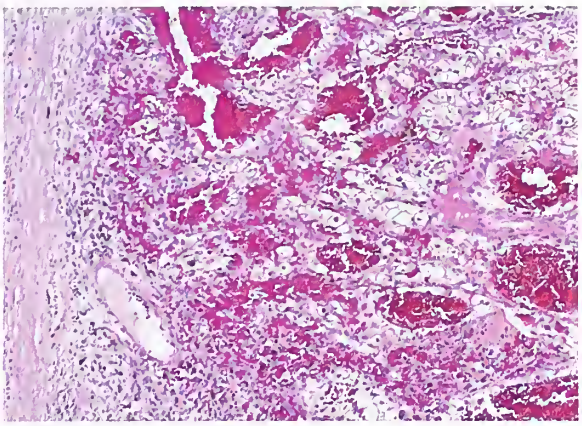

Figure 8-10

RENAL CELL CARCINOMA METASTATIC TO ADRENAL GLAND

Small solitary adrenal metastasis from ipsilateral renal cell carcinoma. The patient had undergone radical nephrectomy for a large renal cell carcinoma. (Fig. 8-10 from Fascicle 19, Third Series.)

as large cell lung carcinoma (see fig. 8-7D–F), renal cell carcinoma, or even hepatocellular carcinoma (fig. 8-9) can simulate an adrenal cortical carcinoma.

Adrenal metastases by renal cell carcinoma have been reported in 2.8 percent (21) to 5.5 percent (22) of patients undergoing nephrectomy (fig. 8-10), and it has been documented in 24 percent of autopsy cases (2). Renal cell carcinoma can involve the ipsilateral adrenal gland by direct extension, and although the metastasis is usually to the ipsilateral adrenal gland, contralateral metastasis also occurs and potentially can cause confusion with an adrenal neoplasm. Rarely, renal cell carcinoma presents with contralateral (fig. 8-11) (23) or bilateral adrenal metastases (24). There can also be an alveolar or nesting pattern similar to that of an adrenal cortical neoplasm, but the optical clarity of the cytoplasm differs from the finely vacuolated cytoplasm seen in many adrenal cortical nodules and tumors. Correlation of clinical, radiologic, and endocrinologic data and intraoperative findings can be important for a correct diagnosis.

The adrenal gland may also be involved by metastatic pancreatic islet cell carcinoma, which can mimic a pheochromocytoma or even an adrenal cortical carcinoma. A very unusual example of adrenal metastasis from adrenohepatic fusion with hepatocellular carcinoma has been reported (25).

There are occasional diagnostic pitfalls in the evaluation of a fine needle aspiration biopsy of an adrenal mass. Metastatic adenocarcinoma can mimic normal adrenal cortical cells (26), and conversely, aspiration of an adrenal cortical nodule can mimic a small cell malignancy (see fig. 3-18) (27). Immunohistochemical stains help to distinguish a metastatic carcinoma from a primary adrenal cortical neoplasm (see fig. 8-7): adrenal cortical carcinoma is usually positive for vimentin, and immunostains for epithelial markers such as cytokeratin and epithelial membrane antigen are usually nonreactive, although there may be exceptions.

INVOLVEMENT OF ADRENAL GLANDS BY MALIGNANT LYMPHOMA AND LEUKEMIA

Secondary involvement of the adrenal glands by malignant lymphoma is seen in 18 to 25 percent of autopsies (28,29), usually in patients who had disseminated disease (fig. 8-12). Unilateral adrenal involvement by malignant lymphoma was found in 5.5 percent of patients with Hodgkin's disease and 8 percent of patients with non-Hodgkin's malignant lymphoma (29); bilateral adrenal involvement has been reported in 9 percent of patients with Hodgkin's disease

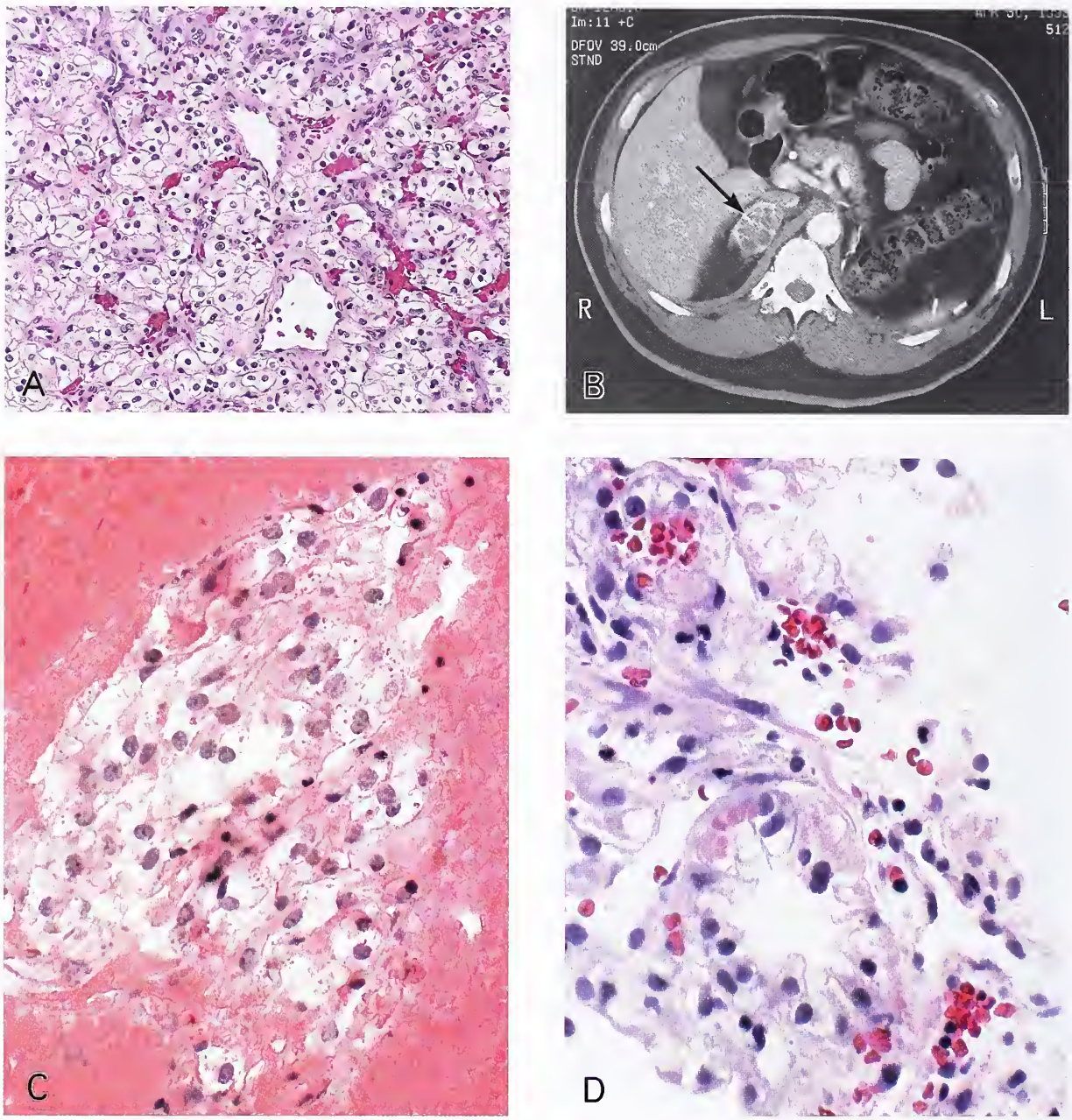

Figure 8-11

RENAL CELL CARCINOMA METASTATIC TO CONTRALATERAL ADRENAL GLAND

A: A 55-year-old man underwent left radical nephrectomy, including the left adrenal gland, for a large renal cell carcinoma measuring 11 cm in diameter. The tumor invaded the renal vein but was entirely resected. Note the tight, solid nesting pattern of the primary renal tumor. Most tumor cells have optically clear cytoplasm. (Fig. 8-11 from Fascicle 19, Third Series.)

B: Ten months later, the same patient was found to have a contralateral right adrenal mass on CT scan which is nonhomogeneous (arrow). The few metal clips mark the surgical bed on the opposite side. There was no evidence of metastases elsewhere.

C: Cell block preparation of fine needle aspiration biopsy shows small nests of metastatic renal cell carcinoma with a prominent bloody background.

D: Separate core biopsy done at the same time as the fine needle aspiration shows metastatic renal cell carcinoma virtually identical to that seen 10 months earlier (A). (B–D: Fig. 8-12 from Fascicle 19, Third Series.)

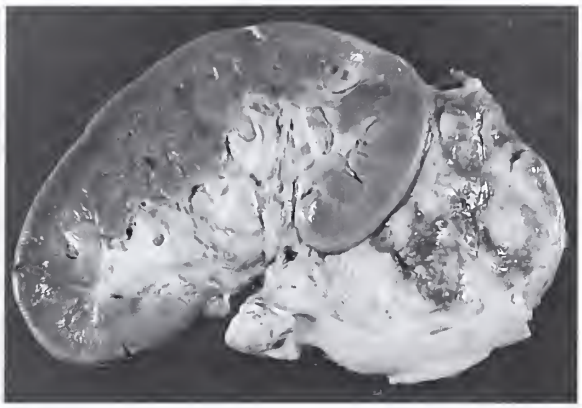

Figure 8-12

MASSIVE ADRENAL INVOLVEMENT BY MALIGNANT LYMPHOMA

This tumor was found at autopsy of a patient with disseminated non-Hodgkin's malignant lymphoma. The bulging, lobulated surface was soft and creamy white on section. (Fig. 10-4A from Travis WD, Oertel JE, Lack EE. Miscellaneous tumors and tumefactive lesions of the adrenal gland. In: Lack EE, ed. Pathology of the adrenal glands. New York: Churchill Livingstone; 1990:351-378.)

at autopsy, and in 12 percent with non-Hodgkin's malignant lymphoma (29). CT scans have demonstrated adrenal involvement by non-Hodgkin's malignant lymphoma in 3 to 4 percent of patients during their disease course (30,31). Massive bilateral adrenal involvement can result in Addison's disease (32), and rarely, this is a presenting manifestation (33). The adrenal insufficiency has been reported to resolve following treatment with combination chemotherapy. Only rarely have extranodal malignant lymphomas presented in the adrenal gland without detectable involvement elsewhere. Spontaneous adrenal hemorrhage is a rare complication (34).

Intravascular lymphomatosis, a peculiar type of non-Hodgkin's malignant lymphoma with destructive angiotropism, can involve the adrenal glands (fig. 8-13) and cause gross enlargement detectable on CT scan. The disorder was originally felt to be a primary endothelial malignancy, hence the term malignant angioendotheliomatosis, but it was shown to be a malignant lymphoma of large cell or immunoblastic type with a B-cell, or less commonly, a T-cell phenotype (35). The malignant cells proliferate within small vessels in most organs, but have an affinity for the central nervous system, with varied neurologic manifestations. There may be massive involvement of the adrenal glands (fig. 8-13B) which can result in Addison's disease, and may account for the fever, hypotension, and electrolyte abnormalities frequently seen in these patients. Plasmacytoma presenting primarily in the adrenal gland is extremely rare (36), and the possibility of a low-grade malignant lymphoma with plasmacytoid features should be considered.

The diagnosis of adrenal involvement by malignant lymphoma can be confirmed on fine needle aspiration biopsy. Problems in the differential diagnosis (e.g., metastatic undifferentiated carcinoma) can usually be resolved by immunohistochemical stains (immunopositive staining for leukocyte common antigen and negative staining for epithelial markers). Involvement of adrenal glands by leukemia is almost always an incidental finding at autopsy (fig. 8-14).

SECONDARY INVOLVEMENT BY OTHER MALIGNANT TUMORS

The adrenal glands are only rarely involved secondarily by mesenchymal neoplasms. The author has observed one case of metastatic leiomyosarcoma to the adrenal gland (unilateral and under 2 cm in size) from a primary arising in the duodenum (fig. 8-15). Angiosarcoma can also involve the adrenal gland secondarily. There may be incidental involvement of the adrenal glands by Kaposi's sarcoma (fig. 8-16) as a manifestation of more widely disseminated tumor in patients with acquired immunodeficiency syndrome (AIDS). Both angiosarcoma and Kaposi's sarcoma may have a sinusoidal pattern with extension between residual columns and cords of cortical cells, and there may be extension outside the gland into periadrenal fat. Meningeal hemangiopericytoma has been reported metastatic to the adrenal gland and is associated with multiple metastases to bones and lungs (37).

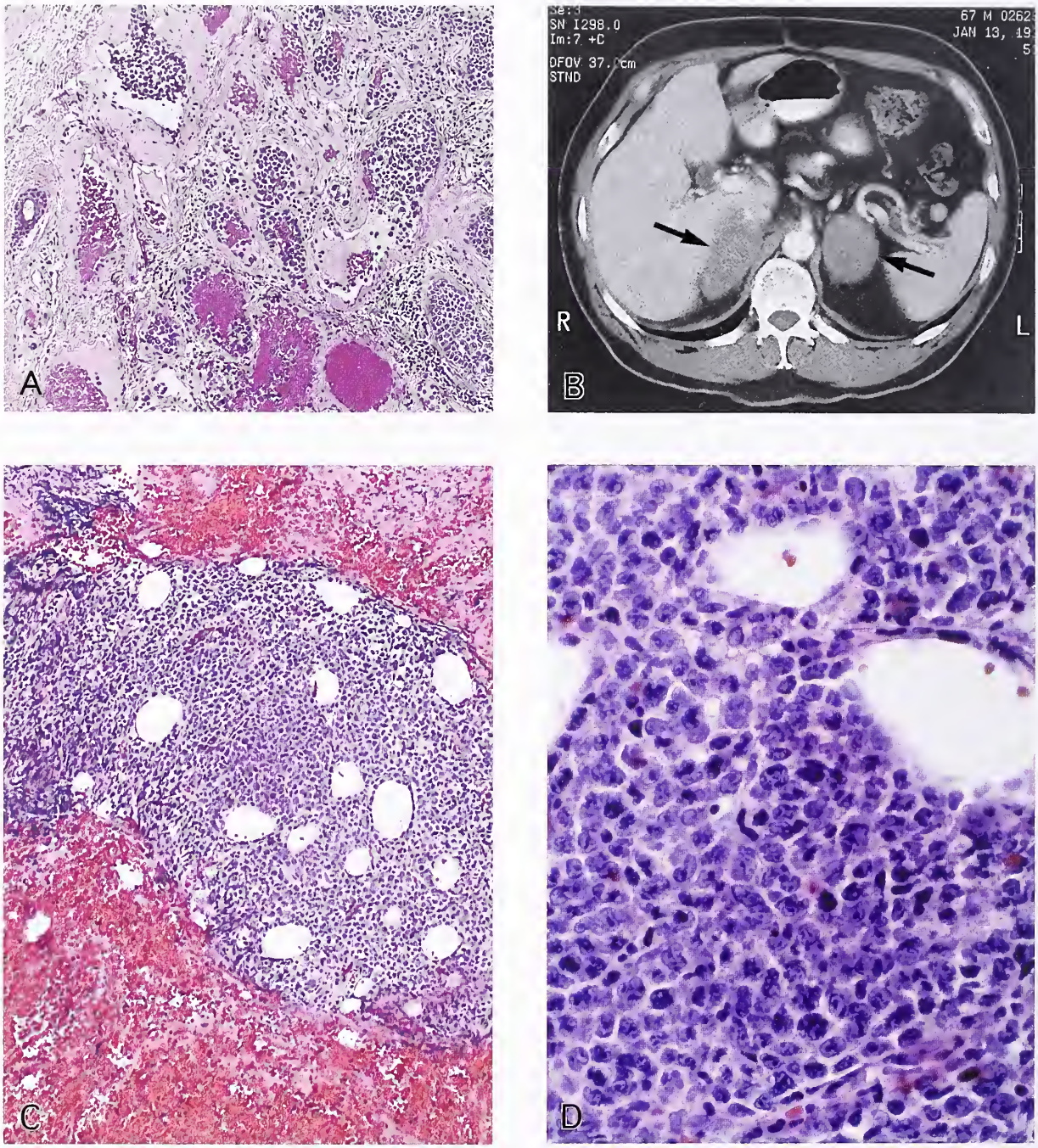

Figure 8-13

INTRAVASCULAR "LYMPHOMATOSIS" INVOLVING ADRENAL GLAND

A: An adult male patient presented with cutaneous cavernous hemangiomas involved by malignant lymphoma, non-Hodgkin's type ("intravascular lymphomatosis"). (A–C: Fig. 8-14 from Fascicle 19, Third Series.)

B: Later, bilateral suprarenal masses (arrows) obliterated both adrenal glands.

C: Fine needle aspiration yielded small fragments of malignant lymphoma in cell block preparations.

D: Higher magnification shows malignant lymphoma, large cell ("histiocytic") type.

Figure 8-14

ACUTE LEUKEMIA INVOLVING ADRENAL GLAND

A: A 51-year-old male with a history of myelofibrosis developed acute leukemic transformation and died of sepsis. The right adrenal gland weighed 18 g and was heavily infiltrated by acute leukemia.

B: Same case showing infiltration of the sinusoids by acute leukemia. (A,B: Fig. 8-16 from Fascicle 19, Third Series.)

C: Patchy areas of fibrosis and dystrophic calcification are present in the adrenal gland.

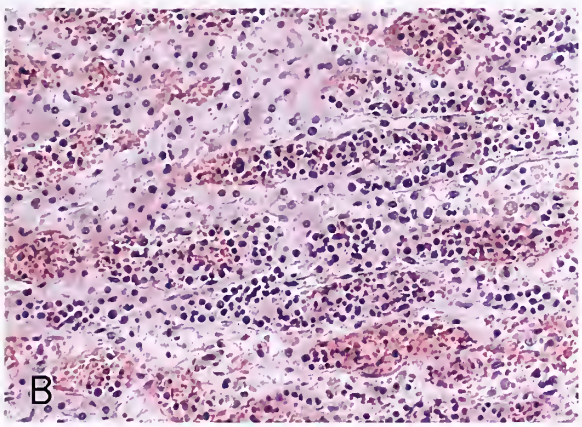

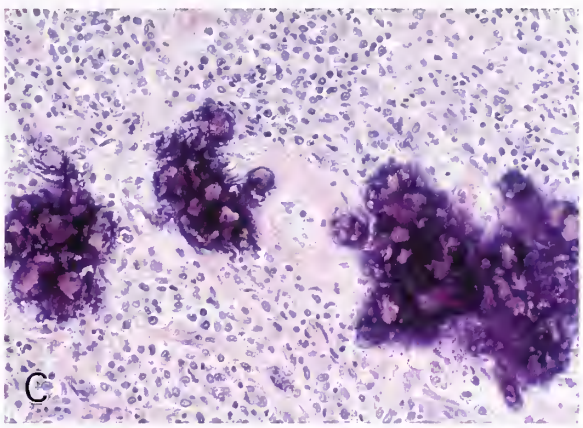

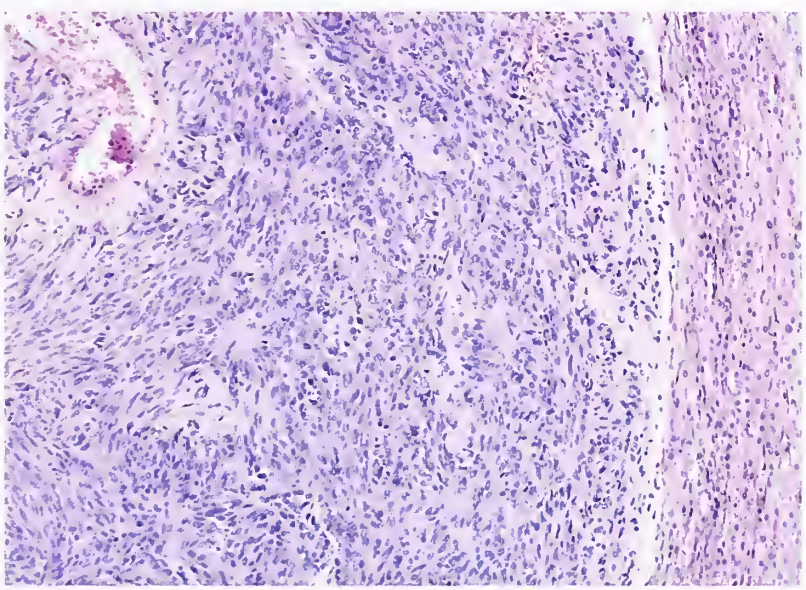

Figure 8-15

LEIOMYOSARCOMA METASTATIC TO ADRENAL GLAND

Metastatic leiomyosarcoma to the adrenal gland from a primary tumor of the duodenum. Specific immunostains were not available at the time to determine whether this was a gastrointestinal stromal tumor. Compressed adrenal cortex is on the right side. (Fig. 8-17 from Fascicle 19, Third Series.)

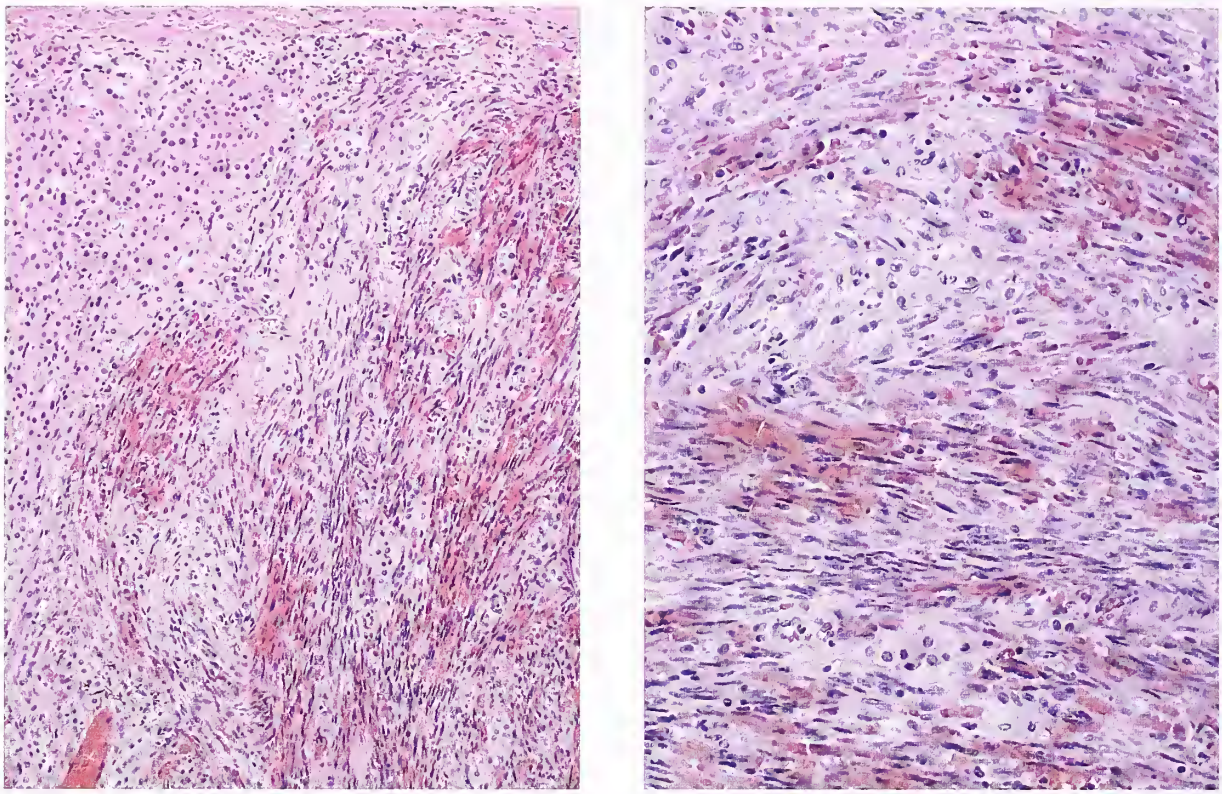

Figure 8-16

KAPOSI'S SARCOMA INVOLVING ADRENAL GLAND

Left: Kaposi's sarcoma involving the adrenal gland of an adult male with acquired immunodeficiency syndrome (AIDS). Right: Residual compressed cortical cells are widely separated by Kaposi's sarcoma. Rare hyaline globules were present. (L&R: Fig. 8-18 from Fascicle 19, Third Series.)

REFERENCES

Incidence and Primary Sites

1. Willis RA. The spread of tumors in the human body, 3rd ed. London: Butterworth; 1973.
2. Abrams HL, Spiro R, Goldstein N. Metastases in carcinoma; analysis of 1000 autopsied cases. Cancer 1950;3:74-85.
3. Sahagian-Edwards A, Holland JF. Metastatic carcinoma to the adrenal glands with cortical hypofunction. Cancer 1954;7:1242-1245.
4. de la Monte SM, Hutchins GM, Moore GW. Influence of age on the metastatic behavior of breast carcinoma. Hum Pathol 1988;19:529-534.
5. de la Monte SM, Hutchins GM, Moore GW. Altered metastatic behavior of small cell carcinoma of the lung after chemotherapy and radiation. Cancer 1988;61:2176-2182.
6. Lack EE. Pathology of the adrenal and extra-adrenal paraganglia. Major problems in pathology, vol 29. Philadelphia: WB Saunders; 1994.
7. McMahon RF. Tumour-to-tumour metastasis: bladder carcinoma metastasizing to an adrenocortical adenoma. Br J Urol 1991;67:216-217.
8. Ilias I, Alesci S, Pacak K. Current views on imaging of adrenal tumors. Horm Metab Res. 2004;36:430-435.
9. Allard, P, Yankaskas, BC, Fletcher, RH, Parker, LA, Halvorsen, RA Jr. Sensitivity and specificity of computed tomography for the detection of adrenal metastatic lesions among 91 autopsied lung cancer patients. Cancer 1990;66:457-462.
10. Kim SH, Brennan MF, Russo P, Burt ME, Coit DG. The role of surgery in the treatment of clinically isolated adrenal metastasis. Cancer 1998;82:389-394.

11. Sarela AI, Murphy I, Coit DG, Conlon KC. Metastasis to the adrenal gland: the emerging role of laparoscopic surgery. Ann Surg Oncol. 2003;10:1191-1196.
12. Gerber E, Dinlenc C, Wagner JR. Laparoscopic adrenalectomy for isolated adrenal metastasis. JSLS. 2004;8:314-319.
13. Mayo-Smith WW, Dupuy DE. Adrenal neoplasms: CT-guided radiofrequency ablation—preliminary results. Radiology. 2004;231:225-230.

Adrenal Cortical Insufficiency (Addison's Disease)

14. Travis WD, Oertel JE, Lack EE. Miscellaneous tumors and tumefactive lesions of the adrenal gland. In: Lack EE, ed. Pathology of the adrenal glands. New York: Churchill Livingstone; 1990:351-378.
15. Lack EE, Kozakewich HP. Embryology, developmental anatomy, and selected aspects of nonneoplastic pathology. In: Lack EE, ed. Pathology of the adrenal glands. New York: Churchill Livingstone; 1990:1-74.
16. Addison T. On the constitutional and local effects of disease of the supra-renal capsules. London: Samuel Highley; 1855.
17. Seidenwurm DJ, Elmer EB, Kaplan LM, Williams EK, Morris DG, Hoffman AR. Metastasis to the adrenal glands and the development of Addison's disease. Cancer 1984;54:552-557.
18. Redman BG, Pazdur R, Zingas AP, Loredo R. Prospective evaluation of adrenal insufficiency in patients with adrenal metastasis. Cancer 1987; 60:103-107.
19. Sheeler LR, Myers JH, Eversman JJ, Taylor HC. Adrenal insufficiency secondary to carcinoma metastatic to the adrenal gland. Cancer 1983;52: 1312-1316.
20. Gufler H, Eichner G, Grossmann A, et al. Differentiation of adrenal adenomas from metastases with unenhanced computed tomography. J Comput Assist Tomogr. 2004;28:818-822.

Pathology and Differential Diagnosis

21. Yokoyama H, Tanaka M. Incidence of adrenal involvement and assessing adrenal function in patients with renal cell carcinoma: is ipsilateral adrenalectomy indispensable during radical nephrectomy? BJU Int. 2005;95:526-529.
22. Siemer S, Lehmann J, Kamradt J, et al. Adrenal metastases in 1635 patients with renal cell carcinoma: outcome and indication for adrenalectomy. J Urol. 2004;171(pt 1):2155-2159.
23. Lau WK, Zincke H, Lohse CM, Cheville JC, Weaver AL, Blute ML. Contralateral adrenal metastasis of renal cell carcinoma: treatment, outcome and a review. BJU Int 2003;91:775-779.
24. Selli C, Carini M, Barbanti G, Barbagli G, Turini D. Simultaneous bilateral adrenal involvement by renal cell carcinoma: experience with 3 cases. J Urol 1987;137:480-482.
25. Okano K, Usuki H, Maeta H. Adrenal metastasis from hepatocellular carcinoma through an adrenohepatic fusion. J Clin Gastroenterol. 2004;38:912.
26. Mitchell ML, Ryan FP Jr, Shermer RW. Pulmonary adenocarcinoma metastatic to the adrenal gland mimicking normal adrenal cortical epithelium on fine needle aspiration. Acta Cytol 1985;29:994-998.
27. Min KW, Song J, Boesenberg M, Acebey J. Adrenal cortical nodule mimicking small round cell malignancy on fine needle aspiration. Acta Cytol 1988;32:543-546.

Secondary Involvement by Malignant Lymphoma, Leukemia and Other Malignant Tumors

28. Rosenberg SA, Diamond HD, Jaslowitz B, Craver LF. Lymphosarcoma: A review of 1269 cases. Medicine (Baltimore) 1961;40:31-84.
29. Richmond J, Sherman RS, Diamond HD, Craver LF. Renal lesions associated with malignant lymphomas. Am J Med 1962;32:184-207.
30. Jafri SZ, Francis IR, Glazer GM, Bree RL, Amendola MA. CT detection of adrenal lymphoma. J Comput Assist Tomogr 1983;7:254-256.
31. Paling MR, Williamson BR. Adrenal involvement in non-Hodgkin lymphoma. AJR Am J Roentgenol 1983;141:303-305.
32. Akcay MN, Tekin SB, Akcay G. Addisonian crisis due to adrenal gland metastasis in Hodgkin's disease. Int J Clin Pract. 2003;57:840-841.
33. Serrano S, Tejedor L, Garcia B, Hallal H, Polo JA, Alguacil G. Addisonian crisis as the presenting feature of bilateral primary adrenal lymphoma. Cancer 1993;71:4030-4033.
34. Kartsios C, Kaloyannidis P, Yannaki E, et al. Spontaneous adrenal haemorrhage as a manifestation of isolated relapse of non-Hodgkin's lymphoma. Acta Haematol. 2003;110:197-199.
35. Glass J, Hochberg FH, Miller DC. Intravascular lymphomatosis. A systemic disease with neurologic manifestations. Cancer 1993;71:3156-3164.
36. Page DL, DeLellis RA, Hough AJ Jr. Tumors of the adrenal. Atlas of Tumor Pathology. 2nd series, Fascicle 23. Washington DC: Armed Forces Institute of Pathology; 1986.
37. Pistolesi S, Fontanini G, Barellini L, et al.. Meningeal hemangiopericytoma metastatic to the adrenal gland with multiple metastases to bones and lungs: a case report. Tumori. 2004; 90:147-150.

9 ADRENAL MEDULLARY HYPERPLASIA AND MULTIPLE ENDOCRINE NEOPLASIA (MEN) SYNDROME TYPE 2

ADRENAL MEDULLARY HYPERPLASIA

Adrenal medullary hyperplasia (AMH) is defined as an increase in the number of chromaffin cells resulting in the expansion of the medullary compartment into areas of the gland where it is not normally present. Expansion in volume of the medullary compartment may result in increased gland size and weight as well as an increased proportion of medulla relative to cortex when viewed in transverse sections. AMH may be diffuse, nodular, or a combination of both. The morphologic features may be symmetric or asymmetric.

AMH may be accompanied by clinical and/or biochemical evidence of hyperfunction, i.e., excess secretion of catecholamines. AMH should not be an unexpected entity since hyperplasia is identified in virtually all other endocrine tissues. AMH is usually seen in association with multiple endocrine neoplasia (MEN) syndrome types 2a and 2b, but it has also been reported in other settings where it can mimic a pheochromocytoma. Hyperplasia of extraadrenal paraganglia of the sympathoadrenal neuroendocrine system has not been well-characterized in humans although it has been noted in the patients with Beckwith-Wiedemann syndrome (1). Anatomic documentation of AMH necessitates careful dissection and weighing of the gland and possible use of morphometric techniques (see chapter 1).

SPORADIC ADRENAL MEDULLARY HYPERPLASIA

There is mounting evidence that AMH exists as a distinct entity, but accurate identification may depend upon rigid morphometric criteria and close correlation with clinical and endocrinologic data (2). The clinical picture may resemble that of pheochromocytoma, with paroxysmal hypertension, diaphoresis, and tachycardia, yet following laparotomy no pheochromocytoma or extraadrenal paraganglioma can be found (3–6). AMH, therefore, is part of the differential diagnosis of pseudopheochromocytoma (2). AMH may be complicated by catecholamine "acute abdomen" with ileus, abdominal distension, and pain (7). Many patients with sporadic AMH experience amelioration of the signs and symptoms of excess catecholamine secretion following surgical resection of one or both adrenal glands. Biochemical documentation of increased catecholamine secretion is a prerequisite for a diagnosis of AMH for some (8). In a review of 15 patients with sporadic (simple) AMH, 7 experienced marked symptomatic improvement following surgery, and 5 had partial reduction in hypertension; 2 of the 3 patients who experienced no benefit from surgery died of cerebral hemorrhage and thrombosis (9). Unilateral AMH has been reported (10). Sporadic bilateral AMH may be detectable on ^{131}I-metaiodobenzylguanidine (^{131}I-MIBG) scan yet show no focal lesion on computerized tomography (CT) or magnetic resonance imaging (MRI) scans (11).

AMH has been noted in patients with cystic fibrosis (fig. 9 -1). In one study, elevated catecholamine levels (mainly epinephrine) were seen on quantitative analysis of medullary tissue at autopsy of patients with cystic fibrosis (12). In this study, a single transverse section of each adrenal gland from six patients with cystic fibrosis proved positive for AMH, although no specific morphometric techniques were described.

An enlarged "mass" of chromaffin cells has been reported in the adrenal medullae of victims of sudden infant death syndrome (SIDS), and has been used as evidence supporting chronic alveolar hypoventilation, along with

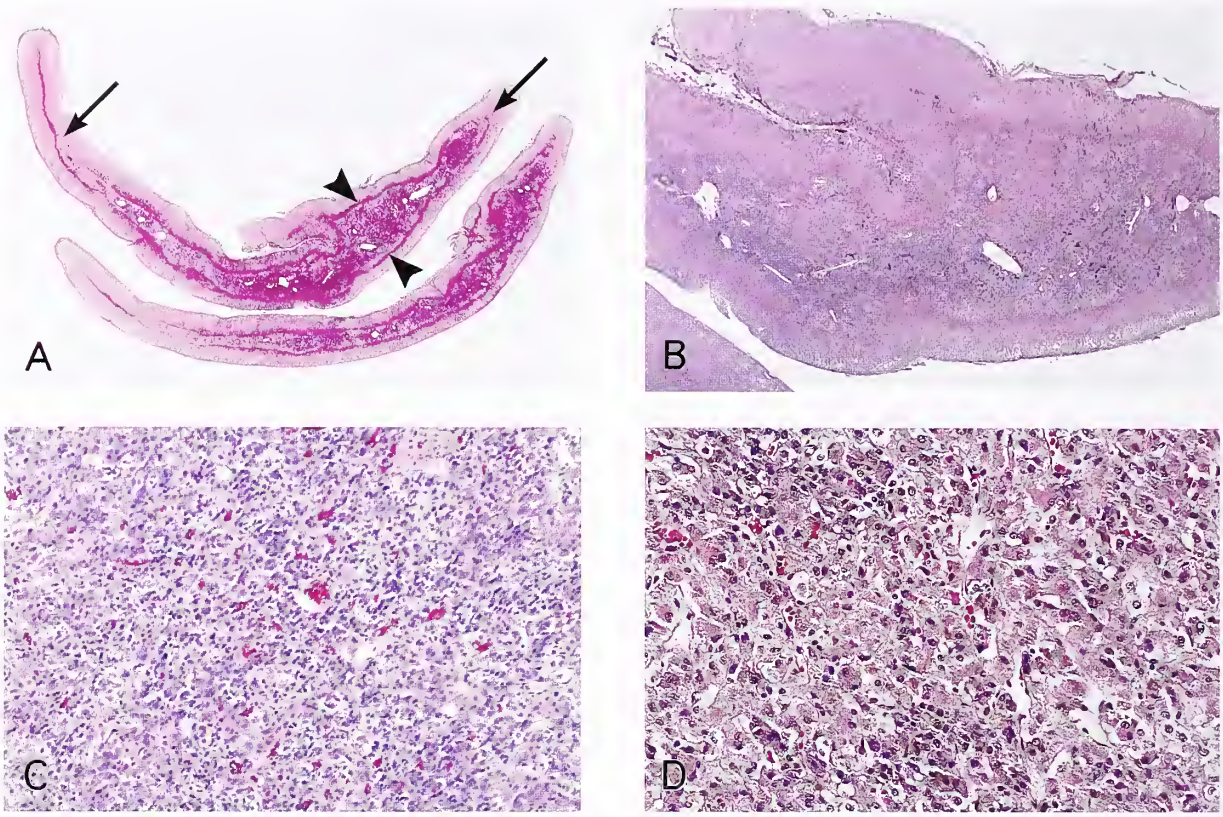

Figure 9-1

DIFFUSE ADRENAL MEDULLARY HYPERPLASIA (AMH)

A: A transverse section from the body of an adrenal gland from a young adult who died of complications of cystic fibrosis. The medullary compartment expands well into both alae (arrows). The corticomedullary junction is indicated by arrowheads.

B: Higher magnification of the diffusely hyperplastic adrenal medulla, close to the head of the adrenal gland. Note the small posterior ridge or crista on the superior aspect of gland. (Fig. 9-1B from Fascicle 19, Third Series.)

C: This section, through the body of the gland, is composed of hyperplastic chromaffin cells.

D: Hyperplastic chromaffin cells vary slightly in size and have a diffuse to vaguely trabecular pattern. (Fig. 9-1C from Fascicle 19, Third Series.)

increased musculature in small pulmonary arteries, abnormal retention of brown fat, and extramedullary hematopoiesis (13). Adrenal corticomedullary hyperplasia has been demonstrated in rats exposed to hypobarism at a simulated altitude of 5,500 m, and is reported to closely resemble some pheochromocytomas (14). There is some suggestion that extraadrenal chromaffin cells may secrete catecholamines in response to hypoxemia (15), but currently there is no evidence of increased medullary activity in humans acclimatized to high altitudes (14). AMH presumably reflects an ongoing need for catecholamines in chronic hypoxemia, but does not necessarily indicate an underlying direct chemoreceptor function (14). Rat pheochromocytoma PC-12 cells have been shown in vitro to undergo hypoxia-induced apoptosis and different signaling pathways seem to be involved in this pattern of cell injury (16).

Sporadic AMH has also been considered a cause of hypertension in the pediatric age group (17). It has been reported in association with Cushing's syndrome due to an adrenal cortical adenoma, and it was speculated that it may have contributed to the hypertension (18).

AMH has also been reported in patients with Beckwith-Wiedemann syndrome (see fig. 2-23) (1); about 85 percent of these cases are sporadic (2). Five of six infants studied by Beckwith (1) had AMH, and in one case there was "definite hyperplasia" of extraadrenal paraganglia. The

adrenal medulla and extraadrenal paraganglia may show an inappropriate degree of development for the infantile age group. A case of malignant giant pheochromocytoma has been reported in association with hemihypertrophy (19).

FAMILIAL ADRENAL MEDULLARY HYPERPLASIA

AMH has been well established as a pathologic entity in patients with the multiple endocrine neoplasia (MEN) syndrome types 2a and 2b, and is regarded as the precursor of pheochromocytomas in these disorders (20–22). The Beckwith-Wiedemann syndrome can also occur in a familial manner. There may be other familial settings in which pheochromocytomas arise, such as von Recklinghausen's disease and von Hipple-Lindau disease, but the precursor lesion (presumably AMH) has not been as well characterized as in MEN type 2 (2).

Multiple Endocrine Neoplasia Syndromes

In 1961, Sipple (23) first noted a significant increase in the incidence of thyroid carcinoma in patients with pheochromocytoma; in 1965, it was shown independently by two groups that the thyroid malignancy was medullary thyroid carcinoma (MTC), a distinctive thyroid malignancy recognized in 1951 by Horn (24) and more fully characterized by Hazard et al. in 1959 (25). C-cell hyperplasia was subsequently shown to be the precursor of MTC in this familial disorder (26). The characteristic neuromas of the oral mucosa were noted by Williams and Pollock along with ganglioneuromatosis of the gastrointestinal tract (27). It was suggested by Steiner et al. (28) that the combination of MTC, pheochromocytoma, and parathyroid disease be referred to as MEN type 2, and the multiple mucosal neuroma complex be designated MEN type 2b or MEN type 3. The presence of AMH and its relation to pheochromocytoma as a precursor lesion is consistent with Knudson's "two mutational event or hit" theory for the initiation of neoplasia, with AMH being the first or genetic mutational event (29,30).

MEN Syndrome Type 2a (Sipple's Syndrome)

MEN syndrome type 2a, also known as *Sipple's syndrome*, has an autosomal dominant mode of inheritance with a high degree of penetrance. The syndrome includes MTC, pheochromocytoma, and parathyroid hyperplasia. About 25 percent of patients have clinical or biochemical evidence of hyperparathyroidism (31); in some patients, the enlarged parathyroid glands are evident during surgery for thyroid cancer (32). The parathyroid mitogenic factor detected in the plasma of patients with MEN type 1 has not been found in patients with MEN type 2, suggesting a different mechanism for promoting parathyroid hyperplasia (33). The MTC is usually the most prominent component of the syndrome, and almost invariably precedes development of the pheochromocytoma. In a recent review, Carney (34) gives a detailed history of the familial MEN syndromes.

MEN Syndrome Type 2b

MEN syndrome type 2b also has an autosomal dominant mode of inheritance, but some cases occur in isolated or sporadic fashion. Explanations for this apparent sporadic occurrence include lack of a careful pedigree analysis and systematic screening of family members or a new genetic mutation that is fatal before the patient passes the syndrome on to a future generation (35). The phenotypic expression of MEN type 2b is very distinctive (see chapter 10), and important to recognize early in the disorder. Patients may have gastrointestinal manifestations, ophthalmologic findings, and the characteristic neuromatous proliferation within the mucosa of lips, tongue, and other mucosal sites including the gastrointestinal tract.

PATHOLOGY OF AMH AND DISTINCTION FROM PHEOCHROMOCYTOMA

The pathologic diagnosis of AMH sometimes requires rigorous application of morphometric criteria (see chapter 1), particularly when morphologic changes are borderline or subtle; at other times, the diagnosis is easily made on gross examination of the gland following transverse sectioning (fig. 9-2). Removal of periadrenal connective tissue and fat, and sectioning of the gland at narrow intervals in the transverse plane, permit more precise evaluation of the amount, character, and distribution of chromaffin tissue. Nodular or diffuse hyperplasia is a characteristic feature of MEN types 2a and 2b, and the pheochromocytomas are frequently multicentric and

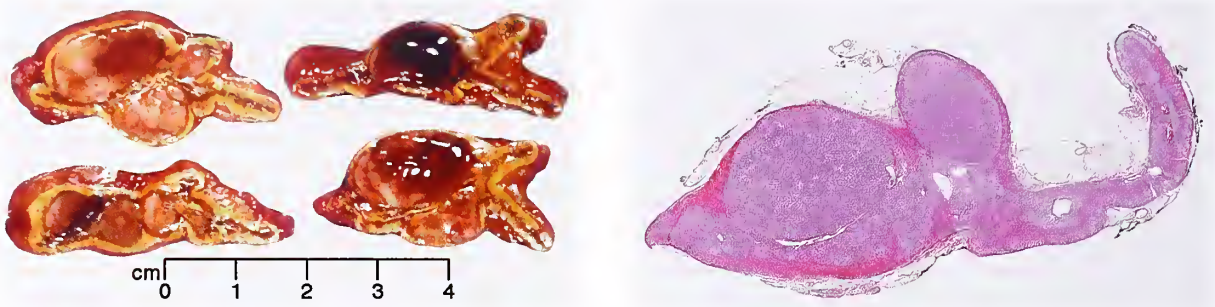

Figure 9-2

NODULAR AMH IN MULTIPLE ENDOCRINE NEOPLASIA (MEN) SYNDROME TYPE 2A

Left: A 36-year-old man with MEN type 2a (Sipple's syndrome) underwent bilateral adrenalectomy. The left adrenal weighed 15 g; the right, 15.4 g. Both glands show numerous nodules of hyperplastic chromaffin cells, some of which are small pheochromocytomas using the "1-cm rule." The nodules have a bulging cut surface in transverse section and vary in color from yellow-tan to deep red-brown.

Right: Diffuse and nodular adrenal medullary hyperplasia with small pheochromocytomas. The largest nodule measured 1.5 cm in diameter.

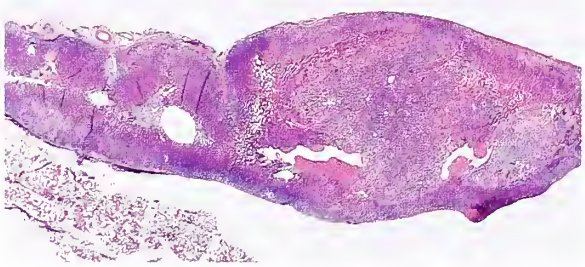

Figure 9-3

DIFFUSE AND NODULAR AMH IN MEN SYNDROME TYPE 2A

Transverse section near the head of the gland shows expansion of the medullary compartment. Small nodules of hyperplastic chromaffin cells compress the cortex.

bilateral. AMH can be nodular or diffuse, with symmetric or asymmetric involvement of the adrenal glands (fig. 9 -3); in a small proportion of cases the glands appear normal. In a study of adrenal glands from 19 patients with MEN type 2 (6 had MEN type 2b), 14 had symmetric involvement (multinodular pheochromocytoma, nodular or diffuse AMH, or normal gland), 4 had asymmetric involvement, and 1 had only unilateral changes (21).

Nodules of AMH may be pale gray to tan and fleshy, but some have a variety of colors and textures (fig. 9-2). On low-power magnification there is often a mixed pattern of diffuse and nodular hyperplasia, with expansion of the medullary compartment into one or both alae (fig. 9-4) or into the tail of the gland. There may be compression or distortion of the adjacent cortex by the nodular expansion of the medulla. An invasive or frankly infiltrative pattern is not seen, but there is typically no histologic evidence of true encapsulation, and sometimes there may be intermingling of cortical and medullary cells. Some nodules of hyperplastic chromaffin cells are partially molded to each other, with merging patterns (fig. 9-5), and some have a more complicated pattern with vague nodules within a larger nodule, suggesting different clones of proliferating chromaffin cells (35). Various architectural patterns can be found in AMH that are similar to those in pheochromocytoma, such as a nesting or alveolar arrangement of cells (fig. 9-6A), anastomosing trabeculae (fig. 9-6B), solid or diffuse growth, or even a spindle cell component (fig. 9-6C). Diffuse hyperplasia may antedate nodular hyperplasia and represent the earliest morphologic correlate of chromaffin cell hyperfunction.

Hyaline globules can be rather conspicuous in AMH associated with MEN type 2 (fig. 9-7). There may also be large numbers of vacuolated or granular cells, possibly reflecting increased secretory activity (2). There may be marked nuclear hyperchromasia and pleomorphism

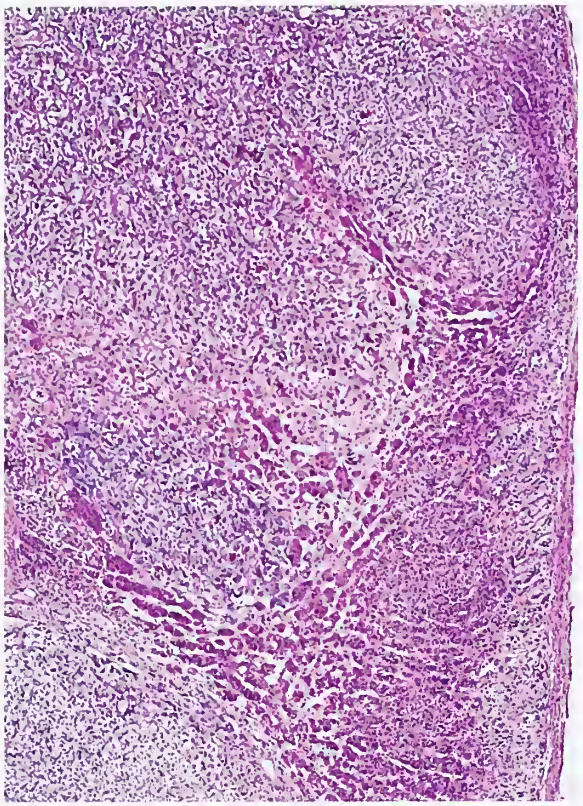

Figure 9-4

DIFFUSE AND NODULAR AMH IN MEN SYNDROME TYPE 2A

Smoothly contoured nodular expansions of chromaffin cells compress the adjacent cortex. Some intermingle with lipid-depleted cortical cells. Occasional hyaline globules were present. (Fig. 9-4 from Fascicle 19, Third Series.)

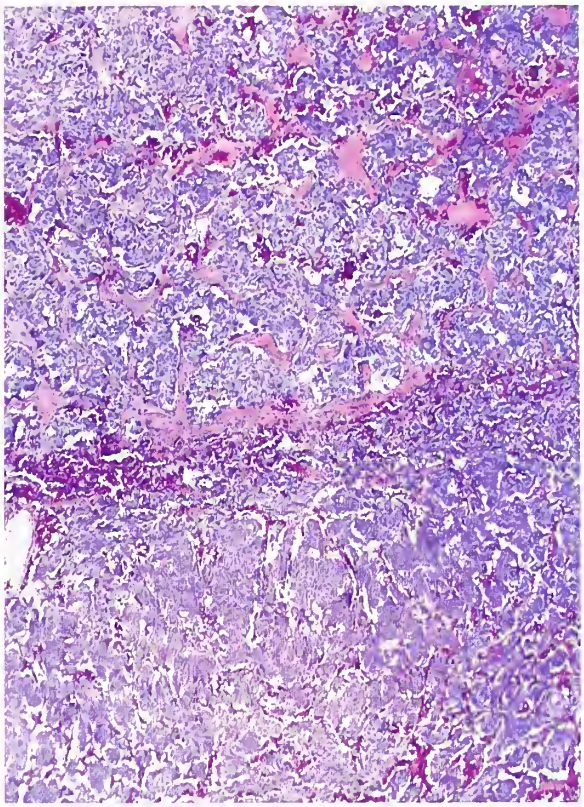

Figure 9-5

NODULAR AMH IN MEN SYNDROME TYPE 2A

Two juxtaposed nodules are present without encapsulation. Both nodules have an anastomosing cell cord pattern.

(fig. 9-8), and mitotic figures are found in some cases, although they are not numerous. In one study, enlarged nuclei were often seen in the juxtacortical area (22). A study of the DNA content in AMH and pheochromocytoma reported diploid or euploid histograms in normal and hyperplastic glands, while 33 of 38 clinically benign pheochromocytomas (87 percent) and all five malignant pheochromocytomas were aneuploid or nondiploid (36).

The distinction between AMH and pheochromocytoma is arbitrary, and it may be very difficult at times to distinguish between the two, particularly when the AMH is nodular (fig. 9-9). Carney et al. (21) designated nodules 1 cm or larger as pheochromocytoma and nodules under 1 cm as nodular AMH; this arbitrary designation was based upon the lower limit in size of pheochromocytoma in the first series Fascicle on adrenal neoplasms published in 1950 (37).

Pheochromocytomas in MEN type 2 are discussed in chapter 10. Some have regarded pheochromocytomas as representing an extreme degree of hyperplasia rather than a true neoplasm (22). In MEN type 2 there may be advanced pathology of the adrenal medulla, without clinical evidence of disease, and laboratory testing may yield variable results (21). These tumors may not even respond to the usual provocative tests used for diagnosing pheochromocytomas (38). One of the early indications of adrenal medullary hyperfunction in MEN type 2 is an elevated ratio of epinephrine to norepinephrine in urine (22,39), or increased levels of epinephrine in tissues of AMH; this is in contrast to sporadic pheochromocytoma where norepinephrine predominates (21). When adrenal medullary disease is detected in

Figure 9-6

NODULAR AMH IN MEN SYNDROME TYPE 2A

A: A vague nesting or alveolar arrangement of cells is present. Some nuclei are enlarged and hyperchromatic, with one having large nuclear pseudoinclusions.

B: Anastomosing trabecular pattern in nodular AMH. The cells have copious lavender cytoplasm. Intracytoplasmic hyaline globules are present in some areas.

C: Spindle cell pattern in nodular AMH. Most nuclei are elongated in the same axis. (Fig. 9-6C from Fascicle 19, Third Series.)

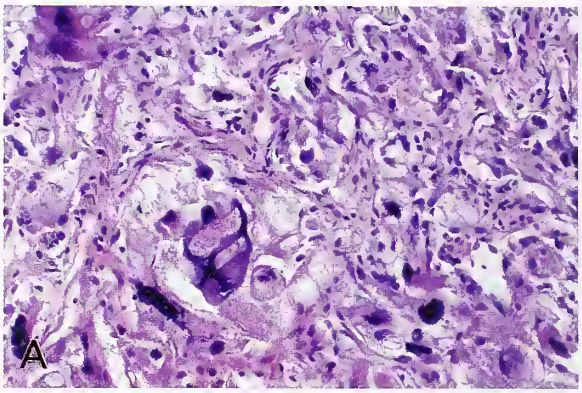

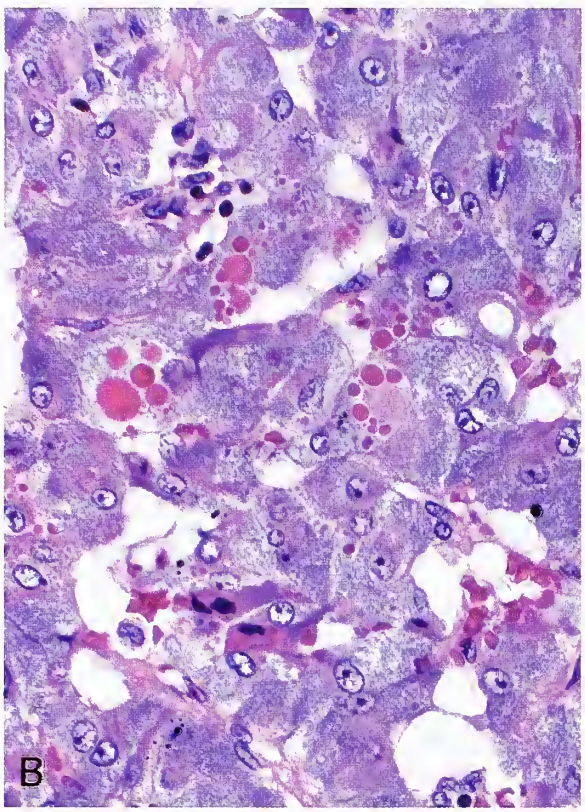

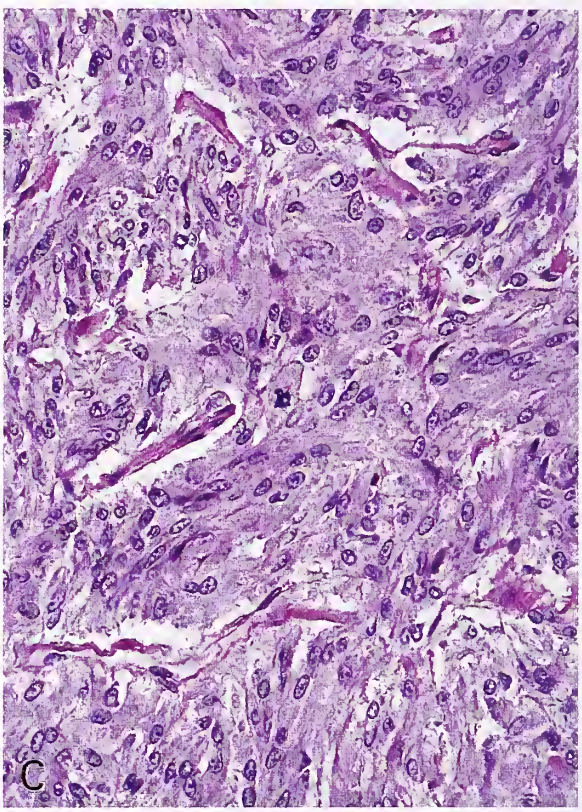

a patient with MEN type 2, some recommend bilateral total adrenalectomy (21). Functional as well as anatomic evidence of adrenal medullary abnormalities can be detected in some patients with the use of ^{131}I-MIBG scintigraphy (40).

PROLIFERATIVE LESIONS OF ADRENAL MEDULLA IN RATS

Diffuse and nodular AMH can develop spontaneously in various strains of aging rats, or be induced experimentally by exogenous xenobiotic agents such as drugs (reserpine, nicotine, growth hormone, estrogen, and retinoids) (41–43) and irradiation (44). The most important endogenous factor appears to be a genetic predisposition (41). Vitamin D3 has been shown to be a potent stimulus of chromaffin cell proliferation in vivo (45). Proliferation of extraadrenal paraganglia has also been reported in older animals (46), although this has not been seen by other investigators (47). Chromaffin cells of the adult rat adrenal gland proliferate in vivo in re-

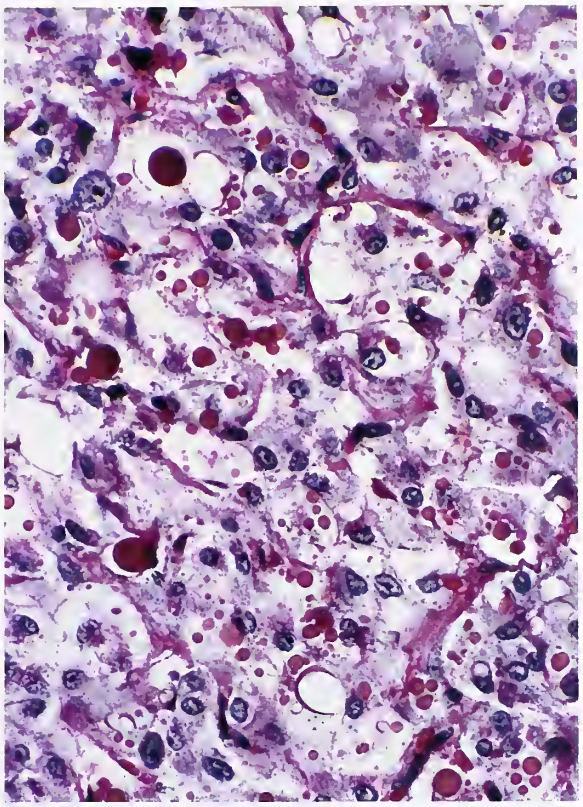

Figure 9-7

NODULAR AND DIFFUSE AMH IN MEN SYNDROME TYPE 2A

Hyperplastic chromaffin cells contain abundant eosinophilic hyaline globules. Some globules appear to reside within the extracellular space, but this is probably artifact. (Fig. 9-7 from Fascicle 19, Third Series.)

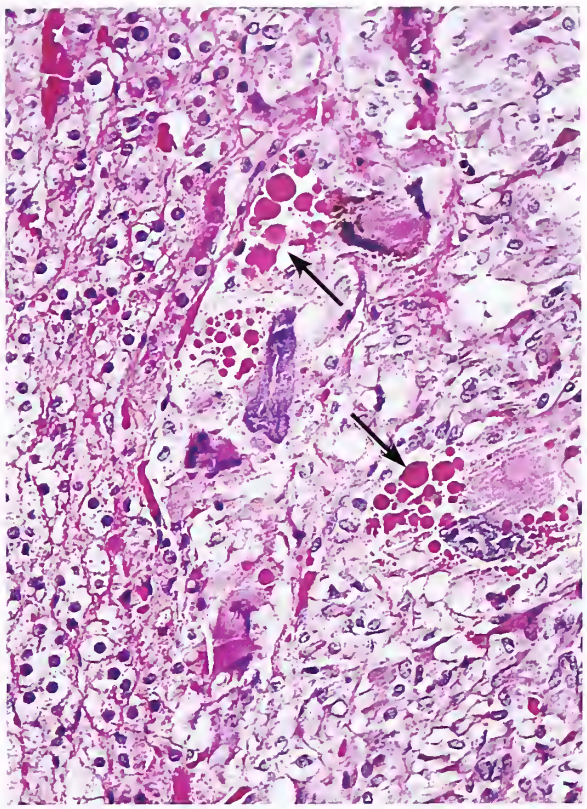

Figure 9-8

NODULAR AMH IN MEN SYNDROME TYPE 2A

Chromaffin cells near the cortex (left) have enlarged pleomorphic nuclei and intracytoplasmic hyaline globules (arrows). (Fig. 9-8 from Fascicle 19, Third Series.)

sponse to neurally derived signals; proliferation in vitro occurs after stimulation by nerve growth factor or by activators of adenylate cyclase or protein kinase C which mimic the effects of neurotransmitters in adrenal medullary nerve endings (48). The highest frequency of medullary proliferative lesions appears to be in Wistar rats, but variation in incidence may be related to age at sacrifice of the animal and vagaries in tissue sampling (41).

Accurate classification of these spontaneous or induced lesions as AMH versus pheochromocytoma are relevant for drug licensing applications (41). Similar to AMH in humans with MEN type 2, it may be very difficult to distinguish AMH in rats from pheochromocytomas. Spontaneous or drug-induced pheochromocytomas in rats are almost invariably norepinephrine producing, and the inability to produce epinephrine may be due to absence or inactivity of phenylethanolamine N-methyltransferase. Advantages of the mouse cell line include expression of substantial levels of phenylethanolamine N-methyltransferase and expression of the receptor tyrosine kinase, Ret, which is characteristic of sporadic and familial pheochromocytomas in humans (49). Most adrenal medullary proliferative lesions in the rat are of the chromaffin cell lineage; an estimated 2 percent of these lesions ultimately metastasize. Neuroblastoma and ganglioneuroblastoma are rare in this experimental animal (41).

Figure 9-9

NODULAR AMH AND EARLY PHEOCHROMOCYTOMAS IN MEN SYNDROME TYPE 2A

A: Bilateral adrenal enlargement was apparent on abdominal computerized tomography (CT) scan in a 31-year-old woman with MEN syndrome type 2a. Enlargement of the left adrenal gland is apparent (arrow); the right adrenal was also enlarged. The patient underwent bilateral adrenalectomy.

B: Transverse section of the left adrenal gland shows multinodular AMH, with the largest nodule measuring 1.5 cm in diameter (i.e., a small pheochromocytoma using the "1-cm rule").

C: Nodules of AMH on the left compress and distort the overlying cortex. (A–C: Fig. 9-9 from Fascicle 19, Third Series.)

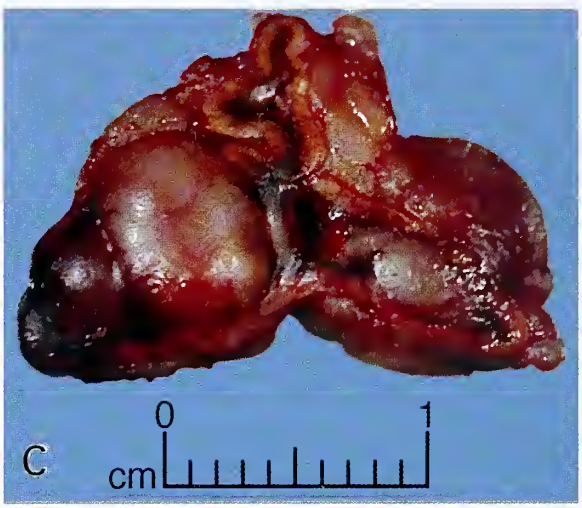

REFERENCES

Sporadic Adrenal Medullary Hyperplasia

1. Beckwith JB. Macroglossia, omphalocele, adrenal cytomegaly, gigantism, and hyperplastic visceromegaly. Birth Defects: Original Article Series 1969;5:188-196.
2. Lack EE. Pathology of adrenal and extra-adrenal paraganglia. Major problems in pathology, vol 29. Philadelphia: WB Saunders; 1994.
3. Montalbano FP, Baronofsky ID, Ball H. Hyperplasia of the adrenal medulla. A clinical entity. JAMA 1962;182:264-267.
4. Rudy FR, Bates RD, Cimorelli AJ, Hill GS, Engleman K. Adrenal medullary hyperplasia: a clinicopathologic study of four cases. Hum Pathol 1980;11:650-657.
5. Kurihara K, Mizuseki K, Kondo T, Ohoka H, Mannami M, Kawai K. Adrenal medullary hyperplasia. Hyperplasia-pheochromocytoma sequence. Acta Pathol Jpn 1990;40:683-686.
6. Dralle H, Schröder S, Gratz KF, Grote R, Padberg B, Hesch RD. Sporadic unilateral adrenomedullary hyperplasia with hypertension cured by adrenalectomy. World J Surg 1990;14:308-316.

7. Chen SX, Zhou ZQ, Zhao JS, Wang SZ, Sun ND. Catecholamine acute abdomen. A case of adrenal medullary hyperplasia accompanied by acute abdomen. Chin Med J (Engl) 1989;102:811-813.
8. Harrison TS, Gann DS. Adrenal medullary hyperplasia: an opinion. Surgery 1979;85:353-354.
9. Wu JP, Xu FJ, Zéng ZP. Adrenal medullary hyperplasia. Long-term follow up of 15 patients. Chin Med J (Engl) 1984;97:653-656.
10. Bailey J, Van Herle AJ, Giuliano A, Schroder S. Unilateral adrenal medullary hyperplasia: another form of curable hypertension? Int J Clin Pract 1999;53:149-151.
11. Yung BC, Loke TK, Tse TW, Tsang MW, Chan JC. Sporadic bilateral adrenal medullary hyperplasia: apparent false positive MIBG scan and expected MRI findings. Eur J Radiol 2000;36:28-31.
12. Bongiovanni AM, Yakovac WC, Steiker DD. Study of adrenal glands in childhood: hormonal content correlated with morphologic characteristics. Lab Invest 1961;10:956-967.
13. Naeye RL. Brain-stem and adrenal abnormalities in the sudden-infant-death syndrome. Am J Clin Pathol 1976;66:526-530.
14. Gosney JR. Adrenal corticomedullary hyperplasia in hypobaric hypoxia. J Pathol 1985;146:59-64.
15. Hervonen A, Korkala O. The effect of hypoxia on the catecholamine content of human fetal abdominal paraganglia and adrenal medulla. Acta Obstet Gynecol Scand 1972;51:7-24.
16. Gozal E, Sachleben LR Jr, Rane MJ, Vega C, Gozal D. Mild sustained and intermittent hypoxia induce apoptosis in PC-12 cells via different mechanisms. Am J Physiol Cell Physiol 2005; 288:C535-542.
17. Bialestock D. Hyperplasia of the adrenal medulla in hypertension of children. Arch Dis Child 1961;36:465-473.
18. Kazama YI, Noguchi T, Kawabe T, et al. A case of Cushing's syndrome associated with possible adrenomedullary hyperplasia. Endocrinol Jpn 1985;32:355-359.
19. Schnakenburg KV, Müller M, Dörner K, Harms D, Schwarze EW. Congenital hemihypertrophy and malignant giant pheochromocytoma—a previously undescribed coincidence. Eur J Pediat 1976;122:263-273.

Familial Adrenal Medullary Hyperplasia

20. Carney JA, Sizemore GW, Tyce GM. Bilateral adrenal medullary hyperplasia in multiple endocrine neoplasia, type 2: the precursor of bilateral pheochromocytoma. Mayo Clin Proc 1975;50:3-10.
21. Carney JA, Sizemore GW, Sheps SG. Adrenal medullary disease in multiple endocrine neoplasia, type 2: pheochromocytoma and its precursors. Am J Clin Pathol 1976;66:279-290.
22. DeLellis RA, Wolfe HJ, Gagel RF, et al. Adrenal medullary hyperplasia. A morphometric analysis in patients with familial medullary thyroid carcinoma. Am J Pathol 1976;83:177-190.
23. Sipple JH. The association of pheochromocytoma with carcinoma of the thyroid gland. Am J Med 1961;31:163-165.
24. Horn RC Jr. Carcinoma of the thyroid: description of a distinctive morphological variant and report of seven cases. Cancer 1951;4:697-707.
25. Hazard JB, Hawk WA, Crile G Jr. Medullary (solid) carcinoma of the thyroid; a clinicopathological entity. J Clin Endocrinol Metab 1959;19:152-161.
26. Wolfe HJ, Melvin KE, Cervi-Skinner SJ, et al. C-cell hyperplasia preceding medullary thyroid carcinoma. N Engl J Med 1973;289:437-441.
27. Williams ED, Pollock DJ. Multiple mucosal neuromata with endocrine tumors: a syndrome allied to von Recklinghausen's disease. J Pathol Bacteriol 1966;91:71-77.
28. Steiner AL, Goodman AD, Powers SR. Study of a kindred with pheochromocytoma, medullary thyroid carcinoma, hyperparathyroidism and Cushing's disease: multiple endocrine neoplasia, type 2. Medicine (Baltimore) 1968;47:371-409.
29. Knudson AG Jr, Strong LC. Mutation and cancer: neuroblastoma and pheochromocytoma. Am J Hum Genet 1972;24:514-532.
30. Cerny JC, Jackson CE, Talpos GB, Yott JB, Lee MW. Pheochromocytoma in multiple endocrine neoplasia type II: an example of the two-hit theory of neoplasia. Surgery 1982;92:849-852.
31. Baylin SB. The multiple endocrine neoplasm syndromes: implications for the study of inherited tumors. Semin Oncol 1978;5:35-45.
32. Keiser HR, Beaven MA, Doppman J, Wells S Jr, Buja LM. Sipple's syndrome: medullary thyroid carcinoma, pheochromocytoma, and parathyroid disease. Studies in a large family. NIH conference. Ann Int Med 1973;78:561-579.
33. Brandi ML, Aurbach GD, Fitzpatrick LA, et al. Parathyroid mitogenic activity in plasma from patients with familial multiple endocrine neoplasia type I. N. Engl J Med 1986;314:1287-1293.
34. Carney JA. Familial multiple endocrine neoplasia: the first 100 years. Am J Surg Pathol 2005;29:254-274.
35. Khairi MR, Dexter RN, Burzynski NJ, Johnston CC Jr. Mucosal neuroma, pheochromocytoma and medullary thyroid carcinoma: multiple endocrine neoplasia type 3. Medicine (Baltimore) 1975;54:89-112.

36. Padberg BC, Garbe E, Achilles E, Dralle H, Bressel M, Schröder S. Adrenomedullary hyperplasia and pheochromocytoma. DNA cytophotometric findings in 47 cases. Virchows Arch A Pathol Anat Histopathol 1990;416:443-446.
37. Karsner HT. Tumors of the adrenal. Atlas of Tumor Pathology, 1st Series, Fascicle 29. Washington DC: Armed Forces Institute of Pathology; 1950.
38. Schimke RN. Multiple endocrine adenomatosis syndromes. Adv Intern Med 1976;21:249-265.
39. Gagel RF, Tashjian AH Jr, Cummings T, et al. The clinical outcome of prospective screening for multiple endocrine neoplasia type 2a. An 18-year experience. N Engl J Med 1988;318:478-484.
40. Valk TW, Frager MS, Gross MD, et al. Spectrum of pheochromocytoma in multiple endocrine neoplasia. A scintigraphic portrayal using 131I-metaiodobenzylguanidine. Ann Int Med 1981;94:762-767.

Proliferative Lesions of Adrenal Medulla in Rats

41. Tischler AS, DeLellis RA. The rat adrenal medulla: II. Proliferative lesions. J Am Coll Toxicol 1988;7: 23-44.
42. Tischler AS, DeLellis RA, Nunnemacher G, Wolfe HJ. Acute stimulation of chromaffin cell proliferation in the adult rat adrenal medulla. Lab Invest 1988;58:733-735.
43. Tischler AS, Ruzicka LA, Donahue SR, DeLellis RA. Chromaffin cell proliferation in the adult rat adrenal medulla. Int J Devl Neurosci 1989;7:439-448.
44. Warren S, Grozdev L, Gates O, Chute RN. Radiation-induced adrenal medullary tumors in the rat. Arch Pathol 1966;82:115-118.
45. Tischler AS, Powers JF, Pignatello M, Tsokas P, Downing JC, McClain RM. Vitamin D3-induced proliferative lesions in the rat adrenal medulla. Toxicol Sci 1999:51:9-18.
46. Partanen M, Chiveh CC, Rapaport SL. Age-related increase in catecholamine-containing paraganglia in male Fischer-344 rats. Anat Rec 1981;201:563-566.
47. Tischler AS, DeLellis RA, Perlman RL, et al. Spontaneous proliferative lesions of the adrenal medulla in aging Long-Evans rats: comparison to PC-12 cells, small granule-containing cells, and human adrenal medullary hyperplasia. Lab Invest 1985;53:486-498.
48. Tischler AS, Riseberg JC, Cherington V. Mitogenic signaling pathways in normal and neoplastic chromaffin cells. Mod Pathol 1994;7:58A.
49. Tischler AS, Powers JF, Alroy J. Animal models of pheochromocytoma. Histol Histopathol 2004; 19:883-895.

10 PHEOCHROMOCYTOMA

Pheochromocytoma is a paraganglioma arising from chromaffin cells of the adrenal medulla. Paragangliomas are named for their anatomic site of origin; adrenal medullary paraganglioma, however, is traditionally referred to as pheochromocytoma. The term pheochromocytoma is also used for extraadrenal paragangliomas of the sympathoadrenal neuroendocrine system, and given the great overlap in morphology, immunohistochemical profile, and ultrastructure, differentiation may be difficult.

INCIDENCE

Using population-based data, the average annual incidence of pheochromocytoma is estimated at 8 cases/million persons/year in the United States; this increased in the Mayo Clinic study to 9.5/million with the inclusion of two additional familial cases (1). In Sweden, the average annual incidence is 2.1 cases/million population (2), and in Denmark it is 1.9/million (3). In a review of population-based data from the SEER (Surveillance, Epidemiology, and End Results) registries of 1973 to 1987, the age-specific incidence of pheochromocytoma for any age group never exceeded 0.1/100,000 population (4).

Pheochromocytomas are uncommon neoplasms and are especially rare in children. Some have suggested that for every pheochromocytoma diagnosed during life, two are discovered incidentally at autopsy. In a review of 54 autopsy-proven cases of pheochromocytoma over a 50-year period at the Mayo Clinic, 24 percent had been diagnosed correctly during life while 76 percent had not been suspected clinically; 75 percent of patients in the latter group died suddenly from either myocardial infarction or cardiovascular catastrophe, with one third of the sudden deaths occurring during or immediately after an unrelated surgical procedure (5). These findings cast serious doubt on the theory that most tumors are "nonfunctional." Heightened clinical awareness and the availability of more sophisticated diagnostic, biochemical, and imaging procedures may lead to more accurate diagnosis during life. Given its relatively high prevalence in autopsy series, pheochromocytoma may be underdiagnosed and the actual annual incidence may be higher than reported (6). In a recent study, pheochromocytomas accounted for about 6 percent of all primary adrenal tumors (7).

AGE, SEX DISTRIBUTION, AND LATERALITY

The peak age at diagnosis is in the fifth decade of life, but pheochromocytomas can affect any age group (8). Most series report a roughly equal sex incidence, but some show a slight predilection for either males or females. In some of the larger studies, the right adrenal gland is involved slightly more often that the left, perhaps reflecting the slightly greater amount of chromaffin tissue that has been reported on that side (8).

Pheochromocytomas have been dubbed the "ten percent tumor": 10 percent bilateral, 10 percent extraadrenal, 10 percent malignant, and about 10 percent occurring in childhood (8). These figures are only an approximation and must be correlated with variables such as proportion of familial cases in any particular series, location of tumor, and age group studied. Others estimate that approximately 15 percent are malignant, 18 percent extraadrenal, and 20 percent familial (9). In a sporadic setting, about 95 percent of pheochromocytomas are solitary, 5 percent are bilateral, and 5 to 10 percent are extraadrenal (Table 10-1) (8). In the familial setting, about 50 percent of tumors are bilateral, and patients tend to be diagnosed at an earlier age. In the pediatric age group there is an increased incidence of bilateral pheochromocytomas as well as multicentric and extraadrenal tumors (10).

PATTERNS OF CATECHOLAMINE SECRETION

The clinical signs and symptoms of patients with pheochromocytoma vary considerably (Table 10-2), but the triad that is most diagnostic is paroxysmal hypertension, headaches, and diaphoresis (11) reflecting an often adrenergic phenotype. Manifestations can mimic many diseases and lead to erroneous diagnoses (9). Norepinephrine-secreting tumors are usually associated with sustained hypertension, while tumors secreting relatively large quantities of epinephrine along with norepinephrine are associated with paroxysmal or episodic hypertension (12). Pure epinephrine-secreting tumors may cause hypotension (12), and may require precise measurement of epinephrine excretion, particularly in patients with multiple endocrine neoplasia (MEN) syndrome type 2. In some normotensive patients, the tumor (which is most often extraadrenal) secretes mainly dopamine, presumably due to decreased activity of dopamine beta-hydroxylase (8,13), and this profile may be associated with malignancy. Extraadrenal paragangliomas usually have a noradrenergic phenotype.

The non-neoplastic adrenal medulla is able to take up ^{131}I-metaiodobenzylguanidine (^{131}I-MIBG) in the presence of a pheochromocytoma with excess catecholamine secretion (8). On rare occasion, spontaneous retroperitoneal hemorrhage by pheochromocytoma occurs (8), and may be accompanied by signs and symptoms of hypercatecholaminemia (see fig. 10-10).

Table 10-1

INCIDENCE OF SOLITARY AND BILATERAL PHEOCHROMOCYTOMAS AND EXTRAADRENAL PARAGANGLIOMAS[a]

	Solitary Adrenal	Bilateral Adrenal	Extra-adrenal
Sporadic (90% of total)	95%	5%	5-10%
Familial (5-10% of total)	<50%	>50%	<10%
Childhood (5-10% of total)	50%	20-25%	15-20%

[a]Table 10-1 from Fascicle 19, Third Series.

PREOPERATIVE LOCALIZATION AND IMAGING CHARACTERISTICS

Preoperative localization of pheochromocytoma and extraadrenal paraganglioma can be accomplished with high resolution computerized tomography (CT) (fig. 10-1) or magnetic resonance imaging (MRI). These have almost eliminated the need for selective arteriography except

Table 10-2

SIGNS AND SYMPTOMS OF PHEOCHROMOCYTOMA[a]

Signs	Frequency	Symptoms	Frequency
Hypertension	76-100%	Headaches	76-100%
Tachycardia or reflex bradycardia	51-75%	Palpitations	51-75%
Postural hypotension	51-75%	Sweating	51-75%
Paroxysmal hypertension	26-50%	Anxiety/nervousness	26-50%
Weight loss	26-50%	Tremulousness	26-50%
Pallor	26-50%	Nausea/emesis	26-50%
Hypermetabolism	26-50%	Pain in chest/abdomen	26-50%
Fasting hyperglycemia	26-50%	Weakness/fatigue	26-50%
Tremor	26-50%	Dizziness	1-25%
Increased respiratory rate	26-50%	Heat intolerance	1-25%
Decreased gastrointestinal motility	26-50%	Paresthesias	1-25%
Psychosis (rare)	1-25%	Constipation	1-25%
Flushing, paroxysmal (rare)	1-25%		

[a]Table 5-1 from Keiser HR, Doppman JL, Robertson CN, Linehan WM, Averbuch SD. Diagnosis, localization, and management of pheochromocytoma. In: Lack EE, ed. Pathology of the adrenal glands. New York: Churchill Livingstone; 1990:237-255. Data from references 1, 5, 16.

in rare instances where it is necessary to delineate the blood supply to the tumor; in those unusual cases it should be done only in patients who are adequately treated with adrenergic blockade to prevent a hypertensive crisis (11).

On CT scan the tumor is usually greater than 3 cm in diameter and has a homogeneous soft tissue density. Necrosis may be present and larger tumors may have a central low density on scan. Contrast enhancement may show heterogeneity better. Sometimes calcifications are seen. On MRI, pheochromocytomas (and other extra-adrenal paragangliomas) tend to show a very high signal intensity on T2-weighted images (fig. 10-2), which is isointense compared to liver on T1-weighted images. Adrenal cortical carcinomas tend to have an intermediate signal intensity and adrenal cortical adenomas a low intensity (11). The imaging on MRI may be nonspecific if hemorrhage occurs within the tumor.

Pheochromocytomas have been likened to an imaging chameleon due to the variety of imaging characteristics, some of which can be misleading (14). Functional imaging using ^{131}I- and ^{123}I-MIBG depends upon uptake of a radiolabeled analogue of guanethidine (fig. 10-3) within the intracellular storage granules (15), but a wide range of neuroendocrine tumors, such as neuroblastoma, medullary thyroid carcinoma, and carcinoid tumors are also localized with this technique. The specificity and sensitivity of ^{131}I- and ^{123}I-MIBG in the localization of pheochromocytomas are reported as 81 percent and 90 percent, respectively (9). Uptake of ^{131}I-MIBG does not appear to correlate with catecholamine secretion as measured in plasma or urine (15,16), but a direct proportional

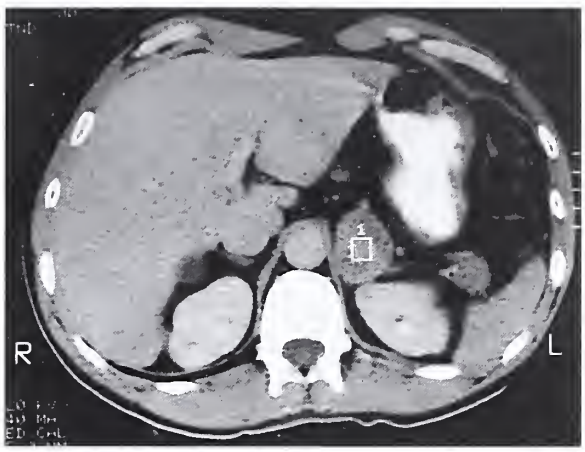

Figure 10-1

PHEOCHROMOCYTOMA

A pheochromocytoma in the left adrenal gland of an adult is well demonstrated by computerized tomography (CT) scan of the abdomen. (Fig. 10-1 from Fascicle 19, Third Series.)

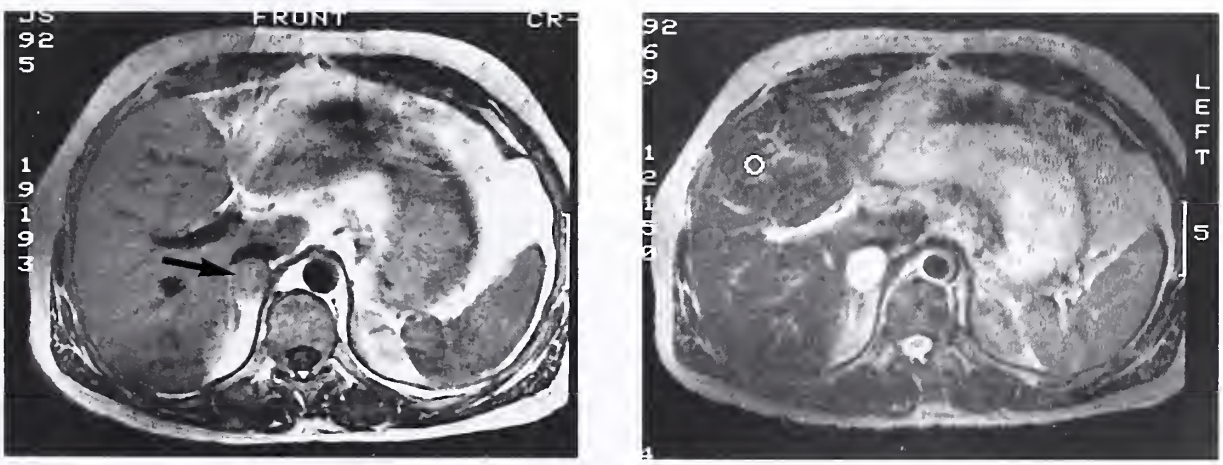

Figure 10-2

PHEOCHROMOCYTOMA

Left: T1-weighted magnetic resonance image (MRI) of the abdomen of a 38-year-old man shows a rounded pheochromocytoma on the right side (arrow) with a low signal intensity. (L&R: Fig. 10-2 from Fascicle 19, Third Series.)

Right: Tumor shows a bright signal on T2-weighted image. The study was prompted by a hypertensive episode during laparoscopic cholecystectomy. The patient was also noted to have "cardiomyopathy" with atrial fibrillation.

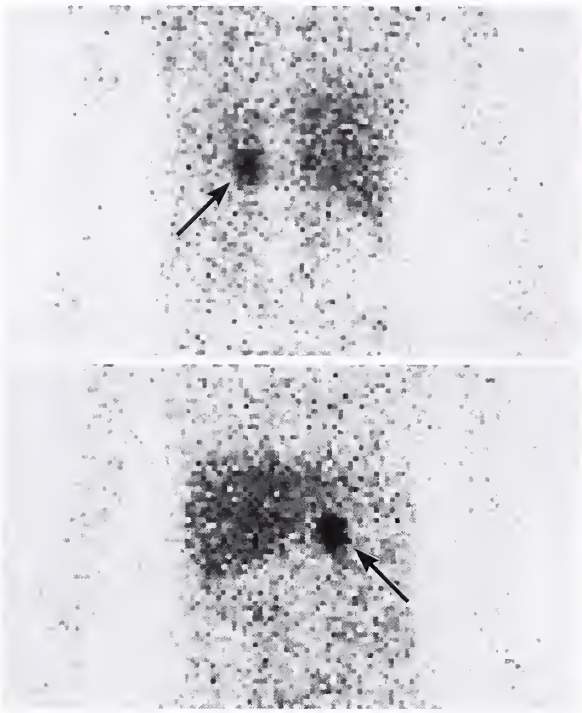

Figure 10-3

PHEOCHROMOCYTOMA

Pheochromocytoma (arrows) of the left adrenal gland is visualized scintigraphically using ^{131}I-metaiodobenzylguanidine. (Fig. 10-3 from Fascicle 19, Third Series.)

correlation has been reported between the percentage of uptake by the tumor and the number of neurosecretory type granules (16). Positron emission tomography (PET) has also been useful in imaging pheochromocytomas using specific ligands such as [8-F]-dopamine (17) and 11C-hydroxyephedrine (18).

SPORADIC PHEOCHROMOCYTOMA

Gross Findings

Pheochromocytoma in the sporadic or nonfamilial setting typically presents as a solitary, rounded, unicentric mass that distorts the adrenal gland, which is usually apparent as an attached remnant (fig. 10-4, top) or splayed over the surface of the tumor (fig. 10-4, bottom). Identification of an adrenal remnant may be difficult with extremely large tumors. Most pheochromocytomas measure 3 to 5 cm in diameter (8), but there is a wide range of from 1 to 10 cm or more. The average weight of pheochromocytomas in several large series (most classified as benign) was 73 g (19), 90 g (20), 113 g (21), and 156.5 g (22); clinically malignant tumors tend to be heavier than benign pheochromocytomas

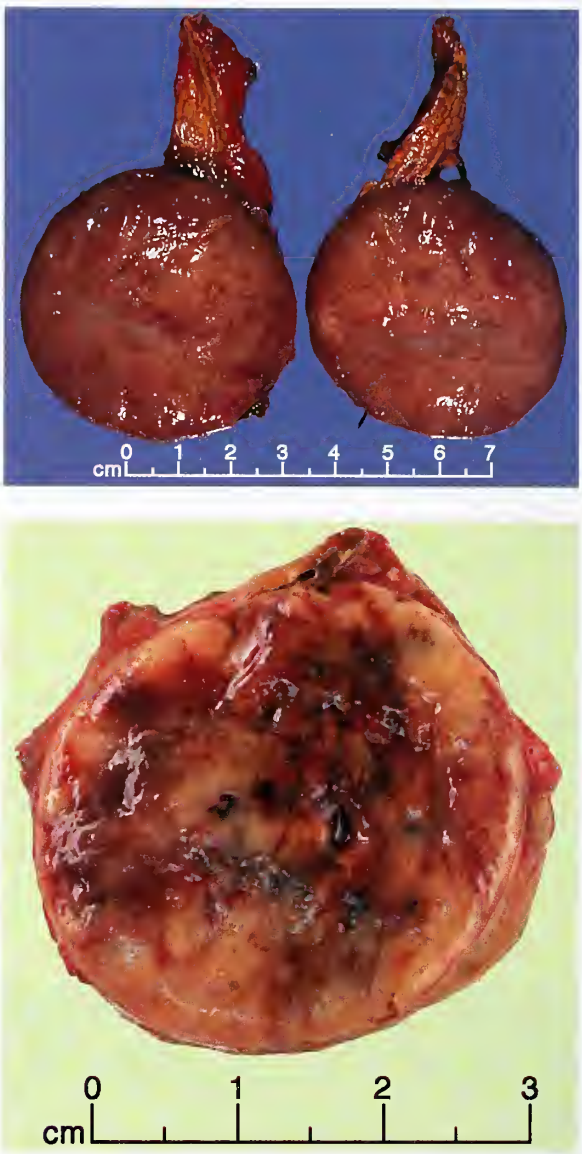

Figure 10-4

PHEOCHROMOCYTOMA

Top: The pheochromocytoma is well-circumscribed and has a bulging tan-brown surface on cross section. An adrenal remnant is attached.

Bottom: The pheochromocytoma in a different case measures about 3 cm in diameter. On cross section, it is glistening tan-white, with irregular mottled areas of congestion. There was a strong chromaffin reaction after immersion of fresh tumor in Zenker's fixative (see figure 10-34). (T&B: Fig. 10-4 from Fascicle 19, Third Series.)

(average 176 g [21], 383 g [19], and 759 g [22]). Given the greater concentration of chromaffin tissue in the head and body of the gland, one would expect most pheochromocytomas to arise in these regions, but in most cases this is impossible to determine with certainty (23).

On cross section, the tumor is usually sharply circumscribed and may even appear encapsulated, but close inspection may reveal a fibrous pseudocapsule or expansion of the adrenal capsule itself. Pheochromocytomas are usually resiliently firm and gray-white, similar to the texture and color of the normal adrenal medulla, but there may be areas of mottled to confluent congestion (fig. 10-5), or even frank hemorrhage within the tumor, sometimes extending out into surrounding adipose tissue. In extreme examples, the tumor grossly resembles a hematoma. Careful inspection of the cut surface of the tumor may reveal punctuate or curvilinear foci, often retracted slightly beneath the surface, which represent vascular structures of various sizes (fig. 10-6).

Central degenerative changes can be seen, particularly in larger tumors, and may appear as zones of remote necrosis, fibrosis, or cystic change (fig. 10-7). The cystic degeneration may appear as nonhomogeneous areas on CT scan (fig. 10-8, top) or ultrasound (fig. 10-8, bottom). Extreme examples of cystic degeneration are unusual and in such cases it may be difficult to identify remnants of the tumor (fig. 10-9). The cyst contents range from thin, blood-tinged fluid to more grumous, red-brown material. Occasionally, a pheochromocytoma may have

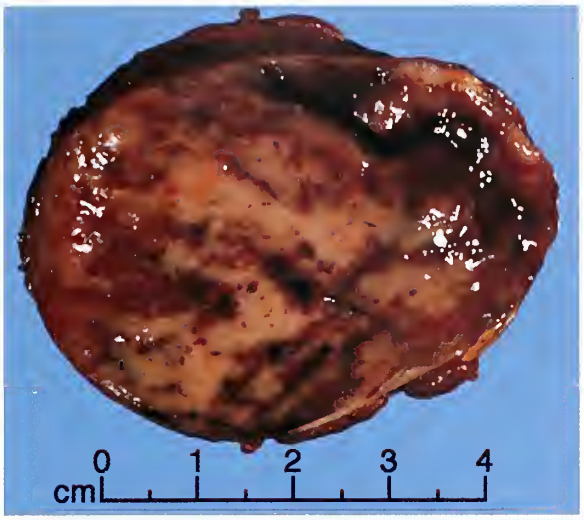

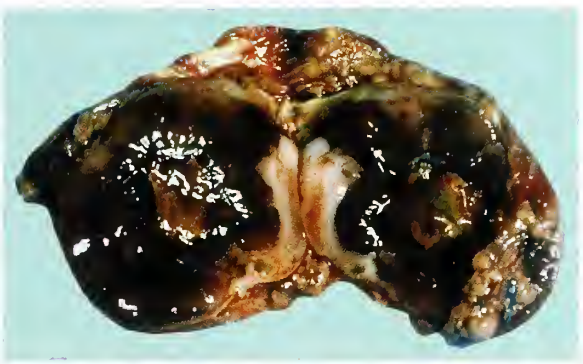

Figure 10-5

PHEOCHROMOCYTOMA

Top: In cross section, this pheochromocytoma shows mottled to confluent areas of hemorrhage. (Fig. 10-5, left from Fascicle 19, Third Series.)

Bottom: A pheochromocytoma from a different patient has a central area of necrosis with surrounding hemorrhage.

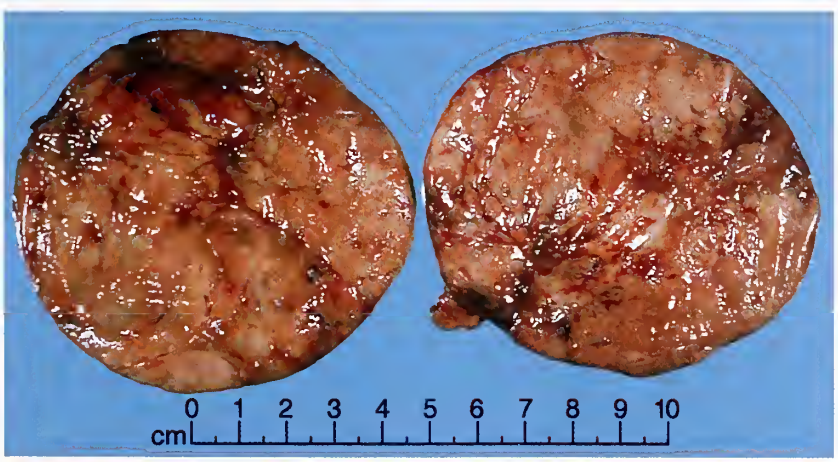

Figure 10-6

PHEOCHROMOCYTOMA

On cross section, the tumor is gray-white to tan, with a finely nodular cut surface due to vascular channels cut in various planes with slight retraction beneath the surface. (Fig. 10-6 from Fascicle 19, Third Series.)

Figure 10-7

PHEOCHROMOCYTOMA

A large central area of degenerative change with fibrosis, edema, and cystic change is seen in a bisected pheochromocytoma. (Fig. 10-7 from Fascicle 19, Third Series.)

areas of dystrophic calcification which may be detected on plain films of the abdomen (23).

Pheochromocytomas can adhere to adjacent structures such as kidney or liver, and frank invasion of adjacent organs or tissues may be an indication of malignancy (8,23). They occasionally extend into the inferior vena cava and even into the right atrium (24); in one case the tumor caused symptoms of recurrent pulmonary emboli (25). The tumor can theoretically gain access to tributaries of the central adrenal vein through discontinuities in the medial smooth muscle (see chapter 1) and cause hemorrhage and infarction (fig. 10-10). Intracaval extension is not necessarily a bad prognostic finding, but may be associated with local recurrence.

Microscopic Findings

Architectural Patterns. Pheochromocytomas usually have a limited array of architectural patterns; one may predominate in a particular tumor or there may be an admixture of patterns in the same neoplasm (8,23). The architectural patterns observed in 98 sympathoadrenal paragangliomas (mostly pheochromocytomas) included a mixture of alveolar and trabecular patterns (36 percent), a predominantly alveolar (nesting or "zellballen") pattern (35 percent) (fig. 10-11), and a predominantly trabecular arrangement of cells (27 percent) (fig. 10-12) (19). A stain for reticulum can accentuate the alveolar (fig. 10-11, right) or anastomosing trabecular patterns (fig. 10-12, right). A spindle cell

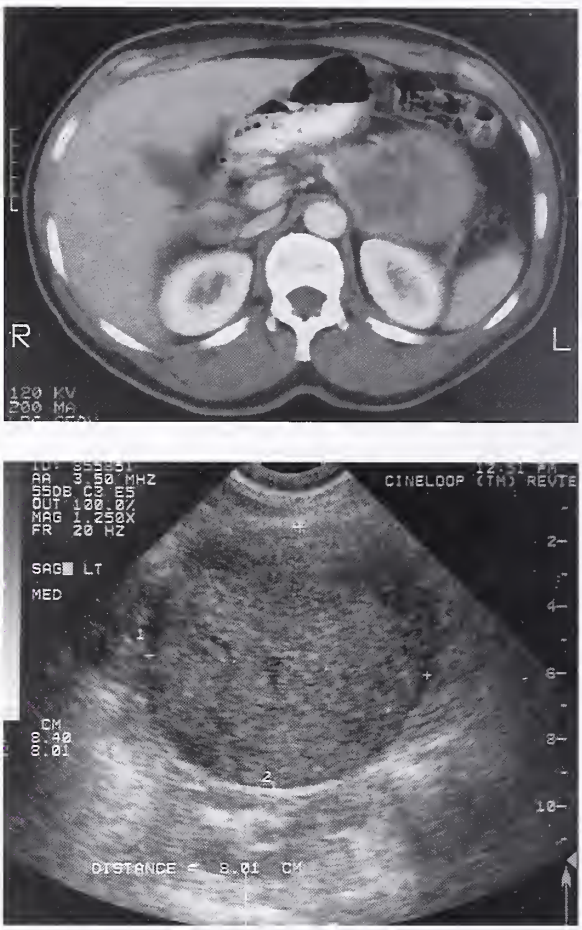

Figure 10-8

PHEOCHROMOCYTOMA

Top: A large pheochromocytoma is apparent on the left side in an abdominal CT scan of a 55-year-old man who presented with flank pain. The tumor is nonhomogeneous after intravenous and gastrointestinal contrast enhancement.

Bottom: Ultrasonograph in same case shows a sharply demarcated mass that is roughly spherical (8.01 x 8.40 cm). (T&B: Fig. 10-8 from Fascicle 19, Third Series.)

pattern has been reported in about 2 percent of tumors (19,21), but it is usually not prominent throughout the tumor. In areas with a spindle cell pattern, the tumor cells have a rounded to ovoid nucleus, or a nucleus elongated in the long axis of the cell (fig. 10-13). Nests of tumor cells may vary considerably in size and shape, and occasional central degenerative change or necrosis is seen (fig. 10-14). Some pheochromocytomas have areas in which the growth pattern is more solid or diffuse (fig. 10-15).

Figure 10-9

PHEOCHROMOCYTOMA

Below: The inner aspect of the markedly cystic pheochromocytoma has a smooth to shaggy appearance. The tumor contained amber, blood-tinged fluid and amorphous soft material. (Fig. 10-9, left from Fascicle 19, Third Series.)

Right: In a different cystic pheochromocytoma, representative sections of the adrenal wall show residual pheochromocytoma. Note the fibrosis with fibrinous matter on the inner aspect of the cyst. The adrenal capsule is at the top.

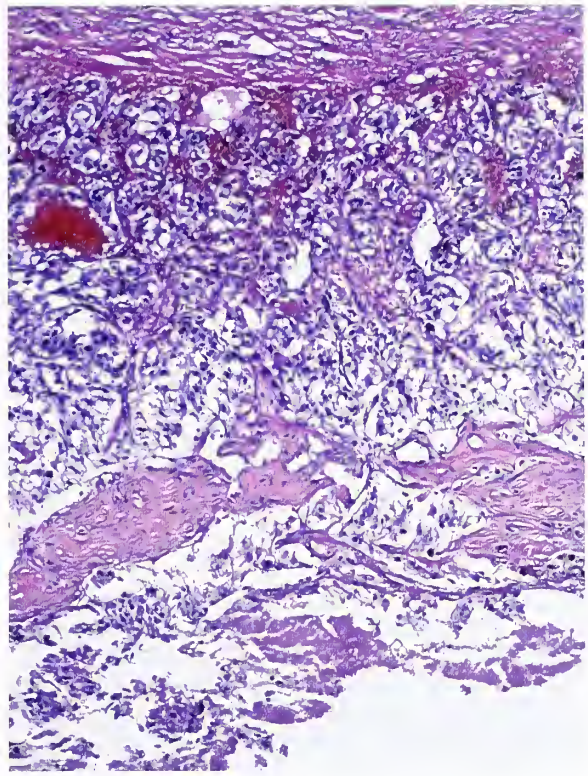

Sections from the periphery of the tumor may reveal a junction between the pheochromocytoma and residual cortex, which is curvilinear or sinuous in contour without any evidence of an intervening fibrous capsule (fig. 10-16, left). Careful examination of these areas may reveal an intermingling of non-neoplastic cortical cells among the tumor cells (fig. 10-16, right). In some tumors, the cytoarchitectural features are similar to those of the adjacent non-neoplastic cortex (fig. 10-17, left) or even the residual adrenal medulla (fig. 10-17, right). Occasionally, the similarity in morphology between pheochromocytomas and adrenal cortical neoplasms can result in misdiagnosis in routine sections. A tumor may also undergo what appears to be spontaneous hemorrhagic necrosis that extensively disrupts the architecture of much of the tumor, making accurate diagnosis difficult without the aid of ancillary stains (fig. 10-18).

Cellular Morphology. The cytoplasm of pheochromocytoma cells is often lightly eosinophilic and finely granular, but it is sometimes amphophilic to basophilic or even lavender in hue with a myriad of minute punctate granules that can barely be seen by light microscopy (fig. 10-19). Tumor cells may be polygonal with sharply defined cell borders, or the cells may interdigitate with indistinct cytoplasmic outlines. Some cells contain large vacuoles which resemble the "pseudoacini" seen in some carotid body type paragangliomas; in many instances this feature does not appear to be an artifact of fixation or processing (fig. 10-20). A potentially confusing picture has been ascribed to lipid degeneration (26), in which the tumor can mimic an adrenal cortical neoplasm with abundant intracytoplasmic lipid (fig. 10-21). Some tumor cells contain such abundant and densely eosinophilic cytoplasm that the tumor has oncocytic features (fig. 10-22). Variation in staining intensity, sometimes in routinely stained sections, gives the impression of a dimorphic population of "light" and "dark" types of cells but this has no known significance. Occasionally, some tumor cells partially envelop other cells ("cell embracing") (fig. 10-23).

The nuclei of some cells contain one or more "pseudoinclusions," which usually appear as a solitary, round to oval structure of variable size having the same tinctorial staining as the remaining cytoplasm (fig. 10-24). These represent

Figure 10-10

PHEOCHROMOCYTOMA

A: Pheochromocytoma from a 32-year-old man shows confluent areas of hemorrhage and necrosis. The hemorrhage extends into the periadrenal adipose tissue. The patient presented with headaches, abdominal pain, and hypertensive crisis. He later underwent total thyroidectomy for medullary thyroid carcinoma. The patient and related family members were undergoing evaluation for multiple endocrine neoplasia (MEN) syndrome type 2.

B: Intravascular protrusion by the pheochromocytoma is associated with a fresh thrombus. A portion of the wall of the central adrenal vein is present.

C: An intact layer of endothelium is over the protruded tumor and portions of the muscular wall of the central adrenal vein are on either side. Intravascular growth of this type may be related to discontinuities in the medial smooth muscle of the tributaries of the central adrenal vein. The patient was alive and well 10 years later. (A–C: Fig. 10-10 from Fascicle 19, Third Series.)

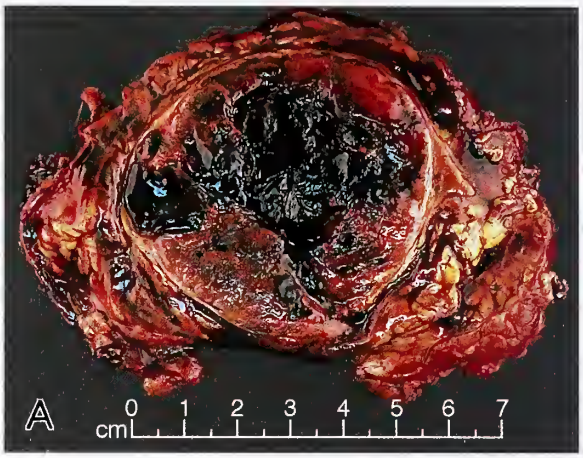

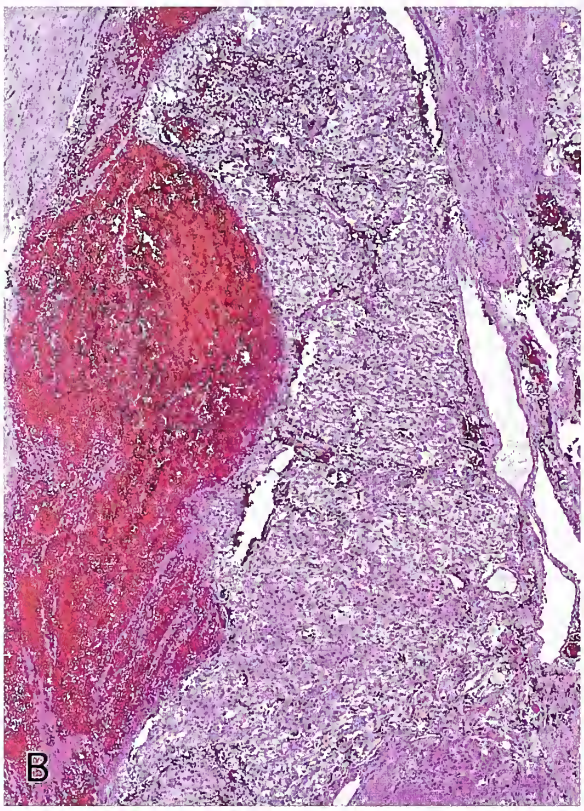

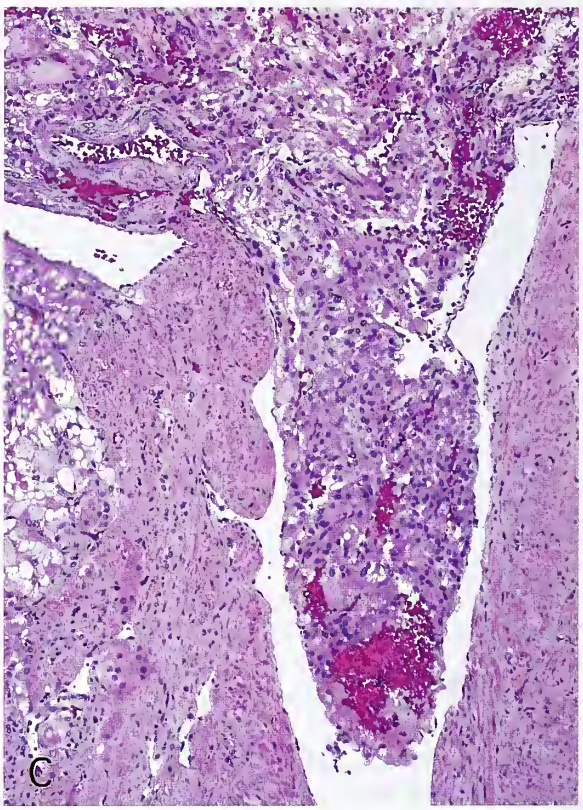

irregular folds or indentations of the nuclear membrane with invagination of cell cytoplasm. Nuclear pseudoinclusions may be central or eccentric when viewed en face, with a smooth or occasionally notched border. There may be a difference in density of cellular organelles within the pseudoinclusion, resulting in variation in staining intensity, and sometimes there are one or more vacuoles. Rarely, there is more than one pseudoinclusion, and in some areas with excessive nuclear folding, the process may be viewed in profile.

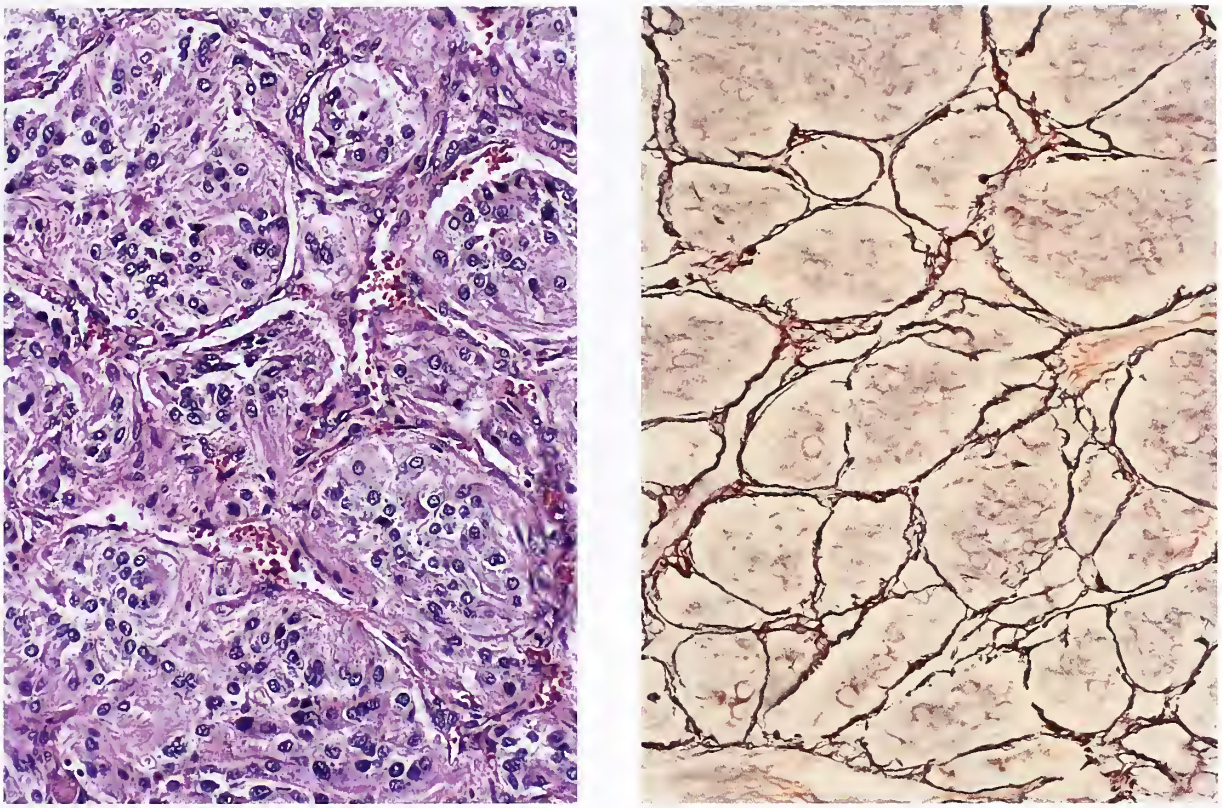

Figure 10-11

PHEOCHROMOCYTOMA

Left: Pheochromocytoma with an alveolar or nesting arrangement of tumor cells. (Fig. 10-11 from Fascicle 19, Third Series.) Right: Reticulum stain clearly accentuates the alveolar pattern and shows distinct nests of cells ("zellballen").

There may be intracytoplasmic hyaline globules which are periodic acid–Schiff (PAS) positive and resistant to diastase predigestion; these globules are identical to those observed in the normal (27) and hyperplastic adrenal medulla. The globules may be numerous (fig. 10-25) or few and very difficult to identify on casual inspection. In one study, globules were detected in 38 of 64 clinically benign and 8 of 34 malignant sympathoadrenal paragangliomas (19). They have been related to secretory activity in some way, but their functional significance is not clear. It is important to remember that intracytoplasmic hyaline globules have also been reported in about 10 percent of adrenal cortical neoplasms, both benign and malignant (28).

Some pheochromocytomas contain cells with moderate to marked nuclear enlargement and hyperchromasia (fig. 10-26, left), and occasionally this nuclear pleomorphism can be a spectacular histologic feature. In several studies, nuclear atypia or pleomorphism has not been shown to have a significant impact on prognosis. Occasional mitotic figures are identified in tumors that prove to be clinically benign (fig. 10-26, right). In the study by Linnoila et al. (19), an average of 1 mitosis per 30 high-power fields was found in clinically benign sympathoadrenal paragangliomas.

Occasionally, cells within an otherwise typical pheochromocytoma have cytologic features resembling neuronal or ganglion cells, with tapering cell processes, eccentric nucleus with nucleolus, and even granular basophilic material at the edge of the cell resembling Nissl substance (fig. 10-27). These and other neural features may be seen in tumors classified as *composite pheochromocytomas*.

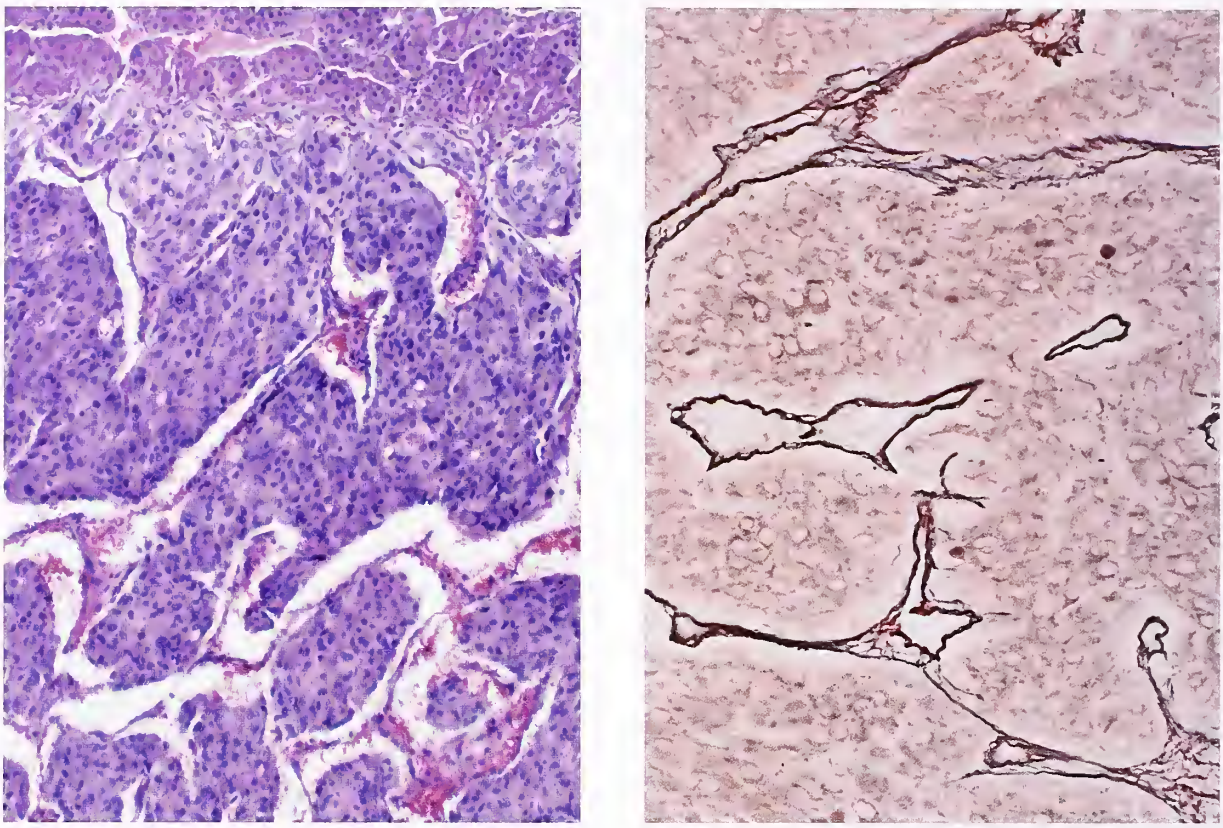

Figure 10-12

PHEOCHROMOCYTOMA

Left: Pheochromocytoma with an anastomosing trabecular pattern. The tumor abuts directly on the adrenal cortex at the top without encapsulation.

Right: Reticulum stain demonstrates the interconnecting or anastomosing trabecular pattern.

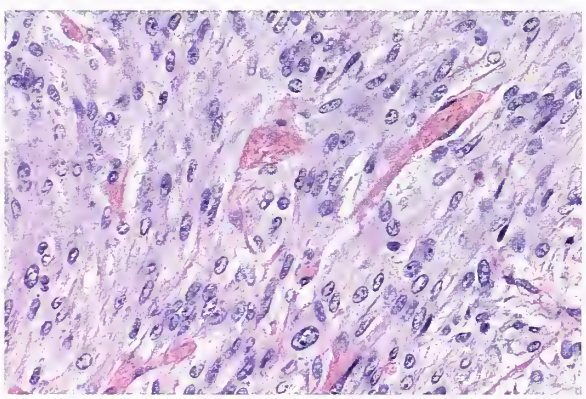

Figure 10-13

PHEOCHROMOCYTOMA

Pheochromocytoma focally has a spindle cell pattern, with elongated tumor cells oriented along the long axis of interconnecting trabeculae. Many tumor cells have nuclei that are elongated in the same axis.

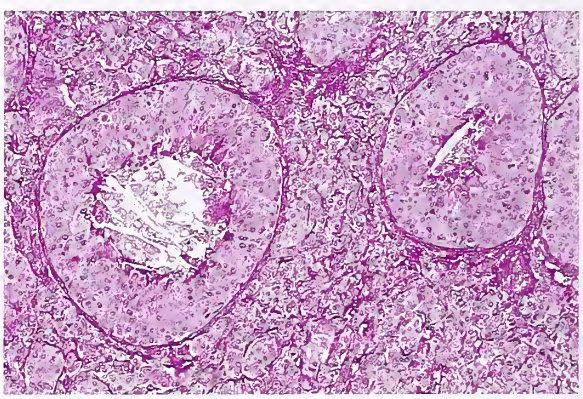

Figure 10-14

PHEOCHROMOCYTOMA

A clinically benign pheochromocytoma has focally enlarged nests of tumor cells with central degenerative change. (Fig. 10-15 from Fascicle 19, Third Series.)

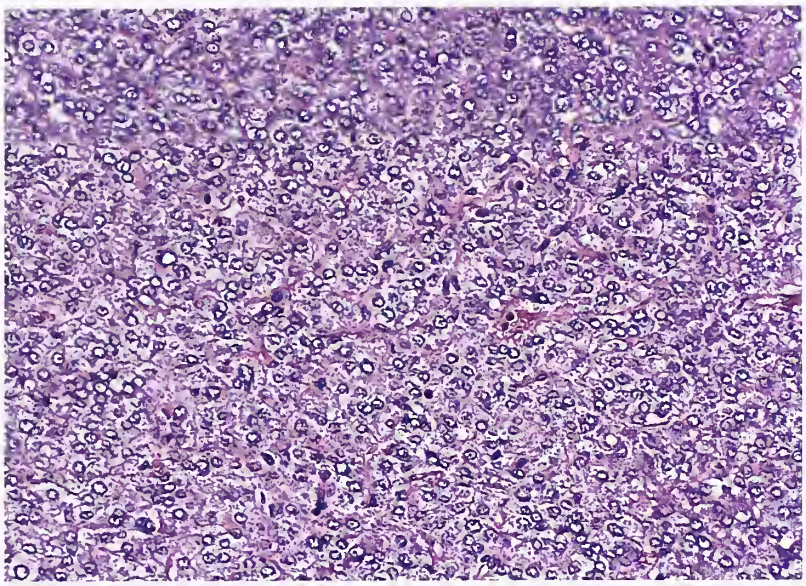

Figure 10-15

PHEOCHROMOCYTOMA

This pheochromocytoma has a more solid or diffuse growth pattern. (Fig. 10-16 from Fascicle 19, Third Series.)

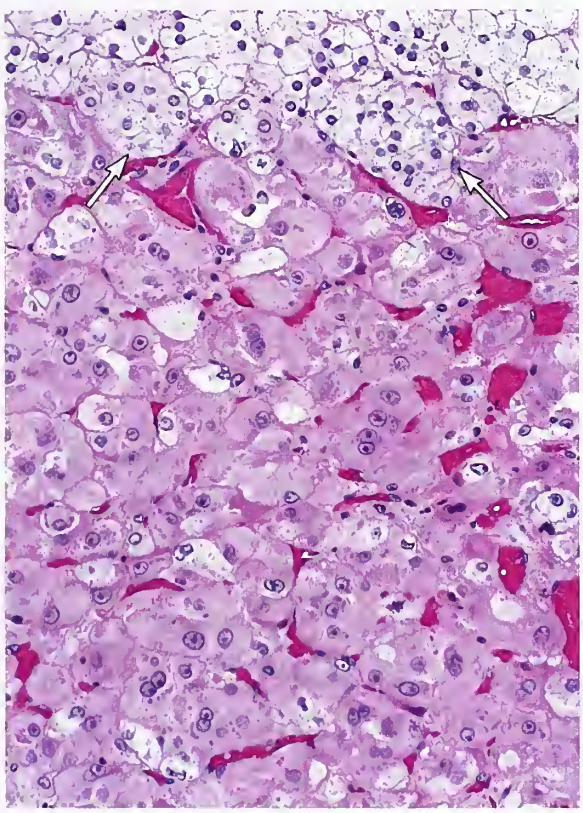

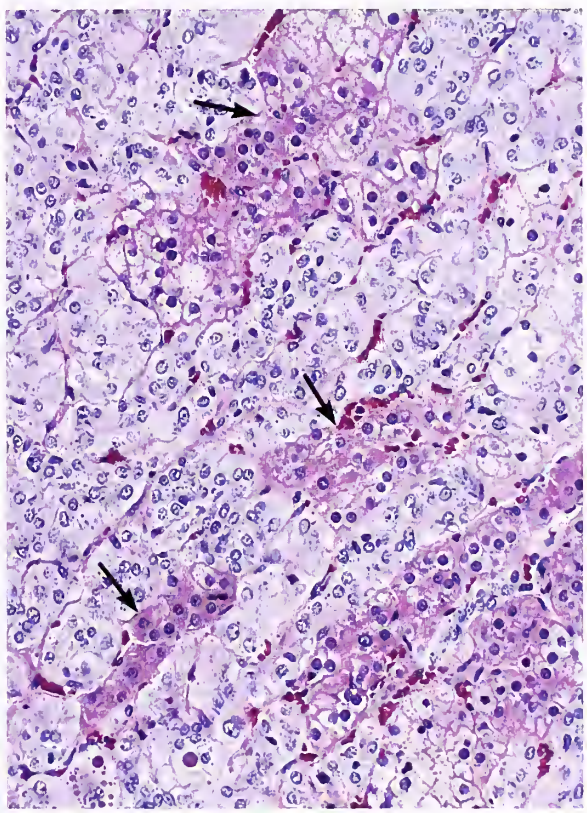

Figure 10-16

PHEOCHROMOCYTOMA

Left: The junction between the pheochromocytoma and the adjacent adrenal cortex (white arrows) is seen. There is no evidence of encapsulation.

Right: A different pheochromocytoma has a pushing border adjacent to the cortex, without evidence of encapsulation. Cortical cells intermingle within the tumor (arrows). (L&R: Fig. 10-17 from Fascicle 19, Third Series.)

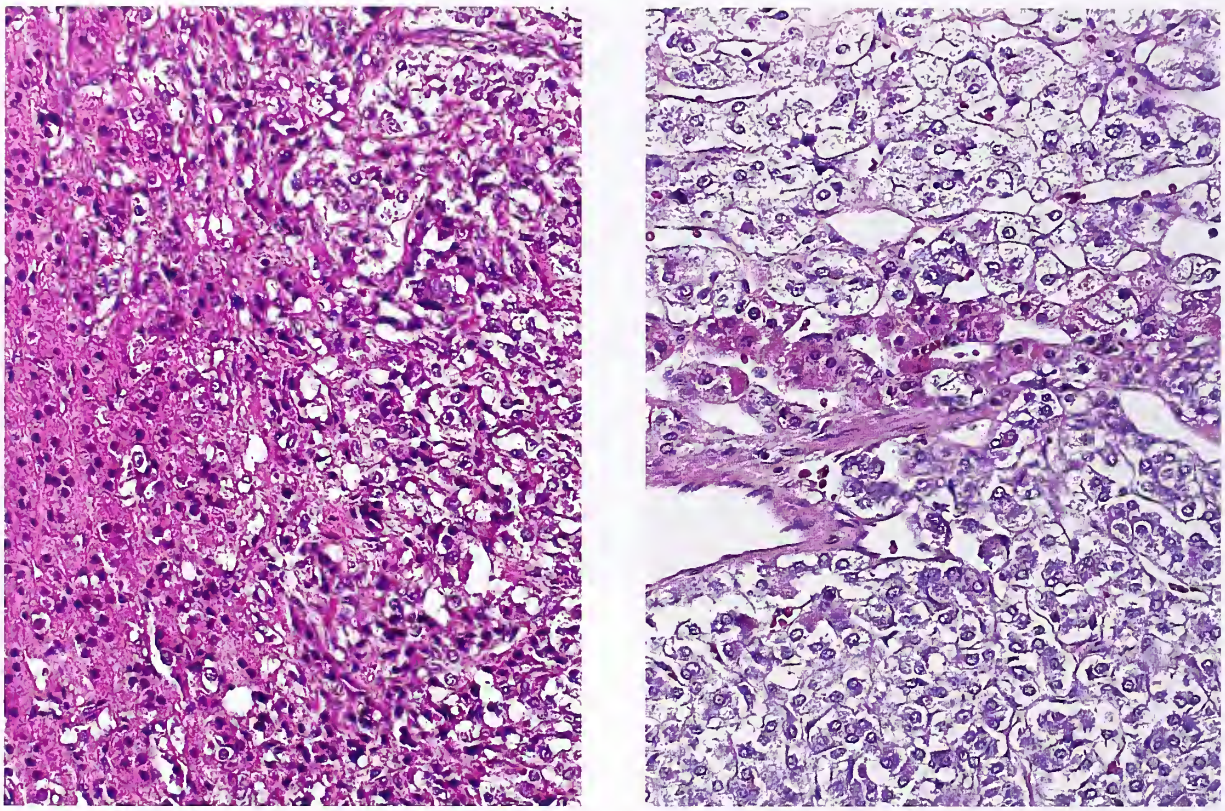

Figure 10-17

PHEOCHROMOCYTOMA

Left: Cells of pheochromocytoma (right of field) and cortex (left of field) have a similar appearance. On rare occasion it may be difficult to distinguish adrenal cortical and medullary neoplasms in routinely stained sections.

Right: Pheochromocytoma in lower half of field resembles the non-neoplastic adrenal medulla at top. A thin zone of residual adrenal cortex is present near the center. (L&R: Fig. 10-18 from Fascicle 19, Third Series.)

The cytoplasm of pheochromocytoma cells (and other paraganglioma cells) is typically argyrophilic with abundant pinpoint granules (fig. 10-28), but with the availability of immunohistochemistry, argyrophilic staining methods (e.g., Grimelius stain) are seldom necessary. Melanin-like pigment has been reported in pheochromocytomas (29); ultrastructurally, melanosomes and premelanosomes were found, but alternative interpretations for this pigment include neuromelanin, lipofuscin, or products related to catecholamine oxidation (29). A grossly pigmented "black" pheochromocytoma was recently reported (30) and is remarkably similar to the pigmented extraadrenal paraganglioma illustrated in chapter 11 (fig. 11-17). The pigment in both cases is most consistent with neuromelanin: argentaffin positive with the Fontana-Masson stain and labile to bleaching procedures using permanganate or picric acid (29). Pigmented pheochromocytomas are rare tumors and common embryogenesis along with melanocytes from the neural crest should not negate the possibility of a shared morphologic phenotype.

Stromal Alterations. Some pheochromocytomas exhibit remarkable alterations in connective tissue stroma, and this may cause problems in diagnosis. Areas of sclerosis may be prominent (fig. 10-29), sometimes in association with cystic degeneration. At times, the sclerosis can have a sinusoidal distribution with accentuation of the alveolar or trabecular pattern of tumor cells. In some tumors the fibrosis can severely distort the architectural arrangement of tumor cells (fig. 10-30).

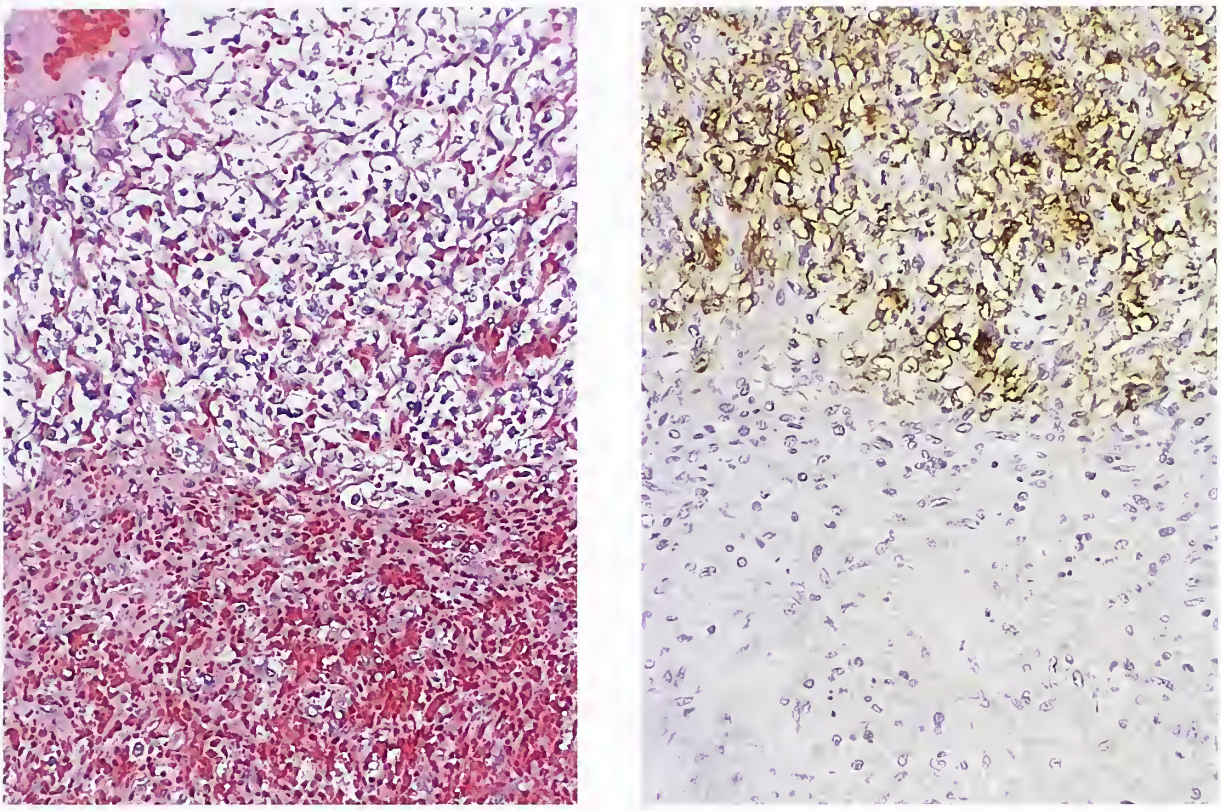

Figure 10-18

PHEOCHROMOCYTOMA

Left: A pheochromocytoma with extensive "spontaneous" hemorrhage and necrosis. Much of the tumor had areas of granulation tissue with organization. Viable tumor is present at top of field. Grossly, the tumor simulated a hematoma.

Right: Residual tumor is strongly immunoreactive for chromogranin A. An area of organizing granulation tissue is in the lower half of the field (avidin-biotin peroxidase method). (L&R: Fig. 10-19 from Fascicle 19, Third Series.)

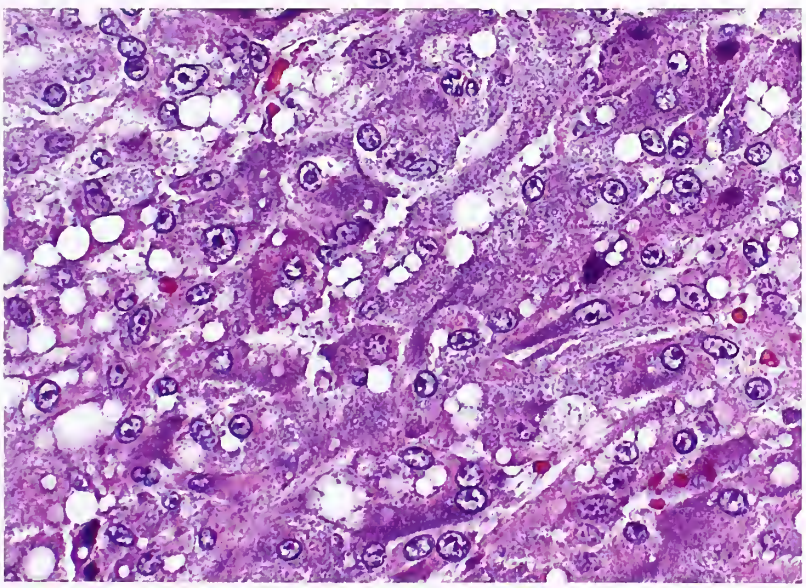

Figure 10-19

PHEOCHROMOCYTOMA

The tumor cells have indistinct cell borders and contain numerous small pinpoint granules. When the granules are numerous, the cytoplasm may acquire a lavender tint. (Fig. 10-20 from Fascicle 19, Third Series.)

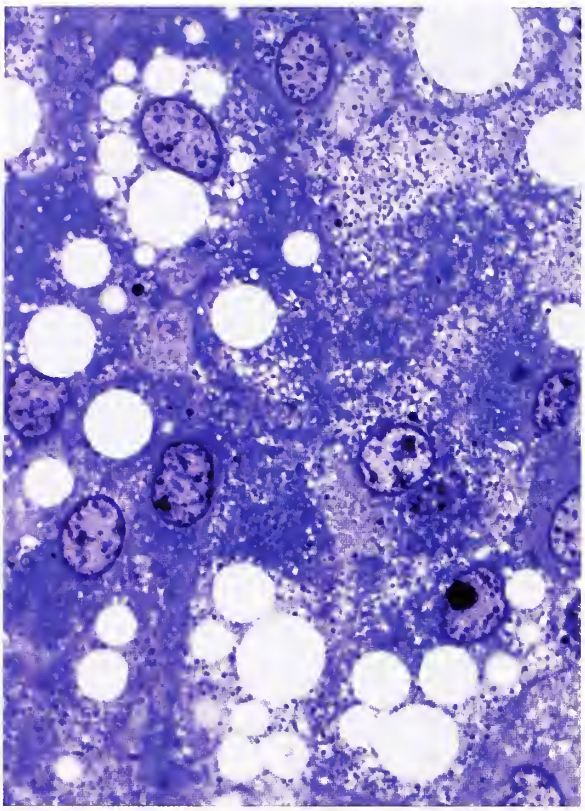

Figure 10-20

PHEOCHROMOCYTOMA

The tumor cells have numerous vacuolar spaces within the cytoplasm (so-called pseudoacini). There are punctate blue-black granules of variable density, most of which were dense-core neurosecretory granules when assessed ultrastructurally. Some cells vary in overall staining of the cytoplasm, giving the impression of "light" and "dark" cells. The specimen was obtained fresh and electron microscopy showed that it was well preserved (toluidine blue stain).

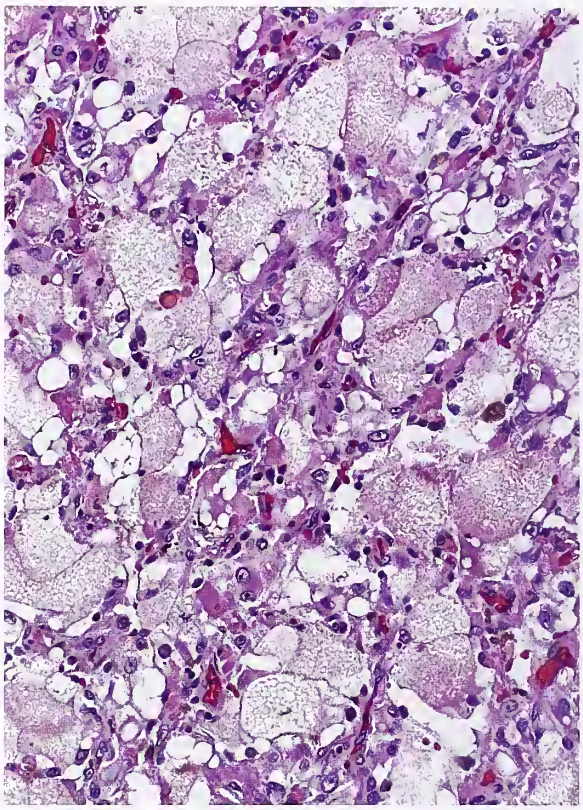

Figure 10-21

PHEOCHROMOCYTOMA

This pheochromocytoma had areas of lipid degeneration, with enlarged cells having finely vacuolated cytoplasm. (Fig. 10-22 from Fascicle 19, Third Series.)

Amyloid has been identified in pheochromocytomas (22,31); in one study it was found in 70 percent of pheochromocytomas and in most cases was considered abundant (31). The amyloid was detected by Congo red stain, but the ultrastructural features were not illustrated. In this author's experience, stromal changes suggesting amyloid are much less frequent and almost never abundant. Another study identified amyloid deposits in 9 percent of pheochromocytomas (32).

Pheochromocytomas (and other paragangliomas) are characteristically highly vascular neoplasms, and hemorrhage within a tumor may artifactually separate clusters of tumor cells. A prominent vascular component with plump endothelial cells may be confused with a vasoformative neoplasm (fig. 10-31). Lakes of eosinophilic proteinaceous material can be seen in occasional pheochromocytomas which have clear vacuoles at the periphery (fig. 10-32); this most likely represents a secondary degenerative change within the tumor. Rarely, there may be gaping sinusoids with a broad anastomosing trabecular arrangement of cells (fig. 10-33), but this should not be confused with the broad trabecular pattern seen in some adrenal cortical carcinomas.

The Chromaffin Reaction. The chromaffin reaction is caused by the oxidation of catecholamines to form adrenochrome pigments. Dichromate-containing fixatives may produce the chromaffin reaction on fresh tumor tissue, resulting in a dark brown color (fig. 10-34). At one time the gross chromaffin reaction was

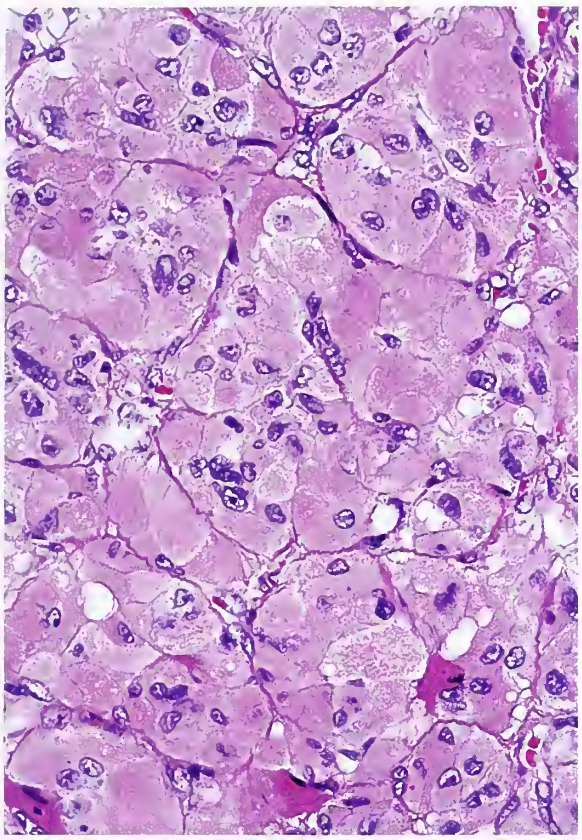

Figure 10-22

PHEOCHROMOCYTOMA

The tumor cells have copious cytoplasm which is densely eosinophilic and finely granular, giving the cells an "oncocytic" appearance.

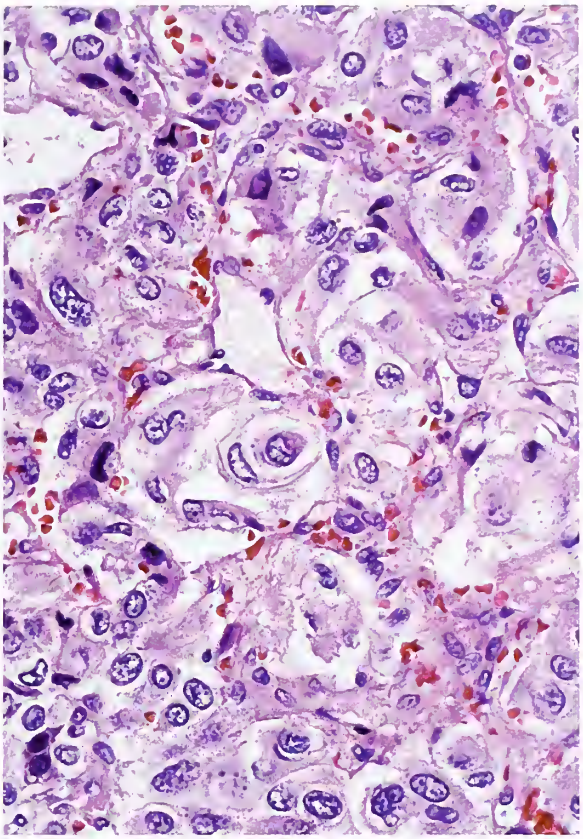

Figure 10-23

PHEOCHROMOCYTOMA

Some tumor cells partially envelop other cells, best seen near the center of the field.

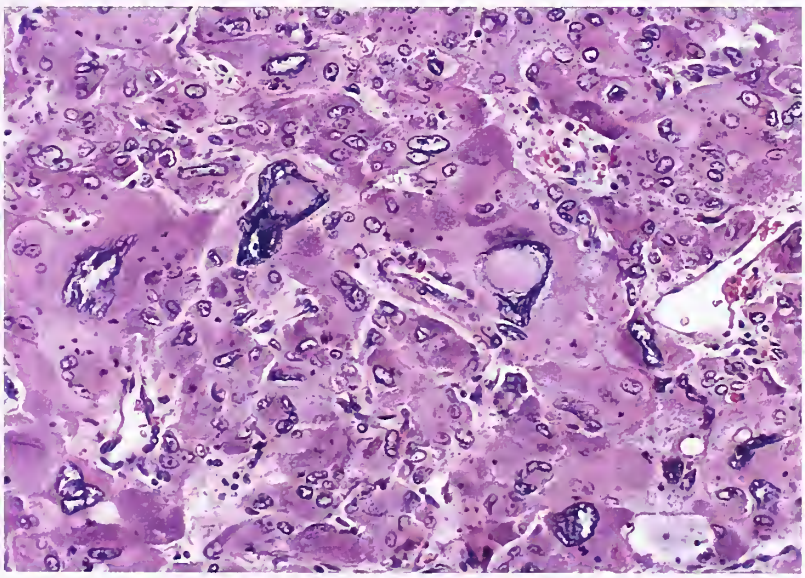

Figure 10-24

PHEOCHROMOCYTOMA

Two tumor cells have large nuclear "pseudoinclusions." There is a moderate degree of nuclear pleomorphism and hyperchromasia. (Fig. 10-25 from Fascicle 19, Third Series.)

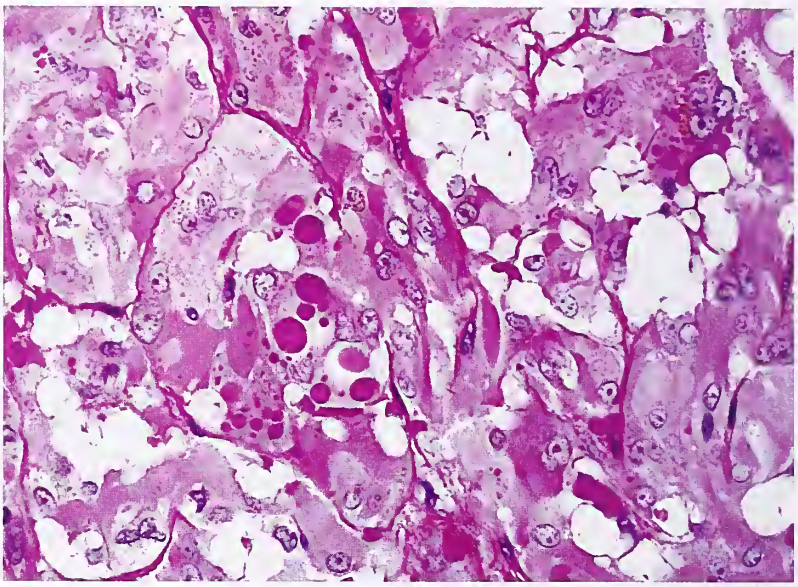

Figure 10-25

PHEOCHROMOCYTOMA

A few tumor cells in this field contain numerous eosinophilic hyaline globules, which vary considerably in size. Some appear to reside in an extracellular location, but this is probably an artifact. (Fig. 10-26 from Fascicle 19, Third Series.)

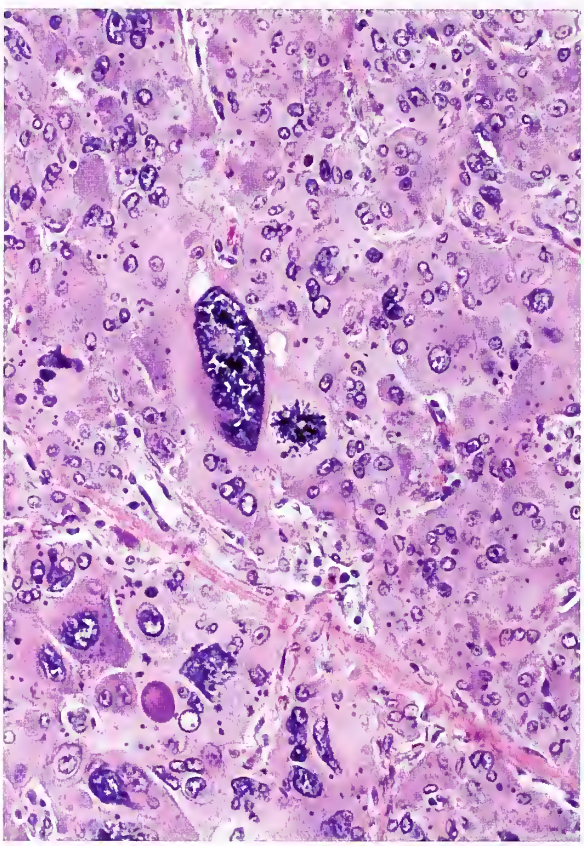

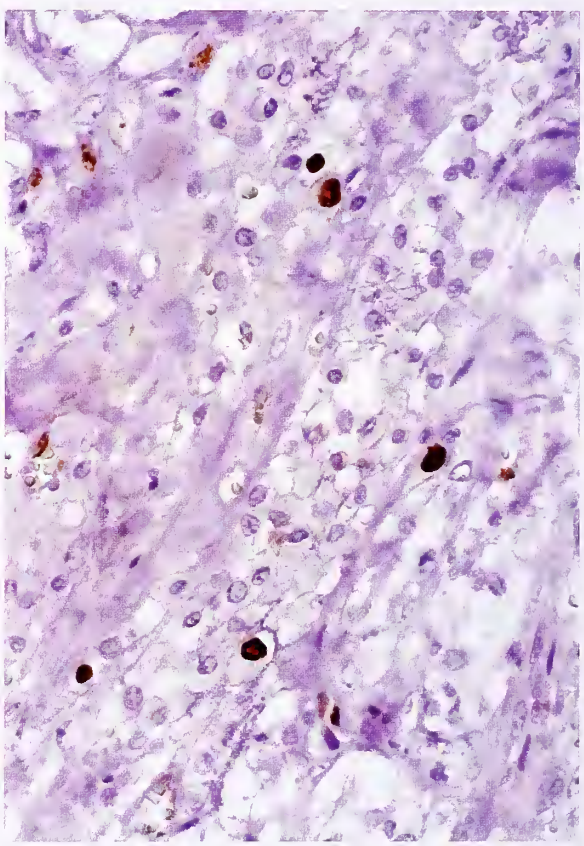

Figure 10-26

PHEOCHROMOCYTOMA

Left: There is a marked degree of nuclear pleomorphism and hyperchromasia. A rare mitotic figure is seen in the center.
Right: The same tumor had a relatively low proliferation index and proved to be clinically benign. Only a few nuclei in this representative field show positive immunolabeling for Ki-67 (MIB-1) (avidin-biotin peroxidase method).

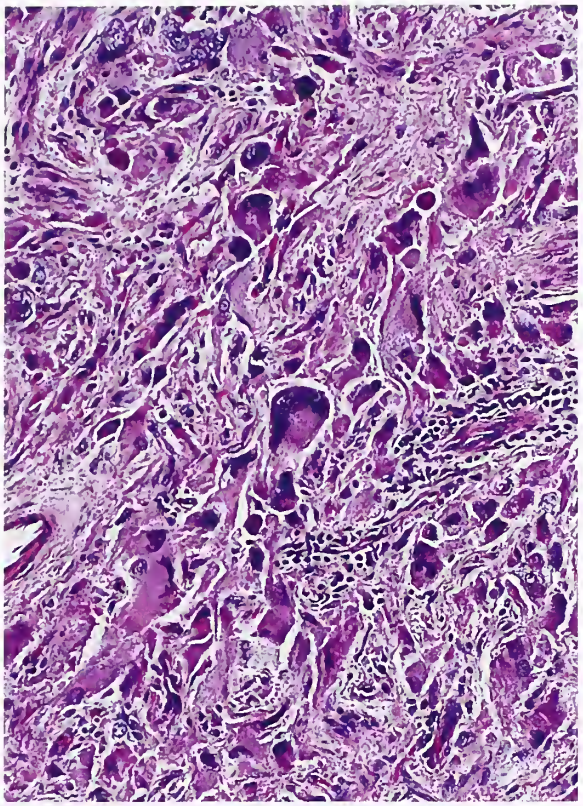

Figure 10-27

PHEOCHROMOCYTOMA

The tumor cells have vague ganglionic or neuronal features. Some cells had prominent nucleoli and basophilic material in the peripheral cytoplasm, which resembled Nissl substance. (Fig. 10-28 from Fascicle 19, Third Series.)

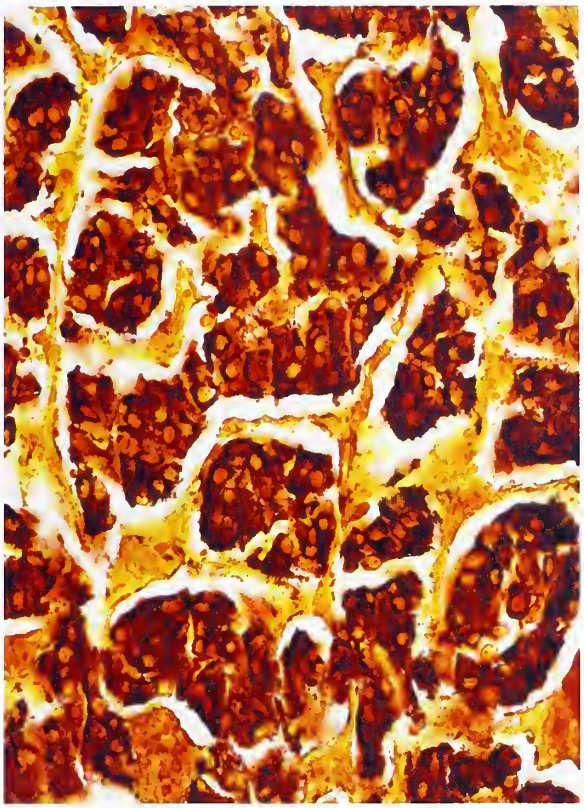

Figure 10-28

PHEOCHROMOCYTOMA

The strong cytoplasmic argyrophilia proved to be a myriad of pinpoint granules on closer view (Grimelius stain).

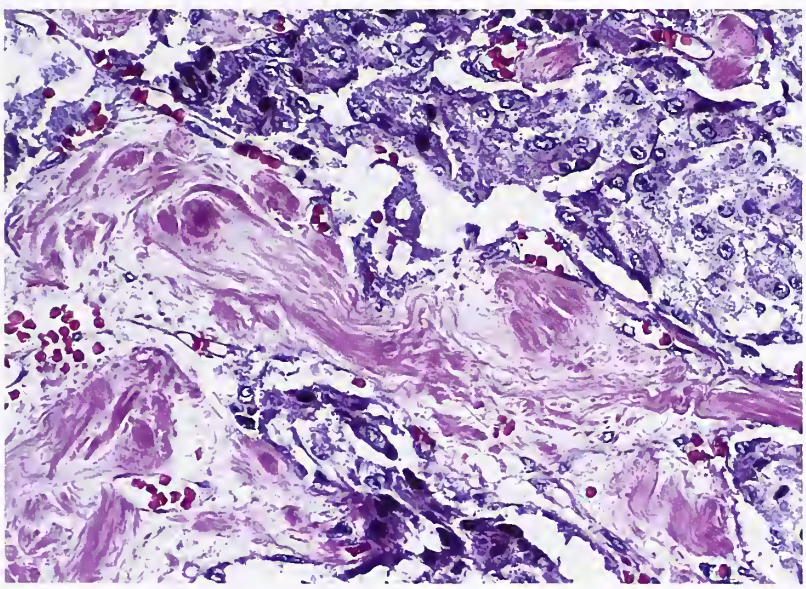

Figure 10-29

PHEOCHROMOCYTOMA

Areas of dense fibrosis separate nests of tumor cells. The fibrotic matrix has a fibrillar quality in areas. The stain for collagen was strongly positive. Amyloid was not identified with the Congo red stain. (Fig. 10-30 from Fascicle 19, Third Series.)

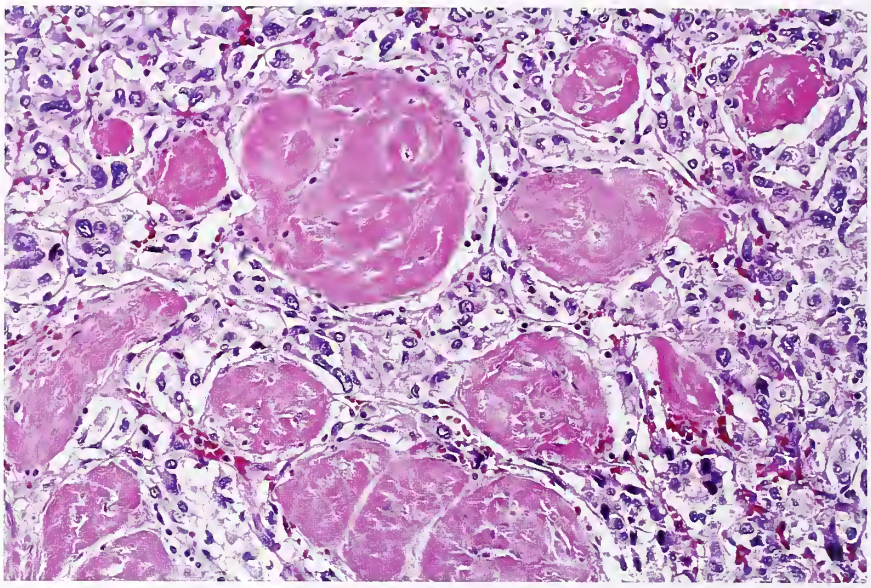

Figure 10-30

PHEOCHROMOCYTOMA

Bundles of dense collagen distort the tumor architecture.

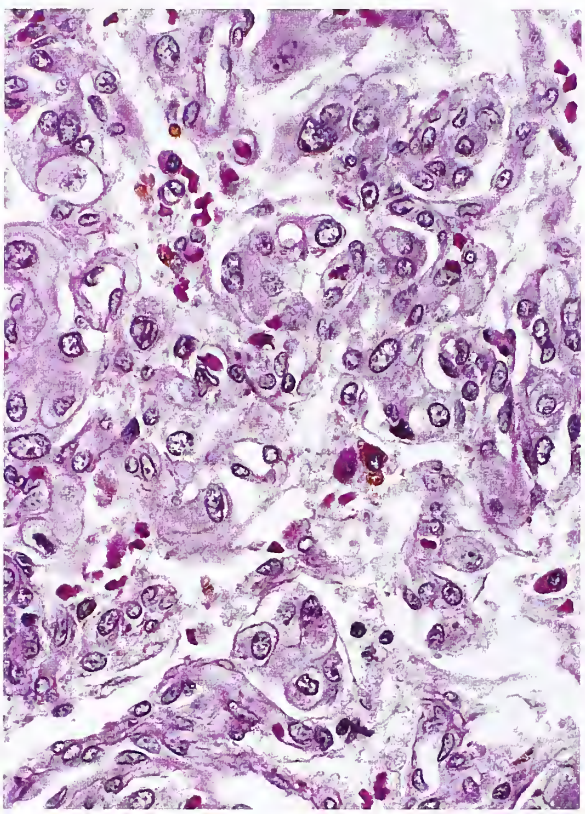

Figure 10-31

PHEOCHROMOCYTOMA

The microvasculature is prominent and plump endothelial cells are seen. Occasional mast cells are also present. (Fig. 10-32 from Fascicle 19, Third Series.)

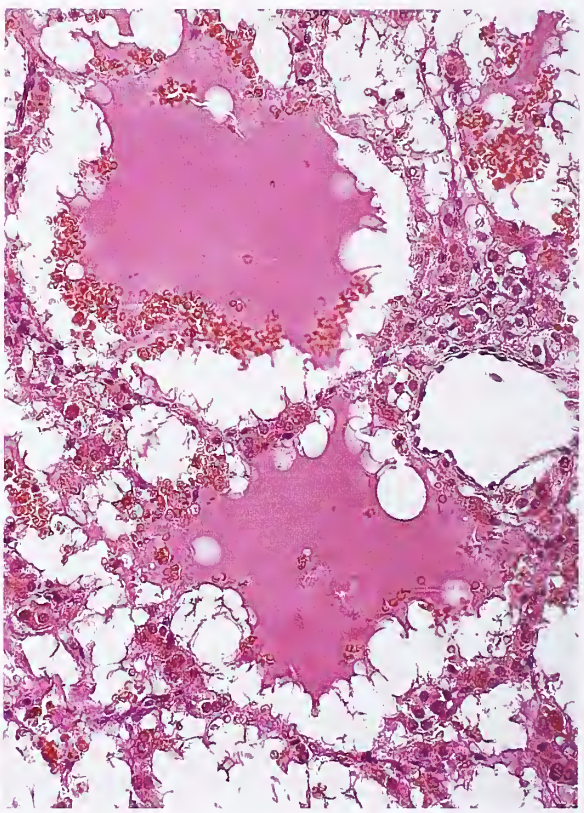

Figure 10-32

PHEOCHROMOCYTOMA

Proteinaceous lakes in pheochromocytoma with peripheral vacuoles or "scalloping." This is probably a degenerative change. (Fig. 10-33 from Fascicle 19, Third Series.)

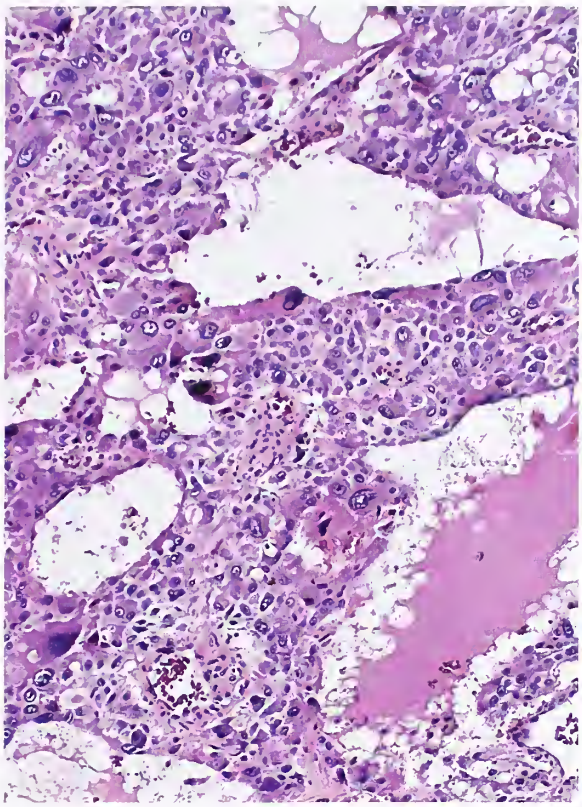

Figure 10-33

PHEOCHROMOCYTOMA

A pheochromocytoma with a trabecular pattern and dilated vascular spaces could be mistaken for an adrenal cortical carcinoma. (Fig. 10-34 from Fascicle 19, Third Series.)

considered the most valuable single procedure in the diagnosis of pheochromocytoma, but currently, with the availability of more sophisticated modern technology, the chromaffin reaction is mainly of historic interest (8). The chromaffin reaction can also be detected microscopically, but with prolonged fixation in aqueous fixatives it may become quite weak due to aqueous extraction of catecholamines. The fixative solution may turn dark brown or the color of cider over time.

Periadrenal Brown Fat. An increased prevalence of periadrenal brown adipose tissue (BAT) has been reported in association with 50 to 88 percent of pheochromocytomas (figs. 10-35, 10-36) (20,22,33). It has been suggested that catecholamines play a significant role in the transformation of periadrenal fat into BAT (34). One study showed no significant difference in the

Figure 10-34

PHEOCHROMOCYTOMA

A positive chromaffin reaction is present following immersion in Zenker's fixative. The same tumor is seen in the fresh, unfixed state in figure 10-4, bottom. The chromaffin reaction is apparent as a dark, mahogany brown color that deepens slightly on exposure to air. (Fig. 10-35 from Fascicle 19, Third Series.)

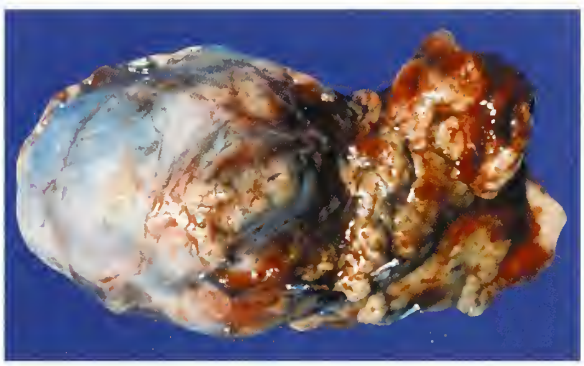

Figure 10-35

PHEOCHROMOCYTOMA

The external aspect of this pheochromocytoma has a prominent amount of adherent brown adipose tissue.

prevalence of BAT in control patients (51 percent) and those with a pheochromocytoma (53 percent), but additional studies need to be done using more critical quantitative evaluation (35). Reactivation of intraabdominal fat in the presence of high circulating norepinephrine levels may

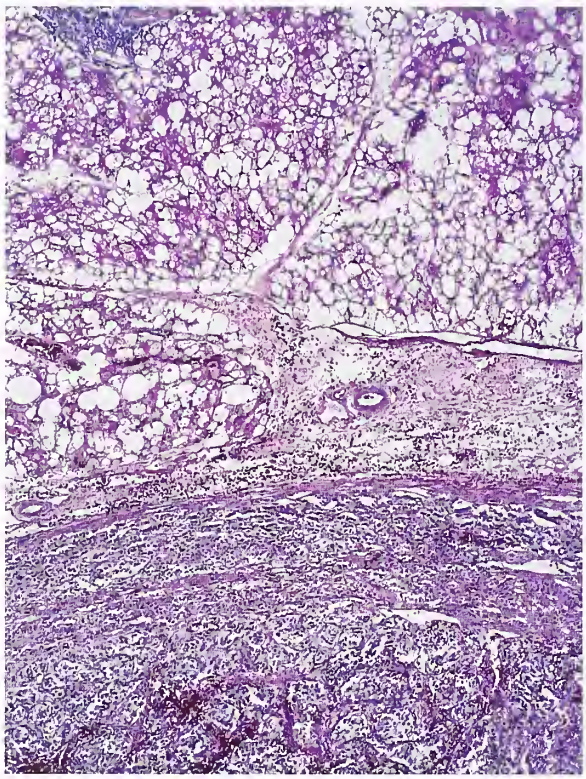

Figure 10-36

PHEOCHROMOCYTOMA

There is abundant periadrenal brown adipose tissue. In the lower half of the field there is a fibrous pseudocapsule and an investing adrenal capsule. (Fig. 10-36 from Fascicle 19, Third Series.)

contribute to the weight loss often observed in patients with pheochromocytoma (34).

Pheochromocytomas have also been reported in association with tumors of brown or fetal fat ("hibernomas") (36). Heat production due to uncoupling of oxidative phosphorylation has been proposed as a mechanism for the fevers that some patients with pheochromocytoma experience, and following surgical resection, the patient may become afebrile due to decreased adrenergic hyperactivity (37).

Other Associated Abnormalities. Catecholamine-associated cardiomyopathy can occur in patients with pheochromocytoma, with associated arrhythmias, cardiac failure, and occasionally even sudden death. There may be myocardial lesions (active catecholamine myocarditis) showing focal degeneration and necrosis of the myocardium along with mild inflammation, particularly involving the inner two thirds of the left ventricular myocardium (38). Other associated abnormalities include fibromuscular dysplasia (39), renal artery stenosis, multiple intracranial aneurysms (40), cholelithiasis (23 percent of patients reported by ReMine et al. [21]), and a variety of constitutional and metabolic abnormalities covered in greater detail elsewhere (41).

FAMILIAL PHEOCHROMOCYTOMA

Familial occurrence of pheochromocytomas has been reported in about 10 percent of cases (42), but the incidence varies depending upon the series examined, referral patterns, and other factors. A recent study indicated that as many as 20 percent of pheochromocytomas occur in a familial setting (9). Familial pheochromocytomas are most notable in patients with MEN syndrome types 2a and 2b (43), but can occur in those with von Recklinghausen's disease and von Hippel-Lindau (VHL) disease. About 5 percent of cases of pheochromocytoma are reported in association with von Recklinghausen's disease, although some estimate the frequency of association is probably 1 percent or less (44). Some reports indicate a higher association of pheochromocytoma in patients with von Recklinghausen's disease who have coexisting hypertension (45). Pheochromocytomas have been reported in 10 percent (46) to 21 percent (47) of patients with VHL disease, and there is an increased incidence of bilateral tumors (48). A bilateral composite pheochromocytoma-ganglioneuroma was reported in a patient with type 1 neurofibromatosis (49), and another patient had a bilateral pheochromocytoma-malignant peripheral nerve sheath tumor (50). There appears to be no firm evidence linking pheochromocytoma with tuberous sclerosis or Sturge-Weber disease. Pheochromocytoma can also occur in a familial setting without any other associated disease (42).

Patients with familial pheochromocytoma in the setting of MEN type 2 and VHL disease tend to be younger at diagnosis than those with sporadic pheochromocytomas (51). The molecular genetic abnormalities associated with these disorders, including MEN type 1, are reviewed in several recent studies (43,51–54). The genetic

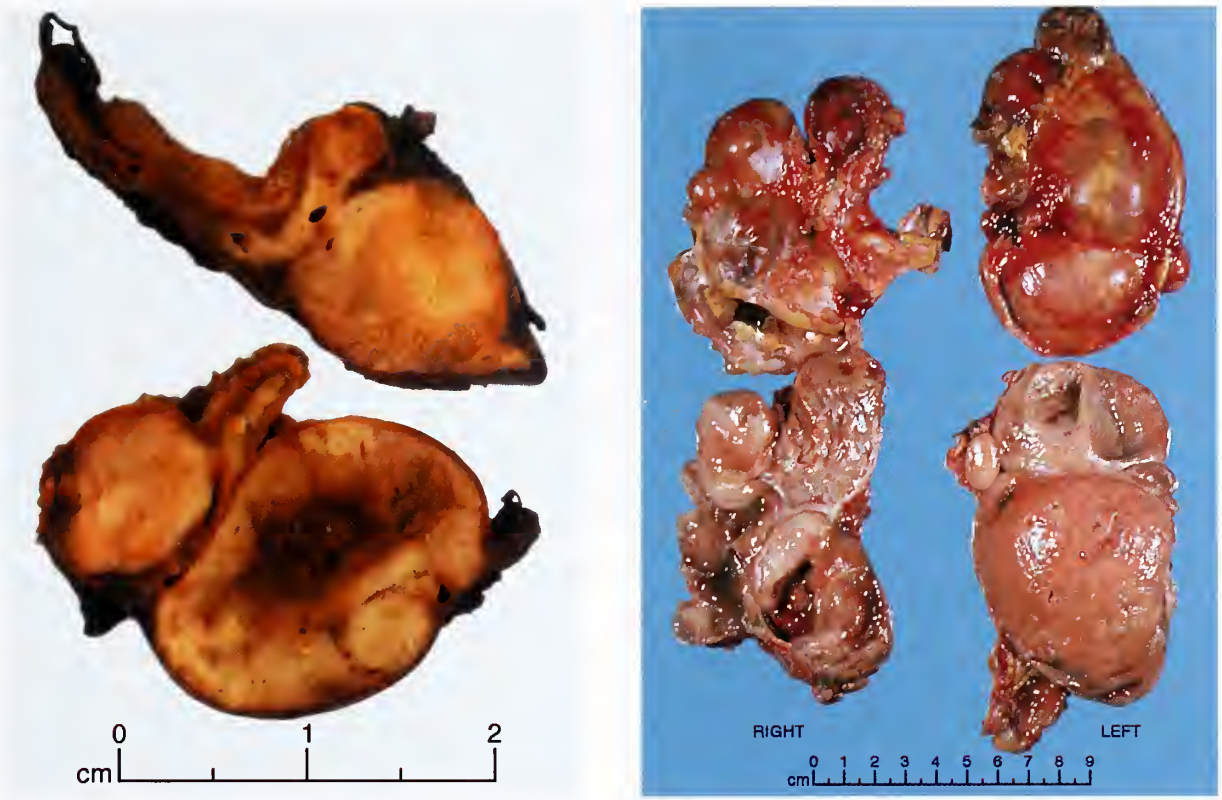

Figure 10-37

BILATERAL PHEOCHROMOCYTOMA

Left: The bilateral pheochromocytomas were multinodular and multicentric. The patient was suspected of having MEN type 2a, but language problems and an impoverished state prevented a full investigation.

Right: Cross section of bilateral pheochromocytomas from a 30-year-old man with MEN type 2a. The right adrenal tumor weighed 168 g and the left, 220 g. Note the distinct multinodular, multicentric pattern of growth on both sides. The external aspect of the tumors is at the top and the cut surface at the bottom on either side. (Fig. 10-37 from Fascicle 19, Third Series.)

basis of pheochromocytoma and paraganglioma is complex: it involves the *VHL* gene (subband 3p25-26), the *NF1* gene (17q11.2), the *RET* protooncogene (MEN syndromes types 2a and b), and several additional genes for extraadrenal paragangliomas (51,55). The first international symposium on pheochromocytoma took place in Bethesda, Maryland, in October 2005 and the conference proceedings will appear as a volume of the Annals of the New York Academy of Sciences in 2006.

Pheochromocytomas in MEN Syndrome Types 2a and 2b

Pheochromocytomas develop in 30 to 50 percent of patients with MEN type 2 (56,57); the tumors are bilateral or multifocal in 60 to 70 percent of cases (58) or more (59). Patients may be asymptomatic (60), and the pheochromocytoma may not respond to the usual provocative tests. The tumors tend to produce more epinephrine than sporadic pheochromocytomas, in which norepinephrine is the predominant catecholamine secreted (61,62). A case of Cushing's syndrome due to ectopic adrenocorticotropic hormone (ACTH) production by bilateral pheochromocytomas has been reported (63).

When the pheochromocytoma is small, there is often extratumoral adrenal medullary hyperplasia, but when the tumor is large, it may not be possible to evaluate the non-neoplastic medulla (fig. 10-37). In a study of 14 pheochromocytomas from 8 patients with VHL disease there was no extratumoral medullary hyperplasia, in contrast to pheochromocytoma in patients with MEN type 2 (64). Extraadrenal

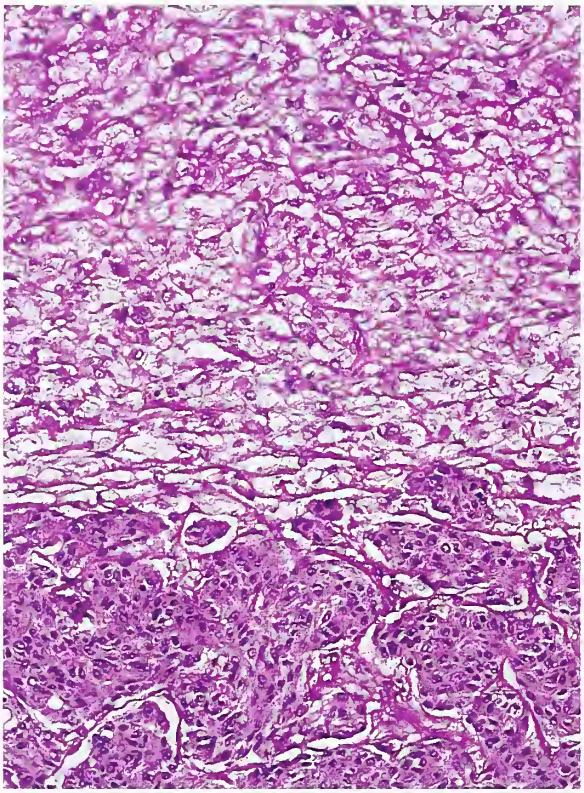

Figure 10-38

MEDULLARY THYROID CARCINOMA METASTATIC TO PHEOCHROMOCYTOMA

Medullary thyroid carcinoma (bottom) metastatic to a pheochromocytoma (top) in a patient with MEN syndrome type 2a. The metastatic tumor was diffusely and strongly positive for thyrocalcitonin. (Fig. 10-38 from Fascicle 19, Third Series.)

paragangliomas have been reported in patients with MEN type 2, but they appear to be uncommon. The gross morphologic features alone may be sufficiently distinctive that the surgical pathologist is alerted to the possibility of MEN type 2a or 2b (65).

Cytogenetic studies in patients with MEN 2a and 2b indicate a genetic linkage to the *RET* gene near the centromere of chromosome 10. The availability of sensitive probes for the *RET* germline mutation has permitted screening of individuals at risk at any age with a high level of certainty (43). The *RET* protooncogene, located in the DNA segment 10q11.2, is reported to be consistently expressed in patients with pheochromocytoma and medullary thyroid carcinoma, and missense mutations of this oncogene have been identified in a high proportion of families with MEN types 2a and 2b (43). Although the MEN types 1 and 2a are considered distinct and separate entities, there may be rare exceptions (8,23). Coexistence of the MEN type 1 gene mutation and *RET* mutation has been documented (66).

The biologic behavior of pheochromocytomas in patients with MEN 2a and 2b varies from series to series (23). Some have suggested that these tumors are extreme examples of adrenal medullary hyperplasia (61). Some data suggest that malignant pheochromocytomas are relatively rare in patients with MEN type 2 (47,58) and possibly VHL disease (47) and in a recent review, the pheochromocytomas were characterized as almost exclusively benign and localized in the adrenal glands (67). In a study by Carney et al. (60), 5 of 19 patients (6 with MEN 2b, 13 with MEN 2a) died as a direct result of the pheochromocytoma (29 percent): 1 due to intracerebral hemorrhage, 2 due to hypotensive crises, and 2 because of pulmonary metastases; 4 patients developed metastases to lung, liver, or bone (21 percent). In a review of 10 series of patients with MEN type 2, the incidence of malignant pheochromocytoma was 4.4 percent (57). Rare tumor to tumor metastases have occurred from medullary thyroid carcinoma to pheochromocytoma (fig. 10-38) (23). Simultaneous hepatic metastases of pheochromocytoma and medullary thyroid carcinoma have been reported (68). In most cases, laparoscopic surgery is the treatment of choice for bilateral pheochromocytomas in patients with MEN type 2, with subtotal (cortical-sparing) adrenalectomy when possible (67).

MEN Syndrome Type 2b

The phenotypic expression of MEN type 2b is very distinctive. The various abnormalities associated with the disease are listed in Tables 10-3 and 10-4. Although this syndrome also has an autosomal dominant pattern of inheritance similar to MEN 2a, not infrequently cases appear to be isolated or sporadic.

Mucosal neuromatous proliferation or neuromas of the oral and labial mucosae are often the first manifestation, usually in the first decade of life. The lower facies may appear elongated with a broad-based nose (fig. 10-39A) and

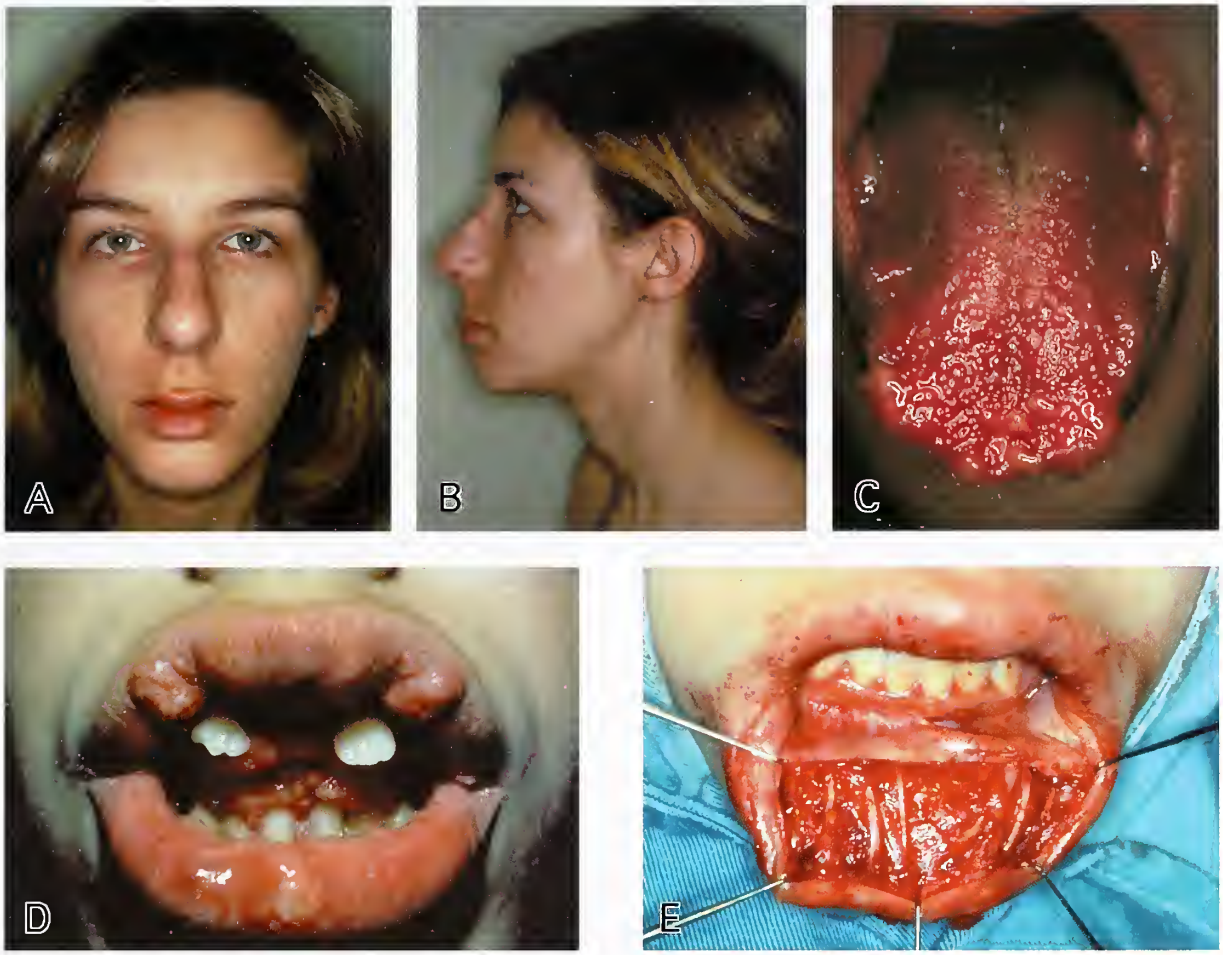

Figure 10-39

MEN SYNDROME TYPE 2B

A: A young female with MEN type 2b has elongated lower facies and a broad-based nose.

B: A mild degree of dolichocephaly is present.

C: Same patient with grotesque mucosal neuromatous nodules. The patient died of widely metastatic medullary thyroid carcinoma. No other immediate family member had MEN syndrome type 2b.

D: A different patient with MEN type 2b has thickened lips with multiple mucosal nodules. Multiple mucosal nodules are seen on the tongue.

E: Attempt at lip reduction to prevent the cosmetic deformity of thickened nodular lips in a different patient with MEN type 2b. Note the thickened nerves, which have been likened to "guy-wires." (D,E courtesy of Dr. Robert J. Gorlin, Minneapolis, MN.)

there may be a mild degree of dolichocephaly (fig. 10-39B). The tongue has multiple nodular or hemispheric fleshy protrusions that characteristically stud the anterior portion and extend along the lateral borders (fig. 10-39C) (8,23). The lips may be thickened and nodular, giving a "blubbery" appearance (fig. 10-39D,E) (69). The nasal, laryngeal, pharyngeal, and conjunctival mucosae may also be involved (fig. 10-40A,B).

The neural lesions are composed of circumscribed but unencapsulated aggregates of hypertrophied, elongated nerves (fig. 10-40C), occasionally with some interstitial edema or myxoid stroma. The lesions only superficially resemble "traumatic" or "amputation" neuromas (8,23). The term *mucosal ganglioneuromatosis* has been used because these lesions may represent just the "tip of the iceberg" in terms of gastrointestinal

Table 10-3

MULTIPLE ENDOCRINE NEOPLASIA SYNDROME TYPE 2B: PHENOTYPIC MANIFESTATIONS[a]

Upper Aerodigestive Tract/Gastrointestinal Tract
Neuromatous proliferation in oral, lingual, and other mucosal sites in upper aerodigestive tract
Ganglioneuromatosis of gastrointestinal tract
Variety of manifestations: motility disorders including megacolon, cholecystitis (calculous or acalculous)
Ocular
Thickened corneal nerves, perilimbal neuromas, keratoconjunctivitis sicca, failing vision (rare)
Conjunctival/eyelid neuromatous proliferation
Neuromuscular
Marfanoid habitus, asthenia with muscular atrophy, somatic and autonomic neuropathy
Musculoskeletal
Elongated facies, dolichocephaly, micrognathia, laxity of joints, congenital dislocation of hip, lordosis, kyphosis, genu valgum, slipped femoral capital epiphysis, coxa valga, pes cavus

[a]Modified from Table 10-3 from Fascicle 19, Third Series.

Table 10-4

MULTIPLE ENDOCRINE NEOPLASIA SYNDROME TYPE 2B: ENDOCRINE MANIFESTATIONS[a]

Medullary Thyroid Carcinoma
Aggressive tumor with metastasis/recurrence: most pernicious component of syndrome
Adrenal Medullary Disease (hyperplasia and pheochromocytoma)
Adrenal medullary disease (34%) with bilateral pheochromocytomas (68%)
Parathyroid Enlargement/Hyperplasia
Very low incidence of clinical/biochemical hyperfunction (4%)

[a]Modified from Table 10-4 from Fascicle 19, Third Series.

involvement (70); ganglion cells, however, are usually not seen in these superficial mucosal lesions (8,23).

The ocular manifestations are also distinctive and include neuromatous nodules on eyelid and conjunctiva; thickening of eyelids, sometimes with eversion of the tarsal plate (fig. 10-40); thickened perilimbal neuromas; and the presence of thickened corneal nerves within a clear corneal stroma (fig. 10-41). Visual impairment due to hypertrophied corneal nerves occasionally occurs (71). A variety of neurologic signs and symptoms may result from the involvement of somatic and sensory nerves or the autonomic nervous system (71). Ganglioneuromatosis of the urinary bladder has been reported with secondary bladder infections (72). There is a low incidence of parathyroid disease (4 percent) (73), and most descriptions of parathyroid hyperplasia are not accompanied by hyperfunction (74).

The gastrointestinal manifestations in MEN 2b are important to recognize since they form a prominent component of the syndrome and often antedate the endocrine neoplasms (75). Manifestations include intestinal dysmotility with constipation, intestinal pseudoobstruction, borborygmi, projectile vomiting, or a clinical picture mimicking megacolon or diverticulitis. Ganglioneuromatosis involves much of the gastrointestinal tract and all layers to a variable extent (fig. 10-42). It can involve other sites as well such as pancreas, salivary gland, adrenal gland (73), and gallbladder. The ganglioneuromatosis consists of a hamartomatous proliferation of Schwann cells, neurites, and ganglion cells, and it has been implicated in motility disturbances. An example of intestinal neuroma causing colonic obstruction has been recently reported (76). Intestinal ganglioneuromatosis (mainly mucosal) can also be found in patients without MEN 2b but with juvenile polyposis (77), colonic polyps, colonic adenocarcinoma, von Recklinghausen's disease, and rarely, as a nonspecific finding in inflamed bowel (78,79). Adrenal ganglioneuroma is a rare occurrence in MEN type 2a and 2b (80).

The most life-threatening component of MEN 2b is medullary thyroid carcinoma which is often aggressive and fatal (43,73,81). In a review by Carney et al. (73), 22 percent of 69 patients with medullary thyroid carcinoma died at an average age of 21 years, and it was suggested that most patients would die of metastatic disease unless total thyroidectomy was performed at an early age. Adrenal medullary disease was diagnosed in 34 percent of patients at an average age of 25 years, and 68 percent of pheochromocytomas were bilateral. Once a diagnosis of adrenal medullary disease is made, total adrenalectomy is recommended (73). Simultaneous bilateral laparoscopic

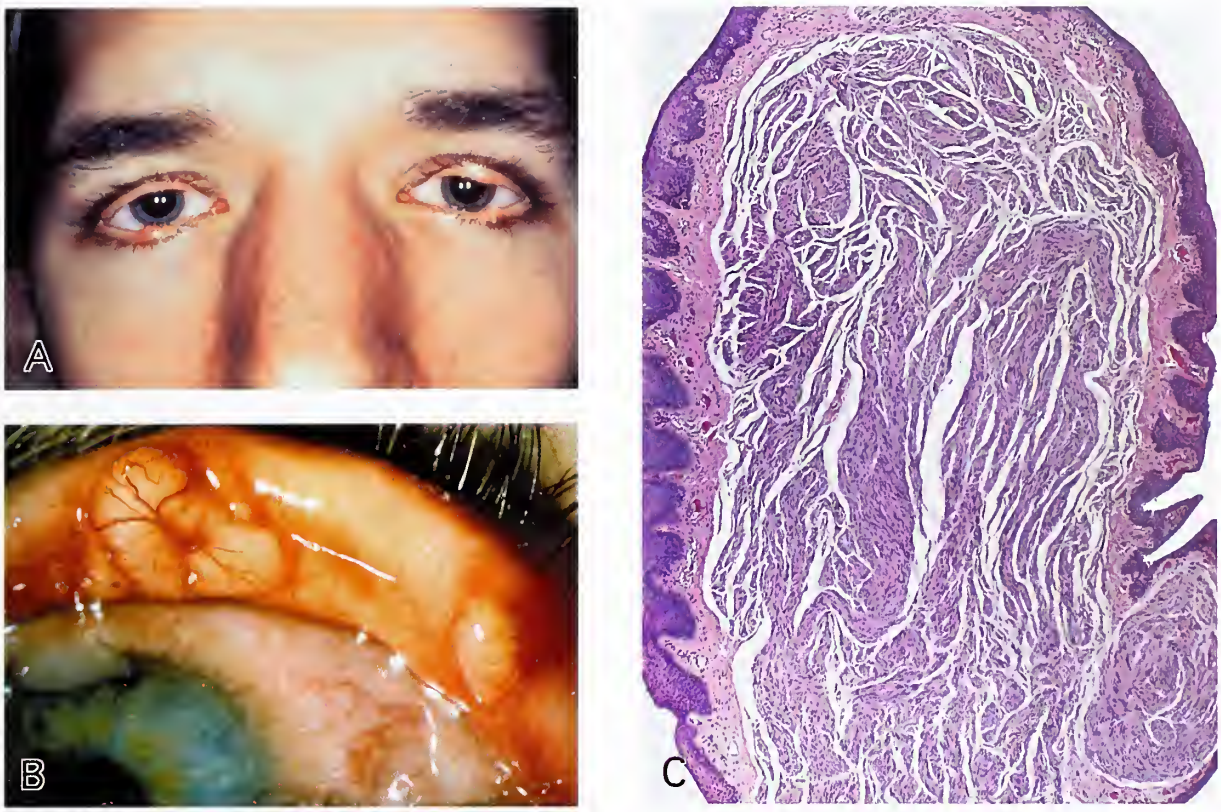

Figure 10-40

MEN SYNDROME TYPE 2B

A: Patient with MEN type 2b has a broad-based nose and multiple neuromatous nodules involving the conjunctiva and eyelids. There is partial eversion of the tarsal plates, and with relative fixation of the lids, the patient may have a "staring" expression.

B: Everted tarsal plate of upper eyelid shows multiple conjunctival nodules. (A,B courtesy of Dr. Robert J. Gorlin, Minneapolis, MN.)

C: Polypoid lesion of the eyelid has irregular bundles of myelinated nerves with slight interstitial edema. No ganglion cells were identified. This neuromatous proliferation is identical to that seen in lips, tongue, and other mucosal sites of the upper aerodigestive tract. (Fig. 10-40 from Fascicle 19, Third Series.)

adrenalectomy has been used (82). A cortical-sparing (subtotal) adrenalectomy may be done if technically feasible to avoid the need for corticosteroid replacement (67,83). A historical perspective of familial endocrine neoplasia has recently appeared (84).

OTHER ASSOCIATED ENDOCRINE DISORDERS

Other endocrine tumors (or hyperplasias) have occurred in association with pheochromocytoma (or other paragangliomas), usually in a sporadic setting. Some have been regarded as a distinct MEN syndrome or a variant of MEN (8). A list of some of these associations is given in Table 10-5.

GASTRIC STROMAL SARCOMA, PULMONARY CHONDROMA, AND EXTRAADRENAL PARAGANGLIOMA (CARNEY'S TRIAD)

This rare but interesting association of three unusual tumors was initially reported in 1977 (85). It occurs most often in young females, but has no established etiology and no known Mendelian inheritance pattern. A recent update raised the possibility of a familial occurrence in some cases (86). Most of the paragangliomas are extraadrenal, in the head and neck region and base of the heart, but pheochromocytomas have also been documented, although the tumor may be periadrenal. The gastric tumors

Figure 10-41

MEN SYNDROME TYPE 2B

Young female with MEN type 2b has thickened, elongated nerves coursing from the limbus in the clear corneal stroma. (Fig. 4-57 from Lack EE. Adrenal medullary hyperplasia and pheochromocytoma. In: Lack EE, ed. Pathology of the adrenal glands. New York: Churchill Livingstone; 1990:173-235.)

Table 10-5

OTHER ENDOCRINE DISORDERS ASSOCIATED WITH PHEOCHROMOCYTOMA[a]

Chemodectoma, bronchial carcinoid tumor, pituitary adenoma, hyperplasia of parathyroid glands, and duodenal gastrin-producing cells
Pituitary adenoma, parathyroid hyperplasia, and multiple functioning extraadrenal paragangliomas
Medullary thyroid carcinoma, multiple parathyroid adenomas, adrenal cortical adenoma, and small cell carcinoma of bronchus
Bilateral pheochromocytoma and pancreatic islet cell tumor
Familial pheochromocytoma and pancreatic islet cell tumor
Pituitary adenoma and pheochromocytoma
Pituitary adenoma, papillary thyroid carcinoma, bilateral carotid body paraganglioma, parathyroid hyperplasia, gastric leiomyoma, and systemic amyloidosis
von Recklinghausen's disease, pheochromocytoma, and duodenal carcinoid tumor
von Recklinghausen's disease, pheochromocytoma, jugulotympanic paraganglioma, and pulmonary paragangliomas
Pheochromocytoma and papillary thyroid carcinoma

[a]Table 10-5 from Fascicle 19, Third Series.

may have an organoid pattern reminiscent of a paraganglioma but they are now classified as stromal sarcomas (gastrointestinal stromal tumor [GIST]) (87).

A recent update of this rare association identified 79 patients (67 females, 12 males) distributed worldwide, with 65 cases having an onset in the first three decades of life (82 percent). A provisional diagnosis is possible if two of the three tumors are present, especially if one or both are multicentric and the affected patient is young and female; a definitive diagnosis is warranted if all three tumors are present. Benign adrenal cortical tumors are a component of the disorder.

The paragangliomas are widely distributed in the head and neck region, chest and abdomen. In one study, 37 patients (47 percent) had 60 paragangliomas; 6 of these patients had pheochromocytomas (adrenal medullary paragangliomas) and 3 had extraadrenal paragangliomas as well (86). Metastases occurred in 4 of the 37 patients (10 percent).

COMPOSITE PHEOCHROMOCYTOMA

Composite pheochromocytoma is a designation for a tumor that is composed, in part, of typical pheochromocytoma, but also has a component resembling neuroblastoma, ganglioneuroblastoma, or typical ganglioneuroma (8,19,23,88, 89). In a series by Linnoila et al. (19), 3 percent of the sympathoadrenal paragangliomas were classified as composite pheochromocytomas (fig. 10-43). A bilateral composite pheochromocytoma-ganglioneuroma has been reported in a patient with type 1 neurofibromatosis (49) and a unilateral example has been reported in association with MEN type 2a (90). Rare examples have been reported in an intraabdominal extraadrenal location. Another distinctive, but even rarer type of composite pheochromocytoma is one that has a component of malignant peripheral nerve sheath tumor (malignant schwannoma) (91,92). Rarely, malignant schwannoma can occur as a primary adrenal tumor (93).

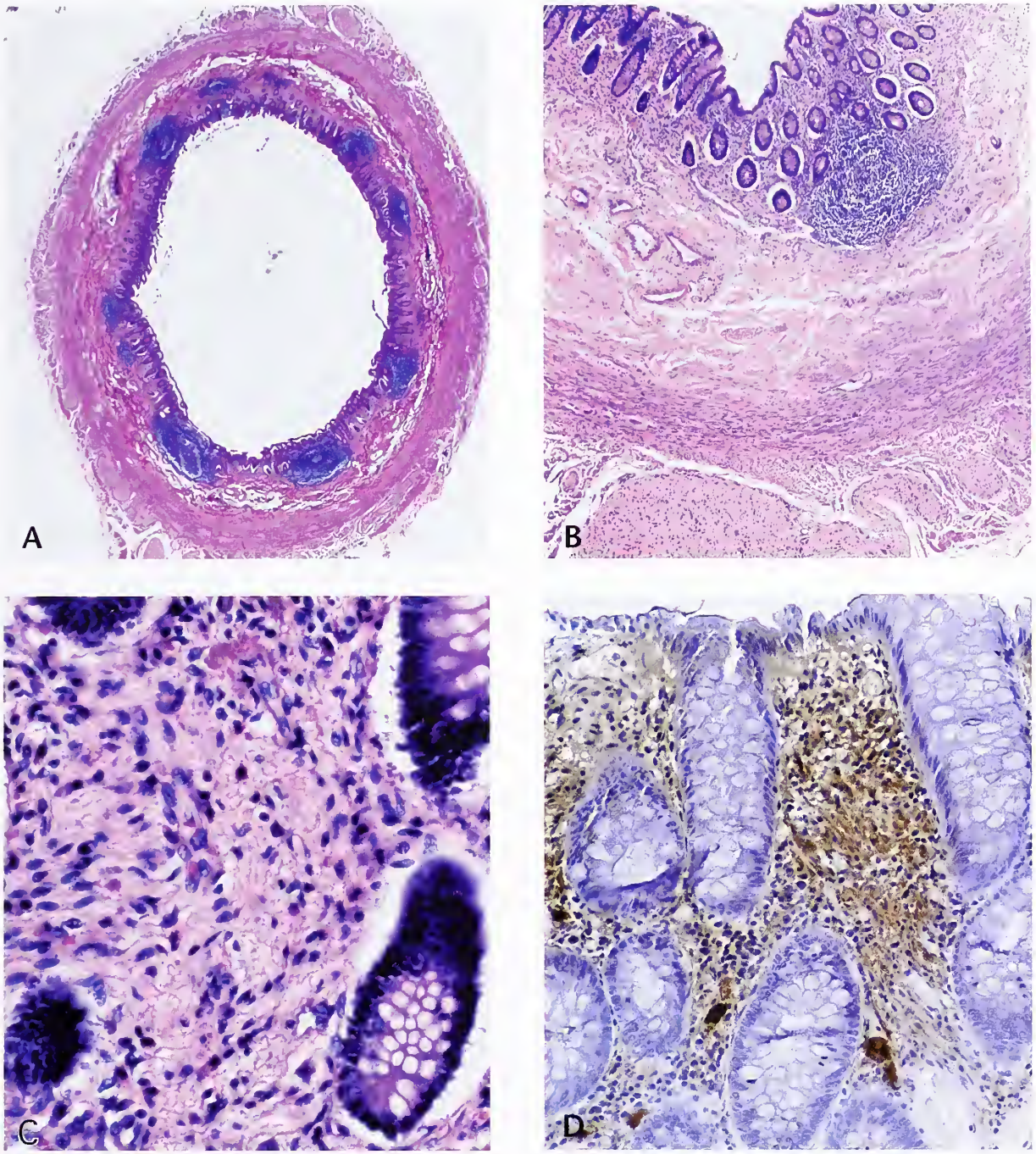

Figure 10-42

MEN SYNDROME TYPE 2

A: Incidental appendectomy specimen from a patient who underwent surgical removal of a pheochromocytoma. Some thickened nerves are present in the serosal aspect as well as in the mesentery.

B: Ganglioneuromatous proliferation is present in a thickened myelinated nerve in the bottom half of the field. Ganglioneuromatosis was also evident in the mucosa of the appendix.

C: Ganglioneuromatosis of lamina propria of appendix.

D: Immunostain for neuron-specific enolase highlights the neural proliferation in the lamina propria and also demonstrates a few intensely stained ganglion cells (avidin-biotin peroxidase method).

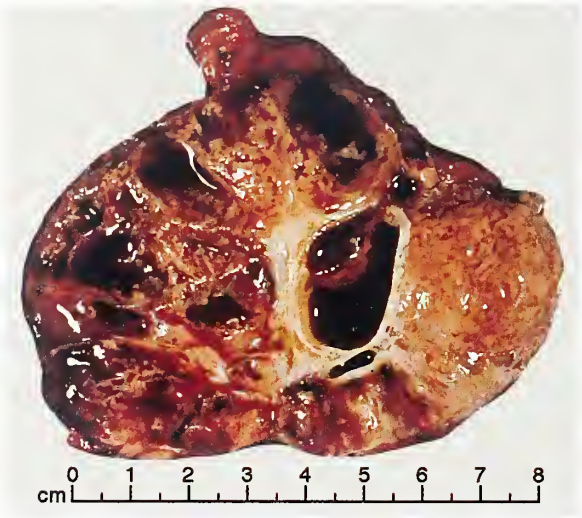

Figure 10-43

COMPOSITE PHEOCHROMOCYTOMA

This composite pheochromocytoma had many areas that microscopically resembled ganglioneuroblastoma. The tumor was resected from a 42-year-old woman who presented with signs and symptoms of excess catecholamine secretion. Irregular areas of cystic degeneration, with congestion and hemorrhage, are seen in cross section. (Fig. 10-42 from Fascicle 19, Third Series.)

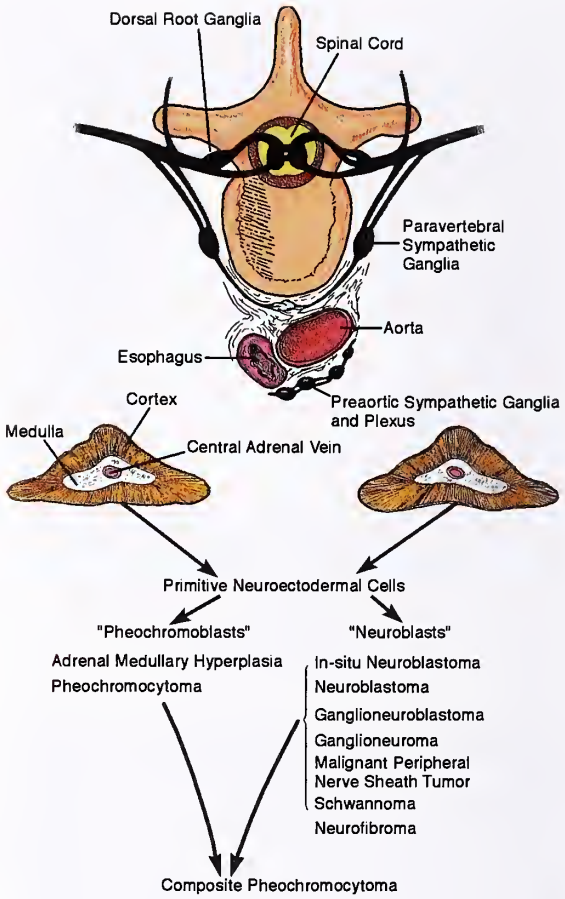

Figure 10-44

COMPOSITE PHEOCHROMOCYTOMA

The fate of the primitive neuroectodermal cells within the developing adrenal gland is variable, but two major lines of cellular differentiation can be envisioned (neural and endocrine) as well as possible types of tumors that may develop. Composite pheochromocytoma consists of dual neural and endocrine cells in various combinations.

Composite pheochromocytomas usually include tumors that have common embryologic ancestry from the neural crest (fig. 10-44), but there are other rare combinations of tumors: mixed adrenal cortical adenoma-pheochromocytoma (corticomedullary mixed tumor) (94), concurrent adrenal cortical adenoma and pheochromocytoma in the same gland (95,96), and composite pheochromocytoma-ganglioneuroma with cortical adenoma (97). A new type of composite pheochromocytoma was recently reported with a neuroendocrine carcinoma component (98).

Composite pheochromocytomas may have areas resembling ganglioneuroblastoma (fig. 10-45), with neuronal or ganglion cell features admixed with a loose fibrillar matrix resembling neuropil. Transition between the different patterns may be gradual or abrupt. Ganglionic cells may contain granular basophilic material corresponding to Nissl substance. The Nissl substance may have an uneven distribution in the perikaryon and occasionally may not even be appreciated in the particular plane of section. The neuronal or ganglionic cells are characterized by relatively abundant light pink cytoplasm with distinct borders and rounded eccentric nuclei, sometimes with a prominent nucleolus (fig. 10-45A). In some fields, the neuronal or ganglionic cells appear suspended in a complex web of matted neuropil (fig. 10-45B,C). There may be a more primitive small cell component resembling neuroblastoma (fig. 10-46).

Composite pheochromocytoma-ganglioneuroma is a rare tumor. The histologic features of both tumors are admixed, often with an abrupt transition (fig. 10-47, left). Ganglion cells may be few and widely scattered, but their presence, coupled with the prominent

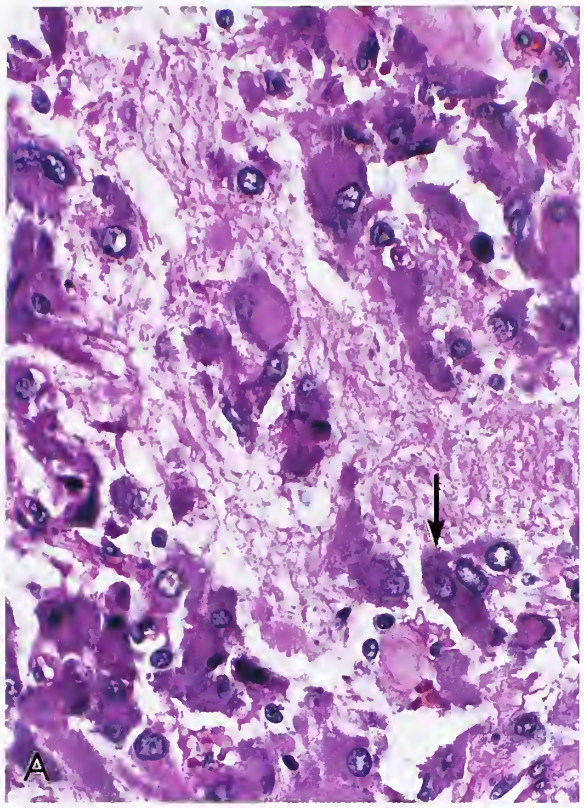

Figure 10-45

COMPOSITE PHEOCHROMOCYTOMA WITH AREAS RESEMBLING GANGLIONEUROBLASTOMA

A: Tumor cells of the pheochromocytoma have neuronal or ganglionic features. The background of fibrillary matrix represents intertwined neuritic cell processes. Some cells with eccentric nuclei have compact cytoplasm with well-defined borders; the basophilic staining near the edge resembles Nissl substance (arrow). Other fields had an appearance more typical of pheochromocytoma.

B: Ganglion-like cells in a background rich in neuropil-like fibrillary matrix. (A,B: Fig. 10-44B,C from Fascicle 19, Third Series.)

C: Ganglion-like cells have a rich neuropil-like fibrillary matrix. Immunostain for neuron-specific enolase highlights the ganglion-like cells and the neurofibrillary matrix.

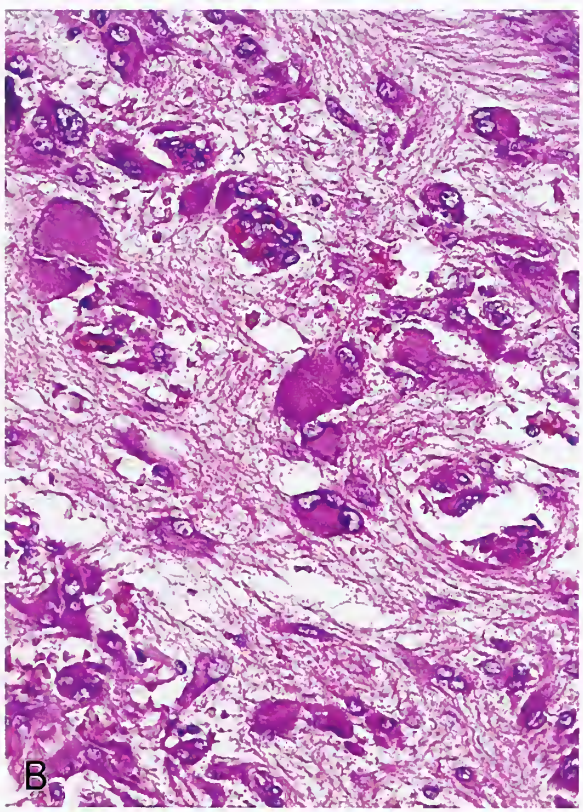

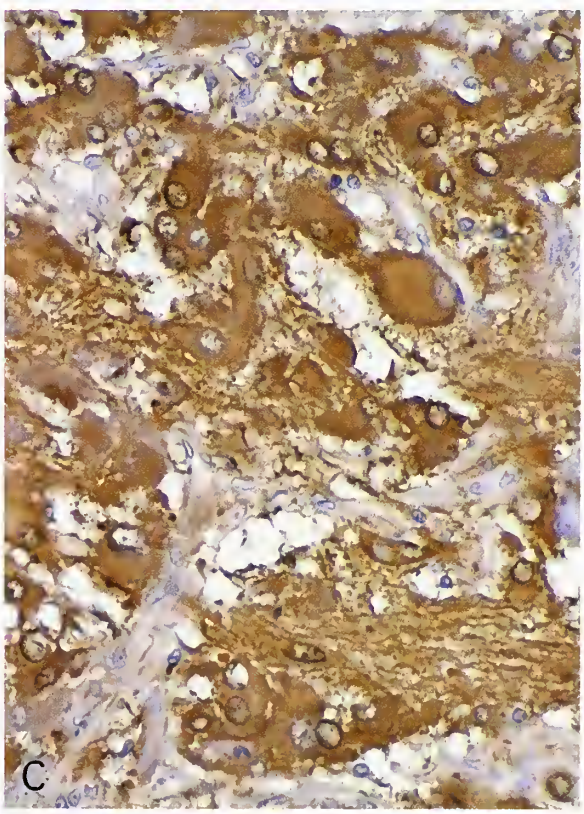

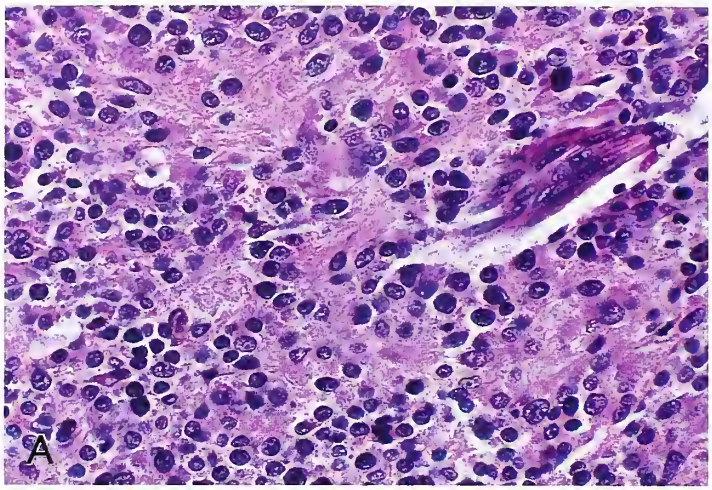

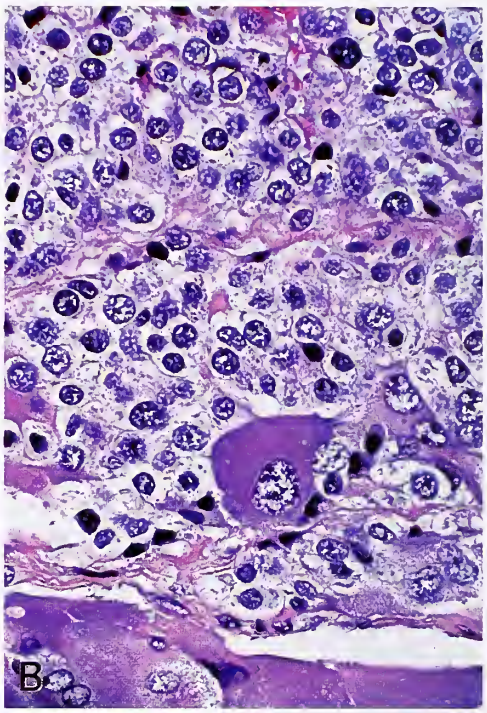

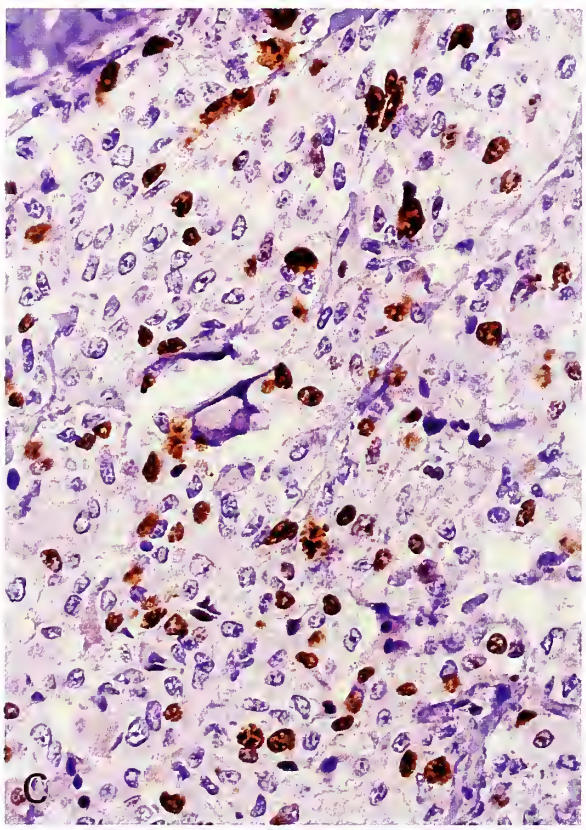

Figure 10-46

COMPOSITE PHEOCHROMOCYTOMA

A: Small, immature cells with a fibrillary matrix represent neuritic cell processes. The pattern resembles neuroblastoma. Other areas showed a morphology typical of pheochromocytoma. (Fig. 10-45 from Fascicle 19, Third Series.)

B: A different tumor has small immature cells and neuronal or ganglion-like cells (bottom). The 71-year-old woman had a 10-cm left adrenal tumor weighing 569 g. The tumor appeared as a thin-walled cystic mass with central hemorrhage and necrosis. Many of the tumor cells have nuclei with stippled ("salt and pepper") nuclear chromatin. In these less-differentiated areas, there was a brisk mitotic rate as well as foci of necrosis. The tumor proved to be biologically aggressive and recurred locally. Areas in the primary tumor had the typical morphology of pheochromocytoma.

C: In areas resembling neuroblastoma, the tumor seen in B had a relatively high labeling index using the proliferation marker Ki-67 (MIB-1). In areas more typical of pheochromocytoma the index was much lower (avidin-biotin peroxidase method).

Schwann cells, is diagnostic (fig. 10-47, right). The pheochromocytoma can grow as small clusters of cells within the neural component of the tumor (fig. 10-48, left), and can readily be detected by staining for cytoplasmic argyrophilia or immunohistochemical stains for neuroendocrine differentiation such as chromogranin A (fig. 10-48, right).

Many of the composite pheochromocytomas reported to date have been functionally active, secreting excess catecholamine. These tumors are occasionally associated with a watery diarrhea syndrome due to the secretion of vasoactive intestinal peptide (VIP) (99,100). Elaboration of VIP has been associated with a neuronal or ganglionic morphologic phenotype, but this is not

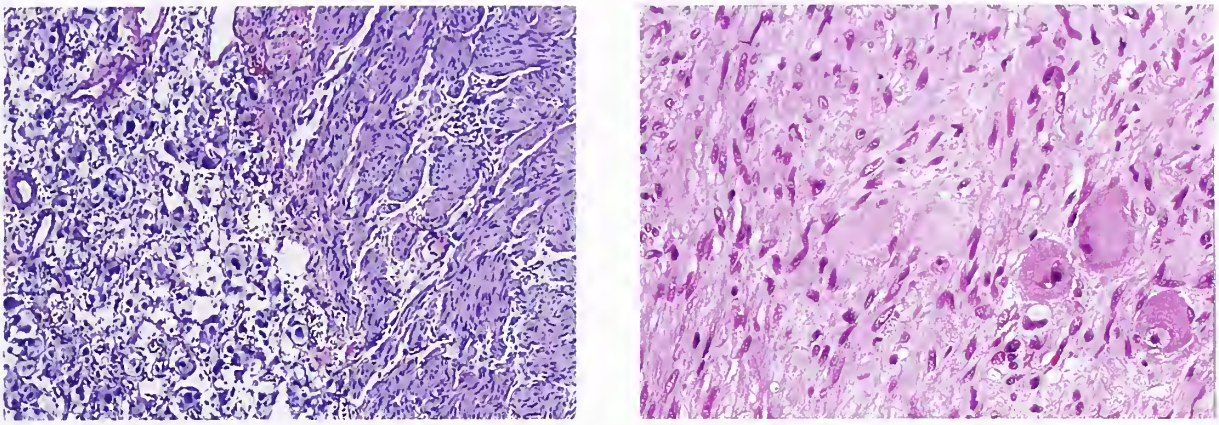

Figure 10-47

COMPOSITE PHEOCHROMOCYTOMA WITH GANGLIONEUROMA

Left: Tumor on the right of the field is a ganglioneuroma and on the left, a pheochromocytoma. The pheochromocytoma was clinically malignant and metastasized to paraaortic lymph nodes. (Fig. 10-46 from Fascicle 19, Third Series.)
Right: Several ganglion cells are apparent in the ganglioneuroma component.

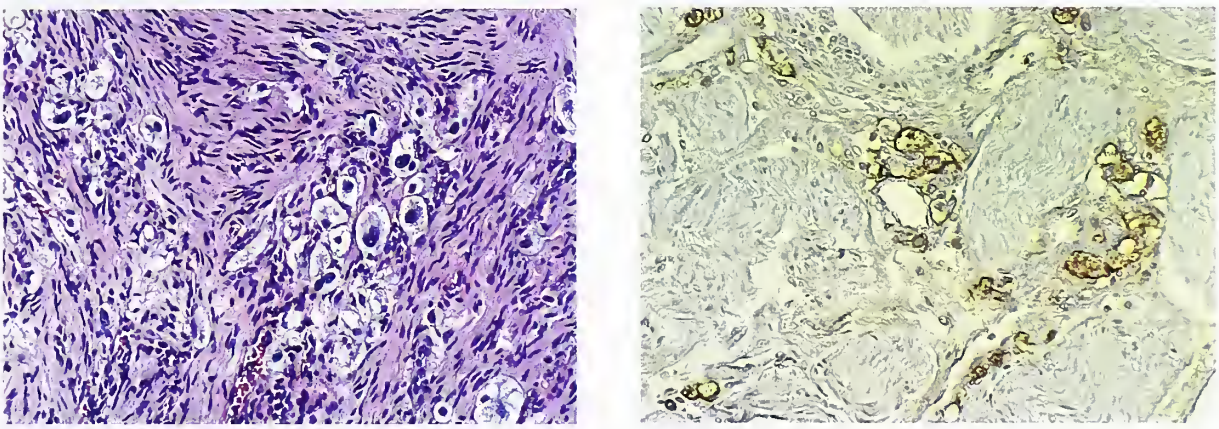

Figure 10-48

COMPOSITE PHEOCHROMOCYTOMA WITH GANGLIONEUROMA

Left: Small nests of pheochromocytoma cells are present between fascicles of Schwann cells.
Right: Immunostain for chromogranin A highlights small nests of pheochromocytoma cells (avidin-biotin peroxidase method). (L&R: Fig. 10-47 from Fascicle 19, Third Series.)

absolute (19); in vitro study of cultured human pheochromocytoma cells has also demonstrated a dissociation between VIP production and outgrowth of neuronal processes (101). Intense immunostaining for VIP is reported in non-neuronal cells, and overall the pattern for VIP reactivity among tumors is less predictable (102).

The existence of pheochromocytomas with composite neural and endocrine features is fascinating; they may be the in vivo counterpart of the neuronal phenotype that can be spontaneous or induced in cultures of human pheochromocytoma cells (101,103). The biologic behavior of composite pheochromocytomas may be as difficult to predict as more traditional pheochromocytomas. Based upon the paucity of cases reported to date, the presence of areas resembling ganglioneuroblastoma or neuroblastoma does not necessarily indicate a poorer prognosis. Some may behave in a malignant

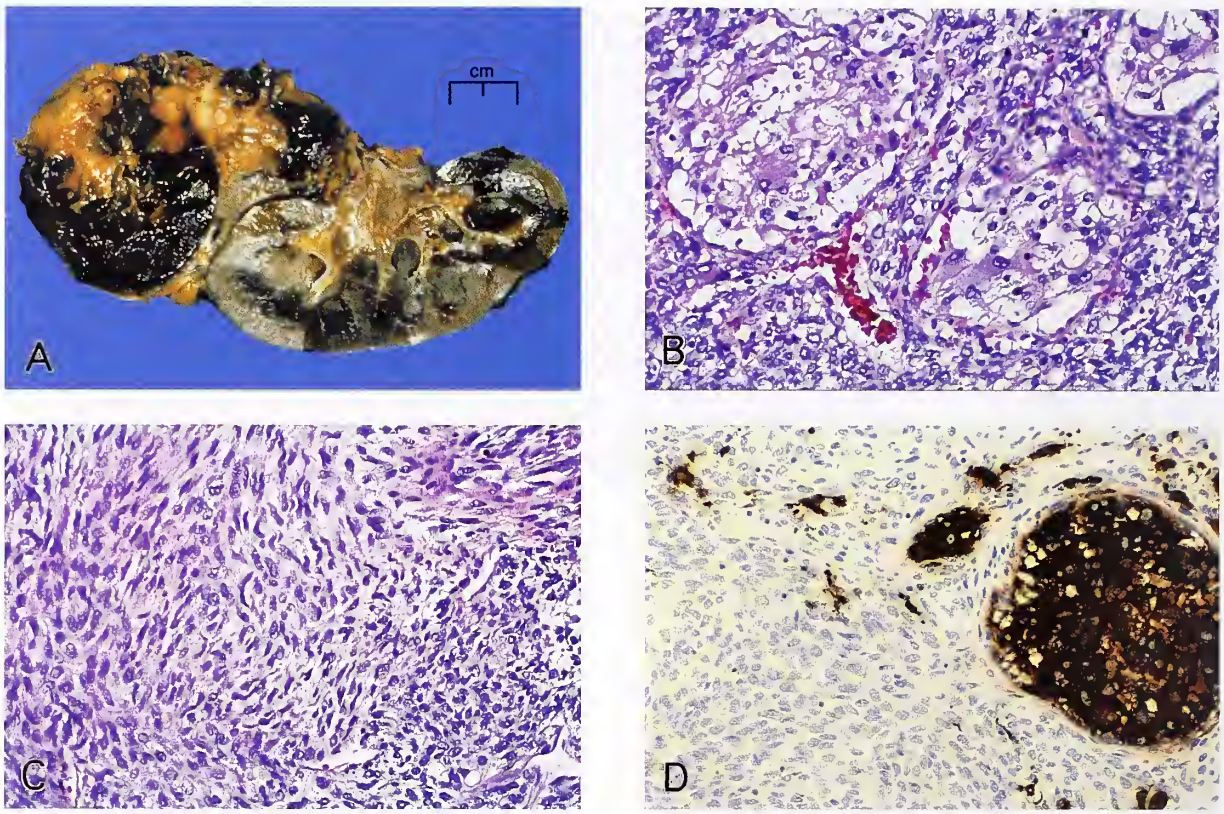

Figure 10-49

COMPOSITE PHEOCHROMOCYTOMA/MALIGNANT PERIPHERAL NERVE SHEATH TUMOR

A: A 27-year-old woman presented with acute right flank pain and was found to have a suprarenal mass; on further investigation there was a 10-fold elevation in the urinary metanephrine level. An adrenal tumor was resected along with the kidney. The adrenal tumor measured almost 10 cm in diameter and on cross section had areas of hemorrhage and necrosis. The tumor also invaded the right adrenal vein.

B: The alveolar or nesting pattern is intermingled with a spindle cell sarcoma. The pheochromocytoma had typical morphology elsewhere.

C: A little over half of the tumor sampled was a spindle cell sarcoma most consistent with malignant peripheral nerve sheath tumor.

D: Immunostain for synaptophysin demonstrates the pheochromocytoma while the sarcoma remains unstained. Some of the neoplastic chromaffin cells are apparent as small, irregular strands and nests within the sarcoma (D–F: avidin-biotin peroxidase method).

fashion with metastasis by a component of the tumor that has neural features. The author has seen only one example of a composite pheochromocytoma-malignant peripheral nerve sheath tumor (fig. 10-49).

PHEOCHROMOCYTOMA IN CHILDHOOD

Pheochromocytomas are uncommon in the pediatric age group. In a review of the first 100 cases reported in children up to 15 years of age, the average age was 11 years and the youngest patient was 5 months old (104). Bilateral pheochromocytomas have been diagnosed in a newborn infant (105). In one series, the tumor was bilateral (fig. 10-50), multicentric (fig. 10-51), or extraadrenal in 32 percent of cases (105). Multicentric paragangliomatosis has been reported in a teenager who had 21 paragangliomas (adrenal and extraadrenal) resected surgically between 13 and 17 years of age, and still had clinical evidence of additional tumors (106). Bilateral pheochromocytomas have been reported in 19 percent (105) to 24 percent (10) of cases. Familial occurrence of some tumors may help

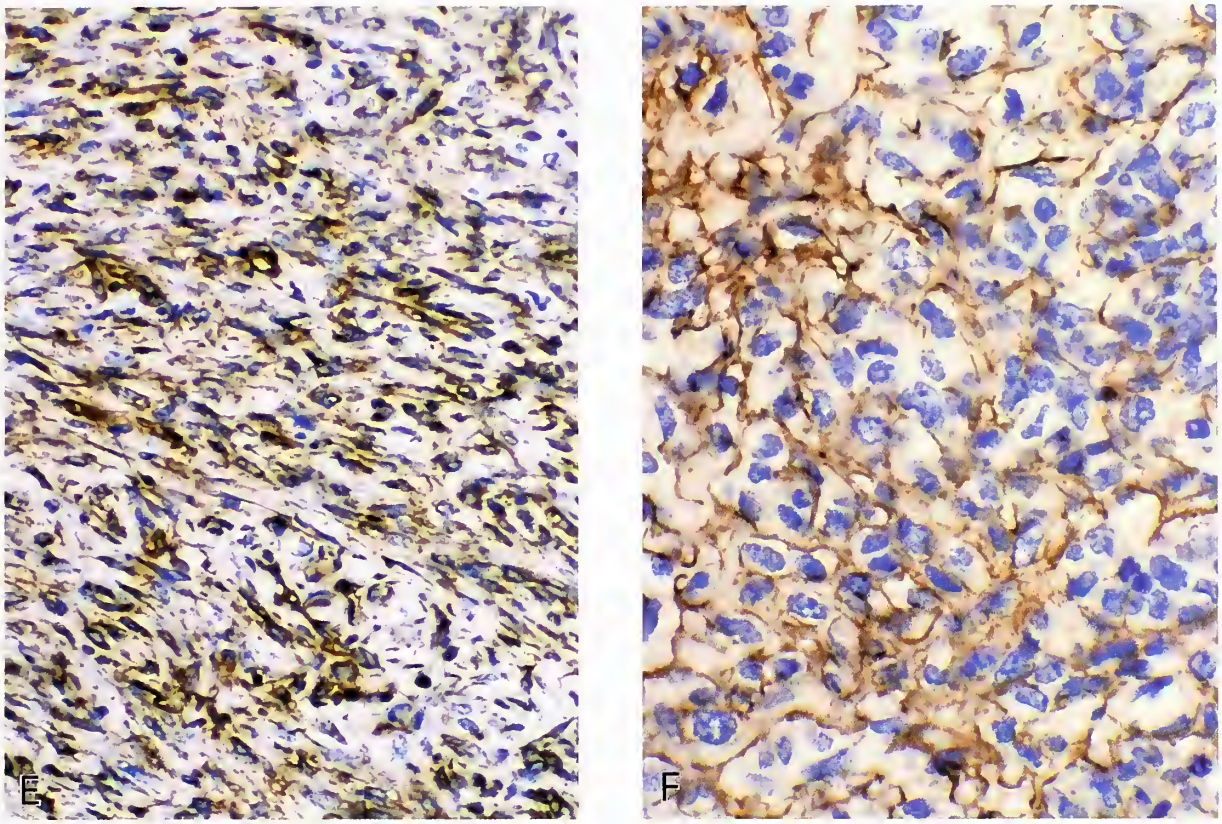

Figure 10-49 (Continued)

E: The sarcoma was strongly positive for vimentin while the endocrine component was nonreactive.
F: The intimate staining pattern for collagen type IV marks basement membrane material in the sarcoma.

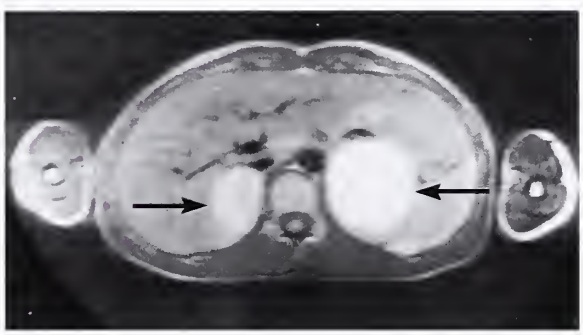

Figure 10-50

BILATERAL PHEOCHROMOCYTOMAS

A 16-year-old boy with history of back pain, nausea, vomiting, and headaches has bilateral pheochromocytomas (arrows). The tumor on the left has some cystic degeneration. Bilateral pheochromocytomas show an intense signal on T2-weighted MRI. (Fig. 4-43B from Lack EE. Adrenal medullary hyperplasia and pheochromocytoma. In: Lack EE, ed. Pathology of the adrenal glands. New York: Churchill Livingstone; 1990:172-235).

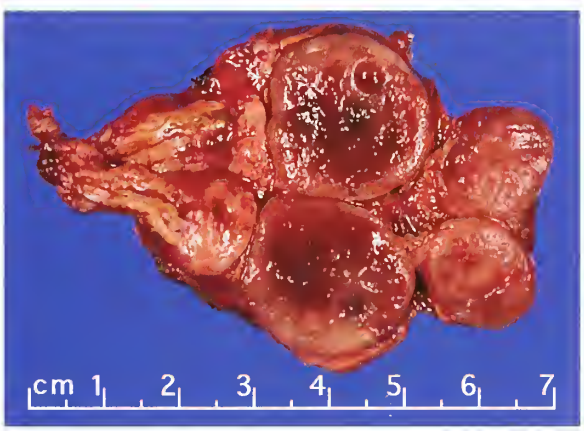

Figure 10-51

BIVALVED PHEOCHROMOCYTOMA

Bivalved pheochromocytoma from a child. Two distinct (multicentric) foci of tumor are apparent, with the larger tumor having mild cystic degeneration. (Fig. 10-50 from Fascicle 19, Third Series.)

to explain the higher incidence of bilaterality. The incidence of malignancy is similar to adults: only 2 of 85 cases (2.4 percent) were malignant in a review by Hume (10). A recent study from the Mayo Clinic reported a higher rate of malignancy and statistically significant risk factors that included extraadrenal location, apparent sporadic occurrence, and tumor size over 6 cm (107).

PSEUDOPHEOCHROMOCYTOMA

Patients with *pseudopheochromocytoma* present with the typical signs or symptoms of a pheochromocytoma, but have no pheochromocytoma or extraadrenal paraganglioma upon surgical exploration. There may be biochemical abnormalities with elevated catecholamines. Adrenal catecholamine-secreting hyperplasia enters into the differential diagnosis, and careful morphometric study may be necessary to exclude this possibility. Other pathologic anatomic lesions with features similar to pseudopheochromocytoma include adrenal myelolipoma, renal cyst (108), coarctation of abdominal aorta (109), and fibrosarcoma of pulmonary artery (110). Acute mercury poisoning (acrodynia) can also mimic pheochromocytoma (111). An unusual cause of pseudopheochromocytoma is surreptitious administration of isoproterenol (112) or epinephrine (113). Pseudopheochromocytoma has also been attributed to overactivity of adrenergic receptors (114). Rarely, adrenal cortical tumors can clinically mimic a pheochromocytoma, resulting in biochemical evidence of elevated catecholamine secretion in serum or urine (fig. 10-52) (115).

MALIGNANT PHEOCHROMOCYTOMA

Clinically *malignant pheochromocytomas* are uncommon. The diagnosis is based on evidence of extensive local invasion, or more reliably, documentation of metastasis to one or more sites where non-neoplastic chromaffin tissue is not normally present (116). Early reviews indicate a 2.5 percent (117) to 2.8 percent (10) rate of malignancy in adults and 2.4 percent in children (10). Other series report an incidence of malignancy of 2.4 percent (118), 7 percent (119), 13 percent (21), and 14 percent (120). Intraabdominal, extraadrenal paragangliomas should be excluded since these tumors tend to be more aggressive clinically (8,23). The intraoperative or perioperative mortality rate in older reports should not be confused with the incidence of clinically malignant tumors (8).

The 5-year survival rate for patients with malignant pheochromocytoma was 44 percent (21) and 53 percent (120) in two sequential series from the Mayo Clinic. The pathologic distinction between clinically benign and malignant pheochromocytomas can be impossible to make. In a study of a large number of sympathoadrenal paragangliomas, only four factors were found to have a significant statistical correlation with malignancy: 1) extraadrenal location; 2) coarse nodularity of the primary tumor; 3) confluent tumor necrosis; and 4) absence of hyaline globules (19). Compared with benign tumors, malignant tumors tend to be larger (average, 383 g versus 73 g); have a higher mitotic count (average, 3 per 30 high-power fields versus 1); and have extensive local or vascular invasion. They also express relatively fewer neuropeptides, as assessed by immunohistochemical studies, than benign tumors (19). The relationship of immunohistochemical findings to prognosis of sympathoadrenal paragangliomas is briefly discussed in chapter 11.

A few recent studies have further addressed features associated with clinically malignant pheochromocytomas (121,122): the series by Thompson (122) evaluated histomorphologic parameters only (Table 10-6) while John et al. (121) included other features such as increased tumor weight and extraadrenal location. Other studies have evaluated the role of immunohistochemical markers of cell proliferation using proliferating cell nuclear antigen (PCNA) and/or Ki-67 (MIB-1) (123,124) and concluded that there was a positive correlation with malignancy.

There may be variations in the methodology and standardization of MIB-1 labeling thus leading to inconsistent conclusions regarding correlation with malignant behavior. In one analysis, a diploid DNA pattern as determined by flow cytometry did not necessarily correlate with benign behavior (123). Tumor angiogenesis in malignant pheochromocytomas was recently evaluated and found to be a rather weak correlate of malignancy (125). In a study by Kimura et al. (126), 146 adrenal and extraadrenal pheochromocytomas were evaluated for prognostic characteristics. A scoring scale of six factors included Ki-67 immunoreactivity and types of

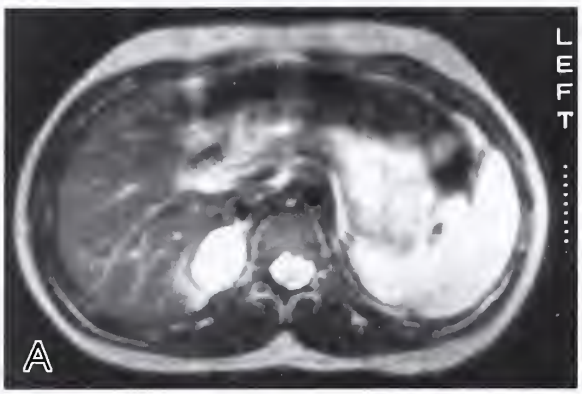

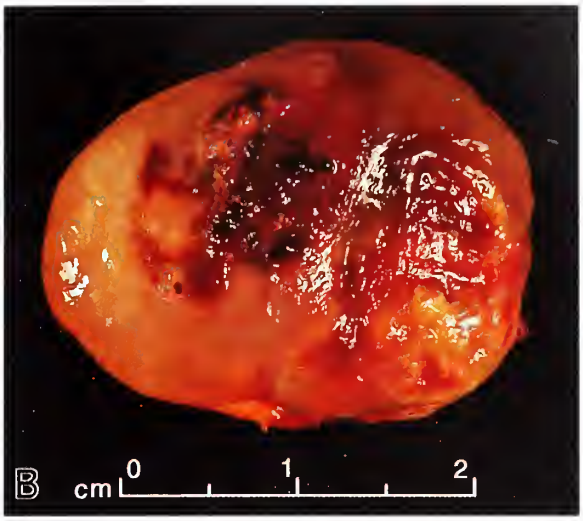

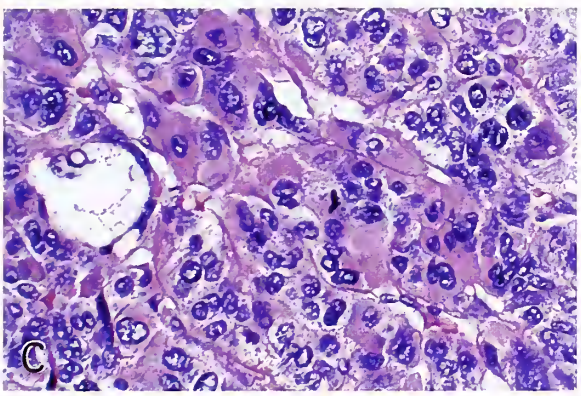

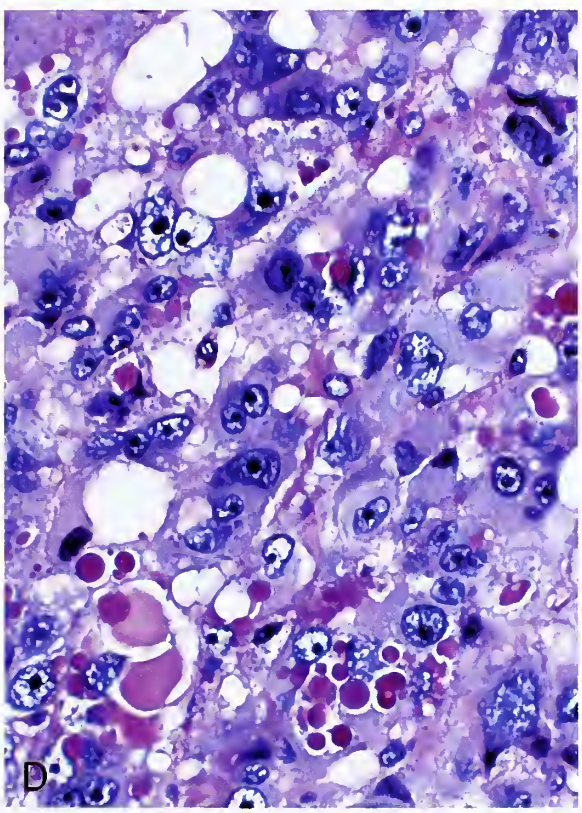

Figure 10-52

ADRENAL CORTICAL ADENOMA MIMICKING A PHEOCHROMOCYTOMA (PSEUDOPHEOCHROMOCYTOMA)

A: A 9-year-old boy presented with systemic hypertension and cardiomegaly documented on chest roentgenogram and electrocardiogram. There was also a history of blurred vision, headaches, sweating, palpitations, and intermittent facial flushing. Serum dopamine was slightly elevated, but levels of other catecholamines were normal. MRI of the upper abdomen showed a right adrenal tumor which was hyperintense on T2-weighted image. The clinical presentation coupled with the imaging characteristics strongly suggested a pheochromocytoma. The child was treated preoperatively with alpha- and beta-adrenergic blockers and the tumor was successfully resected. (Figs. A-D are from the same case.)

B: This 12-g tumor had areas of necrosis and hemorrhage. There were 15 mitoses per 50 high-power fields as well as a few atypical mitotic figures. The patient was alive and well 9 years later. The tumor may have been secreting aldosterone but laboratory evaluation was not done since the tumor was diagnosed preoperatively as a pheochromocytoma.

C: An adrenal cortical adenoma is composed of cells with compact, eosinophilic cytoplasm and are arranged in a trabecular to nested (alveolar) pattern.

D: Other areas of the same tumor had numerous cells with intracytoplasmic hyaline globules, a feature that is more frequently seen in pheochromocytomas. Globules are periodic acid–Schiff (PAS) positive and resistant to diastase predigestion. The immunostains for synaptophysin and neuron-specific enolase were focally positive in this tumor but there was no immunoreactivity for chromogranin (PAS stain after diastase predigestion).

Table 10-6

PHEOCHROMOCYTOMA OF THE ADRENAL GLAND SCORING SCALE (PASS SCORE)[a]

Feature	Score if Present (No. of Points Assigned)[b]
Large nests or diffuse growth (>10% of tumor volume)	2
Central (middle of large nests) or confluent tumor necrosis (not degenerative change)	2
High cellularity	2
Cellular monotony	2
Tumor cell spindling (even if local)	2
Mitotic figures >3/10 HPF	2
Atypical mitotic figures	2
Extension into adipose tissue	2
Vascular invasion	1
Capsular invasion	1
Profound nuclear pleomorphism	1
Nuclear hyperchromasia	1
Total	20

[a]Table 1 from reference 122.

[b]Tumors with PASS score of ≥ 4 have the potential for aggressive behavior; tumors with a PASS score of <4 are benign.

Table 10-7

SCORING SCALE FOR PHEOCHROMOCYTOMAS AND EXTRAADRENAL SYMPATHETIC PARAGANGLIOMAS[a]

Feature	Score
Histologic pattern	
Uniform cell nests	0
Large and irregular nests	1
Pseudorosettes (even if focal)	1
Cellularity	
Low (<150 cells/mm^2)	0
Moderate (150 to 250 cells/mm^2)	1
High (>250 cells/mm^2)	2
Necrosis (confluent or central in large nests)	2
Vascular or capsular invasion	1
Ki-67 immunoreactivity	
>1% or 20 cells per medium-power field	1
>3% or 50 cells per medium-power field	2
Catecholamine phenotype	
Adrenergic	0
Noradrenergic or "nonfunctional"	1
Total	10

[a]Data from reference 126.

catecholamines produced. Tumors were classified (or graded) as well, moderately well, and poorly differentiated. The results correlated with the clinical outcome. Metastases were reported in 13 percent of tumors with scores of 1 to 2, 63 percent with 3 to 6, and 100 percent with 7 to 10. In addition, 5-year survival rates of patients in the three groups were 92, 69, and 0 percent. There is need for a larger, more comprehensive analysis of pheochromocytomas to better determine the morphologic, immunophenotypic, genetic, and other factors that more accurately predict biologic behavior.

Some pheochromocytomas have a lingering or indolent course, thus mandating prolonged follow-up. Pheochromocytomas can metastasize by lymphatic or hematogenous pathways, with involvement of liver, lymph node (fig. 10-53), and bone (8,23). Rarely, a patient may present with an isolated lytic bone metastasis (8,23). A case was recently reported in which the patient survived 26 years with multiple skeletal metastases (127). Pheochromocytoma has been reported growing into the inferior vena cava and extending into the right atrium (128). Another rare complication is endobronchial metastasis (129). Laparoscopic adrenal surgery for pheochromocytoma is an acknowledged therapeutic approach in some cases. A recent report highlighted a previously unreported complication—iatrogenic pheochromocytomatosis due to local spillage of tumor during laparoscopic adrenalectomy (130).

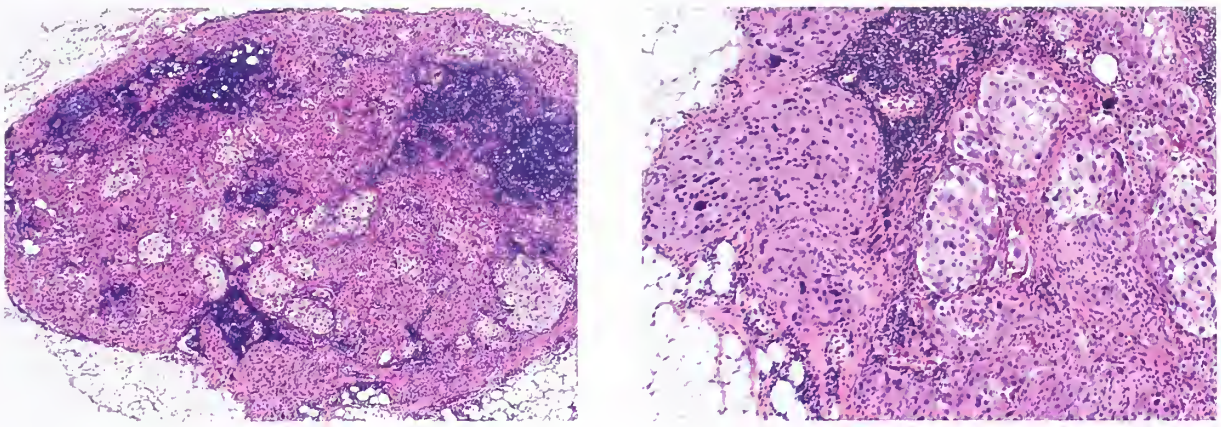

Figure 10-53

METASTATIC PHEOCHROMOCYTOMA

Left: Pheochromocytoma metastatic to a supraclavicular lymph node in a young adult with a history of pheochromocytoma resected several years before.

Right: Higher magnification shows a nesting arrangement of cells. (L&R: Fig. 10-52 from Fascicle 19, Third Series.)

REFERENCES

Incidence of Pheochromocytoma

1. Beard CM, Sheps SG, Kurland LT, Carney JA, Lie JT. Occurrence of pheochromocytoma in Rochester, Minnesota, 1950 through 1979. Mayo Clin Proc 1983;58:802-804.
2. Stenström G, Svardsudd K. Pheochromocytoma in Sweden 1958-1981. An analysis of the National Cancer Registry data. Acta Med Scand 1986;220:225-232.
3. Andersen GS, Lund JO, Toftdahl D, Strandgaard S, Nielsen PE. Pheochromocytoma and Conn's syndrome in Denmark 1977-1981. Acta Med Scand Suppl 1986:714:11-14.
4. Correa P, Chen VW. Endocrine gland cancer. Cancer 1995;75:338-352.
5. Sutton MG, Sheps SG, Lie JT. Prevalence of clinically unsuspected pheochromocytoma. Review of a 50-year autopsy series. Mayo Clin Proc 1981; 56:354-360.
6. Eisenhofer G, Bornstein SR, Brouwers FM, et al. Malignant pheochromocytoma: current status and initiatives for future progress. Endocr Relat Cancer 2004;11:423-436.
7. Patocs A, Karadi E, Toth M, et al.: Clinical and biochemical features of sporadic and hereditary phaeochromocytomas: an analysis of 41 cases investigated in a single endocrine centre. Eur J Cancer Prev 2004;13:403-409.

Clinical Features and Patterns of Catecholamine Secretion

8. Lack EE. Pathology of adrenal and extra-adrenal paraganglia. In: Major problems in pathology, Vol 29. Philadelphia: WB Saunders; 1994.
9. Manger WM, Eisenhofer G. Pheochromocytoma: diagnosis and management update. Curr Hypertens Rep 2004;6:477-484.
10. Hume DM. Pheochromocytoma in the adult and in the child. Am J Surg 1960;99:458-496.
11. Keiser HR, Doppman JL, Robertson CN, Linehan WM, Averbuch SD. Diagnosis, localization, and management of pheochromocytoma. In: Lack EE, ed. Pathology of the adrenal glands. New York: Churchill Livingstone; 1990:237-255.
12. Bravo EL. Pheochromocytoma: new concepts and future trends. Kidney Int 1991;40:544-556.
13. Feldman JM, Blalock JA, Zern RT, et al. Deficiency of dopamine-beta-hydroxylase. A new mechanism for normotensive pheochromocytomas. Am J Clin Pathol 1979;72:175-185.
14. Blake MA, Kalra MK, Maher MM, et al. Pheochromocytoma: an imaging chameleon. Radiographics 2004;24(Suppl 1):S87-S99.
15. Von Moll L, McEwan AJ, Shapiro B, et al. Iodine 131MIBG scintigraphy of neuroendocrine tumors other than pheochromocytoma and neuroblastoma. J Nucl Med 1987;28:979-988.

16. Bomanji J, Levison DA, Flatman WD, et al. Uptake of iodine-123MIBG by pheochromocytomas, paragangliomas and neuroblastomas: a histopathological comparison. J Nucl Med 1987;28:973-978.
17. Ilias I, Pacak K. Anatomical and functional imaging of metastatic pheochromocytoma. Ann N Y Acad Sci 2004;1018:495-504.
18. Trampal C, Engler H, Juhlin C, Bergstrom M, Langstrom B. Pheochromocytomas: detection with 11C hydroxyephedrine PET. Radiology 2004;230:423-428.

Sporadic Pheochromocytoma

19. Linnoila RI, Keiser HR, Steinberg SM, Lack EE. Histopathology of benign versus malignant sympathoadrenal paragangliomas: clinicopathologic study of 120 cases including unusual histologic features. Hum Pathol 1990;21:1168-1180.
20. Sherwin RP. Histopathology of pheochromocytoma. Cancer 1959;12:861-877.
21. ReMine WH, Chong GC, van Heerden JA, Sheps SG, Harrison EG Jr. Current management of pheochromocytoma. Ann Surg 1974;179:740-748.
22. Medeiros LJ, Wolf BC, Balogh K, Federman M. Adrenal pheochromocytoma: a clinicopathologic review of 60 cases. Hum Pathol 1985;16:580-589.
23. Lack EE. Adrenal medullary hyperplasia and pheochromocytoma. In: Lack EE, ed. Pathology of the adrenal glands. New York: Churchill Livingstone; 1990:173-235.
24. Hartgrink HH, Roelfsema F, Tollenaar RA, Hiddema PA, Pijl ME, van de Velde CJ. Primary pheochromocytoma extending into the right atrium: report of a case and review of the literature. Eur J Surg Oncol 2001;27:115-119.
25. Dicke TE, Henry ML, Minton JP. Intracaval extension of pheochromocytoma simulating pulmonary embolism. J Surg Oncol 1987;34:160-164.
26. Unger PD, Cohen JM, Thung SN, Gordon R, Pertsemlidis D, Dikman SH. Lipid degeneration in a pheochromocytoma histologically mimicking an adrenal cortical tumor. Arch Pathol Lab Med 1990;114:892-894.
27. Dekker A, Oehrle JS. Hyaline globules of the adrenal medulla of man. A product of lipid peroxidation? Arch Path 1971;91:353-364.
28. Lack EE, Mulvihill JJ, Travis WD, Kozakewich HP. Adrenal cortical neoplasms in the pediatric and adolescent age group. Clinicopathologic study of 30 cases with emphasis on epidemiological and prognostic factors. Pathol Annu 1992;27(pt 1):1-53.
29. Landas SK, Leigh C, Bonsib SM, Layne K. Occurrence of melanin in pheochromocytoma. Mod Pathol 1993;6:175-178.
30. Bellezza G, Giansanti M, Cavaliere A, Sidoni A. Pigmented "black" pheochromocytoma of the adrenal gland: a case report and review of the literature. Arch Pathol Lab Med 2004;128:125-128.
31. Steinhoff MM, Wells SA Jr, DeSchryver-Kecskemeti K. Stromal amyloid in pheochromocytomas. Hum Pathol 1992;23:33-36.
32. Miranda RN, Wu CD, Nayak RN, Kragel PJ, Medeiros W. Amyloid in adrenal gland pheochromocytomas. Arch Pathol Lab Med 1995;119: 827-830.
33. Melicow MM. Hibernating fat and pheochromocytoma. Arch Pathol Lab Med 1957;63:367-372.
34. Lean ME, James WP, Jennings G, Trayhurn P. Brown adipose tissue in patients with phaeochromocytoma. Int J Obesity 1986;10:219-227.
35. Medeiros LJ, Katsas GG, Balogh K. Brown fat and adrenal pheochromocytoma: association or coincidence? Hum Pathol 1985;16:970-972.
36. English JT, Patel SK, Flanagan MJ. Association of pheochromocytomas with brown fat tumors. Radiology 1973;107:279-281.
37. Klausner JM, Nakash R, Inbar M, Gutman M, Lelcuk S, Rozin RR. Prolonged fever as a presenting symptom in adrenal tumors. Oncology 1988;45:15-17.
38. Van Vliet PD, Burchell HB, Titus JL. Focal myocarditis associated with pheochromocytoma. N Engl J Med 1966;274:1102-1108.
39. Luscher TF, Lie JT, Stanson AW, Houser OW, Hollier LH, Sheps SG. Arterial fibromuscular dysplasia. Mayo Clin Proc 1987;62:931-952.
40. DeSouza TG, Berlad L, Shapiro K, Walsh C, Saenger P, Shinnar S. Pheochromocytoma and multiple intracerebral aneurysms. J Pediatr 1986; 108:947-949.
41. Manger WM, Gifford RW Jr. Pheochromocytoma. New York: Springer-Verlag; 1977.

Familial Pheochromocytoma

42. Greene JP, Guay AT. New perspectives in pheochromocytomas. Urol Clin North Am 1989;16: 487-503.
43. Brandi ML, Gagel RF, Angeli A, et al. Guidelines for diagnosis and therapy of MEN type 1 and type 2. J Clin Endocrinol Metab 2001;86:5658-5671.
44. Riccardi VM. Von Recklinghausen neurofibromatosis. N Engl J Med 1981;305:1617-1627.
45. Kalff V, Shapiro B, Lloyd R, et al. The spectrum of pheochromocytoma in hypertensive patients with neurofibromatosis. Arch Intern Med 1982;142:2092-2098.
46. Horton WA, Wong V, Eldridge R. Von Hippel-Lindau disease: clinical and pathological manifestations in nine families with 50 affected members. Arch Intern Med 1976;136;769-777.

47. Neumann HP, Berger DP, Sigmund G, et al. Pheochromocytomas, multiple endocrine neoplasia type 2, and von Hipple-Lindau disease. N Engl J Med 1993;329:1531-1538.
48. Atuk NO, McDonald T, Wood T, et al. Familial pheochromocytoma, hypercalcemia, and von Hippel Lindau disease. A ten year study of a large family. Medicine (Baltimore) 1979;58:209-2018.
49. Chetty R, Duhig JD. Bilateral pheochromocytoma-ganglioneuroma of the adrenal in type 1 neurofibromatosis. Am J Surg Pathol 1993;17: 837-841.
50. Sakaguchi N, Sano K, Ito M, Baba T, Fukuzawa M, Hotchi M. A case of von Recklinghausen's disease with bilateral pheochromocytoma-malignant peripheral nerve sheath tumors of the adrenal and gastrointestinal autonomic nerve tumors. Am J Surg Pathol 1996;20:889-897.
51. Opocher G, Conton P, Schiavi F, Macino B, Mantero F. Pheochromocytoma in von Hippel-Lindau disease and neurofibromatosis type 1. Fam Cancer 2005;4:13-16.
52. de Krijger RR. Endocrine tumor syndromes in infancy and childhood. Endocr Pathol 2004;15: 223-226.
53. Agarwal SK, Lee Burns A, Sukhodolets KE, et al. Molecular pathology of the MEN 1 gene. Ann N Y Acad Sci 2004;1014:189-198.
54. Marx SJ: Molecular genetics of multiple endocrine neoplasia types 1 and 2. Nat Rev Cancer 2005;5:367-375.
55. Gimm O, Koch CA, Januszewicz A, Opocher G, Neumann HP. The genetic basis of pheochromocytoma. Front Horm Res 2004;31:45-60.
56. Carney JA, Sizemore GW, Tyce GM. Bilateral adrenal medullary hyperplasia in multiple endocrine neoplasia, type 2: the precursor of bilateral pheochromocytoma. Mayo Clin Proc 1975; 50:3-10.
57. Evans DB, Lee JE, Merrell RC, Hickey RC. Adrenal medullary disease in multiple endocrine neoplasia type 2. Appropriate management. Endocrinol Metab Clin North Am 1994;23:167-176.
58. Cance WG, Wells SA Jr. Multiple endocrine neoplasia. Type IIa. Curr Probl Surg 1985;22:8-56.
59. Lips CJ, van der Sluys Veer J, Struyvenberg A, et al. Bilateral occurrence of pheochromocytoma in patients with the multiple endocrine neoplasia syndrome type 2a (Sipple's syndrome). Am J Med 1981;70:1051-1060.
60. Carney JA, Sizemore GW, Sheps SG. Adrenal medullary disease in multiple endocrine neoplasia, type 2: pheochromocytoma and its precursors. Am J Clin Pathol 1976;66:279-290.
61. DeLellis RA, Wolfe HJ, Gagel RF, et al. Adrenal medullary hyperplasia. A morphometric analysis in patients with familial medullary thyroid carcinoma. Am J Pathol 1976;83:177-190.
62. Gagel RF, Tashjian AH Jr, Cummings T, et al. The clinical outcome of prospective screening for multiple endocrine neoplasia type 2a. An 18-year experience. N Engl J Med 1988;318:478-484.
63. Mendonca BB, Arnhold IJ, Nicolau W, Avancini VA, Boise W. Cushing's syndrome due to ectopic ACTH secretion by bilateral pheochromocytomas in multiple endocrine neoplasia type 2A. N Engl J Med 1988;319:1610-1611.
64. Koch CA, Mauro D, Walther MM, et al. Pheochromocytoma in von hippel-lindau disease: distinct histopathologic phenotype compared to pheochromocytoma in multiple endocrine neoplasia type 2. Endocr Pathol 2002;13:17-27.
65. Webb TA, Sheps SG, Carney JA. Differences between sporadic pheochromocytoma and pheochromocytoma in multiple endocrine neoplasia, type 2. Am J Surg Pathol 1980;4:121-126
66. Frank-Raue K, Rondot S, Hoeppner W, Goretzki P, Raue F, Meng W. Coincidence of multiple endocrine neoplasia types 1 and 2: mutations in the RET protooncogene and MEN1 tumor suppressor gene in a family presenting with recurrent primary hyperparathyroidism. J Clin Endocrinol Metab 2005;90:4063-4067.
67. Pacak K, Ilias I, Adams KT, Eisenhofer G. Biochemical diagnosis, localization and management of pheochromocytoma: focus on multiple endocrine neoplasia type 2 in relation to other hereditary syndromes and sporadic forms of the tumour. J Intern Med 2005;257:60-68.
68. Hinze R, Machens A, Schneider U, Holzhausen HJ, Dralle H, Rath FW. Simultaneously occurring liver metastases of pheochromocytoma and medullary thyroid carcinoma—a diagnostic pitfall with clinical implications for patients with multiple endocrine neoplasia type 2a. Pathol Res Pract 2000;196:477-481.
69. Gorlin RJ, Mirkin BL. Multiple mucosal neuromas, pheochromocytoma, medullary carcinoma of the thyroid and marfanoid body build with muscle wasting. Syndrome of hyperplasia and neoplasia of neural crest derivatives—an unitarian concept. Z Kinderheilk 1972;113:313-325.
70. Carney JA, Sizemore GW, Lovestedt SA. Mucosal ganglioneuromatosis, medullary thyroid carcinoma, and pheochromocytoma: multiple endocrine neoplasia, type 2b. Oral Surg Oral Med Oral Pathol 1976;41:739-752.
71. Dyck PJ, Carney JA, Sizemore GW, Okazaki H, Brimijoin WS, Lambert EH. Multiple endocrine neoplasia type 2b: phenotype recognition; neurological features and their pathologic basis. Ann Neurol 1979;6:302-314.

72. Rougier PH, Caillou B, Parmentier C, Lemerle J. Multiple endocrine neoplasia type 2b: experience at Villejuif. In: Humphrey GB, Grindey GB, Dehner LP, Acton RT, Pysher TJ, eds. Adrenal and endocrine tumors in children. Boston: Martinus Nijhoff; 1983:343-347.
73. Carney JA, Sizemore GW, Hayles AB. Multiple endocrine neoplasia, type 2b. Pathobiol Annu 1978;8:105-153.
74. Carney JA, Roth SI, Heath H 3rd, Sizemore GW, Hayles AB. The parathyroid glands in multiple endocrine neoplasia, type 2b. Am J Pathol 1980;99:397-400.
75. Carney JA, Go VL, Sizemore GW, Hayles AB. Alimentary-tract ganglioneuromatosis. A major component of the syndrome of multiple endocrine neoplasia, type 2b. N Engl J Med 1976;295: 1287-1291.
76. Prabhu M, Khouzam RN, Insel J. Multiple endocrine neoplasia type 2 syndrome presenting with bowel obstruction caused by intestinal neuroma: case report. South Med J 2004;97:1130-1132.
77. Mendelsohn G, Diamond MP. Familial ganglioneuromatous polyposis of the large bowel. Report of a family with associated juvenile polyposis. Am J Surg Pathol 1984;8:515-520.
78. d'Amore ES, Manivel JC, Pettinato G, Niehans GA, Snover DC. Intestinal ganglioneuromatosis: mucosal and transmural types. A clinicopathologic and immunohistochemical study of six cases. Hum Pathol 1991;22:276-286.
79. Shekitka KM, Sobin LH. Ganglioneuromas of the gastrointestinal tract. Relation to Von Recklinghausen disease and other multiple tumor syndromes. Am J Surg Pathol 1994;18:250-257.
80. Lora MS, Waguespack SG, Moley JF, Walvoord EC. Adrenal ganglioneuromas in children with multiple endocrine neoplasia type 2: a report of two cases. J Clin Endocrinol Metab 2005;90: 4383-4387.
81. Norton JA, Froome LC, Farrell RE, Wells SR Jr. Multiple endocrine neoplasia type IIb: the most aggressive form of medullary thyroid carcinoma. Surg Clin North Am 1979;59:109-118.
82. Zimmerman P, DaSilva M, Newman T, Marx W, Simon H. Simultaneous bilateral laparoscopic adrenalectomy: a surgical option for multiple endocrine neoplasia (MEN 2) patients with bilateral pheochromocytomas. Surg Endosc 2004; 18:870.
83. Yip L, Lee JE, Shapiro SE, et al. Surgical management of hereditary pheochromocytoma. J Am Coll Surg 2004;198:525-534.
84. Carney JA. Familial multiple endocrine neoplasia: the first 100 years. Am J Surg Pathol 2005;29: 254-274.

Gastric Stromal sarcoma, Pulmonary Chondroma, and Extraadrenal Paraganglioma

85. Carney JA, Sheps SG, Go VL, Gordon H. The triad of gastric leiomyosarcoma, functioning extra-adrenal paraganglioma and pulmonary chondroma. N Engl J Med 1977;296:1517-1518.
86. Carney JA. Gastric stromal sarcoma, pulmonary chondroma, and extra-adrenal paraganglioma (Carney Triad): natural history, adrenocortical component, and possible familial occurrence. Mayo Clin Proc. 1999;74:543-552.
87. Cooper HS. Intestinal neoplasms. In: Mills SE, Carter D, Greenson JK, Oberman HA, Reuter V, Stoler MH, eds. Sternberg's diagnostic surgical pathology, Philadelphia: Lippincott, Williams & Wilkins; 2004:1543-1601.

Composite Pheochromocytoma

88. Franquemont DW, Mills SE, Lack EE. Immunohistochemical detection of neuroblastomatous foci in composite adrenal pheochromocytoma-neuroblastoma. Am J Clin Pathol 1994;102:163-70.
89. Kragel PJ, Johnston CA. Pheochromocytoma-ganglioneuroma of the adrenal. Arch Pathol Lab Med 1985;109:470-472.
90. Brady S, Lechan RM, Schwaitzberg SD, Dayal Y, Ziar J, Tischler AS. Composite pheochromocytoma/ganglioneuroma of the adrenal gland associated with multiple endocrine neoplasia 2A: case report with immunohistochemical analysis. Am J Surg Pathol 1997;21:102-108.
91. Miettinen M, Saari A. Pheochromocytoma combined with malignant schwannoma: unusual neoplasm of the adrenal medulla. Ultrastruct Pathol 1988;12:513-527.
92. Min KW, Clemens A, Bell J, Dick H. Malignant peripheral nerve sheath tumor and pheochromocytoma. A composite tumor of the adrenal. Arch Pathol Lab Med 1988;112:266-270.
93. Ayala GE, Ettinghausen SE, Epstein AH Travis WD, Lack EE. Primary malignant peripheral nerve sheath tumor of the adrenal gland. Case report and literature review. J Urol Pathol 1994; 2:265-272.
94. Wieneke JA, Thompson LD, Heffess CS. Corticomedullary mixed tumor of the adrenal gland. Ann Diagn Pathol 2001;5:304-308.
95. Inoue J, Oishi S, Naomi S, Umeda T, Sato T. Pheochromocytoma associated with adrenocortical adenoma: case report and literature review. Endocrinol Jpn 1986;33:67-74.
96. Sparagana M, Feldman JM, Molnar Z. An unusual pheochromocytoma associated with an androgen secreting adrenocortical adenoma. Evaluation of its polypeptide hormone, catecholamine, and enzyme characteristics. Cancer 1987;60:223-231.

97. Aiba M, Hirayama A, Ito Y, et al. A compound adrenal medullary tumor (pheochromocytoma and ganglioneuroma) and a cortical adenoma in the ipsilateral adrenal gland. A case report with enzyme histochemical and immunohistochemical studies. Am J Surg Pathol 1988;12: 559-566.
98. Juarez D, Brown RW, Ostrowski M, Reardon MJ, Lechago J, Truong LD. Pheochromocytoma associated with neuroendocrine carcinoma. A new type of composite pheochromocytoma. Arch Pathol Lab Med 1999;123:1274-1279.
99. Trump DL, Livingston JN, Baylin SB. Watery diarrhea syndrome in an adult with ganglioneuroma-pheochromocytoma: identification of vasoactive intestinal peptide, calcitonin, and catecholamines and assessment of their biologic activity. Cancer 1977;40:1526-1532.
100. Mendelsohn G, Eggleston JC, Olson JL, Said SI, Baylin SB. Vasoactive intestinal peptide and its relationship to ganglion cell differentiation in neuroblastic tumors. Lab Invest 1979;41:144-149.
101. Tischler AS, Lee YC, Perlman RL, Costopoulos D, Slayton VW, Bloom SR. Production of "ectopic" vasoactive intestinal peptide-like and neurotensin-like immunoreactivity in human pheochromocytoma cell cultures. J Neurosci 1984;4:1398-1404.
102. Tischler AS, Dayal Y, Balogh K, Cohen RB, Connolly JL, Tallberg K. The distribution of immunoreactive chromogranins, S-100 protein, and vasoactive intestinal peptide in compound tumors of the adrenal medulla. Hum Pathol 1987;18:909-917.
103. Tischler AS, Dichter MA, Biales B, DeLellis RA, Wolfe H. Neural properties of cultured human endocrine tumor cells of proposed neural crest origin. Science 1976;192:902-904.

Pheochromocytoma in Childhood

104. Stackpole RH, Melicow MM, Uson AC. Pheochromocytoma in children. Report of 9 cases and review of the first 100 published cases with follow-up studies. J Pediatr 1963;63:315-330.
105. Kaufman BH, Telander RL, van Heerden JA, Zimmerman D, Sheps SG, Dawson B. Pheochromocytoma in the pediatric age group: current status. J Ped Surg 1983;18:879-884.
106. Karasov RS, Sheps SG, Carney JA, van Heerden JA, DeQuattro V. Paragangliomatosis with numerous catecholamine-producing tumors. Mayo Clin Proc 1982;57:590-595.
107. Pham TH, Moir C, Thompson GB, et al. Pheochromocytoma and paraganglioma in children: a review of medical and surgical management at a tertiary care center. Pediatrics 2006;118:1109-1117.

Pseudopheochromocytoma

108. Weaver JC, Kawata N, Hinman F Jr. Renal cyst simulating pheochromocytoma. Post Grad Med 1952;11:294-298.
109. Goldzieher JW, McMahon HE, Goldzieher MA. Coarctation of the abdominal aorta simulating pheochromocytoma. AMA Arch Int Med 1951;88:835-839.
110. Wolf PL, Dickenman RC, Langston JD. Fibrosarcoma of the pulmonary artery, masquerading as a pheochromocytoma. Am J Clin Pathol 1960;34:146-154.
111. Henningsson C, Hoffmann S, McGonigle L, Winter JS. Acute mercury poisoning (acrodynia) mimicking pheochromocytoma in an adolescent. J Ped 1993;122:252-253.
112. Lurvey A, Yussin A, DeQuattro V. Pseudopheochromocytoma after self-administered isoproterenol. J Clin Endocrinol Metab 1973;36: 766-769.
113. Brandenburg RO Jr, Gutnik LM, Nelson RL, Abboud CF, Edis AJ, Sheps SG. Factitial epinephrine-only secreting pheochromocytoma. Ann Intern Med 1979;90:795.
114. Blum I, Weinstein R, Sztern M, Lahav M. Adrenergic receptor hyperactivity—a cause for pseudopheochromocytoma? Med Hypotheses 1987;22:89-96.
115. Alsabeh R, Mazoujian G, Goates J, Medeiros LJ, Weiss LM. Adrenal cortical tumors clinically mimicking pheochromocytoma. Am J Clin Pathol 1995;104:382-390.

Malignant Pheochromocytoma

116. Neville AM. The adrenal medulla. In: Symington T, ed. Functional pathology of the human adrenal glands. Baltimore: Williams & Wilkins; 1969:219-324.
117. Symington T, Goodall AL. Studies in phaeochromocytoma. 1. Pathological aspects. Glasgow Med J 1953;34:75-96.
118. Melicow MM. One hundred cases of pheochromocytoma (107 tumors) at the Columbia-Presbyterian Medical Center, 1926-1976: a clinicopathological analysis. Cancer 1977;40:1987-2004.
119. Modlin IM, Farndon JR, Shepherd A, et al. Phaeochromocytomas in 72 patients: clinical and diagnostic features, treatment and long term results. Br J Surg 1979;66:456-465.
120. van Heerden JA, Sheps SG, Hamberger B, Sheedy PF 2nd, Poston JG, ReMine WH. Pheochromocytoma: current status and changing trends. Surgery 1982;91:367-373.
121. John H, Ziegler WH, Hauri D, Jaeger P. Pheochromocytomas: can malignant potential be predicted? Urology 1999;53:679-683.

122. Thompson LD. Pheochromocytoma of the adrenal gland scaled score (PASS) to separate benign from malignant neoplasms: a clinicopathologic and immunophenotypic study of 100 cases. Am J Surg Pathol 2002;26:551-566.
123. Brown HM, Komorowski RA, Wilson SD, Demeure MJ, Zhu YR. Predicting metastasis of pheochromocytomas using DNA flow cytometry and immunohistochemical markers of cell proliferation: a positive correlation between MIB-1 staining and malignant tumor behavior. Cancer 1999;86:1583-1589.
124. van der Harst E, Bruining HA, Jaap Bonjer H, et al. Proliferative index in phaeochromocytomas: does it predict the occurrence of metastases? J Pathol 2000;191:175-180.
125. Rooijens, PP, de Krijger RR, Bonjer HJ, et al. The significance of angiogenesis in malignant pheochromocytomas. Endocr Pathol 2004;15:39-46.
126. Kimura N, Watanabe T, Noshiro T, Shizawa S, Miura Y. Histological grading of adrenal and extra-adrenal pheochromocytomas and relationship to prognosis: a clinicopathological analysis of 116 adrenal pheochromocytomas and 30 extra-adrenal sympathetic paragangliomas including 38 malignant tumors. Endocr Pathol 2005;16:23-32.
127. Yoshida S, Hatori M, Noshiro T, Kimura N, Kokubun S. Twenty-six-years' survival with multiple bone metastasis of malignant pheochromocytoma. Arch Orthop Trauma Surg 2001;121:598-600.
128. Hartgrink HH, Roelfsema F, Tollenaar RA, Hiddema PA, Pijl ME, van de Velde CJ. Primary pheochromocytoma extending into the right atrium: report of a case and review of the literature. Eur J Surg Oncol 2001;27:115-119.
129. Sandur S, Dasgupta A, Shapiro JL, Arroliga AC, Mehta AC. Thoracic involvement with pheochromocytoma: a review. Chest 1999;115:511-521.
130. Li ML, Fitzgerald PA, Price DC, Norton JA. Iatrogenic pheochromocytomatosis: a previously unreported result of laparoscopic adrenalectomy. Surgery 2001;130:1072-1077.

11 EXTRAADRENAL PARAGANGLIA, PARAGANGLIOMAS, AND OTHER FEATURES OF SYMPATHOADRENAL PARAGANGLIOMAS

EXTRAADRENAL PARAGANGLIA

The sympathoadrenal neuroendocrine system is an integrated complex composed of the sympathetic nervous system, with postganglionic neurons mediating effector responses via the neurotransmitter norepinephrine, and the adrenal medullae, which synthesize and secrete the hormones epinephrine and, in lesser amounts, norepinephrine (1,2). *Extraadrenal paraganglia* of the neuroendocrine system are distributed along the paravertebral and paraaortic axis, closely paralleling the distribution of the sympathetic nervous system (fig. 11-1) (3); tumors arise from the sympathoadrenal paraganglia along this axis. The adrenal medullae are the largest compact collection of paraganglia in this system, and the most common site of paragangliomas (pheochromocytomas).

The nomenclature of extraadrenal paragangliomas is based upon anatomic site of origin. Glenner and Grimley (4) recognized four families of extraadrenal paraganglia: branchiomeric, intravagal, aorticosympathetic, and visceral-autonomic; these families are based upon anatomic distribution, innervation, and microscopic structure. The visceroautonomic paraganglia are poorly defined, and occur in association with visceral organs and blood vessels.

Gross Anatomy

Extraadrenal paraganglia are usually tiny structures, recognizable only with the aid of a microscope. The paraganglia described by Zuckerkandl in 1901 (fig. 11-2), some of which can be detected macroscopically, are an exception (5,6). These paraganglia were identified in the human fetus and newborn on either side of the aorta, with the cephalic component near the origin of the superior mesenteric artery or the renal arteries, and the caudal portion at or just above the aortic bifurcation; they were referred to as aortic bodies (5). In 14.8 percent of cases, these extraadrenal paraganglia are united by an isthmus lying anterior to the aorta just below the superior mesenteric artery (fig. 11-2, right); in other cases they are multiple separate collections (fig. 11-2, left). The multiplicity of

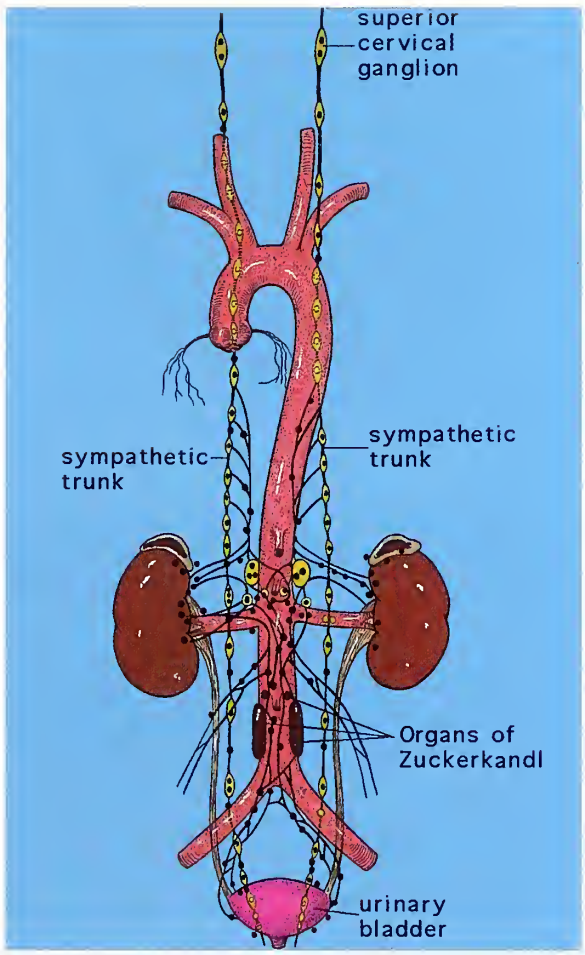

Figure 11-1

ANATOMIC DISTRIBUTION OF SYMPATHOADRENAL PARAGANGLIA

The paraganglia extend from the neck on either side down to the base of the pelvis. (Modified from fig. 64 from Coupland RE. The natural history of the chromaffin cell. Boston: Little, Brown & Co.; 1965:194.)

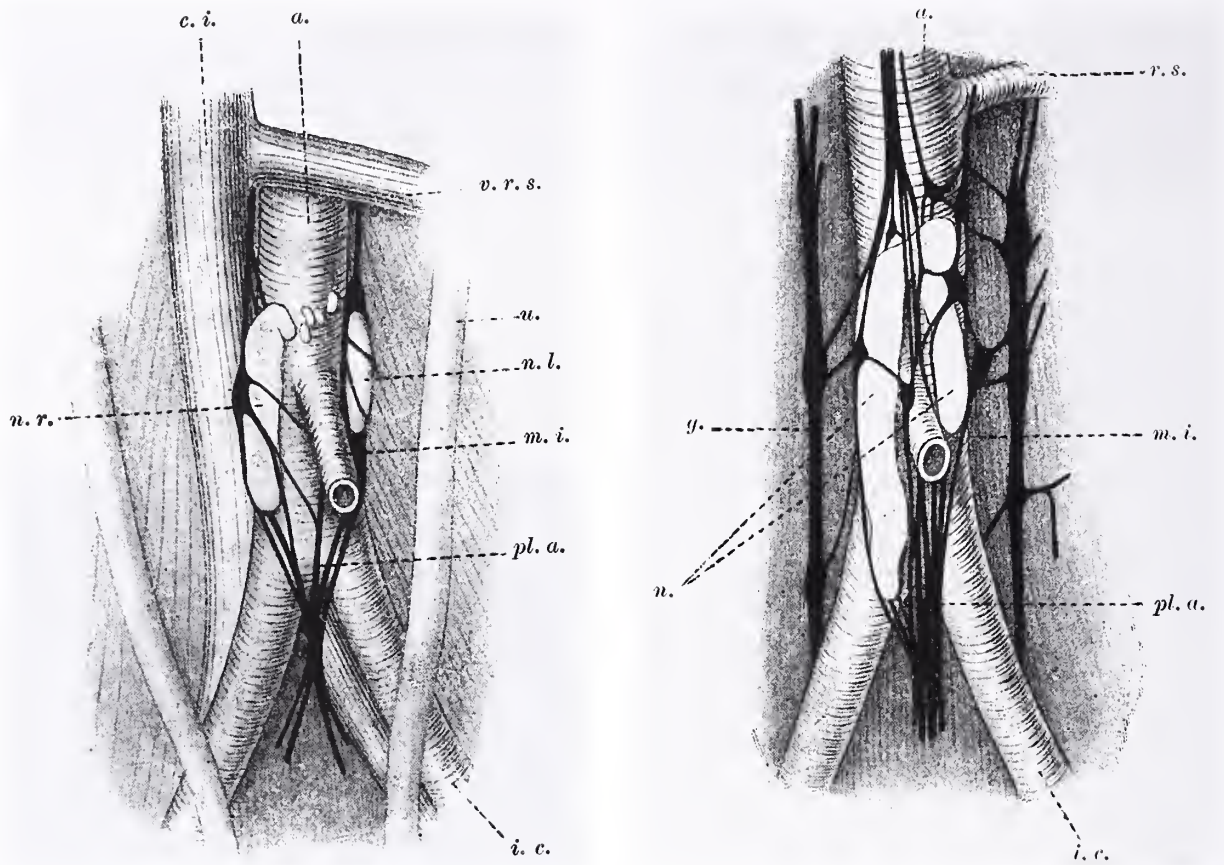

Figure 11-2

ORGANS OF ZUCKERKANDL

Left: Organs of Zuckerkandl in most cases appear as multiple discrete collections of paraganglia on either side of the aorta. Right: In a minority of cases, the paraganglion is a continuous structure forming a partial collarette about the origin of the inferior mesenteric artery. (Figs. 1 and 2 from Zuckerkandl E. Ueber nebenorgane des sympathicus im retroperitonealraum des manschen. Verh Dtsch Anat Ges 1901;15:95-107. [German])

these extraadrenal paraganglia argues against use of the term *"organ" of Zuckerkandl.* In Zuckerkandl's experience, the average length of the right aortic bodies was 11.6 mm and left, 8.8 mm; the number of extraadrenal paraganglia in the abdominal plexuses varied from 12 to 26 (6).

Microscopic Anatomy

The spatial distribution of the organs of Zuckerkandl is shown in figure 11-3 in a human fetus of about 11 weeks' gestational age. In the human fetus, extraadrenal paraganglia such as these are much more prominent than the developing adrenal medulla. These elongated collections of cells on either side of the aorta appear sharply defined, but in most cases are not truly encapsulated (fig. 11-4). There is a delicate microvasculature which subdivides the chromaffin cells into small nests and anastomosing short cords. These cells contrast sharply with the adjacent primitive neuroblasts, many of which will develop into ganglion cells (fig. 11-5). The fact that this chromaffin tissue complex resembles, but is not actually composed of, true ganglia, prompted the designation *paraganglion* by Alfred Kohn in 1903 (7). The developing chromaffin cells have slightly larger nuclei, which are pale staining, and there is an increased cytoplasmic volume with better defined borders. Paraganglia seen elsewhere in the abdomen or in other sites along the sympathetic axis (e.g., intrathoracic region) have a similar

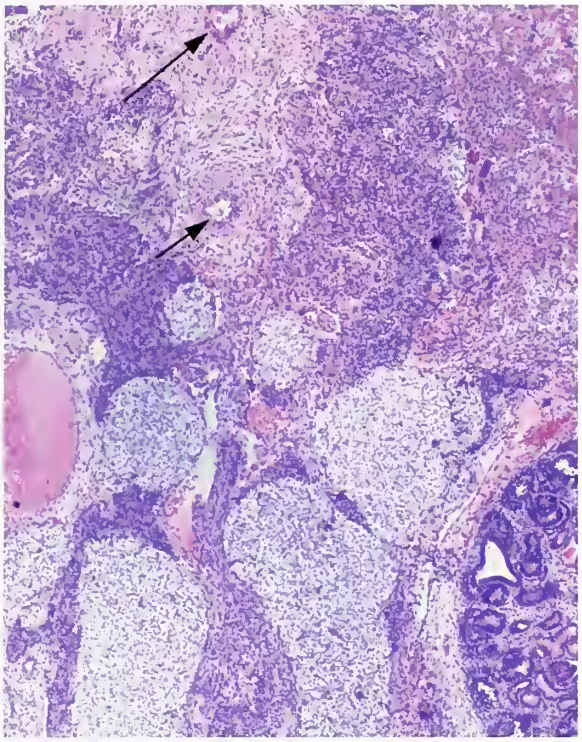

Figure 11-3

ORGANS OF ZUCKERKANDL

Coronal section just anterior to the abdominal aorta in an 11-week-old fetus shows multiple collections of pale-staining paraganglia, with the largest elongated collections in the lower half of the field. The lower pole of the left kidney is evident along with a portion of the developing adrenal gland (right upper corner). The adrenal gland is close to a large paravertebral and paraaortic sympathetic plexus. Near the top of the field is a cross section of the celiac artery (long arrow) and just below it the superior mesenteric artery (short arrow). An oblique section of the adventitia of the inferior mesenteric artery was apparent in other sections.

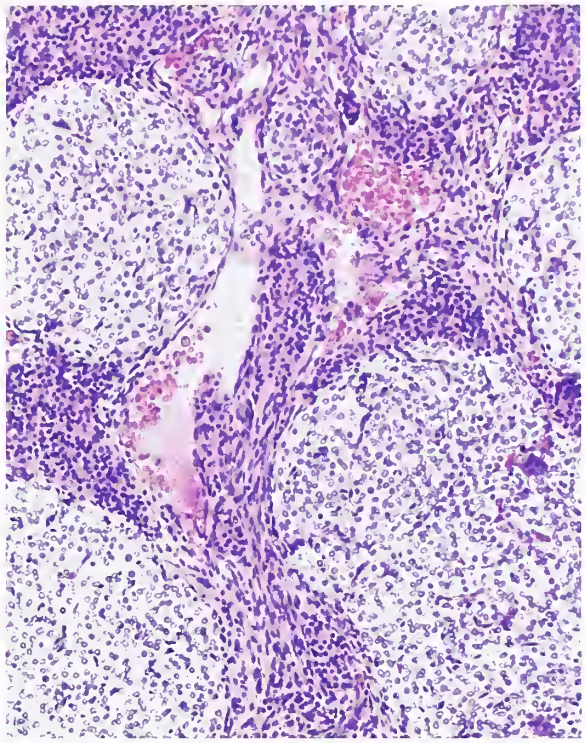

Figure 11-4

ORGANS OF ZUCKERKANDL

Multiple separate paraganglia have cells with pale cytoplasm and are sharply circumscribed but are not truly encapsulated.

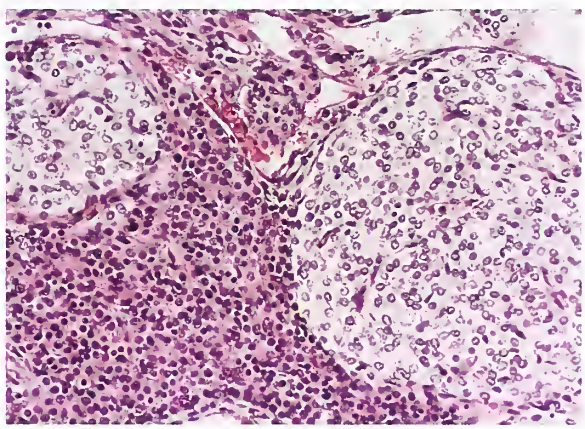

Figure 11-5

ORGANS OF ZUCKERKANDL

The cells of these paraganglia at this early stage of development have pale cytoplasm with relatively indistinct borders. Nuclei are round to oval with dispersed chromatin. Contrast these cells with adjacent neuroblastic cells which are associated with the developing neural plexus. (Fig. 11-5 from Fascicle 19, Third Series.)

microscopic appearance (8). In the older fetus and young infant, these paraganglia become better developed, with more mature chromaffin cells.

Intraabdominal paraaortic paraganglia increase in size in humans up to 3 years of age; between 3 and 5 years they undergo degenerative changes with increased stroma (9). These changes are most marked in the organs of Zuckerkandl, with disintegration and involution by 14 years of age (9). In adults, discrete microscopic collections of extraadrenal chromaffin tissue persist (fig. 11-6) (10,11). The microscopic appearance is virtually identical to that of the adrenal medulla (fig. 11-7A), and occasionally may be associated with ganglion cells (fig. 11-7B) or small

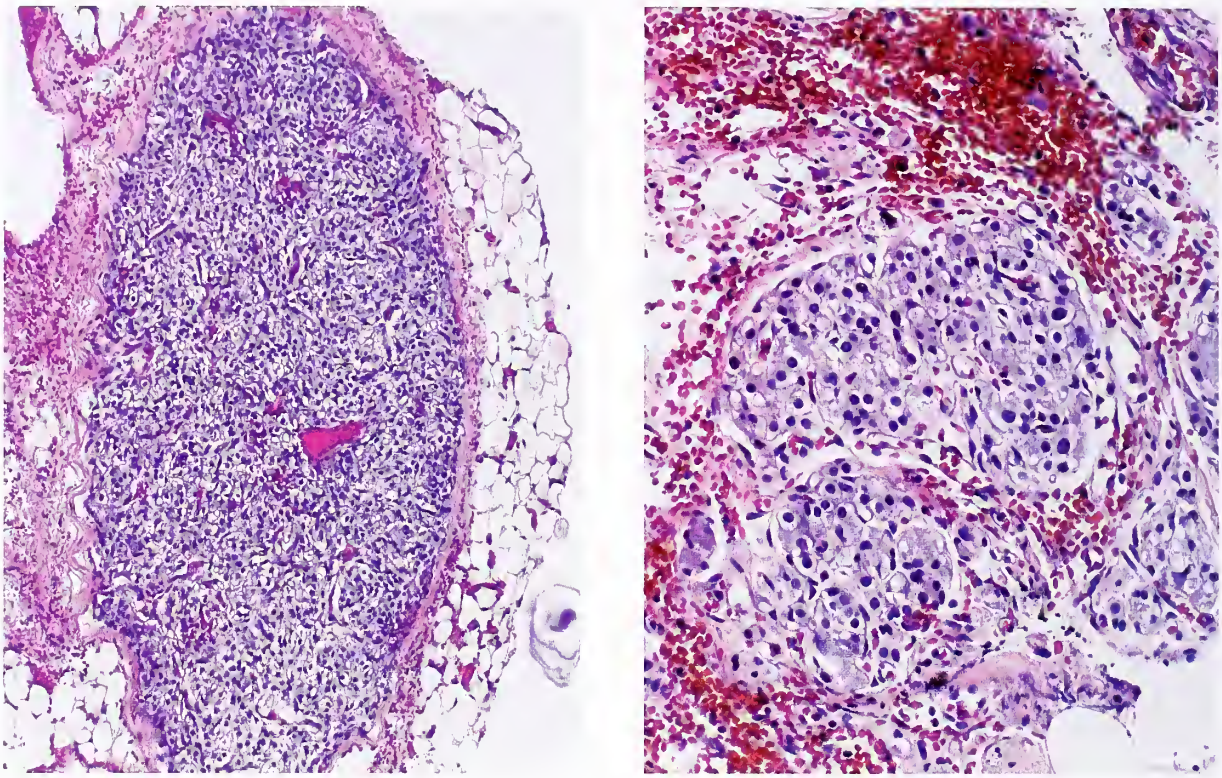

Figure 11-6

EXTRAADRENAL ABDOMINAL PARAGANGLIA IN AN ADULT

Left: Retroperitoneal paraganglion is sharply circumscribed and appears partially encapsulated.
Right: A smaller paraganglion in a different case appears as multiple small nests set within fresh hemorrhage. A small myelinated nerve bundle is present in the lower right corner.

myelinated nerve bundles (fig. 11-7C). The author has seen an intraabdominal paraganglion in an adult with a small component present within the subcapsular sinusoid of an adjacent lymph node (fig. 11-8). Because of their catecholamine storage capacity, formaldehyde-induced fluorescence highlights small collections of extraadrenal chromaffin cells (11,12).

Physiologic Function

The adrenal medullae attain structural maturity much later than the organs of Zuckerkandl (2,13). Extraadrenal paraganglia are sparsely innervated, suggesting that chemical signals of some sort play a predominant role in stimulation (14). Norepinephrine is the predominant catecholamine in extraadrenal chromaffin cells and in the fetal adrenal medulla (13,15). Since this amine is more potent as a pressor agent than epinephrine, it has been thought that the organs of Zuckerkandl in the fetus and newborn may help to maintain vascular tone; later this function gradually is taken over by the adrenal medulla and a more fully mature sympathetic nervous system (13).

Abdominal chemoreceptors have been noted in the experimental animal in association with the vagus nerve (16,17), and the peripheral termination of vagal sensory and efferent fibers suggests that some paraganglia, including those in the adrenal medulla, may be involved in segmental reflex activity and more general homeostatic regulation (18). Hypoxia has been shown to cause a decrease in formaldehyde-induced fluorescence in extraadrenal paraganglia in the human fetus (19) and release of norepinephrine in newborn rabbits exposed to severe asphyxia (20). Hypoxia-induced gene expressions have been identified in experimental pheochromocytoma (PC12) cells (21). A recent review highlights

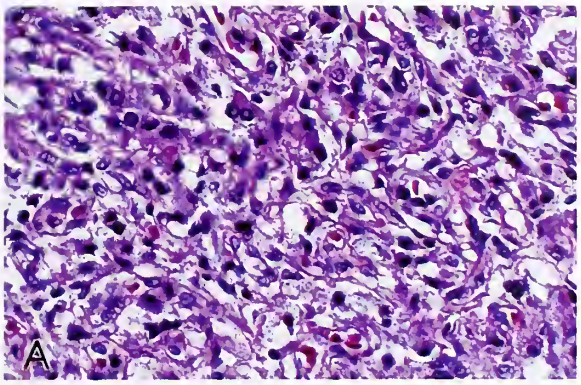

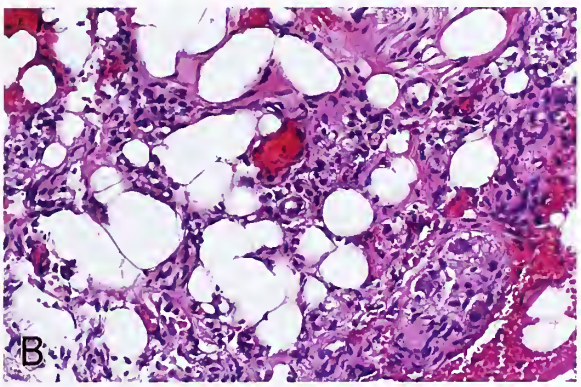

Figure 11-7

RETROPERITONEAL EXTRAADRENAL PARAGANGLIA IN AN ADULT

A: Aside from the lack of circumscription and collections of fat cells (other areas), the histomorphology of this extraadrenal paraganglion closely resembles the adrenal medulla.

B: Small retroperitoneal paraganglion in an adult is admixed with fat and is associated with ganglion cells and a small component of neural tissue. (Fig. 11-7B from Fascicle 19, Third Series.)

C: Small remnants of paraganglionic cells are present as small nests and individual cells admixed with fibrous connective tissue, fat, and small nerves.

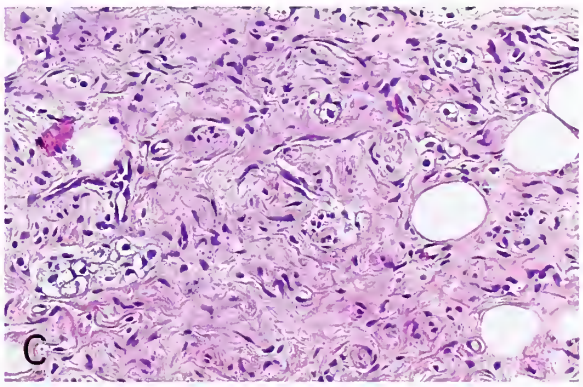

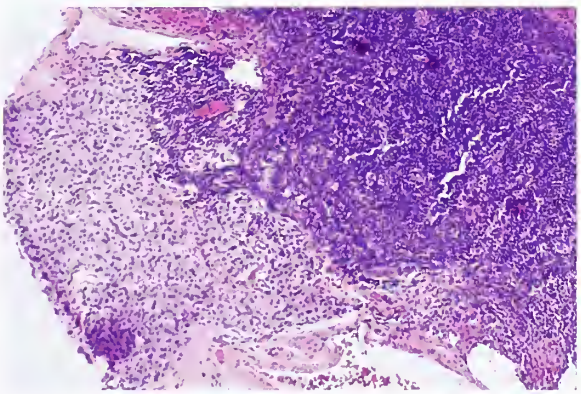

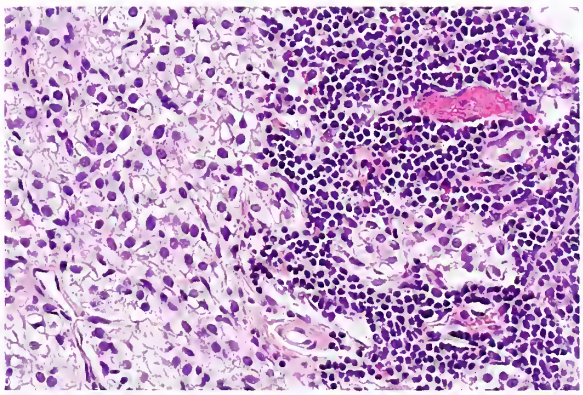

Figure 11-8

EXTRAADRENAL RETROPERITONEAL PARAGANGLION IN AN ADULT

Left: This extraadrenal paraganglion is located within a subcapsular sinusoid and capsule of a small lymph node.
Right: The paraganglion is closely associated with a small lymph node.

some of the paracrine signaling pathways in the endocrine system (22).

Immunohistochemical and Ultrastructural Features

Some of the enzymes involved in catecholamine synthesis have been identified in extraadrenal collections of small, intensely fluorescent cells situated along blood vessels. Similar to neuroblasts of ganglia in the human fetus of 14 to 22 weeks' gestation, positive labeling was observed for tyrosine hydroxylase and dopamine beta-hydroxylase, but not for phenylethanolamine N-methyltransferase,

Figure 11-9

RETROPERITONEAL EXTRAADRENAL PARAGANGLIA IN AN ADULT

A: Extraadrenal paraganglion stains strongly for chromogranin A. Cytoplasmic staining highlights the organoid arrangement of the endocrine cells in nests and short cords. (A–C: avidin-biotin peroxidase method).

B: Endocrine cells of the extraadrenal paraganglion are immunoreactive for synaptophysin.

C: Immunostain for S-100 protein shows dark staining of nuclei and dendritic cell processes of sustentacular cells.

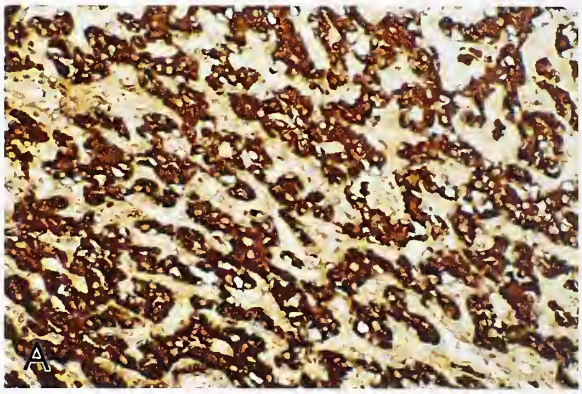

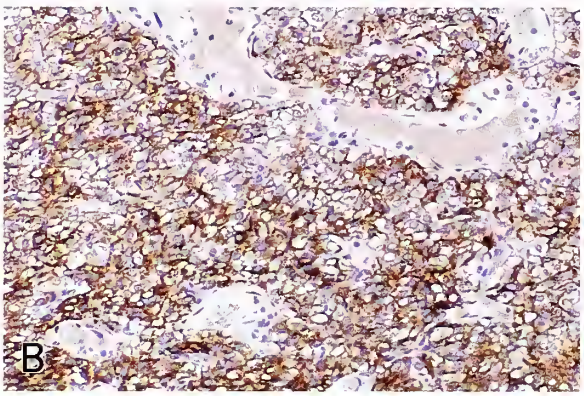

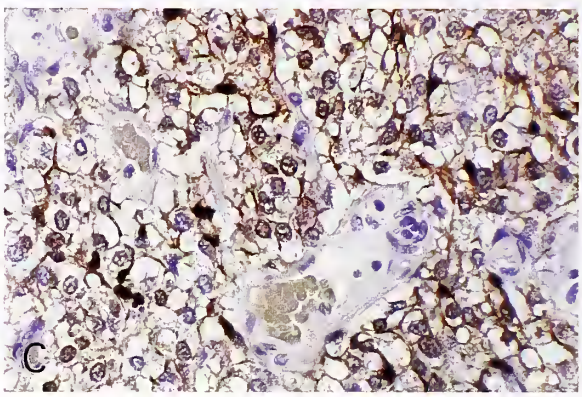

which is consistent with the production of mainly norepinephrine (23). As expected, chromaffin cells of extraadrenal paraganglia stain for neuroendocrine markers such as chromogranin A (fig. 11-9A) and synaptophysin (fig. 11-9B), and contain scattered sustentacular cells which are positive for S-100 protein (fig. 11-9C). The ultrastructural features of paraganglia and the adrenal medulla of the human fetus are covered in detail by Hervonen (24).

EXTRAADRENAL PARAGANGLIOMAS

Extraadrenal paragangliomas of the sympathoadrenal neuroendocrine system are located anywhere from the upper neck to the pelvic floor (25). According to Glenner and Grimley (26), the aorticosympathetic paraganglia are associated with segmental ganglia of the sympathetic chain while visceroautonomic paraganglia are associated with viscera such as urinary bladder, gallbladder, and the intrathoracic area near the base of the heart. Results of a review by Fries and Chamberlin (27) of the distribution of 205 extraadrenal paragangliomas are shown in Table 11-1. Since only 5 to 10 percent of sporadic pheochromocytomas are extraadrenal, the incidence figures shown in Table 11-1 decline considerably if adrenal medullary paragangliomas (pheochromocytomas) are included as a larger subset of sympathoadrenal paragangliomas (25). In a review by Melicow (28), about 98 percent of 107 pheochromocytomas and extraadrenal paragangliomas were intraabdominal, only 2 percent were cervical or intrathoracic, and less than 1 percent arose in the urinary bladder.

Extraadrenal Intraabdominal Paragangliomas

Anatomic Distribution. Extraadrenal paragangliomas of the abdomen are divided into three major groups (29). The largest group, superior paraaortic tumors (45 percent of cases), includes those located adjacent to the adrenal gland, in and around the hilum of the kidney, and the renal pedicle. Inferior paraaortic paragangliomas (30 percent of cases) arise below the inferior pole of the kidneys and extend down the aorta to include the iliac vessels; most extraadrenal paragangliomas in this area arise from remnants of the organs of Zuckerkandl which persist into adult life (30). Some of these

Table 11-1

ANATOMIC DISTRIBUTION OF EXTRAADRENAL PARAGANGLIOMAS (SYMPATHOADRENAL NEUROENDOCRINE SYSTEM)[a]

Area	Incidence
Cervical	3%
Intrathoracic	12%
Intraabdominal	85%
Superior paraaortic	45%
Inferior paraaortic	30%
Urinary bladder	10%

[a]Table 12-1 from Fascicle 19, Third Series.

tumors have a midline or paramedian location anterior to the aorta or over the aortic bifurcation. The last group includes urinary bladder paragangliomas; these are considered separately because of clinical manifestations and what seems to be a somewhat better prognosis. Some have suggested that the anatomic localization of a tumor away from the aorta should essentially exclude a paraganglioma from the differential diagnosis (31), but important exceptions have been reported (30).

Clinical Features. Intraabdominal extraadrenal paragangliomas occur at any age, but most occur in the 3rd to 5th decades of life (31–33). There is a roughly equal sex predilection, although there is a slight male predominance in some series (31–34). Signs and symptoms, most likely due to excess catecholamine secretion, have been reported in 25 to 86 percent of patients (31–33); in some asymptomatic patients the tumor is discovered at autopsy (35). Depending upon size and anatomic location, abdominal or flank pain may be a presenting complaint (32). Other unusual presentations include hydroureteronephrosis due to ureteral obstruction, gross hematuria due to invasion of the hilum of the kidney, obstructive jaundice due to compression of the common bile duct, and acute retroperitoneal hemorrhage (32). The rare patient may present with an osteolytic bony metastasis (36). Renovascular hypertension may result from unilateral compression of the renal artery without any evidence of excess catecholamine secretion (37). A rare case of a malignant retroperitoneal paraganglioma was reported in a 12-year-old girl who had evidence of Cushing's syndrome and virilization (38).

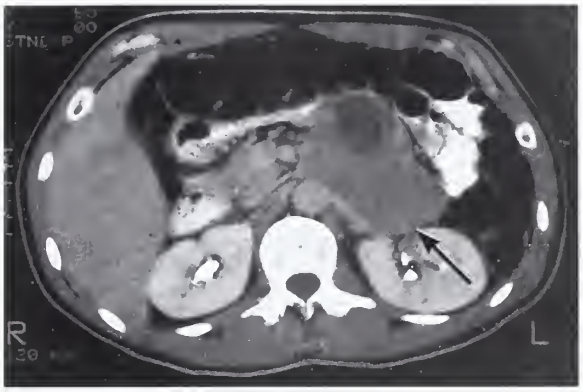

Figure 11-10

EXTRAADRENAL ABDOMINAL PARAGANGLIOMA

Computerized tomography (CT) scan of the upper abdomen of a 28-year-old man who presented with symptoms suggesting pheochromocytoma shows a large preaortic and paraaortic paraganglioma (arrow). The paraganglioma is nonhomogeneous and grossly had areas of cystic degeneration. The ipsilateral adrenal gland was free of tumor. (Fig. 12-1 from Fascicle 19, Third Series.)

Similar to pheochromocytomas, extraadrenal paragangliomas may be localized by imaging modalities other than selective arteriography (fig. 11-10). On magnetic resonance imaging (MRI), the tumors usually have a hyperintense signal on T2-weighted images (fig. 11-11) (39).

Gross and Microscopic Findings. The tumors are usually solitary, particularly in adults, but in a review of nonfunctional, nonchromaffin paragangliomas, two or more separate primary tumors were present in 5 of 21 patients (34). Occasional examples of paragangliomatosis have been reported, with multiple contiguous paragangliomas along the course of the sympathetic chain (31) or distributed from the neck to the pelvis (40,41). An unusual case of paragangliomatosis occurred in a teenager who had 21 separate tumors and evidence of additional paragangliomas (41). The average size of the tumors in two series was about 10 cm (fig. 11-12) (32,33), but there was a broad size range of from 4 to 24 cm. The variety of gross morphologic features is similar to that of pheochromocytoma, although typically an adrenal remnant (entopic or ectopic) is not identified. Some tumors undergo marked cystic degeneration (fig. 11-13), and when the neoplasm shows extensive hemorrhage it can simulate a hematoma.

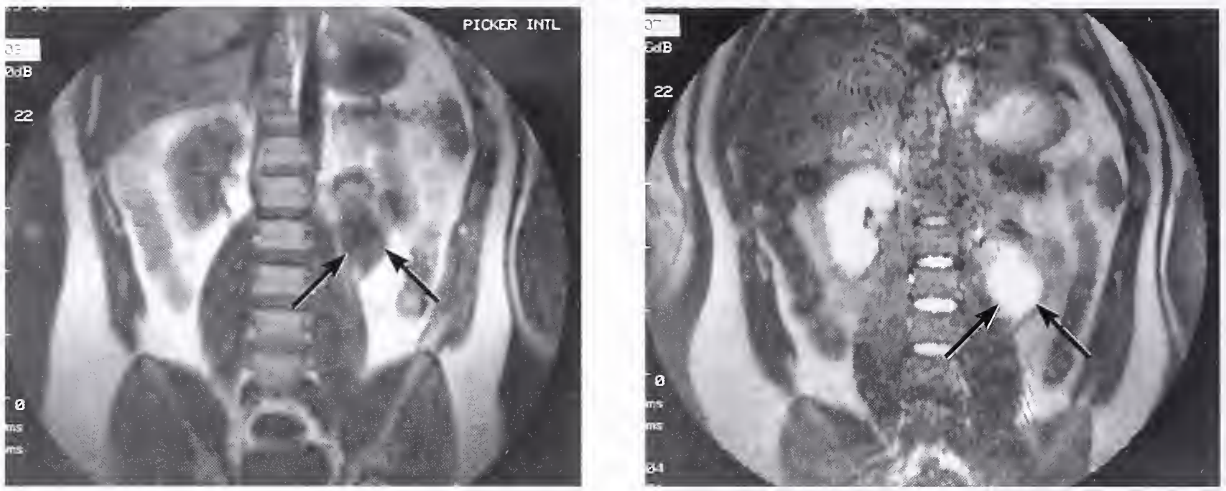

Figure 11-11

EXTRAADRENAL ABDOMINAL PARAGANGLIOMA

Left: This magnetic resonance image (MRI) shows a paraganglioma near the lower border of the kidney on the left side (arrows).

Right: There is an intense signal on a T2-weighted image (arrows). (L&R: Fig. 5-3A,B from Keiser HR, Doppman JL, Robertson CN, Linehan WM, Averbuch SD. Diagnosis, localization, and management of pheochromocytoma. In: Lack EE, ed. Pathology of the adrenal glands. New York: Churchill Livingstone; 1990:237-255.)

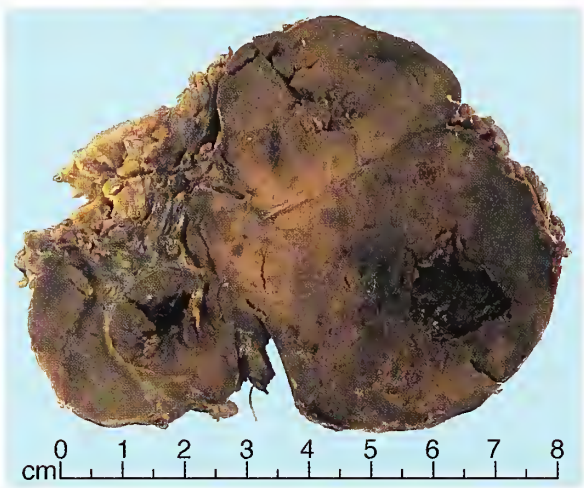

Figure 11-12

EXTRAADRENAL ABDOMINAL PARAGANGLIOMA

In cross section, the paraganglioma seen in figure 11-10 is tan to dark brown with areas of hemorrhage and cystic degeneration. The tumor was 9.5 cm in diameter and weighed 208 g. (Fig. 12-3 from Fascicle 19, Third Series.)

Figure 11-13

EXTRAADRENAL ABDOMINAL PARAGANGLIOMA

This extraadrenal abdominal paraganglioma resected from a 53-year-old man shows marked cystic degeneration on cross section. The tumor had been initially diagnosed as a hemangiopericytoma. It was 20 cm in diameter. The patient was alive and well 5 years later. (Fig. 12-4 from Fascicle 19, Third Series.)

The most characteristic microscopic pattern is a trabecular arrangement with anastomosing cords of tumor cells (fig. 11-14). Some tumors have a diffuse or alveolar (nesting) pattern (fig. 11-15). There is sufficient overlap in architecture and cellular morphology that examination of isolated fields in any particular case may fail to reliably discriminate between an adrenal versus an extraadrenal primary. Finding an attached adrenal remnant is helpful, but some paragangliomas arise in an immediate periadrenal or juxtaadrenal location without intrinsic involvement of the gland. Preoperative localization

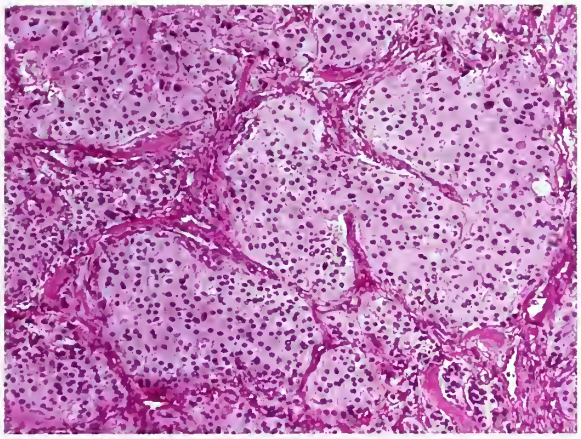

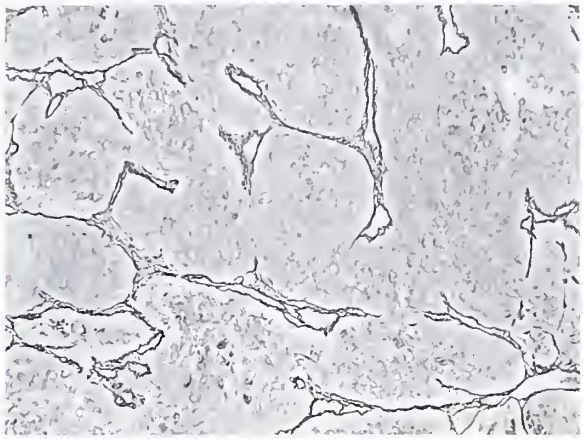

Figure 11-14

EXTRAADRENAL ABDOMINAL PARAGANGLIOMA

Left: An anastomosing trabecular pattern predominates in this field.

Right: The reticulum stain accentuates the interconnecting trabeculae, which form a delicate vascular pattern. (L&R: Fig. 12-5 from Fascicle 19, Third Series.)

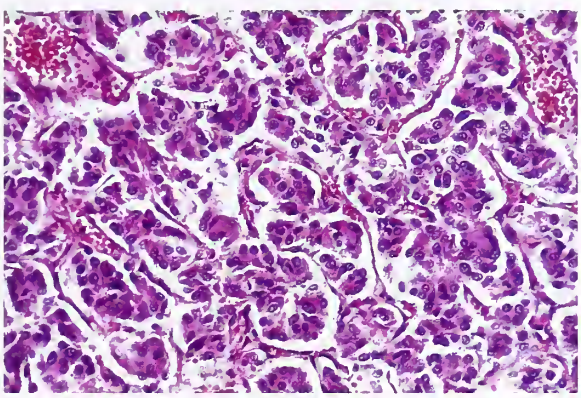

Figure 11-15

EXTRAADRENAL ABDOMINAL PARAGANGLIOMA

There are small, relatively uniform nests of cells. (Fig. 12-6 from Fascicle 19, Third Series.)

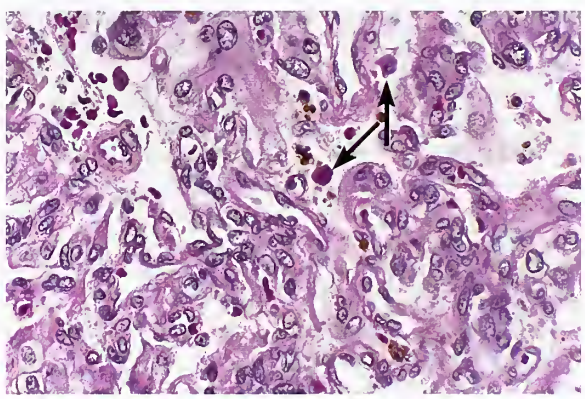

Figure 11-16

EXTRAADRENAL ABDOMINAL PARAGANGLIOMA

The prominent vascular pattern in this extraadrenal abdominal paraganglioma can be misleading due to the component of plump endothelial cells. Note the scattered mast cells (arrows). (Fig. 12-7 from Fascicle 19, Third Series.)

studies or intraoperative findings at the time of laparotomy may distinguish the two (30).

Similar to pheochromocytomas, there may be a remarkable degree of nuclear pleomorphism and even occasional mitotic figures, but these and other morphologic features, such as large size, do not permit reliable classification of the paraganglioma as malignant (30). Intracytoplasmic hyaline globules are present in some tumors, but their frequency in one study was lower (8.3 percent) (32) than the nearly one third incidence for pheochromocytoma (42).

Prominent vascularity with abundance of plump endothelial cells may be mistaken for a primary vasoformative neoplasm (fig. 11-16). Occasionally, a few bundles of myelinated nerve are found within or immediately adjacent to the tumor; this may reflect a close relationship of extraadrenal paraganglia with neural structures, and does not necessarily signify malignancy. An example of a composite extraadrenal paraganglioma-ganglioneuroma has been reported which was clinically malignant (33).

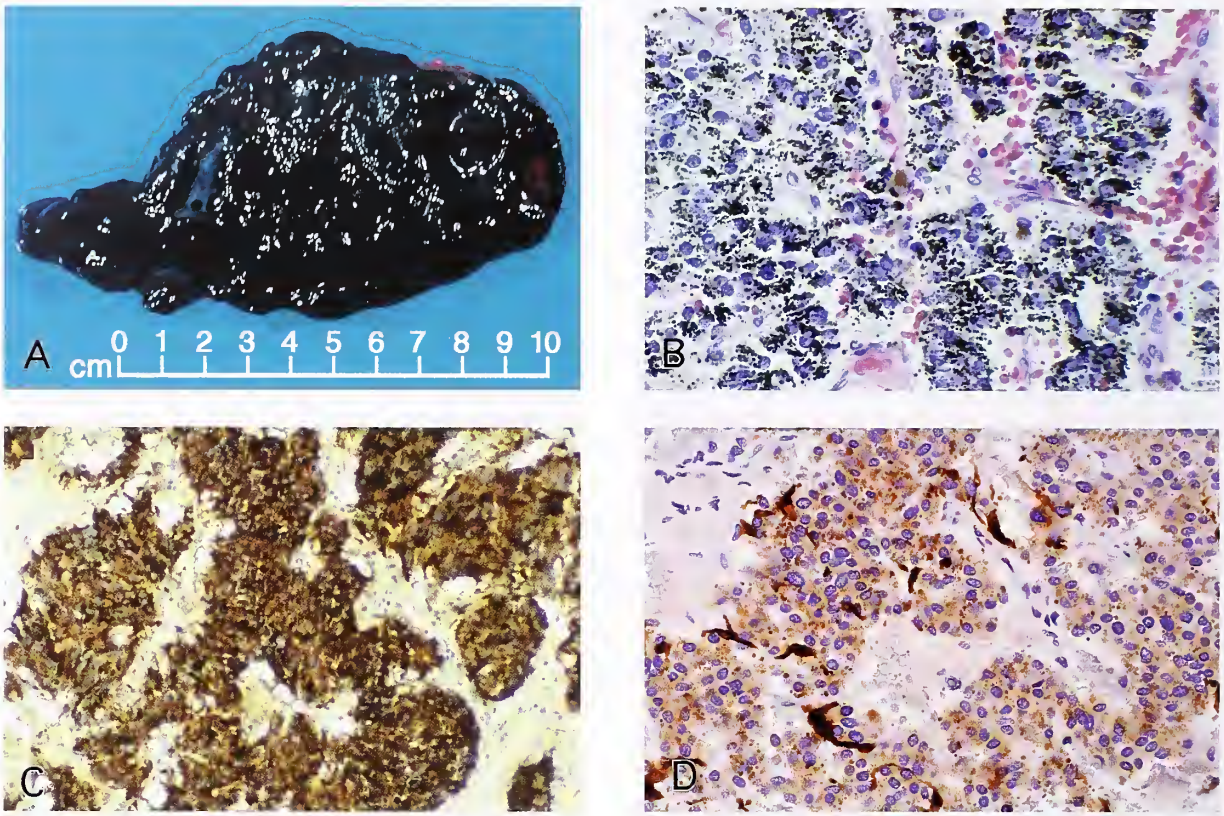

Figure 11-17

PIGMENTED (BLACK) EXTRAADRENAL PARAGANGLIOMA OF RETROPERITONEUM

A: The tumor weighed 225 g and is jet black on cross section. The intact tumor measured 13 x 8 x 4.5 cm. (Fig. 12-8, top from Fascicle 19, Third Series.)

B: Tumor cells contain abundant granular pigment, which on ultrastructural study was most consistent with neuromelanin or lipofuscin. Fine needle aspiration was done preoperatively and the tumor cells containing pigment were thought to be probably malignant melanoma.

C: Tumor cells are strongly positive for chromogranin A. Immunostain for synaptophysin was also positive (avidin-biotin peroxidase method).

D: Scattered sustentacular cells are positive for S-100 protein. Pigment granules can still be seen within the cytoplasm of tumor cells (avidin-biotin peroxidase method).

The author has seen a heavily pigmented retroperitoneal extraadrenal paraganglioma that contained abundant coarse granular pigment within the cytoplasm of most tumor cells, giving the tumor a jet black color (fig. 11-17). Ultrastructural study in this case showed numerous, relatively uniform, dense-core neurosecretory granules as well as electron-dense material consistent with neuromelanin, an electron-dense degradation product of catecholamine metabolism (a lipofuscin type secondary lysosome) (fig. 11-18). No premelanosomes or melanosomes were identified.

Biologic Behavior. Intraabdominal extraadrenal paragangliomas tend to be the most aggressive paragangliomas of the sympathoadrenal neuroendocrine system compared with urinary bladder paragangliomas and probably paragangliomas in rare and exotic sites (there are too few cases to allow for a reliable prognostic profile for these rarer tumors) (30). The incidence of malignancy in six large series was 14 percent (43), 24 percent (44), 29 percent (45), 33 percent (46), 42 percent (47), and 50 percent (48). The mode of spread (fig. 11-19) and pattern of metastasis are similar to that of pheochromocytoma, and

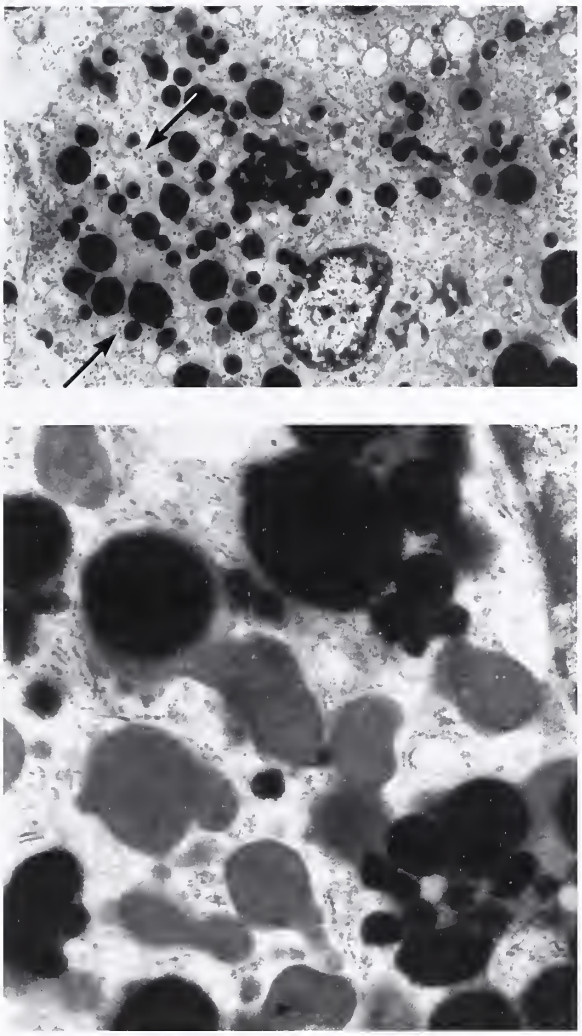

Figure 11-18

PIGMENTED (BLACK) EXTRAADRENAL PARAGANGLIOMA OF RETROPERITONEUM

Top: Tumor cells contain abundant jet black pigment granules of various sizes and shapes. Smaller dense-core neurosecretory granules are also present (arrows).

Bottom: There are jet black pigment granules, some of which appear to be associated with lipid material. The pigment was positive with the Fontana-Masson silver stain and the staining reaction was abolished by a bleaching procedure.

sometimes prolonged follow-up is necessary before metastasis occurs. The 5-year survival rate in one series was 36 percent (48). A relatively high incidence of malignancy has also been reported in children with extraadrenal paragangliomas (49)

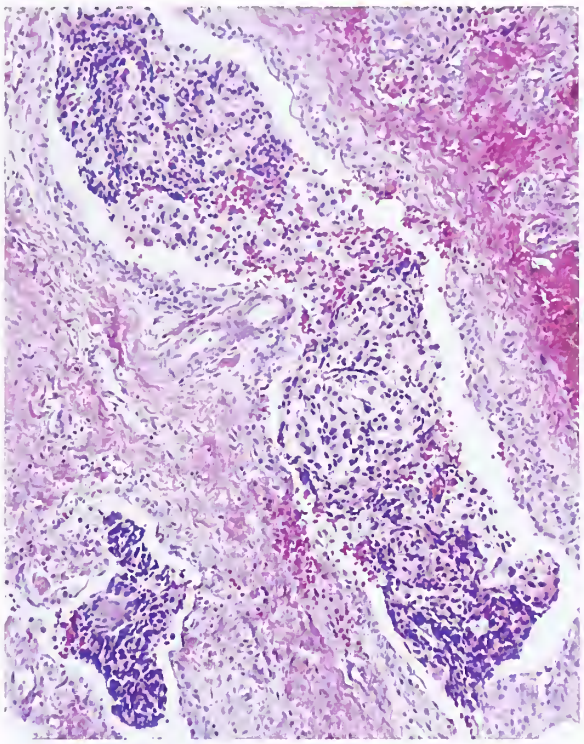

Figure 11-19

EXTRAADRENAL ABDOMINAL PARAGANGLIOMA

This extraadrenal abdominal paraganglioma probably arose from remnants of the organs of Zuckerkandl. There are small foci of vascular invasion. The tumor proved to be clinically malignant. (Fig. 12-9 from Fascicle 19, Third Series.)

Urinary Bladder Paragangliomas

Clinical Features. Urinary bladder paragangliomas account for only 0.06 percent (50) to 0.5 percent (51) of all primary bladder tumors in adults. In a large series and literature review from the Armed Forces Institute of Pathology (AFIP) (50), there was a roughly equal sex predilection, and the average age at diagnosis was about 41 years (range, 11 to 78 years). The tumor is usually located in the trigone near the ureteral orifices, but can also arise in the dome and lateral walls. The clinical triad consists of paroxysmal (or sustained) hypertension, gross intermittent hematuria, and attacks which may be precipitated by micturition although this is not apparent in every case (50). Occasionally, tumors are multifocal in the bladder, are associated with extravesical paragangliomas (52), and occur in a familial setting (53). Cases have been associated with von Recklinghausen's disease, renal

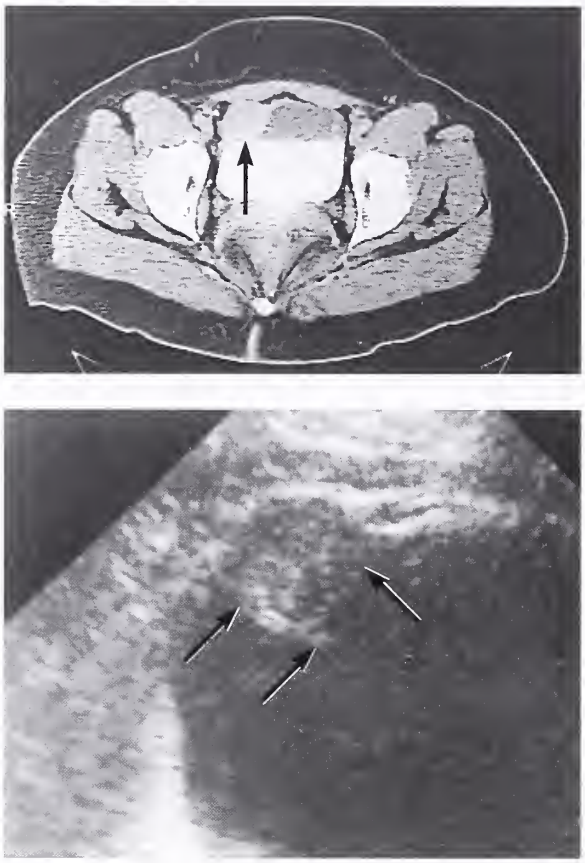

Figure 11-20

URINARY BLADDER PARAGANGLIOMA

Top: CT scan shows an intramural urinary bladder paraganglioma (arrow). Water soluble contrast material layers out in the bladder posteriorly. (Fig. 12-10, top from Fascicle 19, Third Series.)

Bottom: Ultrasound showed a nonhomogeneous mass (arrows) involving the anterior wall of the urinary bladder. (Fig. 5-2B from Keiser HR, Doppman JL, Robertson CN, Linehan WM, Averbuch SD. Diagnosis, localization, and management of pheochromocytoma. In: Lack EE, ed. Pathology of the adrenal glands. New York: Churchill Livingstone; 1990:237-255.)

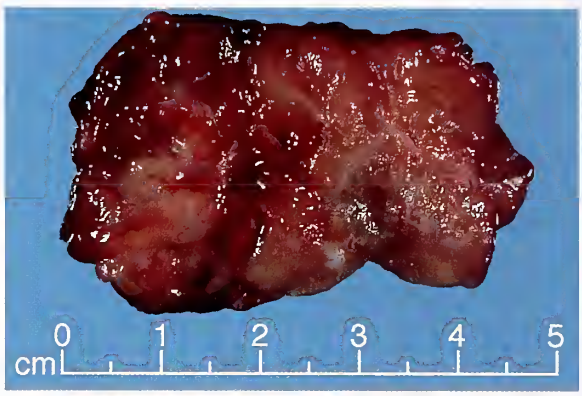

Figure 11-21

URINARY BLADDER PARAGANGLIOMA

This urinary bladder paraganglioma was removed by segmental resection of the bladder wall. The patient had intermittent symptoms of excess catecholamine secretion. (Fig. 12-11 from Fascicle 19, Third Series.)

cell carcinoma, polycystic renal disease, and other conditions (54). A recent case was associated with preeclampsia (55). Imaging studies may provide detailed information regarding the location of the tumor (fig. 11-20).

Gross and Microscopic Findings. Urinary bladder paragangliomas tend to be relatively small, with an average diameter of 1.9 cm in one study, but can be much larger (fig. 11-21). The tumor may project into the bladder lumen. Several of the smaller tumors in the bladder submucosa (50) may represent non-neoplastic paraganglia. Indeed, a normal paraganglion at the base of the bladder interdigitating with smooth muscle can be confused with a paraganglioma. Urinary bladder paragangliomas arise from small nests of paraganglia which have presumably migrated to various parts of the vesicle and bladder base during early embryonic development (fig. 11-22) (54).

Microscopically, urinary bladder paragangliomas usually present little difficulty in diagnosis (fig. 11-23), but problems in interpretation may arise when there is ulceration, crush artifact, suboptimal tissue fixation and processing, or sclerotic stroma (fig. 11-24, left). Some tumors may be misinterpreted as transitional cell carcinoma or even granular cell tumor (myoblastoma) (51). Most urinary bladder paragangliomas are not well circumscribed microscopically, and may interdigitate with bundles of smooth muscle (fig. 11-24, right), an appearance that simulates invasion but is not considered to be reliable evidence of malignancy (54). A case of pigmented composite paraganglioma-ganglioneuroma of the urinary bladder has been reported and the pigment was most consistent with neuromelanin (56).

Biologic Behavior. In the review from the AFIP, metastases were noted in 3 of 58 cases (5 percent) (50). In a review of 87 urinary bladder paragangliomas, regional lymph node metastases

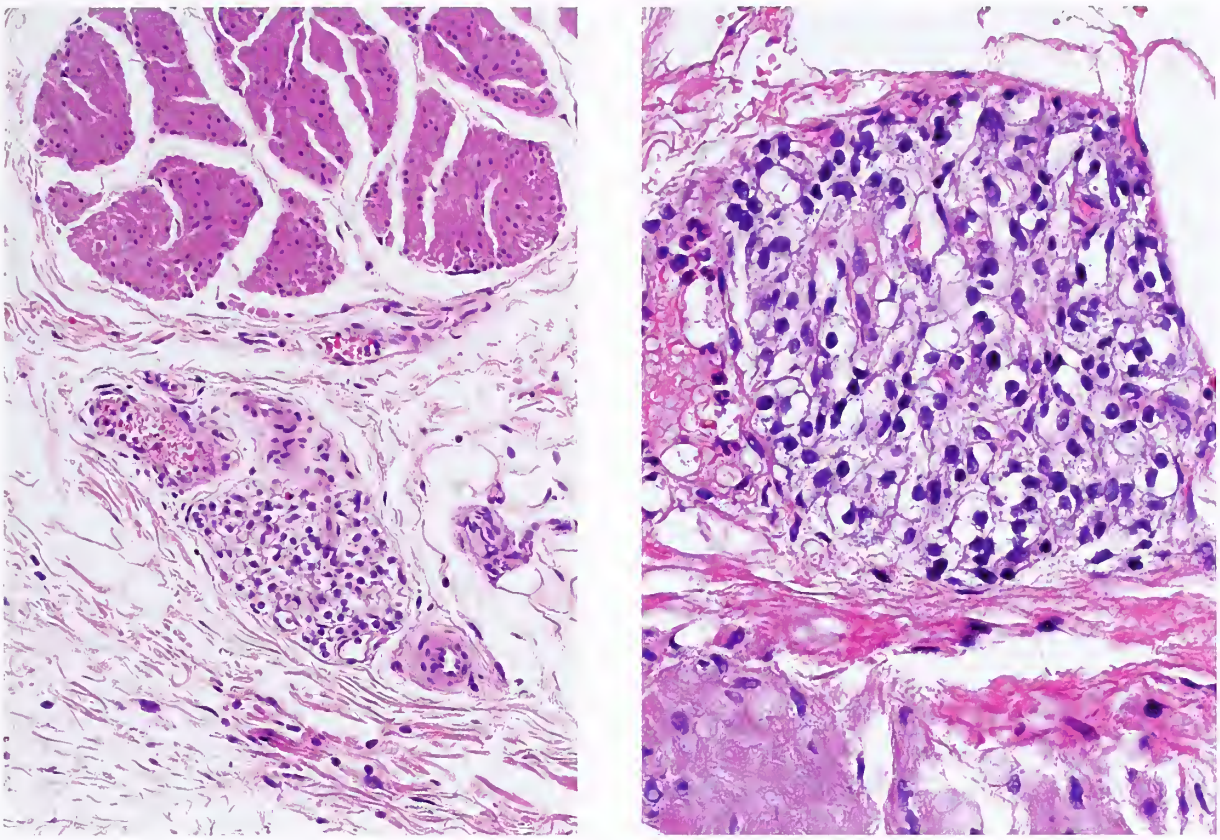

Figure 11-22

NON-NEOPLASTIC PARAGANGLIA OF URINARY BLADDER

Left: Cystectomy specimen shows a paraganglion within the interstitium of edematous bladder submucosa. A portion of the muscularis propria is also present.

Right: Different case showing a paraganglion of the bladder wall adjacent to the muscularis propria.

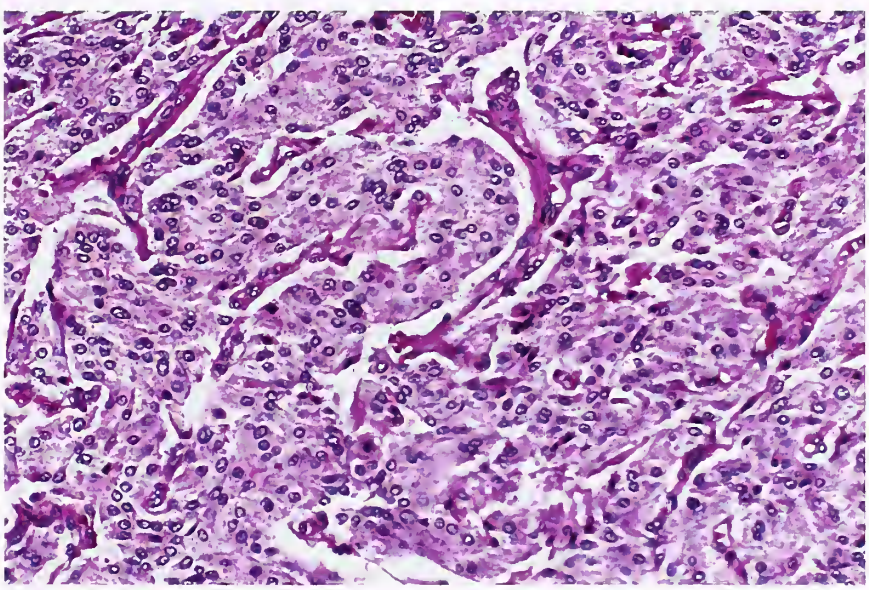

Figure 11-23

URINARY BLADDER PARAGANGLIOMA

A predominant anastomosing trabecular pattern is seen here, but in other areas, a nesting or alveolar arrangement of cells was also apparent. (Fig. 12-13 from Fascicle 19, Third Series.)

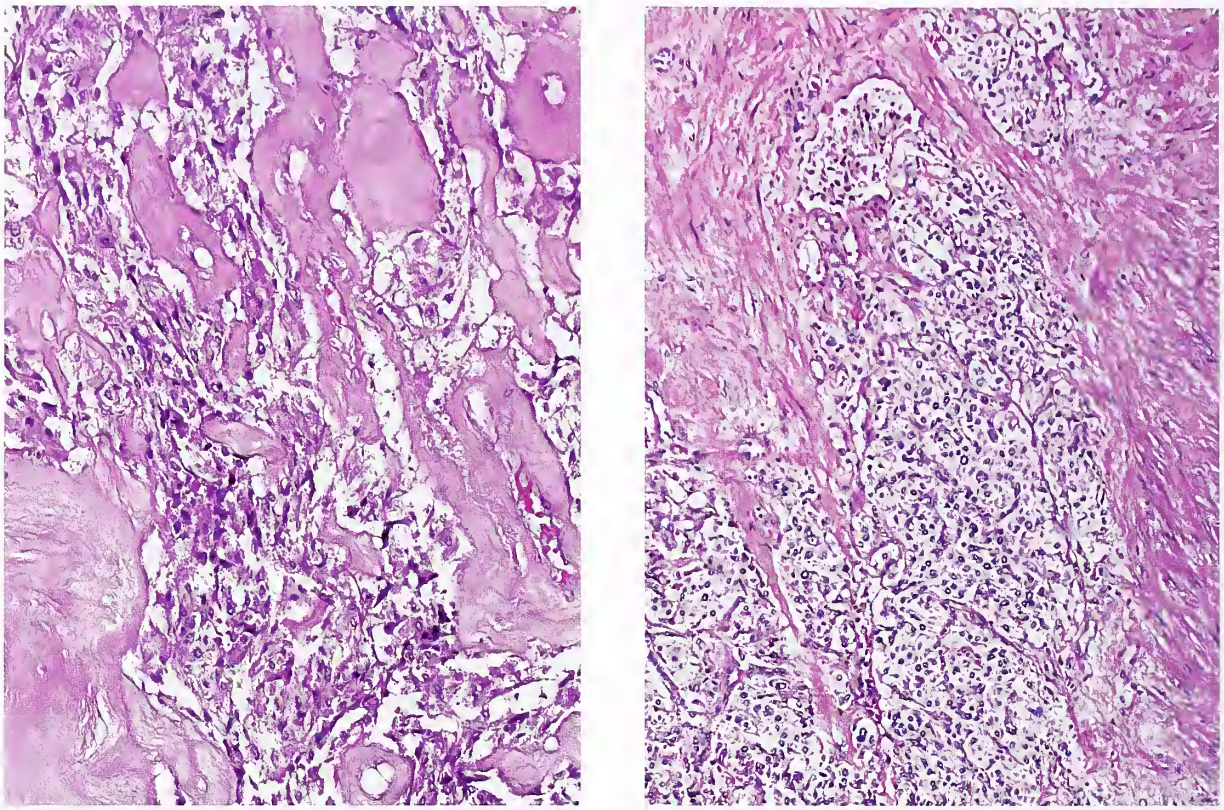

Figure 11-24

URINARY BLADDER PARAGANGLIOMA

Left: The architecture of the tumor is distorted by sclerotic stroma.

Right: In a different case, bundles of smooth muscle in the bladder wall are separated by tumor, which has a predominantly nesting or alveolar pattern. (Fig. 12-14, right from Fascicle 19, Third Series.)

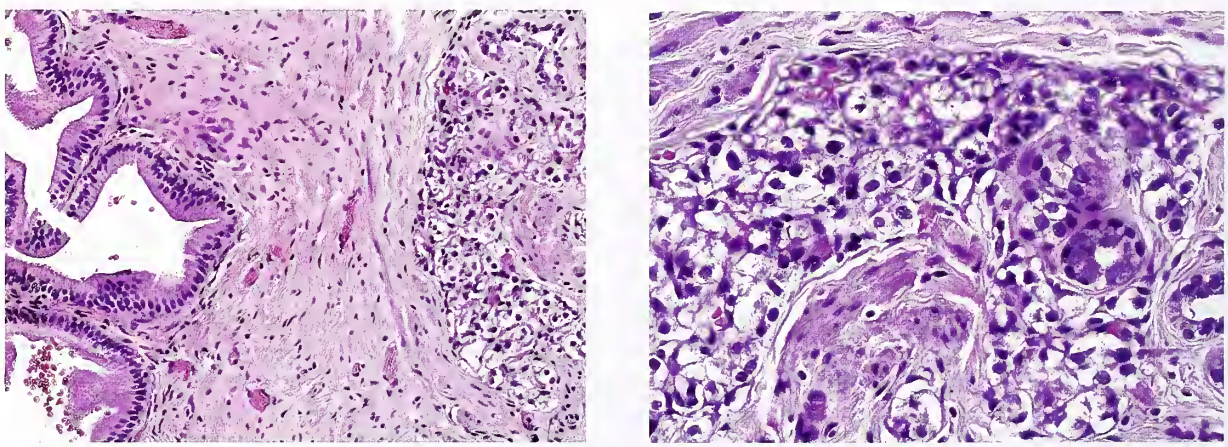

Figure 11-25

NORMAL GALLBLADDER PARAGANGLION

Left: Small paraganglion is present within the muscular layer near the neck of gallbladder.
Right: A paraganglion lies next to small glands in the neck of the gallbladder.

were noted in 12 cases (13.8 percent), but distant metastases occurred in only 2 cases (2.3 percent) (57). In a recent study, the mean MIB-1 labeling index was 1.5 percent (range, 0.03 to 7 percent) (58). Multicentric paragangliomas (vesical and extravesical) should not be overinterpreted as malignant (54).

Unusual Abdominal and Pelvic Sites of Paragangliomas

Paragangliomas have been reported in a number of unusual sites, sometimes where normal paraganglia have yet to be well characterized (59), including various sites in the genitourinary tract such as kidney (60), urethra (61,62), prostate gland (63), and spermatic cord (64). Normal paraganglia have been described immediately adjacent to the human prostate gland or rarely, in prostatic stroma (65) as well as in the wall of the urinary bladder (59). In a recent study of radical prostatectomy specimens, periprostatic paraganglia (median size, 0.9 mm) were identified in about 8 percent of specimens; they were 1 to 3 mm, lateral and slightly posterior to the prostatic capsule, and often associated with neurovascular bundles (65). There have been several reports of gallbladder paragangliomas (66,67); normal paraganglia can occasionally be found within the subserosa of the gallbladder, often close to blood vessels or nerves (67,68) or actually within the wall (fig. 11-25). Other exotic sites for paraganglioma include uterus, ovary (69), vagina, vulva, pancreatico-biliary area (70), and liver parenchyma (71).

Intrathoracic Paravertebral Paragangliomas

Clinical Features. Intrathoracic paravertebral paragangliomas arise in areas closely related to the sympathetic axis (fig. 11-26). In one review the tumors were usually located in the midthoracic region (72). About half of the tumors are functional, with excess catecholamine secretion. Some of the tumors arising in or near the base of the heart (i.e., aorticopulmonary paragangliomas) are also functionally active, thus suggesting a closer alignment with the sympathoadrenal neuroendocrine system; these tumors are considered separately.

There is a predilection for males in the review by Gallivan et al. (72) at an average age at

Figure 11-26

MALIGNANT PARAVERTEBRAL PARAGANGLIOMA

A 50-year-old man presented initially with an osteolytic metastasis to the right hip. Posteroanterior chest roentgenogram shows a primary paravertebral paraganglioma in the costovertebral sulcus in the upper right thorax. (Fig. 1 from Gallivan MV, Chun B, Rowden G, Lack EE. Intrathoracic paravertebral malignant paraganglioma. Arch Pathol Lab Med 1980;104:46-51.) (Figs. 11-26 through 11-30A are from the same case.)

diagnosis of 29 years. Some cases have been reported in the pediatric age group (73). Rarely, Horner's syndrome is noted, and in exceptional cases, an osteolytic metastasis may be the initial presentation (fig. 11-27). Tumors with a "dumbbell" configuration have been described (72); in one case, the tumor located away from the costovertebral sulcus simulated a primary rib tumor (74). Familial cases have occurred, and in some cases paragangliomas are found at other sites, including neck and abdomen (72).

Gross and Microscopic Findings. The average size and weight of the tumors in one review were 5.7 cm and 40 g, respectively; the largest tumor was 13 cm in diameter (72). Most tumors are detected in the right hemithorax (72). The gross appearance of an intrathoracic paravertebral paraganglioma is shown in figure 11-28.

The histologic features are usually diagnostic, although problems can arise in a limited biopsy of a primary tumor or when the presentation is unusual, such as osseous metastasis in

Figure 11-27

OSTEOLYTIC METASTASIS OF INTRATHORACIC PARAVERTEBRAL PARAGANGLIOMA

Intertrochanteric pathologic fracture of the right hip was the initial presentation, and later the patient was found to have a paravertebral intrathoracic paraganglioma. (Fig. 12-15A from Lack EE. Pathology of adrenal and extra-adrenal paraganglia. Major problems in pathology, Vol 29. Philadelphia: WB Saunders Co; 1994:283.)

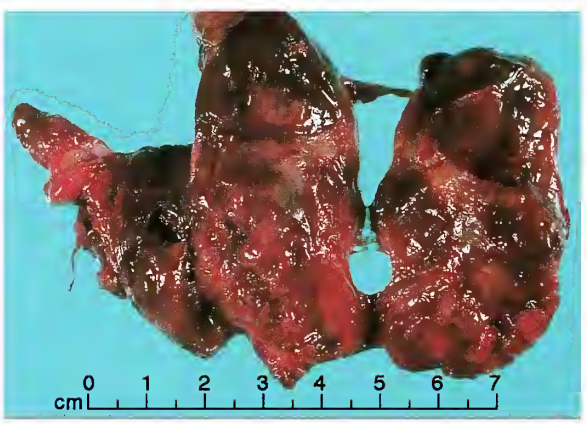

Figure 11-28

INTRATHORACIC PARAVERTEBRAL PARAGANGLIOMA

The tumor appeared well circumscribed, and measured 6.5 cm in diameter. On cross section, the tumor is meaty tan-brown and deeply hemorrhagic in some areas. The tumor was extrapleural, overlying the heads of the first, second, and third ribs on the sympathetic chain. The patient died about 16 months later with multiple bony metastases as well as metastases to lung and liver. (Fig. 12-17 from Fascicle 19, Third Series.)

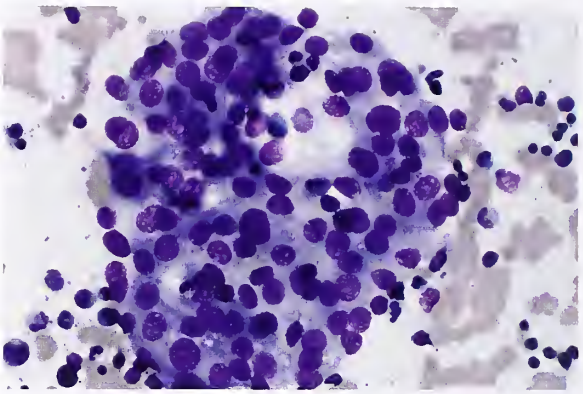

Figure 11-29

METASTATIC INTRATHORACIC PARAVERTEBRAL PARAGANGLIOMA

Intrathoracic paravertebral paraganglioma metastatic to the iliac crest. Bone marrow aspirate of the iliac crest shows relatively cohesive clusters of malignant cells which are difficult to classify accurately without further information or special stains to demonstrate neuroendocrine features (Wright-Giemsa stain). (Fig. 12-18 from Fascicle 19, Third Series.)

which the iliac crest bone marrow biopsy shows clusters of malignant cells which may be difficult to accurately classify (fig. 11-29) (72). On rare occasion, when tumor cells cling to delicate vascular channels with admixed hemorrhage, a paraganglioma may have a pseudopapillary or angiomatous appearance (fig. 11-30A). Special stains can accentuate unusual patterns and provide valuable diagnostic information (fig. 11-30B,C) (75).

Biologic Behavior. An initial review reported that 7 percent of intrathoracic paravertebral paragangliomas are clinically malignant (72), but in another review, 7 of 48 cases were malignant (13 percent) (76). There may be a greater tendency to report malignant paragangliomas arising in rare and exotic locations, thus overestimating the true incidence of malignant behavior.

Cervical Paravertebral Paragangliomas

These tumors are very rare; in a review by Fries and Chamberlin (77) only five cases were identified. Only a few cases have been reported in the pediatric age group, and these may be associated with pheochromocytomas (78). At least two cases have been reported as carotid body type tumors, although the anatomic localization supports an origin from the sympatho-

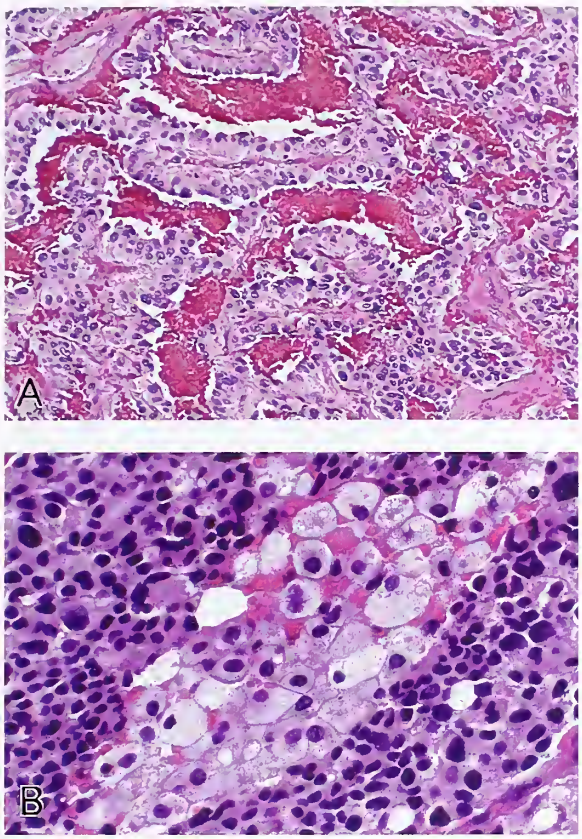

Figure 11-30

INTRATHORACIC PARAVERTEBRAL PARAGANGLIOMA

A: The tumor has a pseudopapillary pattern, with tumor cells clinging to delicate vascular septa. Hemorrhage separated cords of tumor cells. (Fig. 12-19, left from Facicle 19, Third Series.)

B: Different case of a malignant intrathoracic paravertebral paraganglioma shows an enlarged nest of tumor cells with central degenerative change and accumulation of foamy macrophages.

C: Immunostain for chromogranin in same case as B shows intense staining of tumor cells while the macrophages in the center are negative (avidin-biotin peroxidase method).

adrenal neuroendocrine system (79,80). Too few cases have been reported to allow for reliable prognostic assessment (81).

FUNCTIONING PARAGANGLIOMA AND GASTROINTESTINAL STROMAL TUMOR OF THE JEJUNUM

The nonfamilial occurrence of functioning paraganglioma and gastrointestinal stromal tumor (GIST) of the jejunum was recently reported in three women (82). All three patients had intraabdominal extraadrenal paragangliomas and in addition one had bilateral pheochromocytomas. It was unclear whether the tumors were part of a syndrome, a variant of the Carney triad, or coincidental.

ULTRASTRUCTURAL AND OTHER FEATURES OF SYMPATHOADRENAL PARAGANGLIOMAS

Ultrastructural Findings. Examination of 1-µm–thick sections from sympathoadrenal paragangliomas may reveal cells with different cytoplasmic staining characteristics: there may be a "light" and "dark" cell population, as well as some variation in number and distribution of dense-core secretory granules (fig. 11-31). There may be numerous intracytoplasmic, rounded vacuolar spaces of various size which represent pseudoacini, as well as complex interdigitations of cytoplasmic processes (fig. 11-32). Endothelial cells are present and, occasionally, cells consistent with sustentacular cells; the latter are identified by immunostaining for S-100 protein.

The nuclei of paraganglioma cells are round to ovoid, often with some margination of chromatin against the nuclear membrane. The nucleolus may be prominent depending upon the plane of section. The nuclei of some cells have nuclear folds with deep irregular extension or intrusion of cell cytoplasm, forming a nuclear pseudoinclusion. A nuclear pseudoinclusion is viewed in profile in figure 11-33 and en face in figure 11-34 where it is surrounded by a continuous nuclear membrane. The density of cellular organelles within the intranuclear extension of cytoplasm may vary from cell to cell or within a single cell and result in

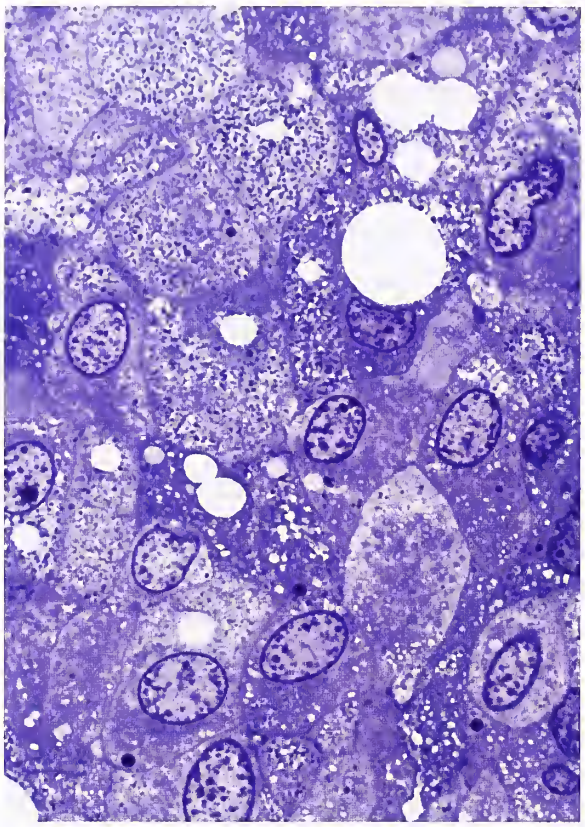

Figure 11-31

PHEOCHROMOCYTOMA

There is a variation in the overall density of the cytoplasm, with "light" and "dark" cells. Most of the dark, pinpoint granules represent dense-core neurosecretory granules. Intracytoplasmic vacuoles are prominent (pseudoacini, see figure 11-38) (toluidine blue stain).

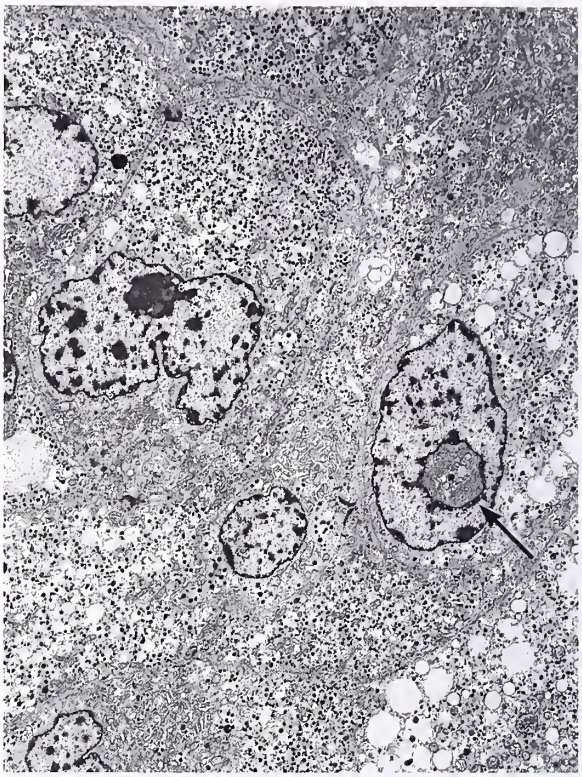

Figure 11-32

PHEOCHROMOCYTOMA

Some tumor cells have complex intertwining cell processes. The dense-core neurosecretory granules vary in density. The nucleus on the left has an irregular contour with infolding of the nuclear membrane while one nucleus on the right has a small nuclear pseudoinclusion (arrow). (Fig. 13-2 from Fascicle 19, Third Series.)

differences in staining. The empty spaces seen at the light microscopic level ultrastructurally represent dilated cisternae of endoplasmic reticulum or nonspecific vacuolar change. There are usually scattered profiles of rough endoplasmic reticulum and occasional lipofuscin. Intercellular junctions are sparse and simple in configuration. There are no true desmosomal attachments with insertion of intermediate filaments.

The hallmark of sympathoadrenal paragangliomas is the presence of dense-core neurosecretory granules, but when sparse, they are difficult to distinguish from small primary lysosomes. Often, the dense-core secretory granules vary in morphology (fig. 11-35). Tannenbaum (83) correlated the ultrastructural morphology of dense-core neurosecretory granules with norepinephrine and epinephrine content in 14 pheochromocytomas. In the tumors that contained predominantly epinephrine, the neurosecretory granules were of uniform type, while in the norepinephrine-containing tumors, they had a distinctive and entirely different appearance, with a prominent eccentric electron-lucent space (or halo) adjacent to the electron-dense core. Granule morphology can vary, however, and correlation with content of any particular hormone or neuropeptide is not reliable. Some granules may be found in close association with a Golgi complex (fig. 11-36); occasionally, intact neurosecretory granules with an investing membrane have been observed outside the cytoplasm of tumor cells,

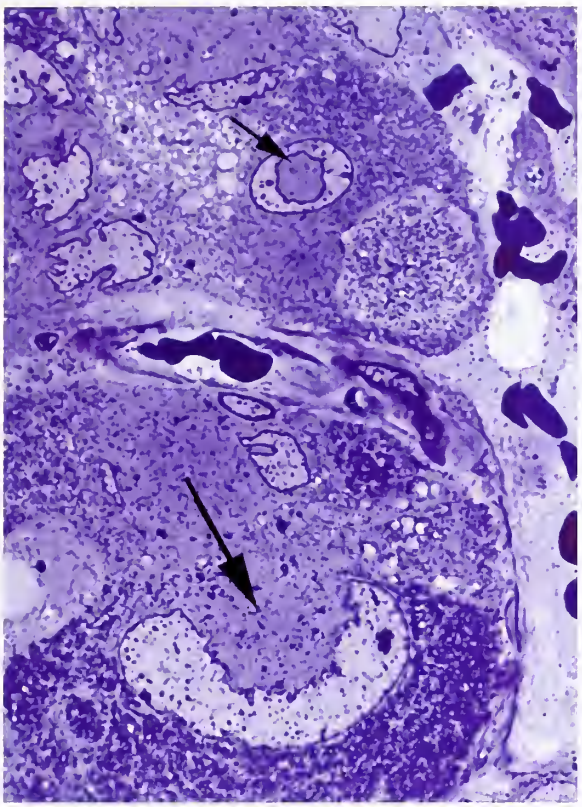

Figure 11-33

PHEOCHROMOCYTOMA

A 1-µm–thick section of a pheochromocytoma shows a deeply notched nucleus at the bottom (long arrow) and a nuclear pseudoinclusion at the top (short arrow) (toluidine blue stain).

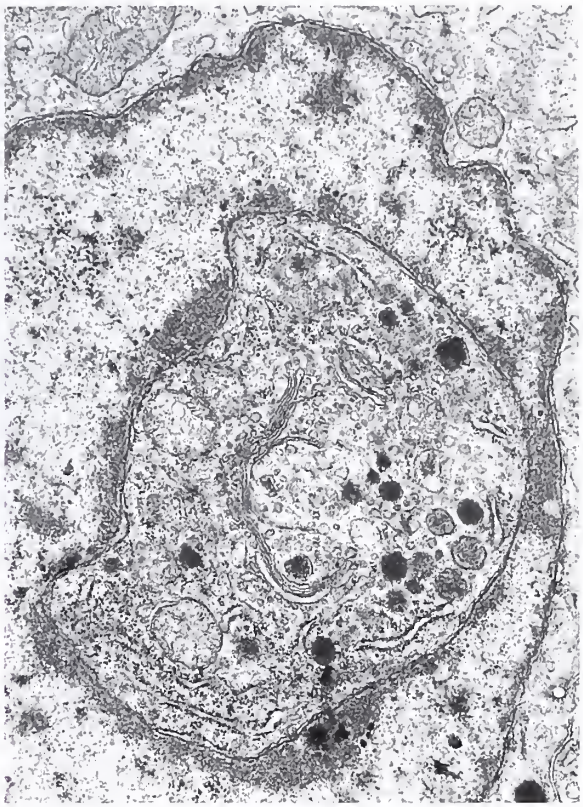

Figure 11-34

PHEOCHROMOCYTOMA

There are few dense-core neurosecretory granules. The increased density of organelles in the nuclear pseudoinclusion includes rough endoplasmic reticulum and a Golgi complex. (Fig. 13-4 from Fascicle 19, Third Series.)

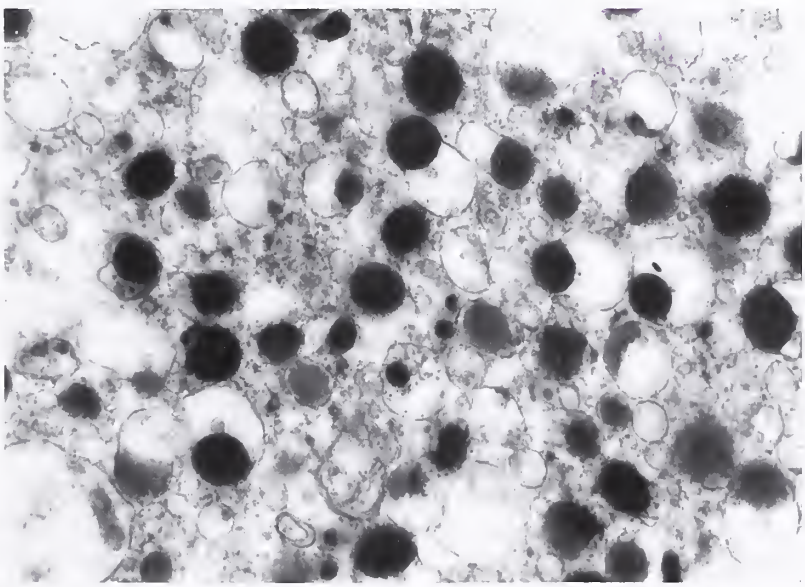

Figure 11-35

PHEOCHROMOCYTOMA

There is a range in morphology of dense-core neurosecretory granules. Some granules have a wide eccentric halo ("norepinephrine type" granules) while others have a more uniform thin halo with an investing membrane ("epinephrine type" granules).

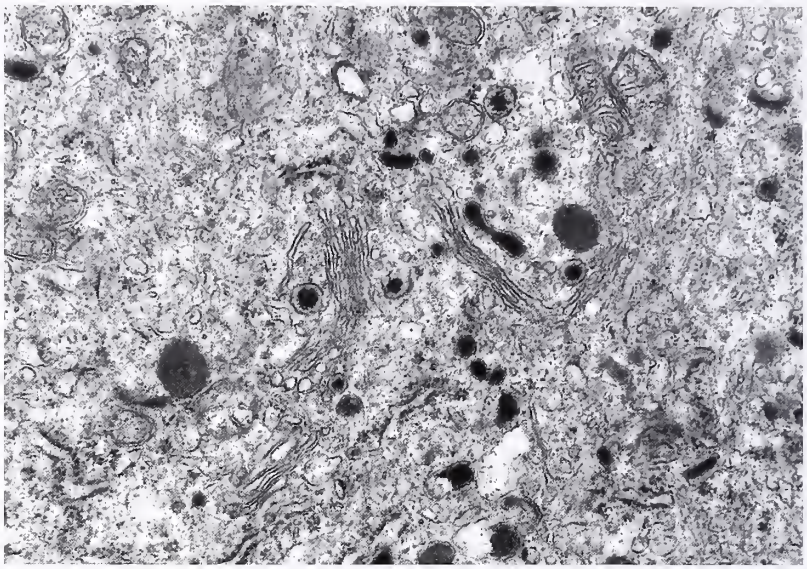

Figure 11-36

PHEOCHROMOCYTOMA

The Golgi complex is evident, with parallel stacks of endoplasmic reticulum and a few areas suggesting granule packaging. (Fig. 13-9 from Lack EE. Pathology of adrenal and extra-adrenal paraganglia. Major problems in pathology, Vol 29. Philadelphia: WB Saunders; 1994:298.)

even within the vascular lumen (83,84), but given the normal sequence of events in fusion and exocytosis of dense-core granules this may be an artifact (84).

In one study, homogenates of normal adrenal medulla revealed an epinephrine level of 4.05 mg/g and norepinephrine of 0.70 mg/g; ultrastructurally, 95 percent of neurosecretory granules were "epinephrine type" and 5 percent "norepinephrine type," a ratio of 20 to 1, which is very different from the ratio in most pheochromocytomas (83). There also appears to be a correlation between the concentration of catecholamines and the density of neurosecretory granules (85). The diameter of dense core granules varies from 127 to 270 nm (83). An ultrastructural study reported 20 of 27 pheochromocytomas had a predominance of type 1 neurosecretory granules (typical for norepinephrine type), while 20 of 23 extraadrenal paragangliomas had neurosecretory granules with type 2 morphology (typical for epinephrine type); on the basis of the differences in granule morphology, the pheochromocytomas were not considered synonymous with extraadrenal paragangliomas (86).

Biochemical analysis has shown that extraadrenal paragangliomas contain predominantly norepinephrine. An immunohistochemical study showed that 6 of 10 pheochromocytomas were positive for the enzyme phenylethanolamine N-methyl transferase (PNMT) (5 had increased levels of epinephrine) while 7 of 7 extraadrenal paragangliomas were negative for PNMT, suggesting a lack of capacity for synthesis of epinephrine (87). In another study of 52 pheochromocytomas and 18 extraadrenal paragangliomas, immunoreactivity for PNMT was limited to the pheochromocytomas, with mixed epinephrine and norepinephrine production (88). Immunoreactivity for PNMT, however, has been demonstrated in some extraadrenal paragangliomas (89).

As already noted, correlation of granule morphology with the storage of a particular catecholamine may not be precise. Granule morphology can vary greatly, with some being elongated, and others having a "dumbbell" or "teardrop" configuration (fig. 11-37) (84). Immunohistochemical studies have shown that pheochromocytomas and extraadrenal paragangliomas are capable of synthesizing or expressing a variety of regulatory peptides and hormones (84). Occasionally, large electron-dense structures are seen which correspond to intracytoplasmic hyaline globules (fig. 11-37). Sometimes there are small curvilinear profiles of structures at the periphery that have an electron density similar to that of neurosecretory granules. It has been suggested that the globules may in some way be related to the secretory activity of the cell (90).

Large vacuolar spaces, or pseudoacini, may be present within the cytoplasm of tumor cells (figs. 11-31, 11-38) (91). Some represent large

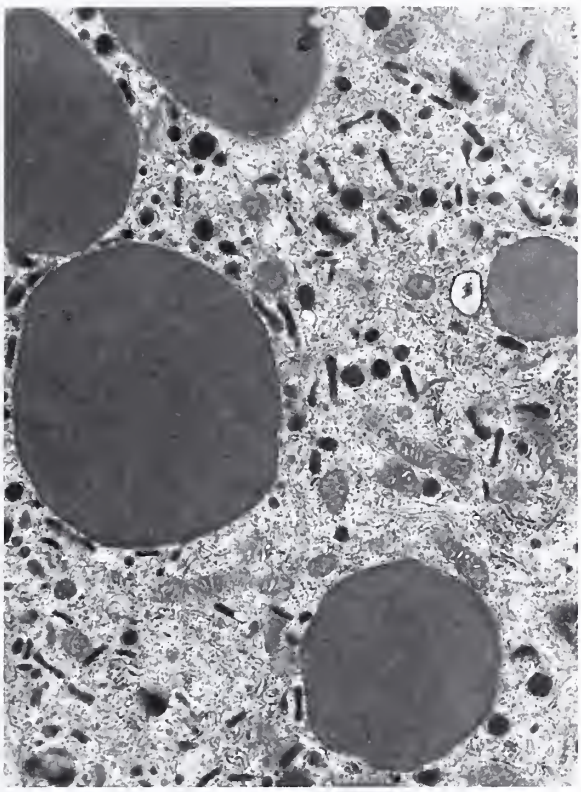

Figure 11-37

PHEOCHROMOCYTOMA

The large electron-dense structures probably represent intracellular hyaline globules. Note the pleomorphism of the dense-core neurosecretory granules. (Fig. 13-7 from Fascicle 19, Third Series.)

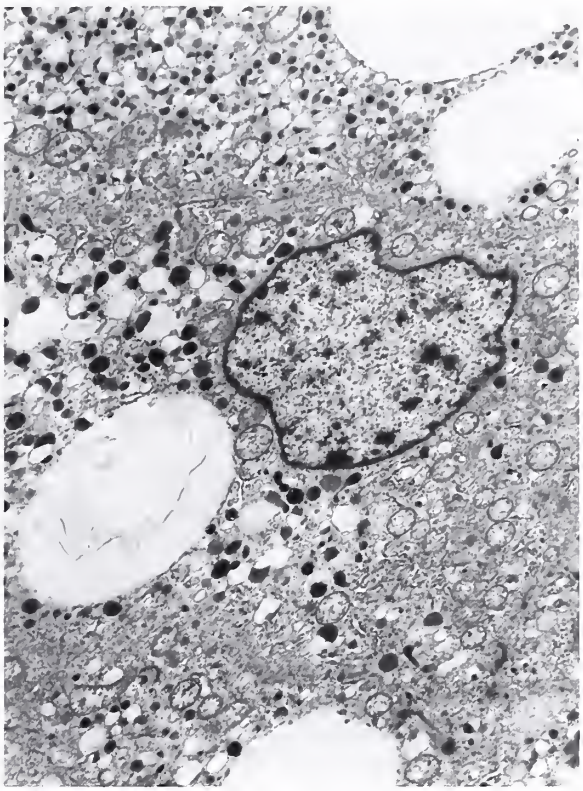

Figure 11-38

PHEOCHROMOCYTOMA

The large vacuolar spaces in this pheochromocytoma are pseudoacini. Some spaces could represent lipid that had been dissolved out during processing. The cells contain a predominance of granules with a wide eccentric halo (norepinephrine type granules).

lipid globules from which the lipid has been dissolved out; smaller ones could be dilated cisternae of endoplasmic reticulum or dilated secretory vesicles that either are empty or contain an eccentric dense core that is not visible in the plane of section.

Several unusual ultrastructural features have been reported, including an unusual glycogen-rich extraadrenal paraganglioma (92). Almost all of these tumors, including pheochromocytomas, usually contain little or no glycogen, at least by light microscopy (84). Neurofibrillary tangles and paired helical filaments, identical to those found in the brain in Alzheimer's disease, have been noted in a pheochromocytoma (93). Another unusual feature is the presence of intracytoplasmic crystalloids similar to structures in alveolar soft-part sarcoma and other cells such as Leydig and juxtaglomerular cells (94).

Immunohistochemical Findings. A wide variety of regulatory peptides and hormones can be localized immunohistochemically in pheochromocytomas and extraadrenal paragangliomas (Table 11-2) (95). All 99 sympathoadrenal paragangliomas studied at the National Cancer Institute (NCI) were positive for neuron-specific enolase (NSE), but similar immunoreactivity can be found in many other tumors. A positive staining reaction for NSE and other neuroendocrine markers can also be found in nuclear pseudoinclusions (fig. 11-39).

Chromogranin A is a member of a family of acidic secretory proteins found in the matrix of dense-core granules; related proteins include chromogranin B (CGB) and secretogranin II (96). Chromogranin A constitutes a large component of the soluble protein in secretory vesicles, and

Table 11-2

IMMUNOHISTOCHEMICAL EXPRESSION OF NEURON-SPECIFIC ENOLASE AND 10 NEUROPEPTIDES IN 99 SYMPATHOADRENAL PARAGANGLIOMAS[a]

	Percent Positive
Neuron-specific enolase	100
[Leu^5]-enkephalin	76
[Met^5]-enkephalin	75
Somatostatin	67
Bovine pancreatic polypeptide	51
Vasoactive intestinal peptide	43
Substance P	31
ACTH[b]	28
Calcitonin	23
Bombesin	15
Neurotensin	12

[a]Table 3-1 from Linnoila RI, Lack EE, Steinberg SM, Keiser HR. Decreased expression of neuropeptides in malignant paragangliomas: an immunohistochemical study. Hum Pathol 1988;19:41-50.
[b]ACTH = adrenocorticotropic hormone.

is a very good marker for neuroendocrine tumors such as sympathoadrenal paragangliomas (fig. 11-40) (97). Chromogranin B and secretogranin II are additional markers for neuroendocrine neoplasms.

Another useful marker is synaptophysin, an integral membrane glycoprotein of secretory vesicles (fig. 11-41) (97); however, adrenal cortical neoplasms, both benign and malignant, can be immunoreactive (98,99) which may be a source of confusion and even lead to misdiagnosis. Immunostain for the neuroendocrine secretory protein-55 (NESP-55), the latest addition to the chromogranin family, apparently has a less widespread distribution in neuroendocrine cells and in a recent study was expressed only in endocrine tumors of the pancreas and adrenal medulla (100). The antilymphocyte antibody leu-7 (HNK-1) (101) and protein gene product (PGP) 9.5 (102) also have been used as neuroendocrine markers.

The most sensitive method for identifying sustentacular cells is by immunostaining for S-100 protein which decorates the nucleus and cytoplasm of elongated, stellate or dendritic sustentacular cells at the periphery of cords and

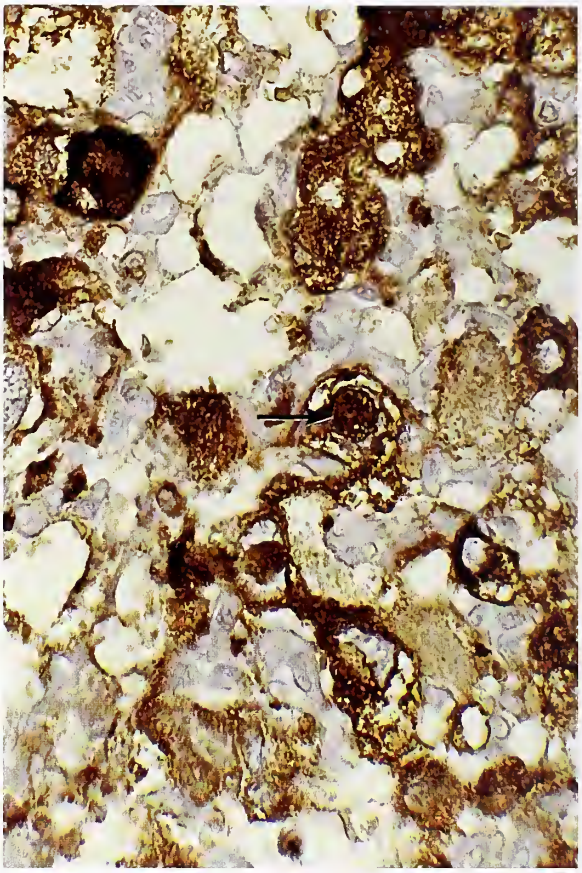

Figure 11-39

EXTRAADRENAL PARAGANGLIOMA OF ABDOMEN

The nuclear pseudoinclusion stains for neuron-specific enolase, similar to the cytoplasm of all tumor cells (avidin-biotin peroxidase method). (Fig. 13-9, right from Fascicle 19, Third Series.)

clusters of tumor cells (fig. 11-42). Recently, a distinctive neoplasm of the adrenal medulla was reported having morphology, immunophenotype, and ultrastructural features suggesting derivation from sustentacular cells; the designation "sustentaculoma" was proposed (103).

Associated Endocrine Syndromes and Other Features. Aside from these neuroendocrine markers, sympathoadrenal paragangliomas are capable of expressing a broad array of neuropeptides and hormones (Table 11-2). Immunostaining for [leu^5]-enkephalin and [met^5]-enkephalin was seen in about 75 percent of tumors studied at the NCI (95). In one study, diffuse adrenal medullary hyperplasia consistently showed leu-enkephalin-like immunoreactivity,

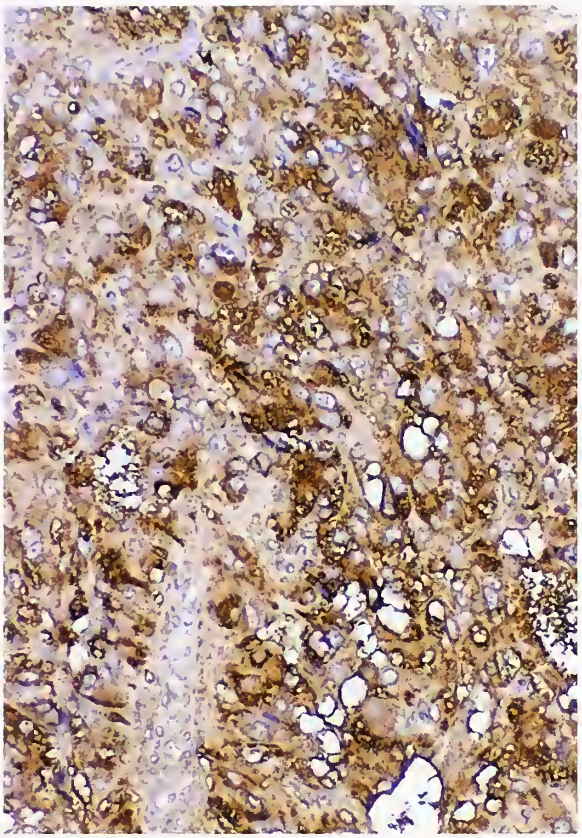

Figure 11-40

COMPOSITE PHEOCHROMOCYTOMA

Composite pheochromocytoma shows strong immunostaining for chromogranin A (avidin-biotin peroxidase method).

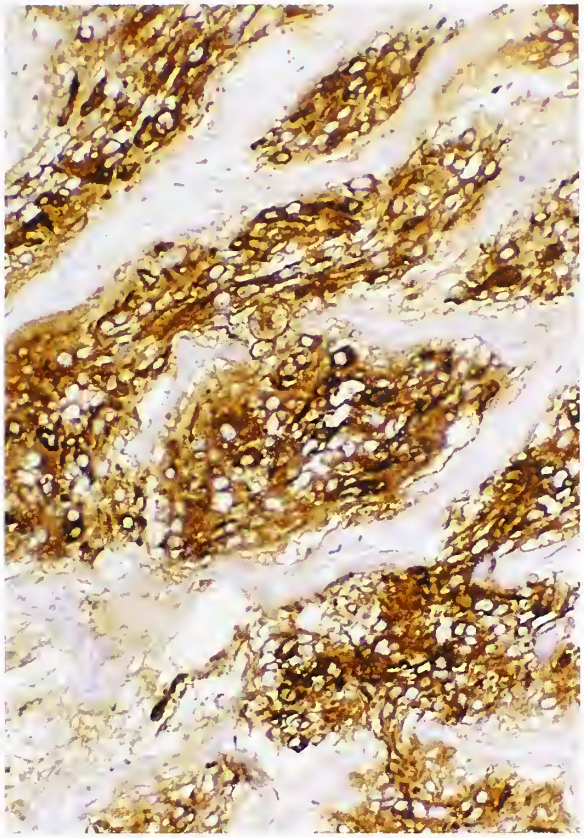

Figure 11-41

EXTRAADRENAL PARAGANGLIOMA OF ABDOMEN

Tumor shows positive immunostaining for synaptophysin (avidin-biotin peroxidase method).

whereas only 50 percent of hyperplastic nodules, pheochromocytomas, and extraadrenal paragangliomas were positive (104). Usually, however, there is no endocrine syndrome or other manifestation ascribed to any particular neuropeptide or hormone with the exception of catecholamines (105,106). In the study at the NCI, 28 percent of sympathoadrenal paragangliomas immunostained for adrenocorticotropic hormone (ACTH), however, rarely have pheochromocytomas been the cause of Cushing's syndrome due to ectopic ACTH production (107,108). Cushing's syndrome due to ectopic production of corticotropin-releasing factor by a pheochromocytoma has been reported (109). ACTH-like immunoreactivity has also been observed in the normal adrenal medulla (106). A review of endocrinologic data associated with ectopic ACTH production by pheochromocytomas indicated that indices of steroid production were markedly elevated in the presence of only modest plasma levels of ACTH, which might be explained by the close proximity of the pheochromocytoma to adrenal cortical sites of ACTH stimulation (110). Evaluation of a patient with Cushing's syndrome and an adrenal mass should include the possibility of an ACTH-producing pheochromocytoma (105).

A watery diarrhea syndrome, also referred to as the Verner-Morrison syndrome (111) or WDHA (watery diarrhea, hypokalemia, achlorhydria) syndrome, has been reported in association with pheochromocytomas (112), and has been attributed to the release of vasoactive intestinal peptide (VIP). In the study at the NCI,

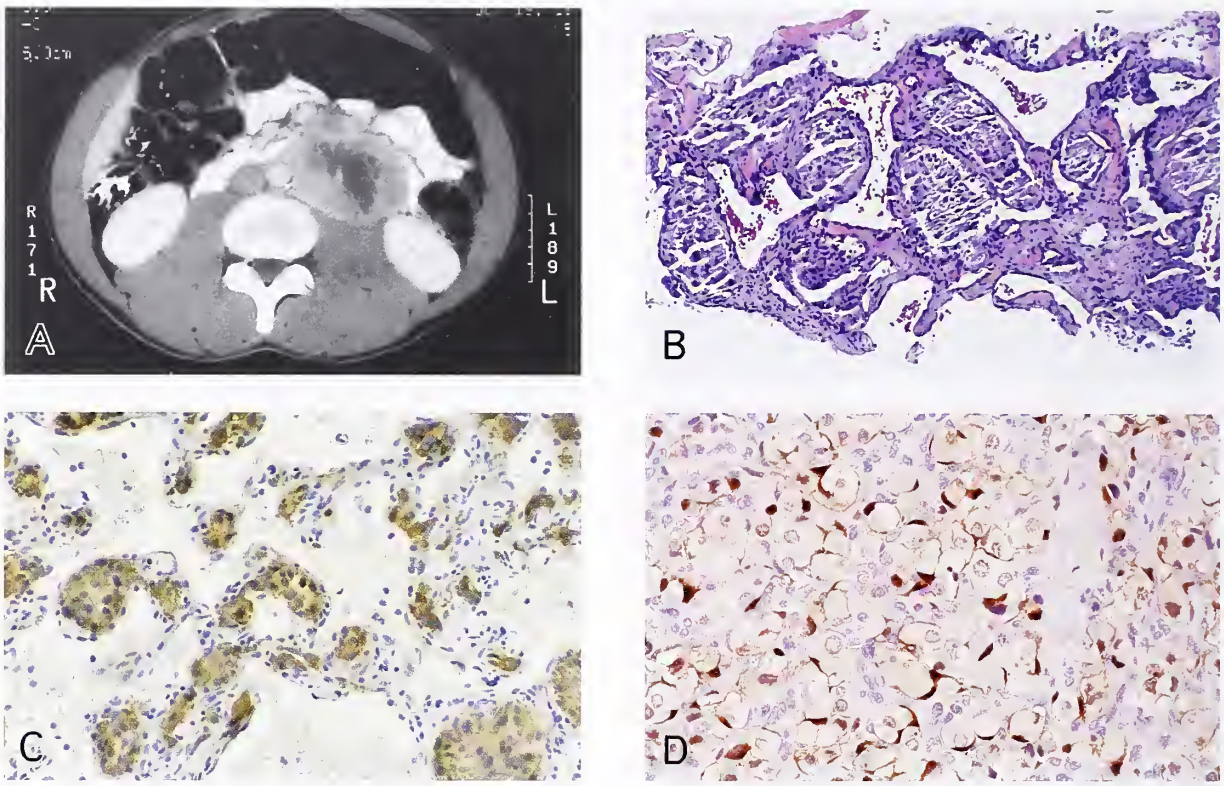

Figure 11-42

EXTRAADRENAL PARAGANGLIOMA ARISING FROM ORGAN(S) OF ZUCKERKANDL

A: Extraadrenal paraganglioma is located near the lower pole of the kidney on the left side and partially encircles the aorta near the midline. The tumor measured 7.5 cm in diameter. On this computerized tomography (CT) scan the tumor is nonhomogenous, suggesting necrosis or cystic degeneration. A percutaneous thin needle core biopsy was obtained.

B: Needle core biopsy shows a nesting arrangement of tumor cells with dilated vascular spaces.

C: An organoid or nesting pattern is accentuated by a positive immunostain for chromogranin A.

D: Immunostain for S-100 protein in same case demonstrates dark staining of the nuclei of sustentacular cells (C,D: avidin-biotin peroxidase method).

43 percent of sympathoadrenal paragangliomas immunostained for VIP, yet none of the patients had the watery diarrhea syndrome (106); few, if any, of the tumors showed any ganglionic or neuronal features. Conversely, a number of tumors do show neuronal or ganglionic features as well as immunoreactivity for VIP, yet there is no associated diarrheal syndrome (fig. 11-43).

Hypercalcemia has also been reported in association with pheochromocytomas (113,114), and in some cases was attributed to the production of a parahormone-like substance (114) or calcitonin (113). Other unusual features associated with pheochromocytoma include polycythemia due to erythropoietin production (115), and diarrhea and steatorrhea (116) possibly due in one case to somatostatin production (117). Secretion of growth hormone-releasing factor has also been described with acromegaly (118).

Other Immunoreactive Substances. Other immunoreactive substances that have been reported in pheochromocytomas (or adrenal medulla) include galanin (119), renin (120), atrial natriuretic polypeptide (121), and insulin-like growth factor (122). Positive immunostaining for J1-beta-tubulin, microtubule-associated protein 2 (MAP-2) (123), and neural cell adhesion molecule (N-CAM) has been reported (124). Pheochromocytomas also join the slowly growing number of tumors, in addition to malignant melanoma, that may be immunoreactive for HMB45 (125).

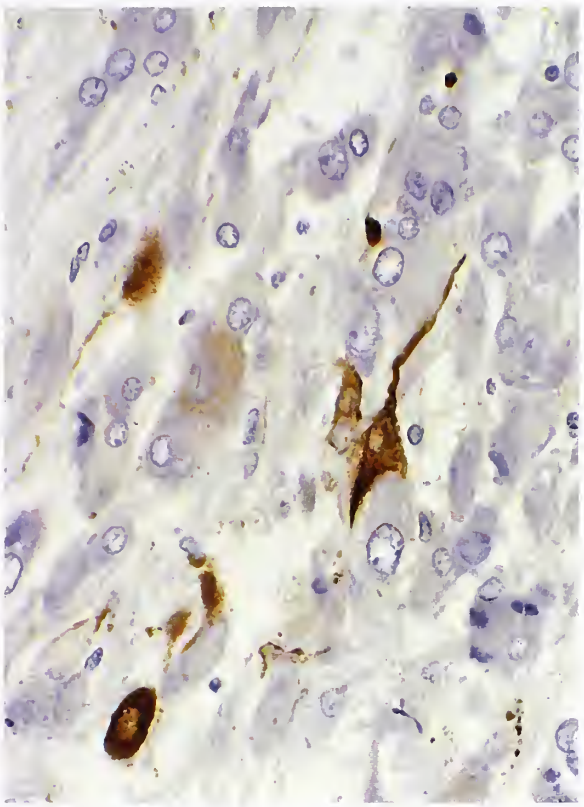

Figure 11-43

COMPOSITE PHEOCHROMOCYTOMA

Some tumor cells with neuronal features show intense immunoreactivity for vasoactive intestinal peptide. Areas elsewhere in the tumor had morphologic features resembling those of a ganglioneuroblastoma (avidin-biotin peroxidase method). (Fig. 13-14 from Fascicle 19, Third Series.)

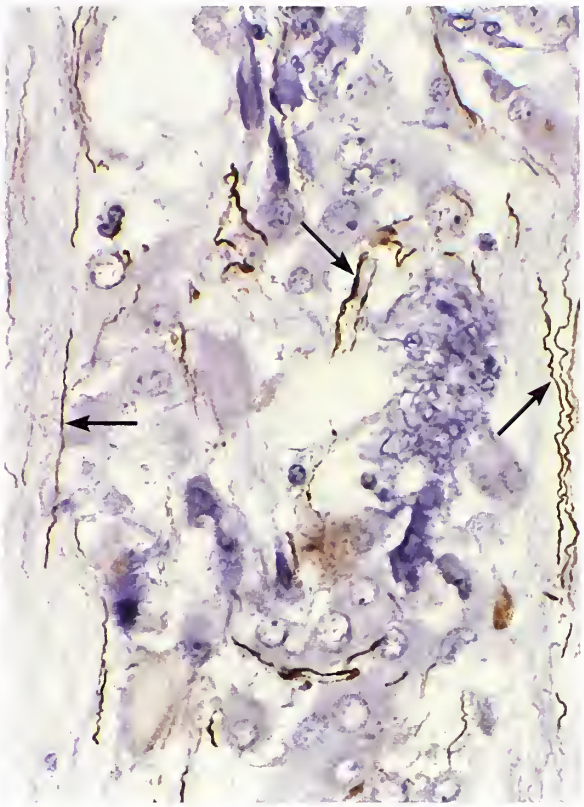

Figure 11-44

COMPOSITE PHEOCHROMOCYTOMA

Positive immunostaining for neurofilament protein is seen mainly in small neuritic processes (arrows). Other areas of the tumor had morphologic features resembling ganglioneuroblastoma (avidin-biotin peroxidase method). (Fig. 13-15 from Fascicle 19, Third Series.)

Intermediate Filament Profile. Neurofilament (NF) proteins have been demonstrated in a high proportion of sympathoadrenal paragangliomas (fig. 11-44) (126–128). In the normal adrenal medulla, positive immunostaining for NF protein has been localized to nerve axons, some ganglion cells, and chromaffin cells (127). In general, immunostaining for vimentin is usually restricted to vascular and connective tissue structures, but staining may be more widespread (129). Vimentin positivity has been reported in pheochromocytomas (126,128). Staining for cytokeratin has also been reported in pheochromocytomas (fig. 11-45) (128), and similar staining has been observed in occasional paragangliomas of the head and neck region using monoclonal antibodies AE1/AE3 and CAM5.2 (130). The rat pheochromocytoma cell line (PC12) expresses markers for cytokeratin (131), and these cells as well as tumor cells of human sympathoadrenal paraganglioma appear capable of coexpressing both epithelial and neuronal immunomarkers. Globules in some pheochromocytomas have been positive for vimentin and glial fibrillary acidic protein (GFAP), and occasional staining has been demonstrated in cells of pheochromocytoma (123) or composite pheochromocytoma, where in addition the neurofibrillary matrix is also positive for NSE (fig. 11-46).

Relation of Immunohistochemistry to Prognosis. Some investigators report a paucity or absence of S-100 protein-positive (sustentacular) cells in clinically aggressive or metastasizing pheochromocytomas and extraadrenal paragangliomas

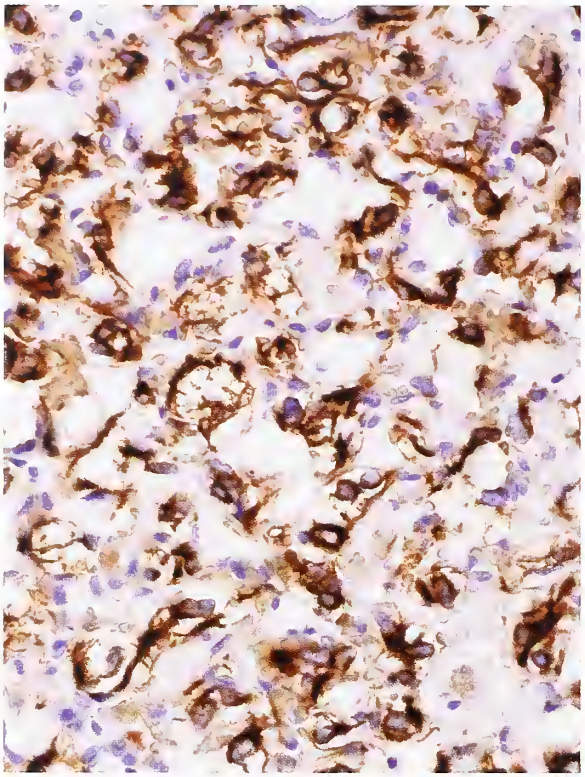

Figure 11-45

PHEOCHROMOCYTOMA

Unusual example of pheochromocytoma in which tumor cells show strong immunoreactivity for the pankeratin marker AE1/AE3, a staining reaction that is unexpected and may on occasion lead to problems in diagnosis (avidin-biotin peroxidase method).

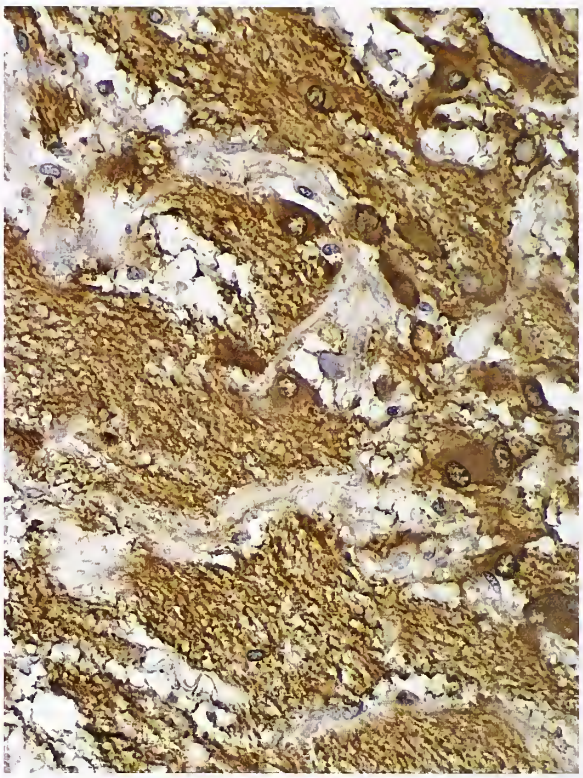

Figure 11-46

COMPOSITE PHEOCHROMOCYTOMA

Composite pheochromocytoma with dense mats of fibrillary matrix resembling neuropil. Scattered tumor cells have neuronal features and along with the fibrillary matrix are strongly positive for neuron-specific enolase (avidin-biotin peroxidase method). (Fig. 13-16 from Fascicle 19, Third Series.)

(132–135). A subsequent study confirmed that clinically malignant tumors tend to have a reduced number of S-100 protein-positive cells, however, the presence or absence of this sustentacular cell population is not an absolutely reliable method for predicting biologic behavior (136). In a study of 64 sympathoadrenal paragangliomas (20 clinically malignant, 44 classified as clinically benign), 37 of the 44 benign tumors contained S-100 protein-positive cells (14 scored as 1+, 13 as 2+, 10 as 3+); the other 7 tumors were negative. There were no S-100 protein-positive cells in 12 of the 20 malignant tumors (60 percent), but in 8 tumors there was a similar spectrum of reactivity (2 scored as 1+, 3 as 2+, 3 as 3+).

Clinically malignant sympathoadrenal paragangliomas have been reported to express significantly fewer neuropeptides compared with benign tumors, although the spectrum of immunostaining is similar (Table 11-3); clinically benign tumors express an average of five neuropeptides compared with two for the malignant tumors (137). A few studies report abnormalities in neuropeptide Y and NSE expression or secretion (138,139). Neuropeptide receptors have been reported in 93 percent of adrenal cortical tumors, 35 percent of pheochromocytomas, and 61 percent of paragangliomas and may be a potential new molecular target for the treatment of malignant tumors (140).

There are recent reports which correlate increased expression of tenascin (141) with malignant pheochromocytomas. The use of region-specific antibodies raised against epitopes in the C-terminal region of chromogranin B and C is

Table 11-3

SIMULTANEOUS EXPRESSION OF MULTIPLE NEUROPEPTIDES IN BENIGN AND MALIGNANT SYMPATHOADRENAL PARAGANGLIOMAS[a]

	Number of Neuropeptides[b]											
	0	1	2	3	4	5	6	7	8	9	10	Index[c]
Benign Tumors	2	2	4	8	9	11	12	5	3	0	0	5
Malignant Tumors	4	3	5	7	2	1	2	0	1	0	0	2

[a]Table 13-2 from Fascicle 19, Third Series.
[b]The presence of the 10 neuropeptides was assessed in two or more blocks of each tumor by immunohistochemistry.
[c]The average number of neuropeptides per tumor.

reported to be potentially useful in the diagnosis of malignant pheochromocytoma (142). Further investigation is needed to identify truly reliable immunomarkers useful in predicting biologic behavior in these neoplasms.

In Situ Hybridization and Other Techniques. In situ hybridization shows great potential as a molecular probe for the diagnosis of sympathoadrenal paraganglioma, offering the pathologist the opportunity to combine molecular and morphologic methodologies (143–145). Detection of mRNA indicates actual production of the gene product by the cell in question rather than secondary absorption, and the technique does not require expression of the gene product because DNA or mRNA gene substance can be detected directly. The polymerase chain reaction (PCR) also has potential application in endocrine pathology for studying oncogene amplification as well as for identifying and analyzing mutations in DNA (146).

Molecular Genetics. About 10 percent of patients with pheochromocytomas and extraadrenal paragangliomas present with a family history of multiple endocrine neoplasia (MEN) type 2, von Hippel-Lindau disease, neurofibromatosis type 1, or one of several paraganglioma syndromes usually involving tumors of the head and neck region which are aligned more closely with the parasympathetic nervous system (147). Germline mutations of the *RET* protooncogene (chromosomal locus 10q11) are responsible for the inheritance of MEN types 2a and 2b in which approximately 50 percent of patients develop pheochromocytomas (147–149). Von Hippel-Lindau disease is characterized by mutations or deletions in the VHL gene (chromosomal locus 3p25); 10 to 34 percent of all patients develop pheochromocytomas or extraadrenal paragangliomas (147). Neurofibromatosis 1 is associated with an abnormality of the NF1 tumor suppressor gene, and loss of neurofibromin affects the same signaling pathway as does overexpression of *RET* (147). The genetic cause of familial paragangliomas aligned with the parasympathetic nervous system involves germline mutations in the succinate dehydrogenase subunits D, C, and B (*SDHD, SDHC,* and *SDHB*) (147). The paraganglioma (PGL) syndromes have been classified on the basis of molecular genetics: *SDHB* mutations predispose to PGL-1, mutations in an unidentified gene on chromosome 11 to PGL-2, *SDHC* mutations to PGL-3, and *SDHB* mutations to PGL-4 (150).

Head and neck paragangliomas are statistically more prevalent among *SDHD* mutation carriers while intraabdominal extraadrenal tumors are more prevalent among *SDHB* mutation carriers. Malignant tumors are more common with *SDHB* mutation-positive individuals. In the combined pheochromocytoma (n = 334) and paraganglioma (n = 83) registries, 49 patients (12 percent) showed a mutation in the *SDHB* or *SDHD* gene (150). Detecting an underlying genetic abnormality hopefully will aid in diagnosis and genetic counseling.

Specific codon mutations in the RET protooncogene may be an important prognostic factor for patients with MEN type 2 (151). A recent review focuses on the varied mutations of the RET proto-oncogene and signaling involved in development of endocrine tumors of the thyroid and adrenal medulla. Deeper understanding of molecular mechanisms may provide targets for the development of novel, specific, and effective small molecule therapeutics to treat RET-mediated tumors (152).

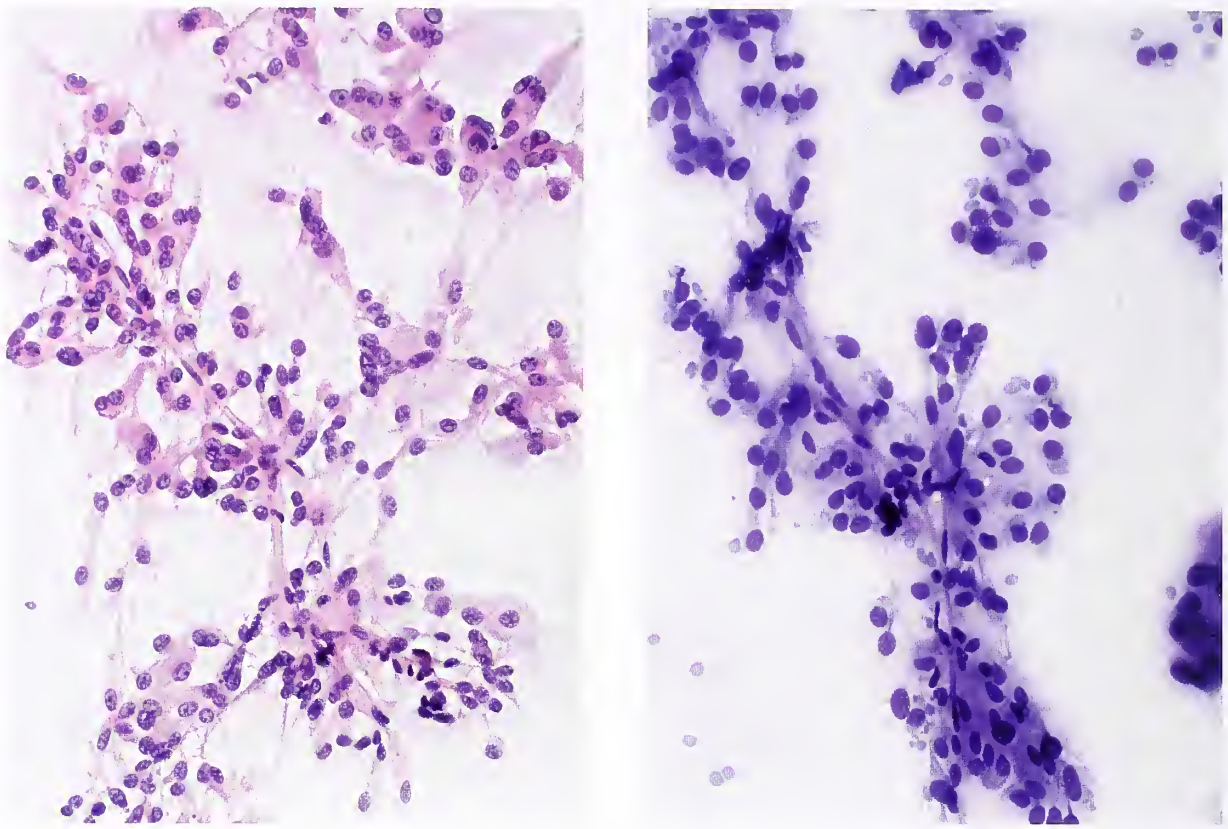

Figure 11-47

PHEOCHROMOCYTOMA

Left: Aspirate smear of a surgically resected pheochromocytoma shows a delicate branching vessel with a surrounding mantle of partially disrupted tumor cells. The nuclear morphology is relatively uniform. The patient had findings of excess catecholamine secretion and underwent pharmacologic blockade prior to surgical resection of the tumor.

Right: Diff Quik stain in the same case.

Cytologic Findings. Cytologic results of fine needle aspiration biopsy (FNAB) of pheochromocytomas and extraadrenal paragangliomas have been reported (153–157), including a case of composite pheochromocytoma-ganglioneuroma (158). Problems occur when malignancy is diagnosed based solely on the interpretation of cytologic atypia, which can be rather marked in these tumors, similar to head and neck paragangliomas. Potentially fatal consequences have been reported with the FNAB procedure, including marked alteration in blood pressure (159–161), sometimes complicated by uncontrollable intraabdominal hemorrhage (159). Due caution is necessary when knowingly aspirating a suspected catecholamine-producing paraganglioma (153,154).

Pheochromocytomas cytologically can feature binucleated or multinucleated cells and prominent intranuclear pseudoinclusions. Precise anatomic localization and close correlation with clinical and endocrinologic data may provide an important advantage in cytologic interpretation, recognizing of course other endocrine tumors that can mimic a paraganglioma, such as a pancreatic endocrine neoplasm (162). Smear/imprint preparations of surgically resected tumors may provide the opportunity to gain familiarity with the cytologic features of these rare tumors (fig. 11-47). Preoperative FNAB of two pheochromocytomas is shown in figure 11-48; the tumors were not associated with excess catecholamine secretion.

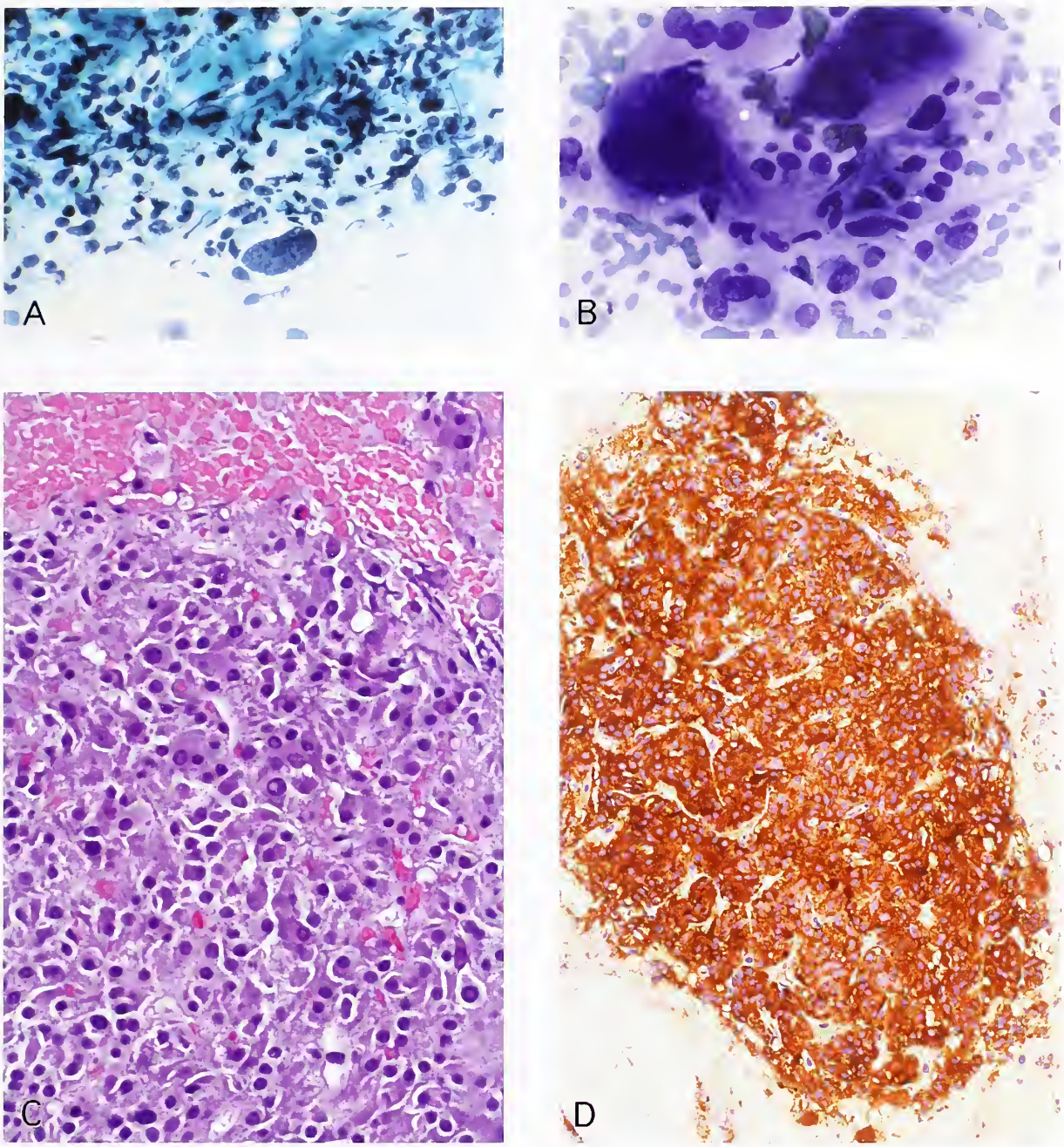

Figure 11-48

PHEOCHROMOCYTOMA

A: The patient had no evidence of excess catecholamine secretion. Preoperative fine needle aspiration biopsy of the adrenal mass shows a relatively cellular smear with occasional enlarged nuclei (Papanicolaou stain).

B: The cells in the same tumor are intact, with enlarged nuclei. The tumor proved to be clinically benign (Diff Quik stain).

C: Fine needle aspiration biopsy of another pheochromocytoma in a patient who also had no evidence of catecholamine hypersecretion. The cell block preparation shows tight organoid clusters of cells with an occasional nuclear pseudoinclusion near the center of the field.

D: Immunostain for chromogranin is markedly positive in same case as C (avidin-biotin peroxidase method).

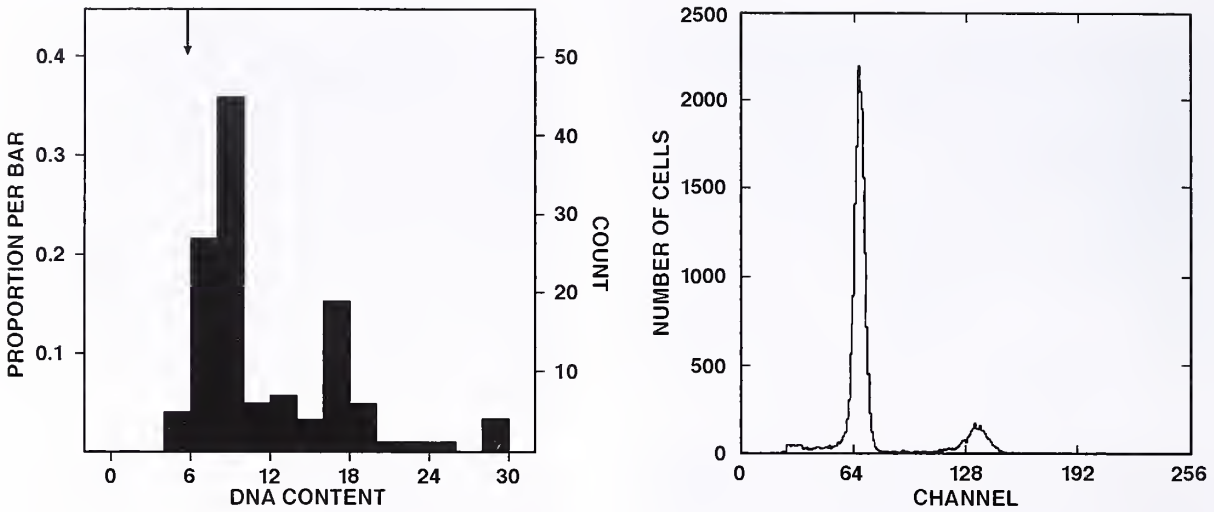

Figure 11-49

CLINICALLY MALIGNANT EXTRAADRENAL ABDOMINAL PARAGANGLIOMA

Left: Static image analysis of DNA content shows aneuploid peaks. (L&R: Fig. 13-19 from Fascicle 19, Third Series.) Right: Flow cytometric analysis of DNA content in same case shows concordance for peak number and placement, although image analysis suggests the presence of a tetraploid subpopulation of cells not evident by flow analysis.

Role of Quantitative DNA Analysis in Prognosis. There have been several studies of the DNA content of pheochromocytomas using flow cytometry or static image analysis of tissue sections (163–173) or cytology specimens (174) in order to predict biologic behavior, but there have been conflicting interpretations (175). Two successive series of DNA flow cytometric analyses from the Mayo Clinic suggest that DNA ploidy patterns offer independent prognostic value for patients with sympathoadrenal paragangliomas (fig. 11-49) (165,169). All 12 patients who died of tumor-related disease had abnormal DNA ploidy, whereas none of the 64 patients with DNA diploid tumors died. These findings are in contrast to other studies using flow cytometry and DNA cytophotometry (fig. 11-50) indicating that on a statistical basis, quantitative DNA analysis does not reliably discriminate between clinically benign and malignant sympathoadrenal paragangliomas (163,166–168,170,173,174). One study documented DNA tetraploidy or aneuploidy in 16 of 72 clinically benign adrenal and extraadrenal paragangliomas (170). Indeed, the surgical pathologist dealing with endocrine tumors in general encounters a significant number of cases with aberrations in nuclear size and shape along with hyperchromasia in which long-term clinical follow-up has indicated a benign course (175).

UNUSUAL NEOPLASMS

Gangliocytic Paraganglioma

This rare tumor was first described by Dahl et al. (176) as a duodenal ganglioneuroma. It was considered to be more closely related to a nonchromaffin paraganglioma (177), and was subsequently designated as gangliocytic paraganglioma (178). About 95 percent of gangliocytic paragangliomas arise in the second portion of the duodenum (179–181), although occasionally in other sites such as jejunum (180), pylorus (181), appendix (182), and even mediastinum and esophagus (183). The tumor may have areas resembling an endocrine tumor, but on close scrutiny this resemblance is superficial (fig. 11-51).

Paraganglioma of Cauda Equina

Paragangliomas of the cauda equina region are rare neoplasms that are usually intradural and limited to the filum terminale. Occasionally they involve the conus medullaris, caudal nerve roots, and thoracic region. Sometimes the

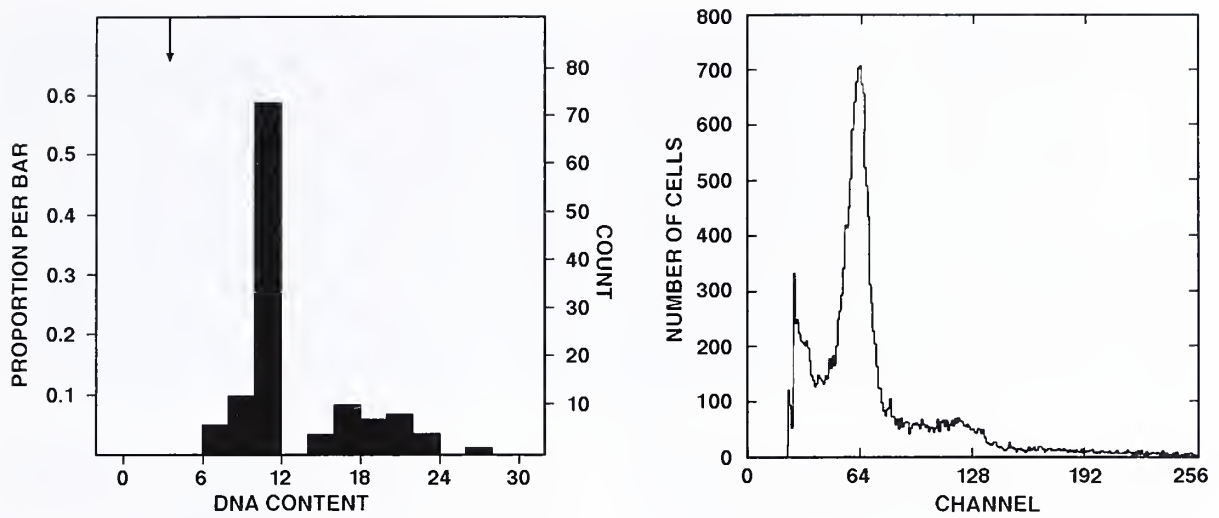

Figure 11-50

CLINICALLY BENIGN PHEOCHROMOCYTOMA

Left: Aneuploidy is evident on static image analysis DNA histogram. (L&R: Fig. 13-20 from Fascicle 19, Third Series.)
Right: Flow cytometric analysis of DNA content in same case. There is better discrimination of aneuploidy by image analysis (left) when the diploid flow peak is obscured due to a paucity of diploid cells or a prevalence of debris.

tumor is epidural. Data from the Mayo Clinic (31 cases) show a slight predilection for males (average age, 51 years). Presenting signs and symptoms include low back pain (87 percent), sensory/motor deficit (35 percent), urinary/fecal incontinence (13 percent), and even paraplegia (6 percent) (184). Most tumors appear to be grossly encapsulated, and the histologic appearance is reported to resemble that of paragangliomas at other sites (184), although the full range of morphology is probably not known. Occasional cases have been reported with neuronal or ganglion cells (185), and ependymal differentiation has been described (186). An oncocytic paraganglioma of the cauda equina has been reported (187) and a germline mutation in succinate dehydrogenase subunit D (SDHD) was recently documented in a paraganglioma of the spinal cord (188). Although occasional pheochromocytomas and extraadrenal paragangliomas express cytokeratin (189), paragangliomas of the cauda equina have a distinctive cytokeratin profile (190).

GLOMUS COCCYGEUM

The glomus coccygeum, first noted by Luschka (191,192), is a small, ovoid structure located near the tip of the coccyx and measuring only a few millimeters in diameter (fig. 11-52). It receives its blood supply from the median sacral artery, and is innervated by the pelvic sympathetic plexus. It is composed of nests of epithelioid cells surrounding small vascular channels (fig. 11-52B,C). The function of this normal anatomic structure is not yet established, and its importance to the pathologist is to know of its existence and not to mistake it for a neoplasm (193–195), including a glomus tumor (196). Immunohistochemical and ultrastructural features indicate that the epithelioid cells are modified smooth muscle cells (197).

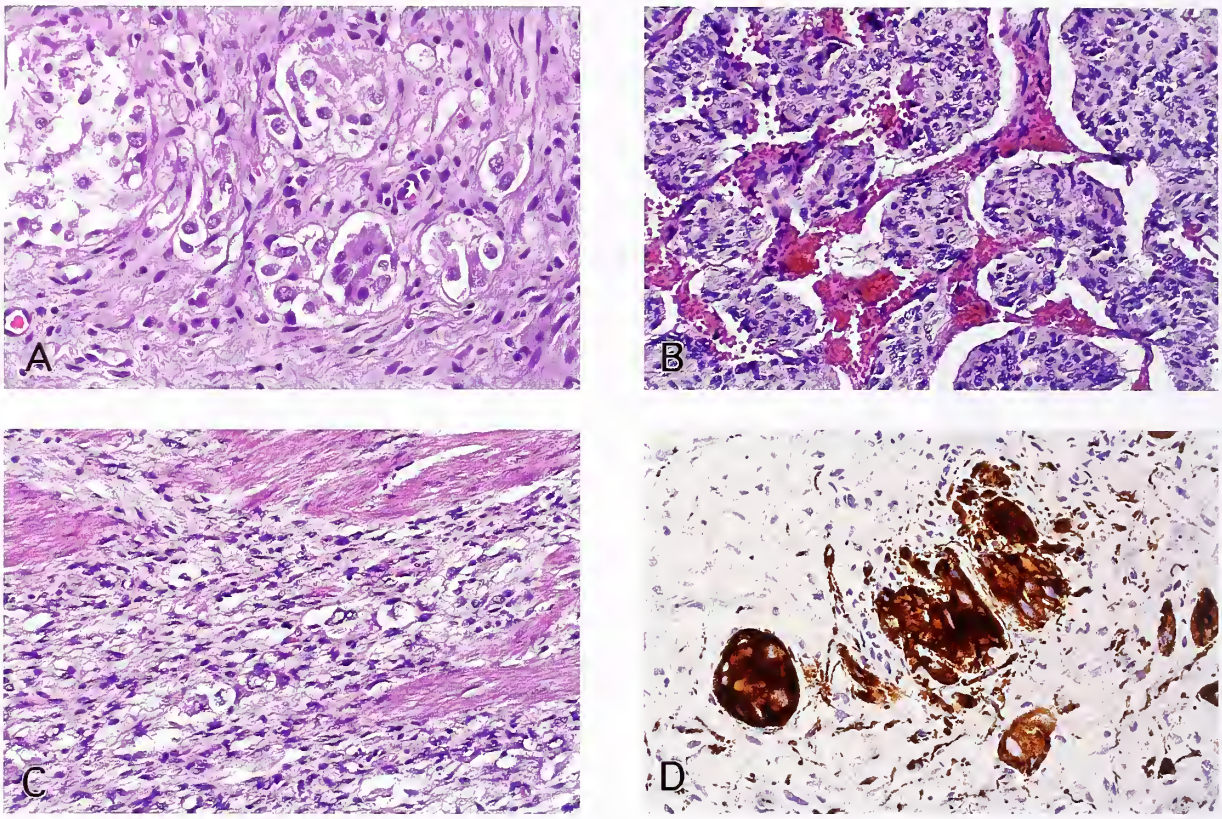

Figure 11-51

GANGLIOCYTIC PARAGANGLIOMA

A: Organoid clusters of epithelioid endocrine cells are set within a spindle cell matrix and resemble Schwann cells.

B: The gangliocytic paraganglioma has a delicate vasculature and organoid clusters of cells.

C: A few cells resemble neuronal or ganglion cells. Spindle cells are also a prominent component. The tumor has extended into the smooth muscle that was adjacent to the ampulla of Vater. (Figs. 22-77A and 22-76B from Lack EE. Pathology of the pancreas, gallbladder, extrahepatic biliary tract, and ampullary region. New York: Oxford University Press; 2003:557-558.)

D: Clusters of endocrine cells are vividly demonstrated by immunostain for synaptophysin (avidin-biotin peroxidase method).

REFERENCES

Extraadrenal Paraganglia

1. Lack EE, Kozakewich HP. Embryology, developmental anatomy, and selected aspects of nonneoplastic pathology. In: Lack EE, ed. Pathology of the adrenal glands. New York: Churchill Livingstone; 1990:1-74.
2. Lack EE. Pathology of adrenal and extra-adrenal paraganglia. Major problems in pathology, Vol. 29. Philadelphia: WB Saunders; 1994.
3. Coupland RE. The natural history of the chromaffin cell. London: Longmans; 1965.
4. Glenner GG, Grimley PM. Tumors of the extra-adrenal paraganglion system (including chemoreceptors). Atlas of Tumor Pathology, 2nd Series, Fascicle 9, Washington, D.C.: Armed Forces Institute of Pathology; 1974.
5. Zuckerkandl E. Ueber nebenorgane des sympathicus im retroperitonaealraum des menschen. Verh Anat Ges 1901;19:95-107.
6. Zuckerkandl E. The development of the chromaffin organs and of the suprarenal bodies. In: Keibel F, Mall FP, eds. Manual of human embryology, Vol. 2. Philadelphia: JB Lippincott; 1912:157-179.

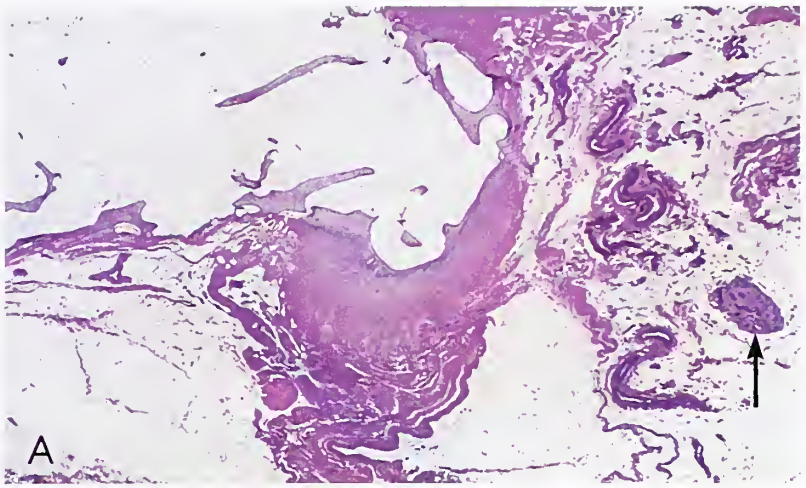

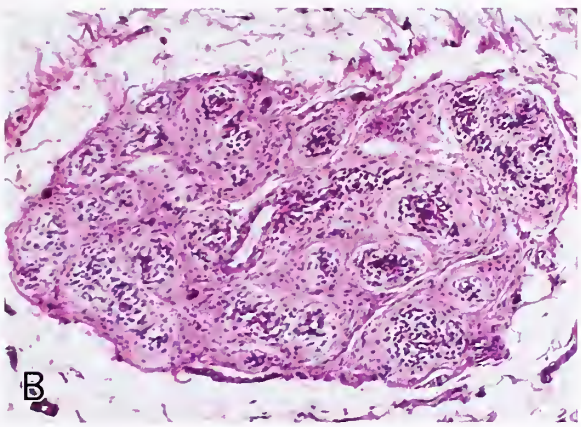

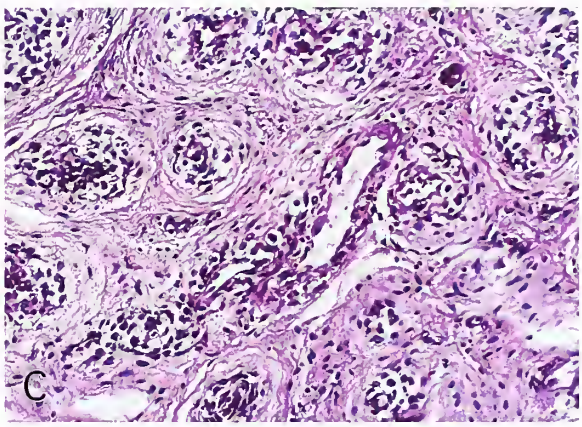

Figure 11-52

NORMAL GLOMUS COCCYGEUM

A: Sagittal section through the coccyx of an adult at autopsy shows a glomus coccygeum (arrow) measuring 2 to 3 mm. (Fig. 12-20A from Fascicle 19, Third Series.)

B: Glomus coccygeum is a well-circumscribed vascular structure with small vessels surrounded by a mantle of epithelioid cells, similar to cutaneous glomera.

C: Glomus coccygeum is not related to paraganglia. This normal anatomic structure near the tip of coccyx should not be confused with a neoplasm.

7. Kohn A. Die paraganglien. Arch f Mikr Anat, Bd 1903:62;263-365.
8. Coupland RE. Persistence of typical chromaffin cells in the human paravertebral sympathetic chain in the child and adult. J Anat 1979;129 (pt 1):196-197. [abstract]
9. Coupland RE. Postnatal fate of the abdominal para-aortic bodies in man. J Anat 1954;88:455-464.
10. Coupland RE. The prenatal development of the abdominal para-aortic bodies in man. J Anat 1952;86:357-372.
11. Hervonen A, Vaalasti A, Partanen M, Kanerva L, Vaalasti T. The paraganglia, a persisting endocrine system in man. Am J Anat 1976;146:207-210.
12. Chiba T. Monoamine fluorescence and electron microscopic studies on small intensely fluorescent (granule-containing) cells in human sympathetic ganglia. J Comp Neurol 1978;179:153-166.
13. West GB, Shepherd DM, Hunter RB, MacGregor AR. The function of the organs of Zuckerkandl. Clin Sci 1953;12:317-325.
14. Tischler AS. Paraganglia. In: Sternberg SS, ed. Histology for pathologists, 2nd ed. Philadelphia: Lippincott-Raven; 1997:1153-1172.
15. Niemineva K, Pekkarinen A. Determination of adrenalin and noradrenalin in the human fetal adrenals and aortic bodies. Nature 1953;171:436-437.
16. Hollinshead WH. Chemoreceptors in the abdomen. J Comp Neurol 1941;74:269-285.
17. Hollinshead WH. The function of the abdominal chemoreceptors of the rat and mouse. Am J Physiol 1946;147:654-660.
18. Coupland RE. The natural history of the chromaffin cell—twenty-five years on the beginning. Arch Histol Cytol 1989;52:331-341.
19. Hervonen A, Korkala O. The effect of hypoxia on the catecholamine content of human fetal abdominal paraganglia and adrenal medulla. Acta Obstet Gynecol Scand 1972;51:7-24.
20. Brundin T. Studies on the preaortal paraganglia of newborn rabbits. Acta Physiol Scand 1966; 290:1-54.

21. Spicer Z, Millhorn DE. Oxygen sensing in neuroendocrine cells and other cell types: pheochromocytoma (PC12) cells as an experimental model. Endocr Pathol 2003;14:277-291.
22. Gratzl M, Breckner M, Prinz C. Mechanisms of storage and exocytosis in neuroendocrine tumors. Endocr Pathol 2004;15:1-16.
23. Hervonen A, Pickel VM, Joh TH, Reis DJ, Linnoila I, Miller RJ. Immunohistochemical localization of the catecholamine-synthesizing enzymes, substance P and enkephalin in the human fetal sympathetic ganglion. Cell Tissue Res 1981;214:33-42.
24. Hervonen A. Development of catecholamine-storing cells in human fetal paraganglia and adrenal medulla. A histochemical and electron microscopical study. Acta Physiol Scand Suppl 1971;368:1-94.

Extraadrenal Paraganglioma

25. Lack EE. Pathology of adrenal and extra-adrenal paraganglia. Major problems in pathology, Vol 29. Philadelphia. WB Saunders; 1994.
26. Glenner GG, Grimley PM. Tumors of the extra-adrenal paraganglion system (including chemoreceptors). Atlas of Tumor Pathology, 2nd Series, Fascicle 9. Washington, D.C.: Armed Forces Institute of Pathology; 1974.
27. Fries JG, Chamberlin JA. Extra-adrenal pheochromocytoma: literature review and report of a cervical pheochromocytoma. Surgery 1968;63:268-279.
28. Melicow MM. One hundred cases of pheochromocytoma (107 tumors) at the Columbia-Presbyterian Medical Center, 1926-1976: a clinicopathologic analysis. Cancer 1977;40:1987-2004.

Extraadrenal Intraabdominal Paragangliomas

29. Fries JG, Chamberlin JA. Extra-adrenal pheochromocytoma: literature review and report of a cervical pheochromocytoma. Surgery 1968;63:268-279.
30. Lack EE. Pathology of adrenal and extra-adrenal paraganglia. Major problems in pathology, Vol 29. Philadelphia: WE Saunders; 1994.
31. Hayes WS, Davidson AJ, Grimley PM, Hartman DS. Extra-adrenal retroperitoneal paraganglioma: clinical, pathologic and CT findings. AJR Am J Roentgenol 1990;155:1247-1250.
32. Lack EE, Cubilla AL, Woodruff JM, Lieberman PH. Extra-adrenal paragangliomas of the retroperitoneum. A clinicopathologic study of 12 tumors. Am J Surg Pathol 1980;4:109-120.
33. Sclafani LM, Woodruff JM, Brennan MF. Extra-adrenal retroperitoneal paragangliomas: natural history and response to treatment. Surgery 1990; 108:1124-1130.
34. Olson JR, Abell MR. Nonfunctional nonchromaffin paragangliomas of the retroperitoneum. Cancer 1969;23:1358-1367.
35. Glenn F, Gray GF. Functional tumors of the organ of Zuckerkandl. Ann Surg 1976;183:578-586.
36. McCarthy EF, Bonfiglio M, Lawton W. A solitary functioning osseous metastasis from a malignant pheochromocytoma of the organ of Zuckerkandl. Cancer 1977;40:3092-3096.
37. Mundis RJ, Bisel HF, Sheps SG, Sheedy PF 2nd, Gaffey TA, Sterioff S. Malignant nonfunctioning paraganglioma of the retroperitoneum producing renovascular hypertension. Mayo Clin Proc 1982;57:661-664.
38. Kitahara M, Mori T, Seki H, et al. Malignant paraganglioma presenting as Cushing's syndrome with virilism in childhood. Production of cortisol, androgens, and adrenocorticotrophic hormone by the tumor. Cancer 1993;72:3340-3345.
39. Keiser HR, Doppman JL, Robertson CN, Linehan WM, Averbuch SD. Diagnosis, localization, and management of pheochromocytoma. In: Lack EE, ed. Pathology of the adrenal glands. New York: Churchill Livingstone; 1990:237-255.
40. Farhi F, Dikman SH, Lawson W, Cobin RH, Zak FG. Paragangliomatosis associated with multiple endocrine adenomas. Arch Pathol Lab Med 1976;100:495-498.
41. Karosov RS, Sheps SG, Carney JA, van Heerden JA, DeAuattro V. Paragangliomatosis with numerous catecholamine-producing tumors. Mayo Clin Proc 1982;57:590-595.
42. Medeiros LJ, Wolf BC, Balogh K, Federman M. Adrenal pheochromocytoma: a clinicopathologic review of 60 cases. Hum Pathol 1985;16: 580-589.

Biologic Behavior

43. Hayes WS, Davidson AJ, Grimley PM, Hartman DS. Extra-adrenal retroperitoneal paraganglioma: clinical, pathologic and CT findings. AJR Am J Roentgenol 1990;155:1247-1250.
44. Glenn F, Gray GF. Functional tumors of the organ of Zuckerkandl. Ann Surg 1976;183:578-586.
45. Kryger-Baggesen N, Kjaergaard J, Sehested M. Nonchromaffm paraganglioma of the retroperitoneum. J Urol 1985;134:536-538.
46. Olson JR, Abell MR. Nonfunctional nonchromaffin paragangliomas of the retroperitoneum. Cancer 1969;23:1358-1367.
47. Lack EE, Cubilla AL, Woodruff JM, Lieberman PH. Extra-adrenal paragangliomas of the retroperitoneum. A clinicopathologic study of 12 tumors. Am J Surg Pathol 1980;4:109-120.
48. Sclafani LM, Woodruff JM, Brennan MF. Extraadrenal retroperitoneal paragangliomas: natural history and response to treatment. Surgery 1990;108:1124-1130.

49. Pham TH, Moir C, Thompson GB, et al. Pheochromocytoma and paraganglioma in children: a review of medical and surgical management at a tertiary care center. Pediatrics 2006;118: 1109-1117.

Urinary Bladder Paraganglioma

50. Leestma JE, Price EB Jr. Paraganglioma of the urinary bladder. Cancer 1971;28:1063-1072.
51. Zhou M, Epstein JI, Young RH. Paraganglioma of the urinary bladder: a lesion that may be misdiagnosed as urothelial carcinoma in transurethral resection specimens. Am J Surg Pathol 2004;28:94-100.
52. Lotz PR, Bogdasarian RS, Thompson NW, Seeger JF, Cho KJ. Paragangliomas of the head, neck, urinary bladder, and pelvis in a hypertensive woman. AJR Am J Roentgenol 1979;132:1001-1004.
53. Spring DB, Palubinskas AJ. Familial pheochromocytoma: a rare case of hydronephrosis and hydroureter in two generations. Br J Radiol 1977;50:596-599.
54. Lack EE. Pathology of adrenal and extra-adrenal paraganglia. Major problems in pathology, Vol 29. Philadelphia: WE Saunders; 1994.
55. Demirkesen O, Cetinel B, Yaycioglu O, Uygun N, Solok V. Unusual cause of early preeclampsia: bladder paraganglioma. Urology 2000;56:154.
56. Dundr P, Dudorkinova D, Povysil C, et al. Pigmented composite paraganglioma-ganglioneuroma of the urinary bladder. Pathol Res Pract 2003;199:765-769.
57. Davaris P, Petraki K, Arvanitis D, Papacharalammpous N, Morakis A, Zorzos, S. Urinary bladder paraganglioma (U.B.P.). Path Res Pract 1986;181:101-105.
58. Cheng L, Leibovich BC, Cheville JC, et al. Paraganglioma of the urinary bladder: can biologic potential be predicted? Cancer 2000;88: 844-852.

Unusual Sites of Paragangliomas

59. Lack EE. Pathology of adrenal and extra-adrenal paraganglia. Major problems in pathology, Vol 29. Philadelphia: WE Saunders; 1994.
60. Lagace R, Tremblay M. Non-chromaffin paraganglioma of the kidney with distant metastases. Can Med Assoc J 1968;99:1095-1098.
61. Badalament RA, Kenworthy P, Pellegrini A, Drago JR. Paraganglioma of urethra. Urology 1991;38:76-78.
62. Cholhan HJ, Cagler H, Kremzier JE. Suburethral paraganglioma. Obstet Gynecol 1991;78:555-558.
63. Nielsen VM, Skovgaard N, Kvist N. Pheochromocytoma of the prostate. Br J Urol 1987;59:478-479.
64. Dharkar D, Kraft JR. Paraganglioma of the spermatic cord. An incidental finding. J Urol Pathol 1994;2:89-93.
65. Ostrowski ML, Wheeler TM. Paraganglia of the prostate. Location, frequency, and differentiation from prostatic adenocarcinoma. Am J Surg Pathol 1994;18:412-420.
66. Miller TA, Weber TR, Appelman HD. Paraganglioma of the gallbladder. Arch Surg 1972;105: 637-639.
67. Wolff M. Paraganglioma of the gallbladder. Arch Surg 1973;107:493.
68. Fine G, Raju UB. Paraganglia in the human gallbladder. Arch Pathol Lab Med 1980;104:265-268.
69. McCluggage WG, Young RH. Paraganglioma of the ovary: report of three cases of a rare ovarian neoplasm, including two exhibiting inhibin positivity. Am J Surg Pathol 2006;30:600-605.
70. Lack EE. Pathology of the pancreas, gallbladder, extrahepatic biliary tract, and ampullary region. New York: Oxford University Press; 2003.
71. Jaeck D, Paris F, Welsch M, et al. Primary hepatic pheochromocytoma: a second case. Surgery 1995;117:586-590.

Intrathoracic Paravertebral Paraganglioma

72. Gallivan MV, Chun B, Rowden G, Lack EE. Intrathoracic paravertebral malignant paraganglioma. Arch Lab Med 1980;104:46-51.
73. Hodgkinson DJ, Telander RL, Sheps SG, Gilchrist GS, Crowe JK. Extra-adrenal intrathoracic functioning paraganglioma (pheochromocytoma) in childhood. Mayo Clin Proc 1980;55:271-276.
74. Smalley JJ, Gallagher WE, Nichols CP. Paraganglioma simulating primary rib tumor. Arch Surg 1977;112:323-325.
75. Lack EE. Pathology of adrenal and extra-adrenal paraganglia. Major problems in pathology, Vol 29. Philadelphia: WE Saunders; 1994.
76. Odze R, Begin LR. Malignant paraganglioma of the posterior mediastinum. A case report and review of the literature. Cancer 1990;65:564-569.

Cervical Paravertebral Paraganglioma

77. Fries JG, Chamberlin JA. Extra-adrenal pheochromocytoma: literature review and report of a cervical pheochromocytoma. Surgery 1968;63: 268-279.
78. Gibbs MK, Carney JA, Hayles AB, Telander RL. Simultaneous adrenal and cervical pheochromocytomas in childhood. Ann Surg 1977;185: 273-278.
79. Glenner GG, Crout JR, Roberts WC. A functional carotid-body-like tumor secreting levarterenol. Arch Pathol 1962;73:230-240.

80. Crowell WT, Grizzle WE, Siegel AL. Functional carotid paragangliomas. Biochemical, ultrastructural and histochemical correlation with clinical symptoms. Arch Pathol Lab Med 1982; 106:599-603.
81. Lack EE. Pathology of adrenal and extra-adrenal paraganglia. Major problems in pathology, Vol 29. Philadelphia: WB Saunders; 1994.

Functioning Paraganglioma and Gastrointestinal Stromal Tumor of the Jejunum

82. Perry CG, Young WF Jr., McWhinney SR, et al. Functioning paraganglioma and gastrointestinal stromal tumor of the jejunum in three women: syndrome or coincidence. Am J Surg Pathol 2006:42-49.

Ultrastructure of Sympathoadrenal Paragangliomas

83. Tannenbaum M. Ultrastructural pathology of adrenal medullary tumors. Pathol Annu 1970; 5:145-171.
84. Lack EE. Pathology of adrenal and extra-adrenal paraganglia. Major problems in pathology, Vol 29. Philadelphia: WB Saunders; 1994.
85. Brown WJ, Barajas L, Waisman J, De Quattro V. Ultrastructural and biochemical correlates of adrenal and extra-adrenal pheochromocytoma. Cancer 1972;29:744-759.
86. Gómez RR, Osborne BM, Ordoñez NG, Mackay B. Pheochromocytoma. Ultrastruct Pathol 1991;15:557-562.
87. Osamura RY, Yasuda O, Kawai K, Hori S, Suemizu H, Onoda N, Joh TH. Immunohistochemical localization of catecholamine-synthesizing enzymes in human pheochromocytomas. Endocr Pathol 1990;1:102-108.
88. Kimura N, Miura Y, Nagatsu I, Nagura H. Catecholamine synthesizing enzymes in 70 cases of functioning and non-functioning pheochromocytoma and extra-adrenal paraganglioma. Virchows Arch A Pathol Anat Histopathol 1992;421:25-32.
89. Lloyd RV, Sisson JC, Shapiro B, Verhofstad AA. Immunohistochemical localization of epinephrine, norepinephrine, catecholamine-synthesizing enzymes, and chromogranin in neuroendocrine cells and tumors. Am J Pathol 1986;125:45-54.
90. Mendelsohn G, Olson JL. Pheochromocytomas. Hum Pathol 1978;9:607-608.
91. Glenner GG, Grimley PM. Tumors of the extra-adrenal paraganglion system (including chemoreceptors). Atlas of Tumor Pathology, 2nd Series, Fascicle 9. Washington DC: Armed Forces Institute of Pathology; 1974.
92. Gordon RE, Taff ML, Schwartz IS, Kleinerman J. Malignant retroperitoneal paraganglioma: unusual light and electron microscopic findings. Mt Sinai J Med 1983;50:507-513.
93. Izumiyama N, Asami E, Itoh Y, Ohtsubo K. Alzheimer's neurofibrillary tangles and paired helical filaments in the pheochromocytoma cells of the adrenal medulla—electron microscopic and immunoelectron microscopic observations. Acta Neuropathol (Berl) 1990;81: 213-216.
94. Kyriacou K, Shipkey FH, Loewen R. Crystalloid structures in retroperitoneal paragangliomas: a light and electron microscopic study. Ultrastr Pathol 1991;15:57-67.

Immunohistochemical Findings in Sympathoadrenal Paragangliomas

95. Linnoila RI, Lack EE, Steinberg SM, Keiser HR. Decreased expression of neuropeptides in malignant paragangliomas: an immunohistochemical study. Hum Pathol 1988;19:41-50.
96. Eiden LE, Huttner WB, Mallet J, O'Connor DT, Winkler H, Zanini A. A nomenclature proposal for the chromogranin/secretogranin proteins. Neuroscience 1987;21:1019-1021.
97. Erickson LA, Lloyd RV. Practical markers used in the diagnosis of endocrine tumors. Adv Anat Pathol 2004;11:175-189.
98. Miettinen M. Neuroendocrine differentiation in adrenocortical carcinoma. New immunohistochemical findings supported by electron microscopy. Lab Invest 1992;66:169-174.
99. Schröder S, Padberg BC, Achilles E, Holl K, Dralle H, Klöppel G. Immunocytochemistry in adrenocortical tumors: a clinicopathological study of 72 neoplasms. Virchows Arch A Pathol Anat Histopathol 1992;420:65-70.
100. Srivastava A, Padilla O, Fischer-Colbrie R, Tischler AS, Dayal Y. Neuroendocrine secretory protein-55 (NESP-55) expression discriminates pancreatic endocrine tumors and pheochromocytomas from gastrointestinal and pulmonary carcinoids. Am J Surg Pathol 2004;28: 1371-1378.
101. Tischler AS, Mobtaker H, Mann K, et al. Antilymphocyte antibody Leu-7 (HNK-1) recognizes a constituent of neuroendocrine granule matrix. J Histochem Cytochem 1986;34:1213-1216.
102. Hamid Q, Varndell IM, Ibrahim NB, Mingazzini P, Polak JM. Extra-adrenal paragangliomas. An immunocytochemical and ultrastructural report. Cancer 1987;60:1776-1781.
103. Lau SK, Romansky SG, Weiss LM. Sustentaculoma: report of a case of a distinctive neoplasm of the adrenal medula. Am J Surg Pathol 2006;30:268-273.

Associated Endocrine Syndromes and Other Features

104. DeLellis RA, Tischler AS, Lee AK, Blount M, Wolfe HJ. Leu-enkephalin-like immunoreactivity in proliferative lesions of the human adrenal medulla and extra-adrenal paraganglia. Am J Surg Pathol 1983;7:29-37.
105. Lack EE. Pathology of adrenal and extra-adrenal paraganglia in major problems in pathology, Vol 29. Philadelphia: WB Saunders; 1994.
106. Linnoila RI, Lack EE, Steinberg SM, Keiser HR. Decreased expression of neuropeptides in malignant paragangliomas: an immunohistochemical study. Hum Pathol 1988;19:41-50.
107. Spark RF, Connolly PB, Gluckin DS, White R, Sacks B, Landsberg L. ACTH secretion from a functioning pheochromocytoma. N Engl J Med 1979;301:416-418.
108. Perry RR, Nieman LK, Cutler GB Jr, et al. Primary adrenal causes of Cushing's syndrome. Diagnosis and surgical management. Ann Surg 1989;210: 59-68.
109. Jessop DS, Cunnah D, Millar JG, et al. A phaeochromocytoma presenting with Cushing's syndrome associated with increased concentrations of circulating corticotrophin-releasing factor. J Endocr 1987;113:133-138.
110. Grizzle WE, Tolbert L, Pittman CS, Siegel AL, Aldrete, JS. Corticotropin production by tumors of the autonomic nervous system. Arch Pathol Lab Med 1984;108:545-550.
111. Verner JV, Morrison AB. Islet cell tumor and a syndrome of refractory watery diarrhea and hypokalemia. Am J Med 1958;25:374-380.
112. Sackel SG, Manson JE, Harawi SJ, Burakoff R. Watery diarrhea syndrome due to an adrenal pheochromocytoma secreting vasoactive intestinal polypeptide. Dig Dis Sci 1985;30:1201-1207.
113. White MC, Hickson BR. Multiple paragangliomata secreting catecholamines and calcitonin with intermittent hypercalcaemia. J R Soc Med 1979;72:532-538.
114. Garbini A, Mainardi M, Grimi M, Repaci G, Nanni G, Bragherio G. Pheochromocytoma and hypercalemia due to ectopic production of parathyroid hormone. N Y State J Med 1986; 86:25-27.
115. Young JD Jr, Qureshi AS, Connor TB, Wiswell JG. Problem lesions in adrenal surgery. J Urol 1969;101:233-240.
116. Interlandi JW, Hundley RF, Kasselberg AG, Orth DN, Salmon WD Jr, Sullivan JN. Hypercortisolism, diarrhea with steatorrhea and massive proteinuria due to pheochromocytoma. South Med J 1985;78:879-883.
117. Thesleff P, Benoni C, Mårtensson H, Nilsson Å, Sundler F, Åkesson B. A mixed endocrine adrenal tumour causing steatorrhea. Gut 1987;28: 1298-1301.
118. Neto LV, Taboada GF, Correa LL, et al. Acromegaly secondary to growth hormone-releasing hormone secreted by an incidentally discovered pheochromocytoma. Endocr Pathol 2007; 18:46-52.

Other Immunoreactive Substances

119. Sano T, Vrontakis ME, Kovacs K, Asa SL, Friesen HG. Galanin immunoreactivity in neuroendocrine tumors. Arch Pathol Lab Med 1991;115: 926-929.
120. Fried G, Wikström LM, Höög A, et al. Multiple neuropeptide immunoreactivities in a renin-producing human paraganglioma. Cancer 1994;74:142-151.
121. Inagaki S, Kubota Y, Kito S, Kangawa K, Matsuo H. Immunoreactive atrial natriuretic polypeptides in the adrenal medulla and sympathetic ganglia. Regul Pept 1986;15:249-260.
122. Haselbacher GK, Irminger JC, Zapf J, Ziegler WH, Humbel RE. Insulin-like growth factor II in human adrenal pheochromocytomas and Wilms' tumors: expression at the mRNA and protein level. Proc Natl Acad Sci U S A1987;84:1104-1106.
123. Franquemont DW, Mills SE, Lack EE. Immunohistochemical detection of neuroblastomatous foci in composite adrenal pheochromocytoma-neuroblastoma. Am J Clin Pathol 1994; 102:163-170.
124. Miettinen M, Cupo W. Neural cell adhesion molecule distribution in soft tissue tumors. Hum Pathol 1993;24:62-66.
125. Unger PD, Hoffman K, Thung SN, Pertsemlides, D, Wolfe, D, Keneko, M. HMB-45 reactivity in adrenal pheochromocytomas. Arch Pathol Lab Med 1992;116:151-153.

Intermediate Filament Profile

126. Franquemont DW, Mills SE, Lack EE. Immunohistochemical detection of neuroblastomatous foci in composite adrenal pheochromocytoma-neuroblastoma. Am J Clin Pathol 1994;102: 163-170.
127. Trojanowski JQ, Lee VM. Expression of neurofilament antigens by normal and neoplastic human adrenal chromaffin cells. N Engl J Med 1985;313:101-104.
128. Kimura N, Nakazato Y, Nagura H, Sasano N. Expression of intermediate filaments in neuroendocrine tumors. Arch Pathol Lab Med 1990;114: 506-510.

129. Azumi N, Battifora H. The distribution of vimentin and keratin in epithelial and nonepithelial neoplasms. A comprehensive immunohistochemical study on formalin- and alcohol-fixed tumors. Am J Clin Pathol 1987;88:286-296.
130. Johnson TL, Zarbo RJ, Lloyd RV, Crissman JD. Paragangliomas of the head and neck: immunohistochemical neuroendocrine and intermediate filament typing. Mod Pathol 1988;1:216-223.
131. Franke WW, Grund C, Achtstätter T. Co-expression of cytokeratins and neurofilament proteins in permanent cell line: cultural rat PC12 cells combine neuronal and epithelial features. J Cell Biol 1986;103:1933-1943.

Relation of Immunohistochemistry to Prognosis

132. Lloyd RV, Blaivas M, Wilson BS. Distribution of chromogranin and S100 protein in normal and abnormal adrenal medullary tissues. Arch Pathol Lab Med 1985;109:633-635.
133. Kliewer KE, Cochran AJ. A review of the histology, ultrastructure, immunohistology, and molecular biology of extra-adrenal paragangliomas. Arch Pathol Lab Med 1989;113:1209-1218.
134. Kliewer KE, Wen DR, Cancilla PA, Cochran AJ. Paragangliomas: assessment of prognosis by histologic, immunohistochemical, and ultrastructural techniques. Hum Pathol 1989;20:29-39.
135. Unger P, Hoffman K, Pertsemlidis D, Thung S, Wolfe D, Kaneko M. S100 protein-positive sustentacular cells in malignant and locally aggressive adrenal pheochromocytomas. Arch Pathol Lab Med 1991;115:484-487.
136. Linnoila RI, Becker RL Jr, Steinberg SM, Kaiser HR, Lack EE. The role of S-100 protein containing cells in the prognosis of sympathoadrenal paragangliomas. Mod Pathol 1993;6: 39A(210).
137. Linnoila RI, Lack EE, Steinberg SM, Keiser HR. Decreased expression of neuropeptides in malignant paragangliomas: an immunohistochemical study. Hum Pathol 1988;19:41-50.
138. Helman LJ, Cohen PS, Averbuch SD, Cooper MJ, Keiser HR, Israel MA. Neuropeptide Y expression distinguishes malignant from benign pheochromocytoma. J Clin Oncol 1989;7:1720-1725.
139. Grouzmann E, Gicquel C, Plouin PF, Schlumberger M, Comoy E, Bohuon C. Neuropeptide Y and neuron-specific enolase levels in benign and malignant pheochromocytomas. Cancer 1990; 66:1833-1835.
140. Korner M, Waser B, Reubi JC. High expression of neuropeptide y receptors in tumors of the human adrenal gland and extra-adrenal paraganglia. Clin Cancer Res 2004;10:8426-8433.
141. Salmenkivi K, Haglund C, Arola J, Heikkila P. Increased expression of tenascin in pheochromocytomas correlates with malignancy. Am J Surg Pathol 2001;25:1419-1423.
142. Portela-Gomes GM, Stridsberg M, Grimelius L, Falkmer UG, Falkmer S. Expression of chromogranins A, B, and C (secretogranin II) in human adrenal medulla and in benign and malignant pheochromocytomas An immunohistochemical study with region-specific antibodies. APMIS 2004;112:663-673.

In Situ Hybridization and Other Techniques

143. Long AA, Mueller J, Andre-Schwartz J, Barrett KJ, Schwartz R, Wolfe H. High specificity in-situ hybridization. Methods and application. Diagn Mol Pathol 1992;1:45-57.
144. Lloyd RV. Introduction to molecular endocrine pathology. Endocr Pathol 1993;4:64-72.
145. DeLellis RA. In situ hybridization techniques for the analysis of gene expression: applications in tumor pathology. Hum Pathol 1994;25:580-585.
146. Templeton NS. The polymerase chain reaction. History, methods, and applications. Diagn Mol Pathol 1992;1:58-72.

Molecular Genetics

147. Dannenberg H, Komminoth P, Dinjens WN, Speel EJ, de Krijger RR. Molecular genetic alterations in adrenal and extra-adrenal pheochromocytomas and paragangliomas. Endocr Pathol 2003;14:329-350.
148. Powers JF, Brachold JM, Tischler AS. Ret protein expression in adrenal medullary hyperplasia and pheochromocytoma. Endocr Pathol 2003;14: 351-361.
149. Emmer T, Volante M, Pagani A, Allia E, Crafa P, Bussolati G. Potential applications of molecular biology in neuroendocrine tumors. Endocr Pathol 2003;14:319-328.
150. Neumann HP, Pawlu C, Peczkowska M, et al. Distinct clinical features of paraganglioma syndromes associated with SDHB and SDHD gene mutations. JAMA 2004;292:943-951. Erratum in: JAMA. 2004;292:1686.
151. Szinnai G, Meier C, Komminoth P, Zumsteg UW. Review of multiple endocrine neoplasia type 2A in children: therapeutic results of early thyroidectomy and prognostic value of codon analysis. Pediatrics. 2003;111:E132-139.
152. Lai AZ, Gujral TS, Mulligan LM. RET signaling in endocrine tumors: delving deeper into molecular mechanisms. Endocr Pathol 2007;18: 57-67.

Cytologic Features and Fine Needle Aspiration

153. Lack EE. Pathology of adrenal and extra-adrenal paraganglia in major problems in pathology, Vol 29. Philadelphia: WB Saunders; 1994.

154. Lack EE. Adrenal medullary hyperplasia and pheochromocytoma. In: Lack EE, ed. Pathology of the adrenal glands. New York: Churchill Livingstone; 1990:173-235.
155. González-Cámpora R, Otal-Salaverri C, Panea-Flores P, Lerma-Puertas E, Galera-Davidson H. Fine needle aspiration cytology of paraganglionic tumors. Acta Cytol 1988;32:386-390.
156. Rupp M, Ehya H. Fine needle aspiration cytology of retroperitoneal paraganglioma with lipofuscin pigmentation. Acta Cytol 1990;34:84-88.
157. Wadih GE, Nance KV, Silverman JF. Fine-needle aspiration cytology of the adrenal gland. Fifty biopsies in 48 patients. Arch Pathol Lab Med 1992;116:841-846.
158. Layfield LJ, Glasgow BJ, Du Puis MH, Bhuta S. Aspiration cytology and immunohistochemistry of a pheochromocytoma-ganglioneuroma of the adrenal gland. Acta Cytologica 1987;31:33-39.
159. McCorkell SJ, Niles NL. Fine-needle aspiration of catecholamine-producing adrenal masses: a possibly fatal mistake. Am J Roentgenol 1985; 145:113-114.
160. Lambert MA, Hirschowitz L, Russell RC. Fine needle aspiration biopsy: a cautionary tale. Br J Surg 1985;72:364.
161. Casola G, Nicolet V, van Sonnenberg E, et al. Unsuspected pheochromocytoma: risk of blood-pressure alterations during percutaneous adrenal biopsy. Radiology 1986;159:733-735.
162. Lack EE. Pathology of the pancreas, gallblader, extrahepatic biliary tract and ampullary region. New York: Oxford University Press; 2003.

Quantitative DNA Analysis

163. Lewis PD. A cytophotometric study of benign and malignant pheochromocytomas. Virchows Arch B Cell Pathol 1971;9:371-376.
164. Klein FA, Kay S, Ratliff JA, White FK, Newsome HH. Flow cytometric determinations of ploidy and proliferation patterns of adrenal neoplasms: an adjunct to histological classification. J Urol 1985;134:862-866.
165. Hosaka Y, Rainwater LM, Grant CS, Farrow GM, van Heerden JA, Lieber MM. Pheochromocytoma: nuclear deoxyribonucleic acid patterns studied by flow cytometry. Surgery 1986;100: 1003-1010.
166. Amberson JB, Vaughan ED Jr, Gray GF, Naus GJ. Flow cytometric differentiation of nuclear DNA content in benign adrenal pheochromocytomas. Urology 1987;30:102-104.
167. Padberg BC, Garbe E, Achilles E, Dralle H, Bressel M, Schröder S. Adrenomedullary hyperplasia and pheochromocytoma. DNA photometric findings in 47 cases. Virchows Arch A Pathol Anat Histopathol 1990;416:443-446.
168. Grignon DJ, Ro JY, Mackay B, et al. Paraganglioma of the urinary bladder: immunohistochemical, ultrastructural, and DNA flow cytometric studies. Hum Pathol 1991;22:1162-1169.
169. Nativ O, Grant CS, Sheps SG, et al. The clinical significance of nuclear DNA ploidy pattern in 184 patients with pheochromocytoma. Cancer 1992;69:2683-2687.
170. Pang LC, Tsao KC. Flow cytometric DNA analysis for the determination of malignant potential in adrenal and extra-adrenal pheochromocytomas or paragangliomas. Arch Pathol Lab Med 1993;117:1142-1147.
171. Linnoila RI, Becker RL Jr, Steinberg SM, Kaiser HR, Lack EE. The role of S-100 protein containing cells in the prognosis of sympathoadrenal paragangliomas. Modern Pathol 1993;6: 39A(210).
172. Hoffman K, Gil J, Barba J, et al. Morphometric analysis of benign and malignant adrenal pheochromocytomas. Arch Pathol Lab Med 1993; 117:244-247.
173. González-Cámpora R, Diazo Cano S, Lerma-Puertas E, et al. Paragangliomas. Static cytometric studies of nuclear DNA patterns. Cancer 1993;71:820-824.
174. Kimura N, Watanabe M, Ookuma T, et al. DNA ploidy of pheochromocytoma on cytology specimen by image analysis. Endocr Pathol 1994;5:178-182.
175. Lack EE. Pathology of adrenal and extra-adrenal paraganglia in major problems in pathology, Vol 29. Philadelphia: WB Saunders; 1994.

Gangliocytic Paraganglioma

176. Dahl EV, Waugh JM, Dahlin DC. Gastrointestinal ganglioneuromas. Brief review with report of a duodenal ganglioneuroma. Am J Pathol 1957;33:953-965.
177. Taylor HB, Helwig EB. Benign nonchromaffin paragangliomas of the duodenum. Virchows Arch Pathol Anat Physiol Klin Med 1962;335: 356-366.
178. Kepes JJ, Zacharias DL. Gangliocytic paragangliomas of the duodenum. A report of two cases with light and electron microscopic examination. Cancer 1971;27:61-70.
179. Perrone T, Sibley RK, Rosai J. Duodenal gangliocytic paraganglioma. An immunohistochemical and ultrastructural study with a hypothesis concerning its origin. Am J Surg Pathol 1985;9: 31-41.
180. Scheithauer BW, Nora FE, Lechago J, et al. Duodenal gangliocytic paraganglioma. Clinicopathologic and immunocytochemical study of 11 cases. Am J Clin Pathol 1986;86:559-565.

181. Burke AP, Helwig EB. Gangliocytic paraganglioma. Am J Clin Pathol 1989;92:1-9.
182. van Eeden S, Offerhaus GJ, Peterse HL, Dingemans KP, Blaauwgeers HL. Gangliocytic paraganglioma of the appendix. Histopathology 2000;36:47-49.
183. Weinrach DM, Wang KL, Blum MG, Yeldandi AV, Laskin WB. Multifocal presentation of gangliocytic paraganglioma in the mediastinum and esophagus. Hum Pathol 2004;35: 1288-1291.

Paraganglioma of Cauda Equina

184. Sonneland PR, Scheithauer BW, Lechago J, Crawford BG, Onofrio BM. Paraganglioma of the cauda equina region. Clinicopathologic study of 31 cases with special reference to immunocytology and ultrastructure. Cancer 1986;58:1720-1735.
185. Djindjian M, Ayache P, Brugières P, Malpert D, Baudrimont M, Poirier J. Giant gangliocytic paraganglioma of the filum terminale. Case report. J Neurosurg 1990;73:459-461.
186. Caccamo DV, Ho KL, Garcia JH. Canda equina tumor with ependymal and paraganglionic differentiation. Hum Pathol 1992;23:835-838.
187. Park DH, Park YK, Oh JI, et al. Oncocytic paraganglioma of the cauda equina in a child. Case report and review of the literature. Pediatr Neurosurg 2002;36:260-265.
188. Masuoka J, Brandner S, Paulus W, et al. Germline SDHD mutation in paraganglioma of the spinal cord. Oncogene 2001;20:5084-5086.
189. Chetty R, Pillay P, Jaichand V. Cytokeratin expression in adrenal phaeochromocytomas and extra-adrenal paragangliomas. J Clin Pathol 1998;51:477-478.
190. Orrell JM, Hales SA. Paragangliomas of the cauda equina have a distinctive cytokeratin immunophenotype. Histopathology 1992;21: 479-481.

Glomus Coccygeum

191. Luschka H. Die steissdrüse des menschen. Arch Pathol Anat Physiol 1860;18:106-115.
192. Luschka H. Ueber die drüsenartige natur des sogenannten ganglion intercaroticum. Arch Anat, Physiol, u Wissensch Med Jahrg 1862:405-414.
193. Bell RS, Goodman SD, Fornasier VL. Coccygeal glomus tumors: a case of mistaken identity? J Bone Joint Surg 1982;64A:595-597.
194. Albrecht S, Zbieranowski I. Incidental glomus coccygeum. When a normal structure looks like a tumor. Am J Surg Pathol 1990;14:922-924.
195. Duncan L, Halverson J, DeSchryver-Kecskemeti K. Glomus tumor of the coccyx. A curable cause of coccydynia. Arch Pathol Lab Med 1991;115: 78-80.
196. Santos LD, Chow C, Kennerson AR. Glomus coccygeum may mimic glomus tumour. Pathology 2002;34:339-343.
197. Gatalica Z, Wang L, Lucio ET, Miettinen M. Glomus coccygeum in surgical pathology specimens: small troublemaker. Arch Pathol Lab Med 1999;123:905-908.

12 PARAGANGLIA OF THE HEAD AND NECK REGION

Extraadrenal paraganglia have a centripetal and roughly symmetric distribution on either side of the midline, extending from the middle ear region and base of the skull to the pelvic floor. All of these endocrine cells are assumed to have common embryogenesis from the neural crest, similar to chromaffin cells of the adrenal medulla and chief cells of the carotid body (1). The sympathoadrenal neuroendocrine system has a different anatomic distribution and mediates rapid adaptions to changes in the environment by a combination of neural (norepinephrine release from postganglionic sympathetic neurons) and hormonal (due to the secretion of catecholamines [mainly epinephrine] from the adrenal medulla) effects.

Paraganglia of the head and neck region are more closely aligned with the parasympathetic nervous system, and often have an intimate association with vascular and neural structures (fig. 12-1). Many paraganglia have a branchiomeric distribution which parallels, in large part, the location of branchial arch mesodermal structures, such as the carotid artery and great vessels near the base of the heart; this anatomic distribution suggests an atavistic relationship to the gill arches of aquatic species which are vital to respiratory function. The strategic location of some of these head and neck paraganglia makes them likely candidates for having a chemoreceptor role, causing reflex changes in respiratory and cardiovascular activity in response to alterations in composition of arterial blood.

Based upon early reports of a positive chromaffin reaction (although notably weaker in the carotid body) and presumed neural connections with the sympathetic nervous system, Kohn (2) regarded the carotid bodies as paraganglia similar to the adrenal medulla. Some have questioned the propriety of the term paraganglia for carotid bodies, and by extrapolation, for similar endocrine structures in the head and neck region that are nonchromaffin and have a chemosensory role. Nonetheless, the term has become widely accepted, although it undoubtedly embraces a wider group of neuroendocrine cells than was originally envisioned by Kohn. Although paraganglia of the head and neck region are structurally and functionally distinct from the sympathoadrenal neuroendocrine system, there is some overlap in morphology

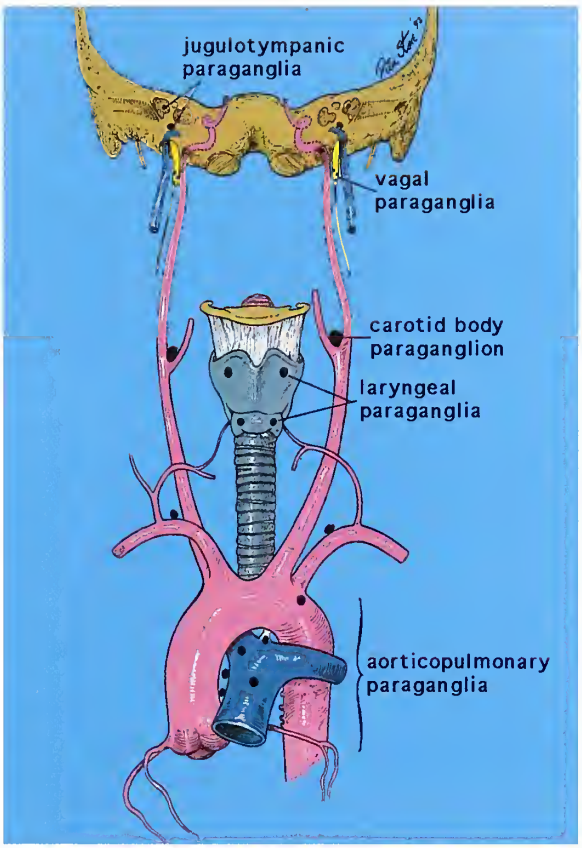

Figure 12-1

ANATOMIC DISTRIBUTION OF PARAGANGLIA IN HEAD AND NECK REGION

Carotid bodies comprise the largest compact collection of paraganglia in this anatomic distribution. There is a close relationship of paraganglia to vascular and neural structures that are embryologically associated with branchial arches. Paragangliomas can arise in sites where normal paraganglia have not yet been adequately characterized (e.g., orbit). (Fig. 14-1 from Fascicle 19, Third Series.)

and some similarity to the immunohistochemical phenotype of normal endocrine cells and the paragangliomas arising from them (3).

PARAGANGLIA AS PART OF A DIFFUSE NEUROENDOCRINE SYSTEM

Paraganglia are members of a very complex and intriguing family of endocrine cells that have a wide anatomic distribution and varied regulatory function. The APUD (amine precursor uptake and decarboxylation) cell concept was introduced by Pearse (4) in an attempt to bond a vast array of endocrine cells having shared metabolic characteristics as well as presumed common embryogenesis from the neural crest. The term "APUDoma" soon became a popular reference to a variety of endocrine tumors. Although no longer in wide use, this concept was an important stimulus for scientific investigation, particularly in the areas of immunology and molecular biology (3).

Feyrter in 1938 (5) recognized certain endocrine cells of the gastrointestinal tract that were presumed to have an influence on neighboring cells (paracrine function), and later postulated that similar endocrine cells of the bronchial mucosa may give rise to carcinoid tumors; this endocrine unit in the gastrointestinal tract was conceptualized as a "diffuse endocrine epithelial organ." The designation *neuroendocrine* has now become popular since it emphasizes the close functional relationship between the nervous system (neurons and ganglion cells) and endocrine cells (6). This diffuse or dispersed neuroendocrine system has evolved as a general unifying concept without focusing on a common path of embryogenesis or shared cytochemical features.

A wide variety of hormones, amines, and regulatory peptides have been identified in endocrine cells of normal paraganglia in the head and neck region as well as their respective paragangliomas. Some of these substances are capable of eliciting a more conventional endocrine effect (e.g., the rare paraganglioma with excess catecholamine secretion), while others mediate a regulatory function on adjacent cells (paracrine action) or an autoregulatory role on the same cells secreting the product (autocrine effect).

The literature dealing with paraganglia is immense, particularly relating to carotid bodies, which have been most accessible to study because of their macroscopic size and relatively constant anatomic location. Investigation of these and other paraganglia in humans has been limited to either autopsy material or, occasionally, tissue obtained during surgery such as therapeutic glomectomy specimens. The first published account of the human carotid body is attributed to Taube, a pupil of Albrecht von Haller, who in 1743 delivered a dissertation on the "ganglion minutum" (7). The carotid body was illustrated by Neubauer in 1772 (8), who portrayed it as a small quadrangular structure in the carotid bifurcation (fig. 12-2). A detailed

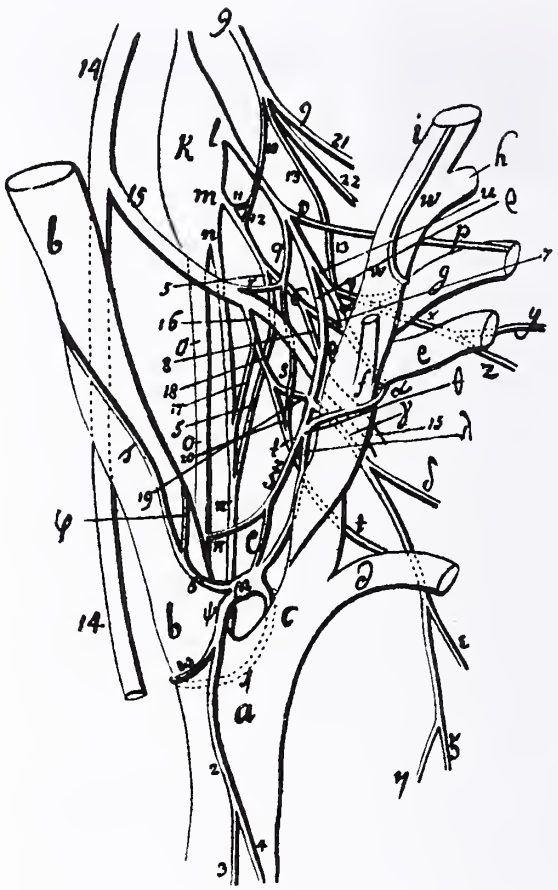

Figure 12-2

CAROTID BODY

In an illustration from 1772, the carotid body appears as a small quadrangular structure at the carotid bifurcation. It has rich neural connections. The carotid body was originally referred to as "ganglion parvum" or "ganglion minutum." (From Neubauer JE. Descriptio anatomica nervorum cardiacorum. Frankfurt, Leipzig: Fleischer. Sectio prima de nervo intercostali cervicali, dextri imprimis lateris; 1772.)

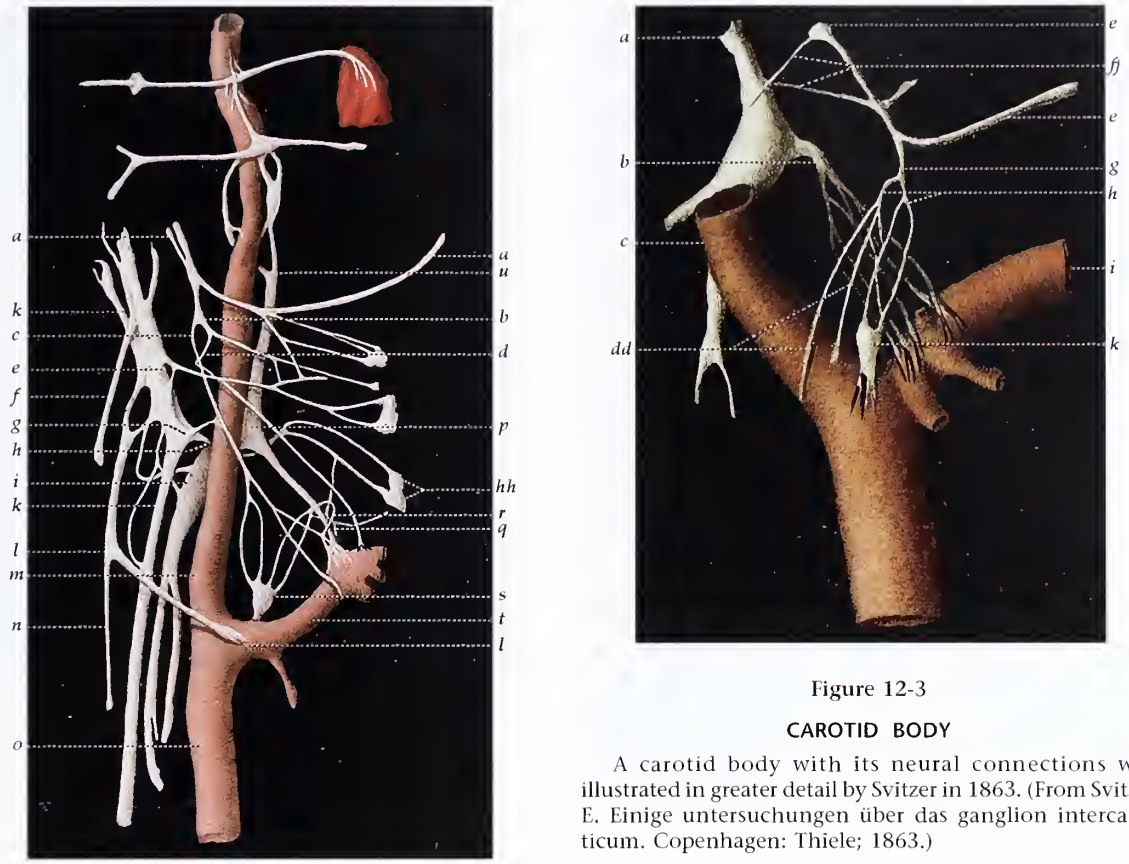

Figure 12-3

CAROTID BODY

A carotid body with its neural connections was illustrated in greater detail by Svitzer in 1863. (From Svitzer E. Einige untersuchungen über das ganglion intercaroticum. Copenhagen: Thiele; 1863.)

account of the early history of the carotid body can be found in the work by Adams (9). Svitzer (10), in his anatomic illustrations, suggested that the carotid body may be innervated solely by the glossopharyngeal nerve without significant sympathetic innervation (fig. 12-3).

For nearly 175 years since the discovery of the carotid body, its physiologic function remained a mystery. De Castro (11) established the predominantly glossopharyngeal innervation of the carotid body in 1926, and in a subsequent study proposed a novel chemoreceptor function for this structure by sensing (or "tasting") alterations in blood. Figure 12-4 shows the neural connections and vascular supply of the carotid body in the experimental animal (12). Conclusive physiologic evidence of chemoreceptor function was provided by Heymans et al. (13) who demonstrated reflex changes in respiration and cardiovascular activity in response to alterations in arterial PaO_2, $PaCO_2$, pH, and other agents. The Nobel Prize in physiology and medicine was awarded to this group in 1938 (14). Other investigators confirmed the chemoreceptor role of carotid bodies as well as small collections of paraganglia located near the base of the heart (15), collectively referred to as aorticopulmonary paraganglia.

PHYSIOLOGIC FUNCTION OF CAROTID BODY IN EXPERIMENTAL ANIMALS

Space constraints in the Fascicle do little justice to the vast literature on the physiology of chemoreceptors in animals, particularly carotid bodies. The peripheral arterial chemoreceptors are responsible for the immediate increase in breathing produced by hypoxia (16). Chemoreceptor discharge along the carotid sinus nerve (nerve of Hering), a branch of the 9th cranial nerve, is stimulated by a decrease in PaO_2, increase in $PaCO_2$, and lowered pH. Other excitatory factors include an increase in temperature or osmotic pressure and a variety of chemical substances. Some agents appear to have a stimulatory effect in some animals while being inhibitory in others. Despite the immense research effort, the

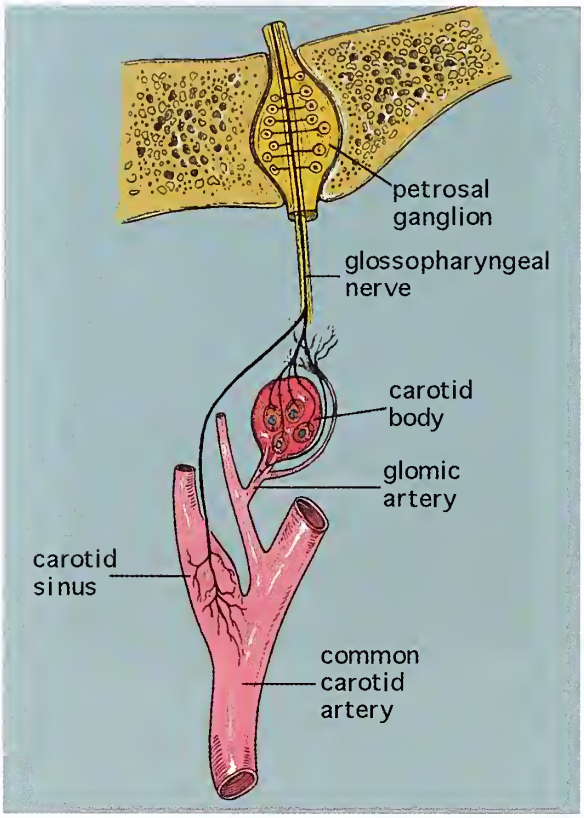

Figure 12-4

NEURAL AND VASCULAR SUPPLY OF CAT CAROTID BODY

Afferent fibers of the glossopharyngeal nerve innervate the baroreceptor apparatus on the left and the carotid body, which also receives its blood supply from the "glomic artery." An arteriovenous anastomosis is also shown. Afferent fibers terminate on or within the cell body of the chief cells (Fig. 10 from DeCastro F. [Sur la structure de la synapse dans les chemorecepteurs: leur mechanisme d'excitation et role dans la circulation sanguine locale.] Acta Physiol Scand 1951;22:14-43. [French])

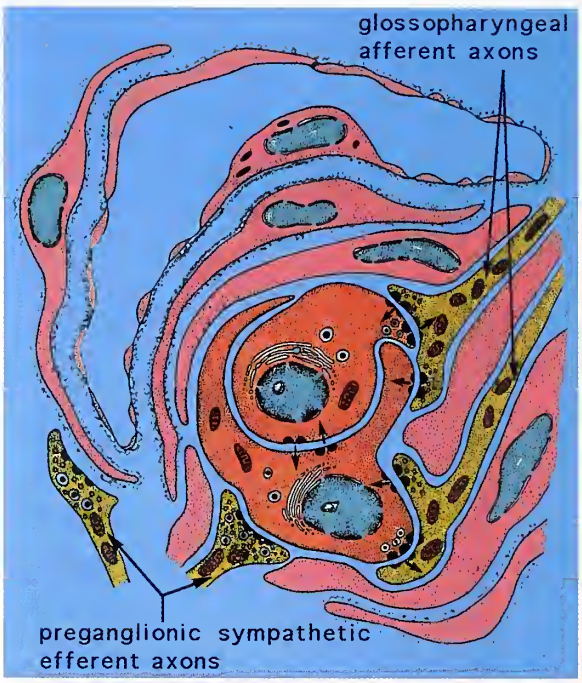

Figure 12-5

NEURAL CONNECTIONS IN THE RAT CAROTID BODY

Schematic diagram of the spatial relationship of carotid body chief cells and afferent terminals of the 9th cranial nerve in the rat. The chief cells are both presynaptic and postsynaptic to glossopharyngeal nerve fibers and the direction of synaptic discharge is indicated by arrows. Synapses between adjacent chief cells are reciprocal. Sustentacular cells envelop chief cells and neural processes. Pericytes and endothelial cells are also present, with the latter having cytoplasmic fenestrations. Note the efferent sympathetic fibers. Based upon this model, the antidromic generation of nerve impulses from the central terminals of chemoreceptor neurons may contribute to efferent activity in the glossopharyngeal nerve even though this nerve is primarily sensory. (Fig. 14-5 from Fascicle 19, Third Series.)

precise mode of chemosensation or transduction in the carotid body is still not entirely clear.

There appears little doubt that chemoreceptor activity involves interaction between nerve endings and chief (glomus type 1) cells. In rats, the chief cell has been regarded as an inhibitory interneuron secreting dopamine which modulates impulse generation along the afferent nerve terminals (fig. 12-5); in this experimental animal the chief cells are both presynaptic and postsynaptic to the nerve terminals, and have reciprocal synapses, features that have not been well characterized for the human carotid body chief cell. Currently, most investigators favor the chief cell as the primary chemosensor or transducer, and some feel that the most likely candidate for a PaO_2 sensor is the respiratory chain in mitochondria of chief cells (17,18).

Carotid body chief cells sense hypoxia through the inhibition of plasmalemmal potassium channels, leading to calcium influx and transmitter release, but the precise mechanism of oxygen sensing remains enigmatic (19). The calcium channels of cultured rat chief cells increase in number under hypoxic conditions (20). The rat pheochromocytoma cell line

(PC12) has become a powerful in vitro model for examining molecular events that occur during hypoxia. Research over the last few years has revealed that the hypoxia response in PC12 cells involves the complex interactions of several signal transduction pathways (e.g., Ca^{2+}/calmodulin-dependent kinases) and a variety of transcription factors (21).

Aorticopulmonary paraganglia have a more pronounced effect on the cardiovascular system, depending upon the animal species studied, but the precise mechanism of chemoreception and transduction is unclear. A chemoreceptor function has also been suggested for vagal paraganglia, perhaps mediated through the ganglion nodosum with reflex changes such as apnea, bradycardia, hypotension, and vomiting (3,22). Laryngeal or endoneurial paraganglia are in an ideal location for regulation of laryngeal airway resistance during hypoxia, but their precise physiologic role is undefined at present (3). A chemoreceptor role has not been established for histologically similar paraganglia elsewhere in the head and neck region.

PHYSIOLOGIC FUNCTION OF CHEMORECEPTORS IN HUMANS

Knowledge about the physiologic role of peripheral arterial chemoreceptors in humans is essentially limited to carotid body paraganglia. Much of the evidence for a chemoreceptor role is based upon the study of ventilatory dynamics in patients who have undergone bilateral glomectomy in an attempt to ameliorate symptoms of obstructive pulmonary disease (e.g., asthma) (23), an operation that is now viewed by many with considerable skepticism regarding its efficacy. Carotid bodies contribute to the sensation of breathlessness which results in a break from breath holding, and following glomectomy, there may be a diminution in exercise hyperpnea as well as a decrease in minute ventilation (3). A relationship with essential hypertension and cluster headaches has also been reported (3). Other important lines of evidence supporting a chemoreceptor role in humans are the hypertrophy and hyperplasia of carotid body paraganglia in individuals dwelling at high altitudes (24,25) and those at sea level with chronic hypoxemia or systemic hypertension (3,26–29), and the increased incidence of carotid body paragangliomas ("chemodectomas") at high altitude (3,25). It has been postulated that attenuated sensitivity of the carotid bodies due to prolonged hypoxia may play a role in the deterioration of the patient with chronic obstructive pulmonary disease (30). Interestingly, autotransplantation of human carotid body cell aggregates into the striatum has been used to treat patients with advanced Parkinson's disease (31).

NOMENCLATURE OF PARAGANGLIOMAS

It is preferable to designate paragangliomas based upon the primary anatomic site of origin. Glenner and Grimley (32) in the second series Fascicle, *Tumors of the Extra-Adrenal Paraganglion System,* recognized several interrelated "families" of paraganglia and corresponding paragangliomas based upon anatomic distribution, innervation, and microscopic anatomy. These families included branchiomeric, intravagal, aorticosympathetic, and visceroautonomic paraganglia and their corresponding paragangliomas. Adrenal medullary paraganglioma (commonly designated pheochromocytoma) was considered separately.

Classification of paragangliomas based upon the chromaffin or nonchromaffin status of the tumor has significant limitations because fresh tissue must be promptly fixed in the appropriate dichromate solution (or exposed to other oxidizing agents), correlation with endocrine function is not always reliable, and a negative reaction does not ensure the absence of catecholamines. The paragangliomas covered in this section, however, are characteristically chromaffin negative. Carotid body paraganglia have been shown to contain catecholamines: dopamine along with lower levels of norepinephrine and only a trace amount of epinephrine (29,33–36); acetylcholine has also been identified. Enzymes involved in catecholamine biosynthesis, such as tyrosine hydroxylase and dopamine beta-hydroxylase, have been localized in chief cells (36), while phenylethanolamine N-methyl transferase (PNMT) is presumed to be present, but in low concentrations since the epinephrine level is so low (33). A negative chromaffin reaction is attributed to the absence or low level of epinephrine, which is responsible for the dark brown color (37). Although norepinephrine has been localized in

some head and neck paragangliomas, along with the expected enzymes involved in the synthesis of this catecholamine, PNMT and its end product epinephrine are identified mainly in cardiac paragangliomas (38). Cardiac paragangliomas are frequently associated with excess catecholamine secretion, as are pheochromocytomas, causing speculation as to whether some of these paraganglia, and their respective tumors, are more closely aligned with the sympathoadrenal neuroendocrine system.

REFERENCES

1. Le Douarin N. The neural crest. London: Cambridge University Press; 1982.
2. Kohn A. Die paraganglien. Arch fur Mikr Anat 1903;62:263-365.
3. Lack EE. Pathology of adrenal and extra-adrenal paraganglia. Major problems in pathology, Vol 29. Philadelphia: WB Saunders; 1994.
4. Pearse AG. The cytochemistry and ultrastructure of polypeptide hormone-producing cells of the APUD series and the embryologic, physiologic and pathologic implications of the concept. J Histochem Cytochem 1969;17:303-313.
5. Feyrter F. [Über die these von den peripheren endokrinen drusen.] Wien z Innere Med Grenzgeb 1946;10:9-36. [German]
6. DeLellis RA, Dayal Y. Neuroendocrine system. In: Sternberg SS, ed. Histology for pathologists. New York: Lippincott Raven; 1997:1133-1151.
7. Haller A. Disputationum anatomicarum selectarum de vera nervi intercostalis origine. Praeside D. Alberto Haller. Gottingae. A Vandenhoeck, Vol II. 1747:939-952.
8. Neubauer JE. Descriptio anatomica nervorum cardiacorum. Frankfurt and Leipzig: Fleischer. Sectio prima de nervo intercostali cervicali, dextri imprimis lateris, 1772.
9. Adams WE. The comparative morphology of the carotid body and carotid sinus. Springfield: Charles C. Thomas; 1958.
10. Svitzer E. Einige untersuchungen über das ganglion intercaroticum. Copenhagen: Thiele Buchdruckerei, 1863.
11. De Castro F. [Sur la structure et l'innervation du sinus carotidien de l'homme et des mammifères. Nouveaux faits sur l'innervation et la fonction du glomus caroticum. Études anatomiques et physiologiques.] Trab Lab Invest Biol Univ Madr 1928;25:331-380.
12. De Castro F. [The structure of the synapse in chemoreceptors: their excitation mechanism and role in local blood circulation.] Acta Physiol Scand 1951;22:14-43. [French.]
13. Heymans C, Bouckhaert JJ, Dautrebande L. [Sinus carotidien et reflexes respiratoires. II. Influences respiratoires reflexes de l'acidose, de l'alkalose, de l'anhydride carbonique, de l'ion hydrogene et de l'anoxéme. Sinus carotidien et echanges respiratoires dans les poumons et au dela des poumons.] Arch Int Pharmacodyn Ther 1930;39:400-450. [French.]
14. Zak FG, Lawson W. The paraganglionic chemoreceptor system. Physiology, pathology and clinical medicine. New York: Springer-Verlag; 1982.
15. Dripps RD Jr, Comroe JH Jr. Physiology: the clinical significance of the carotid and aortic bodies. Am J Med Sci 1944;208:681-694.
16. Berger AJ, Mitchell RA, Severinghaus JW. Regulation of respiration (first of three parts). N Engl J Med 1977;297:92-97.
17. Acker H. Importance of oxygen supply in the carotid body for chemoreception. Biomed Biochim Acta 1987;46:885-898.
18. Biscoe TJ, Duchen MR. Cellular basis of transduction in carotid chemoreceptors. Am J Physiol 1990;258:L271-L278.
19. Lopez-Barneo J. Oxygen and glucose sensing by carotid body glomus cells. Curr Opin Neurobiol 2003;13:493-499.
20. Jiang RG, Eyzaguirre C. Calcium channels of cultured rat glomus cells in normoxia and acute hypoxia. Brain Res 2005;1031:56-66.
21. Spicer Z, Millhorn DE. Oxygen sensing in neuroendocrine cells and other cell types: pheochromocytoma (PC12) cells as an experimental model. Endocr Pathol 2003;14:277-291.
22. Jacobs L, Comroe JH Jr. Reflex apnea, bradycardia, and hypotension produced by serotonin and phenyldiguanide acting on the nodose ganglia of the cat. Circ Res 1971;29:145-155.
23. Fatemian M, Nieuwenhuijs DJ, Teppema LJ, et al. The respiratory response to carbon dioxide in humans with unilateral and bilateral resections of the carotid bodies. J Physiol 2003;549: 965-973.
24. Arias-Stella J, Valcarcel J. Chief cell hyperplasia in the human carotid body at high altitudes; physiologic and pathologic significance. Hum Pathol 1976;7:361-373.

25. Saldana MJ, Salem LE, Travezan R. High altitude hypoxia and chemodectomas. Hum Pathol 1973;4:251-263.
26. Heath D, Edwards C, Harris P. Post-mortem size and structure of the human carotid body. Thorax 1970;25:129-140.
27. Lack EE. Carotid body hypertrophy in patients with cystic fibrosis and cyanotic congenital heart disease. Hum Pathol 1977;8:39-51.
28. Lack EE. Hyperplasia of vagal and carotid body paraganglia in patients with chronic hypoxemia. Am J Pathol 1978;91:497-516.
29. Lack EE, Perez-Atayde AR, Young JB. Carotid body hyperplasia in cystic fibrosis and cyanotic heart disease. A combined morphometric, ultrastructural and biochemical study. Am J Pathol 1985; 119:301-314.
30. Bee D, Howard P. The carotid body: a review of its anatomy, physiology and clinical importance. Monaldi Arch Chest Dis 1993;48(1):48-53.
31. Arjona V, Minguez-Castellanos A, Montoro RJ, et al. Autotransplantation of human carotid body cell aggregates for treatment of Parkinson's disease. Neurosurgery 2003;53:321-328; discussion 328-330.
32. Glenner GG, Grimley PM. Tumors of the extra-adrenal paraganglion system (including chemoreceptors). Atlas of tumor pathology, 2nd Series, Fascicle 9. Washington DC: Armed Forces Institute of Pathology; 1974.
33. Zapata P, Hess A, Bliss EL, Eyzaguirre C. Chemical, electron microscopic and physiological observations on the role of catecholamines in the carotid body. Brain Res 1969;14:473-496.
34. Fidone SJ, Gonzalez C, Yoshizaki K. Putative neurotransmitters in the carotid body: The case for dopamine. Fed Proc 1980;39:2636-2640.
35. Lack EE, Perez-Atayde AR, Young JB. Carotid bodies in sudden infant death syndrome: a combined light microscopic, ultrastructural, and biochemical study. Ped Pathol 1986;6:335-350.
36. Wang ZZ, Stensaas LJ, Dinger B, Fidone SJ. Coexistence of tyrosine hydroxylase and dopamine beta-hydroxylase immunoreactivity in glomus cells of the cat carotid body. J Auton Nerv Syst 1991;32:259-264.
37. Sherwin RP. Histopathology of pheochromocytoma. Cancer 1959;12:861-877.
38. Lloyd RV, Sisson JC, Shapiro B, Verhofstad AA. Immunohistochemical localization of epinephrine, norepinephrine, catecholamine-synthesizing enzymes, and chromogranin in neuroendocrine cells and tumors. Am J Pathol 1986;125:45-54.

13 CAROTID BODY PARAGANGLIA AND PARAGANGLIOMAS

CAROTID BODY PARAGANGLIA

Gross Anatomy

Carotid body paraganglia are distinguished by their location, macroscopic dimensions, compactness, and multilobular architecture; aside from these features, the fundamental microanatomy is virtually identical to that of other paraganglia of the head and neck region. Carotid bodies are round to ovoid or flattened, pale tan to pink structures situated on both sides of the neck close to the medial aspect of the bifurcation of the common carotid artery (fig. 13-1). Occasionally, the carotid body is located along the internal or external branch of the carotid artery or even adjacent to the uppermost part of the common carotid artery, a location that can explain the rare angiographic appearance of a carotid body paraganglioma without significant splaying apart of the carotid artery branches (1).

Carotid body paraganglia are located within the adventitia without being directly connected to the media of the adjacent artery. Their average dimensions are 3.3 x 2.2 x 1.7 mm in adults (2), but they are often considerably smaller in infants. The carotid body sometimes appears bilobed (fig. 13-1) or even trilobed (3). A fibrovascular pedicle (ligament of Mayer) may carry one or more small glomic arteries, which supply the lower pole of the carotid body (4,5), as well as small myelinated nerve bundles (fig. 13-2) (6). The average combined weight of

Figure 13-1

BILATERAL CAROTID BODIES

Bilateral carotid bodies from a 12-year-old boy who died of metastatic malignant melanoma. Combined weight of both carotid bodies was 13.3 mg, and both are located on the medial aspect of the carotid bifurcation. The carotid body on the right is bilobed. (Fig. 2 from Lack EE. Paragangliomas. In: Sternberg SS, ed. Diagnostic surgical pathology, 2nd ed. New York: Raven Press; 1994:600.)

Figure 13-2

CAROTID BODY PARAGANGLION

Common carotid artery with external and internal carotid artery branches from an adult patient at autopsy. Dilation of the proximal internal carotid artery (left) represents a carotid sinus, which has baroreceptor function. An atheromatous plaque has distorted this area. A carotid body paraganglion is present at the top within adventitial connective tissue of the carotid bifurcation (arrow). Small glomic arteries are present in connective tissue near the inferior pole of the carotid body.

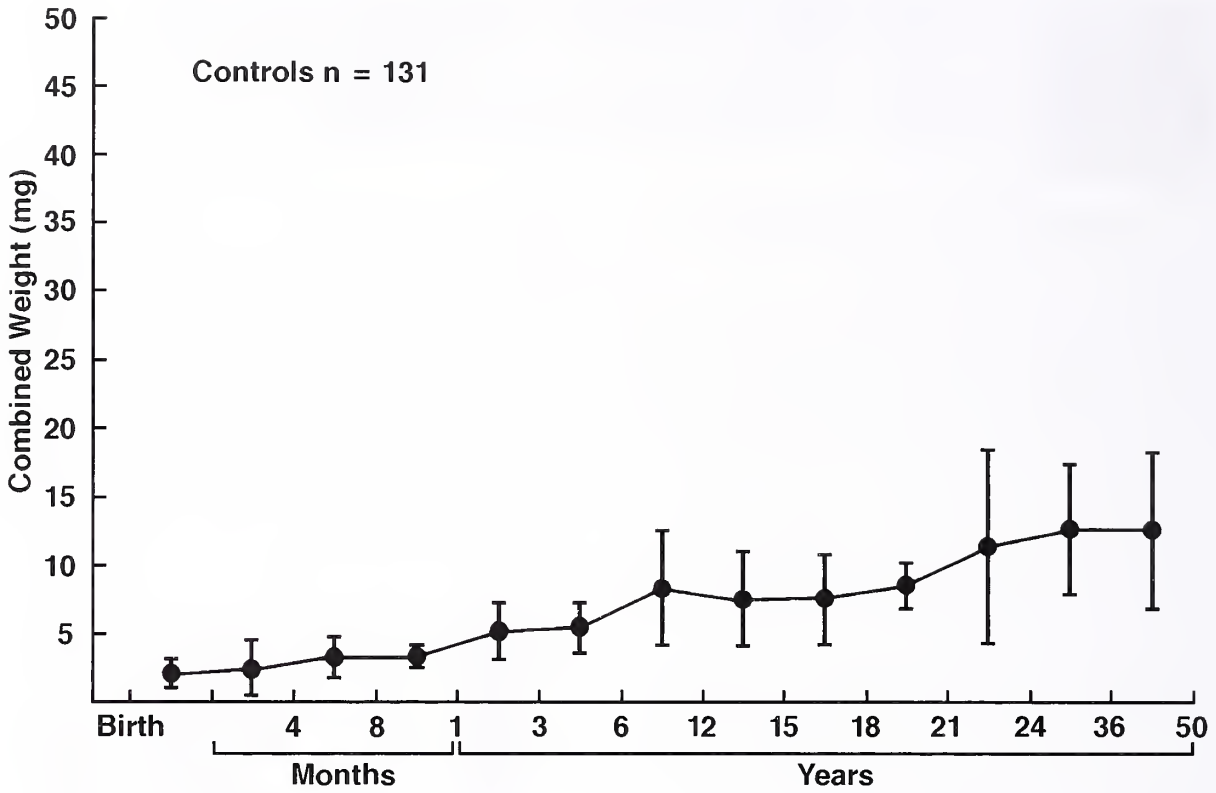

Figure 13-3

AVERAGE COMBINED WEIGHT OF CAROTID BODIES

Average combined weight of both carotid bodies is plotted according to arbitrary age intervals up to 50 years of age. The average combined weight in adults is a little over 12 mg. The control population (n = 131) had no evidence of chronic hypoxemia or systemic hypertension. Vertical bars represent one standard deviation. (Fig. 15-3 from Fascicle 19, Third Series.)

carotid bodies in adult patients under age 50 years is normally a little over 12 mg (fig. 13-3), but this depends upon the effort taken to remove excess connective tissue, preferably with the aid of a dissecting microscope (7,8). The weight of individual carotid bodies on either side is about equal (2,3,7–9).

Microscopic Anatomy

The carotid body is composed of multiple rounded, ovoid, or angular lobules that may appear partially molded to each other (fig. 13-4). The average number of lobules in cross section varies from 11 to 14 for various age intervals into adult life (3). As the individual or combined weights of carotid bodies increase with age, so too does the area of the entire structure in cross section or area occupied by lobules (arbitrarily designated functional parenchyma) (fig. 13-5).

There are two basic types of cells in the carotid body: chief (or glomus type 1) cells and sustentacular (glomus type 2) cells. There is good experimental evidence for a neural crest origin for carotid body chief cells (10), and presumably chief cells of other paraganglia in the head and neck region share a similar line of embryogenesis. Chief cells are arranged in round to elongated nests, and often have an eccentric, dark-staining nucleus with granular eosinophilic or amphophilic cytoplasm (fig. 13-6). Three types of chief cells have been recognized: "light" cells, "dark" cells, and pyknotic cells (subsequently referred to as "progenitor" cells [11]), but there is some question as to whether the nuclear changes may be related to postmortem autolysis (12). At present there is no known functional significance ascribed to these different types of chief cells (1). The marked vascularity of the

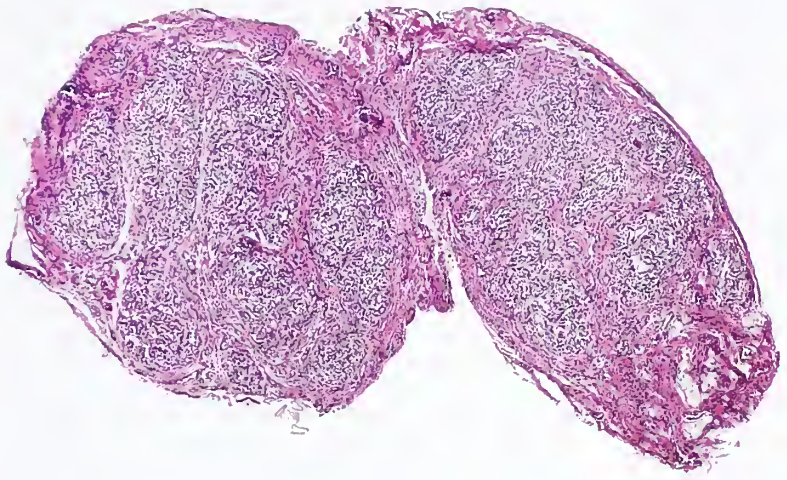

Figure 13-4

CAROTID BODY PARAGANGLIA

Both carotid bodies from a 38-year-old patient are nearly the same size. Note the ovoid shape and multiple lobules. These carotid bodies are well-circumscribed but not truly encapsulated (hematoxylin and eosin [H&E] stain). (Fig. 15-4 from Fascicle 19, Third Series.)

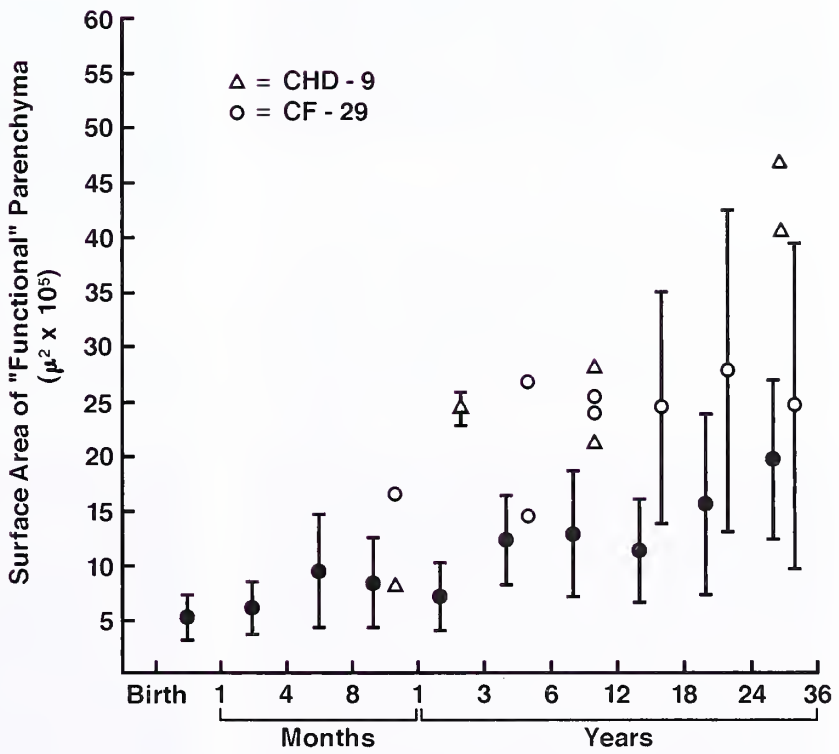

Figure 13-5

AREA OCCUPIED BY CAROTID BODY LOBULES

The area occupied by carotid body lobules has arbitrarily been designated "functional parenchyma" and is plotted according to arbitrary age intervals. Note the gradual increase with age, similar to carotid body weight. The vertical bar represents one standard deviation. (CHD = cyanotic heart disease, CF = cystic fibrosis.) (Fig. 10 from Lack EE, Perez-Atayde AR, Young JB. Carotid body hyperplasia in cystic fibrosis and cyanotic heart disease. A combined morphometric, ultrastructural, and biochemical study. Am J Pathol 1985;119:301-314.)

carotid body is clearly evident in the rare case where there is evidence of vascular telangiectasia and congestion (fig. 13-7).

The sustentacular cells have pale, indistinct cytoplasm with an elongated or crescentic nucleus. They are located at the periphery of clusters of chief cells (fig. 13-6). Ultrastructurally, these cells have been reported to resemble Schwann cells, enough so, in fact, that distinction between the two is not always possible (13). A reliable differential cell count of chief, sustentacular, and other cells can be very difficult (13).

The nesting pattern of the chief cells can be accentuated by staining for cytoplasmic

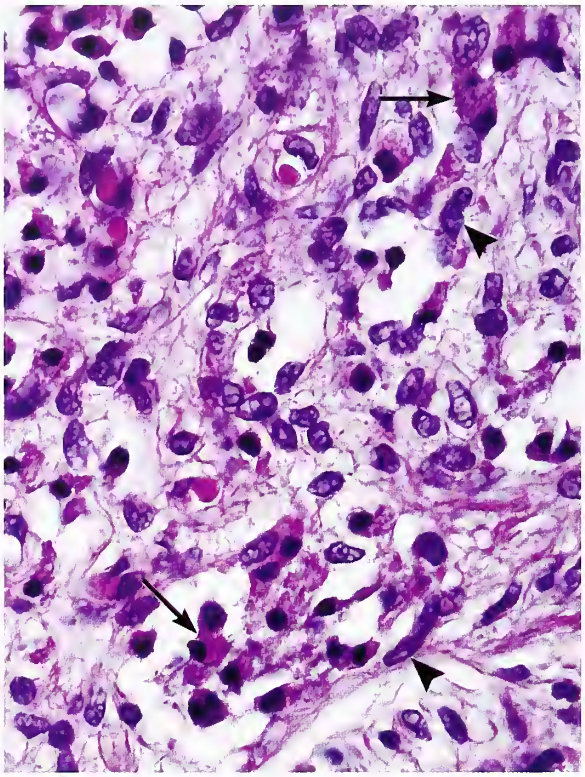

Figure 13-6

CAROTID BODY PARAGANGLION FROM NEWBORN INFANT

There are clusters of chief cells with dark staining nuclei, and eosinophilic, somewhat granular cytoplasm (arrows). Sustentacular cells are in close association with chief cells and have ovoid to elongated, pale-staining nuclei (arrowheads). (Fig. 15-6 from Fascicle 19, Third Series.)

argyrophilia (fig. 13-8); axonal or dendritic neural processes are also seen. Chief cells are most vividly demonstrated by immunostaining for chromogranin (fig. 13-9A) and synaptophysin. The sustentacular cells can be identified by immunostaining for S-100 protein (fig. 13-9B), but given the rich innervation of the carotid body, some of these immunoreactive cells are likely to be Schwann cells. Immunostaining for neurofilament protein highlights the rich innervation of the carotid body (fig. 13-9C).

Carotid body paraganglia contain catecholamines: dopamine is present in the greatest concentration, followed by norepinephrine (3,8,14). The enzymes involved in epinephrine synthesis (e.g., tyrosine hydroxylase) have been localized immunocytochemically in the chief cells (15) along with a variety of neuropeptides (1,15,16). A variety of histologic changes have been described in carotid bodies such as decrease in lobule size and fibrosis with aging (17,18), chronic carotid glomitis (19), vascular telangiectasia (probably agonal due to passive congestion) (fig. 13-7), and Schwann cell proliferation, which may be focal or diffuse in distribution (1). Ganglion cells have only rarely been reported within the interlobular connective tissue of the carotid body (20).

Ultrastructural Anatomy

There have been relatively few ultrastructural studies done on the human carotid body and

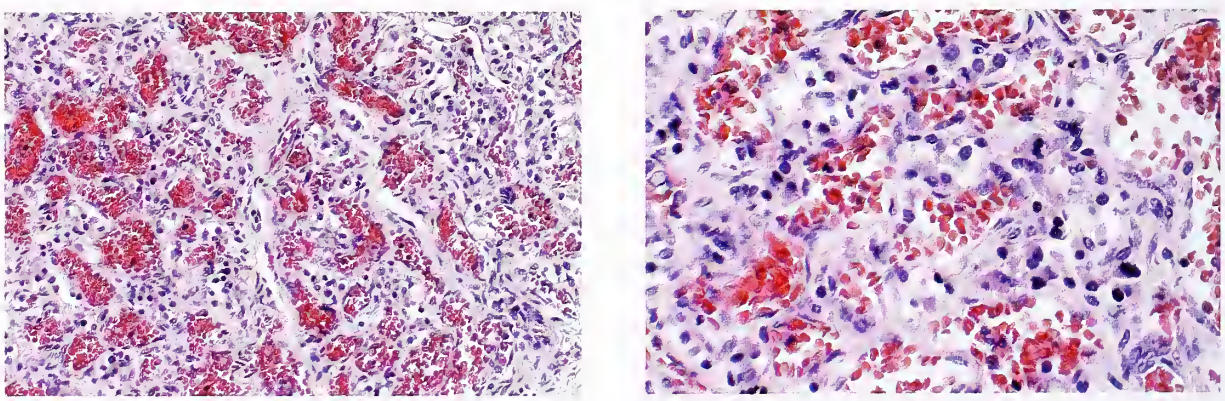

Figure 13-7

CAROTID BODY PARAGANGLION WITH MARKED PASSIVE CONGESTION

Left: Marked vascular telangiectasia and congestion in a carotid body paraganglion. The patient had severe congestive heart failure.

Right: Capillary telangiectasia and congestion underscores the rich vascularity of the carotid body.

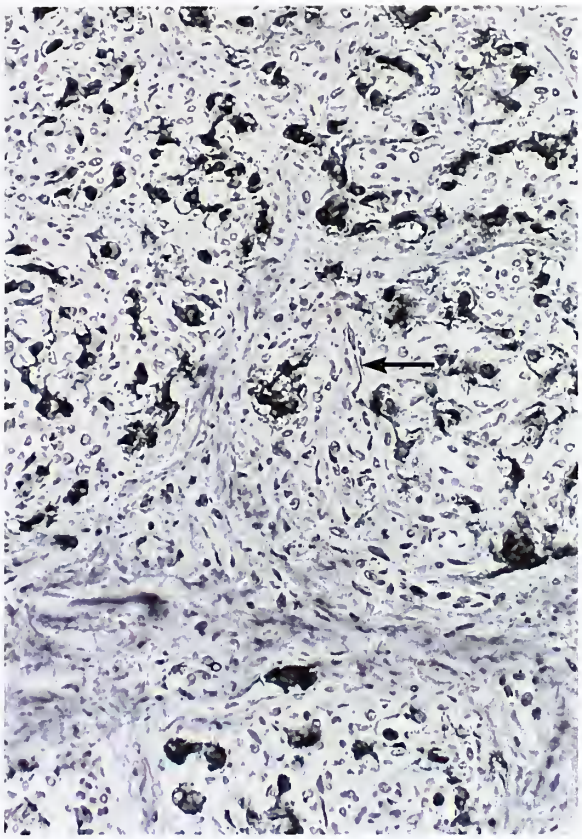

Figure 13-8

NORMAL CAROTID BODY PARAGANGLION

Normal carotid body from an adult shows strong cytoplasmic argyrophilia of the chief cell cytoplasm. The staining reaction shows distinct clusters and cords of chief cells within multiple lobules. Axonal or dendritic neural processes are also well delineated between and within lobules (arrow) (Bodian axon stain). (Fig. 15-8, left from Fascicle 19, Third Series.)

other head and neck paraganglia, and only selected references are cited (3,6,8,21–23). Because of advanced autolysis in postmortem material, there are certain limitations in performing optimal electron microscopy (1). Ultrastructural study of glomectomy specimens obtained surgically from patients with underlying pulmonary disease provide more optimal morphology, but endocrine tissue in this setting may not be entirely normal (1). Survey views show the complexity of carotid body paraganglia, as well as other paraganglia in the head and neck region (fig. 13-10) (6).

Chief cells often show a mosaic interdigitation of cell cytoplasm, sometimes with partial

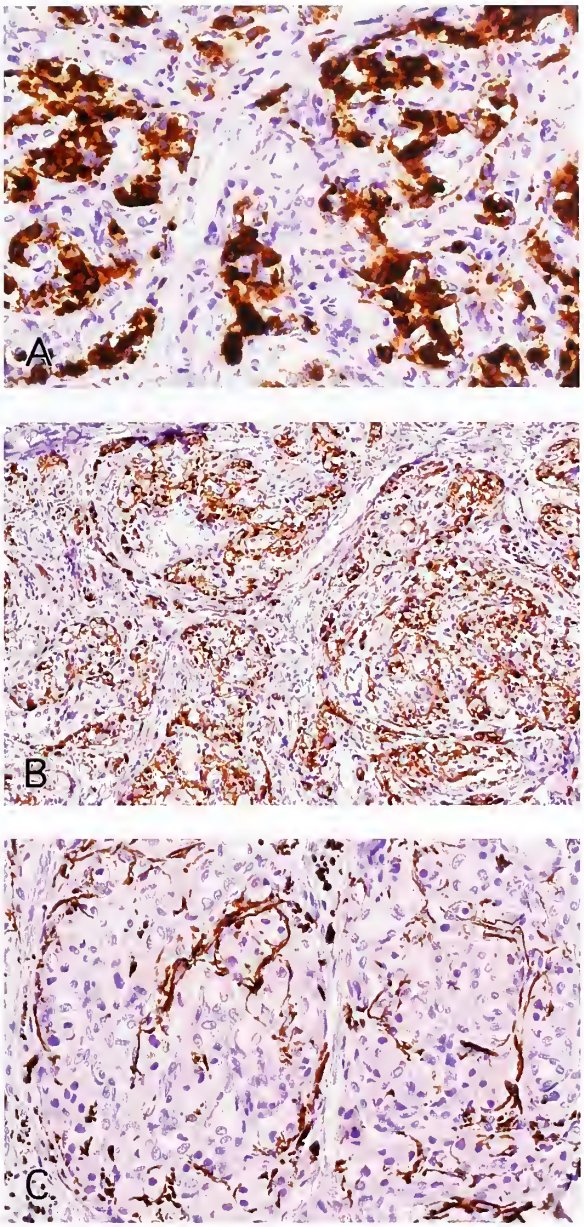

Figure 13-9

NORMAL CAROTID BODY PARAGANGLION

A: Carotid body from an adult at autopsy shows distinct cords and clusters of chief cells with intense cytoplasmic immunostaining for chromogranin A. Several lobules are present.

B: Immunostain for S-100 protein shows cytoplasmic and nuclear staining of numerous cells representing Schwann cells and sustentacular cells.

C: Immunostain for neurofilament protein highlights some of the neuritic processes between and within lobules. This rich neural component and numerous Schwann cells (B) are not features of carotid body paragangliomas. (A–C: avidin-biotin peroxidase method).

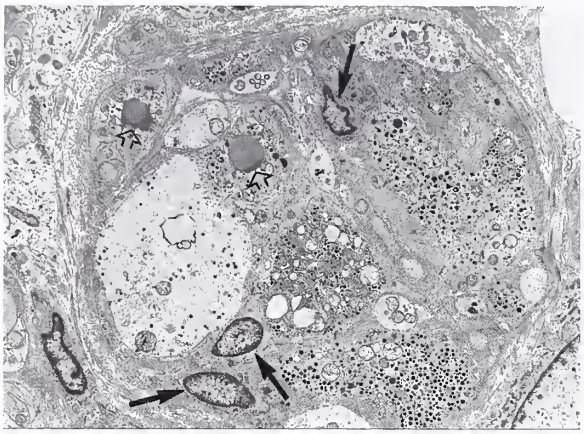

Figure 13-10

ADULT CAROTID BODY OBTAINED AT AUTOPSY

Cluster of chief cells in a carotid body lobule. There is an admixture of both "light" and "dark" chief cells; the latter are increased in number and have a higher density of cellular organelles and dense-core neurosecretory granules. Sustentacular cells (straight arrows) are located at the periphery of clusters of chief cells and have thin, complex cytoplasmic extensions which partially envelope the chief cells. Lipofuscin is indicated by open arrows. (Fig. 15-9 from Fascicle 19, Third Series.)

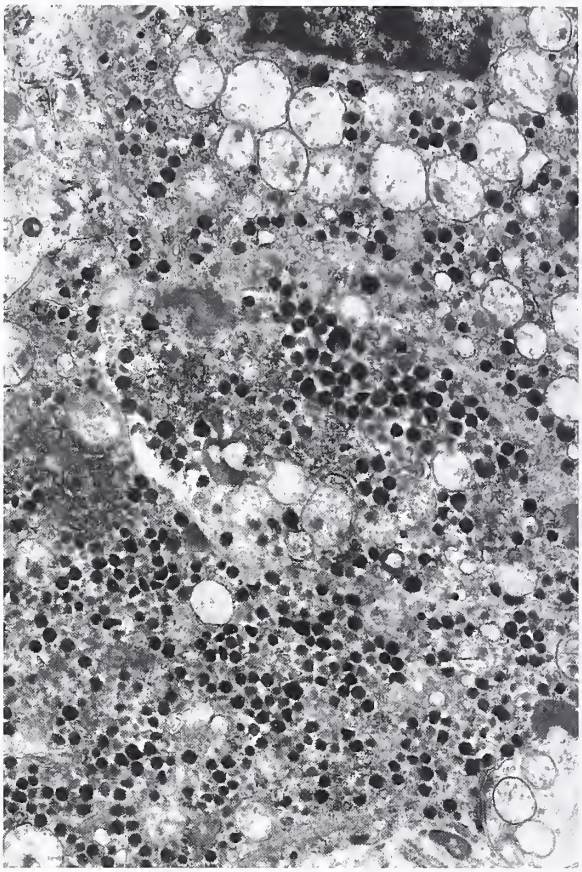

Figure 13-11

CAROTID BODY FROM A VICTIM OF SUDDEN INFANT DEATH SYNDROME (SIDS)

The chief cells contain numerous dense-core neurosecretory granules. There was no evidence of significant depletion of granules compared with carotid bodies from an age-related group without SIDS. (Fig. 2-19 from Lack EE. Pathology of adrenal and extra-adrenal paraganglia. Major Problems in Pathology, Vol 29. Philadelphia: WB Saunders; 1994:28.)

encirclement of one cell by another, the so-called cell embracing, which can also be found in the corresponding paraganglioma (1). Light and dark cells have been identified, with the latter often having numerous dense-core neurosecretory granules (fig. 13-11). Neurosecretory granules usually have a uniform electron-dense core with a narrow symmetric halo between the limiting membrane. Granule diameters usually range from 100 to 200 nm; in a study of the fetal carotid body, the average diameter of neurosecretory granules was 110 nm (6). Some chief cells contain electron-dense material associated with lipid droplets, typical for lipofuscin (1).

Sustentacular cells have sparse cellular organelles with small amounts of rough endoplasmic reticulum and bundles of thin (actin-like) filaments. Sustentacular cells in close proximity to chief cells usually have long, tapering cytoplasmic processes, occasionally forming simple mesaxons with axonal processes. Schwann cells are readily distinguished from sustentacular cells when the myelin sheath is well developed (fig. 13-12). According to Jago et al. (13), the only reliable feature that distinguishes sustentacular cells is the extension of cell processes which envelope chief cells.

Other cells in the carotid body and other head and neck paraganglia include abundant endothelial cells, along with pericytes and occasional mast cells. Efferent type synaptic junctions have been noted in the human fetus; some are probably sympathetic due to very small dense-core granules (23). In the study by Grimley and Glenner (21), afferent type terminals were not identified, although there is compelling experimental data to presume their existence in humans.

Figure 13-12

NORMAL CAROTID BODY PARAGANGLION

At the edge of a carotid body lobule (arrows) is rich innervation with numerous Schwann cells. Well-developed myelin sheaths are present but most processes of Schwann cells have formed simple mesaxons around neural processes. Compare this with figure 13-9B,C. A few fibroblasts are present in left lower field.

HYPERPLASIA OF CAROTID BODY PARAGANGLIA

Definition. *Carotid body hyperplasia* is an increase in the number of chief (glomus type 1) cells, often accompanied by the proliferation of other cell types such as sustentacular (glomus type 2) cells. Cellular proliferation may result in carotid body hypertrophy, which is usually bilateral and roughly symmetrical.

General Comments. Hyperplasia (diffuse or nodular) of the adrenal medulla, with consequent hypertrophy, has been covered in chapter 9, particularly in the setting of multiple endocrine neoplasia (MEN) syndromes type 2a and 2b, in which the pathologic changes clearly antedate the development of pheochromocytomas. The gross and microscopic counterparts of hyperplasia in paraganglia of the head and neck region, particularly carotid bodies, are on a much smaller scale, and the underlying or associated abnormalities for the most part appear to be basically physiologic (24), although carotid body and other types of paragangliomas may have a familial occurrence with varied Mendelian inheritance patterns (1).

A number of pathologic abnormalities have been reported in individuals dwelling at high altitudes (25–31), where a 10-fold increased incidence of "chemodectomas" has been reported (26). A relationship between chronic hypoxemia and carotid body enlargement (sometimes resembling chemodectomas) has been noted in bovines at high altitude (32). Carotid body hypertrophy and hyperplasia have also been reported under normobaric conditions in individuals with chronic obstructive pulmonary disease and systemic hypertension (2,3,33–39), as well as in patients with chronic hypoxemia due to cystic fibrosis and cyanotic heart disease (3,7). Hyperplasia of vagal (1,36) and aorticopulmonary paraganglia (1) has also been described, thus supporting a chemoreceptor role for these paraganglia. Chemodectoma-like tumors have been described in relatively stationary cod fish dwelling in more or less polluted waters, but the etiology of these tumors is unclear (40).

Gross Findings. The hyperplastic carotid body is enlarged, ovoid, often darker in color (fig. 13-13), and occasionally bilobed (fig. 13-13, right). Three criteria have been proposed for the diagnosis of carotid body hyperplasia: 1) combined carotid body weight over 30 mg; 2) mean diameter of lobules greater than 565 μm; and 3) differential count of elongated cells of more than 47 percent over chief cells (9). The individual or combined weight of the carotid bodies should be correlated with an age-related control population, because there is variation in weight and surface area with age (1).

Microscopic Findings. With carotid body hypertrophy and hyperplasia there is an increase in total cross-sectional surface area as well as area occupied by lobules, and in some cases there may be an increase in the number

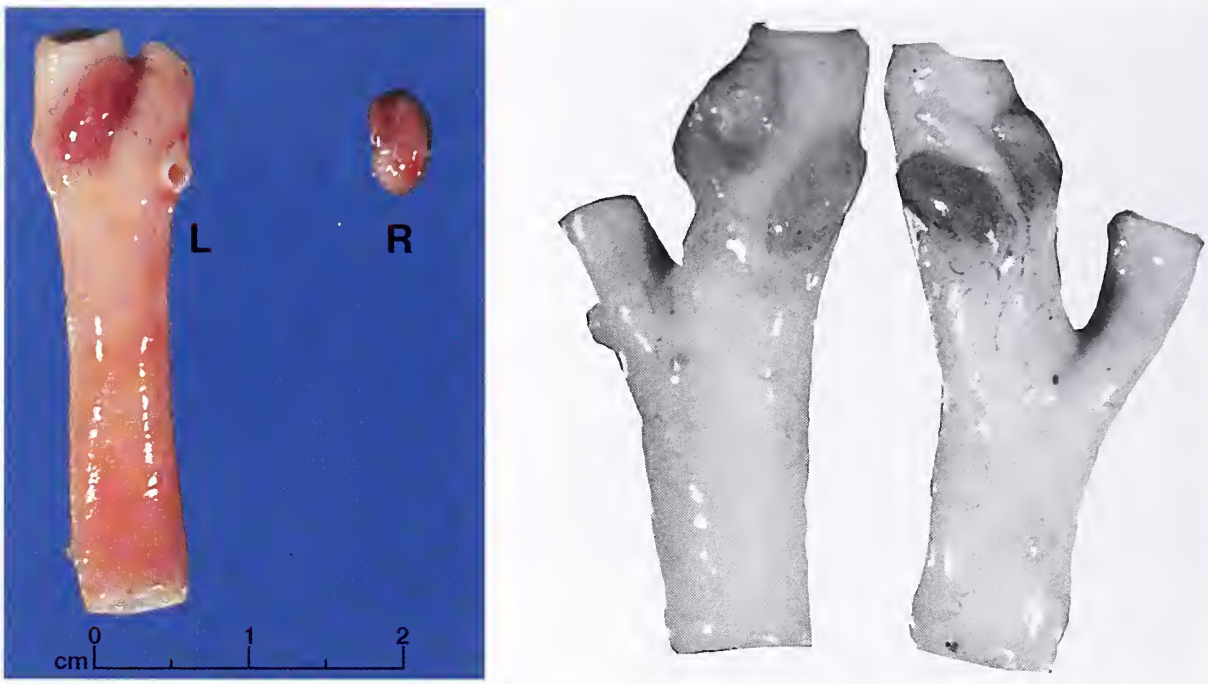

Figure 13-13

HYPERPLASTIC CAROTID BODY

Left: An enlarged hyperplastic carotid body from a 21-year-old woman with cystic fibrosis is located on the medial aspect of the carotid bifurcation on the left side; the contralateral enlarged carotid body is present on the right. The combined weight of both carotid bodies was 70 mg. (Fig. 15-11, left from Fascicle 19, Third Series.)

Right: Enlarged hyperplastic carotid bodies from a 24-year-old woman with cystic fibrosis had a combined weight of 80.3 mg. Both carotid bodies are bilobed and situated along the medial aspect of the internal carotid arteries. The bilobed carotid body on one side has a small vessel emerging from the internal carotid artery. (Modified from fig. 4 from Lack EE. Carotid body hypertrophy in patients with cystic fibrosis and cyanotic congenital heart disease. Hum Pathol 1977;8:39-51.)

of lobules (fig. 13-14). Hyperplasia of lobules may be accompanied by an attenuation in intervening fibrovascular connective tissue, resulting in what appears to be confluence of lobules (1). There tends to be a roughly proportional increase in chief cells as well as sustentacular cells (fig. 13-15). There may be variation in size, shape, and intensity of the nuclear staining of chief cells (1). Depletion of naturally fluorescing biogenic amines has been reported at high altitudes (28); as a corollary to this observation, there may be greatly diminished staining for cytoplasmic argyrophilia (fig. 13-16, left) and chromogranin A immunoreactivity (fig. 13-16, right) compared with controls (1). In adult and elderly patients, some investigators have noted a significant proliferation of elongated cells, mainly sustentacular cells, with a concentric or "onion skin" configuration, and apparent compression of central cores of chief cells (fig. 13-17) (9). Proliferation of dark cells has also been described (41). It is difficult to envision how this type of hyperplasia can progress to the histologic appearance of the chief cell hyperplasia and chemodectomas that have been illustrated in humans (26,28) and bovines at high altitude (32).

Ultrastructural Findings. In a recent study of carotid bodies from eight patients with cystic fibrosis, each showed a moderate to marked decrease in the number of dense-core neurosecretory granules (fig. 13-18), which was either patchy or diffuse throughout the lobules studied (3). In another study, proliferation of sustentacular cells was reported in a patient with carotid body hyperplasia while chief cells were not considered to be abnormal (42). Proliferation of nerve axons has also been described (42,43).

Figure 13-14

HYPERPLASTIC CAROTID BODY PARAGANGLION

Enlarged hyperplastic carotid body from a 21-year-old woman with cystic fibrosis (see fig. 13-13, left). This carotid body contains increased numbers of lobules compared with normal carotid bodies and some lobules appear confluent. Compare the size with normal carotid bodies in figure 13-4 which were photographed at a slightly higher magnification (H&E stain). (Fig. 15-12 from Fascicle 19, Third Series.)

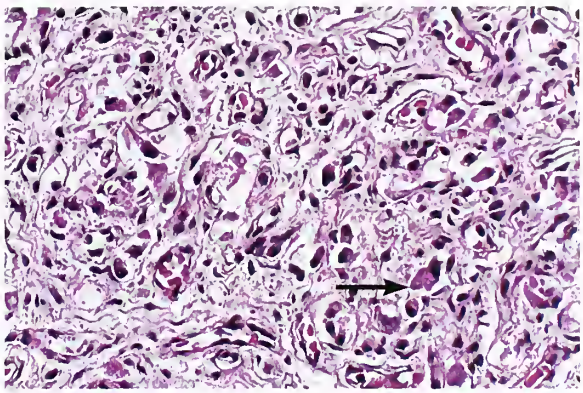

Figure 13-15

HYPERPLASTIC CAROTID BODY

Enlarged, hyperplastic carotid body from a young adult with cystic fibrosis. The lobules were increased in size and appeared to merge. Most chief cell nuclei are hyperchromatic and some are slightly enlarged. Some chief cells had small cytoplasmic vacuoles. (Fig. 15-13 from Fascicle 19, Third Series.)

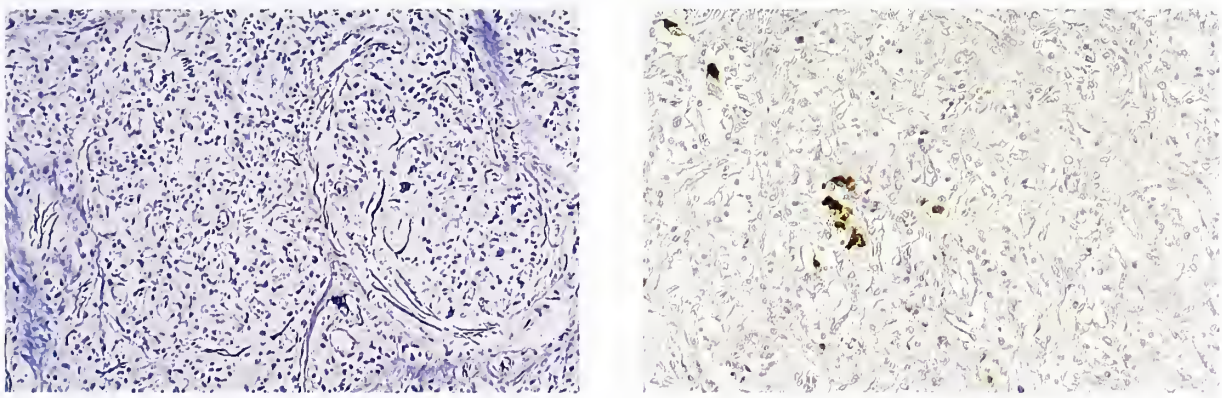

Figure 13-16

CAROTID BODY HYPERTROPHY AND HYPERPLASIA

Left: Carotid body hypertrophy and hyperplasia in a young adult with cystic fibrosis. The chief cell cytoplasm shows a marked decrease in argyrophilia, yet neural processes within and between lobules stain well. Compare with the normal carotid body in figure 13-8 (Bodian axon stain). (L&R: Fig. 15-14 from Fascicle 19, Third Series.)

Right: Hyperplastic carotid body from another patient with cystic fibrosis. There is a marked decrease in immunostaining of chief cells for chromogranin A compared with figure 13-9A (avidin-biotin peroxidase method).

RISK FOR DEVELOPMENT OF CHEMODECTOMA UNDER NORMOBARIC CONDITIONS

There are only anecdotal accounts of carotid body paragangliomas occurring under normobaric conditions in humans with chronic obstructive pulmonary disease (44), systemic hypertension (37), and cyanotic heart disease (45), including a patient with a malignant paraganglioma in another location (46). In general, however, there is currently no convincing evidence of any significant risk of developing a paraganglioma of peripheral arterial chemoreceptors, such as carotid bodies, in patients who have these conditions (1,24).

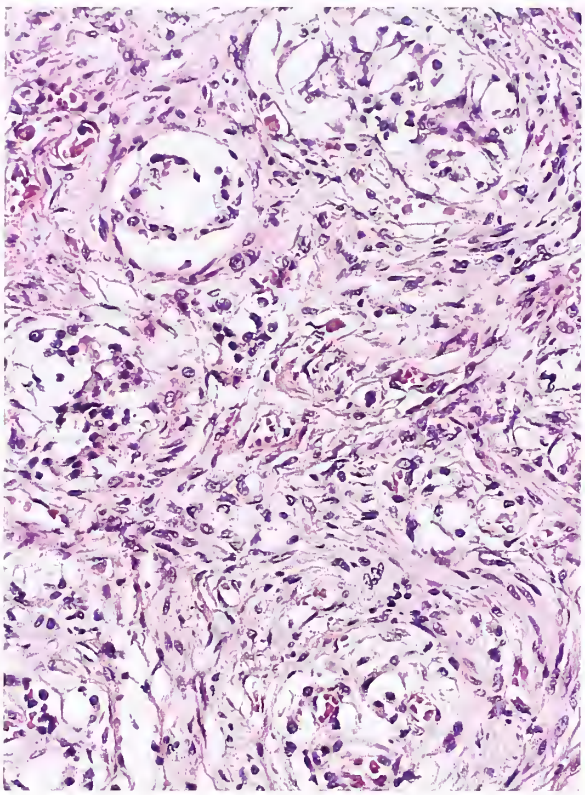

Figure 13-17

HYPERPLASTIC CAROTID BODY

Hyperplastic carotid body from a 54-year-old woman with severe chronic obstructive pulmonary disease. A prominent spindle cell component is seen within a lobule that surrounds clusters of chief cells. (Fig. 15-15 from Fascicle 19, Third Series.)

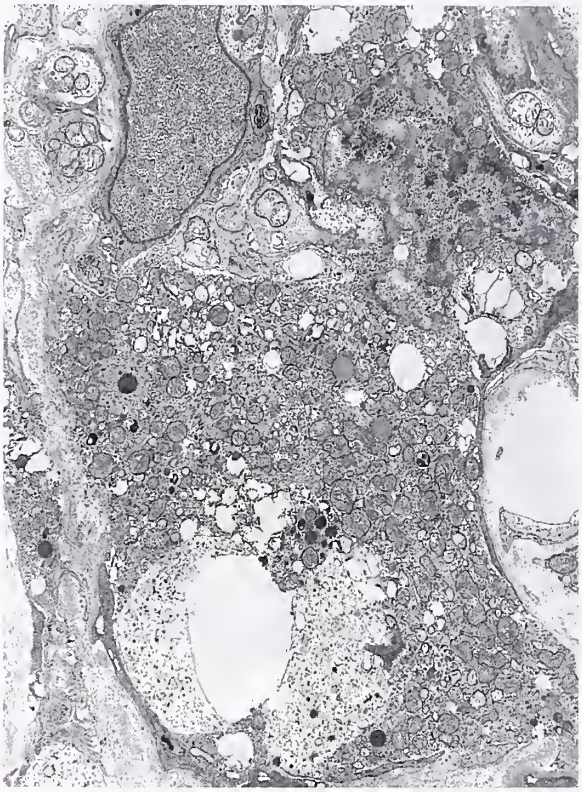

Figure 13-18

HYPERPLASTIC CAROTID BODY

Enlarged hyperplastic carotid body obtained at autopsy from a young adult with cystic fibrosis. On ultrastructural study, the chief cells showed severe depletion of dense-core neurosecretory granules. Compare with figures 13-10 and 13-11. (Fig. 15-16 from Fascicle 19, Third Series.)

CAROTID BODY PARAGANGLIOMA

Carotid body paraganglioma (CBP) is an endocrine neoplasm arising from the chief cells of carotid body paraganglia. It has also been referred to as a *chemodectoma.*

The designation of paragangliomas in the head and neck region is based upon anatomic site of origin. Five families of paraganglia (and the respective paragangliomas) were described by Glenner and Grimley (47): branchiomeric, intravagal, aorticosympathetic, visceroautonomic, and adrenal; the branchiomeric and intravagal are the main groups recognized in the head and neck region. CBP is the prototypic tumor of the head and neck paraganglion system, analogous to pheochromocytoma (adrenal medullary paraganglioma) of the sympathoadrenal neuroendocrine system (48,49). The term chemodectoma (chemeia: infusion; deschesthai: to receive; oma: tumor) was introduced by Mulligan in 1950 (50), but some have objected to its use for a neoplasm such as CBP since none of these tumors have been shown to have any chemoreceptor function (49), and based upon morphologic features, a chemoreceptor role would not even be anticipated. At high altitudes patients with hereditary paraganglioma type 1 and nonsense/splicing mutations of the gene for succinate dehydrogenase D (*SDHD*) had relatively early symptoms due to CBP; since this gene product may be involved in oxygen sensing it was suggested that SDHD mutations impair chemoreception at higher altitudes and result in earlier onset of symptoms (51).

The first CBP was reported by Marchand in 1891 (52), and from the illustration of the resected tumor and carotid vessels (fig. 13-19), it is not surprising that the patient died of complications several days after surgery. Four other patients with CBP were reported from Vienna by Paltauf in the same year (53). These early cases underscore the potential peril to the patient in attempting complete surgical resection because of vascular and neurologic complications; indeed, one is reminded of the intraoperative challenge by the statement of Mathews in 1915 (54), "this rare tumor presents unusual difficulties to the surgeon, and should one encounter it without having suspected the diagnosis, the experience will not soon be forgotten." This poignant phrase is reinforced by intraoperative photographs of a patient undergoing resection of a CBP complicated by excessive bleeding during surgery (fig. 13-20). Scudder in 1903 (55) is credited with the first description of a CBP surgically resected in the United States; the tumor was classified as a variety of angiosarcoma known as perithelioma. Middleton in 1897 (56) gave the first description of a CBP which was most likely bilateral. Historically, CBPs were at one time referred to as "potato tumors" (57), although this designation had been used for fungating tumors of the neck, most of which are probably malignant lymphomas (58).

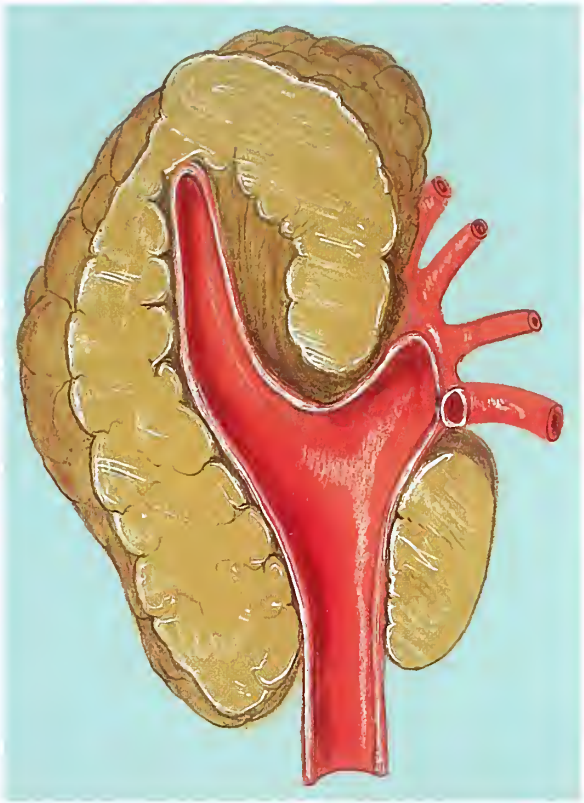

Figure 13-19

CAROTID BODY PARAGANGLIOMA

Cross section of carotid vessels and large carotid body paraganglioma (CBP). (Modification of original illustration of CBP from work by Marchand in 1891.) (Fig. 16-1 from Fascicle 19, Third Series.)

Clinical Features

The sex incidence in most series is roughly equal, although some report a slight predilection for females; the average age is usually in the 5th decade of life (59–62), but CBPs have even been reported in the first year of life (63). Studies of CBPs at high altitude have noted a marked predilection for female patients: in one series of 66 patients there was an overwhelming predominance of females (97 percent) (64).

The most common presentation is a painless, slow-growing neck mass near the angle of the mandible (59,62,65–68), with little to no mobility in the vertical plain (fig. 13-21). Only rarely is the mass painful or tender. Fluctuation in size is also uncommon, but it has been reported in a case associated with upper respiratory tract infections (60,61). There may be signs or symptoms of cranial nerve palsy, usually involving a combination of the 7th, 10th, and 12th nerves (60,66,68). Horner's syndrome is occasionally seen due to involvement of the cervical sympathetic chain (59). The rate of postoperative cranial nerve dysfunction observed at the Mayo Clinic remained relatively unchanged over a 50-year period (rate in the most recent 10 years was 40 percent) (67). The average duration of symptoms usually ranges from 5 (60,61) to nearly 7 years (65), but is sometimes as many as 20 years or more (59–61). The median growth rate is about 1 mm per year with a doubling time of 4.2 years (69). The fraction of Ki-67 (MIB-1) positive tumor cells is generally less than 1 percent in accordance with the slow growth (70). Carotid sinus syndrome with bradycardia and syncopal episodes is uncommon (60,71). A patient with bilateral CBPs presented with transient ischemic attacks (72).

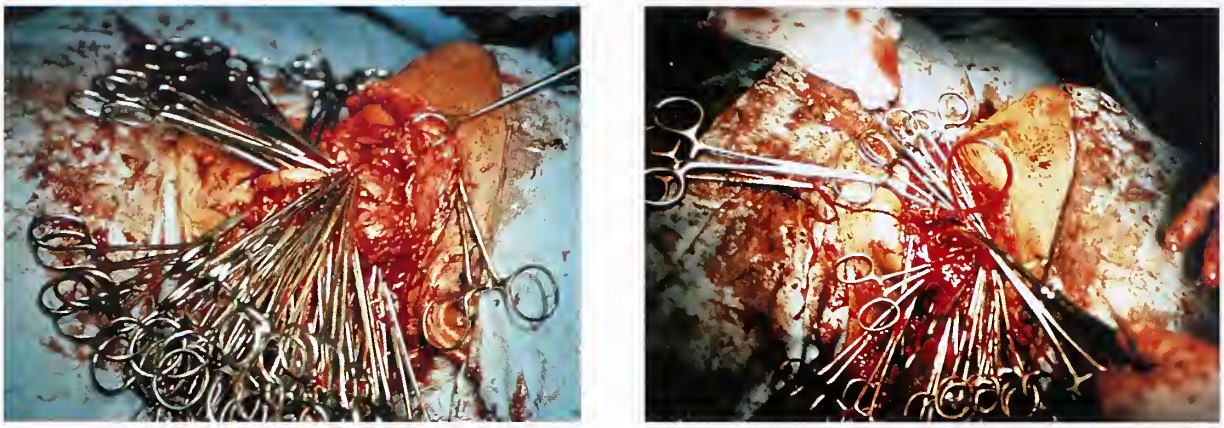

Figure 13-20

CAROTID BODY PARAGANGLIOMA

Left: A 30-year-old man noted a painless neck mass on the left side during the past year. A high-pitched systolic bruit was noted over the carotid vessels, and the carotid arteriogram showed a hypervascular tumor diagnostic of a CBP. During surgical resection, 2,000 mL of blood was lost. The number of hemostats in the field is ample testimony to the difficulty in controlling the bleeding.

Right: A vascular shunt was inserted between the common carotid artery and the internal branch to permit resection of the tumor from the bifurcation. (L&R: Fig. 16-2 from Fascicle 19, Third Series.)

Figure 13-21

CAROTID BODY PARAGANGLIOMA

Left: The patient had a slow-growing, painless mass in the left neck for many years. The tumor is present near the angle of the mandible.

Right: Another patient has a large firm tumor near the angle of the mandible. Note the branching scar over the tumor. An attempt at surgical resection had been done several years ago, but it was incomplete and the tumor continued to grow slowly in the lateral neck.

Unusual functionally active CBPs, vagal and jugulotympanic paragangliomas with excess catecholamine secretion, have been reported (59). In a review of the world literature, Zak and Lawson (73) identified 20 cases of functional paragangliomas of the head and neck region. Some of these reports should be interpreted with caution since some tumors arise along the cervical sympathetic chain (74,75), and are therefore sympathoadrenal paragangliomas. Hypotension has been reported as a prominent feature of a clinically malignant CBP secreting excessive amounts of dopamine (76).

Clinically, the differential diagnosis includes a variety of entities such as salivary gland enlargement, lymphadenopathy, branchial cleft cyst, and even carotid aneurysm (60,61). On physical examination a thrill or bruit is occasionally noted with CBP (and some other head and neck paragangliomas), but it is not a common finding. Medial protrusion by CBP or vagal paraganglioma may simulate tonsillar enlargement or an oropharyngeal mass (fig. 13-22) (60,61). Unusual lesions simulating a CBP are schwannoma (77) and accessory thyroid gland (78).

Preoperative Localization Studies

Preoperative selective angiography is useful for delineating tumor location, defining the blood supply, demonstrating other paragangliomas (79), and providing a route for selective embolization if this is considered prior to surgery. Preoperative embolization has been used to reduce blood loss during surgery (80), but it is not without complications in some cases (81). Characteristically with CPB, there is lateral displacement of the carotid bifurcation and both carotid artery branches (fig. 13-23A), and on lateral view there is widening of the bifurcation with "lyre-like" splaying apart of both branches. The tumor can be intensely vascular (fig. 13-23B), but occasional tumors have a less intense blush during arterial injection of contrast material (fig. 13-23C-E). The diminished and less uniform vascularity may be related to fibrosis within the tumor. On rare occasion, a CBP may be located medial to the bifurcation, without significant widening of the carotid branches. Following selective embolization the vascularization of the CBP can be greatly reduced (fig. 13-24).

Figure 13-22

CAROTID BODY PARAGANGLIOMA

A 31-year-old man presented in 1942 with a 3-year history of a painless neck mass associated with dysphagia. The CBP caused medial protrusion of the soft palate and pharynx. Surgical resection was performed but the patient died on the fourth postoperative day due to complications from the ligation of the major carotid vessels. (Fig. 16-4 from Fascicle 19, Third Series.)

Magnetic resonance imaging (MRI) can be very useful in tumor localization, diagnosis, and identification of multicentric tumors (82). Multiplanar imaging, good tissue contrast, and clear anatomic detail display the CBP in relation to the carotid vessels (fig. 13-25). Computerized tomography (CT) scans also provide valuable information.

Familial and Multicentric Paragangliomas

In the familial setting, about one third of the patients with a CBP have bilateral tumors (fig. 13-26), either synchronous or metachronous, and multicentric paragangliomas may develop at other sites in the head and neck region (fig.

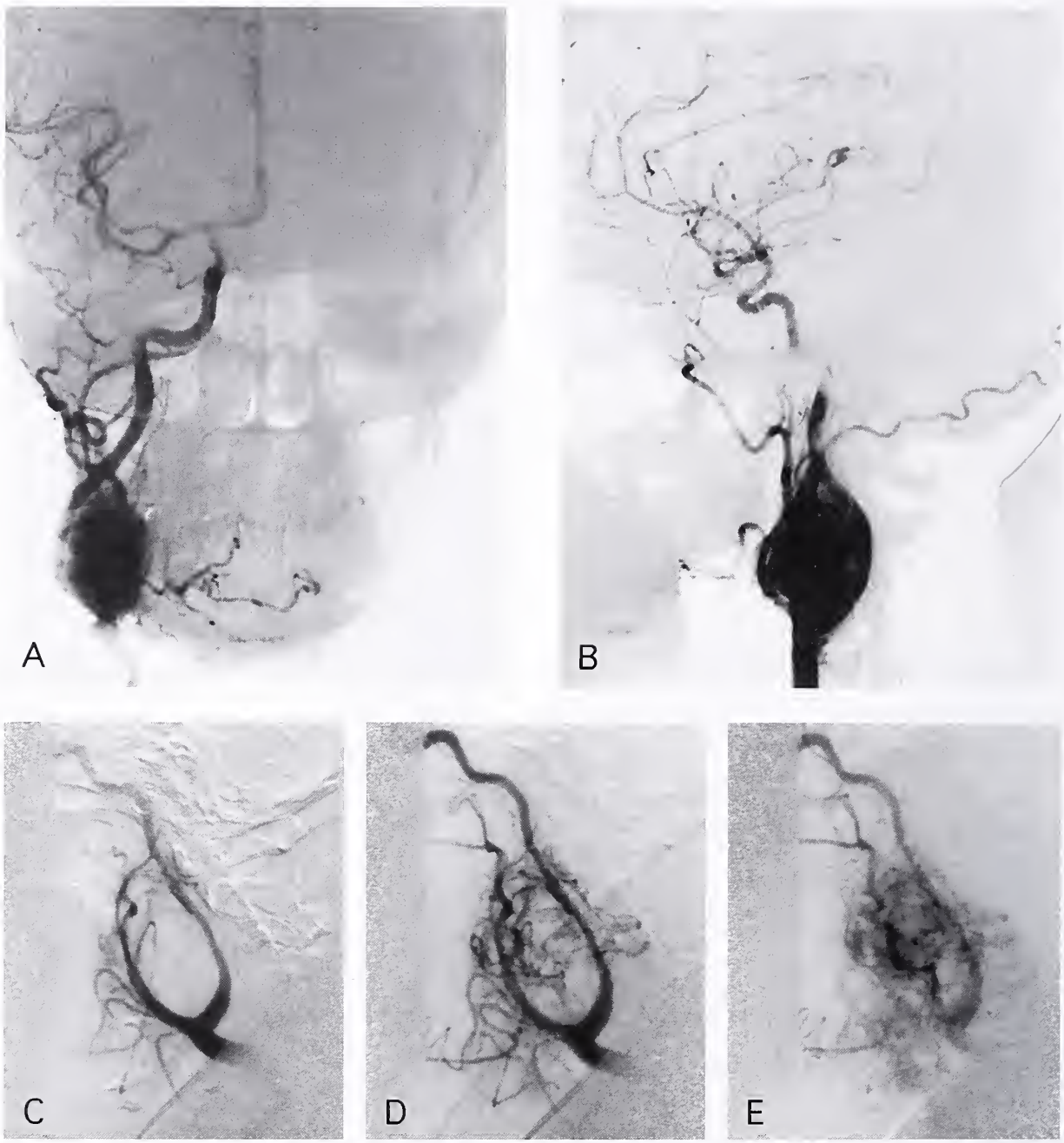

Figure 13-23

CAROTID BODY PARAGANGLIOMA

A: A 40-year-old woman had a right neck mass of about 5 months' duration. Selective right carotid angiogram in the anterior-posterior plane shows a hypervascular mass near the angle of the mandible, with some lateral displacement of the common carotid artery and bifurcation. Digital subtraction enhances contrast with bony densities.

B: Lateral view of the same case shows a mass in the carotid bifurcation which measured 3.5 cm in diameter. (A&B: Fig. 16-5A&B from Fascicle 19, Third Series.)

C: A 52-year-old woman had a painless, slow-growing mass in the left neck. Selective left carotid arteriogram in the early phase shows widening of the bifurcation. Sequences in digital subtraction.

D,E: Later phases of the arteriogram show abnormal vessels in the bifurcation. The tumor measured 7 x 5 x 4 cm and the total resected mass weighed 102 g. Tumor in E shows less intense opacification compared with A and B, which are from a different case.

Figure 13-24

CAROTID BODY PARAGANGLIOMA

Lateral view of CBP after selective embolization. The carotid bifurcation has a "lyre-like" configuration. A small vascular stump at the base of the bifurcation (arrow) represents the ascending pharyngeal artery which had been selectively embolized. The patient had a similar CBP removed from the left neck over a decade earlier, and had a family history of similar tumors. (Fig. 13-9C from Lack EE. Pathology of adrenal and extra-adrenal paraganglia. Major problems in pathology, Vol 29. Philadelphia: WB Saunders; 1994:48.)

13-27). Some studies of family pedigrees indicate an autosomal dominant mode of inheritance with variable penetrance and expressivity (83,84). In some series the sex ratio is nearly equal (83), while in others there is a predilection for females (85,86). At high altitude, CBPs have a distinct predilection for females (87), but familial cases account for only 1 percent of cases (88). Occasionally, tumors are transmitted almost exclusively along the paternal line, and a genomic imprinting hypothesis has been proposed (89). Patients with familial CBP may be diagnosed at a slightly younger age than patients having sporadic tumors (84), and the tumors may develop in childhood (90). In a review of the familial occurrence of head and neck paragangliomas, 78.0 percent were CBPs, 16.0 percent jugular paragangliomas, and 4.5 percent vagal paragangliomas (91). Sympathoadrenal paragangliomas also occur in association with familial paragangliomas of the head and neck region (85). Hereditary deficiencies of

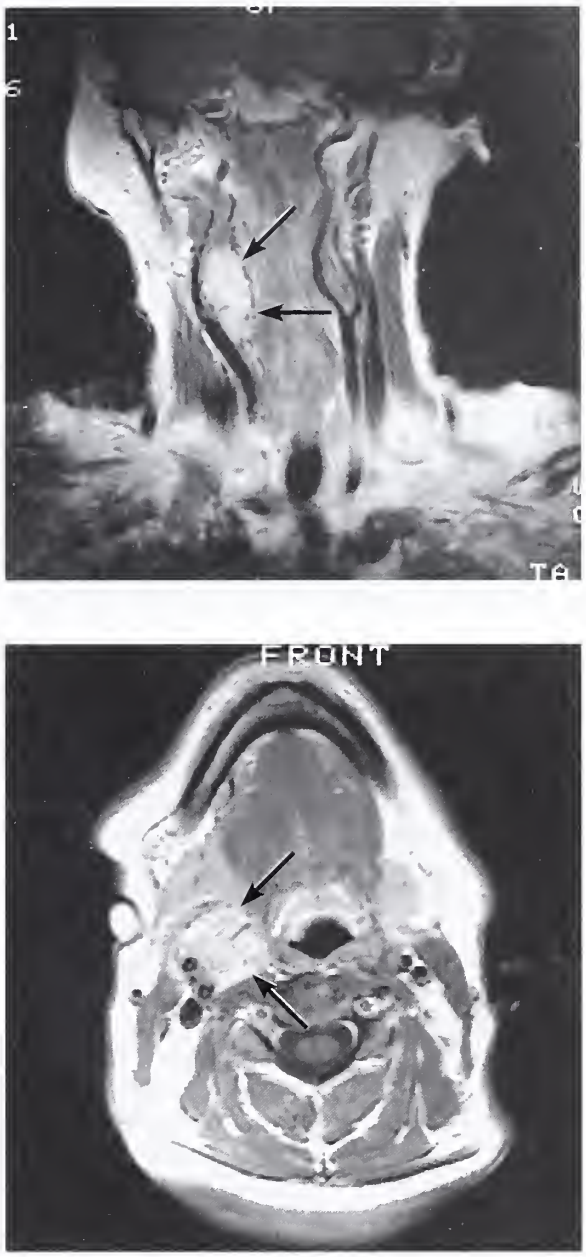

Figure 13-25

CAROTID BODY PARAGANGLIOMA

Top: Magnetic resonance image (MRI) in coronal plane shows a well-demarcated cervical mass (arrows) with bright image after gadolinium contrast administration. The carotid vessels are displaced laterally.

Bottom: MRI in transverse plane after gadolinium contrast administration. The CBP (arrows) was located medial to the carotid vessels and bifurcation. There is no significant widening of the carotid bifurcation, which is very unusual. (T&B: Figs. 3-11B,C from Lack EE. Pathology of adrenal and extra-adrenal paraganglia. Major problems in pathology, Vol 29. Philadelphia: WB Saunders; 1994:50, 51.)

Figure 13-26

CAROTID BODY PARAGANGLIOMA

Familial CBP in a patient with a strong history of similar tumors in related family members. Computerized tomography (CT) scan with intravenous contrast shows a bright image of the left CBP along with the internal and external carotid arteries (arrows) which indent the tumor. Surgical clips are present in the opposite neck where a CBP had been previously resected. (Fig. 16-8 from Fascicle 19, Third Series.)

Figure 13-27

CAROTID BODY AND JUGULOTYMPANIC PARAGANGLIOMA

A 15-year-old girl had a family history of head and neck paragangliomas. Carotid arteriogram on the left side using digital subtraction shows a CBP which measured 2 cm in diameter and a jugulotympanic paraganglioma more cephalad at the skull base. (Fig. 16-9 from Fascicle 19, Third Series.)

clotting factors VII and X have been reported in patients with familial CBP (92).

Recently, the genetics of head and neck paragangliomas has become better defined (93–95). The familial basis of these tumors is firmly established with the identification of at least three genetic loci for paragangliomas (PGL): *PGL1, PGL2,* and *PGL3* (95). The *PGL1* gene at chromosome 11q23 is the most common locus. The *PGL1* gene is succinate dehydrogenase subunit D (SDHD). Germline mutations in the mitochondrial SDHD enzyme complex II have been reported in familial cases and mutations in subunits B and C of succinate dehydrogenase may also predispose to the development of paragangliomas. The mitochondrial succinate dehydrogenase enzyme complex II may have an important role in oxygen sensing and signaling (94).

Multicentric or bilateral paragangliomas also occur in a nonfamilial or sporadic fashion (85); bilateral tumors occur in 4 to 8 percent of patients with CBP (83,84). Recently, baroreflex and chemoreflex dysfunction was reported in a patient who had excision of bilateral CBPs (96).

Association with Other Endocrine Disorders

CBPs have occurred in association with the triad of gastric stromal sarcoma, pulmonary chondroma, and extraadrenal paraganglioma (Carney's triad) (97). Thirty-seven patients (47 percent) had 60 paragangliomas; 7 patients had CBP (one bilateral) and 6 had pheochromocytomas (adrenal medullary paraganglioma). CBPs have also been reported in association with papillary thyroid carcinoma (98), hyperparathyroidism (99), and unusual endocrine disorders raising the possibility of a new pattern of multiple endocrine neoplasia (100,101).

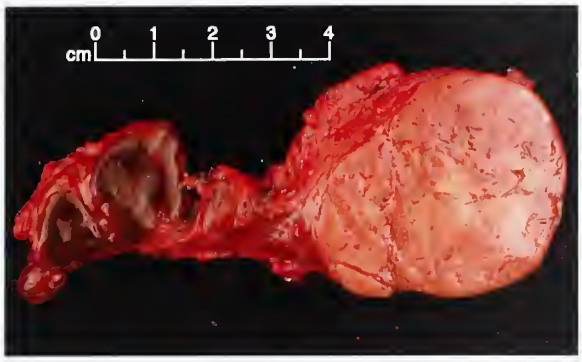

Figure 13-28

CAROTID BODY PARAGANGLIOMA

Cross section of CBP resected from an adult patient with a family history of similar tumors. Grooves on either side represent impressions left by internal and external carotid artery branches. Deeply congested lymph nodes attached to the specimen were negative for tumor. (Fig. 16-10 from Fascicle 19, Third Series.)

Figure 13-29

CAROTID BODY PARAGANGLIOMA

CPB on cross section has a uniform tan appearance.

Pathologic Findings

In general it is not possible to distinguish CBP from other head and neck paragangliomas on purely morphologic grounds, although some gross or microscopic features permit distinction. These features include residual ganglion nodosum at the periphery of a vagal paraganglioma and small irregular fragments of a jugulotympanic paraganglioma with or without bone involvement (102). Details of CBP morphology are covered in this chapter and illustrations of paragangliomas at other sites in the head and neck region emphasize special characteristics or amplify a broader range of morphology.

Gross Findings. CBPs are often sharply demarcated, and occasionally, the tumor gives the impression of true encapsulation, but careful histologic study often shows an expansile border with what is best regarded as a fibrous pseudocapsule. The average size of CBPs in the Memorial Hospital series was 3.8 cm (range, 1.9 to 8.5 cm) (103). In a study of CBP in patients born and living at high altitude, the average dimensions were 3.9 x 2.8 x 2.6 cm; some of the smaller tumors weighed 369 to 550 mg (104).

On external examination there may be an indentation of the surface of the CBP made by one or both carotid vessels (fig. 13-28). CBPs usually have a meaty dull red to light tan appearance (fig. 13-29), but with much mechanical manipulation during surgery, the tumor may become quite congested or frankly hemorrhagic. Close inspection of the cut surface may reveal punctate, linear, or curvilinear profiles of vessels which may be retracted slightly beneath the surface (105). Areas of tumor necrosis are rare, unless of course the tumor has been successfully embolized prior to surgery (fig. 13-30). In one study, there was no significant difference between the surface areas of embolized and nonembolized CBPs, although the intraoperative blood loss was lower in embolized tumors (average, 372 mL versus 609 mL) (106). There may be areas of sclerosis or cystic change (fig. 13-31). On rare occasion, a CBP invades the lumen of the carotid artery or causes total carotid artery occlusion (107,108).

Three groups of CBP have been identified (fig. 13-32) (109). Group I CBPs (26 percent of cases) do not adhere significantly to the vessel adventitia and are relatively small (calculated median volume of tumor, 7 cm^3) (figs. 13-33, 13-34); group II CBPs (46.5 percent of cases) are more adherent to the adventitia of the vessel wall and partially surround one or both carotid vessels (median volume, 11 cm^3); and group III tumors (27.6 percent of cases) intimately adhere to the entire circumference of the bifurcation (median volume, 22 cm^3) (see fig. 13-19) (110). Correlation of increasing size of CBP with each consecutive group has been reported (111).

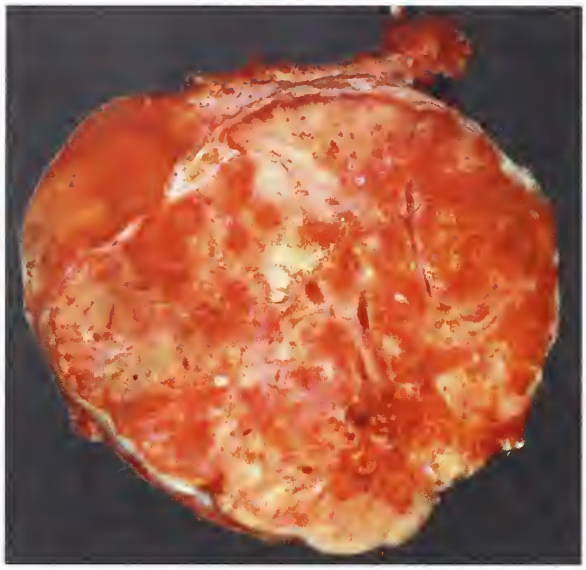

Figure 13-30

CAROTID BODY PARAGANGLIOMA

CBP on cross section has a mottled appearance, with areas of hemorrhage and necrosis. The tumor had been embolized via the ascending pharyngeal artery, resulting in confluent areas of tumor necrosis.

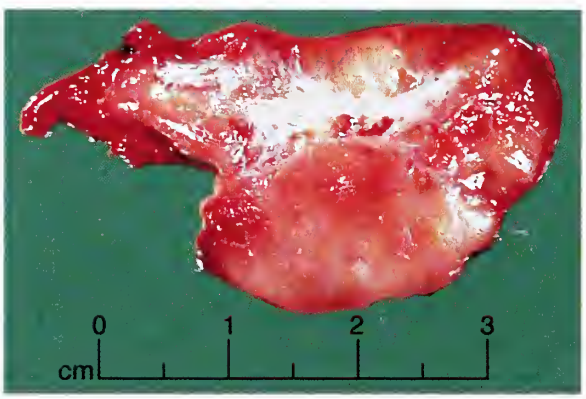

Figure 13-31

CAROTID BODY PARAGANGLIOMA

CBP resected from a young man shows areas of sclerosis and mild cystic degeneration. (Fig. 16-13 from Fascicle 19, Third Series.)

Microscopic Findings. *Architectural and Other Features.* On low-power magnification, CBPs are often well demarcated, with a well-developed fibrous pseudocapsule. Examination of the periphery of the tumor may reveal areas where the fibrous pseudocapsule is deficient, but in general, this should not be regarded as true

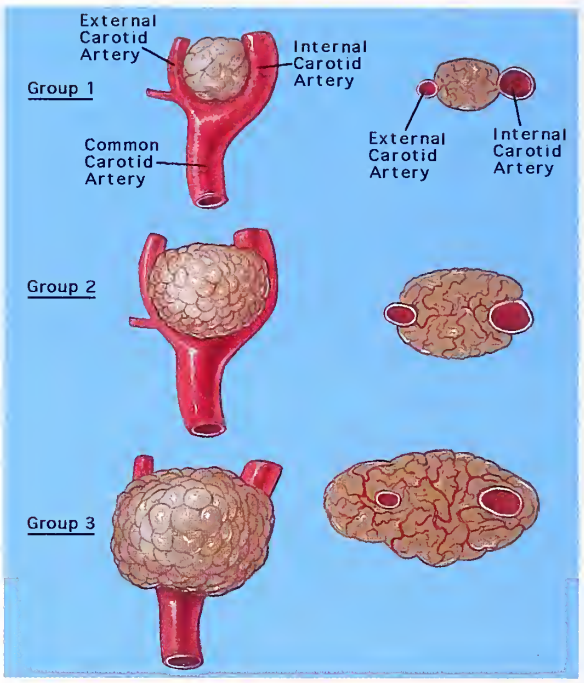

Figure 13-32

CAROTID BODY PARAGANGLIOMA

Three groups of CBP are schematically represented. The tumors get progressively bigger, and in group III the CBP encircles the carotid bifurcation and carotid vessels. (Fig. 16-14 from Fascicle 19, Third Series.)

capsular invasion (fig. 13-35). The tumor may intimately involve the adventitia of one or both carotid artery branches, and complete resection may necessitate vascular grafting. There may not be a discernible plane of dissection from the vessel wall (fig. 13-36).

The most characteristic pattern of CBPs (and other head and neck paragangliomas) is a relatively uniform nesting arrangement of cells or formation of "zellballen" (fig. 13-37), a pattern that can be greatly accentuated in reticulum-stained sections (fig. 13-38). Three basic histologic patterns were recognized by LeCompte (112): usual, adenoma-like, and angioma-like. The occasional artifactual separation of nests of tumor cells from the vascular stroma is probably related to shrinkage during fixation (fig. 13-39). Clusters of neoplastic chief cells may vary in size and shape. The zellballen can focally become quite large and seem to compress adjacent areas within the tumor (fig. 13-40), and extremely large nests of tumor cells may have a

Figure 13-33

CAROTID BODY PARAGANGLIOMA

CBP obtained at autopsy from the left neck of a 52-year-old man who had a CBP on the opposite side for nearly a decade. During surgical resection of the left CBP, the common carotid artery was ligated, and the patient developed a dense hemiplegia which soon proved fatal. There was no family history of other head and neck paragangliomas. (Fig. 16-15 from Fascicle 19, Third Series.)

Figure 13-34

CAROTID BODY PARAGANGLIOMA

A 63-year-old man had a firm nontender cervical mass of the right neck which was felt clinically to be enlarged jugular lymph nodes. The CBP measured 2.2 x 1.2 cm. The tumor has been mobilized from the carotid bifurcation by dissection through the adventitial plane. Preoperative needle aspiration biopsy yielded only blood, a finding that suggests CBP. (Fig. 16-16 from Fascicle 19, Third Series.)

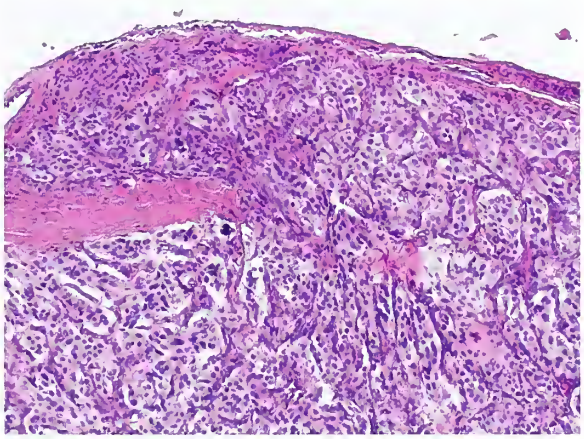

Figure 13-35

CAROTID BODY PARAGANGLIOMA

Clinically benign CBP shows discontinuity in the fibrous pseudocapsule, a feature that mimics true capsular invasion.

central area of degeneration or necrosis (fig. 13-41, left). In tumors that have been selectively embolized there may be confluent areas of necrosis (fig. 13-41, right).

Some CBPs have areas of hemorrhage or fibrosis, which if marked, separate individual clusters of neoplastic chief cells, giving a somewhat misleading picture (fig. 13-42). In sections taken through the periphery of the tumor or fibrous pseudocapsule, small remnants of the normal carotid body may be seen, a feature that shows that the neoplastic process has affected only a portion of the carotid body (fig. 13-43). When the neoplasm has been embolized to decrease vascularity, there may be geographic areas of hemorrhage and necrosis, but this is not always the case. A most unusual pattern is a spindle cell or pseudosarcomatous arrangement of cells (102,105); the author has encountered only two CBPs with this pattern (fig. 13-44).

Cellular Features. CBPs have a high density of neoplastic chief cells, more than the chief cells seen in non-neoplastic carotid body paraganglia. Neoplastic chief cells usually have ample,

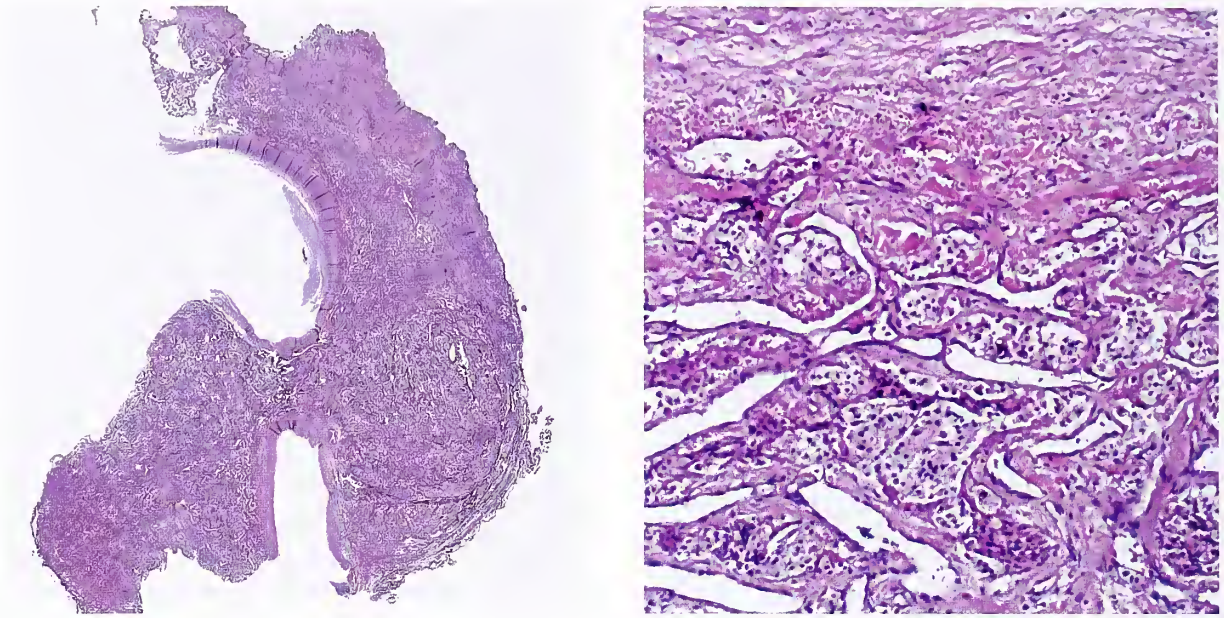

Figure 13-36

CAROTID BODY PARAGANGLIOMA

Left: This CBP almost completely encircled the carotid bifurcation and both the internal and external carotid branches (group III tumor, see figure 13-32). The tumor was firmly adherent to vessels, with no definable plane of dissection. (Fig. 16-19A from Fascicle 19, Third Series.)

Right: CBP is densely adherent to the vessel wall, but does not invade the media.

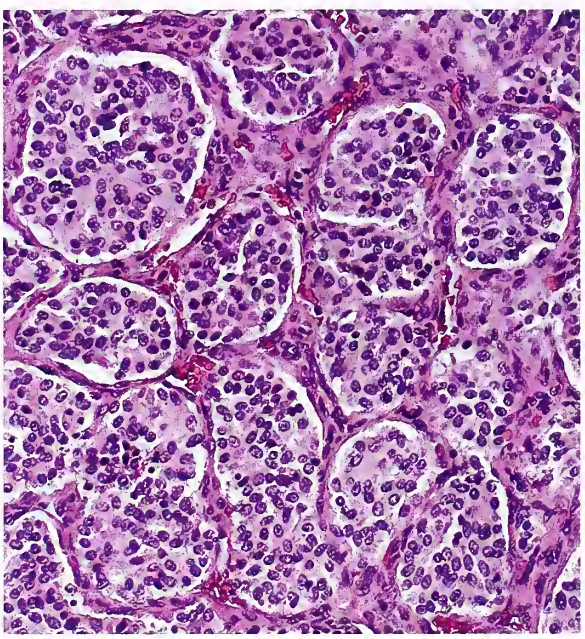

Figure 13-37

CAROTID BODY PARAGANGLIOMA

CBP has distinct nests ("zellballen") of tumor cells. (Fig. 16-20, left from Fascicle 19, Third Series.)

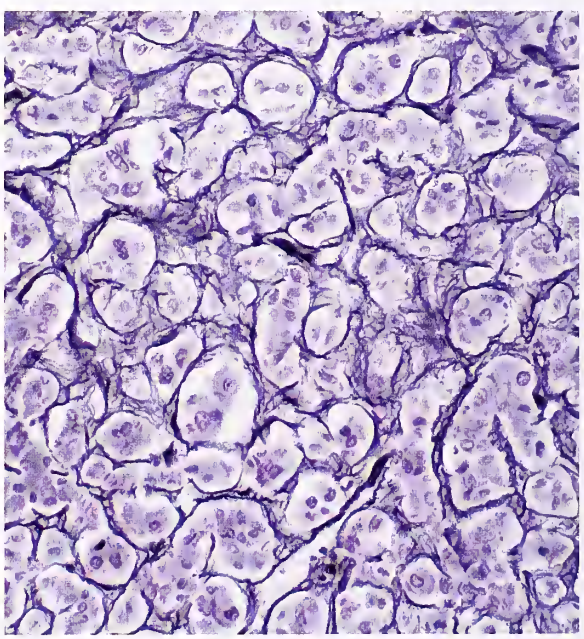

Figure 13-38

CAROTID BODY PARAGANGLIOMA

Stain for reticulum greatly accentuates the nesting pattern of the tumor cells.

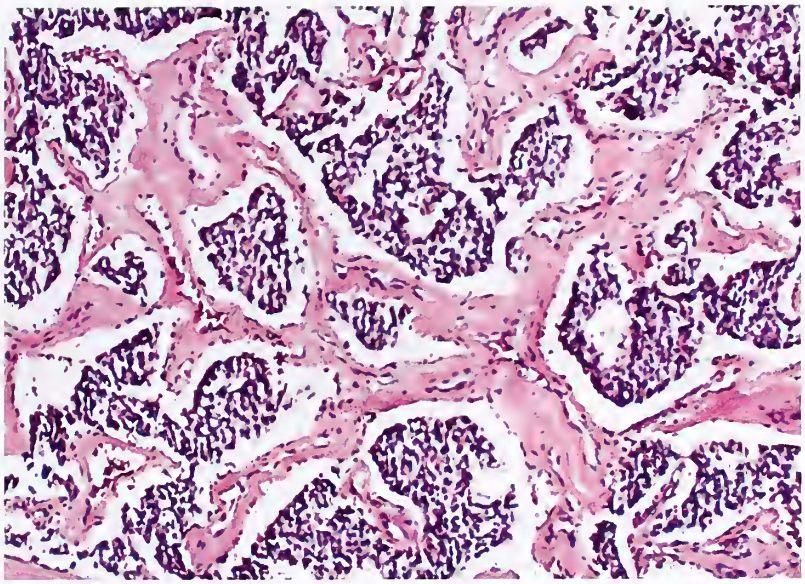

Figure 13-39

CAROTID BODY PARAGANGLIOMA

Clusters of tumor cells show some retraction from the fibrovascular stroma, an artifact of fixation. (Fig. 16-21 from Fascicle 19, Third Series.)

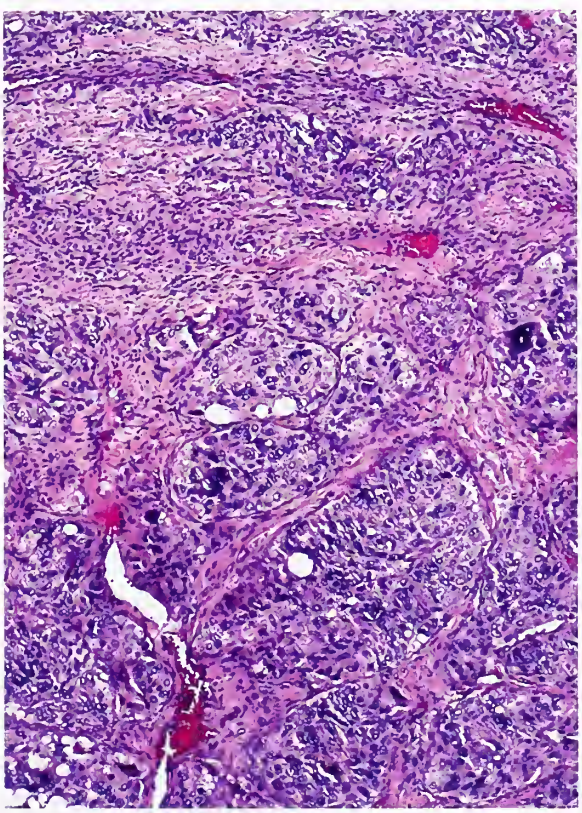

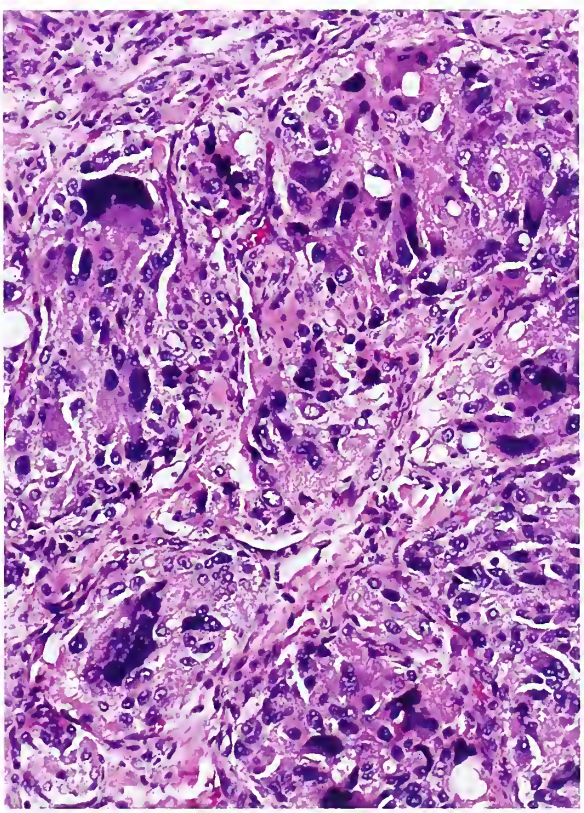

Figure 13-40

CAROTID BODY PARAGANGLIOMA

Left: An area within the CBP shows marked enlargement of zellballen. Contrast the size and irregular shape of these clusters of neoplastic chief cells with the adjacent tumor at the top of the field.

Right: Enlarged hyperchromatic nuclei are present in the same case. The tumor was clinically benign. (L&R: Fig. 16-22 from Fascicle 19, Third Series.)

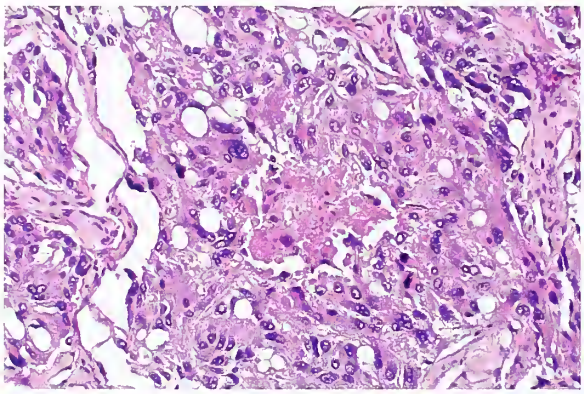

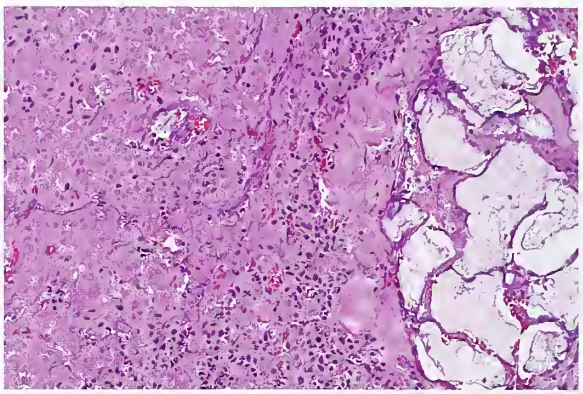

Figure 13-41

CAROTID BODY PARAGANGLIOMA

Left: A few greatly enlarged zellballen, some with central areas of degeneration and necrosis, are present in this CBP. The tumor was clinically benign.

Right: In a different case, the CBP was embolized prior to surgery (see figure 13-30) and had confluent areas of tumor necrosis. Embolic material is present in the vessel at the right.

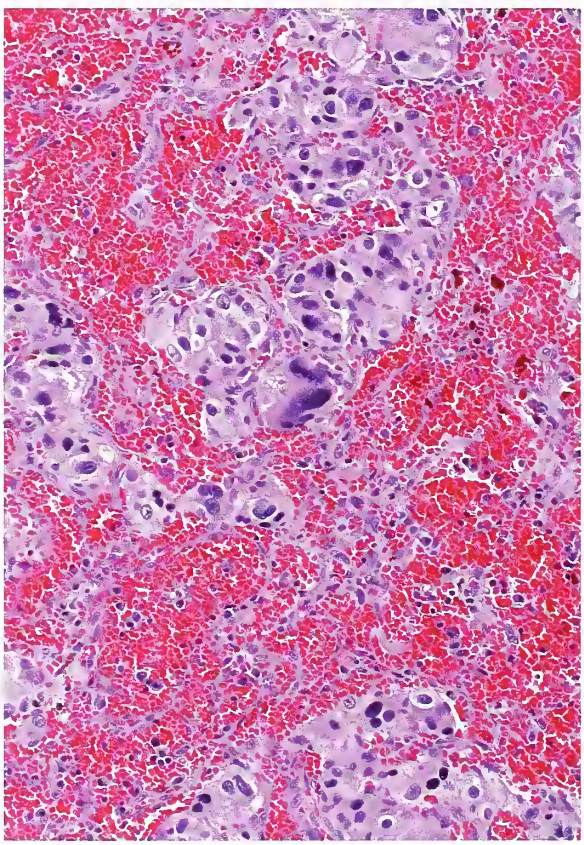

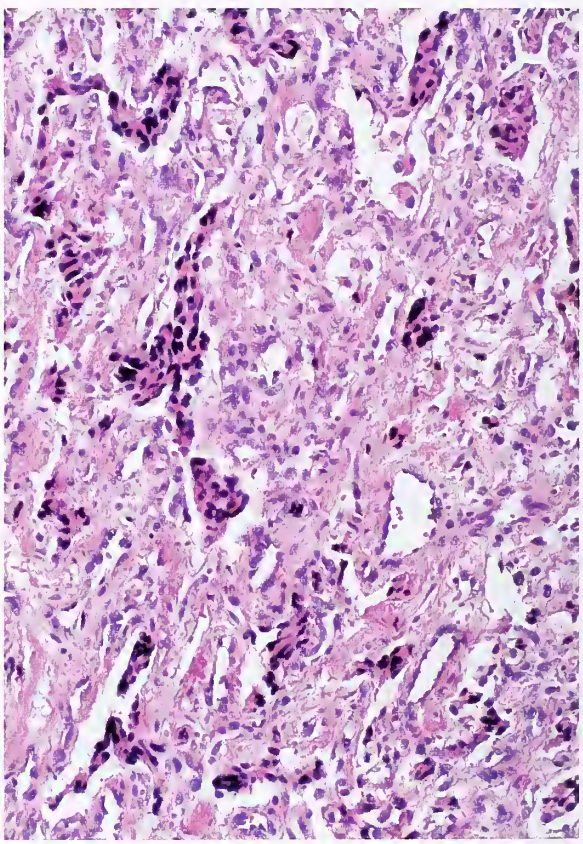

Figure 13-42

CAROTID BODY PARAGANGLIOMA

Left: Marked hemorrhage in this CBP separates nests and cords of tumor cells.

Right: In another CBP, the fibrovascular stroma is prominent and distorts nests and cords of tumor cells.

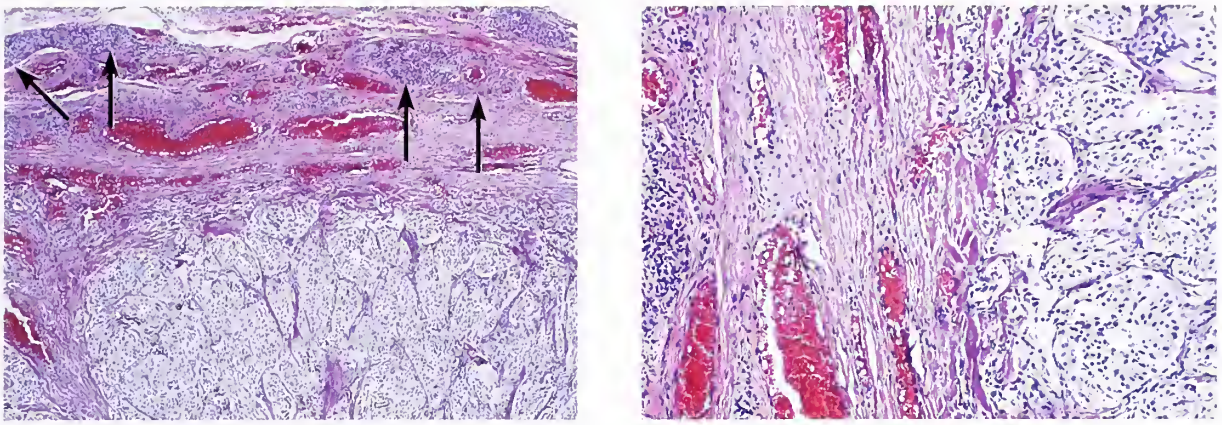

Figure 13-43

CAROTID BODY PARAGANGLIOMA

Left: Residual lobules of non-neoplastic CBP are present within the fibrous pseudocapsule (arrows).
Right: A portion of residual non-neoplastic carotid body is within the fibrous pseudocapsule of the tumor (left side of field). (L&R: Fig. 16-25 from Fascicle 19, Third Series.)

finely granular, eosinophilic cytoplasm; cell borders may be indistinct or at times well defined with polygonal or angular contours. Some tumor cells have such abundant, deeply eosinophilic cytoplasm that the neoplasm appears oncocytic (fig. 13-45), and this has been attributed to the presence of numerous mitochondria. Nuclei may be round to oval and stain uniformly, or there may be conspicuous nuclear pleomorphism and hyperchromasia (fig. 13-46), but these features are not a reliable indication of malignancy. Nuclear "pseudoinclusions," similar to those in sympathoadrenal paragangliomas, are sometimes seen. A vacuolar change in the cytoplasm of tumor cells may be found in the occasional CBP as well as in other paragangliomas; these spaces have been referred to as "pseudoacini" (fig. 13-47) (113). They are also found in some sympathoadrenal paragangliomas.

Sustentacular cells have been estimated to account for 1 to 5 percent of the cells in paragangliomas (114). These cells are almost impossible to identify in routinely stained sections, and they may be difficult to identify even by ultrastructural study (102). A finding that has been noted only rarely is the presence of ganglion cells within a CBP (fig. 13-48) (115). The presence of ganglion cells may be a manifestation of composite neural and endocrine differentiation in vivo, similar to composite pheochromocytomas.

Another unusual histologic feature is significant chronic inflammation. Small perivascular collections of lymphocytes may be present, particularly near the fibrous pseudocapsule, but the presence of chronic inflammatory cells causing architectural distortion within the tumor is rare. One patient in the Memorial Hospital series (105) complained of intermittent swelling of a lateral cervical mass in association with upper respiratory tract infections; on frozen section, the CBP was initially confused with a Hurthle cell carcinoma of the thyroid gland metastatic to a cervical lymph node (fig. 13-49). While some observers have regarded CBPs as representing hyperplastic growths rather than neoplasia (116), the histopathology strongly supports a true neoplasm.

Stromal Features. Alterations in the stromal connective tissue and vascular framework of CBPs and other paragangliomas may be extensive, and at times may partially obscure the diagnosis. Fibrosis may be a conspicuous feature in some cases, and can cause compression and distortion of nests of tumor cells (fig. 13-50). The term sclerosing paraganglioma has been used for tumors with extensive collagen deposition and on occasion the tumor may be mistaken for an invasive malignant neoplasm (117). There may be evidence of old hemorrhage with hemosiderin deposition, and rarely fibrosiderotic nodules (Gamna-Gandy bodies) (105).

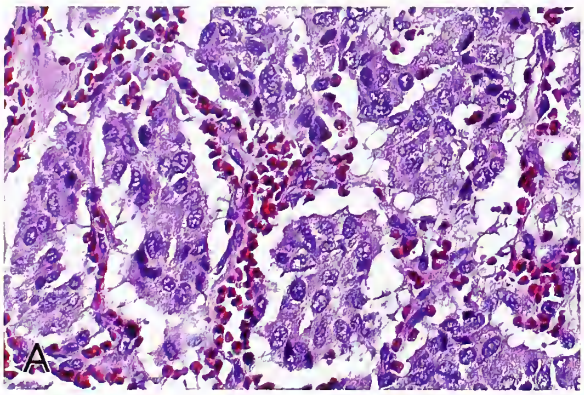

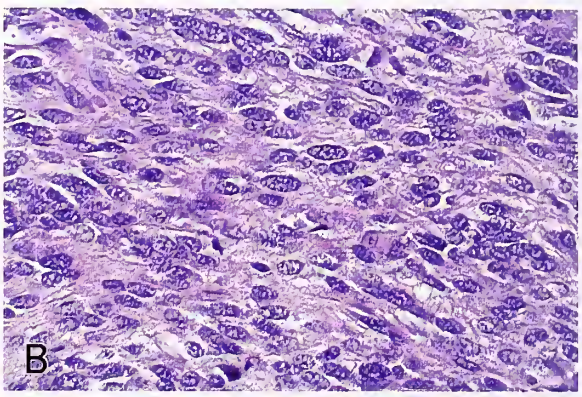

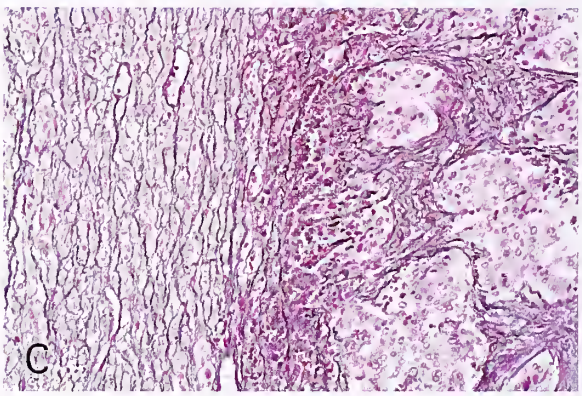

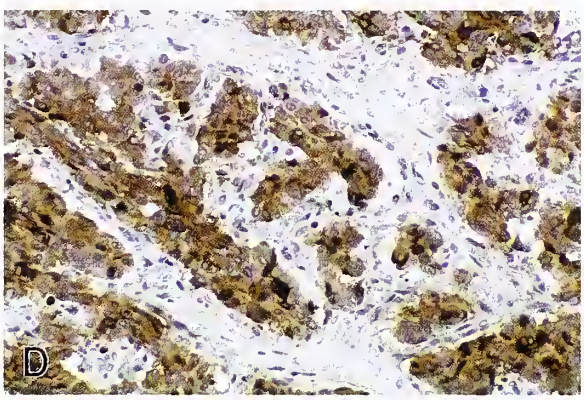

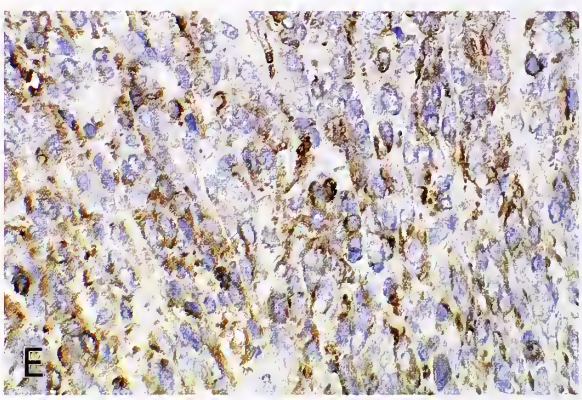

Figure 13-44

SPINDLE CELL CAROTID BODY PARAGANGLIOMA

A: A more typical organoid or nesting pattern is present in roughly half of this spindle cell CBP.

B: The remainder of tumor had a spindle cell or pseudosarcomatous pattern. There was no evidence of mitotic activity.

C: The transition between the spindle cell pattern (left, stained for reticulum) and the more characteristic zellballen pattern is abrupt.

D: Nests and cords of neoplastic chief cells are accentuated by positive immunostain for chromogranin.

E: The spindle cell component in this CBP is also positive for chromogranin but the architecture is markedly different (D,E: avidin-biotin peroxidase method).

Rare foci of metaplastic bone have been reported (105). Alteration in the vascular structures can add to diagnostic difficulties (102). There may be areas of sinusoidal sclerosis, for example, which may cause significant architectural distortion (fig. 13-51). Occasionally, there are arcades of dilated vessels which might be confused with a vascular neoplasm such as hemangiopericytoma or hemangioendothelioma (fig. 13-52). Stromal amyloid deposits have been noted in two CBPs on ultrastructural study, but no illustrations were provided (118).

Treatment and Prognosis

As with paragangliomas in general, complete surgical resection is the treatment of choice for CBPs if it can be done safely (119,120); paragangliomas involving the base of the skull may require adjuvant therapy. Carotid body and other head and neck paragangliomas are seldom malignant. In an early study of CBPs, 50 percent of the tumors were considered malignant based upon histologic findings such as mitotic activity, capsular invasion, and cellular pleomorphism

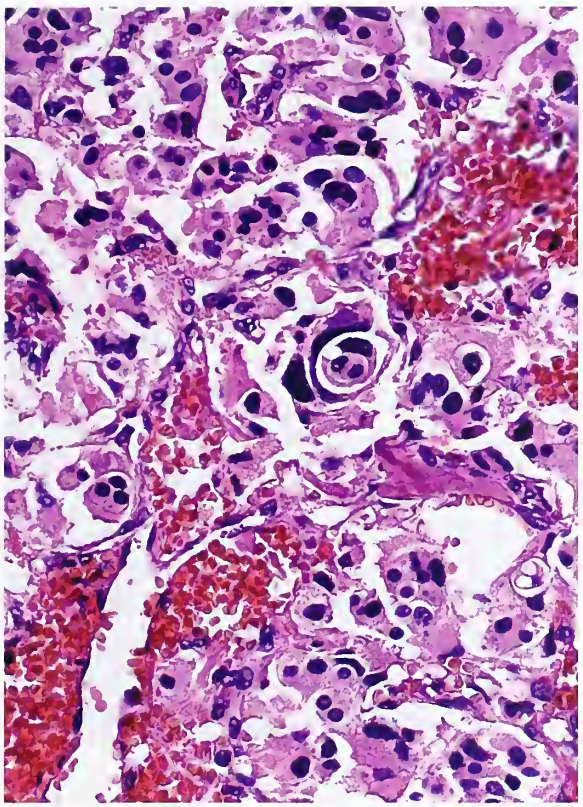

Figure 13-45

CAROTID BODY PARAGANGLIOMA WITH ONCOCYTIC FEATURES

Most nuclei are hyperchromatic and a few are mildly pleomorphic. Some tumor cells encircle other cells, an appearance referred to as "cell embracing." (Fig. 16-27 from Fascicle 19, Third Series.)

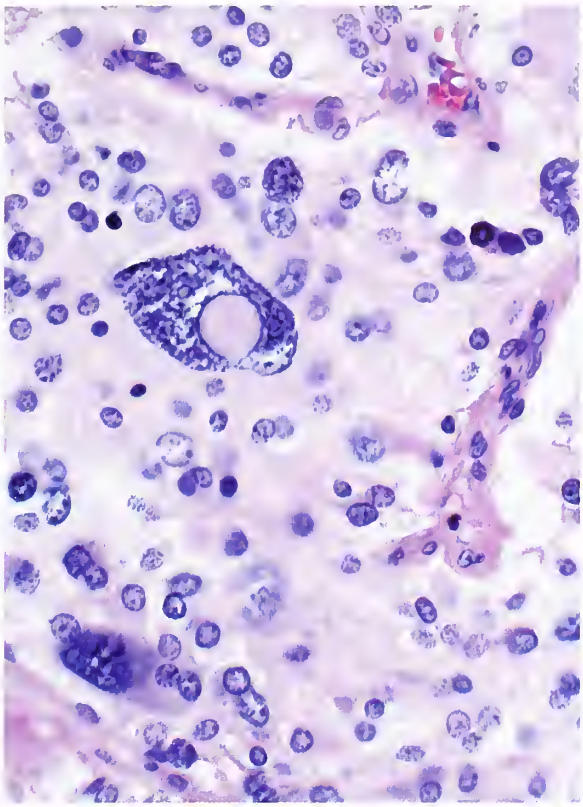

Figure 13-46

CAROTID BODY PARAGANGLIOMA

CBP has focally marked nuclear pleomorphism and hyperchromasia as well as a nuclear "pseudoinclusion."

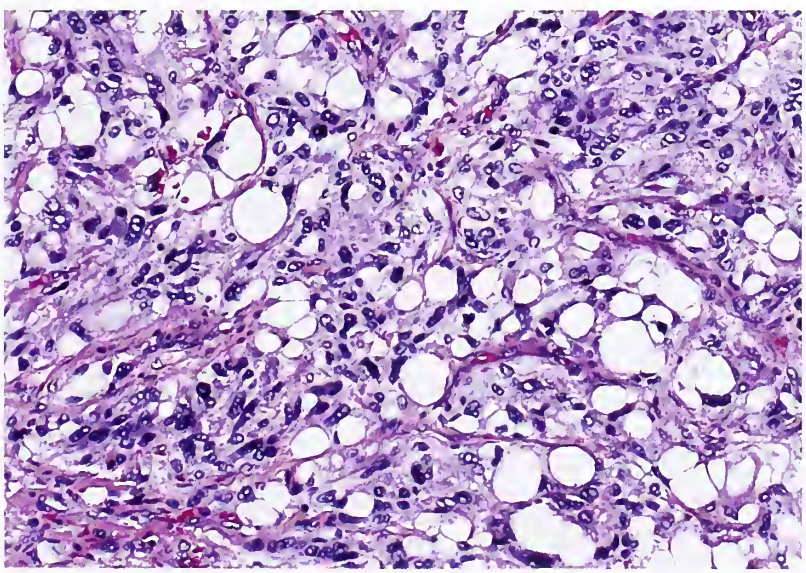

Figure 13-47

CAROTID BODY PARAGANGLIOMA

Nests of neoplastic chief cells have a striking amount of vacuolar spaces. This appearance has been referred to as "pseudoacini." (Fig. 16-29 from Fascicle 19, Third Series.)

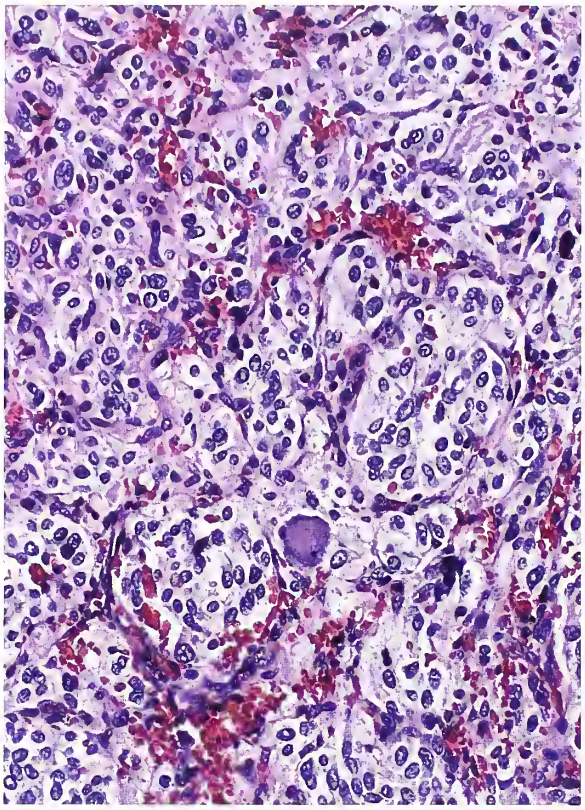

Figure 13-48

CAROTID BODY PARAGANGLIOMA

This CBP contained a few scattered cells with the cytomorphology typical for ganglion cells (lower half of field). (Fig. 16-30 from Fascicle 19, Third Series.)

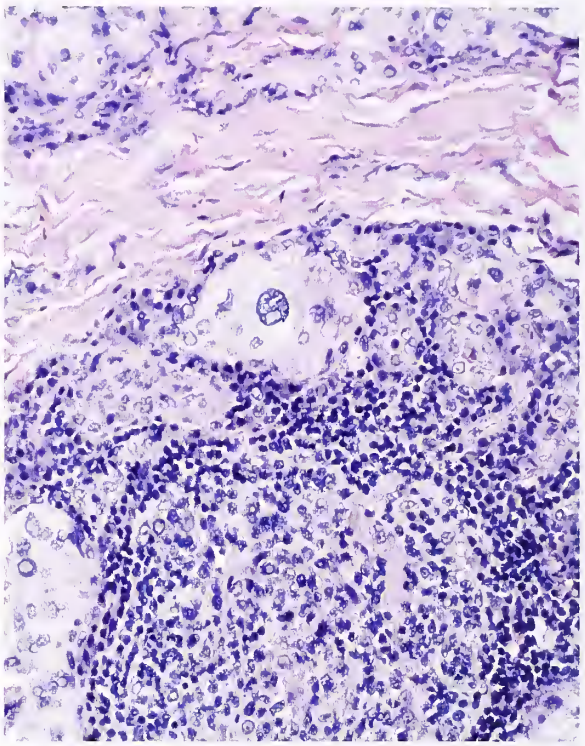

Figure 13-49

CAROTID BODY PARAGANGLIOMA

The patient had intermittent swelling of a painless mass in association with upper respiratory tract infections. The CBP contained abundant lymphocytes, plasma cells, and scattered lymphoid follicles, some with reactive germinal centers (bottom of field). The tumor cells also had oncocytic features. A frozen section of this neck mass was thought to represent Hurthle cell carcinoma of the thyroid gland metastatic to a lymph node.

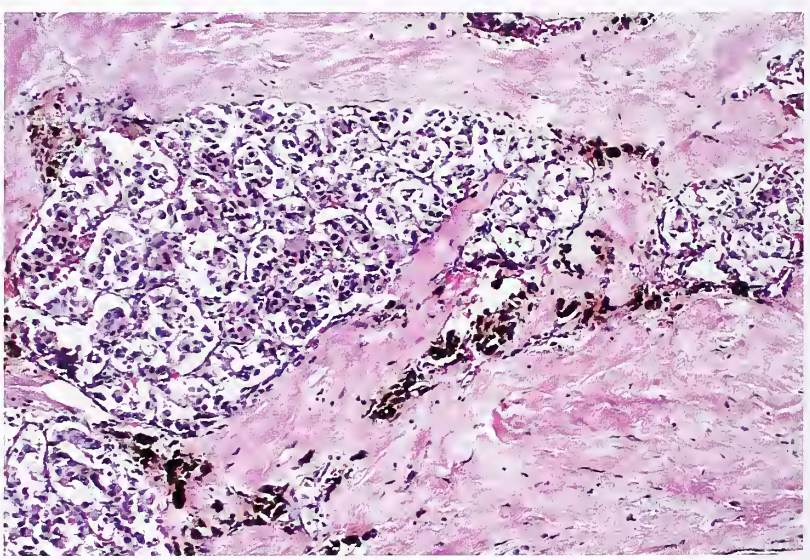

Figure 13-50

CAROTID BODY PARAGANGLIOMA

Multiple areas of marked fibrosis are present along with deposition of hemosiderin due to old hemorrhage. (Fig. 16-32 from Fascicle 19, Third Series.)

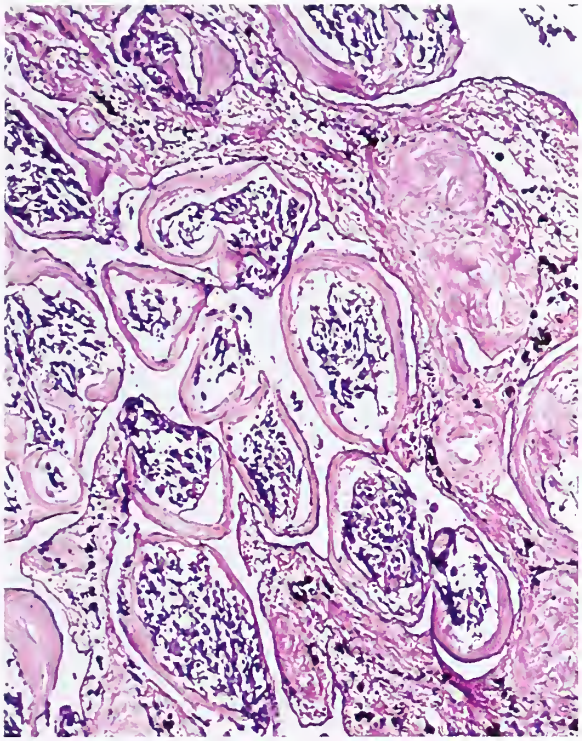

Figure 13-51

CAROTID BODY PARAGANGLIOMA

Sinusoidal sclerosis compresses nests of neoplastic chief cells. The dark granular material in the interstitium of the lower portion of field is hemosiderin. (Fig. 16-33 from Fascicle 19, Third Series.)

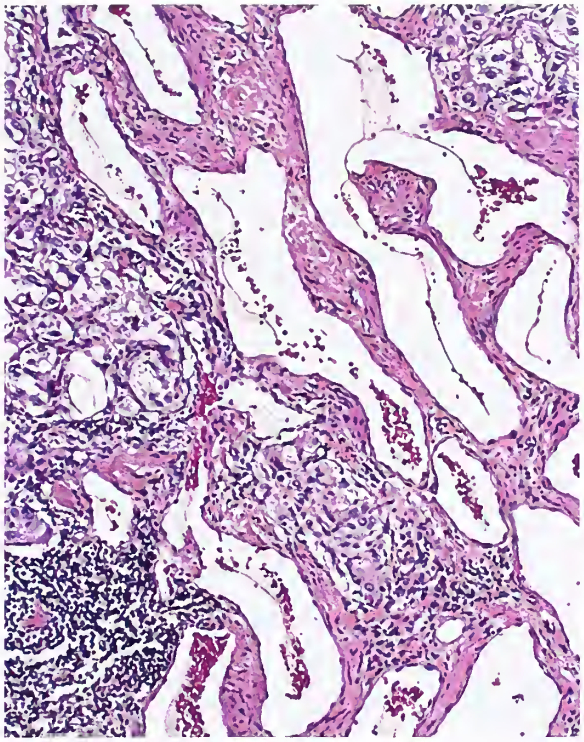

Figure 13-52

CAROTID BODY PARAGANGLIOMA

This CBP has an irregular vascular pattern which might be mistaken for a vasoformative neoplasm such as hemangiopericytoma. There is a small lymphoid aggregate in the lower left corner near the periphery of the tumor. (Fig. 16-34 from Fascicle 19, Third Series.)

(121). Attempts to decrease the vascularity of the tumor preoperatively have included intravascular embolization, direct percutaneous embolization (122), intratumoral injection of cyanoacrylate glue (123), and vascular exclusion of the tumor using stents (124).

Documentation of malignancy usually depends upon the demonstration of metastases to sites such as regional lymph node, liver, lung, or bone (fig. 13-53). Rarely, a patient presents with miliary infiltrates in the lung (125). Aggressive local growth, large tumor size, encirclement of carotid vessels, incorporation of nerves, or invasion near the base of the skull (fig. 13-54) also suggests malignancy, although definitive evidence is provided by metastases. Multicentric paragangliomas must be distinguished from true metastases. The incidence of metastasizing CBPs ranges from 6.4 percent (126) to 11.0 percent (127). A high proportion of malignant CBPs have been reported to have regionally confined metastases (128). Some series report a higher incidence of malignancy (18 percent [129] and 23 percent [130]), or categorically classify all CBPs as malignant (131), but this is an overestimate of the malignant potential of this tumor.

Prolonged follow-up may be necessary since the neoplasm may metastasize after a long interval (132). Data from the Mayo Clinic over two long periods of treatment indicate a 2 percent rate of malignancy (133,134); a relatively low incidence of malignancy was also reported by Padberg et al. (2.7 percent) (135). There is no individual or group of histopathologic findings than can reliably predict metastases (136). Data from Memorial Sloan-Kettering Cancer Center suggest that confluent necrosis, vascular invasion, and increased mitotic activity may be adverse prognostic findings, but these features were not considered to be conclusive (137).

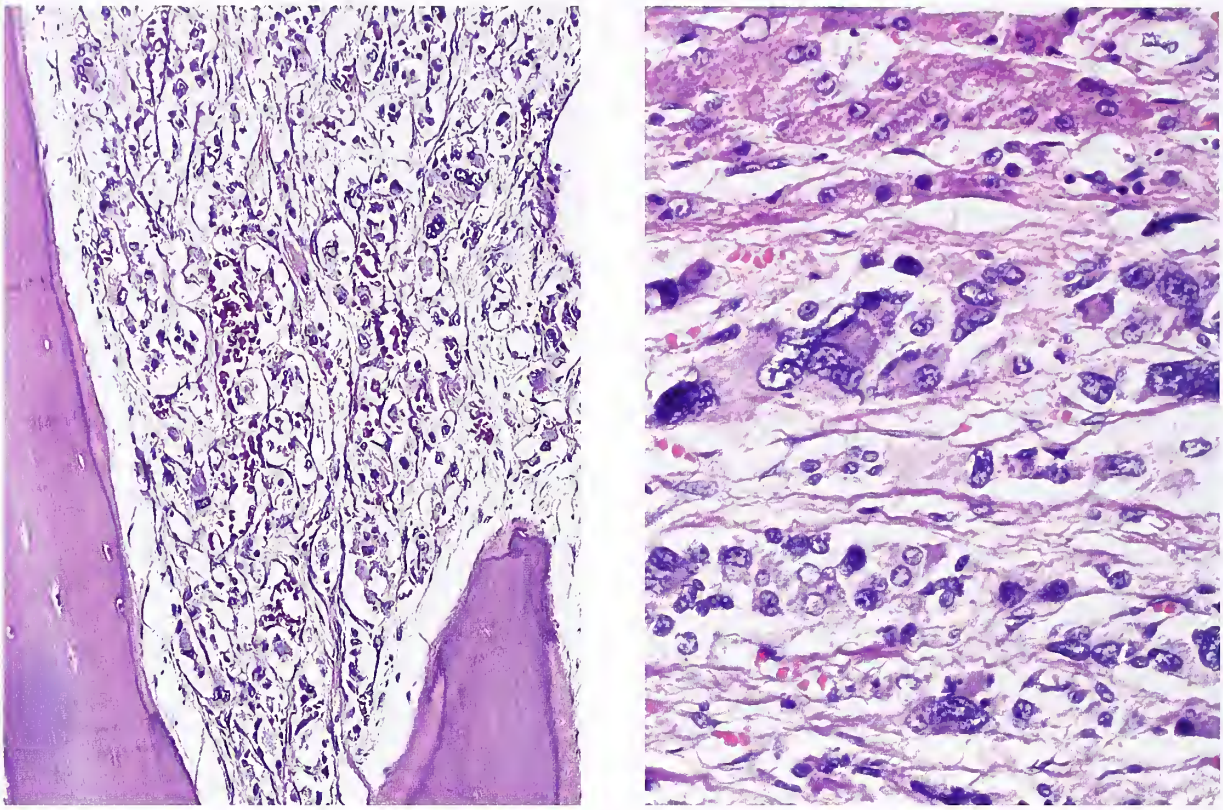

Figure 13-53

CAROTID BODY PARAGANGLIOMA METASTATIC TO BONE AND LIVER

Left: CBP metastatic to rib. The patient had several osteolytic bony metastases. (Fig. 16-35 from Fascicle 19, Third Series.) Right: Same patient at autopsy also had CBP metastatic to liver (compressed at top of field).

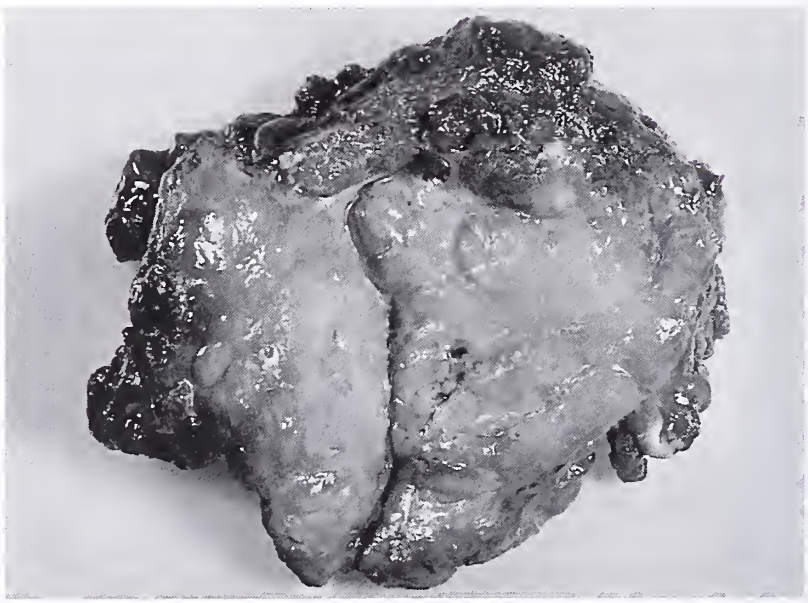

Figure 13-54

CLINICALLY MALIGNANT CAROTID BODY PARAGANGLIOMA

The bisected tumor was adherent to skeletal muscle and fat in the right neck. It recurred locally and extended up to the base of the skull. The patient died almost 3 years later with clinically apparent cervical lymph node metastases. (Fig. 16-36 from Fascicle 19, Third Series.)

REFERENCES

Normal Anatomy of Carotid Body Paraganglia

1. Lack EE. Pathology of adrenal and extra-adrenal paraganglia. Major problems in pathology, Vol 29. Philadelphia: WB Saunders; 1994.
2. Heath D, Edwards C, Harris P. Post-mortem size and structure of the human carotid body. Thorax 1970;25:129-140.
3. Lack EE, Perez-Atayde AR, Young JB. Carotid body hyperplasia in cystic fibrosis and cyanotic heart disease. A combined morphometric, ultrastructural, and biochemical study. Am J Pathol 1985;119:301-314.
4. Heath D, Jago R, Smith P. The vasculature of the carotid body. Cardiovasc Res 1983;17:33-42.
5. Jago R, Heath D, Smith P. Structure of the glomic arteries. J Pathol 1982;138:205-218.
6. Kjaergaard J. Anatomy of the carotid glomus and carotid glomus-like bodies (non-chromaffin paraganglia) with electron microscopy and comparison of human foetal carotid, aorticopulmonary, subclavian, tympanojugular, and vagal glomera. Copenhagen: FADL's Forlag; 1973.
7. Lack EE. Carotid body hypertrophy in patients with cystic fibrosis and cyanotic congenital heart disease. Hum Pathol 1977;8:39-51.
8. Lack EE, Perez-Atayde AR, Young JB. Carotid bodies in sudden infant death syndrome. A combined light microscopic, ultrastructural, and biochemical study. Pediatr Pathol 1986;6:335-350.
9. Smith P, Jago R, Heath D. Anatomical variation and quantitative histology of the normal and enlarged carotid body. J Pathol 1982;137:287-304.
10. Pearse AG, Polak JM, Rost FW, Fontaine J, Le Lievre C, Le Douarin N. Demonstration of the neural crest origin of type I (APUD) cells in the avian carotid body, using a cytochemical marker system. Histochemie 1973;34:191-203.
11. Heath D, Khan Q, Smith P. Histopathology of the carotid bodies in neonates and infants. Histopathology 1990;17:511-520.
12. Pallot DJ, Seker M, Abramovici A. Post-mortem changes in the normal rat carotid body: possible implications for human histopathology. Virchows Arch A Pathol Anat Histopathol 1992:420:31-35.
13. Jago R, Smith P, Heath D. Electron microscopy of carotid body hyperplasia. Arch Pathol Lab Med 1984;108:717-722.
14. Steele RH, Hinterberger H. Catecholamines and 5-hydroxytryptamine in the carotid body in vascular, respiratory, and other diseases. J Lab Clin Med 1972;80:63-70.
15. Tischler AS. Paraganglia. In: Sternberg SS, ed. Histology for pathologists, 2nd ed. Philadelphia: Lippincott-Raven; 1997:1153-1172.
16. Smith P, Gosney J, Heath D, Burnett H. The occurrence and distribution of certain polypeptides within the human carotid body. Cell Tissue Res 1990;261:565-571.
17. Hurst G, Heath D, Smith P. Histological changes associated with ageing of the human carotid body. J Pathol 1985;147:181-187.
18. Lowe P, Heath D, Smith P. Relation between histological age-changes in the carotid body and atherosclerosis in the carotid arteries. J Laryngol Otol 1987;101:1271-1275.
19. Heath D, Khan Q. Focal chronic thyroiditis and chronic carotid glomitis. J Pathol 1989;159:29-34.
20. Pryse-Davies J, Dawson IM. Some morphologic, histochemical, and chemical observations on chemodectomas and the normal carotid body, including a study of the chromaffin reaction and possible ganglion cell elements. Cancer 1964;17:185-202.
21. Grimley PM, Glenner GG. Ultrastructure of the human carotid body. A perspective on the mode of chemoreception. Circulation 1968;37:648-665.
22. Böck P, Stockinger L, Vyslonzil E. [The fine structure of the human carotid body.] Z Zellforsch Mikrosk Anat 1970;105:543-568. [German.]
23. Hervonen A, Korkala O. Fine structure of the carotid body of the midterm human fetus. Z Anat Entwicklungsmach Gesch 1972;138:135-144.

Hyperplasia of Carotid Body Paraganglia

24. Lack EE. Paraganglioma. In: Mills SE, Carter D, Greenson JK, Oberman HA, Reuter VE, Stoler MH, eds. Sternberg's diagnostic surgical pathology, 4th ed, vol 1. Philadelphia: Lippincott Williams & Wilkins; 2004:669-698
25. Arias-Stella J. Human carotid body at high altitude. Am J Pathol 1969;55:82a.
26. Saldana MJ, Salem LE, Travezan R. High altitude hypoxia and chemodectomas. Hum Pathol 1973;4:251-263.
27. De La Vega J, Takano J. Tumores del corpusculo carotideo en el hombre de las grandes alturas. Presented at the Ninth Latin-American Congress of Pathology, Merida, Yucatan, Mexico, Noviembre 25-30, 1973.
28. Arias-Stella J, Valcarcel J. Chief cell hyperplasia in the human carotid body at high altitudes: physiologic and pathologic significance. Hum Pathol 1976;7:361-373.

29. Rodriguez-Cuevas H, Lau I, Rodriguez HP. High altitude paragangliomas, diagnostic and therapeutic considerations. Cancer 1986;57:672-676.
30. Gaylis H, Davidge-Pitts K, Pantanowitz D. Carotid body tumours. A review of 52 cases. S Afr Med J 1987;72:493-496.
31. Pacheco-Ojeda L, Darango E, Rodriquez C, Vivar N. Carotid body tumors at high altitudes: Quito, Ecuador, 1987. World J Surg 1988;12:856-860.
32. Arias-Stella J, Bustos F. Chronic hypoxia and chemocectomas in bovines at high altitudes. Arch Pathol Lab Med 1976;100:636-639.
33. Lange F. [Enlargement of the glomus caroticum in all forms of hypertension.] Dtsch Med Wochenschr 1962;87:13-16. [German.]
34. Edwards C, Heath D, Harris P. The carotid body in emphysema and left ventricular hypertrophy. J Pathol 1971;104:1-13.
35. Janzer RC, Schneider J. The influence of chronically hypoxemic states on human carotid body structure and cardiac hypertrophy. Virchows Arch A Path Anat and Histol 1977;376:75-87.
36. Lack EE. Hyperplasia of vagal and carotid body paraganglia in patients with chronic hypoxemia. Am J Pathol 1978;91:497-516.
37. Heath D, Smith P, Jago R. Hyperplasia of the carotid body. J Pathol 1982;138:115-127.
38. Kluge P. Vascularization and morphology of carotid bodies in patients with essential hypertension. Acta Physiol Pol 1985;36:76-82.
39. Habeck JO. Morphological findings at the carotid bodies of humans suffering from different types of systemic hypertension or severe lung diseases. Anat Anz 1986;162:17-27.
40. Lange E, Johannessen JV. Histochemical and ultrastructural studies of chemodectoma-like tumors in the cod (Gadus morrhua L.). Lab Invest 1977;37:96-104.
41. Heath D, Smith P, Jago R. Dark cell proliferation in carotid body hyperplasia. J Pathol 1984;142:39-49.
42. Jago R, Smith P, Heath D. Electron microscopy of carotid body hyperplasia. Arch Pathol Lab Med 1984;108:717-722.
43. Fitch R, Smith P, Heath D. Nerve axons in carotid body hyperplasia. A quantitative study. Arch Pathol Lab Med 1985;109:234-237.

Chemodectomas Under Normobaric Conditions

44. Chedid A, Jao W. Hereditary tumors of the carotid bodies and chronic obstructive pulmonary disease. Cancer 1974;33:1635-1641.
45. Nissenblatt MJ. Cyanotic heart disease: "low altitude" risk for carotid body tumor? Johns Hopkins Med J 1978;142:12-21.
46. Bockelman HW, Arya S, Gilbert EF. Cyanotic congenital heart disease with malignant paraganglioma. Cancer 1982;50:2513-2517.

Carotid Body Paraganglioma

47. Glenner GG, Grimley PM. Tumors of the extra-adrenal paraganglion system (including chemoreceptors). Atlas of Tumor Pathology, 2nd Series, Fascicle 9. Washington DC: Armed Forces Institute of Pathology; 1974.
48. Lack EE. Adrenal medullary hyperplasia and pheochromocytoma. In: Lack EE, ed. Pathology of the adrenal glands. New York: Churchill Livingstone; 1990:173-235.
49. Lack EE. Pathology of adrenal and extra-adrenal paraganglia. Major problems in pathology, Vol 29. Philadelphia: WB Saunders; 1994.
50. Mulligan RM. Chemodectoma in the dog. Am J Pathol 1950;26:680-681. [abstract]
51. Astrom K, Cohen JE, Willett-Brozick JE, Aston CE, Baysal BE. Altitude is a phenotypic modifier in hereditary paraganglioma type 1: evidence for an oxygen-sensing defect. Hum Genet 2003;113:228-237.
52. Marchand F. Beiträge zur kenntniss der normalen und pathologischen anatomie der glandula carotica und der nebennieren. Internat Beitr z Wissensch Med Festschr R Virchow 1891;1:535-581.
53. Paltauf R. Ueber geschwülste der glandula carotica nebst einem beitrage zur histologie und entwickelungsgeschichte derselben. Ziegler's Beitr z path Anat u alleg Path, Jena 1891-1892;11:260-301.
54. Mathews FS. Surgery of the neck. In: Johnson AB, ed. Operative therapeusis, vol 3. New York: Appleton & Co; 1915:377-413.
55. Scudder CL. Tumor of the intercarotid body. A report of one case, together with all cases in the literature. Am J Med Sci 1903;126:384-389.
56. Middleton WD. Some curiosities in surgical pathology. Trans Iowa State Med Soc 1897;15:91-98.
57. Gilford H, Davis KL. "Potato" tumours of the neck and their origin as endotheliomata of carotid body, with account of three cases. Practioner, Lond 1904;73:729-739.
58. Robson AW. Sarcomatous tumours under the upper part of the sterno-mastoid (potato-like tumours), vol 3. Illust Med News, Lond 1889:194.

Clinical Features of Carotid Body Paragangliomas and Preoperative Localization

59. Lack EE. Pathology of adrenal and extra-adrenal paraganglia. Major problems in pathology, Vol 29. Philadelphia: WB Saunders; 1994.

60. Lack EE, Cubilla AL, Woodruff JM, Farr HW. Paragangliomas of the head and neck region: a clinical study of 69 patients. Cancer 1977;39: 397-409.
61. Lack EE, Cubilla AL, Woodruff JM. Paragangliomas of the head and neck region. A pathologic study of tumors from 71 patients. Hum Pathol 1979;10:191-218.
62. Lack EE. Paragangliomas. In: Mills SE, Carter D, Greenson JK, Oberman HA, Reuter VE, Stoler MH, eds. Diagnostic surgical pathology, 4th ed. Philadelphia: Lippincott Williams & Wilkins; 2004:669-696.
63. Fletcher WE, Arnold JH. Carotid body tumors: a review of the literature and report of an unusual case. Am J Surg 1954;87:617-619.
64. Luna-Ortiz K, Rascon-Ortiz M, Villavicencio-Valencia V, Granados-Garcia M, Herrera-Gomez A. Carotid body tumors: review of a 20-year experience. Oral Oncol 2005;41:56-61.
65. Shamblin WR, ReMine WH, Sheps SG, Harrison EG Jr. Carotid body tumor (chemodectoma). Clinicopathologic analysis of ninety cases. Am J Surg 1971;122:732-739.
66. Padberg FT Jr, Cady B, Persson AV. Carotid body tumor. The Lahey Clinic experience. Am J Surg 1983;145:526-528.
67. Hallett JW Jr, Nora JD, Hollier LH, Cherry KJ Jr, Pairolero PC. Trends in neurovascular complications of surgical management of carotid body and cervical paragangliomas: a fifty-year experience with 153 tumors. J Vasc Surg 1988;7:284-291.
68. Nora JD, Hallett JW Jr, O'Brien PC, Naessens JM, Cherry KJ Jr, Pairolero PC. Surgical resection of carotid body tumors: long-term survival, recurrence, and metastasis. Mayo Clin Proc 1988;63: 348-352.
69. Jansen JC, van den Berg R, Kuiper A, van der Mey AG, Zwinderman AH, Cornelisse CJ. Estimation of growth rate in patients with head and neck paragangliomas influences the treatment proposal. Cancer 2000;88:2811-2816.
70. Dekker PB, Kuipers-Dijkshoorn N, Hogendoorn PC, van der Mey AG, Cornelisse CJ. G2M arrest, blocked apoptosis, and low growth fraction may explain indolent behavior of head and neck paragangliomas. Hum Pathol 2003;34: 690-698.
71. Patel AK, Yap VU, Fields J, Thomsen JH. Carotid sinus syncope induced by malignant tumors in the neck. Emergence of vasodepressor manifestations following pacemaker therapy. Arch Intern Med 1979;139:1281-1284.
72. Chamorro Sanchez A, Varela de Seijas E, Matesarz Matesanz J, Trapero VL. Carotid body tumor: unusual cause of transient ischemic attacks. Stroke 1988;19:102-103.
73. Zak FG, Lawson W. The paraganglionic chemoreceptor system. Physiology, pathology, and clinical medicine. New York: Springer-Verlag; 1982.
74. Glenner GG, Crout JR, Roberts WC. A functional carotid-body-like tumor secreting levarterenol. Arch Pathol 1962;73:230-240.
75. Crowell WT, Grizzle WE, Siegel AL. Functional carotid paragangliomas. Biochemical, ultrastructural, and histochemical correlation with clinical symptoms. Arch Pathol Lab Med 1982;106:599-603.
76. Koch CA, Rodbard JS, Brouwers FM, Eisenhofer G, Pacak K. Hypotension in a woman with a metastatic dopamine-secreting carotid body tumor. Endocr Pract 2003;9:310-314.
77. Wang CP, Hsiao JK, Ko JY. Splaying of the carotid bifurcation caused by a cervical sympathetic chain schwannoma. Ann Otol Rhinol Laryngol 2004;113:696-699.
78. Hollander EJ, Visser MJ, van Baalen JM. Accessory thyroid gland at carotid bifurcation presenting as a carotid body tumor: case report and review of the literature. J Vasc Surg 2004;39:260-262.
79. Duncan AW, Lack EE, Deck MF. Radiological evaluation of paragangliomas of the head and neck. Radiology 1979;132:99-105.
80. Liapis CD, Evangelidakis EL, Papavassiliou VG, et al. Role of malignancy and preoperative embolization in the management of carotid body tumors. World J Surg 2000;24:1526-1530.
81. van der Mey AG, Jansen JC, van Baalen JM. Management of carotid body tumors. Otolaryngol Clin North Am 2001;34:907-924.
82. Lustrin ES, Palestro C, Vaheesan K. Radiographic evaluation and assessment of paragangliomas. Otolaryngol Clin North Am 2001;34:881-905.

Familial and Multicentric Paragangliomas

83. Grufferman S, Gillman MW, Pasternak LR, Peterson CL, Young WG. Familial carotid body tumors: case report and epidemiologic review. Cancer 1980;46:2116-2122.
84. Parry DM, Li FP, Strong LC, et al. Carotid body tumors in humans: genetics and epidemiology. JNCI 1982;68:573-578.
85. Lack EE. Pathology of adrenal and extra-adrenal paraganglia. Major problems in pathology, Vol 29. Philadelphia: WB Saunders; 1994.
86. Jensen JC, Choyke PL, Rosenfeld M, et al. A report of familial carotid body tumors and multiple extra-adrenal pheochromocytomas. J Urol 1991;145:1040-1042.
87. Luna-Ortiz K, Rascon-Ortiz M, Villavicencio-Valencia V, Granados-Garcia M, Herrera-Gomez A. Carotid body tumors: review of a 20-year experience. Oral Oncol 2005;41:56-61.

88. Rodriguez-Cuevas S, Lopez-Garza J, Labastida-Almendaro S. Carotid body tumors in inhabitants of altitudes higher than 2000 meters above sea level. Head Neck 1998;5:374-378.
89. van der May AG, Maaswinkel-Mooy PD, Cornelisse CJ, Schmidt PH, van de Kamp JJ. Genomic imprinting in hereditary glomus tumors: evidence for new genetic theory. Lancet 1989; 2:1291-1294.
90. Ophir D. Familial multicentric paragangliomas in a child. J Laryngol Otol 1991;105:376-380.
91. van Baars F, van den Broek P, Cremers C, Veldman J. Familial non-chromaffin paragangliomas (glomus tumors): clinical aspects. Laryngoscope 1981;91:988-996.
92. Kroll AJ, Alexander B, Cochios F, Pechet L. Hereditary deficiencies of clotting factors VII and X associated with carotid body tumors. N Engl J Med 1964;270:6-13.
93. Baysal BE, Ferrell RE, Willett-Brozick JE, et al. Mutations in SDHD, a mitochondrial complex II gene, in hereditary paraganglioma. Science 2000;287:848-851.
94. Baysal BE. Genetics of familial paragangliomas: past, present, and future. Otolaryngol Clin North Am 2001;34:863-879.
95. Dannenberg H, Komminoth P, Dinjens WN, Speel EJ, de Krijger RR. Molecular genetic alterations in adrenal and extra-adrenal pheochromocytomas and paragangliomas. Endocr Pathol 2003;14:329-350.
96. Timmers HJ, Karemaker JM, Wieling W, Marres HA, Folgering HT, Lenders JW. Baroreflex and chemoreflex function after bilateral carotid body tumor resection. J Hypertens 2003;21:591-599.

Association with Other Endocrine Disorders

97. Carney JA. Gastric stromal sarcoma, pulmonary chondroma, and extra-adrenal paraganglioma (Carney triad): natural history, adrenocortical component, and possible familial occurrence. Mayo Clin Proc 1999;74:543-552.
98. Parry DM, Li FP, Strong LC, et al. Carotid body tumors in humans: genetics and epidemiology. JNCI 1982;68:573-578.
99. Steely WM, Davies RS, Brigham RA. Carotid body tumor and hyperparathyroidism. A case report and review of the literature. Amer Surg 1987;53:337-338.
100. Berg B, Biörklund A, Grimelius L, et al. A new pattern of multiple endocrine adenomatosis: chemodectoma, bronchial carcinoid, GH-producing pituitary adenoma, and hyperplasia of the parathyroid glands, and antral and duodenal gastric cells. Acta Med Scand 1976;200:321-326.
101. Larraza-Hernandez O, Albores-Saavedra J, Benavides G, Krause LG, Perez-Merizaldi JC, Ginzo A. Multiple endocrine neoplasia. Pituitary adenoma, multicentric papillary thyroid carcinoma, bilateral carotid body paraganglioma, parathyroid hyperplasia, gastric leiomyoma, and systemic amyloidosis. Am J Clin Pathol 1982;78:527-532.

Pathologic Findings

102. Lack EE. Pathology of adrenal and extra-adrenal paraganglia. Major problems in pathology, Vol 29. Philadelphia: WB Saunders; 1994.
103. Lack EE, Cubilla AL, Woodruff JM, Farr HW. Paragangliomas of the head and neck region: a clinical study of 69 patients. Cancer 1977;39: 397-409.
104. Saldana MJ, Salem LE, Travezan R. High altitude hypoxia and chemodectomas. Hum Pathol 1973;4:251-263.
105. Lack EE, Cubilla AL, Woodruff JM. Paragangliomas of the head and neck region. A pathologic study of tumors from 71 patients. Hum Pathol 1979;10:191-218.
106. LaMuraglia GM, Fabian RL, Brewster DC, et al. The current surgical management of carotid body paragangliomas. J Vasc Surg 1992;15:1038-1045.
107. Sacher M, Som PM, Lanzieri CF, Biller HF. Total internal carotid artery occlusion by a benign carotid body tumor: a rare occurrence. J Comput Assist Tomogr 1985;9:213-217.
108. Warshawski SJ, de Souza FM. The carotid body tumor. J Otolaryngol 1989;18:306-310.
109. Shamblin WR, ReMine WH, Sheps SG, Harrison EG Jr. Carotid body tumor (chemodectoma). Clinicopathologic analysis of ninety cases. Am J Surg 1971;122:732-739.
110. Nora JD, Hallett JW Jr, O'Brien PC, Naessens JM, Cherry KJ Jr, Pairolero PC. Surgical resection of carotid body tumors: long-term survival, recurrence, and metastasis. Mayo Clin Proc 1988;63: 348-352.
111. Plukker JT, Brongers EP, Vermey A, Krikke A, van den Dungen AM. Outcome of surgical treatment for carotid body paraganglioma. Br J Surg 2001;88:1382-1386.
112. Le Compte PM. Tumors of the carotid body and related structures (chemoreceptor system), Atlas of Tumor Pathology, 1st Series, Fascicle 16. Washington DC: Armed Forces Institute of Pathology; 1951.
113. Glenner GG, Grimley PM. Tumors of the extra-adrenal paraganglion system (including chemoreceptors). Atlas of Tumor Pathology, 2nd Series, Fascicle 9. Washington DC: Armed Forces Institute of Pathology; 1974.

114. Capella C, Riva C, Cornaggia M, Chiaravalli AM, Frigerio B. Histopathology, cytology and cytochemistry of pheochromocytomas and paragangliomas including chemodectomas. Pathol Res Pract 1988;183:176-187.
115. Pryse-Davies J, Dawson IM, Westbury G. Some morphologic, histochemical, and chemical observations on chemodectomas and the normal carotid body, including a study of the chromaffin reaction and possible ganglion cell elements. Cancer 1964;17:185-202.
116. Rodriguez-Cuevas H, Lau I, Rodriguez HP. High-altitude paragangliomas diagnostic and therapeutic considerations. Cancer 1986;57:672-676.
117. Plaza JA, Wakely PE Jr, Moran C, Fletcher CD, Suster S. Sclerosing paraganglioma: report of 19 cases of an unusual variant of neuroendocrine tumor that may be mistaken for an aggressive malignant neoplasm. Am J Surg Pathol 2006;30:7-12.
118. Capella C, Solcia E. Optical and electron microscopical study of cytoplasmic granules in human carotid body, carotid body tumors and glomus jugulare tumors. Virchows Arch B Cell Pathol 1971;7:37-53.

Treatment and Prognosis

119. Sniezek JC, Sabri AN, Netterville JL. Paraganglioma surgery. Complications and treatment. Otolaryngologic Clin North Am 2001;34:993-1005.
120. Dardik A, Eisele DW, Williams GM, Perler BA. A contemporary assessment of carotid body tumor surgery. Vasc Endovascular Surg 2002;36:277-283.
121. Harrington SW, Clagett OT, Dockerty MB. Tumors of the carotid body. Clinical and pathologic considerations of twenty tumors affecting nineteen patients (one bilateral). Ann Surg 1941;114:820-833.
122. Harman M, Etlik O, Unal O. Direct percutaneous embolization of a carotid body tumor with n-butyl cyanoacrylate: an alternative method to endovascular embolization. Acta Radiol 2004;45:646-648.
123. Abud DG, Mounayer C, Benndorf G, Piotin M, Spelle L, Moret J. Intratumoral injection of cyanoacrylate glue in head and neck paragangliomas. Am J Neuroradiol 2004;25:1457-1462.
124. Tripp HF Jr, Fail PS, Beyer MG, Chaisson GA. New approach to preoperative vascular exclusion for carotid body tumor. J Vasc Surg 2003;38:389-391.
125. Tu H, Bottomley, RH. Malignant chemodectoma presenting as a miliary infiltrate. Cancer 1974;33:244-249.
126. Staats EF, Brown RL, Smith RR. Carotid body tumors, benign and malignant. Laryngoscope 1966;76:907-915.
127. Zbaren P, Lehmann W. Carotid body paraganglioma with metastases. Laryngoscope 1985;95:450-454.
128. Lee JH, Barich F, Karnell LH, et al. National Cancer Data Base report on malignant paragangliomas of the head and neck. Cancer 2002;94:730-737.
129. Gaylis H, Davidge-Pitts K, Pantanowitz D. Carotid body tumours. A review of 52 cases. S Afr Med J 1987;72:493-496.
130. Martin CE, Rosenfeld L, McSwain B. Carotid body tumors: a 16-year follow-up of seven malignant cases. South Med J 1973;66:1236-1243.
131. Pantanowitz D, Davidge-Pitts K, Gaylis H, Hale MJ. Are carotid body tumours malignant? S Afr J Surg 1990;28:97-99.
132. North CA, Zinreich ES, Christensen WN, North RB. Multiple spinal metastases from paraganglioma. Cancer 1990;66:2224-2228.
133. Shamblin WR, ReMine WH, Sheps SG, Harrison EG Jr. Carotid body tumor (chemodectoma). Clinicopathologic analysis of ninety cases. Am J Surg 1971;122:732-739.
134. Nora JD, Hallett JW Jr, O'Brien PC, Naessens JM, Cherry KJ Jr, Pairolero PC. Surgical resection of carotid body tumors: long-term survival, recurrence, and metastasis. Mayo Clin Proc 1988;63:348-352.
135. Padberg FT Jr, Cady B, Persson AV. Carotid body tumor. The Lahey Clinic experience. Am J Surg 1983;145:526-528.
136. Lack EE. Pathology of adrenal and extra-adrenal paraganglia. Major problems in pathology, Vol 29. Philadelphia: WB Saunders; 1994.
137. Lack EE, Cubilla AL, Woodruff JM. Paragangliomas of the head and neck region. A pathologic study of tumors from 71 patients. Hum Pathol 1979;10:191-218.

14 JUGULOTYMPANIC PARAGANGLIOMA

The first description of a "carotid body tumor" located in the middle ear and mastoid, was by Rosenwasser in 1945 (1), but it was Otani who actually made the pathologic diagnosis (1,2). The tumor was considered to arise from the minute paraganglia located near the base of the skull that had been described by Guild (3). Several other carotid body–like tumors of the middle ear and base of the skull were reported over the next few years, including the first case associated with carotid body paraganglioma (4).

JUGULOTYMPANIC PARAGANGLIA

In 1941, Guild (3) described microscopic structures that resembled the carotid body that were located in the adventitia of the dome of the jugular bulb beneath the bony floor of the middle ear or along the ramus tympanicus of the glossopharyngeal nerve. In a subsequent study in 1953 (5), Guild examined 88 temporal bones from 44 individuals and identified 248 collections of paraganglia, 135 of which were closely associated with the tympanic branch of the 9th cranial nerve (nerve of Jacobson) and 113 were near the auricular branch of the 10th cranial nerve (nerve of Arnold) (fig. 14-1). He believed that previous reports by Krause (6) and Valentin (7) did not validly document "glomus jugulare."

This minor historical dispute aside, the study published in 1953 provided valuable anatomic data regarding number, size, and distribution of the paraganglia in humans (5). An average of 2.82 paraganglia were identified in each temporal bone (range, 0 to 12), but this was probably a low estimate; 7 of 82 temporal bones contained more than 6 paraganglia (5). A little over half of the paraganglia were present in the adventitia of the dome of the jugular bulb and along the course of the nerves of Jacobson and

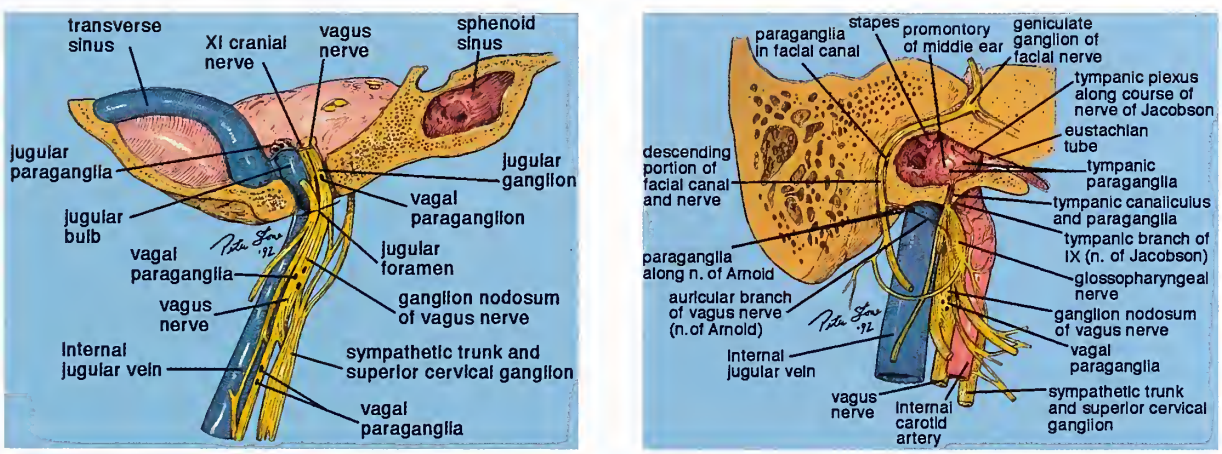

Figure 14-1

JUGULOTYMPANIC PARAGANGLIA

Left: The diagram shows the plane of section through the base of the skull and lateral temporal bone. Jugulotympanic paraganglia are present within the adventitia near the jugular bulb. Vagal paraganglia are seen in relation to the ganglion nodosum of the vagus nerve and a vagal paraganglion is seen higher up in or near the superior jugular ganglion.

Right: A different plane of section through the base of the skull shows paraganglia within the facial canal, middle ear over the promontory, and along the nerves of Arnold and Jacobson. The vagal paraganglia are in close association with the ganglion nodosum of the vagus nerve. (L&R: Fig. 17-1 from Fascicle 19, Third Series.)

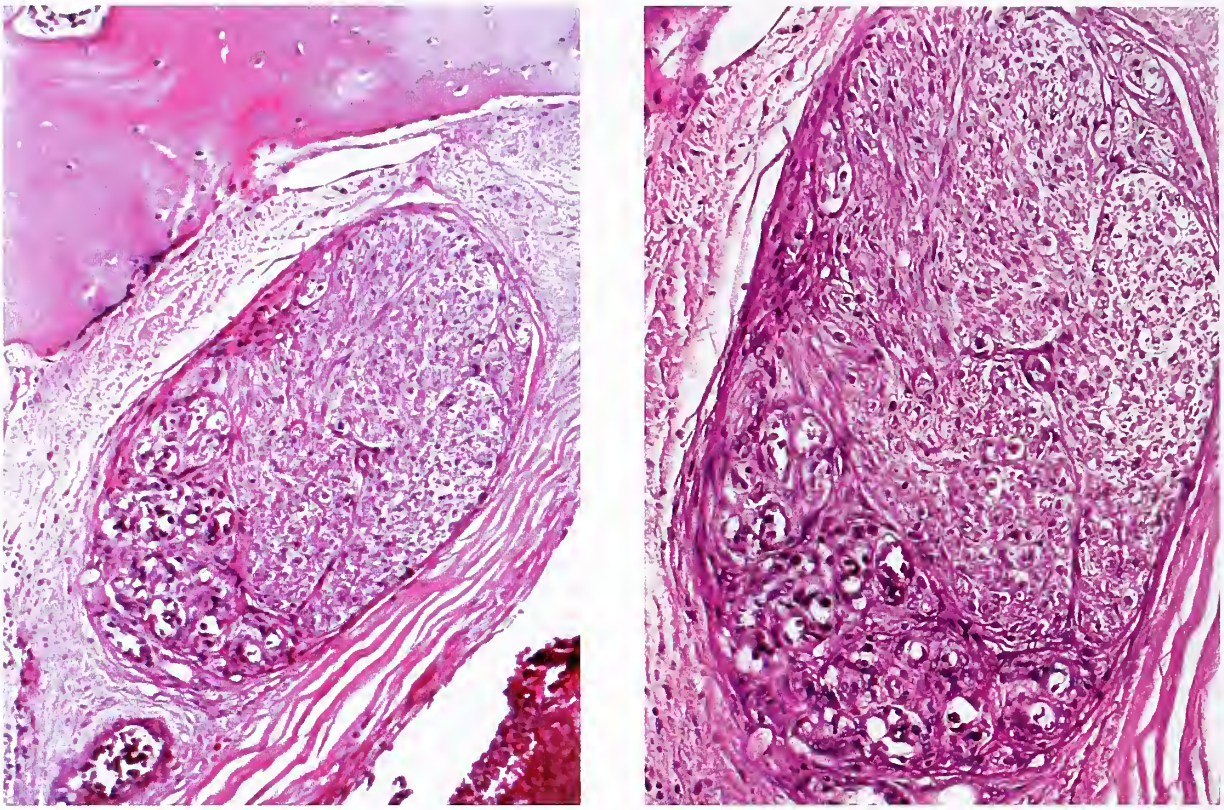

Figure 14-2

SMALL JUGULOTYMPANIC PARAGANGLION

Left: This small paraganglion is located in a paraneural space along the nerve of Jacobson. Note the dense bone of the skull base.

Right: The cytoarchitecture of this jugulotympanic paraganglion is identical to that of a portion of a carotid body lobule. The chief cells have eccentric, dark-staining nuclei. (Fig. 17-2 from Fascicle 19, Third Series.)

Arnold, and 25 percent were within mucosa of the cochlear promontory in association with the tympanic plexus of the nerve of Jacobson (fig. 14-1, right).

The microanatomy of jugulotympanic paraganglia is virtually identical to that of carotid body paraganglia except for smaller size and lack of multilobulation (fig. 14-2); most are ovoid or flattened and measure 0.5 mm or less in diameter (5). A chemoreceptor role has been postulated in response to changes in gas composition of the middle ear, but inconsistency of anatomic localization has cast some doubt on this proposal (8). The ultrastructural features of jugulotympanic paraganglia in the human fetus are essentially identical to those of carotid body paraganglia (9).

JUGULOTYMPANIC PARAGANGLIOMA

Jugular and tympanic paragangliomas arise from anatomically dispersed paraganglia near the base of the skull and middle ear. *Jugulotympanic paragangliomas* (JTPs) usually occur in adults in the 5th to 6th decade of life (10,11), but have been diagnosed even in early childhood (12). A distinct predilection for female patients has been reported: in one large series the female to male ratio was 6 to 1 (198 females, 33 males), with an average age of 55 years at diagnosis (11). At the Mayo Clinic, 55 patients (43 females, 12 males) were evaluated for a tympanic paraganglioma at an average age of 52 years (range, 22 to 81 years) (13). There is no apparent bias in laterality: JTPs have a roughly equal distribution on either side.

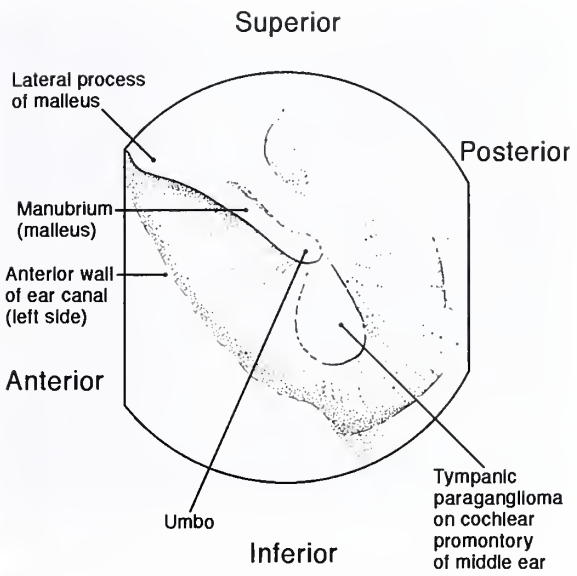

Figure 14-3

TYMPANIC PARAGANGLIOMA

Left: Jugulotympanic paraganglioma appears as a small, deeply congested lesion on the cochlear promontory of the middle ear. The tumor is apparent through the intact tympanic membrane.

Right: Schematic diagram of the anatomic relationship of the tympanic paraganglioma shown at left. (L&R: Fig. 17-3A,B from Fascicle 19, Third Series.)

Tympanic Paraganglioma

Tympanic paragangliomas (TPs) are usually located along the course of Jacobson's nerve in the middle ear cavity. They are often associated with tinnitus or aural pulsations, and may cause conduction type hearing loss due to involvement of the middle ear ossicles. Other manifestations include ear fullness or pain, otorrhea, vertigo/dizziness, and symptoms of chronic otitis media. Facial palsy has also been noted in a small number of patients. A TP can be quite small on the promontory of the middle ear (figs. 14-3, 14-4) or be large enough to fill the middle ear cavity, engulf the middle ear ossicles, bulge or protrude through the tympanic membrane, and present as an aural polyp in the external ear canal. Biopsy of such a lesion can result in brisk, copious bleeding. TP can also extend into the orifice of the eustachian tube or aditus ad antrum.

The lesion can be visualized using high resolution computerized tomography (CT) scans (fig. 14-5). Magnetic resonance imaging (MRI) also provides high resolution, but is less sensitive for identifying bone erosion or destruction. Direct visualization of the middle ear mass or bulging tympanic membrane typically shows a red, pink, or bluish lesion. Problems associated with hemorrhage are clearly conveyed in a report of surgery on a young girl with a JTP: "... the most vivid vascular experience we have ever encountered requiring 6 hours and 17 bottles of blood" (14).

Jugular Paraganglioma

Jugular paragangliomas (JPs) involve the lateral temporal bone at the base of the skull (fig. 14-6). They may grow within the petrous bone, sometimes extending intracranially (15) and simulating a cerebellopontine angle tumor or a mass in the middle cranial fossa. The tumor may have a dumbbell configuration, grow through the jugular foramen, and occasionally occlude the superior part of the internal jugular vein and bulb. The tumor may extend as a sausage-like projection into the lumen of the internal jugular vein (fig. 14-7), and present as a neck mass (16). Theoretical complications include contiguous extension into the right heart or fatal embolization at the time of surgery or even during the course of radiation treatment. In one

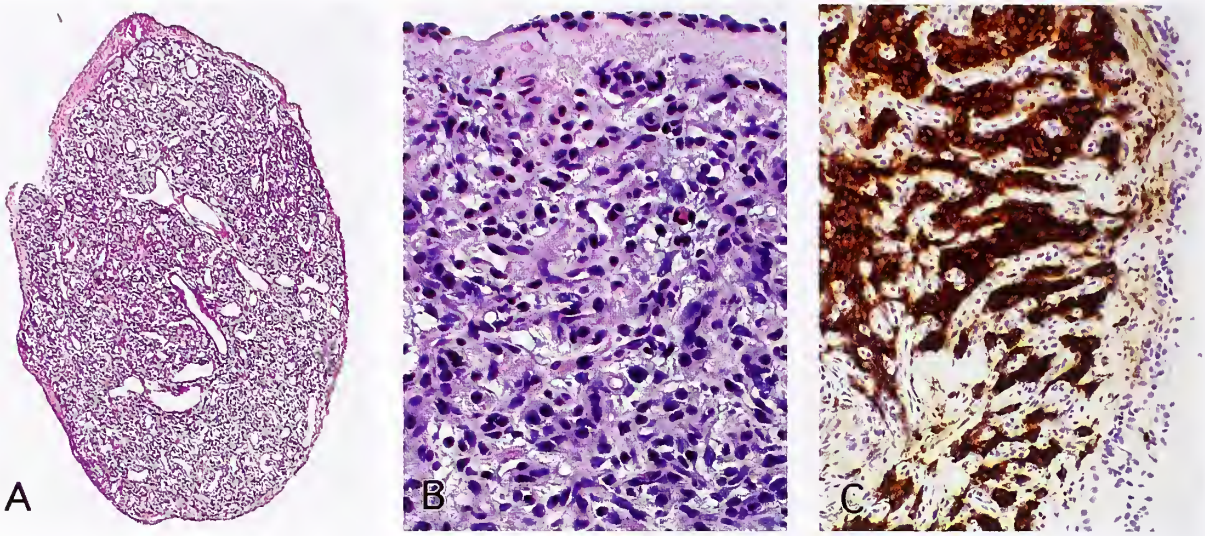

Figure 14-4

TYMPANIC PARAGANGLIOMA

A: Small tympanic paraganglioma was removed by transmeatal approach from the cochlear promontory of the middle ear. (Fig. 17-3C from Fascicle 19, Third Series.)

B: Tympanic paraganglioma in different case filled much of the middle ear and grows beneath attenuated middle ear mucosa. The tumor may be difficult to diagnose in biopsy material that is limited in amount or partially crushed.

C: Same case as B showing intense immunoreactivity of neoplastic chief cells for synaptophysin (avidin-biotin peroxidase method).

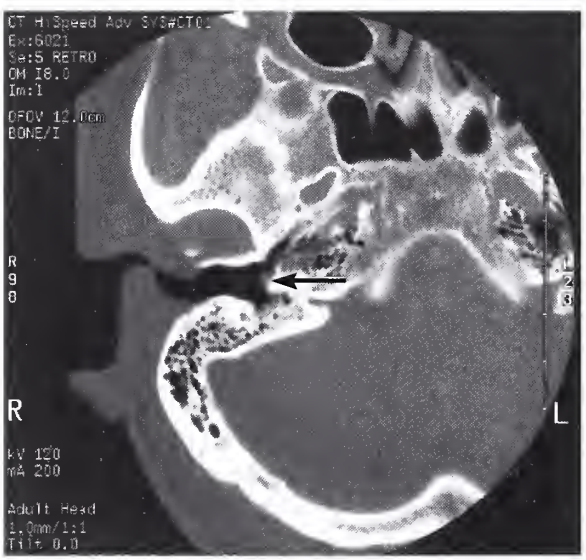

Figure 14-5

TYMPANIC PARAGANGLIOMA

Axial, or horizontal, plane of computerized tomography (CT) scan shows a small tympanic paraganglioma (arrow) on the promontory of the middle ear.

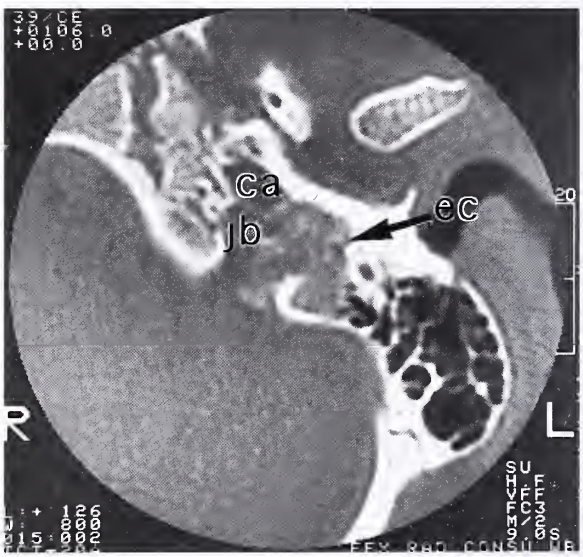

Figure 14-6

JUGULAR PARAGANGLIOMA

CT scan in horizontal (axial) plane shows a jugular paraganglioma (JP) (arrow) on the left side in a 15-year-old girl with a family history of head and neck paragangliomas. The patient also had an ipsilateral carotid body paraganglioma. Jugular bulb (jb), internal carotid artery (ca), and external ear canal (ec) are indicated. (Fig. 17-5 from Fascicle 19, Third Series.)

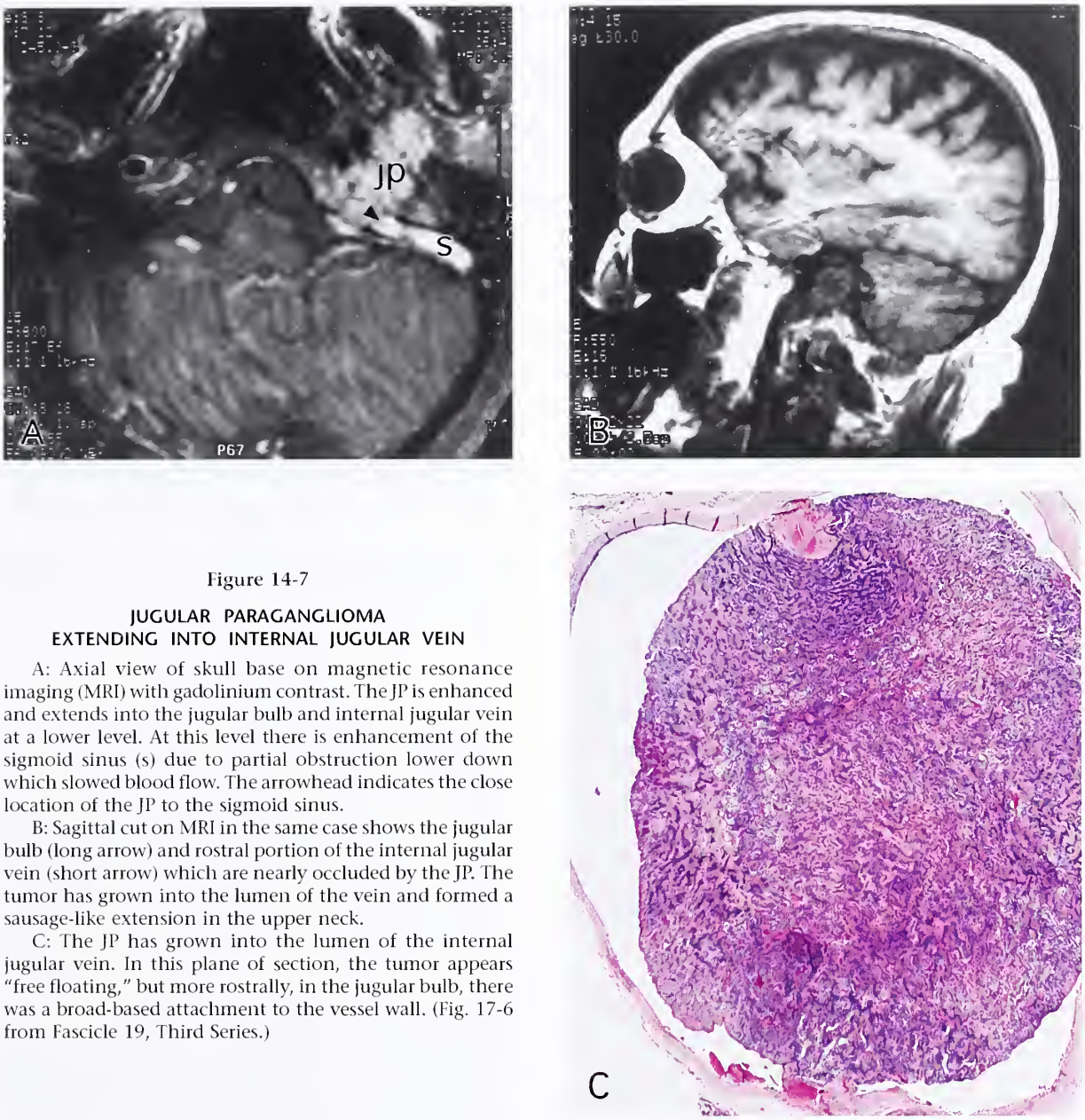

Figure 14-7

JUGULAR PARAGANGLIOMA EXTENDING INTO INTERNAL JUGULAR VEIN

A: Axial view of skull base on magnetic resonance imaging (MRI) with gadolinium contrast. The JP is enhanced and extends into the jugular bulb and internal jugular vein at a lower level. At this level there is enhancement of the sigmoid sinus (s) due to partial obstruction lower down which slowed blood flow. The arrowhead indicates the close location of the JP to the sigmoid sinus.

B: Sagittal cut on MRI in the same case shows the jugular bulb (long arrow) and rostral portion of the internal jugular vein (short arrow) which are nearly occluded by the JP. The tumor has grown into the lumen of the vein and formed a sausage-like extension in the upper neck.

C: The JP has grown into the lumen of the internal jugular vein. In this plane of section, the tumor appears "free floating," but more rostrally, in the jugular bulb, there was a broad-based attachment to the vessel wall. (Fig. 17-6 from Fascicle 19, Third Series.)

case, the tumor caused extensive bone destruction at the base of the skull, and extended in a continuous fashion into the internal jugular vein, superior vena cava, and on into the right atrium; the surgically resected tumor measured 15 cm in length and 3 cm in diameter when it was transected near the base of the skull (17). A retrograde venous jugulogram can document intravenous growth by the tumor (18). The jugular foramen syndrome may occur and result in paresis due to compression of the 9th to 12th cranial nerves in various combination.

Ragged erosion of the jugular fossa or foramen is important radiographic evidence of a JP (fig. 14-8), but erosion should not be confused with simple asymmetry in size and shape of the jugular foramen, which can occur under normal conditions (19,20). JPs can also erode the thin bony plate overlying the dome of the jugular fossa, and present as an aural or middle ear

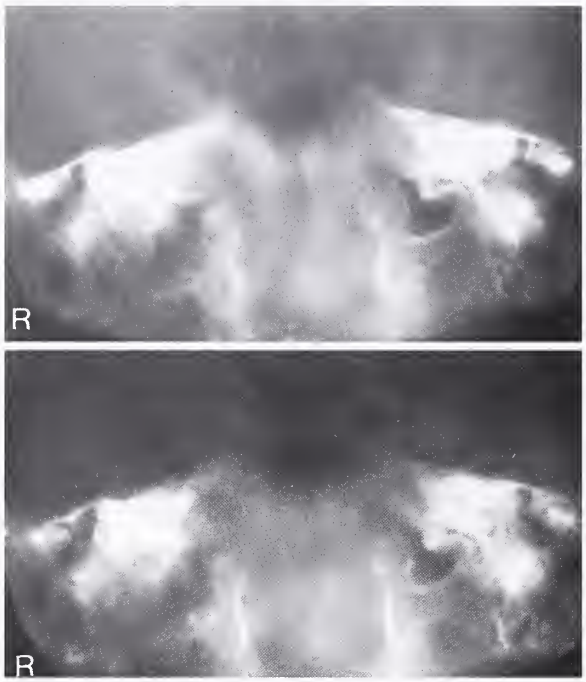

Figure 14-8

JUGULAR PARAGANGLIOMA

Tomogram of the base of the skull of a woman with a JP on the right side that irregularly eroded the jugular fossa or foramen. (Fig. 5 from Duncan AW, Lack EE, Deck MF. Radiological evaluation of paragangliomas of the head and neck region. Radiology 1979;132:99-105.)

polyp (fig. 14-9). The tumor has also been reported to cause parotid swelling, and mimic an acinic cell neoplasm on pathologic examination of the parotidectomy specimen (21). Upper cervical growth may cause medial deviation of nasopharyngeal soft tissue. Small biopsy specimens of JP may be misinterpreted as meningioma, and in one case the tumor radiographically simulated a meningioma, extending medially to the area of the foramen magnum with extensive calcification (22). Ossification of JP has also occurred (23).

Based upon extent and location of some paragangliomas of the skull base, it may not be possible to neatly designate the tumor as tympanic or jugular, hence, the composite designation jugulotympanic paraganglioma (JTP). Some vagal paragangliomas are difficult to distinguish from JTPs, because of the close spatial relationship of the ganglion nodosum and jugular foramen and the fact that vagal paraganglia sometimes occur rostral to this ganglion, or even within the jugular ganglion of the vagus nerve (24). Due to the complexities of these paragangliomas of the skull base, and some controversy regarding optimal treatment regimens, several clinical classification schemes have been proposed (13,25) in an attempt to promote consistency in communication, and permit a more standardized analysis of treatment results.

Hormonal Manifestations of JTPs

Rare examples of functionally active or catecholamine-producing paragangliomas of the skull base or infratemporal fossa have been reported (26,27), and wide fluctuations in systemic blood pressure during surgical removal of JTPs has prompted some observers to advise that "gentle handling" of all large glomus jugulare tumors is imperative (28). A case has also been reported with the carcinoid syndrome, but there was no biochemical documentation (29). Norepinephrine (30) and dopamine (31) have been detected in several JTPs.

Pathologic Findings of JTPs

Gross Findings. Surgically resected JTPs are often small or fragmentary. A TP that appears significant in size to the surgeon using an operating microscope during transmeatal resection may be small (see fig. 14-4), but can cause significant symptoms for the patient. Massive JTPs with petrosal extension and intracranial impingement causing fatal consequences are rare. Selective tumor embolization and radiation therapy may also limit the gross characterization of JTP. The rare JTP that extends intravenously may be more significant in terms of gross pathology.

Microscopic Findings. Microscopically, JTPs are similar to paragangliomas at other sites in the head and neck region, although sometimes there are features that allow prediction of anatomic location with relative assurance. Examples include the circumscribed small tumor removed from the cochlear promontory on transmeatal approach (see fig. 14-3), or a portion of attached tympanic membrane or middle ear mucosa. JTPs tend to be more vascular (32), and cell nests are less uniform and frequently smaller, with small chief cell nuclei compared with other paragangliomas (figs. 14-10, 14-11) (33). A remarkable feature of some JTPs (and

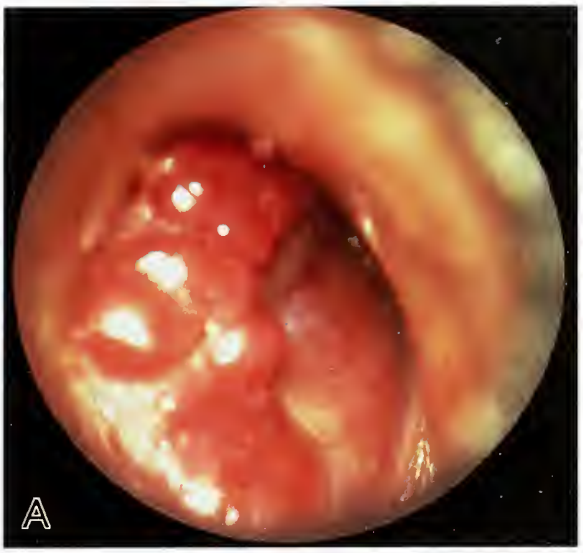

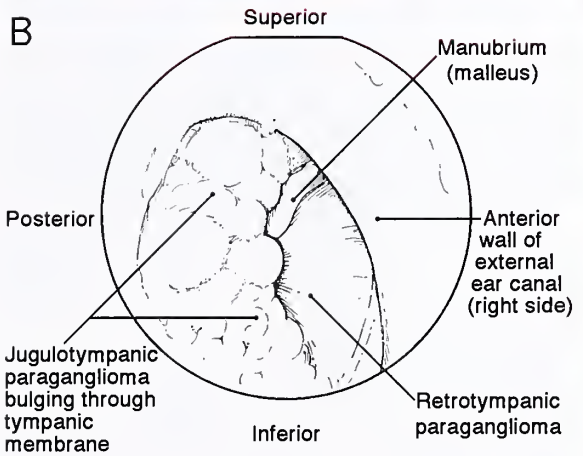

Figure 14-9

JUGULAR PARAGANGLIOMA

A: JP appears as a lobulated, deeply congested mass bulging out of the tympanic membrane. The tumor completely filled the middle ear cavity.

B: Diagram depicting the anatomic relationships of the tumor in A. There was also involvement of bone at the skull base.

C: The paraganglioma protrudes behind the tympanic membrane. There is a well-developed organoid arrangement of neoplastic chief cells. (A–C: Fig. 17-8 from Fascicle 19, Third Series.)

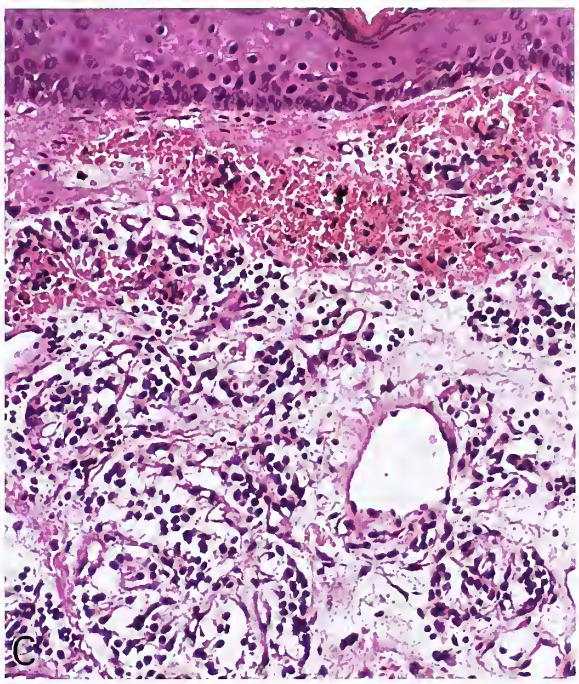

also some vagal paragangliomas) is the degree of sclerosis that is present (fig. 14-12) (34). In a review of a large number of head and neck paragangliomas, stromal sclerosis was most marked in JTPs and vagal paragangliomas (35). Due to their location at the skull base with access to bony recesses and foramina, JTPs can involve adjacent bone, causing pressure erosion and marked bony destruction (fig. 14-13) (34). Occasionally, JTPs show extensive calcification (36) or ossification (37). The rare small cell, almost neuroblastic component replete with a fibrillary matrix resembling neuropil (fig. 14-14) may represent a divergent path of differentiation, analogous to composite pheochromocytomas (see chapter 10).

Differential Diagnosis of JTPs

An important neoplasm to consider in the differential diagnosis is a middle ear adenoma or adenomatous neoplasm (38), an indolent tumor that arises in the middle ear and often causes conductive type hearing loss (fig. 14-15, left). These tumors may have a neuroendocrine component as shown by immunohistochemistry and electron microscopy and may be confused with paragangliomas. The adenoma/adenomatous neoplasm is usually associated with an intact tympanic membrane, and is composed of remarkably uniform cuboidal or cylindrical cells often in thin anastomosing cords or trabeculae (fig. 14-15, right). The neoplasm is usually

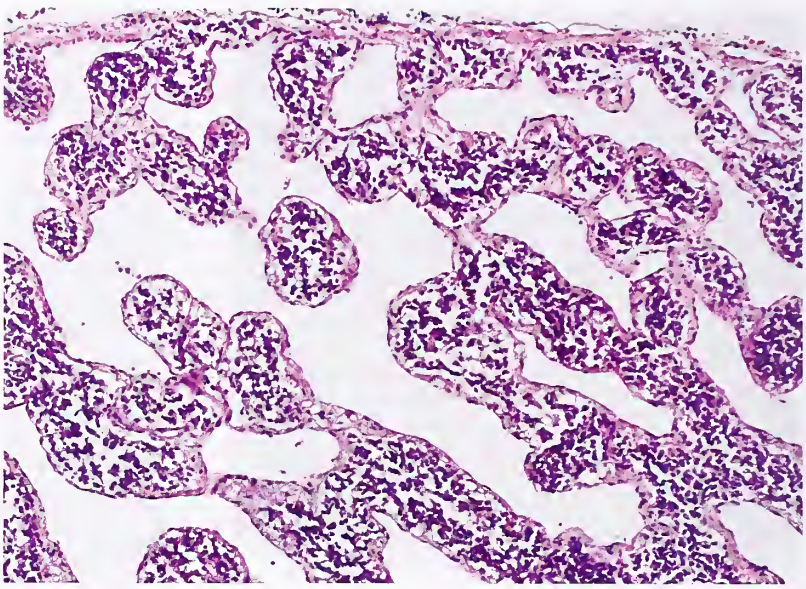

Figure 14-10

JUGULOTYMPANIC PARAGANGLIOMA

Anastomosing arcades of relatively small tumor cells were focally evident in this jugulotympanic paraganglioma (JTP). The vascular channels appear devoid of blood, an artifactual effect of mechanical manipulation of the tumor during surgery. (Fig. 17-9 from Fascicle 19, Third Series.)

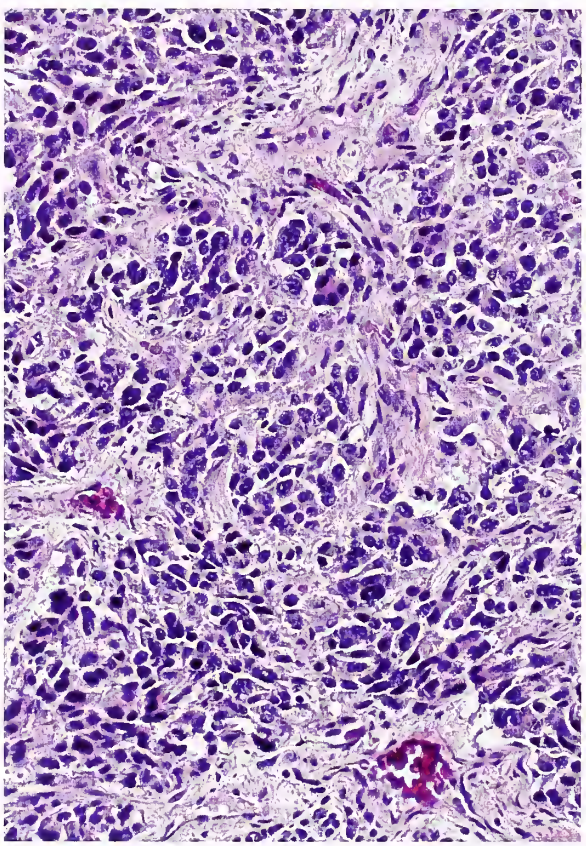

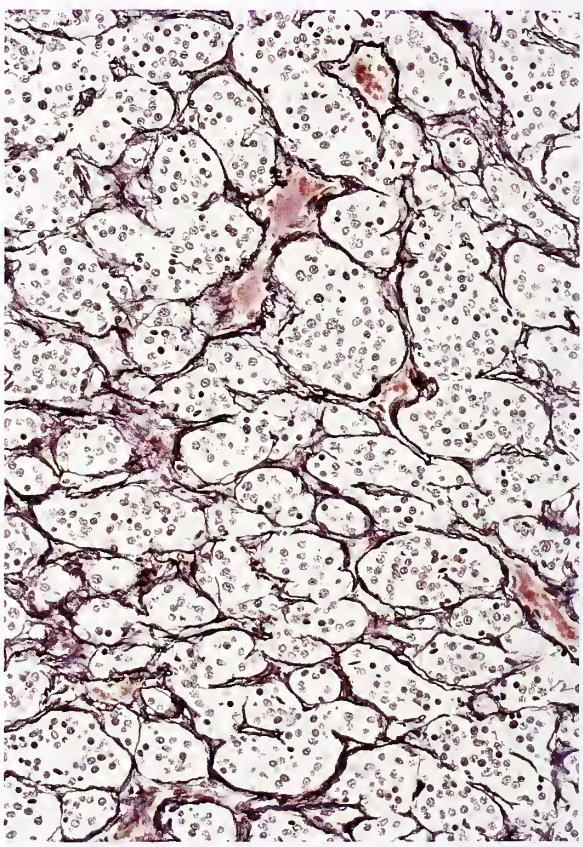

Figure 14-11

JUGULOTYMPANIC PARAGANGLIOMA

Left: Other areas of the tumor seen in figure 14-10 show a more organoid or nesting pattern with formation of small "zellballen." The tumor cells have relatively uniform hyperchromatic nuclei.

Right: Stain for reticulum greatly accentuates the small nests (or zellballen) of tumor cells.

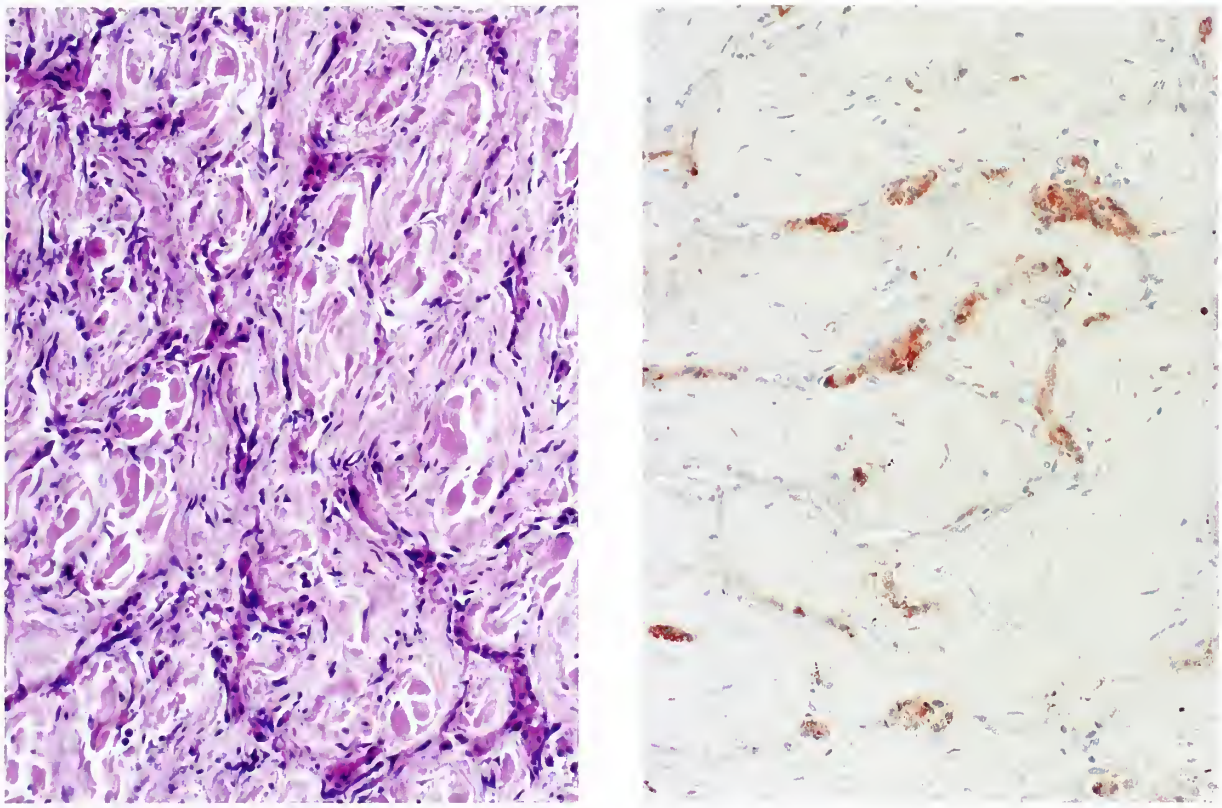

Figure 14-12

JUGULOTYMPANIC PARAGANGLIOMA

Left: There were areas of marked sclerosis within the tumor with significant architectural distortion.

Right: Immunoreactivity for chromogranin highlights the thin cords and strands of compressed tumor cells (streptavidin-alkaline phosphatase method). (Fig. 17-11 from Fascicle 19, Third Series.)

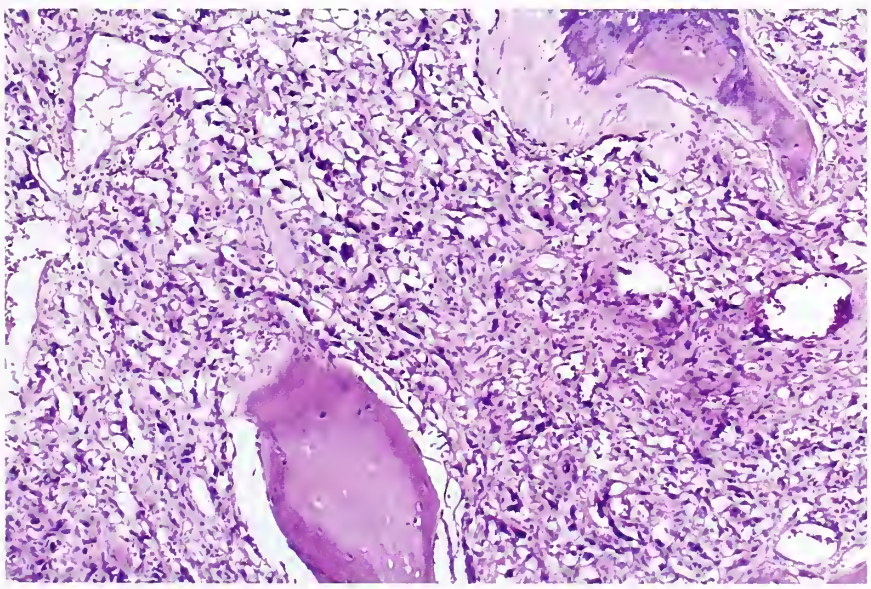

Figure 14-13

JUGULOTYMPANIC PARAGANGLIOMA

JTP invades bony structures at the base of the skull, with some evidence of bone remodeling. This represents local invasion, not metastasis.

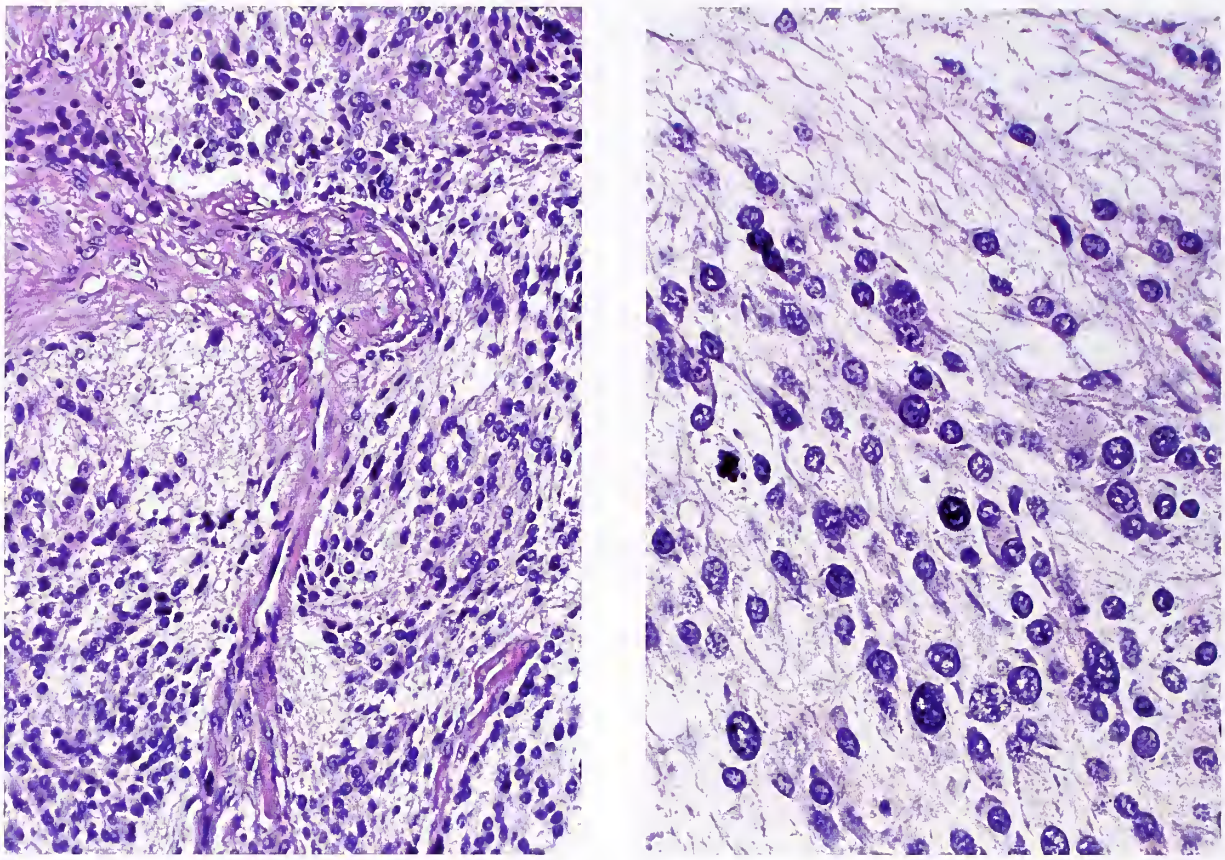

Figure 14-14

JUGULOTYMPANIC PARAGANGLIOMA

Left: A few areas of tumor are composed of small "neuroblast-like" cells associated with a distinct fibrillary matrix resembling neuropil.

Right: A different area in the same JTP shows small cells with neuronal features. The fibrillary background represents neuritic cell processes. Other areas had more typical histologic features of JTP. The morphologic features resemble those of composite pheochromocytoma (see chapter 10).

not as vascular as a paraganglioma. The histogenesis is apparently from the epithelium lining the middle ear (38).

Other tumors in the differential diagnosis are meningioma (or meningeal hemangiopericytoma) (fig. 14-16), metastatic renal cell carcinoma (39), and several non-neoplastic entities such as lateral aberrant internal carotid artery (or aneurysmal intrapetrosal internal carotid artery), which can present in the middle ear as a "blue" retrotympanic lesion (40), and aberrant jugular bulb due to anatomic extension into the middle ear (41,42). Meningiomas involving the jugular foramen can mimic the more common JP (43). Schwannoma can also involve the jugular foramen (44).

Treatment and Prognosis of JTPs

JTPs can be locally aggressive neoplasms that destroy bone and extend intracranially, and they may recur (or persist) locally. They extend in a centrifugal pattern following multiple pathways simultaneously, with growth along paths of least resistance as offered by bony fissures, air cells, vascular channels, and neural foramina (45). Regional and distant metastases are uncommon: in a literature review by Alford and Guilford (46), only 1.9 percent of tumors metastasized; others estimate 3 percent of tumors to be clinically malignant (47). The true incidence of malignancy, however, may be even lower since there is a greater tendency to report

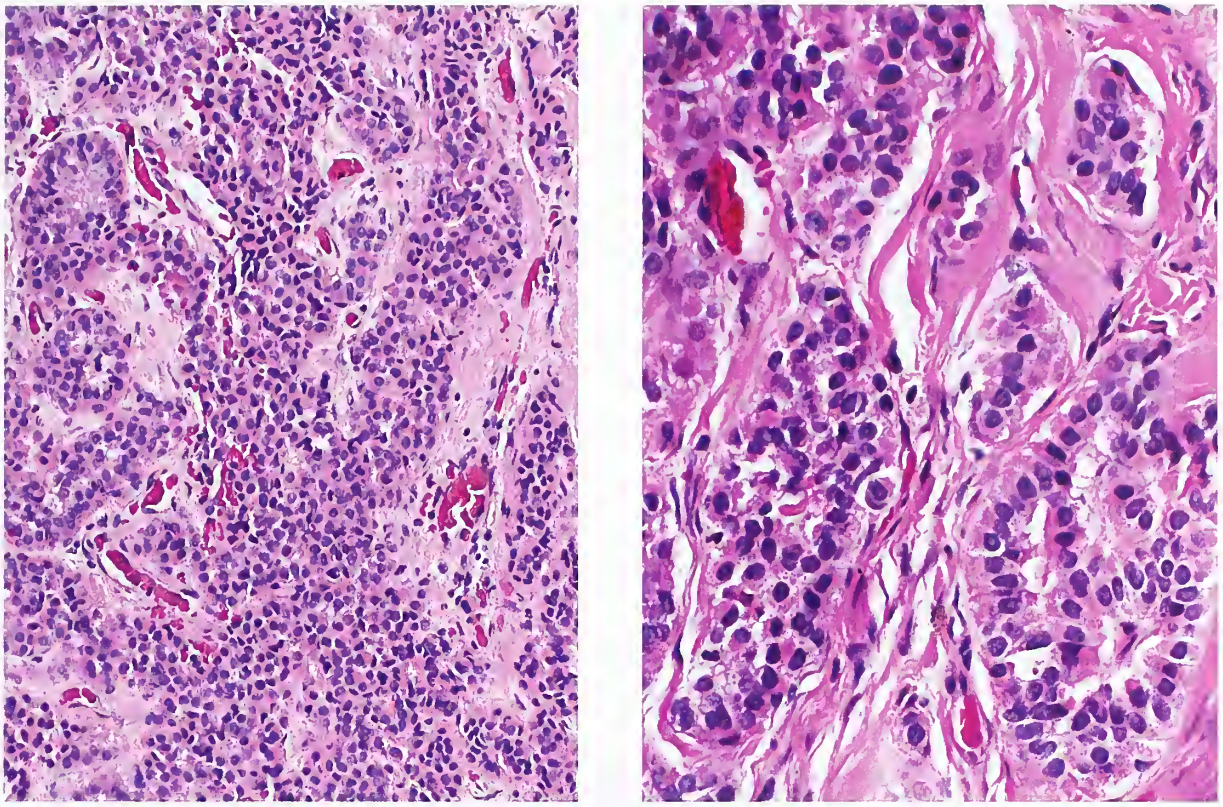

Figure 14-15

MIDDLE EAR ADENOMA

Left: An adenoma or adenomatous neoplasm of the middle ear from a woman with conductive type hearing loss. The tumor is composed of uniform cells arranged in anastomosing trabeculae. Mucicarminophilic material was present in gland-like spaces in some areas of the tumor. (Fig. 17-14 from Fascicle 19, Third Series.)

Right: The nuclei of the tumor cells are round to oval and relatively uniform. No mitotic figures were identified. (Fig. 17-15 from Fascicle 19, Third Series.)

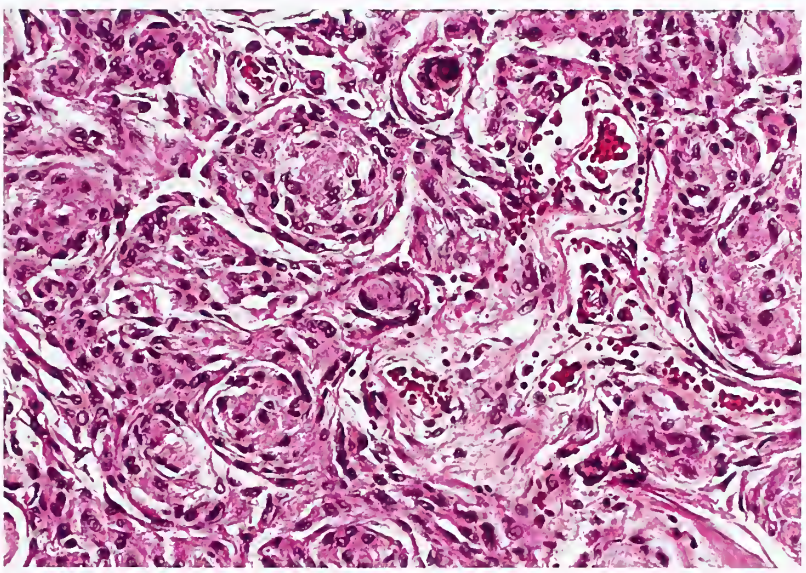

Figure 14-16

MENINGIOMA

Tight clusters of cells with areas having a whorl-like configuration in a meningioma. This tumor may occasionally enter into the differential diagnosis of a paraganglioma. (Fig. 17-16 from Fascicle 19, Third Series.)

clinically malignant tumors. None of the patients reported by Larson et al. (48) with TPs had a clinically malignant tumor with metastases. A most unusual mode of spread is extension through the dura with seeding and dissemination within the subarachnoid space via the cerebrospinal fluid (49).

Because of inherent problems in safe, complete resection of some JTPs, much has been written about the relative efficacy of radiation treatment, with or without surgery (50). In one literature review, local control rates were similar for surgery alone (86 percent), radiation before and after surgery (90 percent), and radiation alone (93 percent), but there was a higher incidence of treatment-related morbidity following surgical resection (51). Radiation in some studies may not entirely obliterate the tumor (52). The rationale for surgical management is provided in a recent review by Jackson (53). Stereotactic radiosurgery has also been successfully used in treating these tumors (54).

OTHER INTRACRANIAL PARAGANGLIOMAS

Rare *intrasellar* and *parasellar paragangliomas* have been reported (55). Rarely, the tumor is associated with increased catecholamine secretion (56). *Intracerebral paraganglioma* has been reported (57) and paraganglioma has also been reported in the region of the pineal gland (58), but the histopathology in the latter case was somewhat atypical. Expanding the concept of tumors of "glomic" tissue, Zak (59) referred to tumors arising from aberrant cranial "glomera" over the cerebral convexity, in the ventricular lumen, and in other locations, and questioned whether some meningiomas and hemangioblastomas were of glomic origin. This concept has never been accepted, since these tumors have specific histopathologic features distinct from those of paragangliomas.

REFERENCES

Paraganglia

1. Rosenwasser H. Carotid body tumor of the middle ear and mastoid. Arch Otolaryngol 1945;41: 64-67.
2. Rosenwasser H. Glomus jugulare tumors. II. Pathology. Arch Otolaryngol 1968;88:32-36.
3. Guild SR. A hitherto unrecognized structure, the glomus jugularis, in man. Anat Rec 1941;79:28.
4. Kipkie GF. Simultaneous chromaffin tumors of the carotid body and the glomus jugularis. Arch Path 1947;44:113-118.
5. Guild SR. The glomus jugulare, a nonchromaffin paraganglion in man. Ann Otol Rhinol Laryngol 1953;62:1045-1071.
6. Krause W. Die glandula tympanica des menschen. Centralbl f. d. Med Wissenschaften 1878;16:737-739.
7. Valentin G. Ueber eine gangliöse anschwellung in der Jacobsonschen anastomose des menschen. Arch f Anat Physiol u Wissensch Med 1840:287-290.
8. Rockley TJ, Hawke M. The glomus tympanicum: A middle ear chemoreceptor? J Otolaryngol 1989;18:370-373.
9. Kjaergaard J. Tympanojugular glomus. Anatomy of the carotid glomus-like bodies (nonchromaffin paraganglia): with electron microscopy and comparison of human foetal carotid, aorticopulmonary, subclavian, tympanojugular, and vagal glomera. Copenhagen: FADL's Forlag; 1973:76-92.

Jugulotympanic Paraganglioma

10. Alford BR, Guilford FR. A comprehensive study of tumors of the glomus jugulare. Laryngoscope 1962;72:765-787.
11. Brown JS. Glomus jugulare tumors revisited: a ten-year statistical follow-up of 231 cases. Laryngoscope 1985;95:284-288.
12. Choa DI, Colman BH. Paraganglioma of the temporal bone in infancy. A congenital lesion? Arch Otolaryngol Head Neck Surg 1987;113:421-424.
13. Larson TC 3rd, Reese DF, Baker HL Jr, McDonald TJ. Glomus tympanicum chemodectomas: radiographic and clinical characteristics. Radiology 1987;163:801-806.
14. Parkinson D. Intracranial pheochromocytomas (active glomus jugulare). Case report. J Neurosurg 1969;31:94-100.
15. Jackson CG, Kaylie DM, Coppit G, Gardner EK. Glomus jugulare tumors with intracranial extension. Neurosurg Focus 2004;17:E7.

16. Husband AD, Spedding A, Davis AE. Neck mass caused by an intraluminal jugular paraganglioma. J Laryngol Otol 2000;114:389-391.
17. Chretien PB, Engleman K, Hoye RC, Geelhoed GW. Surgical management of intravascular glomus jugulare tumor. Am J Surg 1971;122:740-743.
18. Gejrot T, Laurén T. Retrograde jugulariography in diagnosis of glomus tumours in the jugular region. Acta Otolaryngol 1964;58:191-207.
19. Lack EE. Pathology of adrenal and extra-adrenal paraganglia. In: Major problems in pathology, vol. 29. Philadelphia: WB Saunders; 1994.
20. Phelps PD, Stansbie JM. Glomus jugulare or tympanicum? The role of CT and MR imaging with gadolinium DTPA. J Laryngol Otol 1988; 102:766-776.
21. Brandrick JT, Das Gupta AR, Singh R. Jugulotympanic paraganglioma (glomus jugulare tumour) presenting as a parotid neoplasm (a case report and review of the literature). J Laryngol Otol 1988;102:741-744.
22. Moody DM, Ghatak NR, Kelly DL Jr. Extensive calcification in a tumor of the glomus jugulare. Neuroradiology 1976;12:131-135.
23. Goel A, Panchwagh J, Desai K. Ossified glomus jugulare tumour: Case report. Br J Neurosurg 1997;11:337-340.
24. Birrell JH. The jugular body and its tumour. Aust NZ J Surg 1955;24:195-206.
25. Jackson CG. Glomus tympanicum and glomus jugulare tumors. Otolaryngol Clin North Am 2001;34:941-970.

Hormonal Manifestations of JTPs

26. Cantrell RW, Kaplan MJ, Atuk NO, Winn HR, Jahrsdoerfer RA. Catecholamine-secreting infratemporal fossa paraganglioma. Ann Otol Rhinol Laryngol 1984;93:583-588.
27. Matishak, MZ, Symon, L, Cheeseman, A, Pamphlett, R. Catecholamine-secreting paragangliomas of the base of the skull. Report of two cases. J Neurosurg 1987;66:604-608.
28. Brown JS. Glomus jugulare tumors revisited: a ten-year statistical follow-up of 231 cases. Laryngoscope 1985;95:284-288.
29. Farrior JB 3rd, Hyams VJ, Benke RH, Farrior JB. Carcinoid apudoma arising in a glomus jugulare tumor: Review of endocrine activity in glomus jugulare tumors. Laryngoscope 1980;90:110-119.
30. DeLellis RA, Roth JA. Norepinephrine in a glomus jugulare tumor. Histochemical demonstration. Arch Path 1971;92:73-75.
31. Azzarelli B, Felten S, Muller J, Miyamoto R, Purvin V. Dopamine in paragangliomas of the glomus jugulare. Laryngoscope 1988;98:573-578.

Pathologic Findings of JTPs

32. Glenner GG, Grimley PM. Tumors of the extra-adrenal paraganglion system (including chemoreceptors). Atlas of Tumor Pathology, 2nd Series, Fascicle 9. Washington DC: Armed Forces Institute of Pathology; 1974.
33. Oberman HA, Holtz F, Sheffer LA, Magielski JE. Chemodectomas (nonchromaffin paragangliomas) of the head and neck. A clinicopathologic study. Cancer 1968;21:838-851.
34. Lack EE. Pathology of adrenal and extra-adrenal paraganglia. In: Major problems in pathology, vol. 29. Philadelphia: WB Saunders; 1994.
35. Bitterman P, Sherman M, Lack EE. Paragangliomas of the head and neck region. Clinicopathologic and immunohistochemical evaluation of 88 cases. International Congress of IAP, Madrid, Spain, October, 1992.
36. Moody DM, Ghatak NR, Kelly DL Jr. Extensive calcification in a tumor of the glomus jugulare. Neuroradiology 1976;12:131-135.
37. Goel A, Panchwagh J, Desai K. Ossified glomus jugulare tumour: Case report. Br J Neurosurg 1997;11:337-340.

Differential Diagnosis of JTPs

38. Wenig BM. The ear. In: Mills SE, Carter D, Greenson JK, Oberman HA, Reuter VE, Stoler MH, eds. Sternberg's diagnostic surgical pathology, vol 4, 4th ed. Philadephia: Lippincott Williams & Wilkins; 2004:1033-1072.
39. Boileau MA, Grotta JC, Borit A, et al. Metastatic renal cell carcinoma simulating glomus jugulare tumor. J Surg Oncol 1987;35:201-203.
40. Goldman NC, Singleton GT, Holly EA. Aberrant internal carotid artery presenting as a mass in the middle ear. Arch Otolaryngol 1971;94:269-273.
41. West JM, Bandy BC, Jafek BW. Aberrant jugular bulb in the middle ear cavity. Arch Otolaryngol 1974;100:370-372.
42. Rauch SD, Xu WZ, Nadol JB Jr. High jugular bulb: implications for posterior fossa neurotologic and cranial base surgery. Ann Otol Rhinol Laryngol 1993;102:100-107.
43. Gilbert ME, Shelton C, McDonald A, et al. Meningioma of the jugular foramen: glomus jugulare mimic and surgical challenge. Laryngoscope 2004;114:25-32.
44. Ramina R, Maniglia JJ, Fernandes YB, et al. Jugular foramen tumors: diagnosis and treatment. Neurosurg Focus 2004;17:E5.

Treatment and Prognosis of JTPs

45. Spector GJ, Sobol S, Thawley SE, Maisel RH, Ogura JH. Panal discussion: glomus jugulare tumors of the temporal bone: patterns of invasion in the temporal bone. Laryngoscope 1979;89: 1628-1639.
46. Alford BR, Guilford FR. A comprehensive study of tumors of the glomus jugulare. Laryngoscope 1962;72:765-787.
47. Zak FG, Lawson W. The paraganglionic chemoreceptor system: physiology, pathology, and clinical medicine. New York: Springer-Verlag; 1982: 372-375.
48. Larson TC 3rd, Reese DF, Baker HL Jr, McDonald TJ. Glomus tympanicum chemodectomas: radiographic and clinical characteristics. Radiology 1987;163:801-806.
49. Welsh LW, Welsh JJ, Huck GF Jr. Glomus jugulare tumor. Disseminated form in the central nervous system. Arch Otolaryngol 1976;102:507-510.
50. Michael LM 2nd, Robertson JH. Glomus jugulare tumors: historical overview of the management of this disease. Neurosurg Focus 2004;17:E1.
51. Springate SC, Haraf D, Weichselbaum RR. Temporal bone chemodectomas—comparing surgery and radiation therapy. Oncology (Williston Park) 1991;5:131-137.
52. Spector GJ, Compagno J, Perez CA, Maisel RH, Ogura JH. Glomus jugulare tumors: effects of radiotherapy. Cancer 1975;35:1316-1321.
53. Jackson CG. Glomus tympanicum and glomus jugulare tumors. Otolaryngol Clin North Am 2001;34:941-970.
54. Sheehan J, Kondziolka D, Flickinger J, Lunsford LD. Gamma knife surgery for glomus jugulare tumors: an intermediate report on efficacy and safety. J Neurosurg 2005;102(Suppl):241-246.

Other Intracranial Paragangliomas

55. Salame K, Ouaknine GE, Yossipov J, Rochkind S. Paraganglioma of the pituitary fossa: diagnosis and management. J Neurooncol 2001;54:49-52.
56. Nelson MD, Kendall BE. Intracranial catecholamine-secreting paragangliomas. Neuroradiology 1987;29:277-282.
57. Reithmeier T, Gumprecht H, Stölzle A, Lumenta CB. Intracerebral paraganglioma. Acta Neurochir (Wien). 2000;142:1063-1066.
58. Smith WT, Hughes B, Ermocilla R. Chemodectoma of the pineal region, with observations on the pineal body and chemoreceptor tissue. J Pathol Bacteriol 1966;92:69-72.
59. Zak FG. An expanded concept of tumors of glomic tissue. N Y State J Med 1954;54:1153-1165.

15 VAGAL PARAGANGLIOMA

VAGAL PARAGANGLIA

Anatomy of the Rostral Vagus Nerve

The vagus nerve is a mixed sensory and motor nerve which exits the medulla as fila radicularia. It consists of 10 to 18 small nerve bundles which converge to form the larger vagal trunk (fig. 15-1). The ganglion nodosum is a fusiform expansion of the nerve, measuring about 1.5 cm in length in adults; it contains cell bodies of visceral afferent fibers from pharynx, larynx, and trachea as well as intrathoracic and intraabdominal viscera (1). The superior or jugular ganglion of the vagus nerve contains cell bodies of somatic efferent nerve fibers. The vagus nerve also has special visceral efferent fibers to the voluntary musculature of the upper aerodigestive tract, and has an important role in the regulation and control of respiratory, cardiovascular, and gastrointestinal function. Among sensory ganglia, those of the vagus nerve are seemingly unique in containing paraganglionic tissue (1).

Distribution and Normal Microanatomy of Vagal Paraganglia

The terms *vagal body* and *vagal body paraganglia* collectively refer to the multiple, spatially dispersed paraganglia usually found at or just below the lower border of the ganglion nodosum (fig. 15-2). Muratori (2) described vagal paraganglia in birds in 1932, and White (3) identified them in humans in 1935 within the rostral vagus nerve in juxtaposition to ganglion cells (3). Because these paraganglia do not form a single compact structure, the term vagal body is technically a misnomer. These paraganglia are microscopic structures that have virtually the same microanatomy as subunits of the carotid body (fig. 15-3). The varied anatomic locations of paraganglia adjacent to or within the substance of nerve bundles of the vagus nerve may help to explain some of the characteristic clinicopathologic features of vagal paragangliomas and the problems inherent in complete surgical resection.

Paraganglia have also been identified higher in the vagus nerve, in or near the jugular ganglion (4), and vagal paragangliomas arising in this more rostral location may have radiographic and clinical features suggesting a jugular paraganglioma (1). Paraganglia have also been identified well below the inferior pole of the nodose ganglion (5,6), even in laryngeal nerves (6,7).

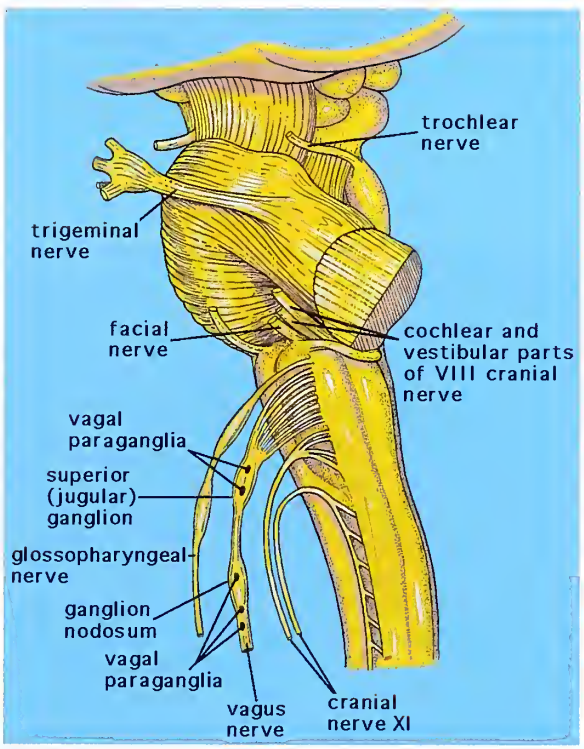

Figure 15-1

BRAIN STEM AND VAGUS NERVE

Lateral view of brain stem and upper cervical spinal cord. The trunk of the vagus nerve is formed after the confluence of the fila radicularia. The position of the superior (jugular) ganglion and ganglion nodosum (inferior ganglion) are indicated. Vagal paraganglia are usually found at or near the lower border of the ganglion nodosum. (Fig. 18-1 from Fascicle 19, Third Series.)

Figure 15-2

VAGUS NERVE

Rostral portion of the vagus nerve from an infant. The ganglion nodosum is seen as a fusiform expansion of nerve between the arrows. Vagal paraganglia are usually located near the lower border of the ganglion.

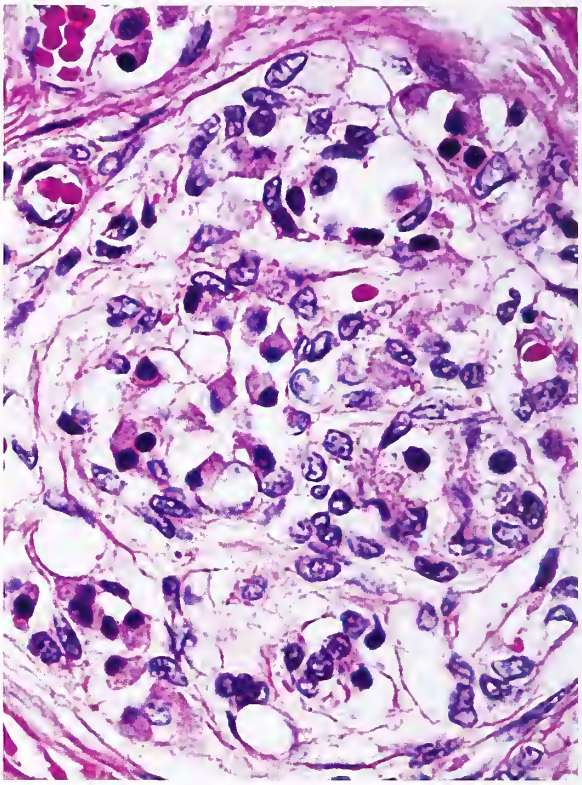

Figure 15-3

VAGAL PARAGANGLION

A vagal paraganglion is present within the interstitium of the vagus nerve; small bundles of myelinated nerve are adjacent to it. The paraganglion is identical to the lobular subunit of the carotid body. Clusters of chief cells are seen along with a few sustentacular cells. (Fig. 18-3 from Fascicle 19, Third Series.)

In the experimental animal paraganglia are associated with the abdominal portion of the vagus nerve and even the hilum of the liver (8).

In a study in humans using a step sectioning technique (9), an average of seven separate paraganglia were found on the left side of the vagus nerve and six on the right. They are usually ovoid structures with average dimensions in adults of about 160 x 350 µm, but tend to be smaller in young children (10). Vagal paraganglia are located within the interstitial connective tissue of the nerve (fig. 15-3), within large nerve trunks just beneath the perineurium, partially surrounding small nerve bundles within the vagus nerve (fig. 15-4A), or occasionally, immediately adjacent to ganglion cells of the ganglion nodosum (fig. 15-4B).

Chief cells in normal vagal paraganglia show distinct cytoplasmic argyrophilia (fig. 15-4C) identical to carotid body chief cells. Rarely, an intravascular protrusion of a vagal paraganglion is covered by an intact continuous layer of endothelial cells (fig. 15-5). An ultrastructural study of vagal paraganglia in the human fetus showed morphologic features indistinguishable from those of the carotid body (11).

Hyperplasia of Vagal Paraganglia

Hyperplasia of vagal paraganglia has been reported in some patients with chronic hypoxemia due to chronic obstructive pulmonary disease (9), and has been observed in some patients with cystic fibrosis (fig. 15-6) and cyanotic heart disease (fig. 15-7). The hyperplasia tends to parallel similar changes in carotid body paraganglia, but the findings are not always concordant (1). Hyperplasia provides additional support for

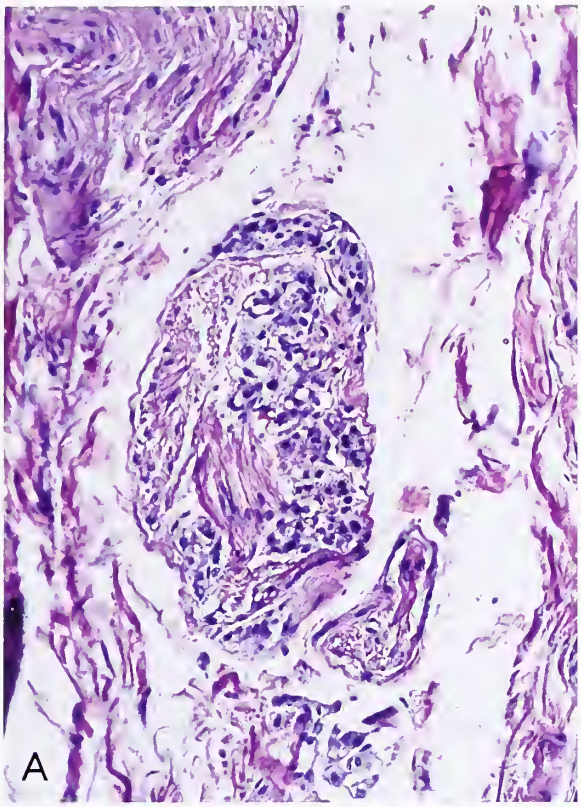

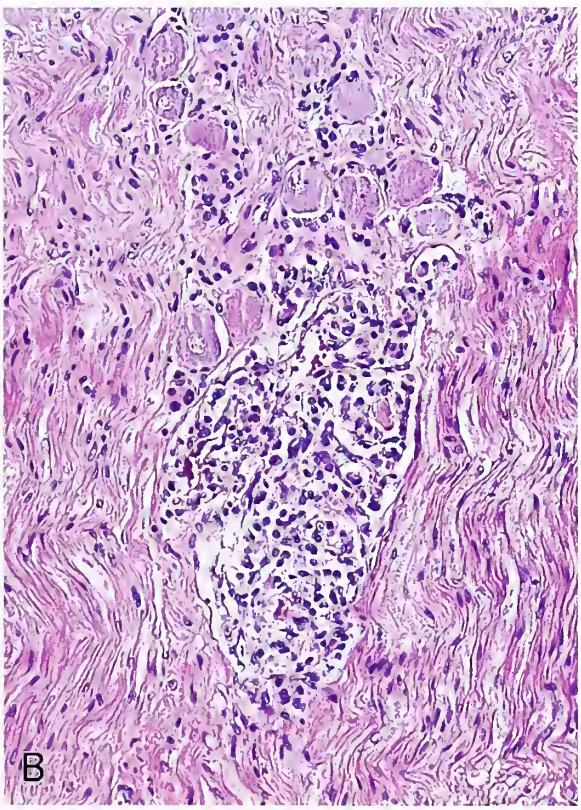

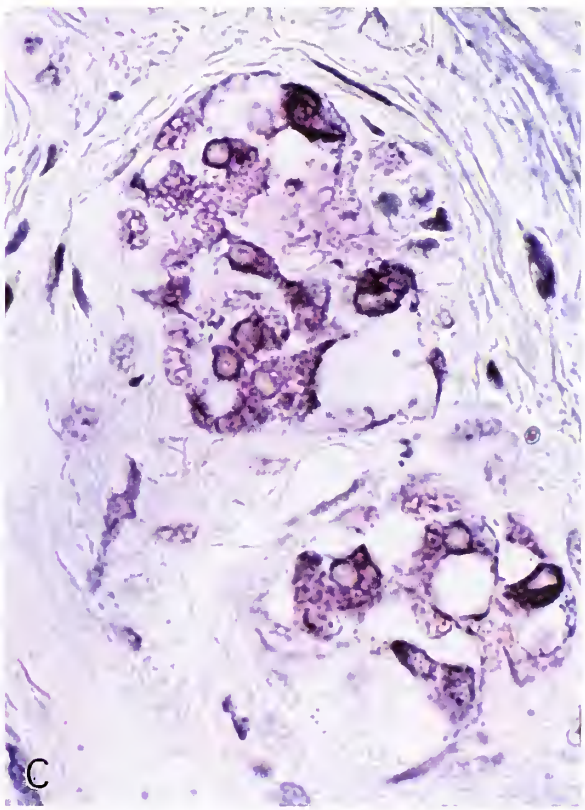

Figure 15-4

VAGAL PARAGANGLIA

A: A small vagal paraganglion partially surrounds a myelinated nerve bundle.

B: This vagal paraganglion is located at the lower border of the ganglion nodosum immediately adjacent to ganglion cells. (A,B: Fig. 18-4B,C from Fascicle 19, Third Series.)

C: Chief cells of a vagal paraganglion show finely granular cytoplasmic argyrophilia (Bodian axon stain).

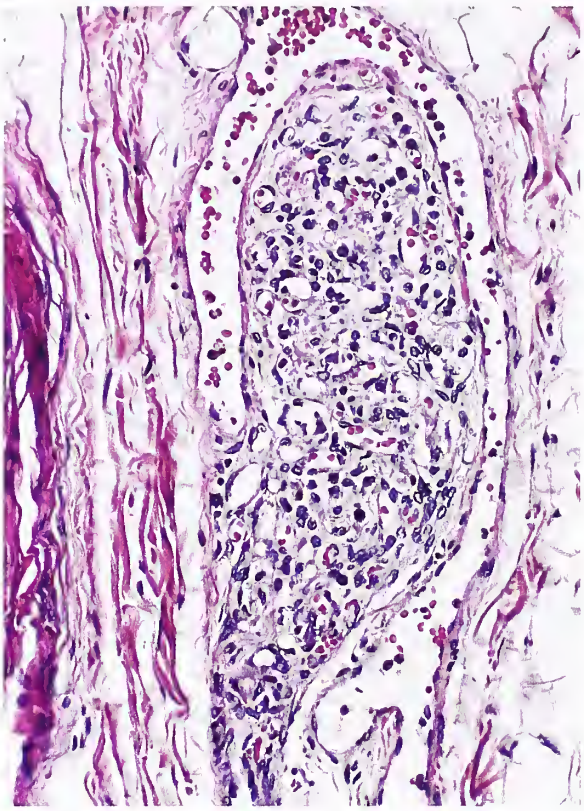

Figure 15-5

INTRAVASCULAR POLYPOID PROTRUSION BY NORMAL VAGAL PARAGANGLION

The intraluminal surface is covered by a continuous layer of endothelial cells. (Fig. 18-5 from Fascicle 19, Third Series.)

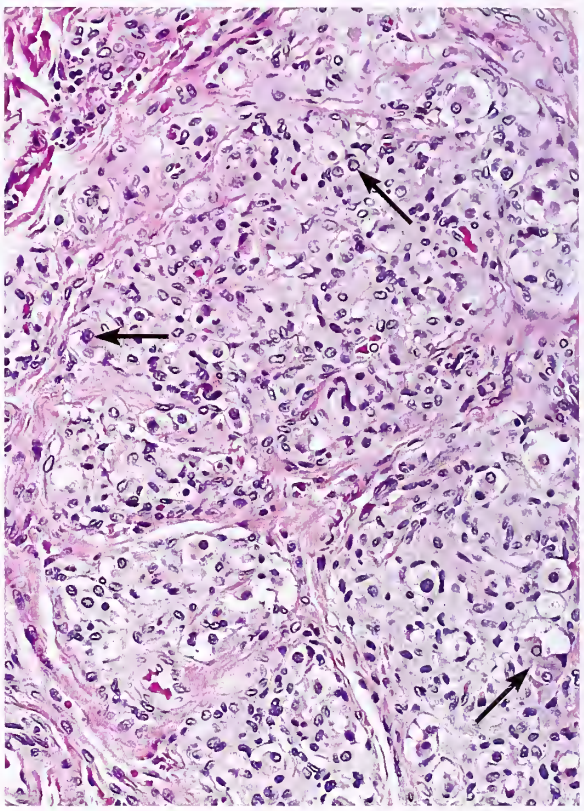

Figure 15-6

ENLARGED HYPERPLASTIC VAGAL PARAGANGLION

Enlarged hyperplastic vagal paraganglion in a young adult with cystic fibrosis. Chief cells are indicated by arrows. (Fig. 18-6 from Fascicle 19, Third Series.)

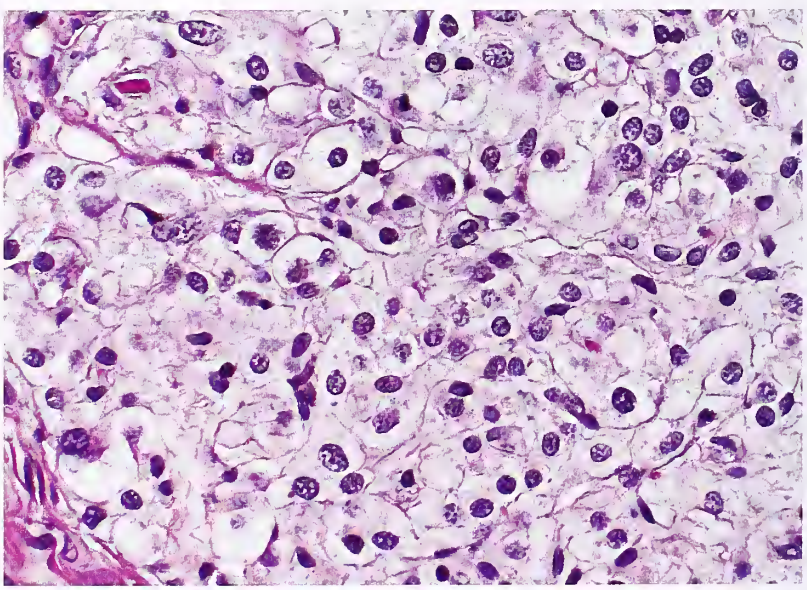

Figure 15-7

HYPERPLASIA OF VAGAL PARAGANGLION

Hyperplasia of vagal paraganglion in a young patient who had digital clubbing and cyanosis due to congenital heart disease. The patient had a simple left ventricle with transposition of the great vessels. The paraganglion shown was enlarged, cellular, and measured 320 x 1,100 µm. Enlarged hyperplastic chief cells predominate throughout the field. (Fig. 18-7 from Fascicle 19, Third Series.)

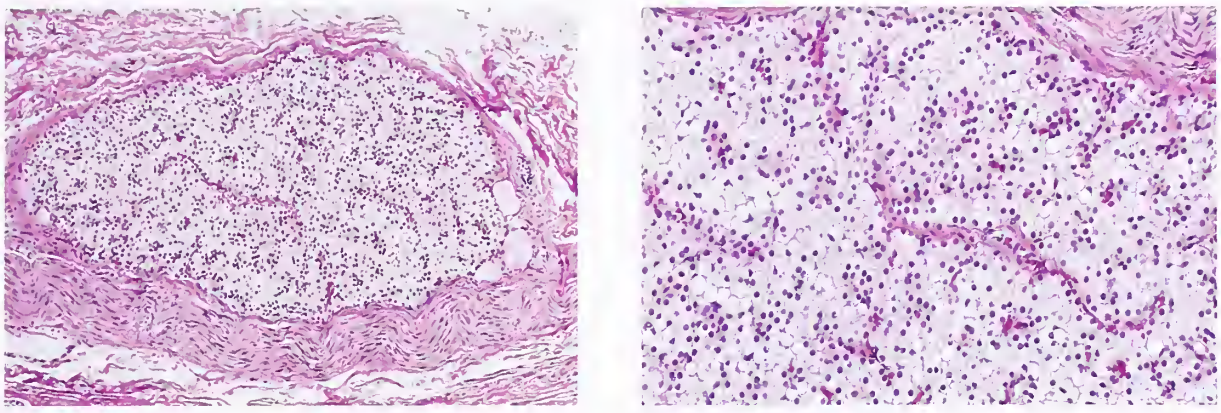

Figure 15-8

ECTOPIC PARATHYROID TISSUE WITHIN THE VAGUS NERVE

Left: The ectopic parathyroid tissue is located beneath the perineurium of the rostral portion of the vagus nerve. The tissue is subdivided by small, branching vascular channels.

Right: Higher magnification shows uniform round nuclei and distinct cell borders. Small cytoplasmic vacuoles are present, probably due to lipid accumulation. (L&R: Fig. 18-8 from Fascicle 19, Third Series.)

a chemoreceptor role for vagal paraganglia, but there are essentially no data available to indicate a relationship between hyperplasia and the development of a paraganglioma, even at high altitude (1). A brief discussion of possible physiologic functions of vagal paraganglia is provided elsewhere (1).

PARATHYROID TISSUE WITHIN THE VAGUS NERVE

A small collection of uniform parathyroid chief cells is sometimes seen in sections of the rostral vagus nerve (fig. 15-8) (9,12,13). Parathyroid ectopic tissue has been reported in the cervical vagus nerve in 4 percent of adults (9) and 6 percent of children in the first year of life (13). These collections of cells vary in size (fig. 15-9A); some are small enough to evade detection on casual inspection (fig. 15-9B). They may simulate a vagal paraganglion, but their cytologic uniformity, distinct cell borders, and pale-staining or clear cytoplasm should permit distinction. The cells lack the distinct cytoplasmic argyrophilia of chief cells (fig. 15-9C) and contain abundant intracytoplasmic glycogen (fig. 15-9D,E). There is positive staining for chromogranin and parathormone (fig. 15-10) (13). Rare examples of aberrant parathyroid adenoma with primary hyperparathyroidism have been reported within the cervical vagus nerve (14–16). Intravagal supernumerary parathyroid hyperplasia has also been reported (17). Ectopic parathyroid tissue has also been noted within a cervical ganglion (probably related to the vagus nerve) in a patient undergoing surgery for papillary thyroid carcinoma (18).

VAGAL PARAGANGLIOMA

Definition. *Vagal paraganglioma* (VP) arises from dispersed paraganglia located within or immediately adjacent to the vagus nerve, especially the most rostral portion of the nerve in relation to the ganglion nodosum. The tumor is also referred to as *vagal body paraganglioma.*

Clinical Features. VP is the third most frequent paraganglioma of the head and neck region. There is a distinct predilection for female patients, usually in the 4th and 5th decades of life (19–24). The patient may present with a painless, slowly growing neck mass, and there may be medial deviation of tonsillar or oropharyngeal tissue. In a recent case, a VP mimicked a peritonsillar abscess and following incision there was intractable hemorrhage (25). There may be a variety of cranial nerve palsies, mostly involving the vagus nerve, with ipsilateral vocal cord dysfunction, hoarseness, or dysphagia (1); local expansion by a VP can compress other nerves in the jugular foramen with paresis of the 9th, 11th, and 12th cranial nerves in various combination (26). An occasional patient may have ipsilateral Horner's syndrome. A rare VP may have a dumbbell configuration and

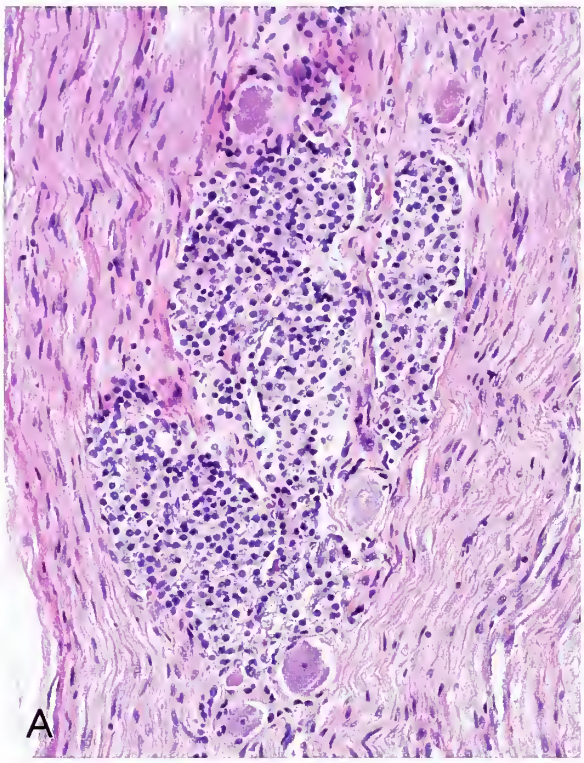

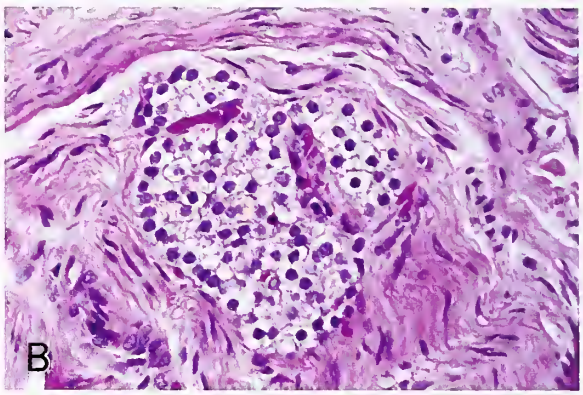

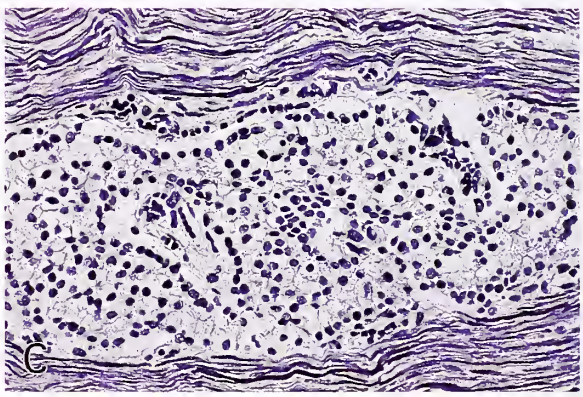

Figure 15-9

ECTOPIC PARATHYROID TISSUE WITHIN THE VAGUS NERVE

A,B: Small collections of parathyroid chief cells are present within a myelinated nerve bundle of the vagus nerve. The cells have relatively clear cytoplasm with distinct cell borders and small uniform nuclei. Ganglion cells are present in A.

C: Ectopic parathyroid tissue within the vagus nerve has no cytoplasmic argyrophilia (compare with figure 15-4C). Nerve bundles on either side of the parathyroid tissue are richly stained for axons (Bodian axon stain).

D: Ectopic parathyroid tissue contains abundant glycogen (periodic acid–Schiff [PAS] stain).

E: The glycogen is completely abolished by pretreatment of the section with diastase (PAS following diastase predigestion).

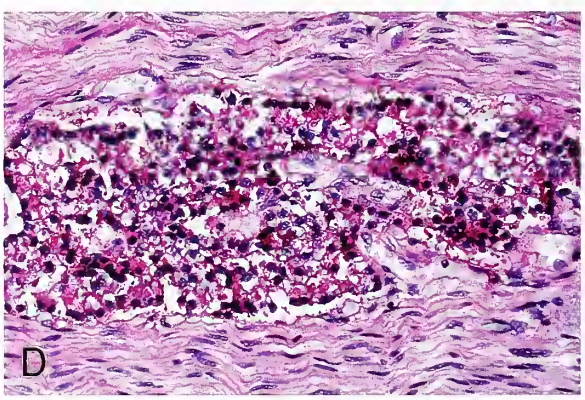

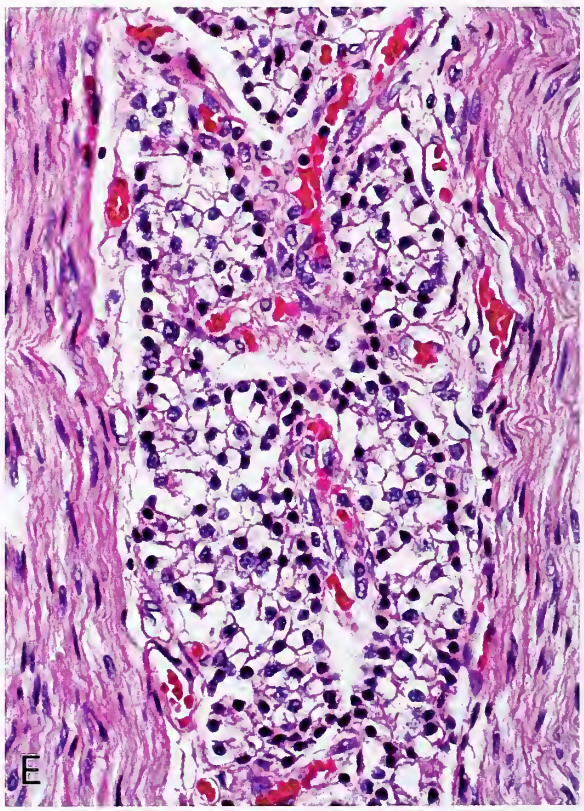

extend into the jugular foramen (27), or arise above the level of the ganglion nodosum (28). Functionally active VPs are occasionally reported, causing signs and symptoms of excess catecholamine secretion (22,29–32). Intraoperative traction on the vagus nerve can be complicated by cardiac arrest, probably related to bradycardia (33). A rare clinical presentation is cardiovascular syncope (34).

On selective arteriography, VPs typically cause anterior displacement of the carotid vessels without direct involvement of the bifurcation (figs. 15-11, 15-12) (35); in lateral views, therefore, there is no "lyre-like" widening of the common carotid artery bifurcation as expected with a carotid body paraganglioma. Other effective means of tumor localization are computerized tomography (CT) (fig. 15-13) and magnetic resonance imaging (MRI).

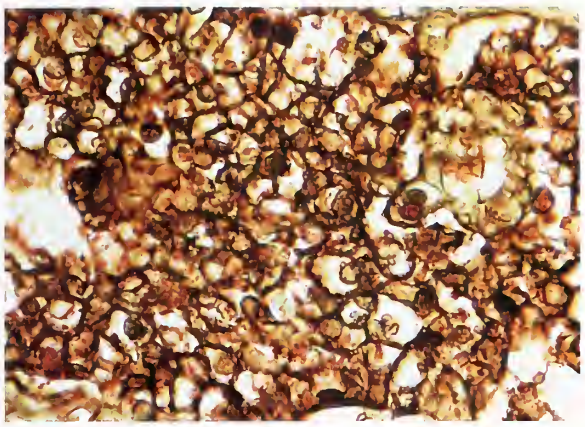

Figure 15-10

INTRAVAGAL PARATHYROID CHIEF CELLS

The intravagal parathyroid chief cells immunostain strongly for parathormone (avidin-biotin peroxidase method). (Fig. 18-10, right from Fascicle 19, Third Series.)

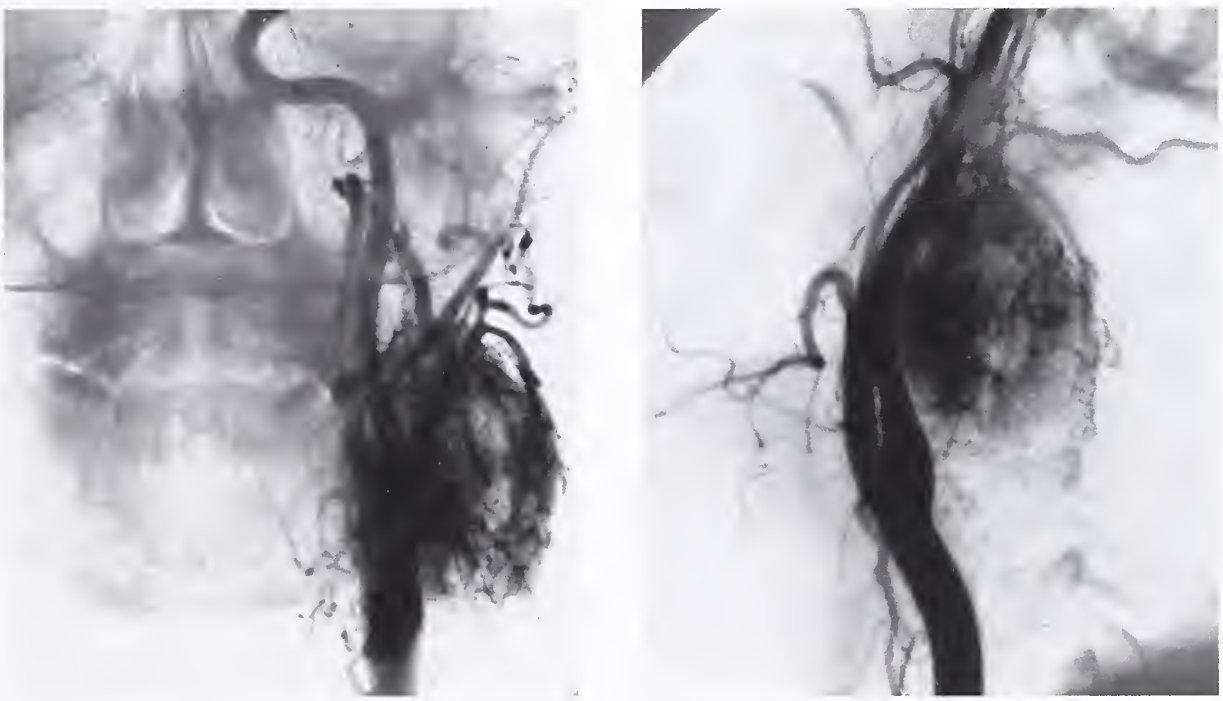

Figure 15-11

VAGAL PARAGANGLIOMA

Left: Vagal paraganglioma in the left neck in a 29-year-old patient who presented with a 3-year history of a painless, slow-growing mass associated with dysphagia. Selective carotid arteriogram in the anteroposterior projection shows a distinct tumor blush near the angle of mandible without lateral displacement of the carotid vessels. (Fig. 18-11, left from Fascicle 19, Third Series.)

Right: Lateral view of the same vagal paraganglioma shows anterior bowing of both internal and external carotid artery branches without direct involvement of the carotid bifurcation. (Fig. 5-11B from Lack EE. Pathology of adrenal and extraadrenal paraganglia. Major problems in pathology, Vol 29. Philadelphia: WB Saunders Co, 1994:105.) (Figs. 15-11 and 15-13 are from the same case.)

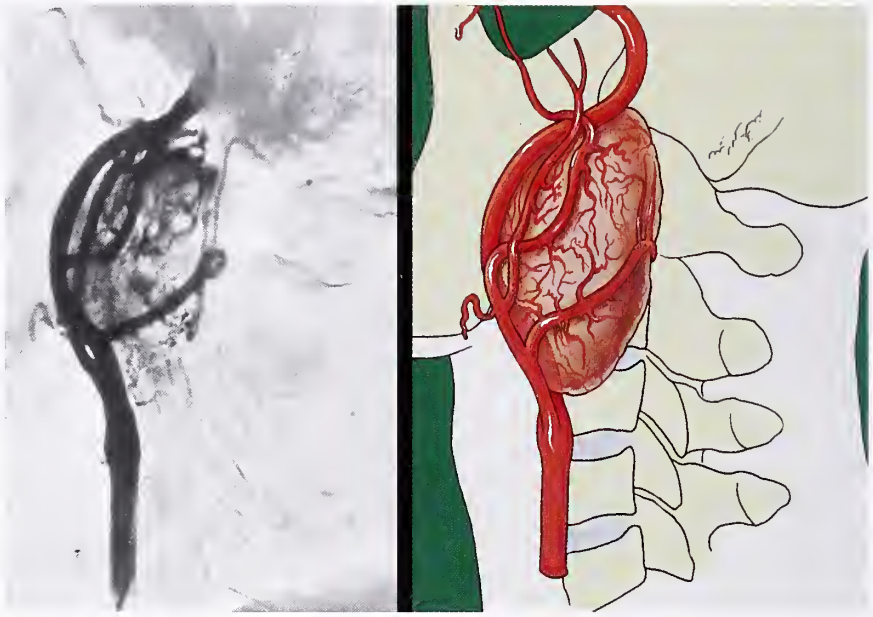

Figure 15-12

VAGAL PARAGANGLIOMA

The schematic diagram illustrates the relationship of a vagal paraganglioma to the carotid vessels. The tumor does not directly involve the carotid bifurcation and is located more cephalad than carotid body paragangliomas. (Fig. 18-12 from Fascicle 19, Third Series.)

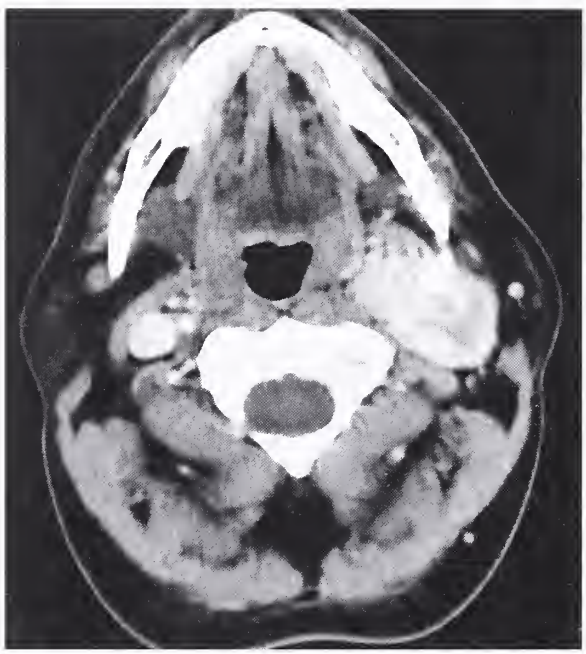

Figure 15-13

VAGAL PARAGANGLIOMA

On CT scan, the vagal paraganglioma appears as a bright ovoid mass that has imaging intensity similar to the carotid artery and internal jugular vein with intravenous contrast. (Fig. 18-13 from Fascicle 19, Third Series.)

VPs may be associated with other paragangliomas and occur in a familial setting (1). In a recent series, 44 of 48 patients with VP had multiple paragangliomas that were considered hereditary (24). Bilateral VPs have been reported as a component of Carney's triad in a patient with a family history of Hirschsprung's disease (36).

Gross Findings. VPs may have a fusiform or globular configuration and abut directly onto the base of the skull. When the tumor grows directly within the vagus nerve and nerve bundles splay out over much or all of the surface of the paraganglioma (fig. 15-14), it may be impossible to simply "shellout" the tumor at surgery (24). In some cases, the tumor causes lateral displacement of the vagus nerve, thus permitting preservation of much of the nerve (1,22). The cut surface of VP is similar grossly to other head and neck paragangliomas, although the VP may be quite sclerotic, similar to jugulotympanic paragangliomas (1). The gross identification of a stump of resected vagus nerve suggests the anatomic site of origin (fig. 15-15).

Microscopic Findings. The organoid arrangement of tumor cells is similar to that of other head and neck paragangliomas; the pattern seen in figure 15-16, left, emphasizes the disparity in the size of the "zellballen." Staining for reticulum highlights zellballen to better advantage (fig. 15-16, right). Microscopic sections may reveal a close relationship with a large ganglion (fig. 15-17), helping in the localization of the VP. Multiple myelinated nerve bundles may be seen in sections taken from the

Figure 15-14

VAGAL PARAGANGLIOMA

Left: The tumor is apparent as a fusiform expansion of the vagus nerve. It extended up to the base of the skull.

Right: The forcep in the left portion of field is elevating the trunk of the vagus nerve at the lower aspect of the tumor. Bundles of vagus nerve were splayed over the surface of tumor, and were densely adherent to the fibrous pseudocapsule. The left vagus nerve was sacrificed during surgery. (L&R: Fig. 18-14 from Fascicle 19, Third Series.)

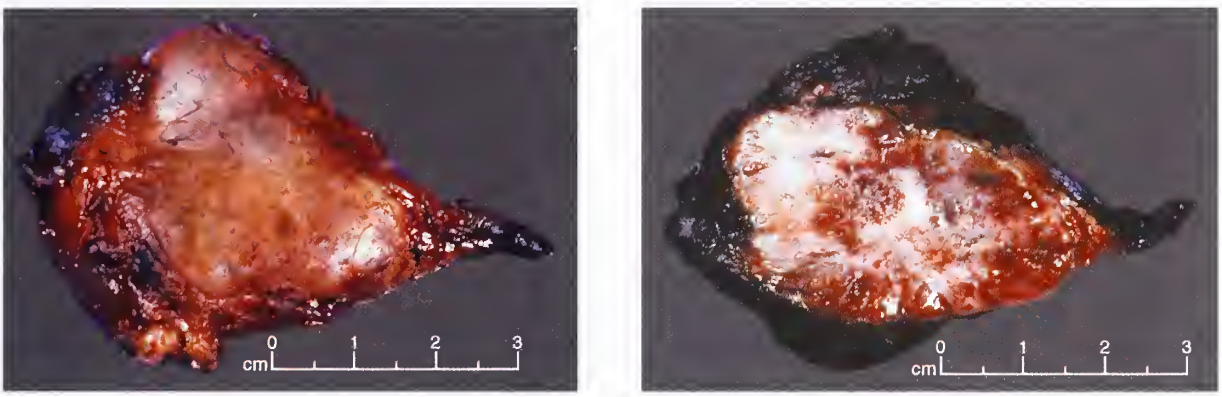

Figure 15-15

VAGAL PARAGANGLIOMA

Left: The external aspect of the tumor in figure 15-14 is relatively smooth. The distal vagus nerve is on the right side with India ink applied to it. The left inked side represents the portion of tumor that was at the skull base near the jugular foramen. This is where the proximal vagus nerve was transected.

Right: Longitudinal section of tumor shows much fibrosis. Ink has been applied to the outer surface of the tumor. The tumor had been selectively embolized before surgery and there was some evidence of ischemic necrosis in areas.

periphery of the tumor (fig. 15-18); these represent components of the vagus nerve. Other head and neck paragangliomas may have nerve bundles at the periphery of the tumor (e.g., carotid body tumors) or actually incorporate them within the substance of the tumor. Because of the anatomic location of vagal paraganglia within myelinated nerve bundles of the vagus nerve, there is occasional close paraneural, or even intraneural (fig. 15-19), growth by neoplastic chief cells (19,20). This does not necessarily indicate malignancy. Stromal changes such as sclerosis may be prominent in some tumors (fig. 15-20) and the presence of interstitial edema with prominent vascularity may cause difficulty in accurate diagnosis.

The first VP was reported by Stout in 1935 (37) in a 52-year-old woman; the tumor cells were reported to contain brown pigment, presumably melanin. The same case was reported

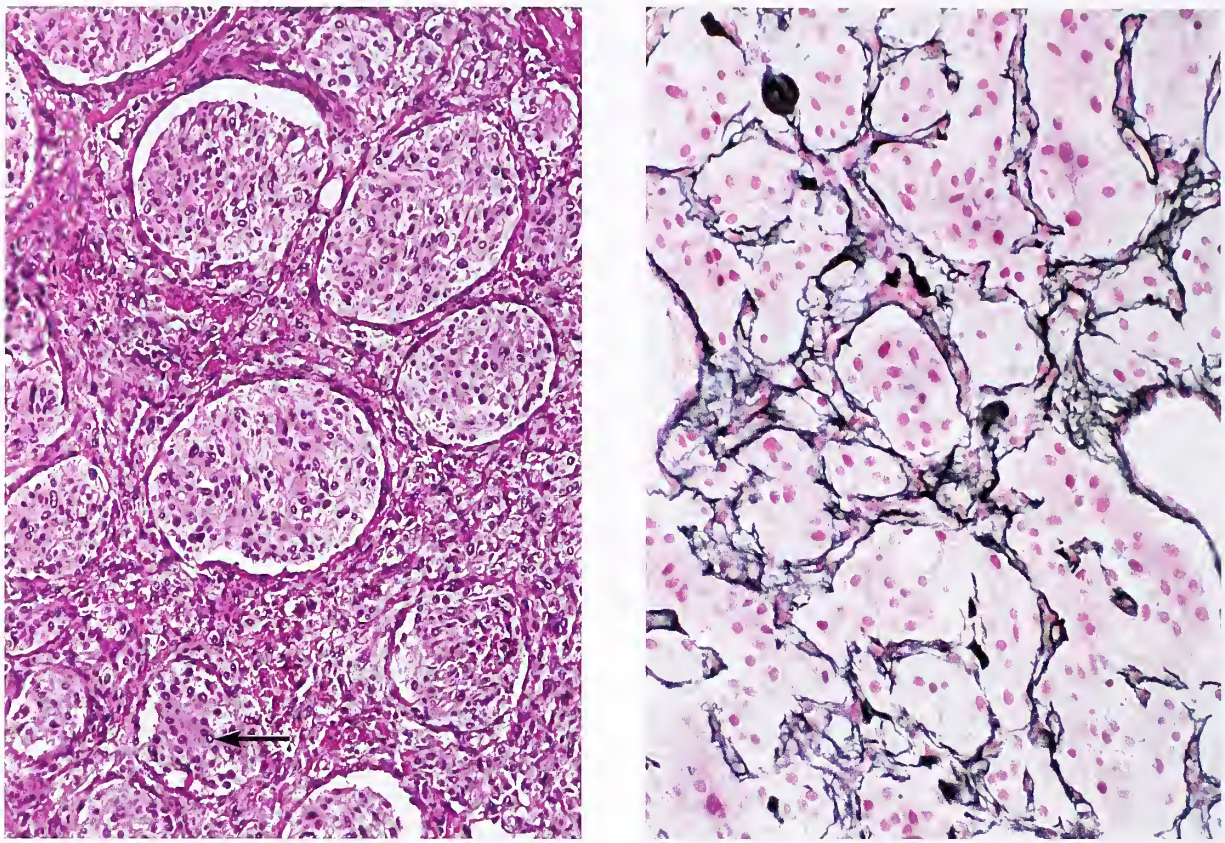

Figure 15-16

VAGAL PARAGANGLIOMA

Left: Vagal paraganglioma shows "zellballen" of varying sizes, with some being quite small and difficult to identify. Note the nuclear "pseudoinclusions" (arrow). (Fig. 18-16, left from Fascicle 19, Third Series.)

Right: In another case, reticulum highlights oval to elongated nests of neoplastic cells.

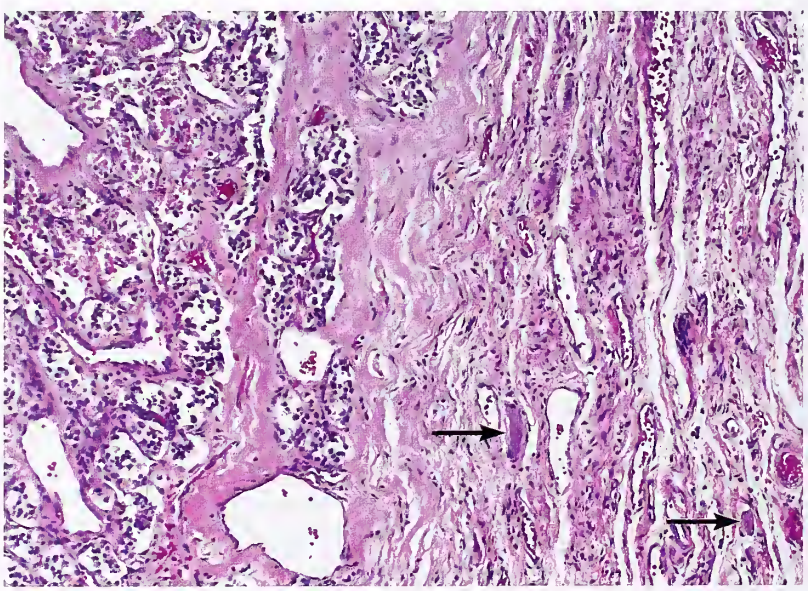

Figure 15-17

VAGAL PARAGANGLIOMA

The tumor compresses the adjacent ganglion nodosum of the vagus nerve. Scattered ganglion cells (arrows) are present. (Fig. 18-17 from Fascicle 19, Third Series.)

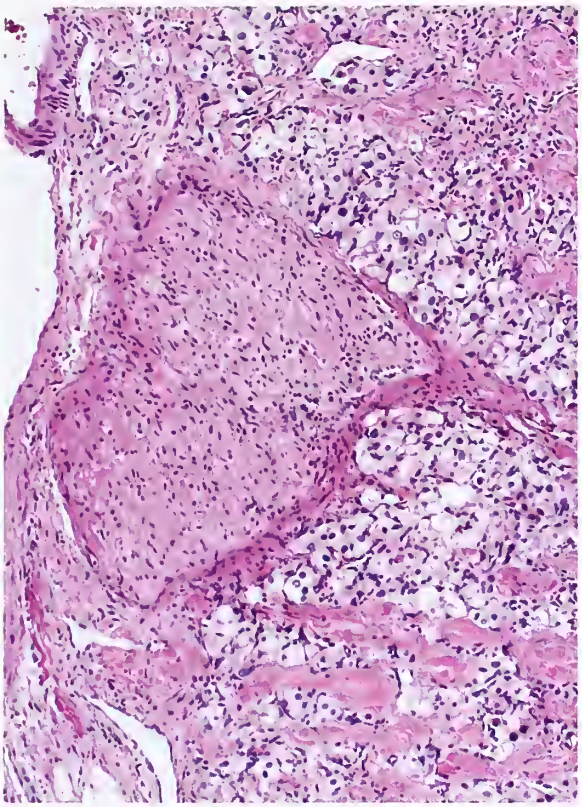

Figure 15-18

VAGAL PARAGANGLIOMA

Section taken through the periphery of the tumor shows several bundles of myelinated nerve, some of which are compressed and distorted. (Fig. 18-18 from Fascicle 19, Third Series.)

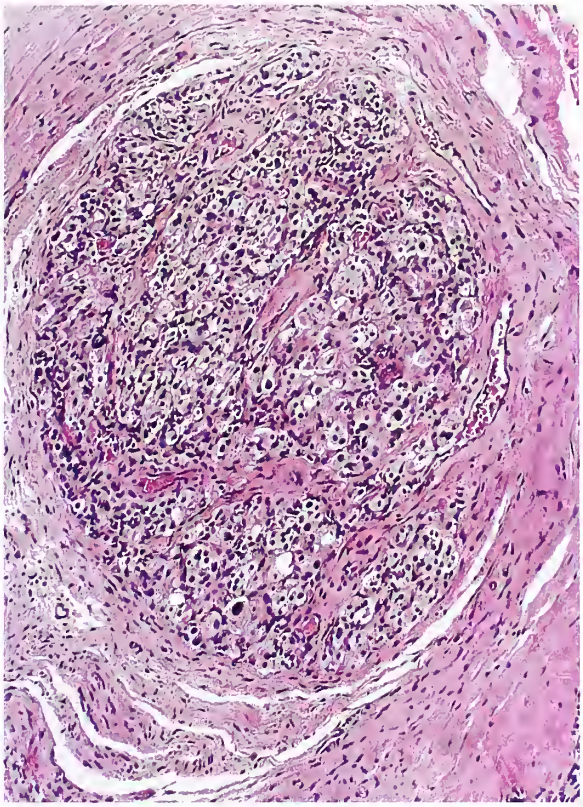

Figure 15-19

VAGAL PARAGANGLIOMA

There is a focus of intraneural growth along with some sclerosis. The tumor proved to be clinically benign. (Fig. 18-19 from Fascicle 19, Third Series.)

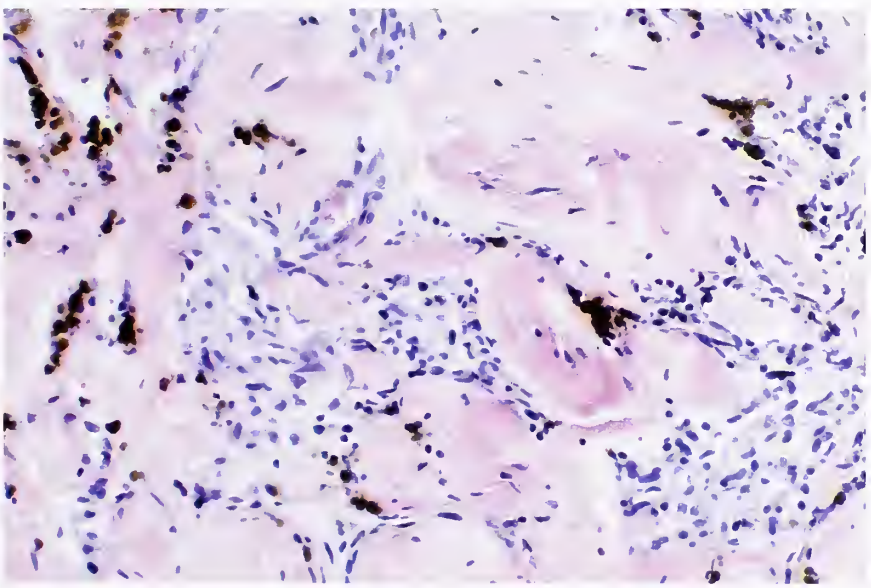

Figure 15-20

VAGAL PARAGANGLIOMA

The tumor was densely sclerotic in many areas. Hemosiderin deposition is evidence of old hemorrhage.

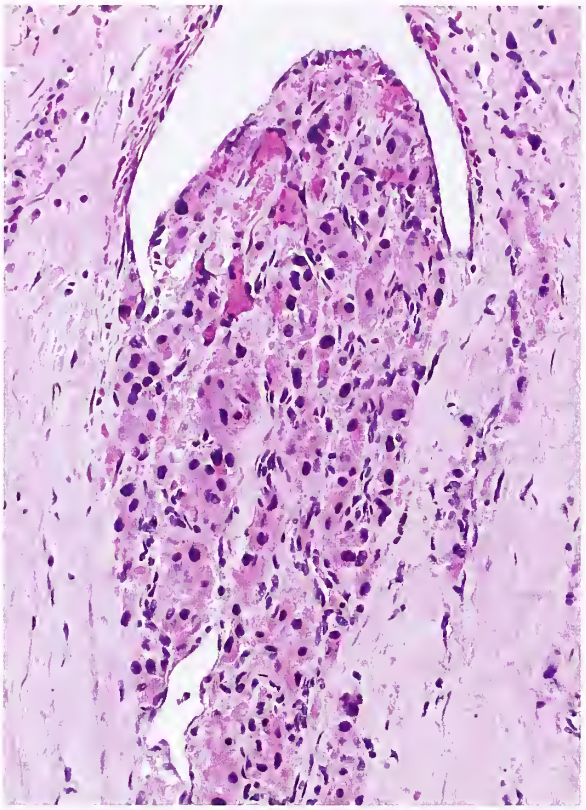

Figure 15-21

VAGAL PARAGANGLIOMA

Intravascular extension (or protrusion) is present. The tumor was benign after a follow-up of nearly 6 years. (Fig. 18-21 from Fascicle 19, Third Series.)

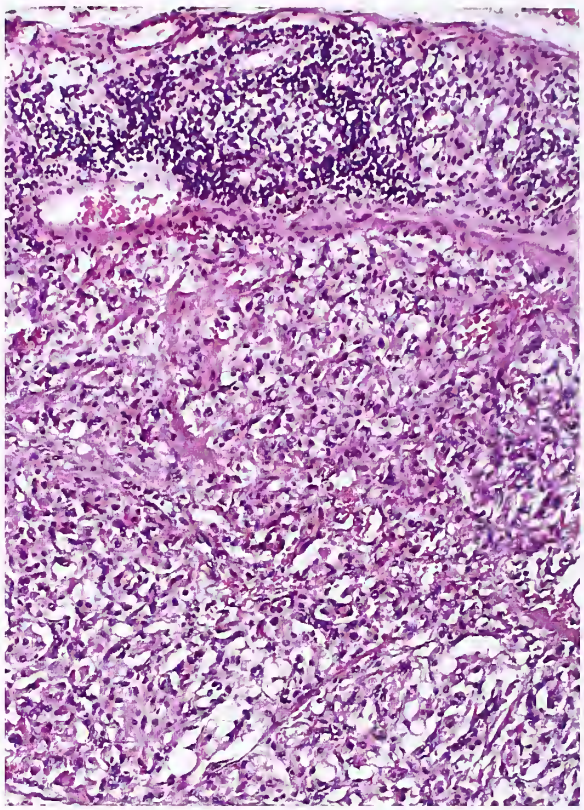

Figure 15-22

MALIGNANT VAGAL PARAGANGLIOMA

This malignant vagal paraganglioma in a 49-year-old female metastasized to a regional cervical lymph node. (Fig. 18-22 from Fascicle 19, Third Series.)

again by Lattes in 1950 (38), and the tumor proved to be clinically benign after a 19-year follow-up, despite the fact that in the original article intravascular plugs of tumor were shown side by side in vein and artery (37). A pigmented VP was recently reported (39). Occasional foci may suggest angioinvasion by a VP (or other head and neck paragangliomas), but it is unclear whether that illustrated in figure 15-21 is true vascular invasion or merely intravascular protrusion (see fig. 15-5).

Treatment and Prognosis. In general, the optimal treatment for VP is complete surgical resection. Radiation therapy may be reserved for elderly patients and patients at risk for bilateral cranial nerve deficits (21). Complications may result from intraoperative hemorrhage or postoperative sequelae due to the sacrifice of the 10th cranial (or other) nerves. Adjuvant therapy may provide some palliation.

Although some have felt that VPs are hyperplastic rather than truly neoplastic (4), these tumors are considered to be authentic neoplasms (1). The actual or true incidence of malignant behavior of VPs may be slightly inflated because of the increased tendency to report individual cases of a rare malignant tumor. Heinrich et al. (40) identified 151 VPs reported in the English language literature: 10.6 percent were malignant (15 tumors), of which 73 percent metastasized to one or more cervical lymph nodes (fig. 15-22); distant metastases to sites such as lung and bone occurred in 4 of the 15 cases.

REFERENCES

Vagal Paraganglia

1. Lack EE. Pathology of adrenal and extra-adrenal paraganglia. In: Major problems in pathology, Vol 29. Philadelphia: WB Saunders; 1994.
2. Muratori G. Contributo all' innervazione del tessuto paragangliare annesso al sistema del vago (glomo carotico, paragangli estravagali, ed intravagali) e all' innervazione del seno carotideo. Anat Anz 1932;75:115-123.
3. White EG. Die struktur des glomus caroticum, seine pathologie und physiologie und seine beziehung zum nervensystem. Beitr Path Anat 1935;96:177-227.
4. Birrell JH. Jugular body and its tumour. Aust N Z J Surg 1955;24:195-206.
5. Marcuse PM, Chamberlin JA. Multicentric paragangliomas: case report with demonstration of intravagal paraganglionic tissue at a previously undescribed level. Cancer 1956;9:288-292.
6. Plenat F, Leroux P, Floquet J, Floquet A. Intra and juxtavagal paraganglia: a topographical, histochemical, and ultrastructural study in the human. Anat Rec 1988;221:743-753.
7. Dahlqvist A, Carlsoo B, Hellstrom S. Paraganglia of the human recurrent laryngeal nerve. Am J Otolaryngol 1986;7:366-369.
8. Goormaghtigh N. On the existence of abdominal vagal paraganglia in the adult mouse. J Anat 1936;71:77-90.
9. Lack EE. Hyperplasia of vagal and carotid body paraganglia in patients with chronic hypoxemia. Am J Pathol 1978;91:497-516.
10. Lack EE. Microanatomy of vagal body paraganglia in infancy including victims of sudden infant death syndrome. Ped Pathol 1989;9:373-386.
11. Kjaergaard J. Anatomy of the carotid glomus and carotid glomus-like bodies (nonchromaffin paraganglia). With electron microscopy and comparison of human fetal carotid, aorticopulmonary, subclavian, tympanojugular, and vagal glomera. Copenhagen: FADL's Forlag; 1973.

Parathyroid Tissue Within the Vagus Nerve

12. Gilmour JR. Some developmental abnormalities of the thymus and parathyroids. J Pathol Bacteriol 1941;52:213-218.
13. Lack EE, Delay S, Linnoila RI. Ectopic parathyroid tissue within the vagus nerve. Incidence and possible clinical significance. Arch Pathol Lab Med 1988;112:304-306.
14. Reiling RB, Cady B, Clerkin EP. Aberrant parathyroid adenoma within vagus nerve. Lahey Clin Bull 1972;21:158-162.
15. Doppman JL, Shawker TH, Fraker DL, et al. Parathyroid adenoma within the vagus nerve. AJR Am J Roentgenol 1994;163:943-945.
16. Pawlik TM, Richards M, Giordano TJ, Burney R, Thompson N. Identification and management of intravagal parathyroid adenoma. World J Surg 2001;25:419-423.
17. Hung CJ, Lin PW, Lee PC, Chen HH, Chen FF. Supernumerary intravagal parathyroid hyperplasia. Surgery 2002;131:359-361.
18. Michal M. Ectopic parathyroid within a neck paraganglion. Histopathology 1993;22:85-87.

Vagal Paraganglioma

19. Lack EE, Cubilla AL, Woodruff JM. Paragangliomas of the head and neck region. A pathologic study of tumors from 71 patients. Hum Pathol 1979;10:191-218.
20. Lack EE, Cubilla AL, Woodruff JM, Farr HW. Paragangliomas of the head and neck region: a clinical study of 69 patients. Cancer 1977;39:397-409.
21. Netterville JL, Jackson CG, Miller FR, Wanamaker JR, Glasscock ME. Vagal paraganglioma: a review of 46 patients treated during a 20-year period. Arch Otolaryngol Head Neck Surg 1998;124:1133-1140.
22. Miller RB, Boon MS, Atkins JP, Lowry LD. Vagal paraganglioma: the Jefferson experience. Otolaryngol Head Neck Surg 2000;122:482-487.
23. Sniezek JC, Netterville JL, Sabri AN. Vagal paragangliomas. Otolaryngol Clin North Am 2001;34:925-939.
24. Bradshaw JW, Jansen JC. Management of vagal paraganglioma: is operative resection really the best option? Surgery 2005;137:225-228.
25. Rajan GP, Fischer U, Schmid S. Intractable hemorrhage after incision of a vagal paraganglioma mimicking a peritonsillar abscess. Otolaryngol Head Neck Surg 2005;132:161-162.
26. Lawson W. Glomus bodies and tumors. N Y State J Med 1980;80:1567-1575.
27. Black FO, Myers EN, Parnes SM. Surgical management of vagal chemodectomas. Laryngoscope 1977;87:1259-1269.
28. Perez PE, Harrison EG Jr, ReMine WH. Vagal-body tumor (chemodectoma of the glomus intravagale). N Engl J Med 1960;263:1116-1121.
29. Tannir NM, Cortas N, Allam C. A functioning catecholamine-secreting vagal body tumor. A case report and review of the literature. Cancer 1983;52:932-935.

30. Green JD Jr, Olsen KD, DeSanto LW, Scheithauer BW. Neoplasms of the vagus nerve. Laryngoscope 1988;98(Pt. 1):648-654.
31. Levin RJ, Hamill NJ, Grenko RT, Huang MY, Fedok FG. Dopamine-secreting glomus vagale: a case report and histopathologic correlation. Head Neck. 1998;20:753-757.
32. Groblewski JC, Thekdi A, Carrau RL. Secreting vagal paraganglioma. Am J Otolaryngol 2004; 25:295-300.
33. Wong GT, Stokes BA, Khangure MS, Apsimon HT, Sterrett GF. Glomus intravagale tumour: aspects of management. Aust NZ J Surg 1987;57: 199-204.
34. Okmen E, Erdinler I, Oguz E, Akyol A, Cam N. An unusual cause of reflex cardiovascular syncope: vagal paraganglioma. Ann Noninvasive Electrocardiol 2003;8:173-176.
35. Duncan AW, Lack EE, Deck MF. Radiological evaluation of paragangliomas of the head and neck. Radiology 1979;132:95-105.
36. Scopsi L, Collini P, Muscolino G. A new observation of the Carney's triad with long follow-up period and additional tumors. Cancer Detect Prev 1999;23:435-443.
37. Stout AP. Malignant tumors of peripheral nerves. Am J Cancer 1935;25:1-36.
38. Lattes R. Nonchromaffin paraganglioma of ganglion nodosum, carotid body, and aortic-arch bodies. Cancer 1950;3:667-694.
39. Reddy CE, Panda NK, Vaiphei K, Powari M. Pigmented vagal paraganglioma. J Laryngol Otol 2003;117:584-587.
40. Heinrich MC, Harris AE, Bell WR. Metastatic intravagal paraganglioma. Case report and review of the literature. Am J Med 1985;78:1017-1024.

16 LARYNGEAL PARAGANGLIOMA

LARYNGEAL PARAGANGLIA

Laryngeal paraganglia are microscopic structures that have a variable anatomic distribution in relation to the cricoid and thyroid cartilages (1,2). They are divided into a superior and inferior group (fig. 16-1) (3); the size and location of the superior laryngeal paraganglia are more constant. A midline paraganglion is designated as the "anterior laryngeal glomus" (2). Laryngeal paraganglia are sometimes found immediately adjacent to the thyroid gland or as ovoid structures within the capsule of the gland (4). They have also been described within the recurrent laryngeal nerve (5). Laryngeal paraganglia seem to be radioresistant since there are no detectable structural changes following therapeutic doses of radiation (4). Their basic histology is virtually identical to that of paraganglia elsewhere in the head and neck region (fig. 16-2) (6).

The precise physiologic role of laryngeal paraganglia is not known. The larynx has been characterized as a respirator effector organ capable of regulating the respiratory flow of air, particularly during expiration (7). Fine motor control of the vocal cords modulates changes in airway resistance during the respiratory cycle; vagal innervation appears to be important in keeping laryngeal resistance low during hypoxia, and may help to prevent partial airway obstruction, and thereby blunt the ventilatory work load (8). Some have postulated that endoneurial paraganglia function as chemoreceptors, and that the chemosensory input to the central nervous system during hypoxia may represent a summation of stimuli from a variety of chemoreceptor sites (9).

LARYNGEAL PARAGANGLIOMA

Definition. *Laryngeal paragangliomas* (LPs) arise from dispersed paraganglia located near the larynx.

Clinical Features. LPs present as a submucosal mass in the supraglottic larynx that may impinge on the glottic airway (fig. 16-3). The usual presenting complaint is hoarseness; other signs and symptoms include dysphagia, dyspnea, stridor, dysphonia, hemoptysis, and a cervical mass (10,11). Throat pain is a prominent symptom in some cases (12).

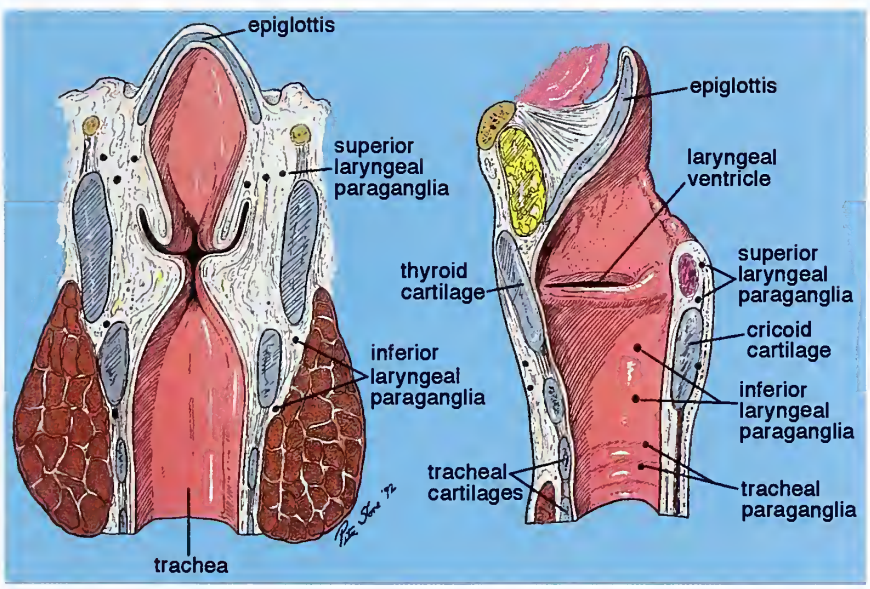

Figure 16-1

DISTRIBUTION OF HUMAN LARYNGEAL AND TRACHEAL PARAGANGLIA

Most paraganglia are paired structures located in superior and inferior locations in the lateral larynx. (Fig. 19-1 from Fascicle 19, Third Series.)

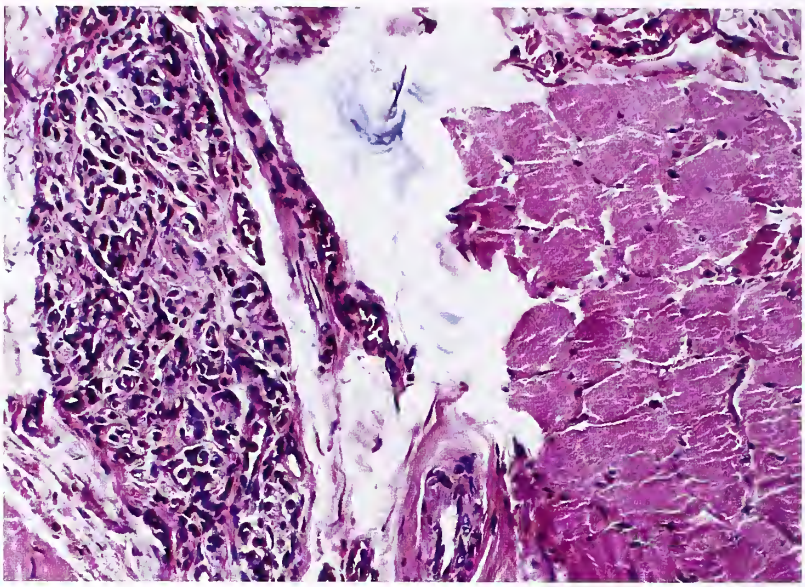

Figure 16-2

NORMAL LARYNGEAL PARAGANGLION

The normal laryngeal paraganglion is ovoid, and is morphologically identical to a lobule of carotid body. (Fig. 19-2 from Fascicle 19, Third Series.)

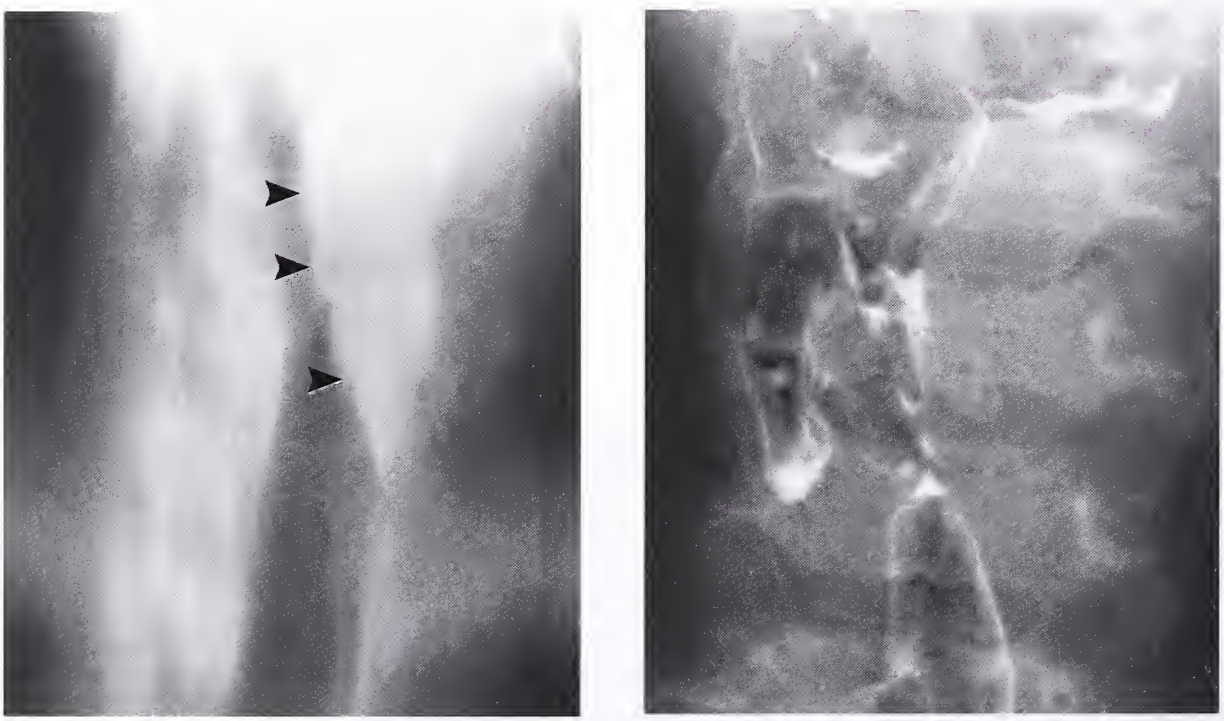

Figure 16-3

LARYNGEAL PARAGANGLIOMA

Left: A 26-year-old woman presented with progressive hoarseness of 5 months' duration. A tomogram of the larynx shows a soft tissue mass (arrows) impinging on the glottic airway.

Right: Laryngogram shows the mass effect of a laryngeal paraganglioma (LP) with smooth overlying mucosa. The tumor originated in the area of the left pyriform sinus and measured 4 x 6 cm. (Figs. 1A, B from Gallivan MV, Chun B, Rowden G, Lack EE. Laryngeal paraganglioma. Case report with ultrastructural analysis and literature review. Am J Surg Pathol 1979;3:85-92.)

In a critical review of the literature on LPs, Barnes (13) identified 81 cases, of which 34 were considered acceptable for analysis. There was a predilection for females (25 females, 9 males), average age at diagnosis of 47 years (range, 14 to 80 years), and average duration of symptoms of 26 months. One LP was reported in a 5-year-old child (14). A subsequent review added eight new cases (15). Only 15 percent of LPs were primary in the subglottis and 3 percent in the glottis. One LP may have been hormonally active since the patient experienced hypertension and tachycardia, but there was no biochemical documentation of excess catecholamine secretion (16). The likelihood of an LP being a familial tumor or multicentric appears to be remote (17), although, LPs have been associated with carotid body and other paragangliomas (18). An inferior LP presenting as a plunging goiter has been recently reported (19).

Pathologic Findings. The average size of the LPs reviewed by Barnes (13) was 2.5 cm (range, 0.5 to 6 cm); most arose in the right side of the larynx. One LP reported with a dumbbell configuration extended into the larynx and prelaryngeal space adjacent to the thyroid gland (20). There may be multicentric paragangliomas at other sites (21), but several of these cases were excluded in the review by Barnes (including a tracheal paraganglioma); cases were also excluded if the tumor had not been illustrated or the pictures were not considered confirmatory of the diagnosis.

LPs are described as a red or blue-red submucosal mass. On cross section, they may have a meaty dull red to tan appearance, with areas of congestion and hemorrhage (fig. 16-4).

The histologic appearance is typical for a paraganglioma, but the unusual location or a prominent vascular pattern with plump endothelial cells can cause problems in interpretation (fig. 16-5). Accurate diagnosis is also hindered by technical alterations induced by a limited biopsy or crush artifact. In the review by Barnes (13), mitotic figures were few. Frank invasion into adjoining soft tissues is uncommon and should raise the possibility of another type of laryngeal neuroendocrine neoplasm with more aggressive behavior (6).

Biologic Behavior. Gallivan et al. (10) found that 25 percent of laryngeal tumors reported as

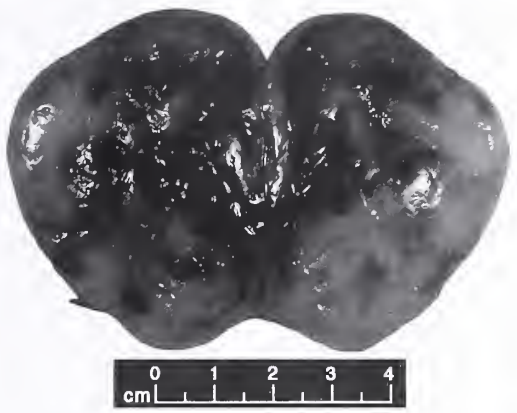

Figure 16-4

LARYNGEAL PARAGANGLIOMA

Bisected LP from a 57-year-old woman who presented with a 3-year history of hoarseness and dysphagia. The preoperative diagnosis was a laryngeal chondroma. The patient was alive and well 15 years following surgical resection of the tumor. In cross section, mottled areas of hemorrhage are seen. (Fig. 19-4 from Fascicle 19, Third Series.)

LPs were clinically malignant. This incidence was considered to be "spuriously high." The increased incidence of malignancy is attributed to the fact that some of the cases reported as LP were actually atypical laryngeal carcinoid tumors (13,22–24). Based upon the updated world literature review by Myssiorek et al. (25), LPs have a significantly lower incidence of malignancy than previously reported. In an earlier review by Barnes (13), recurrent LP was noted in 5 of 30 patients (17 percent); only one tumor was malignant (3 percent) with metastasis to the lumbar spine 16 years after diagnosis of the primary tumor (26,27).

Differential Diagnosis. The differential diagnosis includes a variety of tumors such as malignant melanoma, either primary (28) or metastatic to the larynx (29), and hemangiopericytoma (30). The primary neoplasm that has caused the greatest diagnostic confusion with LP, however, is the laryngeal atypical carcinoid tumor (LAC) (31), which has also been referred to as large cell (32) or moderately differentiated neuroendocrine carcinoma (33,34). The average size of LAC in the review by Woodruff and Senie (31) was 1.6 cm. An organoid or trabecular pattern in a LAC can be readily confused with an LP (fig. 16-6) (6), and similar to LP, neuroendocrine

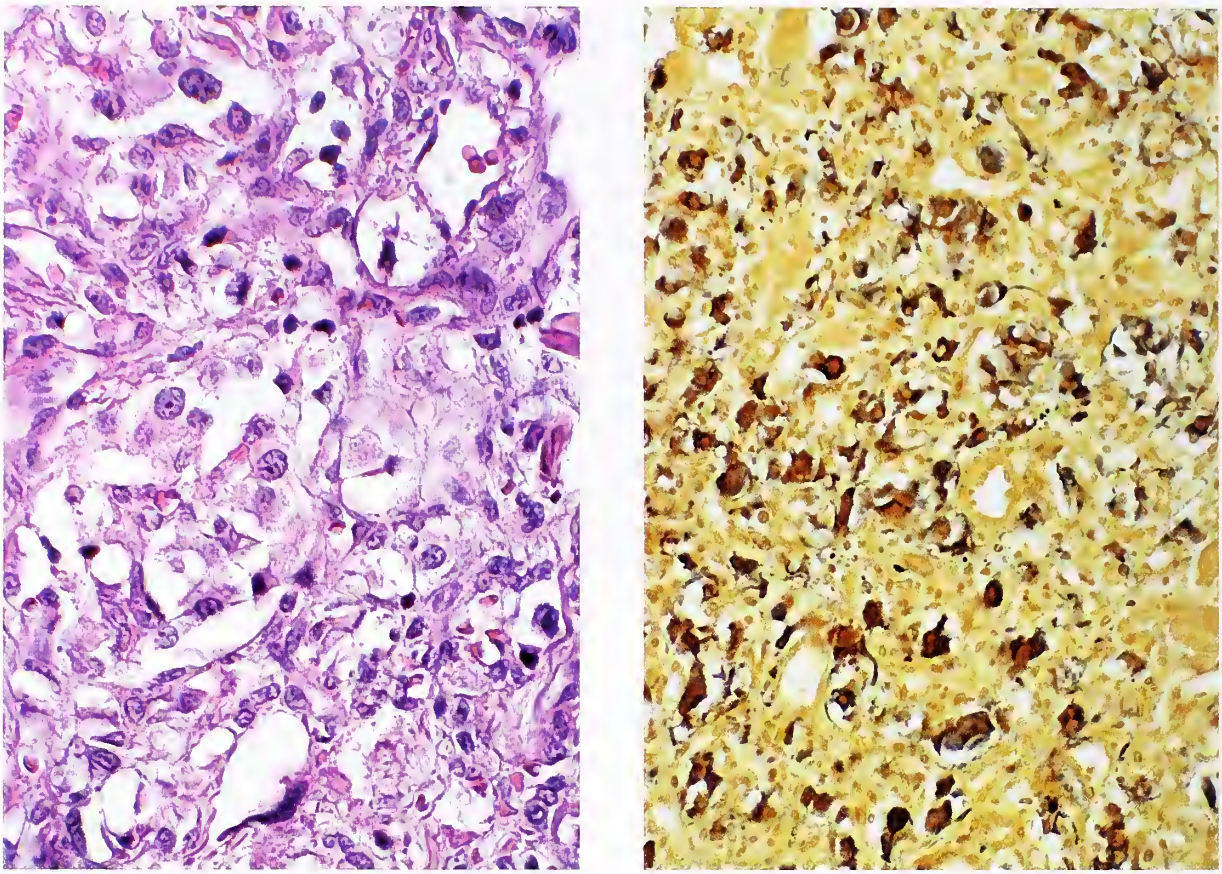

Figure 16-5

LARYNGEAL PARAGANGLIOMA

Left: The tumor has a nested arrangement of cells with pale eosinophilic cytoplasm. Initially, the tumor had been misinterpreted as a hemangioendothelioma because of the prominent vasculature and retraction spaces simulating vascular spaces.

Right: Tumor cells are better delineated due to distinct cytoplasmic argyrophilia. This is the Grimelius technique for cytoplasmic argyrophilia which was popular for staining endocrine neoplasms but is illustrated only a few times in this Fascicle since it has largely been replaced by immunostains for neuroendocrine differentiation (Grimelius stain).

neoplasms of the larynx can express markers such as chromogranin (fig. 16-7, left), protein gene product 9.5, and neuron-specific enolase. The LAC, however, is typically positive for epithelial markers such as cytokeratin (fig. 16-7, right) (31,33,35) and carcinoembryonic antigen (35). Positive staining for S-100 protein was found in 20 percent of LACs in the study by Wenig et al. (33), while in LPs, S-100 protein–positive cells are sustentacular cells and are distributed at the periphery of clusters of neoplastic chief cells (6). In a comprehensive review of LACs, the survival rate at 5 years was 48 percent and at 10 years, 30 percent; a poorer survival rate was noted for patients having tumors over 1 cm in diameter and tumors involving skin and subcutaneous tissue (31).

There has been some attempt at standardization for nomenclature of neuroendocrine neoplasms of the upper respiratory tract: group 1 tumors are subclassified as 1) well-differentiated neuroendocrine carcinoma (carcinoid tumor), 2) moderately differentiated neuroendocrine carcinoma (atypical carcinoid tumor), and 3) poorly differentiated neuroendocrine carcinoma, small and large cell type (34). Tracheal paraganglioma has also been described (36).

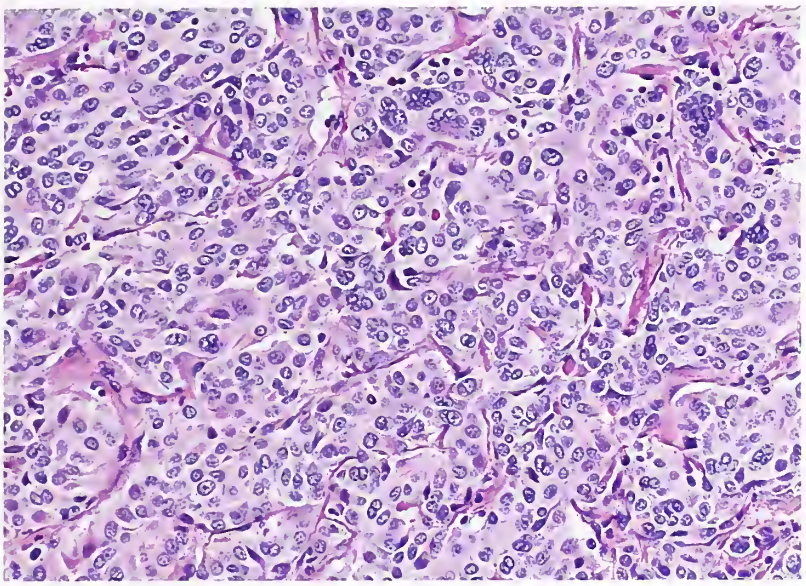

Figure 16-6

LARYNGEAL ATYPICAL CARCINOID

A 66-year-old female had a 1-cm tumor in the submucosa of the supraglottic larynx. There is a nested and trabecular arrangement of cells with ample, granular eosinophilic cytoplasm. The vague organoid pattern can cause confusion with LP. (Figs. 16-6 and 16-7 are from the same case.) (Fig. 19-6, right from Fascicle 19, Third Series.)

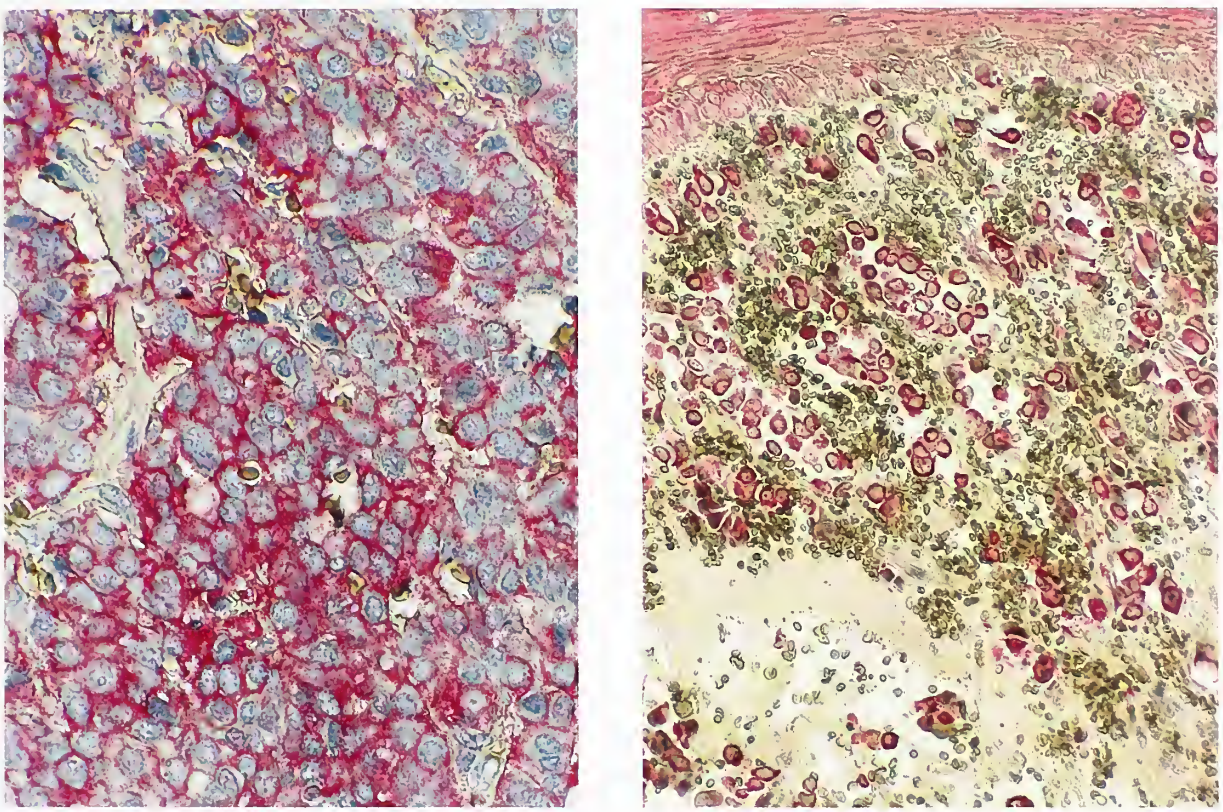

Figure 16-7

LARYNGEAL ATYPICAL CARCINOID

Left: Laryngeal atypical carcinoid shows positive immunostain for chromogranin (L&R: avidin-biotin peroxidase method). Right: Same case with diffuse cytoplasmic immunoreactivity for cytokeratin. (L&R: Fig. 19-7 from Fascicle 19, Third Series.)

REFERENCES

Laryngeal Paraganglia

1. Watzka M. Uber die paraganglion in der plica ventricularis des menschlichen kehlkopfes. Dtsch Med Forsch 1963;1:19-20.
2. Kleinsasser O. [The inferior laryngeal glomus. A nonchromaffin paraganglion, unknown so far, of the structures of the so-called carotid gland in human larynx.]. Archiv Ohren Nasen Kehlkopfheilk 1964;184:214-224. [German.]
3. Lawson W, Zak FG. The glomus bodies ("paraganglia") of the human larynx. Laryngoscope 1974;84:98-111.
4. Zak FG, Lawson W. Glomic (paraganglionic) tissue in the larynx and capsule of the thyroid gland. Mt Sinai J Med 1972;39:82-90.
5. Dahlqvist A, Carlsoo B, Hellstrom S. Paraganglia of the human recurrent laryngeal nerve. Am J Otolaryngol 1986;7:366-369.
6. Lack EE. Pathology of adrenal and extra-adrenal paraganglia. Major problems in pathology, Vol 29. Philadelphia: WE Saunders; 1994.
7. Bartlett D Jr, Remmers JE, Gautier H. Laryngeal regulation of respiratory airflow. Respir Physiol 1973;18:194-204.
8. Bartlett D. Effects of vagal afferents on laryngeal responses to hypercapnia and hypoxia. Respir Physiol 1980;42:189-198.
9. Dahlqvist A, Pequignot JM, Hellstrom S, Carlsoo B, Peyrin L. Catecholamines of endoneurial laryngeal paraganglia in the rat. Acta Physiol Scand 1986;127:257-261.

Laryngeal Paraganglioma

10. Gallivan MV, Chun B, Rowden G, Lack EE. Laryngeal paraganglioma. Case report with ultrastructural analysis and literature review. Am J Surg Pathol 1979;3:85-92.
11. Lack EE, Cubilla AL, Woodruff JM. Paragangliomas of the head and neck region. A pathologic study of tumors from 71 patients. Hum Pathol 1979;10:191-218.
12. Stanley RJ, Weiland LH, Neel HB 3rd. Pain-inducing laryngeal paraganglioma: report of the ninth case and review of the literature. Otolaryngol Head Neck Surg 1986;95:107-112.
13. Barnes L. Paraganglioma of the larynx. A critical review of the literature. ORL J Otorhinolaryngol Relat Spec 1991;53:220-234.
14. Thirlwall AS, Bailey CM, Ramsay AD, Wyatt M. Laryngeal paraganglioma in a five-year-old child—the youngest case ever recorded. J Laryngol Otol. 1999;113:62-64.
15. Ferlito A, Barnes L, Wenig BM. Identification, classification, treatment, and prognosis of laryngeal paraganglioma. Review of the literature and eight new cases. Ann Otol Rhinol Laryngol 1994;103:525-536.
16. Laudadio P. [Chemodectoma (paraganglioma, noncromaffin) of the superior glomus laryngeus.] Otolaringol Ital 1972;39:19-31. [Italian.]
17. Myssiorek D, Halaas Y, Silver C. Laryngeal and sinonasal paragangliomas. Otolaryngol Clin North Am 2001;34:971-981.
18. Rubin AD, Cheng SS, Bradford CR. Laryngeal paraganglioma in a patient with multiple head and neck paragangliomas. Otolaryngol Head Neck Surg 2005;132:520-522.
19. Aribas OK, Kanat F, Avunduk MC. Inferior laryngeal paraganglioma presenting as plunging goiter. Eur J Cardiothorac Surg 2004;25:655-657.
20. Googe PB, Ferry JA, Bhan AK, Dickersin GR, Pilch BZ, Goodman M. A comparison of paraganglioma, carcinoid tumor, and small-cell carcinoma of the larynx. Arch Pathol Lab Med 1988;112:809-815.
21. Hartmann E. [Chemodectoma laryngis.] Acta Otolaryngol 1960;51:528-532. [German.]
22. Justrabo E, Michiels R, Calmettes C, et al. An uncommon apudoma: a functional chemodectoma of the larynx. Report of a case and review of the literature. Acta Otolaryngol 1980;89:135-143.
23. Marks PV, Brookes GB. Malignant paraganglioma of the larynx. J Laryngol Otol 1983;97: 1183-1188.
24. Milroy CM, Rode J, Moss E. Laryngeal paragangliomas and neuroendocrine carcinomas. Histopathology 1991;18:201-209.
25. Myssiorek D, Rinaldo A, Barnes L, Ferlito A. Laryngeal paraganglioma: an updated critical review. Acta Otolaryngol 2004;124:995-999.
26. Azevedo-Gamas A, Gloor F. [A very unusual case of tumor of the larynx. Unexpected anatomopathologic diagnosis.] Ann Otolaryngol (Paris) 1968;85:329-335. [French.]
27. Rufenacht H, Mihatsch MJ, Jundt K, Gachter A, Tanner K, Heitz PU. Gastric epithelioid leiomyomas, pulmonary chondroma, non-functioning metastasizing extra-adrenal paraganglioma and myxoma: a variant of Carney's triad. Report of a patient. Klin Wochenschr 1985;63:282-284.

Differential Diagnosis

28. Reuter VE, Woodruff JM. Melanoma of the larynx. Laryngoscope 1986;94:389-393.
29. Ferlito A, Caruso G, Recher G. Secondary laryngeal tumors. Report of seven cases with review of the literature. Arch Otolaryngol Head Neck Surg 1988;114:635-639.
30. Schwartz MR, Donovan DT. Hemangiopericytoma of the larynx: a case report and review of the literature. Otolaryngol Head Neck Surg 1987;96:369-372.
31. Woodruff JM, Senie RT. Atypical carcinoid tumor of the larynx. A critical review of the literature. ORL J Otorhinolaryngol Relat Spec 1991;53:194-209.
32. Woodruff JM, Huvos AG, Erlandson RA, Shah JP, Gerold FP. Neuroendocrine carcinomas of the larynx. Am J Surg Pathol 1985;9:771-790.
33. Wenig BM, Hyams VJ, Heffner DK Moderately differentiated neuroendocrine carcinoma of the larynx. A clinicopathologic study of 54 cases. Cancer 1988;62:2658-2676.
34. Mills SE. Neuroectodermal neoplasms of the head and neck with emphasis on neuroendocrine carcinomas. Mod Pathol 2002;15:264-278.
35. Ferlito A, Friedmann I. Contribution of immunohistochemistry in the diagnosis of neuroendocrine neoplasms of the larynx. ORL J Otorhinolaryngol Relat Spec 1991;53:235-244.
36. Jones TM, Alderson D, Sheard JD, Swift AC. Tracheal paraganglioma: a diagnostic dilemma culminating in a complex airway management problem. J Laryngol Otol 2001;115:747-749.

17 AORTICOPULMONARY PARAGANGLIOMA AND PARAGANGLIOMAS AT OTHER SITES IN THE HEAD AND NECK REGION

AORTICOPULMONARY PARAGANGLIA

There have been descriptions of paraganglia in various sites near the base of the heart and great vessels, collectively referred to as *aorticopulmonary paraganglia*. Early descriptions by Wiesel (1), Busacchi (2), Penitschka (3), and others (4) leave little doubt that these microscopic structures have a varied anatomic distribution. They may be very difficult to recognize in histologic sections unless systematically searched for. In a study by Blessing (5), several thousand serial sections from the supracardiac region in an infant revealed 56 separate paraganglia (fig. 17-1). Boyd (6) subdivided aorticopulmonary paraganglia into three groups at the base of the heart, while in an extensive study by Becker (7), four groups were recognized, including those located along the course of the left coronary artery in adventitia of the pulmonary trunk.

If some (or all) of these aorticopulmonary paraganglia have a chemoreceptor function, the nature of the vascular supply may be important. Although there was some controversy in early studies (8), and some consider the blood supply to be derived from the pulmonary artery trunk (9), several studies in humans have convincingly demonstrated that the arterial supply is systemic and originates from the left coronary artery via the intertruncal branch (7,10) or the aorta (7). Aorticopulmonary paraganglia are also found in or near the interatrial septum (11,12), as well as along the proximal course of the left coronary artery (12); the subgroup of tumors designated cardiac paragangliomas may originate from some of these paraganglia.

Aorticopulmonary paraganglia are microscopic structures that are histologically identical to the lobular subunits of carotid bodies. These paraganglia may be closely associated with small vascular units (fig. 17-2, left) or myelinated nerve bundles (fig. 17-2, right). The precise dimensions and histologic appearance of aorticopulmonary paraganglia have not been systematically correlated with age or any specific disease process. In the human fetus and newborn the maximum size of paraganglia ranges from 140 to 250 μm (7); in another study, 14 fetal paraganglia ranged in size from 45 to 180 μm (13). It is estimated that collectively the aorticopulmonary paraganglia make up a total volume about one third that of the carotid body. The ultrastructural appearance is very similar to that of other head and neck paraganglia.

Hyperplasia of aorticopulmonary paraganglia has been observed in some patients with cystic fibrosis (4). The largest paraganglion measured 1,360 by 1,800 μm. Hyperplasia is evidenced by

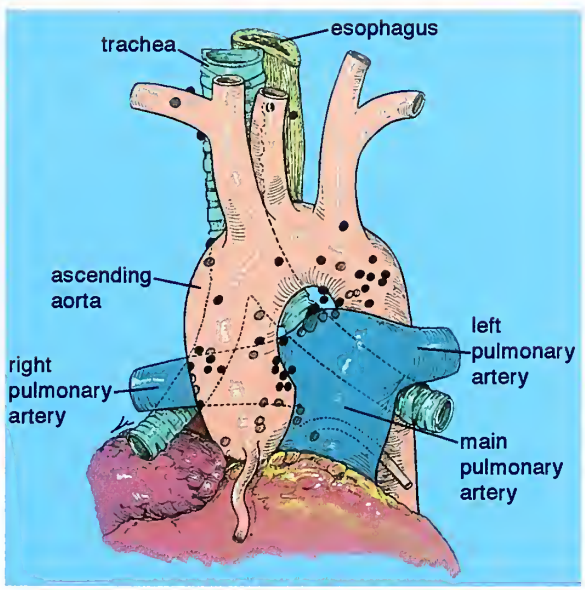

Figure 17-1

ANATOMIC DISTRIBUTION OF AORTICOPULMONARY PARAGANGLIA

Cross-hatched dots indicate the distribution of aorticopulmonary paraganglia on the dorsal aspect, while solid black dots show the location on the ventral aspect. Some paraganglia are located on the superior aspect of the aortic arch and more cephalad near the subclavian artery. (Modified from fig. 1 from Blessing MH. Uber glomuszellen im suprakardialraum. Klin Wochenschr 1963;41:1025-1026.)

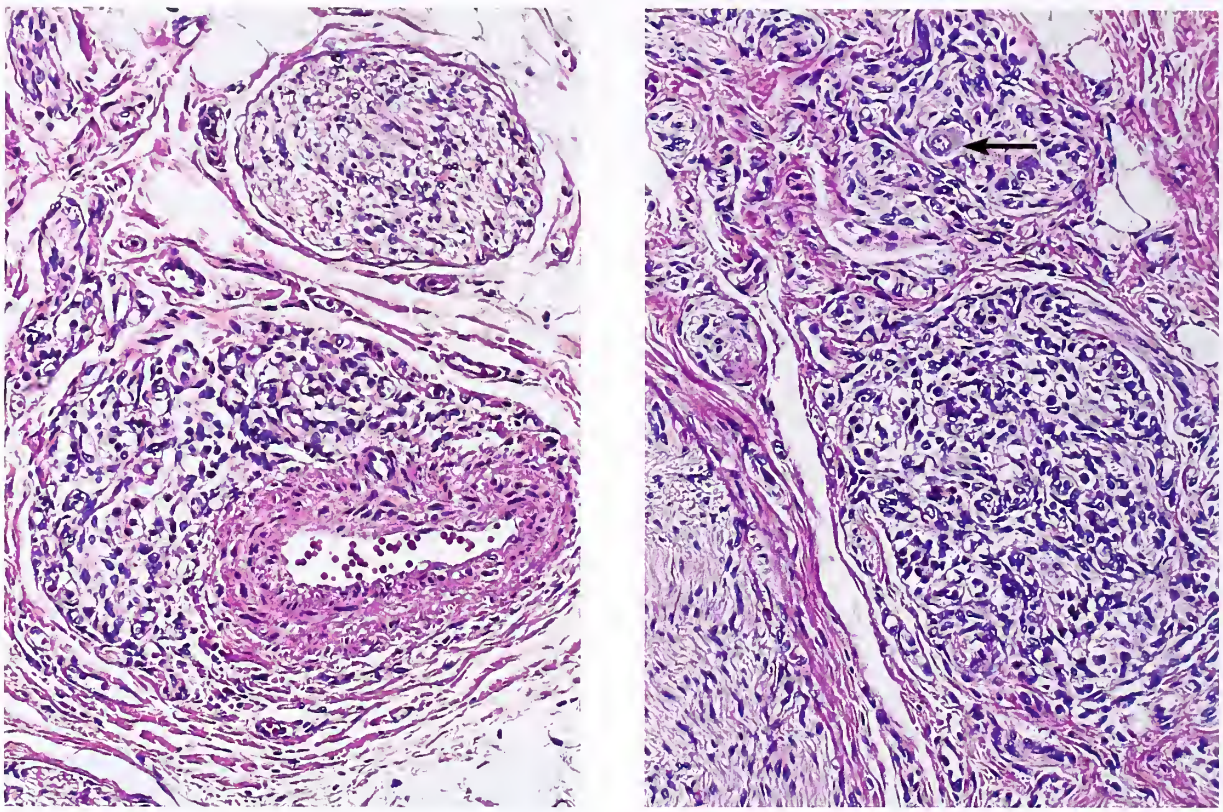

Figure 17-2

AORTICOPULMONARY PARAGANGLIA

Left: Aorticopulmonary paraganglion is morphologically identical to the lobular subunit of the carotid body. Note the small vascular channel in the lower field. Chief cells are arranged in small clusters and many have small nuclei.

Right: Small lobules of an aorticopulmonary paraganglion are located adjacent to myelinated nerve bundles. Note the ganglion cell (arrow). (L&R. Fig. 20-2 from Fascicle 19, Third Series.)

an increase in size, sometimes with multilobulation; chief cells may be prominent (fig. 17-3). It would be very interesting to systematically study these and other extracarotid paraganglia in the head and neck region in individuals residing at high altitude or in individuals with altered physiologic function resulting in chronic hypoxemia (4). Morphologic alterations of some aorticopulmonary paraganglia have been reported in victims of sudden unexpected death, and it has been suggested on theoretical grounds that these alterations could lead to disturbance of cardiac rhythm, conduction, or repolarization (14).

AORTICOPULMONARY PARAGANGLIOMA

Definition. *Aorticopulmonary paragangliomas* (APPs) arise from paraganglia near the base of the heart and great vessels.

General Comments. APPs arise from paraganglia that are intracardiac, usually at the level of the atria; intrapericardial but extracardiac; or in more diverse sites, above or below the aortic arch (fig. 17-1). The collective group of APPs can be subdivided into *cardiac* and *extracardiac paragangliomas*. These tumors account for about 1 percent of all primary mediastinal neoplasms (15). The term APP is not used for paragangliomas located in the paravertebral sulcus paralleling the sympathetic chain (16).

Clinical Features. *Cardiac Paraganglioma.* Over 40 primary cardiac paragangliomas have been reported, some more than once (see 17–31). This subset of APP may require special techniques for surgical management, such as cardiopulmonary bypass with cardioplegia and coronary artery reconstruction; human cardiac

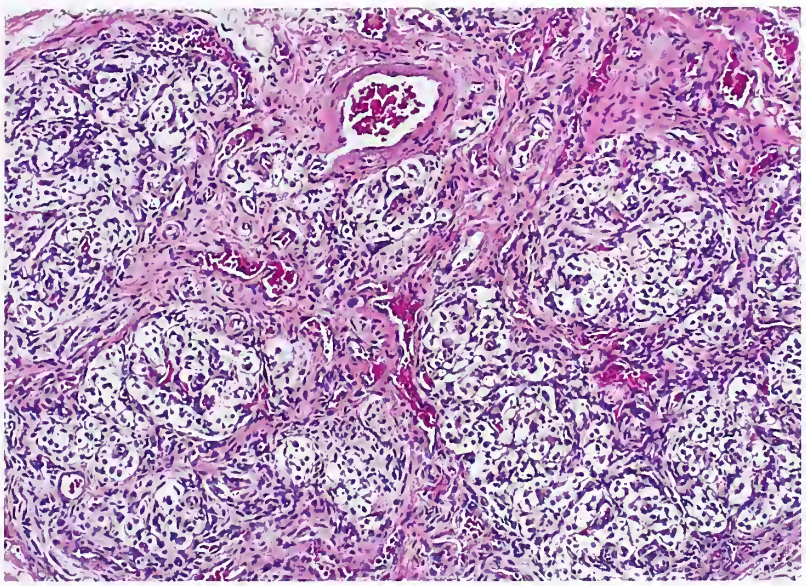

Figure 17-3

HYPERPLASTIC AORTICOPULMONARY PARAGANGLION

A portion of a hyperplastic aorticopulmonary paraganglion in an 18-year-old man with cystic fibrosis. The lobular architecture is accentuated and there is a prominent array of chief cells. (Fig. 20-3 from Fascicle 19, Third Series.)

explantation and autotransplantation have even been attempted following resection of a large atrial paraganglioma (20,22). Cardiac paragangliomas arise within the pericardium and involve some intrinsic aspect of the heart.

In a review by Mikolaenko et al. (25), there was a roughly equal sex distribution and the average age at diagnosis was 39 years. Some of the presenting signs or symptoms include cardiomegaly, retrosternal pain, hemoptysis, cardiac murmur, and palpitations. A few patients have symptoms of ischemic heart disease (21, 26). Occlusion of the left anterior descending coronary artery has been reported, probably due to extrinsic compression by the tumor (27).

About half of the reported cardiac paragangliomas have been associated with signs or symptoms of excess catecholamine secretion; some of these tumors (and the associated paraganglia) may be more closely aligned with sympathoadrenal paragangliomas (4). Several patients have undergone failed abdominal exploration for suspected pheochromocytoma (18,28). Cardiac paragangliomas can involve the walls of the atria, interatrial septum or groove, and the pericardium overlying the right or left ventricle toward the base of the heart. Some are not detectable by routine tomography or computerized tomography (CT) scan (18), and in some cases ^{131}I-metaiodobenzylguanidine (MIBG) scintigraphy has been useful in localizing iodine uptake in the cardiac region (29–31).

Extracardiac Paragangliomas. Extracardiac paragangliomas are located outside the pericardial cavity in relation to the base of the heart and great vessels (figs. 17-4, 17-5) (32–41). The first cases were reported in 1950 (32,33). A slight female predominance is apparent, with an age distribution similar to that of cardiac paragangliomas (4). In a study of 16 mediastinal paragangliomas, there was slight male predominance, but most of the tumors were located in the posterior mediastinum (40), raising the possibility that some were paravertebral paragangliomas of the sympathoadrenal neuroendocrine system. Hoarseness, dysphagia, cough, and chest pain are common manifestations, and occasionally patients present with superior vena cava syndrome (37).

Occasionally, both cardiac and extracardiac paragangliomas are associated with paragangliomas in other sites (17,21,32,40) including pheochromocytoma (28) or extraadrenal abdominal paraganglioma (42), and some patients may have a family history of similar tumors (17). A number of APPs have been reported in association with Carney's triad of gastric stromal sarcoma, pulmonary chondroma, and extraadrenal paraganglioma (43,44). In one study, 37 patients (47 percent) had 60 paragangliomas (multicentric in 8 patients); 14 tumors arose in the chest, 20 in the head and neck (most often carotid body paraganglioma), and 26 arose in the abdomen (including 6 pheochromocytomas) (44).

Figure 17-4

AORTICOPULMONARY PARAGANGLIOMA

Chest radiograph with barium esophagogram in an 11-year-old girl with an aorticopulmonary paraganglioma. A middle mediastinal mass impinging on the esophagus was initially interpreted as a vascular structure. (Fig. 20-4 from Fascicle 19, Third Series.) (Figs. 17-4 and 17-5 are from the same case.)

Figure 17-5

AORTICOPULMONARY PARAGANGLIOMA

Anteroposterior radiograph of the chest 4 years later shows enlargement of the mediastinal mass seen in figure 17-4. The left lower lobe infiltrate most likely represents pneumonitis secondary to compression of the mainstem bronchus. The patient had complained of recent cough with sputum production. There was no evidence of excess catecholamine secretion. (Fig. 2 from Lack EE, Stillinger RA, Colvin DB, Groves RM, Burnette DG. Aortico-pulmonary paraganglioma. Report of a case with ultrastructural study and review of the literature. Cancer 1979;43:269-278.)

Gross Findings. APPs range considerably in size, from 1.2 (32) to 17.0 cm, but are usually 5 to 7 cm in diameter (4,37). They may be rounded to ovoid and sharply demarcated, or flattened and expansile with indistinct borders and a tenacious attachment to vital structures, making complete surgical removal a major problem (4). Because of their location, APPs may encircle or partially envelop large vascular channels or encase or displace neural structures (4). Unless the pericardium is opened, some cardiac paragangliomas escape detection if they are flattened and easily compressed. An occasional tumor may have a polyploid configuration and protrude into the atrium.

Microscopic Findings. With adequate tissue sampling, the diagnosis of APP can be readily made based upon the organoid clustering of neoplastic cells forming "zellballen" (fig. 17-6), but with small biopsy specimens the diagnosis may be difficult, particularly if there is crush artifact. A sustentacular cell population can be demonstrated in APPs and other paragangliomas by staining for S-100 protein. Intracytoplasmic hyaline globules are rare in these and other head and neck paragangliomas. An unusual spindle cell pattern has been reported (40).

The presence of apparent "infiltration" of cardiac connective tissue or muscle is not considered a reliable indicator of malignancy (19). A pigmented cardiac paraganglioma was thought to contain melanin (25). A variety of other neoplasms enter into the differential diagnosis of APP, and several of these are discussed elsewhere (4).

Biologic Behavior. The incidence of malignancy of APPs with metastasis has been estimated at 13 (37) to 20 percent (45) of cases (fig. 17-7); however, the rarity of these tumors, particularly the malignant ones, may make them more likely to be reported and hence result in an overestimation of the true malignant potential. An even greater problem, however, is the relatively high rate of unresectability due to the dense adherence to or direct involvement of vital structures (4). Only 60 percent of patients with APPs have had complete surgical resection (45); this figure varies with APP size

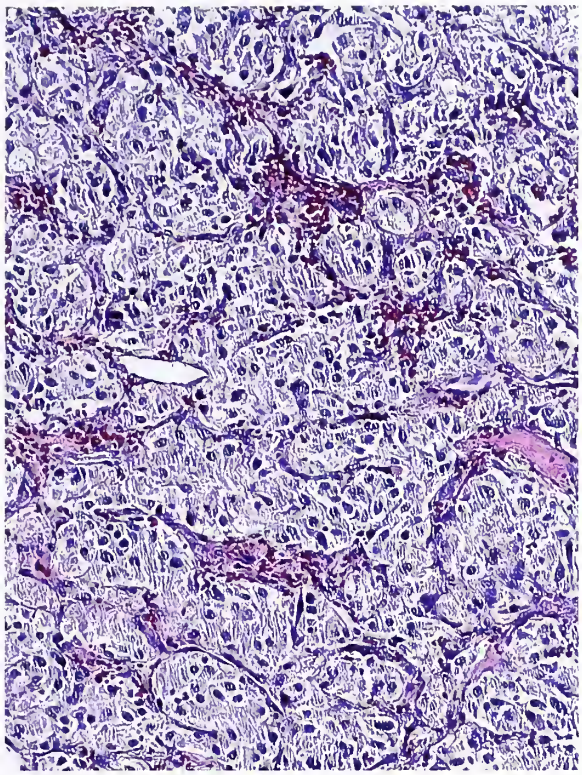

Figure 17-6

AORTICOPULMONARY PARAGANGLIOMA

The tumor cells have a nesting pattern with relatively abundant granular cytoplasm. Small nests and short cords of tumor cells were highlighted by staining for reticulum. (Fig. 20-6 from Fascicle 19, Third Series.)

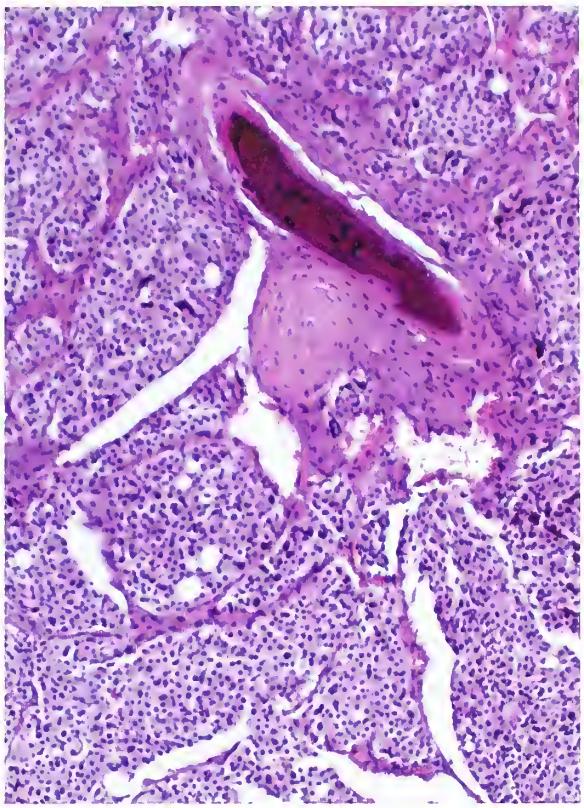

Figure 17-7

AORTICOPULMONARY PARAGANGLIOMA

Rib metastasis from aorticopulmonary paraganglioma arising near the root of the lung. Tumor retains a well-developed nesting ("zellballen") pattern.

and precise anatomic location. Surgical resection of cardiac paragangliomas may necessitate cardiopulmonary bypass with removal of portions of the heart involved by tumor, and fatalities have occurred intraoperatively due to excess bleeding (20,29). Preoperative embolization of an APP has been reported (46).

THE ENDOCRINE LUNG AND PULMONARY CHEMORECEPTORS: INNERVATED CLUSTERS OF PULMONARY NEUROENDOCRINE CELLS

Pulmonary neuroendocrine cells are solitary or arranged in small, discrete collections referred to as neuroepithelial bodies. They form ovoid to triangular corpuscles intercalated within the respiratory mucosa (fig. 17-8), and in experimental animals have been shown to be innervated by sensory nerve fibers of the vagus nerve (47). The corpuscular cell appears presynaptic to the nerve ending, thus permitting discharge of nerve impulses to the central nervous system (48). It has been proposed that innervated clusters of neuroendocrine cells (i.e., neuroepithelial bodies) may function as pulmonary airway chemoreceptors sensitive to hypoxia (49). It is clear from experimental data, coupled with results of a symposium on pulmonary neuroendocrine cells in health and disease (50), that the bronchopulmonary tree has physiologic functions and is not merely an airway conduit.

Structural changes, including hyperplasia of pulmonary neuroendocrine cells, have been reported in experimental animals (51), in humans living at high altitude (52), and in those with chronic bronchitis, emphysema (53), and pulmonary hypertension (54). A study of high altitude dwellers and lowlanders found no significant differences in structure, number,

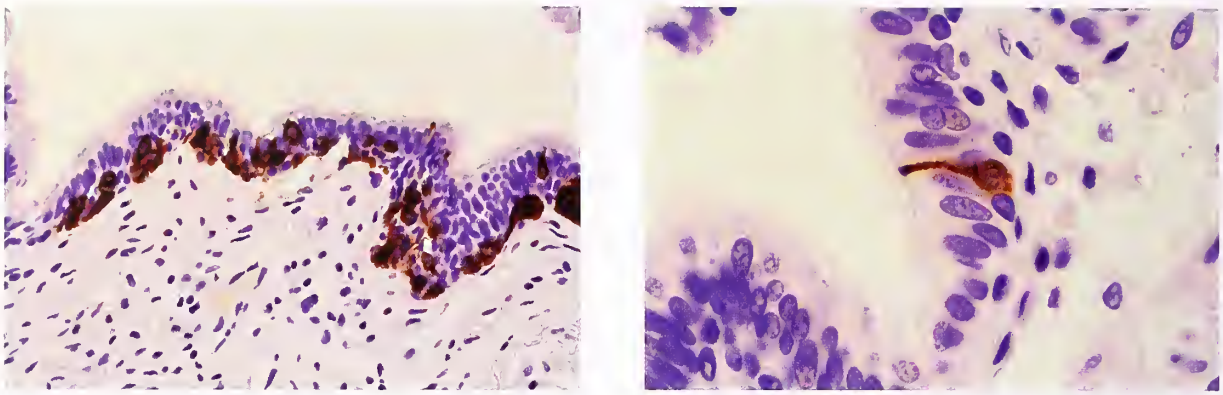

Figure 17-8

PULMONARY NEUROENDOCRINE CELLS

Left: Scattered collections of neuroendocrine cells are oriented along the basement membrane within the bronchial mucosa. Immunostain for chromogranin clearly delineates these cells (avidin-biotin peroxidase method).

Right: A solitary neuroendocrine cell is present near the basement membrane. A thin cytoplasmic extension courses up to the surface of airway (avidin-biotin peroxidase method).

content, or distribution of pulmonary neuroendocrine cells, but the number of cases was small and subtle changes may not achieve statistical significance (55). Presently, there does not appear to be sufficient data from human studies to draw any valid conclusions on the effects of high altitude on pulmonary neuroendocrine cells (56).

PULMONARY PARAGANGLIA

There are very few references to *pulmonary paraganglia* in the literature, and they are difficult to document in humans (4). In a study by Blessing and Hora (57) involving over 5,000 serial sections of a newborn human lung, 68 separate pulmonary paraganglia were identified (fig. 17-9). These paraganglia were in close proximity to blood vessels and nerves, and were often located near the pulmonary artery, especially in areas of branching. Based upon most of the illustrations, these appear to be genuine paraganglia, and the authors considered them to be chemoreceptors involved in regulating respiration and pulmonary blood flow (57). It is important to note that these paraganglia were not identified within the interstitium of alveolar walls or in conducting airway epithelium.

PULMONARY PARAGANGLIOMA

If the occurrence of normal paraganglia within the lung in association with blood vessels and nerves is accepted, then it follows that *pulmonary paragangliomas* exist as well, and indeed a number of such tumors have been reported in the literature (58–65), including one associated with ectopic adrenocorticotropic hormone (ACTH) hypersecretion (66). The author has not personally seen a case of primary pulmonary paraganglioma. A meaningful review of the clinical and pathologic features of these tumors is not possible because: 1) some reports lack detailed illustrations of pathology; 2) the tumors are difficult (if not impossible) to distinguish from some bronchial carcinoid tumors (fig. 17-10); and 3) distinction from metastatic paraganglioma to lung is difficult (4). Some of the reported pulmonary paragangliomas appear to have the typical architectural patterns seen in paragangliomas elsewhere in the head and neck region.

Differential Diagnosis. Pulmonary paragangliomas may be difficult to distinguish from bronchial carcinoid tumors. There are a number of morphologic features seen in bronchial carcinoid tumors that are not typical for a paraganglioma, but distinguishing the two may be more of an academic exercise since bronchial carcinoid tumors and most paragangliomas of the head and neck region have relatively limited malignant potential (4).

Another lesion in the differential diagnosis of a primary pulmonary paraganglioma is carcinoid tumorlet. These are usually peripheral in the lung and microscopic in size or only a few millimeters

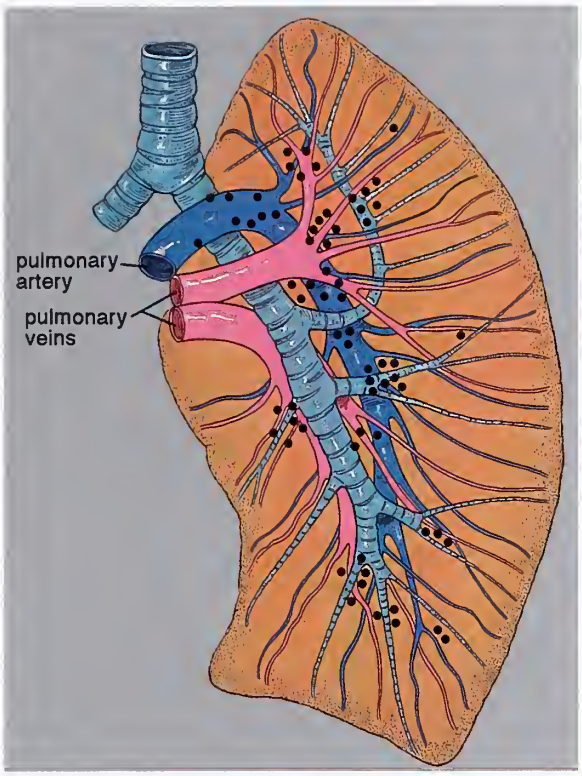

Figure 17-9

PULMONARY PARAGANGLIA

Distribution of pulmonary paraganglia in human fetal lung. Most have a centripetal location in relation to vessels and nerves. (Modified from fig.1 from Blessing MH, Hora BI. Glomera in der lunge des menschen. Z Zellforsch Mikrosk Anat 1968;87:562-70.) (Fig. 20-8 from Fascicle 19, Third Series.)

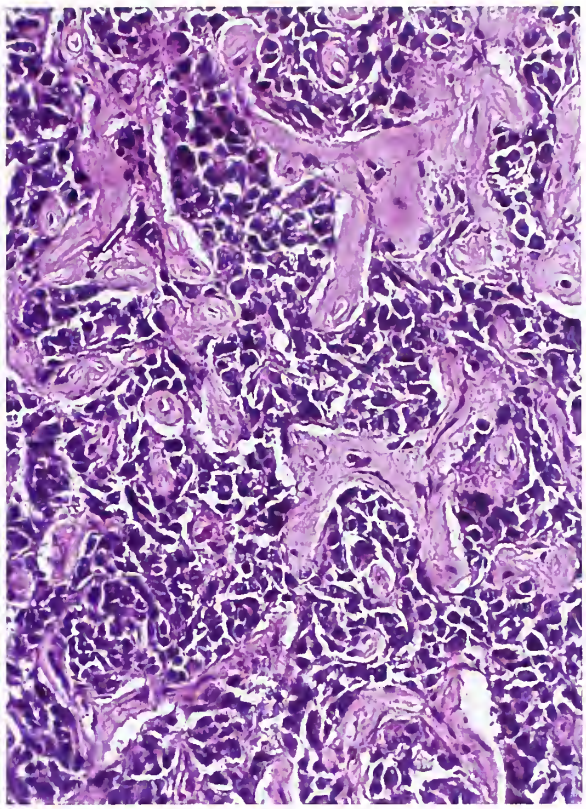

Figure 17-10

BRONCHIAL CARCINOID TUMOR MIMICKING PARAGANGLIOMA

The nesting arrangement of cells in a bronchial carcinoid tumor can mimic a paraganglioma. A small amount of fibrosis is present. (Fig. 20-9 from Fascicle 19, Third Series.)

in diameter (fig. 17-11). Carcinoid tumorlets are often related to bronchial or bronchiolar epithelium; they may progress to luminal obliteration or extend to involve adjacent lung parenchyma, with proliferation of connective tissue including elastosis (67). The organoid clustering of cells faintly resembles a paraganglioma, but close sectioning reveals continuity of one nest with another (68). Neurosecretory type granules have been demonstrated by electron microscopy (67–70). Carcinoid tumorlets are usually incidental findings, sometimes in lung parenchyma involved by bronchiectasis or other inflammatory processes, and are of no consequence to the patient. Metastases of carcinoid tumorlet to regional hilar lymph nodes occur occasionally (71); 2 of 85 cases originally reported by Whitwell in 1955 metastasized (72).

Minute meningothelial-like nodules (MMNs) were described by Korn et al. in 1960 (73), and were regarded as minute pulmonary tumors resembling chemodectomas. MMNs have been reported in 1 of 60 (74) to 1 of 300 autopsies (73), and there appears to be an increased frequency in lungs from patients with cardiac failure, chronic bronchitis, emphysema (73,75), and thromboemboli (76). A number of other investigators have regarded these as pulmonary chemoreceptors or chemodectomas analogous to the carotid body (76–79). Some even report an intensely positive argentaffin reaction within MMNs consistent with hyperplasia of endocrine type chemoreceptor tissue (78), although a subsequent ultrastructural study provided different conclusions and suggested a pleural origin (80). There is no relationship to paraganglia or

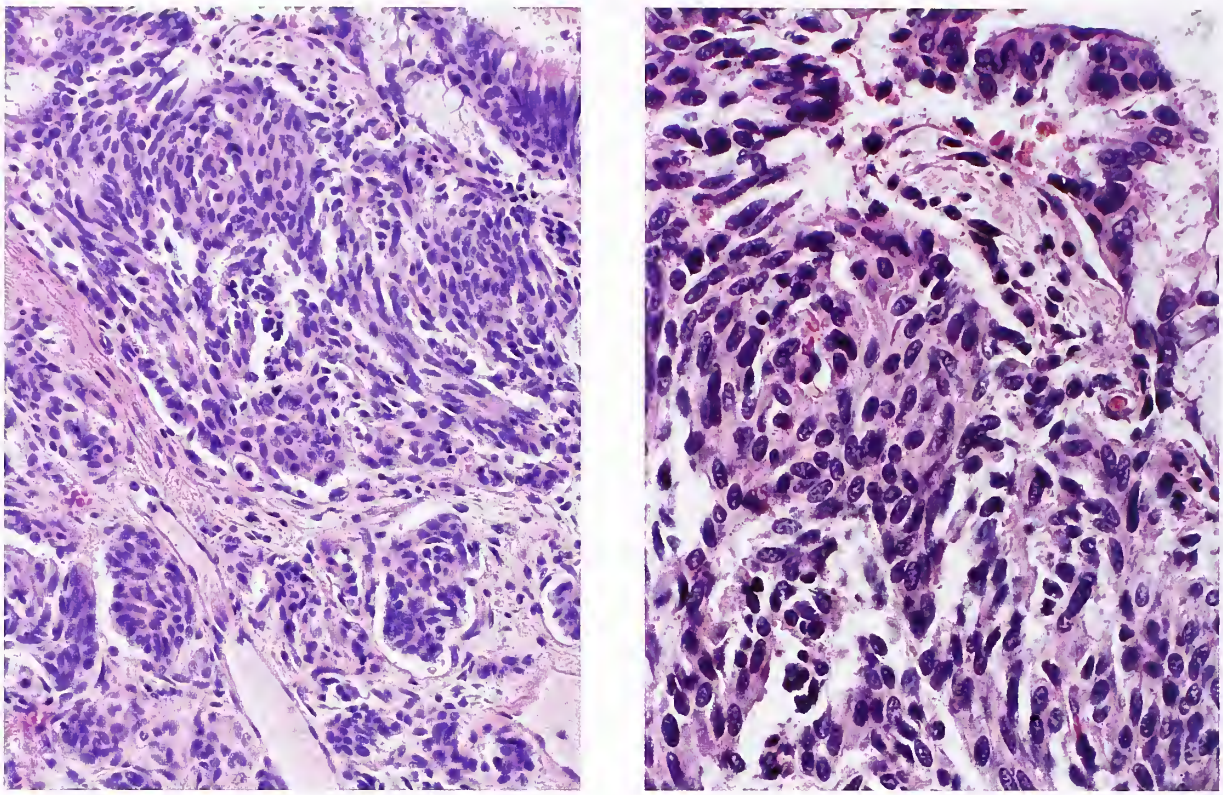

Figure 17-11

CARCINOID TUMORLET OF LUNG

Left: Multiple carcinoid tumorlets were found incidentally in a lobectomy specimen from a patient with bronchiectasis. The lesion abuts the epithelial lining of a terminal bronchiole. Nests of spindle to ovoid cells are separated by collagenous stroma.

Right: The carcinoid tumorlet has oval to elongated nuclei, many of which have finely stippled nuclear chromatin. (Fig. 20-11 from Fascicle 19, Third Series.)

paraganglioma. Other ultrastructural studies have confirmed the nonendocrine nature of these cells and proposed a strong resemblance to meningothelial cells (81,82). MMN often appears as a 1- to 3-mm, tan-yellow lesion that may be detected on gross examination. It is characteristically located in the pulmonary interstitium, expanding the alveolar septa (fig. 17-12). The cells have bland oval nuclei, often with a small dot-like nucleolus, and pale eosinophilic cytoplasm with indistinct borders, which may be arranged in nests, or "zellballen" (73). The existence of MMNs may help to explain the rare occurrence of primary pulmonary meningiomas (83). A recent study showed that isolated MMNs lacked mutations consistent with a reactive origin (84). In another recent study, diffuse meningotheliomatosis was diagnosed in patients who presented with dyspnea and shortness of breath and were evaluated for diffuse bilateral interstitial lung infiltrates (85).

PARAGANGLIOMAS AT OTHER SITES IN THE HEAD AND NECK REGION

Paragangliomas of the head and neck region occasionally occur in unusual or unexpected sites where normal paraganglia have not been documented in humans, and may pose a formidable diagnostic challenge for the pathologist (4). Brief consideration is given to some of these rare tumors.

Orbital Paraganglioma

General Comments. The orbit is one of a number of anatomic sites in which the existence of normal paraganglia is not well documented in humans (4). A ciliary paraganglion has been noted in the chimpanzee (86), and an intraorbital

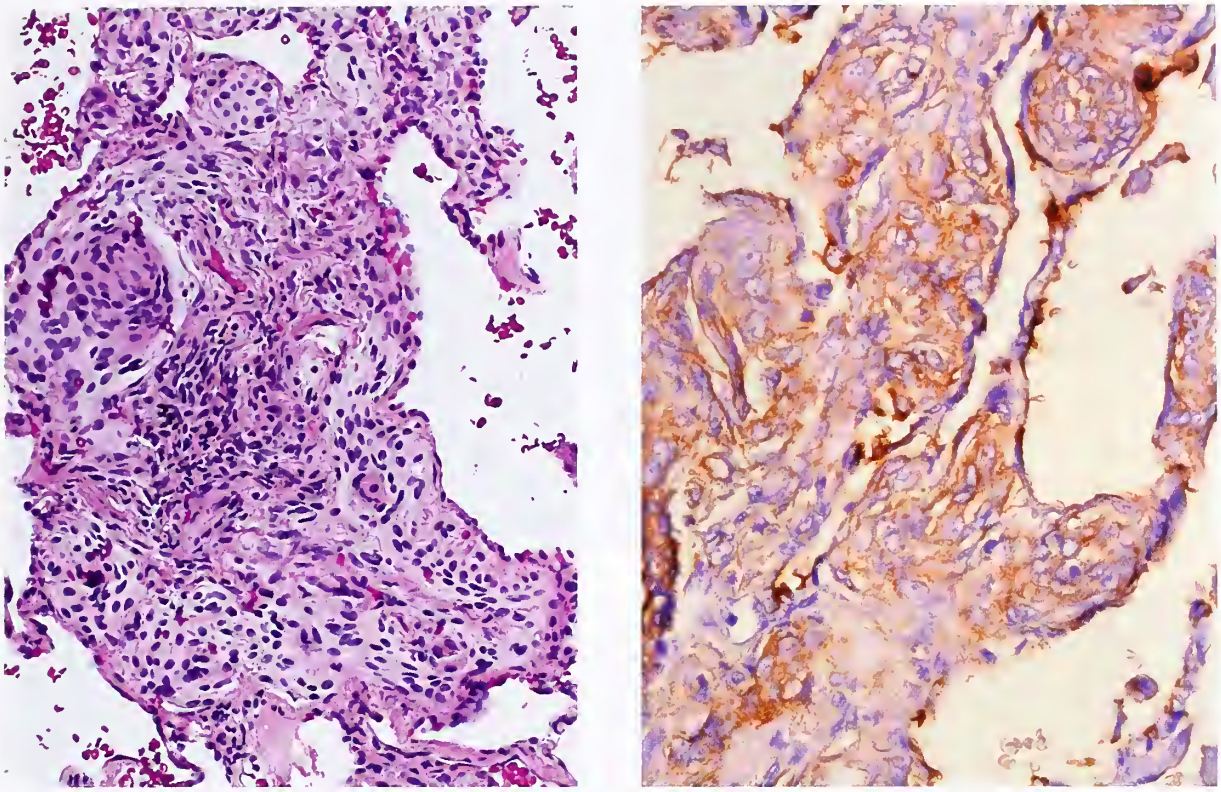

Figure 17-12

MINUTE MENINGOTHELIAL-LIKE NODULE

Left: The lesion formerly referred to as pulmonary "chemodectoma" is composed of nests of oval uniform cells which expand the interstitium of alveolar septa. (Fig. 20-12 from Fascicle 19, Third Series.)

Right: Immunostain for epithelial membrane antigen highlights the cytoplasmic borders of the meningothelial-like cells (avidin-biotin peroxidase method).

paraganglion was reported in a human newborn (87), but the normal anatomic distribution and microanatomy of orbital paraganglia in humans are essentially unknown. Several studies of retroorbital tissues in both adults and infants have failed to identify paraganglia, however, some orbital paragangliomas seem to arise at this site.

The first orbital paraganglioma was reported in 1952 by Fisher and Hazard (88). Zak and Lawson (89) identified 17 cases in the 25-year period since that initial report. Additional cases have been reported in various languages (4), with one reported twice in the same year (90, 91). Intense scrutiny of the literature will undoubtedly reveal additional cases with different designations. A melanotic paraganglioma of the orbit has also been reported (92), but the histopathology deviates significantly from that of traditional paragangliomas.

Clinical and Pathologic Findings. A review of orbital paragangliomas showed a roughly equal distribution with regard to sex and laterality, and a varied range in age at diagnosis (93). Establishing a clinical and pathologic profile of these tumors is difficult since some cases have marginal pathologic documentation and follow-up information may be quite limited (4). Some tumors would be reclassified as alveolar soft-part sarcoma, an important tumor to consider in the differential diagnosis of orbital paraganglioma.

The most common presenting sign of orbital paraganglioma is proptosis (94), which may be pulsatile (4,93). The tumor may be situated in any quadrant of the orbit and retrobulbar space, and it may cause disturbance in ocular mobility, visual loss, or diplopia. Other manifestations include conjunctival redness, photophobia, and papilledema (93). Orbital paragangliomas have

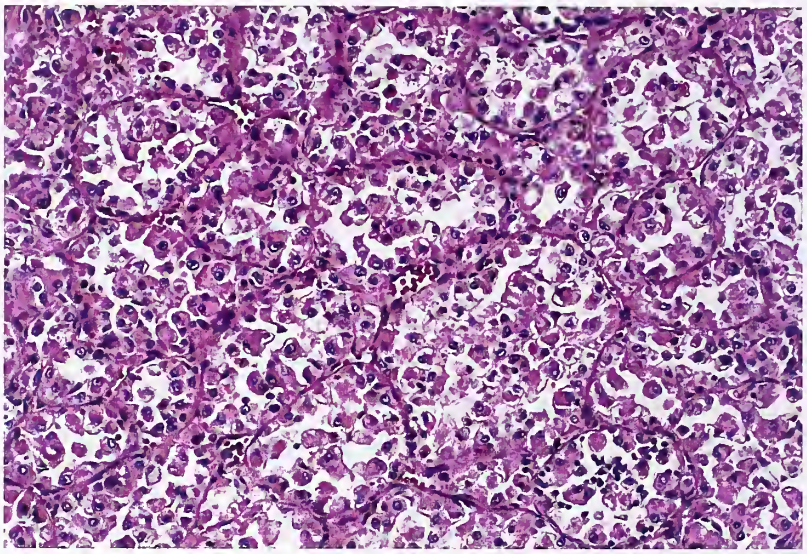

Figure 17-13

ALVEOLAR SOFT-PART SARCOMA

There is a rigid alveolar pattern with discohesion of tumor cells. This tumor was formerly regarded as a malignant nonchromaffin paraganglioma. (Fig. 21-1 from Fascicle 19, Third Series.)

been reported in association with other paragangliomas such as carotid body paraganglioma (95) and jugulotympanic paraganglioma (93). In a study of 53 neurogenic orbital tumors, 1 was classified as an orbital paraganglioma (96). An intracranial paraganglioma with secondary orbital extension has been reported (97).

The pathologic features of orbital paraganglioma in well-documented cases are typical for paragangliomas in general. Other tumors that should be considered in the differential diagnosis include alveolar soft-part sarcoma and carcinoid tumors (4). Metastasis of orbital paraganglioma can occur, but it appears to be unusual; a greater problem is local recurrence (or persistence) of tumor following attempt at surgical resection including orbital exenteration (93).

Differential Diagnosis. A number of orbital tumors classified as orbital paraganglioma (chemodectoma or nonchromaffin paraganglioma) are in fact alveolar soft-part sarcomas (98–100). The latter designation was given by Christopherson et al. (101) for a distinctive neoplasm of uncertain histogenesis; the same tumor had been classified by Smetana and Scott (102) as a malignant nonchromaffin paraganglioma. The tumor occurs in a wide variety of sites, usually in the lower extremities in association with a large muscle group (103), but may arise in the retroperitoneum and orbit.

Regardless of anatomic site of origin, the histopathology of alveolar soft-part sarcoma is distinctive, with a rigid organoid pattern and delicate microvasculature (fig. 17-13). Tumor cells may be discohesive, with exfoliation into the alveolar spaces. The architectural pattern can be confused with a paraganglioma, particularly when the alveolar spaces are not as conspicuous. Tumor cells tend to have relatively abundant granular eosinophilic cytoplasm, a round to ovoid nucleus with vesicular chromatin, and a prominent nucleolus. A characteristic feature is the presence of intracytoplasmic crystalline material that is periodic acid-Schiff (PAS) positive and resistant to diastase predigestion (fig. 17-14). This material has been noted in 22 percent (104) to 80 percent (105) of tumors. On ultrastructural study, the crystals are electron-dense rhomboid or rod-like structures that are membrane bound; they have a parallel crystalline array of rigid "fibers" with a diameter of about 5 nm and periodicity of about 10 nm (103,106). There may be a morphologic transition between the small, membrane-bound granules and the larger rhomboid crystals (103). A number of immunohistochemical studies provide support for a myogenous phenotype, although results are not entirely consistent in each case, and a few studies do not confirm myogenic origin. Recently, aberrantly strong nuclear immunoreactivity for the C-terminal portion of *TFE3* (a transcription factor gene) was reported for a group of tumors including alveolar soft-part sarcoma and a specific subset of renal carcinomas (107).

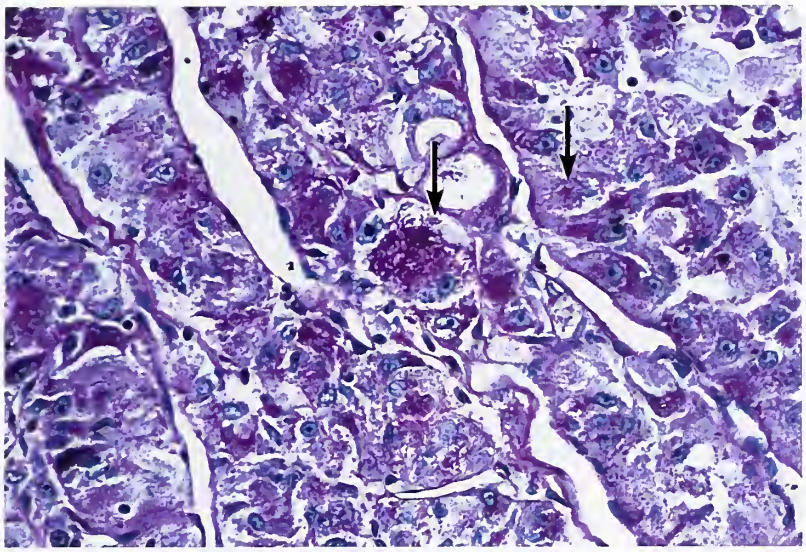

Figure 17-14

ALVEOLAR SOFT-PART SARCOMA

Many tumor cells contain darkly stained, amorphous to needle-shaped structures (arrows) (periodic acid–Schiff [PAS] stain following diastase predigestion). (Fig. 21-2 from Fascicle 19, Third Series.)

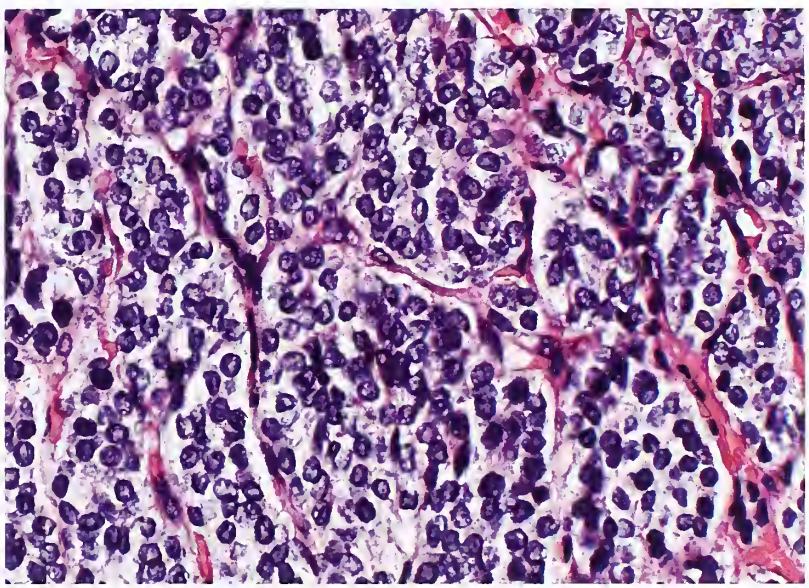

Figure 17-15

CARCINOID TUMOR

This orbital tumor was initially interpreted as a nonchromaffin paraganglioma, but is considered most likely a carcinoid tumor. The patient had no evidence of a primary tumor elsewhere. Ultrastructural study showed dense-core neurosecretory type granules. (Fig. 21-3 from Fascicle 19, Third Series.)

Carcinoid Tumors

Carcinoid tumors involving the eye and orbit are usually metastatic from a bronchial primary (108), occasionally from the ileum, and rarely the colon. The orbit is rarely cited as the primary site for a carcinoid tumor (109). One patient seen at Memorial Hospital complained of eye swelling of a few months' duration and on examination had pulsatile exophthalmos (110,111). There was evidence of destruction of the lateral wall and roof of the orbit, and carotid angiogram revealed a large vascular mass extending deep into the orbital cone. The biopsy showed a tumor that had initially been diagnosed as a "nonchromaffin paraganglioma" (110), but later was considered to be a carcinoid tumor (fig. 17-15) (111). The patient developed skeletal metastases several years following diagnosis, but there was still no evidence of a primary tumor elsewhere.

Paraganglioma of Nasal Cavity and Nasopharynx

Rare paragangliomas have been reported primary in the nasopharynx and paranasal sinus

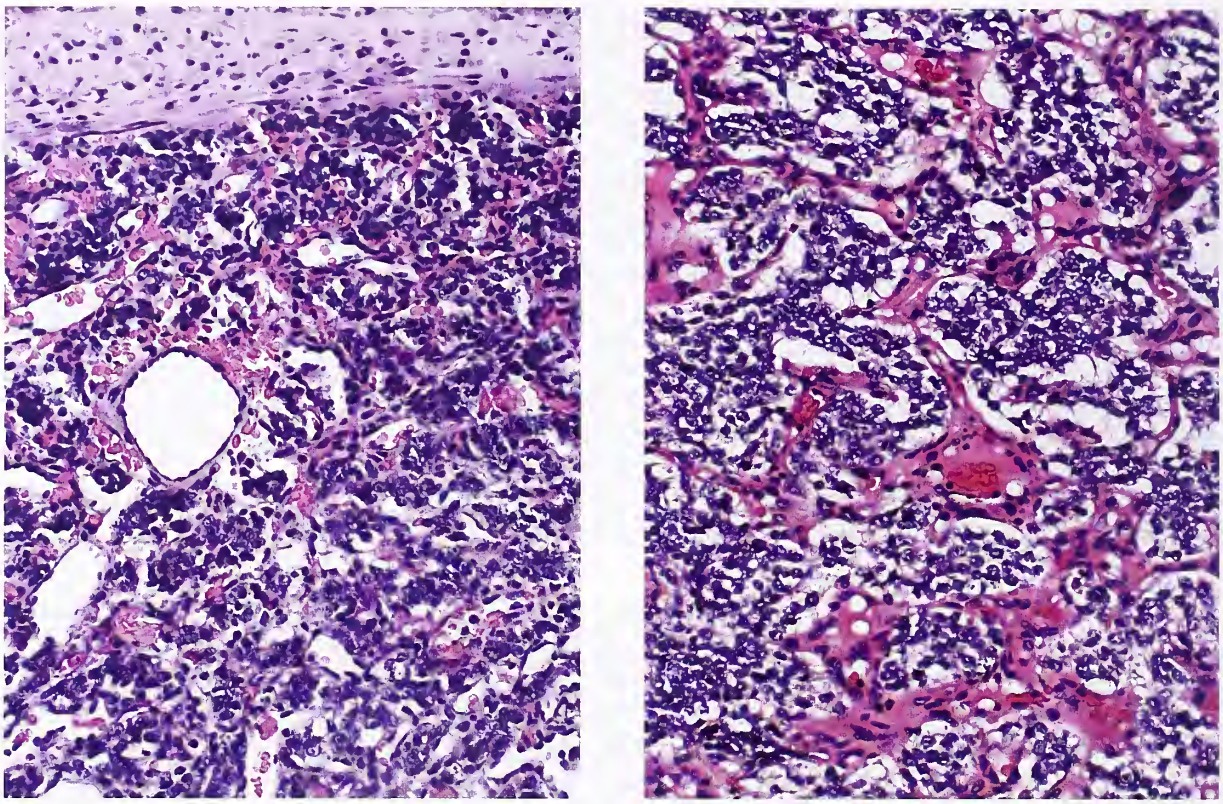

Figure 17-16

PRIMARY NASAL PARAGANGLIOMA

Left: Primary nasal paraganglioma had recurred locally on three occasions and at final surgery appeared as a polypoid mass attached to the cribriform plate. Respiratory type mucosa was present over a portion of the tumor.

Right: A prominent nesting pattern with "zellballen" is present. Most of the intervening vascular spaces appear devoid of blood. (L&R: Fig. 21-4 from Fascicle 19, Third Series.)

(112,113) as well as soft palate (114) and pterygopalatine fossa (115). A few paragangliomas reported in the nasopharynx were presumed to originate in the area of the ganglion nodosum and hence may be vagal paragangliomas (116).

Most patients are female, and the range in age at diagnosis is quite wide. In most cases, the tumor is a polypoid or exophytic mass ranging in size from 1.5 to 4.0 cm (116). Profuse bleeding may occur either spontaneously or during attempted surgery.

Normal paraganglia have not been well documented to explain the varied anatomic locations of these paragangliomas (116). One nasal paraganglioma recurred several times over a 4-year period (117,118), and was diagnosed by the late Dr. Frank W. Foote as a "carotid body-type tumor" (fig. 17-16).

Primary Thyroid Paraganglioma

There have been a small number of paragangliomas originating within thyroid parenchyma (119–123) or immediately adjacent to the gland (124). The study by Zak and Lawson (125) documents the presence of paraganglionic tissue adjacent to (fig. 17-17) or within the thyroid capsule, but there is no documentation of paraganglia actually within the substance of the gland. Some have regarded these paraganglia as misplaced inferior laryngeal paraganglia and advocate grouping thyroid paragangliomas with inferior laryngeal paragangliomas (126). In one case the thyroid paraganglioma was associated with bilateral carotid body paragangliomas (127), while in another case, a papillary thyroid carcinoma and a parathyroid adenoma were present (128).

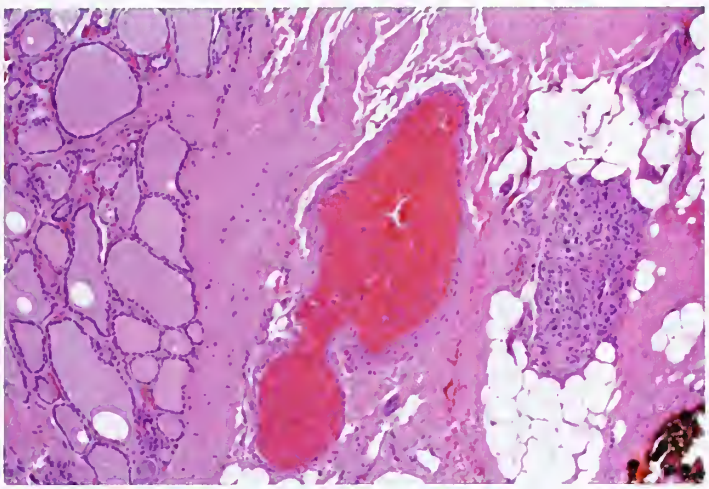

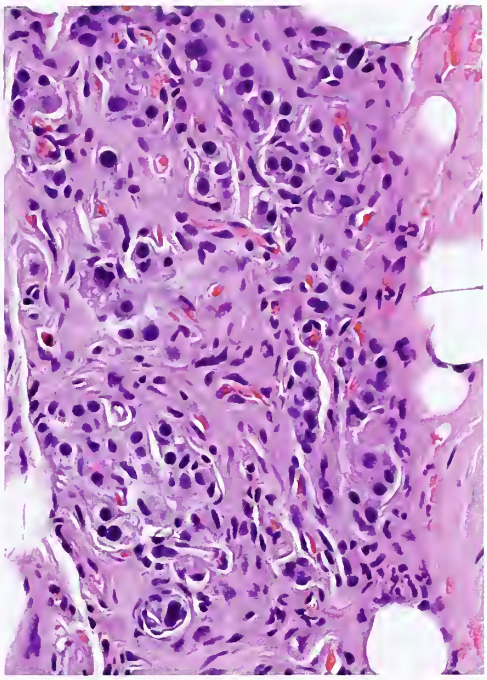

Figure 17-17

NORMAL PARAGANGLION ADJACENT TO THYROID

Above: The paraganglion is located within fibrofatty connective tissue adjacent to the thyroid gland.

Right: The normal paraganglion contains small nests of chief cells.

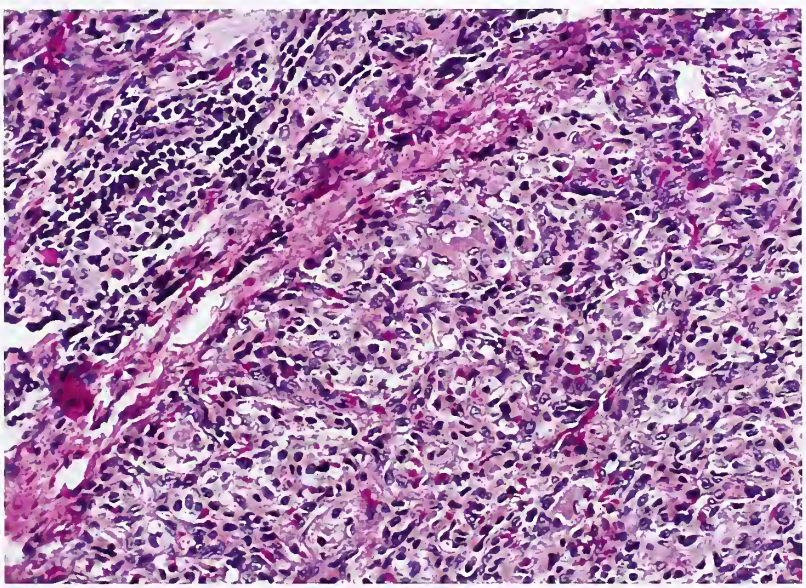

Figure 17-18

PRIMARY THYROID PARAGANGLIOMA

This primary thyroid paraganglioma in a 56-year-old woman was originally regarded as medullary thyroid carcinoma. The tumor has fine interlacing fibrous stroma with distinct nests of neoplastic epithelioid chief cells. Residual inflamed thyroid is present at the top left. (Fig. 21-5 from Fascicle 19, Third Series.) (Figs. 17-18 through 17-21 are from the same case.)

Thyroid paraganglioma can be mistaken for medullary thyroid carcinoma, but the classic nesting pattern (figs. 17-18, 17-19) and absence of amyloid stroma are features of paraganglioma. Immunohistochemical staining for chromogranin is usually positive in both tumors (fig. 17-20), but the demonstration of abundant sustentacular cells at the periphery of clusters of chief cells is a feature more characteristic of thyroid paraganglioma (fig. 17-21). A recent case of medullary thyroid carcinoma was reported with S-100 protein–positive sustentacular-like cells, which might make distinction from paraganglioma more problematic (129). The tumor illustrated in figures 17-18 through 17-21 was negative for thyrocalcitonin, carcinoembryonic antigen, and cytokeratin. Of thyroid paragangliomas reported to date, two were locally invasive (121,130).

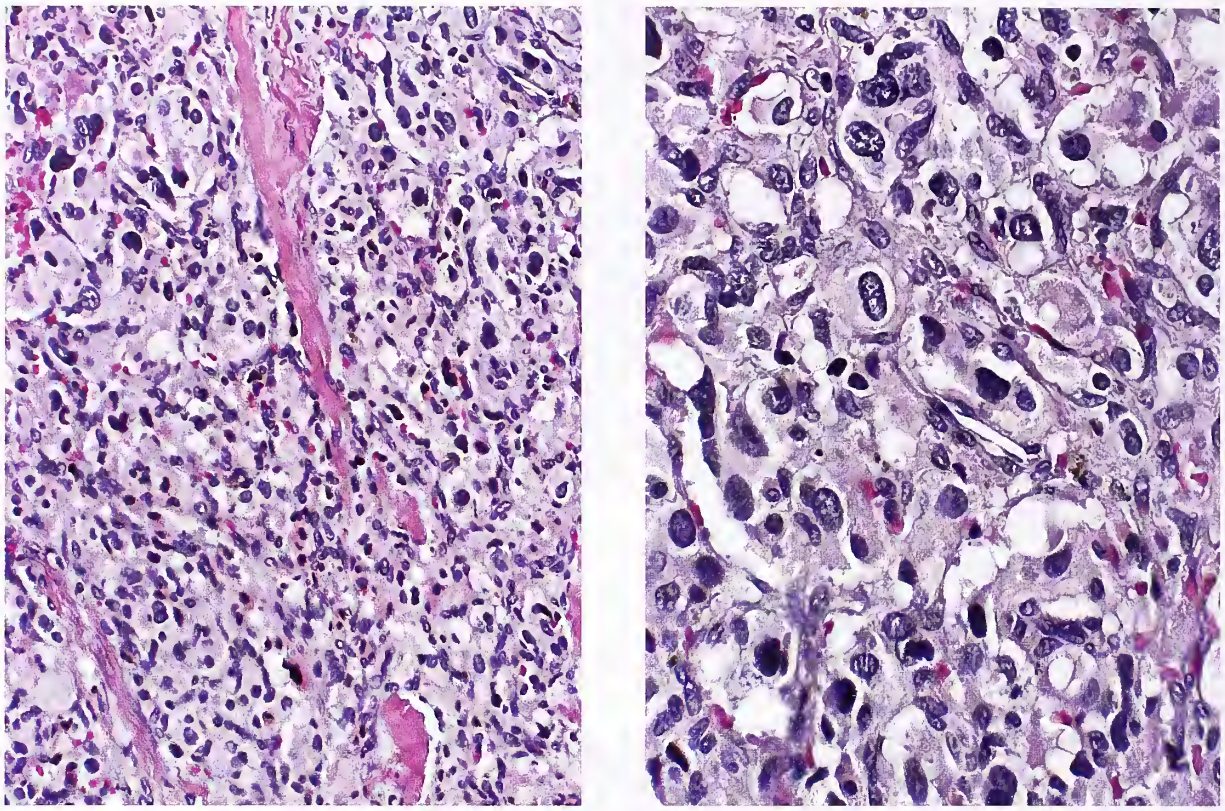

Figure 17-19

PRIMARY THYROID PARAGANGLIOMA

Left: Organoid clusters of cells have a prominent microvasculature.

Right: The histologic features are indistinguishable from those of paragangliomas elsewhere in the head and neck region. (L&R: Fig. 21-6 from Fascicle 19, Third Series.)

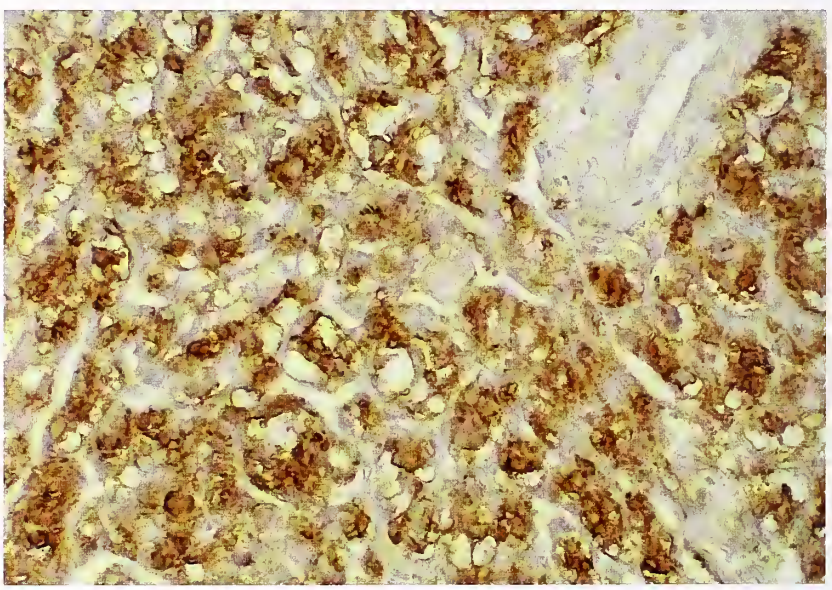

Figure 17-20

PRIMARY THYROID PARAGANGLIOMA

Recurrent primary thyroid paraganglioma contains numerous cells that are strongly immunoreactive for chromogranin (avidin-biotin peroxidase method). (Fig. 21-7 from Fascicle 19, Third Series.)

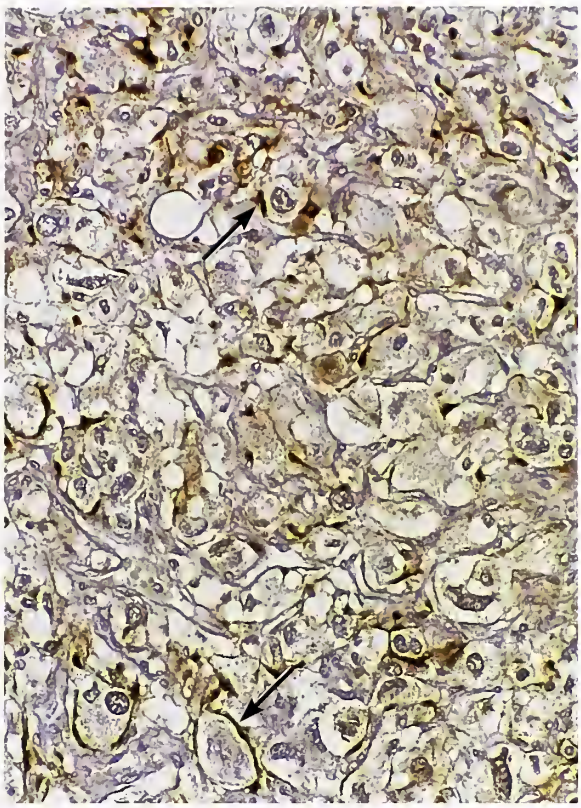

Figure 17-21

PRIMARY THYROID PARAGANGLIOMA

Immunostain for S-100 protein shows numerous slender to dendritic sustentacular cells (both nucleus and cytoplasm are immunoreactive) at the periphery of clusters of neoplastic chief cells (arrows) (avidin-biotin peroxidase method). (Fig. 21-8 from Fascicle 19, Third Series.)

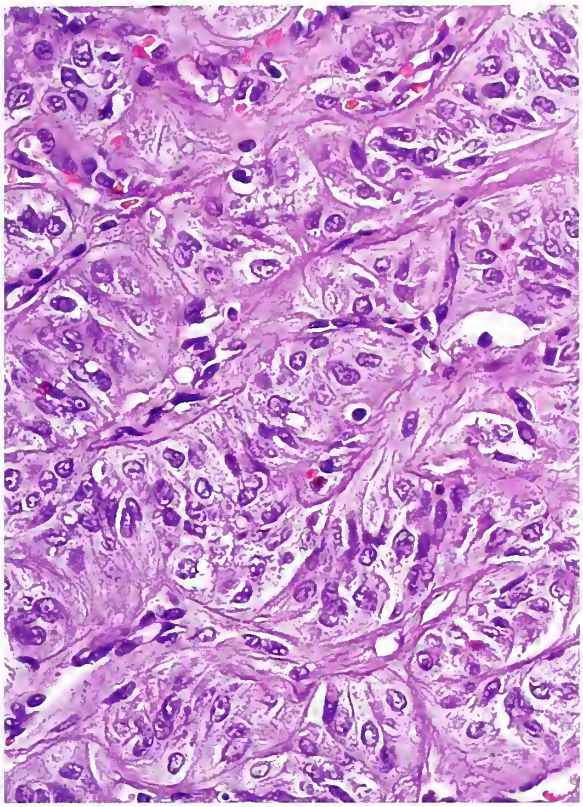

Figure 17-22

HYALINIZING TRABECULAR ADENOMA

The organoid trabecular pattern consists of elongated cells arranged around capillaries. The patient had multifocal areas of papillary thyroid carcinoma elsewhere in the gland.

Another thyroid lesion that may mimic a primary thyroid paraganglioma is hyalinizing trabecular tumor (HTT) or adenoma (HTA) of the thyroid (fig. 17-22) (131,132). Bronner et al. (133) refer to this lesion of the thyroid, which may have histologic features resembling paraganglioma, as "paraganglioma-like adenoma of the thyroid." The specificity of this lesion might be questioned since a HTT-like pattern has been reported in adenomatous nodules (119), lymphocytic thyroiditis (134), and thyroid adenoma, and some have identified malignant features in HTT (135). HTT of the thyroid may be regarded as a reasonably distinct variant of thyroid adenoma when it occurs as a solitary, well-circumscribed or encapsulated mass. An encapsulated variant of medullary thyroid carcinoma has been described which also resembles the HTT of the thyroid (136). Some feel that the HTT is a morphologic variant of papillary thyroid carcinoma based upon the finding of a gene rearrangement (137). A recent review of HTT summarized some of the controversial and complex relationships with papillary thyroid carcinoma (138).

Paragangliomas in Other Locations

Paragangliomas have been reported in exotic sites such as face (139), external ear (140), tongue (141), cheek (142), intracerebral (pineal gland and area of the sella) (143), cerebellum (144), and esophagus (145), anatomic sites in which normal paraganglionic tissue is not well documented. Paraganglioma of trachea has been

documented, and if the tumor arises superiorly near the thyroid or cricoid cartilage it could originate from paraganglia normally residing there. A case of paraganglioma arising within a parathyroid gland has also been reported (146).

REFERENCES

Aorticopulmonary Paraganglia

1. Wiesel J. Über erkrankungen der koronararterien im verlaufe akuter infektionskrankheiten. Wien Klin Wochenschr 1906;19:723-725.
2. Busacchi P. I corpi cromaffini del cuore umano. Arch Ital Anat Embriol 1912-1913;11:352-376.
3. Penitschka W. Paraganglion aorticum supracardiale. Z Mikros Anat Forsch 1931;24:24-37.
4. Lack EE. Pathology of adrenal and extra-adrenal paraganglia. Major problems in pathology, Vol 29. Philadelphia: WB Saunders; 1994.
5. Blessing MH. [On glomus cells in the supracardial space.] Klin Wochenschr 1963;41:1025-1026. [German.]
6. Boyd JD. The inferior aortico-pulmonary glomus. Brit Med Bull 1961;17:127-131.
7. Becker AE. The glomera in the region of the heart and great vessels. A microscopic-anatomical and histochemical study. MD thesis, Laboratory of Pathological Anatomy of the University of Amsterdam; 1966.
8. Edwards C, Heath D. Microanatomy of glomic tissue of the pulmonary trunk. Thorax 1969;24: 209-217.
9. Krahl VE. The glomus pulmonale: its location and microscopic anatomy. In: De Reuck AU, O'Connor M, eds. Ciba foundation symposium on pulmonary structure and function. Boston: Little Brown and Co; 1962:53-76.
10. Edwards C, Heath D. Site and blood supply of the intertruncal glomera. Cardiovasc Res 1970;4:502-508.
11. Dail WG Jr, Palmer GC. Localization and correlation of catecholamine-containing cells with adenyl cyclase and phosphodiesterase activities in the human fetal heart. Anat Rec 1973;177:265-288.
12. Gobbi H, Barbosa AJ, Teixeira VP, Almeida HO. Immunocytochemical identification of neuroendocrine markers in human cardiac paraganglion-like structures. Histochemistry 1991;95:337-340.
13. Kjaergaard J. Anatomy of the carotid glomus and carotid glomus-like bodies (nonchromaffin paraganglia) with electron microscopy and comparison of human foetal carotid, aorticopulmonary, subclavian, tympanojugular, and vagal glomera. Copenhagen: FADL's Forlag; 1973.
14. James TN. Degenerative lesions of a coronary chemoreceptor and nearby neural elements in the hearts of victims of sudden death. J Am Coll Cardiol 1986;8:12A-21A.

Aorticopulmonary Paraganglioma

15. Benjamin SP, McCormack LJ, Effler DB, Groves LK. Primary tumors of the mediastinum. Chest 1972;62:297-303.
16. Kwon HJ, Park JH, Jin GY, et al. Posterior mediastinal paraganglioma with bilateral adrenal pheochromocytoma. Respir Med 2004;98:574-576.
17. Del Fante FM, Watkins E Jr. Chemodectoma of the heart in a patient with multiple chemodectomas and familial history. Case report and survey of literature. Lahey Clin Found Bull 1967; 16:224-229.
18. Hodgson SF, Sheps SG, Subramanian R, Lie JT, Carney JA. Catecholamine-secreting paraganglioma of the interatrial septum. Am J Med 1984;77:157-161.
19. Johnson TL, Lloyd RV, Shapiro B, et al. Cardiac paragangliomas. A clinicopathologic and immunohistochemical study of four cases. Am J Surg Pathol 1985;9:827-834.
20. Cooley DA, Reardon MJ, Frazier OH, Angelini P. Human cardiac explantation and autotransplantation: application in a patient with a large cardiac pheochromocytoma. Tex Heart Inst J 1985; 12:171-176.
21. Dunn GD, Brown MJ, Sapsford RN, et al. Functioning middle mediastinal paraganglioma (phaeochromocytoma) associated with intercarotid paragangliomas. Lancet 1986;1:1061-1064.
22. Hui G, McAllister HA, Angelini P. Left atrial paraganglioma: report of a case and review of the literature. Am Heart J 1987;113:1230-1234.
23 Sawka AM, Young WF Jr, Schaff HV. Cardiac phaeochromocytoma presenting with severe hypertension and chest pain. Clin Endocrinol (Oxf) 2001;54:689-692.
24. Meunier JP, Tatou E, Bernard A, Brenot R, David M. Cardiac pheochromocytoma. Ann Thorac Surg 2001;71:712-713.
25. Mikolaenko I, Galliani CA, Davis GG. Pigmented cardiac paraganglioma. Arch Pathol Lab Med 2001;125:680-682.

26. Orenstein HH, Green GE, Kancherla PL. Aortocoronary paraganglioma. Anatomic relationship of left coronary artery to paraganglia of aorta. N Y State J Med 1984;84:33-36.
27. Levi B, Cain AS, Dorzab WE. Coronary paraganglioma. Clin Cardiol 1982;5:505-510.
28. Wilson AC, Bennett RC, Niall JF, Clarebrough JK, Doyle AE, Louis WJ. An unusual case of intrathoracic pheochromocytoma. Aust N Z J Surg 1974;44:27-32.
29. Orringer MB, Sisson JC, Glazer G, et al. Surgical treatment of cardiac pheochromocytomas. J Thorac Cardiovasc Surg 1984;89:753-757.
30. Sheps SG, Brown ML. Localization of mediastinal paragangliomas (pheochromocytoma). Chest 1985;87:807-809.
31. Swensen SJ, Brown ML, Sheps SG, et al. Use of 131I-MIBG scintigraphy in the evaluation of suspected pheochromocytoma. Mayo Clin Proc 1985;60:299-304.
32. Lattes R. Nonchromaffin paraganglioma of ganglion nodosum, carotid body, and aortic-arch bodies. Cancer 1950;3:667-694.
33. Monro RS. The morphology of the branchial glomera and their tumours, with a report of a case of aortico-pulmonary glomus tumour. Br J Surg 1950;38:105-109.
34. MacDonald RA. A carotid-body-like tumor on the left subclavian artery. AMA Arch Pathol 1956;62:107-111.
35. Pachter MR. Mediastinal nonchromaffin paraganglioma. A clinicopathologic study based on eight cases. J Thorac Cardiovasc Surg 1963;45:152-160.
36. Olson JL, Salyer WR. Mediastinal paragangliomas (aortic body tumor). A report of four cases and a review of the literature. Cancer 1978;41:2405-2412.
37. Lack EE, Stillinger RA, Colvin DB, Groves RM. Burnette DG. Aortico-pulmonary paraganglioma: report of a case with ultrastructural study and review of the literature. Cancer 1979;43:269-278.
38. Cueto-Garcia L, Shub C, Sheps SG, Puga FJ. Two-dimensional echocardiographic detection of mediastinal pheochromocytoma. Chest 1985;87: 834-836.
39. Flickinger FW, Yuh WT, Behrendt DM. Magnetic resonance imaging of mediastinal paraganglioma. Chest 1988;94:652-654.
40. Moran CA, Suster S, Fishback N, Koss MN. Mediastinal paragangliomas. A clinicopathologic and immunohistochemical study of 16 cases. Cancer 1993;72:2358-2364.
41. Hann U, Geist-Barth B, Menon AK, Greschniok A, Hoffmann J, Raygrotzki S. Aortico-pulmonary paraganglioma associated with bilateral carotid body tumors. Diagnostic presentation and clinical implications. J Cardiovasc Surg (Torino) 2001; 42:131-134.
42. Shapiro B, Sisson J, Kalff V, et al. The location of middle mediastinal pheochromocytomas. J Thorac Cardiovasc Surg 1984;87:814-820.
43. Carney JA. The triad of gastric epithelioid leiomyosarcoma, pulmonary chondroma, and functioning extra-adrenal paraganglioma: a five-year review. Medicine (Baltimore) 1983;62:159-169.
44. Carney JA. Gastric stromal sarcoma, pulmonary chondroma, and extra-adrenal paraganglioma (Carney triad): natural history, adrenocortical component, and possible familial occurrence. Mayo Clin Proc 1999;74:543-552.
45. Zak FG, Lawson W. The paraganglionic chemoreceptor system physiology, pathology and clinical medicine. New York: Springer-Verlag; 1982.
46. Rakovich G, Ferraro P, Therasse E, Duranceau A. Preoperative embolization in the management of a mediastinal paraganglioma. Ann Thorac Surg 2001;72:601-603.

The Endocrine Lung and Pulmonary Chemoreceptors

47. Lauweryns JM, Van Lommel AT, Dom RJ. Innervation of rabbit intrapulmonary neuroepithelial bodies. Quantitative and qualitative ultrastructural study after vagotomy. J Neurol Sci 1985;67:81-92.
48. Lauweryns JM, Van Lommel A. Ultrastructure of nerve endings and synaptic junctions in rabbit intrapulmonary neuroepithelial bodies: a single and serial section analysis. J Anat 1987;151:65-83.
49. Lauweryns JM, Cokelaere M. Hypoxia-sensitive neuro-epithelial bodies. Intrapulmonary secretory neuroreceptors, modulated by the CNS. Z Zellforsch Mikrosk Anat 1973;145:521-540.
50. Workshop on pulmonary neuroendocrine cells in health and disease. Proceedings. Bethesda, Maryland, Sept. 5-6, 1991. Anat Rec 1993;236:1-256.
51. Taylor W. Pulmonary argyrophil cells at high altitude. J Pathol 1977;122:137-144.
52. Memoli VA, Linnoila I, Warren WH, Rios-Dalenz J, Gould VE. Hyperplasia of pulmonary neuroendocrine cells and neuroepithelial bodies [Abstract]. Lab Invest 1983;48:57A.
53. Gosney JR, Sissons MC, Allibone RO, Blakey AF. Pulmonary endocrine cells in chronic bronchitis and emphysema. J Pathol 1989;157:127-133.
54. Gosney J, Heath D, Smith P, Harris P, Yacoub M. Pulmonary endocrine cells in pulmonary arterial disease. Arch Pathol Lab Med 1989;113:337-341.
55. Williams D, Heath D, Gosney J, Rios-Dalenz J. Pulmonary endocrine cells of Aymara indians from the Bolivian Andes. Thorax 1993;48:52-56.

56. Gosney JR. Pulmonary neuroendocrine cells in species at high altitude. Anat Rec 1993:236:105-107.

Pulmonary Paraganglia

57. Blessing MH, Hora BI. [Glomera in the human lung.] Z Zellforsch Mikrosk Anat 1968;87:562-570. [German.]

Pulmonary Paraganglioma

58. Heppleston AG. A carotid-body-like tumour in the lung. J Pathol Bacteriol 1958;75:461-464.
59. Blessing MH, Borchard F, Lenz W. [Glomus tumour (so-called chemodectomas of the lung. Pathological and biological findings.] Virchows Arch A Pathol Anat 1973; 359:315-329. [German.]
60. Fawcett FJ, Husband EM. Chemodectoma of lung. J Clin Pathol 1967;20:260-262.
61. Singh G, Lee RE, Brooks DH. Primary pulmonary paraganglioma: report of a case and review of the literature. Cancer 1977;40:2286-2289.
62. Hangartner JR, Loosemore TM, Burke M, Pepper JR. Malignant primary pulmonary paraganglioma. Thorax 1989;44:154-156.
63. Saeki T, Akiba T, Joh K, et al. An extremely large solitary primary paraganglioma of the lung: report of a case. Surg Today 1999;29:1195-1200.
64. Aubertine CL, Flieder DB. Primary paraganglioma of the lung. Ann Diagn Pathol 2004;8: 237-241.
65. Shibahara J, Goto A, Niki T, Tanaka M, Nakajima J, Fukayama M. Primary pulmonary paraganglioma: report of a functioning case with immunohistochemical and ultrastructural study. Am J Surg Pathol 2004;28:825-829.
66. Dahir KM, Gonzalez A, Revelo MP, Ahmed SR, Roberts JR, Blevins LS Jr. Ectopic adrenocorticotropic hormone hypersecretion due to a primary pulmonary paraganglioma. Endocr Pract 2004;10:424-428.
67. Churg A, Warnock ML. Pulmonary tumorlet. A form of peripheral carcinoid. Cancer 1976;37: 1469-1477.
68. Ranchod M. The histogenesis and development of pulmonary tumorlets. Cancer 1977;39:1135-1145.
69. Bonikos DS, Archibald R, Bensch KG. On the origin of the so-called tumorlets of the lung. Hum Pathol 1976;7:461-469.
70. Pelosi G, Zancanaro C, Sbabo L, Bresaola E, Martignoni G, Bontempini L. Development of innumerable neuroendocrine tumorlets in pulmonary lobe scarred by intralobar sequestration. Immunohistochemical and ultrastructural study of an unusual case. Arch Pathol Lab Med 1992; 116:1167-1174.
71. Hausman DH, Weimann RB. Pulmonary tumorlet with hilar lymph node metastasis. Report of a case. Cancer 1967;20:1515-1519.
72. Whitwell F. Tumorlets of the lung. J Pathol Bacteriol 1955;70:529-541.
73. Korn D, Bensch K, Liebow AA, Castleman B. Multiple minute pulmonary tumors resembling chemodectomas. Am J Pathol 1960;37:641-672.
74. Gaffey MJ, Mills SE, Askin FB. Minute pulmonary meningothelial-like nodules. A clinicopathologic study of so-called minute pulmonary chemodectoma. Am J Surg Pathol 1988;12:167-175.
75. Churg AM, Warnock ML. So-called "minute pulmonary chemodectoma": a tumor not related to paragangliomas. Cancer 1976;37:1759-1769.
76. Spain DM. Intrapulmonary chemodectomas in subjects with organizing pulmonary thromboemboli. Am Rev Respir Dis 1967;96:1158-1164.
77. Zak FG, Chabes A. Pulmonary chemodectomatosis. JAMA 1963;183:887-889.
78. Barroso-Moguel R, Costero I. Some histochemical tests in Zak's chemoblastosis. Am J Path 1964; 44:17a.
79. Edwards C, Heath D. Pulmonary venous chemoreceptor tissue. Br J Dis Chest 1972;66:96-100.
80. Costero I, Barroso-Moguel R, Martinez-Paloma A. Pleural origin of some of the supposed chemodectomoid structures of the lung. Beitr Pathol 1972;146:351-365.
81. Kuhn C 3rd, Askin FB. The fine structure of so-called minute pulmonary chemodectomas. Hum Pathol 1975;6:681-691.
82. Torikata C, Mukai M. So-called minute chemodectoma of the lung. An electron microscopic and immunohistochemical study. Virchows Archiv A Pathol Anat Histopathol 1990;417:113-118.
83. Drlicek M, Grisold W, Lorber J, Hackl H, Wuketich S, Jellinger K. Pulmonary meningioma. Immunohistochemical and ultrastructural features. Am J Surg Pathol 1991;15:455-459.
84. Ionescu DN, Sasatomi E, Aldeeb D, et al. Pulmonary meningothelial-like nodules: a genotypic comparison with meningiomas. Am J Surg Pathol 2004;28:207-214.
85. Suster S, Moran CA. Diffuse pulmonary meningiotheliomatosis. Am J Surg Pathol 2007;31: 624-631.

Orbital Paraganglioma

86. Botár J, Pribék L. Corpuscle paraganglionnaire dans l'orbite. Ann D'Anat Path 1935;12:227-228.
87. Mawas J. Sur un organe épithélial non décrit, le paraganglion infra-orbitaire. C R Hebd Seances Acad Sci 1936;202:977-978.
88. Fisher ER, Hazard JB. Nonchromaffin paraganglioma of the orbit. Cancer 1952;5:521-524.
89. Zak FG, Lawson W. The paraganglionic chemoreceptor system: physiology, pathology, and clinical medicine. New York: Springer-Verlag; 1982: 419-423.

90. Deutsch AR, Duckworth JK. Nonchromaffin paraganglioma of the orbit. Am J Opthalmol 1969; 68:659-663.
91. Thacker WC, Duckworth JK. Chemodectoma of the orbit. Cancer 1969;23:1233-1238.
92. Paulus W, Jellinger K, Brenner H. Melanotic paraganglioma of the orbit: a case report. Acta Neuropathol (Berl) 1989;79:340-346.
93. Archer KF, Hurwitz JJ, Balogh JM, Fernandes BJ. Orbital nonchromaffin paraganglioma. A case report and review of the literature. Ophthalmology 1989;96:1659-1666.
94. Bednar MM, Trainer TD, Aitken PA, et al. Orbital paraganglioma: case report and review of the literature. Br J Ophthalmol 1992;76:183-185.
95. Lattes R, McDonald JJ, Sproul E. Non-chromaffin paraganglioma, of carotid body and orbit; report of a case. Ann Surg 1954;139:382-384.
96. Gunalp I, Gunduz K, Duruk K, Kanpolat Y. Neurogenic tumors of the orbit. Jpn J Ophthalmol 1994;38:185-190.
97. Laquis SJ, Vick V, Haik BG, Fleming JC, Wilson MW. Intracranial paraganglioma (glomus tumor) with orbital extension. Ophthal Plast Reconstr Surg 2001;17:458-461.
98. Nirankari MS, Greer CH, Chaddah MR. Malignant non-chromaffin paraganglioma in the orbit. Brit J Ophthalmol 1963;47:357-363.
99. Varghese S, Nair B, Joseph TA. Orbital malignant non-chromaffin paraganglioma. Alveolar soft tissue sarcoma. Br J Ophthalmol 1968;52: 713-715.
100. Wu BF. Orbital chemodectoma. Clinical and pathologic analysis of 2 cases. Chinese Med J 1981;94:419-422.
101. Christopherson WM, Foote FW, Stewart FW. Alveolar soft-part sarcomas; structurally characteristic tumors of uncertain histogenesis. Cancer 1952;5:100-111.
102. Smetana HF, Scott WF Jr. Malignant tumors of nonchromaffin paraganglia. Mil Surg 1951;109: 330-349.
103. Lieberman PH, Brennan MF, Kimmel M, Erlandson RA, Garin-Chesa P, Flehinger BY. Alveolar soft part sarcoma. A clinico-pathologic study of half a century. Cancer 1989;63:1-13.
104. Lieberman PH, Foote FW Jr, Stewart FW, Berg JW. Alveolar soft part sarcoma. JAMA 1966;198: 1047-1051.
105. Weiss SW, Goldblum, JR. Enzinger and Weiss's soft tissue tumors, 4th ed. St. Louis: Mosby; 2001:1509-1521.
106. Shipkey FH, Lieberman PH, Foote FW Jr, Stewart FW. Ultrastructure of alveolar soft part sarcoma. Cancer 1964;17:821-830.
107. Amin MB, Patel RM, Oliveira P, et al. Alveolar soft-part sarcoma of the urinary bladder with urethral recurrence: a unique case with emphasis on differential diagnoses and diagnostic utility of an immunohistochemical panel including TFE3. Am J Surg Pathol. 2006;30:1322-1325.

Carcinoid Tumors of the Eye and Orbit

108. Riddle PJ, Font RL, Zimmerman LE. Carcinoid tumors of the eye and orbit: a clinicopathologic study of 15 cases, with histochemical and electron microscopic observations. Hum Pathol 1982;13:459-469.
109. Zimmerman LE, Stangl R, Riddle PJ. Primary carcinoid tumor of the orbit. A clinicopathologic study with histochemical and electron microscopic observations. Arch Ophthalmol 1983;101: 1395-1398.
110. Lack EE, Cubilla AL, Woodruff JM, Farr HW. Paragangliomas of the head and neck region: a clinical study of 69 patients. Cancer 1977;39: 397-409.
111. Lack EE, Cubilla AL, Woodruff JM. Paragangliomas of the head and neck region. A pathologic study of tumors from 71 patients. Hum Pathol 1979;10:191-218.

Paragangliomas of Nasal Cavity and Nasopharynx

112. Welkoborsky HJ, Gosepath J, Jacob R, Mann WJ, Amedee RG. Biologic characteristics of paragangliomas of the nasal cavity and paranasal sinuses. Am J Rhinol 2000;14:419-426.
113. Mevio E, Bignami M, Luinetti O, Villani L. Nasal paraganglioma. A case report. Acta Otorhinolaryngol Belg 2001;55:247-249.
114. Dasgupta G, Deodhare SG. Chemodectoma of the soft palate. Int Surg 1977;62:366-367.
115. Walker PJ, Fagan PA. Catecholamine-secreting paraganglioma of the pterygopalatine fossa: case report. Am J Otol 1993;14:306-308.
116. Lack EE. Pathology of adrenal and extra-adrenal paraganglia. Major problems in pathology, Vol 29. Philadelphia: WB Saunders; 1994.
117. Lack EE, Cubilla AL, Woodruff JM, Farr HW. Paragangliomas of the head and neck region: a clinical study of 69 patients. Cancer 1977;39: 397-409.
118. Lack EE, Cubilla AL, Woodruff JM. Paragangliomas of the head and neck region. A pathologic study of tumors from 71 patients. Hum Pathol 1979;10:191-218.

Primary Thyroid Paraganglioma

119. Lack EE. Pathology of adrenal and extra-adrenal paraganglia. Major problems in pathology, Vol 29. Philadelphia: WB Saunders; 1994.
120. LaGuette J, Matias-Guiu X, Rosai J. Thyroid paraganglioma: a clinicopathologic and immunohistochemical study of three cases. Am J Surg Pathol 1997;21:748-753.
121. Kronz JD, Argani P, Udelsman R, Silverberg L, Westra WH. Paraganglioma of the thyroid: two cases that clarify and expand the clinical spectrum. Head Neck 2000;22:621-625.

122. Corrado S, Montanini V, De Gaetani C, Borghi F, Papi G. Primary paraganglioma of the thyroid gland. J Endocrinol Invest 2004;27:788-792.
123. Zantour B, Guilhaume B, Tissier F, et al. A thyroid nodule revealing a paraganglioma in a patient with a new germline mutation in the succinate dehydrogenase B gene. Eur J Endocrinol 2004;151:433-438.
124. Kay S, Montague JW, Dodd RW. Nonchromaffin paraganglioma (chemodectoma) of thyroid region. Cancer 1975:36:582-585.
125. Zak FG, Lawson W. Glomic (paraganglionic) tissue in the larynx and capsule of the thyroid gland. Mt. Sinai J Med 1972;39:82-90.
126. Hinojar AG, Prieto JR, Munoz E, Hinojar AA. Relapsing paraganglioma of the inferior laryngeal paraganglion: case report and review of the literature. Head Neck 2002;24:95-102.
127. Haegert DG, Wang NS, Farrer PA, Seemayer TA, Thelmo W. Non-chromaffin paragangliomatosis manifesting as a cold thyroid nodule. Am J Clin Pathol 1974;61:561-570.
128. Cayot F, Bastien H, Justrabo E, et al. [Multiple paragangliomas of the neck localized in the thyroid region. Papillary thyroid cancer associated with parathyroid adenoma.] Sem Hop 1982;58: 2004-2007. [French.]
129. Bockhorn M, Sheu SY, Frilling A, Molmenti E, Schmid KW, Broelsch CE. Paraganglioma-like medullary thyroid carcinoma: a rare entity. Thyroid 2005;15:1363-1367.
130. Mitsudo SM, Grajower MM, Balbi H, Silver C. Malignant paraganglioma of the thyroid gland. Arch Pathol Lab Med 1987;111:378-380.
131. Carney JA, Ryan J, Goellner JR. Hyalinizing trabecular adenoma of the thyroid gland. Am J Surg Pathol 1987;11:583-591.
132. Goellner JR, Carney JA. Cytologic features of fine-needle aspirates of hyalinizing trabecular adenoma of the thyroid. Am J Clin Pathol 1989;91:115-119.
133. Bronner M, LiVolsi VA, Jennings T. Plat: paraganglioma-like adenomas of the thyroid. Surg Pathol 1988;1:383-389.
134. Chetty R, Beydoun R, LiVolsi V. Paraganglioma-like nodular proliferations in chronic lymphocytic thyroiditis. Mod Pathol 1993;6:38A(203).
135. Sambade C, Franssila KO, Cameselle-Teijeiro J, Nesland JM, Sobrinho-Simões M. Hyalinizing trabecular adenoma. A misnomer for a peculiar tumor of the thyroid gland. Endocr Pathol 1991;2:83-91.
136. Huss LJ, Mendelsohn G. Medullary carcinoma of the thyroid gland: an encapsulated variant resembling the hyalinizing trabecular (paraganglioma-like) adenoma of thyroid. Mod Pathol 1990;3:581-585.
137. Cheung CC, Boerner SL, MacMillan CM, Ramyar L, Asa SL. Hyalinizing trabecular tumor of the thyroid: a variant of papillary carcinoma proved by molecular genetics. Am J Surg Pathol 2000;24:1622-1626.
138. Galgano MT, Mills SE, Stelow EB. Hyalinizing trabecular adenoma of the thyroid revisited: a histologic and immunohistochemical study of thyroid lesions with prominent trabecular architecture and sclerosis. Am J Surg Pathol 2006;30:1269-1273.

Paragangliomas in Other Locations

139. Milroy EJ. Chemodectoma (non-chromaffin paraganglioma) of the face. Brit J Surg 1969;56: 510-512.
140. Volchek GB, Bolotnaia RD. Chemodectoma of the auricular concha. Vestnik Otorinolaryngol 1970;32:103-104.
141. Scopelliti G, Camera A, Barbato U. [Chemodectoma of tongue: differential diagnostic and histogenic criteria.] Ann Stomatol (Roma) 1970;19: 819-834. [Italian.]
142. DeLozier HL. Chemodectoma of the cheek. A case report. Ann Otol Rhinol Laryngol 1983;92: 109-112.
143. Reithmeier T, Gumprecht H, Stolzle A, Lumenta CB. Intracerebral paraganglioma. Acta Neurochir (Wien) 2000;142:1063-1066.
144. Prayson RA, Chahlavi A, Luciano M. Cerebellar paraganglioma. Ann Diagn Pathol 2004;8:219-223.
145. Harries K, Nunn T, Shah V, Richards D, Manson JM. First reported case of esophageal paraganglioma. A review of the literature of gastrointestinal tract paraganglioma including gangliocytic paraganglioma. Dis Esophagus 2004;17:191-195.
146. McCluggage WG, Cameron CH, Brooker D, O'Hara MD. Paraganglioma: an unusual tumour of the parathyroid gland. J Laryngol Otol 1996;110:196-199.

18 ULTRASTRUCTURAL AND OTHER FEATURES OF PARAGANGLIOMAS OF THE HEAD AND NECK REGION

GENERAL FEATURES

Paragangliomas of the head and neck region (including non-neoplastic paraganglia such as carotid bodies) are typically nonchromaffin (1). They are typically negative for phenylethanolamine N-methyltransferase (PNMT), except for cardiac paragangliomas (2), and the excess catecholamine secretion seen with some of these tumors suggests a closer alignment with paragangliomas of the sympathoadrenal neuroendocrine system. For diagnostic purposes, it is not essential to document the presence of catecholamines within head and neck paragangliomas. The demonstration of cytoplasmic argyrophilia is seldom needed in diagnosis; positive cytoplasmic argyrophilia was observed focally or diffusely in virtually all paragangliomas studied at Memorial Hospital in which paraffin blocks were available (3). The tumors are typically argentaffin negative. Sensitive and specific immunohistochemical markers and various molecular probes can establish a diagnosis if routine morphology is equivocal.

ULTRASTRUCTURAL FINDINGS

The ultrastructure of various paragangliomas (and paraganglia) from different sites in the head and neck region is similar, and it is not possible to distinguish one particular tumor from another based upon fine structural characteristics (1,3–11). Examination of 1-μm–thick sections provides some insight into the different types of cells found in these paragangliomas. In general, neoplastic chief cells greatly outnumber other cell types, a ratio not seen with normal or hyperplastic paraganglia (figs. 18-1, 18-2). Reliable identification of sustentacular cells is difficult in routine or ultrathin sections, and they may be difficult to recognize on ultrastructural study as well. The easiest way to detect these cells is by immunohistochemical staining for S-100 protein (or occasionally glial fibrillary acidic protein [GFAP]).

Ultrastructurally, paragangliomas are not as complicated as normal or hyperplastic paraganglia. Clusters of neoplastic chief cells appear sharply demarcated, and may be subtended by thin, continuous or discontinuous extensions of sustentacular cell cytoplasm (fig. 18-3). The nuclei of the chief cells may have irregular folds

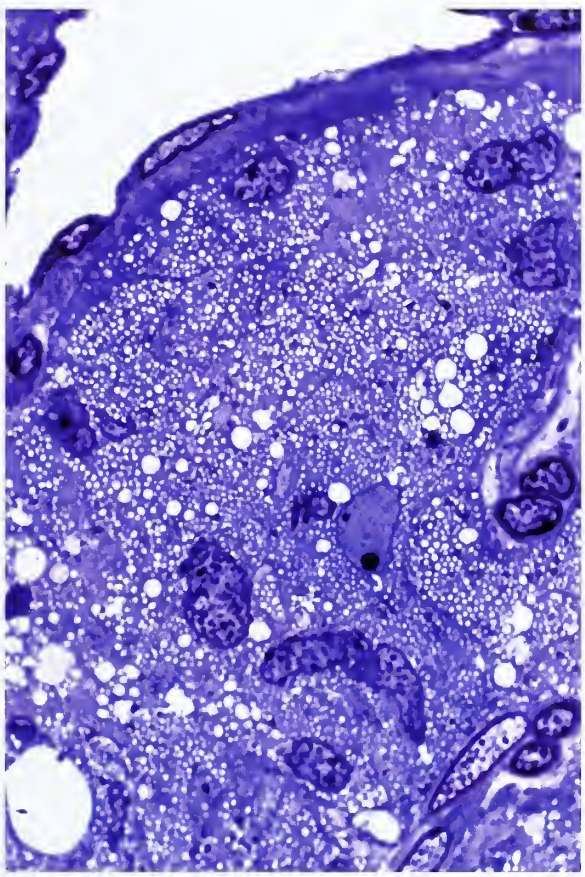

Figure 18-1

CAROTID BODY PARAGANGLIOMA

Neoplastic chief cells adjacent to a capillary channel have a nesting pattern. Endothelial cells are easily seen but other cell types (e.g., sustentacular cells) are difficult to identify in 1-μm–thick pilot sections for electron microscopy (toluidine blue stain).

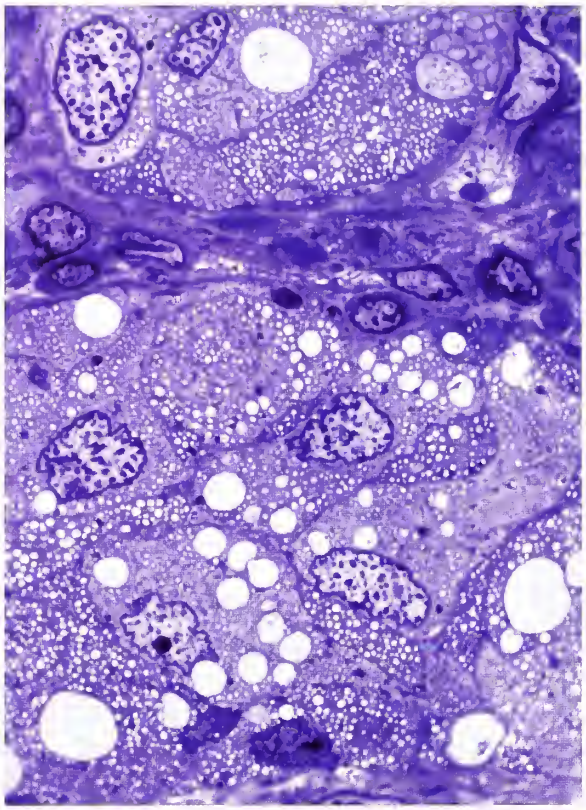

Figure 18-2

CAROTID BODY PARAGANGLIOMA

Many neoplastic chief cells contain medium to large cytoplasmic vacuoles, so-called pseudoacini. Occasional mast cells were seen in the delicate interstitium in other fields (toluidine blue stain).

and indentations, which when marked, may result in the formation of nuclear pseudoinclusions as seen with sympathoadrenal paragangliomas. It is advantageous when identifying cell types other than neoplastic chief cells to examine profiles of vascular channels and then proceed into nests of neoplastic chief cells (fig. 18-4). Endothelial cells are ubiquitous, and may have small cytoplasmic fenestrations. Pericytes are present in close relation to endothelial cells. Examination of the interstitium adjacent to the vascular spaces may reveal occasional mast cells, and the heterogeneous, scroll-like, lamellar or curvilinear granules should not be confused with neurosecretory type granules of chief cells (fig. 18-5). Interstitial collagen may be a prominent feature. Amyloid deposits have been reported, but not illustrated (6).

The cell cytoplasm of neoplastic chief cells may show a variation in overall electron density, giving the impression of two polar cell populations of "light" and "dark" cells (1). This has been ascribed to a variation in density of hyaloplasm, or disparity in compactness or density of cellular organelles such as mitochondria and even neurosecretory granules (fig. 18-6) (4). Forms transitional in cellular density have been described. There does not appear to be any biologic significance attached to this cellular variation at the ultrastructural level (1). Irregular profiles of rough and smooth endoplasmic reticulum, some appearing slightly dilated, may be seen.

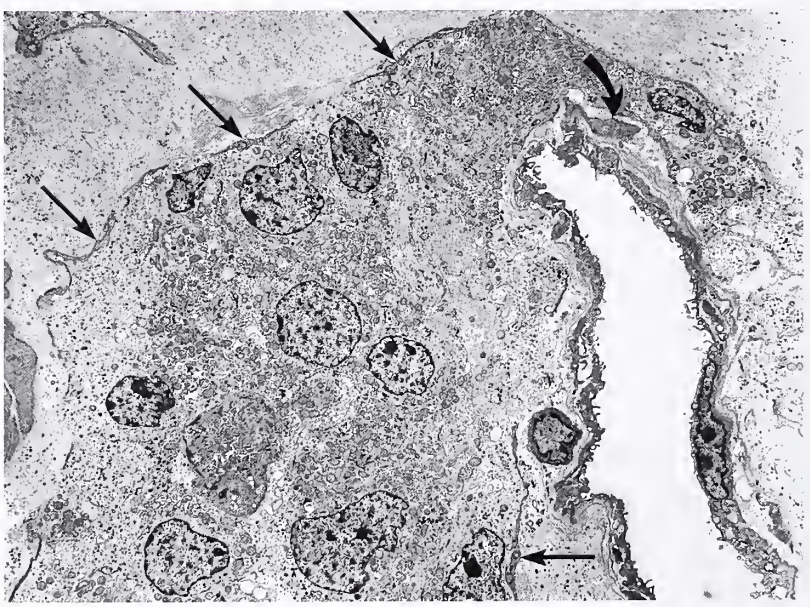

Figure 18-3

CAROTID BODY PARAGANGLIOMA

An ultrastructural survey view shows rounded to ovoid nuclei of neoplastic chief cells, some with an irregular contour, and an occasional nucleolus. Slender, discontinuous wisps of cytoplasm are around the outer aspect of a cluster of tumor cells (straight arrows), which are cellular extensions of sustentacular cells. A portion of pericyte cytoplasm is evident near an endothelial cell (curved arrow). (Fig. 9-3 from Lack EE. Pathology of adrenal and extra-adrenal paraganglia. Major problems in pathology, Vol 29. Philadelphia: WB Saunders; 1994:168.)

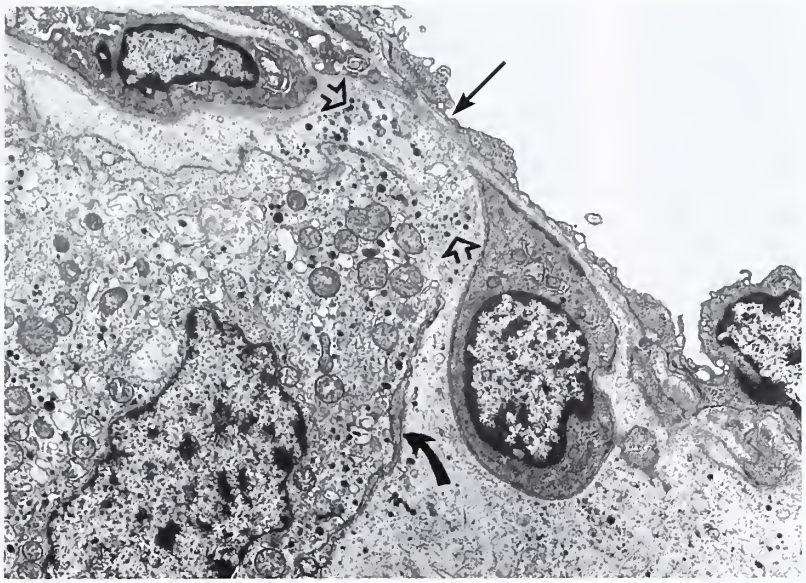

Figure 18-4

CAROTID BODY PARAGANGLIOMA

Attenuated endothelial lining of a vascular channel is seen, with a few cytoplasmic fenestrations (straight arrow). Several pericytes are present with plasmalemmal densities, a few pinocytotic vesicles, and a layer of continuous basement membrane. Note the slender extension of a sustentacular cell (curved arrow) and the presence of dense-core neurosecretory granules free in the interstitium (open arrows). This may be artifactual due to mechanical disruption of the cytoplasm. (Fig. 9-8 from Lack EE. Pathology of adrenal and extra-adrenal paraganglia. Major problems in pathology, Vol 29. Philadelphia: WB Saunders; 1994:172.)

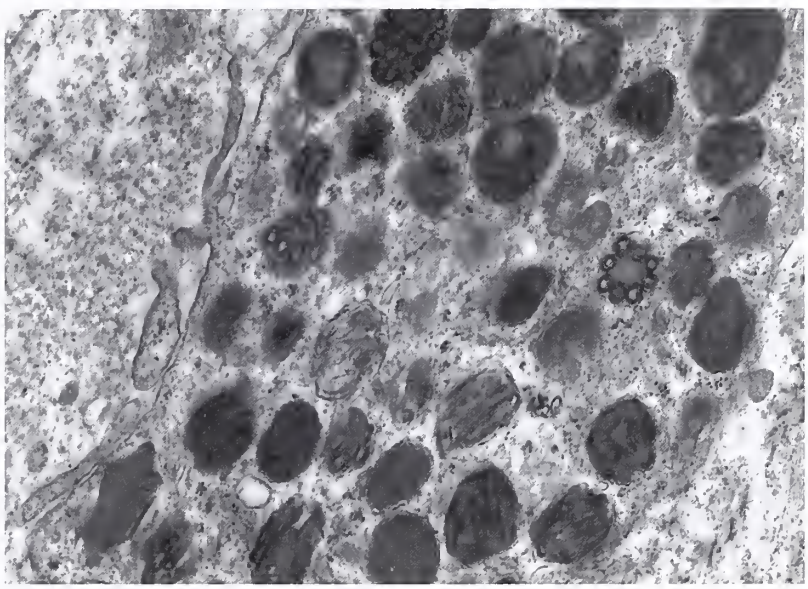

Figure 18-5

CAROTID BODY PARAGANGLIOMA

A mast cell is seen within the interstitium near a vascular channel in a carotid body paraganglioma. The cytoplasm contains numerous electron-dense structures which have scroll-like, lamellar, or curvilinear profiles. Because of the large size and heterogeneity, the mast cell granules should not be confused with neurosecretory granules. (Fig. 9-11 from Lack EE. Pathology of adrenal and extra-adrenal paraganglia. Major problems in pathology, Vol 29. Philadelphia: WB Saunders; 1994:173.)

Free polyribosomes may also be seen. Some cells have simple intercellular junctions without the formation of true desmosomal attachments (fig. 18-7), but they are usually sparse.

The diagnostic feature of the neoplastic chief cells is the presence of dense-core neurosecretory type granules; however, the distribution and density of these granules can vary considerably. Some secretory vesicles appear empty since tangential sectioning or vagaries in fixation can give an inaccurate impression (1). Most neurosecretory type granules are relatively uniform in size (70 to 200 nm) and shape, depending upon the precise plane of section (1). Some granules have a wide, asymmetric halo between the limiting membrane which may simulate "norepinephrine type" granules (fig. 18-8), but correlation of granule morphology with content of particular catecholamine or neuropeptide is unreliable (1). There may be some variability in granule morphology, with an elongated or "sausage" shape (1). Close association of neurosecretory type granules with a Golgi complex may be seen.

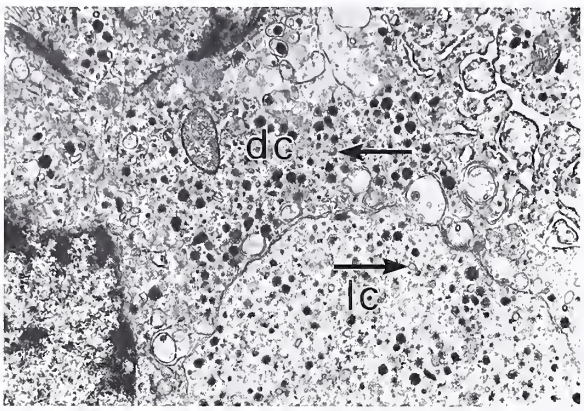

Figure 18-6

CAROTID BODY PARAGANGLIOMA

There is a slightly greater density of cellular organelles in the "dark" cell (dc), including dense-core neurosecretory granules, compared with the adjacent "light" cell (lc). The cells contain a few empty vesicles (arrows). Profiles of dilated rough endoplasmic reticulum are also present. (Fig. 9-4 from Lack EE. Pathology of adrenal and extra-adrenal paraganglia. Major problems in pathology, Vol 29. Philadelphia: WB Saunders; 1994:169.)

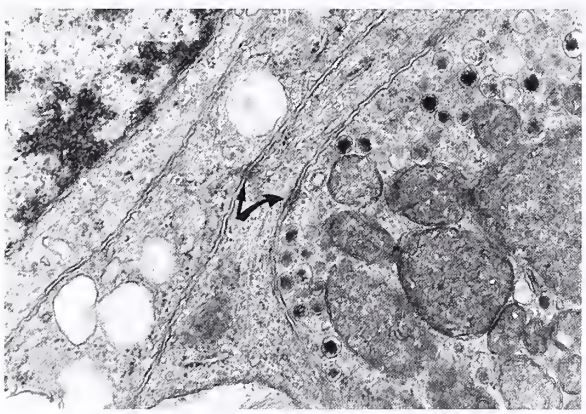

Figure 18-7

CAROTID BODY PARAGANGLIOMA

Simple belt-like intercellular attachments are present between neoplastic chief cells (branching arrows). Occasional profiles of smooth endoplasmic reticulum were present along with free polyribosomes. Note the electron-dense neurosecretory granules.

Occasionally dense-core granules are observed in an extracellular location (see fig. 18-4), and some investigators have speculated that this represents release of catecholamines during surgical manipulation of the tumor. A synaptic connection between nerve fibers and neoplastic chief cells is not a feature of true paragangliomas (1). An extraordinary case of jugulotympanic paraganglioma (JTP) was reported: there were membrane-bound, rhomboid crystals nearly identical to those seen in alveolar soft-part sarcoma, and a similar mode of origin from smaller dense-core granules was postulated (10).

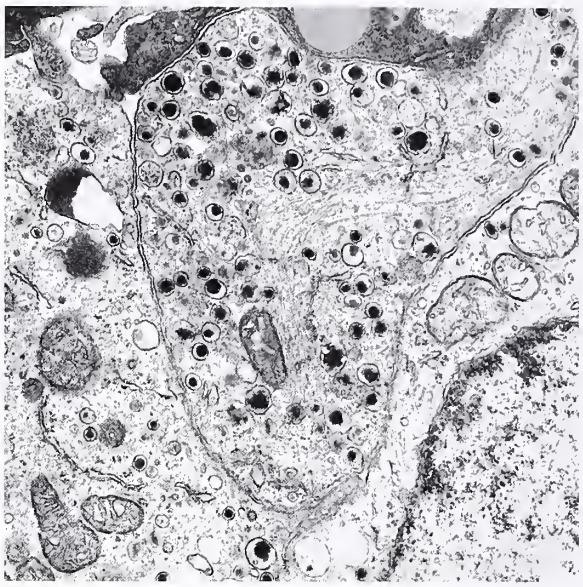

Figure 18-8

CAROTID BODY PARAGANGLIOMA

Some dense-core neurosecretory granules have a symmetric halo beneath the limiting membrane while other granules have a wider, somewhat asymmetric halo. (Fig. 9-5 from Lack EE. Pathology of adrenal and extra-adrenal paraganglia. Major problems in pathology, Vol 29. Philadelphia: WB Saunders; 1994:170.)

IMMUNOHISTOCHEMICAL FINDINGS

The immunohistochemical profile of paragangliomas displays a diversity similar to that of sympathoadrenal paragangliomas (Table 18-1) (12–14). In the diagnostic interpretation of these immunohistochemical stains, artifacts and technical problems may occur, and caution should be exercised when contradicting an opinion based upon sound clinical information and experienced evaluation of morphology (15).

There are a number of good, reliable immunomarkers for neuroendocrine differentiation (16). Staining for neuron-specific enolase is uniformly positive under optimal conditions (fig. 18-9), but the lack of specificity limits its diagnostic value. An immunoprofile using a selected battery of

Table 18-1

IMMUNOPROFILE FOR CAROTID BODY (N = 11) AND JUGULOTYMPANIC (N = 7) PARAGANGLIOMAS[a]

Markers	No. Positive
Neuron-specific enolase	18/18
Serotonin	13/18
Leu-enkephalin	10/18
Gastrin	7/18
Substance P	7/18
Vasoactive intestinal peptide	7/18
Somatostatin	5/18
Bombesin	2/18
Alpha-MSH	2/18
Calcitonin	2/18
Adrenocorticotrophic hormone	0/18
Glucagon	0/18
Human chorionic gonadotrophin	0/18
Insulin	0/18
Vasopressin	0/18

[a]Table 1 from Warren WH, Lee I, Gould VE, Memoli VA, Jao W. Paragangliomas of the head and neck: ultrastructural and immunohistochemical analysis. Ultrastr Pathol 1985;8:336.

stains may yield more specific results when using monoclonal antibodies directed against chromogranin A (fig. 18-10) (or related substances such as chromogranin B) or synaptophysin, an integral and specific component of the membranes of presynaptic vesicles (fig. 18-11). Given the localization of chromogranin A in the matrix of granules and not in the investing membranes, staining may be granular, and differences in intensity or distribution of staining (under optimal conditions) may reflect a variation in content or density of neurosecretory type granules. Molecular probes may detect mRNA for the chromogranin and secretogranin family of acidic proteins in endocrine tumors which have a paucity of neurosecretory granules (17). Results of immunostaining for various neuroendocrine markers in the study of Johnson et al (14) involving 29 head and neck paragangliomas are shown in Table 18-2.

A study using specific antibodies against chromogranin A and B and secretogranin II revealed divergent staining patterns in parasympathetic paragangliomas (i.e., carotid body paragangliomas [CBP] and JTP) versus

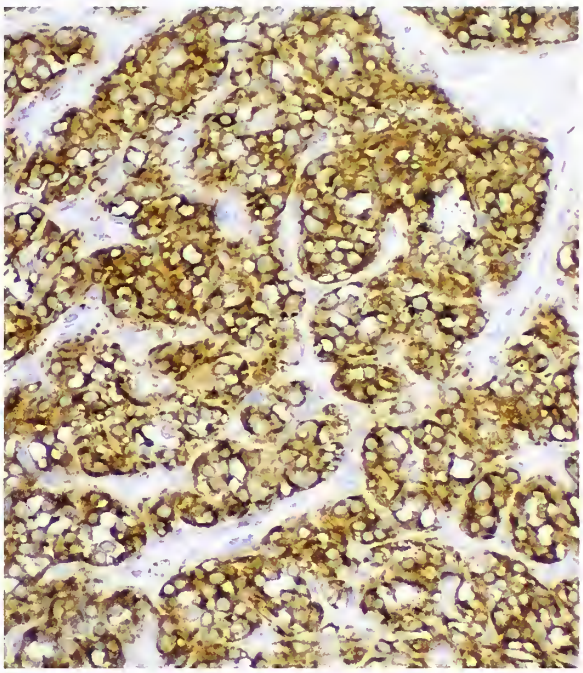

Figure 18-9

JUGULAR PARAGANGLIOMA

Immunoreactivity for neuron-specific enolase is diffusely strong within the cytoplasm of tumor cells (avidin-biotin peroxidase method).

Table 18-2

NEUROENDOCRINE MARKERS AND INTERMEDIATE FILAMENT TYPING FOR CAROTID BODY (N = 9) AND JUGULOTYMPANIC (N = 20) PARAGANGLIOMAS[a,b]

Neuroendocrine Markers	No. Positive
Neuron-specific enolase	29/29
Chromogranin A	26/29
Synaptophysin	28/29
Serotonin	25/29
S-100 protein	29/29
Sustentacular vs. chief cells (100%) (24%)	
Intermediate Filaments	**No. Positive**
Cytokeratin	3/29
Neurofilament	0/29
Desmin	0/29
Vimentin	rarely + in chief cells
Glial fibrillary acidic protein	0/29

[a]Table 22-2 from Fascicle 19, Third Series.
[b]Data from reference 14.

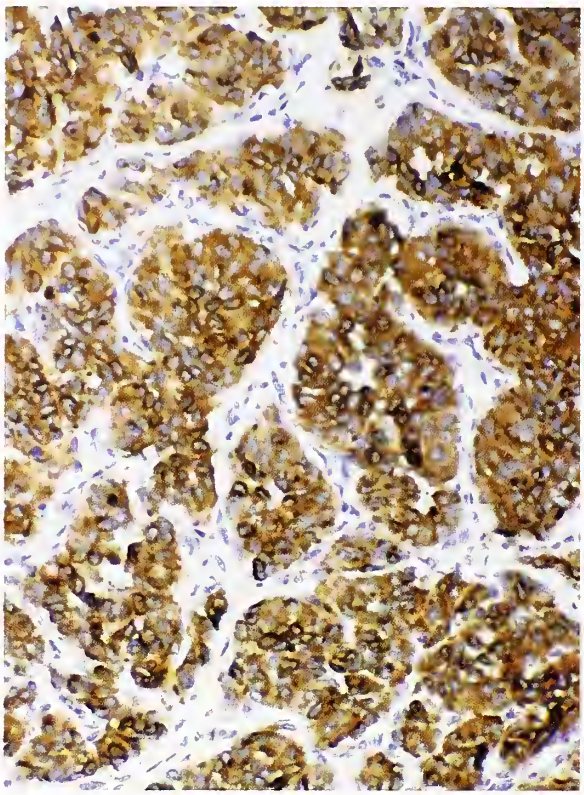

Figure 18-10

VAGAL PARAGANGLIOMA

There is strong immunoreactivity for chromogranin A in this vagal paraganglioma. On high magnification, the staining of most tumor cells has a finely granular quality (avidin-biotin peroxidase method).

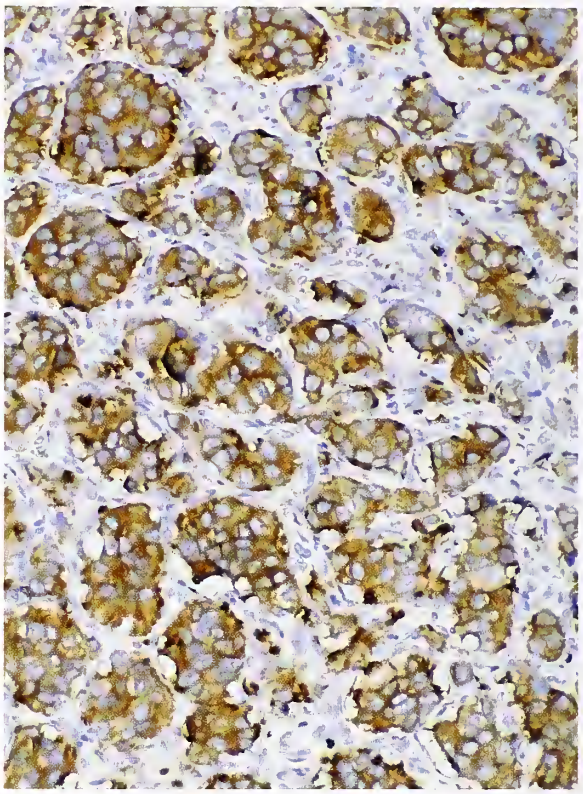

Figure 18-11

CAROTID BODY PARAGANGLIOMA

There is diffuse but somewhat less intense immunostaining for somatostatin in this carotid body paraganglioma (avidin-biotin peroxidase method).

sympathetic (extraadrenal) paragangliomas. The parasympathetic tumors expressed both chromogranin B and secretogranin II in most neoplastic chief cells of all 14 tumors while chromogranin A reactivity was strong in only 2 tumors and weak to absent in the rest; 12 of 12 sympathetic paragangliomas showed immunoreactivity for chromogranin A and 11 of 12 for chromogranin B while secretogranin II was found in less than half (18). Immunoreactivity of endocrine cells with the antilymphocyte antibody leu-7 (HNK-l) has also been reported (19).

Intermediate filament typing has been reported in paragangliomas of the head and neck region (14). Some tumors stain for neurofilament protein (20). Vimentin staining is occasionally noted in chief and sustentacular cells (14), but positive results are most notable in endothelial cells in which the stain highlights the organoid arrangement of neoplastic chief cells. Immunostaining for cytokeratin has been reported to be positive in a small number of JTPs and CBPs (fig. 18-12) using a combination of monoclonal antibodies including CAM5.2; in difficult cases this may be a potential source of immunohistochemical misinterpretation unless a panel of markers is used (14). GFAP has been used as a marker for sustentacular cells (fig. 18-13), but the staining reaction appears to have variable results (14).

Based upon a number of studies, the identification of sustentacular cells is most reliably done by immunostaining for S-100 protein. These cells characteristically appear as elongated or dendritic cells at the periphery of neoplastic chief cells and may demonstrate nuclear or cytoplasmic positivity, or both (fig. 18-14). Ultrastructurally, sustentacular cells closely "embrace" neoplastic

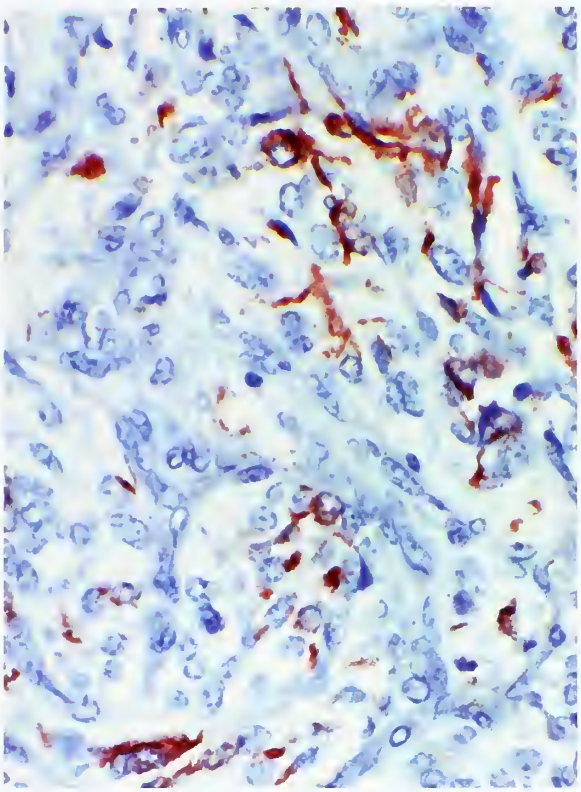

Figure 18-12

CAROTID BODY PARAGANGLIOMA

Some cells in this paraganglioma are immunoreactive for cytokeratin (AE1/AE3) monoclonal antibodies. Some have a stellate or dendritic configuration. Some ovoid cells could be neoplastic chief cells (avidin-biotin peroxidase method).

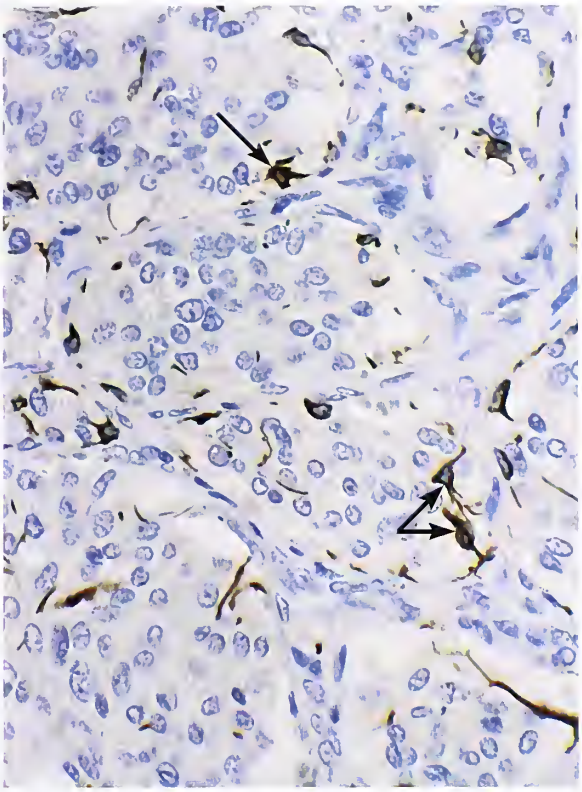

Figure 18-13

CAROTID BODY PARAGANGLIOMA

Glial fibrillary acidic protein intensely stains the stellate to dendritic cells near the vascular channels (arrows), the characteristic distribution for sustentacular cells (avidin-biotin peroxidase method). (Fig. 22-14 from Fascicle 19, Third Series.)

chief cells with slender wisp-like extensions of cytoplasm (fig. 18-15); these cells have relatively sparse numbers of cellular organelles and lack neurosecretory type granules. Some chief cells have also been reported to be immunoreactive for S-100 protein (14,20). The role of in situ hybridization and other molecular probes has been briefly referred to in chapter 11.

S-100 PROTEIN–POSITIVE CELLS AND PROGNOSIS

Some investigators have reported a decrease in density of S-100 protein–positive sustentacular cells in clinically malignant paragangliomas of the head and neck region (21–25). In a study by Kliewer et al. (23), paragangliomas were assigned three grades (Table 18-3); JTPs (n = 10) accounted for over 50 percent of all recurrent or locally aggressive tumors, and were reported to have strikingly few sustentacular cells regardless of behavior. In a recent study of over 50 head and neck paragangliomas, semiquantitative analysis of overall density of S-100 protein was not considered to be a reliable means of distinguishing clinically benign from malignant (i.e., metastasizing) paragangliomas (26), and a number of JTPs contained demonstrable sustentacular cells (fig. 18-16). A similar study of benign and malignant sympathoadrenal paragangliomas showed no statistically significant difference in density of S-100 protein–positive sustentacular cells, although there was a trend for decreased density in malignant tumors (27). A malignant CBP has been reported with high sustentacular cell density in both the primary tumor and the pulmonary metastases (28).

Figure 18-14

PRIMARY MALIGNANT THYROID PARAGANGLIOMA

S-100 protein is intensely reactive in numerous slender to curvilinear sustentacular cells that are closely applied to the microvasculature at the periphery of neoplastic chief cells. The tumor recurred locally, with extensive invasion of laryngotracheal structures (avidin-biotin peroxidase method). (Fig. 22-15 from Fascicle 19, Third Series.)

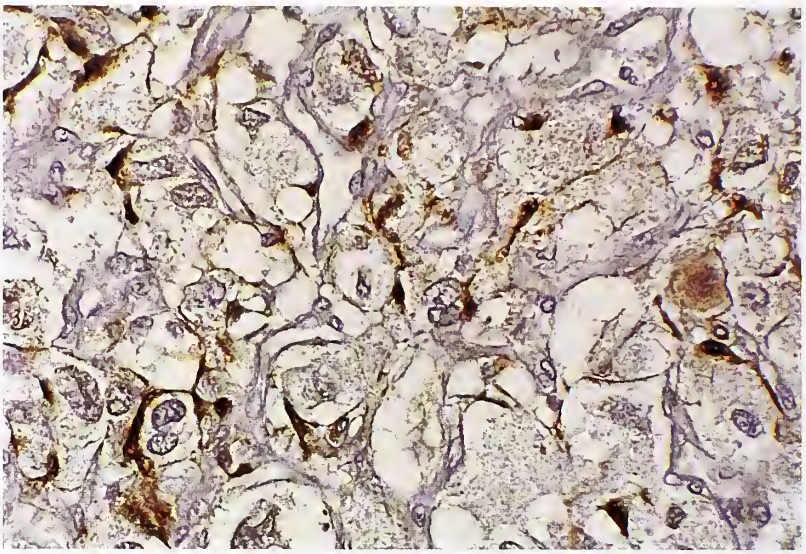

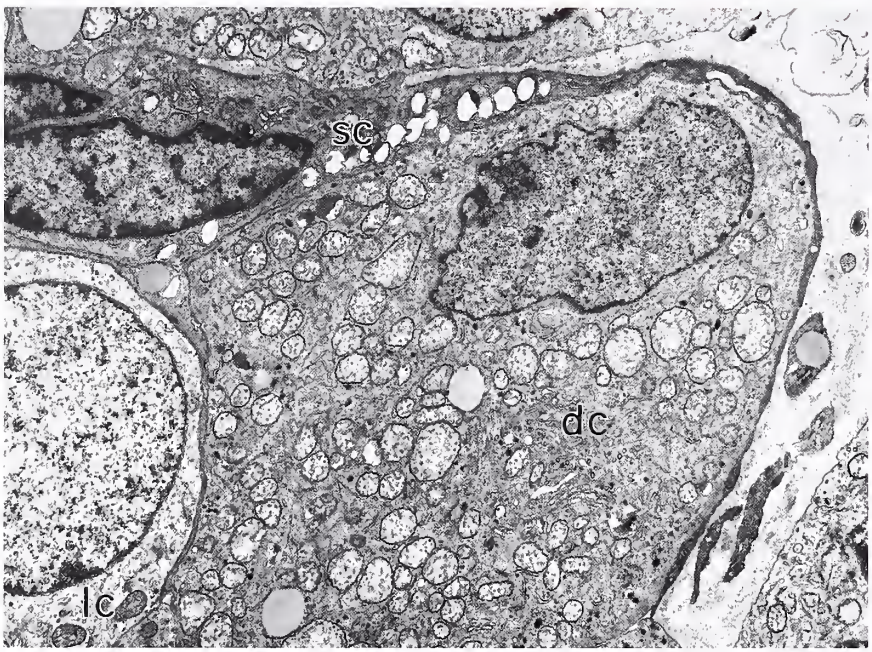

Figure 18-15

CAROTID BODY PARAGANGLIOMA

Nests of neoplastic dark (dc) and light (lc) chief cells are partially surrounded by cytoplasmic extensions of a sustentacular cell (sc). Both chief cells contained sparse dense-core neurosecretory type granules, but the sustentacular cell contained none. (Fig. 9-9 from Lack EE. Pathology of adrenal and extraadrenal paraganglia. Major problems in pathology, Vol 29. Philadelphia: WB Saunders; 1994:172.)

A recent study showed that clinically benign pheochromocytomas contain an increased density of HLA-DR–positive and S-100 protein–negative cells (double immunostaining technique), whereas relatively few such cells are seen in tumors that are aggressive or metastasize; one clinically benign CBP also had few dendritic cells (29). Another study reported positive immunostaining for tyrosine hydroxylase in two primary CBPs and one JTP, but cervical lymph node metastases in two cases were negative, suggesting an immature phenotype for the more aggressive component of the tumors (30).

MOLECULAR GENETICS

Germline mutations have been identified in genes of the mitochondrial succinate dehydrogenase (SDH) enzyme complex ll. These genes encode protein subunits of cytochrome b in the mitochondrial respiratory chains A, B, C, and D (31–33). Germline mutations in *SDHA* cause Leigh's syndrome, an early-onset progressive neurologic disorder, while mutations in *SDHB*,

Table 18-3

GRADING SCHEME PROPOSED FOR VARIOUS PARAGANGLIOMAS OF THE HEAD AND NECK REGION[a,b]

Paragangliomas (n = 42; 37 patients)
CBP[c] - 46%; JTP - 27%; VP-1, LP-1, NP-1, other
Low grade = benign, nonrecurrent (n = 24)
Intermediate grade = recurrent, locally aggressive (n = 8)
High grade = metastasizing (n = 5)
Conclusions using panel of immunohistochemical stains
1) Useful in confirming diagnosis
2) Decline in relative proportion of type II (sustentacular) cells (S-100 protein, GFAP)[d] correlates with aggressive behavior/metastases

[a]Table 22-3 from Fascicle 19, Third Series.

[b]Data from reference 23.

[c]CBP = carotid body paraganglioma; JTP = jugulotympanic paraganglioma; VP = vagal paraganglioma; LP = laryngeal paraganglioma; NP = nasal paraganglioma.

[d]GFAP = glial fibrillary acidic protein.

SDHC, and *SDHD* are strongly associated with familial paragangliomas and in 8 to 35 percent of apparently sporadic paragangliomas (33). The pheochromocytoma/paraganglioma syndrome is characterized by adrenal pheochromocytoma and/or a catecholamine-secreting extraadrenal paraganglioma or biochemically silent paragangliomas such as CBP (34). The syndrome is caused by germline mutations in *SDHB*, *SDHC*, and *SDHD*. Germline mutations in *SDHB* and *SDHD* (less commonly *SDHC*) account for up to 70 percent of familial head and neck paragangliomas and perhaps 8 percent of sporadic head and neck paragangliomas and pheochromocytomas.

Three familial paraganglioma syndromes can be identified by three genetic loci: *PGL1*, *PGL2*, and *PGL3*. The *PGL1* gene at chromosome band 11q23 is the most common locus and corresponds to *SDHD* (31).

Aside from mutations in SDH enzyme complex II, little is known about the molecular genetics that predispose to the development of paragangliomas. Early-onset renal cell carcinoma has been reported as a novel extraparaganglial component of SDHB-associated heritable paraganglioma (35). Loss of chromosome 11 is the only recurrent chromosomal aberration (36). Recurrent loss of 8p22-23 has also been reported (37). The pheochromocytoma (PC12) cell line is a potentially useful model for studying oxygen sensing in neuroendocrine cells and a recent review highlights the signal transduction pathways and transcription factors involved (38).

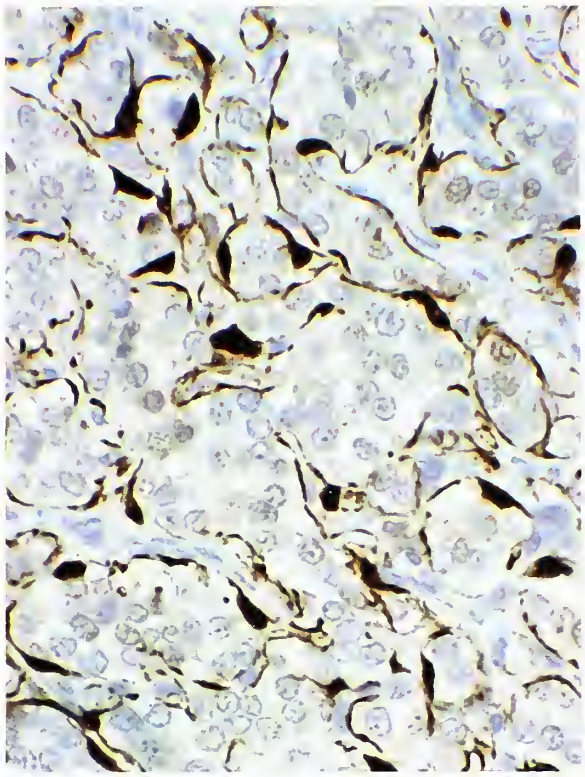

Figure 18-16

JUGULOTYMPANIC PARAGANGLIOMA

This jugulotympanic paraganglioma contains scattered sustentacular cells easily recognizable by strong nuclear and cytoplasmic immunostaining for S-100 protein (avidin-biotin peroxidase method).

FINE NEEDLE ASPIRATION BIOPSY AND CYTOLOGIC FINDINGS

It can be very difficult (or even impossible) to specifically diagnose a paraganglioma without heightened clinical suspicion, pertinent correlation with clinical history (e.g., positive family history of similar tumors), or precise anatomic localization. Without additional information, the variability in nuclear size, shape, and intensity of staining may easily lead to a mistaken diagnosis of malignancy (fig. 18-17A,B) or of an entirely different neoplasm, either benign or malignant. Fine needle aspiration biopsy (FNAB) has been performed on head and neck paragangliomas prior to surgery. There have

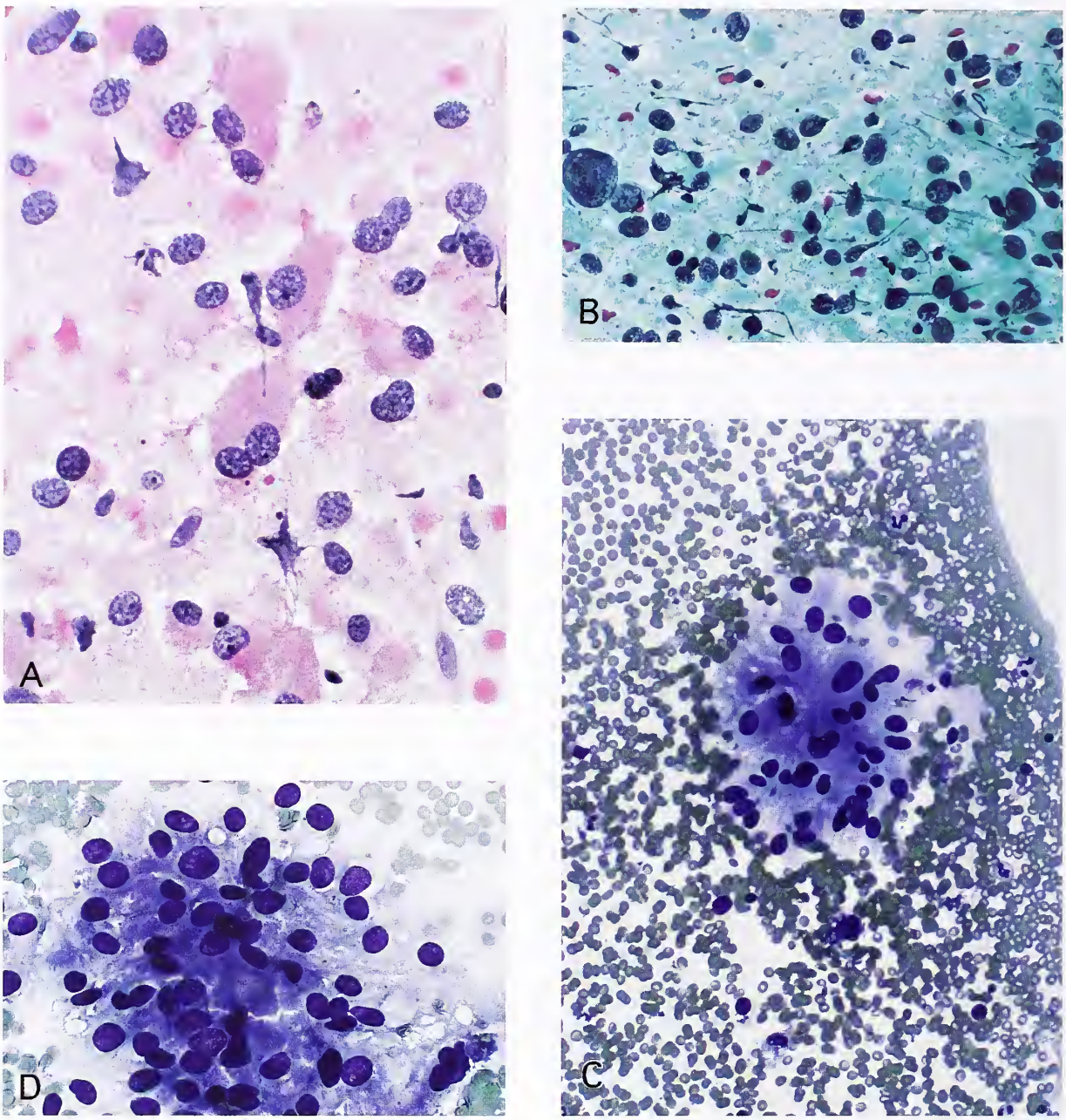

Figure 18-17

CAROTID BODY PARAGANGLIOMA

A: Smear/imprint of a surgically resected carotid body paraganglioma (CBP). The cells have a mild degree of nuclear pleomorphism and hyperchromasia and where intact, the cytoplasm is deeply eosinophilic.

B: Smear/imprint of a different surgically resected CBP. The variability in nuclear size might be confused with malignancy (Papanicolaou stain).

C: Preoperative fine-needle aspiration of a different CBP. A small cluster of loosely cohesive tumor cells is present within a bloody background. Small vacuolar spaces give a lattice-like appearance. The nuclei are darkly stained, with a mild degree of irregularity in size and shape (Diff Quik stain).

D: Same case as C shows a bloody background and a greater degree of variation in nuclear size. A heightened clinical suspicion for paraganglioma, along with correlation with clinical findings and anatomic localization, is critical in making an accurate diagnosis (Diff Quik stain). (B,C,D: Fig. 22-18 from Fascicle 19, Third Series.)

been significantly different views on the efficacy or role of this procedure in diagnosing CBP, a neoplasm which can simulate an enlarged cervical lymph node or a variety of other lesions (fig. 18-17C,D). Some regard the procedure as a safe (39,40) and accurate means of diagnosing CBP (39); to enhance accuracy, skill in interpretation of aspirates must be coupled with in-depth knowledge of surgical pathology. Still, the importance of the factors embodied in the first sentence of this paragraph cannot be emphasized enough.

Complications appear to be extremely rare with FNAB, but include hemorrhage and thrombosis of the common carotid artery with cerebral embolism and death (41). In a Memorial Hospital review of 73 head and neck paragangliomas, 15 patients had undergone FNAB (15 CBPs; 4 vagal paragangliomas), and the diagnosis was strongly suggested in 6 (40 percent) (1,42). Needle aspiration of tumors had been performed at Memorial Hospital since 1926 (43); Stewart (44) studied smears of material from 2,500 tumors obtained by aspiration with an 18-gauge needle, but there was no specific reference to head and neck paragangliomas.

One important clue to a paraganglioma is the presence of much blood in the aspirate (45). Aspirates often yield only a few clusters of tumor cells, and strands of cytoplasm may give a lattice-like appearance (40). Nuclei may appear "naked" or stripped of cytoplasm (46), and the presence of prominent nuclear vacuoles (nuclear pseudoinclusions) can simulate a papillary thyroid carcinoma (47). Rarely, tumor cells envelop one another (cell embracing) (47). Immunohistochemical stains may aid in the diagnosis of aspirates or cell block preparations if a paraganglioma is suspected (1,48).

QUANTITATIVE DETERMINATION OF DNA CONTENT

Quantification of DNA content in paragangliomas of the head and neck region has been done using flow cytometry or static image analysis of Feulgen-stained tissue sections. Several studies have shown that CBPs and other paragangliomas commonly have an abnormal content of DNA, and that DNA ploidy is not reliable in determining malignant potential (49–54). Some clinically malignant CBPs have even been reported to have normal diploid DNA (49). In a large study of 99 paragangliomas from 77 patients (average duration of follow-up, 10 years or more), aneuploidy was noted in 37 tumors (37 percent), none of which proved to be clinically malignant (52). While DNA aneuploidy in hereditary and sporadic paragangliomas does not reliably predict malignant behavior, it does provide strong support that these paragangliomas are truly neoplastic (52).

There also appears to be no relation between DNA ploidy and location of the paraganglioma in the neck (52). Cytogenetic analysis of a head and neck paraganglioma has seldom been reported and in a case of bilateral familial CBP, no evidence of numerical or structural alteration was seen (49).

In a recent study of six head and neck paragangliomas, multiparameter DNA flow cytometry was performed utilizing S-100 protein labeling as a selective marker of the sustentacular fraction simultaneously with DNA content measurement. The S-100 protein–labeled cell fraction was diploid and retained the wild type *SDHD* allele while there was loss of this allele in the S-100 protein–negative fractions (55). The results strongly suggested that the sustentacular cell population was non-neoplastic and may be induced as a tumor-specific stromal component by the neoplastic chief cells (55).

REFERENCES

General and Ultrastructural Features

1. Lack EE. Pathology of adrenal and extra-adrenal paraganglia. Major problems in pathology, Vol 29. Philadelphia: WB Saunders; 1994.
2. Lloyd RV, Sisson JC, Shapiro B, Verhofstad AA. Immunohistochemical localization of epinephrine, norepinephrine, catecholamine-synthesizing enzymes, and chromogranin in neuroendocrine cells and tumors. Am J Pathol 1986;125:45-54.
3. Lack EE, Cubilla AL, Woodruff JM. Paragangliomas of the head and neck region. A pathologic study of tumors from 71 patients. Hum Pathol 1979;10:191-218.
4. Grimley PM, Glenner GG. Histology and ultrastructure of carotid body paragangliomas. Comparison with the normal gland. Cancer 1967;20: 1473-1488.
5. Grimley PM, Glenner GG. Ultrastructure of the human carotid body. A perspective on the mode of chemoreception. Circulation 1968;37:648-665.
6. Capella C, Solcia E. Optical and electron microscopical study of cytoplasmic granules in human carotid body, carotid body tumours and glomus jugulare tumours. Virchows Arch B Cell Pathol 1971;7:37-53.
7. Kjaergaard J. Anatomy of the carotid glomus and carotid glomus-like bodies (non-chromaffin paraganglia). With electron microscopy and comparison of human foetal carotid, aorticopulmonary, subclavian, tympanojugular, and vagal glomera. Copenhagen: FADL's Forlag; 1973.
8. Stiller D, Katenkamp D, Kuttner K. Jugular body tumors: hyperplasias or true neoplasms? Light and electron microscopical investigations. Virchows Arch A Pathol Anat Histol 1975;365:163-177.
9. Kahn LB. Vagal body tumor (nonchromaffin paraganglioma, chemodectoma, and carotid body-like tumor) with cervical node metastasis and familial association: ultrastructural study and review. Cancer 1976;38:2367-2377.
10. Horváth KK, Ormos J, Ribári O. Crystals in a jugulotympanic paraganglioma. Ultrastr Pathol 1986;10:257-254.
11. Archer KF, Hurwitz JJ, Balogh JM, Fernandes BJ. Orbital nonchromaffin paraganglioma. A case report and review of the literature. Ophthalmology 1989;96:1659-1666.

Immunohistochemical Findings

12. Warren WH, Lee I, Gould VE, Memoli VA, Jao W. Paragangliomas of the head and neck: ultrastructural and immunohistochemical analysis. Ultrastruct Pathol 1985;8:333-343.
13. Capella C, Riva C, Cornaggia M, Chiaravalli AM, Frigerio B, Solcia E. Histopathology, cytology and cytochemistry of pheochromocytomas and paragangliomas including chemodectomas. Pathol Res Pract 1988;183:176-187.
14. Johnson TL, Zarbo RJ, Lloyd RV, Crissman JD. Paragangliomas of the head and neck: immunohistochemical neuroendocrine and intermediate filament typing. Mod Pathol 1988;1:216-223.
15. Erlandson RA. Diagnostic immunohistochemistry of human tumors. An interim evaluation. Am J Surg Pathol 1984;8:615-624.
16. Lloyd RV. Practical markers used in the diagnosis of neuroendocrine tumors. Endocr Pathol 2003;4:293-302.
17. Lloyd RV, Jin L, Kulig E, Fields K. Molecular approaches for the analysis of chromogranins and secretogranins. Diagn Mol Pathol 1992;1:2-15.
18. Schmid KW, Schröder S, Duckhorn-Dworniczak B, et al. Immunohistochemical demonstration of chromogranin A, chromogranin B, and secretogranin II in extra-adrenal paragangliomas. Mod Pathol 1994;7:347-353.
19. Tischler AS, Mobtaker H, Mann K, et al. Anti-lymphocyte antibody leu-7 (HNK-1) recognizes a constituent of neuroendocrine granule matrix. J Histochem Cytochem 1986;34:1213-1216.
20. Martinez-Madrigal F, Bosq J, Micheau C, Nivet P, Luboinski B. Paragangliomas of the head and neck. Immunohistochemical analysis of 16 cases in comparison with neuroendocrine carcinomas. Pathol Res Pract 1991;187:814-823.

S-100 Protein-Positive Cells and Prognosis

21. Kliewer KE, Cochran AJ, Wen DR, Cheng L, Cancilla PA. An immunohistochemical study of 37 paragangliomas. Med Sci Res 1987;15:87-88.
22. Korat O, Trojanowski JQ, LiVolsi VA, Merino MJ. Antigen expression in normal paraganglia and paragangliomas. Surg Pathol 1988;1:33-40.
23. Kliewer KE, Wen DR, Cancilla PA, Cochran AJ. Paragangliomas: assessment of prognosis by histologic, immunohistochemical, and ultrastructural techniques. Hum Pathol 1989;20:29-39.
24. Kliewer KE, Cochran AJ. A review of the histology, ultrastructure, immunohistology, and molecular biology of extra-adrenal paragangliomas. Arch Pathol Lab Med 1989;113:1209-1218.
25. Bhansali SA, Bojrab DI, Zarbo RJ. Malignant paragangliomas of the head and neck: clinical and immunohistochemical characterization. Otolaryngol Head Neck Surg 1991;104:132.

26. Bitterman P, Sherman M, Lack EE. Paragangliomas of the head and neck region: clinicopathologic and immunohistochemical evaluation of 88 cases. Patologia 1992;25:493A.
27. Linnoila RI, Becker RL Jr, Steinberg SM, Kaiser HR, Lack EE. The role of S-100 protein containing cells in the prognosis of sympathoadrenal paragangliomas [Abstract]. Mod Pathol 1993;6:39A.
28. Granger JK, Houn HY. Head and neck paragangliomas: a clinicopathologic study with DNA flow cytometric analysis. South Med J 1990;83: 1407-1412.
29. Furihata M, Ohtsuki Y. Immunohistochemical characterization of HLA-DR-antigen positive dendritic cells in pheochromocytomas and paragangliomas as a prognostic marker. Virchows Archiv A Pathol Anat Histopathol 1991;418:33-39.
30. Takahashi H, Nakashima S, Kumanishi T, Ikuta F. Paragangliomas of the craniocervical region. An immunohistochemical study on tyrosine hydroxylase. Acta Neuropathol (Berl) 1987;73: 227-232.

Molecular Genetics

31. Baysal BE. Genetics of familial paragangliomas: past, present, and future. Otolaryngol Clin North Am 2001;34:863-879.
32. van Nederveen FH, Dannenberg H, Sleddens HF, de Krijger RR, Dinjens WN. p53 alterations and their relationship to SDHD mutations in parasympathetic paragangliomas. Mod Pathol 2003;16:849-856.
33. Dannenberg H, Komminoth P, Dinjens WN, Speel EJ, de Krijger RR. Molecular genetic alterations in adrenal and extra-adrenal pheochromocytomas and paragangliomas. Endocr Pathol 2003;14:329-350.
34. McWhinney SR, Pilarski RT, Forrester SR, et al. Large germline deletions of mitochondrial complex II subunits SDHB and SDHD in hereditary paraganglioma. J Clin Endocrinol Metab 2004;89:5694-5699.
35. Vanharanta S, Buchta M, McWhinney SR, et al. Early-onset renal cell carcinoma as a novel extraparaganglial component of SDHB-associated heritable paraganglioma. Am J Hum Genet 2004;74:153-159.
36. Dannenberg H, de Krijger RR, Zhao J, et al. Differential loss of chromosome 11q in familial and sporadic parasympathetic paragangliomas detected by comparative genomic hybridization. Am J Pathol 2001;158:1937-1942.
37. Cascon A, Ruiz-Llorente S, Rodriguez-Perales S, et al. A novel candidate region linked to development of both pheochromocytoma and head/neck paraganglioma. Genes Chromosomes Cancer 2005;42:260-268.
38. Spicer Z, Millhorn DE. Oxygen sensing in neuroendocrine cells and other cell types: pheochromocytoma (PC12) cells as an experimental model. Endocr Pathol 2003;14:277-291.

Fine Needle Aspiration and Cytologic Findings

39. Fleming MV, Oertel YC, Rodriguez ER, Fidler WJ. Fine-needle aspiration of six carotid body paragangliomas. Diagn Cytopathol 1993;9:510-515.
40. Qizilbash AH, Young JE. Guides to clinical aspiration biopsy. Head and neck. New York: Igaku-Shoin; 1988:279-289.
41. Engzell U, Franzén S, Zajicek J. Aspiration biopsy of tumors of the neck II. Cytologic findings in 13 cases of carotid body tumor. Acta Cytol 1971; 15:25-30.
42. Lack EE, Cubilla AL, Woodruff JM, Farr HW. Paragangliomas of the head and neck region: a clinical study of 69 patients. Cancer 1977;39: 397-409.
43. Martin HE, Ellis EB. Biopsy by needle puncture and aspiration. Ann Surg 1930;92:169-181.
44. Stewart FW. The diagnosis of tumors by aspiration. Am J Pathol 1933;9:801-812.
45. Farr HW. Carotid body tumors. A thirty year experience at Memorial Hospital. Am J Surg 1967; 114:614-619.
46. González-Cámpora R, Otal-Salaverri C, Panea-Flores P, Lerma-Puertas E, Galera-Davidson H. Fine needle aspiration cytology of paraganglionic tumors. Acta Cytol 1988;32:386-390.
47. Mincione GP, Urso C. Carotid body paraganglioma (chemodectoma): cytologic remarks. Pathologica 1989;81:179-183.
48. Zaharopoulos P. Diagnostic challenges in the fine-needle aspiration diagnosis of carotid body paragangliomas: report of two cases. Diagn Cytopathol 2000;23:202-207.

Quantitative Determination of DNA Content

49. Granger JK, Houn HY. Head and neck paragangliomas: a clinicopathologic study with DNA flow cytometric analysis. South Med J 1990;83: 1407-1412.
50. Granger JK, Houn HY. Bilateral familial carotid body paragangliomas. Report of a case with DNA flow cytometric and cytogenetic analyses. Arch Pathol Lab Med 1990;114:1272-1275.
51. Barnes L, Taylor SR. Carotid body paragangliomas. A clinicopathologic and DNA analysis of 13 tumors. Arch Otolaryngol Head Neck Surg 1990;116:447-453.
52. van der Mey AG, Cornelisse CJ, Hermans J, Terpstra JL, Schmidt PH, Fleuren GJ. DNA flow cytometry of hereditary and sporadic paragangliomas (glomus tumours). Br J Cancer 1991;63: 298-302.

53. Milroy CM, Williams RA, Charlton IG, Moss E, Rode J. Nuclear ploidy in neuroendocrine neoplasms of the larynx. ORL J Otorhinolaryngol Relat Spec 1991;53:245-249.
54. González-Cámpora R, Diaz Cano S, Lerma-Puertas E, et al. Paragangliomas. Static cytometric studies of nuclear DNA patterns. Cancer 1993;71:820-824.
55. Douwes Dekker PB, Corver WE, Hogendoorn PC, van der Mey AG, Cornelisse CJ. Multiparameter DNA flow-sorting demonstrates diploidy and SDHD wild-type gene retention in the sustentacular cell compartment of head and neck paragangliomas: chief cells are the only neoplastic component. J Pathol 2004;202:456-462.

19 NEUROBLASTOMA, GANGLIONEUROBLASTOMA, AND OTHER RELATED TUMORS

NEUROBLASTOMA AND GANGLIONEUROBLASTOMA

Neuroblastoma (NB) is a primitive neoplasm of neuroectodermal origin that arises in anatomic sites paralleling the distribution of the sympathoadrenal neuroendocrine system. *Ganglioneuroblastoma* (GNB) is a closely related neoplasm showing variable cytodifferentiation into ganglion cells, often accompanied by a spindle cell schwannian matrix. The term *neuroblastic* or *peripheral neuroblastic tumor* has been used to embrace the full morphologic range of NB and GNB and even the most mature and histologically benign ganglioneuroma.

Epidemiology

NB and GNB are the fourth most common malignant tumors in childhood after leukemia, brain tumors, and malignant lymphoma (1). The incidence of NB in the United States is estimated to be 8.7/million white population and of GNB, 1.8/million, with a slightly lower incidence in blacks. About 85 percent of all cases of NB and GNB occur in the first 4 years of life; there are no sex-related differences in incidence rates (2). Both NB and GNB make up 7.9 percent of the 9,308 childhood cancers followed by the Surveillance, Epidemiology, and End Result (SEER) program in children younger than age 15 years (3). In a series of 118 patients, 88 percent were 5 years of age or younger at diagnosis, with a median age of 21 months (fig. 19-1) (4). These tumors are very uncommon in the 2nd decade, and are rare in adult life, although NB and GNB have been reported at nearly every age (1).

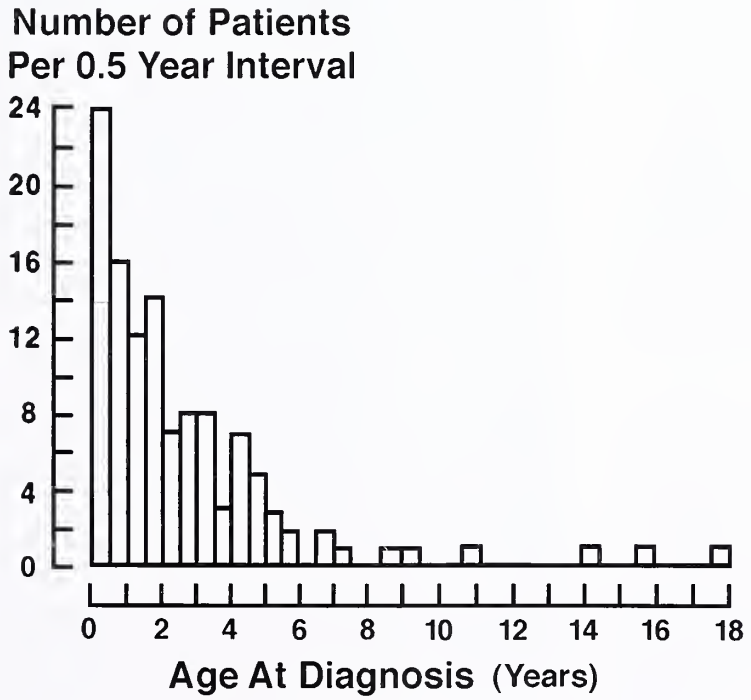

Figure 19-1

AGE DISTRIBUTION OF 118 PATIENTS WITH NEUROBLASTOMA

Nearly 90 percent of patients are 5 years of age or younger at diagnosis. The median age at diagnosis is 21 months. (Fig. 1 from Rosen EM, Cassady JR, Frantz CN, Kretschmar C, Levey R, Sallen SE. Neuroblastoma: The Joint Center For Radiation Therapy/ Dana-Farber Cancer Institute/Children's Hospital experience. J Clin Oncol 1984;2: 719-732.)

Table 19-1

UNUSUAL MANIFESTATIONS OR ASSOCIATIONS WITH CHILDHOOD NEUROBLASTOMA[a]

Congenital neuroblastoma
Cutaneous metastases and "blueberry muffin" baby
Placental enlargement with hydrops fetalis
Neuroblastoma "leukemia"
Opsoclonus/myoclonus
Alopecia
Heterochromia iridis
Horner's syndrome
Watery diarrhea (vasoactive intestinal peptide [VIP] secretion)
Cushing's syndrome
Asymmetric crying facies
Central hypoventilation syndrome ("Ondine's curse")
Late recurrence and death
Familial neuroblastoma
Association with von Recklinghausen's disease

[a]Table 14-1 from Lack EE. Pathology of adrenal and extraadrenal paraganglia. Major problems in pathology, Vol. 29. Philadelphia: WB Saunders; 1994:318.

NB has an unusual geographic distribution, with a low incidence in certain areas, particularly the "Burkitt lymphoma belt" of Africa (5). Familial occurrence of NB has been reported (6), and in some cases appears to have an autosomal dominant pattern of inheritance; however, there are obvious difficulties in determining the incidence and penetrance of an inherited susceptibility for this neoplasm given its capacity for regression, maturation, and early death, and the treatment complications that preclude reproduction and prevent multigenerational pedigrees for evaluation (7). Some studies indicate essentially no risk of offspring of surviving patients with NB or GNB developing similar tumors (8). Using the two-mutation model of cancer genesis, nonhereditary NBs and pheochromocytomas have both events occurring in somatic cells and the tumor is characteristically solitary, whereas in hereditary cases, the tumors may be multiple (9).

There are a variety of disorders or unusual manifestations associated with these tumors (Table 19-1) (1). A watery diarrhea syndrome has been reported with NB, GNB, ganglioneuroma, and pheochromocytoma, with or without composite features (1). This diarrheal syndrome has been reported in 6 percent of children with NB and GNB (4) and secretion of vasoactive intestinal peptide (VIP) has been implicated as an etiologic agent (1). Ganglion cell differentiation has been considered a prerequisite for VIP production, but as indicated for pheochromocytomas, this may not always be true. Adrenergic overactivity due to excess catecholamine secretion is uncommon with NB and GNB, and in one series only 4 percent of patients were hypertensive at the time of diagnosis (4). Opsoclonus/myoclonus ("dancing eyes, dancing feet") is present in 2 to 7 percent of patients with NB and GNB, and has been associated with a favorable prognosis, but may present a diagnostic dilemma in a child without a palpable mass or abnormalities in excretion of catecholamines or their metabolites (4). In a large series of 1,187 children (0 to 15 years) with previously untreated neuroblastic tumors, 15 (1.3 percent) had opsoclonus-myoclonus syndrome at presentation (10). In that study, factors contributing to a favorable prognosis included ganglioneuroblastoma intermixed subtype, lack of *N-myc* oncogene amplification, and the presence of abundant lymphoid infiltrates. Heterochromia iridis is a rare, but potentially important sign associated with cervical or mediastinal NB or GNB (1), and has even been reported in a patient with paravertebral neurilemoma (fig. 19-2); the heterochromia results from prenatal or postnatal interruption of sympathetic tracts that apparently mediate pigmentation of the iris (11).

Mass Screening Programs for Neuroblastoma

Mass screening for NB began in Kyoto, Japan in 1974 (12), and other screening programs have been subsequently developed in other areas of Japan and other countries. Mass screening in infancy, usually at 6 months of age, with a qualitative vanillylmandelic acid (VMA) spot test, has resulted in an increased annual detection rate of 93/million compared with a baseline annual rate of 13.3/million without screening (13). Screening for urinary catecholamine metabolites and dopamine has been done earlier (14) and at 12 (15) and 14 months of age (16), but the usefulness of general screening has been questioned in terms of decreasing the mortality rate from neuroblastoma (14,15).

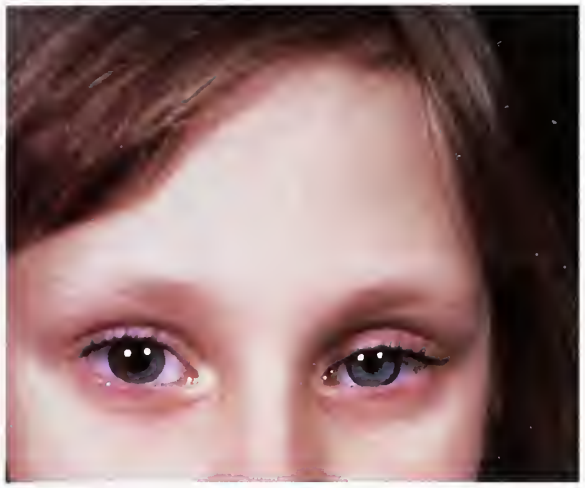

Figure 19-2

HETEROCHROMIA IRIDIS ASSOCIATED WITH INTRATHORACIC PARAVERTEBRAL NEURILEMOMA

A 7-year-old-girl had Horner's syndrome on the right side and heterochromia iridis. The patient had an upper thoracic paravertebral neurilemoma on the left side measuring 4 cm in diameter. Half of the right iris was brown, and the other half blue, while the left iris was blue throughout. (Fig. 23-2 from Fascicle 19, Third Series.)

Table 19-2

INCIDENCE AND SURVIVAL DATA BASED UPON PRIMARY ANATOMIC SITE OF NEUROBLASTOMA[a,b]

Primary Site	Incidence (%)	Survival (%)
Head	2	33
Neck	5	15
Thorax	14	61
Abdomen	54	20
Adrenal	36	9
Nonadrenal	18	32
Pelvis	5	41
Other	10	21
Unknown	10	17

[a]Table 23-2 from Fascicle 19, Third Series.
[b]Data from reference 19.

The prognosis for children with NB detected by screening is clearly favorable, and important factors are low clinical stage and early age at diagnosis (1,17). Tumors that are not detected through screening but are diagnosed clinically after 12 months of age are of predominantly unfavorable histology with poor outcomes (over 1 year of age and advanced stage). Some have recommended additional screening of infants over 12 months of age to detect tumors that may have been missed during earlier screening (18). More data are needed to tell whether preclinical detection will truly result in a decline in population-based mortality for patients with NB (14,15).

Anatomic Distribution of Primary Tumors

The anatomic distribution of NB and GNB closely parallels that of the sympathoadrenal neuroendocrine system with which they are so closely aligned (1). Data on anatomic site compiled from 10 reference sources by Jaffe (19) are shown in Table 19-2. The anatomic distribution of NB and GNB in 118 patients is shown in figure 19-3 (4). Unusual anatomic sites of origin include orbit (1), intrarenal (20), and ovary (cystic teratoma) (21). A better survival rate has been noted for patients with NB and GNB located in the neck, thorax (fig. 19-4) (22), and pelvis, but this may be attributed in large part to early stage disease and younger age at diagnosis. Thoracic NB has been reported to contain more complex gangliosides of the b series and few monosialogangliosides, suggesting a more differentiated cellular composition (23). Only about 2 to 3 percent of all primary tumors arise in the cervical area (4) of the sympathetic chain (fig. 19-5); these tumors may encase the ganglion nodosum of the vagus nerve and occasionally cause Horner's syndrome (24).

There may be intraspinal extension of NB and GNB with compression of spinal cord, and extradural intraspinal extension has also been reported with ganglioneuroma. King et al. (25) found intraspinal extension ("dumbbell" NB) in 10 percent of abdominal NBs, 28 percent of thoracic tumors (fig. 19-6), and one of four cervical tumors (25 percent).

Staging Systems

The staging system proposed by Evans et al. (26) has been very popular and continues to provide valuable information regarding prognosis, but other staging classifications have been proposed and comparative studies of many of them have been reported (27). An international NB staging system, very similar to the original Evans classification, may avoid some disparities in staging criteria (Table 19-3) (28). Based

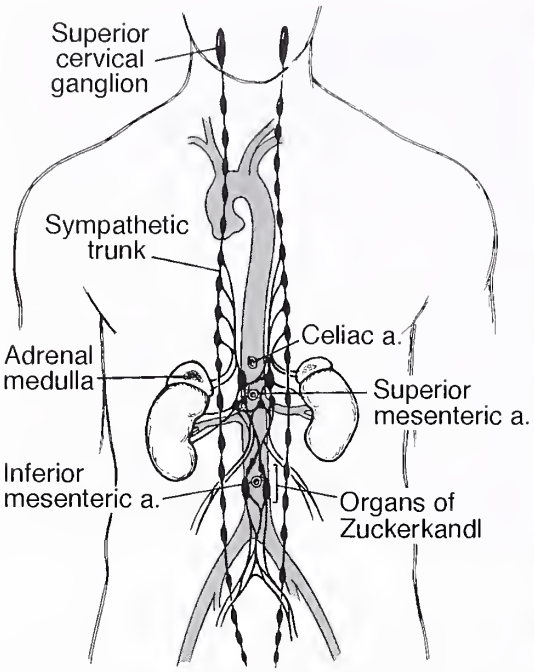

Site	Number	(%)
Unknown	6	(5.1)
Cervical	4	(3.4)
Thoracic	24	(20.3)
Abdomen	80	(67.8)
Adrenal	45	(38.1)
Extraadrenal	35	(29.7)
Pelvic	4	(3.4)
All sites	**118**	**(100.0)**

Figure 19-3

ANATOMIC DISTRIBUTION OF PRIMARY NEUROBLASTOMA AND GANGLIONEUROBLASTOMA IN 118 PATIENTS

Most tumors were intraabdominal, arising in adrenal glands or upper abdomen. (Table data from Rosen EM, Cassady JR, Frantz CN, Kretschmar C, Levey R, Sallan SE. Neuroblastoma: the Joint Center for Radiation Therapy/ Dana-Farber Cancer Institute/Children's Hospital experience. J Clin Oncol 1984;2:719–32.) (Fig. 23-3 from Fascicle 19, Third Series.)

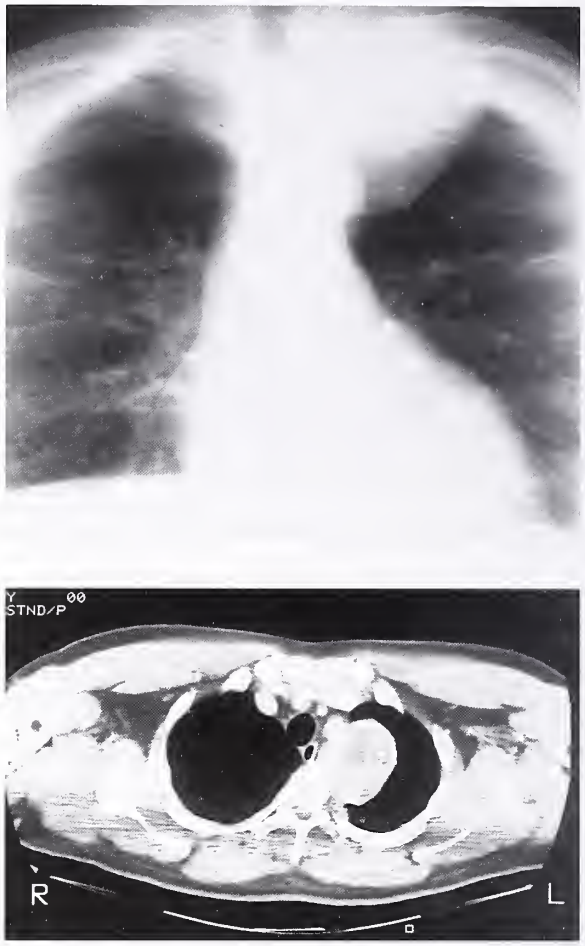

Figure 19-4

STROMA-POOR NEUROBLASTOMA

Top: A 25-year-old-man presented with a history of dry cough and on chest roentgenogram had a large intrathoracic, paravertebral mass. The tumor was a stroma-poor neuroblastoma (NB) in the original Shimada classification (57) with 5 percent differentiating elements and a low mitosis-karyorrhexis index (MKI). (Fig. 14-2 from Lack EE. Pathology of adrenal and extra-adrenal paraganglia. Major problems in pathology, Vol. 29. Philadelphia: WB Saunders; 1994:316.)

Bottom: Computerized tomography (CT) scan in the same case showed the tumor in the paravertebral sulcus on the left side. The tumor is nonhomogeneous and has areas of dystrophic calcification. An earlier biopsy of a left supraclavicular lymph node showed metastatic NB. (Fig. 23-4, bottom from Fascicle 19, Third Series.)

upon several clinical series, the relative proportion of patients at each stage at diagnosis is 6 to 8 percent at stage I, 9 to 24 percent at stage II, 9 to 23 percent at stage III (4,29,30), 48 to 52 percent at stage IV, and 8 to 12 percent at stage IV-S (S = special) (4,31–33). Between 60 and 70 percent of patients with NB and GNB have advanced stage disease or metastases at presentation (i.e., stages IV and IV-S), while 30 to 40 percent have more localized disease (i.e., stages I, II, and III) (27,29,30). In a study of 128 children with peripheral neuroblastic tumors, 52

Table 19-3

INTERNATIONAL STAGING SYSTEM FOR NEUROBLASTOMA[a,b]

Stage I	Localized tumor confined to the area of origin; complete gross excision, with or without microscopic residual disease; identifiable ipsilateral and contralateral lymph nodes negative microscopically
Stage IIA	Unilateral tumor with incomplete gross excision; identifiable ipsilateral and contralateral lymph nodes negative microscopically
Stage IIB	Unilateral tumor with complete or incomplete gross excision; positive ipsilateral regional lymph nodes; identifiable contralateral lymph nodes negative microscopically
Stage III	Tumor infiltrating across the midline without regional lymph node involvement; or unilateral tumor with contralateral regional lymph node involvement; or midline tumor with bilateral lymph nodes negative
Stage IV	Dissemination of tumor to distant lymph nodes, bone, bone marrow, liver, and/or other organs (except as defined in stage IV-S)
Stage IV-S	Localized primary tumor as defined for stage I or II with dissemination limited to liver, skin, and/or bone marrow

[a]Table 23-3 from Fascicle 19, Third Series.
[b]Data from reference 28.

Figure 19-5

CONGENITAL CERVICAL NEUROBLASTOMA

A newborn female with a large congenital NB in the right neck. The tumor was stroma-poor with a low MKI, a favorable subgroup in the original Shimada classification. (Fig. 14-6 from Lack EE. Pathology of adrenal and extra-adrenal paraganglia. Major problems in pathology, Vol. 29. Philadelphia: WB Saunders; 1994:320.)

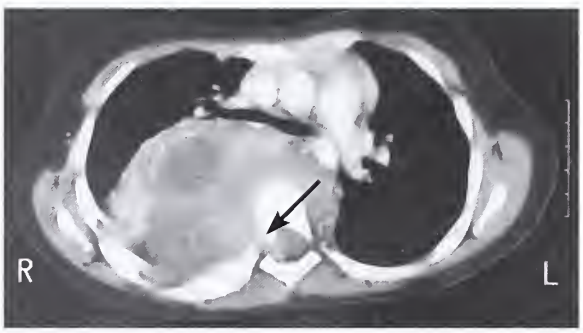

Figure 19-6

INTRATHORACIC GANGLIONEUROBLASTOMA

A large intrathoracic ganglioneuroblastoma (GNB) in a 5-year-old girl partially destroyed the rib posteriorly and extended across the midline. There are spotty areas of calcification within the tumor as well as erosion of the intervertebral foramen on the right side (arrow) due to intraspinal extradural extension by tumor. (Fig. 23-6 from Fascicle 19, Third Series.)

percent had localized disease, 41 percent were stage IV, and 7 percent were stage IV-S; the 5-year overall survival rate was 65 percent (34). The IV-S category includes patients with any extent of bone marrow involvement; although it is not limited to the age of 1 year, few patients are older than this (28). Bone marrow involvement in stage IV-S should be minimal (i.e., less than 10 percent of total nucleated cells identified as malignant on bone marrow biopsy or marrow aspirate). More extensive marrow involvement is considered stage IV (35). Chronic NB has been regarded as a relatively indolent stage IV disease in children since there is prolonged survival in the wake of complex therapeutic programs that incorporate novel treatments (36).

Figure 19-7

IN SITU NEUROBLASTOMA

A: Incidental in situ NB in a 26-day-old girl who died of congenital heart disease. The tumor measured 6 mm in diameter. The junction with residual adult or definitive cortex is indicated by arrows.

B: This in situ NB is composed of sheets of monotonous primitive cells.

C: Secondary degenerative features can sometimes be found, such as edema and microcystic change. (A–C: Fig. 23-7 from Fascicle 19, Third Series.)

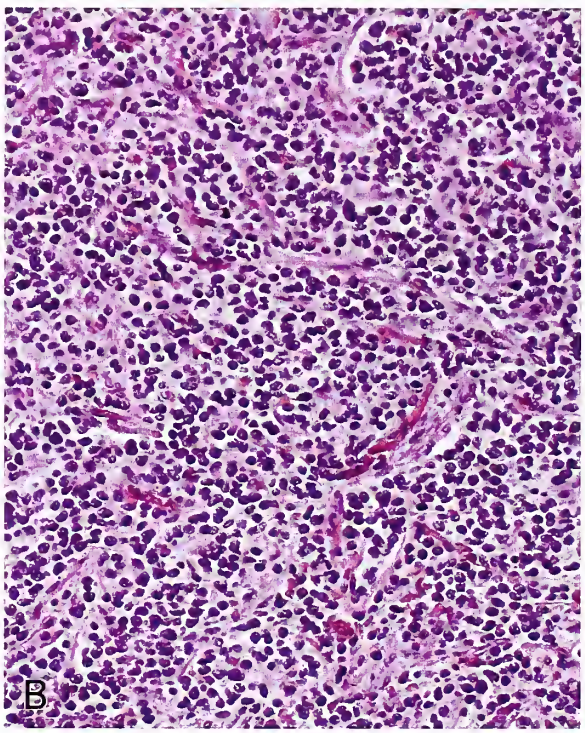

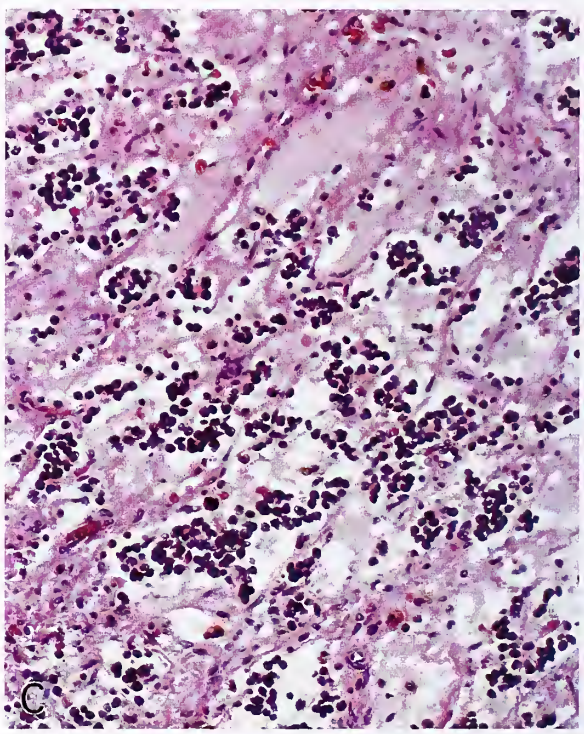

In Situ Neuroblastoma

The concept of *in situ NB* was introduced by Beckwith and Perrin (37) for a small nodule of NB cells within the adrenal gland (fig. 19-7) that was histologically indistinguishable from childhood NB, but without evidence of tumor anywhere else. The size of the in situ NBs in their study ranged from 0.7 to 9.5 mm. In situ NB has been found in from 1 in 39 (38) to 1 in 244 autopsies (37) of infants less than 3 months of age, an incidence that is much higher than that of clinically overt NB, suggesting that the lesion involutes or matures "spontaneously" or otherwise remains clinically occult. The increased frequency reported in the study by Guin et al. (38) is due to careful prospective evaluation of adrenal glands yielding 5 to 12 blocks from each gland. Other possibilities for a higher incidence of in situ NBs include evolution into an adrenal cyst or a calcified scar. In situ NB has been reported associated with an adrenal cyst, very similar to cystic NB (39). The nodules of neuroblasts that are an integral part of the normal development of the adrenal gland (see chapter 1) may be hard to distinguish from in situ NB (40,41).

Stage IV-S Neuroblastoma

Stage IV-S NB is a distinctive subgroup with distant metastases to liver (fig. 19-8), skin (fig. 19-9), or bone marrow without evidence of bone metastases (see Table 19-3) (42). These children usually have a small intraabdominal adrenal primary, but in about 10 percent of cases no primary tumor is identified (43). Stage IV-S NB usually occurs in infants of a median age of about 3 months (44), but is occasionally found in those over the age of 1 year. The prognosis is good, with survival rates of 80 percent (42,43,45) despite an immense tumor burden. Spontaneous regression has been documented, and some have proposed that stage lV-S NB represents hyperplastic nodules of nonmalignant neural tissue bearing a mutation that interferes with normal development, and a second "hit" or further event could transform the lesions into malignant neoplasms such as malignant schwannoma or NB (46). No significant cytogenetic abnormalities have been described (47), and the patients usually lack the adverse prognostic findings associated with stage IV NB or the high frequency of *N-myc* oncogene amplification (48), although exceptions have been noted (49).

ln 1901, Pepper (50) described six infants who in the first 6 weeks of life had abdominal distension and massive liver enlargement due to "congenital sarcoma of the liver and suprarenal," which proved fatal 10 days to 16 weeks later. These patients had the "high-risk" type of stage lV-S NB with massive enlarging hepatomegaly and secondary complications such as compromise of cardiac, respiratory, or renal function (45). Low-dose radiotherapy or chemotherapy may be of benefit in stage lV-S disease; surgical procedures, such as formation of a silastic pouch to relieve intraabdominal pressure, may also help (fig. 19-10) (42,45). The designation of IV-P (P = Pepper) has been proposed for this high-risk group (45).

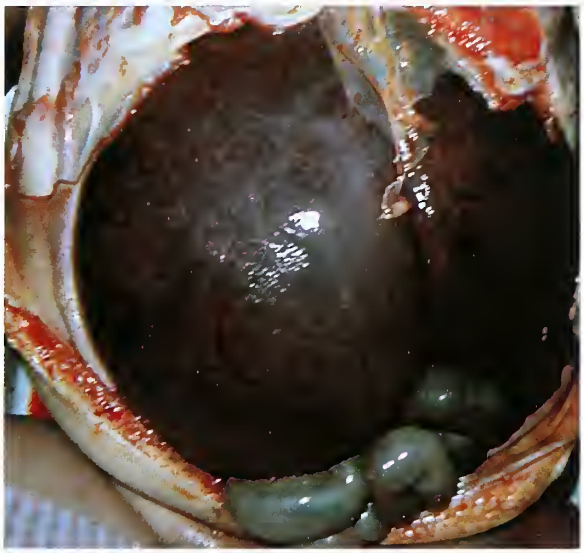

Figure 19-8

STAGE IV-S NEUROBLASTOMA

An infant with stage IV-S NB has massive involvement of liver at autopsy. Marked hepatomegaly such as this can compromise function of vital organs and result in death. (Fig. 23-8 from Fascicle 19, Third Series.)

Figure 19-9

STAGE IV-S NEUROBLASTOMA

Infant with stage IV-S NB has multiple cutaneous metastases which appear as mobile blue-gray nodules. (Fig. 23-9 from Fascicle 19, Third Series.)

Figure 19-10

STAGE IV-S NEUROBLASTOMA

This infant has massive hepatomegaly due to metastatic NB. Intraabdominal pressure is partially relieved by a silastic pouch. (Fig. 23-10 from Fascicle 19, Third Series.)

Gross Findings

The gross morphology of NB and GNB can vary considerably from a relatively circumscribed ovoid mass to a massive multilobulated tumor measuring 10 cm or larger (51). A recent study correlated the gross morphology of NB and GNB with radiographic and other imaging characteristics (51). A very small adrenal primary may give the impression of "encapsulation," but part of the perceived capsule may be the adrenal capsule proper. On cross section, NB may be hemorrhagic with vague bulging lobules (fig. 19-11). Some tumors are massive (fig. 19-12), and entirely eclipse the associated adrenal gland, making it difficult or impossible to determine the precise anatomic site of origin (fig. 19-13).

The tumor is usually a solitary, unicentric mass or contiguous aggregation of large nodules; bilateral adrenal NB or GNB or multicentric nondisseminated tumors are very unusual (52,53). Several examples of NB extending into the inferior vena cava have been reported, including one extending into the right atrium (54). The color and consistency of the tumor in cross section depend upon the extent of hemorrhage or necrosis and the amount and distribution of stromal component, be it the fibrillary component resembling neuropil or a cellular, schwannian matrix (fig. 19-14). Some tumors are composed of strikingly different areas, with one portion well differentiated (e.g., ganglioneuroma) and one or more areas of NB;

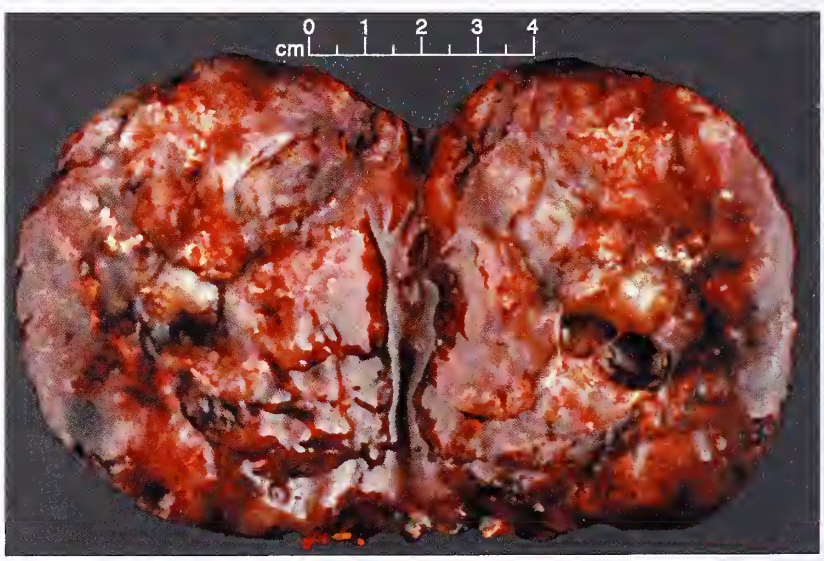

Figure 19-11

ADRENAL NEUROBLASTOMA

Large adrenal NB in a 7-year-old girl. The tumor measured 11 cm in diameter and weighed 237 g. The cut surface has a lobulated appearance with areas of hemorrhage. The tumor replaced almost the entire adrenal gland.

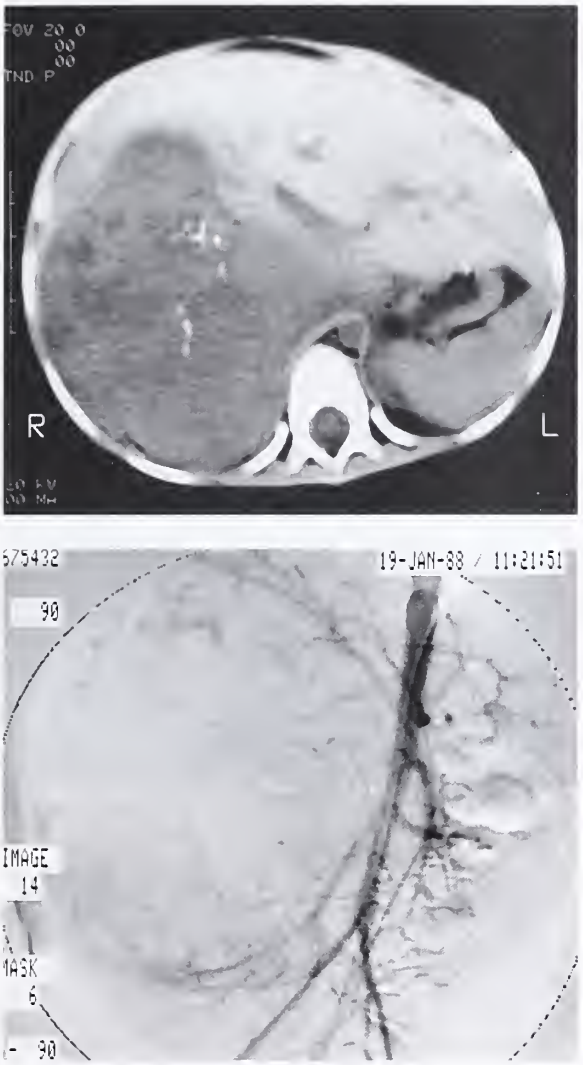

Figure 19-12

ABDOMINAL NEUROBLASTOMA

Top: Abdominal CT scan from a 2-year-old girl with a large NB in the right hemiabdomen that extended across the midline and displaced the aorta somewhat. Note also the irregular calcifications within the tumor.

Bottom: Aortogram in same case shows tenting and stretching of vessels by a large abdominal NB. (Fig. 14-14A,B from Lack EE. Pathology of adrenal and extra-adrenal paraganglia. Major problems in pathology, Vol 29. Philadelphia: WB Saunders; 1994:327.)

Figure 19-13

HEMORRHAGIC NEUROBLASTOMA

Cross section of a large hemorrhagic NB of the left adrenal gland at autopsy. The tumor replaced the entire adrenal gland and invaded the renal parenchyma. Note the coarse lobulations on cross section, with bulging nodules showing irregular areas of hemorrhage. The tumor had a soft, almost encephaloid, texture. Several regional lymph nodes are involved by metastases. (Fig. 23-13 from Fascicle 19, Third Series.)

such tumors were referred to as *composite GNB* by Stout (55,56), and are included under the stroma-rich nodular grouping in the classification described by Shimada et al. (57).

On close inspection, bulging lobules of tumor may be deeply congested or hemorrhagic, and have a soft, almost encephaloid consistency (fig. 19-15). Cystic degeneration can be seen in some tumors, and on rare occasion, a NB can rupture, leading to retroperitoneal hemorrhage and shock (58). Calcification may be apparent on gross inspection as punctate, opaque foci (fig. 19-15). In some tumors this is a conspicuous feature which can be readily appreciated on gross examination (fig. 19-16, left); on sectioning it may impart a gritty sensation.

A specimen radiograph may vividly demonstrate calcifications (fig. 19-16, right). In a study of 106 adrenal masses of all types in all age groups, NBs were the most common calcified masses seen on radiographs, sonography, or computerized

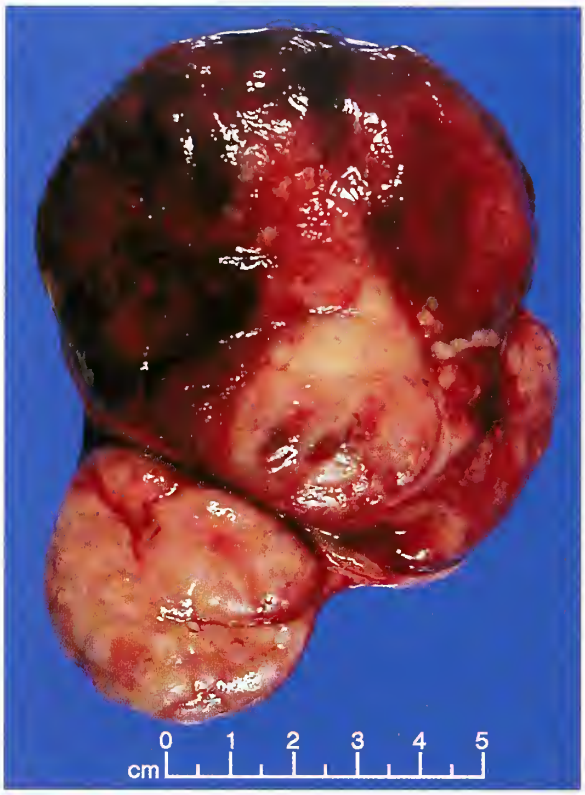

Figure 19-14

STROMA-POOR NEUROBLASTOMA

This tumor on cross section shows a variation from hemorrhagic, bulging, irregular lobules to more pale, homogeneous foci. Because of ganglion cell differentiation, this tumor in older terminology would be classified as GNB. (Fig. 23-14 from Fascicle 19, Third Series.)

Figure 19-15

STROMA-POOR NEUROBLASTOMA OF UPPER ABDOMEN IN A TEENAGE PATIENT

Bulging nodules of tumor are congested and hemorrhagic. Punctate yellowish areas represent dystrophic calcification. (Fig. 23-15 from Fascicle 19, Third Series.)

tomography (CT) scan (59). Calcification has been reported to be detectable in at least 30 percent of NBs on plain radiography and approximately 80 to 90 percent on CT scan (51).

Microscopic Findings

Architectural Pattern. NBs and GNBs often have a lobular growth pattern, with delicate, often incomplete fibrovascular septa (fig. 19-17) (1). Sometimes there are areas with a more diffuse or solid pattern. A distinct organoid pattern has been described in which a thin fibrovascular meshwork isolates regular nests of NB cells; this is reported to be an indicator of good prognosis in younger children (60). Immunostaining for S-100 protein shows a prominent spindle cell component, suggesting a close relationship between NB and Schwann cells (60).

There is a continuum of microscopic morphology between undifferentiated NB (fig. 19-18) and GNB (61): at one end of the spectrum is the prototypical small, "blue cell" tumor of childhood with a range of patterns that merge imperceptibly with GNB (fig. 19-19); at the other end are tumors that are so highly differentiated (in part or throughout) that they resemble ganglioneuroma (fig. 19-20). Most clinical series of childhood NBs include all neoplasms that fall within this wide spectrum (1). The correct diagnosis may be difficult, particularly with undifferentiated neuroblastomas, tumors that have been poorly fixed, or in biopsy specimens with crush artifact.

Cytomorphology. One of the most characteristic features of NB is the formation of Homer Wright rosettes or pseudorosettes (fig. 19-21)

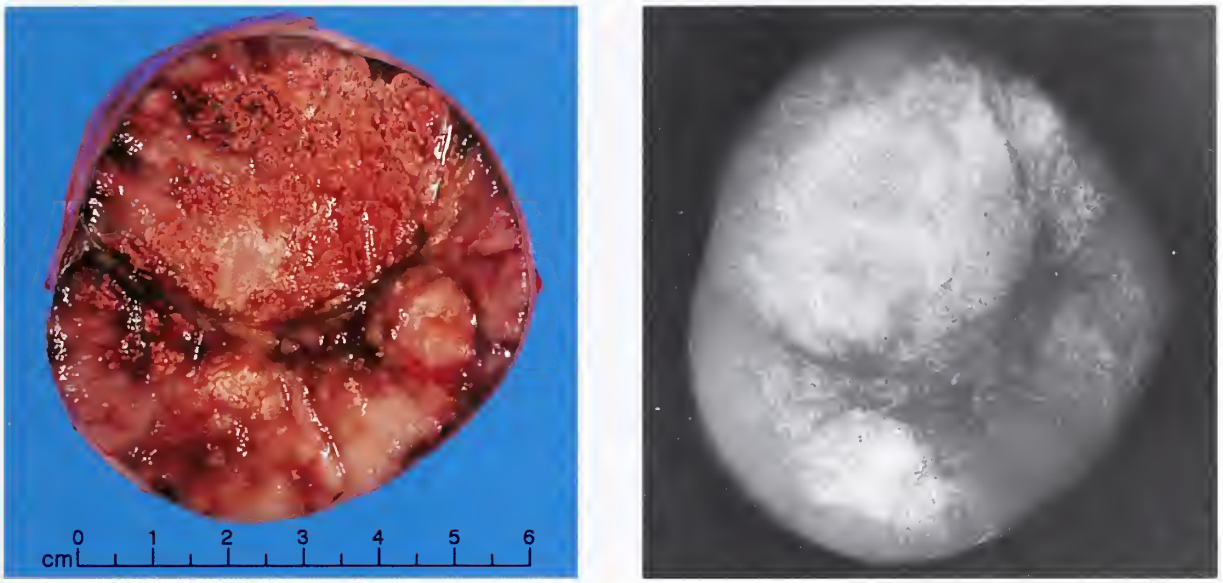

Figure 19-16

ADRENAL NEUROBLASTOMA

Left: Cross section of a 174-g adrenal NB from a 5-month-old boy. There is extensive calcification within the tumor, which appears as yellowish coarse granular areas. (Fig. 23-16A from Fascicle 19, Third Series.)

Right: Specimen radiograph with identical orientation shows extensive foci of dystrophic calcification. (Fig. 7-6B from Lack EE, Kozakewich HP. Adrenal neuroblastoma, ganglioneuroblastoma, and related tumors. In Lack EE, ed. Pathology of the adrenal glands. New York: Churchill Livingstone; 1990:282).

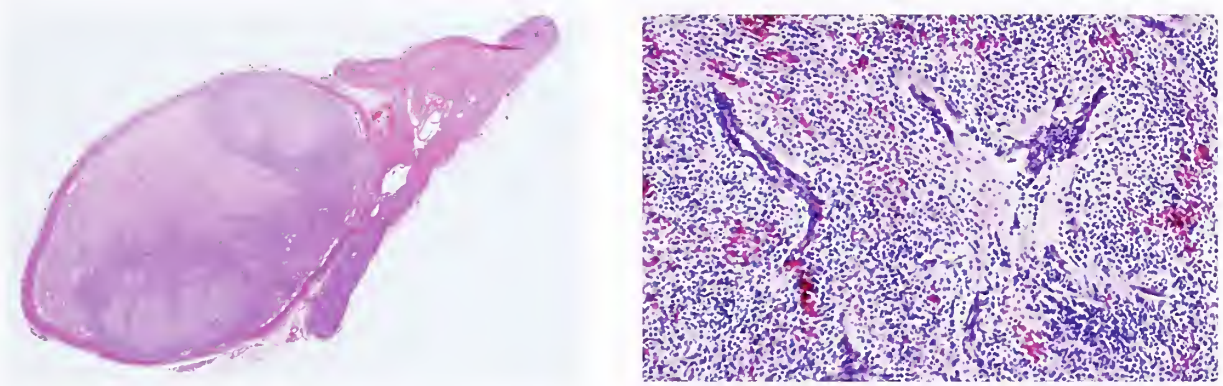

Figure 19-17

ADRENAL NEUROBLASTOMA

Left: The stroma-poor NB is relatively small and well circumscribed. The two darker nodular areas are less differentiated while the paler areas were rich in fibrillary matrix resembling neuropil.

Right: The NB has a lobular architecture, but it is not as well developed and organoid as pheochromocytomas or extraadrenal paragangliomas. The section is from one of the darker nodules.

(62,63), although in actual practice, well-formed rosettes are often difficult to identify. The rosettes are circular, ovoid, or angular zones of pale-staining, fibrillar material flanked circumferentially by tumor cell nuclei. The fibrillar matrix represents a tangled skein of neuritic cell processes. Sometimes there is a small vascular channel or collagenous tissue within the fibrillar zone, which is sometimes referred to as a pseudorosette (fig. 19-22). Because of the alignment of

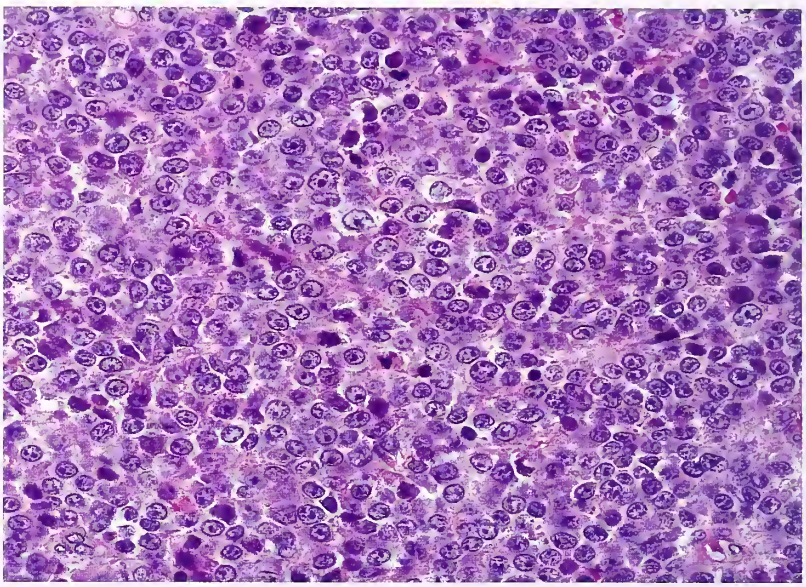

Figure 19-18

UNDIFFERENTIATED NEUROBLASTOMA

Closely packed, poorly differentiated neuroblasts form solid sheets. Patterns such as this may cause confusion with other childhood neoplasms such as malignant lymphoma. Most nuclei have a single, small nucleolus. The tumor had been fixed in B-5 fixative. (Fig. 23-18 from Fascicle 19, Third Series.)

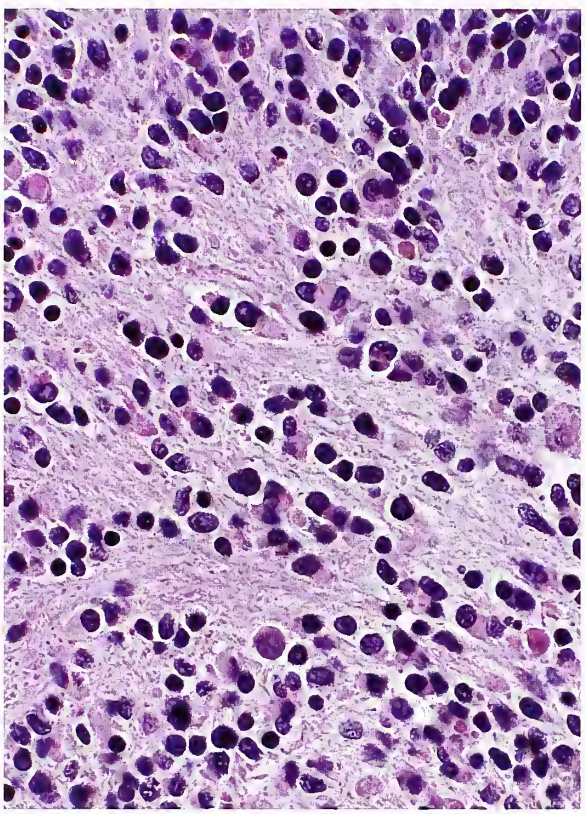

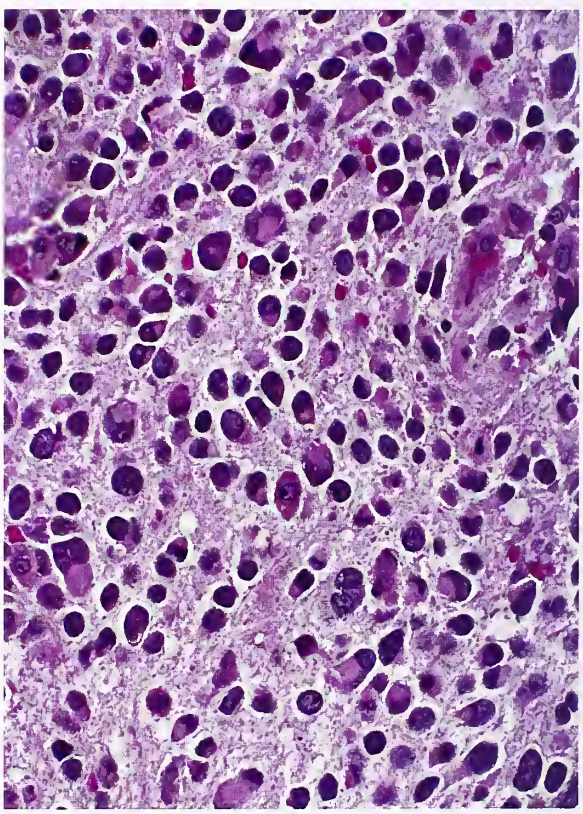

Figure 19-19

STROMA-POOR NEUROBLASTOMA

Left: The tumor cells are separated by pale pink fibrillar material representing neuritic cell processes. The tumor was largely undifferentiated with only rare cells showing early ganglion cell differentiation.

Right: A different tumor with abundant, relatively immature ganglion cells. (L&R: Fig. 23-19 from Fascicle 19, Third Series.)

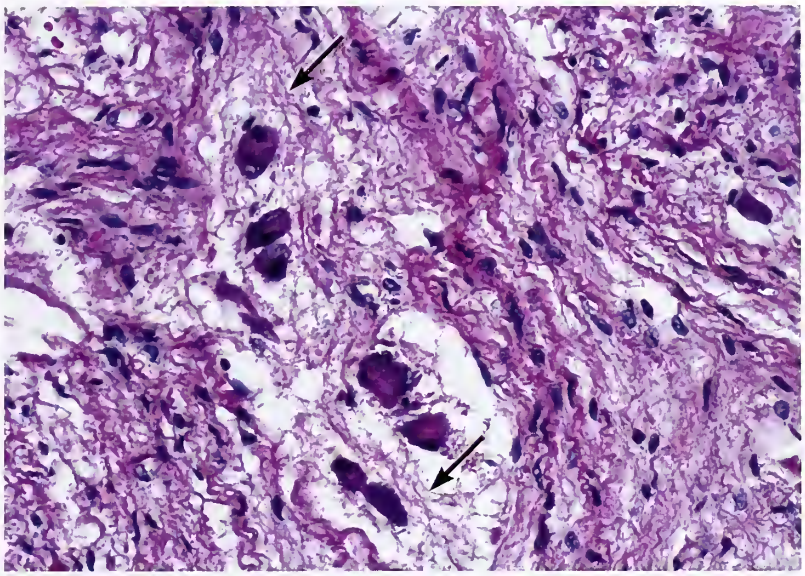

Figure 19-20

STROMA-RICH TUMOR

A high level of ganglion cell differentiation was apparent along with a prominent schwannian spindle cell stroma, but the tumor is still incompletely differentiated as evidenced by the fibrillary matrix (arrows). (Fig. 23-20 from Fasicle 19, Third Series.)

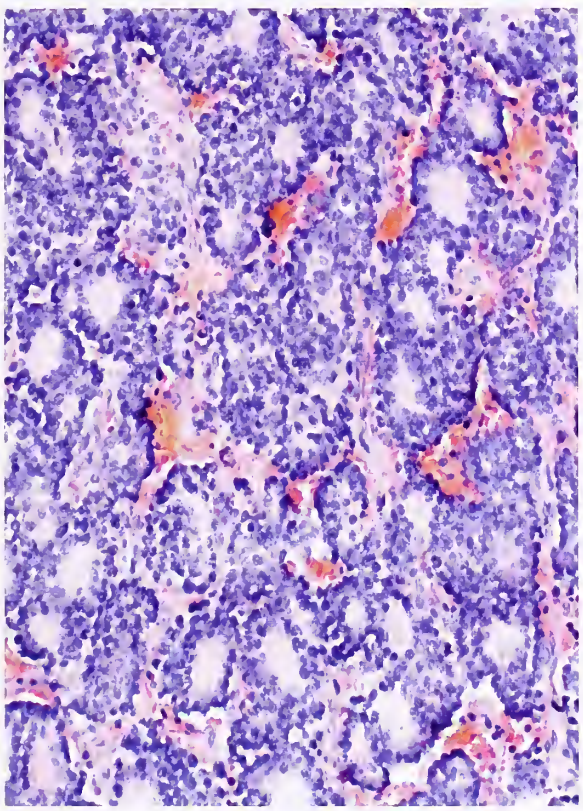

Figure 19-21

NUMEROUS HOMER WRIGHT ROSETTES IN A NEUROBLASTOMA

Areas contain numerous Homer Wright rosettes, a relatively rare occurrence in these tumors. Nuclei are grouped in a ring-like structure around a pale pink center composed of tangled, intertwining neuritic processes.

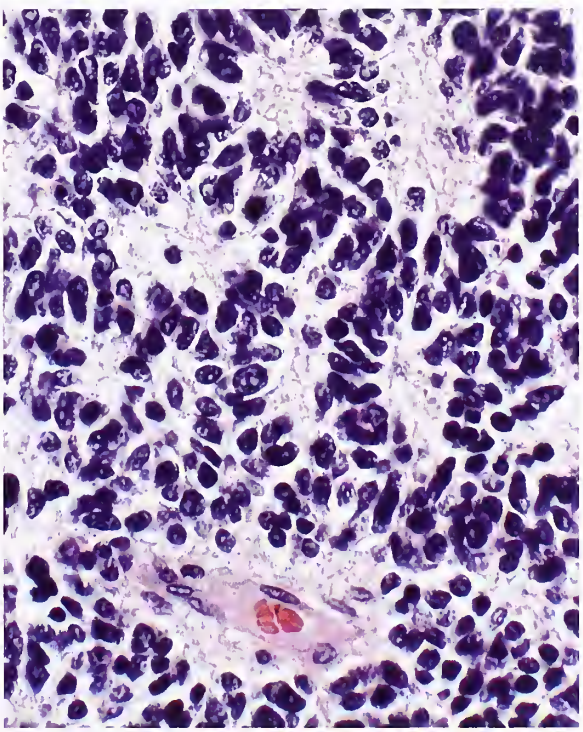

Figure 19-22

HOMER WRIGHT ROSETTES IN A NEUROBLASTOMA

These Homer Wright rosettes appear as nuclei grouped about a pale pink fibrillar zone, which is characteristically roughly circular or ovoid. The central area corresponds to a tangled skein of neuritic cell processes. This is a preexisting structure similar to the small vessel near the bottom and hence these structures could appropriately be regarded as pseudorosettes. (Fig. 23-21 from Fascicle 19, Third Series.)

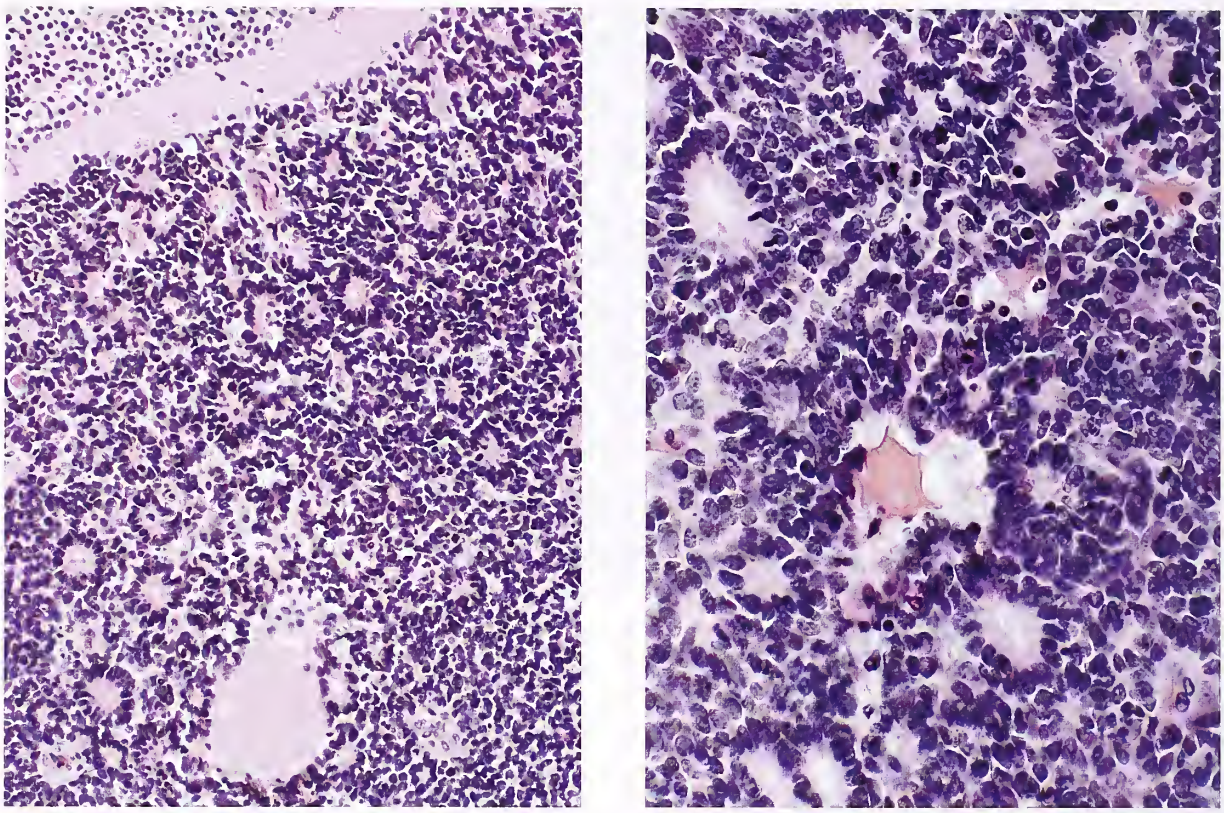

Figure 19-23

RETINOBLASTOMA WITH FLEXNER-WINTERSTEINER ROSETTES

Flexner-Wintersteiner rosettes are characterized by a roughly circular alignment of short columnar cells around a central lumen. (Fig. 23-22 from Fascicle 19, Third Series.)

tumor cells about this preformed tangle of neuritic processes, the term pseudorosette has been considered most appropriate. Homer Wright rosettes contrast sharply with the Flexner-Wintersteiner true rosettes seen in retinoblastoma (fig. 19-23). Rarely, the Homer Wright rosettes have a prominent rhythmic or palisaded arrangement (fig. 19-24).

Nuclei of typical NB cells are rounded or ovoid, often with dispersed nuclear chromatin, which gives a stippled appearance or one likened to "salt and pepper" (fig. 19-25). Rarely, eosinophilic inclusions within nuclei have been reported (64). Anaplasia has been noted in some NBs with a striking degree of cellular and nuclear pleomorphism (fig. 19-26), which is different from the large maturing cells with ganglionic differentiation (65). Although anaplasia, as rigidly defined in Wilms' tumor (nephroblastoma), has important prognostic implications, at least before the use of more intensive chemotherapy, it appears doubtful that anaplasia in NB can be tested as a prognostic factor until more effective treatment is available (66). One study reported no statistically significant differences in survival with regard to anaplasia in stage III and IV NB (67). Foci of spindle-shaped neuroblasts have also been reported (64), and may resemble those of rhabdomyosarcoma. Large cell neuroblastoma, defined as a tumor with large cells with sharply outlined nuclear membranes and one to four prominent nucleoli, is a rare tumor with apparent aggressive clinical behavior (68).

The nuclei of most NB cells are usually larger than nuclei of mature lymphocytes. Aggregates of lymphocytes may be seen in NB, GNB, and ganglioneuroma, and should not be confused with small primitive neuroblasts; if confusion arises, immunostaining for lymphoid markers quickly resolves the issue (fig. 19-27A,B). Rarely,

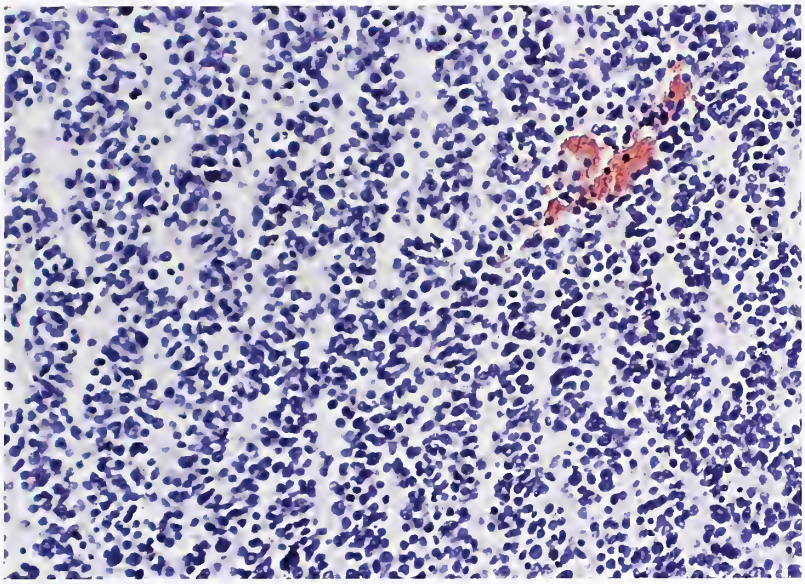

Figure 19-24

NEUROBLASTOMA WITH PALISADING ROSETTES

Palisading of Homer Wright rosettes in an almost parallel array is a very unusual pattern in NB. A similar pattern can occur in medulloblastoma. (Fig. 23-23 from Fascicle 19, Third Series.)

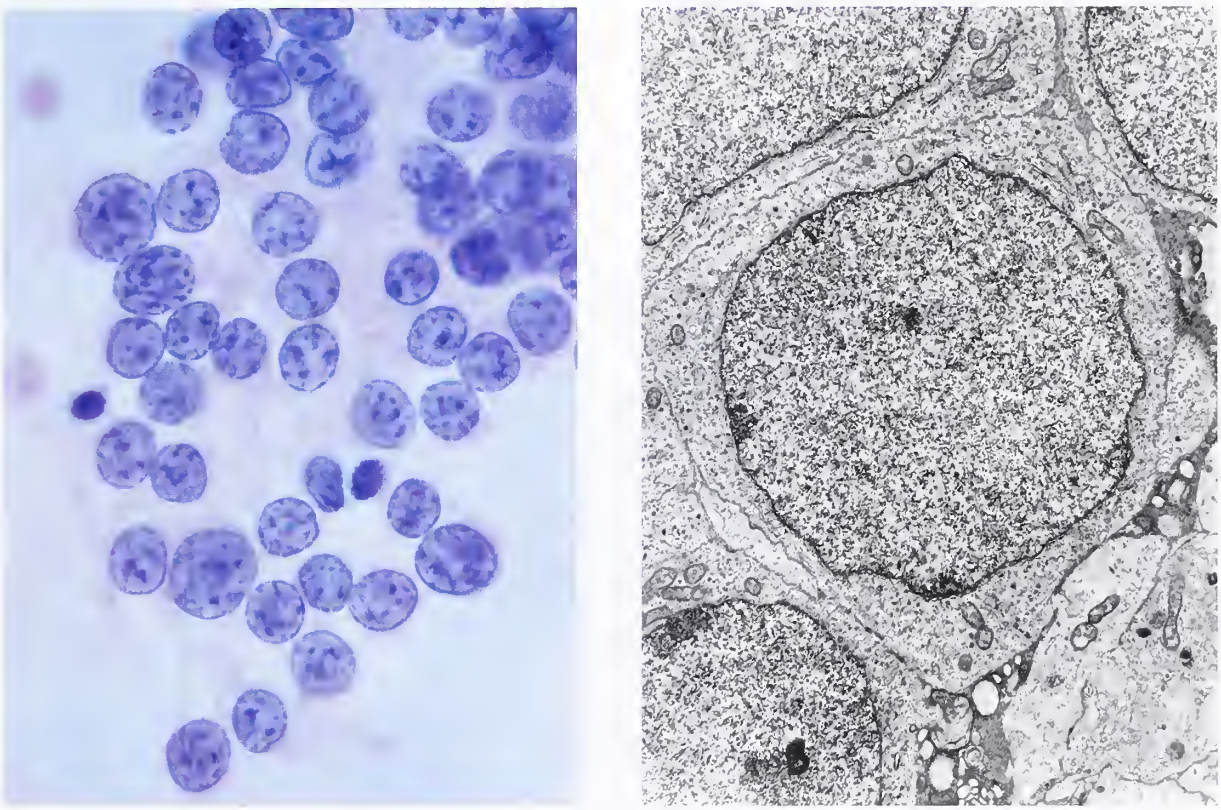

Figure 19-25

DISPERSED CHROMATIN PATTERN IN NEUROBLASTOMA

Left: Touch imprint of a NB shows nuclei that are round to oval and variable in size, with a stippled nuclear chromatin pattern. Some cells have shaggy strands of pale cytoplasm. Cell borders are indistinct. (Fig. 23-24 from Fascicle 19, Third Series.)

Right: Dispersed nuclear chromatin in a NB. Small, denser structures represent chromocenters. No nucleoli are present.

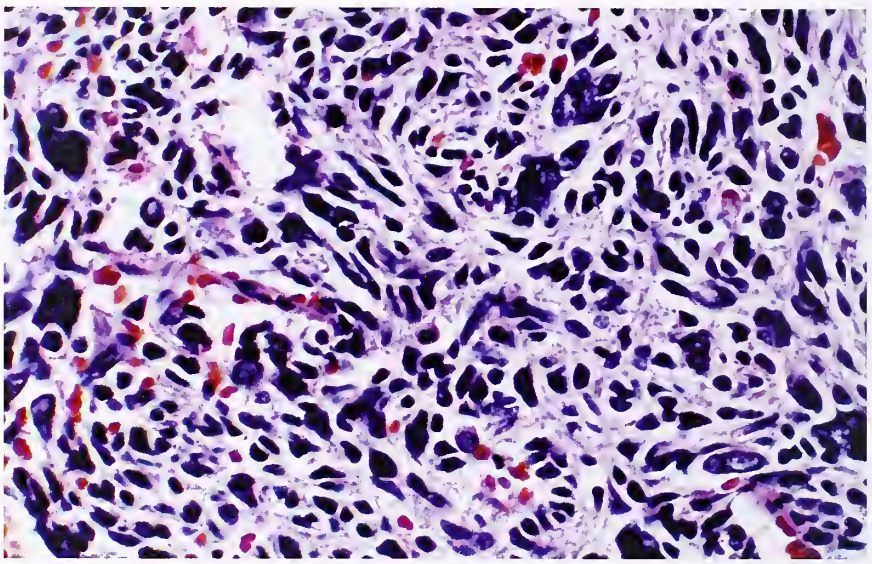

Figure 19-26

ANAPLASTIC NEUROBLASTOMA

Tumor cells have pleomorphic, hyperchromatic nuclei.

the lymphocytic and plasma cell infiltrate can be so intense that there may be some obliteration of the primary tumor (fig. 19-27C) (64).

Cytomorphologic evidence of ganglion cell differentiation includes nuclear enlargement along with increasing amounts of eosinophilic cytoplasm and distinct cell borders. Nuclei may be eccentric in location, with prominent nucleoli. Granular amphophilic material in the peripheral cytoplasm represents Nissl substance, which is a concentration of rough endoplasmic reticulum; metachromatic stains may accentuate this material (fig. 19-28) (1). A GNB may be composed almost purely of fibrillar matrix and scattered ganglion cells (fig. 19-29), but this is uncommon. Occasionally, there is prominent, brown, finely granular pigment that is probably neuromelanin (53). Interestingly, the phenotype of NB cells in vitro may be schwannian and even melanocytic, replete with pigmented cells containing melanosomes (69).

A most unusual example of a childhood NB was recently reported in which the tumor had chromaffin cell differentiation similar to pheochromocytoma (70). This occurred following intensive chemotherapy and radiation therapy, but neuronal to chromaffin metaplasia has also been reported under the influence of hypoxia in vitro (71). This recalls the somewhat plastic morphologic phenotype of composite pheochromocytomas (see chapter 10).

Alterations in Stroma. Hemorrhage or necrosis may be a conspicuous feature in these tumors, and frequently there is dystrophic calcification which appears as fine, dust-like basophilic stippling or coarse, plaque-like areas (fig. 19-30). Intensely hemorrhagic NB may mimic a hematoma, with wide separation of nests of neuroblasts (fig. 19-31, left); rarely, an angiomatoid pattern is seen (fig. 19-31, right). An angiomatoid NB with intracytoplasmic glycogen has been reported (72). Some NBs undergo marked cystic alteration and simulate an adrenal cyst (fig. 19-32) or hematoma. A recent review of cystic NBs indicated a favorable prognosis (73). A focal sclerosing pattern has been reported (64).

Grading and Other Prognostic Factors

Grading and Prognostic Subgrouping of Peripheral Neuroblastic Tumors. Various grading schemes have been proposed over the last several decades for NB and GNB (74–76); some studies have combined biochemical and histologic determinants in an attempt to predict prognosis (77). The proportion of fibrillary (neuropil-like) matrix has also been incorporated as a factor in prognosis (77,78), as well as the number of neurosecretory granules and urinary excretion pattern of catecholamines in "undifferentiated" NB (79). Survival has also been correlated with stage, level of serum ferritin, and favorable versus unfavorable histology in the Shimada age-linked classification (57). Dehner (80) has suggested that cytogenetic and molecular biologic findings may render purely histopathologic classification obsolete, but

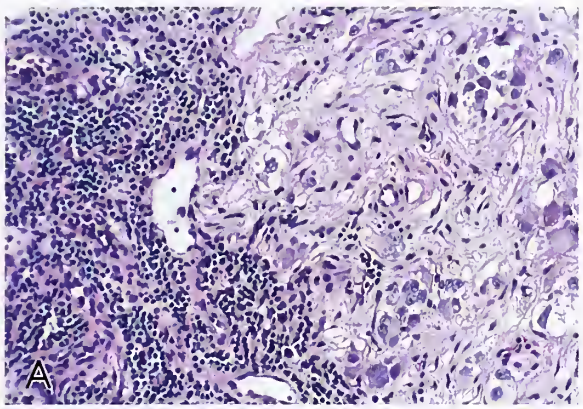

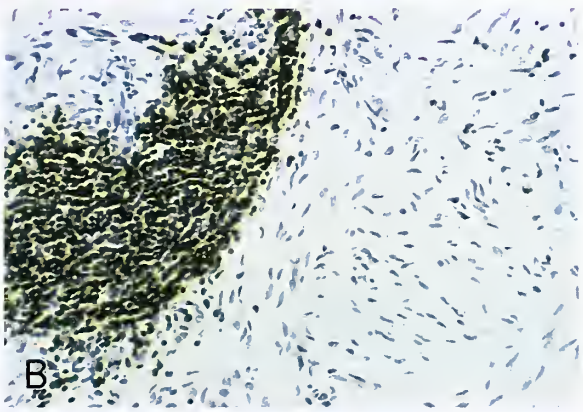

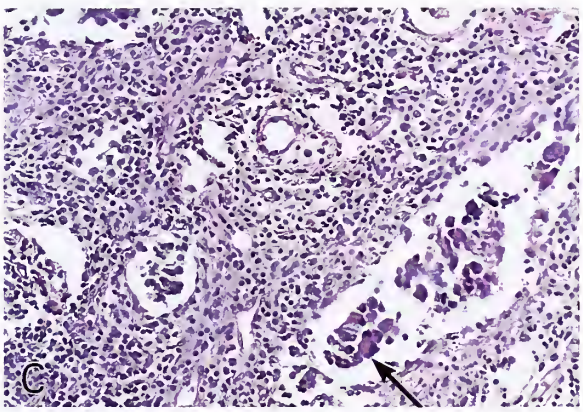

Figure 19-27

GANGLIONEUROBLASTOMA

A: The perivascular aggregates of small cells with darkly stained nuclei are lymphocytes and not primitive neuroblasts.

B: Immunostain for CD45 (leukocyte common antigen) highlights the aggregates of lymphocytes (avidin-biotin peroxidase method).

C: Primary adrenal GNB had abundant lymphocytes and scattered lymphoid follicles with reactive germinal centers. This area of tumor had dense infiltrates of lymphocytes. A few residual islands of tumor show some ganglion cell differentiation (arrow). (A–C: Fig. 23-26 from Fascicle 19, Third Series.)

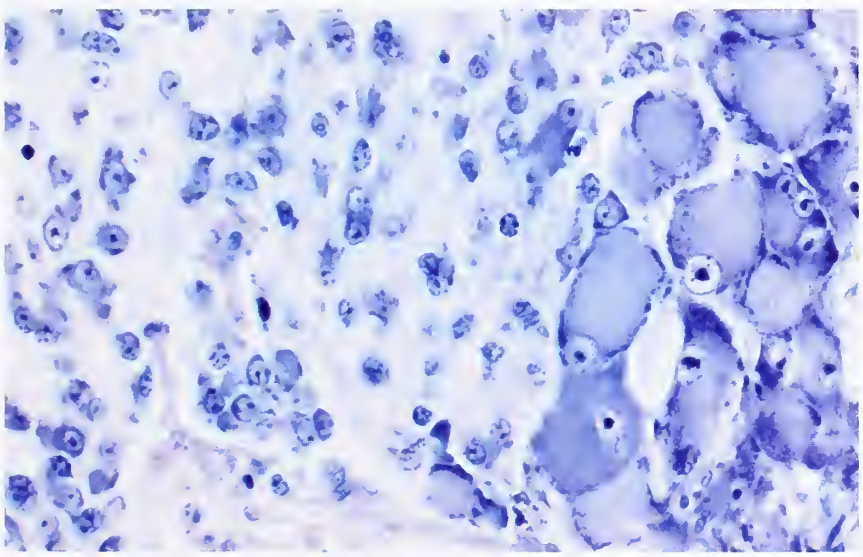

Figure 19-28

GANGLIONEUROBLASTOMA

There is a high level of ganglion cell differentiation in this tumor (right side of field). The coarsely granular material near the cell borders (Nissl substance) has similar tinctorial staining as the prominent nucleoli (toluidine blue stain).

combining morphologic parameters with clinical (e.g., age) or other factors may be valuable, particularly with respect to prognosis.

An age-linked classification of NB and GNB was introduced in 1984 by Shimada et al. (57), and initially involved subcategorization into stroma-rich and stroma-poor tumors; stroma-rich tumors have an extensive growth of schwannian, spindle cell stroma (fig. 19-33). Three subgroups of tumors were recognized in

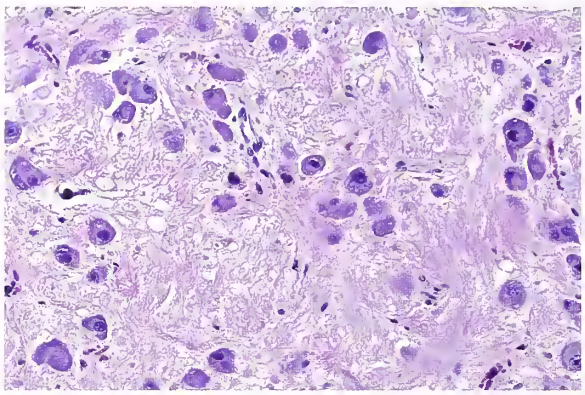

Figure 19-29

GANGLIONEUROBLASTOMA

GNB, a stroma-poor tumor in the Shimada classification, occurred in a 4-year-old child who had watery diarrhea and an elevated level of serum vasoactive intestinal peptide (VIP). There was a low MKI and a high proportion of differentiating elements, placing the tumor in a favorable subgroup.

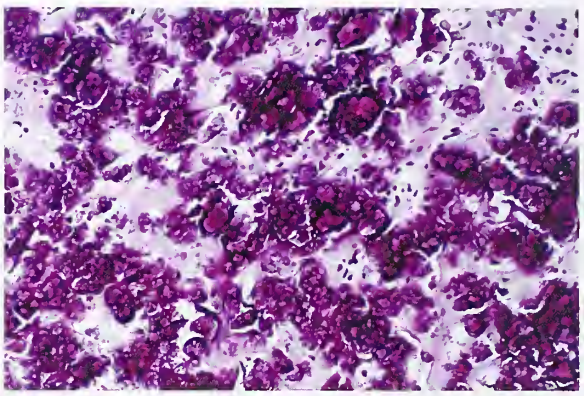

Figure 19-30

NEUROBLASTOMA

The tumor had extensive areas of dystrophic calcification. Prominent mineralization such as this may give the tumor a gritty consistency on sectioning.

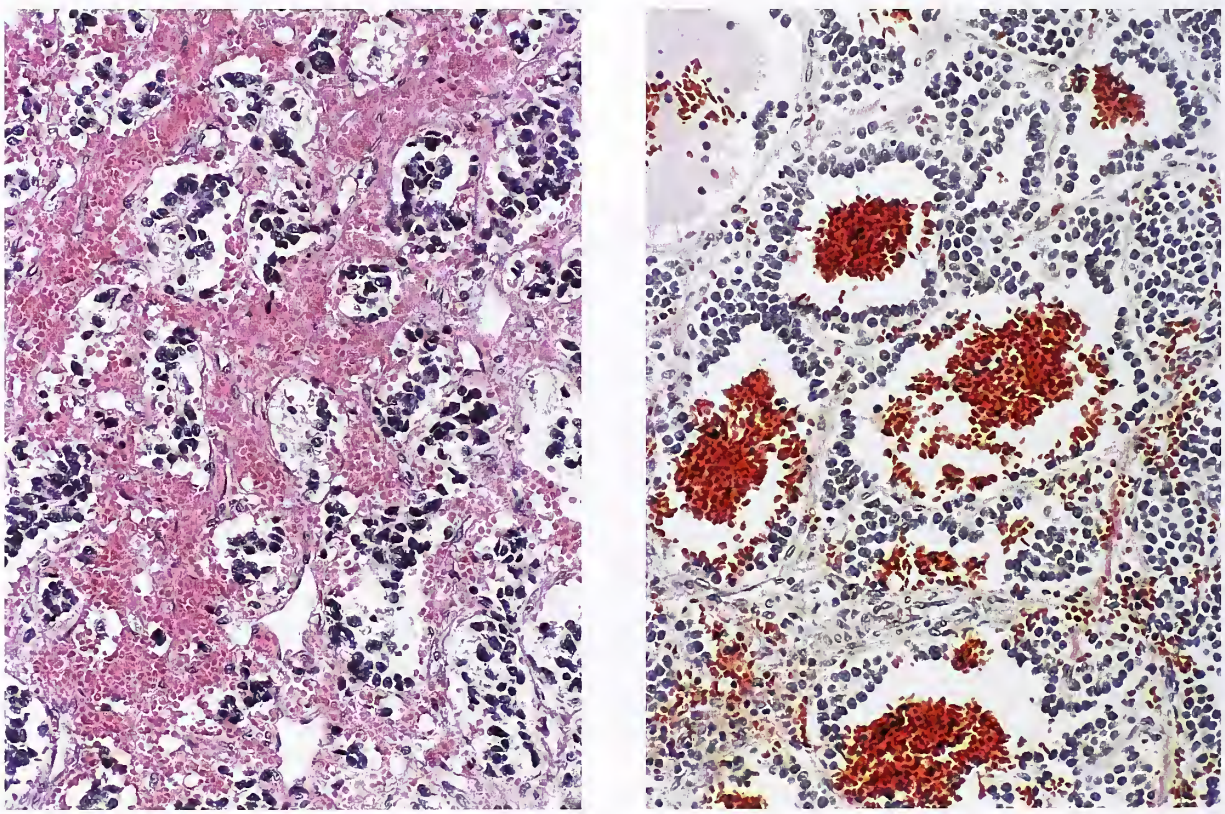

Figure 19-31

NEUROBLASTOMA

Left: Marked hemorrhage separates small irregular nests of tumor cells.
Right: NB has an angiomatoid pattern. (L&R: Fig. 23-31 from Fascicle 19, Third Series.)

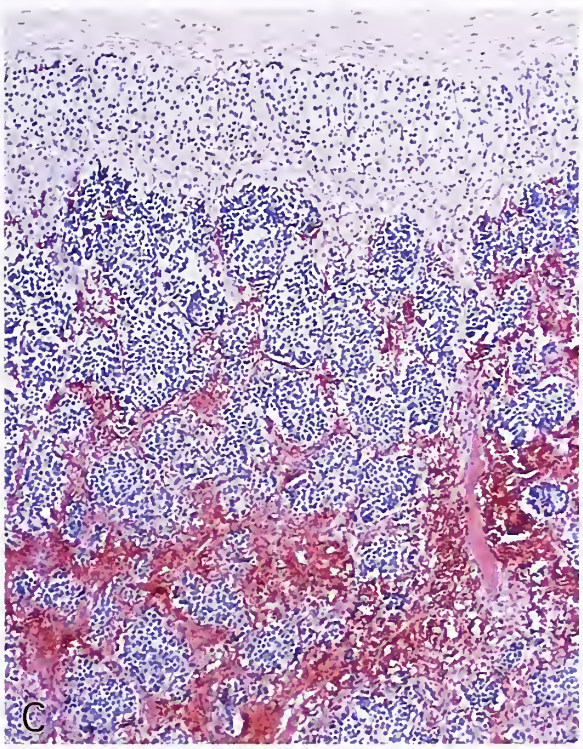

Figure 19-32

CONGENITAL CYSTIC NEUROBLASTOMA

A: Coronal plane on MRI of a newborn infant with a large cystic suprarenal mass on the left side. Tumor had been detected in utero by ultrasonography. (Fig. 7-13 from Lack EE, Kozakewich HP. Adrenal neuroblastoma, ganglioneuroblastoma, and related tumors. In: Lack EE, ed. Pathology of the adrenal glands. New York: Churchill Livingstone; 1990:287.)

B: Congenital cystic NB was filled with blood-tinged fluid. The inner surface is relatively smooth and glistening. The adrenal remnant stretches over the top of the cystic tumor. (B,C: Fig. 23-32B,C from Fascicle 19, Third Series.)

C: The wall of congenital cystic NB has residual adrenal cortex at the top and a narrow rim of hemorrhagic NB below it.

the stroma-rich group: well-differentiated, intermixed, and nodular. The well-differentiated and intermixed stroma-rich tumors can grossly resemble a ganglioneuroma (fig. 19-34). The well-differentiated stroma-rich tumors have only a few randomly distributed aggregates of immature neuroblastic cells (see fig. 19-20), while the intermixed group has ganglioneuromatous tissue interspersed with scattered nests of variably differentiated neuroblastic cells, which are sharply

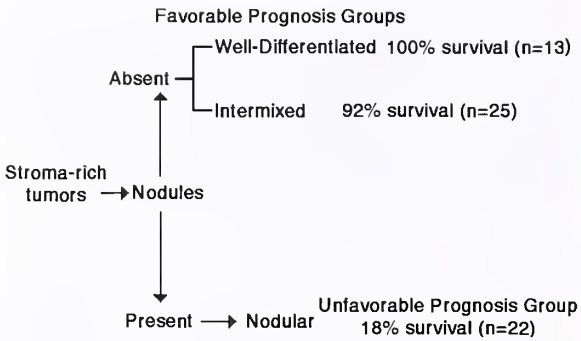

Figure 19-33

SUBGROUPING OF STROMA-RICH TUMORS

Subgrouping of stroma-rich tumors using the age-linked classification of Shimada (57). Survival data in favorable and unfavorable prognosis groups are indicated. (Fig. 23-47 from Fascicle 19, Third Series.)

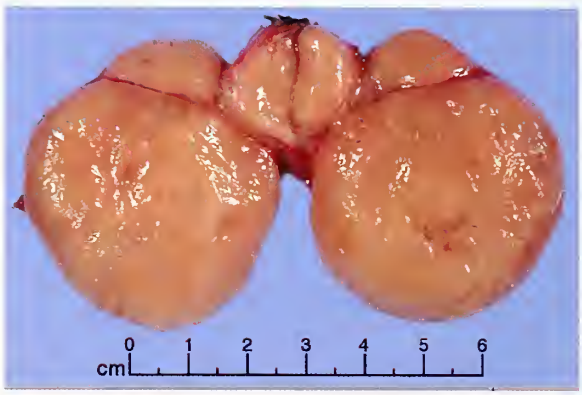

Figure 19-34

GANGLIONEUROBLASTOMA

Paravertebral intraabdominal GNB from a 3-year-old girl was stroma-rich intermixed in the Shimada classification. The tumor grossly resembles a ganglioneuroma. (Fig. 23-48 from Fascicle 19, Third Series.)

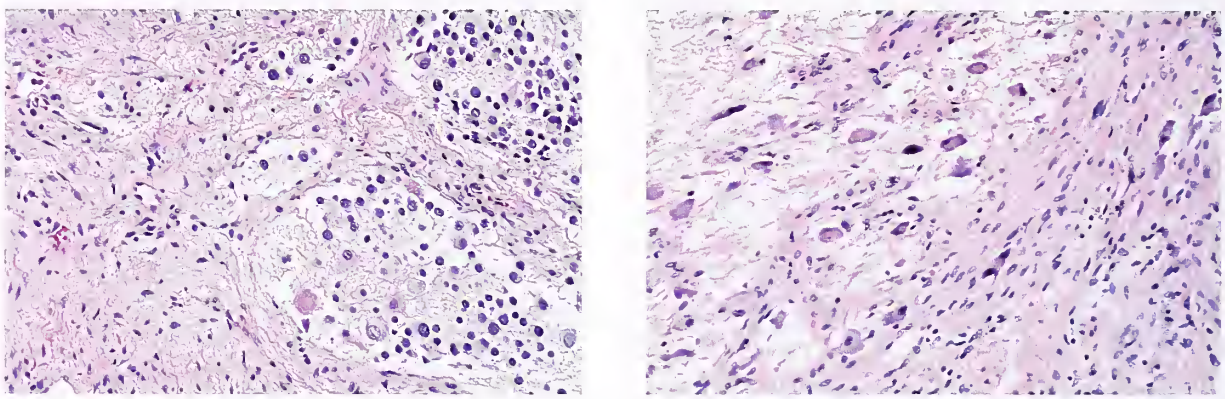

Figure 19-35

GANGLIONEUROBLASTOMA

Left: This tumor conforms to the stroma-rich intermixed subgroup in the Shimada classification. Abundant spindle cell (schwannian) stroma is seen in the left half of the field and immature cells and fibrillary matrix in the right half. A very small proportion of cells shows ganglion cell differentiation.

Right: Different tumor in the stroma-rich intermixed subgroup shows a much higher proportion of differentiation in the form of ganglion cells, but fibrillary matrix is still evident.

defined, making a "space" in the stroma (fig. 19-35). Nodular stroma-rich tumors have a grossly identifiable component of mature and immature tumor, with either one component within the other in the primary tumor (fig. 19-36), or one in the primary tumor and one in the metastasis (57,81); this subgroup largely corresponds to the composite tumors reviewed by Stout in 1947 (55). Favorable and unfavorable prognosis groups are indicated along with survival data in figure 19-33.

Stroma-poor tumors (fig. 19-37) are divided into two prognostic subgroups based upon age at diagnosis, degree of cytologic differentiation (i.e., maturation into ganglion cells), and the mitosis-karyorrhexis index (MKI) (Table 19-4) (57). Since it is often difficult to distinguish mitotic figures from karyorrhexis, these are counted together as mitosis-karyorrhexis and quantified as an index (i.e., counting of 5,000 cells in randomly selected fields). The MKI was introduced to decrease the interobserver and

intraobserver variability in identifying and counting mitotic figures (57), but a less rigorous method for counting may be possible (81). Stroma-poor tumors have more of the typical gross and histologic features of NB and GNB already illustrated. Using the Shimada classification, stage IV-S NBs are classified in a favorable prognosis group of stroma-poor tumors (82). Although problems may exist in the original Shimada classification, such as determination of histologic details, interobserver discrepancy can be reduced considerably if the tumor is assigned to a particular prognostic subgroup (i.e., favorable versus unfavorable histology) because of age at diagnosis (81). A high level of consensus agreement has been reported by others (83).

Another age-linked classification of childhood NBs has been reported (84), along with

Table 19-4

HISTOLOGIC FACTORS INVOLVED IN CLASSIFICATION OF STROMA-POOR NEUROBLASTOMAS[a,b]

Levels of differentiation
Undifferentiated: less than 5% differentiating elements
Differentiating: 5% or greater differentiating elements
Mitosis-karyorrhexis index (MKI)[c]
Low: less than 100
Intermediate: less than 200
High: greater than 200

[a]Table 23-4 from Fascicle 19, Third Series.
[b]Data from reference 57.
[c]Originally based upon 5,000 cell count in random fields.

Figure 19-36

COMPOSITE ADRENAL GANGLIONEUROBLASTOMA

Composite adrenal GNB, or stroma-rich nodular in the Shimada classification. Note the adrenal remnant (arrow). The patient was a 7-year-old girl who died of widespread metastases to liver, lung, spleen, lymph nodes, and bone. The bulging, hemorrhagic nodule on the right is typical NB while the remainder of the tumor was completely differentiated ganglioneuroma. (Modified from fig. 7-19 from Lack EE, Kozakewich HP. Adrenal neuroblastoma, ganglioneuroblastoma, and related tumors. In Lack EE, ed. Pathology of the adrenal glands. New York: Churchill Livingstone; 1990:291.)

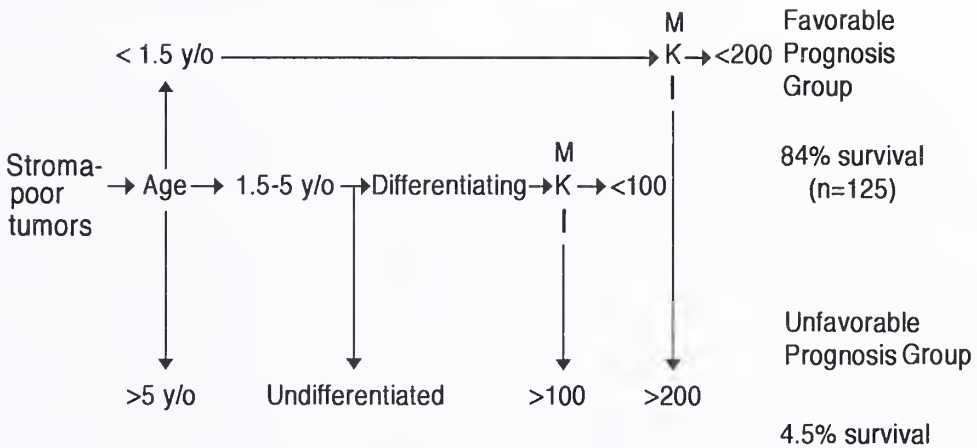

Figure 19-37

PROGNOSIS FOR PATIENTS WITH STROMA-POOR TUMORS

Stroma-poor tumors in the Shimada classification can be subdivided into favorable and unfavorable prognosis groups based upon age at diagnosis, proportion of differentiating cells, and MKI. Survival data are indicated. (Fig. 23-51 from Fascicle 19, Third Series.)

some modification in terminology and reinstitution of the terms NB and GNB (84,85). NB is divided into undifferentiated, poorly differentiated, or differentiating on the basis of the proportion of differentiating neuroblasts (0 percent, 5 percent or less, and more than 5 percent). Neuroblasts and neuropil constitute the predominant (over 50 percent) or exclusive component of the tumor. GNB is divided into nodular, intermixed, or borderline tumors and is composed of a predominantly (greater than 50 percent) ganglioneuromatous component and a small neuroblastomatous component. Low mitotic rate (10 or fewer mitoses per 10 high-power fields) and the presence of calcification are the most significant prognostic features. Grading of the neoplasms is based upon mitotic rate and the presence or absence of calcification, with two risk groups being identified. A correlation between dystrophic calcification and improved survival has been noted in other studies (81,86). Grade 1 tumors have a low mitotic rate (10 or less per 10 high-power fields) with identifiable calcifications; grade 2 tumors also have a low mitotic rate or contain calcifications; and grade 3 tumors have a high mitotic rate (more than 10 per 10 high-power fields) and no calcifications. The low-risk group is defined as grade 1 NB (1 year or less or greater than 1 year of age) or grade 2 NB (1 year or less of age), and the high-risk group is grade 2 NB (over 1 year of age) or grade 3 NB (1 year or less or greater than 1 year of age) (84).

The authors of this classification scheme found a high degree of interobserver concordance in the low-risk versus high-risk groups, and the favorable and unfavorable histologic subgroups in the original Shimada age-linked classification; the survival curves, therefore, are very similar. The availability of adequate and representative histologic material from a primary tumor prior to treatment is obviously of importance in grading or assigning a tumor to an unfavorable (high-risk) or favorable (low-risk) category. Adequate histologic sampling has been defined as one section for each centimeter of the longest dimension of resected primary tumor (87). This grading system could not be used for GNB since a low mitotic rate is present in the predominantly ganglioneuromatous component of these tumors, and calcification is present in most tumors (85.7 percent) (84).

The age-linked classification of peripheral neuroblastic tumors has continued to evolve based upon the framework of the original Shimada classification with minor modifications (88–92). A recent revision of the International Neuroblastoma Pathology Classification (INPC) is shown in figure 19-38. GNB, nodular, comprises one of the categories of peripheral neuroblastic tumors and can be divided into two prognostic subsets, favorable and unfavorable (88,92). The morphologic features used for evaluation of the nodular histology are the same as those used for the prognostic distinction of conventional NB (stroma-poor tumors) and include grade of neuroblastic differentiation (undifferentiated, poorly differentiated, differentiating) and MKI (low MKI, less than 2 percent or less than 100 per 5,000 cells; intermediate MKI, 2 to 4 percent or 100 to 200 per 5,000 cells; high MKI, greater than 4 percent or more than 200 per 5,000 cells) (88,92). A recent report of the protocol for examination of neuroblastic tumors summarizes the biologic and clinical risk factors (35). The latest analysis of the INPC disclosed a cut-off in age of around 18 months for optimal prognostic distinction, but the INPC added independent prognostic information beyond the prognostic contribution of age (93).

Other Prognostic Factors including Cytogenetics and Immunohistochemistry. A variety of adverse nonhistologic and histologic factors have been identified in childhood NB and GNB, but space limitations herein preclude a detailed consideration of each of them. A list of some of these factors is shown in Table 19-5. Age at diagnosis and stage of disease are two powerful, independent prognostic factors that have been shown to exert a great influence on overall survival. From an overview of treatment results for NB, the estimated survival rates are indicated in Table 19-6 based upon the stage of the tumor at diagnosis (94).

NB has been more extensively studied than any other childhood solid cancer and a perplexing array of tumor genetic and other biologic factors have been shown to play important roles in tumor development (95). A number of cytogenetic abnormalities have been described in NB (95–97): 1) loss of distal chromosome 1p and gain of distal 17q with variable simple deletion and unbalanced translocation; 2) sequence

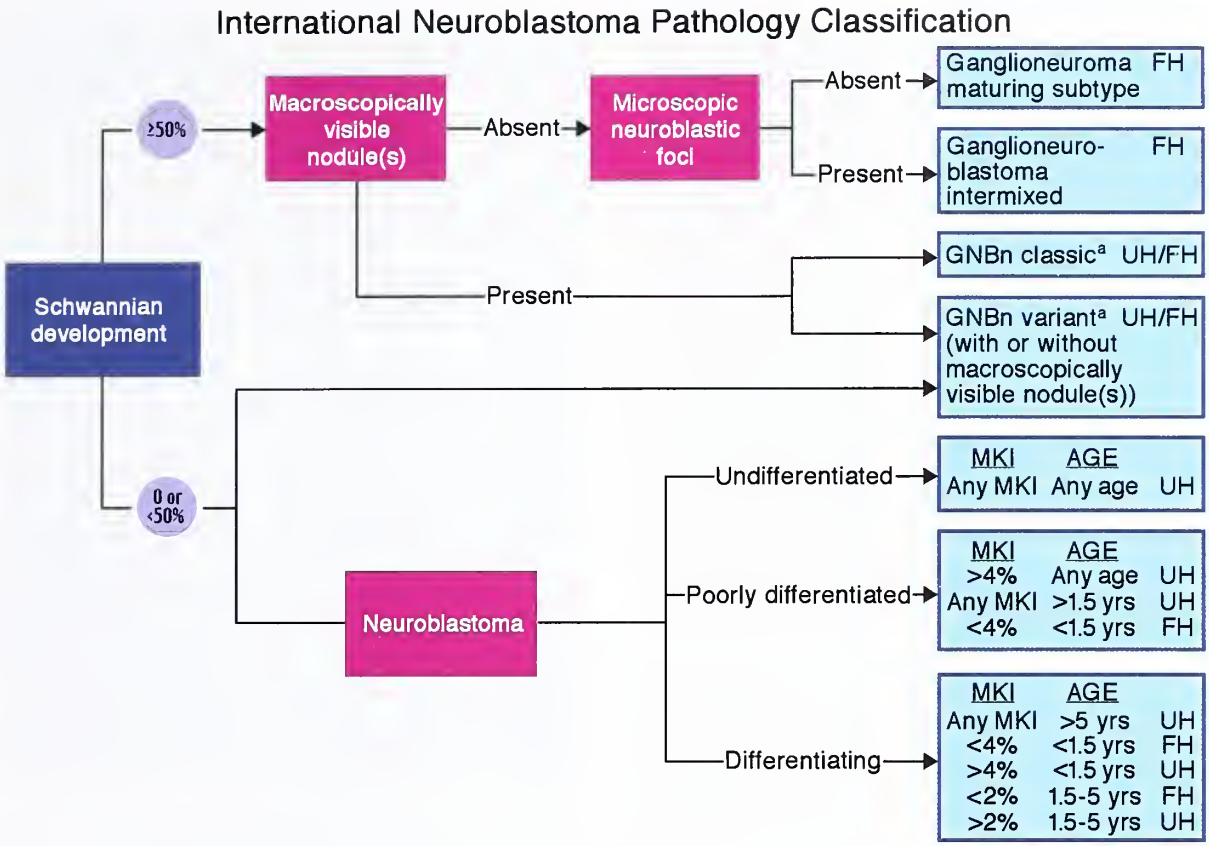

Figure 19-38

REVISION OF THE INTERNATIONAL NEUROBLASTOMA PATHOLOGY CLASSIFICATION (INPC)

This classification system uses many of the features of the original Shimada system, but has various modifications. FH: favorable histology; UH: unfavorable histology; GNBn: ganglioneuroblastoma, nodular; MKI: mitosis-karyorrhexis index (MKI: 2%, 100 of 5,000 cells; 4%, 200 of 5,000 cells). For prognostic evaluation of GNBn see references 89 and 92. (Figure modified from reference 92.)

Table 19-5

ADVERSE NONHISTOLOGIC AND HISTOLOGIC FACTORS IN NEUROBLASTOMA[a]

Older age at diagnosis (e.g., older than 1 year)
Advanced stage of disease
High histologic grade of tumor
Unfavorable or high-risk category using age-linked classification
N-myc oncogene amplification
Diploid DNA value
Pattern of urinary catecholamine excretion (e.g., decreased ratio of vanillylmandelic acid to homovanillic acid)
Increased serum levels of: neuron-specific enolase, ferritin, lactate dehydrogenase, chromogranin A, creatine kinase BB
Cytogenetic abnormalities of chromosomes 1 and 17
Establishment of a permanent cell line in vitro or establishment of a xenograft
Abnormalities in ganglioside composition
Lack of high-affinity nerve growth factor receptors ($gp140^{TRK-A}$)
Other

[a]Table 23-5 from Fascicle 19, Third Series.

Table 19-6

INTERNATIONAL STAGING SYSTEM FOR WORKING PARTY[a]

	Incidence (%)	Survival at 5 Years
Stage I	5	≥90%
Stage IIa Stage IIb	10	70-80%
Stage III	25	40-70% (depending on completeness of surgical resection)
Stage IV	60	>60% if less than 1 year; 20% if 1 to 2 years; 10% if older than 2 years[b]
Stage IVS	5	>80%

[a]Table 23-6 from Fascicle 19, Third Series; data from reference 94.

[b]Children with stage IV neuroblastoma diagnosed when over 1 to 2 years of age have a poor survival rate compared to those under 1 year of age.

losses from the long arm of chromosome 11 oncogene; 3) amplification of the *N-myc* protooncogene (98) or expression of *N-myc* without gene amplification; 4) hyperdiploidy or near triploidy; and 5) expression of trkA, a transmembrane tyrosine kinase that acts as a receptor for the neurotrophin nerve growth factor. Recently, unbalanced loss of heterozygosity (LOH) for 11q and 1p36 was independently associated with a worse outcome in patients with NB (99).

In an early study, LOH for chromosome 1 band p36 and *N-myc* amplification were more common in children over the age of 1 year with advanced stage disease. When these abnormalities were combined with assessment of DNA content, three distinct genetic subsets were recognized: 1) a hyperdiploid or near triploid modal karyotype and few if any cytogenetic rearrangements—patients were generally less than 1 year of age with localized disease and a good prognosis; 2) a near-diploid karyotype with no consistent abnormality identified—patients usually were older with more advanced disease which was progressive and often fatal; and 3) near-diploid or tetraploid karyotype with deletions or LOH for 1p36, amplification of *N-myc* or both—patients were usually older with advanced stages of disease that were rapidly progressive (100). Chromogenic in situ hybridization (CISH) has been used to evaluate tumor cell heterogeneity of *N-myc* copy number; this heterogeneity may reflect different tumor clones. Some methods to estimate the number of *N-myc* genes based on pooled cells do not address copy number heterogeneity at the cellular level and may underestimate or even miss amplification (101).

Lack of trkA expression has been shown to be associated with rapid disease progression in patients with NB, particularly those with tumors showing amplification of the *N-myc* proto-oncogene (102). A recent study of levels of trkA expression did not add significant information to prognostic grouping as defined by the combination of clinical stage, histopathology, and *N-myc* status (103). Other factors have been associated with disease progression such as overexpression of the Brn-3b transcription factor (104), low expression of human tubulin tyrosine ligase (105), and elevated blood level of the heparin-binding growth factor midkine (106). High activin A expression has been correlated with favorable outcome (107). A variety of other factors may influence cell growth and differentiation such as galanin (108), insulin-like growth factor-I (109), and delta-like gene and protein (110). A tabular summary of some of the molecular genetics is provided elsewhere (111). Therapy stratification based upon selected genetic markers is becoming increasingly important, making reliable and accurate determination of markers all the more essential (112).

Study of cell proliferation in peripheral neuroblastic tumors has been reported to aid in distinguishing prognostic subgroups (113,114). Use of the cellular proliferation marker Ki-67 in one study showed that the proliferation index had greater predictive power than the *N-myc* status (113).

Spontaneous Regression or Maturation

Childhood neuroblastic tumors are complex neoplasms that occasionally undergo complete regression or maturation to ganglioneuroma (fig. 19-39). In a review of the incidence of spontaneous regression of cancer in humans, Everson and Cole (115) indicated that the figures for childhood NB may be variable and cited an overall incidence of 1 to 2 percent. The term "spontaneous" may be a misnomer since therapeutic efforts may have been inadequate, or there may be

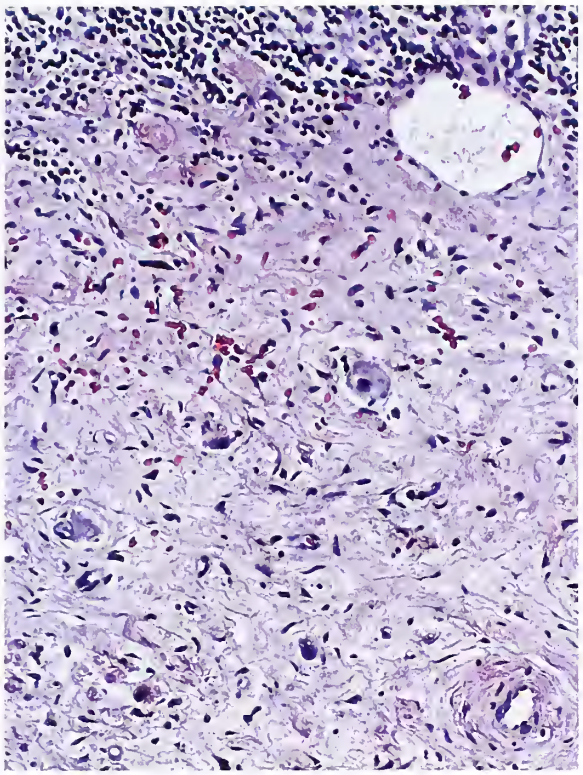

Figure 19-39

CERVICAL LYMPH NODE PARTIALLY REPLACED BY GANGLIONEUROMA

Cervical lymph node from a young adult is partially replaced by fully mature ganglioneuroma. The patient had advanced stage NB as a young child. (Fig. 23-53 from Fascicle 19, Third Series.)

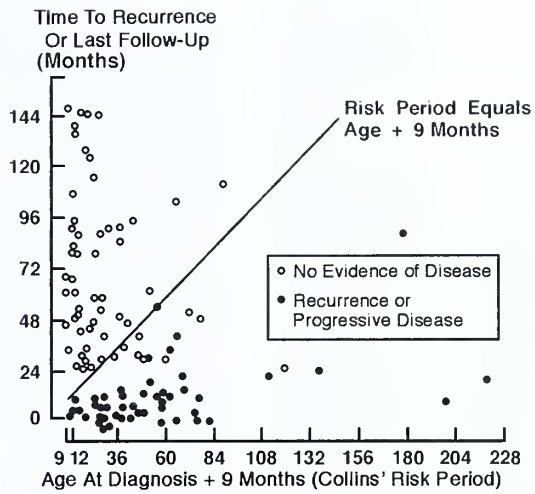

Figure 19-40

GRAPH OF 118 PATIENTS WITH NEUROBLASTOMA BASED UPON COLLINS' RISK PERIOD

Fifty-three patients had recurrent or progressive tumor (closed circles), all within Collins' risk period of age at diagnosis plus 9 months. (Fig. 2 from Rosen EM, Cassady JR, Frantz CN, Kretscharr C, Levey R, Sallan SE. Neuroblastoma: The Joint Center for Radiation Therapy/Dana-Farber Cancer Institute/Children's Hospital experience. J Clin Oncol 1984;2:719-32.)

an underlying biologic explanation which remains undetected. The first documented case of tumor maturation was reported by Cushing and Wolbach in 1927 (116) in a child who had cerebellar symptoms with nystagmus. In a follow-up report by Fox et al. (117), the same patient was apparently free of residual or recurrent tumor nearly 46 years later; the other patient in their report had multiple subcutaneous nodules of metastatic NB along with a large adrenal GNB diagnosed at 7 months of age, and biopsy of one of the skin nodules nearly 20 years later showed fully mature ganglioneuroma.

An understanding of the factors that cause NBs to spontaneously regress is predicted to provide molecular markers of tumor behavior and also to lead to the development of successful treatments. Immunologic mechanisms and tumor maturation have been used to explain regression; NBs have been shown to undergo spontaneous regression in which two types of programmed cell death play a role: caspase-dependent apoptosis and H-ras-mediated autophagic degeneration, but further investigation is clearly indicated (118).

Survival and Patterns of Metastasis

Approximate survival data are indicated in Table 19-6. The concept of Collins' law (119) has been used to predict survival for children with NB (fig. 19-40). Based upon a period of risk equal to the patient's age at diagnosis plus 9 months, it predicts that a child who has not been cured will relapse within this time span.

Metastases in NBs usually involve bone marrow (78 percent), bone (69 percent) (fig. 19-41), lymph nodes (42 percent) (figs. 19-42, 19-43), liver (20 percent), skin (2 percent), testis (2 percent), and intracranial structures (7 percent) (120). Ovarian metastases also occur (121). Bone marrow biopsy (fig. 19-44A,B), usually bilateral, has been shown to be more reliable

Figure 19-41

WIDELY METASTATIC NEUROBLASTOMA

The bony metastases seen here (in a 4-year-old boy) involve predominantly the metaphyses of the upper tibia and lower femur on both sides. (Fig. 23-55 from Fascicle 19, Third Series.)

Figure 19-42

METASTATIC NEUROBLASTOMA

Widely metastatic NB in a 4-year-old child. Posterior view of viscera shows an adrenal NB replacing the right adrenal gland and invading the kidney. The tumor extensively involved the paraaortic lymph nodes. (Fig. 7-27 from Lack EE, Kozakewich HP. Adrenal neuroblastoma, ganglioneuroblastoma, and related tumors. In: Lack EE, ed. Pathology of the adrenal glands. New York: Churchill Livingstone; 1990:298.)

than bone marrow aspiration (fig. 19-44C) in detecting tumor, but ancillary techniques such as immunohistochemistry may enhance sensitivity (1). Cranial involvement is essentially limited to calvarial bone, leptomeninges, and dura (fig. 19-45), while intrinsic involvement of brain parenchyma is uncommon (1,122). Secondary encroachment on adjacent venous sinuses or extension into brain parenchyma may occur from leptomeningeal or dural sites of involvement. "Neuroblastomatosis" of basal leptomeninges can also occur (123). In a review of NB metastatic to the central nervous system there was a strong association with diagnostic lumbar punctures in patients with known bone marrow disease, raising the possibility that circulating or epidural microscopic tumor cells may seed the craniospinal axis (124). Pulmonary metastases by NB are uncommon, and usually signify widely disseminated tumor and a grave prognosis. Rare cases of NB metastatic to lung have been associated with possible reinfusion of malignant cells at the time of autologous bone marrow transplantation for adjuvant treatment of advanced stage disease (125).

NB metastatic to bones of the skull, with involvement of the vault and base of the skull, was characterized as a clinical syndrome by Hutchison (126). In fact two "syndromes" of metastatic NB can be found in the literature: Pepper's syndrome with massive hepatic metastases, and Hutchison's syndrome with skull metastases usually at a later age (127). There is no correlation between the laterality of the adrenal tumor and the pattern of metastases, so the concept of these "syndromes" is obsolete. Patients with disseminated NB may present with metastases to periorbital bone or

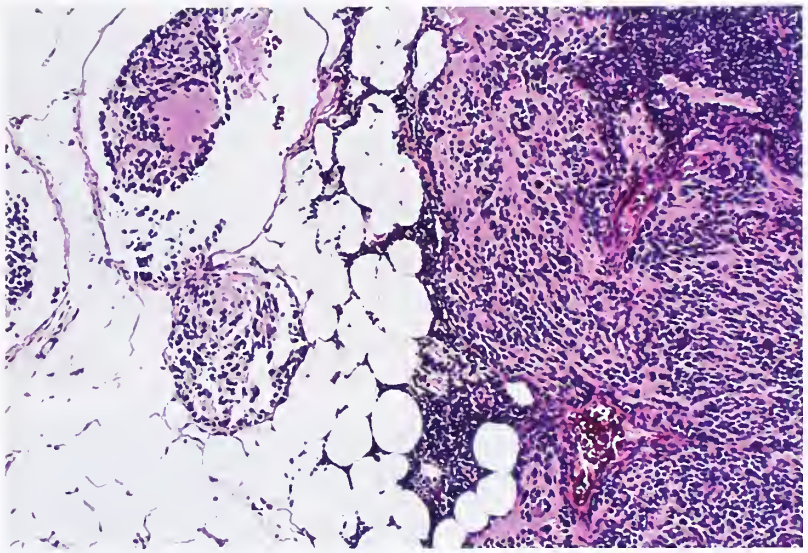

Figure 19-43

METASTATIC NEUROBLASTOMA

Metastatic NB extensively involves the lymph node. Areas of permeation are adjacent to the node (left). (Fig. 23-57 from Fascicle 19, Third Series.)

Figure 19-44

NEUROBLASTOMA METASTATIC TO BONE AND BONE MARROW

A: Metastatic NB extensively involved bone and bone marrow.

B: Tumor cells have small, darkly stained nuclei with the important diagnostic hallmark of neuritic cell processes. (Fig. 23-58, left from Fascicle 19, Third Series.)

C: Bone marrow aspirate has an aggregate of metastatic NB cells with finely dispersed nuclear chromatin. The cluster of cells in the center is almost forming a Homer Wright rosette or pseudorosette.

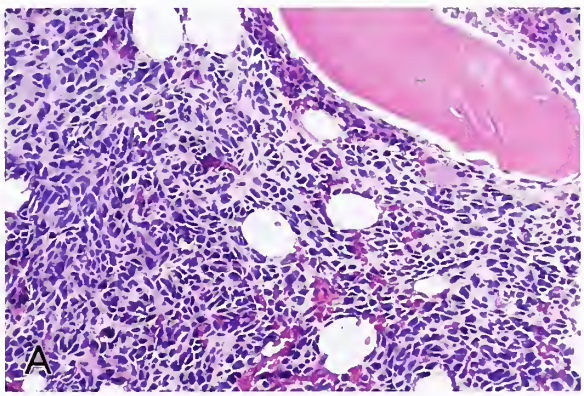

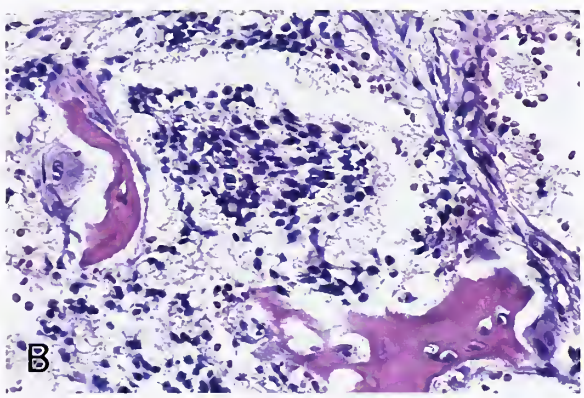

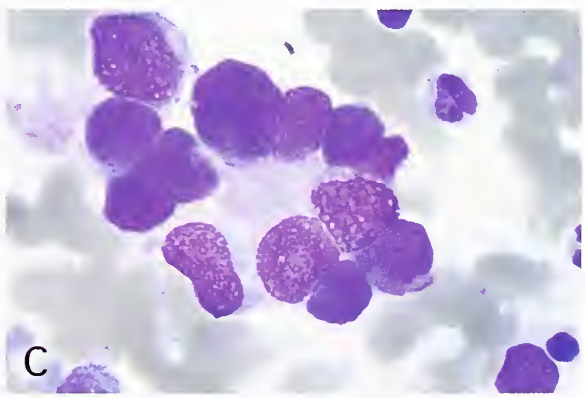

soft tissue that result in proptosis, periorbital ecchymosis, or swelling (fig. 19-46) (1). Metastases are often bilateral, but the clinical findings may be asynchronous and subtle. Metastases have also been reported to placenta (128), umbilical cord (129), and skin, sometimes with blanching cutaneous nodules (130). The appearance of the multiple blue-gray mobile skin nodules has been likened to a "blueberry muffin" (see fig. 19-9) (131). NB cells can also be detected in blood (132), and rarely, NB can simulate leukemia (133).

Figure 19-45

NEUROBLASTOMA METASTATIC TO CALVARIAL BONE AND DURA MATER

The leptomeninges over the cerebral convexities were free of tumor and there were no brain metastases. (Fig. 7-30 from Lack EE, Kozakewich HP. Adrenal neuroblastoma, ganglioneuroblastoma, and related tumors. In: Lack EE, ed. Pathology of the adrenal glands. New York: Churchill Livingstone; 1990:300.)

Figure 19-46

STAGE IV NEUROBLASTOMA

Top: Young child has bilateral orbital ecchymoses and swelling due to metastatic NB.

Bottom: Child is bed-ridden and cachectic in the terminal phase of stage IV NB. Orbital swelling is marked on the right side with proptosis. There were numerous bone metastases, two of which caused visible deformity of the chest wall.

Differential Diagnosis of Neuroblastoma

The differential diagnosis of NB includes a variety of other small cell neoplasms of childhood, such as rhabdomyosarcoma, malignant lymphoma, Ewing's sarcoma, and a variety of other neoplasms. The differential diagnosis of NB at the least differentiated end of the morphologic spectrum includes an impressive array of small "blue cell" tumors, and accurate diagnosis frequently mandates ancillary diagnostic techniques, even electron microscopy. The scope of this differential diagnosis goes well beyond the material that can be covered in this chapter. A small minority of tumors are so undifferentiated at various levels of investigation, and some may have overlapping features on molecular and cytogenetic investigation, that precise classification remains a problem.

Ewing's sarcoma, both skeletal and extraskeletal, and primitive neuroectodermal tumor (PNET) have been the focus of rather intense scrutiny in terms of better defining histogenesis. Studies indicate a shared or overlapping immunophenotypic profile and other phenotype features that support neuronal or neuroectodermal differentiation (134). In one review, 3 of 26 PNETs originated in the adrenal gland and had a clinical outcome which was not typical for NB (135). There is a very broad age range for patients with PNET, but the young adult age group is affected most often. PNETs have been reported in various sites such as the thoracopulmonary area, pelvis, retroperitoneum, extremities, and neck. Ewing's sarcoma and PNET can be regarded as members of the same family of small cell tumors, with the latter arising more commonly in soft tissues and being biologically more aggressive (1,134). A recent study of the morphologic and immunohistochemical diversity of Ewing's sarcoma/PNET placed these sarcomas in the "Ewing family of tumors" (136). Studies have pointed to more immunophenotypic

similarities between Ewing's sarcoma and PNET than differences, and most tumors have the same translocation t(11;22)(q24;q12) (134, 136). Rosettes or pseudorosettes have been described in PNET, occasionally the Homer Wright type, with pale eosinophilic cores and less commonly, the Flexner-Wintersteiner type of true rosettes (135). Rosette formation has also been observed in osseous and extraosseous Ewing's sarcoma. Genetic confirmation seems essential for the diagnosis of unusual morphologic variants of Ewing's sarcoma/PNET such as the "adamantinoma-like," spindled sclerosing, and clear cell/anaplastic variants (136). Classic childhood NB, however, differs in bioenzymatic traits, cytogenetic abnormalities, and protooncogene products as well as other features (1).

The desmoplastic small round cell tumor (DSRCT) is yet another member of the evolving family of small, round blue cell tumors of childhood; it occurs predominantly in young adult males (137,138). Most tumors are localized to the abdominal cavity and present with multiple peritoneal implants, and are characterized by a nesting pattern of growth with intense desmoplasia. A unique translocation, t(11;22) p13;q12 or q11.2 has been reported in a few cases of DSRCT, which is different from Ewing's sarcoma/PNET, although the chromosome 22 breakpoint involves the same gene (*EWS*) (139).

Renal and extrarenal malignant rhabdoid tumors can also enter into the differential diagnosis of childhood NB. The usual morphology is a solid or diffuse proliferation of monotonous tumor cells with vesicular nuclei, prominent nucleoli, and intracytoplasmic inclusions consisting of whorls of intermediate filaments representing vimentin. Nine major morphologic patterns have been described for malignant rhabdoid tumors of the kidney (140). Some studies cast doubt on the validity of extrarenal malignant rhabdoid tumors as a specific diagnostic entity (141), but more investigation is needed. NB and GNB of the central nervous system is covered in another Fourth Series Fascicle along with central neurocytoma and olfactory NB (142). Rare neurilemomas have neuroblastoma-like features due to a predominance of small, round, hyperchromatic Schwann cells with scant cytoplasm, but areas of more conventional neurilemoma can be found (143).

GANGLIONEUROMA

Clinical Features. *Ganglioneuroma* (GN) is a fully mature benign neoplasm that usually occurs in an older age group than NB; many patients are 7 years of age (144) or older (145,146). Most GNs arise in the posterior mediastinum (146) followed by the retroperitoneum, particularly the presacral space (fig. 19-47) (147), but can occur in a variety of other locations (145) including cervical and parapharyngeal area, urinary bladder (148), prostate (149), bone (150), pancreas (151), skin (152), orbit (153), paratesticular area (154), and even the appendix (155). A polyploid form of GN has been described in the gastrointestinal tract as a small (2 cm or less usually), sessile or pedunculated lesion and appears to be a hamartoma or choristoma (156). Symmetric, dumbbell-shaped GNs of cervical spine that extend intradurally have been recently reported in a patient with von Recklinghausen's disease (157). Only a relatively small proportion of GNs are adrenal in origin (146). Calcification has been detected by radiographic study in 41 percent of GNs (158), and in some cases may be detected on gross examination (159).

Gross Findings. GN is characteristically well-circumscribed, and is described by some as encapsulated (144,160) or having a fibrous capsule (147), but microscopic study of sections taken from the periphery of some tumors may not bear this out entirely (1). GNs vary in size from an average of about 8 cm (159) to individual tumors measuring 15 cm (161); some GNs in the retroperitoneum weigh over 5,000 g (147). The tumors are firm and resilient, and on cross section are gray-white to tan-yellow (fig. 19-48A). Occasionally, there is a trabecular or whorled appearance reminiscent of a leiomyoma (fig. 19-48B,C). In some cases, particularly in children, a GN should be carefully examined to exclude a type of stroma-rich GNB, which may grossly and microscopically resemble a GN (1). Adrenal GNs may be sharply circumscribed and delimited by residual adrenal cortex and capsule, but the tumor may extend focally beyond the confines of the capsule (fig. 19-48D).

Microscopic Findings. GNs contain a variable admixture of mature or mildly dysmorphic ganglion cells and an overabundance of mature Schwann cells (fig. 19-49); the latter often ensheathe neuritic processes as is seen

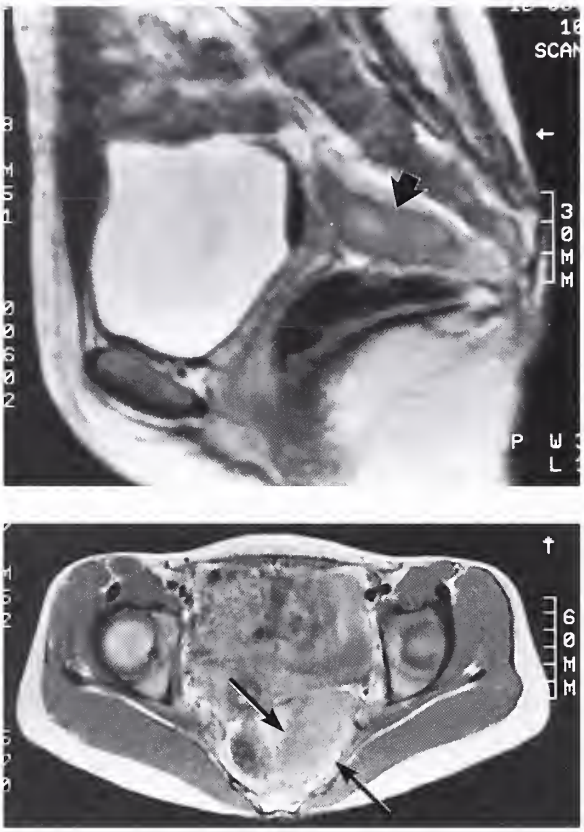

Figure 19-47

PELVIC GANGLIONEUROMA

Top: Sagittal view on MRI of a 28-year-old woman with a pelvic ganglioneuroma located in the convexity of the sacrum (arrow) adjacent to the rectum. The patient had symptoms due to local pressure on the rectum.

Bottom: Tumor in the axial view has an ovoid shape (arrows), and was slightly adherent posteriorly to soft tissues of the sacrum. A transrectal needle biopsy showed ganglioneuroma.

ultrastructurally. The Schwann cell component may be arranged in small fascicles which intersect at various angles, and the bundles of cells may be separated by loose myxoid stroma.

There is considerable variation in distribution and number of ganglion cells. A paucity or absence of these cells may give the mistaken impression of a neurofibroma (1); by contrast, a chance section of a neurofibroma may reveal a secondarily incorporated ganglion which might lead to a mistaken diagnosis of a GN (147). Rare GNs have one or more ganglia or myelinated nerve bundles that are secondarily incorporated into peripheral areas of the tumor (fig. 19-50). It is possible that rare foci such as this may represent an unusually high level of differentiation within the GN. The amount and distribution of Nissl substance may be sparse or uneven in the perikaryon of ganglion cells, and it may be absent in a particular plane of section. Well-differentiated ganglion cells have compact, eosinophilic cytoplasm with distinct cell borders and a single eccentric nucleus with a prominent nucleolus. Occasional ganglion cells are dysmorphic, with single or multiple pyknotic nuclei. Occasionally, locules of mature adipose tissue are seen in some tumors; these may be more conspicuous in sections taken at the periphery (fig. 19-51).

In adrenal GNs, the tumor may be sharply demarcated from adjacent adrenal tissue such as cortical cells (fig. 19-52, left) or it can insinuate between adjacent cells (fig. 19-52, right). There may be some mild variation in cellularity, but cellular atypia, mitotic activity, and necrosis are not features of a fully mature GN. Mast cells may be seen in some GNs (fig. 19-53), similar to neurofibromas (1). Some ganglion cells contain prominent, finely granular brown to golden brown pigment consistent with lipofuscin or neuromelanin (fig. 19-54). In some cases, a partial or complete encirclement of elongated cells typical for satellite cells can be found (fig. 19-54). In occasional GNs, areas of densely collagenized stroma are seen (fig. 19-55). As with other peripheral neuroblastic tumors, areas of chronic inflammation may be present (see fig. 19-27), which should not be mistaken for primitive neuroblasts.

There is still some controversy as to whether GN arises de novo or by maturation or differentiation of a preexisting NB or GNB; the latter has certainly been well documented (see fig. 19-39). Others feel that GNs arise de novo given the significant differences in age distribution and location compared with childhood NBs (146).

Malignant Transformation. There have been rare examples of malignant transformation of ganglioneuroma into malignant peripheral nerve sheath tumor (MPNST, malignant schwannoma), either de novo (162–165) or following abdominal radiation for NB or GNB (1,166, 167). An MPNST has been reported in an adrenal GN in an adult male homosexual (168).

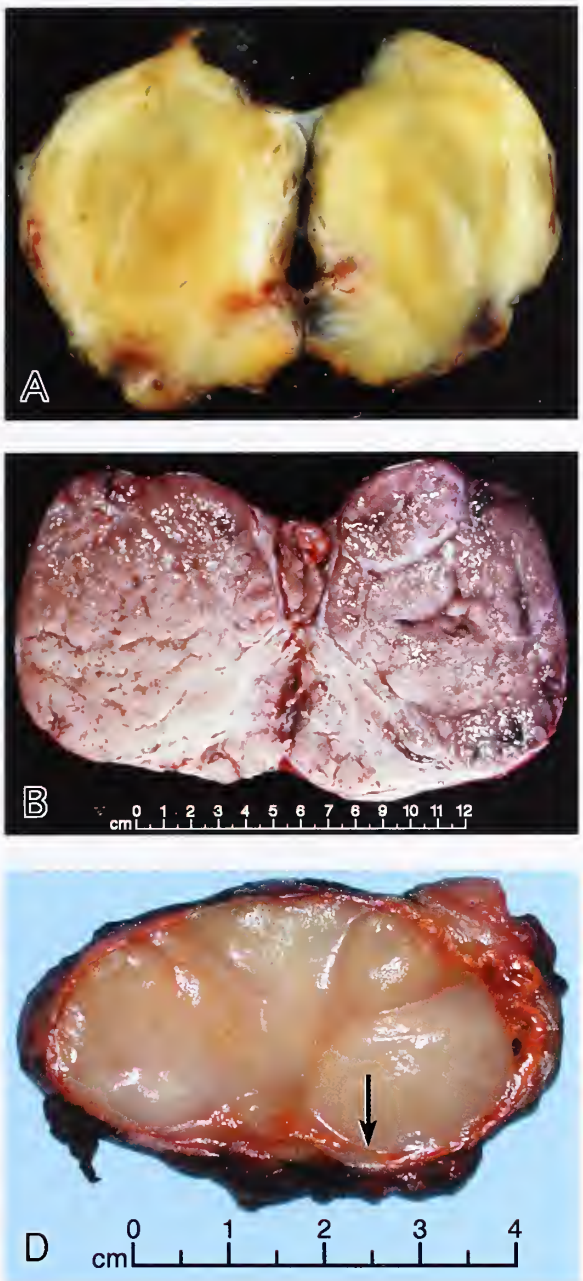

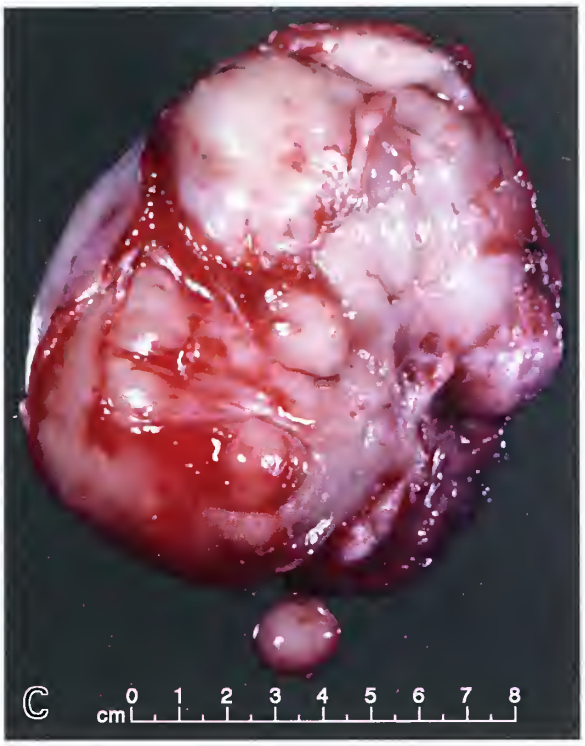

Figure 19-48

GANGLIONEUROMA

A: Bisected ganglioneuroma has a smooth, glistening, tan-yellow surface. The tumor measured 9 cm in diameter. (Same case as figure 19-47.)

B: A different ganglioneuroma in cross section has a trabecular and lobular appearance reminiscent of a smooth muscle neoplasm.

C: The external aspect of another ganglioneuroma has coarse lobulations.

D: Adrenal ganglioneuroma in a 59-year old woman is vaguely lobulated on cross section and has a uniform pale appearance. The tumor intermingled freely in areas with compressed residual cortex and focally extended through the capsule without evidence of true encapsulation (arrow). There were small locules of adipose tissue as well as a small focus of myelolipomatous metaplasia.

Several other cases have been described, but there was no mention of antecedent radiation treatment. Rhabdomyosarcoma was recently reported arising from a dormant dumbbell-shaped GN of the lumbar spine (169). Figure 19-56 shows an example of an MPNST arising in a GN 17 years following abdominal radiation for a large unresectable NB that was initially diagnosed when the patient was 13 months of age (1). The presumed sequence of events in this case is radiation-induced or -associated maturation of NB to GN, and then after a latency of 17 years, evolution to MPNST from the Schwann cell component (1).

Masculinizing Ganglioneuroma

Masculinizing adrenal GNs (fig. 19-57) are rare neoplasms in which there is an admixture of GN along with Leydig cells containing pathognomonic crystalloids of Reinke (170), or strands

Figure 19-49

GANGLIONEUROMA

Ganglioneuroma is composed of multiple ganglion cells and abundant Schwann cells. These tumors can vary considerably in the distribution and number of ganglion cells. Some of the mature ganglion cells have Nissl substance in the peripheral cytoplasm.

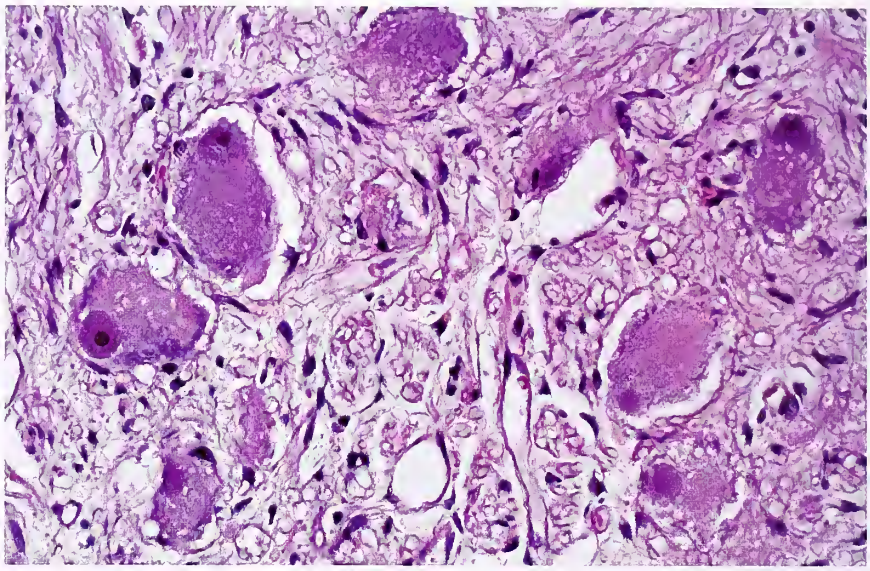

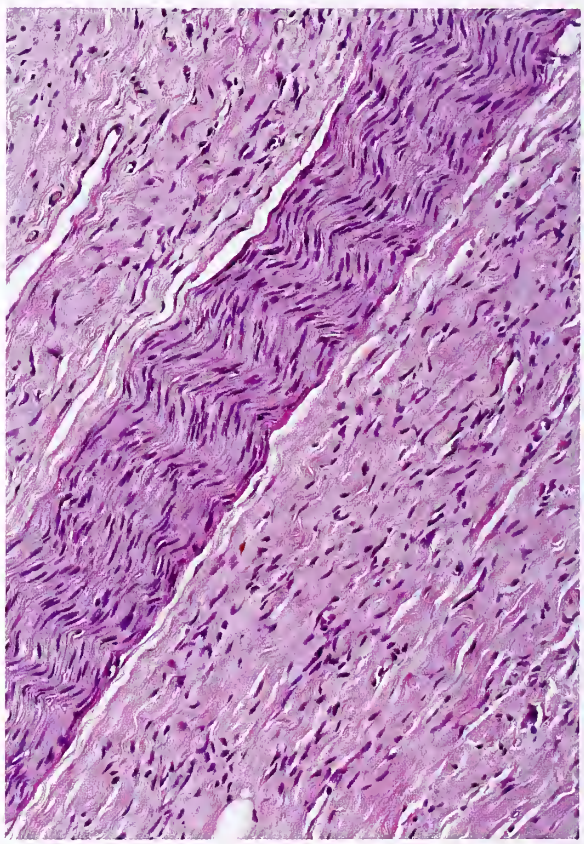

Figure 19-50

GANGLIONEUROMA

Left: This ganglioneuroma contained a few small ganglia. A small myelinated nerve is present at one pole of a ganglion. The ganglion is probably incorporated secondarily in the tumor.

Right: A large bundle of myelinated nerve is present in this ganglioneuroma and is most likely secondarily incorporated in the tumor.

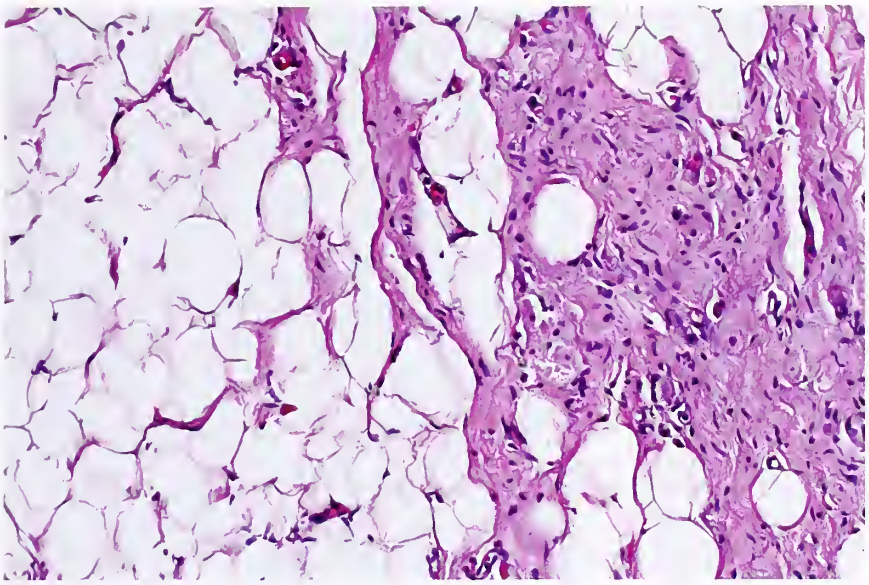

Figure 19-51

GANGLIONEUROMA

Mature adipose tissue is seen in sections taken near the periphery of the ganglioneuroma, perhaps due to secondary incorporation by the tumor.

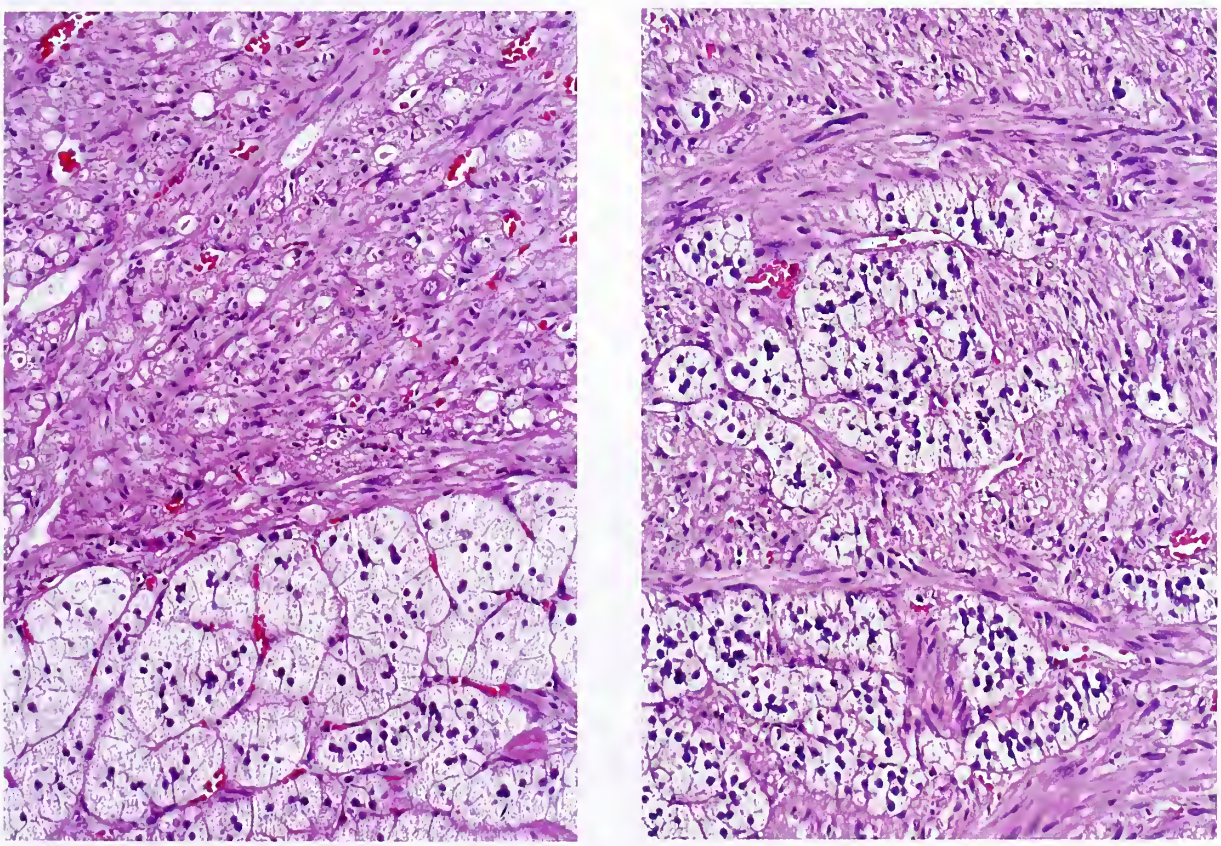

Figure 19-52

ADRENAL GANGLIONEUROMA

Left: The tumor is sharply demarcated from the adjacent adrenal cortex.
Right: In other areas, the tumor is unencapsulated and intersects nests of cortical cells.

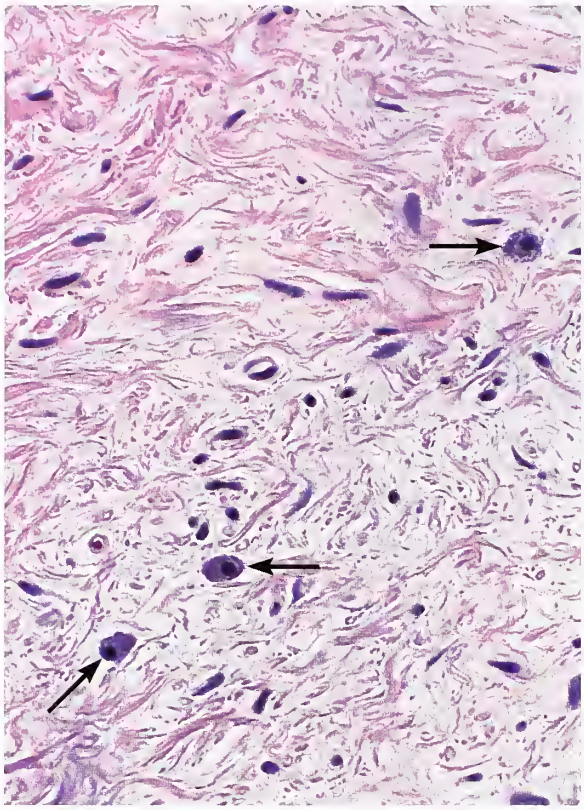

Figure 19-53

GANGLIONEUROMA

Mast cells (arrows) are identifiable. (Fig. 23-67 from Fascicle 19, Third Series.)

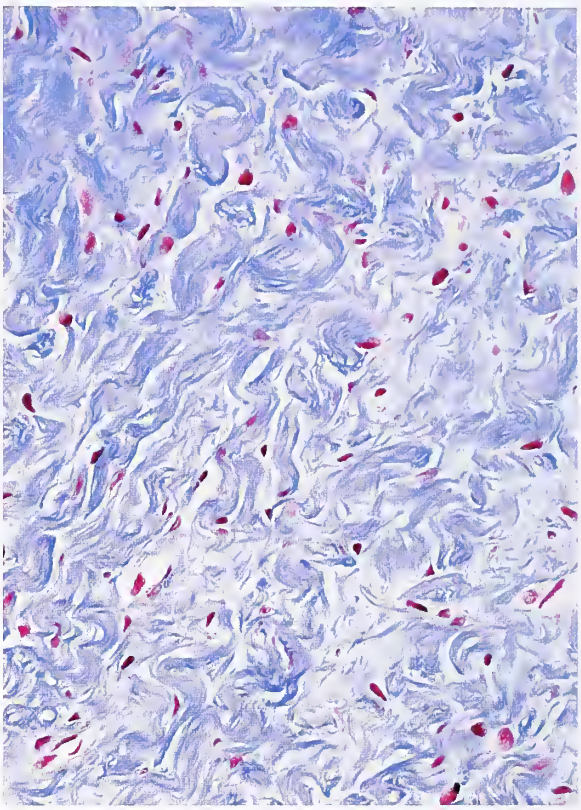

Figure 19-55

GANGLIONEUROMA

The stroma contains abundant collagen. Other parts of the tumor had loose, more cellular areas with ganglion cells (trichrome stain).

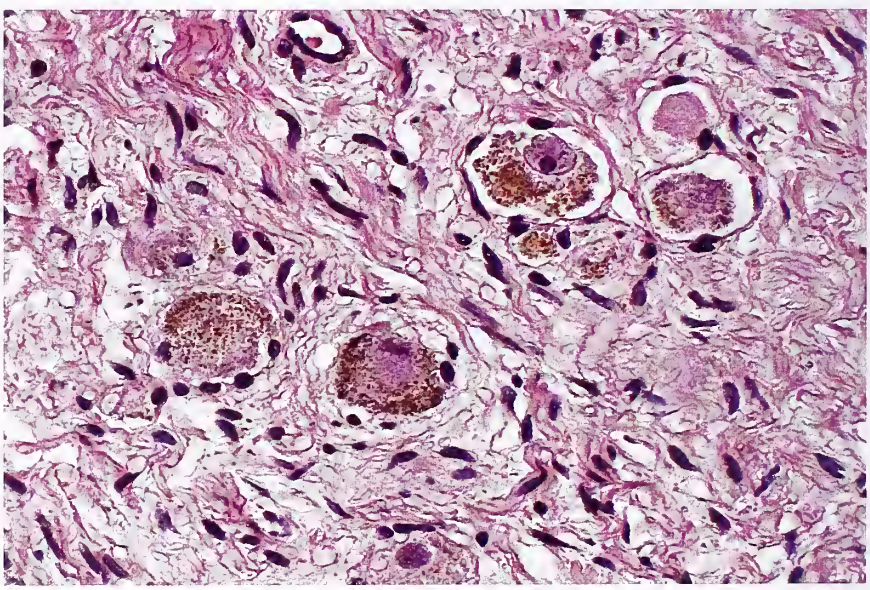

Figure 19-54

GANGLIONEUROMA

The ganglion cells of this ganglioneuroma contain abundant granular pigment consistent with lipofuscin or neuromelanin. Mature ganglion cells are encircled by satellite cells. (Fig. 23-68 from Fascicle 19, Third Series.)

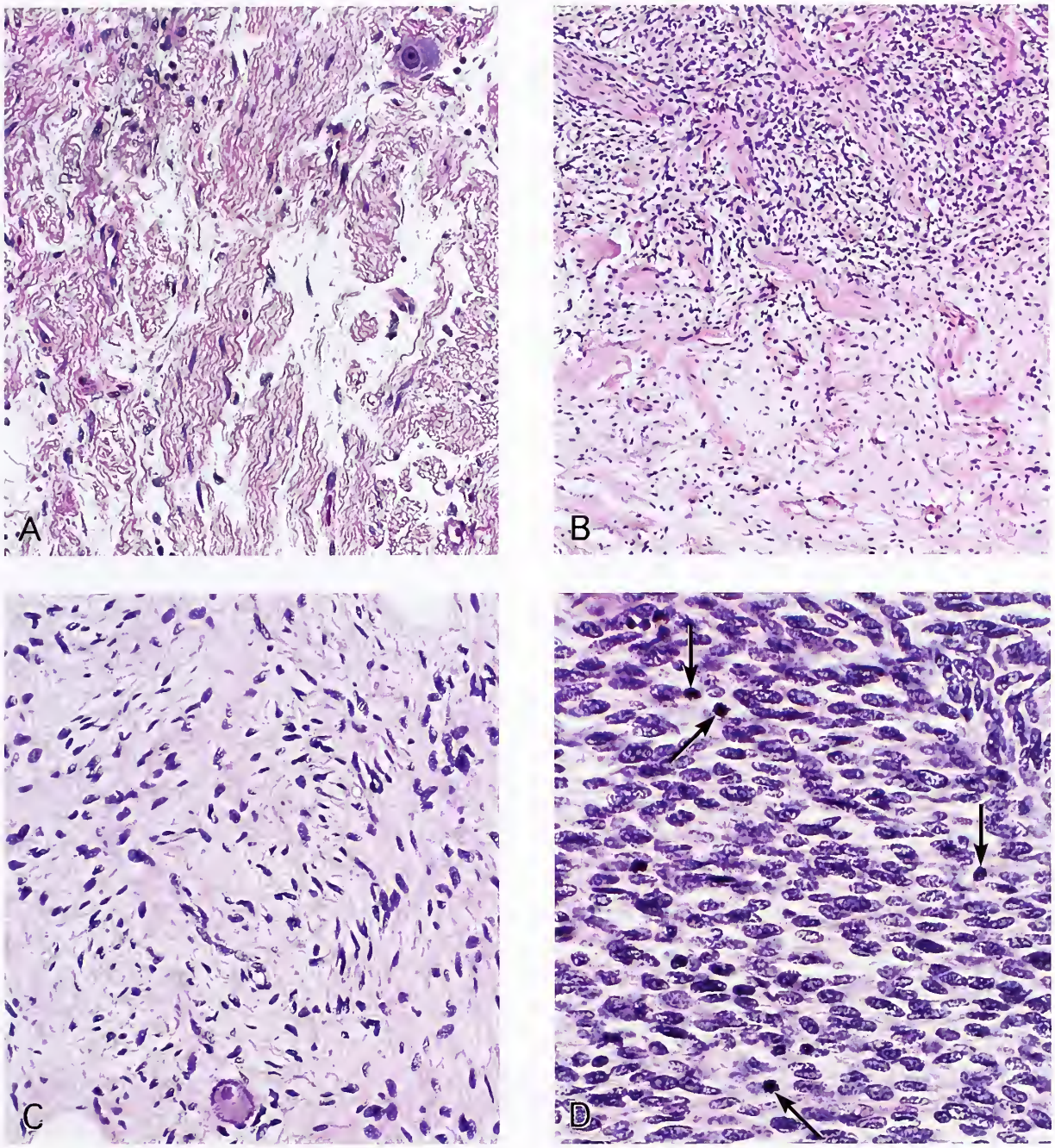

Figure 19-56

MALIGNANT TRANSFORMATION OF A GANGLIONEUROMA

Malignant transformation of a ganglioneuroma 17 years after abdominal mega-voltage radiation for unresectable abdominal NB in a 13-month-old patient.

A: Mature ganglioneuroma was seen in much of the resected tumor when the patient was a little over 18 years of age during a "debulking" procedure.

B: Other areas of the same tumor show transition to a malignant peripheral nerve sheath tumor.

C: Transition zone of a malignant peripheral nerve sheath tumor.

D: Some areas show pure malignant peripheral nerve sheath tumor with numerous mitotic figures (arrows) while other areas were necrotic. (A–D: Fig. 23-69 from Fascicle 19, Third Series.)

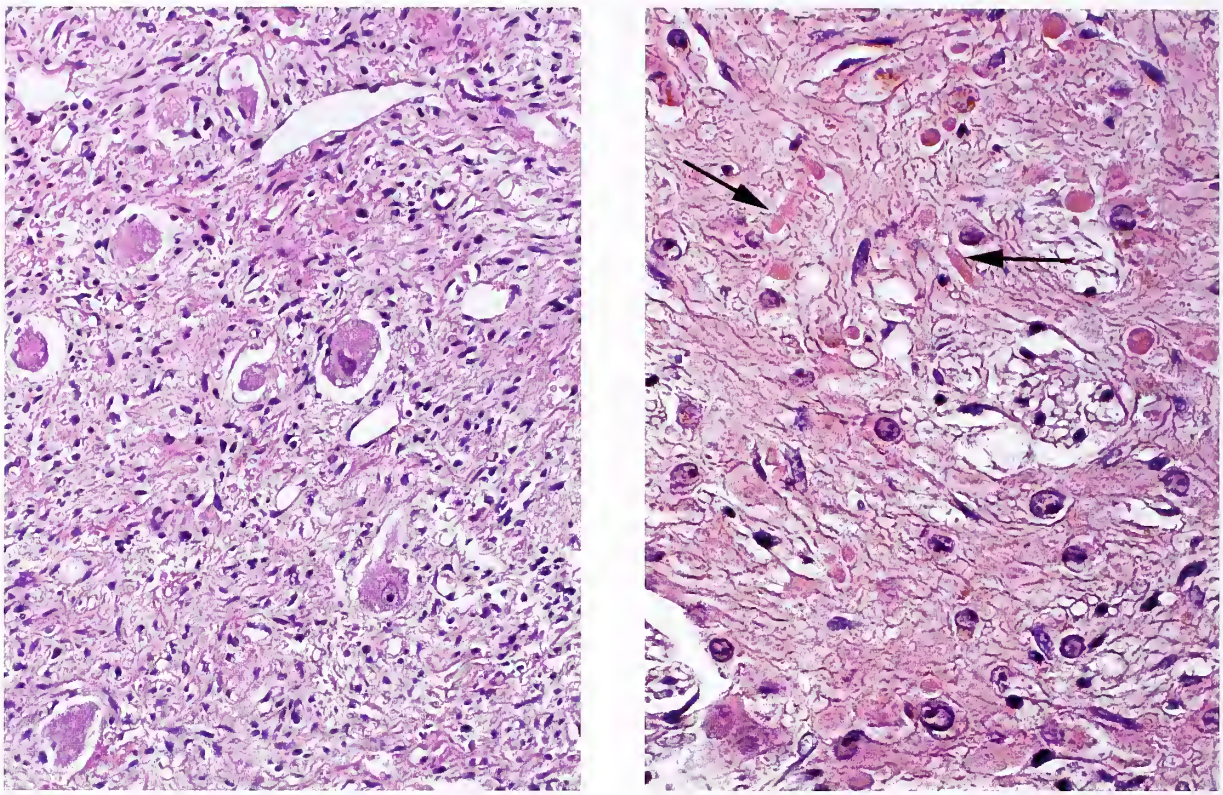

Figure 19-57

ADRENAL GANGLIONEUROMA WITH HILUS (OR LEYDIG) CELLS

Left: This testosterone-secreting adrenal ganglioneuroma contains numerous ganglion cells with interspersed fascicles of Schwann cells. There were other fields with hilus (or Leydig) cells.

Right: Typical hilus (or Leydig) cells with Reinke crystalloids (arrows) are seen in the same tumor. Some of the crystalloids have a globular shape.

or clusters of cells resembling adrenal cortical cells (171). Scully and Cohen (172) reported a case of GN containing cells morphologically identical to hilus cells in a 50-year-old woman, but there was no evidence of virilization; the 3.5-cm adrenal tumor was an incidental finding in a patient whose symptoms suggested biliary tract disease (172). On rare occasion, heterotopic hilus (or Leydig) cells have been identified within the adrenal gland (see chapter 1).

REFERENCES

Neuroblastoma and Ganglioneuroblastoma

1. Lack EE. Pathology of adrenal and extra-adrenal paraganglia in major problems in pathology, Vol 29. Philadelphia: WB Saunders; 1994.
2. Young JL Jr, Ries LG, Silverberg E. Horm JW, Miller RW. Cancer incidence, survival, and mortality for children younger than age 15 years. Cancer 1986;58:598-602.
3. Miller RW, Young JL Jr, Novakovic B. Childhood cancer. Cancer 1995;75:395-405.
4. Rosen EM, Cassady JR, Frantz CN, Kretschmar C, Levey R, Sallan SE. Neuroblastoma. The Joint Center for Radiation Therapy/Dana-Farber Cancer Institute/Children's Hospital experience. J Clin Oncol 1984;2:719-732.
5. Miller RW. Ethnic differences in cancer occurrence: genetic and environmental influences with particular reference to neuroblastoma. In: Mulvihill JJ, Miller RW, Fraumeni JF Jr, eds. Genetics of human cancer. New York: Raven Press; 1977:1-14.

6. Hardy PC, Nesbit ME Jr. Familial neuroblastoma: report of a kindred with a high incidence of infantile tumors. J Pediatr 1972;80:74-77.
7. Kushner BH, Gilbert F, Helson L. Familial neuroblastoma. Case reports, literature review and etiologic considerations. Cancer 1986;57:1887-1893.
8. Bundey S, Evans K. Survivors of neuroblastoma and ganglioneuroma and their families. J Med Genet 1982;19:16-21.
9. Knudson AG Jr, Strong LC. Mutation and cancer: neuroblastoma and pheochromocytoma. Am J Hum Genet 1972;24:514-532.
10. Gambini C, Conte M, Bernini G, et al. Neuroblastic tumors associated with opsoclonus-myoclonus syndrome: histological, immunohistochemical and molecular features of 15 Italian cases. Virchows Arch 2003;442:555-562.
11. Sayed AK, Miller BA, Lack EE, Sallan SE, Levey RH. Heterochromia iridis and Horner's syndrome due to paravertebral neurilemona. J Surg Oncol 1983;22:15-16.
12. Sawada T. Past and future of neuroblastoma screening in Japan. Am J Ped Hematol Oncol 1992;14:320-326.
13. Sawada T, Kidowaki T, Sugimoto T, Kusunoki T. Incidence of neuroblastoma in infancy in Japan. Med Pediatr Oncol 1984;12:101-103.
14. Woods WG, Gao RN, Shuster JJ, et al. Screening of infants and mortality due to neuroblastoma. N Engl J Med 2002;346:1041-1046.
15. Schilling FH, Spix C, Berthold F, et al. Neuroblastoma screening at one year of age. N Engl J Med 2002;346:1047-1053.
16. Nishi M, Miyake H, Takeda T, Hanai J, Kikuchi Y, Hirama T. Mass screening for neuroblastoma targeting children age 14 months in Sapporo City: a preliminary report. Cancer 1998;82:1973-1977.
17. Ijiri R, Tanaka Y, Kato K, et al. Clinicopathologic study of mass-screened neuroblastoma with special emphasis on untreated observed cases: a possible histologic clue to tumor regression. Am J Surg Pathol 2000;24:807-815.
18. Hayashi Y, Hanada R, Yamamoto K. Biology of neuroblastomas in Japan found by screening. Am J Pediatr Hematol Oncol 1992;14:342-347.
19. Jaffe N. Neuroblastoma: review of the literature and an examination of factors contributing to its enigmatic character. Cancer Treat Rev 1976;3:61-82.
20. Shende A, Wind ES, Lanzkowsky P. Intrarenal neuroblastoma mimicking Wilms' tumor. N Y State J Med 1979;79:93.
21. Reid H, van der Walt JD, Fox H. Neuroblastoma arising in a mature cystic teratoma of the ovary. J Clin Pathol 1983;36:68-73.
22. Filler RM, Traggis DG, Jaffe N, Vawter GF. Favorable outlook for children with mediastinal neuroblastoma. J Ped Surg 1972;7:136-143.
23. Shochat SJ, Corbelletta NL, Repman MA, Schengrund CL. A biochemical analysis of thoracic neuroblastomas: a Pediatric Oncology Group study. J Pediatr Surg 1987;22:660-664.
24. Ogita S, Tokiwa K, Takahashi T, Imashuku S, Sawada T. Congenital cervical neuroblastoma associated with Horner syndrome. J Pediatr Surg 1988;23:991-992.
25. King D, Goodman J, Hawk T, Boles ET Jr, Sayers MP. Dumbbell neuroblastomas in children. Arch Surg 1975;110:888-891.

Staging Systems

26. Evans AE, D'Angio GJ, Randolph J. A proposed staging for children with neuroblastoma. Children's Cancer Study Group A. Cancer 1971;27: 374-378.
27. Evans AE, D'Angio GJ, Sather HN, et al. A comparison of four staging systems for localized and regional neuroblastoma: a report trom the Childrens Cancer Study Group. J Clin Oncol 1990;8:678-688.
28. Brodeur GM, Seeger RC, Barret A, et al. International criteria for diagnosis, staging and response to treatment in patients with neuroblastoma. J Clin Oncol 1988;6:1874-1881.
29. Hayes FA, Green A, Hustu HO, Kumar M. Surgicopathologic staging of neuroblastoma: Prognostic significance of regional lymph node metastases. J Pediatr 1983;102:59-62.
30. Thomas PR, Lee JY, Fineberg BB, et al. An analysis of neuroblastoma at a single institution. Cancer 1984;53:2079-2082.
31. Evans AE, Chatten J, D'Angio GJ, Gerson JM, Robinson J, Schnaufer L. A review of 17 IV-S neuroblastoma patients at the Children's Hospital of Philadelphia. Cancer 1980;45:833-839.
32. Stokes SH, Thomas PR, Perez CA, Vietti TJ. Stage IV-S neuroblastoma. Results with definitive therapy. Cancer 1984;53:2083-2086.
33. Tsuchida Y, Yokomori K, Saito S, Kaku H, Bessho F. Stage IV-S neuroblastoma involving the liver and ectopic liver. Report of an unusual case. Cancer 1984;53:1609-1611.
34. Lau L. Neuroblastoma: a single institution's experience with 128 children and an evaluation of clinical and biological prognostic factors. Pediatr Hematol Oncol 2002;19:79-89.
35. Qualman SJ, Bowen J, Fitzgibbons PL, Cohn SL, Shimada H. Cancer Committee, College of American Pathologists. Protocol for the examination of specimens from patients with neuroblastoma and related neuroblastic tumors. Arch Pathol Lab Med 2005;129:874-883.

36. Kushner BH, Kramer K, Cheung NK. Chronic neuroblastoma. Cancer 2002;95:1366-1375.

In Situ Neuroblastoma

37. Beckwith JB, Perrin EV. In situ neuroblastoma: a contribution to the natural history of neural crest tumors. Am J Pathol 1963;43:1089-1104.
38. Guin GH, Gilbert EF, Jones B. Incidental neuroblastoma in infants. Am J Clin Pathol 1969;51: 126-136.
39. Tubergen DG, Heyn RM. In situ neuroblastoma associated with an adrenal cyst. J Pediatr 1970;76:451-453.
40. Turkel SB, Itabashi HH. The natural history of neuroblastic cells in the fetal adrenal gland. Am J Pathol 1974;76:225-236.
41. Lack EE, Kozakewich HP. Embryology, developmental anatomy, and selected aspects of nonneoplastic pathology. In: Lack EE, ed. Pathology of the adrenal glands. New York: Churchill Livingstone; 1990:1-74.

Stage IV-S Neuroblastoma

42. Nickerson HJ, Matthay KK, Seeger RC, et al. Favorable biology and outcome of stage IV-S neuroblastoma with supportive care or minimal therapy: a Children's Cancer Group study. J Clin Oncol 2000;18:477-486.
43. Evans AE, Baum E, Chard R. Do infants with stage IV-S neuroblastoma need treatment? Arch Dis Child 1981;56:271-274.
44. Kretschmar CS. Childhood neuroblastoma: clinical and prognostic features. In: Lack EE, ed. Pathology of the adrenal glands. New York: Churchill Livingstone; 1990:257-275.
45. Stephenson SR, Cook BA, Mease AD, Ruymann FB. The prognostic significance of age and pattern of metastases in stage IV-S neuroblastoma. Cancer 1986;58:372-375.
46. Knudson AG Jr, Meadows AT. Sounding board. Regression of neuroblastoma IV-S: a genetic hypothesis. N Engl J Med 1980;302:1254-1256.
47. Balaban G, Gilbert F. Neuroblastoma IV-S: a chromosome analysis. N Engl J Med 1983;309: 989.
48. Garvin J Jr, Bendit I, Nisen PD. N-myc oncogene expression and amplification in metastatic lesions of stage IV-S neuroblastoma. Cancer 1990;65:2572-2575.
49. Nakagawara A, Sasazuki T, Akiyama H, et al. N-myc oncogene and stage IV-S neuroblastoma. Preliminary observations in ten cases. Cancer 1990;65:1960-1967.
50. Pepper W. Study of congenital sarcoma of the liver and suprarenal. Am J Med Sci 1901;121: 287-299.

Gross and Microscopic Pathology

51. Lonergan GJ, Schwab CM, Suarez ES, Carlson CL. Neuroblastoma, ganglioneuroblastoma, and ganglioneuroma: radiologic-pathologic correlation. Radiographics 2002;22:911-934.
52. Leape LL, Lowman JT, Loveland GC. Multifocal nondisseminated neuroblastoma. Report of two cases in siblings. J Pediatr 1978;92:75-77.
53. Gonzalez-Crussi F, Hsueh W. Bilateral adrenal ganglioneuroblastoma with neuromelanin. Clinical and pathologic observations. Cancer 1988;61:1159-1166.
54. Day DL, Johnson R, Cohen MD. Abdominal neuroblastoma with inferior vena caval tumor thrombus: report of three cases (one with right atrial extension). Pediatr Radiol 1991;21:205-207.
55. Stout AP. Ganglioneuroma of the sympathetic nervous system. Surg Gynecol Obstet 1947;84: 101-110.
56. Bove KE, McAdams AJ, Composite ganglioneuroblastoma. An assessment of the significance of histological maturation in neuroblastoma diagnosed beyond infancy. Arch Pathol Lab Med 1981;105:325-330.
57. Shimada H, Chatten J, Newton WA Jr, et al. Histopathologic prognostic factors in neuroblastic tumors: definition of subtypes of ganglioneuroblastoma and age-linked classification of neuroblastomas. J Natl Cancer Inst 1984;73:405-416.
58. Brock CE, Ricketts RR. Hemoperitoneum from spontaneous rupture of neonatal neuroblastoma. Am J Dis Child 1982;136:370-371.
59. Kenney PJ, Stanley RJ. Calcified adrenal masses. Urol Radiol. 1987;9:9-15.
60. Hachitanda Y, Tsuneyoshi M. Neuroblastoma with a distinct organoid pattern: a clinicopathologic, immunohistochemical, and ultrastructural study. Hum Pathol 1994;25:67-72.
61. Adam A, Hochholzer L. Ganglioneuroblastoma of the posterior mediastinum. A clinicopathologic review of 80 cases. Cancer 1981;47:373-381.
62. Wright JH. Neurocytoma or neuroblastoma, a kind of tumor not generally recognized. J Experim Medicine 1910;12:556-561.
63. Lee RE, Young RH, Castleman B. James Homer Wright. A biography of the enigmatic creator of the Wright stain on the occasion of its centennial. Am J Surg Pathol 2002;26:88-96.
64. Joshi VV, Silverman JF, Altshuler G, et al. Systematization of primary histopathologic and fine-needle aspiration cytologic features and description of unusual histopathologic, features of neuroblastic tumors: a report from the Pediatric Oncology Group. Hum Pathol 1993;24: 493-504.

65. Cozzutto C, Carbone A. Pleomorphic (anaplastic) neuroblastoma. Arch Pathol Lab Med 1988; 112:621-625.
66. Dehner LP. Anaplasia in solid malignant tumors of childhood. Arch Pathol Lab Med 1989; 113:11-12.
67. Chatten J. Anaplastic neuroblastoma. Arch Pathol Lab Med 1989;113:9-10.
68. Tornoczky T, Kalman E, Kajtar PG, et al. Large cell neuroblastoma: a distinct phenotype of neuroblastoma with aggressive clinical behavior. Cancer 2004;100:390-397.
69. Tsokos M, Scarpa S, Ross RA, Triche TJ. Differentiation of human neuroblastoma recapitulates neural crest development. Study of morphology, neurotransmitter enzymes, and extracellular matrix proteins. Am J Pathol 1987;128:484-496.
70. Miyauchi J, Kiyotani C, Shioda Y, et al. Unusual chromaffin cell differentiation of a neuroblastoma after chemotherapy and radiotherapy: report of an autopsy case with immunohistochemical evaluations. Am J Surg Pathol. 2004;28:548-553.
71. Hedborg F, Ulleras E, Grimelius L, et al. Evidence for hypoxia-induced neuronal-to-chromaffin metaplasia in neuroblastoma. FASEB J 2003;17:598-609.
72. Koppersmith DL, Powers JM, Hennigar GR. Angiomatoid neuroblastoma with cytoplasmic glycogen: a case report and histogenic considerations. Cancer 1980;45:553-560.
73. Kozakewich HP, Perez-Atayde AR, Donovan MJ, et al. Cystic neuroblastoma: emphasis on gene expression, morphology, and pathogenesis. Pediatr Dev Pathol 1998;1:17-28.

Grading and Other Prognostic Factors

74. Beckwith JB, Martin RF. Observations on the histopathology of neuroblastomas. J Ped Surg 1968;3:106-110.
75. Hughes M, Marsden HB, Palmer MK. Histologic patterns of neuroblastoma related to prognosis and clinical stage. Cancer 1974;34:1706-1711.
76. Mäkinen J. Microscopic patterns as a guide to prognosis of neuroblastoma in childhood. Cancer 1972;29:1637-1646.
77. Gitlow SE, Dziedzic LB, Strauss L, Greenwood SM, Dziedzic SW. Biochemical and histologic determination in the prognosis of neuroblastoma. Cancer 1973;32:898-905.
78. Moragas A, Toran N. Image analysis of neuroblastomas—discrimination of prognostic patterns. Diagn Histopathol 1982;5:53-57.
79. Romansky SG, Crocker DW, Shaw KN. Ultrastructural studies on neuroblastoma: evaluation of cytodifferentiation. Cancer 1978;42:2392-2398.
80. Dehner LP. Classic neuroblastoma: histopathologic grading as a prognostic indicator. The Shimada system and its progenitors. Am J Ped Hematol Oncol 1988;10:143-154.
81. Chatten J, Shimada H, Sather HN, Wong KY, Siegel SE, Hammond GD. Prognostic value of histopathology in advanced neuroblastoma: a report from the Childrens Cancer Study Group. Hum Pathol 1988;19:1187-1198.
82. Hachitanda Y, Ishimoto K, Shimada H. Stage IV-S neuroblastoma: histopathology of 27 cases compared with conventional neuroblastomas. Lab Invest 1991;64:5P(26).
83. Joshi VV, Chatten J, Sather HN, Shimada H. Evaluation of the Shimada classification in advanced neuroblastoma with a special reference to the mitosis-karyorrhexis index: a report from the Childrens Cancer Study Group. Mod Pathol 1991;4:139-147.
84. Joshi VV, Cantor AB, Altshuler G, et al. Age-linked prognostic categorization based on a new histologic grading system of neuroblastomas. A clinicopathologic study of 211 cases from the Pediatric Oncology Group. Cancer 1992;69: 2197-2211.
85. Joshi VV, Cantor AB, Altshuler G, et al. Recommendations for modification of terminology of neuroblastic tumors and prognostic significance of Shimada classification. A clinicopathologic study of 213 cases from the Pediatric Oncology Group. Cancer 1992;69:2183-2196.
86. Joshi VV, Cantor AB, Brodeur GM, et al. Correlation between morphologic and other prognostic markers of neuroblastoma. A study of histologic grade, DNA index, N-myc gene copy number, and lactic dehydrogenase in patients in the Pediatric Oncology Group. Cancer 1993;71: 3173-3181.
87. Joshi VV, Silverman JF, Altshuler G, et at. Systemization of primary histopathologic and fine-needle aspiration cytologic features and description of unusual histopathologic features of neuroblastic tumors: a report from the Pediatric Oncology Group. Hum Pathol 1993;24:493-504.
88. Shimada H, Ambros IM, Dehner LP, et al. The International Neuroblastoma Pathology Classification (the Shimada system). Cancer 1999;86: 364-372.
89. Umehara S, Nakagawa A, Matthay KK, et al. Histopathology defines prognostic subsets of ganglioneuroblastoma, nodular. Cancer. 2000;89: 1150-1161.
90. Shimada H, Umehara S, Monobe Y, et al. International neuroblastoma pathology classification for prognostic evaluation of patients with peripheral neuroblastic tumors: a report from the Children's Cancer Group. Cancer 2001;92:2451-2461.
91. Goto S, Umehara S, Gerbing RB, et al. Histopathology (International Neuroblastoma Pathology Classification) and MYCN status in patients with peripheral neuroblastic tumors: a report from the Children's Cancer Group. Cancer 2001;92:2699-2708.

92. Peuchmaur M, d'Amore ES, Joshi VV, et al. Revision of the International Neuroblastoma Pathology Classification: confirmation of favorable and unfavorable prognostic subsets in ganglioneuroblastoma, nodular. Cancer. 2003;98:2274-2281.
93. Sano H, Bonadio J, Gerbing RB, et al. International neuroblatoma pathology classificatin adds independent prognostic information beyond the prognostic contribution of age. Eur J Cancer 2006;42:1113-1119.
94. Philip T. Overview of current treatment of neuroblastoma. Am J Ped Hematol Oncol 1992;14: 97-102.
95. Schwab M, Westermann F, Hero B, Berthold F. Neuroblastoma: biology and molecular and chromosomal pathology. Lancet Oncol 2003;4: 472-480.
96. Stark B, Jeison M, Glaser-Gabay L, et al. der(11)t(11;17): a distinct cytogenetic pathway of advanced stage neuroblastoma (NBL) detected by spectral karyotyping (SKY). Cancer Lett 2003;197:75-79.
97. Mora J, Alaminos M, de Torres C, et al. Comprehensive analysis of the 9p21 region in neuroblastoma suggests a role for genes mapping to 9p21-23 in the biology of favourable stage 4 tumours. Br J Cancer 2004;91:1112-1118.
98. Seeger RC, Brodeur GM, Sather H, et al. Association of multiple copies of the N-myc oncogene with rapid progression of neuroblastomas. N Engl J Med 1985;313:1111-1116.
99. Attiyeh EF, London WB, Mosse YP, et al. Chromosome 1 p and 11q deletions and outcome in neuroblastoma. N Engl J Med 2005;353:2243-2253.
100. Brodeur GM, Azar C, Brother M, et al. Neuroblastoma. Effect of genetic factors on prognosis and treatment. Cancer 1992;70:1685-1694.
101. Thorner PS, Ho M, Chilton-MacNeill S, Zielenska M. Use of chromogenic in situ hybridization to identify MYCN gene copy number in neuroblastoma using routine tissue sections. Am J Surg Pathol 2006;30:635-642.
102. Suzuki T, Bogenmann E, Shimada H, Stram D, Seeger RC. Lack of high-affinity nerve growth factor receptors in aggressive neuroblastomas. J Natl Cancer Inst 1993;85:377-384.
103. Shimada H, Nakagawa A, Peters J, et al. TrkA expression in peripheral neuroblastic tumors: prognostic significance and biological relevance. Cancer 2004;101:1873-1881.
104. Irshad S, Pedley RB, Anderson J, Latchman DS, Budhram-Mahadeo V. The Brn-3b transcription factor regulates the growth, behavior, and invasiveness of human neuroblastoma cells in vitro and in vivo. J Biol Chem 2004;279:21617-21627.
105. Kato C, Miyazaki K, Nakagawa A, et al. Low expression of human tubulin tyrosine ligase and suppressed tubulin tyrosination/detyrosination cycle are associated with impaired neuronal differentiation in neuroblastomas with poor prognosis. Int J Cancer 2004; 112:365-375.
106. Ikematsu S, Nakagawara A, Nakamura Y, et al. Correlation of elevated level of blood midkine with poor prognostic factors of human neuroblastomas. Br J Cancer 2003;88:1522-1526.
107. Schramm A, von Schuetz V, Christiansen H, et al. High activin A-expression in human neuroblastoma: suppression of malignant potential and correlation with favourable clinical outcome. Oncogene 2005;24:680-687.
108. Perel Y, Amrein L, Dobremez E, Rivel J, Daniel JY, Landry M. Galanin and galanin receptor expression in neuroblastic tumours: correlation with their differentiation status. Br J Cancer 2002;86:117-122.
109. Kuo YH, Chen TT. Novel activities of pro-IGF-I E peptides: regulation of morphological differentiation and anchorage-independent growth in human neuroblastoma cells. Exp Cell Res 2002;280:75-89.
110. Hsiao CC, Huang CC, Sheen JM, et al. Differential expression of delta-like gene and protein in neuroblastoma, ganglioneuroblastoma and ganglioneuroma. Mod Pathol 2005;18:656-662.
111. DeLellis RA, Mangray S. The adrenal glands. In: Mills SE, Greenson JK, Oberman HA, Reuter V, Stoler MH, eds. Sternberg's diagnostic surgical pathology, 4th ed. Philadelphia: Lippincott Williams & Wilkins; 2004:621-667.
112. Ambros IM, Benard J, Boavida M, et al. Quality assessment of genetic markers used for therapy stratification. J Clin Oncol 2003;21:2077-2084.
113. Krams M, Hero B, Berthold F, Parwaresch R, Harms D, Rudolph P. Proliferation marker KI-S5 discriminates between favorable and adverse prognosis in advanced stages of neuroblastoma with and without MYCN amplification. Cancer 2002;94:854-861.
114. Korja M, Finne J, Salmi TT, et al. Chromogenic in situ hybridization-detected hotspot MYCN amplification associates with Ki-67 expression and inversely with nestin expression in neuroblastomas. Mod Pathol 2005;18:1599-1605.

Spontaneous Regression or Maturation

115. Everson TC, Cole WH. Spontaneous regression of cancer; a study and abstract of reports in the world medical lliterature and of personal communications concerning spontaneous regression of malignant disease. Philadelphia: WB Saunders; 1966:88-163.

116. Cushing H, Wolbach SB. The transformation of a malignant paravertebral sympathicoblastoma into a benign ganglioneuroma. Am J Path 1927;3:203-216.
117. Fox F, Davidson J, Thomas LB. Maturation of sympathicoblastoma into ganglioneuroma: report of 2 patients with 20- and 46-year survivals respectively. Cancer 1959;12:108-116.
118. Koizumi H, Hamano S, Doi M, et al. Increased occurrence of caspase-dependent apoptosis in unfavorable neuroblastomas. Am J Surg Pathol 2006;30:249-257.

Survival and Patterns of Metastasis

119. Collins VP. Wilms' tumor: its behavior and prognosis. J La State Med Soc 1955;107:474-480.
120. Berthold F. Overview: biology of neuroblastoma. In: Pochedly C, ed. Neuroblastoma. Tumor biology and therapy. Boca Raton: CRC Press; 1990:2-27.
121. Young RH, Kozakewich HP, Scully RE. Metastatic ovarian tumors in children: a report of 14 cases and review of the literature. Int J Gynecol Pathol 1993;12:8-19.
122. de la Monte SM, Moore GW, Hutchins GM. Nonrandom distribution of metastases in neuroblastic tumors. Cancer 1983;52:915-925.
123. Feldges AJ, Stanisic M, Morger R, Waidelich E. Neuroblastoma with meningeal involvement causing increased intracranial pressure and coma in two children. Am J Pediatr Hematol Oncol 1986;8:355-357.
124. Kramer K, Kushner B, Heller G, Cheung NK. Neuroblastoma metastatic to the central nervous system. The Memorial Sloan-Kettering Cancer Center experience and a literature review. Cancer. 2001;91:1510-1519.
125. Glorieux P, Bouffet E, Philip I, et al. Metastatic interstitial pneumonitis after autologous bone marrow transplantation. A consequence of reinjection of malignant cells? Cancer 1986;58: 2136-2139.
126. Hutchison R. On suprarenal sarcoma in children with metastases in the skull. Q J Med 1907; 1:33-38.
127. Willis RA. The spread of tumours in the human body, 3rd ed. London: Butterworth & Co. Ltd.; 1973:102-105.
128. Smith CR, Chan HS, deSa DJ. Placental involvement in congenital neuroblastoma. J Clin Pathol 1981;34:785-789.
129. Andersen HJ, Hariri J. Congenital neuroblastoma in a fetus with multiple malformations. Metastasis in the umbilical cord as a cause of intrauterine death. Virchows Arch A Pathol Anat Histopathol 1983;400:219-222.
130. Lucky AW, McGuire J, Komp DM. Infantile neuroblastoma presenting with cutaneous blanching nodules. J Am Acad Dermatol 1982;6:389-391.
131. Shown TE, Durfee MF. Blueberry muffin baby: neonatal neuroblastoma with subcutaneous metastases. J Urol 1970;104:193-195.
132. Moss TJ, Sanders DG. Detection of neuroblastoma cells in blood. J Clin Oncol 1990;8:736-740.
133. Pereira F, Crist W, McKaig S. Neuroblastoma "leukemia" a rarity? Report of a case. Clin Pediatr 1978;17:701-704.

Differential Diagnosis of Neuroblastoma

134. Dehner LP. Primitive neuroectodermal tumor and Ewing's sarcoma. Am J Surg Pathol 1993; 17:1-13.
135. Marina NM, Etcubanas E, Parham DM, Bowman LC, Green A. Peripheral primitive neuroectodennal tumor (peripheral neuroepithelioma) in children. A review of the St. Jude experience and controversies in diagnosis and management. Cancer 1989;64:1952-1960.
136. Folpe AL, Goldblum JR, Rubin BP, et al. Morphologic and immunophenotypic diversity in Ewing family tumors: a study of 66 genetically confirmed cases. Am J Surg Pathol 2005;29: 1025-1033.
137. Gerald WL, Miller HK, Battifora H, Miettinen M, Silva EG, Rosai J. Intra-abdominal desmoplastic small round-cell tumor. Report of 19 cases of a distinctive type of high-grade polyphenotypic malignancy affecting young individuals. Am J Surg Pathol 1991;15:499-513.
138. Lae ME, Roche PC, Jin L, Lloyd RV, Nascimento AG. Desmoplastic small round cell tumor: a clinicopathologic, immunohistochemical, and molecular study of 32 tumors. Am J Surg Pathol 2002;26:823-835.
139. Ladanyi M, Gerald W. Fusion of the EWS and WTl genes in the desmoplastic small round cell tumor. Cancer Res 1994;54:2837-2840.
140. Weeks DA, Beckwith JB, Mierau GW, Luckey DW. Rhabdoid tumor of kidney. A report of 111 cases from the National Wilms' Tumor Study Pathology Center. Am J Surg Pathol 1989;13: 439-458.
141. Parham DM, Weeks DA, Beckwith JB. The clinicopathologic spectrum of putative extrarenal rhabdoid tumors. An analysis of 42 cases studied with immunohistochemistry or electron microscopy. Am J Surg Pathol 1994;18:1010-1029.
142. Burger PC, Scheithauer BW. Tumors of the central nervous system. Atlas of Tumor Pathology, 4th Series, Fascicle 6. Washington, DC: American Registry of Pathology; 2007.
143. Goldblum JR, Beals TF, Weiss SW. Neuroblastoma-like neurilemoma. Am J Surg Pathol 1994;18:266-273.

Ganglioneuroma

144. Bove KE, McAdams AJ, Composite ganglioneuroblastoma. An assessment of the significance of histological maturation in neuroblastoma diagnosed beyond infancy. Arch Pathol Lab Med 1981;105:325-330.

145. Stout AP. Ganglioneuroma of the sympathetic nervous system. Surg Gynecol Obstet 1947;84: 101-110.
146. Weiss SW, Goldblum JR, eds. Enzinger and Weiss's soft tissue tumors, 4th ed. St. Louis: Mosby; 2001:1284-1288.
147. Carpenter WB, Kernohan JW. Retroperitoneal ganglioneuromas and neurofibromas. A clinicopathological study. Cancer 1963;16:788-797.
148. Wyman HE, Chappell BS, Jones WR Jr. Ganglioneuroma of bladder: report of a case. J Urol 1950;63:526-532.
149. Nassiri M, Ghazi C, Stivers JR, Nadji M. Ganglioneuroma of the prostate. A novel finding in neurofibromatosis. Arch Pathol Lab Med 1994;118:938-939.
150. Mithofer K, Grabowski EF, Rosenberg AE, Ryan DP, Mankin HJ. Symptomatic ganglioneuroma of bone. A case report. J Bone Joint Surg 1999; 81:1589-1595.
151. Christein JD, Kim AW, Jakate S, Deziel DJ. Central pancreatectomy for a pancreatic ganglioneuroma in a patient with previous neuroblastoma. Pancreatology 2002;2:557-560.
152. Wallace CA, Hallman JR, Sangueza OP. Primary cutaneous ganglioneuroma: a report of two cases and literature review. Am J Dermatopathol 2003;25:239-242.
153. Cannon TC, Brown HH, Hughes BM, Wenger AN, Flynn SB, Westfall CT. Orbital ganglioneuroma in a patient with chronic progressive proptosis. Arch Ophthalmol 2004;122:1712-1714.
154. Pardalidis NP, Grigoriadis K, Papatsoris AG, Kosmaoglou EV, Horti M. Primary paratesticular adult ganglioneuroma. Urology 2004;63: 584-585.
155. Zarabi M, LaBach JP. Ganglioneuroma causing acute appendicitis. Hum Pathol 1982;13:1143-1146.
156. Shekitka KM, Sobin LH. Ganglioneuromas of the gastrointestinal tract. Relation to von Reckinghausen disease and other multiple tumor syndromes. Am J Surg Pathol 1994;18:250-257.
157. Kyoshima K, Sakai K, Kanaji M, et al. Symmetric dumbbell ganglioneuromas of bilateral C2 and C3 roots with intradural extension associated with von Recklinghausen's disease: case report. Surg Neurol 2004;61:468-473.
158. Hamilton JP, Koop CE. Ganglioneuromas in children. Surg Gynec Obstet 1965;121:803-812.
159. Pachter MR, Lattes R. Neurogenous tumors of the mediastinum: a clinicopathologic study based on 50 cases. Dis Chest 1963;44:79-87.
160. Abell MR, Hart WR, Olson JR. Tumors of the peripheral nervous system. Hum Pathol 1970; 1:503-551.
161. Ackerman LV, Taylor FH. Neurogenous tumors within the thorax; a clinicopathologic evaluation of forty-eight cases. Cancer 1951;4:669-691.

Malignant Transformation of Ganglioneuroma

162. Fletcher CD, Fernando IN, Braimbridge MV, McKee PH, Lyall JR. Malignant nerve sheath tumor arising in a ganglioneuroma. Histopathology 1988;12:445-458.
163. Banks E, Yum M, Brodhecker C, Goheen M. A malignant peripheral nerve sheath tumor in association with a paratesticular ganglioneuroma. Cancer 1989;64:1738-1742.
164. Ghali VS, Gold JE, Vincent RA, Cosgrove JM. Malignant peripheral nerve sheath tumor arising spontaneously from retroperitoneal ganglioneuroma: a case report, review of the literature, and immunohistochemical study. Hum Pathol 1992;23:72-75.
165. de Chadarevian JP, MaePascasio J, Halligan GE, et al. Malignant peripheral nerve sheath tumor arising from an adrenal ganglioneuroma in a 6-year-old boy. Pediatr Dev Pathol 2004;7:277-284.
166. Ricci A Jr, Parham DM, Woodruff JM, Callihan T, Green A, Erlandson RA. Malignant peripheral nerve sheath tumors arising from ganglioneuromas. Am J Surg Pathol 1984;8:19-29.
167. Keller SM, Papazoglou S, McKeever P, Baker A, Roth JA. Late occurrence of malignancy in a ganglioneuroma 19 years following radiation therapy to a neuroblastoma. J Surg Oncol 1984; 25:227-231.
168. Chandrasoma P, Shibata D, Radin R, Brown LP, Koss M. Malignant peripheral nerve sheath tumor arising in an adrenal ganglioneuroma in an adult male homosexual. Cancer 1986;57: 2022-2025.
169. Kimura S, Kawaguchi S, Wada T, Nagoya S, Yamashita T, Kikuchi K. Rhabdomyosarcoma arising from a dormant dumbbell ganglioneuroma of the lumbar spine: a case report. Spine 2002;27:E513-517.

Masculinizing Ganglioneuroma

170. Aguirre P, Scully RE. Testosterone-secreting adrenal ganglioneuroma containing Leydig cells. Am J Surg Pathol 1983;7:699-705.
171. Mack E, Sarto GE, Crummy AB, Carlson IH, Curet LB, Wu J. Virilizing adrenal ganglioneuroma. JAMA 1978;239:2273-2274.
172. Scully RE, Cohen RB. Ganglioneuroma of adrenal medulla containing cells morphologicaly identical to hilus cells (extraparenchymal Leydig cells). Cancer 1961;14:421-425.

20 ULTRASTRUCTURAL, IMMUNOHISTOCHEMICAL, AND OTHER FEATURES OF NEUROBLASTOMAS AND RELATED TUMORS

ULTRASTRUCTURAL FINDINGS

Neuroblastoma and Ganglioneuroblastoma

Ultrastructural studies are still of value in the diagnosis of relatively undifferentiated neuroblastoma (NB) if the diagnosis is not readily evident by light microscopic evaluation or urinary catecholamine study, especially given the variable specificity of immunostaining (1). On survey views of NB, cytoplasmic organelles are generally sparse, with few mitochondria, and small amounts of rough endoplasmic reticulum and free ribosomes (fig. 20-1). The neuritic extensions of the cell cytoplasm can be impressive, with a prominent fibrillary matrix at the light microscopic level, and where there is matted neuropil-like matrix, a complicated, seemingly haphazard intertwining of cell processes may be seen ultrastructurally. An example of this is seen with the Homer Wright rosette or pseudorosette (fig. 20-2). Nuclei are often rounded, have a regular contour and finely dispersed chromatin with some margination at the periphery; occasionally, the nuclear membrane is slightly irregular or indented, and one or more small nucleoli may be present.

A characteristic morphologic feature of NB and ganglioneuroblastoma (GNB) is the presence of small, dense-core neurosecretory granules, usually within neuritic cell processes, but they may be sparse, and on occasion difficult to distinguish from primary lysosomes (fig. 20-3, left) (1–3). The neuritic cell processes can be rudimentary or short. Neurosecretory granules are

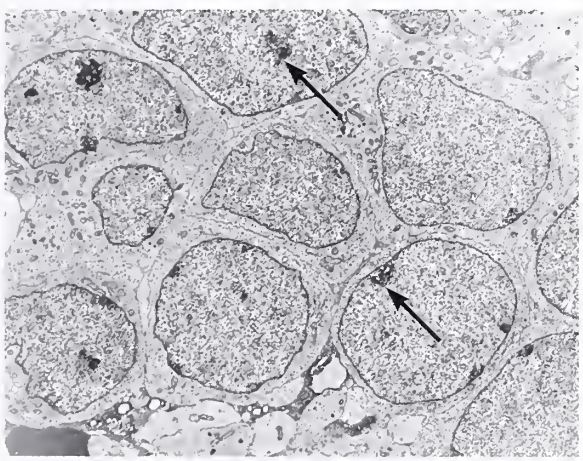

Figure 20-1

NEUROBLASTOMA

A survey view of neuroblastoma (NB) shows nuclei with a finely dispersed pattern of nuclear chromatin and a few small chromocenters (arrows). Neuritic processes are present in the upper right and lower fields. There are a few cellular organelles, mainly mitochondria. (Fig. 15-1 from Lack, EE. Pathology of adrenal and extra-adrenal paraganglia. Major problems in pathology, Vol 29. Philadelphia: WB Saunders; 1994:372.)

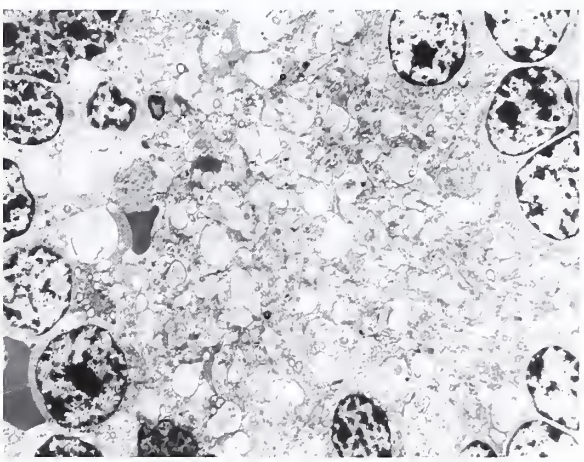

Figure 20-2

HOMER WRIGHT ROSETTE OR PSEUDOROSETTE

The nuclei of this NB have coarser chromatin with larger chromocenters and surround a space filled with complex intertwined neuritic processes. It is in areas such as this that there may be a denser concentration of dense-core neurosecretory type granules. Compare the light microscopic appearance of Homer Wright rosettes or pseudorosettes in figures 19-21 and 19-22.

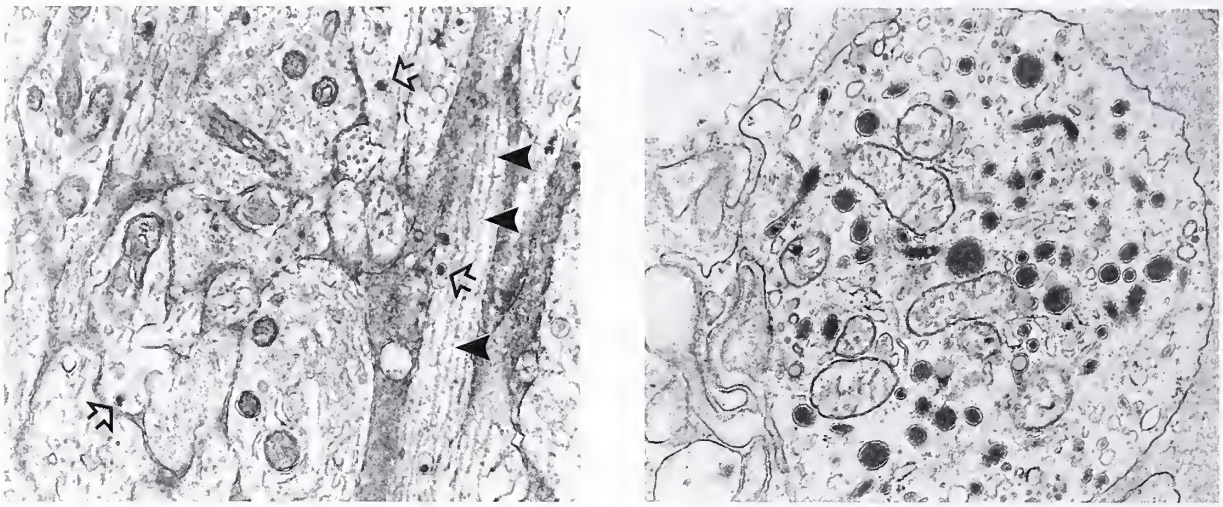

Figure 20-3

NEUROBLASTOMA

Left: Sparse neurosecretory type granules are present within neuritic processes (open arrows) and there are microtubules in longitudinal alignment (arrowheads). Scattered mitochondria are present.

Right: A neuritic process contains mildly pleomorphic dense-core neurosecretory type granules along with several empty vesicles.

occasionally recognized in the perinuclear cytoplasm or perikaryon. The granules are usually small and uniform, and one third to half the size of dense-core neurosecretory granules in pheochromocytomas (4). The average size of the granules in one study was 100 nm (5). On occasion, the dense-core neurosecretory granules are mildly pleomorphic (fig. 20-3, right). The diagnostic features include the presence of dense-core neurosecretory granules (which may be sparse in number) along with neuritic cell processes with fine neurofilaments 8 to 12 nm in width and neurotubules 24 to 26 nm in diameter (1,2,6,7). A positive correlation has been shown between the number of neurosecretory type granules in undifferentiated NB and prognostically favorable histochemical excretory patterns (5).

With advancing levels of cellular differentiation in GNB, some cells acquire structural features resembling ganglionic cells in a fully mature ganglioneuroma. The nucleus has an eccentric location, a prominent nucleolus, and often margination of heterochromatin against the nuclear membrane (fig. 20-4). There may be small, disorderly profiles of rough endoplasmic reticulum, particularly in the peripheral cytoplasm, and only rarely are there the orderly stacks or lamellar profiles that are found in a fully mature ganglion cell (Nissl substance) (3). Thin cytoplasmic processes can partially envelope cells with ganglionic differentiation consistent with satellite cells. It is uncommon to obtain a ganglion cell with an attached neuritic or neuronal extension in the same plane of section. The term "neuritic" or "neuronal" is appropriately noncommittal for the cytoplasmic extensions since it is not possible to be specific as to whether the process is a classic axon or dendrite (3). In GNBs with a spindle cell, schwannian matrix, there are Schwann cells with a well-developed myelin sheath enclosing neuritic cell processes, or simple infolding of the plasma membrane forming a mesaxon (fig. 20-5).

Glycogen has been noted within some NBs (8,9) but is uncommon. In a large study of nearly 100 NBs, intracytoplasmic glycogen was noted in less than 5 percent of cases (10); if abundant intracellular glycogen is noted, consideration should be given to other neoplasms in the differential diagnosis (3). Primitive intercellular junctions have been described (10).

Ganglioneuroma

Fully mature ganglioneuroma (GN) is composed of ganglion cells that may be difficult to recognize in random sampling of tissue submitted

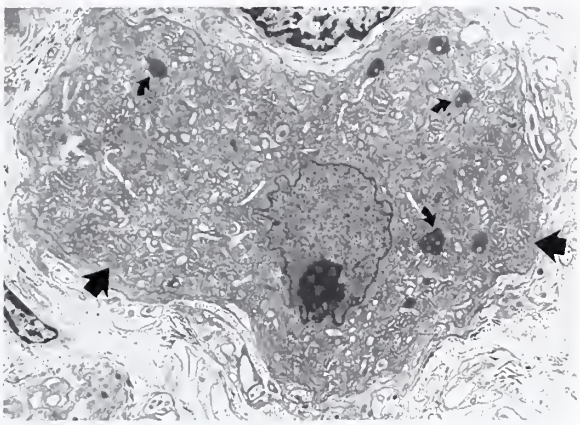

Figure 20-4

GANGLIONEUROBLASTOMA, OR STROMA-RICH TUMOR IN THE SHIMADA CLASSIFICATION

Ganglion cell differentiation is illustrated. The nucleus is eccentric with a prominent nucleolus. Stacks of rough endoplasmic reticulum are concentrated in the peripheral cytoplasm (arrows), which may be detected at the light microscopic level as Nissl substance (see fig. 19-28). The electron-dense material in the cytoplasm is lipofuscin or neuromelanin (curved arrows), which may become very prominent in ganglion cells (see figure 19-54). The tumor was a ganglioneuroblastoma (GNB), or a well-differentiated stroma-rich tumor in the Shimada classification, and closely resembled a ganglioneuroma.

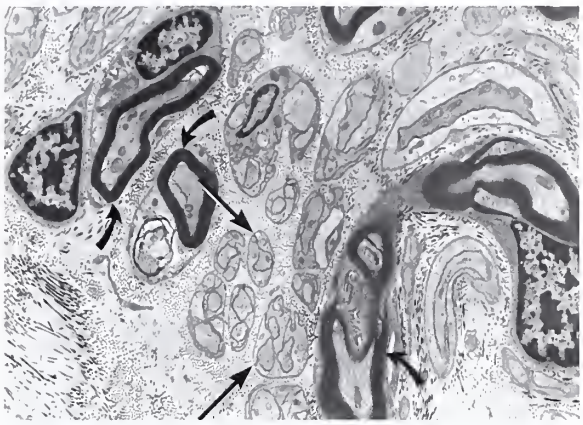

Figure 20-5

GANGLIONEUROBLASTOMA, OR STROMA-RICH INTERMIXED TUMOR IN THE SHIMADA CLASSIFICATION

There is a rich spindle cell schwannian matrix in this tumor. Numerous neuritic processes from neuroblasts and differentiating ganglion cells are ensheathed by the cytoplasm of Schwann cells. Mesaxons are present (straight arrows) along with well-developed myelin sheaths (curved arrows). (Fig. 23-36 from Fascicle 19, Third Series.)

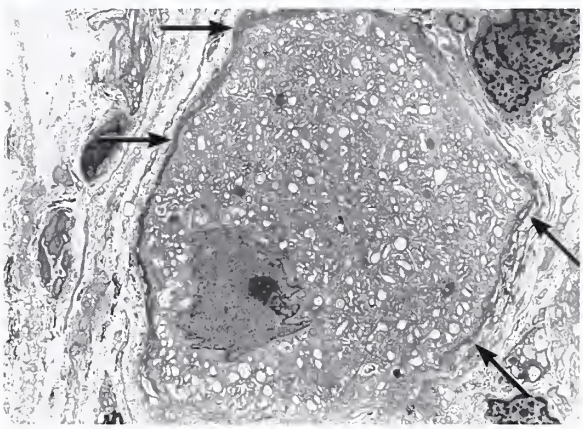

Figure 20-6

GANGLION CELL SURROUNDED BY SATELLITE CELL

The ganglion cell has an eccentric nucleus and prominent nucleolus. Irregular profiles of rough endoplasmic reticulum are present but are not arranged in parallel stacks as is seen with Nissl substance. Thin cytoplasmic processes partially surround the ganglion cell (arrows) and represent satellite cells. (Fig. 15-5 from Lack EE. Pathology of adrenal and extra-adrenal paraganglia. Major problems in pathology, Vol 29, Philadelphia: WB Saunders; 1994:374.)

for ultrastructural study unless a more directed search is made in multiple pilot sections preparatory to fine structural study. The morphologic features of note are ganglion cells sometimes enveloped by satellite cells (fig. 20-6), Schwann cells, and neuritic cell processes. Schwann cells may be numerous, with a continuous basement membrane around cytoplasmic processes (fig. 20-7). The vast majority of GNs are diagnosed by routine histologic sections and rarely is examination by electron microscopy necessary. The ultrastructure of GN is addressed in several other works (7,11). Rarely, mast cells are seen in these tumors, and the large, nonhomogeneous granules should not be confused with dense-core neurosecretory granules (3).

IMMUNOHISTOCHEMICAL FINDINGS

Sometimes the primitive cytomorphology of undifferentiated NB has muted or equivocal immunophenotypic "signals" of diagnostic value, and careful correlation with other findings such as ultrastructure may be indicated (3). Immunostaining for neuron-specific enolase is usually readily apparent in NB and GNB (3), with highlighting of neuritic extensions in the form of rosettes (or pseudorosettes), matted

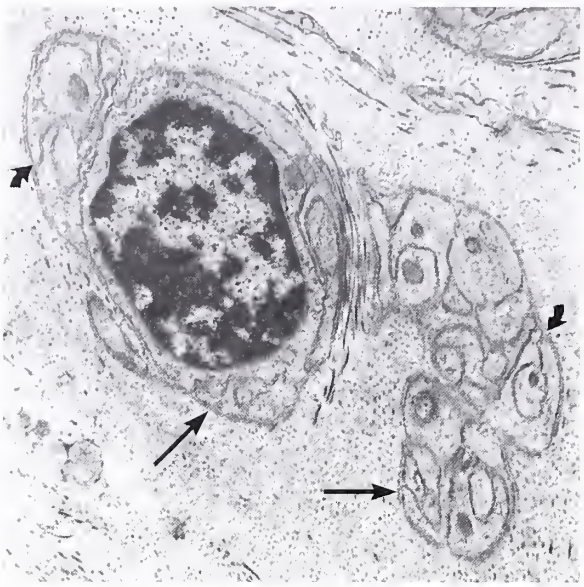

Figure 20-7

GANGLIONEUROMA

Schwann cell ensheathes numerous neuritic processes and has formed mesaxons in a number of areas (curved arrows). A continuous basement membrane is present around the Schwann cell and its cytoplasmic processes (straight arrows). Collagen is relatively abundant.

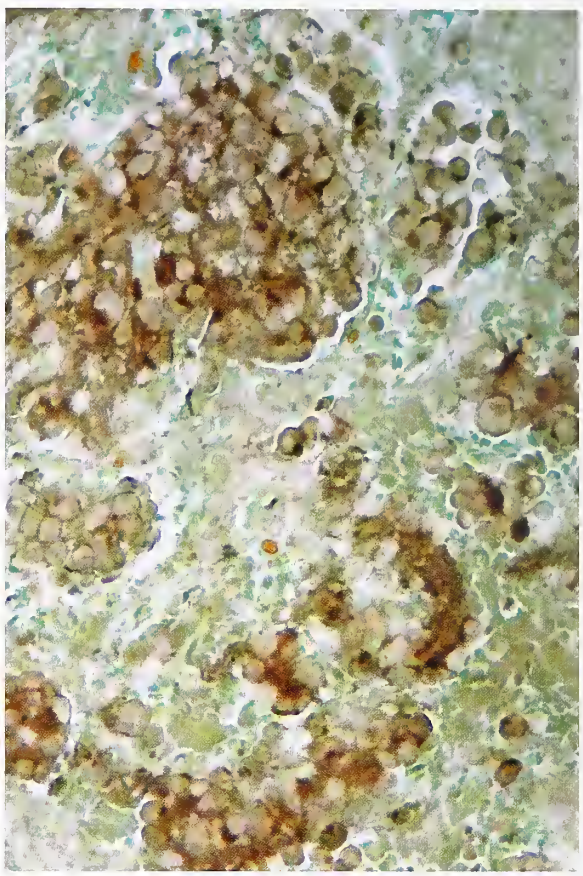

Figure 20-8

STAGE IV-S HEMORRHAGIC NEUROBLASTOMA

Virtually all of the tumor cells are immunoreactive for neuron-specific enolase. The tumor cells are separated by edema and hemorrhage (avidin-biotin peroxidase method).

neuropil, or sparse intercellular fibrillar matrix (fig. 20-8). Cells with neuronal or ganglionic differentiation may also be immunoreactive. The wide range of structures stained with neuron-specific enolase may mandate correlation with routine morphology and other features to ensure specificity.

Virtually all NBs have an adrenergic, cholinergic, or mixed neurotransmitter enzyme profile, thus indicating a close phenotypic relationship to the autonomic nervous system, while tumors generically grouped as primitive neuroectodermal tumors (PNETs) appear to represent relatively primitive derivatives of the neural crest (12). Several immunohistochemical studies have identified markers of PNETs (13); these tumors are characteristically positive for CD99 and may be positive for cytokeratin; using reverse transcriptase-polymerase chain reaction, the *EWS/FLI-1* fusion transcripts are detected (13,14).

Immunohistochemical staining for catecholamine synthesizing enzymes has been reported in NB, GNB, and GN, including tyrosine hydroxylase (15,16) and dopamine beta-hydroxylase, but some studies report negative results for phenylethanolamine N-methyltransferase (PNMT) (17). Immunohistochemical stains have also been uniformly positive for norepinephrine and negative for epinephrine, but some of the staining for norepinephrine might be related to neuronal uptake of this catecholamine (17). Detection of intracytoplasmic catecholamines is possible by fluorescence methods using formaldehyde or glyoxylic acid, but because of technical problems and availability of other diagnostic tests, this is seldom necessary (12).

Human NB cells in vitro have been shown to have a diverse morphologic phenotype including: 1) neuronal cells having neuritic processes and neurosecretory granules; 2) cells resembling Schwann cells; and 3) melanocytic cells replete with melanosomes (18). Interconversion (or

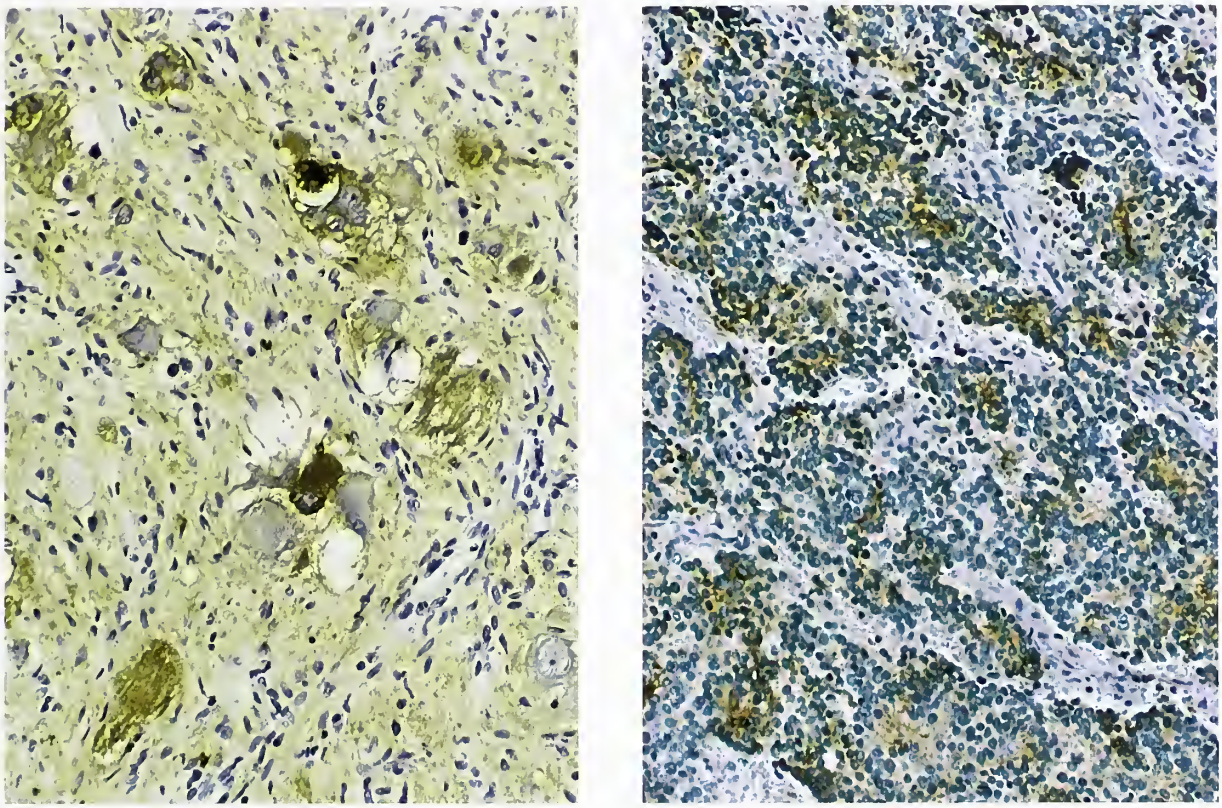

Figure 20-9

STROMA-RICH INTERMIXED NEUROBLASTOMA AND STROMA-POOR NEUROBLASTOMA

Left: In this stroma-rich NB, immunoreactivity for chromogranin A is most evident in scattered ganglion cells, but could also be seen in pale fibrillar areas with overlapping, intertwining neuritic processes (avidin-biotin peroxidase method).

Right: The stroma-poor NB stains for chromogranin A, particularly in the Homer Wright rosettes or pseudorosettes where there is intertwining and overlapping of neuritic processes. This allows for density concentration of dense-core neurosecretory type granules (avidin-biotin peroxidase method). (Fig. 23-38 from Fascicle 19, Third Series.)

transdifferentiation) of nonadrenergic cells and melanocytic cells has been demonstrated as well as an intermediate cell type, possibly representing a multipotential precursor (19). In normal adrenal neuroblasts, the sequential expression of genes coding for tyrosine hydroxylase, chromogranin A, pG2, and beta-2-microglobulin marks successive stages in maturation of the chromaffin cell lineage. Cells of NB are "arrested" in this sequence, thus raising the possibility that malignant transformation of cells at different stages of maturation may account for some of the phenotypic diversity that characterizes these tumors (20).

Immunostaining for chromogranin A has been demonstrated in NBs, GNBs (fig. 20-9, left) (21–24), and GNs (21); positive results are expected where the concentration of neurosecretory granules is greatest, such as ganglionic cells with active synthesis or areas with overlapping or intertwining of numerous neuritic processes (e.g., Homer Wright rosettes or pseudorosettes) (fig. 20-9, right) or matted neuropil. Immunohistochemical staining has also been demonstrated for other neuroendocrine markers, such as other members of the chromogranin family (22), synaptophysin (21,24), protein gene product (PGP) 9.5 (15), HNK-1 (3), and HISL (15). There may be immunostaining for neurofilament protein(s) (fig. 20-10), with some variability in staining for the three subgroups (21,25). Monoclonal antibodies to neuronal microtubule-associated proteins (MAP-1 and MAP-2) may be strongly reactive with neuroblasts (fig. 20-11),

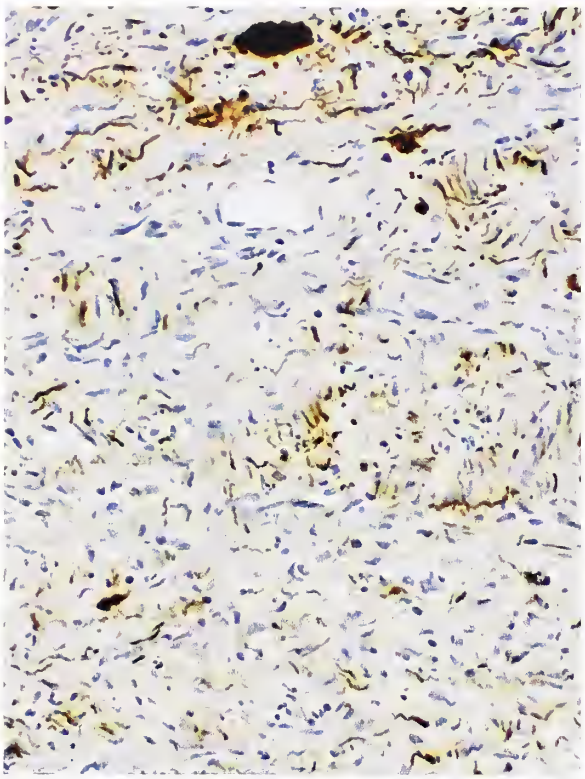

Figure 20-10

GANGLIONEUROBLASTOMA

Immunostain for neurofilament protein highlights slender to plump neuritic processes. The cytoplasm of an occasional cell body also stains intensely (top) (avidin-biotin peroxidase method).

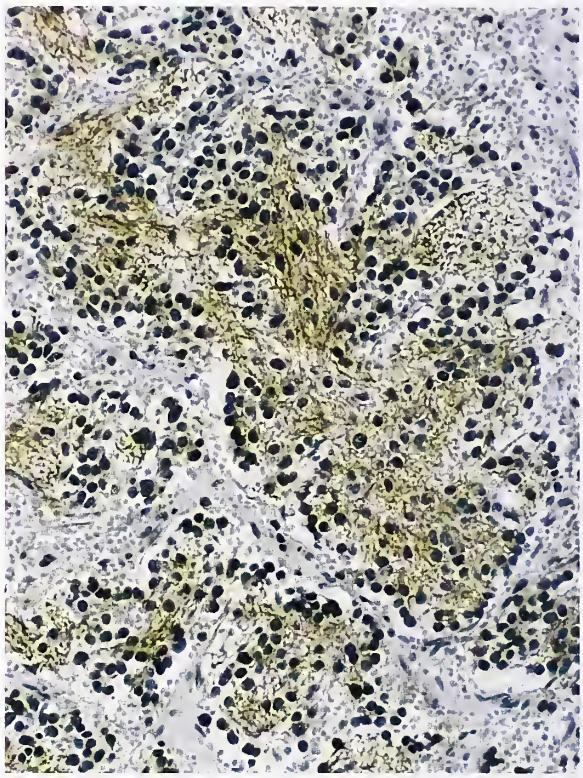

Figure 20-11

STROMA-POOR NEUROBLASTOMA

Immunostain for microtubule-associated protein (MAP-2) highlights abundant neuritic processes. A nearly identical pattern was seen with a stain for J-1 tubulin (avidin-biotin peroxidase method). (Fig. 23-40 from Fascicle 19, Third Series.)

ganglion cells, and neurofibrils; staining for alpha- and beta-tubulin may show a similar pattern of reactivity (26). Immunostaining has also been reported for peripherin, a type of intermediate filament expressed in the peripheral nervous system (27); it has been regarded as evidence of cell maturation in NB and enhanced expression is associated with an improved prognosis. High expression of neuropeptide Y receptors has been reported in 90 percent of NBs; these receptors are potential new molecular targets for the treatment of these malignant tumors (28).

As noted in chapter 19, some tumors may be associated with a watery diarrhea syndrome, due to the secretion of vasoactive intestinal peptide (VIP); VIP can be demonstrated in cells usually showing neuronal and ganglionic differentiation (fig. 20-12). The distribution of VIP mRNA is usually confined to the cytoplasm of cells with ganglionic differentiation and not to undifferentiated neuroblastic cells (29). Increased VIP levels in NB have been correlated with cellular differentiation and favorable tumor stage (30), and there is some suggestion that both VIP and somatostatin may function as autocrine growth factors at the cellular level, with perhaps some modulation of differentiation (30).

P glycoprotein, encoded by the *mdr-1* gene, has a role in multidrug resistance to chemotherapy through a drug efflux pump at the cellular level which is ATP dependent; it has been expressed immunohistochemically in stage IV NB, but was not detected in a study of stage IV-S NB (31). Expression of mdr-1/p-glycoprotein is reported to be increased in differentiating cells such as mature ganglion cells (32). The protein encoded by the *N-myc* oncogene (12) or N-myc RNA expression (12) can also be detected, and

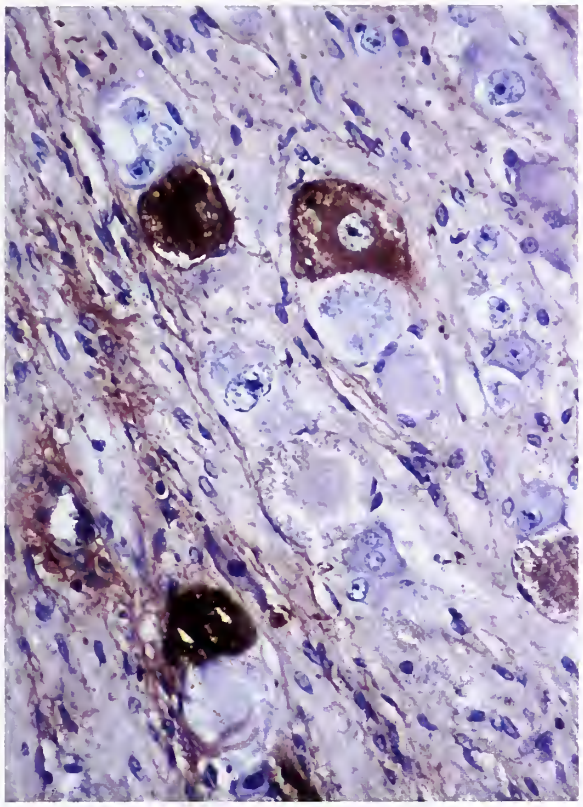

Figure 20-12

GANGLIONEUROBLASTOMA, STROMA-RICH TUMOR

GNB, or stroma-rich intermixed tumor in the Shimada classification, was associated with watery diarrhea syndrome and elevated serum level of vasoactive intestinal peptide (VIP). Immunostain for VIP is positive in several ganglionic cells (avidin-biotin peroxidase method). (Fig. 23-41 from Fascicle 19, Third Series.)

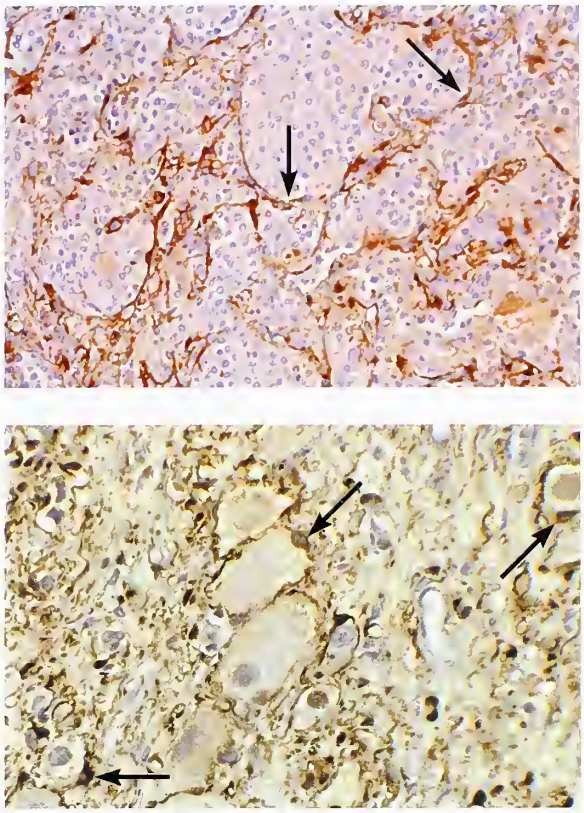

Figure 20-13

NEUROBLASTOMA AND GANGLIONEUROBLASTOMA

Top: In this NB, stellate to dendritic cells immunoreactive for S-100 protein are adjacent to vascular septa (arrows). Cells are consistent with Schwann (or sustentacular) cells.

Bottom: In this GNB, cells in intimate contact with ganglion cells (arrows) stain intensely for S-100 protein and are in a typical location for satellite cells. A few other cells are immunoreactive, and are probably Schwann cells. (T&B: avidin-biotin peroxidase method.)

quantification of this protein may be correlated with prognosis. A significant proportion of aggressive NBs lack genomic amplification of *N-myc*, yet some tumors can express N-myc RNA and protein (33). A recent study indicated that tumor cells with enlarged and prominent nucleoli are associated with *N-myc* amplification in a subset of NBs (undifferentiated/poorly differentiated with a high mitosis-karyorrhexis index) (34).

Immunostaining for S-100 protein may demonstrate small to elongated dendritic-shaped cells in NB and GNB, particularly in the fibrovascular septa separating nests of tumor cells (fig. 20-13, top) (35). These have been regarded as Schwann cells or precursor cells, suggesting an avenue of differentiation within the tumor. These S-100 protein–positive cells are also situated in the same area as sustentacular cells in paragangliomas. Some cells in close proximity to neuronal or ganglion cells are consistent with satellite cells, and may also be immunoreactive for S-100 protein (fig. 20-13, bottom). Immunoreactivity for S-100 protein has been used to evaluate differentiation of NB cells into Schwann cells, and may provide some information regarding prognosis (36), even though it is not entirely specific for Schwann cells.

Immunoreactivity for S-100 protein has been correlated with other prognostic factors such as age and mitosis-karyorrhexis index (MKI), and favorable and unfavorable stroma-rich

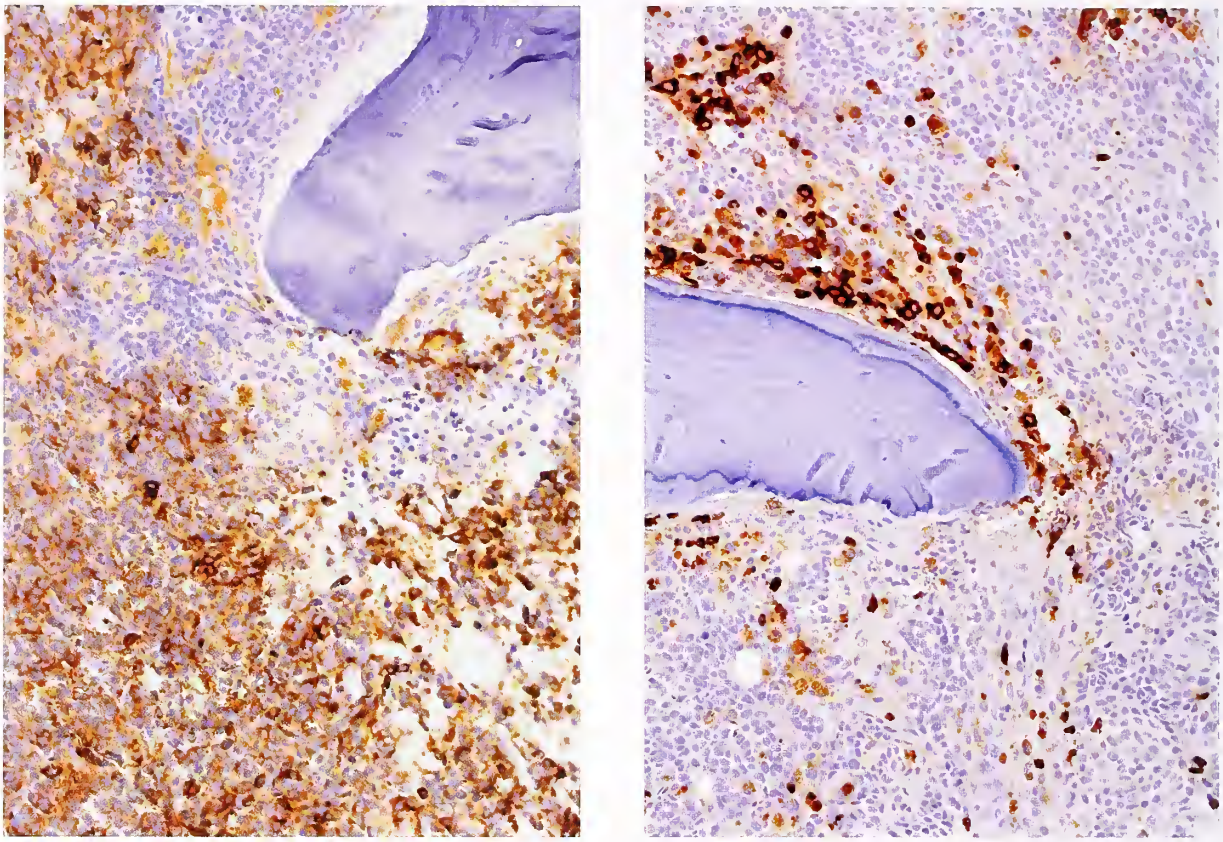

Figure 20-14

NEUROBLASTOMA METASTATIC TO BONE

Left: Immunostain for synaptophysin was of aid in demonstrating the extent of metastatic NB in this case and distinguishing the immunoreactive neuroblasts from immature myeloid cells.

Right: Immunostain for myeloperoxidase demonstrates immature myeloid cells while most of the nonreactive cells are metastatic NB (L&R: avidin-biotin peroxidase method).

categories in the Shimada classification (36). An inverse relationship has been reported between immunopositivity for S-100 protein and ferritin, with an increased number of ferritin-positive cells (stromal septa and NB cells) associated with an unfavorable outcome (36). Selected immunostains may be useful in delineating metastatic neuroblastoma in bone marrow (fig. 20-14).

Differentiating neuronal or ganglionic cells of NB are strongly positive for transforming growth factors beta-1 and beta-3, a group of regulatory proteins with a variable effect on cell growth and differentiation (37). Expression of other molecular markers such as trk-A (38) and lack of high-affinity nerve growth factor receptors (39) may have some influence on prognosis. Hopefully, future studies will shed additional light on the molecular aspects of these tumors and lead to major advances in treatment (3). Immunostains in GN can highlight satellite cells in close relationship to ganglion cells (fig. 20-15, left) and also demonstrate neuronal processes emanating from ganglion cells (fig. 20-15, right).

FINE NEEDLE ASPIRATION BIOPSY AND CYTOLOGIC FINDINGS

Fine needle aspiration biopsy (FNAB) or exfoliative cytology of NB and GNB typically shows a cellular specimen with small primitive cells having a high nuclear to cytoplasmic ratio (fig. 20-16); amorphous fibrillar material may be seen in the background or attached directly to the cells. There may be one or two small nucleoli or small aggregates of chromatin that

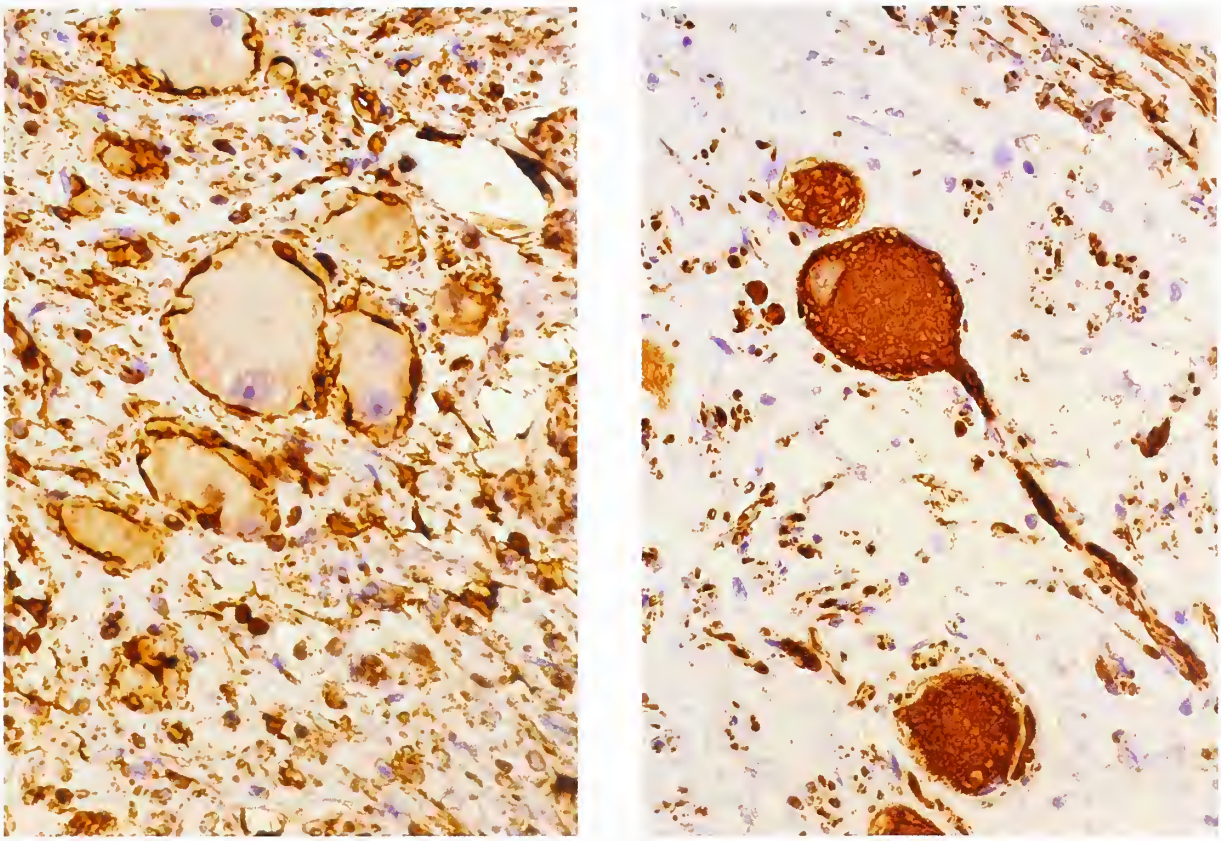

Figure 20-15

GANGLIONEUROMA

Left: There is intense S-100 protein immunostaining of most cells in the field except for the ganglion cells. The cells encircling ganglion cells are satellite cells and the remaining immunoreactive cells are Schwann cells.

Right: Immunostain for neurofilament protein highlights ganglion cells and neuritic cell processes (L&R: avidin-biotin peroxidase method).

form chromocenters. Smear/imprint preparations of surgically resected specimens may provide valuable cytologic information (fig. 20-17). It is very uncommon to see Homer Wright rosettes or pseudorosettes in aspiration specimens (40,41), and when found, they may be poorly formed (42).

Ancillary diagnostic techniques such as electron microscopy and immunohistochemistry may be necessary to ensure accuracy of interpretation in difficult cases, and of course close clinical correlation is always indicated. Small tissue fragments obtained during FNAB may provide valuable morphologic information, and in this context, cell block preparation may yield diagnostic material and enable immunohistochemical study. In one series of exfoliative cytology specimens of malignant tumors in children, over half of the specimens positive for NB were from cerebrospinal fluid (see fig. 20-16), followed by peritoneal fluid and two positive urine cytologies (43). GN has also been diagnosed by FNAB (fig. 20-18, left), but one must be aware of some of the stroma-rich tumors in which definitive resection may overturn a benign cytologic interpretation (3). Some tumors are accessible by disposable trucut needle biopsy as seen in figure 20-18, right.

QUANTIFICATION OF DNA AND NUCLEOLAR ORGANIZER REGIONS

Quantitative analysis of DNA has been shown to have prognostic value in patients with NB (44–50), with the most favorable group

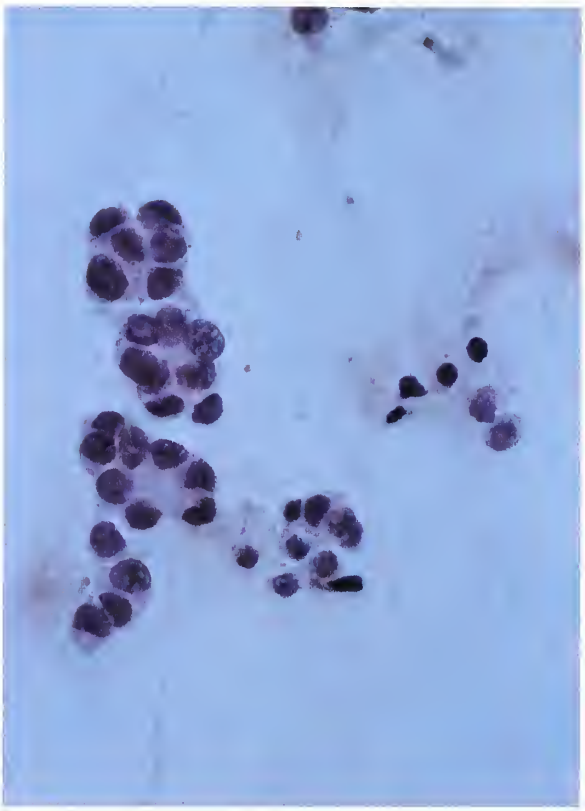

Figure 20-16

NEUROBLASTOMA

Neuroblastoma cells are evident in an exfoliative cytology preparation of cerebrospinal fluid. (Fig. 23-43 from Fascicle 19, Third Series.)

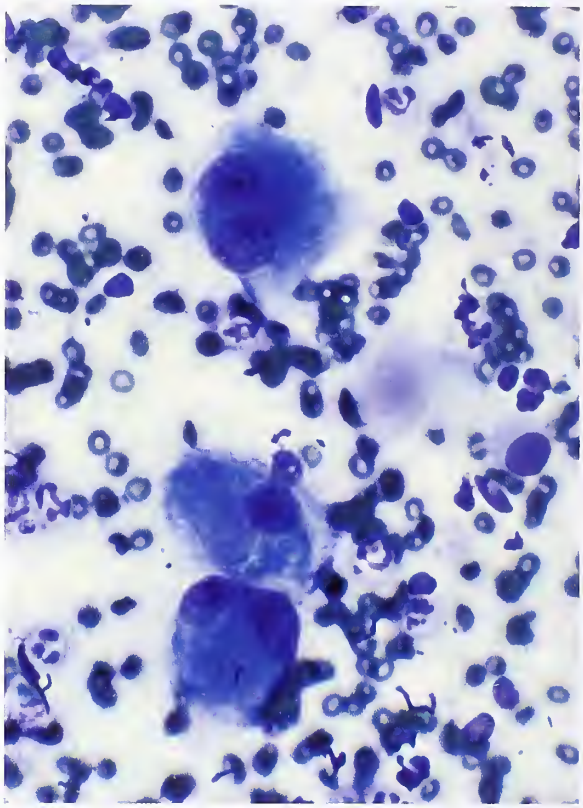

Figure 20-17

SMEAR/IMPRINT OF A GANGLIONEUROBLASTOMA

Cells show ganglionic features with ample cytoplasm and eccentric nuclei; some cells in other areas had a single prominent nucleolus (Diff Quik stain).

of tumors having hyperdiploid or aneuploid DNA histograms. Abnormal DNA content has also been reported in GNs when a significant number of ganglion cell nuclei are recovered (51). A favorable clinical outcome has been associated with an aneuploid stemline and a low percentage of cells in the S, G2, and M phases of the cell cycle (45). In some studies, favorable stage and DNA aneuploidy have been found to be independent prognostic indicators (51). Evaluation of DNA ploidy along with *N-myc* gene amplification may be complementary and together provide useful information regarding prognosis (49).

A significant correlation has been noted between the mean number of nucleolar organizer regions (AgNORs) with differentiation and MKI in stroma-poor tumors, while stroma-rich tumors had the lowest average number of AgNORs (52). Increased numbers of AgNORs correlate with poor survival (50,52,53): it has been reported to be lowest in the primary tumor, intermediate in regional lymph node metastases, and highest in distant metastases (50).

CYTOGENETIC STUDIES AND MOLECULAR PATHOLOGY

Cytogenetic markers may aid in the differential diagnosis of small round cell tumors, and because of its potential role in predicting clinical outcome, it is likely to assume increasing importance as cancer therapies are stratified on the basis of prognostic variables. Chromosomal abnormalities have been documented in NB, mainly a deletion in the short arm of chromosome 1 involving bands 1p36.1-2 (54,55). The current literature supports a strong association between an unbalanced gain of chromosome 17q and an adverse clinical outcome (56).

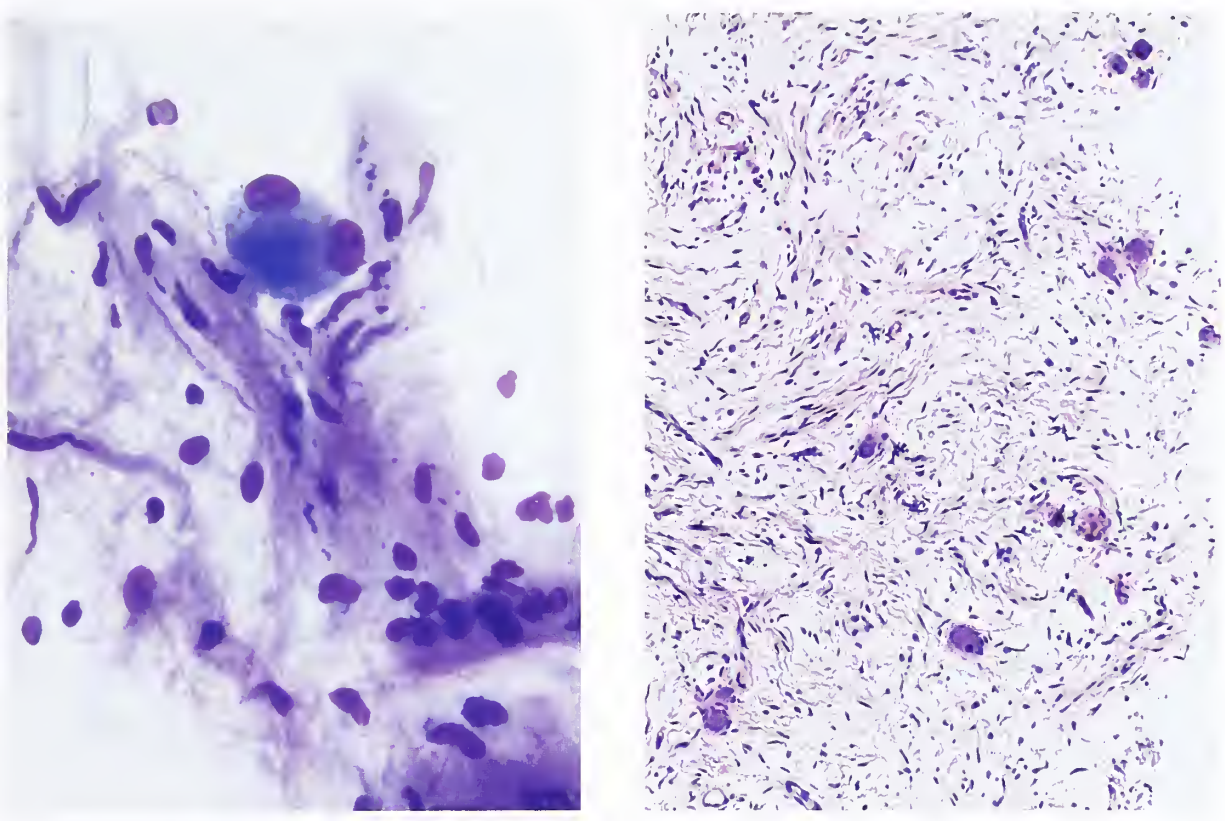

Figure 20-18

GANGLIONEUROMA

Left: Fine-needle aspiration shows ganglion cells with a spindle cell component representing Schwann cells. The diagnosis of ganglioneuroma was subsequently confirmed on pathologic examination of the resected tumor (Diff Quik stain).

Right: Transrectal biopsy of a presacral ganglioneuroma. The ganglion cells are set within a loose spindle cell matrix composed of Schwann cells (same case as in figure 19-47).

In addition to conventional cytogenetics, there are other abnormalities that can be detected by fluorescence in situ hybridization (FISH) (57) and quantitative polymerase chain reaction (58). In a study by Bown et al. (59), 15 of 36 NBs had clonal karyotype abnormalities in tumor cells, 15 had normal karyotypes, and cytogenetic analysis failed in 6. The NB-associated oncogene *N-myc* is normally found on chromosome 2, but it appears to be translocated to the short arm of chromosome 1 and may become amplified, which helps explain the chromosome 1p abnormalities and poor prognosis compared with patients who have normal chromosome 1p and hyperdiploidy (12).

As discussed previously, three distinct genetic subsets of NB have been recognized (see chapter 19). Less than half of all patients who present with or who later develop metastatic NB show *N-myc* amplification (60). There appears to be great variability in modulation of gene expression which may offer insight into differences in clinical behavior of NB (61). The locus of the NB tumor suppressor gene has been mapped to 1p36 on the distal arm of chromosome 1 in a constitutional cytogenetic study done on blood lymphocytes (62). Other genetic abnormalities reported in NBs include hyperdiploidy, "double minute" chromosomes (dmin), and "homogeneously staining regions" (hsrs); the dmin and hsrs usually represent amplification of the oncogene *N-myc* (59). Schwann cells in maturing NBs have been shown to be genetically different from neuronal cells, suggesting that these cells may be a reactive population of normal cells that invade the NB (63).

Identification of the role of *N-myc* oncogene amplification in rapid tumor progression in many (but not all) patients with NB (64) has been a major step in better understanding the molecular biology of this tumor and has been confirmed in a number of other studies. *N-myc*-amplification is seen in about 40 percent of stages III and IV NBs and in only 5 to 10 percent of stage I, II, or IV-S disease (65). In some cases, *N-myc* expression is associated with poor clinical outcome even in the absence of gene amplification (66). For the individual patient, therefore, lack of *N-myc* amplification does not exclude a poor prognosis. Patients with NB and opsoclonus/myoclonus have been reported to have a good prognosis independent of stage or age at diagnosis, and tumors from several patients have shown no evidence of *N-myc* gene amplification (67). *N-myc* amplification and expression have been noted in localized, stroma-rich GNBs, suggesting that morphologic differentiation in vivo is not necessarily associated with decreased expression or an adverse prognosis (68). Other cytogenetic alterations have been described involving the *ras* (69), the *c-src* (70), and the *ret* protooncogenes (70).

Newer techniques exist for more rapid and direct determination of single copy chromosome 17q gain, *N-myc* amplification, chromosome 1 copy number, presence of 1p deletion, and ploidy than FISH and quantitative polymerase chain reaction (56,71). Chromogenic in situ hybridization (CISH) has recently been used to detect *N-myc* amplification; interpretation appeared to be relatively easy because the preparations were viewed with an ordinary light microscope with good preservation of the tissue morphology (65). It is, therefore, possible to define distinct prognostic groups on the basis of this genetic information and other parameters, and thus permit stratification in therapies. Molecular detection of the GD2-synthase transcript by polymerase chain reaction may improve the detection of minimal residual tumor whether in bone marrow or in peripheral blood (72). In a recent review of the biology of NBs, there was discussion of the role of overexpressed oncogenes like *N-myc* and cyclin D, and the mechanisms leading to decreased apoptosis like overexpression of bcl-2, survivin, NM23, and epigenetic silencing of caspase 8 (73).

REFERENCES

Ultrastructural Findings

1. Qualman SJ, Bowen J, Fitzgibbons PL, Cohn SL, Shimada H. Cancer Committee, College of American Pathologists. Protocol for the examination of specimens from patients with neuroblastoma and related neuroblastic tumors. Arch Pathol Lab Med 2005;129:874-883.
2. Triche TJ. Differential diagnosis of neuroblastoma and related tumors. In: Lack EE, Pathology of the adrenal glands. New York: Churchill Livingstone; 1990:323-350.
3. Lack EE. Pathology of adrenal and extra-adrenal paraganglia. Major Problems in Pathology, Vol 29. Philadelphia: WB Saunders Co; 1994.
4. Tannenbaum M. Ultrastructural pathology of adrenal medullary tumors. Pathol Annu 1970;5: 145-171.
5. Romansky SG, Crocker DW, Shaw KN. Ultrastructural studies on neuroblastoma: evaluation of cytodifferentiation and correlation of morphology and biochemical and survival data. Cancer 1978;42:2392-2398.
6. Taxy JB. Electron microscopy in the diagnosis of neuroblastoma. Arch Pathol Lab Med 1980;104: 355-360.
7. Erlandson RA. Diagnostic transmission electron microscopy of tumors. New York: Raven Press; 1994.
8. Triche TJ, Ross WE. Glycogen-containing neuroblastoma with clinical and histopathologic features of Ewing's sarcoma. Cancer 1978;41:1425-1432.
9. Yunis EJ, Agostini RM Jr, Walpusk JA, Hubbard JD. Glycogen in neuroblastomas. A light- and electron-microscopic study of 40 cases. Am J Surg Pathol 1979;3:313-323.
10. Mierau GW, Berry PJ, Orsini EN. Small round cell neoplasms: can electron microscopy and immunohistochemical studies accurately classify them? Ultrastr Pathol 1985;9:99-111.

11. Ricci A Jr, Parham DM, Woodruff JM, Callihan T, Green A, Erlandson RA. Malignant peripheral nerve sheath tumors arising from ganglioneuromas. Am J Surg Pathol 1984;8:19-29.

Immunohistochemical Findings

12. Triche TJ. Neuroblastoma and other childhood neural tumors: A review. Pediatr Pathol 1990;10: 175-193.
13. Sorensen PH, Liu XF, DeLattre O, et al. Reverse transcriptase PCR amplification of EWS/FLI-1 fusion transcripts as a diagnostic test for peripheral primitive neuroectodermal tumors of childhood. Diagn Mol Pathol 1993;2:147-157.
14. Hasegawa T, Hirose T, Ayala AG, et al. Adult neuroblastoma of the retroperitoneum and abdomen: clinicopathologic distinction from primitive neuroectodermal tumor. Am J Surg Pathol 2001;25:918-924.
15. Wirnsberger GH, Becker H, Ziervogel K, Höfler H. Diagnostic immunohistochemistry of neuroblastic tumors. Am J Surg Pathol 1992;16:49-57.
16. Grossman DM, Jin L, Heidelberger KP, Lloyd RV. Expression of chromogranin A protein and messenger RNA and tyrosine hydroxylase protein in paraffin-embedded sections of neuroendocrine neoplasms. Endocr Pathol 1991;2:148-154.
17. Lloyd RV, Sisson JC, Shapiro B, Verhofstad AA. Immunohistochemical localization of epinephrine, norepinephrine, catecholamine-synthesizing enzymes, and chromogranin in neuroendocrine cells and tumors. Am J Pathol 1986;125:45-54.
18. Tsokos M, Scarpa S, Ross RA, Triche TJ. Differentiation of human neuroblastoma recapitulates neural crest development. Study of morphology, neurotransmitter enzymes and extracellular matrix proteins. Am J Pathol 1987;128:484-496.
19. Ciccarone V, Spengler BA, Meyers MB, Biedler JL, Ross RA. Phenotypic diversification in human neuroblastoma cells: expression of distinct neural crest lineages. Cancer Res 1989;49:219-225.
20. Cooper MJ, Hutchins GM, Cohen PS, Helman LJ, Mennie RJ, Israel MA. Human neuroblastoma tumor cell lines correspond to the arrested differentiation of chromaffin adrenal medullary neuroblasts. Cell Growth Differ 1990;1:149-159.
21. Molenar WM, Baker DL, Pleasure D, Lee VM, Trojanowski JQ. The neuroendocrine and neural profiles of neuroblastomas, ganglioneuroblastomas, and ganglioneuromas. Am J Pathol 1990;136:375-382.
22. Pagani A, Forni M, Tonini GP, Papotti M, Bussolati G. Expression of members of the chromogranin family in primary neuroblastomas. Diagn Mol Pathol 1992;1:16-24.
23. Franquemont DW, Mills SE, Lack EE. Immunohistochemical detection of neuroblastomatous foci in composite adrenal pheochromocytoma-neuroblastoma. Am J Clin Pathol 1994;102:163-170.
24. Erickson LA, Lloyd RV. Practical markers used in the diagnosis of endocrine tumors. Adv Anat Pathol 2004;11:175-189.
25. Osborn M, Dirk T, Käser H, Weber K, Altmannsberger M. Immunohistochemical localization of neurofilaments and neuron-specific enolase in 29 cases of neuroblastoma. Am J Pathol 1986; 122:433-442.
26. Caccamo D, Katsetos CD, Herman MM, Frankfurter A, Collins VP, Rubinstein LJ. Immunohistochemistry of a spontaneous murine ovarian teratoma with neuroepithelial differentiation. Neuron-associated beta-tubulin as a marker for primitive neuroepithelium. Lab Invest 1989;60:390-398.
27. Pedersen WA, Becker LE, Yeger H. Expression and distribution of peripherin protein in human neuroblastoma cell lines. Int J Cancer 1993;53: 463-470.
28. Korner M, Waser B, Reubi JC. High expression of neuropeptide y receptors in tumors of the human adrenal gland and extra-adrenal paraganglia. Clin Cancer Res 2004;10:8426-8433.
29. Yoshioka M, Nagano I, Nakamura S, Imaizumi M, Kimura N. Detection of vasoactive intestinal polypeptide messenger RNA in ganglioneuroblastoma by in situ hybridization. Endocr Pathol 1990;1:51-57.
30. Qualman SJ, O'Dorisio MS, Fleshman DJ, Shimada H, O'Dorisio TM. Neuroblastoma. Correlation of neuropeptide expression in tumor tissue with other prognostic factors. Cancer 1992;70:2005-2012.
31. Chan HS, Haddad G, Thorner PS, et al. P-glycoprotein expression as a predictor of the outcome of therapy for neuroblastoma. N Engl J Med 1991;325:1608-1614.
32. Bates SE, Shieh CY, Tsokos M. Expession of mdr-1/P-glycoprotein in human neuroblastoma. Am J Pathol 1991;139:305-315.
33. Wada RK, Seeger RC, Brodeur GM, et al. Human neuroblastoma cell lines that express N-myc without gene amplification. Cancer 1993;72: 3346-3354.
34. Kobayashi C, Monforte-Munoz HL, Gerbing RB, et al. Enlaged and prominent nucleoli may be indicative of MYCN amplification: a study of neuroblatoma (Schwannian stroma-poor), undifferentiated/poorly differentiated subtype with high mitosis-karyorrhexis index. Cancer 2005; 103:174-180.

35. DeLellis RA, Mangray S. The adrenal glands. In: Mills SE, Carter D, Greenson JK, Oberman HA, Reuter V, Stoler MH, eds. Sternberg's diagnostic pathology, 4th ed. Philadelphia: Lippincott Williams & Wilkins; 2004:621-667.
36. Aoyama C, Qualman ST, Regan M, Shimada H. Histopathologic features of composite ganglioneuroblastoma. Immunohistochemical distinction of the stromal component is related to prognosis. Cancer 1990;65:255-264.
37. McCune BK, Patterson K, Chandra RS, Kapur S, Sporn MB, Tsokos M. Expression of transforming growth factor-ß isoforms in small round cell tumors of childhood. An immunohistochemical study. Am J Pathol 1993;142:49-59.
38. Brodeur GM. TRK-a expression in neuroblastomas: a new prognostic marker with biological and clinical significance. J Natl Cancer Inst 1993; 85:344-345.
39. Suzuki T, Bogenmann E, Shimada H, Stram D, Seeger RC. Lack of high-affinity nerve growth factor receptors in aggressive neuroblastomas. J Natl Cancer Inst 1993;85:377-383.

Fine Needle Aspiration Biopsy and Cytologic Findings

40. Miller TR, Bottles K, Abele JS, Beckstead JH. Neuroblastoma diagnosed by fine needle aspiration biopsy. Acta Cytol 1985;29:461-468.
41. Akhtar M, Ali MA, Sabbah RS, Bakry M, Sackey K, Nash EJ. Aspiration cytology of neuroblastoma. Light and electron microscopic correlations. Cancer 1986;57:797-803.
42. Silverman JF, Dabbs DJ, Ganick DJ, Holbrook CT, Geisinger KR. Fine needle aspiration cytology of neuroblastoma, including peripheral neuroectodermal tumor, with immunocytochemical and ultrastructural confirmation. Acta Cytol 1988;32:367-376.
43. Geisinger KR, Hajdu SI, Helson L. Exfoliative cytology of nonlymphoreticular neoplasms in children. Acta Cytol 1984;28:16-28.

Quantification of DNA and AgNORs

44. Look AT, Hayes FA, Nitschke R, McWilliams NB, Green AA. Cellular DNA content and predictor of response to chemotherapy in infants with unresectable neuroblastoma. N Engl J Med 1984; 311:231-235.
45. Gansler T, Chatten J, Varello M, Bunin GR, Atkinson B. Flow cytometric DNA analysis of neuroblastoma. Correlation with histology and clinical outcome. Cancer 1986;58:2453-2458.
46. Abramowsky CR, Taylor SR, Anton AH, Berk AI, Roerderer M, Murphy RF. Flow cytometry, DNA ploidy analysis and catecholamine secretion profiles in neuroblastoma. Cancer 1989;63:1752-1756.
47. Look AT, Hayes FA, Shuster JJ, et al. Clinical relevance of tumor cell ploidy and N-myc gene amplification in childhood neuroblastoma: a Pediatric Oncology Group study. J Clin Oncol 1991;9:581-591.
48. Naito M, Iwafuchi M, Ohsawa Y, et al. Flow cytometric DNA analysis of neuroblastoma: prognostic significance of DNA ploidy in unfavorable group. J Pediatr Surg 1991;26:834-837.
49. Muraji T, Okamoto E, Fujimoto J, Suita S, Nakagawara A. Combined determination of N-myc oncogene amplification and DNA ploidy in neuroblastoma. Cancer 1993;72:2763-2768.
50. Shimotake T, Iwai N, Tokiwa K, Deguchi E, Sawada T, Fushiki S. Increased numbers of argyrophilic nucleolar organizer regions between primary and metastatic sites predict tumor progression in stage IV and IV-S neuroblastoma. Cancer 1994;73:3103-3107.
51. Taylor SR, Blatt J, Costantino JP, Roederer M, Murphy RF. Flow cytometric DNA analysis of neuroblastoma and ganglioneuroblastoma. A 10-year retrospective study. Cancer 1988;62:749-754.
52. Egan M, Raafat F, Crocker J, Williams D. Comparative study of the degree of differentiation of neuroblastoma and mean numbers of nucleolar organizer regions. J Clin Pathol 1988;41:527-531.
53. Brookes CN, Ooms BC, McGill F, England K, Hinchliffe SA, van Velzen D. Ploidy independence of Ag-NOR number in neuroblastoma. Lab Invest 1992;67:243-245.

Cytogenetic Studies and Molecular Pathology

54. Schneider NR. Cytogenetic evaluation of childhood neoplasms. Arch Pathol Lab Med 1993;117: 1220-1224.
55. Stark B, Jeison M, Bar-Am I, et al. Distinct cytogenetic pathways of advanced-stage neuroblastoma tumors, detected by spectral karyotyping. Genes Chromosomes Cancer 2002;34:313-324.
56. Morowitz M, Shusterman S, Mosse Y, et al. Detection of single-copy chromosome 17q gain in human neuroblastoma using real-time quantitative polymerase chain reaction. Mod Pathol 2003;16:1248-1256.
57. Sartelet H, Grossi L, Pasquier D, et al. Detection of N-myc amplification by FISH in immature areas of fixed neuroblastomas: more efficient than Southern blot/PCR. J Pathol 2002;198:83-91.
58. De Preter K, Speleman F, Combaret V, et al. Quantification of MYCN, DDX1, and NAG gene copy number in neuroblastoma using a real-time quantitative PCR assay. Mod Pathol 2002;15:159-166.

59. Bown NP, Reid MM, Malcolm AJ, Davison EV, Craft AW, Pearson AD. Cytogenetic abnormalities of small round cell tumours. Med Ped Oncol 1994;23:124-129.
60. McConville CM, Dyer S, Rees SA, et al. Molecular cytogenetic characterization of two non-MYCN amplified neuroblastoma cell lines with complex t(11;17). Cancer Genet Cytogenet 2001;130:133-140.
61. Raetz EA, Kim MK, Moos P, et al. Identification of genes that are regulated transcriptionally by Myc in childhood tumors. Cancer 2003;98:841-853.
62. Biegel JA, White PS, Marshall HN, et al. Constitutional 1p36 deletion in a child with neuroblastoma. Am J Hum Genet 1993;52:176-182.
63. Ambros IM, Zellner A, Roald B, et al. Role of ploidy, chromosome 1p, and Schwann cells in the maturation of neuroblastoma. N Engl J Med 1996;334:1505-1511.
64. Seeger RC, Brodeur GM, Sather H, et al. Association of multiple copies of the N-myc oncogene with rapid progression of neuroblastomas. N Engl J Med 1985;313:1111-1116.
65. Tsai HY, Hsi BL, Hung IJ, et al. Correlation of MYCN amplification with MCM7 protein expression in neuroblastomas: a chromogenic in situ hybridization study in paraffin sections. Hum Pathol 2004;35:1397-1403.
66. Wada RK, Seeger RC, Brodeur GM, et al. Human neuroblastoma cell lines that express N-myc without gene amplification. Cancer 1993;72:3346-3354.
67. Cohn SL, Salwen H, Herst CV, et al. Single copies of the N-myc oncogene in neuroblastomas from children presenting with the syndrome of opsoclonus-myoclonus. Cancer 1988;62:723-726.
68. Fabbretti G, Valenti C, Loda M, et al. N-myc gene amplification/expression in localized stroma-rich neuroblastoma (ganglioneuroblastoma). Hum Pathol 1993;24:294-297.
69. Ireland CM. Activated N-ras oncogenes in human neuroblastoma. Cancer Res 1989;49:5530-5533.
70. Benz CC, Liu ET. Oncogenes and tumor supressor genes in human malignancies. Boston: Kluwer Academic Pub.; 1993:108-118.
71. Taylor CP, McGuckin AG, Bown NP, et al. Rapid detection of prognostic genetic factors in neuroblastomas using fluorescence in situ hybridization on tumour imprints and bone marrow smears. United Kingdom Children's Cancer Study Group. Br J Cancer 1994;69:445-451.
72. Lo Piccolo MS, Cheung NK, Cheung IY. GD2 synthase: a new molecular marker for detecting neuroblastoma. Cancer 2001;92:924-931.
73. van Noesel MM, Versteeg R. Pediatric neuroblastomas: genetic and epigenetic 'danse macabre'. Gene 2004;325:1-15.

Index*

*In a series of numbers, those in boldface indicate the main discussion of the entity.

B

C

F

G

H

N

O

P

S

T

U

V

W

Z

ISBN-13: 978-1-881041-01-6
ISBN-10: 1-881041-01-8
EAN
9 781881 041016 16000 >